SIDISA 2024

XII International Symposium on Environmental Engineering

PALERMO

October 1st - 4th

Book of Abstract

Università degli Studi di Palermo

GITISA
Gruppo Italiano di Ingegneria Sanitaria Ambientale

ANDIS
ASSOCIAZIONE NAZIONALE DI INGEGNERIA SANITARIA AMBIENTALE

SCIENTIFIC COMMITTEE

Michele Torregrossa (IT) - Chair
Abdeltif Amrane (FR)
Gianni Andreottola (IT)
Renato Baciocchi (IT)
Juan Antonio Baeza Labat (ES)
Damià Barceló (ES)
Vincenzo Belgiorno (IT)
Giorgio Bertanza (IT)
Maria Rosaria Boni (IT)
Paolo Salvatore Calabrò (IT)
Roberto Canziani (IT)
Andrea Giuseppe Capodaglio (IT)
Marco Capodici (IT)
Alessandra Carucci (IT)
Stefano Caserini (IT)
Stefano Cernuschi (IT)
Diana Cocarta (RO)
Fabio Conti (IT)
Santo Fabio Corsino (IT)
Philippe Corvini (CH)
Alida Cosenza (IT)
Raffaello Cossu (IT)
Frederic Coulon (UK)
Adriana Del Borghi (IT)
Glen Daigger (USA)
Joana Maria Dias (PT)
Gaetano Di Bella (IT)
Daniele Di Trapani (IT)
Cigdem Eskicioglu (CAN)
Giovanni Esposito (IT)
Anna Laura Eusebi (IT)
Massimiliano Fabbricino (IT)
Francesco Fatone (IT)
Margherita Ferrante (IT)
Filipa Maria Ferreira (PT)
Grazia Ghermandi (IT)
Daniele Goi (IT)
Renato Iannelli (IT)
Pavel Jenicek (CZ)
Ioannis Katsoyiannis (EL)
Dana Kominkova (CZ)
Gregory Korshin (USA)
Maria Cristina Lavagnolo (IT)
Juan M. Lema Rodicio (ES)
Geoffroy Lesage (FR)
Francesco Lombardi (IT)

SCIENTIFIC COMMITTEE

Jörg Londong (DE)
Claudio Lubello (IT)
Roberta Maffettone (IT)
Elena Magaril (RU)
Jacek Mąkinia (PL)
Francesca Malpei (IT)
Ignazio Marcello Mancini (IT)
Giorgio Mannina (IT)
Salvatore Masi (IT)
Anuska Mosquera Corral (ES)
Lotfi Mouni (DZ)
Aldo Muntoni (IT)
Vincenzo Naddeo (IT)
Zoran Nakić (HR)
Monia Niero (IT)
Patryk Oleszczuk (PL)
Antonio Panico (IT)
Francesco Pirozzi (IT)
Alessandra Polettini (IT)
Sebastià Puig (ES)
Roberto Raga (IT)
Marco Race (IT)
Marco Ragazzi (IT)
Ezio Ranieri (IT)
Harsha Ratnaweera (NO)
Paolo Roccaro (IT)
Aurora Santos Lopez (ES)
Rajandrea Sethi (IT)
Alessio Siciliano (IT)
Piero Sirini, (IT)
José Antonio Sobrino (ES)
Sabrina Sorlini (IT)
Danilo Spasiano (IT)
Jean Philippe Steyer (FR)
Fabio Tatano (IT)
Sergio Teggi (IT)
Alberto Tiraferri (IT)
Vincenzo Torretta (IT)
Cristina Trois (ZA)
Federico Vagliasindi (IT)
Paola Verlicchi (IT)
Gaspare Viviani (IT)
Jiri Wanner (CZ)
Mariachiara Zanetti (IT)
Najla Sadfi Zouaoui (TN)

ORGANIZING COMMITTEE

Michele Torregrossa
Gaspare Viviani
Giorgio Mannina
Gaetano Di Bella
Daniele Di Trapani
Alida Cosenza
Santo Fabio Corsino
Marco Capodici

PALERMO
October 1st - 4th

XII International Symposium on Environmental Engineering

SUPPORT TO ORGANIZING COMMITTEE

Daniele Di Trapani
(Coordinator)
Michele Carabillò
Federica De Marines
Sara Mulone
Manuela Russo Tiesi
Maria Castiglione
Giuseppe Beringheli
Alice Sorrenti
Giovanni Vinti

SUPPORTED BY

ARS

Regione Siciliana
PRESIDENZA

Città di Palermo

ORDINE DEGLI INGEGNERI
DELLA PROVINCIA DI PALERMO

EWA
EUROPEAN WATER ASSOCIATION

ARPA SICILIA
AGENZIA REGIONALE PER LA PROTEZIONE DELL'AMBIENTE

IWA
the international water association
YOUNG WATER PROFESSIONALS ITALY

Aiat
Associazione Ingegneria Ambiente e Territorio - APS

MINISTERO DELL'AMBIENTE
E DELLA SICUREZZA ENERGETICA

COMMISSARIO
STRAORDINARIO UNICO
PER LA DEPURAZIONE

CONAI
CONSORZIO NAZIONALE IMBALLAGGI

SPONSORS

OWAC
ENGINEERING COMPANY

AMAP S.p.A.

ACQUAENNA
Gruppo iren

Agesp
servizi ambientali

Calcestruzzi Ericina Libera
SOCIETÀ COOPERATIVA

caltaqua
Acque di Caltanissetta S.p.A.

EVONIK
Leading Beyond Chemistry

FN Ingegneria S.r.l.

GIGLIO srl

HACH
Be Right™

MANN+HUMMEL

minsait
An Indra company

OBLYSIS
new wastewater era

ORION
WWW.ORION-SRL.IT

SHIMADZU
Excellence in Science

xylem
Let's Solve Water

vermicon
solutions for microbiology

SUMMARY

PARALLEL SESSION: A1

Wastewater treatment

Anaerobic digestion

Title: Comparison between poly aluminum chloride and aluminum sulfate in sludge anaerobic digestion: impacts and drawbacks of Al-based inorganic coagulants in a circular economy perspective

Author(s): Francesco Pasciucco*[1], Erika Pasciucco[1], Alessio Castagnoli[1], Renato Iannelli[1] and Isabella Pecorini[1]

[1] Department of Energy, Systems, Territory and Construction Engineering (DESTEC), University of Pisa, 56122 Pisa, Italy isabella.pecorini@unipi.it

Keyword(s): anaerobic digestion, inorganic aluminum coagulant, energy recovery, wastewater treatment.

Abstract

The current paradigm changes that wastewater treatment plants (WWTPs) are confronting from a linear to a circular economy has made WWTPs a topic of much discussion [1].

In fact, wastewater facilities will be required to adopt a biorefinery model [2], encouraging process sustainability by including the design of infrastructures [3] and byproduct recycling [4].

Because of that, WWTPs should meet two goals: minimizing the use of non-renewable resources and safeguarding human health [5]. The facility's treatments should be designed to prevent or lessen negative impacts on other processes, since compliance with standard requirements is achieved through treatment chains that may clash with one another [6].

The coagulation and flocculation techniques are widely employed in wastewater treatment to remove pollutants, comprising emerging pollutants [7] or nutrients [8], because they are simple to apply and effective.

Through the use of two processes - fast coagulant mixing and gentle agitation, respectively - the treatment promotes the aggregation of colloidal particles into larger settleable flocs. Based on earlier testing, the operation times of the two phases are determined. Generally, these times fall between 1 and 10 minutes and 10 and 30 minutes, respectively [9, 10, 11].

Because of their established efficacy, availability, and affordability, coagulants based on aluminum (Al) and iron (Fe) are frequently utilized [12, 13, 14].

Conversely, the majority of coagulants condense and gather in sludge. Previous studies reports that Fe and Al concentrations in waste activated sludge ranged from 1.9 to 15.4 and from 2.6 to 28.8 mg/g, respectively [15, 16, 17]. These concentrations may have an adverse effect in sludge anaerobic digestion, which is one of the most used technologies for sludge treatment [18, 19].

The literature has shown a significant deal of interest in this topic in the previous few years. The impact of poly ferric sulfate on sludge anaerobic digestion was investigated by Liu et al. [14]. The roles of ferric chloride were examined by Zhan et al. [20]. Wu et al. [21] compared poly ferric sulfate and poly aluminum chloride's effects. Among the studies mentioned above, only Zhan et al. [20] found an improvement in biomethane generation due to the presence of coagulant.

To the best of the authors' knowledge, the effects of poly aluminum chloride and aluminum sulfate on biomethane yield were not compared by prior studies, notwithstanding the most recent advancements. The impacts of these two flocculants on aerobic granules production were examined by Liu et al. [25], but a comparison on the anaerobic digestion process has not yet been addressed.

By supplying triplicate reactors with varying concentrations of coagulants (up to 20 mg Al/g TS), the effects of poly aluminum chloride and aluminum sulfate on waste activated sludge anaerobic digestion were compared in this study. In the control group, reactors had no coagulants added to them. The findings showed that biomethane production was hindered by Al-based coagulants, and the inhibition increased with increasing coagulant addition. In comparison to the control (167.8$\pm$1.9 mL CH_4/g VS), biomethane generation was significantly more inhibited in aluminum sulfate reactors, with maximum decreases up to 32% around. The presence of flocculants changed the starting characteristics of the reactors, affecting the solubilization and hydrolysis, as shown by analytical analysis, FTIR, and SEM examinations. Moreover, the suppression of biomethane phase was significantly influenced by the enormous production of H_2S in reactors that were conditioned with aluminum sulfate.

However, the application of coagulant can encourage nutrient recovery, particularly with regard to phosphorus. Our research will increase the body of knowledge in this area and help stakeholders select coagulants for full-scale plants. Subsequent investigations ought to concentrate on diminishing the impact of coagulants on biomethane generation by the alteration or examination of novel flocculants.

References

[1] F. Pasciucco, I. Pecorini, and R. Iannelli, “Planning the centralization level in wastewater collection and treatment: A review of assessment methods,” J. Clean. Prod., vol. 375, 2022, doi: 10.1016/j.jclepro.2022.134092.
[2] I. Owusu-Agyeman et al., “Conceptual system for sustainable and next-generation wastewater resource recovery facilities,” Sci. Total Environ., vol. 885, 2023, doi: 10.1016/j.scitotenv.2023.163758.
[3] F. Pasciucco, I. Pecorini, and R. Iannelli, “Centralization of wastewater treatment in a tourist area: A comparative LCA considering the impact of seasonal changes,” Sci. Total Environ., vol. 897, 2023, doi: 10.1016/j.scitotenv.2023.165390.
[4] E. Rossi, F. Pasciucco, R. Iannelli, and I. Pecorini, “Environmental impacts of dry anaerobic biorefineries in a Life Cycle Assessment (LCA) approach,” J. Clean. Prod., vol. 371, 2022, doi: 10.1016/j.jclepro.2022.133692.
[5] F. Pasciucco, I. Pecorini, and R. Iannelli, “A comparative LCA of three WWTPs in a tourist area: Effects of seasonal loading rate variations,” Sci. Total Environ., vol. 863, 2023, doi: 10.1016/j.scitotenv.2022.160841.
[6] E. Albini, I. Pecorini, and G. Ferrara, “Improvement of digestate stability using dark fermentation and anaerobic digestion processes,” Energies, vol. 12, no. 18, 2019, doi: 10.3390/en12183552.
[7] N. Girish, N. Parashar, and S. Hait, “Coagulative removal of microplastics from aqueous matrices: Recent progresses and future perspectives,” Sci. Total Environ., vol. 899, 2023, doi: 10.1016/j.scitotenv.2023.165723.
[8] G. A. Zoumpouli, D. Herron, A. Thornton, B. Jefferson, and P. Campo, “The role of coagulation on the fate of PFAS, brominated flame retardants and other trace contaminants in tertiary wastewater treatment for phosphorus control,” Sci. Total Environ., vol. 887, 2023, doi: 10.1016/j.scitotenv.2023.163982.
[9] O. S. Amuda and I. A. Amoo, “Coagulation/flocculation process and sludge conditioning in beverage industrial wastewater treatment,” J. Hazard. Mater., vol. 141, no. 3, pp. 778–783, 2007, doi: 10.1016/j.jhazmat.2006.07.044.
[10] C. Y. Teh, P. M. Budiman, K. P. Y. Shak, and T. Y. Wu, “Recent Advancement of Coagulation-Flocculation and Its Application in Wastewater Treatment,” Ind. Eng. Chem. Res., vol. 55, no. 16, pp. 4363–4389, 2016, doi: 10.1021/acs.iecr.5b04703.
[11] V. Saritha, N. Srinivas, and N. V. Srikanth Vuppala, “Analysis and optimization of coagulation and flocculation process,” Appl. Water Sci., vol. 7, no. 1, 2017, doi: 10.1007/s13201-014-0262-y.
[12] John Bratby, Coagulation and Flocculation in Water and Wastewater Treatment – Third Edition. 2016.
[13] Y. Chen, H. Lin, W. Yan, J. Huang, G. Wang, and N. Shen, “Alkaline fermentation promotes organics and phosphorus recovery from polyaluminum chloride-enhanced primary sedimentation sludge,” Bioresour. Technol., vol. 294, 2019, doi: 10.1016/j.biortech.2019.122160.
[14] X. Liu et al., “Mechanistic insights into the effect of poly ferric sulfate on anaerobic digestion of waste activated sludge,” Water Res., vol. 189, 2021, doi: 10.1016/j.watres.2020.116645.
[15] Y. J. Chen et al., “Effects of Al-coagulant sludge characteristics on the efficiency of coagulants recovery by acidification,” Environ. Technol. (United Kingdom), vol. 33, no. 22, pp. 2525–2530, 2012, doi: 10.1080/09593330.2012.679696.
[16] G. Zhen, X. Yan, H. Zhou, H. Chen, T. Zhao, and Y. Zhao, “Effects of calcined aluminum salts on the advanced dewatering and solidification/stabilization of sewage sludge,” J. Environ. Sci., vol. 23, no. 7, pp. 1225–1232, 2011, doi: 10.1016/S1001-0742(10)60539-6.
[17] C. Park, C. D. Muller, M. M. Abu-Orf, and J. T. Novak, “The Effect of Wastewater Cations on Activated Sludge Characteristics: Effects of Aluminum and Iron in Floc,” Water Environ. Res., vol. 78, no. 1, pp. 31–40, 2006, doi: 10.2175/106143005x84495.
[18] Z. Wang, T. Wang, B. Si, J. Watson, and Y. Zhang, “Accelerating anaerobic digestion for methane production: Potential role of direct interspecies electron transfer,” Renew. Sustain. Energy Rev., vol. 145, 2021, doi: 10.1016/j.rser.2021.111069.
[19] F. Pasciucco, G. Francini, I. Pecorini, A. Baccioli, L. Lombardi, and L. Ferrari, “Valorization of biogas from the anaerobic co-treatment of sewage sludge and organic waste: Life cycle assessment and life cycle costing of different recovery strategies,” J. Clean. Prod., vol. 401, p. 136762, 2023, doi: 10.1016/j.jclepro.2023.136762.
[20] W. Zhan et al., “Mechanistic insights into the roles of ferric chloride on methane production in anaerobic digestion of waste activated sludge,” J. Clean. Prod., vol. 296, 2021, doi: 10.1016/j.jclepro.2021.126527.
[21] Y. Wu et al., “Insights into how poly aluminum chloride and poly ferric sulfate affect methane production from anaerobic digestion of waste activated sludge,” Sci. Total Environ., vol. 811, 2022, doi: 10.1016/j.scitotenv.2021.151413.

[22] A. Cainglet et al., “The influence of coagulant type on the biological treatment of sewage sludge,” Sci. Total Environ., vol. 869, 2023, doi: 10.1016/j.scitotenv.2023.161706.
[23] H. Luo et al., “Impacts of aluminum- and iron-based coagulants on municipal sludge anaerobic digestibility, dewaterability, and odor emission,” Water Environ. Res., vol. 94, no. 1, 2022, doi: 10.1002/wer.1684.
[24] Y. Chen et al., “Understanding the mechanisms of how poly aluminium chloride inhibits short-chain fatty acids production from anaerobic fermentation of waste activated sludge,” Chem. Eng. J., vol. 334, pp. 1351–1360, 2018, doi: 10.1016/j.cej.2017.11.064.
[25] Z. Liu et al., “Impact of Al-based coagulants on the formation of aerobic granules: Comparison between poly aluminum chloride (PAC) and aluminum sulfate (AS),” Sci. Total Environ., vol. 685, pp. 74–84, 2019, doi: 10.1016/j.scitotenv.2019.05.306.

Title: Optimizing the Ultrasound Treatment of Anaerobic Digestate for its wider valorization: Impact of a Flow-Through Configuration with a Rod-Shaped Transducer

Author(s): Enrica Ciotola*, Alessandra Cesaro, Giovanni Esposito, Francesco Pirozzi

Department of Civil, Architectural and Environmental Engineering, Napoli, Italy, e-mails: enrica.ciotola@unina.it, alessandra.cesaro@unina.it, giovanni.esposito1@unina.it, francesco.pirozzi@unina.it

Keyword(s): sonolysis, Digestate, reactor configuration, Trace Organic Contaminants, Biogas production, Energy recovery.

Abstract

Anaerobic digestion (AD) technology is highly effective in stabilizing the organic matter content of residual sludge, besides enabling sludge reduction [1]. One of the most interesting aspects of the AD process is undoubtedly the opportunity to recover energy in the form of methane. Moreover, the AD byproduct, digestate, contains a significant amount of nutrients in the form of ammonia nitrogen, and ortho-phosphates that make it a valuable fertilizer [2]. For these reasons, the improvement of the efficiency of the AD biochemical process, both in terms of energy production and quality of the digestate produced, aligns with the evolving objectives of the scientific community. These objectives aim to minimize sludge disposal while maximizing its reuse as a valuable source of nutrients and energy [3].

Since the early 2000s, the ultrasound (US) treatment of sewage sludge has been studied to investigate potential strategies aimed at increasing methane yields and accelerating the AD rate-limiting step, namely hydrolysis [4]. The intensification of AD via US pre-treatment of waste activated sludge (WAS) before AD has been demonstrated in numerous works over the years [4]. This achievement has been associated with the disintegration of organic matter caused by the fierce collapse of transient acoustic cavitation bubbles and its secondary effects such as the reaching of high local temperatures and pressures, the formation of highly reactive radicals, and most of all intense shear forces [5]. At the same time, two main reasons have been found to negatively affect the process efficiency: the attenuation of the acoustic cavitation due to the high solids content of thickened WAS (4-6%) [6] entering the anaerobic digester and the non-selectivity of the US sound waves [7]. Therefore, the techno-economic analysis of theUS sludge pre-treatment before AD showed an unattractive net energy balance for the application in full-scale facilities [8].

Recently, a few works have delved into the study of US treatment of municipal digestates; according to the literature, the characteristic TS content of digestate (2-3%) is in the optimum range for US treatment [9]. Moreover, in this way it is possible to focus the energy input on the recalcitrant organic matter that has not been degraded during the AD process [10]. As a consequence, the possible recirculation of the treated digestate to the AD could increase the overall energy potential of the biochemical process. Specifically, batch studies have shown better biomethane potential increase [7] and acoustic cavitation field [11] compared to WAS. Nonetheless, at a laboratory scale the US process has been mainly studied in static conditions, while only a study [6] has explored digestate treatment in a flow-through configuration. In this case, a novel design was tested, in which the types of transducers used, as well as the intensity and wavelengths of the ultrasonic field emitted were significantly different from the US

devices usually tested in static conditions.

In addition to its investigation as a treatment for enhancing biogas production, ultrasound treatment has also been studied in terms of reducing and potentially degrading emerging contaminants in wastewater treatment [12]. The studies showed how the physico-mechanical action of US induces effective desorption of trace organic contaminants, which from the solid phase tend to be released into solution, being then more susceptible to potential chemical attack both by the radicals formed due to the US cavitation phenomenon itself, and by further advanced oxidation treatments, which can potentially be coupled to the US [13]. Additionally, the organic contaminant presence in solution in relatively low concentration could also provide additional substrate for the anaerobic biochemical reactions. Nevertheless, this kind of study has never been performed on digested sludge.

Following the aforementioned, US treatment could open up broad prospects for application. Nonetheless, since the complexity of the process is reflected both in its strong dependence on geometrical factors and configuration, that influence its intensity and dissipated energy and in the matrix treated, more efforts are needed to understand whether the US can have real potential in sludge treatment.

This work aims to compare for the first time the effect of US treatment on anaerobic digestate under static and flow conditions, using the same transducer. Specifically, the most commonly used transducer at full-scale is the rod-shaped one, which guarantees high ultrasonic field intensities [14]. For this reason, a sonotrode was chosen as US device. The laboratory-scale configuration has been designed to carry out both batch and plug flow tests under the same operating conditions (i.e. geometry of the sonicated chamber, probe diameter, energy input and amplitude of the sound wave). In the proposed flow-through configuration, the ultrasonic field is emitted in countercurrent to the incoming sludge flow rate to maximize cavitation effects. The effect of ultrasound will then be evaluated holistically, considering: (a) the yields in terms of solubilization of organic matter, evaluating parameters such as soluble COD, dissolved proteins and carbohydrates constituting the extracellular polymeric substances released during treatment and their different transfer in static or flow conditions; (b) the possible increase of the biodegradability of the digestate through biomethanation tests; (c) the reduction of the concentrations of emerging target contaminants, for the safe reuse of digestate as fertilizer.

The ultimate goal of the following research is to understand the maximum potential of the US technology in terms of organic matter solubilization in digestate due to ultrasound effects, and the resulting efficiencies in terms of increased biogas production and reduction of trace contaminants under varying operational conditions. In this way, the proposed configuration (Figure 1) would contribute to the advancement in sustainable sludge treatment technologies.

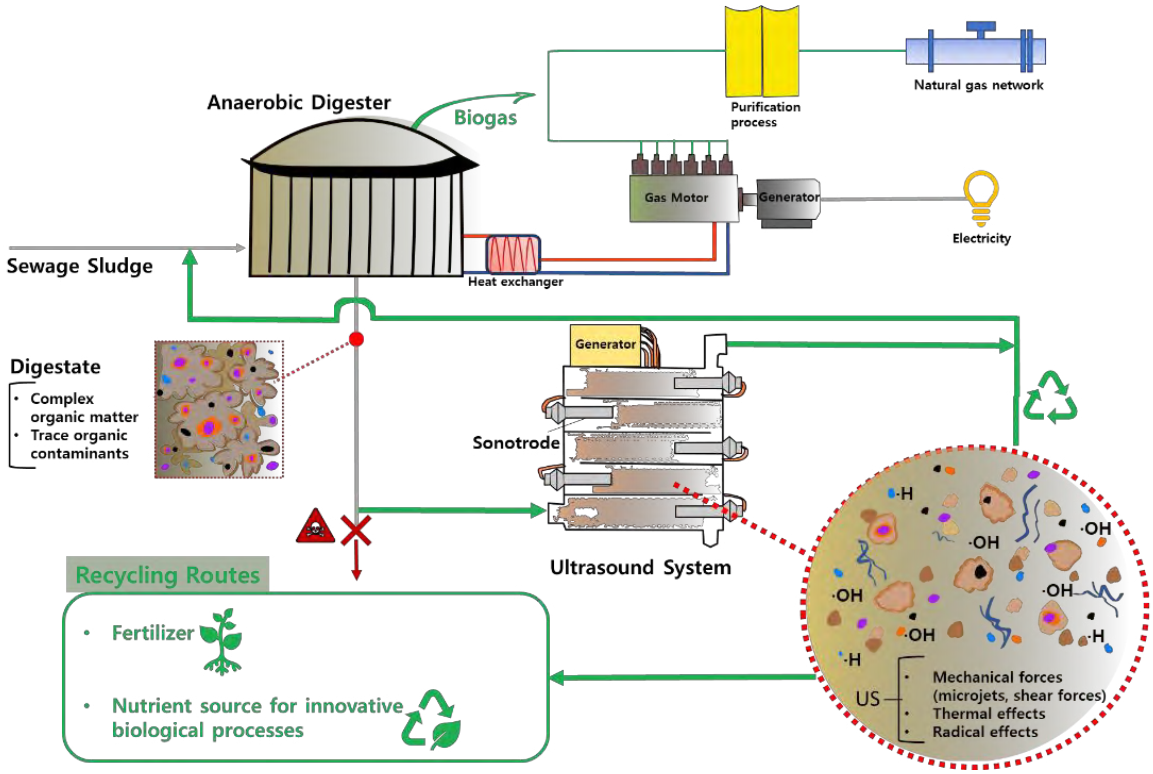

Figure 1. Graphical Abstract

References

[1] Zhang J., Long Z., Liu X., He H., Zhang G., Tian Y., "Structure and composition of dissolved organic matters in sludge by ultrasonic treatment", Journal of Environmental Management, 356, 120589, (2024).
[2] Di Costanzo N., Cesaro A., Di Capua F., Mascolo M.C., Esposito G., "Application of high-intensity static magnetic field as a strategy to enhance the fertilizing potential of sewage sludge digestate", Waste Management 170, 122–130, (2023).
[3] Ruiz-Hernando M., Vinardell S., Labanda J., LLorens J., " Effect of ultrasonication on waste activated sludge rheological properties and process economics", Water Research, 208, 117855, (2022).
[4] Pilli S., Bhunia P., Yan S., LeBlanc R.J., Tyagi R.D., Surampalli R.Y., "Ultrasonic pretreatment of sludge: A review", Ultrasonic Sonochemistry 18, 1–18, (2011).
[5] Carpenter J., Badve M., Rajoriya S., George S., Saharan V.K., Pandit A.B., "Hydrodynamic cavitation: An emerging technology for the intensification of various chemical and physical processes in a chemical process industry", Reviews in Chemical Engineering, 33, 433–468, (2017).
[6] Lippert T., Bandelin J., Xu Y., Liu Y.C., Robles G.H., Drewes J.E., Koch K., "From pre-treatment to co-treatment - How successful is ultrasonication of digested sewage sludge in continuously operated anaerobic digesters?", Renewable Energy, 166, 56–65, (2020).
[7] Koch K., Lippert T., Hauck Sabadini N., Drewes J.E., "Tube reactors as a novel ultrasonication system for trouble-free treatment of sludges", Ultrasonic Sonochemistry 37, 464–470, (2017).
[8] Ruiz-Hernando M., Vinardell S., Labanda J., Llorens J., "Effect of ultrasonication on waste activated sludge rheological properties and process economics", Water Research 208, 117855, (2022).
[9] Show K., Mao T., Lee D., "Optimisation of sludge disruption by sonication", Water Research, 41, 4741-4747, (2007).

[10] Garoma T., Pappaterra D., “An investigation of ultrasound effect on digestate solubilization and methane yield”, Waste Management 71, 728–733, (2018).
[11] Bandelin J., Lippert T., Drewes J.E., Koch K., “Cavitation field analysis for an increased efficiency of ultrasonic sludge pre-treatment using a novel hydrophone system”, Ultrasonic Sonochemistry 42, 672–678, (2018).
[12] de Andrade F.V., Augusti R., de Lima G.M., “Ultrasound for the remediation of contaminated waters with persistent organic pollutants: A short review”, Ultrasonic Sonochemistry, 78, (2021).
[13] Serna-Galvis E.A., Botero-Coy A.M., Martínez-Pachón D., Moncayo-Lasso A., Ibáñez M., Hernández F., Torres-Palma R.A., “Degradation of seventeen contaminants of emerging concern in municipal wastewater effluents by sonochemical advanced oxidation processes”, Water Research, 154, 349–360, (2019).
[14] Le N.T., Julcour-Lebigue C., Delmas H., “An executive review of sludge pretreatment by sonication”, Journal of Environmental Sciences, 37, 139–153, (2015).

Production of Volatile Fatty Acids from the Source Separated Organic Fraction of Municipal Solid Waste and Wastewater Sludge: Semi-continuous Tests Results

Domenica Pangallo[1], Mariastella Ferreri[2], Altea Pedullà[2] , Demetrio Zema[1], Paolo S. Calabrò[2]

[1] Università Mediterranea degli Studi di Reggio Calabria, Department Agraria, Reggio Calabria, Italy
[2] Università Mediterranea degli Studi di Reggio Calabria, Department of Civil, Energy, Environmental and Materials Engineering, Reggio Calabria, Italy

Abstract

Volatile fatty acids (VFAs) are intermediates in anaerobic digestion, valued for their versatility and utility. These chemical building blocks have numerous industrial applications. VFAs can be produced both synthetically from petrochemical derivatives and also through biological routes. In this regard, co-fermentation of thickened and raw excess sludge with the organic fraction of municipal solid waste (OFMSW) not only lead to VFA production, but can also help achieving both resource recovery and sustainable and innovative waste and wastewater management. In the paper are presented the results of semi-continuous experiments, according to the results the production of VFAs greatly depend on the amount of OFMSW in the mixture between sludge and OFMSW.

Keywords: Anaerobic Digestion; Organic Fraction of Municipal Solid Waste; Wastewater Sludge; Volatile fatty acids

Introduction

Volatile fatty acids (VFAs) are chemical building blocks that are experiencing a significant surge in market demand. Recently, a growing focus on the biological production and recovery of volatile fatty acids (VFAs) has been emerging. VFAs such as acetic, propionic, and butyric acids find extensive industrial application in several fields such as pharmaceutic, food, and chemical [1],[2]. Moreover, VFAs serve as valuable raw materials for diverse products including biogas [3], biodiesel [4], bioplastics [5], biohydrogen [6], and even electricity generation through microbial fuel cells [7].

Conventionally, VFAs production as commercial pure chemicals mainly relies on the synthesis from fossil-based (petroleum-based) resources through petrochemical pathways [8]. Due to the continuously increasing environmental consciousness and the dwindling global petroleum reserves, economically viable alternative production methods have emerged. Following the transition to the circular economy, the biorefinery approach for VFAs production highlights their provision flexibility and sustainability. The biorefinery strategy for producing VFAs involves fermentation processes provided by pure cultures of specific anaerobic bacterial strains [9].

The aim of this paper is to present the results of semi-continuous tests evaluating VFAs production from the co-fermentation of OFMSW and excess sludge from wastewater treatment.

MATERIALS AND METHODS

Substrates

In order to reproduce real conditions, samples of real OFMSW collected in the city of Reggio Calabria were used. OFMSW was grab sampled, shredded (reproducing the mechanical pre-treatment by a pulper used in full scale plants) and then stored at 4 °C.

Samples of wastewater sludge were collected from a full-scale plant situated in the Municipality of Reggio Calabria. The plant, with a capacity of 30,000 population equivalents (PE), provides for physico-mechanical pre-treatments and a secondary treatment system employing pre-denitrification.

Two different wastewater sludges were tested: thickened sludge (TKS) and raw excess sludge (RS).

Substrates characteristics are summarized in Table 1.

Table 1. Substrates Characteristics

	OFMSW	TKS	RS
Total Solids [%]	31,4 ± 1,62	3,2 ± 0,22	1,1 ± 0,02
Volatile Solids [$\%_{TS}$]	90,5 ± 0,50	77,3 ± 0,38	76,9 ± 0,61
pH	5,6 ± 0,02	6,5 ± 0,02	7,0 ± 0,02

Semi-continuous tests

Fermentation tests were carried out using glass reactors with a net volume of about 2.0 L equipped with a mechanical mixing system and immersed in a thermostatic bath at 35°C. Reactors were operated in a semi-continuous mode, were fed three times a week, during the feeding the fermented material was also collected.
Fermentation tests were conducted by modifying the initial pH, the Hydraulic Retention Time (HRT), the type of sludge used (TKS and/or RS) and the sludge-to-OFMSW ratio.
The predetermined quantities of sludge and OFMSW were combined directly within the reactor and gently stirred. Subsequently, the pH was measured and eventually adjusted using analytical-grade H_2SO_4 or NaOH (Sigma-Aldrich) or kept at its natural value.
The design of the experiments is summarized in Table 2; a total of 6 semi-continuous tests were carried out.

Table 2. Design of the experiments

Reactor	HRT [days]	Initial pH	Sludge tested	V_{Sludge}:V_{OFMSW}
A	7	9,0	TKS	30:70
B	7	5,0	TKS	30:70
C	7	6,9*	RS	90:10
D	7	6,3*	TKS	90:10
E	4	6,2*	RS	90:10
F	4	6,3*	TKS	90:10

*not adjusted

Volatile Fatty Acids (VFAs) were quantified once a week using a titration technique [10], [11] which proved effective even with very low initial pH levels (e.g. close to 4).
The results have been evaluated in terms of approximate concentration of volatile acids expressed as acetic acid.

Results and discussion

VFAs production from the co-fermentation of excess sludge and OFMSW is summarized in Figure 1. Analysing the results and comparing them to the volumetric ratio between sludge and OFMSW, a clear predominace of the 30:70 ratio arises. The change in retention time from 7 to 4 days causes a slight reduction in VFA concentration.
Considering the variation in pH, initial correction seems to increase VFAs production, but the difference is minimal. Moreover this is not enough to justify the costs required for initial pH correction.
The co-fermentation with TKS shows VFAs production slightly higher than RS at an HRT of 7 days while with an HRT of 4 days the situation is opposite.

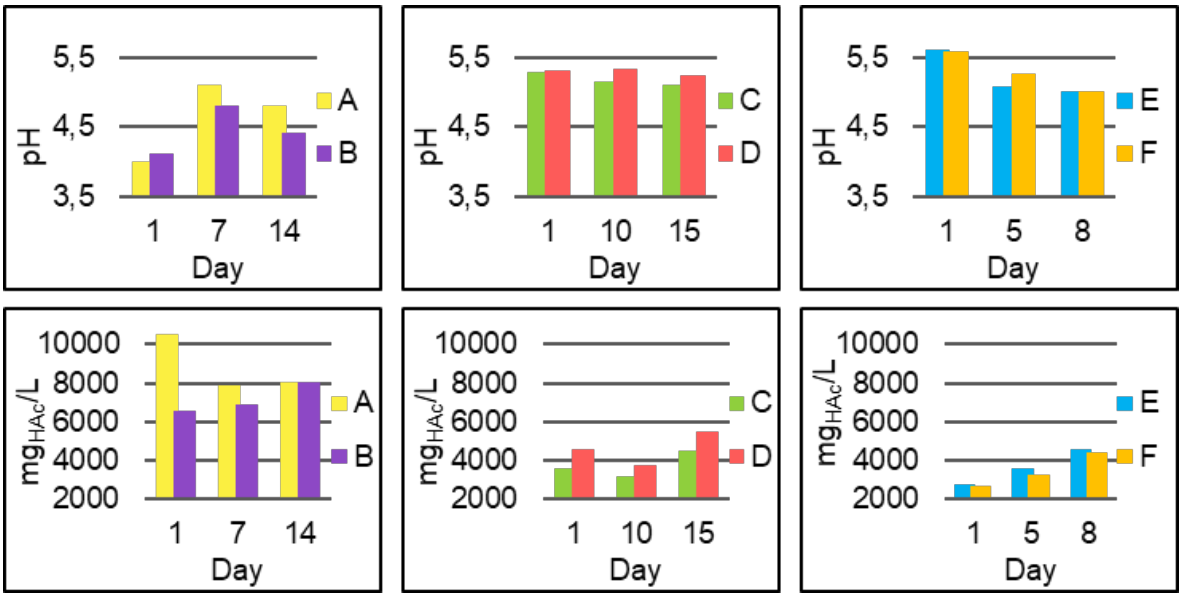

Figure 1. Semicontinuous tests results

CONCLUSION

The results demonstrate that the best performance was achieved for volumetric ratio between TKS sludge and OFMSW of 70:30, with both an alkaline or acid initial pH, for hydraulic retention times of 7 days.

ACKNOWLEDGMENT

This work was financially supported by Fondazione AMGA – Genova, through the call “Project 4.0 – third edition”. Financed project “Joint valorisation of the organic fraction of municipal solid waste from separated collection and of excess sludge for the production of biogas and volatile fatty acids”.

References

[1] M. Atasoy, I. Owusu-Agyeman, E. Plaza, e Z. Cetecioglu, «Bio-based volatile fatty acid production and recovery from waste streams: Current status and future challenges», *Bioresour. Technol.*, vol. 268, pp. 773–786, 2018.
[2] F. Valentino, G. Munarin, M. Biasiolo, C. Cavinato, D. Bolzonella, e P. Pavan, «Enhancing volatile fatty acids (VFA) production from food waste in a two-phases pilot-scale anaerobic digestion process», *J. Environ. Chem. Eng.*, vol. 9, fasc. 5, p. 106062, ott. 2021, doi: 10.1016/j.jece.2021.106062.
[3] S. Begum, G. R. Anupoju, S. Sridhar, S. K. Bhargava, V. Jegatheesan, e N. Eshtiaghi, «Evaluation of single and two stage anaerobic digestion of landfill leachate: Effect of pH and initial organic loading rate on volatile fatty acid (VFA) and biogas production», *Bioresour. Technol.*, vol. 251, pp. 364–373, mar. 2018, doi: 10.1016/j.biortech.2017.12.069.
[4] D. L. Fortela *et al.*, «Extent of inhibition and utilization of volatile fatty acids as carbon sources for activated sludge microbial consortia dedicated for biodiesel production», *Renew. Energy*, vol. 96, pp. 11–19, ott. 2016, doi: 10.1016/j.renene.2016.04.068.
[5] J. C. Fradinho, A. Oehmen, e M. A. M. Reis, «Photosynthetic mixed culture polyhydroxyalkanoate (PHA) production from individual and mixed volatile fatty acids (VFAs): Substrate preferences and co-substrate uptake», *J. Biotechnol.*, vol. 185, pp. 19–27, set. 2014, doi: 10.1016/j.jbiotec.2014.05.035.
[6] E. B. Sydney *et al.*, «Screening and bioprospecting of anaerobic consortia for biohydrogen and volatile fatty acid production in a vinasse based medium through dark fermentation», *Process Biochem.*, vol. 67, pp. 1–7, 2018.
[7] X. Zheng, Y. Chen, X. Wang, e J. Wu, «Using Mixed Sludge-derived Short-chain Fatty Acids Enhances Power Generation of Microbial Fuel Cells», *Energy Procedia*, vol. 105, pp. 1282–1288, mag. 2017, doi: 10.1016/j.egypro.2017.03.458.
[8] W. S. Lee, A. S. M. Chua, H. K. Yeoh, e G. C. Ngoh, «A review of the production and applications of waste-derived volatile fatty acids», *Chem. Eng. J.*, vol. 235, pp. 83–99, 2014.
[9] K. Dai, J.-L. Wen, F. Zhang, e R. J. Zeng, «Valuable biochemical production in mixed culture fermentation: fundamentals and process coupling», *Appl. Microbiol. Biotechnol.*, vol. 101, fasc. 17, pp. 6575–6586, set. 2017, doi: 10.1007/s00253-017-8441-z.
[10] R. DiLallo e O. E. Albertson, «Volatile acids by direct titration», *J. Water Pollut. Control Fed.*, pp. 356–365, 1961.
[11] T. E. Baxter, «Approximate Volatile Acids by Titration (Standard Operating Procedure AMBL-101-A).», Flagstaff, AZ, USA:Northern Arizona University, 2014. [Online]. Disponibile su: https://www.cefns.nau.edu/~teb/ambl/sop/SOP_AMBL_101A_AppoxVolatileAcids.pdf

Title: Valorization of secondary sludge through hydrothermal carbonization and acidogenic fermentation: influence of reactors configurations and process parameters

Author(s): Marco Pesenti*[1], Matteo Grana[1], Alisar Kiwan[2], Daniele Pirini[2], Maria Jose Hernandez Sanchez[1], Elena Ficara[1], Andrea Turolla[1]

[1] Politecnico di Milano, Dipartimento di Ingegneria Civile e Ambientale (DICA), Piazza Leonardo da Vinci 32, 20133 MI, Italy (E-mail: marco1.pesenti@polimi.it, matteo.grana@polimi.it, mariajose1.hernandez@mail.polimi.it, elena.ficara@polimi.it, andrea.turolla@polimi.it)
[2] B-Plas S.b.r.l, Via Lanfranco Gessi, 16, 48022 Lugo RA, Italy (E-mail: alisar.kiwan@b-plas.it, daniele.pirini@b-plas.it)

Keyword(s): resource recovery, volatile fatty acids, thermochemical processes

Abstract

Sewage sludge from wastewater treatment plants presents significant treatment and disposal challenges. Hydrothermal carbonization (HTC) as sludge treatment produces process liquid and hydrochar with several interesting properties, as enhanced filterability and fermentability. This study investigates HTC benefits for volatile fatty acids (VFAs) production from sewage sludge. Three fermentation reactor configurations operated in continuous were compared: a sequencing batch reactor (SBR) and two continuously stirred tank reactors (CSTR). Results indicated that HTC significantly boosts methane production potential for process liquid and hydrochar with respect to raw sludge, promising for VFAs production. The SBR exhibited the highest VFAs productivity, while no different acidification yields were observed. No significant advantage was found for filtered HTC liquid over unfiltered liquid.

Introduction

Sewage sludge from wastewater treatment plants (WWTP) poses significant operational challenges due to its treatment and disposal costs. Resource recovery is crucial for environmental and economic sustainability, with common strategies including biological treatments, thermochemical conversion, and land application of stabilized biosolids [1]. Recently, anaerobic fermentation for volatile fatty acids (VFAs) production has gained interest for carbon recovery, with VFAs used in WWTPs to enhance nutrient removal and for producing polyhydroxyalkanoates, as substitutes of fossil-based plastics [2].

Hydrothermal carbonization (HTC) is a promising wet thermochemical technology used as sludge treatment for promoting its filterability and fermentability. In HTC reactors sludge is processed at high temperatures (170-350 °C) and pressures (5-25 MPa) for minutes to hours [3]. HTC produces process liquid, rich in dissolved organic macromolecules, and a carbonaceous product, named hydrochar.

Few studies have examined HTC as a pretreatment for improving sludge fermentability, with mixed results ([3], [4]). This work aims to elucidate the benefits of HTC for more sustainable sewage sludge management, exploring valorization options for both the recovered process liquid and hydrochar.

Materials and methods

Microbial inoculum and sewage sludge were sampled from a WWTP in northern Italy. The microbial inoculum for fermentation was sourced from the anaerobic digester. To inhibit methanogenic activity,

the inoculum was pre-treated at 80°C for 1 hour, and 2-Bromoethanesulfonic acid was added at a concentration of 0.2 g/L during the acclimation period. The sludge underwent HTC pre-treatment in a high-pressure laboratory reactor (treating 5 L of sludge) at 180°C for 1 hour. Following the HTC process, the liquid fraction was obtained via pressure filtration. Mesophilic biomethane potential (BMP) tests were conducted on HTC sludge, HTC process liquid, and hydrochar using a volumetric device (AMPTS II, Bioprocess Control®).

Three different fermentation reactor configurations were operated in continuous under thermophilic conditions (50 °C): (i) one sequencing batch reactor (SBR) and two continuously stirred tank reactors (CSTRs). The SBR reactor had 0.7 L volume, with HRT of 2 days and SRT of 4 days. Each CSTR reactor had a volume of 2 L, with both HRT and SRT set at 4 days. The difference between CSTR reactors consisted in the absence (CSTR1) or presence (CSTR2) of an upstream solid-liquid separation phase (filter press) for solid removal. Samples of feedstock and fermentate were collected from the reactors and characterized weekly in terms of TS, VS, volatile suspended solids (VSS), total suspended solids (TSS), pH, VFAs, sCOD, NH_4^+, and PO_4^{3-}.

Results and discussion

Figure 1 presents the BMP test results for various streams before and after HTC treatment at 180°C. HTC treatment significantly enhanced the methane production potential of the secondary sludge. Additionally, both the process liquid and the hydrochar showed a higher BMP than the raw sludge, indicating the promising properties for VFA production, as BMP tests can be an early indicator of anaerobic degradability. The stream with the highest BMP was the untreated HTC product.

Figure 2 reports the soluble COD (sCOD) and VFAs in the fermented liquor for the three reactors configurations tested. The sCOD and VFA data suggested stable process performance after the initial acclimation period, likely because HTC pretreatment solubilized most of the COD, making organic carbon more available for bacterial assimilation and VFA conversion. This stability was also reflected in the VFA composition of the mixture in the SBR (Figure 3a), which stabilized after the first two weeks. The higher net VFA production in the two CSTRs during the second part of testing was due to the use of a different batch of HTC feedstock with higher sCOD concentration then the one that was been used for the SBR.

To compare the different configurations, experimental data were processed to calculate productivity, acidification yield, and the COD mass balance for each reactor. Figure 3b displays the COD mass balance between the inlet and outlet COD for the three reactors after the acclimation period. The percentage of COD lost to methanogenesis is low, but less than 30% of the fed COD is converted into VFAs. Productivity, shown in Figure 4a, was calculated as the ratio of net VFA production to the reactor HRT expressed per unit of volume. The SBR exhibited the highest average productivity among the three configurations. This is because, despite having the same SRT, the SBR configuration allows for a decoupled and halved HRT, resulting in a higher average organic loading rate of 12.1 g sCOD/L compared to 6.5 g sCOD/L in the other two reactors. The acidification yield, shown in Figure 4b, was calculated as the ratio of net VFA production to the total COD. All reactors exhibited a similar yield of around 0.25 g COD-VFA per g CODin. There was no noted advantage in feeding the CSTR reactor with filtered HTC process liquid over the unfiltered process liquid (CSTR1 vs CSTR2).

Conclusions

This study demonstrated that the process liquid resulting from HTC treatment of secondary sludge (180°C, 1 hour) can enhance anaerobic biodegradability and improve acidogenic fermentation efficiency for VFA production. The lab-scale fermentation reactors fed with this process liquid achieved stable VFA

production during the testing period but were unable to convert all the anaerobically usable COD into VFAs. Future work should focus on adjusting reactor operating conditions, such as HRT and pH, to maximize acidification yield and minimize wasted sCOD.

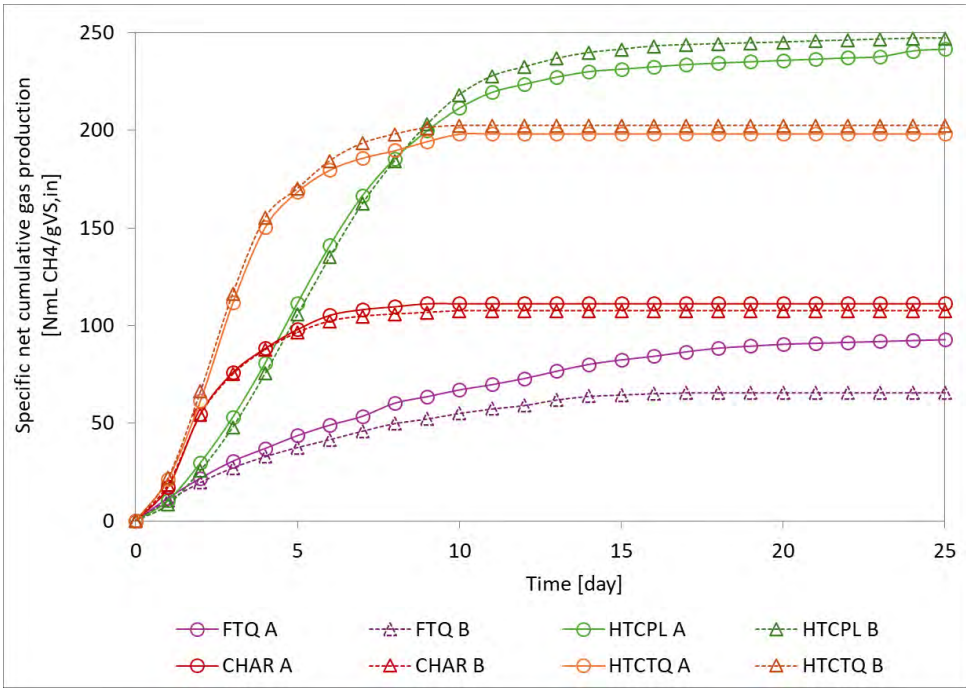

Figure 1. BMP tests of samples for different streams: (i) FTQ= secondary sludge, (ii) CHAR= hydrochar from HTC, (iii) HTCPL= filtered process liquid, (iv) HTCTQ= total process liquid.

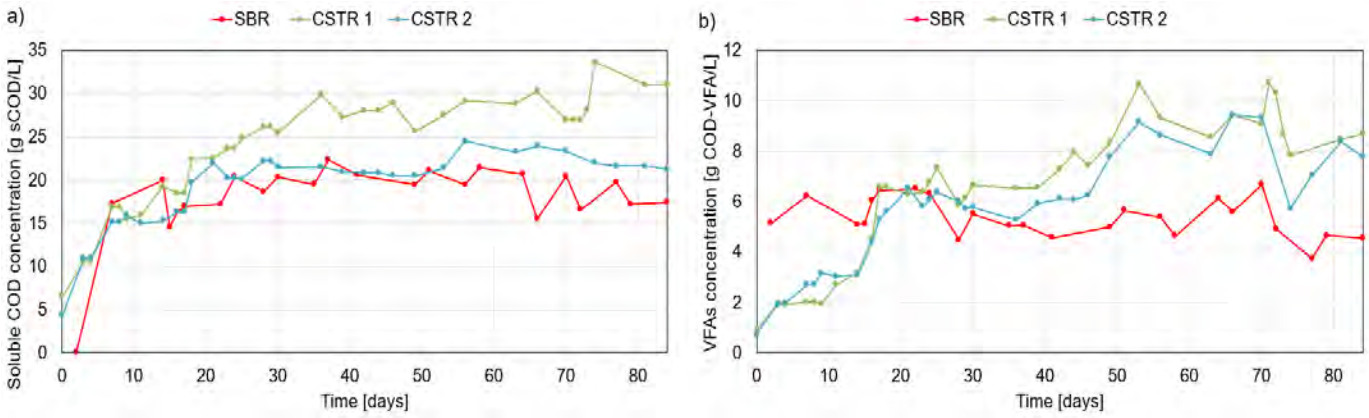

Figure 2. sCOD (a) and VFAs (b) concentrations inside the three reactors.

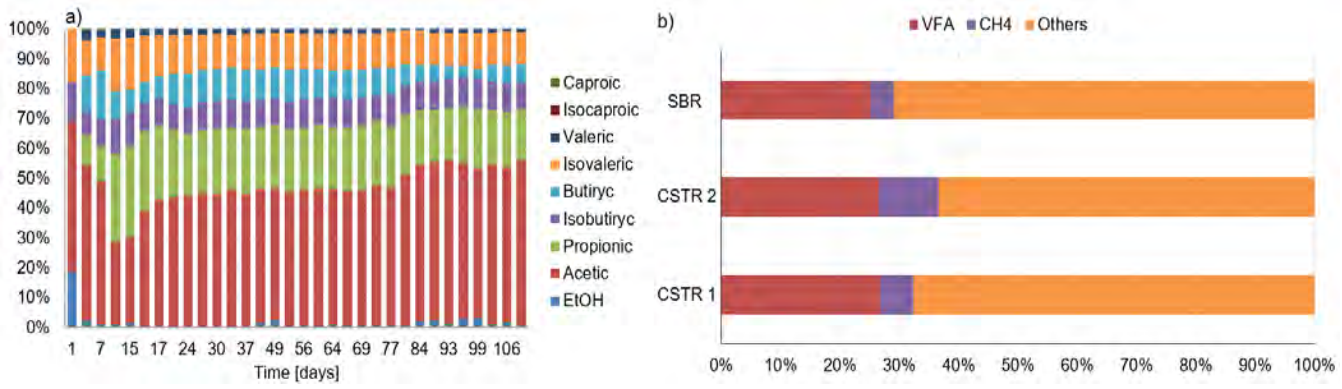

Figure 3. (a) Evolution over time of VFAs composition of the SBR effluent. (b) COD balance between outputs of the 3 different configurations.

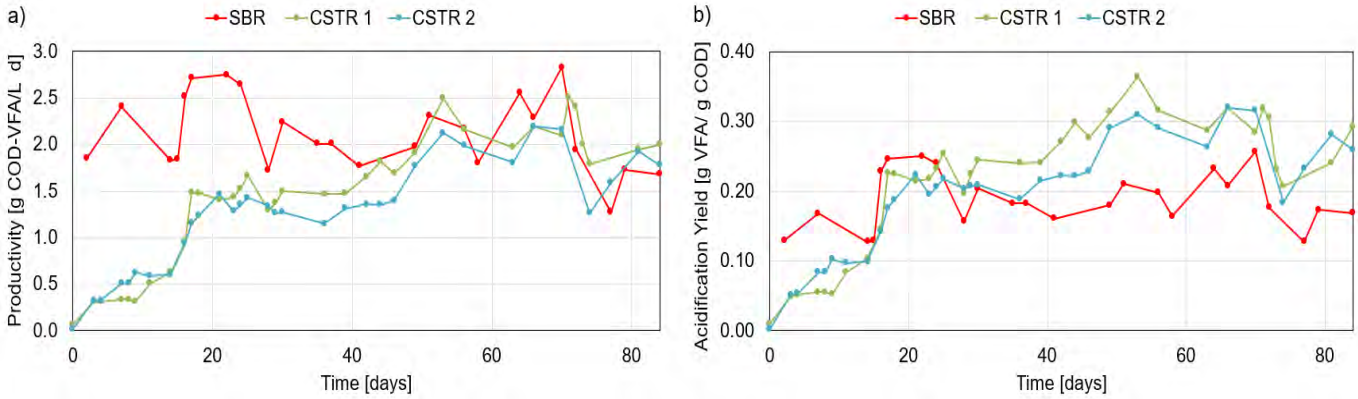

Figure 4. Productivity (a) and acidification yield (b) for the 3 different configurations.

References

[1] Bora, R.R., Richardson, R.E., You, F., 2020. Resource recovery and waste-to-energy from wastewater sludge via thermochemical conversion technologies in support of circular economy: a comprehensive review. BMC Chemical Engineering 2, 8.

[2] Atasoy, M., Owusu-Agyeman, I., Plaza, E., Cetecioglu, Z., 2018. Bio-based volatile fatty acid production and recovery from waste streams: Current status and future challenges. Bioresource Technology 268, 773–786.

[3] Chen, Z., Rao, Y., Usman, M., Chen, H., Białowiec, A., Zhang, S., Luo, G., 2021. Anaerobic fermentation of hydrothermal liquefaction wastewater of dewatered sewage sludge for volatile fatty acids production with focuses on the degradation of organic components and microbial community compositions. Science of The Total Environment 777, 146077.

[4] Castro-Fernandez, A., Taboada-Santos, A., Balboa, S., Lema, J.M., 2023. Thermal hydrolysis pre-treatment has no positive influence on volatile fatty acids production from sewage sludge. Bioresource Technology 376, 128839.

PARALLEL SESSION: B1

Drinking water

Removal and control of emerging contaminants

Title: Sampling devices for MPs analysis in sources of water for human consumption, with focus on the Tiber river

Author(s): Margherita Barchiesi[1], Francesca Mangiagli*[2], Camilla Di Marcantonio[3], Agostina Chiavola[4], Maria Rosaria Boni[5]

[1] *Department of Civil, Building and Environmental Engineering, Sapienza University of Rome, Rome, Italy, francesca.mangiagli@uniroma1.it*
[2] *Department of Civil, Building and Environmental Engineering, Sapienza University of Rome, Rome, Italy, margherita.barchiesi@uniroma1.it*
[3] *Department of Civil, Building and Environmental Engineering, Sapienza University of Rome, Rome, Italy, camilla.dimarcantonio@uniroma1.it*
[4] *Department of Civil, Building and Environmental Engineering, Sapienza University of Rome, Rome, Italy, agostina.chiavola@uniroma1.it*
[5] *Department of Civil, Building and Environmental Engineering, Sapienza University of Rome, Rome, Italy, mariarosaria.boni@uniroma1.it*

Keyword(s): microplastics, analysis, sampling

Introduction

Microplastics (MPs) are considered as a contaminant of emerging concern that came recently under the spotlight of the scientific community due to its persistence and ubiquity. The public outreach of the issue is wide and it is resulting in a series of actions by governmental and non-governmental organizations to address the issue and satisfy the need for understanding and control. Regarding regulators, the European Union is challenging the issue introducing MPs in many of its Directives, implementing bans (e.g. the proposed restriction on intentionally added MPs), but also actions for the standardization of analytical protocols and monitoring. Indeed, MPs are specifically mentioned in the new Drinking Water Directive (2020/2184) [1] and the review of the Urban Wastewater Directive [2]. The former imposes the definition of an analytical protocol for MPs analysis in drinking water and the subsequent monitoring in water to be destined to human consumption by 2024. The latter mentions the Wastewater Treatment Plants (WWTPs) as a possible source of release of MPs to the environment and therefore also as a possible control point. The European Commission Delegated Decision with specific indication on MPs analysis in water to be destined to human consumption is available as from March 2024 [3]. The first quest for MPs analysis and monitoring is set by the European Union on water to be destined to human consumption. The international attention to drinking water is linked to the concern of health risks associated with MPs. Water to be destined to human consumption is however just a step of the urban water cycle, where rivers often represent the core: they are not only suppliers of drinking water but also receivers of wastewater and stormwater runoff [4]. Urban rivers are also rich ecosystems whose resilience is being pushed to the brim by human activity [5]. Finally, they are a source of pollutants for the marine environments [6].

MPs analysis in water is necessarily structured in four phases: sampling, pre-treatments, identification-quantification-characterization, reporting.

Sampling is a crucial moment of the MPs analysis protocol as it is the first step that defines the MPs subsample analysable. MPs are indeed solid particles, suspended in the liquid matrix, which can be described by many environmentally relevant parameters, such as size, shape, mass, volume, surface

area, chemical composition, density. Sampling extracts only a definite number of MPs from the pool in the matrix of interest. Therefore, two are the aspects that need to be defined, which have not been assessed definitively yet by the studies conducted so far: (1) the volume of sample to be considered representative and (2) the collection sampling device specific for the water source systems (which are characterized by variable characteristics in time and space). Therefore, the purpose of this research is twofold:

- Goal 1: design of a sampling device optimized for river monitoring, with the following characteristics:
  - Portability
  - Easy assembly and dismantling
  - Reduced contamination
  - Possible reuse in the same sampling campaign reducing the chance of cross contamination.
  - Possible use of the device afar from electric and transport infrastructure (off-grid)
  - Modularity for adjustment to different water qualities
  - Economically feasible and appealing for monitoring and control authorities.
  - Able to retrieve representative MPs sample in the interval 20-300µm
  - Simplified MPs transfer from the sampling device (laboratory post-processing and activities)
  - Materials and methods
- Goal 2: field testing of the designed device.

Furthermore, this research aims at discussing the feasibility of MPs monitoring in surface water for MPs in the size range 20-300µm. The case study of the research is the Tiber river, one of the major Italian rivers and possible source of water for the Italian Capital in the years to come.

Methodology

The research is structured as follows:

- Literature research on the main scientific database (Science Direct, google scholar)
- Selection of the most promising sampling systems for surface waters
- Construction and optimization of the sampling systems
- Data acquisition on the Tiber river and analysis of the MPs with the aid of a µ-Raman
- Critical evaluation of the results, highlighting pros and cons of the different sampling systems
- New sampling system proposal

The two systems chosen are:

- Stack of sieves, following Mintenig et al. 2020 [7]: two sieves, of 300 and 20µm (Giuliani, Italy), are stacked and water is directed on them with a centrifugal pump (Efco 3000, Italy). Water flow expected is approximately 10L/min (Figure 1, system A). A water flow meter (Gioanola, Italy) is used to measure the volume filtered. A funnel is used to reduce the environmental contamination.
- Positive pressure filters in series 300-10µm. cartridge filters, with brass cups (Euroacque, Italy) following Pittroff et al. [8], adapting the system to surface waters (Figure 1, system B). Again, a water meter is used to keep track of the volume sampled; at least 100L will be sampled and the expected flow is >10L/min.

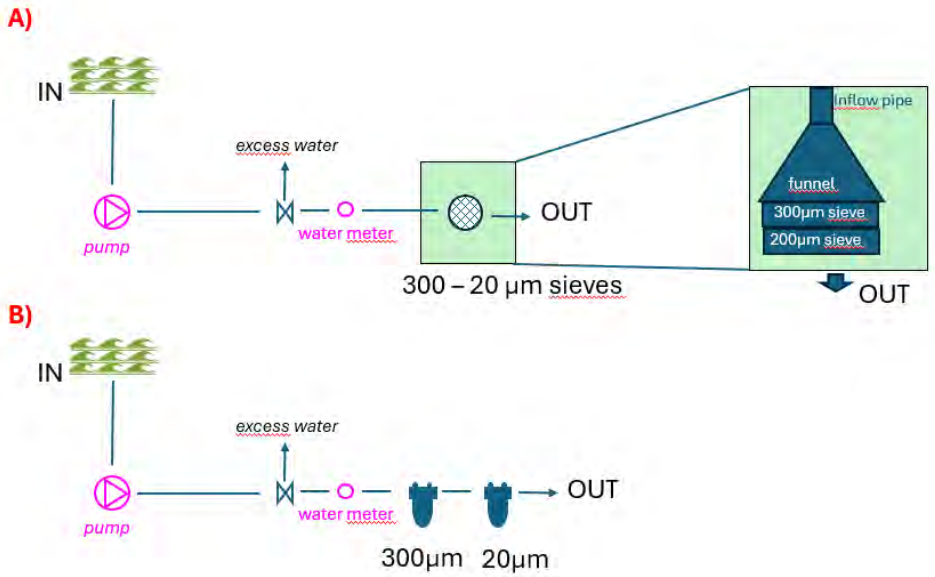

Figure 1. Sampling systems for MPs in surface water considered in this study

Preliminary results and conclusions

As mentioned in the Materials and Methods section, the sampling systems chosen among those reported in the literature are one based on a stack of sieves and another based on cascading filtration in positive pressure filters. Pros and cons of such systems are already mentioned in general in Almutharam et al. 2022 [9]. When considering the specificity of the surface water matrix, high-capacity filters are needed, hence the choice of stacked sieves or cartridge filters. The comparison between the two systems with reference to monitoring is ongoing. The main aspects that are taken into consideration are their portability, possible environmental contamination, sampling time. The critical comment to the two systems and the results of their application to monitoring campaigns will be presented for the first time during SIDISA 2024.

Acknowledgment

The study is funded by Sapienza University of Rome (Progetti piccoli di Ateneo 2023)

References

[1] The European Parliament and the Council of the European Union, “Directive (EU) 2020/2184, EU (revised) Drinking Water Directive. Annex 1. Part B.,” *Off. J. Eur. Communities*, vol. 2019, no. December, p. 35, 2020, [Online]. Available: https://eur-lex.europa.eu/eli/dir/2020/2184/oj.

[2] European Commission, “Proposal for a revised Urban Wastewater Treatment Directive,” vol. 0345. p. 69, 2022, [Online]. Available: https://environment.ec.europa.eu/publications/proposal-revised-urban-wastewater-treatment-directive_en%0Ahttps://oeil.secure.europarl.europa.eu/oeil/popups/ficheprocedure.do?reference=2022/0345(COD)&l=en%0Ahttps://www.europarl.europa.eu/RegData/etudes/BRI.

[3] European commission, “Commission Delegated Decision supplementing Directive (EU) 2020/2184 of the European Parliament and of the Council by laying down a methodology to measure microplastics in water intended for human consumption.” 2024.

[4] J. Marsalek, B. . Jiménez-Cisneros, P.-A. Malmquist, M. Karamouz, J. Goldenfum, and B. Chocat, “Urban

Water Cycle Processes and Interactions," *Urban Water Cycle Process. Interact.*, no. January, 2014, doi: 10.1201/9781482288544.

[5] R. A. Francis, "Urban rivers : novel ecosystems , new challenges," *WIREs Water*, vol. 1, no. February, pp. 19–29, 2014, doi: 10.1002/wat2.1007.

[6] H. A. Leslie, S. H. Brandsma, M. J. M. van Velzen, and A. D. Vethaak, "Microplastics en route: Field measurements in the Dutch river delta and Amsterdam canals, wastewater treatment plants, North Sea sediments and biota," *Environ. Int.*, vol. 101, pp. 133–142, 2017, doi: 10.1016/j.envint.2017.01.018.

[7] S. M. Mintenig *et al.*, "A systems approach to understand microplastic occurrence and variability in Dutch riverine surface waters," *Water Res.*, vol. 176, p. 115723, Jun. 2020, doi: 10.1016/j.watres.2020.115723.

[8] M. Pittroff, Y. K. Müller, C. S. Witzig, M. Scheurer, F. R. Storck, and N. Zumbülte, "Microplastic analysis in drinking water based on fractionated filtration sampling and Raman microspectroscopy," *Environ. Sci. Pollut. Res.*, 2021, doi: 10.1007/s11356-021-12467-y.

[9] H. Almuhtaram and R. C. Andrews, "Sampling Microplastics in Water Matrices: A Need for Standardization," *ACS ES T Water*, vol. 2, no. 8, pp. 1276–1278, 2022, doi: 10.1021/acsestwater.2c00236.

Title: Spectroscopic indexes developed for controlling DBPs precursors in drinking water processes

Authors: Antonino Di Bella[1], Saida Martí[2], Pere Emiliano[3], Fernando Valero[3], Maria José Farré [2], Paolo Roccaro*[1]

[1] *Department of Civil Engineering and Architecture, University of Catania, Catania, Italy*
[2] *ICRA, Catalan Institute for Water Research, Girona, Spain*
[3] *Ens d'Abastament d'Aigua Ter-Llobregat, ATL, Spain*

* *paolo.roccaro@unict.it*

Keywords: DBPs monitoring; fluorescence; Natural Organic Matter.

Abstract

Water unavailability poses a significant challenge for many communities around the world, impacting health, hygiene, and overall quality of life. In response to the need for safe and accessible water, chlorination emerged as a groundbreaking advancement in water treatment processes. Introduced in the early 20th century, chlorination involves adding chlorine to water to kill harmful pathogens, making it safe to drink. This method drastically reduced waterborne diseases, transforming public health and enabling reliable access to potable water for millions of people globally. However, one of the most important problems associated with chlorinated water is the formation of disinfection byproducts (DBPs). When chlorine reacts with natural organic matter (NOM) present in the water, it forms DBPs, such as trihalomethanes (THMs) and haloacetic acids (HAAs), which are potentially harmful. These compounds can form throughout the water distribution system, posing health risks such as cancer and reproductive issues. Managing the balance between effective disinfection and minimizing DBP formation remains a critical challenge in water treatment.

Given the complexity and variability of NOM, various surrogate parameters have been employed to measure NOM reactivity in halogenation reactions and DBP formation. Spectroscopic methods, including absorbance and fluorescence spectroscopy, have become essential tools for monitoring DBP formation. These techniques allow for the real-time detection and quantification of DBP precursors and by-products. Absorbance spectroscopy measures the light absorption by organic compounds, indicating the presence of NOM that can react to form DBPs. Among these parameters, the absorbance of ultraviolet light at 254 nm (A_{254}) and its specific value ($SUVA_{254}$), which is the ratio of A_{254} to dissolved organic carbon (DOC), are likely the most widely used [1]. Fluorescence spectroscopy, on the other hand, detects the emission of light from NOM, providing a sensitive and rapid means of monitoring water quality [2]. These methods offer valuable insights into the dynamics of DBP formation and help in optimizing treatment processes to minimize health risks. Spectroscopy-based indices have been utilized in the literature to monitor natural organic matter (NOM) in water treatment and distribution lines [3]. These indices allow for real-time and in situ monitoring, enabling operators to adjust treatment processes dynamically to control DBP levels effectively. By using these indices, water treatment facilities can better predict and manage the formation of harmful byproducts, ensuring safer drinking water.

The aim of this study is to assess the effectiveness and application of absorbance and fluorescence-

based surrogates in predicting and controlling DBP formation during water chlorination under various conditions. The findings indicate that these surrogates are valuable for real-time, in situ monitoring of DBP formation and speciation. For instance, changes in fluorescence excitation emission matrix (EEM) during full-scale water treatment (as shown in Figure 1) were used to develop predictive indices for DBP precursors. In particular, two indexes have been selected from EEM data as indicators of NOM reactivity in DBPs formation, namely I3 (255,440) and I5 (325,450), which are representative of fluvic- and humic-like material, respectively. These two indexes have been found to correlate with DBPFP in chlorinated waters. For instance, Figure 2 shows a correlation between either ΔI3 or ΔI5 and the DBPFP obtained from chlorination of ATL water samples collected at different points of the WTP on two different sampling days. The determination coefficients obtained for ΔI3 or ΔI5 indexes are very high, especially for HAA5 and HAA9, while for THM are lower. The high correlation is due to the fact that the changes in I3 or I5 during chlorination, measured by the differential approach [4,5] is related to the halogenation process and subsequent release of DBPs [6]. Furthermore, also the absolute values of such fluorescence indexes I3 and I5 are correlated with DBPFP with similar determination coefficients to those observed for the differential indexes (Figure 3).

The latter result is highly significant because it suggests that the absolute values of the fluorescence indices I3 and I5 can be effectively used to monitor the reactivity of natural organic matter (NOM) in real-time during water treatment processes. This capability, facilitated by online sensors, allows for continuous, dynamic adjustments in the treatment process, thereby optimizing the balance between effective disinfection and minimizing the formation of harmful disinfection by-products (DBPs). Such advancements enhance the overall safety and quality of drinking water.

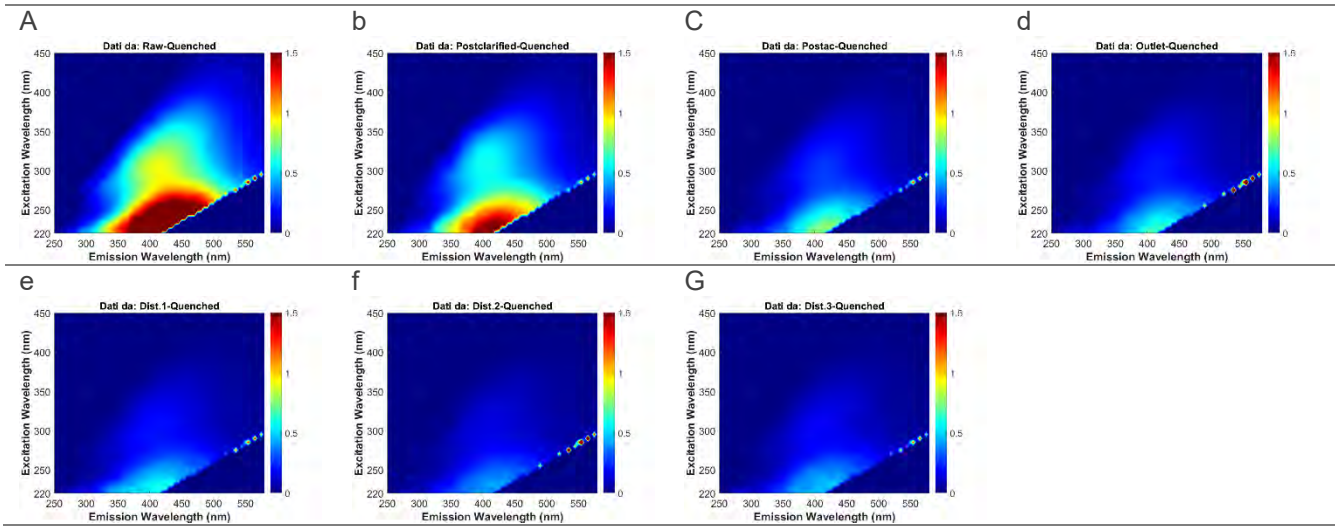

Figure 1 - EEM of Quenched samples from Drinking Water Treatment Plant (TDWTP) in Barcellona : a) raw water, b) Post clarifield, c) Post AC, d) Outlet, e) Distribution 1, f) Distribution 2, g) Distribution 3

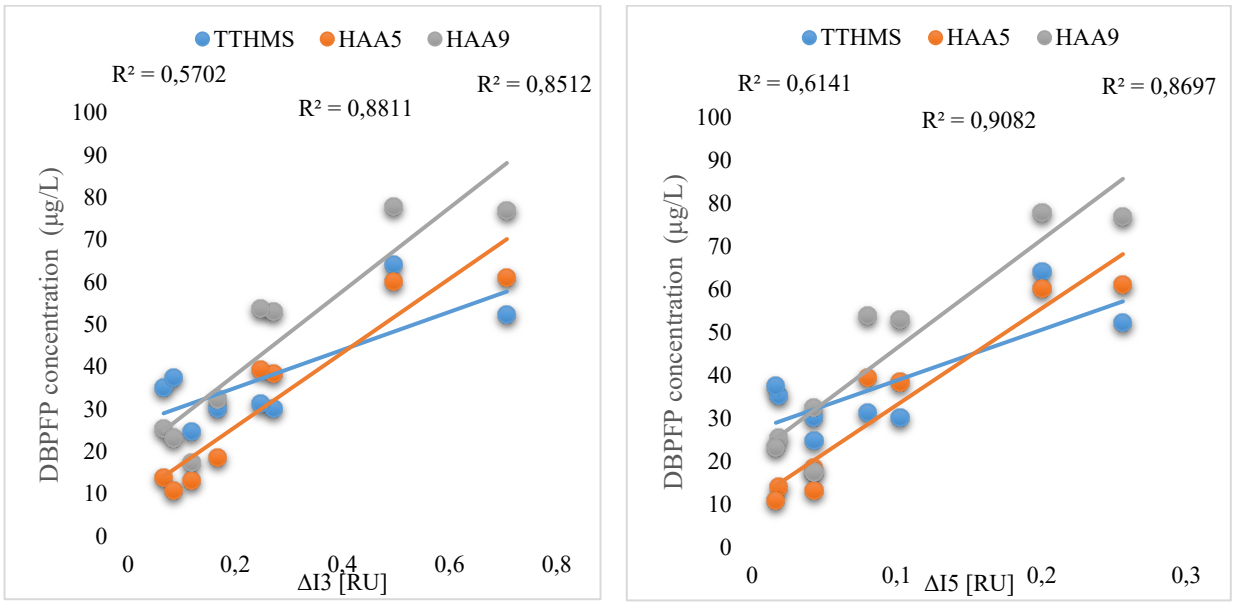

Figure 2. Correlation between ΔI3 or ΔI5 and DBPFP in chlorinated waters (raw, clarified, GAC filtered, outlet) in two different sampling days

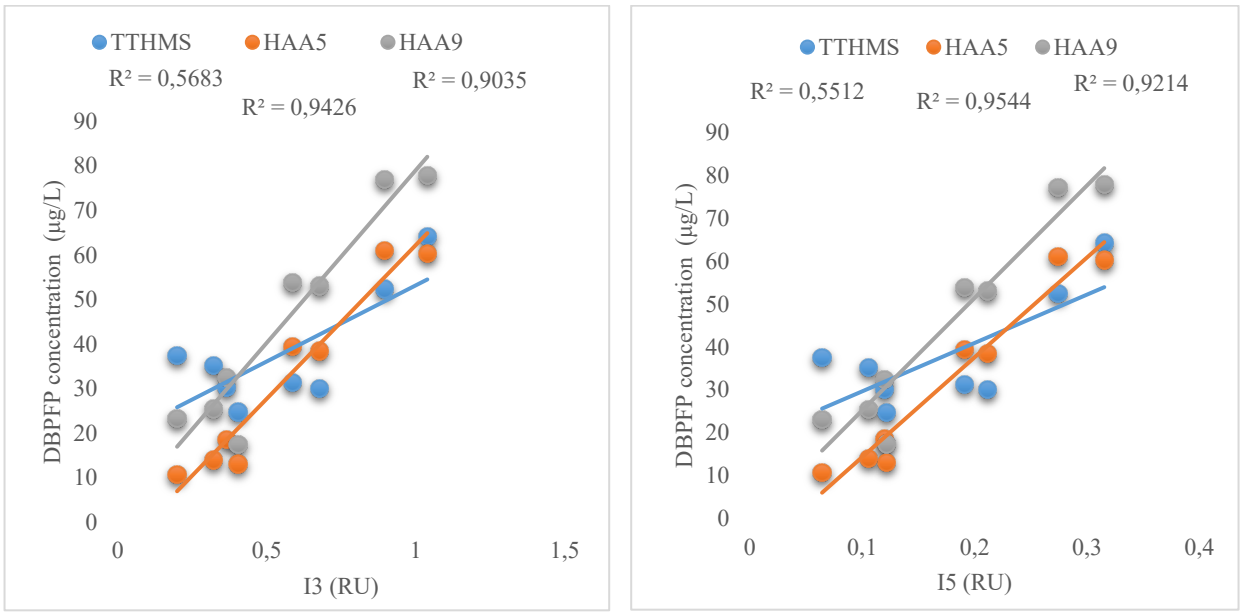

Figure 3. Correlation between I3 or I5 and DBPFP in chlorinated waters (raw, clarified, GAC filtered, outlet) in two different sampling days

Table 1 – R^2 and equations between Fluorescence Indices and DBP concentrations

Correlation	Equation	R^2
ΔI3-TTHMS	y = 34,169x + 19,03	0,5683
ΔI3-HAA5	y = 68,99x - 6,7373	0,9426
ΔI3-HAA9	y = 77,501x + 1,5703	0,9035
ΔI5-TTHMS	y = 112,52x + 18,437	0,5512
ΔI5-HAA5	y = 232,14x - 8,8035	0,9544
ΔI5-HAA9	y = 261,7x - 0,913	0,9214
I3-TTHMS	y= 44.917x+26.069	0,5702
I3-HAA5	y= 87,538x + 8,3251	0,8811
I3-HAA9	y= 98,722x + 18,387	0,8512
I5-TTHMS	y = 117,95x + 26,999	0,6141
I5-HAA5	y = 224,9x + 10,61	0,99082
I5-HAA9	y = 252,52x + 21,07	0,8697

References

[1] Weishaar JL, Aiken GR, Bergamaschi BA, Fram MS, Fujii R, Mopper K. Evaluation of Specific Ultraviolet Absorbance as an Indicator of the Chemical Composition and Reactivity of Dissolved Organic Carbon. Environ Sci Technol 2003;37:4702–8. https://doi.org/10.1021/es030360x.

[2] Johnstone DW, Miller CM. Fluorescence Excitation–Emission Matrix Regional Transformation and Chlorine Consumption to Predict Trihalomethane and Haloacetic Acid Formation. Environmental Engineering Science 2009;26:1163–70. https://doi.org/10.1089/ees.2009.0035.

[3] Sgroi M, Roccaro P, Korshin GV, Vagliasindi FGA. Monitoring the Behavior of Emerging Contaminants in Wastewater-Impacted Rivers Based on the Use of Fluorescence Excitation Emission Matrixes (EEM). Environ Sci Technol 2017;51:4306–16. https://doi.org/10.1021/acs.est.6b05785.

[4] Roccaro P, Vagliasindi FGA. Differential vs. absolute UV absorbance approaches in studying NOM reactivity in DBPs formation: Comparison and applicability. Water Research 2009;43:744–50. https://doi.org/10.1016/j.watres.2008.11.007.

[5] Roccaro P, Vagliasindi FGA, Korshin GV. Changes in NOM Fluorescence Caused by Chlorination and their Associations with Disinfection by-Products Formation. Environ Sci Technol 2009;43:724–9. https://doi.org/10.1021/es801939f.

[6] Zhang C, Roccaro P, Yan M, Korshin GV. Interpretation of the formation of unstable halogen-containing disinfection by-products based on the differential absorbance spectroscopy approach. Chemosphere 2021;268:129241. https://doi.org/10.1016/j.chemosphere.2020.129241.

Acknowledgments

This study was partially supported by the European Union through the intoDBP project (Project 101081728). However, the manuscript has not been subjected to peer and policy review of the agency and therefore, does not necessarily reflect its views.

Title: Research into determining and removing microplastics from tap water: the AQUApLASt project.

Author(s): **Oliveri Conti Gea[1,5*], Eloise Pulvirenti [1,2], Paola Rapisarda[1,2], Giovanna Deiana[3], Giuseppe Mancini[4], Maria Anna Coniglio[1], Paolo Castiglia[3], Antonio Azara[3], Margherita Ferrante[1], Marco Dettori [3]**

[1]Department of Medical, Surgical Sciences and Advanced Technologies "G.F. Ingrassia", University of Catania, Catania, Italy, olivericonti@unict.it; marfer@unict.it; maria.coniglio@unict.it; giuseppe.mancini@unict.it.
[2]Hearth and Environmental Sciences PhD Couse. Department of Biological, Geological and Environmental Sciences, University of Catania, Catania, Italy. eloise.pulvi@gmail.com; paolarapisarda5@gmail.com.
[3]Department of Biomedical Sciences, University of Sassari. Sassari. Italy. madettori@uniss.it; azara@uniss.it; castigli@uniss.it; g.deiana31@studenti.uniss.it
[4]Electric, Electronic and Informatic Department of University of Catania. Catania. Italy.
[5]Marco Dettori (PI) e Gea Oliveri Conti (co-PI) contributed equally.

Keyword(s): tap water, microplastics, water treatment, public health

Abstract

Microplastics (MPs) derive from the degradation of plastic waste [1]. MPs have recently been included as emerging contaminants in EU Directive 2020/2184 on water intended for human consumption.
As the MPs could be uptaked both at the tissue and cellular level [2], and recent studies demonstrated that are toxic [3], we are studying the presence and remotion of MPs by inlet and outlet water plant. The AQUApLASt (PRIN-PNRR - P2022XE857) is the first National study intended for analyse the presence of MPs in tap water and to carry out a risk assessment, calculating the concentrations of MPs for Sardinian (surface supply waters) and Sicilian drinking waters (groundwaters), respectively.
Both the type of raw water and of water treatment can influence the content of MPs in final tap water. With the AQUApLASt project, not only the quality of water intended for human consumption is evaluated, but also what the best treatments could be that minimize the presence of MPs in output from the drinking water system. In fact, a capture and filtration system has already been validated with a capability to remove MPs up to 3 µm, and which can be combined with the output of the water purifier with a retention efficiency of 98%. Both water MPs detection that filters validations were performed using the patent PCT/IB2019/051,838 of 7 March 2019 - METHOD FOR THE EXTRACTION AND THE DETERMINATION OF MICROPLASTICS IN SAMPLES WITH ORGANIC AND INORGANIC MATRICES [4].
The calculated Estimated Daily Intakes (EDIs) of MPs through the AQUApLASt project highlight the urgent issue both for consumers and environment. The project will permit to reduce the Estimated Daily Intakes (EDIs) of MPs by tap water consumption, with important public health impacts and savings in terms of environmental contamination.

References

[1] Oliveri Conti, G., Rapisarda, P. & Ferrante, M. Relationship between climate change and environmental microplastics: a one health vision for the platysphere health. One Health Adv. 2, 17 (2024).
[2] Oliveri Conti G, Ferrante M, Banni M, Favara C, Nicolosi I, Cristaldi A, Fiore M, Zuccarello P. Micro- and nano-

plastics in edible fruit and vegetables. The first diet risks assessment for the general population. Environ Res. 2020 Aug;187:109677.
[3] Eloise Pulvirenti, Margherita Ferrante, Nunziata Barbera, Claudia Favara, Erica Aquilia, Marco Palella, Antonio Cristaldi, Gea Oliveri Conti, Maria Fiore. Effects of Nano and Microplastics on the Inflammatory Process: In Vitro and In Vivo Studies Systematic Review. Front. Biosci. (Landmark Ed) 2022, 27(10), 287.
[4] https://patentscope.wipo.int/search/en/detail.jsf?docId=WO2019171312

Title: Innovative regeneration based on microwave irradiation for PFAS-loaded GAC

Author(s): Erica Gagliano*[1,2], Pietro P. Falciglia[2], Nazmiye C. Birben[3], Yeakub Zaker[3], Tanju Karanfil[3], Paolo Roccaro[2]

[1] *Department of Civil, Chemical and Environmental Engineering, University of Genoa, Italy erica.gagliano@unige.it*
[2] *Department of Civil Engineering and Architecture, University of Catania, Italy*
[2] *Department of Environmental Engineering and Earth Science, Clemson University, United States of America*

Keyword(s): Adsorption; granular activated carbon (GAC); microwave (MW) irradiation; per- and polyfluoroalkyl substances (PFAS); regeneration.

Introduction

Per- and poly-fluoroalkyl substances (PFAS) have been historically used in every-day consumer products such as non-stick cookware, food packaging, carpets, waterproof fabrics, masking tape, pesticides, and firefighting foams due to their unique chemical properties [1,2].
Nicknamed as “forever chemicals”, PFAS have received particular attention due to their global occurrence and harmful impact on human health and ecosystems. Moreover, it is extensively documented PFAS recalcitrant behavior to conventional water treatment processes [1].
Several regulations have been recently introduced, which restrict both the manufacture and use of PFAS, however their occurrence in the environment is ubiquitous. Recently, the European Drinking Water Directive (EU 2020/2184) has come into force setting a limit value of 100 ng L^{-1} for the sum of twenty PFAS (including both long- and short-chain compounds) and U.S. EPA is proposing the first-ever national standard to limit PFAS in drinking water [3,4]. Consequently, the need for efficient PFAS removal from contaminated water is a growing need because of the increasing regulatory attention and the general concern regarding the exposure effects.
To date, adsorption through granular activated carbon (GAC) is considered a well-established treatment for PFAS removal from contaminated water [1,5]. Due to fast breakthrough observed at full-scale GAC filters, the regeneration of PFAS-exhausted GACs is still challenging [1,6]. Landfilling or incineration of PFAS-saturated GACs are not sustainable approaches leading to potential secondary contamination risks. Thermal treatment could be feasible to treat PFAS-laden media (e.g., soils, sludge, including exhausted GACs). However, PFAS degradation pathways under thermal conditions are still under investigations [5,6]. Moreover, thermal regeneration based on conventional heating and performed under oxidative gases could negatively affect carbon porous structure, causing the changes in carbon functional groups and the loss of carbon mass due to attrition and washout. The subsequent decline in the adsorption capacity was also extensively pointed out [5,7].
Microwave (MW) irradiation has been recently proposed as an innovative technique and alternative to conventional thermal heating for the regeneration GACs [5,8]. A preliminary laboratory investigation has investigated the performance of MW irradiation in regenerating PFOA- and PFOS-exhausted GACs demonstrating promising findings [9].
In this study, the performance of MW irradiation performed at varying operational conditions (power and time applied) was investigated on GAC samples loaded with synthetic solution of individual compound belonging to PFAS group (i.e., PFBA, PFOA, PFBS, and PFOS). Changes in GAC properties in terms of surface area and porosity were also assessed to evaluate the effect of MW irradiation on carbon.

Materials and methods

Samples of bituminous coal-based GAC (particle size of 10-20 mesh) were loaded with solutions of single compound in deionized water (PFOA, PFBA, PFBS, and PFOS) (initial concentration of 500 mg L^{-1}). The mixtures were kept stirred (180 rpm) at room temperature (25 ±1 °C) for 24 h [9].
A 2.45 GHz microwave oven (maximum power of 1.25 kW) was employed to perform the regeneration of PFAS-loaded GAC. Based on preliminary investigations, MW irradiation was performed at two different experimental conditions, 250 W x 1.75 min and 250 W x 3 min. A type-k thermocouple was used for recording GAC temperatures.
Off-gases were collected during MW irradiation and the trap solvent samples were analysed by using ionic chromatography (IC) to measure fluoride contents (defluorinated products) and LC-MS/MS to check PFAS degradation products.
The removal percentage of each compound was calculated based on the adsorption capacity on GAC during adsorption experiments (the amount of compound adsorbed), the amount of degradation products measured in solvent traps and in system washing. Moreover, the potential release of target compounds and other related shorter compounds from MW-regenerated GAC samples was measured by soaking MW-regenerated samples in 200 mL of methanolic ammonium acetate solution for 48 h, then the residual concentration of PFAS in liquid samples were analyzed through LC-MS/MS [9,10].Changes in GAC physical properties (before and after MW irradiation) were analysed through N_2 adsorption isotherms (ASAP 2020, Micromeritics Instrument Corp.).

Results and discussion

GAC samples reached high temperatures due to MW irradiation as shown in Figure 1 demonstrating the strong ability of GAC to convert the absorbed MW power into a fast temperature increase.
Specifically, the temperatures reached by PFAS-saturated GACs ranged from 289 to 435 °C at a MW power of 250 W and irradiation time of 1.75 min. Highest temperatures (~700-800 °C) were reached by increasing the irradiation time to 3 min.
These findings are similar to previously observed and supported the key factors of the regeneration technique based on MW irradiation such as high heating rates and short treatment time [9,11]. Figure 1 also reported GAC weight loss (WL, %) due to MW irradiation. Overall, the weight loss of PFAS-laden GAC samples increased with the temperature reached and it does not depend on the type of adsorbed compound. The obtained results are in agreement with other findings reported in literature [9,11] pointing out that the WL does not represent a drawback of MW regeneration technology and it is lower than that ascribed to conventional thermal regeneration technology [7].

Figure 2 shows the removal percentages of PFAS from GAC due to MW irradiation. It can be noted that at lower temperatures (~300 °C) the amount of PFAS removal might depend on the chain length and the functional group. Indeed, PFOA (long-chain PFCA) was better removed than PFBA (short-chain PFCA) their removal percentages were ~96 % and ~82 %, respectively. PFOS (long-chain PFSA) removal was higher than PFBS (short-chain PFSA) with removal percentages of ~61 % and ~45 %, respectively. All four compounds were almost completely removed from GAC samples at temperatures of ~700-800 °C and PFAS removal percentages were >90%. Specifically, PFBA=99.8%, PFOA=100%, PFBS= 90.6%, and PFOS= 91.8% (Figure 2).

As whole, PFCAs (e.g., PFOA and PFBA) were better removed than PFSAs (e.g., PFOS and PFBS). As previously demonstrated, higher temperatures are needed to PFSAs removal than PFCAs as reported elsewhere [5,10].

Indeed, as reported in the literature, temperatures in the range of 400-700 °C were suitable to desorb several compounds belonging to PFAS class (including PFOS, PFOA, PFBS and PFBA) from contaminated soils and GAC [5,12]. Moreover, it can be inferred that the stripping mechanism linked to

the evaporation of interstitial water can contribute to PFAS desorption enhancing MW regeneration efficiency [5,9].

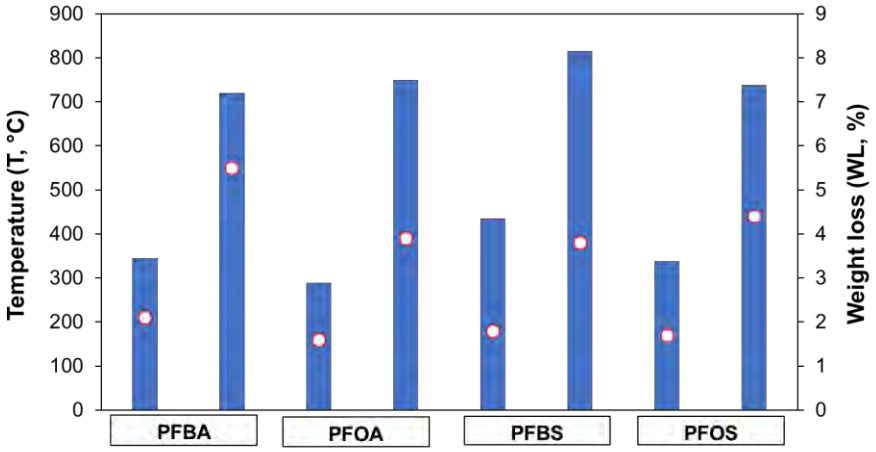

Figure 1. Temperatures reached by GAC samples at 250 W x 1.75 min and 250 W x 3 min. Points represent the recorded WL.

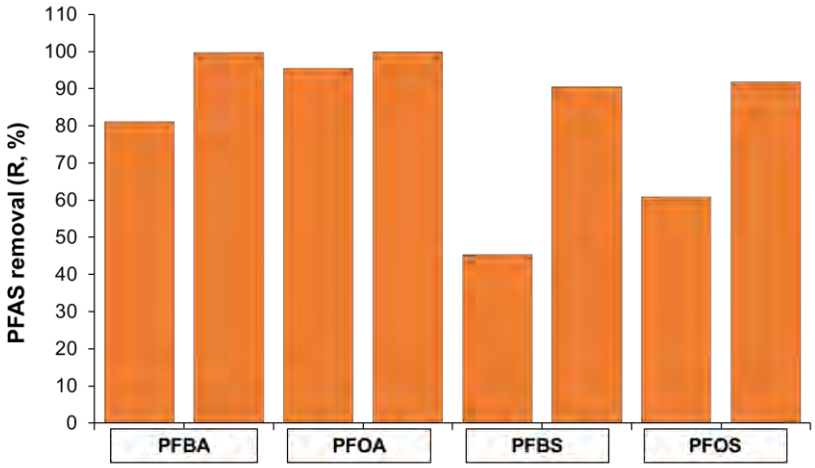

Figure 2. PFAS removal percentages at experimental conditions investigated.

BET surface area and porosity of GACs were analyzed through N_2 adsorption isotherms to understand the changes on the physical properties of GACs ascribed to MW irradiation. The values of BET area and porosity remained within ±5% as compared to virgin F400 values. Consequently, no significant change on the physical characteristics of GAC samples might be ascribed to MW irradiation. Moreover, the variation did not depend on the kind of PFAS adsorbed on GAC samples.

Conclusion and future perspectives

The obtained findings demonstrated that PFAS-loaded GAC reached high temperatures in short irradiation times (~3 min) due to MW irradiation. This evidence demonstrates the strong ability of GAC to convert MW irradiation into rapid temperature increase with Furthermore, in agreement with findings reported in the literature, the reached temperatures are eligible to desorb PFAS. Some differences in terms of PFAS removal percentages could be identified looking at carbon chain length and functional

group. Multi-cycle adsorption/MW regeneration experiments and the investigation of MW efficiency for the regeneration of real field PFAS-exhausted GACs are ongoing to further assess the MW regeneration performance and the feasibility of technology scaling-up.

Indeed, despite the advancement in knowledge on PFAS degradation pathways, further investigation is strongly advised to systematically assess the interplay between PFAS and co-adsorbed compounds (both organic and inorganic species). Moreover, to avoid PFAS-loaded GAC transportation and/or disposal and their potential contamination risks, further efforts are needed to develop and pursue on-site regeneration.

References

[1] E. Gagliano, M. Sgroi, P.P. Falciglia, F.G.A. Vagliasindi, P. Roccaro, Removal of poly- and perfluoroalkyl substances (PFAS) from water by adsorption: Role of PFAS chain length, effect of organic matter and challenges in adsorbent regeneration, Water Research 171 (2020) 115381. https://doi.org/10.1016/j.watres.2019.115381.
[2] N. Belkouteb, V. Franke, P. McCleaf, S. Köhler, L. Ahrens, Removal of per- and polyfluoroalkyl substances (PFASs) in a full-scale drinking water treatment plant: Long-term performance of granular activated carbon (GAC) and influence of flow-rate, Water Research 182 (2020) 115913. https://doi.org/10.1016/j.watres.2020.115913.
[3] DIRECTIVE (EU) 2020/2184 OF THE EUROPEAN PARLIAMENT AND OF THE COUNCIL on the quality of water intended for human consumption, 2020.
[4] U.S. EPA, Proposed PFAS National Drinking Water Regulation. U.S. Environmental Protection Agency., 2023. https://www.epa.gov/sdwa /and-polyfluoroalkyl-substances-pfas.
[5] E. Gagliano, P.P. Falciglia, Y. Zaker, N.C. Birben, T. Karanfil, P. Roccaro, State of the research on regeneration and reactivation techniques for per- and polyfluoroalkyl substances (PFAS)-laden granular activated carbons (GACs), Current Opinion in Chemical Engineering 42 (2023) 100955–100955. https://doi.org/10.1016/j.coche.2023.100955.
[6] J. Wang, Z. Lin, X. He, M. Song, P. Westerhoff, K. Doudrick, D. Hanigan, Critical Review of Thermal Decomposition of Per- and Polyfluoroalkyl Substances: Mechanisms and Implications for Thermal Treatment Processes, Environmental Science and Technology 56 (2022) 5355–5370. https://doi.org/10.1021/acs.est.2c02251.
[7] O. Zanella, I.C. Tessaro, L.A. Féris, Desorption- and decomposition-based techniques for the regeneration of activated carbon, Chemical Engineering and Technology 37 (2014) 1447–1459. https://doi.org/10.1002/ceat.201300808.
[8] G. Durán-Jiménez, L.A. Stevens, G.R. Hodgins, J. Uguna, J. Ryan, E.R. Binner, J.P. Robinson, Fast regeneration of activated carbons saturated with textile dyes: Textural, thermal and dielectric characterization, Chemical Engineering Journal 378 (2019) 121774. https://doi.org/10.1016/j.cej.2019.05.135.
[9] E. Gagliano, P.P. Falciglia, Y. Zaker, T. Karanfil, P. Roccaro, Microwave regeneration of granular activated carbon saturated with PFAS, Water Research 198 (2021) 117121. https://doi.org/10.1016/j.watres.2021.117121.
[10] F. Xiao, P.C. Sasi, B. Yao, A. Kubátová, S.A. Golovko, M.Y. Golovko, D. Soli, Thermal Stability and Decomposition of Perfluoroalkyl Substances on Spent Granular Activated Carbon, Environmental Science & Technology Letters 7 (2020) 343–350. https://doi.org/10.1021/acs.estlett.0c00114.
[11] P.P. Falciglia, E. Gagliano, V. Brancato, G. Malandrino, G. Finocchiaro, A. Catalfo, G. De Guidi, S. Romano, P. Roccaro, F.G.A. Vagliasindi, Microwave based regenerating permeable reactive barriers (MW-PRBs): Proof of concept and application for Cs removal, Chemosphere 251 (2020) 126582. https://doi.org/10.1016/j.chemosphere.2020.126582.
[12] E. Crownover, D. Oberle, M. Kluger, G. Heron, Perfluoroalkyl and polyfluoroalkyl substances thermal desorption evaluation, Remediation 29 (2019) 77–81. https://doi.org/10.1002/rem.21623.

PARALLEL SESSION: C1

Climate change

Climate change and water quality

Title: Analysing changes in precipitation trends across northern Italy's climatic divide

Author(s): Sofia Costanzini*[1], Mauro Boccolari[1], Francesca Despini[1], Luca Lombroso[1], Stephanie Vega Parra[2], Sergio Teggi[1]

[1] *University of Modena and Reggio Emilia, Via Università 4, 41121 Modena (Italy)*
[2] *PhD in Sustainable Development and Climate change, IUSS Pavia School, Piazza della Vittoria 15, 27100 Pavia (Italy)*

Keyword(s): Precipitation Trends, Extreme Indices, Teleconnection Patterns, Po Valley, Apennines, Tyrrhenian area

Abstract

Introduction

This study delves into the analysis of precipitation changes in northern Italy, a strategic area located between central Europe and the Mediterranean region. The region is characterized by diverse geographical and climatic features, making it an ideal setting for comparative studies of precipitation trends.

Data set

We explore the precipitation series from four stations, representing different geographical and climatic characteristics:

- Geophysical Observatory of Modena (MO) at 64 m.a.s.l. and Observatory of Collegio Alberoni (AL) in Piacenza at 50 m.a.s.l., both located in the densely urbanized and industrialized Po Valley.
- Pontremoli Observatory (PO) at 257 m.a.s.l. on the Tyrrhenian side of the Apennines, managed by the Italian Society for Meteorology.
- Sestola Meteorological Station (SE) at 1020 m.a.s.l. located in the Apennines at the base of Mount Cimone, near the watershed between Emilia-Romagna and Tuscany, offering views overlooking the Po Valley.

The territory framed across these stations provides an ideal setting for comparative studies of precipitation trends. This is due to the Apennine watershed that creates a climatic division between two distinct regions. The Tyrrhenian side, directly exposed to maritime air masses predominantly from the south-west, contrasts with the Adriatic side, facing the Po Valley plain and influenced by continental-origin eastern currents [1].

MO, managed by the University of Modena and Reggio Emilia, was established by Duke Francesco IV D'Este and has been recording daily precipitation since 1830. AL was founded at the Alberoni College in 1751 through the initiative of Cardinal Giulio Alberoni, with regular meteorological observations

commencing in 1802. Both MO and AL maintain uninterrupted, homogeneous, and unblended series of data, demonstrating their longstanding commitment to meteorological observations. These stations have been recognized as Long-Term Observing Stations by the World Meteorological Organization (WMO).

PO has been recording data since 1920. The meteorological parameters measured at this station represent a blended and homogeneous series, initiated at the Episcopal Seminary (Verdeno) from 1920 to 1956, and continued at SS. Annunziata from 1957 to 1981, and resumed in Verdeno from 1982 to the present.

To characterize the Apennine region, we initially intended to use the time series of accumulated daily precipitation collected at the Mount Cimone Observatory, situated at 2165 m.a.s.l. on the highest peak in the Northern Apennines. Data from this observatory have been available since 1951. However, the series contains numerous missing measurement days, particularly in the last decade, and fails homogeneity tests. Furthermore, the literature suggests a likely underestimation of precipitation at this high-altitude station due to extreme climatic conditions at the summit, including winds reaching intensities of 216 km/h [1]. Consequently, we decided to use data from the Sestola station, located approximately 7 km from Mount Cimone. This data set is a blended, yet homogenized, series comprising information from the National Hydrographic and Mareographic Service, a research station at the University of Modena and Reggio Emilia active in the 1990s, and the ERACLITO dataset [2] provided by ARPAE.

Methodology

The methodology applied in this study begins with the examination of accumulated precipitation series (grouped by season and year) recorded by all stations, covering the period from 1951 to 2018, for which consistent observations are available. The entire period was also divided into sub-periods, specifically 1951-1981 and 1981-2018, to highlight differences in the trends of the examined quantities.
We then focused on computing the trends and their statistical significance for the four series of accumulated precipitation (both seasonal and annual) during the three periods: 1951-1981, 1981-2018, and 1951-2018. The non-parametric Theil-Sen median slope estimator was applied for trend estimation, and statistical significance was assessed using the modified Mann-Kendall non-parametric trend test [3,4].
Furthermore, we selected and applied indices from the ETCCDI to the precipitation datasets of each station. These indices, encompassing fixed-value thresholds, absolute measures, percentiles, and duration parameters, were utilized to examine shifts in extreme climate patterns. Several indices were calculated, including Precipitation sum (RR), Wet days (RR1), Simple daily intensity index (SDII), Maximum number of consecutive wet days (CWD), heavy precipitation days (R10mm), and very heavy precipitation days (R20mm), among others. The trends of annual climate extreme indices of precipitation were computed for the periods 1951-2018, 1951-1980, and 1981-2018.

Finally, correlations were estimated between the seasonal precipitation series recorded at the studied stations and indices associated with various teleconnection patterns. These patterns are recurrent and persistent large-scale pressure and circulation anomalies that extend over vast geographical areas. While they typically persist from several weeks to several months, they can sometimes have significant impacts over several consecutive years. These patterns are crucial in understanding the interannual and interdecadal variability of atmospheric circulation, which in turn influences precipitation.
The correlations were evaluated over the entire period (1951-2018) and in two sub-periods (1951-1980 and 1981-2018).

The teleconnection patterns considered include the Scandinavia Pattern, North Atlantic Oscillation, Arctic Oscillation, East Atlantic/Western Russia Pattern, Polar - Eurasia Pattern, East Atlantic Pattern, Western Mediterranean Oscillation, Southern Oscillation Index, West Pacific Pattern, Pacific/North American Teleconnection Pattern, Tropical/Northern Hemisphere Pattern, Pacific Transition Pattern, East Pacific - North Pacific Pattern, and Atlantic Multidecadal Oscillation.

Results and discussion

Trends in precipitation were assessed across three periods: 1951-1981, 1981-2018, and 1951-2018 for the entire annual period (ANN) and the four meteorological seasons:

- Winter (DJF) - December, January, February
- Spring (MAM) - March, April, May
- Summer (JJA) - June, July, August
- Fall (SON) - September, October, November

No trends reached significance at the 99% confidence level across all periods, with only limited significance observed at the 95% level, notably at AL during 1951-1980. Significant trends at the 90% confidence level were identified as follows: MO and AL in SON for 1951-2018; SE in ANN and MAM for 1951-2018; PO in ANN and AL in JJA for 1951-1980; MO in DJF and PO in JJA for 1981-2018. Notably, while statistical significance was limited, seasonal variations were observed: for 1981-2018, the annual summer trend differed from other seasons, being negative overall (except for PO in MAM) where it showed positive trends. Similarly, during 1951-1980, negative trends were observed for PO, contrasting with positive trends at other sites.

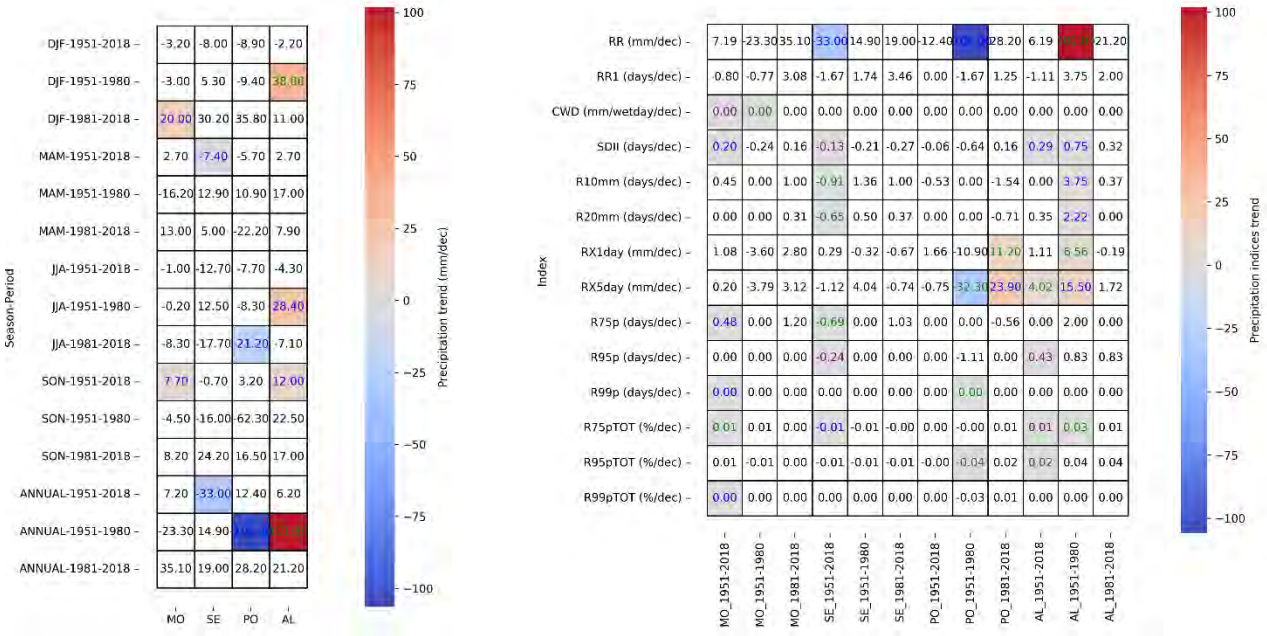

Figure 1. Annual and seasonal precipitation trends for the periods 1951-1981, 1981-2018, and 1951-2018 (left). Extreme index trends evaluated for the same periods (right). The values in purple are significant at the 99% level, those in green are significant at the 95% level, and those in blue are significant at the 90% level.

Regarding extreme index values, no statistically significant values are observed for the period 1981-2018, except for RX5p in PO. However, for the period 1951-2018, several statistically significant values are noted in MO, SE, and AL (also in PO, but the values are close to zero). Generally, these values are

positive for MO (albeit low), negative for SE, and positive for AL.
Concerning teleconnection patterns, for all three periods, there were no statistically significant correlations (> 90%) with the West Pacific Pattern, Pacific/North American Pattern, Tropical/Northern Hemisphere Pattern, Pacific Transition Pattern, or Atlantic Multidecadal Oscillation, with a few exceptions for specific stations and periods. A statistically significant correlation (> 99%) with the Scandinavia Pattern was found for all stations during the entire period (1951-2018) and the last period (1981-2018), with lower significance during 1951-1980. Significant correlations (≥ 95%) were also observed with the North Atlantic Oscillation, the Atlantic Oscillation and the East Atlantic/Western Russia Pattern in DJF for the entire period, with slightly lower significance in the sub-periods.

Conclusions

The findings on precipitation trends, extreme indices, and teleconnection patterns presented in this paper are part of a preliminary study aimed primarily at analyzing the similarities and differences observed in the geographical contexts of the respective stations. Our study underscores the importance of long-term observations and the integration of multiple data sources to assess precipitation trends. The observed trends and correlations with teleconnection patterns provide valuable insights into the factors driving precipitation changes in northern Italy.
However, future outlooks will involve comparing these results with the latest literature and considering a possible new subdivision of the time series into intervals to better understand trends and their variations.

References

[1] Rapetti, F., Vittorini, S., 1988. Differenze pluviometriche tra i versanti tirrenico e adriatico lungo l'allineamento Livorno-Monte Cimone-Modena. Geografia fisica e Dinamica quaternaria, 11(2), 105-115.
[2] Antolini, G., Auteri, L., Pavan, V., Tomei, F., Tomozeiu, R., Marletto, V., 2016. A daily high-resolution gridded climatic data set for Emilia-Romagna, Italy, during 1961–2010. International Journal of Climatology 36, 1970–1986. https://doi.org/10.1002/joc.4473
[3] Wilks, D.S., 2006. Statistical methods in the atmospheric sciences, 2nd ed, International geophysics series. Academic Press, Amsterdam ; Boston.
[4] Pohlert, T., 2023. Non-Parametric Trend Tests and Change-Point Detection. CC BY-ND, 2016, 4: 1-18.

Title: Water Safety Plan as a tool for climate resilient water supply: a case study in Nepal

Authors: Maria Pezzato*[1], Sabrina Sorlini[1]

[1] *Department of Civil, Environmental, Architectural Engineering and Mathematics, University of Brescia, Brescia, Lombardy, Italy*

Keywords: climate change, water security, resilience, tools, developing countries

Introduction

Extreme weather events are increasing all over the world in frequency and (or) severity due to climate change. These include extreme rainfall events, prolonged heat and more frequent and stronger cyclones and hurricanes. The terrible consequences of these occurrences, such as floods, heavy rainfall, landslides, fires, droughts, melting and thawing of cryosphere, are exacerbated by many factors (e.g. population growth, poverty, urbanisation, environmental degradation) that are exposing to catastrophes, every year, millions of people and assets, especially in fragile and conflict-affected areas.
Furthermore, the global water cycle is affected by climate change that directly impacts water resources and the availability and quality of water, threatening water scarcity and concerning water security.
Moreover, increasing extremes due to climate change, have great potential to damage Water, Sanitation and Hygiene (WASH) infrastructure (e.g. inundation of facilities, sedimentation of reservoirs, and loss of electricity), especially in developing countries, where infrastructures are much more susceptible to damage and pollution. Therefore, these events are linked to increased incidence and outbreaks of water-related diseases. The Intergovernmental Panel on Climate Change (IPCC) demonstrated that in developing countries, the incidence of diarrhoea is expected to increase by around 5 percent for every 1°C increase in temperature [1].
Water security is also critical for meeting Sustainable Development Goals (SDGs) since water is central to almost all of them. Water is explicitly referred to in SDG6 (clean water and sanitation) and SDG11 (sustainable communities and cities), while meeting SDG11 (sustainable cities and communities) will require reducing the impacts from water-related disasters. SDG13 focuses on measures to face climate change and its impacts, including strengthening resilience and adaptive capacity to climate-related hazards, actions that are also required in the water sector.
Due to a combination with political, geographical, economic, and social factors, Nepal is recognized as vulnerable to climate change impacts (e.g. floods, landslides, storms, extreme temperatures, droughts) that are all projected to intensify over the 21st century [2]. Indeed, weakness in effective response mechanisms and strategies for dealing with natural hazards has exacerbated this vulnerability leading to drastic forecasting of economic repercussions [3]. The water management susceptibility to disasters underscores the urgent need for adaptation and mitigation measures and resilient water supply systems in Nepal to improve water safety and security for all, and directly contribute to sustainable development. However, these resilience measures require different processes, including guiding concepts, frameworks, tools, and integrated approaches that reflect on the interdependencies between the different risks experienced or predicted and aim to make water resources, physical infrastructure, institutions, and finance more sustainable and durable [4].
The present work presents a feasibility assessment for the use of Water Safety Plans (WSPs) as a tool to strengthen climate resilience of water supply systems and communities in Nepal.

Methodology

The study was conducted in November 2023 in collaboration with Oxfam and the NGO NEEDS Nepal

as a part of the “Strengthening Community Preparedness, Rapid Response and Recovery” (SCOP-R3) project.
The research focuses on six communities in Bhimdatta, a municipality in the Kanchanpur district of Sudhurpaschim Province, South-West Nepal. The 2021 census reports Kanchanpur's population at around 500,000, with Bhimdatta housing about 122,000 residents. The study targets six small disaster-affected communities:

- Khalla, Tudikhel, and Masseti in the hilly rural area.
- Bhujela and Pipraiya in the rural plains.
- Bhagatpur in the urban plain area.

The area is mainly rural with diverse, economically disadvantaged ethnic groups like Tharu, Madhesi, and Dalits. The district faces social challenges and relies on agriculture, including rice and wheat, as well as business, day labor, remittances, and livestock farming. Health facilities are insufficient, and clean drinking water is scarce, with only 43 water supply infrastructures and no treatment plants in the district [5]. Nearly 15% lack access to safe drinking water, with most using private shallow tubewells with hand pumps. Regarding the study, the key water systems used in the hilly areas are gravity-fed systems from unprotected springs and surface water collection, primarily used daily by marginalized groups and during emergencies, while the system used in the plain areas is shallow tubewells with hand pumps.
The Terai region, where the study area is located, has elevations below 500 meters and experiences hot monsoon and tropical climates. Annual precipitation ranges from 1,100-3,000 mm, mostly from June to September, with dry weather from November to December. The average annual temperature is 20-25°C, with high temperatures from May to July and cold temperatures from December to January [6].
These areas experience drought post-monsoon and face landslides and disruptive floods during monsoons, given their location in the lower Mahakali River basin, as seen in past events (e.g. 2014, 2016, 2018, 2021). The impacts of these disasters result in fatalities, infrastructure damages and economical losses that are exacerbated by socio-economic vulnerabilities and governance [7].
The aim of the visit was to collect information and data on the Drinking Water Supply Systems (DWSS) to carry out a proper description, an identification and assessment of the hazardous and climate induced events and of the hazards.
The methodology employed adheres to the World Health Organization (WHO) WSP guidelines [8,9]. WSPs are proactive and comprehensive risk assessment and management tools that cover the entire water supply chain, from catchment to consumer.
The WSP approach was adopted due to its documented effectiveness in addressing risks to water availability, quality, and system functionality posed by climate-related hazards, as highlighted in the literature. The flexibility of this methodology, in fact, can be exploited to integrate climate risk screening as part of the WSP continuous improvement cycle. In this way, climate risk assessment is best addressed as an incremental step within existing planning assessments and processes. For example, the governments of Fiji and Vanuatu and the United Nations Children's Fund (UNICEF), implemented a Drinking Water Safety Planning (DWSP) [10]. DWSP approach combines the concepts of water security with the Water Safety Plan (WSP) method, and it has been valuated as appropriate to ensure sustainable access to safe water in a disaster affected area as Fiji and Vanuatu. WHO has also developed guidance for Climate-resilient Water Safety Plans, emphasizing the importance of considering climatic hazards such as heavy rain, floods, and droughts in hazard identification and risk assessment [11].
Moreover, pilots of climate-resilient WSPs in Nepal, Bangladesh, Ethiopia and Jordan have demonstrated the effectiveness of the WSP process in addressing risks to water supply systems brought about by climate change and other disasters in developing countries [12, 13, 14, 15].

Results

At this stage of the research, the implementation of the WSP has not been completed. Instead, the focus

has been on the initial steps of the methodology, particularly the identification and assessment of hazards and the impacts of disasters on the DWSS of the villages.
The study revealed that floods, inundations, erosion, fires, landslides, and droughts are the main hazards impacting drinking water supply and affecting water quality (e.g. microbial contamination, water turbidity), water quantity (e.g. drying of the springs, decreasing groundwater level), and the infrastructures (e.g. damages, submerging handpumps, sweeping away pipes).
Key findings reveal a spectrum of challenges impacting the safely management of water supply systems and disasters in the study area. These challenges include lack of awareness about safe water and hygiene practices (e.g. absence of water treatment); inadequate water supply systems and poor infrastructure maintenance and workmanship; issues related to water privatization and prioritization during water scarcity. To further enhance disaster management, key areas to focus on include increasing awareness of climate change, disasters, and their impacts; improving community preparedness; strengthening communication, such as early warning systems; enhancing the accessibility of villages during disasters and developing emergency planning procedures. Additionally, governance issues such as political instability, inadequate training, and a lack of data, as well as socio-economic vulnerabilities including gender disparities, ethnic discrimination, and budgetary constraints, exacerbate water and disaster management challenges.

Conclusions

In conclusion, the complexity of this case study highlights the urgent need to enhance the resilience of water supply services and communities against disasters through the implementation of preventive and long-term plans. Providing decision-support tools is crucial to help policymakers and practitioners assess existing water supply systems, identify associated climate risks, and develop and monitor plans for enhancing the climate resilience of these systems.
However, it is important to note that the WSP approach, while effective in ensuring safe water by focusing on technical and managerial aspects of water supply systems, lacks a multi-sectoral perspective. It does not adequately consider external factors such as political, social, and economic aspects.
Future work recommendations include conducting studies using comprehensive and inclusive frameworks that consider the multi-sectoral dimensions of water risks and externalities. These frameworks should encompass financial, physical, technical, political, institutional, social, and environmental aspects. Examples of such frameworks include the UNICEF-Global Water Partnership (GWP) WASH Climate Resilient Development Strategic Framework (2022) [16], the United States Agency for International Development (USAID) Water Security Improvement Framework (2021) [17], and the Pacific Institute Water Resilience Assessment Framework (2021) [18]. It is essential to include the WSP methodology in these frameworks as a vital tool for risk assessment, necessary for improving the climate resilience of water supply systems.

Acknowledgments: This study was written within the project “Strengthening Community Preparedness, Rapid Response and Recovery” (SCOP-R3), implemented with the contribution of Oxfam Nepal and the collaboration of the NGO NEEDS Nepal.

References

[1] Caretta M.A., et al., Water. In: Climate Change 2022: Impacts, Adaptation and Vulnerability. Contribution of Working Group II to the Sixth Assessment Report of the Intergovernmental Panel on Climate Change, Cambridge University Press, pp. 551–712, (2022).
[2] Iyer P., Water Dilemmas: The Cascading Impacts of Water Insecurity in a heating world, Oxfam International, (2023)
[3] WDB/ADB, Climate Risk Country Profile: Nepal, (2021).
[4] Morris-Iveson L., Day S.J., Resilience of Water Supply in Practice: Experiences from the Frontline, IWA

Publishing, London (2021).
[5] NEEDS/OXFAM, Pre-crisis Market Analysis (PCMA) Report, (2021).
[6] Government of Nepal, Climate Change Related Indicators of Nepal, (2022).
[7] Government of Nepal, Nepal's Third National Communication to the UNFCCC, (2021).
[8] WHO, A field guide to improving small drinking-water supplies: water safety planning for rural communities, WHO Regional Office for Europe, Copenhagen (2022).
[9] WHO/IWA, Water safety plan manual: step-by-step risk management for drinking-water suppliers, second edition, World Health Organization, Geneva (2023).
[10] UNICEF Pacific, Pacific WASH Resilience Guidelines: A practical tool for all those involved in addressing the resilience of water, sanitation and hygiene services in the Pacific, UNICEF Pacific Multi Country Office, Suva (2018).
[11] WHO, Climate-resilient water safety plans: managing health risks associated with climate variability and change, World Health Organization, Geneva (2017).
[12] Government of Nepal, Climate Resilient Water Safety Plans Guideline: Rural Water Supply System, Kathmandu (2017).
[13] Shamsuzzoha Md., et al., "Implementation of Water Safety Plan Considering Climatic Disaster Risk Reduction in Bangladesh: A Study on Patuakhali Pourashava Water Supply System" in Proceedings of 7th International Conference on Building Resilience, Using scientific knowledge to inform policy and practice in disaster risk reduction, Bangkok, 27 – 29 November 2017, (2018).
[14] Rickert B., van den Berg H., Climate resilient water safety plans: compilation of potential hazardous events and their causes, Umweltbundesamt, (2021).
[15] UNICEF Jordan, Climate resilient Water Safety Plan for Madaba, Jordan, UNICEF Jordan, Jordan (2020).
[16] GWP, UNICEF., 2022 WASH Climate Resilient Development Strategic Framework, Ed. GWP - Stockholm UNICEF - New York (2022).
[17] USAID, SWP., Water Security Improvement (WSI) process, (2022).
[18] Chapagain A., et al., Water Resilience Assessment Framework, Alliance for Global Water Adaptation, CEO Water Mandate, International Water Management Institute, Pacific Institute, and World Resources Institute (2021).

Impacts of Climate Change on Italian Drinking Water Supply Systems: Experiences and Adaptation Strategies of Water Utilities

Author(s): Sabrina Sorlini, Hoan Thi Kim Tran, Seemab Mujahid

Department of Civil Engineering, Architecture, Land and Environment and Mathematics, University of Brescia, Brescia, Italy.

Email: sabrina.sorlini@unibs.it, h.tranthikim@unibs.it; s.mujahid@studenti.unibs.it

Keyword(s): Drinking water Supply System, Climate change, water treatment

Abstract

Italy's water resources are distributed unevenly, with the northern regions having the highest share, followed by the south and central areas [1]. Water management in Italy aligns with the EU's Water Framework Directive [15], but climate change is posing significant challenges, particularly in the Alpine region where glaciers are rapidly melting[4]. Italy has the highest drinking water consumption in Europe [12], and droughts, inefficient water management, and extreme weather events like floods further strain water resources.[5].Severe droughts, inefficient water management, and debris accumulation in dams have led to water scarcity issues. Flooding, such as the 2023 events in Emilia-Romagna, also presents risks, with significant populations exposed to flood hazards [6]. Climate change affects different treatment phases in drinking water plants, necessitating adjustments to maintain water quality [11]. Regarding treatment processes, it is necessary to identify suitable technological or engineering solutions to address climate change impacts on water treatment. Several studies ([8], [14]) suggested upgrading treatment plants, enhancing water treatment processes and technologies, and increasing chemical dosages to counteract anticipated reductions in source water quality due to climate change.

The main conclusion is that a degradation trend of drinking water quality in the context of climate change leads to an increase of at risk situations related to potential health impact [3].Variations in the intensity and frequency of rainfall events could exceed treatment capacity, leading to additional deterioration in water quality and flooding of utility assets [7]. Lyle [10] highlighted the challenges faced by drinking water utilities in ensuring water quality amidst changing climatic conditions, particularly extreme rainfall events, which are more exposed to vulnerability. Drinking water utilities are widely recognized as exceptionally dependable entities due to their ability to fulfill consumers' needs for water quantity and quality in both routine and emergency situations [2] [13]. Water treatment plants play a vital role in public health by ensuring clean water distribution, but climate change is challenging their processes and networks [9]. This study examines the impacts of climate change on Italy's water sector and measures taken by managers to adapt their water supply systems. By understanding these challenges and responses, the research contributes to efforts for resilient and sustainable water management in Italy.

Results and Discussions:

Climate change is increasingly impacting drinking water supply systems, challenging conventional water management practices. This study analyzes responses from 40 anonymous managers (Table 1) through a questionnaire to identify key climate-related issues affecting drinking water sources, treatment

processes, and distribution systems. The findings underscore the need for innovative control measures to ensure safe and reliable water supply.

Table 1: Location of managers

Number of managers	Regions
1	Abruzzo
1	Campania
3	Emilia Romagna
1	Friuli Venezia Giulia
1	Lazio
2	Liguria
9	Lombardy
1	Molise
6	Piemonte
1	Sardinia
2	Sicily
2	Tuscany
1	Trentino Alto Adige
1	Umbria
7	Veneto
1	Not identified

General Characteristics of Supply Systems

The survey revealed that the managers oversee diverse water supply systems, with varying capacities and service areas. While some managers are responsible for over 100 purification plants, others focus solely on distribution. The majority of these supply systems (97%) rely on underground aquifers, with a smaller proportion utilizing spring water, rivers, and artificial reservoirs. Climate change impacts have been reported across all types of water sources, notably with increased drought periods, rising temperatures, and intensified rainfall affecting supply capacities.

Impacts on Treatment Phases

Climate change has significant effects on various stages of water treatment. A key observation is the reduction in water levels across different sources, leading to increased turbidity and microbial contamination. During the pre-oxidation phase, 10 out of 11 managers noted increased oxidant demand, while the coagulation-flocculation phase saw higher coagulant demand due to rising turbidity. In granular filtration, more than half of the respondents reported increased suspended solids, attributed to increase of turbidity in raw water on of algal contamination due to climate factors. In the final disinfection phase, there was a marked increase in demand for disinfectants, with heightened microbiological contamination and increased formation of disinfection by-products (DBPs).

Impacts on Distribution Systems

The effects of climate change extend to the distribution systems, where the primary concern is rising water temperatures, reported by 15 out of 23 managers. This temperature increase has led to changes in microbiological quality, increased disinfectant consumption, and instances of biofilm growth. Other issues include chemical quality changes and biocorrosion of pipes. Certain managers also reported night-time breakages and temporary service interruptions due to water shortages, linked to drought conditions.

Non-Compliance Episodes and Control Measures

The climatic impacts on treatment and distribution have led to episodes of non-compliance with Italy's Legislative Decree 31/2001 (now Legislative Decree 18/2023), which governs drinking water safety. Cases of non-compliance were noted in total coliforms, *E. coli*, and other contaminants, and in some cases water companies faced issues with aluminium and chloride levels. In response, companies have adopted various control measures, ranging from enhanced monitoring and introduction of water safety plans (PSA or WSP) to new technologies and treatment procedures. Examples include one utility studying groundwater levels and considering online probes for turbidity monitoring in spring water, one utility distributing water with tankers during droughts, and one utility using mobile reverse osmosis units to reduce salinity in the Po River.

The adaptation measures highlight the industry's proactive response to the ongoing challenges posed by climate change, illustrating a commitment to ensuring the safety and reliability of drinking water supply systems. The results of this study contribute to a broader understanding of the climate-related challenges faced by water management systems and the innovative solutions employed to address them.

Conclusion:

The impacts of climate change on drinking water supply systems in Italy are widespread and multifaceted, as evidenced by the experiences reported by 40 water managers surveyed in this study. Nearly all respondents (97%) have observed climate-related effects, with increased drought periods being the most prevalent phenomenon. Decreased water levels across sources like aquifers, springs, rivers, and reservoirs are the primary consequence, accompanied by heightened microbial and algal contamination.

Within treatment plants, various unit processes are affected, with increased oxidant demand in pre-oxidation, higher coagulant needs and turbidity in coagulation-flocculation, more suspended solids in granular filtration, higher contaminant loads in activated carbon filtration, and elevated disinfectant requirements and microbial loads in the final disinfection phase. Distribution networks also face challenges like increased water temperatures, deteriorated microbiological quality, higher disinfectant consumption, and disinfection by-product formation.

To mitigate these impacts and ensure a reliable and safe water supply, Italian water utilities have implemented a range of adaptive measures. These include enhanced monitoring, risk assessment procedures like Water Safety Plans, and the adoption of new treatment technologies such as membrane filtration. Strategies like interconnections between systems, mobile treatment units, and network upgrades have also been employed to maintain service during crises.

Overall, this nationwide study highlights the significant vulnerability of Italy's drinking water sector to climate change impacts. It underscores the need for continued research, innovation, and proactive measures to bolster the resilience of water supply systems against the evolving challenges posed by a changing climate. Collaborative efforts among utilities, policymakers, and stakeholders will be crucial in safeguarding access to safe and sustainable drinking water resources for Italy's population.

Reference:

[1] Antonio Massarutto Dipartimento di Scienze Economiche, Università di Udine. *Agriculture, water resources and water policies in Italy*. Retrieved February 4, 2024 from https://citeseerx.ist.psu.edu/document?doi=268721044973f710f82c0267e4a547f8726713b7&repid=rep1&type=pdf

[2] Roland Bradshaw, Áine M. Gormley, Jeffrey W. Charrois, Steve E. Hrudey, Nancy J. Cromar, Daniel Jalba, and Simon J. T. Pollard. 2011. Managing incidents in the water utility sector – towards high reliability? *Water Supply* 11, 5 (December 2011), 631–641. https://doi.org/10.2166/ws.2011.069

[3] I. Delpla, A.-V. Jung, E. Baures, M. Clement, and O. Thomas. 2009. Impacts of climate change on surface water quality in relation to drinking water production. *Environment International* 35, 8 (November 2009), 1225–1233. https://doi.org/10.1016/j.envint.2009.07.001

[4] Elizabeth Miller. 2011. Climate Change Is Acidifying and Contaminating Drinking Water and Alpine Ecosystems.

[5] European Commission. Joint Research Centre. 2024. *Drought in the Mediterranean region: January 2024 : GDO analytical report.* Publications Office, LU. Retrieved April 18, 2024 from https://data.europa.eu/doi/10.2760/384093

[6] Filomena Fotia. 2023. Le principali siccità nella storia italiana. Retrieved from https://www.meteoweb.eu/2023/10/le-principali-siccita-nella-storia-italiana/1001318459/

[7] Matilde García-Valdecasas Ojeda, Fabio Di Sante, Erika Coppola, Adriano Fantini, Rita Nogherotto, Francesca Raffaele, and Filippo Giorgi. 2022. Climate change impact on flood hazard over Italy. *Journal of Hydrology* 615, (December 2022), 128628. https://doi.org/10.1016/j.jhydrol.2022.128628

[8] Monica Garnier and Ian Holman. 2019. Critical Review of Adaptation Measures to Reduce the Vulnerability of European Drinking Water Resources to the Pressures of Climate Change. *Environmental Management* 64, 2 (August 2019), 138–153. https://doi.org/10.1007/s00267-019-01184-5

[9] Gary Bonnett. 2023. A Guide to Understanding Water Treatment. Retrieved from https://safetyculture.com/topics/water-treatment/

[10] Zia J. Lyle, Jeanne M. VanBriesen, and Constantine Samaras. 2023. Drinking Water Utility-Level Understanding of Climate Change Effects to System Reliability. *ACS EST Water* 3, 8 (August 2023), 2395–2406. https://doi.org/10.1021/acsestwater.3c00091

[11] Manuela Perrone. 2024. Il commissario Dell'Acqua: «Siccità scongiurata grazie alle nevicate ma urge intervento sugli invasi». Retrieved from [4] https://www.ilsole24ore.com/art/il-commissario-dell-acqua-rischio-siccita-scongiurato-ma-urge-interno-dighe-e-invasi-AFdpdD9C

[12] V. Niccolucci, S. Botto, B. Rugani, V. Nicolardi, S. Bastianoni, and C. Gaggi. 2011. The real water consumption behind drinking water: The case of Italy. *Journal of Environmental Management* 92, 10 (October 2011), 2611–2618. https://doi.org/10.1016/j.jenvman.2011.05.033

[13] Avi Ostfeld, Dimitri Kogan, and Uri Shamir. 2002. Reliability simulation of water distribution systems – single and multiquality. *Urban Water* 4, 1 (March 2002), 53–61. https://doi.org/10.1016/S1462-0758(01)00055-3

[14] Lucas Augusto Pereira Rodrigues, Fernando Aparecido Dias Radomski, Rodrigo Felipe Bedim Godoy, Elias Trevisan, and Enzo Luigi Crisigiovanni. 2021. Correlations between water quality and precipitation in areas with different levels of human occupation. *International Journal of Energy and Water Resources* 5, 1 (2021), 25–31. https://doi.org/10.1007/s42108-020-00097-y

[15] WFD,2000. Water Framework Directive. Retrieved from https://environment.ec.europa.eu/topics/water/water-framework-directive_en

Acknowledgement:

Thanks to Matteo Donghi, who developed this survey during his master thesis at the University of Brescia. The survey was developed by GdL working group (https://impiantitrattamentoacque.unibs.it/) with the involvement of the PhD students Thi Kim Hoan Tran and Seemab Mujahid enrolled in the Ph.D. Programme in Civil, Environmental Engineering, International Cooperation and Mathematics (DICACIM) at the University of Brescia.

Title: Carbon dioxide removal strategies and ocean alkalinity enhancement: a review of a developing and promising field of research

Author(s): Stefano Caserini*[1]

[1] *Department of Engineering and Architecture, University of Parma, Parma, Italy, stefano.caserini@unipr.it*

Keyword(s): climate change, climate mitigation, negative emission technologies, CO_2, climate action

Abstract

Greenhouse gas (GHG) emissions are heavily affecting the global climate, and at the same time are acidifying the oceans. In particular, the concentration of carbon dioxide (CO_2), the most important greenhouse gas (GHG) by radiative forcing, is significantly and continuously rising due to human activities such as the use of fossil fuels and ongoing deforestation. Further greenhouse gas (GHG) emissions and consequent warming are expected in the coming decades. Rapid and far-reaching transitions in energy, land, urban infrastructure, and industrial systems are urgently needed to decrease emissions and limit global warming. Furthermore, to keep the increase of global temperature "well below 2°C", as agreed with Article 2 of the Paris Agreement, and thus net-zero CO_2 emission by around 2050-2060, it is now clear that there is the need to remove from the atmosphere a large amount of CO_2 already present in the atmosphere, through "negative emission technologies" (NETs), also called "Carbon Dioxide Removal" (CDR) strategies. The latest IPCC assessment report emphasizes the need for CDR [1], stating: "*The deployment of CDR to counterbalance hard-to-abate residual emissions is unavoidable if net zero carbon dioxide or greenhouse gas emissions are to be achieved*".

It is now clear that to provide many Gt of carbon removal per year, a portfolio of NETs is needed. Many strategies have been proposed, such as afforestation and reforestation, land management to increase carbon in soils, bioenergy with carbon capture and storage (BECCS), direct air carbon capture and storage (DACCS), enhanced weathering, ocean alkalinity enhancement and ocean fertilization [1, 2]. A categorization of CDR strategies based on the removal process and storage medium is shown in Figure 1 [3].

The comparison of the different pros and cons, co-benefits and side effects of the various options is a developing field of research. It is widely recognized that the tremendous amount of CO_2 research needed should be devoted not only to current frontrunners, i.e. BECCS and DACCS, but also to approaches less formally evaluated in terms of cost, effectiveness, resource availability and acceptability [4].

Methods and levels of CDR deployment in global modelled mitigation pathways vary depending on assumptions about costs, availability and constraints. According to the last IPCC-WG3 report, in modelled pathways that report CDR and that limit warming to 1.5°C (>50%) with no or limited overshoot, global cumulative CDR during 2020–2100 from BECCS and DACCS amount to 30–780 $GtCO_2$ and 0–310 $GtCO_2$, respectively [1].

This large amount of carbon removal depends on how swiftly global emissions will be reduced, the level of residual emissions and how these residual emissions will be restricted over time. This raises questions among experts about whether CDR is a necessary requirement or could act as a dangerous distraction from limiting GHG emissions [5].

Several studies, and the summary of the latest IPCC report [3], have discussed the risks and co-benefits

of the different strategies, including environmental impacts and costs.

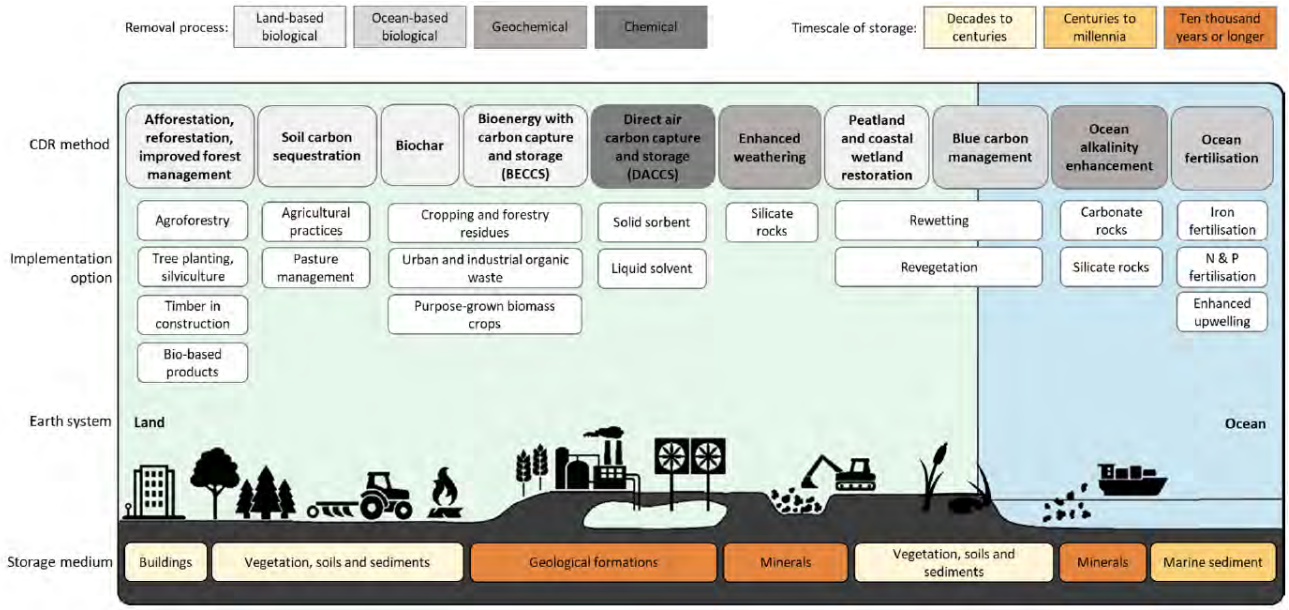

Figure 1. Carbon dioxide removal taxonomy. Methods are categorized based on the removal process (grey shades) and storage medium (for which timescales of storage are given, yellow/brown shades). Source: Babiker et al., 2023.

This review discusses in detail a promising ocean-based CDR option, ocean alkalinity enhancement (OAE) through the direct discharge of $Ca(OH)_2$ (calcium hydroxide, slaked lime, SL) in seawater, also called ocean liming. One of the reasons for the interest in ocean liming is that it has the potential of removing atmospheric CO_2 and, at the same time, counteracting ocean acidification, an often-forgotten consequence of the exploitation of fossil fuels. While the chemical processes of OAE are theoretically known, and many authors indicate a large potential for carbon removal, further research is needed to evaluate the environmental benefits and trade-offs, technological challenges, potential side effects and economic feasibility. Some of these researches have been developed in the framework of the DESARC (DEcreasing Seawater Acidification Removing Carbon)-MARESANUS project.
Potential strategies to discharge slaked lime and remove CO_2 have been evaluated, suggesting that the global potential of CO_2 removal from SL discharge by existing or new ships is estimated at several Gt/year, depending on the discharge rate [6]. A modelling simulation of ocean liming on the Mediterranean Sea through SL discharged along current shipping routes shows the potential of nearly doubling the carbon-dioxide uptake rate of the Mediterranean Sea after 30 years of alkalinization, and of neutralizing the mean surface acidification trend of the baseline scenario without alkalinization over the same time span [7].
Likewise other climate strategies, the overriding issues with the implementation at the global of ocean liming are costs and energy requirements; for this reason, the research has investigated the possibilities of optimizing the whole chain of ocean liming, from calcium hydroxide production to its discharge by vessels, in different contexts and scales. A detailed analysis of each operation shows that grinding, transport, and calcination are the most energy-expensive phases with great energy-saving potential. Optimization of the logistics of limestone transport and spreading requires different types of knowledge,

i.e. limestone availability, current maritime traffic, ocean circulation and efficiency of CO_2 uptake in different regions of the world's ocean. The analysis of the data extracted from the global lithological map database [8] shows that the global availability of pure carbonates is vast, although with uneven distribution, and it could largely satisfy the requirement for large-scale development of ocean liming; a large fraction of pure limestone resources that could be exploitable are within 50 km from the coastline; the fraction below bare ground or scrub/shrub, preferred for the logistics of exploitation, account for about 600,000 km2, and could provide about 15.000 Gt of limestone. A conservative assessment of the total world production of mineral raw materials is around 44 Gt y^{-1}. Limestone yearly production, estimated to be more than 6 Gt from deposits scattered all around the world, is the same order of magnitude as coal. The required up-scaling of limestone production compared to the actual level is limited, much lower than what would be needed for ocean alkalinity enhancement with other raw materials that could be used, such as olivine, magnesite and brucite

To assess the overall performance of ocean liming in removing atmospheric CO_2, as well as other potential environmental impacts connected to slaked lime production and transport, a life-cycle assessment (LCA), based on a "cradle-to-grave" approach has been applied to a process that combines biomass gasification, limestone calcination, CO_2/H_2 separation and CO_2 storage [9] and a process based on renewable electric calcination. The results show that the process has a potential negative impact on the Climate change category, i.e. there is a benefit for the environment in terms of CO_2 removal from the atmosphere [10].

Since one limiting factor of ocean liming through the dispersion of slaked lime is the availability of safe and permanent storage for the CO_2 produced during the calcination of limestone, and the geological CO_2 storage is not developing at the required pace, alternative methods for the capture and storage of CO_2 in the form of bicarbonates have been proposed, and are currently under scrutiny or development, such as accelerated weathering of limestone [11], buffered accelerated weathering of limestone [12, 13] or the Limenet process [14].

Although slaked lime (e.g., calcium hydroxide) may be the most appropriate option for OAE also considering the lower content of potentially toxic elements and thus fewer environmental concerns compared to other minerals, such as olivine, besides metal toxicity impacts on marine ecosystems are largely unknown, especially regarding alkalinization process. Some studies have defined a relationship between slaked lime sparging rate, and the corresponding pH increase in seawater [6], but understanding whether these short-lasting pH spikes could substantially affect marine organisms is challenging based on current literature since it principally addresses the relationship between climate change and ocean acidification. Only recently, research papers discussing the short-term effects of these pH spikes on marine organisms have emerged, and show that at pH 9 for short exposure times (<6 h), no negative effects were observed [15].

Anyway, ocean alkalinity enhancement still faces many challenges, such as the implementation of loading facilities in ports, or international legislative constraints that could limit its deployment.

In conclusion, it's worth remembering that the world's oceans have already helped in the fight against climate change, absorbing about 30% of anthropogenic CO_2 emissions and 90% of the resulting excess heat trapped in the climate system. The growing interest in using oceans for enhanced climate action, i.e. through ocean alkalinity enhancement, aims to leverage the ocean's natural processes to reduce CO_2 concentrations in the atmosphere and safely store that carbon in the ocean. For this reason, they deserve attention as necessary carbon dioxide removal options to pursue to keep the Paris Agreement goal of "well below 2.5 °C" within reach.

References

[1] IPCC – Intergovernmental Panel on Climate Change (2022). Summary for policymakers. In P. R. Shukla, J. Skea, R. Slade, A. Al Khourdajie, R. van Diemen, D. McCollum, M. Pathak, S. Some, P. Vyas, R. Fradera, M.

Belkacemi, A. Hasija, G. Lisboa, S. Luz, & J. Malley (Eds), Climate change 2022: Mitigation of climate change. Contribution of working group III to the sixth assessment report of the intergovernmental panel on climate change. Cambridge University Press. doi: 10.1017/9781009157926.001

[2] Minx, J.C. et al., 2018: Negative emissions - Part 1: Research landscape and synthesis. Environ. Res. Lett., 13(6), 063001, doi:10.1088/1748-9326/aabf9b

[3] Babiker, M., G. Berndes, K. Blok, B. Cohen, A. Cowie, O. Geden, V. Ginzburg, A. Leip, P. Smith, M. Sugiyama, F. Yamba, 2022: Cross-sectoral perspectives. In IPCC, 2022: Climate Change 2022: Mitigation of Climate Change. Contribution of Working Group III to the Sixth Assessment Report of the Intergovernmental Panel on Climate Change [P.R. Shukla, J. Skea, R. Slade, A. Al Khourdajie, R. van Diemen, D. McCollum, M. Pathak, S. Some, P. Vyas, R. Fradera, M. Belkacemi, A. Hasija, G. Lisboa, S. Luz, J. Malley, (eds.)]. Cambridge University Press, Cambridge, UK and New York, NY, USA. doi: 10.1017/9781009157926.005

[4] Rau,G. (2019). The race to remove CO2 needs more contestants. Nat. Clim. Change 9:256. doi: 10.1038/s41558-019-0445-5

[5] Anderson, K., Buck, H.J., Fuhr, L. et al. Controversies of carbon dioxide removal. Nat Rev Earth Environ 4, 808–814 (2023). https://doi.org/10.1038/s43017-023-00493-y

[6] Caserini, S., Pagano, D., Campo, F., Abbá, A., Serena, D. M., Righi, D., Renforth P., Grosso M. (2021) Potential of maritime transport for ocean liming and atmospheric CO2 removal. Frontiers in Climate. 3:575900. https://doi.org/10.3389/fclim.2021.575900

[7] Butenschön M., Lovato T., Masina S., Caserini S. and Grosso M. (2021) Alkalinization scenarios in the Mediterranean sea for efficient removal of atmospheric CO2 and the mitigation of ocean acidification. Frontiers in Climate. 3, 614537. https://doi.org/10.3389/fclim.2021.614537

[8] Caserini S., Storni N., Grosso M. (2022) The availability of limestone and other raw materials for ocean alkalinity enhancement. Global Biogeochemical Cycles, 36, 5. https://doi.org/10.1029/2021GB007246

[9] Caserini S., Barreto B., Lanfredi C., Cappello G., Ross Morrey D., Grosso M. (2019) Affordable CO2 negative emission through hydrogen from biomass, ocean liming, and CO2 storage. Mitigation and Adaptation Strategies for Global Change. 24(7), 1231-1248. https://doi.org/10.1007/s11027-018-9835-7

[10] Campo F., Caserini S., Pagano D., Dolci G., Grosso M. (2020) Analisi del ciclo di vita di un processo per rimuovere la CO2 atmosferica e contrastare l'acidificazione del mare. Ingegneria dell'Ambiente, 7, 1, 7-22. https://dx.doi.org/10.32024/ida.v7i1.230

[11] Rau G, Knauss K, Langer W, Caldeira K (2007) Reducing energy-related CO2 emissions using accelerated weathering of limestone. Energy 32:1471–1477. https://doi.org/10.1016/j.energy.2006.10.011

[12] Caserini S., Capello G., Righi D., Raos G., Campo F., De Marco S., Renforth P., Varliero S., Grosso ; (2021) Buffered accelerated weathering of limestone for storing CO2: Chemical background. International Journal of Greenhouse Gas Control, 112, 103517. https://doi.org/10.1016/j.ijggc.2021.103517

[13] De Marco S., Varliero S., Caserini S., Cappello G., Raos G., Campo F., Grosso M. (2023) Techno-economic evaluation of buffered accelerated weathering of limestone as a CO2 capture and storage option. Mitigation and Adaptation Strategies for Global Change, 28:17, https://doi.org/10.1007/s11027-023-10052-x

[14] www.limenet.tech

[15] Camatti E., Valsecchi S., Caserini S., Barbaccia E., Santinelli S., Basso D., Azzellino A., (2024) Short-term impact assessment of ocean liming: A copepod exposure test. Marine Pollution Bulletin, 198, 115833. https://doi.org/10.1016/j.marpolbul.2023.115833.

PARALLEL SESSION: D1

Municipal and industrial waste

Energy recovery and production

Bioenergy potential from green waste through lab-scale anaerobic digestion: Thermophilic versus mesophilic conditions

Adele Folino[1], Antonio Randazzo[2], Franco Tassi[2,3], Fabio Tatàno*[1], Sandro de Rosa[4], Alma Gambioli[4]

[1] DiSPeA - Department of Pure and Applied Sciences, Section ChEM - Chemistry, Environment, and Materials, University of Urbino "Carlo Bo", Campus Scientifico "E. Mattei", 61029 Urbino, Italy, adelefolino@gmail.com, fabio.tatano@uniurb.it
[2] DST - Department of Earth Sciences, University of Florence, via G. La Pira 4, 50121 Firenze, Italy, antonio.randazzo@unifi.it, franco.tassi@unifi.it
[3] IGG - Institute of Geosciences and Earth Resources, CNR - National Research Council of Italy, via G. La Pira 4, 50121 Firenze, Italy
[4] ASET S.p.A. public multi-utility group, via E. Mattei 17, 61032 Fano, Italy, s.derosa@asetservizi.it, a.gambioli@asetservizi.it

Keywords: anaerobic digestion; biochemical methane potential; biogas; characterisation; green waste; thermophilic vs mesophilic conditions; VOCs

Abstract

The anaerobic digestion (AD) is a suitable management option to valorise biomass resources and organic waste by generating renewable bioenergy. Considering the overall organic fraction of municipal waste (MW), a key component is represented by the green waste (GW), typically consisting of grass, leaves, and pruning residues originating from private gardens and public parks.
Although being a sustainable and renewable alternative to fossil fuels, biogas production through AD poses still some technical-scientific and management challenges, such as: (1) the comprehensive analysis of the chemical composition (in terms of the main gaseous components and volatile organic compounds - VOCs) of the biogas and its evolution during the AD process; (2) the consequential evaluation of the impact of possible biogas escapes eventually occurring due to leakages from digester plants or possible damages in engine systems finalised to the direct energy recovery; (3) the consequential optimisation of possible cleaning approaches for the alternative option of biogas upgrading to biomethane; and (4) the consideration of the initial and final characteristics of the organic substrate and digestate, respectively, in the overall evaluation of the AD process. Clearly, the mentioned points should be attentively investigated for both the relevant design and implementation options of mesophilic and thermophilic AD.
In this study, a peculiar AD test on a GW substrate at lab-scale in batch mode (Figure 1, left), adapted from the volumetric (eudiometric) approach for determining the biochemical methane potential (BMP) [1], was conducted under thermophilic conditions. The results were compared with those from a similar test under the alternative mesophilic conditions performed in a previous, initial work presented at the 2021 Edition of the "SIDISA, International Symposium on Environmental Engineering" [2].
The GW substrate sample was obtained at the GW collection and initial management centre of the Fano town district in the Marche Region (Central Italy, Adriatic Sea side), which is operated by the "ASET" public multi-utility group. The GW substrate to inoculum (anaerobic sludge) ratio was fixed at 2:1 on a volatile solids (VS) basis, as in the previous mesophilic AD test [2], whilst the operating temperature was higher (55 °C instead of 38 °C). Both the GW substrate and the inoculum were characterised in

terms of moisture, total solids (TS), VS, total Kjeldahl nitrogen (TKN), total ammoniacal nitrogen (TAN), total phosphorus (TP), total potassium (TK), and heavy metals (Cd, Cr, Cu, Hg, Ni, Pb, and Zn). Similar analytical determinations were performed on the separated solid (or fibre) and liquid (or liquor) fractions of the obtained whole digestate. All the previous analytical determinations were conducted in triplicate.
During the thermophilic AD test, which lasted 60 days, biogas samples were periodically collected from the headspace of a selected digester containing the mixture of GW substrate and inoculum following the sampling procedure by [3]: a needle, connected to a syringe through a three-way-valve, was inserted in the digester headspace from a pertaining, pierceable rubber cap (Figure 1, right). Isotope ($^{13}C/^{12}C$ in CO_2 and CH_4 - $\delta^{13}C\text{-}CO_2$ and $\delta^{13}C\text{-}CH_4$, respectively) and main chemical (CH_4, CO_2, N_2, A_r, and O_2) composition of biogas samples was determined along with the identification and quantification of VOCs (as species and related functional groups).

Figure 1. Overall view of the lab-scale system used for the AD experiment (left) and particular view of the biogas sampling from the headspace of one digester (right)

By properly adapting the eudiometric measurements with the lab-scale system of Figure 1 (left) to the effective methane contents based on the modelling of the analyses of main gaseous components in the selected biogas samples, the thermophilic AD of the GW sample exhibited a BMP equal to 167.5 Nml CH_4 g VS^{-1}. As expected, the GW biogas samples were dominated by CH_4, except at the beginning of thermophilic AD where N_2 and (subsequently) CO_2 were the dominant gaseous components. After the beginning of thermophilic AD and until its end, CH_4 showed uninterrupted ^{12}C-enrichment, whilst CO_2 exhibited the opposite trend (i.e., ^{13}C-enrichment). This may suggest the establishment of hydrogenotrophic methanogenesis that, interestingly, occurred almost 10 days earlier than the mesophilic AD.
The thermophilic BMP resulted lower than the value of 178.2 Nml CH_4 g VS^{-1} from the mesophilic AD of a GW sample (obtained from the same collection centre) performed in the mentioned initial work [2], although the relative difference was limited to 6% (calculated as $[(BMP_{GW\text{-}mesophilic} - BMP_{GW\text{-}thermophilic})/(BMP_{GW\text{-}mesophilic})] \times 100$). The lower BMP obtained in thermophilic AD could be concurrently attributed to: (1) the larger risk of ammonia inhibition, as indicated by the resulting higher TAN content in the digestate solid fraction from the thermophilic AD test compared to that from the initial mesophilic AD test; (2) the mentioned anticipation of hydrogenotrophic methanogenesis, that is expected to give a lower contribution to the overall methane generation compared to the alternative acetate-dependent

methanogenesis [4]; (3) the resulting condition of pH located externally at the upper limit of the optimal range for methanogens [5] in the last temporal phase of the thermophilic AD test; and (4) the expected higher transfer of CO_2 to the gas phase with increasing temperature [4], as confirmed by the resulting higher CO_2 volumetric percentages detected in the biogas samples of thermophilic AD, compared to mesophilic AD, during the predominant time of test durations.
Up to 29 different VOC species were detected in the GW biogas samples from the thermophilic AD test. In terms of functional groups, they were dominated by alkanes, aromatics, and terpenes, whilst alkenes, cyclics, halogenated, and O-substituted compounds occurred in subordinate amounts. Such a compositional VOC pattern differed from that observed for mesophilic conditions (dominated, instead, by terpenes, alkanes, alkenes, and cyclics), clearly indicating a strong effect of the temperature regime on VOC release from AD of GW.
These results pointed out the pivotal role of temperature in controlling the extent and evolution of the whole AD process and, subsequently, the BMP values and chemical composition of the generated biogases.
This overall study is part of a multi-year research cooperation evaluating the bioenergy potential through AD from organic residues and waste having territorial consistency or value.

Acknowledgements

The “BO-ASET, Biological Organic Anaerobic System for Energy Technologies” lab-scale system (for the thermophilic and mesophilic AD experiments) was conceived by the Sanitary-Environmental Engineering Research Unit at the University of Urbino ‘‘Carlo Bo” and logistically located at the Environmental Analysis Laboratory of ASET in Fano (Marche Region, Italy). The detailed biogas characterisation was performed at the Laboratory of Fluid Geochemistry of the University of Florence based on the initial biogas sampling procedure optimised by the same Laboratory. The authors are grateful to Dr. M. Gabrielli, Dr. V. Bacchiocchi, Dr. G. Tombari, and Dr. A. Piersimoni at the ASET for the support in conducting the analytical characterisation of GW, inoculum, and digestate samples. The authors thank Mr. M. Di Domenico at the Hera in Rimini (Emilia-Romagna Region, Italy) for providing the anaerobic sludge samples.

References

[1] Carchesio M., Di Addario M., Tatàno F., de Rosa S., Gambioli A., Evaluation of the biochemical methane potential of residual organic fraction and mechanically-biologically treated organic outputs intended for landfilling, Waste Management, 113, 20-21 (2020).
[2] Folino, A., Randazzo, A., Tassi, F., Tatàno, F., de Rosa, S., Gambioli, A., Bioenergy from green waste through anaerobic digestion: Substrate, biogas, and digestate characterization at lab-scale. In: Proceedings ‘‘SIDISA 2021, XI International Symposium on Environmental Engineering”, Turin, Italy, June 29 - July 2 (2021).
[3] Randazzo, A., Folino, A., Tassi, F., Tatàno, F., de Rosa, S., Gambioli, A., Volatile organic compounds from green waste anaerobic degradation at lab-scale: Evolution and comparison with landfill gas, Detritus, 19, 63-74 (2022).
[4] Angelidaki, I., Batstone, D.J., Anaerobic digestion: Process. In: Christensen, T.H. (Ed.), Solid Waste Technology & Management, vol. 2, John Wiley & Sons Ltd., Chichester, UK, pp. 583–600 (2010).
[5] Weiland, P., Biogas production: Current state and perspectives, Applied Microbiology and Biotechnology, 85, 849–860 (2010).

Title: Dual-Purpose Valorization of Olive Pomace: Energy Production and Agricultural Application via Hydrothermal Carbonization

Authors: Gianluigi Farru*[1], Daniele Cabras[1], Mona Ghaslani[1], Alessandro Orsini[2], Giovanna Cappai[1]

[1] *Department of Civil and Environmental Engineering and Architecture, University of Cagliari, Via Marengo 2,09123 Cagliari, Italy.* gianluigi.farru@unica.it, mona.ghaslani@unica.it, gcappai@unica.it
[2] *Sotacarbo S.p.A., Grande Miniera di Serbariu, Carbonia, 09013, Italy.* alessandro.orsini@sotacarbo.it

Keywords: Hydrothermal carbonization, waste management, organic waste, olive pomace

Abstract

This study explores the hydrothermal carbonization (HTC) of olive pomace under varying conditions of temperature (180, 200, and 220 °C) and holding time (0 and 1 h) to identify the best valorization path for the resulting by-products. The hydrochars produced displayed a higher carbon content and lower oxygen and ash content compared to the feedstock, resembling the characteristics of solid fuels and suggesting their potential as sustainable energy sources. The liquid by-product (process water), was assessed for its effects on the germination of cress seeds (*Lepidium sativum* L.), revealing that while lower concentrations enhance seedling growth, higher concentrations exhibit significant phytotoxic effects. The study concludes that with appropriate dilution, process water can be effectively utilized in agriculture, aligning with sustainable waste management practices, and contributing to a circular approach.

Introduction

The cultivation of olive trees and the production of olive oil hold significant global agricultural value, particularly in Mediterranean regions where about 11 million hectares are under cultivation. According to the International Olive Council, olive oil production totalled 3 million tons in 2021 and 2022, with Mediterranean countries contributing 90% of this output [1]. However, the extraction process generates substantial waste that impacts soil microbes, aquatic ecosystems, and air quality, emphasizing the need for effective waste management and sustainable practices using advanced technology. Parallel to agricultural developments, the global energy demand has surged since the early twentieth century due to industrial growth and technological advances, historically met by non-renewable fossil fuels. This reliance has increased energy costs and highlighted the unsustainability of continued fossil fuel use, pushing for a shift towards more economically and environmentally sustainable energy sources. The European Union, through initiatives like the European Green Deal, aims to achieve climate neutrality by 2050, promoting a modern, sustainable economy. This includes the diversification of energy production to include renewable sources. Additionally, biomass, particularly residual biomass, is gaining attention as a dual solution for renewable energy production and waste management, despite its challenges, like heterogeneous composition and lower energy density. This study focuses on the potential of converting olive pomace (OP), a problematic waste by-product, into valuable materials through hydrothermal carbonization. This process could transform the OP into hydrochar, usable as solid fuel, and process water, which could serve as a fertilizer [2]. This research not only aims to manage olive waste sustainably but also explores how different operating parameters affect the quality of the resulting products.

Materials and methods

Olive pomace produced after the extraction of the oil in a two-and-a-half-phase mill in Sardinia, Italy, was used as feedstock for the application of the hydrothermal carbonization process. The olive pomace

consists of a slurry with a water content of about 84%. The HTC tests were conducted using a pressurized 1.5L-stainless steel reactor (Berghof BR-1000), without water addition. For the execution of the tests, 6 different combinations of temperature (180, 200, and 220 °C) and residence time (0 and 1 h) were studied. For each combination, the triple tests were carried out to ensure replicability. The residence time was assessed from the time the set point temperature was reached. In the zero-time test (0 h), in fact, the reactor was shut down as soon as the desired temperature was reached. In each trial, 1 kg of OP was treated. Once the test was completed and the reactor was cooled down, the three products obtained (hydrochar, process water, and gas) were quantified and a mass balance was performed. While the gas was released through a valve, the hydrochar produced was separated from the process water through a press lined with a food-grade filter. The wet hydrochar was dried at 105 °C for 24 h, while the process water was stored at 4 °C. The samples were labelled with codes indicating their contents and the HTC parameters used. For example, the sample treated at 200 °C for one hour was labelled with the initials OP_200_1. Solid materials (feedstock and hydrochars) were characterized by elemental composition, thermogravimetric analysis (TGA), and higher heating value (HHV), while process waters were assessed for pH and electrical conductivity (EC), total organic carbon (TOC) and total nitrogen (TN), and ion chromatography to assess the presence of dissolved ions. Moreover, process waters were used in germination tests (according to UNI EN 16086-2) using cress (*Lepidium sativum* L.) seeds to assess their phytotoxicity or ability to improve germination and seedling growth. Process water dilutions (50, 10 and 4%) were carried out. In addition, tests with 100% process water and a control with 100% distilled water were carried out.

Results and discussion

From the analysis and comparison between the various tests, temperature and time affected the solid yield results. Solid yields ranged from 96.68% to 62.79%, decreasing as the severity of the process conditions increased. Comparing the tests with the two different times analyzed, longer times produce lower solid yields, in fact, comparing two identical temperatures at different times they differ by 20%. This happens because over time an increasing part of the starting solid matrix is transformed into the liquid and gaseous phase. In the same way, as the temperature increases, a more effective decomposition of the material occurs during the process, due to the fragmentation and solubilization of the pomace macromolecules, thus obtaining a decrease in the solid yield. The elemental composition showed an increase in the carbon content from 54.92% in the feedstock to a range of 56.62 - 65.96% in the hydrochars and a reduction of oxygen from 32.63% in the feedstock up to 23.49% in OP_220_1. Consequently, the atomic ratios H/C and O/C are reduced so that the resulting hydrochars in a Van Krevelen diagram (Fig.1) are positioned in the typical region of lignite. Thermogravimetric analyses revealed a reduction in ash from 4.31% in feedstock to a range of 1.46 - 1.89% in hydrochars and an increase in fixed carbon from 20.4% to between 21.01 and 26.83% with higher values for higher temperature but shorter holding time. The carbonization process produced a material with calorific value higher than the feedstock (23.63 MJ/kg) and influenced by the applied temperature and residence time. In tests conducted at time zero, the calorific value increased slightly as the temperature increases. In one-hour tests, the HHV was consistently higher than in zero-time tests, and it increased further as the temperature rose. In OP_220_1, HHV values (31.71 MJ/kg) similar to or higher than common fuels used for energy production are obtained (bituminous coal = 30.6 MJ/kg, anthracite = 33.2 MJ/kg [3]).
Process waters were characterized by an acid pH (around 4) and an EC ranging from 64.83 to 79.02 mS/cm. Through hydrothermal carbonization, process water with a high organic carbon content is obtained, given the fact that the feedstock is partially solubilized. The TOC increases compared to the feedstock (18.46 g/L, measured in the liquid part) reaching concentrations in the range of 23.65 - 30.16 g/L. By increasing the temperature of the test, a decrease in TOC can be noticed due to the gradual mineralization of organic carbon [4], which is greater with tests lasting one hour.

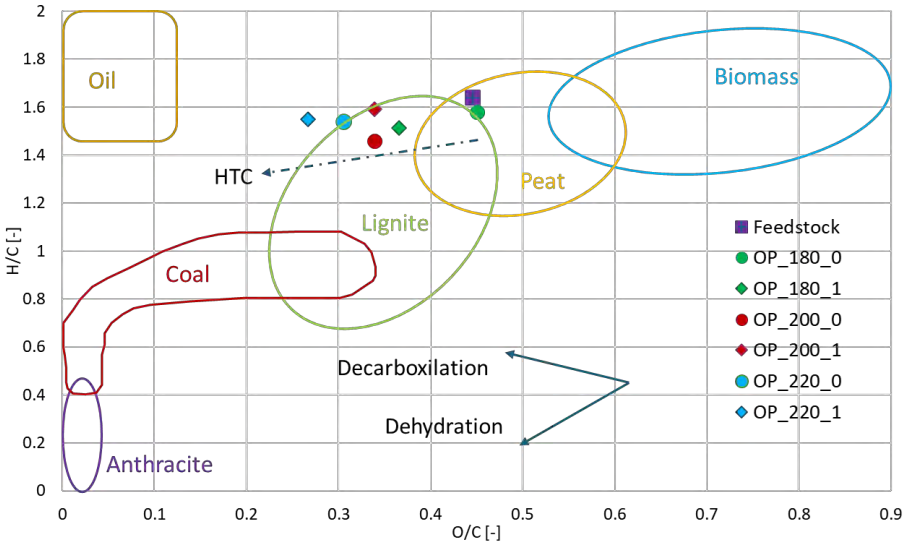

Figure 1. Van Krevelen diagram of the feedstock and hydrochars obtained from the different HTC tests.

The opposite trend can be shown for the total nitrogen, which increased compared to the feedstock (73.2 mg/L) with the increase of the temperature and time (up to 640.3 mg/L in OP_220_0 and 717.8 in OP_220_1). The ion chromatography revealed the presence and quantity of anions and cations within the process water. A high concentration of potassium and phosphates is noted (almost 5 g/L and 1.2 g/L, respectively). These are crucial nutrients for plant growth. For this reason, given their high concentration in the process water, they could be recovered and used for agriculture. In Fig.2, the root index (RI) and Munoo-Liisa vitality index (MLV) from germination tests are reported.

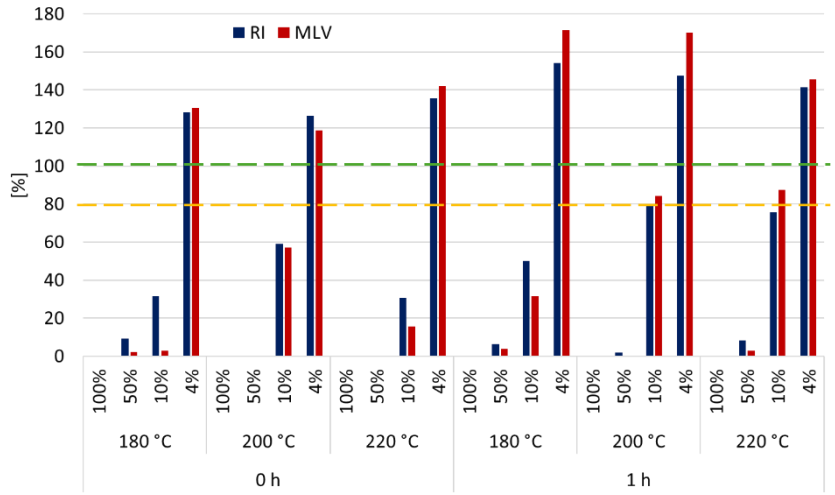

Figure 2. Germination tests results. Values between the yellow and green lines (80 and 100%) can be considered similar to the control, while higher values are considered better than the control.

Process water not diluted (100%) and those with 50% dilutions strongly inhibited seed germination and root growth. Also, the tests with 10% dilution showed partial inhibition of seed germination and plant growth, with the only exception of samples produced at 200 °C where the MLV index slightly exceeded 80% presenting values similar to those of the control The best results were obtained with 4% dilutions,

where the indices are all above 100% and in two cases 150% values are exceeded, specifically in the tests carried out at one hour with temperatures of 180 and 200 °C. This shows that toxicity decreases as reaction time increases. In addition, by analyzing the effect of temperature, lower toxicity can be observed at temperatures not exceeding 200 °C.

Conclusions

The aim of the experimentation carried out in this work was to provide a contribution to the sustainable management of waste from olive oil production. This was achieved through the application of the hydrothermal carbonization process, which converts organic waste into higher-value products for market reintroduction. The produced hydrochars possess a higher carbon and fixed carbon content and a lower oxygen and ash content than the feedstock. In addition, hydrochars are similar to solid fuels such as coal in terms of HHV. These characteristics make hydrochars potentially usable as solid fuels in energy production, replacing non-renewable sources [5]. Another important result concerns process water, which must be properly managed, as it constitutes the majority of the flow leaving the HTC process. The process water is rich in organic matter and nutrients. From the germination tests, it can be concluded that using significant quantities of process water results in considerable toxicity for the germination of the seeds, inhibiting their growth. On the contrary, dilutions of 4% promote seed germination and root growth, suggesting that low concentrations can be beneficial. Therefore, this water can be used for fertigation in low concentrations, improving its management by reducing the consumption of water [6]. Further investigation, including analysis for potential soil pollutants, is needed to confirm this hypothesis. In conclusion, the hydrothermal carbonization process applied to olive pomace could reduce the environmental impact related to its disposal and allow using the obtained products as a resource, bringing a double benefit from the perspective of a circular economy and the reduction of emissions.

Acknowledgement

We acknowledge financial support under the National Recovery and Resilience Plan (NRRP), Mission 4 Component 2 Investment 1.5 - Call for tender No.3277 published on December 30, 2021 by the Italian Ministry of University and Research (MUR) funded by the European Union – NextGenerationEU. Project Code ECS0000038 – Project Title eINS Ecosystem of Innovation for Next Generation Sardinia – CUP F53C22000430001- Grant Assignment Decree No. 1056 adopted on June 23, 2022 by the Italian Ministry of Ministry of University and Research (MUR).

References

[1] A. Dahdouh, Y. Le Brech, I. Khay, A. El Maakoul, and M. Bakhouya, “Hydrothermal liquefaction of Moroccan two-phase olive mill waste (*alperujo*): Parametric study and products characterizations,” *Industrial Crops and Products*, vol. 205, p. 117519, Dec. 2023, doi: 10.1016/j.indcrop.2023.117519.

[2] J. A. Libra *et al.*, “Hydrothermal carbonization of biomass residuals: a comparative review of the chemistry, processes and applications of wet and dry pyrolysis,” *Biofuels*, vol. 2, no. 1, pp. 71–106, Jan. 2011, doi: 10.4155/bfs.10.81.

[3] A. Plaisant, A. Orsini, and R. Cara, “Caratterizzazione sistemi di campionamento e analisi a supporto delle attività di impianto,” p. 49, Sep. 2012.

[4] M. Langone, G. Sabia, L. Petta, L. Zanetti, P. Leoni, and D. Basso, “Evaluation of the aerobic biodegradability of process water produced by hydrothermal carbonization and inhibition effects on the heterotrophic biomass of an activated sludge system,” *Journal of Environmental Management*, vol. 299, p. 113561, Dec. 2021, doi: 10.1016/j.jenvman.2021.113561.

[5] G. Farru *et al.*, “Hydrothermal carbonization of hemp digestate: influence of operating parameters,” *Biomass Conv. Bioref.*, May 2022, doi: 10.1007/s13399-022-02831-4.

[6] G. Farru, C. H. Dang, M. Schultze, J. Kern, G. Cappai, and J. A. Libra, “Benefits and Limitations of Using Hydrochars from Organic Residues as Replacement for Peat on Growing Media,” *Horticulturae*, vol. 8, p. 325, 2022, doi: https://doi.org/10.3390/horticulturae8040325.

Title: Biohydrogen production from organic waste using wine lees as inoculum for the dark fermentation process

Author(s): Francesco Bianco*[1], Marco Race[1]

[1] Department of Civil and Mechanical Engineering, University of Cassino and Southern Lazio, Via Di Biasio 43, Cassino, 03043, Italy
** Email address (francesco.bianco@unicas.it)*

Keyword(s): Organic waste; Wine lees; Dark Fermentation; Biohydrogen; Volatile fatty acids.

Abstract

The depletion of fossil fuel resources and their negative environmental impact have led to increased interest in hydrogen as a promising energy source. However, currently, 96% of hydrogen production comes from non-renewable sources, making it an unsustainable and not eco-friendly energy source [1]. The Dark Fermentation process is a sustainable method to produce hydrogen that offers significant advantages over other production technologies. It is characterized by low energy consumption and effective management of organic waste. The yield of hydrogen production depends on the operational conditions of this process, such as the type of substrate, inoculum, organic load variation, and pH variation [2]. However, some national regulations do not allow the use of conventional inocula, such as sewage sludge, as it can be identified as waste. Also, such inoculum requires pre-treatment processes to select useful microorganisms for dark fermentation, thus increasing management costs [3].
The objective of this experimental study is to develop a Dark Fermentation process using the metabolic process of microorganisms contained in wine lees as an inoculum. The use of wine lees aims to introduce an already active and selected microbial community that inhibits the growth of methanogenic bacteria, thus reducing pre-treatment costs. Anaerobic digestion was subsequently applied downstream of the dark fermentation process to produce biomethane, which further increased the energy recovery and reduced the concentration of volatile fatty acids (VFAs) in the effluent before discharge into the receiving body [4].
The experimental activity was carried out for a total of 145 days, during which two phases of the described biological process took place. The different substrates analyzed in this study were collected from various agri-food industries located in the Campania region. These substrates were no longer suitable for commercialization due to obvious signs of deterioration. The following substrates were used in the experimental phases: *a*) Red tomatoes (PR); *b*) Green tomatoes (PV); *c*) Bell peppers (P); *d*) Green beans (F); *e*) Zucchini (Z); *f*) Peas (PI); *g*) Eggplants (M). The biochemical hydrogen production (BHP) tests were conducted to evaluate the biohydrogen production from individual substrates. Batch cultivation was deemed the most suitable mode and was used in the laboratories for preliminary investigations into optimal conditions for dark fermentation. These reactors allow easy control of process parameters such as temperature, pH, and other fermentation parameters. The experimental phases were carried out using hermetically sealed glass serum bottles. The reactors were prepared in triplicate in 250 mL bottles with a final working volume of 150 mL. The inoculum and substrate concentrations were implemented appropriately correlated in terms of grams of volatile solids (VS): *Phase 1*) during the dark fermentation, the reactors were fed with a 1:1 inoculum/substrate ratio; *Phase 2*) for the anaerobic digestion, the reactors were fed with an inoculum/substrate ratio of 2:1 [5]. In each experimental phase,

biogas production was measured using a blank control consisting solely of inoculum. The bottles were manually agitated at the beginning of the test and during each daily measurement of biogas production until a stationary phase was reached in the cumulative biogas production curve. The volume of biogas produced was measured using the liquid displacement method [6]. Additionally, the composition of the biogas was determined by collecting biogas from each bottle and analyzing it to determine the percentage content of H_2, CH_4, and CO_2 using a Varian-Agilent 3400 GC-TCD gas chromatograph equipped with a Restek Packed column, using argon as the carrier gas [7]. Periodic sampling was conducted to determine the concentration of VFAs. The analyses were performed using high-performance liquid chromatography (HPLC) with an LC-20AD instrument (Shimadzu, Japan) equipped with a Rezex ROA- Organic Acid H+ column (Phenomenex, USA) [7].

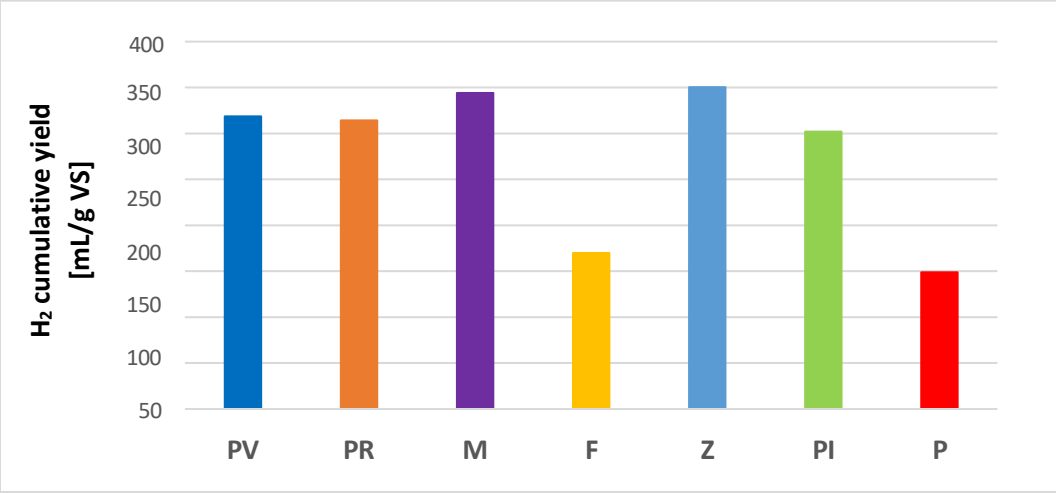

Figure 1. Cumulative biohydrogen yield for each organic substrate.

Based on the results obtained (as shown in Fig. 1), it can be observed that green tomatoes, red tomatoes, eggplants, and zucchinis produced almost similar yields, with a maximum production of 319 mL/g VS, 314 mL/g VS, 344 mL/g VS, and 350 mL/g VS, respectively. Lower yields were recorded for bell peppers (i.e., 149 mL/g VS), which were only included in the second experimental phase, and green beans, which had a maximum yield of 170 mL/g VS. If we compare the results of this study with the BHP of similar substrates reported in the scientific literature [8], it clearly emerges that the hydrogen yields in the BHP tests conducted in this study were significantly higher ($p < 0.05$). The production of H_2 is influenced by the carbohydrate content and biodegradability of the substrate. The type of substrate used, and microbial metabolism also affect the fermentation pathways and final biohydrogen yields. Waste products such as food scraps, vegetables, or kitchen waste, which have a high carbohydrate content, are likely to produce larger amounts of H_2. In contrast, waste products that have a higher protein content, such as slaughterhouse waste which contains high amounts of cellulose, hemicellulose, and total lignocellulosic material, and nitrogen (48% of total solids), tend to exhibit slower degradation rates [9].

Table 1. Final biogas constituents [%].

Experimental conditions	H_2 [%]	CO_2 [%]
PR	84.29	15.71
PV	86.55	13.45
F	83.05	16.95
Z	83.26	16.74
PI	82.81	17.19
M	77.84	22.16
P	8.06	91.94

According to the analysis of biogas constituents in Phase I, it was observed that there was a higher production of hydrogen, while CO_2 production decreased (as shown in Table 1). This resulted in a lower volumetric concentration of CO_2, which in turn led to an increased concentration of other combustible components like hydrogen, ultimately improving the calorific value of the biogas. These benefits not only make biogas more sustainable as an energy source but also contribute to its increased competitiveness and efficiency by reducing purification costs. During anaerobic fermentation, volatile fatty acids (VFA) are produced along with other byproducts such as alcohols and reduced end products like ethanol, butanol, and lactate [10]. These end products contain hydrogen atoms that are not released as gas and, as a result, reduce the H2 yield. Acetic acid, butyric acid, and propionic acid were the fatty acids that showed the highest accumulation in this phase, while smaller amounts of isobutyric acid and valeric acid were also observed. This information confirms the findings of previous studies conducted with mixed cultures, which indicated that these metabolic pathways predominantly involve routes that include acetate and/or butyrate [11].

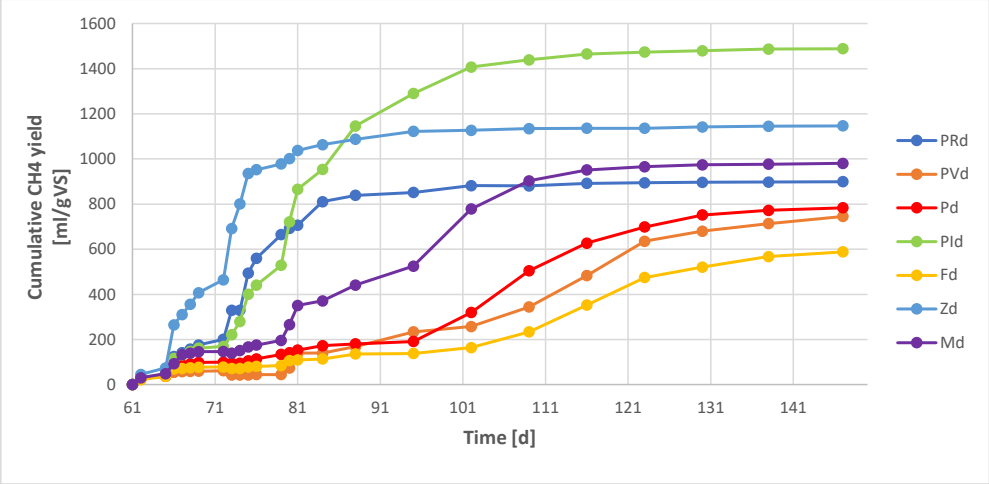

Figure 2. Cumulative biomethane yield for each experimental condition.

As shown in the graph (Fig. 2), the methanogenesis phase was initiated by raising the pH to values close to pH 8 from day 61 onwards. The graph shows that during the first four days of adaptation, there was limited biogas production. However, from day 65 onwards, a significant increase in methane production was observed, particularly for the zucchini waste substrate, with a yield of 1147 mL CH4/g VS. Peas, on the other hand, achieved the highest yield of 1489 mL CH4/g VS, but only after a total

process duration of 145 days. This can be attributed to a different VFA accumulation among the experimental conditions investigated.
In conclusion, this study shows that biohydrogen can be produced by employing wine lees without any pretreatment. Future research on this topic must focus on integrating aspects related to continuous plant processes and managing the significant variability and seasonal availability of substrates. This variability is closely tied to the fluctuations in waste mass throughout the year, and it plays an essential role in maintaining process stability. It's important to note that different substrates can vary significantly between seasons and among companies, each having different quantities and types of materials available to them. Therefore, developing a predictive tool capable of estimating the range within which different substrates can be blended to maintain optimal or sub-optimal hydrogen production based on specific needs and availabilities would significantly help in the efficient management of processes of this kind.

References

[1] S. Sharma, S. Agarwal, A. Jain, Significance of Hydrogen as Economic and Environmentally Friendly Fuel, Energies. 14 (2021) 7389. https://doi.org/10.3390/en14217389.
[2] L. Sillero, W.G. Sganzerla, T. Forster-Carneiro, R. Solera, M. Perez, A bibliometric analysis of the hydrogen production from dark fermentation, Int. J. Hydrogen Energy. 47 (2022) 27397–27420. https://doi.org/10.1016/j.ijhydene.2022.06.083.
[3] J.F. Soares, T.C. Confortin, I. Todero, F.D. Mayer, M.A. Mazutti, Dark fermentative biohydrogen production from lignocellulosic biomass: Technological challenges and future prospects, Renew. Sustain. Energy Rev. 117 (2020) 109484. https://doi.org/10.1016/j.rser.2019.109484.
[4] O. García-Depraect, R. Muñoz, J.B. van Lier, E.R. Rene, V.F. Diaz-Cruces, E. León-Becerril, Three-stage process for tequila vinasse valorization through sequential lactate, biohydrogen and methane production, Bioresour. Technol. (2020). https://doi.org/10.1016/j.biortech.2020.123160.
[5] C. Holliger, M. Alves, D. Andrade, I. Angelidaki, S. Astals, U. Baier, C. Bougrier, P. Buffière, M. Carballa, V. de Wilde, F. Ebertseder, B. Fernández, E. Ficara, I. Fotidis, J.-C. Frigon, H.F. de Laclos, D.S.M. Ghasimi, G. Hack, M. Hartel, J. Heerenklage, I.S. Horvath, P. Jenicek, K. Koch, J. Krautwald, J. Lizasoain, J. Liu, L. Mosberger, M. Nistor, H. Oechsner, J.V. Oliveira, M. Paterson, A. Pauss, S. Pommier, I. Porqueddu, F. Raposo, T. Ribeiro, F. Rüsch Pfund, S. Strömberg, M. Torrijos, M. van Eekert, J. van Lier, H. Wedwitschka, I. Wierinck, Towards a standardization of biomethane potential tests, Water Sci. Technol. 74 (2016) 2515–2522. https://doi.org/10.2166/wst.2016.336.
[6] F. Bianco, H. Şenol, S. Papirio, H. Zenk, A. Kara, S. Atasoy, Combined ultrasonic–hydrothermal pretreatment to improve the biomethane potential of hazelnut shell, Biomass and Bioenergy. 165 (2022) 106554. https://doi.org/10.1016/j.biombioe.2022.106554.
[7] F. Bianco, M. Race, S. Papirio, G. Esposito, Removal of polycyclic aromatic hydrocarbons during anaerobic biostimulation of marine sediments, Sci. Total Environ. 709 (2020) 136141. https://doi.org/10.1016/j.scitotenv.2019.136141.
[8] A. Ghimire, L. Frunzo, F. Pirozzi, E. Trably, R. Escudie, P.N.L. Lens, G. Esposito, A review on dark fermentative biohydrogen production from organic biomass: Process parameters and use of by-products, Appl. Energy. 144 (2015) 73–95. https://doi.org/10.1016/j.apenergy.2015.01.045.
[9] M. Karrabi, F.M. Ranjbar, B. Shahnavaz, S. Seyedi, A comprehensive review on biogas production from lignocellulosic wastes through anaerobic digestion: An insight into performance improvement strategies, Fuel. 340 (2023) 127239. https://doi.org/10.1016/j.fuel.2022.127239.
[10] M. Worwag, A. Kwarciak-Kozłowska, Volatile fatty acid (VFA) yield from sludge anaerobic fermentation through a biotechnological approach, in: Ind. Munic. Sludge, Elsevier, 2019: pp. 681–703. https://doi.org/10.1016/B978-0-12-815907-1.00029-5.
[11] R.A. Gonzalez-Garcia, R. Aispuro-Castro, E. Salgado-Manjarrez, J. Aranda-Barradas, E.I. Garcia-Peña, Metabolic pathway and flux analysis of H2 production by an anaerobic mixed culture, Int. J. Hydrogen Energy. 42 (2017) 4069–4082. https://doi.org/10.1016/j.ijhydene.2017.01.043.

Title: Biohydrogen production from Municipal Solid Waste (MSW): paving the way for a sustainable future according to the circular economy and energy transition

Author(s): Fabiana Romano*[1,2], Vincenzo Naddeo[1], Vincenzo Belgiorno[1], Octavio García-Depraect[2], Raúl Muñoz[2], Tiziano Zarra[1].

[1] *Sanitary Environmental Engineering Division (SEED), Department of Civil Engineering, University of Salerno, Italy*
[2] *Institute of Sustainable Processes, University of Valladolid, Dr. Mergelina, s/n, 47011 Valladolid, Spain*

Keyword(s): hydrogen production pathways, biological processes, food waste, biohydrogen, circular economy

Abstract

Hydrogen is one of the key resources for the energy transition with a view to mitigating climate change. It has emerged as a promising alternative energy carrier due to its high energy density and potential for clean production. Among various pathways for hydrogen production, such as physical, chemical and biological processes, biohydrogen generation by using food waste has garnered significant attention owing to its environmental sustainability and ability to utilize organic waste as a feedstock. The research presents an overview of the main processes for hydrogen production with specific attention on biological processes, because of their potential to promote climate changes reductions. The use of waste materials, such as municipal solid waste (MSW), is also presented, as sustainable option from the perspective of applying the circular economy approach. Food Waste (FW), as part of MSW, is highlighted as suitable feedstock for the production of high-value products via fermentation owing to its high energy content and carbon density. Dark Fermentation (DF) as biological process is underlined allowing the valorization of FW not only through the production of renewable hydrogen but also of carboxylic acids that can be further used to produce other high added value products. In this context, the production of medium-chain carboxylic acids (MCCAs) opens new routes for FW valorization into green chemicals. A case study is presented with reference to the production of biohydrogen through dark fermentation, focusing on its efficiency, feasibility, and environmental implications. Key factors influencing biohydrogen production are reported. The challenges and opportunities associated with scaling up biohydrogen production systems for industrial applications are mentioned. The research aims to contribute to the comprehensive understanding of biohydrogen generation and to offer valuable guidance for advancing sustainable hydrogen production technologies.

1. Introduction

Hydrogen (H_2), as an energy carrier, is recognised as one of the main solutions for achieving climate neutrality [1, 2]. The first element in the periodic table and the most abundant in the universe, H_2 is present, combined with other elements, in compounds such as water or mineral substances, hydrocarbons and biological molecules. In addition to forming about 75% of matter, it is the primary ingredient of the sun, of which it makes up about 90%. H_2 is a light, storable and efficient fuel, and above all it can be used without producing direct emissions of greenhouse gases (GHG) [3]. H_2 is only found in nature bound to other molecules, and current techniques to extract and isolate it require enormous amounts of energy [4]. Overall, hydrogen production processes fall into three macro-categories: physical, chemical and biological [5]. Physical processes concern the possible changes to which a substance can be subjected without changing its constitution or properties. These can be changes in

terms of state, volume, shape or motion during movement. While chemical processes, which, as their name suggests, make use of chemical substances to produce H_2. Finally, biological processes allow hydrogen to be produced using microorganisms, such as algae or bacteria [6]. Currently, the main hydrogen production technologies include gasification, steam reforming, steam reforming with carbon dioxide capture, pyrolysis, and electrolysis [7]. Depending on the energy source from which it is obtained, and the production process employed, hydrogen is classified using different colour conventions [8]. One of the most popular colour scales is the one that adopts a 7-colour grouping (Figure 1): grey, brown, blue, yellow, violet, turquoise and green.

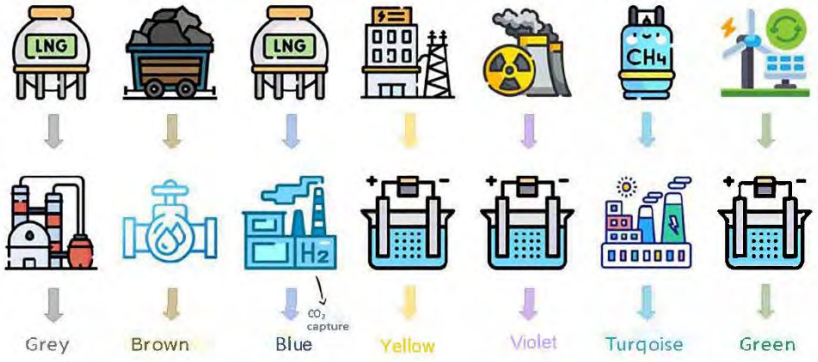

Figure 1. Hydrogen 7-colour classification

There are many processes for producing H_2 from renewable sources [9]. Some technologies are based on biomass, along with water splitting approaches. In the face of escalating environmental concerns and energy demands, the search for sustainable and renewable energy sources has intensified. BioH_2, generated through biological processes, emerges as a promising candidate owing to its high energy content, carbon neutrality, and minimal environmental impact [10]. BioH_2 can be produced through various biological pathways, including dark fermentation, photofermentation, and microbial electrolysis. DF involves the anaerobic breakdown of organic substrates by bacteria such as Clostridium spp., yielding H_2, CO_2, and VFAs. BioH_2 production through dark fermentation offers a promising avenue for sustainable energy generation, utilizing organic substrates such as food waste to produce H_2 gas.

2. Lactate Driven Dark Fermentation on Food Waste for biohydrogen production

The research presents the investigation of the feasibility of employing Lactate Driven Dark Fermentation (LD-DF) on restaurant food waste to yield bioH_2. In order to assess the efficacy of the proposed approach for bioH_2 production, intensive experimental activities were conducted in a continuous mode.

2.1. Material and methods

46-days tests were conducted to evaluate continuous hydrogen production. Daily measure of the liquid and gas phase were conducted during the experiment, to analyse respectively the liquid and gas composition. Following batch activation, the inoculum was transferred to a fermentation setup equipped with a stirred-tank bioreactor. The reactor was operated under anaerobic conditions with controlled temperature and pH to facilitate optimal microbial activity. The FW slurry, supplemented with lactate as a readily fermentable substrate, served as the feedstock for continuous fermentation. Periodic feeding of fresh food waste was employed to maintain reactor stability and substrate availability. Simulated FW was used as a model substrate following the recipe reported by Neves et al. [11] to mimic restaurant FW. This FW was based on a grinded mixture of potato flakes (78%), chicken breast (14%), white cabbage (4%) and pork lard (4% w/w), as a source of carbohydrates, proteins, and lipids, respectively. A batch experiment was performed in a 1 L stirred tank reactor with a working volume of 0.8 L. The LD-DF of FW was carried out at 37°C under magnetic stirring at ≈ 180 rpm. The fermentation was conducted

with a cultivation broth initially composed of 720 mL synthetic FW (previously minced with a blender), and inoculum at 10 % (v/v) with a Volatile Suspended Solids (VSS) concentration of 0.43 ± 0.01 g/L. The hydrogenogenic inoculum was preincubated overnight at 37°C using lactose as the sole carbon source at a concentration of 10 g/L in 2 L gas-tight glass flasks with 0.9 L of mineral salt medium (the pre-inoculum size was 10 % v/v). During the experiment, the TS content was fixed at 5 % and the influence of pH on the LD-DF of FW was investigated by automatically controlling it at 7.0, 6.5, and 6.0. Several Hydraulic Retention Times, HRT, that exerted a significant effect on process performance, were tested to find the one that better promotes biohydrogen production. The performance of the process was measured based on the rates and yields of hydrogen production, VS removal efficiency and organic acids profile. HRTs of 24-, 20-, 16-, 12-h were investigated.

2.2. Analytical methods

Gas composition (i.e., H_2, CO_2 and CH_4) was measured by gas chromatography using a Varian CP-3800 gas chromatograph (GC) coupled with a Thermal Conductivity Detector (TCD) and equipped with a Varian CP-Molsieve 5A capillary column (15 m × 0.53 mm × 15 µm) interconnected with a Varian CP-PoreBOND Q capillary column (25 m × 0.53 mm × 10 µm), using helium as the carrier gas, according to Alcantara et al. [12]. Organic acids (i.e., lactic acid, acetic acid, formic acid, propionic acid, butyric acid, isobutyric acid, valeric acid, isovaleric acid, caproic acid, isocaproic acid, and heptanoic acid) were measured by High-Performance Liquid Chromatography (HPLC) using a Alliance HPLC system (model e2695, USA) equipped with an ultraviolet (UV) detector (214 nm) and an Aminex chromatographic column kept at 75°C (HPX-87H, Bio Rad, USA), preceded by a Micro-Guard Cation H^+ refill cartridge of 30 × 4.6 mm (Bio Rad, USA) as a pre-column. Sulfuric acid 25 mM was used as the eluent at a flow rate of 0.7 mL/min.

2.3. Results and discussion

Figure 2 highlights VFAs (2a) and the hydrogen production rate (HPR) (2b), measured during the investigated fermentation process overall the experimental analysis conducted.

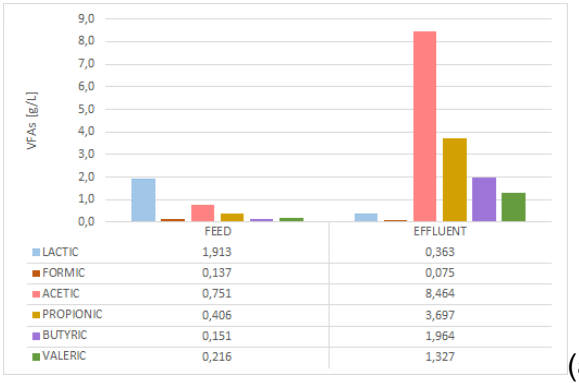

(a)

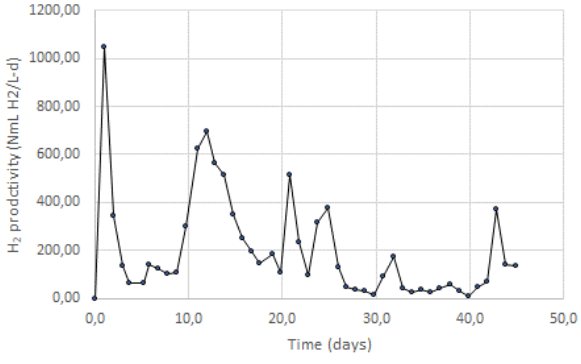

(b)

Figure 2. (a) VFAs comparing feeding and effluent phase
(b) hydrogen production rate (HPR)

Results show how the recorded HPR peaked at the beginning of the operation at 1046.8 mL H_2/L-d before decreasing to 62.16 mL H_2/L-d (Fig. 2b). This behaviour of HPR is typically observed in healthy DF systems and tends to occur because the kinetics of hydrogen production are promoted in a discontinuous manner [13] reason why the trend describing hydrogen production is erratic. The profile

of carboxylic acids showed well-defined trends throughout the experiment. Lactose is consumed in order to promote the production of acetic, butyric, propionic and valeric acids, a signal that attests to the promotion of the acidogenic phase (Fig. 2a), in which H_2 is produced during the fermentation process.

3. Conclusion

H_2, generated through biological processes, emerges as a promising alternative and sustainable energy carrier, thanks to its high carbon neutrality and reduced environmental pressures. The production of biohydrogen from a LD-DF process is presented. High potential for co-producing H_2 and organic acids including MCCAs from FW is proven. Operating parameters such as pH, HRT and TS% have a great influence on H_2 production by the DF process. Optimizing the behaviour among the above 3 parameters is fundamental to increase bioH_2 production and carboxylic acids profile. Lactate consumption, followed by the production of MCCAs, has been identified as the main pathway for H_2 production.

References

[1] Ivanenko, A. A., Laikova, A. A., Zhuravleva, E. A., Shekhurdina, S. V., Vishnyakova, A. V., Kovalev, A. A., Kovalev, D. A., Trchounian, K. A., & Litti, Y. V. Biological production of hydrogen: From basic principles to the latest advances in process improvement. *International Journal of Hydrogen Energy*, *55*, 740–755, (2024).
[2] Ballesteros, F. C., Li, C.-W., Hasan, S. W., Belgiorno, V., & Naddeo, V. Advances in technological control of greenhouse gas emissions from wastewater in the context of circular economy. Science of The Total Environment, 792, 148479 2021).
[3] Pasquarelli, F., Oliva, G., Mariniello, A., Buonerba, A., Li, C.-W., Belgiorno, V., Naddeo, V., & Zarra, T. Carbon neutrality in wastewater treatment plants: An integrated biotechnological-based solution for nutrients recovery, odour abatement and CO2 conversion in alternative energy drivers. Chemosphere, 354, 141700 (2024).
[4] Ramprakash, B., Lindblad, P., Eaton-Rye, J. J., & Incharoensakdi, A. Current strategies and future perspectives in biological hydrogen production: A review. *Renewable and Sustainable Energy Reviews*, *168*, 112773 (2022).
[5] Hassan, Q., Abdulateef, A. M., Hafedh, S. A., Al-samari, A., Abdulateef, J., Sameen, A. Z., Salman, H. M., Al-Jiboory, A. K., Wieteska, S., & Jaszczur, M. Renewable energy-to-green hydrogen: A review of main resources routes, processes and evaluation. *International Journal of Hydrogen Energy*, *48*(46), 17383–17408, (2023).
[6] Oliva, G., Buonerba, A., Grassi, A., Hasan, S. W., Korshin, G. V., Zorpas, A. A., Belgiorno, V., Naddeo, V., & Zarra, T. Microalgae to biodiesel: A novel green conversion method for high-quality lipids recovery and in-situ transesterification to fatty acid methyl esters. Journal of Environmental Management, 357, 120830 (2024).
[7] da Silva Veras, T., Mozer, T. S., da Costa Rubim Messeder dos Santos, D., & da Silva César, A. Hydrogen: Trends, production and characterization of the main process worldwide. *International Journal of Hydrogen Energy*, *42*(4), 2018–2033 (2017).
[8] Incer-Valverde, J., Korayem, A., Tsatsaronis, G., & Morosuk, T. “Colors” of hydrogen: Definitions and carbon intensity. Energy Conversion and Management, 291, 117294 (2023).
[9] Matamba, T., Tahmasebi, A., Yu, J., Keshavarz, A., Abid, H. R., & Iglauer, S. A review on biomass as a substitute energy source: Polygeneration influence and hydrogen rich gas formation via pyrolysis. *Journal of Analytical and Applied Pyrolysis*, *175*, 106221 (2023).
[10] Ananthi, V., Bora, A., Ramesh, U., Yuvakkumar, R., Raja, K., Ponnuchamy, K., Muthusamy, G., & Arun, A. A review on the technologies for sustainable biohydrogen production. Process Safety and Environmental Protection, 186, 944–956 (2024).
[11] Neves, L., Gonçalo, E., Oliveira, R., & Alves, M. M. Influence of composition on the biomethanation potential of restaurant waste at mesophilic temperatures. *Waste Management*, *28*(6), 965–972 (2008).
[12] Alcántara, C., Fernández, C., García-Encina, P. A., & Muñoz, R. Mixotrophic metabolism of Chlorella sorokiniana and algal-bacterial consortia under extended dark-light periods and nutrient starvation. *Applied Microbiology and Biotechnology*, *99*(5), 2393–2404 (2015).
[13] Regueira-Marcos, L., García-Depraect, O., & Muñoz, R. Elucidating the role of pH and total solids content in the co-production of biohydrogen and carboxylic acids from food waste via lactate-driven dark fermentation. Fuel, 338, 127238 (2023).

PARALLEL SESSION: A2

Wastewater treatment

Wastewater reuse

Title: Interdisciplinary assessment for crops irrigation with reclaimed wastewater

Authors: Francesca Mangiagli*[1], Camilla Di Marcantonio[1], Margherita Barchiesi[1], Andrea Martelli[2], Filiberto Altobelli[2], Eduardo Di Marcantonio[3], Massimo Marchiesi[3], Luigi Dallai[3], Simona Bongirolami[4], Jessica Bartolucci[4], Roberto Romano[4], Agostina Chiavola[1], Maria Rosaria Boni[1]

[1] *Sapienza University of Rome, Department of Civil, Building and Environmental Engineering, Rome, Italy,* francesca.mangiagli@uniroma1.it, camilla.dimarcantonio@uniroma1.it, margherita.barchiesi@uniroma1.it, agostina.chiavola@uniroma1.it, mariarosaria.boni@uniroma1.it

[2] CREA Research Centre for Agricultural Policies and Bioeconomy, Rome, Via Barberini 36, Italy andrea.martelli@crea.gov.it, filiberto.altobelli@crea.gov.it

[3] *Department of the Earth Sciences, Rome, Italy,* eduardo.dimarcantonio@uniroma1.it, massimo.marchiesi@uniroma1.it, luigi.dallai@uniroma1.it

[4] *ACQUA PUBBLICA SABINA S.p.A., Rieti, Italy* s.bongirolami@acquapubblicasabina.it, j.bartolucci@acquapubblicasabina.it

Keywords: Contaminants of Emerging Concern; European Regulation; Uptake; Risk Assessment

Abstract

The pressure on water supply is steadily increasing and the problem of water scarcity is becoming more central and urgent. Treated wastewater, also called reclaimed wastewater (RWW), could replace primary water, especially in agriculture, one of the major source of water consumption worldwide [1], playing a key role in the ecological transition to a circular economy ([2], [3]). In 2023 a new European Regulation for water reuse entered into effect for regulating and promoting RWW reuse, defining the minimum requirements for a safe water reuse in agriculture and introducing a 'fit for purpose' approach based on 'scientific evidence' to establish additional water requirements, especially for contaminants of emerging concern (CECs) [4]. CECs, indeed, could persist even after treatment in wastewater treatment plants (WWTPs) ([5], [6]) potentially leading to their uptake and bioaccumulation by crops when the effluent is reused for irrigation, posing risks to both the environment and human health ([2], [7]).

The aim of this study is to develop an effect-based experimental methodology to evaluate the use of RWW in Lazio region (Italy) applying the EU Regulation 2020/741. A pilot-scale experimental set up was designed, with *Eruca vesicaria* plants (commonly known as Rocket) being irrigated using treated wastewater sourced from a WWTP in central Italy. Both positive and negative effects of wastewater irrigation on crops were evaluated, considering the content of CECs, assessing associated risks, and examining their interactions with crops. This evaluation also made use of an innovative combination of different tools, such as stable isotope tracing, phytotoxicity assessment and chemical data. In the actual absence of official protocols for evaluating the risks to human health and environment (a fundamental aspect of risk management, KRM5) ([8], [9]), a well-established procedure was used to estimate the potential risk to two exposed receptors (adults and children) from consuming edible crops irrigated with RWW [8].

Material and Methods

1. WWTP of study

The WWTP considered in the study is located in Central Italy. The plant has a treatment capacity of 5000 P.E., corresponding to an average flow rate of 1000 m^3/d. It has a conventional activated sludge treatment lay-out, consisting of pre-treatments, anoxic and aerobic tanks, final sedimentation and chlorination; sludge treatment is carried out by thickening. The WWTP was selected being representative of common situations in Italy, where around 40% of the existing WWTPs have a treatment capacity lower than 5000 P.E. [10]. Additionally, it is located in a rural area where the reuse of RWW for crop irrigation can represent a valuable option for the local community. The WTTP will be soon upgraded with an innovative advanced biological treatment. Therefore, it also offers the possibility to test the suitability of the RWW from this system for irrigation.

2. Experimental set-up

The experimental set-up was designed to be agronomically representative and automatable. It is composed by 3 lines with 3 cultivation tanks each (100x120x100 cm): the first line (Test 1) is irrigated with reclaimed water from the existing WWTP; the second line (Test 2) is irrigated with reclaimed water from the new advanced biological treatment; the third line is used as a control and therefore irrigated with tap water. Each cultivation tank was filled with 15 cm of drainage material (gravel) at the bottom and 65 cm of agricultural soil above, with the remaining 20 cm are available for the growth of the chosen crop. The soil was real agricultural soil collected from a farm near the WWTP.

3. Crop selection

The *Eruca vesicaria* (known as Rocket) was selected as the crop for the investigation. The sowing period of this plant is April-May; it produces during the entire summer, ensuring several harvesting cycles. Rocket is also a fourth-range crop, which means that it is a type of cultivation used for preparation of food products, such as fruits and vegetables. For this reason, it has a relevant economic interest. Additionally, since rocket is a leafy vegetable, it is expected to accumulate higher levels of micropollutants as compared to other types of crops, putting under spotlight the evaluation of the effects.

4. Calculation of risk to human health

The risk quotient (RQ) was calculated following the procedure proposed by Prosser and Sibley [8], using the Estimated Daily Intake (EDI) and the Acceptable Daily Intake (ADI), according to the following equation:

$$RQ = \frac{EDI}{ADI} \quad (1)$$

The ADI value was calculated based on the lowest therapeutic dose or the oral reference dose, divided by a safety factor. These values were collected from the World Health Organization and the European Food Safety Authority (not here reported). The EDI value was calculated as a function of several parameters (not here reported), including the concentration of CECs in plant tissue (C_{food}, ng/g dry weight). C_{food} was estimated considering the concentration of contaminants in RWW (C_{RWW}) and the BioConcentration Factor (BCF) as follows:

$$C_{food} = C_{\mathrm{RWW}} \times \mathrm{BFC} \quad (2)$$

Four contamination scenarios were evaluated based on the values of the CECs concentration in RWW (using literature data and the concentration measured in the effluent of the WWTP) and of the BCF: *A) literature average*: average of mean C_{RWW} from literature and average of mean BCFs from literature; *B)*

literature worst: average of the maximum C_{RWW} from literature and maximum of mean BCFs from literature; *C) measured average*: C_{RWW} measured in the WWTP effluent and average of mean BCFs; *D) measured worst:* C_{RWW} in WWTP effluent and maximum of mean BCFs. The final receptors were assumed to be adults (70kg of body weight) and children (15kg body weight).

Preliminary results and discussion

The experimental setup (Figure 1) was designed, built, tested and verified in all its components. Then, the first sowing of rocket was carried out on the 4th April 2024, starting the experiment.

Figure 1 - Experimental setup

1. *Characterization of matrices*

Characterization analyses of the soil and water were conducted by a certified laboratory (Ecopoint Srl). These analyses comprised parameters such as organic carbon content, nitrogen species, phosphorus, and solids. Additionally, the δ15N, as total nitrogen, was determined in water, soil and rocket vegetable tissue samples. Finally, concentrations of four target CECs (Caffeine, Sulfamethoxazole, Carbamazepine and Benzotriazole) were measured in both the influent and effluent of the plant using grab samples, which were then analyzed by a certified laboratory (Ecopoint Srl) utilizing a UHPLC–MS/MS system.

2. *Risk analysis*

Five years (2018-2022) monitoring data of the WWTP's final effluent showed that this can be classified as belonging to Class B, according to Regulation EU 2020/741. This quality classification permits the use of the treated water for irrigating crops intended for raw consumption, provided that the edible portion grows above ground and it is not in direct contact with refined water.

Considering this, a preliminary risk analysis was conducted, taking into account data from both literature sources and the initial characterization of influent and effluent from the WWTP.

From the results of the risk analysis, it emerged that Carbamazepine and Benzotriazole could present the highest risk when the estimate was carried out based on literature data, especially in the worst-case scenario. However, for the measured scenario (real WWTP), the risk exceeds the unacceptable

threshold only for Benzotriazole in the worst-case scenario, particularly when considering children as receptors.

The risk evaluation should be regarded only as a preliminary because of the few data from the real case. Therefore, once the real data will be provided from the experimental activity, the risk analysis can be refined.

Conclusions

The experimental activity is ongoing and the pilot-scale experimental setup is being irrigated periodically with the WWTP effluent. Data from this activity will be used to validate the results obtained from the theoretical risk assessment. Furthermore, they will be combined with the data from the water phytotoxicity tests, CECs uptake assessment and nitrogen stable isotope tracing. This innovative combination of different tools will allow to acquire the full knowledge necessary to assess the feasibility of RWW reuse for irrigation and the specific conditions for its safe application in various scenarios. The first results are expected by the end of June 2024.

References

[1] EEA, 'Water use in Europe — Quantity and quality face big challenges'. Accessed: Jan. 31, 2024. [Online]. Available: https://www.eea.europa.eu/signals-archived/signals-2018-content-list/articles/water-use-in-europe-2014
[2] M. Mainardis *et al.*, 'Wastewater fertigation in agriculture: Issues and opportunities for improved water management and circular economy', *Environ. Pollut.*, vol. 296, no. December 2021, p. 118755, Mar. 2022, doi: 10.1016/j.envpol.2021.118755.
[3] A. Poustie, Y. Yang, P. Verburg, K. Pagilla, and D. Hanigan, 'Reclaimed wastewater as a viable water source for agricultural irrigation: A review of food crop growth inhibition and promotion in the context of environmental change', *Sci. Total Environ.*, vol. 739, p. 139756, Jun. 2020, doi: 10.1016/j.scitotenv.2020.139756.
[4] The European Parliament, 'Regulation (EU) 2020/741 on minimum requirements for water reuse', 2020.
[5] C. Di Marcantonio *et al.*, 'Occurrence, seasonal variations and removal of Organic Micropollutants in 76 Wastewater Treatment Plants', *Process Saf. Environ. Prot.*, vol. 141, pp. 61–72, Sep. 2020, doi: 10.1016/j.psep.2020.05.032.
[6] C. Di Marcantonio *et al.*, 'A step forward on site-specific environmental risk assessment and insight into the main influencing factors of CECs removal from wastewater', *J. Environ. Manage.*, vol. 325, no. PA, p. 116541, 2023, doi: 10.1016/j.jenvman.2022.116541.
[7] R. Delli Compagni *et al.*, 'Risk assessment of contaminants of emerging concern in the context of wastewater reuse for irrigation: An integrated modelling approach', *Chemosphere*, vol. 242, p. 125185, 2020, doi: 10.1016/j.chemosphere.2019.125185.
[8] R. S. Prosser and P. K. Sibley, 'Human health risk assessment of pharmaceuticals and personal care products in plant tissue due to biosolids and manure amendments, and wastewater irrigation', *Environ. Int.*, vol. 75, pp. 223–233, 2015, doi: 10.1016/j.envint.2014.11.020.
[9] Joint Research Centre (European Commission), R. Maffettone, and B. M. Gawlik, *Technical guidance water reuse risk management for agricultural irrigation schemes in Europe*. Publications Office of the European Union, 2022. Accessed: Apr. 17, 2024. [Online]. Available: https://data.europa.eu/doi/10.2760/590804
[10] 'Waterbase - UWWTD: Urban Waste Water Treatment Directive – reported data', EEA geospatial data catalogue. Accessed: Apr. 17, 2024. [Online]. Available: https://sdi.eea.europa.eu/catalogue/srv/api/records/6244937d-1c2c-47f5-bdf1-33ca01ff1715

Title: **Development of innovative multifunctional filters for pre- and post- irrigation water treatment.**

Author(s): S. Filice[1*], V. Scuderi[1], E.L. Sciuto[2], R. A. Farina[1], S. Libertino[1], M.A. Coniglio[3] and S. Scalese[1]

[1] Consiglio Nazionale delle Ricerche, Istituto per la Microelettronica e Microsistemi (CNR-IMM), Ottava Strada n.5, 95121 Catania, Italy
[2] Dipartimento di Scienze Chimiche, Biologiche, Farmaceutiche e Ambientali, Università di Messina, V.le Stagno d'Alcontres, 31, 98166 Messina - Italy
[3]Department of Medical and Surgical Sciences and Advanced Technologies "G.F. Ingrassia", University of Catania, Via Sofia 87, 95123 Catania, Italy

Keyword(s):
Nexar, sulfonated copolymer, water, coating, filtration, adsorption, antibiofouling

Abstract

Agricultural water consumption is expected to increase in the next future to accommodate population growth and a larger number of food varieties, but freshwater sources are limited and unsustainable to meet the increasing water demand [1]. New alternative water sources are needed and one solution could be the use of appropriately treated municipal wastewater, brackish water, seawater. In the present work, we show the possibility of obtaining irrigation water by (i) purification of dirty water by adsorption, photocatalysis and filtration and (ii) by the reduction of salinity of seawater.

For this purpose, a sulfonated pentablock copolymer (s-PBC, commercially named Nexar™) was investigated as innovative multifunctional coating for improving the performance of commercial water filters towards different kinds of contaminants [2]. Innovative multifunctional coatings represent an emerging appealing technology aiming to improve the performance of commercial filters [1] for water purification. The filtration technology is very easy and straightforward to use, it is cost effective since it does not require high maintenance costs and it does not affect the odor and taste of the water with respect to other purification technologies, such as adsorption and photocatalysis, and does not introduce nanoparticles (NP) in water, avoiding the issue of NP safe recovery [2]. In particular, Figure 1 shows polypropylene commercial filters coated by s-PBC solution in polar solvent by solvent casting. Furthermore, graphene oxide (GO) flakes were added to casting solution in order to increase the active sites for contaminants adsorption/filtration. Indeed, GO is formed by oxidation of graphite resulting in the introduction of oxygen functional groups on graphene planes. representing not only active sites for contaminants removal but also showing antimicrobial properties [3].

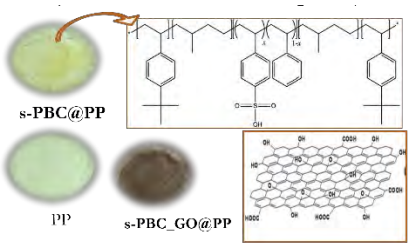

Figure 1. Photos of initial PP filter and after coating with polymeric solutions named s-PBC@PP and s-PBC_GO@PP. The structures of s-PBC and GO are reported in the schemes.

The first effect of coating the initial PP filter with s-PBC is the formation of a hydrophilic surface (PP is, instead, hydrophobic), as also demonstrated by the increasing of water uptake. This is a fundamental parameter for the application of these materials in water purification field. Measured values are reported in Table 1.

Table 1. Water Uptake WU(%) = $[(m_{wet} – m_{dry})/m_{dry}] * 100$

Material	WU (%)
PP	3
s-PBC@PP	160
s- PBC_GO@PP	230

Chemical composition of coating layers and their morphologies were characterized by IR and SEM analysis, respectively, and these are reported in Figure 2. No chemical modifications of polymer composition was induced by the preparation procedure and the PP filter (that is formed by fibers) was completely coated by the polymeric layer.

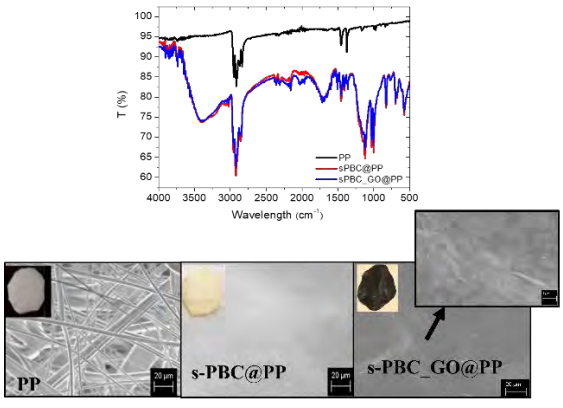

Figure 2. IR spectra (on the top) and SEM images (on the bottom) of PP filters before and after being coated with S-PBC and s-PBC_GO solutions [6].

We will provide an overview of s-PBC coated filters potentialities for the selective removal of cationic/anionic organic molecules (Methylene Blue and Methyl Orange, respectively) and bacteria such as *Pseudomonas aeruginosa* and *L. pneumophila*. Figure 3 reports the UV-Vis absorbance spectra of dyes solution before and after the filtration process and the zone of inhibition tests of coated and uncoated filters against two different bacteria.

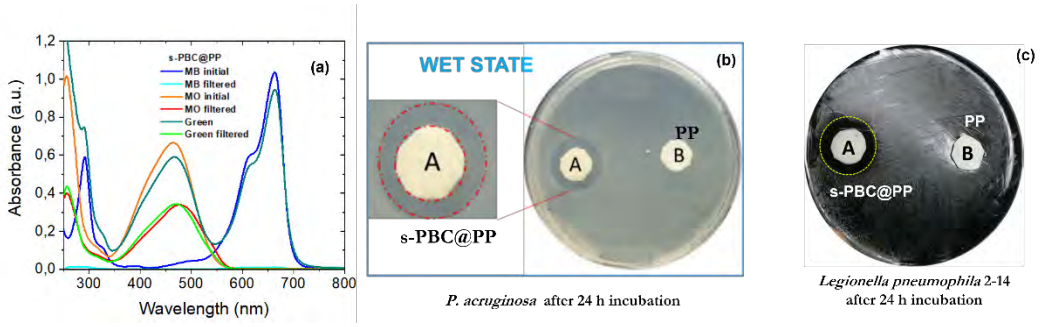

Figure 3 (a) UV-Vis absorbance spectra of dyes solution before and after the filtration process with uncoated and coated PP filters and the zone of inhibition tests for the same materials against *Pseudomonas* (b) and *Legionella* (c) bacteria.

The coated filters showed selectivity for the removal of cationic species and the coating layer acts as antimicrobic and antibiofouling surface [2,4-6]. Considering their selectivity for cationic species, the same filters were tested for the removal of metal ions (e.g. Co^{2+} and Fe^{3+} ions). The dispersion of GO flakes into s-PBC polymeric layer shows an evident effect only on the adsorption of Co^{2+} ions according to the different affinity of cations and polymeric nanocomposites. Furthermore, we report a study on the modification of s-PBC and s-PBC_GO coating by UV treatment to further improve its removal efficiencies of cobalt and iron ions in filtration/adsorption processes [6]. The UV irradiation of coating surface increases its hydrophilicity (-15%), however modifies its interaction with Co^{2+} ions suggesting the formation of oxysulfur radicals. These species could find application in photocatalytic degradation processes.

Preliminary results on s-PBC removal activity of other typical pollutants in agriculture, such as pesticides, will be also shown.

[1] Edirisooriya, E.; Wang, H.; Banerjee, S.; Longley, K.; Wright, W.; Mizuno, W.; Xu, P.cEconomic feasibility of developing alternative water supplies for agricultural irrigation,c*Current Opinion in Chemical Engineering*, **2024**, 43, 100987.

[2] Filice, S.; Scuderi, V.; Libertino, S.; Zimbone, M.; Galati, C.; Spinella, N.; Gradon, L.; Falqui, L.; Scalese, S. Sulfonated Pentablock Copolymer Coating of Polypropylene Filters for Dye and Metal Ions Effective Removal by Integrated Adsorption and Filtration Process. *Int. J. Mol. Sci.* **2022**, *23*, 11777.

[3] Buccheri, M.A., D'Angelo, D., Scalese, S., Spanò, S.F., Filice, S., Fazio, E., Compagnini, G., Zimbone, M., Brundo, M. V., Pecoraro, R., Alba, A., Sinatra, F., Rappazzo, G., Privitera, V. Modification of graphene oxide by laser irradiation: a new route to enhance antibacterial activity. *Nanotechnology* **2016**, 27, 245704 – 245716.

[4] Sciuto, E.L.; Filice, S.; Coniglio, M.A.; Faro, G.; Gradon, L.; Galati, C.; Spinella, N.; Libertino, S.; Scalese, S. Antimicrobial s-PBC Coatings for Innovative Multifunctional Water Filters. *Molecules* **2020**, *25*, 5196.

[5] Filice, S.; Sciuto, E.L.; Scalese, S.; Faro, G.; Libertino, S.; Corso, D.; Timpanaro, R.M.; Laganà, P.; Coniglio, M.A. Innovative Antibiofilm Smart Surface against Legionella for Water Systems. *Microorganisms* **2022**, *10*, 870.

[6] Filice, S.; Scuderi, V.; Zimbone, M.; Libertino, S.; La Piana, L.; Farina, R.; Scalese, S. Sulfonated pentablock copolymer with graphene oxide for Co2+ ions removal: efficiency, interaction mechanisms and secondary reaction products. *Coatings* **2023**, *13*(10), 1715.

Risk assessment in the case of reuse of reclaimed water – A proposed methodology

Author(s): Paola Verlicchi[1]*, Vittoria Grillini[1], Vítor Vilar[2,3], M. Pilar Castro[4], Cristina Sáez[4], Manuel A. Rodrigo[4] Pawel Krzeminski[5]

[1] *Department of Engineering, University of Ferrara, Via Saragat 1, 44122, Ferrara, Italy*
paola.verlicchi@unife.it, vittoria.grillini@unife.it
[2] *LSRE-LCM – Laboratory of Separation and Reaction Engineering – Laboratory of Catalysis and Materials, Faculty of Engineering, University of Porto, Rua Dr. Roberto Frias, 4200-465 Porto, Portugal*
[3] *ALiCE – Associate Laboratory in Chemical Engineering, Faculty of Engineering, University of Porto, Rua Dr. Roberto Frias, 4200-465 Porto, Portugal*
vilar@fe.up.pt
[4] *Department of Chemical Engineering. Faculty of Chemical Sciences &Technologies. University of Castilla-La Mancha, Campus Universitario s/n, 13071 Ciudad Real, Spain.*
[5] *Norwegian Institute for Water Research (NIVA), Urban Environments and Infrastructure Section, Økernveien 94, N-0579, Oslo, Norway*

Keyword(s): emerging contaminants, FMEA, reclamation facility, risk assessment, risk management plan, water reuse.

Introduction –
The reuse of reclaimed water from urban wastewater treatment plants (WWTPs) might be a valid solution to address water scarcity due to increasing droughts and to reduce the pressure on water bodies. European Regulation [1] and national ones, as discussed in [2], support the reuse of reclaimed water for agricultural irrigation as it is a precious alternative water source. The main reasons limiting this practice are the high investment and operation costs and the public concerns related to potential human and environmental risks. At the same time, the occurrence in the reclaimed water of contaminants of emerging concern (CECs), most of them still unregulated, may increase the public distrust due their accumulation in the environment. CECs include not only organic compounds, but also microbial contaminants, among them antibiotic-resistant bacteria (ARB) and antibiotic resistance genes (ARGs). Therefore, it becomes fundamental to develop a human health and environmental risk assessment to identify the main hazards and hazardous events and to evaluate their occurrence (likelihood) and the magnitude (severity) of hazard impacts on the exposed receptors.
The EU Regulation [1] requires the implementation of a Water Reuse Risk Management Plan (WRRMP) in reclamation facilities that includes not only the development of the risk assessment, but also the risk management to ensure the safe use of reclaimed water and minimize the risks to the environment and human health (workers, outside population, and crop end users). A set of indications is reported in the EC Guideline [3] and in [4]. The WRRMP includes: *i)* a detailed description of the water reuse system, *ii)* the identification of all potential hazards and hazardous events with the receptors (environments and populations at risk) and the related routes of exposure, *iii)* the human and environment risk assessment, and *iv*) the management of the assessed risks with the use of existing or new preventive measures to remove or reduce them.
The risk (*R*) is defined by eq. 1:

$$R = L \times M \qquad \text{eq. 1}$$

where *L* is the likelihood, that is the probability of occurrence of a hazardous event, and *M* is the magnitude or severity, i.e. the potential adverse health and environmental effects due to the exposure to a hazard [5].

According to [1], a hazard is a pollutant or pathogen, and a hazardous event is any failure of treatment, accidental leakage, or contamination of the water reuse system that can cause harm to human and animal health and/or the environment. WHO [6] and JRC [4] also list bad weather conditions related to the occurrence of hazardous events. Once the hazardous events are identified, a risk assessment can be done following qualitative, semi-quantitative or quantitative approaches [1].

Proposed methodology for assessing the risks related to wastewater treatments for reusing reclaimed water

Within the framework outlined by the European regulation, a simplified methodology was developed to assess the main risks for the reclamation facility aiming to produce an effluent adequate for irrigation needs.

The identification of the hazardous events is carried out by means of the Failure Mode and Effect Analysis (FMEA): a *qualitative methodology* able to identify failure modes and their effects on the system (leakage, breakage, release, reduction in the removal efficiency, etc), which can result in a worse quality of the final effluent with potential adverse effects on the environment and human health [7]. The results of this analysis are reported in a table in terms of descriptions of the identified failure modes and their consequences. This table represents the basis for the developing of the methodology. According to eq. 1, the risk is defined as the product of the likelihood of occurrence of a failure mode and the severity of its consequences. Due to the lack of data of likelihood of occurrence of failures and of parameters which measures the consequences, *a semi-quantitative approach* was adopted as suggested in [6], and the risk was evaluated on the basis of scores assigned to occurrence S_1 and severity S_2 following eq. 2, which derives from eq. 1 where $L=S_1$ and $M= S_2$. Eq. 2 provides the risk score S.

$$S = S_1 \times S_2 \qquad \text{eq. 2}$$

According to [6], S_1 varies between 1 and 5 and S_2 may assume the values: 1, 2, 4, 8 and 16. The values are defined on the basis of the opinions of interviewed experts.

As shown in Table 1, the higher the likelihood, the higher S_1 and the higher the severity, the higher S_2.

Table 1. Risk assessment matrix, according to [6]. Green =low, orange = medium, red= high and purple= very high risk

Likelihood score, S_1	**Magnitude score S_2**				
	1 (insignificant)	2 (minor)	4 (moderate)	8 (major)	16 (catastrophic)
1 (rare)	1	2	4	8	16
2 (unlikely)	2	4	8	16	32
3 (possible)	3	6	12	24	48
4 (likely)	4	8	16	32	64
5 (almost certain)	5	10	20	40	80
Risk Score *S*	<6	6–12	13-32		>32
Risk level	Low	Medium	High		Very high

On the basis of the obtained S values for the identified failure modes, the risk can be considered low, medium, high and very high as reported in Table 1. In particular: the risk is low for S in the range 1-5; medium with S in the range 6 – 12, high for the range 13-32 and very high with $S > 32$

Those failure modes with the highest value of S correspond to the most critical ones. For these, an in-depth analysis of the existing preventive safety measures must be carried out to evaluate the capacity of the system to return the plant to normal operation, and if necessary, further (preventive and mitigative) safety measures must be implemented. The described approach is a semi-quantitative methodology that can be useful for a first and rough risk assessment in the case of wastewater treatment trains, including options for reuse of reclaimed water as shown in the following section. It represents a first

attempt to develop a Sanitation Safety Plan for reuse purposes which has recently become mandatory in reuse projects [8].

Application to a polishing treatment

This methodology was applied to a new polishing treatment, developed within the European project SERPIC (https://www.serpic-project.eu/), to identify the main malfunctions and failures in the different components of the treatment and to evaluate the main risks associated with them for the final effluent quality, and consequently the most critical components of the new technology.

The SERPIC technology aims to reduce organic and microbial CECs concentrations and produce a final effluent adequate for direct reuse for irrigation needs and another effluent to be directly released in surface water. It consists of two routes: Route A fed by a secondary effluent treated by a membrane nanofiltration (NF) unit and disinfected by ozone produced electrochemically for the effluent destinated to the reuse, and Route B fed by NF concentrate consisting of a membrane photoreactor (Figure 1) for effective removal of CECs from the stream to be directly released.

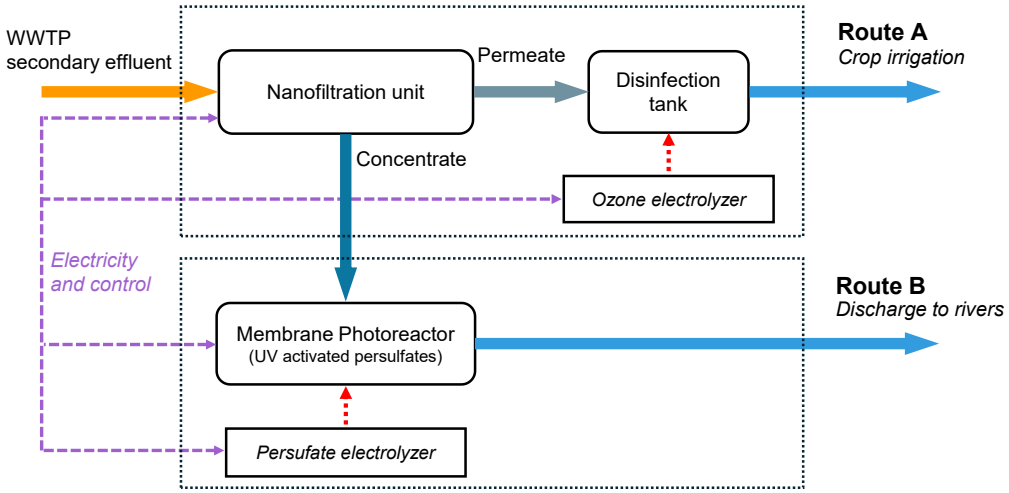

Figure 1. Treatments under investigation within the SERPIC project for direct reuse (Route A) and release in surface water (Route B).

Table 2 contains the results of the FMEA for some components of the SERPIC technology in terms of failure modes of the components and the potential effects on the treatment systems and the quality of the final effluent. It refers to nanofiltration membrane, power supply to ozone electrolyzer and gas diffusers. The same approach must be applied to all the components of the two routes, and the final effluent quality, to which the analysis refers, is that required for the reuse of reclaimed water or the release in the environment.

The CECs to monitor were selected by means of the methodology described in [9], and include 4 organic CECs (diclofenac, iopromide, sulfamethoxazole, venlafaxine), 1 ARB (*E. coli*) and 1 ARG (*sul*1).

The following step consists in assigning the scores to the expected likelihood of occurrence of the failure modes and to the severity of their consequences. Due to the lack of experimental data, the scores will be assigned on the basis of interviews to experts in the field (practitioners, environmental engineers working in the field of water reclamation, water company staff, and researchers). This phase is under development and results of the application of the methodology to SERPIC technology will be presented at the conference as well as the uncertainties connected to the score assignment. The strength of this study is that it represents a first attempt to identify the main critical failure modes which can lead to an effluent inadequate for the reuse and to evaluate if the adopted measures to prevent these events or mitigate their consequences are sufficient or further actions must be adopted to improve the reliability

of the plant.

Table 2. Failures mode and their potential effects for some components of the SERPIC technology.

Components	Failure Mode	Effects on the treatment performance	Effect on the final effluent quality
NF membrane	Membrane breakage	Low or very poor retention of CECs in the NF unit	High concentration of of organic and microbial pollutants, including CECs, in the NF effluent
	Membrane clogging	Membrane may seriously damage or break	High concentration of organic and microbial CECs in the NF effluent Reduced or lack of water supply
	Membrane aging	Reduced rejection capabilities	High concentration of organic and microbial pollutants, including CECs, in the NF effluent
Power supply to ozone electrolyzer	Low electricity	Insufficient ozone production, insufficient disinfection	High concentration of microbial CECs
	No electricity	No disinfection	High concentration of microbial CECs
Gas diffusers in the disinfection tank	Clogging of diffusers	Low ozone produced Lower rate of oxidation and disinfection	High concentrations of organics and microbial CECs

References

[1] Regulation (EU) 2020/741 of the European Parliament and of the Council of 25 May 2020 on minimum requirements for water reuse, Office of the European Union, (2020), https://eur-lex.europa.eu/legal-content/EN/TXT/PDF/?uri=CELEX:32020R0741&from=EN.

[2] Ramm, K. and Smol, M. Water Reuse—Analysis of the Possibility of Using Reclaimed Water Depending on the Quality Class in the European Countries. Sustainability (2023), 15, 12781. https://doi.org/10.3390/su151712781.

[3] EC Guidelines 2022/C 298/01, Commission Notice - Guidelines to support the application of Regulation 2020/741 on minimum requirements for water reuse, Office of the European Union, (2022), https://eur-lex.europa.eu/legal-content/EN/TXT/PDF/?uri=CELEX:52022XC0805(01)&from=EN.

[4] Maffettone, R. and Gawlik, B.M., Technical Guidance: Water Reuse Risk Management for Agricultural Irrigation Schemes in Europe, European Commission, Luxembourg, (2022), JRC 129596.

[5] CCPS, Guidelines for hazard evaluation procedures, Wiley, 2008. 3rd edition. ISBN 978-0-471-97815-2

[6] WHO, Sanitation safety planning: step-by-step risk management for safely managed sanitation systems, World Health Organization, Genova, (2022), https://www.who.int/publications/i/item/9789240062887.

[7] Stamatis, D.H., Failure mode and effect analysis: FMEA from theory to execution, ASQ Quality Press, New York (2003), ISBN: 9780873895989.

[8]Commission Delegated Regulation (EU) 2024/1765 of 11 March 2024 supplementing Regulation (EU) 2020/741 of the European Parliament and of the Council with regard to technical specifications of the key elements of risk management. OJ L, 2024/1765, 20.6.2024

[9] Verlicchi, P., Grillini, V., Lacasa, E., Archer, E., Krzeminski, P., Gomes, A.I., Vilar, V.J.P., Rodrigo, M.A., Gäbler, J., Schäfer, L., Selection of indicator contaminants of emerging concern when reusing reclaimed water for irrigation — A proposed methodology, Science of the Total Environmental, 873, 162359, (2023), https://doi.org/10.1016/j.scitotenv.2023.162359.

Title: Water Re-use after treatment of industrial water resulting from the Peroxide and Peracetic Acid production

Author(s): M.G.Chieti*[1,2], A.Cherubini[1], N.Ciuccoli[1], D.Caterino[1], M.Sgroi[1], F.Ulivari[3], A.L.Eusebi[1], F.Fatone[1]

[1]*Dipartimento di Scienze ed Ingegneria della Materia, dell'Ambiente ed Urbanistica*, *Facoltà di Ingegneria – Università Politecnica delle Marche, Ancona (AN), Italy*
[2] *Dipartimento di Ingegneria Civile e Architettura*, *Facoltà di Ingegneria – Università di Catania, Catania (CT), Italy*
[3]*Società Solvay Chimica Italia S.p.A., Rosignano Solvay (LI), Italy*

Abstract

In recent years, the European Union has promoted numerous initiatives to encourage the transition from a linear economy to a circular economy to minimize the waste production. As regards production processes, public-industrial symbiosis plays a key role in the EU Circular Economy Action Plan, or a process of business interaction aimed at obtaining competitive advantages resulting from the transfer of resources between two or more actors. In this framework, the main objective of testing WAPEREUSE pilot plant as part of the European H2020 AquaSPICE (Adavancing Sustainability of Process Industries through Digital and Circular Water Use Innovations) project is the optimization of the industrial wastewater treatment to recover water for reuse. The goal is also to reduce costs and energy consumption through process optimization to increase the sustainability of the treatment process. This objective is achieved thanks to the real-time reading of the quality parameters of the effluent water via sensors. This indirect monitoring system will track functional parameters using sensors, allowing optimal management of the pilot plant and resulting in cost reductions. Based on the quality that can be obtained at the output, the best feasible value chain route is suggested: 1. discharge into sewer systems; 2. discharge at the head of the ARETUSA water recovery plant; 3. intra-loop reuse at Solvay Chimica Italia S.p.a., a chemical industrial plant. It was observed that the possibility of implementing the three value chains depends on the quality of the incoming wastewater.

Keyword(s): circular economy, industrial symbiosis, industrial wastewater treatment, wastewater reuse, pilot plant

Introduction

Circular economy model is based on increasing resource efficiency, minimizing waste production, in order to decoupling economic growth from resource use [1]. Industrial symbiosis engages traditionally separate industries in cooperative approaches for managing resource flows that improve their overall environmental performance [2]. By organizing industry according to the model of an ecosystem, the transition from a linear to a circular economy system is encouraged. Rosignano Solvay hosts an industrial symbiosis through a concrete regional synergy with the implementation of the circular economy concept. The Rosignano Solvay industrial site produces sodium carbonate, sodium bicarbonate, calcium chloride, chlorine, hydrochloric acid, chloromethane, polyethylene, hydrogen peroxide and peracetic acid. In order to deliver more sustainable water management, Consorzio ARETUSA was established in 2001 as partnership between water utility (ASA Livorno), industry (Solvay Chimica Italia) and tech provider (Termomeccanica). Thanks to ARETUSA, since more than 15 years

the Solvay chemical plant is implementing a utility-industry (public-private) symbiosis system for optimizing the regional water cycle, by reusing about 3 million cubic meters per year of urban wastewater treated in the ARETUSA reclamation plant. The existing Wastewater Reuse Plant (WWRP) contains flocculation, sedimentation, filtration, activated carbon filter (GAC) and UV disinfection. Industrial water cycles may still be optimized towards increased energy and carbon efficient water re-use. In this context the WAPEREUSE pilot-scale has be validated for the treatment of the industrial used water (water from Hydrogen Peroxide and Peracetic Acid production) up to the limits for discharge in municipal sewers. Furthermore, the pilot was implemented with a dense network of sensors for setting treatments and continuous and remote monitoring in order to optimize the various processes. Therefore, specific goals of the pilot system were: (i) pH Neutralization, (ii) H_2O_2 removal and increase of COD biodegradability, (iii) COD and Nitrates removal and (iv) additional NO_3^- removal by refinements steps (v) control, management and optimization of the main parameters of the processes by Digital Twin.

Materials and Methods

The pilot system has been installed at the experimental demo hall of the “Università Politecnica delle Marche – UNIVPM”, and it is located at the municipal wastewater treatment plant (WWTP) of Falconara Marittima (Italy). The process chain used for the influent treatments consists of: Neutralization, AOP filtration, biological treatment and GAC/IEX filtration. While the sensors that are used for the good control of the processes include: pH, redox potential, total suspended solids (TSS), UV absorbance at 254 nm (UV254), dissolved oxygen (DO), nitrates, water level in the tanks, flowrate measurements, pressure in the membrane compartment. All process logics implemented in the PLC were developed based on on-site sensor measurements. In fact, for each operating unit the control takes place depending on the different process parameters monitored by the sensors. The graphical interface shows process layouts with different variables that can be selected and modified. Thanks to this technological solution it is possible to monitor the pilot even remotely. (**Figure 1**)

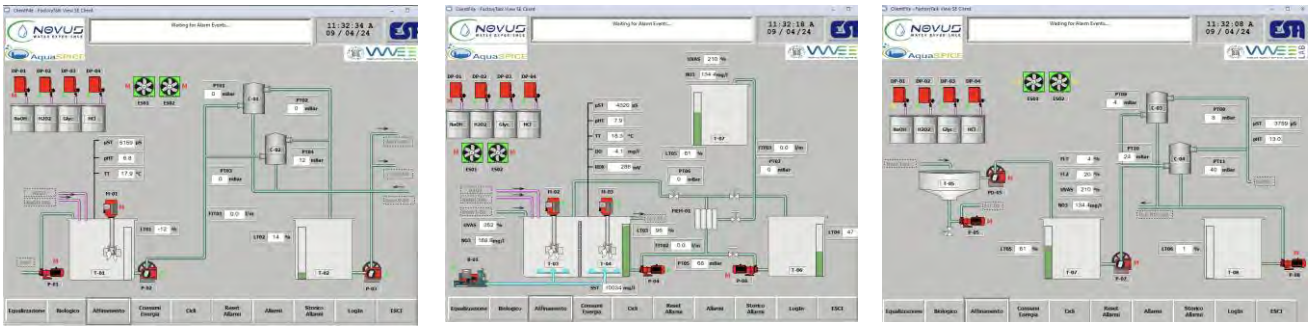

Figure 1. The interactive interface of the PLC

Table 1 summarizes the main quality parameters of Solvay industrial wastewater, which is treated by the WAPEREUSE pilot system within the H2020 AquaSPICE project.

Table 1. Solvay wastewater characterization

Parameters	U.m.	Typical	Min	Max
pH	-	2.0	1.5	3.0
TOC	mg/l	350	50	500
COD	mg O_2/l	1000	500	1800
NO_3^-	mg NO_3/l	850	600	1300
SO_4^{2-}	mg/l	511	297	1110

H_2O_2	g/l	0.3	0.1	0.8
Al_3^+	mg/l	0.5	0.2	1
Fe_2^+	mg/l	0.6	0.2	1.2

The pilot system can be operated with an average flowrate of 1 m^3/d. The wastewater is characterized by relevant concentrations of TOC/COD, nitrates, sulphates, and hydrogen peroxide. Great attention must be paid to the organic fraction that consists mainly of acids, alcohols, and aromatic compounds. Therefore, the influent to the pilot was treated through four treatment steps:

1. *Neutralization*: the wastewater from the peroxidate production cycle has a pH of 2-3, which must be neutralized before entering the biological compartment. In this first step, Soda at 30% will be dosed to neutralize or to reach the suitable pH for subsequent treatments.
2. *AOP filtration*: this unit involves the use of columns containing Granular Ferric Hydroxide (GFH), for the removal/degradation of H_2O_2 and recalcitrant COD, while providing a heterogeneous Fenton reaction.
3. *Biological compartment*: The operation of the biological reactor involves three steps: A) wastewater feeding; B) biological process and C) solid-liquid separation. The logic of the biological reactor can be set to control the process based on i) time or ii) sensor measurements. Hence, different logics were developed to control the process related to sensors measurements or according to defined times interval of operation. The Biological compartment has been designed to allow different process configurations. Particularly, step B "biological process" involves two phases: 1) Denitrification, for the removal of nitrates in anoxic conditions by the addition of external carbon (glycerol); 2) Oxidation, for the removal of COD in aerobic conditions. Tanks can work under identical or different operating conditions. Depending on the working configuration of tanks, the operation of the biological reactor can be distinguished as:
   a. Intermittent aeration (tanks work under the same conditions);
   b. Separated phases (tanks work under different conditions).
   The solid-liquid separation can be performed by membranes, hence, the system work as MBR. The control logic for the biological process can be selected via PC interface as shown in **Figure 1**. Particularly, the logics can be selected for intermittent aeration or separated phases working conditions. Hence, it is possible to decide if the two tanks of the biological reactor can work under identical or different conditions.
4. *GAC/IEX filtration*: The aim of this treatment unit is to further reduce COD, nitrates and, if needed, to eliminate sulphates from the effluent of the biological compartment. The treatment is optional and could be implemented in order to reach the limits for reuse.

Results

Water quality parameters such as nitrates, phosphates, alkalinity, pH and conductivity are monitored by laboratory analysis in influent and in effluent streams. Mixed liquor suspended solids (MLSS) and mixed liquor volatile suspended solids (MLVSS) measurements are obtained by laboratory analysis once per week. Spectroscopic measurements such as UV absorbance at 254 nm (UV254) are tested to validate their use as surrogate parameters to monitor COD removal during wastewater treatments. Indeed, UV254 sensors have been installed in the WAPEREUSE pilot system for the real-time monitoring of COD removal during the industrial wastewater treatment. Nitrates, redox, pH, conductivity and TSS are also collected in real time by in situ probes. Regarding the neutralization process, the treated Solvay influent reached a pH of 6.8 with a dosage of 0.21 l/min of 30% soda, suitable for entry into the biological reactor. In the **Figure 2**, it is possible to observe the trend in nitrates concentrations during absence of oxygen (i.e., denitrification phase) and air bubbling (i.e., oxidation phase) by varying the hours of the cycles according to the dosage and the reduction of nitrates achieved. During the period in consideration a reduction in nitrates (90-95%) below the law limit (20 mgN-NO_3/L) has been obtained, using the dosing

pump at 50% of its power and varying with an external carbon dosage of 0.35 l/min. After an initial stabilization phase of the system in which the dosage was set at 6 min with a cycle of 10h of oxidation and 8h of denitrification, the dosage was decreased first to 3 min, then to 2 min by changing the cycle to 12h of oxidation and 4h of denitrification, to then maintain the same cycle with a glycerol dosage of 1 min. The COD reduction efficiency achieved is approximately 60%.

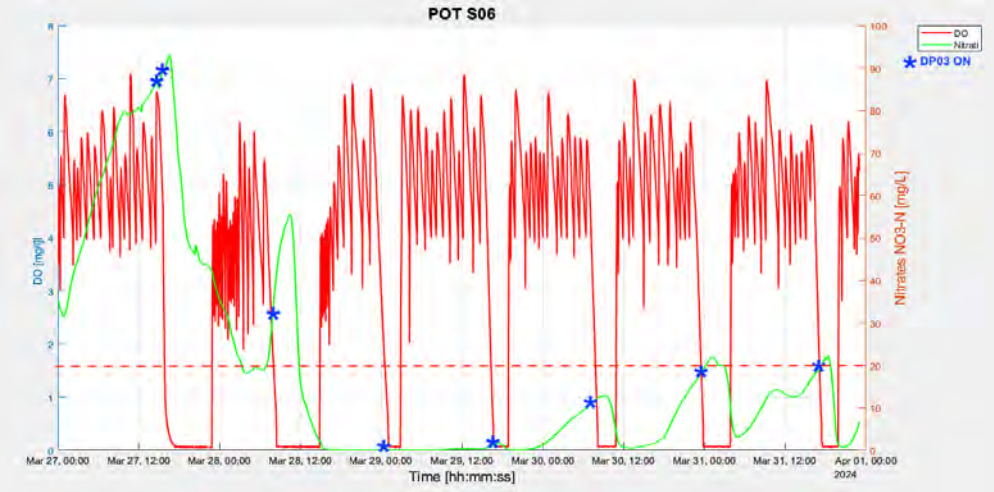

Figure 2. Observed Nitrates removal during different cycles

All data collected in real-time by sensors are shared in the AquaSPICE RTM platform. The aims is to create a digital twin model that can predict optimal operational conditions to reduce reagent and energy consumption. Consumption of reagents include: 1.2 l/m^3 of external carbon, 1.7 l/m^3 of soda, 0.1 l/m^3 of acid.

Conclusion

The results obtained demonstrate that the WAPEREUSE pilot plant can treat the industrial wastewater resulting from the peroxide and peracetic acid production at Solvay plant, reaching the law limits following the Table 3 of Annex V - Third Part of Dllgs.152/2006 for COD and nitrates (500 mgO_2/l and 30 mgN/l) for the discharge into public sewage. The logic implemented based on the sensors has proven to be an innovative solution useful for managing and controlling the functional parameters of the processes even remotely.

Acknowledgement

Authors would like to acknowledge the H2020 project AquaSPICE for funding the present work under Grant Agreement 958396.

References

[1] B. G. Arias, N. Merayo, A. Millán, and C. Negro, “Sustainable recovery of wastewater to be reused in cooling towers: Towards circular economy approach,” Journal of Water Process Engineering, vol. 41, p. 102064, Jun. 2021, doi: 10.1016/j.jwpe.2021.102064.

[2] M. R. Chertow, W. S. Ashton, and J. C. Espinosa, “Industrial Symbiosis in Puerto Rico: Environmentally Related Agglomeration Economies,” Reg Stud, vol. 42, no. 10, pp. 1299–1312, Dec. 2008, doi: 10.1080/00343400701874123.

Title: Water reuse opportunities and challenges for *Galdieria sulphuraria* cultivation

Author(s): Marco Malaguti*[1], Michele Carone[1], Mariachiara Zanetti[1] Alberto Tiraferri[1], Vincenzo Riggio[1]

[1] Department of Environment, Land and Infrastructure Engineering - DIATI, Politecnico di Torino, Corso Duca degli Abruzzi, 24, 10129 – Torino, Italy

Keyword(s): water reuse, microalgae cultivation, microalgae dewatering, energy requirements.

Abstract

Microalgae biomass cultivation interest is consistently growing due to its potential for several commercial applications [1]. As relevant examples, microalgae are capable of accumulating significant amounts of carbohydrates, proteins, and lipids, making them a promising energy feedstock [2]. However, one of the main challenges that nowadays tackle the microalgae sector in the field of sustainability is the large amount of high purity water required for the biomass production itself [3]. In detail, one of the main water intensive aspects is the continuous need of freshwater inside photobioreactors that promote the growth of algae. In this context, an optimization of biomass harvesting processes is considered fundamental to assess and critically evaluate the feasibility of a direct water reuse scenario that would lead to the reduction of both environmental and management costs moving consequently the sector towards a circular economy approach. Among the various strains, the red microalga *Galdieria sulphuraria* has gained increasing attention. The main characteristics of this strain are the blue-green colour mainly attributed to the presence of blue phycobiliproteins C-phycocyanin (C-PC) that represents a valuable feature making it a promising candidate for its production as a food source, and the ability to grow and survive in extreme conditions in terms of low pH (until 0.2) and high temperatures (until 57°) [4]. Seen these characteristics, the cultivation medium requires low pH values that are commonly reached by the addition of sulphuric acid. This directly leads to acidic wastewaters related to the cultivation phases which typically exceed wastewater discharge law limits (as an example the Italian limits for industrial wastewater discharge after biomass harvesting (Annex 5, Third Section, Legislative Decree n. 152/2006, (Italian Legislative Decree No. 152 approving the Code on the Environment, n.d.)).
Consequently, the scope of this research is to investigate the performance and the differences of two of the most widely used separation techniques, centrifugation and membrane microfiltration, with the target of assessing the potential to extract water to be reused as a new cultivation medium. In details, different fractions of reused water are assessed together with the effects of multiple growth cycles in reused water at pilot scale. In conclusion, a fair and systematic comparison between the two downstream processes for microalgae dewatering is provided in terms of water recovery capabilities and energy requirements with the aim to provide a guide toward the choice of the most suitable water reuse technology for each specific case.
The obtained results in terms of biomass growth in the reused medium are summarized. Figure 1 shows *G. sulphuraria* growth capability in control conditions, i.e. in the ideal cultivation medium inside the photobioreactor (PBR), and in each consecutive cycle of growth in partially reused water from centrifugation. The term partially is used to highlight that in this first stage only 25% of the water used for cultivation comes from the centrifugation process consequent to past cultivation cycles. The time evolution of the biomass dry weight shows that after 16 days of cultivation, a biomass concentration of 3.26 g/L was reached in control conditions with a consequent biomass productivity (Px) of 0.21 g/L/day.

On the other hand, growth in partially reused water showed minor differences when compared to the ideal medium condition since average Px were 0.22, 0.20, and 0.20 g/L/day for the three cycles. The same trends were registered when biomass was cultivated in reused water from microfiltration. The growth results are reported in Figure 2 where average Px values were 0.22, 0.24, and 0.21 g/L/day for the first, second, and third cultivation cycle, respectively.

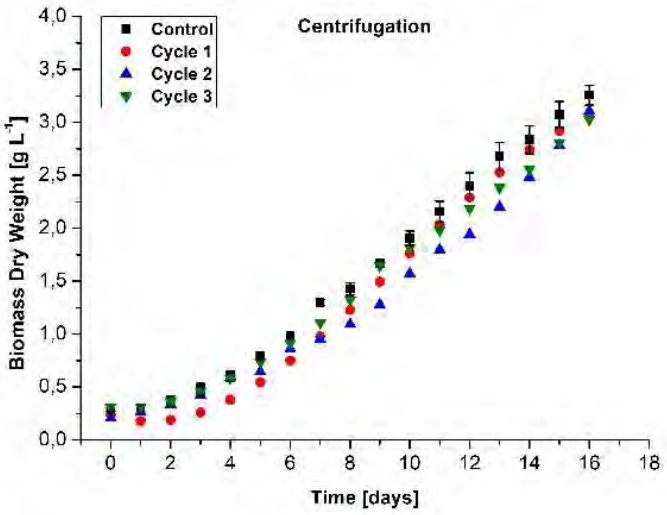

Figure 1. Biomass concentration measured over time during cultivation relative of cycles of partially reused water from centrifugation. Black squares: control (n =3). Red circles: 1st cycle of 25% water recycling. Blue triangles: 2nd cycle of 25% water recycling. Green triangles: 3rd cycle of 25% water recycling.

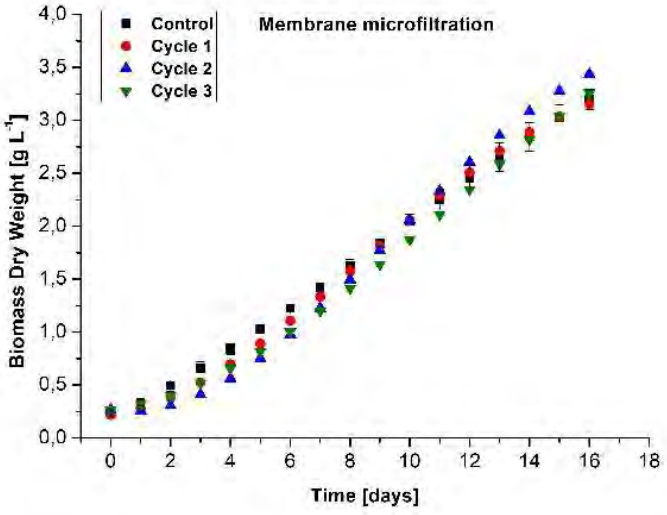

Figure 2. Biomass concentration measured over time during cultivation relative of cycles of partially reused water from membrane microfiltration. Black squares: control (n =3). Red circles: 1st cycle of 25% water recycling. Blue triangles: 2nd cycle of 25% water recycling. Green triangles: 3rd cycle of 25% water recycling.

Seen the strength of the results displayed above, the two downstream processes for algae concentration were further investigated. In particular, growth cycles utilizing as cultivation substrate the maximum amount of reused water achievable with the two dewatering processes were performed. This corresponded to cultivation substrates composed by 98% and 71.5% of reused water for the centrifugation and for the membrane microfiltration, respectively. The results reported in Figure 3 show that *G. sulphuraria* growth performance were not affected by the reused water in none of the two cases. Quantitatively, the averaged Px were 0.25, 0.24, and 0.24 g/L/day for the control batches, the growth in reused water from centrifugation, and the growth in microfiltration reused water, respectively. However, to strengthen the finding, further experiments may be useful to address the feasibility of directly reusing the water for consecutive cycles.

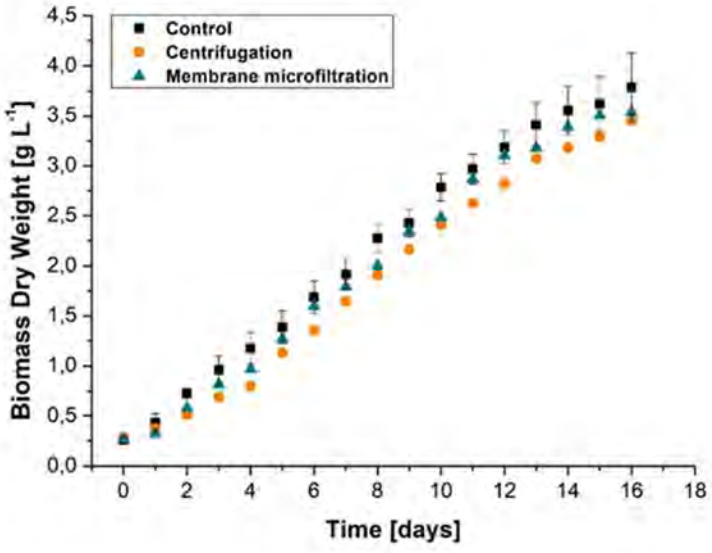

Figure 3. Biomass concentration over time during cultivation in reused water. Black squares: control (n =3). Orange circles: growth in 98 % reused water from centrifugation (n = 2). Green triangles: growth in 71.5 % reused water from microfiltration.

Another crucial aspect that needs to be addressed when choosing a microalgae biomass harvesting technology, is the energy consumption. However, a direct energy comparison between the two investigated techniques is far from being straightforward because of the intrinsically differences in their separation mechanism. However, two parameters that are expected to significantly impact the energy performance are the cultivation volumes (or flow rates) and the starting and final biomass concentrations (or concentration factor). In details, the effect of system size on the specific electrical energy consumption (SEEC) can be highlighted comparing lab-scale results performed in non-optimized conditions in terms of system design with real-scale applications. In details, in this research the SEEC recorded when using the membrane separation was approximately 23 kWh/m^3 calculated considering the power absorbed by the pump (~ 0.3 kW) and that the system needed 150 min to recover approximately 32.2 L of water out of 40 L of biomass. On the other hand, the SEEC of the centrifuge was approximately 14 kWh/m^3 considering that the power absorption (~2.2 kW) and that it recovered 39.2 L of water out of 40 L of biomass in 15 min. On the other hand, SEEC values reported in the published results for pilot-scale membrane filtration systems span from 0.97 kWh/m^3 to 2.5 kWh/m^3 while considering available data of commercial centrifuge systems these values span from 0.9 kWh/m^3 to 4.4 kWh/m^3. The numbers just presented point out that the membrane system value cover an ample

range of different energy consumption values seen the intrinsic modularity of the systems: the higher is the active area of the membranes the more energetically efficient is the process. For centrifugation system instead, this trend seems to be reduced implying that even if the centrifuge dimension plays a role, its impact is lower if compared to membrane units. For what concerns the impact of the concentration factor on energy consumption the discussion starts highlighting that microfiltration is limited when to objective is to reach concentrations higher than ~ 50 g/L [5]. On the other hand, centrifugation consistently shown final concentration of at least 150 g/L and ideally up to 1000 g/L. To summarize the discussion, the main guidelines that may be extrapolated by this research are that for biomass plants producing < ~10 m^3 of algae suspension daily, a harvesting system composed by a single centrifugation step may represent the best option while for larger involved volumes membrane systems become competitive in terms of energy consumption representing an effective solution to pre-concentrate the biomass suspension before centrifugation. This two-step approach would merge the ability membrane systems to extract large volumes of water while operating at low SEEC values, and the ability of centrifuge systems to reach highly concentrate biomass values.

References

[1] Spolaore, P., Joannis-Cassan, C., Duran, E., Isambert, A., 2006. Commercial applications of microalgae. J Biosci Bioeng 101, 87–96

[2] Gimpel, J.A., Henríquez, V., Mayfield, S.P., 2015. In metabolic engineering of eukaryotic microalgae: Potential and challenges come with great diversity. Front Microbiol 6, 1–14.

[3] Batan, L., Quinn, J.C., Bradley, T.H., 2013. Analysis of water footprint of a photobioreactor microalgae biofuel production system from blue, green and lifecycle perspectives. Algal Res 2, 196–203.

[4] Abiusi, F., Trompetter, E., Hoenink, H., Wijffels, R.H., Janssen, M., 2021. Autotrophic and mixotrophic biomass production of the acidophilic Galdieria sulphuraria ACUF 64. Algal Res 60.

[5] Malaguti, M., Craveri, L., et al., 2023. Dewatering of Scenedesmus Obliquus Cultivation Substrate with Microfiltration: Potential and Challenges for Water Reuse and Effective Harvesting, Engineering.

Title: Membrane Bioreactor as a cost-effective solution for water reuse and bacteria, viruses, and micro pollutants removal

Author(s): Andreas Fischer*[1], Dominik Schreier[2], Maximilian Werner[3], Alexander Merz[4]

[1] Engineering, Mann+Hummel, Wiesbaden, Germany, Andreas.Fischer2@mann-hummel.com
[2] Engineering, Mann+Hummel, Wiesbaden, Germany, Dominik.Schreier@mann-hummel.com
[3]Engineering, Mann+Hummel, Wiesbaden, Germany, Maximilian.Werner2@mann-hummel.com
[4] Engineering, Mann+Hummel, Wiesbaden, Germany, Alexander.Merz@mann-hummel.com

Keyword(s): MBR, micro pollutants, water reuse

MANN+HUMMEL has specialized in the development of new membranes at its Wiesbaden site since 1966 and has been developing and selling membrane bioreactors (MBRs) since 2006. The main advantages of MBRs are the lower footprint required compared to conventional activated sludge systems (CAS) and the higher effluent quality (Figure 1).

Due to the increasingly competitive situation in this sector, the flow performance of MBRs is becoming an ever more decisive factor. The flow performance has a direct influence on the operating and investment costs. In addition, the high separation performance of particles, micro pollutants and (antibiotic resistant) bacteria for the reuse of wastewater, e.g. for irrigation in agriculture.

Water Reuse by using Membrane Bioreactors

The reuse of wastewater is one of the major drivers to reduce water shortage. In order to demonstrate the technical feasibility for water reuse, Mann+Hummel conducted performance and effluent quality testing at a municipal wastewater treatment, a casino called Angel of the Winds (state Washington in USA). The target was to fulfil water reuse criteria based on Tier 1, Water Research Foundation 4997 [1].

Mann+Hummel installed two membrane modules of the newly released product generation BIO-CEL L+480 with 480 m² in January 2023 (Figure 1). The process flow of the wastewater treatment plant includes a 2 mm fine screening, an equalization basin, biology, MBR and finally a UV disinfection. The filtrate is stored in a filtrate storage tank. Turbidity was measured online, and all virus, bacteria and protozoa samples were taken and analyzed by an accredited laboratory.

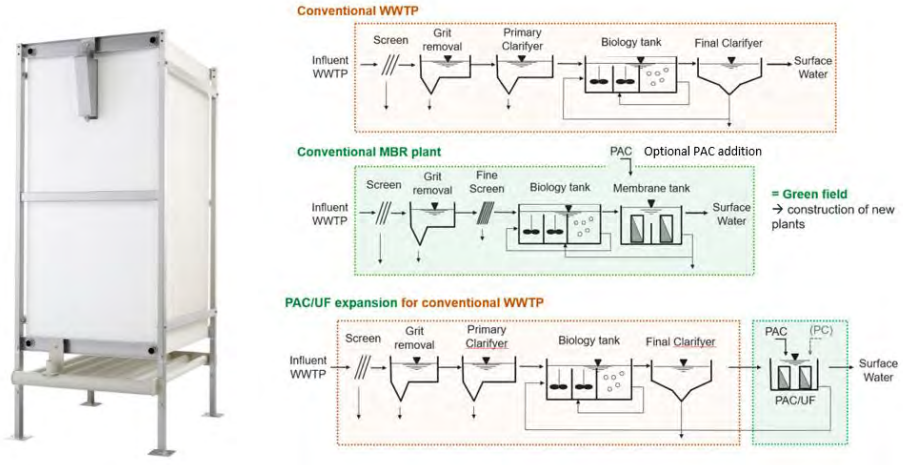

Figure 1. BIO-CEL L+480 and process Combinations for advanced wastewater treatment

In order to obtain a higher flow during the effluent testing, just one of the two membrane modules were operated to generate a higher specific flux (flow divided by available membrane area). The flux was therefore increased from 12 to 24 L/m^2/hrs throughout the trial period from October 2023 to End of January 2024.

The permeability and flux are shown in Figure 2. For the purposes of the trial, a recovery clean with 2,000 mg/L hypochlorite and four hours exposure was conducted before the trial on October 4, 2023, and prior to peak flux testing on January 8, 2024. This second clean was not required based on specific permeability which had remained typically at 500 L/m^2/hrs/bar at 20 degrees Celsius across the entire 96-day CIP interval observed. Instead, the second CIP was conducted to ensure that during peak flux sampling, the membranes were in as clean as possible state and should therefore exhibit conservative removal performance of indicator organisms. That is, removal was not improved via accumulated foulants.

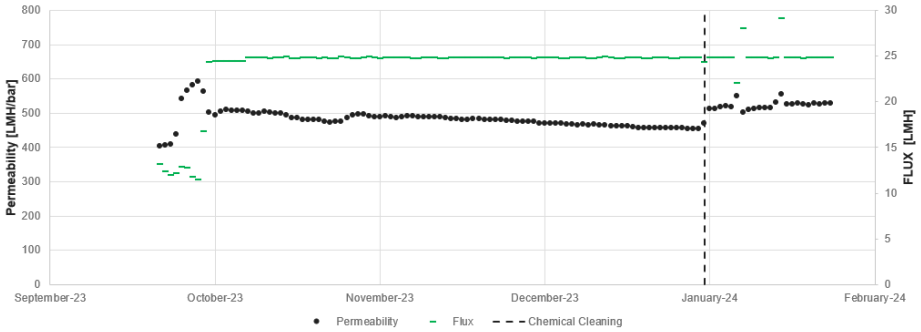

Figure 2. Permeability during Peak-Flux and Effluent Quality Testing

A key criterion for membrane filtered water per the expired California Title 22 recycled water regulations – which is considered in the Tier 1 criteria – is that filtrate turbidity should be:

- Less than 0.2 NTU at the 95th percentile
- Not to exceed 0.5 NTU.

Typically, this is based on online monitored data that is to be collected at no less than 15-minute intervals.

A 5-minute average turbidity data was translated into a probability plot and is shown in Figure 3. Based on the entire observation period, MBR filtrate turbidity was 0.135 NTU at the 95th percentile. The limits of Title 22 of 0.2 and 0.5 NTU were not exceeded until the 98th and after the 99.9th percentiles when considering the entire data set. The values plotted included elevated turbidity that were suspected of being falsely high readings during the peak flux testing and as such are anticipated to be conservative estimates of typical turbidity.

The above analysis suggests that the MBR product meets the requirements for filtered water turbidity outlined in California Title 22 and WRF 4997.

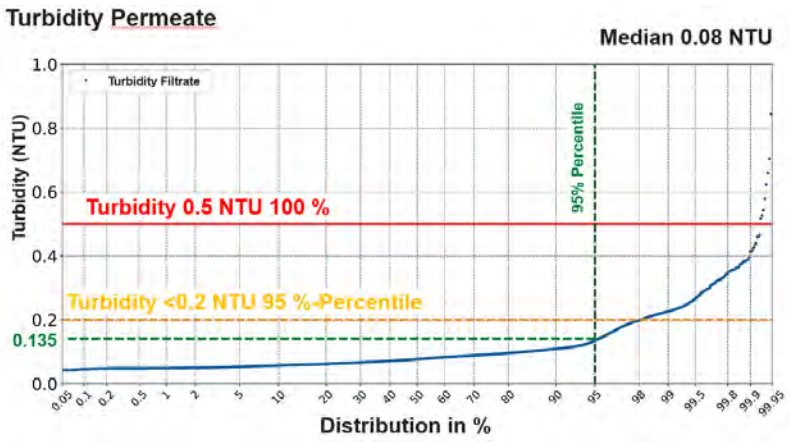

Figure 3. Data for the figure was compiled from the historized MBR filtrate turbidity five-minute averages during the observation period (October 1, 2023, to January 31, 2024).

MBRs typically have a hydraulic retention time and solids retention time that are long enough that there is some uncertainty on the appropriateness of pairing raw wastewater (Raw WW) and MBR filtrate samples to calculate removal. To address this limitation, probability density functions can be fit to microorganism in the Raw WW and MBR filtrate and Monte Carlo simulation used to calculate a LRV. For this data set, the value of the detection limit was assumed to be appropriate to be substituted for any non-detect values. This is ultimately conservative as it means that a higher than true value for microorganism concentration is assumed for the filtrate. This calculation method is consistent with the analysis conducted in WRF 4997 to set default Tier 1 LRV values and was used to calculate LRVs at the 5th percentile.

Statistics of the resulting LRV distributions from Monte Carlo simulation are shown relative to prior MBR validation guidance in Table 1. Male-specific coliphage was only detected in one of 14 filtrate samples. Consequently, the distribution of LRVs for this indicator virus is likely a significant underestimate.

Table 1. Median LRVs for Each Organism Compared to Tier 1 Benchmarks

Pathogen Group	Organism	Median LRV(4)	5th Percentile LRV(5)	Tier 1 LRV
Virus	Somatic coliphages	4.9	3.5	>1.0(1)
	Male-specific coliphages(2)	>3.1	>1.9	
Bacteria	Total coliforms	6.4	4.6	>4.0(3)
	E. coli	6.3	4.5	
Protozoa	C. perfringens	5.8	4.7	>2.5(1)

Notes:
(1) Tier 1 virus and protozoa credit from Salveson, A., Trussell, S., Linden, K., (2021)" Membrane Bioreactor Validation Protocols for Water Reuse - WRF Project 4997", Water Research Foundation, Denver, CO.
(2) Male-specific coliphage was only detected once in the filtrate at the detection limit in 14 samples and the LRVs above are likely underestimates.
(3) Tier 1 bacteria credit from WaterSecure. 2017. Membrane Bio-Reactor WaterVal Validation Protocol. Australian WaterSecure Innovations Ltd, Brisbane, Australia.
(4) LRVs were calculated using Monte Carlo simulation consistent with the methods outline in WRF 4997.

Advanced Wastewater Treatment by micro pollutant and antibiotic resistant germs removal

Micro pollutant removal can be achieved by combining a MBR with Powdered Activated Carbon (PAC), which is directly dosed into the MBR (Figure 1). In addition, an existing conventional wastewater treatment plant (WWTP) can be equipped with a post-treatment step combining a submerged ultrafiltration and PAC dosage.

The European union has defined a reference list for micro pollutants to be monitored [2]. Additional screening was conducted for a PAC/UF expansion as outlined in Figure 1. During these tests two PAC types were used. The target value of 80 % micro pollutant removal was achieved by using PAC 2 in a dosage rate between 12 to 18 mg/l (Figure 4).

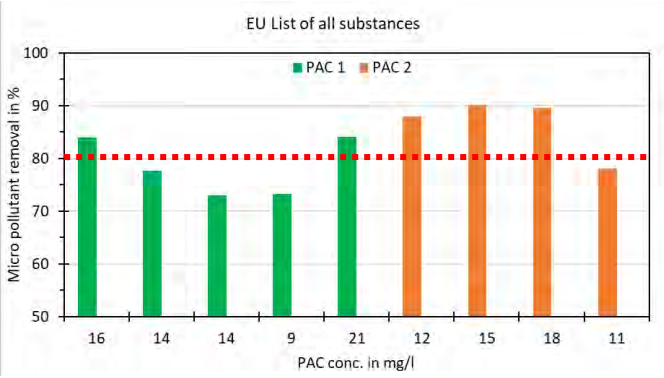

Figure 4. Micro pollutant removal dependent on PAC conc. dosage in reference to EU target list of all substances to be monitored

Summary, Conclusion

The results show that the BIO-CEL L+ 480 satisfactorily fulfils and furthermore exceeds the Tier 1 requirements. Furthermore, the trials showed a stable operation at a conservative flux of 24 L/m^2/hrs throughout the trial period without the necessity of a chemical cleaning.

By dosing powdered activated carbon (PAC) to the MBR, micro pollutants can be efficiently removed. It is concluded, that MBR is an economic solution for advanced wastewater treatment for water reuse and micropollutant and bacteria removal.

References

[1] Salveson, A., Trussell, S., Linden, K., (2021)" Membrane Bioreactor Validation Protocols for Water Reuse - WRF Project 4997", Water Research Foundation, Denver, CO.

PARALLEL SESSION: B2

Drinking water

Emerging challenges in operation

Title: Hydrogenotrophic denitrification of nitrate-contaminated supply water using anaerobic granular sludge in up-flow bioreactors

Authors: Emanuele Marino*[1], Armando Oliva[1], Stefano Papirio[1], Giovanni Esposito[1], Francesco Pirozzi[1]

[1] *Department of Civil, Architectural and Environmental Engineering, University of Naples Federico II, Via Claudio 21, 80125, Naples, Italy, (emanuele.marino@unina.it, armando.oliva@unina.it, stefano.papirio@unina.it, giovanni.esposito1@unina.it, francesco.pirozzi@unina.it)*

Keywords: Hydrogenotrophic denitrification; Anaerobic granular sludge; Supply water; Nitrate removal; Greenhouse gas emissions

Abstract

Nitrate (NO_3^-) concentration in the supply water is significantly increasing due to human alteration of the nitrogen (N) cycle [1]. Besides, NO_3^- is the precursor of nitrite (NO_2^-), which is responsible for several diseases, such as methemoglobinemia [2]. The EU directive 2020/2184 on drinking water established that NO_3^- and NO_2^- shall not exceed respectively 50 and 0.5 mg/L in waters intended for human consumption [3]. Hydrogenotrophic denitrification (H_2Den) is an interesting biological technology to remove NO_3^- from supply water lacking in organic carbon as an alternative to traditional physicochemical treatments, which are generally more expensive and impactful on the environment [4]. H_2Den is a four-stage process in which NO_3^- is step by step reduced to nitrite (NO_2^-), nitric oxide (NO), nitrous oxide (N_2O), and N_2 through reductase enzymes [5]. Although hydrogen (H_2) is characterised by low solubility and hazardous handling, it has several advantages as electron donor, such as no production of toxic by-products, high diffusivity through biofilm, and low sludge production [6].

In this study, an anaerobic granular sludge (AnGS) was used for H_2Den to exploit the granular sludge's compact structure and density which enhance NO_3^- removal and facilitate the downstream separation of biomass from treated water [7]. AnGS H_2Den was investigated for the treatment of highly nitrate-contaminated synthetic supply water in semi-continuous up-flow bioreactors with a working volume of 0.5 L. Two recirculation channels, i.e., i) for liquid and ii) gaseous phases, were implemented to enhance i) the contact between the influent and the granules and ii) H_2 solubilisation. Two bioreactors were operated as duplicates under several experimental conditions for 115 days, as reported in *Table 1*. The bioreactors (D: 5.5 cm, H: 44 cm) were filled with 15% (*w/v*) inoculum. The synthetic supply water was prepared ensuring an initial concentration of 200 mg NO_3^-/L. The anoxic conditions were ensured using

Argon as gas inert to ventilate the headspace. The initial pH was adjusted to 8.0 ± 0.2. NO_3^- and NO_2^- concentrations were measured by ion chromatography. The headspace composition at the end of the batch tests was evaluated through mass spectrometry to assess the presence of gaseous intermediates, such as N_2O and NO, as well as N_2 production and H_2 utilisation.

Table 1 – Process parameters maintained in each experimental phase. Hydrogen (H_2) excess was defined as the extra H_2 provided with respect to the stoichiometric reaction.

Experimental phase	**Time interval** (days)	**H_2 excess** (%)	**Hydraulic Retention Time** (days)	**Changes in the experimental configuration**
Phase I	0-18	100	4	Manual NO_3^- refeeding 5/7
Phase II	18-39	100	4	Automatic NO_3^- refeeding 7/7
Phase III	39-55	100	4	Gas recirculation OFF
Phase IV	55-70	100	3	Gas recirculation ON
Phase V	70-73	100	2	-
Phase IV*	73-83	100	3	-
Phase VI	83-91	100	3	Automatic H_2 dosing 7/7
Phase IV*	91-94	100	3	Back to manual H_2 dosing 5/7
Phase VII	94-115	150	3	-

*Phase IV conditions were reestablished when the newly investigated experimental parameters did not allow a stable operation of the bioreactors under the regulatory limits for NO_3^- and/or NO_2^-.

In Phases I and II, a 4-day hydraulic retention time (HRT) with 100% excess in H_2 was maintained. Nevertheless, in Phase II a higher NO_3^- load than in Phase I was used in both bioreactors. In both phases, the reactors showed great performances, ensuring a NO_3^- removal efficiency of up to 99% (Figure 1A) and very low NO_2^- accumulation (Figure 1B), namely, after the initial week, in this phase, the higher NO_2^- concentration was about 0.5 mg/L. In Phase III, the AnGS H_2Den was experimented with no gas recirculation (Table 1). In this phase, an increase in NO_2^- accumulation was noticed (up to 6.1 mg NO_2^-/L) (Figure 1B), pointing out the need to implement gas recirculation to enhance H_2 solubilisation. Indeed, in Phase III, a residual H_2 percentage in the headspace was constantly observed (up to 11.8%), suggesting scarce utilisation of the electron donor. In Phases IV and V, the HRT was lowered respectively to 3 and 2 days. In Phase IV, the NO_3^- concentration was constantly below 50 mg/L reaching a NO_3^- removal efficiency of up to 99.4% (Figure 1A). Nevertheless, the NO_2^- limit was often exceeded (Figure 1B). On the other hand, in Phase V, both NO_3^- and NO_2^- were surpassed (Figure 1A and 1B). In Phase VI, H_2 was supplied 7 days a week (7/7) through a pump introduced in the reactor

set-up, but a further increase in NO_3^- and NO_2^- concentrations in the bioreactors was observed (Figure 1A and 1B). The failure of this experimental phase can be likely attributed to leakages in the gas bags used to store the H_2, which limited the electron donor availability for microorganisms. During Phase VII, the H_2 excess was increased to 150% to guarantee a greater electron donor availability, ensuring a minimal NO_2^- accumulation as intermediate in the liquid phase (Figure 1B) and reaching a NO_3^- removal efficiency of up to 99.5% (Figure 1A). In the gaseous phase, the production of the intermediates NO and N_2O, potent greenhouse gases, was minimal. The gas recirculation from the headspace to the liquid phase ensured a lower H_2 accumulation in the headspace reactors as a result of the improved H_2 solubilisation.

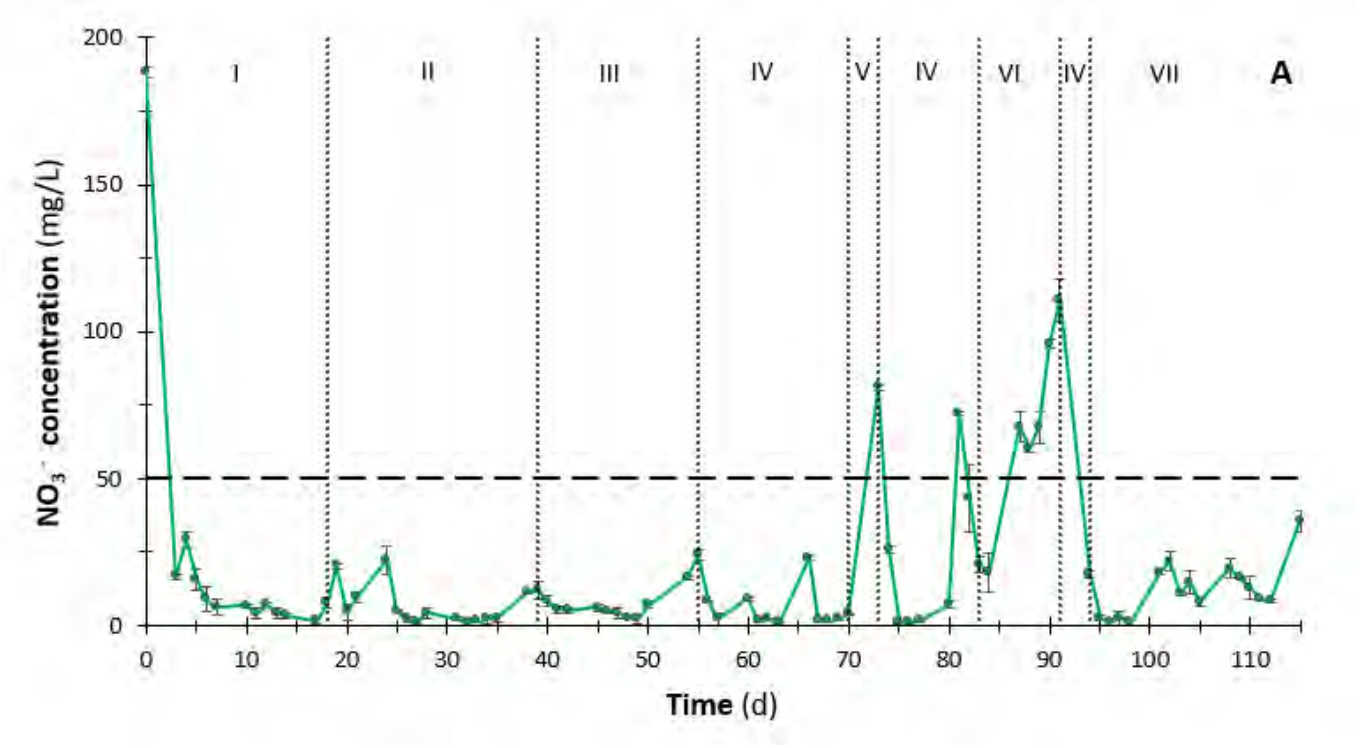

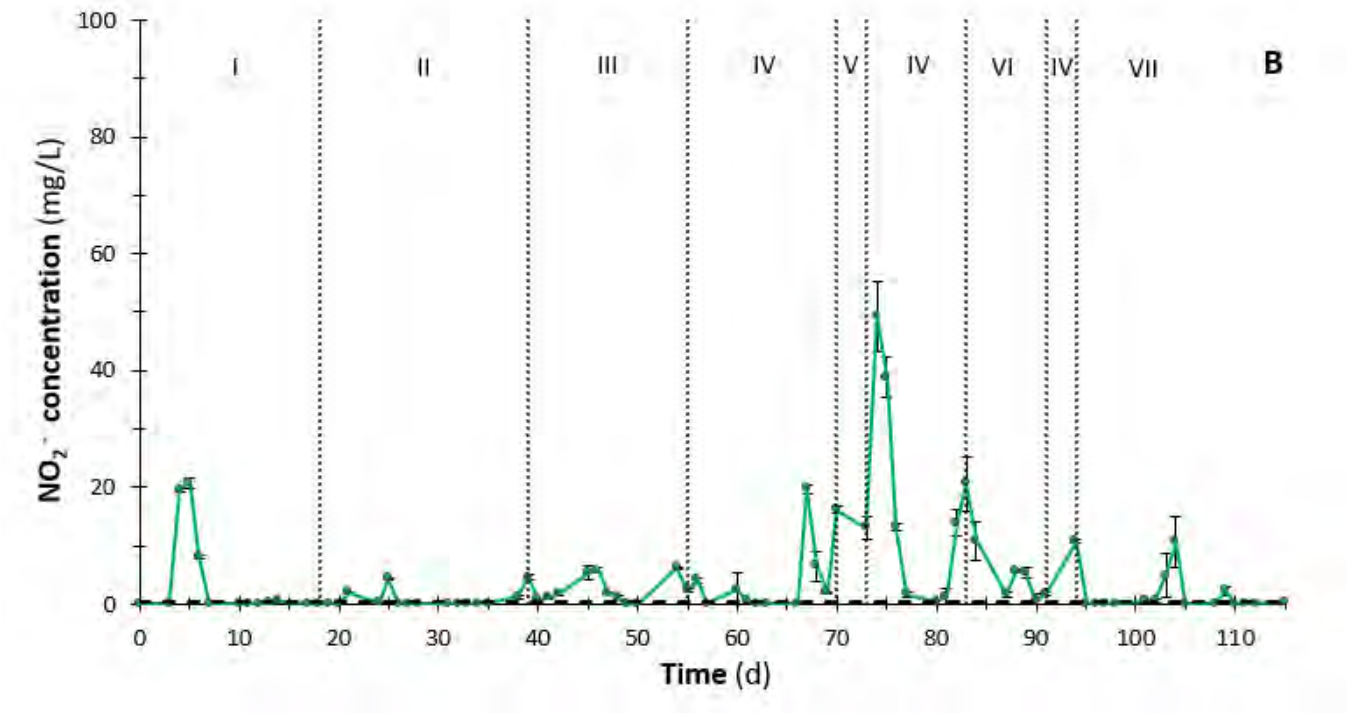

Figure 1 – Mean nitrate (NO_3^-) (A) and nitrite (NO_2^-) (B) concentration trend during the operation of the two bioreactors. Daily concentration (●), NO_3^- and NO_2^- regulatory limit (....).

References

[1] E. Abascal, L. Gómez-Coma, I. Ortiz, and A. Ortiz, "Global diagnosis of nitrate pollution in groundwater and review of removal technologies," *Sci. Total Environ.*, vol. 810, 2022, doi: 10.1016/j.scitotenv.2021.152233.

[2] L. Wu *et al.*, "Denitrifying biofilm processes for wastewater treatment: Developments and perspectives," *Environ. Sci. Water Res. Technol.*, vol. 7, no. 1, pp. 40–67, 2021, doi: 10.1039/d0ew00576b.

[3] T. H. Le-Lam, H. H. Lam, H. P. Phan, T. Nguyen, and T. Dang-Bao, "Thioglycolic acid-functionalized gold nanoparticles: Capping agent-affected color perception stability towards nitrate sensing purpose," *Mater. Today Proc.*, vol. 66, pp. 2720–2725, 2022, doi: 10.1016/j.matpr.2022.06.502.

[4] R. Eamrat, Y. Tsutsumi, T. Kamei, W. Khanichaidecha, T. Ito, and F. Kazama, "Microbubble application to enhance hydrogenotrophic denitrification for groundwater treatment," *Environ. Nat. Resour. J.*, vol. 18, no. 2, pp. 156–165, 2020, doi: 10.32526/ennrj.18.2.2020.15.

[5] P. Li, Y. Wang, J. Zuo, R. Wang, J. Zhao, and Y. Du, "Nitrogen Removal and N 2 O Accumulation during Hydrogenotrophic Denitri fi cation : In fl uence of Environmental Factors and Microbial Community Characteristics," 2017, doi: 10.1021/acs.est.6b00071.

[6] F. Di Capua, F. Pirozzi, P. N. L. Lens, and G. Esposito, "Electron donors for autotrophic denitrification," *Chem. Eng. J.*, vol. 362, no. 3, pp. 922–937, 2019, doi: 10.1016/j.cej.2019.01.069.

[7] S. Mills *et al.*, "Unifying concepts in methanogenic, aerobic, and anammox sludge granulation," *Environ. Sci. Ecotechnology*, vol. 17, 2024, doi: 10.1016/j.ese.2023.100310.

Title: Management of the drinking water supply chain under climate change: new threats require new strategies

Author(s): Beatrice Cantoni[1,*], Marco Matracchi[1], Mattia Stefanoni[1], Beatrice Bastante[1], Ilenia Epifani[2], Manuela Antonelli[1]

[1] *Politecnico di Milano, Department of Civil and Environmental Engineering (DICA), Piazza Leonardo da Vinci 32, 20133 Milan, Italy*
[2] *Politecnico di Milano, Department of Mathematics (DMAT), Piazza Leonardo da Vinci 32, 20133 Milan, Italy*

Keyword(s): adsorption; climate change; contaminants of emerging concern; disinfection; microorganisms; natural organic matter

Abstract

Direct consequences of climate change are represented by both the increase of air and water temperature and the alteration of precipitation patterns, characterized by longer droughts periods and more intense precipitations. These modifications impact on water quality, affecting the presence of microorganisms, natural organic matter (NOM), and contaminants of emerging concern (CECs). Such quality parameters are indeed crucial to provide consumers with safe drinking water, making the understanding of their variation patterns of paramount importance, to tune proper treatment schemes to minimize the human health risk. The goal of this work is to develop a holistic approach to increase the overall preparedness of the drinking water sector with respect to the need of upgrading the drinking water supply systems, comprising the plants and the distribution networks. Concerning CECs and NOM removal, the adsorption process was assessed by: (i) meta-analysis of literature isotherm data to predict CECs removal extent, and (ii) lab experiments to optimize NOM removal with respect to the type of activated carbon and the EBCT value. Then, an analysis of full-scale monitoring data from an Italian Water Utility was performed to support operators in the correct management of distribution network, identifying the most vulnerable monitoring locations with respect to both microbiological and chemical risk.

Introduction

Climate change has impacts not only on water quantity, but also on water quality, such as Natural Organic Matter (NOM), microorganisms and contaminant of emerging concern (CECs) [1,2,3].
If NOM is not properly removed, a greater extent of by-products formation could be assumed during disinfection; actually, an increase of the biological activity supported by the higher content of NOM could also be expected, (i) representing a threat for not-disinfected drinking water distribution networks, or (ii) increasing the disinfectant demand in disinfected networks. In addition, CECs spread cannot be overlooked, requiring proper removal processes, being adsorption on activated carbon, eventually coupled to ozonation, presently considered the best option [4].
Our goal is to provide some insights about adsorption and disinfection processes, to increase the overall preparedness of the drinking water sector with respect to the need of upgrading drinking water supply systems, comprising the treatment plants and the distribution networks. Since adsorption on activated carbon represents a valid strategy for reducing both CECs and NOM, considered as main precursors of

chlorination by-products, we focused on the evaluation of the performance of this process on both selected CECs, by a meta-model based on literature data, and NOM by lab experiments. Then, we focused also on the prioritization of the most vulnerable monitoring points within a distribution network to minimize chemical and microbiological risk for consumers.

Materials and Methods

Firstly, a literature review was performed retrieving isotherms data for 10 per- and poly-fluorinated substances (PFAS) and 23 pharmaceuticals and personal care products (PPCPs). These data were processed by a meta-analysis, clustering based on two climate-affected water characteristics (initial target CECs and NOM concentrations) and one operating parameter (activated carbon dose). The Kruskal-Wallis test was used to evaluate the differences in the distributions of the adsorption capacity (q_e, $\mu g_{CEC}/mg_{AC}$) within different clusters.
About lab experiments, the Rapid Small Scale Column Test (RSSCT) apparatus was adopted, varying the Empty Bed Contact Time (EBCT) and assuming the constant diffusivity model. The EBCT values (8 to 15 minutes) were selected based on a statistical analysis considering the full-scale adsorbers EBCT managed by the Water Utility that provided monitoring data. Tests were performed comparing three activated carbons, with a different porosity, and varying the concentration and type of NOM, evaluated by absorbance and fluorescence spectroscopic methods.
As for prioritization of monitoring locations, water quality data (residual chlorine, electrical conductivity at 20°C, pH, temperature, *E. coli*, *Pseudomonas aeruginosa*, total trihalomethanes TTHMs) provided by an Italian Water Utility, over a period of 14 years, were analysed through a clustering analysis.

Results and Discussion

Based on available literature studies about climate change impacts on the most common water quality parameters (Figure 1), a general increasing trend is highlighted, with the exception of NOM content.

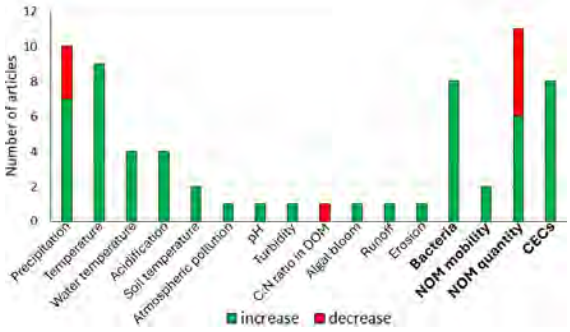

Figure 1. Number of literature studies concerning the effects of climate change on different water quality parameters (green bar: the parameter is expected to increase; red bar: the parameter is expected to decrease).

Having in mind the expected CECs concentration increase, we explored the possibility to gain insights on the potential changes in CECs adsorption performance in climate change scenarios, exploiting data obtained in experiments adopting high CECs concentrations, depending on NOM content. A cluster analysis was conducted on isotherms data: five clusters were identified characterized by different experimental conditions and adsorption capacity q_e, as shown in Figure 2. Clusters 4 and 5 group 70.4% of the data: they are characterized by very high CECs concentrations, but no NOM content, providing not reliable information about CECs removal extent. However, focusing on clusters 1 to 3, the initial CECs concentration is comparable, while the NOM content decreases, as well as the adsorption capacity q_e, from 0.25 µg/mg in cluster 3 to 0.07 µg/mg in cluster 1. This relevant reduction can be

attributed to NOM competition, suggesting worst adsorption performances towards CECs in case of NOM increase due to climate change.

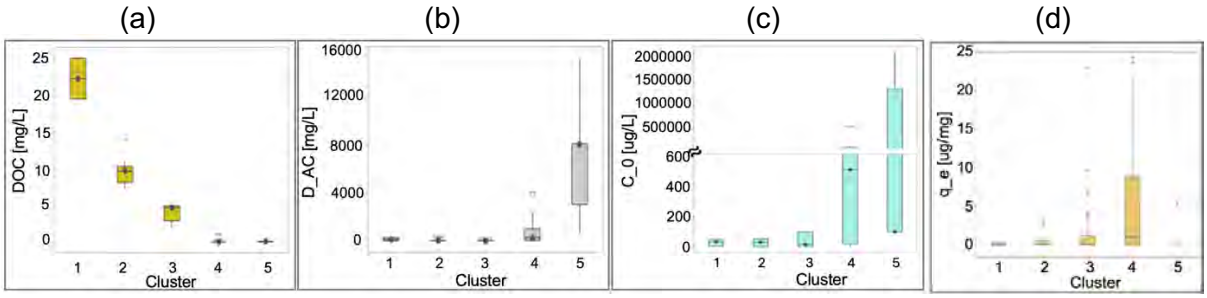

Figure 2. Distributions among the identified clusters of: (a) NOM concentration expressed as Dissolved Organic Carbon (DOC), (b) activated carbon dose, (c) initial CECs concentration, (d) adsorption capacity q_e.

As for NOM removal, we compared a real water matrix, sampled in a drinking water treatment plant managed by the Water Utility that provided monitoring data, with the same water matrix spiked with Suwannee River NOM (SRNOM) and Humic Acid (HA), both at a concentration of 3 mg/L. Figure 3 illustrates the obtained breakthrough curves as a function of NOM content, activated carbon type and EBCT. Macroporous activated carbon proved to be the most efficient in NOM removal with longer operating times, particularly adopting mid-to-high EBCT values, compared to microporous and mesoporous activated carbons: fixing the breakthrough at 50% of the initial NOM concentration and the EBCT at 11 min, the bed volumes (volume of treated water normalized with respect to the carbon bed volume) were <500, 500-1000 and >3000 respectively for the microporous, mesoporous and macroporous activated carbons.

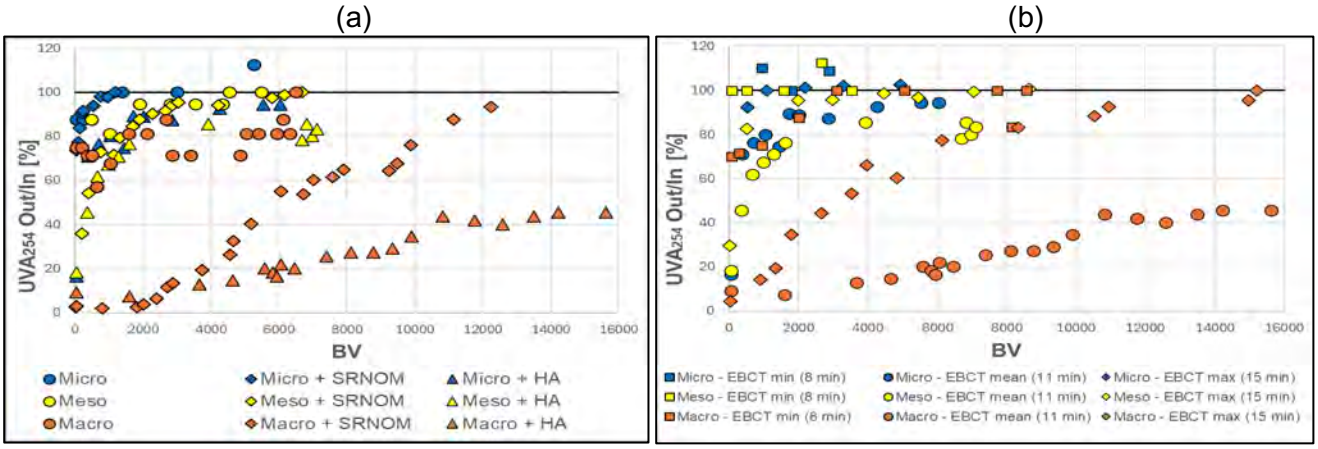

Figure 3. Breakthrough curves (referred to absorbance at 254 nm, 1 cm optical path) testing different (a) types of NOM (EBCT = 11 min) and (b) EBCT values (real water matrix, without spikes).

Finally, we focused on prioritizing the monitoring locations along the distribution network which could be more vulnerable for the concentration of disinfection by-products and/or the bacterial load. Results of the cluster analysis are shown in Figure 4. Five clusters were identified. It can be noted that cluster 3 is the one characterized by the higher residual chlorine values, mostly above 0.08 mg/L. Grouping data according to residual chlorine concentration under (lowCl_2) or above (highCl_2) 0.08 mg/L, we evaluated the bacterial load summarized in Table 1 and the concentration of TTHMs shown in Figure 4b. It emerges that the bacterial load tends to increase when the residual chlorine concentration is lower,

while the TTHMs tends to decrease, even if many outliers are present. This suggests the importance of a correct management of the disinfection process, to find the optimal trade-off between microbiological and chemical risk.

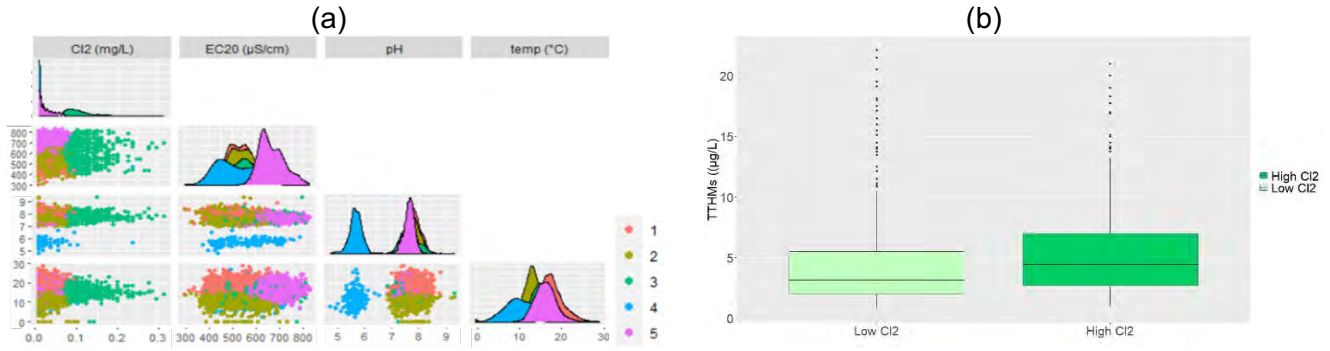

Figure 4 (a) Cluster analysis by residual chlorine (Cl_2), electrical conductivity (EC20), pH and temperature. (b) Boxplots of TTHMs concentration in monitoring points grouped for residual chlorine concentration under ($LowCl_2$) and over ($HighCl_2$) 0.08 mg/L.

Table 1 Descriptive statistics (mean ± standard deviation) of bacteria in monitoring points along the distribution network depending on residual chlorine concentration under ($LowCl_2$) and over ($HighCl_2$) 0.08 mg/L.

	E. coli (CFU/100 mL)	**Enterococci** (CFU/100 mL)	**Coliforms @ 37°C** (CFU/100 mL)	***P. aeruginosa*** (CFU/250 mL)
$LowCl_2$	0.001±0.033	0.006±0.090	0.15±1.78	0.02±0.18
$HighCl_2$	-	0.003±0.052	0.04±0.73	-

Conclusions

We presented three key findings: (i) meta-analysis on isotherm data stressed how adsorption on activated carbon becomes less effective in removing CECs, due to competition effects in case of NOM content increase; (ii) the porosity of activated carbon revealed to be essential for an efficient NOM removal; (iii) the challenge to identify an optimal trade-off for final disinfection to balance microbiological and chemical risk. This underscores the need for further investigation into the impact of climate change on NOM dynamics and the development of modelling tools to help balancing the microbiological and chemical risk during the management of the distribution network.

This work has been carried out within the safeCREW project (grant agreement 101081980) and the AXA Research Fund Post-Doctoral Fellowship.

References

[1] Creed I.F., Bergström A., Trick C.G., Grimm N.B., Hessen D.O., Karlsson J., Kidd K.A., Kritzberg E., McKnight D.M., Freeman E.C., Senar O.E., Andersson A., Ask J., Berggren M., Cherif M., Giesler R., Hotchkiss E.R., Kortelainen P., Palta M.M., Vrede T., Weyhenmeyer G.A. “Global change-driven effects on dissolved organic matter composition: Implications for food webs of northern lakes”, Global Change Biology, 24, 3692-3714 (2018)
[2] Lipczynska-Kochany E. ”Effect of climate change on humic substances and associated impacts on the quality of surface water and groundwater: A review”, Science of the Total Environment, 640-641, 1548-1565 (2018)
[3] O’Flynn, D., Lawler, J., Yusuf, A., Parle-Mcdermott, A., Harold, D., Mc Cloughlin, T., Holland, L., Regan, F., White, B. A review of pharmaceutical occurrence and pathways in the aquatic environment in the context of a changing climate and the COVID-19 pandemic", Analytical Methods, 13(5), 575-594 (2021)
[4] Cantoni B., Ianes J., Bertolo B., Ziccardi S., Maffini F., Antonelli M. “Adsorption on activated carbon combined with ozonation for the removal of contaminants of emerging concern in drinking water”, J. Environ. Manage., 350, 119537 (2024)

A validated and upgraded turbidity robustness index aligned with the new drinking water EU Directive 2020/2184

Authors: Federica De Marines*[1], Santo Fabio Corsino[1], Alida Cosenza[1], Marco Capodici[1], Michele Torregrossa[1], Gaspare Viviani[1]

[1] *Department of Engineering, University of Palermo, Palermo, Italy, federica.demarines@unipa.it*

Keyword(s): Drinking water, Drinking water treatment plant, Robustness index, Turbidity

Abstract

This study has introduced a turbidity robustness index (TRI), named TRI_{95B}, designed to serve as an early warning tool capable of identifying potential issues by detecting deviations from water quality standards. A comprehensive three-year monitoring program dataset at an operational drinking water treatment plant (DWTP) was used for comparison and validation against existing TRIs.

Introduction

Drinking water treatment plants (DWTPs) play a critical role in providing safe drinking water to communities. In recent years, climate change has exacerbated challenges by affecting the quality of raw water sources [1]. This poses operational challenges for DWTPs to meet regulatory standards [2, 3]. Thus, compliance with turbidity regulations is essential to mitigate health risks and disinfection by-product formation. The EU Directive 2020/2184 [4] strengthened drinking water safety by imposing stricter monitoring and control measures. In more detail, turbidity at the water supply plant must be lower than 0.3 NTU in 95% of samples and none must exceed 1 NTU. This represents a notable improvement over previous regulations, emphasizing the need for DWTPs to exhibit robustness in maintaining water quality despite external factors. Previous literature [5,6] has proposed some Turbidity Robustness Indices (TRIs) to address the ability of a process within a DWTP to maintain performance despite variations in source water quality and changing conditions. Previous TRIs proposed by Huck and Coffey [7] and Li and Huck [8] (TRI_{90E} and TRI_{90D}, respectively), had limitations due to arbitrary weighting scores and complexity. Advancements (TRI_{90J}) introduced by Hartshorn et al. [9] consider the percentage of time turbidity meets goals but overlooks performance variability during regulation compliance. In this light, this study aimed to assess existing TRIs considering new regulations. Additionally, a modified TRI was proposed and validated to address previous limitations and comply with regulatory demands. The new TRI was compared with those already available in the literature and validated using a dataset derived from an intensive three-year monitoring program performed at a DWTP.

Materials and Methods

Table 1 reports the main TRI existing in the literature. The values assumed by the TRI are categorized into six classes that define the class of system operation quality [8] (Table 1).
The new TRI, from now called TRI_{95B}, proposed in this study took inspiration from the model proposed by Hartshorn and co-authors [9]. The TRI_{95B} is reported below:

$$TRI_{95B} = \left\{\left[B \times \left(1 - \frac{G\%}{100}\right) \times \frac{T_{95}}{T_{goal}}\right] + \left[B \times \frac{T_{50}}{T_{goal}} \times \frac{G\%}{100}\right] + \left[(1-B)\left(\frac{T_{100}}{T_{max}} + 1\right)\right]\right\} \times 100$$

Table 1. Classification of system operation with robustness index value and mathematical significance

Existing TRIs

$$TRI_{90E} = \frac{1}{2}\left(\frac{T_{90}}{T_{50}} + \frac{T_{50}}{T_{goal}}\right) \quad [7]$$

$$TRI_{90D} = \left(A_1\frac{T_{90}}{T_{50}} + A_2\frac{T_{50}}{T_{goal}}\right) \times 100 \quad [8]$$

$W \leq N \rightarrow$ if $\frac{T_{90}}{T_{50}} \leq \frac{T_{50}}{T_{goal}} \rightarrow$ then A1 = 0.9; A2 = 0.1;
$W \leq N \rightarrow$ if $\frac{T_{90}}{T_{50}} > \frac{T_{50}}{T_{goal}} \rightarrow$ then A1 = 0.1; A2 = 0.9;
$W > N \rightarrow$ if $\frac{T_{90}}{T_{50}} \leq \frac{T_{50}}{T_{goal}} \rightarrow$ then A1 = 0.1; A2 = 0.9;
$W > N \rightarrow$ if $\frac{T_{90}}{T_{50}} > \frac{T_{50}}{T_{goal}} \rightarrow$ then A1 = 0.9; A2 = 0.1

$$W = \left(\frac{T_{50}}{T_{goal}} + \frac{T_{60}}{T_{goal}} + \frac{T_{70}}{T_{goal}} + \frac{T_{80}}{T_{goal}} + \frac{T_{90}}{T_{goal}}\right) \times 10$$

$N = 50$

$$TRI_{90J} = \left\{\left[\left(1 - \frac{G\%}{100}\right) \times \frac{T_{90}}{T_{50}}\right] + \left[\frac{T_{50}}{T_{goal}} \times \frac{G\%}{100}\right]\right\} \times 100 \quad [9]$$

G% is the percentage time below the turbidity goal within the run

Class	TRI	Mathematical significance
Very stable	<60	$T_{50} << T_{goal}$ and T_{90} < 50% of T_{goal}
Stable	60–100	T_{50} = 60-75% of T_{goal} and $T_{90} \approx T_{goal}$
Slightly disturbed	100–130	$T_{50} < T_{goal}$ and T_{90} = 30% over T_{goal}
Moderately disturbed	130–160	T_{50} = 20% over T_{goal} and T_{90} = 60-80% over T_{goal}
Upset	160–200	T_{50}, T_{90} = 60-80% over T_{goal}
Severely upset	>200	T_{50}, T_{90} = 100% over T_{goal}

The main modifications involved replacing the 90th percentile with the 95th to align the index with the new regulation. Furthermore, a new term T_{100}/T_{max} has been added, which indicated if the maximum turbidity value measured in a run exceeded the threshold value that must not be exceeded according to the EU regulation (1 NTU). The DWTP selected for the present study was located in Sicily (Italy), full-scale plant data (including turbidity) were collected for 3 years (2021-2023). Turbidity data for TRIs assessment were considered at the outlet of the disinfection tank. All the above TRIs were calculated with reference to the new regulation (T_{goal} < 0.3 NTU).

Results

Turbidity data collected from the SCADA system in the effluent water are reported in Figure 1.

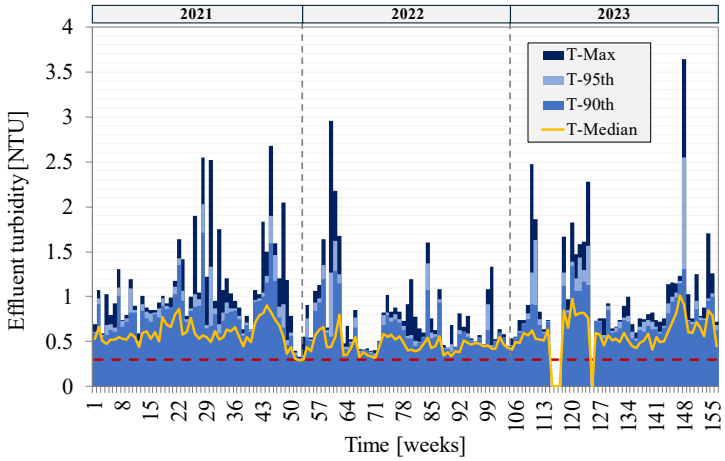

Figure 1. Trends of the main statistics (maximum, 95,90 percentiles, and median) of turbidity data in effluent water (the red dotted line indicates the limit set by the EU 2020/2184 of 0.30 NTU)

While median turbidity remained relatively stable at 0.55±0.15 NTU, the 95th percentile and maximum values showed greater fluctuations, averaging at 0.81±0.34 NTU and 1.01±0.54 NTU respectively.

Although the median turbidity stayed below the 1 NTU limit set by the old Directive 98/83, several exceedances occurred when considering the 95th percentile, as required by new regulations. This pointed out the importance of the plant's ability to handle turbidity fluctuations, as mandated by the new regulation, which demands a more cautious approach. Overall, the plant demonstrated a lower capacity to maintain consistent effluent turbidity when considering the 95th percentile, highlighting the need for a thorough analysis of its robustness in compliance with the new regulation.
The trends of the TRIs are shown in Figure 2, whereas the frequency of TRIs occurrence within the robustness classes is reported in Table 2.

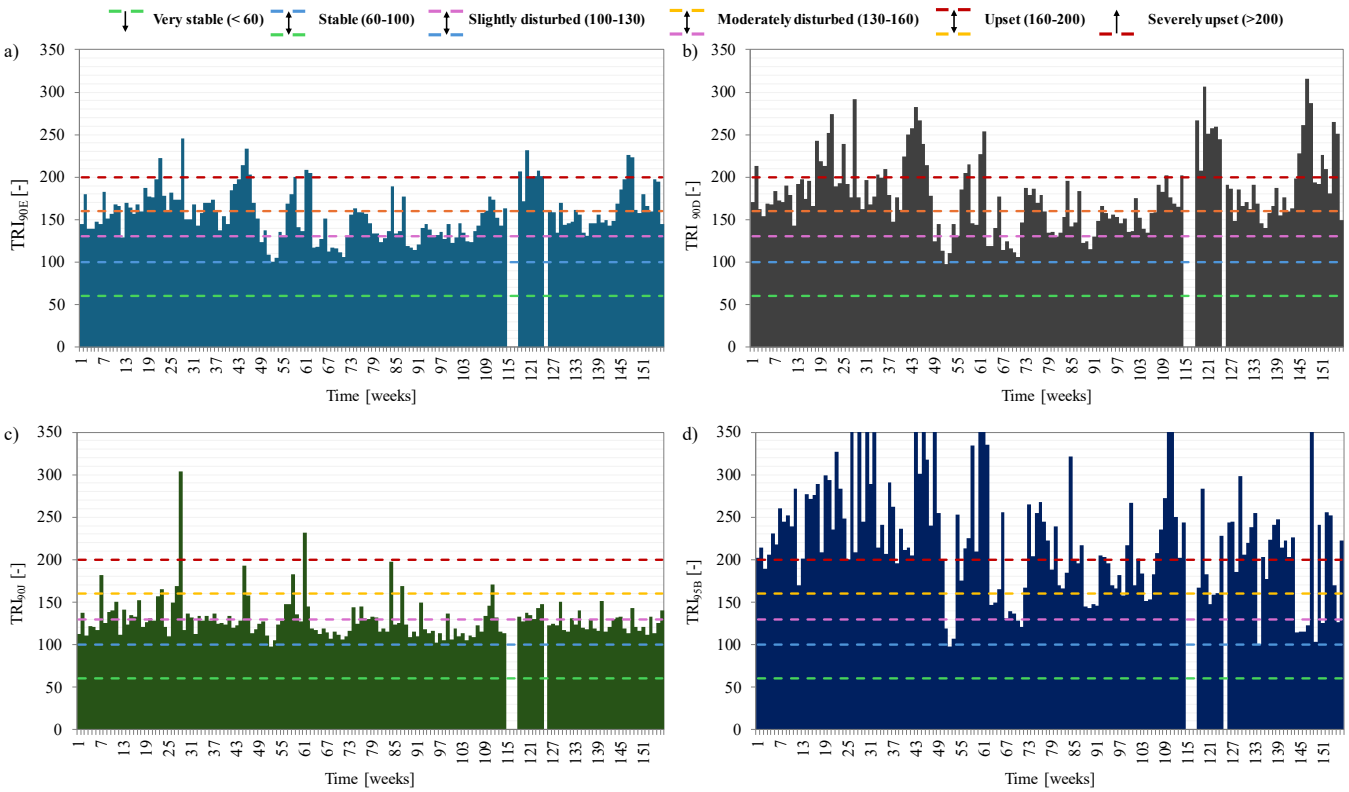

Figure 2. Trends of TRIs scores during the 2021-2023 period assuming a T_{goal} of 0.3 NTU

Table 2. Occurrence of TRIs within a class of system operation quality (T_{goal} = 0.3 NTU)

TRI class	TRI_{90E}	TRI_{90D}	TRI_{90J}	TRI_{95B}
Very stable	0	0	0	0
Stable	0	1	1	1
Slightly disturbed	25	15	91	12
Moderately disturbed	66	38	50	14
Upset	46	60	8	24
Severely upset	15	38	2	101
Not available	4	4	4	4
Total	156	156	156	156

TRI_{90E} and TRI_{90J} resulted quite low, with average values of 157±29 and 129±23, respectively. Thus, according to the response provided by those TRI, the plant fell mainly within the "slightly disturbed" and "moderately disturbed" classes (Table 2), despite the main statistical indicators of the effluent turbidity

(median and T_{90}) consistently exceeded the 0.30 NTU limit. The results provided by the TRI_{90E} indicated that the DWTP was affected by process instability. However, the absolute values of the index were generally low, and only in a few runs indicated an "upset" class or higher. Similarly, regarding TRI_{90J} this occurrence was even more evident. As reported in previous studies, TRI_{90J} was not a reliable indicator of performance against a target because it favoured variation rather than performance against a goal [9, 10]. TRI_{90D} was higher compared to the previous TRIs (180±45). However, it still highlighted the same criticalities arose for the previous indices, mainly linked to the fact that the T_{goal} exceedance was not adequately identified by the TRI value. TRI_{95B} resulted much higher compared to the other TRIs, averaging 228±84. Overall, TRI_{95B} was the index that fell more frequently (101 out of 156 weeks) into the "severely upset" class (Table 2), indicating a significant exceedance of the maximum turbidity value at the DWTP outlet. Unlike the previous TRIs, TRI_{95B} showed a closely correspondence to the real plant performances.

Conclusions

This study introduces TRI_{95B}, a robustness index designed for DWTPs to address limitations of existing indices amidst evolving regulatory standards. TRI_{95B} exhibits enhanced accuracy and reliability, particularly in aligning with new regulations requiring turbidity lower than 0.30 NTU. It effectively identified deviations from desired water quality standards, offering a robust diagnostic tool for assessing plant performance. Its implementation could be helpful to reduce DWTP vulnerability and ensures continuous delivery of safe drinking water to consumers.

References

[1] Calero Preciado, C., Boxall, J., Soria-Carrasco, V., Martínez, S., Douterelo, I., 2021. Implications of Climate Change: How Does Increased Water Temperature Influence Biofilm and Water Quality of Chlorinated Drinking Water Distribution Systems? Front. Microbiol. 12. https://doi.org/10.3389/fmicb.2021.658927.
[2] Quevedo-Castro, A., Bustos-Terrones, Y.A., Bandala, E.R., Loaiza, J.G., Rangel-Peraza, J.G., 2022. Modeling the effect of climate change scenarios on water quality for tropical reservoirs. J. Environ. Manage. 322, 116137. https://doi.org/10.1016/j.jenvman.2022.116137.
[3] Doménech, E., Martorell, S., Kombo-Mpindou, G.O.M., Macián-Cervera, J., Escuder-Bueno, I., 2022. Risk assessment of Cryptosporidium intake in drinking water treatment plant by a combination of predictive models and event-tree and fault-tree techniques. Sci. Total Environ. 838. https://doi.org/10.1016/j.scitotenv.2022.156500.
[4] Directive EU 2184/2020, 2020. Directive (EU) 2020/2184 of the European Parliment and of the Council of 16 December 2020 on the quality of water intended for human consumption. Off. J. Eur. Union 2020, 1–62.
[5] Hurst, A.M., Edwards, M.J., Chipps, M., Jefferson, B., Parsons, S.A., 2004. The impact of rainstorm events on coagulation and clarifier performance in potable water treatment. Sci. Total Environ. 321, 219–230. https://doi.org/10.1016/j.scitotenv.2003.08.016.
[6] Jung, D., Lee, S., Kim, J.H., 2019. Robustness and water distribution system: State-of-the-art review. Water (Switzerland) 11, 1–12. https://doi.org/10.3390/w11050974.
[7] Huck, P.M., Coffey, B.M., 2004. The importance of robustness in drinking-water systems, in: Journal of Toxicology and Environmental Health - Part A. Taylor & Francis, pp. 1581–1590. https://doi.org/10.1080/15287390490491891.
[8] Li, T., Huck, P.M., 2008. Improving the evaluation of filtration robustness. J. Environ. Eng. Sci. 7, 29–37. https://doi.org/10.1139/S07-032.
[9] Hartshorn, A.J., Prpich, G., Upton, A., Macadam, J., Jefferson, B., Jarvis, P., 2015. Assessing filter robustness at drinking water treatment plants. Water Environ. J. 29, 16–26. https://doi.org/10.1111/wej.12094.
[10] Nemani, K.S., Peldszus, S., Huck, P.M., 2023. Practical Framework for Evaluation and Improvement of Drinking Water Treatment Robustness in Preparation for Extreme-Weather-Related Adverse Water Quality Events. ACS ES T Water 3, 1305–1313. https://doi.org/10.1021/acsestwater.2c00627.

Title: Effect of applied current on simultaneous bioelectrochemical denitrification and desalination of groundwater

Author(s): Seyedmehdi Hosseini*[1], Alessandra Carucci[1], Cristiano Armas[1], Narcis Pous[2], Sebastià Puig[2], Stefano Milia[3]

[1]Department of Civil-Environmental Engineering and Architecture (DICAAR), University of Cagliari, Cagliari, Italy, seyedmehdi.hosseini@unica.it, carucci@unica.it, cristiano.armas@unica.it
[2]Laboratory of Chemical and Environmental Engineering (LEQUiA), Institute of the Environment, University of Girona, Girona, Spain, narcis.pous@udg.edu, sebastia.puig@udg.edu
[3]Institute of Environmental Geology and Geoengineering, National Research Council, Cagliari, Italy, stefano.milia@cnr.it

Keyword(s): bioelectrochemical systems, nitrate, salinity, groundwater, chlorine recovery

Abstract

High levels of nitrate and salinity in groundwater, often derived from agricultural and industrial sources, pose significant environmental and health risks, limiting its usage. Bioelectrochemical systems (BES) have emerged as a promising technology for electro bioremediating nitrate-contaminated groundwater due to their cost-effectiveness and minimal secondary pollution. This study evaluated the ability of BES to remove nitrates and reduce salinity from synthetic groundwater using a three-chamber cell. The research focused on optimizing the applied current, a crucial operational factor, for simultaneous denitrification at the bio-cathode, desalination in the central chamber, and production of free chlorine in the anodic chamber. The currents tested were 6, 8, 10, and 12 mA. Increasing the current from 6 to 12 mA enhanced both nitrate removal rate and efficiency from 66.8±12.1 gNO_3^--N $m^{-3}d^{-1}$ (69±8%) to 100.5±0.7 gNO_3^--N $m^{-3}d^{-1}$ (99±2%), electrical conductivity (EC) removal from 12.7±2.1% to 18.5±3.5%, and free chlorine production rate from 0.6±0.02 mg $L^{-1}d^{-1}$ to 3.7±0.1 mg $L^{-1}d^{-1}$. These findings open the door to scaling up the technology.

Introduction

Nitrate is a prevalent pollutant in groundwater resources worldwide, originating from various sources such as agricultural fertilizers, manure, solid waste infiltration, and sewage leakage [1]. Additionally, high salinity levels in groundwater-often related to industrial and agricultural activities-can severely limit its potential uses [2]. Bioelectrochemical systems (BES) represent a cost-effective, environmentally friendly technology for the remediation of nitrate-contaminated groundwater through autotrophic denitrification at the bio-cathode [3,4]. Extensive research on autotrophic denitrification via BES has been conducted, ranging from initial proof of concept to studies on underlying mechanisms and potential technological applications [5]. This study investigates the effect of the applied current on a three-chamber BES treating model groundwater for simultaneous nitrate and salinity removal, while also creating a valuable resource, such as chlorine, which can be used as a disinfectant.

Materials and methods

A three-chamber bioelectrochemical cell made of polycarbonate was operated. It consisted of an anodic

chamber (8x8x2 cm^3), a bio-cathodic chamber (8x8x2 cm^3), and a central chamber (8x8x0.5 cm^3). The central compartment was separated from the cathodic and anodic compartments by a cation exchange membrane (CEM, 64 cm^2) and an anion exchange membrane (AEM, 64 cm^2), respectively. Carbon felt (64 cm^2) served as the bio-cathode (working electrode), paired with an Ag/AgCl reference electrode. The counter-electrode was a titanium mesh (area of 14 cm^2) coated with mixed metals oxide (Ti-MMO). A synthetic medium, prepared according to [6], was mixed in an 80:20 v/v ratio with the effluent from a parent denitrifying BES reactor (50:50 v/v during startup) and fed continuously to the bio-cathode chamber under intense recirculation. The resulting influent NO_3^--N concentration and conductivity were 28.1±2.3 mg L^{-1} and 3.9±0.2 mS cm^{-1}, respectively. The effluent from the cathodic compartment was directed to the central chamber for desalination. The anodic compartment was filled with tap water and operated in batch mode with intense recirculation. Tap water was replaced weekly to prevent excessive accumulation of chlorine [6]. The pH in the cathodic chamber was kept below 8 by injecting 1M HCl into the cathode recirculation line. All electrodes were connected to a multichannel potentiostat set to galvanostatic mode. Four different currents (i.e. 6, 8, 10, and 12 mA, corresponding to the current density of 1.2-2.4 A $m^{-2}_{membrane}$) were applied, maintaining a constant hydraulic retention time (HRT) of 7 hours, considering the volumes of the biocathode and central chambers.

Results and discussion

The effect of applied current on the denitrification and desalination performance was investigated. The average removal efficiencies for NO_3^--N, EC, chloride, and the consumption of acid with different currents are presented in Figure 1. Denitrification occurred in the biocathode chamber, while the electromigration of ions through the membranes, resulting in desalination, occurred in the central chamber. The results indicated that increasing the applied current from 6 to 12 mA enhanced the nitrate removal rate from 66.8±12.1 gNO_3^--N $m^{-3}d^{-1}$ to 100.5±0.7 gNO_3^--N $m^{-3}d^{-1}$, the nitrate removal efficiency from 68.6±8.2% to 99.1±1.8%, and the EC removal efficiency from 12.7±2.1% to 18.5±3.5%. These findings are consistent with those reported by Puggioni et al. [6]. Notably, no nitrite nor nitrous oxide were detected throughout the experiment, suggesting full conversion of nitrates into dinitrogen gas (N_2). However, an increasing trend in acid dosage from 9.4 mL d^{-1} to 15.8 mL d^{-1} was observed with increasing current from 6 to 12 mA.

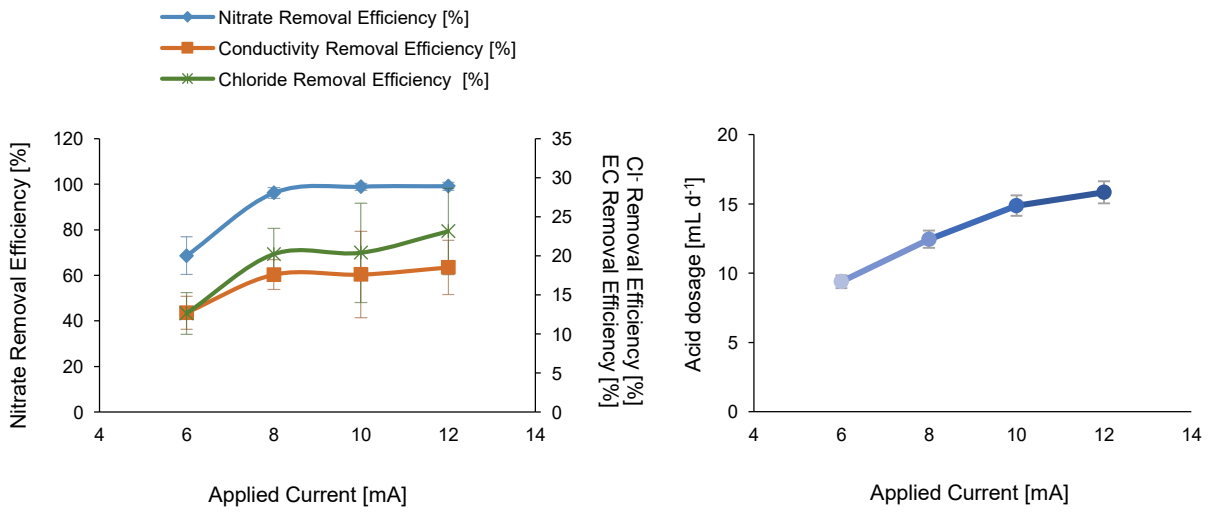

Figure 1. The effect of applied current on NO_3^--N, EC, and Cl^- removal efficiencies and acid dosage

The coulombic efficiency increased with the applied current, and it was always above 100%, as all the tested currents were higher than the theoretically required for nitrate removal (approx. 5.8 mA). The specific energy consumption (SEC) increased from $4.06\times10^{-2}\pm0.69\times10^{-2}$ to $5.85\times10^{-2}\pm0.86\times10^{-2}$ kWh $g^{-1}NO_3^-$-$N_{removed}$ as the current increased from 6 to 12 mA. This is comparable to a SEC of approx. 8×10^{-2} kWh $g^{-1}NO_3^-$-$N_{removed}$ reported by Puggioni et al. [4] with an applied current of 10 mA and an HRT of 7.3 h (further decreasing the HRT to 2.4 h led to a lower SEC of $5.1\times10^{-2}\pm0.7\times10^{-2}$ kWh $g^{-1}NO_3^-$-$N_{removed}$, but also to the formation of intermediates which indicated the worsening of denitrification performance). In terms of water treated, the SEC at an applied current of 12 mA was 1.33 kWh m^{-3}, comparable to SEC values observed in conventional membrane techniques for nitrate removal [7]. Under these conditions, based on an energy cost of 0.18 € kWh^{-1} (Eurostat, 2023, Semester II), the energy-related cost was 0.24 € m^{-3}.

Changes in the concentration of Na^+, K^+, and Cl^- in the influent, biocathode chamber, and effluent at different current levels are depicted in Figure 2. As the current increased, the accumulation of cations in the biocathode chamber increased. Though significant Cl^- removal was obtained in the central compartment, the effluent's chloride concentration increased relative to the influent levels due to HCl dosing for pH control in the biocathode. This caused the effluent EC to remain above the threshold limit of 2.5 mS cm^{-1} as specified by the 98/83/EC Directive. Furthermore, the migration of chloride ions into the anodic chamber increased with the current, enhancing chlorine production, which is economically beneficial and offers practical potential for water disinfection [8].

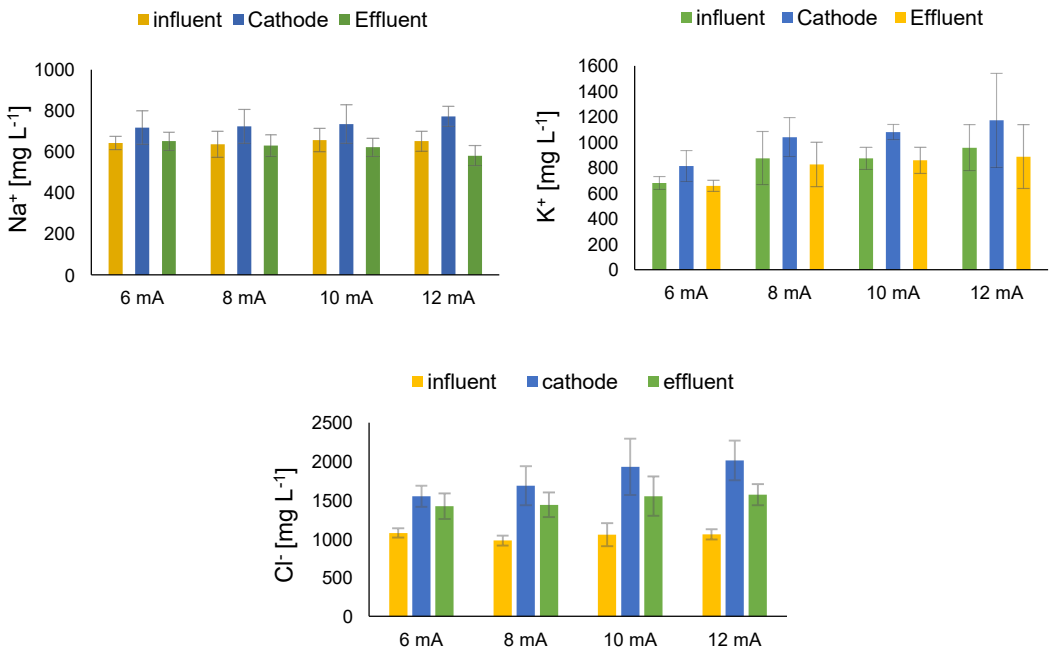

Figure 2. The concentration of Na^+, K^+, and Cl^- in the influent, biocathode, and effluents

Last but not least, the effect of the applied current on creating a concomitant valuable by-product (chlorine as a disinfectant) was assessed in Figure 3. As a catalytic process the higher the current applied, the higher the chlorine production rate which increased from 0.59±0.02 mg $L^{-1}d^{-1}$ to 3.65± 0.09 mg $L^{-1}d^{-1}$. Such product could be used *in situ* in water treatment plants reducing the need for additional chemical treatments, improving the overall water quality, and lowering operational costs.

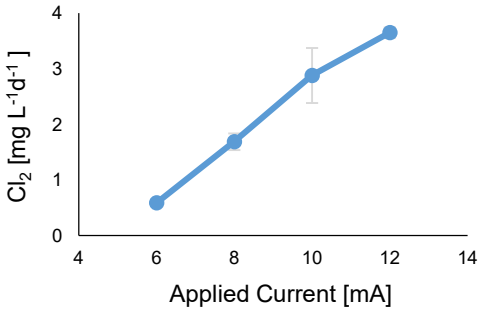

Figure 3. Effect of applied currents on free chlorine production rate

Conclusion

As the current intensity increased from 6 to 12 mA, improvements in denitrification and desalination performance were observed, alongside an increase in acid consumption. Although the nitrate removal efficiency reached 99.1±1.8% at 12 mA, the EC levels remained above the threshold limit of 2.5 mS cm^{-1}, suggesting that further process optimization is necessary. Additionally, the progressive accumulation of chloride ions in the anodic chamber resulted in enhanced free chlorine production, which offers economic benefits for water disinfection. When performing cost-effectiveness analyses for the investigated cell, it is crucial to consider both the benefits associated with chlorine production and the costs related to energy consumption and acid dosage, which should be carefully balanced.

Acknowledgements

We acknowledge financial support under the National Recovery and Resilience Plan (NRRP), Mission 4 Component 2 Investment 1.5 - Call for tender No.3277 published on December 30, 2021 by the Italian Ministry of University and Research (MUR) funded by the European Union – NextGenerationEU. Project Code ECS0000038 – Project Title eINS Ecosystem of Innovation for Next Generation Sardinia – CUP F53C22000430001- Grant Assignment Decree No. 1056 adopted on June 23, 2022 by the Italian Ministry of University and Research (MUR). Sebastià Puig is a Serra Hunter Fellow (UdG-AG-575) and acknowledges funding from the ICREA Academia award. LEQUiA [2021-SGR-01352] has been recognised as consolidated research group by Catalan Government.

References

[1] Cecconet D., Sabba F., Anastasi V., Bolognesi S., Callegari A., He Z., Capodaglio A.G., “Integrated experimental and modeling evaluation of removal efficiency and energy consumption for an autotrophic denitrifying biocathode”, Environ. Sci.: Water Res. Technol., 8, 1466, (2022).
[2] Li C., Gao X., Li S., Bundschuh J., “A review of the distribution, sources, genesis, and environmental concerns of salinity in groundwater”, Environ. Sci. Pollut. R., 27, 41157–41174, (2020).
[3] Xue L., Chen N., Zhao J., Yang C., Feng C., “Rice husk-intensified cathode driving bioelectrochemical reactor for remediating nitrate-contaminated groundwater”, Sci. Total Environ., 837, 155917, (2022).
[4] Puggioni G., Milia S., Unali V., Ardu R., Tamburini E., Pous N., Carucci A., Puig S., “Effect of hydraulic retention time on the electro-bioremediation of nitrate in saline groundwater”, Sci. Total Environ., 845, 157236, (2022).
[5] Ceballos-Escalera A., Pous N., Chiluiza-Ramos P., Korth B., Harnisch F., Bañeras L., Balaguer M.D., Puig S., “Electro-bioremediation of nitrate and arsenite polluted groundwater”, Water Res., 190, 116748, (2021).
[6] Puggioni G., Milia S., Dessì E., Unali V., Pous N., Balaguer M.D., Puig S., Carucci A., “Combining electro-bioremediation of nitrate in saline groundwater with concomitant chlorine production”, Water Res., 206, 117736, (2021).
[7] Mrabet H.E., Elazhar F., Kitanou S., Elazhar M., Mokhtari A., Taky M., Elmidaoui, A., “Comparison of diverse direct and hybrid membrane processes for nitrate removal from brackish water”, Desal. Water Treat., 273, 73-80, (2022).
[8] Batlle-Vilanova P., Rovira-Alsina L., Puig S., Balaguer M.D., Icaran P., Monsalvo V.M., Rogalla F., Colprim J., “Biogas upgrading, CO2 valorisation and economic revaluation of bioelectrochemical systems through anodic chlorine production in the framework of wastewater treatment plants”, Sci. Total Environ., 690, 352–360, (2019).

Title: Application of potassium ferrate to address emerging challenges in drinking water treatment plant

Author(s): Federica De Marines*[1], Maria Castiglione[1], Marco Capodici[1], Santo Fabio Corsino[1], Michele Torregrossa[1].

[1] *Department of Engineering, University of Palermo, Palermo, Italy, federica.demarines@unipa.it*

Keyword(s): Drinking water, ferrate, climate changes, manganese, turbidity, algal bloom.

Abstract

Besides quantitative impacts (e.g., floods and droughts), it is widely recognized that surface water quality is also affected by climate change. This results in higher concentrations of soluble metals, natural organic matter (NOM), turbidity, and algal blooms. Such changes place increasing strain on conventional water treatment systems, highlighting the need for more innovative approaches. Ferrate(VI) has been studied as a potential solution to address water crises triggered by climate change, either alone or in combination with traditional treatment chemicals to ensure safe drinking water.
The study shows that Fe(VI) offers significant promise, both as an alternative and a complement to conventional methods, helping to overcome climate-related challenges while preserving high standards of potable water quality.

Introduction

The latest Intergovernmental Panel on Climate Change (IPCC) report reveals that climate change is widespread, rapid, and intensifying [1]. Besides quantitative impacts (e.g., floods and droughts), it is widely recognized that surface water quality is also affected by climate change. According to a throughout literature review, it arose that the main effects of climate change in terms of water quality impacts are referred to three main concerns: (i) increase of soluble metals (Fe, Mn, Al) which are released from lake sediments under anoxic conditions [2,3], (ii) algal bloom due to the increase of water temperature in nutrients rich lakes [4], (iii) increase of natural organic matter (NOM) concentration and turbidity as a consequence of extreme precipitation events [5].
Manganese is commonly removed by using strong oxidants that convert soluble manganese (Mn^{2+}) into insoluble (Mn^{4+}) that can be separated through filtration [6]. Removal of NOM in drinking water treatment plant is of particular concern. Although NOM is not toxic, its presence in drinking water sources is highly detrimental because it is an important source of disinfection byproducts (DBP) precursors. To this aim, pre-oxidation is commonly performed to partially oxidize NOM and DBP before clariflocculation process. However, conventional oxidants, like ozone (O_3 manganate (MnO_4), chlorine compounds (e.g., ClO_2) might lead to disadvantages among which high production costs and complex onsite generation facilities (ozone), byproducts generation (chlorine compounds) and overproduction of particulate manganese (permanganate) [7]. Furthermore, due to the heterogeneity of pollutants and the inability to predict in some cases the sudden increase in their concentrations, it is necessary to rely on oxidizing agents capable of acting on a wide range of compounds and being ready for use in any situation. In addition, the recent entry into force of Directive (EU) 2020/2184, concerning the quality of water intended for

human consumption, has posed additional challenges for water treatment plants, with reference to the imposition of much stricter limits, especially regarding turbidity (<0.30 NTU). To cope with the above issues and meet the more stringent regulations/standards of drinking water, ferrate(VI) (i.e., FeO_4^{2-}) has been recently proposed as one of the most broad-spectrum chemical toward several contaminants [8,9]. The main advantage of Fe(VI) is that nontoxic by-products are formed after the reduction of Fe(VI). Besides, Fe(VI) reduction process provides reaction iron-intermediates which may accelerate oxidation process (Fe^{5+} and Fe^{4+}) or act as useful precipitants (Fe^{3+}), thus reducing the required dose of conventional chemicals [10].

Materials and methods

Jar test experimental procedure was used to assess the effect of Fe (VI) for removing manganese, NOM and algae. For all the experiments, jar test procedure involved a rapid mixing at 200 rpm for 1 minute followed by a slow mixing at 30 rpm for 20 minutes and finally a settled period for 60 minutes. At the end of settling phase, a sample from the supernatant of each test was withdrawn and stored for the analyses. Each of the above pollutants was studied individually to eliminate possible interference or synergistic effects.
Stoichiometry of soluble manganese (Mn(II)) oxidation by potassium ferrate and permanganate was assessed by carrying out 15 experimental repetitions for each chemical.
The initial Mn(II) concentration ranged between 2 and 14 µM (100–900 mg/L), whereas oxidants (Fe(VI) and Mn (VII)) doses were in the range 2–10 µM. At the end of the settling phase, the residual concentrations of the Mn(II) and Fe(VI) in the filtrated water were measured to assess the moles of manganese oxidized per mole of Fe(VI) or Mn(VII) reduced.
The same experimental approach was used to assess the removal of Mn(II) using Fe(III). Fe(II) was measured to prove Mn(II) oxidation by ferric chloride via a colorimetric method.
To assess NOM removal by Fe(VI), six batch reactors were filled with deionized water and the supernatant derived from compost elution until reaching a target TOC vale of approximately 7 mg/L. Then Fe(VI) was supplied at different doses between 0 and 2 mgFe(VI)/L. This assay was replicated by adding a constant dose of soluble manganese (0.90 mgMn(II)/L) to assess Fe(VI) reactivity in presence of a reducing agent.
Turbidity removal assays were carried out on real water samples collected at the entrance of a drinking water treatment plant. Initial turbidity of samples was approximately 6.5 NTU and pH was close to 7.6.
Jar test procedure was carried out on 18 samples without any pH adjustment.
Specifically, in six batch reactors increasing conventional coagulant/flocculant (polyaluminum chloride - PACl) between 5 and 25 mg/L and a constant dose of cationic polyelectrolyte (0.10 mg/L) were dosed. The same test was replicated twice while adding a constant dose of potassium ferrate (2.5 and 4 mgFe(VI)/L).
A mixture of natural algae was used to artificially contaminate deionized water and simulate algal bloom. Six batch reactors were filled with deionized water and a mixture of natural algae (initial Chl-a concentration of 0.45 µg/L), then Fe(VI) and Mn(VII) were dosed at different doses (0–15 mg/L).
The removal effect of algae by Fe(VI) was also evaluated synergis tically with conventional coagulant/flocculant agents used in drinking water treatment plants.

Results

Results for Mn(II) oxidation by potassium ferrate and permanganate are depicted in Figure 1.
The above results indicated that the overall molar stoichiometry of the Mn (II) oxidation by Fe(VI) and

Mn(VII) without any other oxidant demand was approximately 2:3 according to the following global reactions:

$$2K_2FeO_4 + 3MnCl_2 + 2H_2O \rightarrow 2FeCl_3 + 4KOH \quad (1)$$

$$2KMnO_4 + 3MnCl_2 + 2H_2O \rightarrow 5MnO_2 + 2KCl + 4HCl \quad (2)$$

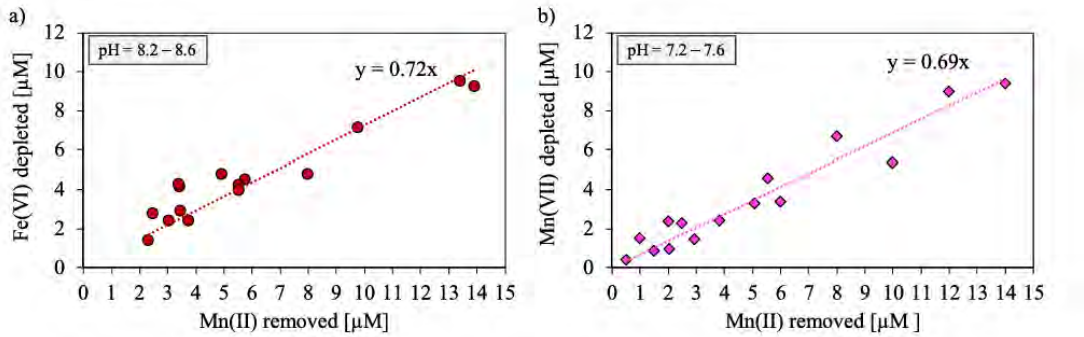

Figure 1. Relationship between the Fe(VI) (a) and Mn(VII) (b) depleted and the Mn(II) oxidized

Batch assays performed with potassium ferrate solution at neutral pH revealed that Fe(III) was the main iron compound derived from Fe(VI) decay/reduction. Fig. 2 shows the results for Mn(II) removal by Fe(III). This result indicated that Fe(III) underwent one electron transfer to Fe (II) and Mn(II) was oxidized to Mn(IV) as consequence. Based on the above results, the stoichiometry of Mn(II) removal by Fe(III) was hypothesized:

$$2FeCl_3 + MnCl_2 + 2H_2O \rightarrow MnO_2 + 2FeCl_2 + 4HCl \quad (3)$$

However, in the assays carried out with Fe(VI), no contribution of Fe(III) to the overall oxidation reaction of Mn(II) was observed. This is due to the fact that the kinetics of Mn(II) removal with Fe(IV) is much faster than with Fe(III). In the presence of NOM only in the water, the TOC removal efficiency was found to be very modest, and results were comparable with those obtained with Mn(VII). When soluble manganese was also added to the medium (Mn(II) = 0.9 mg/L), the TOC removal efficiency increased significantly, reaching around 55 % (Figure 2).

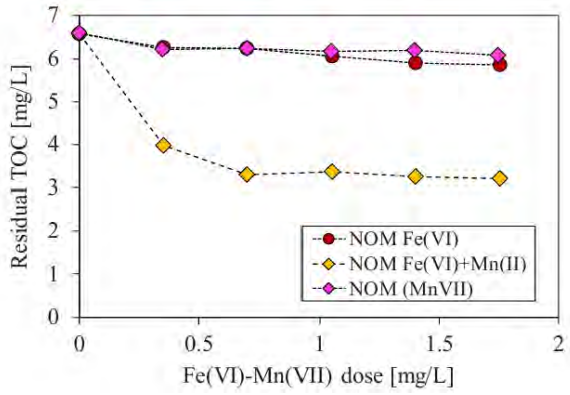

Figure 2. Trend of residual TOC at increasing dose of permanganate and ferrate with or without Mn(II)

Conclusions

The obtained results confirmed that Fe(VI) can achieve high removal efficiencies for all the examined contaminants, often outperforming conventionally used reagents. Specifically, for manganese removal, the Fe(VI) dose can be lower than the stoichio metric dose (< 2 mol of Fe(VI) per 3 mol of Mn(II)), as the reaction by- products (Fe(III)) can contribute to further Mn(II) removal. Activation of Fe(VI) is required for NOM removal, which can be achieved through the simultaneous presence of soluble manganese in the water. Furthermore, the use of Fe(VI) allows for a reduction of approximately 50 % in the quantity of oxidizing/coagulating agents required for algae and turbidity removal. Therefore, treating drinking water with Fe(VI) rep resents a promising process that can be used as an alternative or in conjunction with conventional methods to address the challenges posed by climate change, ensuring high quality standards and process sustainability.

References

[1] B. Ma, C. Hu, J. Zhang, M. Ulbricht, S. Panglisch, Impact of climate change on drinking water safety, ACS Environ. Sci. Technol. Water 2 (2022) 259–261, https://doi.org/10.1021/acsestwater.2c00004.

[2] O. Freeman, O. Ovie, I. Omoregie, Effect of climate change through temperature increase on heavy metals concentrations in water and sediment of Ekpan Creek, Delta State, Nigeria, Adv. Res. 10 (2017) 1–16, https://doi.org/10.9734/air/2017/ 34754.

[3] J. Jarsj¨o, Y. Andersson-Sk¨old, M. Fr¨oberg, J. Pietro´ n, R. Borgstr¨om, Å. L¨ov, D. B. Kleja, Projecting impacts of climate change on metal mobilization at contaminated sites: controls by the groundwater level, Sci. Total Environ. 712 (2020), https://doi.org/10.1016/j.scitotenv.2019.135560.

[4] C.J. Gobler, Climate change and harmful algal blooms: insights and perspective, Harmful Algae 91 (2020) 101731, https://doi.org/10.1016/j.hal.2019.101731.

[5] Y. Hashempour, M. Nasseri, A. Mohseni-Bandpei, S. Motesaddi, M. Eslamizadeh, Assessing vulnerability to climate change for total organic carbon in a system of drinking water supply, Sustain. Cities Soc. 53 (2020) 101904, https://doi.org/ 10.1016/j.scs.2019.101904.

[6] J.E. Tobiason, A. Bazilio, J. Goodwill, X. Mai, C. Nguyen, Manganese removal from drinking water sources, Curr. Pollut. Rep. 2 (2016) 168–177, https://doi.org/ 10.1007/s40726-016-0036-2.

[7] J. Ma, B. Jia, S. Li, Y. Kong, Y. Nie, H. Zhang, M. Xiao, T. Gao, Enhanced coagulation of covalent composite coagulant with potassium permanganate oxidation for algae laden water treatment: algae and extracellular organic matter removal, Chem. Eng. J. Adv. 13 (2023) 100427, https://doi.org/10.1016/j. ceja.2022.100427.

[8] B. Li, R. Guo, J. Tian, Z. Wang, R. Qu, New findings of ferrate(VI) oxidation mechanism from its degradation of alkene imidazole ionic liquids, Environ. Sci. Technol. 55 (2021) 11733–11744, https://doi.org/10.1021/acs.est.1c03348.

[9] C.V. Marbaniang, K. Sathiyan, T.J. McDonald, E. Lichtfouse, P. Mukherjee, V. K. Sharma, Metal ion-induced enhanced oxidation of organic contaminants by ferrate: a review, Environ. Chem. Lett. 21 (2023) 1729–1743, https://doi.org/ 10.1007/s10311-023-01584-4.

[10] X. Zhang, M. Feng, C. Luo, N. Nesnas, C.H. Huang, V.K. Sharma, Effect of metal ions on oxidation of micropollutants by ferrate(VI): enhancing role of FeIVSpecies, Environ. Sci. Technol. 55 (2021) 623–633, https://doi.org/10.1021/acs. est.0c04674.

Title: Application of flow cytometry for groundwater quality monitoring within the Water Safety Plans

Author(s): Michele Menghini*[1], Simona Vezzoli[1], Barbara Lovisetto[2], Roberta Pedrazzani[1]

[1] *DIMI-Department of Mechanical and Industrial Engineering, University of Brescia, Brescia, Italy, michele.menghini@unibs.it; simona.vezzoli@unibs.it; roberta.pedrazzani@unibs.it*
[2] *ETRA S.p.A., Bassano del Grappa, VI, Italy, b.lovisetto@etraspa.it*

Keyword(s): Bacteria, Drinking Water, Nucleic Acid Content, Biological stability, Online measurements, Microbial water quality.

Abstract

Groundwater are crucial aquatic sources globally [1], [2], [3], [4]. Protecting these freshwater supplies is crucial to prevent contamination, thereby reducing the need for downstream treatment [5], [6], [7]. The Water Safety Plans (WSPs) promote comprehensive risk management from catchment to consumer [8]. Understanding water source characteristics is vital to identify potential hazards, particularly microbial threats [9], [10], [11]. Due to their labour-intensive and time-consuming nature, conventional monitoring methods such as the Heterotrophic Plate Count (HPC) are inadequate for the early detection of contamination events [12], [13], [14], [15], [16]. Therefore, high-throughput, cultivation-free methods, especially flow cytometry (FCM), have been developed to address these challenges [2], [17], [18], [19]. FCM provides rapid, real-time, and detailed analysis of microbial communities [20], [21], [22], including total cell count and differentiation of intact cells based on nucleic acid content, which can indicate bacterial activity levels[13]. Despite its potential, the widespread adoption of FCM is hindered by high costs, non-standardized data processing, and limitations in identifying specific bacterial strains [12], [23], [24]. Nevertheless, advancements in FCM and the establishment of standardized protocols have increased their significance in water monitoring [25], [26].

This work focused on the application of FCM for online raw groundwater monitoring. Located in the Po River catchment area. Microbiological water quality was assessed using both online high-frequency flow cytometry (FCM) and conventional methods. As far as FCM is concerned, samples were automatically collected every 2 to 6 hours and analysed using a BactoSense® flow cytometer (Sigrist-Photometer AG, Switzerland), equipped with a 488 nm solid-state laser, a side scatter detector (SSC: 488/10), and two fluorescence detectors (FL1: 525/45, FL2: 715 LP). Prior to analysis, samples were treated with SYBR Green I and incubated for 10 minutes at 37 °C.

Figure 1 BactoSense® displays the results of a single measurement: the fluorescence signals (F1 and F2) were elaborated in order to estimate the intact cell counts (ICC) as well as high nucleic acid (HNA) content bacteria and low nucleic acid (LNA) content bacteria.

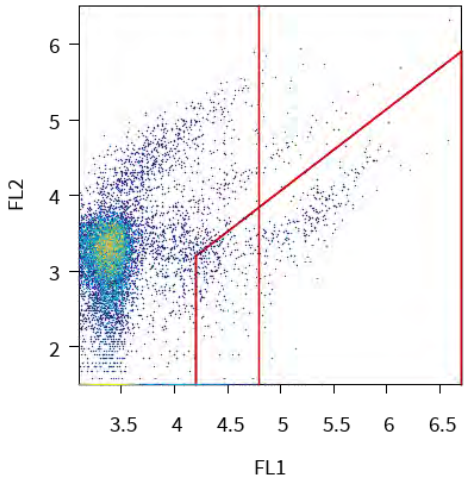

Figure 1. Fingerprint of a groundwater sample

Data were post-processed in R studio (v4.3.3) in order to identify a customized gate, able to better exclude the background noise due to debris typical of these types of groundwater sources. The customized gates allow to increase accuracy of the results in terms of ICC, HNA, and LNA.
The measurements were performed over time, in order to acquire long-term trends of ICC, HNA, and LNA (see Figure 2). Different environmental parameters (e.g., the daily mean value of precipitation height, air, relative air humidity) and physical-chemical parameters (such as temperature, pH, electrical conductivity, turbidity, chlorides, DOC, etc.) were measured in parallel, to obtain a comprehensive description of groundwater.

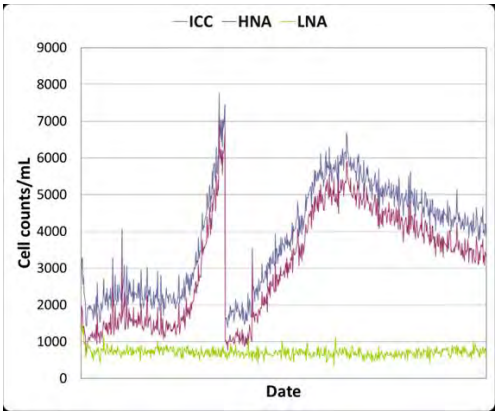

Figure 2. Long-term trend of ICC, HNA and LNA, from 26/01/2023 to 03/03/2023, in a groundwater source of the Po catchment area.

As reported in the scientific literature, flow cytometry appears to be a suitable early warning system for DWTPs management thanks to real-time information about microbiological water quality, thus providing a solid basis for implementing preventive actions.
In conclusion, the integration of flow cytometry into standard water monitoring protocols might represent a significant advancement in public health protection. Water treatment facilities adopting this technology may benefit from FCM rapid detection capabilities, enabling prompter responses to microbiological threats. Finally, what is even more important in the management of the supply chain of water intended

for human consumption, the FCM technique allows the creation of a historical series of data which, together with the climatic-environmental and chemical-physical surveys, allows to critically evaluate whether the quality of the water remains biologically stable.

References

[1] S. S. D. Foster and P. J. Chilton, “Groundwater: the processes and global significance of aquifer degradation.,” *Philosophical Transactions of the Royal Society B: Biological Sciences*, vol. 358, no. 1440, p. 1957, Dec. 2003, doi: 10.1098/RSTB.2003.1380.

[2] M. D. Besmer, J. Epting, R. M. Page, J. A. Sigrist, P. Huggenberger, and F. Hammes, “Online flow cytometry reveals microbial dynamics influenced by concurrent natural and operational events in groundwater used for drinking water treatment,” *Sci Rep*, vol. 6, 2016, doi: 10.1038/srep38462.

[3] Q. Luo *et al.*, “Spring protection and sustainable management of groundwater resources in a spring field,” *J Hydrol (Amst)*, vol. 582, Mar. 2020, doi: 10.1016/J.JHYDROL.2019.124498.

[4] L. Vucinic, D. O’Connell, R. Teixeira, C. Coxon, and L. Gill, “Flow Cytometry and Fecal Indicator Bacteria Analyses for Fingerprinting Microbial Pollution in Karst Aquifer Systems,” *Water Resour Res*, vol. 58, no. 5, 2022, doi: 10.1029/2021WR029840.

[5] D. M. Oliver, C. D. Clegg, P. M. Haygarth, and A. L. Heathwaite, “Assessing the Potential for Pathogen Transfer from Grassland Soils to Surface Waters,” *Advances in Agronomy*, vol. 85, pp. 125–180, 2005, doi: 10.1016/S0065-2113(04)85003-X.

[6] H. R. Safford and H. N. Bischel, “Flow cytometry applications in water treatment, distribution, and reuse: A review,” *Water Res*, vol. 151, pp. 110–133, 2019, doi: 10.1016/j.watres.2018.12.016.

[7] WHO, “Guidelines for drinking-water quality, 4th edition, incorporating the 1st addendum. Geneva: World Health Organization. Geneva, Switzerland,” *World Health Organization*, 2017, Accessed: May 30, 2024. [Online]. Available: https://www.who.int/publications/i/item/9789241549950

[8] “Water safety plan manual: step-by-step risk management for drinking-water suppliers, second edition.” Accessed: May 30, 2024. [Online]. Available: https://www.who.int/publications/i/item/9789240067691

[9] M. Sinreich, M. Pronk, and R. Kozel, “Microbiological monitoring and classification of karst springs,” *Environ Earth Sci*, vol. 71, no. 2, 2014, doi: 10.1007/s12665-013-2508-7.

[10] P. R. Hunter, “Climate change and waterborne and vector-borne disease,” *J Appl Microbiol*, vol. 94 Suppl, no. 32, 2003, doi: 10.1046/J.1365-2672.94.S1.5.X.

[11] T. van den Hoven and C. Kazner, “TECHNEAU: Safe Drinking Water from Source to Tap State of the art & Perspectives,” *Water Intelligence Online*, vol. 8, Jul. 2009, doi: 10.2166/9781780401782.

[12] S. Van Nevel *et al.*, “Flow cytometric bacterial cell counts challenge conventional heterotrophic plate counts for routine microbiological drinking water monitoring,” *Water Res*, vol. 113, pp. 191–206, Apr. 2017, doi: 10.1016/j.watres.2017.01.065.

[13] F. Hassard, R. Whitton, B. Jefferson, J. Fawell, and P. Jarvis, “Understanding the Use of Flow Cytometry for Monitoring of Drinking Water,” 2019.

[14] F. Hammes and T. Egli, “Cytometric methods for measuring bacteria in water: Advantages, pitfalls and applications,” *Analytical and Bioanalytical Chemistry*, vol. 397, no. 3. 2010. doi: 10.1007/s00216-010-3646-3.

[15] K. De Roy, L. Clement, O. Thas, Y. Wang, and N. Boon, “Flow cytometry for fast microbial community fingerprinting,” *Water Res*, vol. 46, no. 3, pp. 907–919, Mar. 2012, doi: 10.1016/J.WATRES.2011.11.076.

[16] C. Schleich *et al.*, “Mapping dynamics of bacterial communities in a full-scale drinking water distribution system using flow cytometry,” *Water (Switzerland)*, vol. 11, no. 10, 2019, doi: 10.3390/w11102137.

[17] M. Vital, M. Dignum, A. Magic-Knezev, P. Ross, L. Rietveld, and F. Hammes, “Flow cytometry and adenosine tri-phosphate analysis: Alternative possibilities to evaluate major bacteriological changes in drinking water treatment and distribution systems,” *Water Res*, vol. 46, no. 15, pp. 4665–4676, 2012, doi: 10.1016/j.watres.2012.06.010.

[18] E. I. Prest, J. El-Chakhtoura, F. Hammes, P. E. Saikaly, M. C. M. van Loosdrecht, and J. S. Vrouwenvelder, “Combining flow cytometry and 16S rRNA gene pyrosequencing: A promising approach for drinking water monitoring and characterization,” *Water Res*, vol. 63, pp. 179–189, 2014, doi: 10.1016/j.watres.2014.06.020.

[19] J. Ihssen, N. Jovanovic, T. Sirec, and U. Spitz, “Real-time monitoring of extracellular ATP in bacterial cultures using thermostable luciferase,” *PLoS One*, vol. 16, no. 1 January, 2021, doi: 10.1371/journal.pone.0244200.

[20] P. Boi *et al.*, “Strategies for Water Quality Assessment: A Multiparametric Analysis of Microbiological Changes in River Waters,” *River Res Appl*, vol. 32, no. 3, 2016, doi: 10.1002/rra.2872.

[21] R. Props, P. Monsieurs, M. Mysara, L. Clement, and N. Boon, “Measuring the biodiversity of microbial communities by flow cytometry,” *Methods Ecol Evol*, vol. 7, no. 11, 2016, doi: 10.1111/2041-210X.12607.

[22] M. Gabrielli, A. Turolla, and M. Antonelli, “Bacterial dynamics in drinking water distribution systems and flow cytometry monitoring scheme optimization,” *J Environ Manage*, vol. 286, 2021, doi: 10.1016/j.jenvman.2021.112151.

[23] H. A. Keserue, A. Baumgartner, R. Felleisen, and T. Egli, “Rapid detection of total and viable Legionella pneumophila in tap water by immunomagnetic separation, double fluorescent staining and flow cytometry,” *Microb Biotechnol*, vol. 5, no. 6, pp. 753–763, Nov. 2012, doi: 10.1111/J.1751-7915.2012.00366.X.

[24] S. Müller and G. Nebe-Von-Caron, “Functional single-cell analyses: Flow cytometry and cell sorting of microbial populations and communities,” *FEMS Microbiology Reviews*, vol. 34, no. 4. 2010. doi: 10.1111/j.1574-6976.2010.00214.x.

[25] E. I. Prest, F. Hammes, S. Kötzsch, M. C. M. van Loosdrecht, and J. S. Vrouwenvelder, “Monitoring microbiological changes in drinking water systems using a fast and reproducible flow cytometric method,” *Water Res*, vol. 47, no. 19, 2013, doi: 10.1016/j.watres.2013.07.051.

[26] M. D. Besmer and F. Hammes, “Short-term microbial dynamics in a drinking water plant treating groundwater with occasional high microbial loads,” *Water Res*, vol. 107, 2016, doi: 10.1016/j.watres.2016.10.041.

PARALLEL SESSION: C2

Climate change

Climate change effects preventing and control

Algal photobioreactors: advanced CO_2 valorisation biotechnology in an ecological transition perspective to control climate change

Author(s): Federica Pasquarelli*[1], Giuseppina Oliva[1], Vincenzo Belgiorno[1], Vincenzo Naddeo[1], Tiziano Zarra[1]

[1] *Sanitary Environmental Engineering Division (SEED), Department of Civil Engineering, University of Salerno, via Giovanni Paolo II, Fisciano, SA, Italy*

Keyword(s): carbon dioxide; greenhouse gases, biofixation; biomass; microalgae

Abstract

Climate change is the result of greenhouse gas emissions, which are growing rapidly. It is therefore an increasingly topical issue, the scope of which will grow in the absence of concrete action. Among greenhouse gases, CO_2 is the main factor contributing to climate change, and this makes it necessary to find solutions that can reduce the current concentration in the atmosphere and its future emissions. The paper presents the study of advanced CO_2 capture and utilization technologies, with particular reference to microalgal biological systems, with the dual objective of climate change mitigation and production of exploitable biomass. In particular, a comparison between two photobioreactors, PBR and mPBR, is discussed in order to evaluate the best performance in terms of CO_2 biofixation and microalgal biomass production.

1. Introduction

Emissions of greenhouse gases (GHGs) into the atmosphere are considered to be among the most urgent problems to be remedied as the main driver of global climate change [1]. Climate change is a natural phenomenon, but in recent years the most marked and sudden changes in the climate system have been caused by man, mainly due to the increase in greenhouse gas emissions by industrial plants. Carbon dioxide (CO_2) accounted for about 82% of total GHGs emissions in 2017, while the remaining 18% is attributable to methane (CH_4), fluorinated gases and nitrous oxide (N_2O) [2]. The fight against climate change is the objective n.13 ("Promoting action at all levels to combat climate change") of the Agenda 2030 for Sustainable Development, adopted in 2015 by the Member States of the United Nations and divided into 17 Sustainable Development Goals (SDGs), which considers the three dimensions of sustainable development equally, namely economic, social and ecological [3,4].
To help achieve climate change mitigation, there are several technologies including carbon capture and storage (CCS) and carbon capture and utilization (CCU). The difference between CCS and CCU lies in the final destination of the captured CO_2: in the CCS it is transferred to a suitable and safe place for long-term storage, while in the CCU it is converted into a commercial product [5]. In particular, the CCU method can be biological and, in this case, it is called Biological Carbon Capture and Utilization (BCCU). Biogical-CCU using microalgae has proven to be a promising biotechnology that significantly reduces CO_2 emissions [6]. In fact, carbon dioxide can be converted, through the process of photosynthesis and without damaging the environment, into organic matter using sunlight as an energy source [7,8]. CO_2 biofixation and biomass production differ significantly for the different species of microalgae, but also in view of the different growth conditions and cultivation parameters (pH, lighting, CO_2 input concentration) [9]. In addition, microalgal biomass is considered a promising energy raw material with multiple applications in the production of biofuels, nutraceuticals and health supplements [10]. The current

challenge concerns the development of new technologies for the cultivation of microalgae in order to optimize their productivity and the collection of biomass. The research activities are focused on the study, analysis and comparison of two microalgal biological systems, modifying the main operating and process conditions in order to evaluate the different biofixation efficiencies of CO_2.

2. Materials and methods

2.1 Experimental set-up

The experimental plant consists of two cylindrical plexiglass reactors (PBR and mPBR; external diameter of 30 cm, internal diameter of 29 cm, height of 60 cm), with a working volume of 40 L; a membrane has been inserted into a reactor (mPBR; external dimensions of 30x18 cm, internal dimensions of 26x11 cm, mesh porosity of 30μm), useful for the collection of microalgal biomass. The membrane is connected to a peristaltic pump (Watson-Marlow 323S equipped with two 313x heads), useful for the recirculation of microalgal broth, and to a pressure transducer for transmembrane pressure monitoring. In coupling to each reactor there is an absorption column (AC; external diameter of 7 cm, internal diameter of 6 cm, height of 290 cm), made of plexiglass and PVC, with a working volume of 8 L. Four white LEDs with a power of 24 W and a distance of 5 cm are used for the illumination of each photobioreactor. An air compressor is used for the injection of air into the system (Stanley DST 100/8/6). In addition, there is a liquid line, equipped with a peristaltic pump (Watson-Marlow 323S equipped with two 313x heads) for the recirculation of the liquid culture medium from the reactor to the absorption column, and a gas line for the introduction of the gaseous mixture into the AC module. The gas mixture entering the system, regulated through a flow meter, is obtained by combining a dosed flow of CO_2 (derived from a CO_2 cylinder; 99.99% and degree of purity 4.0) and compressed air (obtained from the air compressor). In addition, there are two liquid sampling points (LSP1 and LSP2), used to take samples for analysis of physical-chemical parameters, total suspended solids (TSS), chlorophyll and turbidity, and three gas sampling points (GSP1, GSP2 and GSP3), used for the determination of the CO_2 concentrations inlet and outlet of the column.

2.2 Operating conditions

During the experimental activities the luminous intensity was maintained at a value of 8000 LUX and a light/dark cycle of 12 hours was adopted. Chlorella Vulgaris (strain CCAP 211/11B), which was purchased by the Culture Collection of Algae and Protozoa (CCAP) of the Scottish Association for Marine Science (Scotland), was used as a microalgae species due to the high tolerance to CO_2 found in the scientific literature. The experimental activities were conducted with the operating conditions shown in Table 1.

Table 1. Programme of the experimental activity

Stage	Air flowrate [mL m^{-1}]	Liquid flowrate [mL m^{-1}]	CO_2 inlet concentration [%]	L/G Ratio	Mineral renewal rate [mL d^{-1}]
I	100	500	5	5	250
II	100	1000	5	10	250
III	100	2000	5	20	250

System feeding time for each stage is 8 hours/day. Modified Bold's Basal Medium (mBBM) is used as mineral renewal for both photobioreactors (a stocks solution per 400 mL of (1) 10.0 g of $NaNO_3$; (2) 3.0 g of $MgSO_4 \cdot 7H_2O$; (3) 1.0 g of NaCl; (4) 3.0 g of K_2HPO_4; (5) 7.0 g of KH_2PO_4; (6) 1.0 g of $CaCl_2 \cdot 2H_2O$; (7) trace elements solution (g/L); $ZnSO_4 \cdot 7H_2O$ (8.82 g), $MnCl_2 \cdot 4H_2O$ (1.44 g), $(NH_4)_6MO_7)_4 \cdot 4H_2O$ (0.87 g), $CuSO_4 \cdot 5H_2O$ (1.57 g), $CoCl_2 \cdot 6H_2O$ (0.38); (8) H_3BO_3 11.42 g/L; (9) 50.0 g/L of EDTA and 31.0 g/L of KOH; and (10) 4.98 g/L of $FeSO_4 \cdot 7H_2O$).

2.3 Analytical methods

The concentration of CO_2 was determined at GSP1, GSP2 and GSP3 using the GC - TCD (TRACETM 1300 Gas Chromatograph, Thermo Fisher). The pH, dissolved oxygen and temperature trend were monitored using the multiparameter probe (HI9829, Hanna Instruments), while the monitoring of total suspended solids (TSS) was carried out according to the standard 2540 D method. The turbidity of the algal broth and the permeate obtained through membrane filtration were measured using a turbidimeter (Hach 2100 N). All analyses were carried out at the Sanitary Environmental Engineering Division (SEED) Laboratory of the Department of Civil Engineering of the University of Salerno.

3. Results and Discussion

Microalgae require a source of inorganic carbon for photosynthesis. Therefore, CO_2 was provided for 8 hours a day. Figure 1 shows the average removal of CO_2 during the three stages of the experimental activity. The graph shows an increasing trend of CO_2 removal efficiencies (RE) in the different stages, with similar percentages for the two systems: 65% for both PBR and mPBR in stage I; 73% for PBR and 76% for mPBR in stage II; 83% for PBR and 82% for mPBR in stage III. Despite the CO_2 concentration has been maintained at 5% of the air flow of 100 mL min^{-1} for the entire experimental activity, the percentages of CO_2 removal are different as the algal broth recirculation factor has been changed (L/G) starting with a flow value of 500 mL min^{-1} for the first stage up to a value of 2 L min^{-1} for the third stage, resulting in an increase in turbulence in the absorption column and therefore both a greater contact time gas-liquid that a greater mass transfer coefficient (kLa). Removal efficiencies have been evaluated from monitoring CO_2 inlet and outlet concentrations for both configurations. In both cases the trends were similar, with maximum inlet CO_2 concentrations of 185.34 g m^{-3} for PBR and 194.68 g m^{-3} for mPBR obtained in stage III, at which the minimum outlet CO_2 concentrations were also obtained, 30.52 g m^{-3} for PBR and 34.60 g m^{-3} for mPBR.

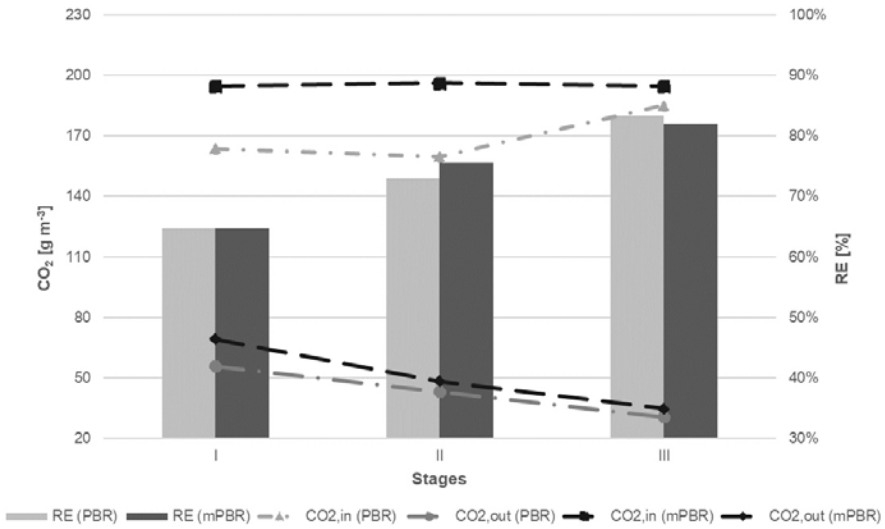

Figure 1. Inlet and outlet concentrations of CO_2 from PBR and mPBR and their removal efficiencies

In addition, it was found that the maximum biomass production value is obtained for the mPBR configuration with a value of 64.48 g d^{-1}, compared to the PBR configuration for which a value of 52.29 g d^{-1} was obtained. In addition, the presence of the membrane has allowed a direct recovery of biomass unlike the PBR configuration, in which recovery has taken place in several steps (sampling phase, sedimentation and subsequent centrifugation of microalgae).

4. Conclusions

Microalgae have been identified as single-celled photoautotrophic microorganisms that, through photosynthetic activity, demonstrate a high biofixation efficiency of carbon dioxide, which is recognized as the main cause of climate change. Microalgae cultivation is associated with the design of cultivation systems and the scientific literature confirms that the greatest efficiency is obtained through closed systems also called photobioreactors (PBR). The research activities concerned the study of closed microalgal systems, with an in-depth and detailed analysis on the development, efficiency and optimization of PBR and mPBR (membrane photobioreactor) systems. The results of the experimental activities carried out reveal a high CO_2 removal efficiency for both technological configurations of photobioreactors studied at laboratory scale. In particular, the efficiency of CO_2 removal by the two configurations was more or less similar, with values of 74% for the PBR configuration and 75% for the mPBR configuration. The results obtained show that the proposed solutions are environmentally friendly in accordance with the principles of ecological transition and the climate neutrality objectives promoted by Agenda 2030, but the mPBR configuration proved more efficient in terms of biomass production due to the presence of the membrane.

References

[1] C.R. Cattaneo, R. Muñoz, G.V. Korshin, V. Naddeo, V. Belgiorno, T. Zarra, Biological desulfurization of biogas: A comprehensive review on sulfide microbial metabolism and treatment biotechnologies, Science of The Total Environment 893 (2023) 164689. https://doi.org/10.1016/j.scitotenv.2023.164689.
[2] E.F. Oteng-Abayie, E. Duodu, G. Mensah, P.B. Frimpong, Natural resource abundance, environmental sustainability, and policies and institutions for environmental sustainability in sub-Saharan Africa, Resources Policy 79 (2022) 103097. https://doi.org/10.1016/j.resourpol.2022.103097.
[3] T. Bennich, Å. Persson, R. Beaussart, C. Allen, S. Malekpour, Recurring patterns of SDG interlinkages and how they can advance the 2030 Agenda, One Earth 6 (2023) 1465–1476. https://doi.org/10.1016/j.oneear.2023.10.008.
[4] C. Magazzino, G. Cerulli, I. Haouas, J.O. Unuofin, S.A. Sarkodie, The drivers of GHG emissions: A novel approach to estimate emissions using nonparametric analysis, Gondwana Research 127 (2024) 4–21. https://doi.org/10.1016/j.gr.2023.10.004.
[5] G. Oliva, M.G. Galang, A. Buonerba, S.W. Hasan, V. Belgiorno, V. Naddeo, T. Zarra, Carbon capture and utilization in waste to energy approach by leading-edge algal photo-bioreactors: The influence of the illumination wavelength, Case Studies in Chemical and Environmental Engineering 7 (2023) 100348. https://doi.org/10.1016/j.cscee.2023.100348.
[6] V. Senatore, A. Buonerba, T. Zarra, G. Oliva, V. Belgiorno, J. Boguniewicz-Zablocka, V. Naddeo, Innovative membrane photobioreactor for sustainable CO2 capture and utilization, Chemosphere 273 (2021) 129682. https://doi.org/10.1016/j.chemosphere.2021.129682.
[7] F. Pasquarelli, G. Oliva, A. Mariniello, A. Buonerba, C.-W. Li, V. Belgiorno, V. Naddeo, T. Zarra, Carbon neutrality in wastewater treatment plants: An integrated biotechnological-based solution for nutrients recovery, odour abatement and CO2 conversion in alternative energy drivers, Chemosphere 354 (2024) 141700. https://doi.org/10.1016/j.chemosphere.2024.141700.
[8] M.V.A. Corpuz, L. Borea, V. Senatore, F. Castrogiovanni, A. Buonerba, G. Oliva, F. Ballesteros, T. Zarra, V. Belgiorno, K.-H. Choo, S.W. Hasan, V. Naddeo, Wastewater treatment and fouling control in an electro algae-activated sludge membrane bioreactor, Science of The Total Environment 786 (2021) 147475. https://doi.org/10.1016/j.scitotenv.2021.147475.
[9] L. Aditya, H.P. Vu, M. Abu Hasan Johir, T.M.I. Mahlia, A.S. Silitonga, X. Zhang, Q. Liu, V.-T. Tra, H.H. Ngo, L.D. Nghiem, Role of culture solution pH in balancing CO2 input and light intensity for maximising microalgae growth rate, Chemosphere 343 (2023) 140255. https://doi.org/10.1016/j.chemosphere.2023.140255.
[10] G. Oliva, R.R. Pahunang, G. Vigliotta, T. Zarra, F.C. Ballesteros, A. Mariniello, A. Buonerba, V. Belgiorno, V. Naddeo, Advanced treatment of toluene emissions with a cutting-edge algal bacterial photo-bioreactor: Performance assessment in a circular economy perspective, Science of The Total Environment 878 (2023) 163005. https://doi.org/10.1016/j.scitotenv.2023.163005.

Title: An innovative wireless tool (LESSDRONE) for multipurpose investigations aimed at optimizing water resource recovery facilities (WRRFs) aeration process

Author(s): R. Gori[1], I. Ducci[1], S. Dugheri[2], C. Caretti[1]

[1] Civil and Environmental Engineering Department, University of Florence, Via di Santa Marta 3, 50139 Florence, Italy, riccardo.gori@unifi.it, cecilia.caretti@unifi.it, iacopo.ducci@unifi.it
[2] Experimental and Clinical Medicine Department, University of Florence, Largo Brambilla 3, 50134, Florence, Italy, stefano.dugheri@unifi.it

Keyword(s): aeration efficiency, energy saving, GHGs, odour, VOCs, WRRFs

Abstract

Introduction

Water resource recovery facilities (WRRFs) make it possible to achieve the quality objectives of superficial water bodies but are also a source of greenhouse gas (GHG) emissions. These include direct emissions arising from the biological processes, and indirect emissions largely but not exclusively associated with the energy consumption of the various treatment processes [1]. Aerobic/anoxic processes with activated sludge, and their variations, are the most widely used technology for wastewater treatment. The aeration compartment of oxidation tanks is the most energy-intensive and is responsible for indirect emissions of the plants [2]. As far as direct emissions are concerned, the main GHGs emitted by aerated tanks are carbon dioxide (CO_2) produced by oxidation of organic compounds, nitrous oxide (N_2O) produced by nitrification and denitrification of compounds containing nitrogen [3, 4], and methane (CH_4). Methane develops in anaerobic sections of the plant and may also be released to the atmosphere from oxidation tanks due to aeration. Optimisation of the aeration process can significantly reduce energy costs and the carbon footprint (CF) of WRRFs. It is therefore fundamental that plant managers have reliable instruments to measure aeration system performance in terms of oxygen transfer efficiency and overall GHG emissions [5]. Within the LESSWATT project (LIFE16 ENV/IT/000486), of which the Department of Civil and Environmental Engineering (University of Florence) was the coordinator, an innovative wireless tool for measuring direct and indirect contributions to the CF of oxidation tanks of WRRFs was developed. The tool allows to offer solutions to minimise the energy consumption and GHG emissions from water resource recovery facilities.
In this paper we present some of the results of measurement campaigns carried out in the last five years (both during the project and in its after-life), highlighting the different application options for limiting energy consumption and mitigating the environmental impacts of WRRFs.

Material and methods

The developed instrument (LESSDRONE) is an automated device that moves on the surface of the oxidation tank and is able to capture the gas that comes out of it (off-gas). It evaluates the oxygen transfer efficiency under standard conditions and in process water (αSOTE) by means of the «off-gas method», which is based on a mass balance in gas phase between the oxygen content of reference gas (atmospheric air) and off-gas [6], and measures GHG concentrations (CO_2, CH_4, N_2O) through infrared absorption sensors.

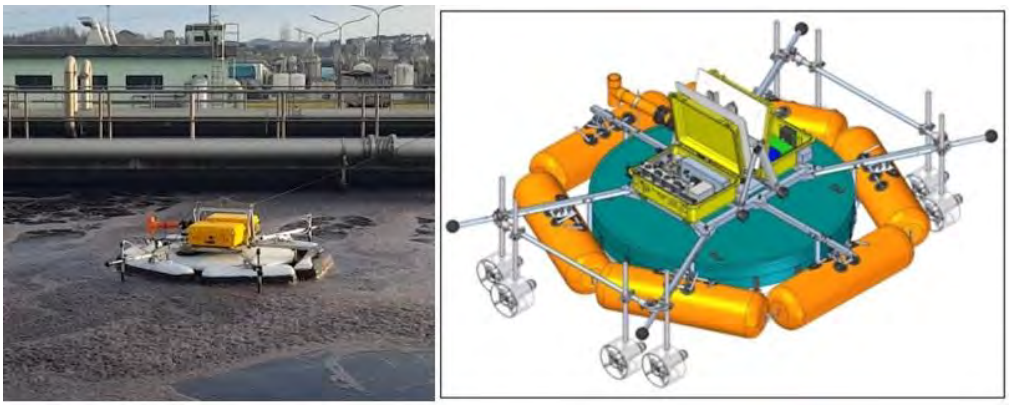

Figure 1. The LESSDRONE

The instrument also measures the dissolved oxygen and the temperature in the mixed liquor (LDO sensor), and the air flow speed (hot-wire anemometer), from which it is possible to calculate the flow rate of air blown into the oxidation tank. The movement of the LESSDRONE is ensured by the thrust of 8 double-wing propeller engines and the control is managed via a special remote control.
Since the LESSDRONE is able to measure the off-gas flow rate, it is possible to calculate GHG direct emissions in terms of mass flow ($kgCO_{2,eq}/d$). The GHG indirect emissions can be estimated in case the electricity consumption for aeration (blowers) is known, using the specific emission factor for electricity production ($kgCO_{2,eq}/kWh$).

Results and conclusions

Generally, a measurement campaign consists of a “point” test and a “stationary” test. The first one is performed at constant air flow rate and consists of measurements on several points of the oxidation tank. At each point, the αSOTE, the air flow, the DO and the GHGs are measured; in this case the spatial distribution of the parameters in the tank is measured. The second one consists, instead, of a measurement in a significant single point in the tank for a prolonged period (at least one week) under ordinary management conditions. The parameters are measured to evaluate their temporal distribution in the various operating conditions (working day/holiday, night/day, high/low load, etc.). As an example, the results of a standard measurement campaign are shown below.

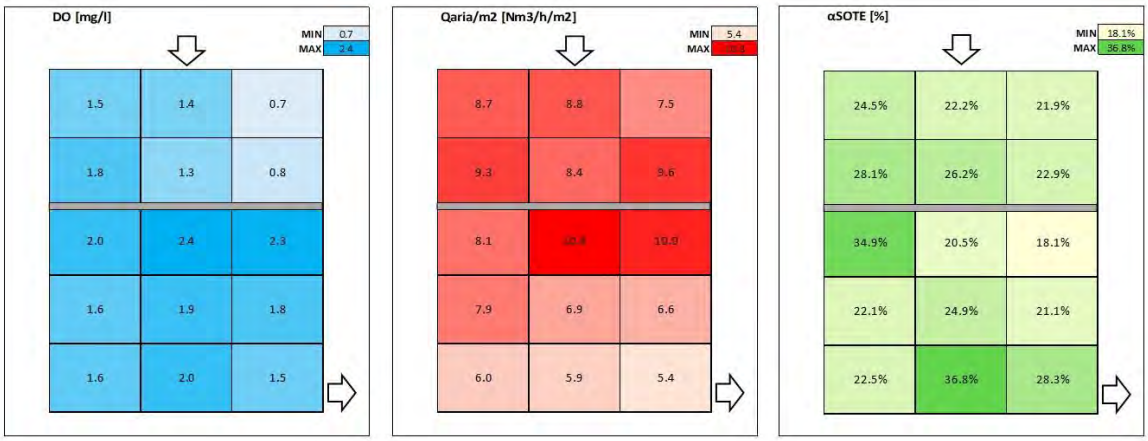

Figure 2. Point test result

The oxygen transfer efficiency measured at different points of the same tank allows to obtain a more detailed estimation of the overall efficiency of the system and to highlight any differences due to hydrodynamics, concentration of contaminants and air distribution. The test is carried out by keeping the flow rate of air blown as constant as possible so as not to influence the measurements at different points. It is possible to carry out multi-point tests at different levels of air flow rate, to experimentally determine an operating curve of the air diffusers by correlating the oxygen transfer efficiency with the air flow rate.

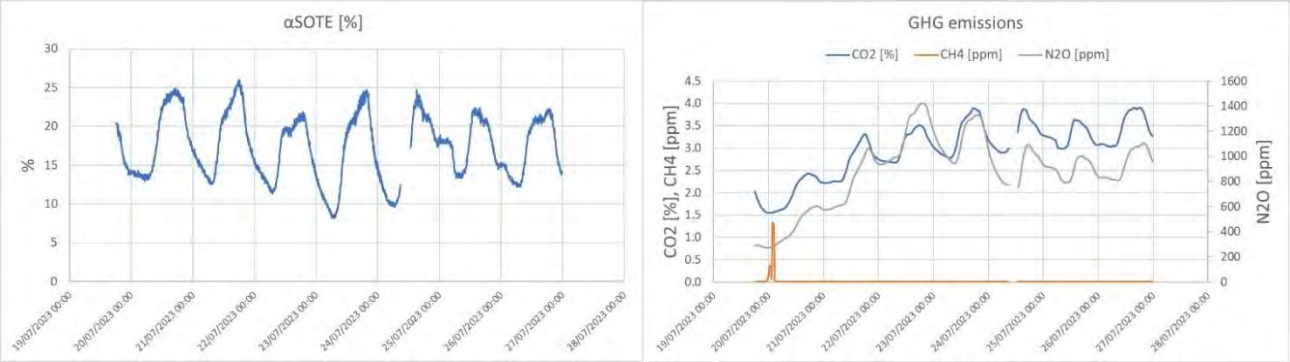

Figure 3. Stationary test result

The αSOTE trend shows a daily cycling pattern, reaching the maximum values in the late afternoon hours and the minimums in the night or early morning hours, in accordance with the trend of the influent load (considering the WRRF hydraulic residence time). This variability also appears evident in the trends in GHG concentrations, with an increasing trend for both CO_2 and N_2O.
The repetition of the measurement campaign after a few months has the main objectives of evaluating the decrease in the oxygen transfer efficiency into the tank over time and of evaluating the seasonal variability of GHG emissions. If the air diffusers have been cleaned, repeating the measurement campaign also has the purpose of evaluating the loss of the benefits of cleaning and therefore optimizing the interventions frequency. It is possible to identify the management scenarios aimed at improving the oxygen transfer efficiency and minimizing energy consumption (and indirect emissions) and evaluate the environmental and economic impacts.

In this regard, an example of a result obtained from a measurement carried out to evaluate the effectiveness of cleaning the air diffusers is reported.

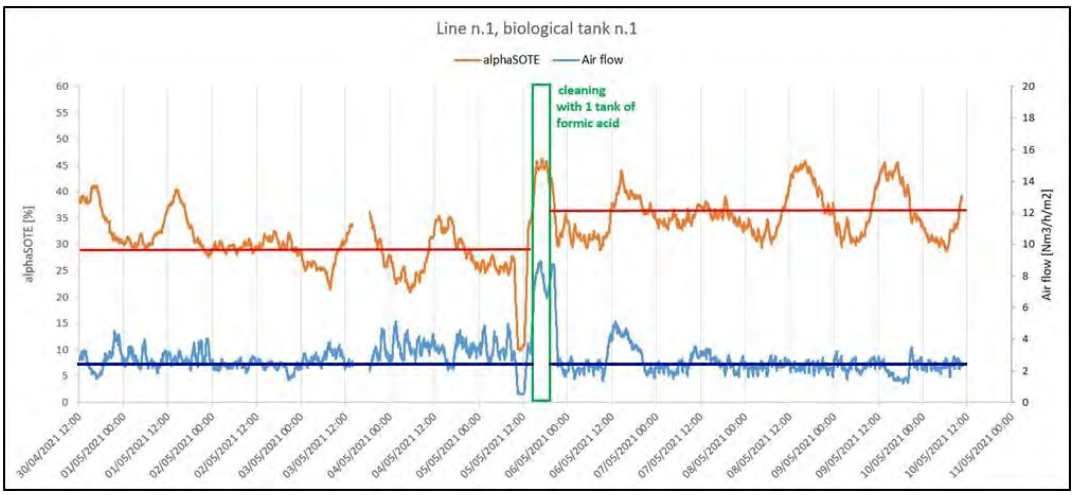

Figure 4. Air diffusers cleaning result

In this case, the air diffusers were cleaned by injecting a formic acid solution into the air supply pipes, so as not to manually clean the diffusers by emptying the tank. The evaluation of the effectiveness of cleaning is made by considering the average levels at which the αSOTE trend stands, eliminating the wide daily variability. In fact, there is an average increase in αSOTE after cleaning (+35%), for the same amount of air flow rate blown into the oxidation tank.

Referring to the evaluation of direct GHG emissions, the LESSDRONE, with its ability to directly measure GHG emissions, overcomes the limitations of generic emission factors provided by scientific literature. These factors do not account for the specific characteristics of wastewater and the management of the WRRFs, particularly in the case of industrial wastewaters.

The LESSDRONE is also used to sample off-gas using nalophan bags. These gas samples are subsequently analyzed for Volatile Organic Compound (VOCs) by gas chromatography and mass spectrometry, hydrogen sulphide (H_2S) by gas chromatography and pulsed flame photometric detector and odour units by SM100i portable automatic olfactometer. These investigations are becoming increasingly interesting as WRRFs are important sources of VOCs and odours. VOCs include all odorous compounds generated by the degradation of organic matter in wastewater. Complaints about smelly emissions from communities living near the WRRFs have steadily increased. Thus, in recent years, the monitoring of odorous emissions has also become important in the WFFRs management.

References

[1] Mannina G., Ekama G., Caniani D., Cosenza A., Esposito G., Gori R., Garrido-Baserba M., Rosso D., Olsson G. (2016) Greenhouse gases from wastewater treatment - A review of modelling tools. Science of the Total Environment 551–552, 254–270.

[2] Vaccari M., Foladori P., Nembrini S., Vitali F. (2018) Benchmarking of energy consumption in municipal wastewater treatment plants - A survey of over 200 plants in Italy. Water Science and Technology 77, 2242–2252.

[3] Foley J., de Haas D., Yuan Z., Lant P. (2010) Nitrous oxide generation in full-scale biological nutrient removal wastewater treatment plants. Water Research 44, 831–844.

[4] Daneshgar, S., Amerlinck, Y., Amaral, A., De Mulder, C., Di Nisio, A., Bellandi, G., ... & Torfs, E. (2024). An innovative model-based protocol for minimisation of greenhouse gas (GHG) emissions in WRRFs. Chemical Engineering Journal, 483, 148327.

[5] Gori R., Balducci A., Caretti C., Lubello C. (2014) Monitoring the oxygen transfer efficiency of full-scale aeration systems: Investigation method and experimental results. Water Science and Technology 70, 8–14.

[6] Redmon, D., Boyle, W. C., & Ewing, L. (1983). Oxygen transfer efficiency measurements in mixed liquor using off-gas techniques. Journal (Water Pollution Control Federation), 1338-1347.

Title: Garden streets in urban areas - pilot project in the city of Antwerp

Author(s): Gert Luyckx*[1], Liselotte De Waele[1]

[1] *Aquafin, Aartselaar, Belgium, Gert.Luyckx@aquafin.be*

Keyword(s): climate resilience, urban area, blue-green measures, citizen participation

Abstract

Due to the predicted climate change, we are forced to look for solutions to our environment in relation to flooding, prolonged droughts and heat stress. We must continuously look for ways to make our environment as climate-resilient as possible. In highly urbanised areas, it is not always easy to find obvious solutions.

For this reason, the city of Antwerp started with the idea of garden streets in 2017. These are not streets where renovation is only thought of as the construction of a separate drainage system, but where a number of additional parameters are taken into account. In the first phase, 5 garden streets were selected.

Recognising the importance of such projects, the Flemish government decided to grant government subsidies to this pilot project on executing these 5 garden streets in the city of Antwerp.

Figure 1. Picture of garden street ‘Aziëlaan’ - before & after

Technical preconditions

From an engineering point of view, solving the technical issues is the most obvious problem.
The rainwater is handled according to the following principle:

- only the strictly necessary paved surfaces are laid out
- necessary pavements are laid as much as possible in permeable material
- drained rainwater is initially drained into a reuse system
- the excess rainwater is further directed to an infiltration facility which is preferably above ground.

The overall system is conceived in such a way that no rainwater leaves the project area. Only for very heavy rainfall events (return period above 20 years), an overflow to the sewer system is allowed. Monitoring is carried out to verify that this condition is reached..

Figure 2. Picture of garden street 'Lange Riddersstraat' (south-side) - before & after

The fact that above-ground infiltration measures are emphasized creates a linkage opportunity for green measures. For example, solutions are found in rain gardens, sunken planting areas, tree growth sites, herb and vegetable gardens, lawns, climbing plants,... Different combinations of these measures are executed in the different garden street projects.

Social part

A completely different aspect of the project is the involvement of the residents.
For example, they are asked to think about possible solutions from the start of the project. They can indicate whether they want to maintain part of the green zone on public property as their own garden, whether they are interested in a rainwater cistern in front of their door or whether they opt for a lawn maintained by the municipality - as in regular projects. On a weekly basis, the residents are informed about the status of the project and they can also provide additional insights.

The ultimate goal is that the street will have a higher amenity value after the project has been completed and that it will create greater social cohesion for the residents.

Figure 3. Picture of garden street ‘Lange Riddersstraat’ (north-side) - before & after

Follow-up and next steps

The 5 different garden streets were installed in the period 2021-2022. Since then, the evaluation period has started. After all, this was part of the subsidy project.

The following parameters will be further monitored during the use phase of the newly created public domain - as a garden street:

- What about the green spaces? Are they well maintained by the residents where it was agreed? Can the public green space be properly maintained?
- How does the infiltration capacity of the different structures change over time? Are there any problems with the Maintenance of it?
- Are the public rainwater cisterns being used sufficiently? Were any problems reported?
- Does the rainwater actually stay within the project area or does the emergency overflow work more often than expected?
- What about the general satisfaction of the residents?

The answers to these questions will be looked at from two sides. First of all, it will be checked whether there are any optimizations in the garden streets as they were carried out. But it is more important to check whether the follow-up research gives rise to improved guidelines and adapted cooperation with the residents. After all, in order to continue to construct garden streets in a successful way in the future, both aspects must be on point. Technically, the design must be correct, but - perhaps more importantly - the residents must support the choices made by the design team.

Title: Normalized measurement proposal for carbon footprint quantification in combined sewer system

Author(s): Lorenzo Tombolini*[1,2], Daniele Caterino[1], Lucia De Simoni[1], Jonathan Domizi[1], Mattia Camerini[3], Cristian Cecchetto[3], Massimiliano Sgroi[1], Giovanna Darvini[4], Anna Laura Eusebi[1], Francesco Fatone[1]

[1]Dipartimento di Scienze ed Ingegneria della Materia, dell'Ambiente ed Urbanistica, Facoltà di Ingegneria – Università Politecnica delle Marche, Ancona (AN), Italy, f.fatone@staff.univpm.it, a.l.eusebi@staff.univpm.it,
[2]Dottorato Nazionale Scientific,Technological and Social Methods Enabling Circular Economy-Università degli studi di Padova, Padova (PD), Italy, lorenzo.tombolini@studenti.unipd.it,
[3]ATS | Servizio idrico integrato | Alto Trevigiano Servizi Spa, Treviso (TV), Italy, c.cecchetto@altotrevigianoservizi.it, m.camerini@altotrevigianoservizi.it
[4]Dipartimento di Ingegneria Civile, Edile e Architettura, Facoltà di Ingegneria – Università Politecnica delle Marche, Ancona (AN), Italy, g.darvini@univpm.it

Keyword(s): Greenhouse gases, sewer network management, carbon footprint, emission factors

Introduction

The overall contribution of the water sector to global greenhouse gas emissions is limited, notwithstanding the wastewater management could represent a significant portion of the urban greenhouse gas emissions inventory [1]. According to parametric evaluation, the European wastewater treatment plants can be considered responsible for about 34 million t CO_2e/year of GHG emissions [2]. Of this amount, about 14 million is due to the carbon footprint of the sewer networks and cannot be reduced through a more targeted operation of WWTPs especially in case of combined sewer systems. Also diffuse CH_4 emissions from the collection networks cannot be controlled through the operation of WWTPs. An improved understanding of the emission of CH_4 and N_2O in the sewer system is apparently needed to identify possible design solutions for their reduction or valorisation. Moreover, the integrated analysis of carbon footprint in the sewerage network is fully aligned with new urban wastewater directive [3] supporting monitoring analysis of GHG and initiatives to achieve energy neutrality. In this sense, the integrated approach allows to fully understand the environmental impact of the entire wastewater cycle and implement effective measures to reduce greenhouse gas emissions. However, a normalized methodology still lacks to quantify these emissions in the sewer networks, both for separated and for combined configurations. In 2017, Italian National Regulatory Authority for Energy, Networks, and Environment (ARERA) implemented the 'Carbon Footprint' (CF) of the wastewater treatment service as crucial performance indicator for the technical management of urban water services. This initiative is aligned with the ISO 14064-1:2019 standard [4], that provides guidelines for organizations to quantify, monitor, report, and verify greenhouse gas (GHG) emissions. The aim of this work is to provide a normalized approach to quantify the carbon footprint of combined sewage system in a territory of 70.000 PE. The method includes a specific sampling campaign and assessment of dissolved and direct emissions of methane, nitrous oxides and carbon dioxides from the sewer system both during the dry and the wet periods.

Materials and method

The proposal for Carbon Footprint Assessment in Sewer Network involves the determination of different impacts categories. Several aspects and steps need to be followed to implement the ISO standard at the organizational level: (1) defining reporting boundaries, (2) aggregating direct and indirect emissions from imported energy, transportation of waste and internal maintenance, (3) quantifying different greenhouse gases (e.g. CO_2, CH_4, N_2O) associated with the type of organization, (4) distinguishing between the anthropogenic biogenic, non-anthropogenic biogenic, or fossil origin of CO_2, (5) the definition of quantitative and/or qualitative uncertainty related to the methodology used for quantifying emissions [5]. In the Table 1, the direct and undirect emission related to this study are shown following the guidelines of the ISO 14064.

Table 1 - ISO 14064 emissions and categories for CF determination in sewer network

EMISSION TYPE - 14064	CATEGORY	GHG's	EF	ref.
DIRECT EMISSION	Direct fugitive emissions	CH_4, CO_2, N_2O	measurements	This study
UNDIRECT EMISSION	Indirect emissions related to energy consumption	tonCO_2eq/ GWh	parametric analysis	National and International databases [6]
	Indirect emissions from transportation for waste disposal and internal maintenance	gN_2O/km, gCH_4/km, gCO_2/km	parametric analysis	National databases [7]
	Indirect emissions from sewerage network	CH_4, CO_2, N_2O	measurements	This study

In this study, a dry weather measurement campaign in the sewer system is conducted to quantify Specific Emission Factors for N_2O, CH_4, and CO_2, related to both direct fugitive emissions into the air and dissolved emissions in the sewer. The assessment is conducted in the urban area of Castelfranco (TV), which comprises four distinct sewer districts served by combined and separate sewerage systems. During the sampling period, from September 2023 to January 2024, are collected five liquid grab samples for each junction (50 samples) and five gaseous grab samples (25 samples). The investigated flowmeters are arranged sequentially from the beginning of the network (P1) down to the final stage of the sewerage (P5), near the Castelfranco Veneto wastewater treatment plant. The samples are analysed in UNIVPM laboratories using Standard IRSA CNR methods to determine analytical parameters such as N_2O, CH_4, and CO_2 as dissolved and direct gas emissions, as well as Ntot, TKN, COD, and TSS for physico-chemical characterization. The dissolved emissions are extrapolated from the liquid through a stripping process and then analysed with an Infrared Photoacoustic Detector (IPD) (Brüel & Kjaer, Multi-gas Monitor Type 1302) [8], while direct emissions are directly measured in the IPD. Then, specific emission factors are evaluated by correlating emissions measurements with physico-chemical characterization results. The campaign yields EF values for dissolved and direct GHG emissions, expressed as kgN_2O/kgTKN; kgCH_4/kgCOD; kgCO_2/kgCOD.

Results

In this section, the results of the analysis are expressed as the average value for each flowmeter investigated during the campaign. In the Table 2, all the data sampled during the sampling period are summarized.

Table 2 - Physico-chemical characterization, gas emissions and emission factors

	P1	P2	P3	P4	P5
PHYSICO-CHEMICAL CHARACTERIZATION					
TSS [mg/l]	43.9 ± 14.2	218.3 ± 417.3	36.1 ± 12.9	1533.2	65.0 ± 11.8
COD [mg/l]	215.2 ± 133.1	1293.6 ± 1804.3	218.6 ± 141.3	1901.8± 1194.7	1287.6 ± 1172.2
TKN [mg/l]	41.3 ± 10.3	80.5 ± 50.8	42.3 ± 8.2	128.9 ± 33.3	61.5 ± 15.8
Ntot [mg/l]	43.3 ± 10.2	68.9 ± 21.9	45.4 ± 5.2	129.2 ± 33.4	63.0 ± 16.4
DISSOLVED AND DIRECT GAS EMISSION					
Dissolved CH_4 [mg/l]	0.64 ± 0.28	1.14 ± 1.05	0.56 ± 0.57	1.12 ± 0.75	3.29 ± 6.83
Dissolved CO_2 [mg/l]	74.07 ± 28.34	106.86 ± 71.72	88.34 ± 23.83	171.8 ± 87.68	125.53 ± 72.18
Dissolved N_2O [mg/l]	3.18 ± 1.86	5.73 ± 7.74	2.74 ± 3.30	4.85 ± 4.82	5.28 ± 4.15
Direct CH_4 [mg/l]	0.040 ± 0.043	0.523 ± 1.216	0.769 ± 0.759	0.755 ± 0.561	2.406 ± 2.868
Direct CO_2 [mg/l]	2.348 ± 1.87	1.014 ± 1.118	7.716 ± 8.348	4.592 ± 2.34	2.699 ± 3.802
Direct N_2O [mg/l]	0.004 ± 0.005	0.002 ± 0.003	0.007 ± 0.007	0.005 ± 0.005	0.005 ± 0.005
EF DISSOLVED GAS					
EF_{CH4} (CH_4/COD)	0.007 ± 0.009	0.004 ± 0.006	0.004 ± 0.003	0.001 ± 0.001	0.003 ± 0.004
EF_{CO2} (CO_2/COD)	0.6 ± 0.503	0.448 ± 0.528	1.063 ± 1.308	0.11 ± 0.077	0.213 ± 0.218
EF_{N2O} (N_2O/TKN)	0.073 ± 0.034	0.06 ± 0.043	0.065 ± 0.078	0.027 ± 0.02	0.09 ± 0.078
EF DIRECT GAS					
EF_{CH4} (CH_4/COD)	0.0002 ± 0.0001	0.0004 ± 0.0006	0.004 ± 0.002	0.001 ± 0.0004	0.002 ± 0.001
EF_{CO2} (CO_2/COD)	0.013 ± 0.005	0.001 ± 0.018	0.040 ± 0.025	0.003 ± 0.002	0.002 ± 0.002
EF_{N2O} (N_2O/TKN)	0.0001 ± 0.0001	0.00003 ± 0.00004	0.0002 ± 0.0002	0.0001 ± 0.00004	0.0001 ± 0.0001

The highest concentrations of COD are in points P2, P4, P5 of the network. The TKN and Ntot concentration fluctuates with the maximum peak in the point P4. TSS values are highest in the point P4. The trend of dissolved gas emission suggests the straight relation between the concentration of macropollutants with the dissolved emission in the sewerage. On the other hand, the direct gas emissions of CO_2 and N_2O have their own peaks in the point 3, while the CH_4 direct emission has the peak in the wastewater treatment plant (sampling point P5). The last part of the results relates to the Emission Factors. The results show how the emission factor of the direct gas emission are significantly lower compared to the EF for dissolved gas in all the sampled points. In the case of dissolved gas emissions, the EF_{CH4} decreases from sampling point 1 to sampling point 4 and then increases again near the treatment plant. The EF_{CO2} are significantly higher in respect to the others with a peak in the point 3 of about 1.063 $kgCO_2/kgCOD$.

Table 3 - Main results of the correlation matrix

X	Y	r - Sperman correlation coefficient	p - Significance test
CO_2 dissolved [mg/l]	Conducibility [µS/cm]	0.964	0.000
CO_2 direct [mg/l]	N_2O direct [mg/l]	0.862	0.000
CH_4 direct [mg/l]	N_2O direct [mg/l]	0.668	0.005
CO_2 direct [mg/l]	i [%]	0.547	0.002
CH_4 direct [mg/l]	TKN [mg/l]	0.540	0.004
CH_4 direct [mg/l]	CO_2 direct [mg/l]	0.533	0.003
CH_4 direct [mg/l]	COD [mg/l]	0.498	0.006
CH_4 dissolved [mg/l]	CH_4 direct [mg/l]	0.493	0.007
CO_2 dissolved [mg/l]	pH	-0.818	0.004

The EF_{N2O} remain constant up to the sampling point 3 and then decrease in the point 4 and increase again near the wastewater treatment plant. The EF_{N2O} and EF_{CH4} are respectively one and two order of magnitude lower than EF_{CO2} but still present as dissolved gases in sewer. Regarding direct gas the EF_{CO2} are always the highest while EF_{N2O} are an order of magnitude lower compared to those of EF_{CH4}. There is a huge difference among the EF_{N2O} of dissolved and direct emission and suggests that N_2O emissions are the less fugitive from the liquid flow. To better understand the different correlations, specific statistical matrix was developed among all the data analysed during the campaign. The Spearman correlation test, conducted with a two-tailed approach, assesses the presence of a monotonic relationship between two variables without presuming its direction. It ranges from -1 to 1, where 1 indicates a perfect positive correlation, 0 indicates no correlation and -1 indicates a perfect negative correlation. A low p-value (typically less than 0.05-0.07) indicates stronger evidence against the null hypothesis, suggesting that the observed correlation is statistically significant. The results of the main evidence are expressed in Table 3. The strong direct relationship between dissolved CO_2 and conductivity and the resulting inverse relationship with pH should be probably linked to the CO_2 behaviour and partition in the liquid with possible formation of H_2CO_3. This compound, through chemical equilibrium, releases H^+ ions into the liquid flow by decreasing the pH. On the contrary, an increment of ionic forms results in a higher conductivity. The fugitive emissions of all greenhouse gases (CH_4, CO_2 and N_2O) are correlated each other and they increase at higher concentrations of the liquid macropollutants (COD, TKN) in the flow. The CH_4 is the only GHG that has a positive and significative relation among its own dissolved and the direct emission. As a final indication, the direct emission of CO_2 increases with the slope, probably caused by the correlation between the more elevated turbulent flow and the enhancing of the stripping gas phenomena. Continuous measurement by CH_4 and N_2O probes were carried out.

Conclusion

In conclusion, the proposed methodology represents a possible option to face the current lack of a normalized method for carbon footprint estimation in the sewer network service. Regarding the results, the dissolved emissions in the sewer system are always higher in respect to the direct emissions. The highest concentration of dissolved GHG's in the sewer network is CO_2 followed by N_2O and CH_4 while in the case of direct emissions the more elevated value is always related to CO_2, CH_4 and N_2O. Possible correlations with pH, macropollutants amounts and sewer system slope were found.

Acknowledgements

The water utility ATS and EU-PNRR as PRIN 2022 (N4En project. CUP: B53D23005590006) are kindly acknowledged for financial and technical support.

References

[1] Liu Y. Quantification and Modelling of Fugitive Greenhouse Gas Emissions from Urban Water Systems, 2022.
[2] Parravicini V, Nielsen PH, Thornberg D, Pistocchi A. Evaluation of greenhouse gas emissions from the European urban wastewater sector, and options for their reduction. Science of The Total Environment 2022;838:156322. https://doi.org/10.1016/J.SCITOTENV.2022.156322.
[3] Council of the European Union. Proposal for a Directive of the European Parliament and of the Council concerning urban wastewater treatment 2024.
[4] 14064-1. Greenhouse gases - Part 1: specification for the quantification, monitoring 2019.
[5] Marinelli E, Radini S, Foglia A, Lancioni N, Piasentin A, Eusebi AL, et al. Validation of an evidence-based methodology to support regional carbon footprint assessment and decarbonisation of wastewater treatment service in Italy. Water Res 2021;207:117831. https://doi.org/10.1016/J.WATRES.2021.117831.
[6] ISPRA. Fattori di emissione atmosferica di gas a effetto serra e altri gas nel settore elettrico, 2018.
[7] SINANET. SINANET 2017. http://www.sinanet.isprambiente.it/it (accessed May 2, 2024).
[8] Costa A. Definition of emission factor for methane(CH4) from manure management from swine husbandry. ID 421096: http://www.ipcc-nggip.iges.or.jp/EFDB/find_ef_main.php, 2010.

Title: Modelling spatial changes of Soil Organic Carbon in Flanders, Belgium

Authors: Stefano Spotorno*[12], Anne Gobin[3], Fien Vanongeval[3], Adriana Del Borghi[1], Michela Gallo[1].

[1]*Department of Civil, Chemical and Environmental Engineering (DICCA), University of Genoa, Genova, Italy (Email: adriana.delborghi@unige.it, michela.gallo@unige.it)*
[2]*University School for Advanced Studies IUSS, Italy, Pavia (Email: Stefano.spotorno@iusspavia.it)*
[3]*Division of Soil and Water Management, Department of Earth- and Environmental Sciences, Katholieke Universiteit Leuven, Leuven, Belgium (Email: anne.gobin@kuleuven.be, fien.vanongeval@kuleuven.be)*

Abstract: Carbon sequestration in soils is essential for mitigating climate change and promoting sustainable soil management. The European Union emphasizes reducing greenhouse gas emissions in agriculture, highlighting the need for innovative carbon sequestration methods. This study used the RothC model to analyse Soil Organic Carbon (SOC) in Flanders, Belgium, showing that cover crops and improved crop rotations could reduce soil emissions by up to 60%. Key variables influencing outcomes were Business As Usual carbon inputs and initial carbon content.

Keywords: Carbon sequestration in soils; Soil Organic Carbon (SOC); RothC.

1. INTRODUCTION

Carbon sequestration in soils is a crucial strategy for mitigating climate change and promoting sustainable soil management by removing CO_2 from the atmosphere and storing it in stable carbon pools[1]. This process not only helps mitigate climate change but also enhances soil fertility, nutrient cycling, biodiversity, and ecosystem services, while reducing erosion and improving water management. The global technical mitigation potential for agriculture is significant, with soil carbon sequestration contributing about 89% of the potential reduction in CO_2 emissions [2]. The European Union (EU) is actively pursuing strategies to reduce greenhouse gas emissions from agriculture, which constitutes 11% of its total emissions. The EU's Common Agricultural Policy (CAP) has been revised to emphasize environmental sustainability and promote carbon sequestration practices. Carbon Farming (CF) has emerged as a promising approach, encompassing practices such as agroforestry, improved crop rotations, peatland restoration, and nutrient management on croplands and grasslands [3]. These practices aim to sequester carbon in soils and biomass, reduce emissions, and enhance agricultural resilience to climate impacts. To accurately quantify and monitor soil carbon sequestration, robust methodologies, computational models, and monitoring frameworks are essential [4]. The RothC model is one such tool used to assess carbon sequestration in soils [5]. This study utilized the RothC model to evaluate the impact of sustainable soil management practices on soil organic carbon (SOC) changes in the topsoil of Flanders, Belgium. The model's simulations aimed to provide reliable estimations of SOC changes over twenty years, facilitating participation in carbon markets and supporting the implementation of CF practices. The study's objectives included modeling sustainable soil management practices, assessing their spatial variability, and identifying the most sensitive model variables affecting SOC changes. The findings underscore the potential of CF practices to contribute significantly to climate mitigation in agricultural soils and highlight the importance of accurate baseline definitions for effective carbon credit schemes. By enhancing the understanding of SOC dynamics and the impact of various practices, this research supports the broader adoption of CF and contributes to achieving sustainable development goals related to climate action and sustainable agriculture.

2. MATERIALS & METHODS

RothC-26.3 is a process-based model that simulates organic carbon dynamics in non-waterlogged topsoils with a monthly time-step. Implemented in R using the RothC Model function from the SoilR package [6], the model was modified to include soil cover effects and can run in both inverse and forward modes. It tracks changes in five organic carbon pools. The model requires inputs on soil texture, carbon inputs, climate, vegetation cover, and plant material decomposability. Climate data was processed from the Royal Meteorological Service, and potential evapotranspiration was calculated using the Penman-Monteith equation [7]. Initial SOC data, considered representative for 2004, was sourced from sampling in Flanders, excluding outliers for better accuracy. Clay content was obtained from ISRIC SoilGrids, and land use data from the ESA, focusing on agricultural land. Vegetation cover data was retrieved from MODIS NDVI products [8], using Google Earth Engine for processing. The modelling phase, based on the GSOCseq technical manual [9], began with a 10,000-year inverse run ("spin-up phase") to estimate yearly carbon (C) inputs needed to reach 2004 SOC equilibrium levels using 1985-2004 climate data. To minimize variability and account for climate changes up to 2022, a "warm-up phase" adjusted C inputs based on changes in NPP [10]. The forward phase then simulated SOC dynamics for the next 20 years using 2005-2020 climate data. The model scenarios analyzed include business-as-usual (BAU) conditions and two alternative soil carbon enrichment strategies: improved crop rotations and cover crops. The BAU scenario uses C inputs derived from the spin-up and warm-up phases, assuming no changes in climate or land use. The alternative scenarios evaluate the impact of different crop rotations and the use of cover crops, such as yellow mustard, on soil organic carbon (SOC) stocks. Crop-specific C inputs and decomposability ratios were adapted based on data from Belgium, and the use of cover crops was assumed to increase C inputs by 12% over the BAU scenario [11]. The SOC sequestration potential is calculated as the difference between SOC stocks in the alternative scenarios and the BAU scenario, with simulations conducted across all arable agricultural land in Flanders. The RothC model's performance was assessed using SOC measurements from the LUCAS survey conducted in 2009 [12], 2015 [13], and 2018 [14]. Bulk density estimates were used to calculate SOC stocks, which were compared with model simulations from 2005 to the respective survey years. Evaluation metrics included coefficient of determination (R^2), Mean Absolute Error (MAE), Root Mean Squared Error (RMSE), and Cohen's d. ΔSOC (difference between final and initial SOC in 2004) was used for comparison. Statistical correlation analysis was conducted between model variables and ΔSOC.

3. RESULTS AND DISCUSSION

Under Business-As-Usual (BAU) conditions, agricultural soils in Flanders exhibit a decreasing trend (**Figure 1**) in soil organic carbon (SOC) stocks, indicating net carbon emissions. Both scenarios incorporating cover crops (CC) and enriched crop rotations show decreasing SOC stocks over time. In the BAU scenario, a release of up to 9 tC/ha is expected in twenty years. Although the use of CC mitigates this loss, a net loss of 6.5 tC/ha is still projected. Different crop rotations influence the rate of decrease, with rotation 1 resulting in a slower decrease compared to others, reaching a net loss of 2.5 tC/ha in twenty years, significantly lower than other rotations. Rotation 2, 3, and 4 show higher net losses of 10.5 tC/ha, 7.5 tC/ha, and 7.5 tC/ha respectively. The SOC sequestration potential after 20 years, compared to the BAU scenario, is reported in maps (**Figure 2**) where white to green indicates SOC accumulation and white to red indicates SOC loss. Cover crops (CC) can increase SOC stocks by 3 tC/ha evenly across Flanders, while improved rotation 1 shows a homogeneous increase of up to 8.5 tC/ha. However, rotations 2, 3, and 4 display spatial variations, with rotation 2 showing marked SOC loss, especially in central zones, while rotations 3 and 4 exhibit higher SOC accumulation in the south.

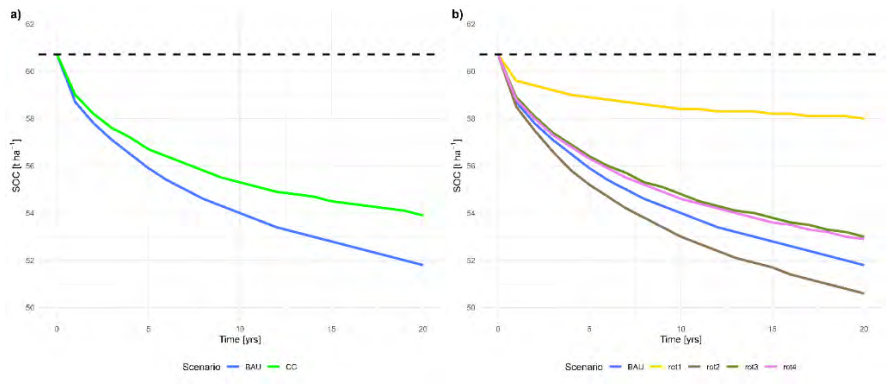

Figure 1. SOC trends under different management scenarios: a) Use of cover crops (CC) compared to the BAU scenario; b) improved rotations1, 2, 3 and 4 compared to the BAU scenario. See Table 1 for the crops in rotation.

Spatial variability of SOC stock in 2022 is significant, with higher values in the northwest and central-eastern regions, peaking at 90 tC/ha. BAU C inputs vary spatially, ranging from 1.37 to 7.36 tC/ha/yr, with peaks in central-eastern areas and lowest values in the southern region.

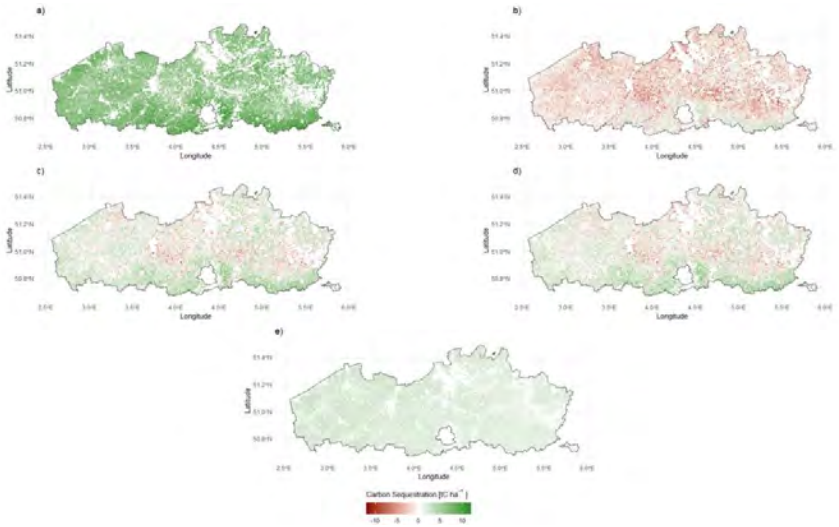

Figure 2. SOC sequestration potential at twenty years with respect to the BAU (relative change): a) Improved rotation 1; b) improved rotation 2; c) Improved rotation 3; d) improved rotation 4; e) cover crops.

Table 1: coefficient of determination (R2), Mean Absolute Error (MAE), Root Mean Squared Error (RMSE) and Cohen's d (d).

Year	Number of observations	R^2	MAE [$tCha^{-1}$]	RMSE [$tCha^{-1}$]	d [$tCha^{-1}$]
2009	11	0.20	0.92	1.18	0.64
2015	31	0.52	0.92	1.33	0.75
2018	26	0.40	0.72	1.03	0.75
Aggregate	68	0.53	0.93	1.22	0.83

The statistical correlation (R^2) of individual years is weaker than that of the aggregate. The year 2018 has lower values in terms of MAE and RMSE than all the other years, hence it shows a better performance. The effect size is large for each year and for the aggregate values, except for the year 2009, which has the lowest value of d (**Table 1**).

4. CONCLUSIONS AND FUTURE PERSPETCIVES

This study used the RothC model to predict changes in soil organic carbon (SOC) stocks in Flanders' agricultural soils. Results showed that Flanders' soils are net carbon emitters, especially in the Business-As-Usual (BAU) scenario, aligning with previous observations. Cover crops (CC) mitigated SOC loss by about 20%, as observed in similar studies in western Germany [11]. Improved rotations, particularly rotation 1 (grain maize monoculture), effectively reduced SOC losses. Spatial variability analysis showed CC implementation led to uniformly distributed SOC accumulation, while rotation 1 was effective throughout the region. BAU C inputs strongly influenced SOC changes, with areas of higher inputs showing less response to accumulation. Correlation analysis highlighted the influence of initial SOC, clay content, and climate variables on SOC changes. Validation showed the RothC model performed well, despite limitations in data availability and model scope. Overall, while sustainable soil practices reduced emissions, they couldn't fully reverse trends, emphasizing the need for targeted interventions and improved data for carbon farming initiatives.

References

[1] Lal, R., “Soil carbon sequestration impacts on global climate change and food security”, *Science 304*(5677), 2004, pp. 1623–1627.
[2] Smith et al., “(PDF) Chapter 8 Greenhouse Gas Mitigation in Agriculture”, 2007.
[3] Mcdonald, H., A. Frelih-Larsen, A. Lóránt, et al., “Carbon farming Making agriculture fit for 2030 Policy Department for Economic, Scientific and Quality of Life Policies Directorate-General for Internal Policies”, 2021.
[4] Paustian, K., J. Lehmann, S. Ogle, D. Reay, G.P. Robertson, and P. Smith, “Climate-smart soils”, *Nature 532*(7597), 2016, pp. 49–57.
[5] Coleman, K., and D.S. Jenkinson, “RothC-26.3 - A Model for the turnover of carbon in soil”, *Evaluation of Soil Organic Matter Models*, Springer (1996), 237–246.
[6] Carlos A. Sierra, Markus Mueller, and Susan E. Trumbore, “Models of soil organic matter decomposition: the SoilR package, version 1.0”, *Geoscientific Model Development 5*(4), 2012, pp. 1045–1060.
[7] Gobin, A., and H. Van De Vyver, “Spatio-temporal variability of dry and wet spells and their influence on crop yields”, *Agricultural and Forest Meteorology 308–309*, 2021, pp. 108565.
[8] Didan, K., “MOD13A2 MODIS/Terra Vegetation Indices 16-Day L3 Global 1km SIN Grid V006”, 2015. https://lpdaac.usgs.gov/products/mod13a2v006/
[9] FAO, “Technical Specifications and Country Guidelines for Global Soil Organic Carbon Sequestration Potential Map (GSOCseq)”, 2020.
[10] Smith, J., P. Smith, M. Wattenbach, et al., “Projected changes in mineral soil carbon of European croplands and grasslands, 1990–2080”, *Global Change Biology 11*(12), 2005, pp. 2141–2152.
[11] Seitz, D., L.M. Fischer, R. Dechow, M. Wiesmeier, and A. Don, “The potential of cover crops to increase soil organic carbon storage in German croplands”, *Plant and Soil 488*(1), 2023, pp. 157–173.
[12] European Commission. Joint Research Centre. Institute for Environment and Sustainability., *LUCAS topsoil survey: methodology, data and results.*, Publications Office, LU, 2013.
[13] European Commission. Joint Research Centre., *LUCAS 2015 topsoil survey: presentation of dataset and results.*, Publications Office, LU, 2020.
[14] Fernandez, U.O., S. Scarpa, A. Orgiazzi, et al., “LUCAS 2018 Soil Module”, *JRC Publications Repository*, 2022. https://publications.jrc.ec.europa.eu/repository/handle/JRC129926

Energy efficiency in wastewater treatment plant: benchmark analysis on more than 50 plants in Sicily

Author(s): Daniele Di Trapani[1], Marco Carciola[1], Santo Fabio Corsino[1], Alida Cosenza[1], Gaetano Di Bella[2], Gianfranco Gravina[3], Luigi Gurreri[4], Giuseppe Mancini[4], Antonella Luciano[5], Michela Langone[6], Davide Mattioli[6], Luigi Petta[6], Gianpaolo Sabia*[6], Giovani Sciortino[7], Michele Torregrossa[1], Gaspare Viviani[1]

[1] *Department of Engineering, University of Palermo, Palermo, Italy,*
[2] *Faculty of Engineering and Architecture, University of Enna "Kore", Enna, Italy*
[3] *ACQUAENNA S.C.p.A., Via Sant'Agata, 65/71, 94100 Enna, Italy.*
[4] *Department of Electrical, Electronic and informatic Engineering, University of Catania, Catania, Italy*
[5] *Laboratory Instruments for the Sustainability and Circularity of Productive and Territorial Systems, Italian National Agency for New Technologies, Energy and Sustainable Economic Development (ENEA), CR Casaccia, Via Anguillarese, 301, 00123 Santa Maria di Galeria, Roma, Italy.*
[6] *Laboratory Technologies for the Efficient Use and Management of Water and Wastewater, Italian National Agency for New Technologies, Energy and Sustainable Economic Development (ENEA), CR Bologna, Via dei Mille, 21, 40121, Bologna, Italy.* gianpaolo.sabia@enea.it
[7] *AMAP S.p.A., Via Volturno, 2, 90138 Palermo, Italy.*

Keyword(s): benchmarking, energy efficiency, wastewater treatment, performance indicators, smart WWTP

Abstract

Nowadays, the water and wastewater sectors are facing pivotal challenges, resulting from aging and ineffective processes, which promote high electric energy consumption and significant carbon emissions [1]. Moreover, the above issues have been worsened by climate change impacts and increasing population [2]. At the same time, the reference legislation in the wastewater sector is currently being developed at both European and Italian levels, seeking to promote ambitious targets in terms of WWTP energy neutrality and stricter discharge limits. An approximate estimate suggests that more than 2% of the world's electrical energy is utilized for water supply and wastewater treatment globally [3,4]. Municipal wastewater treatment plants (WWTPs), being a prominent segment of water utilities, significantly contribute to the total energy consumption in this sector. The overall WWTP electricity use in Europe (only plants with no less than 2.000 population equivalent (PE) have been considered) was estimated at 24.747 GWh yr^{-1}, about 0,8% of the electricity consumption in the EU-28 [5]. A substantial portion of primary energy, primarily derived from fossil fuels, is employed in WWTPs to adhere to strict standards concerning effluent water quality, albeit this contributes to environmental issues like global warming and climate change. In 2018, wastewater treatment in the EU produced 34,45 million tons of CO_2 equivalent annually, accounting for 0,86% of the EU's total greenhouse gas emissions. This included 4% of methane (CH_4) and 3% of nitrous oxide (N_2O) emissions. Operational activities contributed approximately 13 million tons of CO_2 equivalent per year, with 4,6 million tons from energy use for wastewater collection and treatment, and 8,4 million tons from the treatment process itself [6]. In this context, it is crucial to implement measures aimed at simultaneously maintaining high-quality effluents while enhancing energy efficiency in WWTPs. The benchmark of energy consumption in WWTPs serves as a powerful management tool for energy saving, employing specific indicators to ascertain optimal performance or assess plants energy efficiency in comparison to other plants or reference standard values [7,8]. Currently, there is no universal benchmarking system for energy performance in WWTPs at the international level, and the few available benchmarking studies are often fragmented and conducted locally based on national or regional surveys. Additionally, very few studies

are available on the water-energy nexus specifically associated with energy demand and, subsequently, greenhouse gas (GHG) emissions [9]. A broad survey in the Italian context has been presented by Vaccari et al. [10], where a total of 289 municipal WWTPs were included in the study. Nevertheless, as the authors are aware, no benchmark information is available for WWTPs located in the Sicilian territory. Therefore, the present study aims to provide new knowledge and data on a benchmark of energy consumption in WWTPs located in an area (Sicily) that requires remarkable efforts to respond in the near future to the need for energy-efficient WWTPs. Moreover, according to the available data set, the present study provides a preliminary evaluation of the carbon footprint (CF) of WWTPs, specifically related to energy demands. The results of the present study have been achieved within the research project "Smart Energy-Efficiency wastewater treatment Plants (SMARTEE-PLANTS)", whose final aim is to pursue energy efficiency of WWTPs throughout the Sicilian territory, with a special focus on the metropolitan areas of Catania, Enna and Palermo.
The survey included 54 WWTPs located in Sicily. Data were obtained through specific questionnaires compiled by the treatment plant operators from 2 large multi-utility bodies. P.E. served by the plants (P.E.s) were calculated in this study referring to a per capita contribution of 60 $gBOD_5$ $P.E.^{-1}$ d^{-1}. Data variables over time were collected as average values on an annual basis. For each plant, a minimum dataset of three years of operation was requested from the WWTPs operators. Moreover, information about plant configuration were collected, especially regarding biological processes applied as secondary treatment for COD and nutrient removal, as well as for sludge stabilisation. WWTPs exhibiting uncommon characteristics or lacking sufficient information or consistency were omitted from the sample, resulting in a final sample of 42 plants considered for the following elaborations.
The study was based on the calculation of specific energy consumption indicators (ECIs), commonly defined, with reference to a specific time basis, as the ratio between the energy consumption and one relevant parameter in the plant, according to the reference literature [8]. Three ECIs were calculated for each WWTP according to the following expressions (Table 1):

Table 1: Energy consumption indicators

Energy consumption indicators	Units	Equation n.
$ECI_{m3} = \frac{Energy\ consumption\ [\frac{KWh}{y}]}{Treated\ wastewater\ flowrate\ [\frac{m^3}{y}]}$	$\left[\frac{KWh}{m^3}\right]$	(eq.1)
$ECI_{COD} = \frac{Energy\ consumption\ [\frac{KWh}{y}]}{COD\ load\ removed\ [\frac{kgCOD_{rem}}{y}]}$	$\left[\frac{KWh}{kgCOD_{rem}}\right]$	(eq.2)
$ECI_{PE} = \frac{Energy\ consumption\ [\frac{KWh}{y}]}{Population\ equivalent\ [P.E.s]}$	$\left[\frac{KWh}{P.E.s\ year}\right]$	(eq.3)

Data analysis was carried out after partitioning the surveyed WWTPs into four classes of design-based plant size: (1) class with P.E.< 2.000, which comprises 7 plants; (2) class with 2.000 < P.E. < 10.000, which comprises 22 plants; (3) class with 10.000 < P.E. < 50.000, which comprises 10 plants; (4) class with P.E. > 50.000, which comprises 3 plants. Once the ECI values for each class were calculated, the statistics of mean, 25° and 75° percentiles, minimum, and maximum were elaborated, and the results were graphically represented using box plots and compared with respective benchmark corresponding to the mean value of a representative sample of EU WWTPs [11], [12]. With reference to the box plots (Figure 1), for all the considered ECIs, the sample of plants examined is on average less energy efficient than the respective benchmark. Specifically, in comparison with other EC indicators, the ECI_{m3} showed the closest values to the relevant benchmark references, for all WWTP's size classes; on the other

hand, for ECI_{COD}, values are generally outlying the corresponding benchmark, showing higher energy consumptions, mainly related to the generally low COD values in the raw wastewater fed to the plants. According to the available data set, the carbon footprint (CF) of each plant was estimated by quantifying the Direct (DE) and Indirect (IE) Emissions.

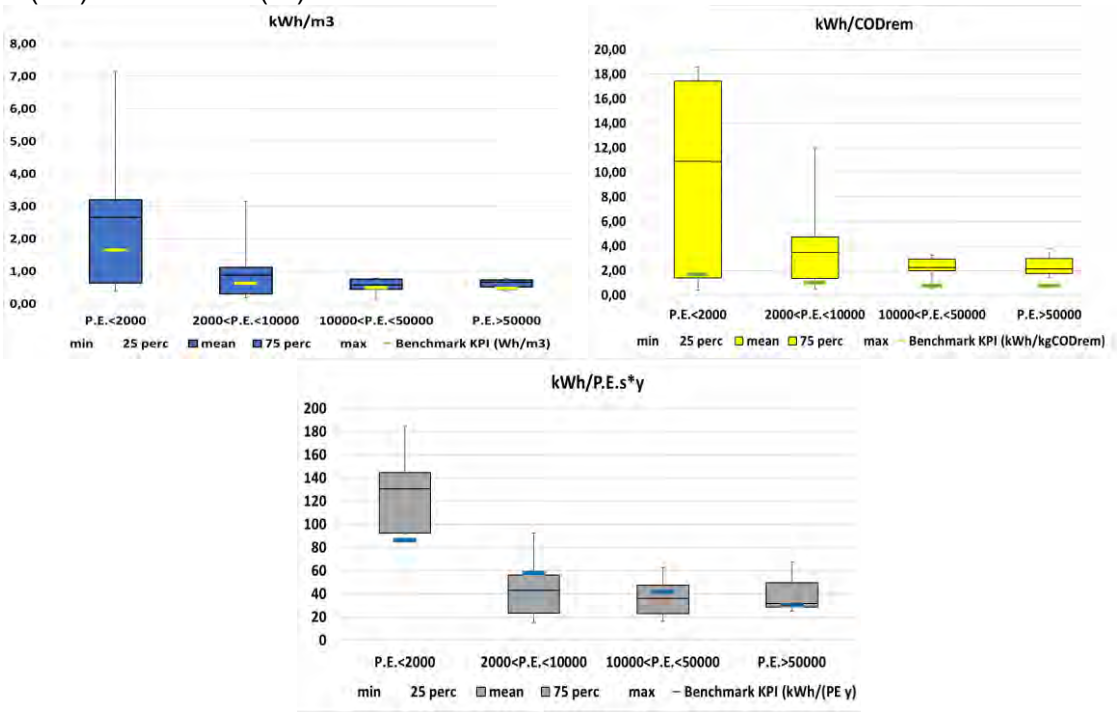

Figure 1. Boxplot for the different ECIs considered in the study

Specifically, DE were evaluated taking into consideration: the equivalent CO_2 due to the bio-treatment (including organic carbon oxidation, endogenous respiration and, separately, the contribution of N_2O emission, [13] [14]) and to CH_4 emission generated along the whole treatment line [13]; IE were determined by summing the equivalent CO_2 due to energy consumption according to [16], using an emission factor as reported in [17]. Also, for such evaluations, WWTPs lacking sufficient information were omitted. The total WWTP emissions, expressed as CO_2 equivalents (CO_{2e}), were grouped according to the defined plant size classes to derive the related emission factor per P.E. served (Table 2). The outcomes highlighted the higher impacts of small WWTPs.

Table 2: Calculated GHG emissions and emission factors per plant size classes.

WWTP Class Size	n. of WWTPs	$kgCO_{2e}/y$	Total served P.E.	$kgCO_{2e}$/served P.E./y
P.E.<2.000	2	396.021	3.910	101,3
2.000≤ P.E.<10.000	14	2.572.035	47.492	54,2
10.000≤ P.E.<50.000	7	5.244.946	109.400	47,9
P.E.≥50.000	3	28.760.276	472.764	60,8

The incidence of different GHG sources was also assessed. In smaller WWTPs the use of energy (IE) represents the major contribution to total emissions. In contrast, the bio-treatment emissions (and particularly, the removal of organic and nitrogen loads, and biomass activity, DE) account for the higher share in greater plants.
The work allowed to derive a first framework of the energy requirements and GHG emissions of a sample

of 42 WWTPs located in the Sicilian territory. The information gained show a lower energy efficiency of the assessed WWTPs than sector benchmarks, also resulting in higher impacts in terms of climate gas emissions. Further in-depth assessments will be aimed at identifying the specific treatment units to be improved and defining strategies and actions to improve energy efficiency and GHG impacts.

Conclusions

From the achieved results, the most suitable indicator of the specific energy consumption is expressed as kWh/m^3 while the indicator expressed as kWh/COD_{rem} appeared misleading because plants with very low COD values in the feeding wastewater appear erroneously less energy efficient. The emission analysis highlighted that direct emissions represent the major contributor.

Acknowledgements

This study was carried out within the SMARTEE-PLANT Research Project and received funding from the European Union FESR (Project n. n. 08CT3600000330 - CUP G57H18002050006). Authors warmly thank Dr. Alessio Librizzi for his precious support with data processing.

References

[1] Borzooei, S., Campo, G., Cerutti, A., Meucci, L., Panepinto, D., Ravina, M., Riggio, V., Ruffino, B., Scibilia, G., Zanetti, M., 2019. Optimization of the wastewater treatment plant: from energy saving to environmental impact mitigation. Sci. Total Environ. 691, 1182–1189.
[2] Haldar, K., Kujawa-Roeleveld, K., Acharjee, T.K., Datta, D.K., Rijnaarts, H., 2022. Urban water as an alternative freshwater resource for matching irrigation demand in the Bengal delta. Sci. Total Environ. 835, 155475
[3] Olsson, G. 2012. Water and Energy: Threats and Opportunities. IWA Publishing, London, UK.
[4] Zib, L., Byrne, D. M., Marston, L. T., Chini, C. M., 2021. Operational carbon footprint of the U.S. water and wastewater sector's energy consumption, Journal of Cleaner Production, 321, 128815,
[5] Ganora et al (2019). Opportunities to improve energy use in urban wastewater treatment: a European-scale analysis. Environmental Research letters 14 044028.
[6] Impact Assessment accompanying the document Proposal for a Directive of the European Parliament and of the Council concerning urban wastewater treatment (recast) {COM (2022) 541 final} - {SEC (2022) 541 final} - {SWD (2022) 544 final}.
[7] Krampe, J. 2013 Energy benchmarking of South Australian WWTPs. Water Science & Technology 67 (9), 2059–2066.
[8] Torregrossa, D., Schutz, G., Cornelissen, A., Hernández-Sancho, F. & Hansen, J. 2016. Energy saving in WWTP: daily benchmarking under uncertainty and data availability limitations. Environmental Research 148, 330–337.
[9] Chini, C., Excell, L., Stillwell, A., 2020. A review of energy-for-water data in energy-water nexus publications. Environ. Res. Lett. 15, 123011.
[10] Vaccari, M., Foladori, P., Nembrini, S., Vitali, F. 2018. Benchmarking of energy consumption in municipal wastewater treatment plants – a survey of over 200 plants in Italy. Water Science & Technology, 77.9. doi: 10.2166/wst.2018.035.
[11] G. Sabia, L. Petta, F. Avolio, E. Caporossi (2020) Energy saving in wastewater treatment plants: A methodology based on common key performance indicators for the evaluation of plant energy performance, classification and benchmarking. Energy Conversion and Management 220 (2020) 113067. https://doi.org/10.1016/j.enconman.2020.113067
[12] M. Canditelli, M. Ferraris, P. G. Landolfo, L. Luccarini, D. Mattioli, F. Musmeci, L. Petta, G. Sabia (2016) Gestione efficiente della risorsa idrica e del rifiuto organico in una smart city Report RdS/PAR2016/027
[13] IPCC. 2019 Refinement to the 2006 IPCC Guidelines for National Greenhouse Gas Inventories.
[14] Snip, L.J.P. (2010) Quantifying the Greenhouse Gas Emissions of Waste Water Treatment Plants. Thesis Project Systems and Control, MES (Environmental Sciences), Wageningen, The Netherlands.
[15] Bridle Consulting. (2007). Development of a process model to predict GHG emissinos from the water corporation metropolitan WWTPs.
[16] Mannina, G., Rebouças, T. F., Cosenza, A., & Chandran, K. (2019). A plant-wide wastewater treatment plant model for carbon and energy footprint: model application and scenario analysis. Journal of Cleaner Production,

217, 244-256.
[17] ISPRA Rapporto 363/2022 Indicatori di efficienza e decarbonizzazione del sistema energetico nazionale e del settore elettrico ISBN: 978-88-448-1107-5

PARALLEL SESSION: D2

Municipal and industrial waste

Material recovery

Title: Vermicomposting applied to OFMSW: study with laboratory-scale vermicomposters

Author(s): Enrico Licitra[1], Gaetano Di Bella*[1]

[1] Department of Engineering and Architecture, University of Enna "Kore", Cittadella Universitaria, 94100 Enna, Italy, enrico.licitra@unikore.it, gaetano.dibella@unikore.it

Keyword(s): Vermicomposting; OFMSW; Eisenia Fetida; Soil improver; Heavy metals

Abstract

Composting is the most widely used and studied biological process for the managing of organic fraction of municipal solid waste (OFMSW) **[1]**. It is a process of aerobic biodegradation of organic waste carried out by microorganisms, in which organic waste is converted into soil improver, containing mineral compounds such as CO_2, H_2O, NH_4, as well as organic compounds rich in humus **[2]**. On the other hand, vermicomposting is inspired by a similar biological (aerobic) process operated by the combined activity of worms and bacteria, thanks to whom nutrients in organic waste are transformed into a stable, available, and nutrient-rich product for plant growth **[3]**. In particular, in vermicomposting, the oxidation and biological stabilization of organic waste depend on the interaction between worms and microorganisms in the mesophilic transformation processes **[4]**. Typically, worms process the most substantial amounts of soil in nature; they consume dead plant debris, animal excrement, and thereby they contribute to positive soil transformation and to promote the mineralization of dead plant matter. However, despite the variety and abundance of worms in nature, the controlled use of worms to enhance the biological treatment of organic waste has so far been largely limited to vermiculture of animal manure and, to a lesser extent, domestic food waste **[5]**.

In municipal solid waste, usually, there are other more recalcitrant vegetable fractions such as leaf waste, weeds, crop residues, and also toxic elements derived from imperfect upstream separation. Despite vermicomposting is an inherently cleaner process than composting, as it requires much less energy due to lower temperatures reached during the process and does not require periodic turning of piles or forced aeration thanks to the activity of worms, there are many doubts about long-term results and the real negative influences due to the presence of certain pollutants in municipal waste, even if selected **[6]**. Currently, the mainly application of vermicomposting is correlated to the transformation of waste from zootechnics such as bovine manure. Indeed, the presence of potential toxic elements, such as heavy metals contained in the waste, can affect soil quality and worm's growth. Nevertheless, the biochemical transformations of heavy metals during vermicomposting process are still controversial, despite the current compost standard setting limits on total concentrations of toxic metals. Several studies have reported increases in total concentrations of heavy metals during vermicomposting **[7,8]**, while other studies have obtained a completely opposite behavior, in which the activity of worms can influence the real solubility and bioavailability of heavy metals, modifying the speciation of vermicast **[9]**.

However, considering the large volume of OFMSW produced and the need for proper management and transformation of these waste materials into reusable and environmentally friendly products, this study aims to evaluate the combined process of composting-vermicomposting for the management of OFMSW, using *Eisenia Fetida* species and complementing the process with the addition of preselected organic matter. The experimental work was based on laboratory batch tests using pilot vermicomposting systems, in which the physical-chemical parameters, worm growth rate, and their growth characteristics

(accumulation of metals in tissues, production of worm tea, etc.) were monitored and measured during the transformation processes of real matrices derived from a composting plant, placed in the province of Catania (Italy), with receptive capacity of about 150,000 tons per year of OFMSW. The processing line of composting plant includes: 1) weighting and reception; 2) unloading and storage of lignocellulosic waste; 3) wood shredding and storage of shredded wood; 4) unloading and storage of OFMSW; 5) waste mixing; 6) accelerated and intermediate bio-oxidation; 7) stabilization, maturation, and storage of raw compost; 8) final screening; 9) storage of finished compost.

Specifically, the experimental study was carried out at the *Laboratory of Environmental Sanitary Engineering* of the University of Enna and it involved the use of "prefabricated" vermicomposters provided by the CONITALO company, a leader in the vermiculture sector since 1979 (https://www.conitalo.it/). The worms, *Eisenia Fetida*, were provided by the same company that supplied the vermicomposters. The provided worms were young and kept in the mother culture in 200-grams packages. Initially, the worm biomass was taken and acclimated in mixed cultures of rabbit manure and selected organic material before being placed in the vermicomposters. Each vermicomposting unit consisted of a lower compartment for leachate accumulation, and three additional compartments (of which only two were utilized for the purposes of the proposed study) for placing the composting matrices. The bio-treatment compartment was essentially comprised of a bedding system in which the worms could be introduced within a thin layer of organic material that would be consumed over time. Additional layers were added to the upper platforms in day 0 of the experimental study, which were accessible to the worms residing in the lower layers. It was important that the various layers of organic material in each compartment were not too thick (maximum size 4-5 cm) to allow the worms to colonize and degrade the entire depth. Five tests were planned using five different composting units, studying for 180 days the transformation of different organic matters: OFMSW, before the mixing phase with bulking agents (shredded wood); PRE-COMPOST, collected after the accelerated bio-oxidation phase; COMPOST, stabilized fraction collected after the maturation phase, before the screening phase.

In order to facilitate a comparative experimental investigation with “regular matrices”, a sample of organic selected material from household waste was concurrently prepared. This sample represents the "blank" reference, free from impurities. The analytical characterization of each (initial) sample is shown in Table 1.

Table 1. Initial characteristics of organic substrates

Parameters	*MU*	*OFMSW*	*Pre-compost (PC)*	*Compost (C)*	*selected Organic Material (OM)*
Organic content (O.C.)	[g/kg$_{dm}$]	323.52	284.87	268.47	321.76
Nitrogen content (N)	[g/kg$_{dm}$]	10.97	12.89	13.84	7.54
Phosphorus content (P)	[g/kg$_{dm}$]	0.525	0.809	0.881	0.389
O.C./N	--	29.5	22.1	19.4	42.7
N/P	--	20.9	15.9	15.7	19.4
pH	--	4.0	6.0	6.0	5.5
Moisture	%	85	85	85	95

Five tests were planned using five different vermicomposting units and each vermicomposter was initiated with 3 kg of organic matter. The layout of the vermicomposters and the experimental setup are illustrated in Figure 1. Measurements of humidity, pH, and temperature were carried out using insertion probes directly on the solid matrix. Nitrogen content was evaluated using a standardized method **[10]**, including the grinding of the organic matrices, a preliminary assessment of its moisture for the mixing with deionized water, an agitation phase and then a spectrophotometrically analysis (using the chromotropic acid method). Phosphorus and heavy metals content was evaluated using ICP (*Inductively Coupled Plasma*) spectrometry. Organic Carbon (O.C.) content and organic matter content were analyzed using the Walkley-Black method (Violante, 2000). Carbon/Nitrogen ratios have been referenced to the organic carbon content.

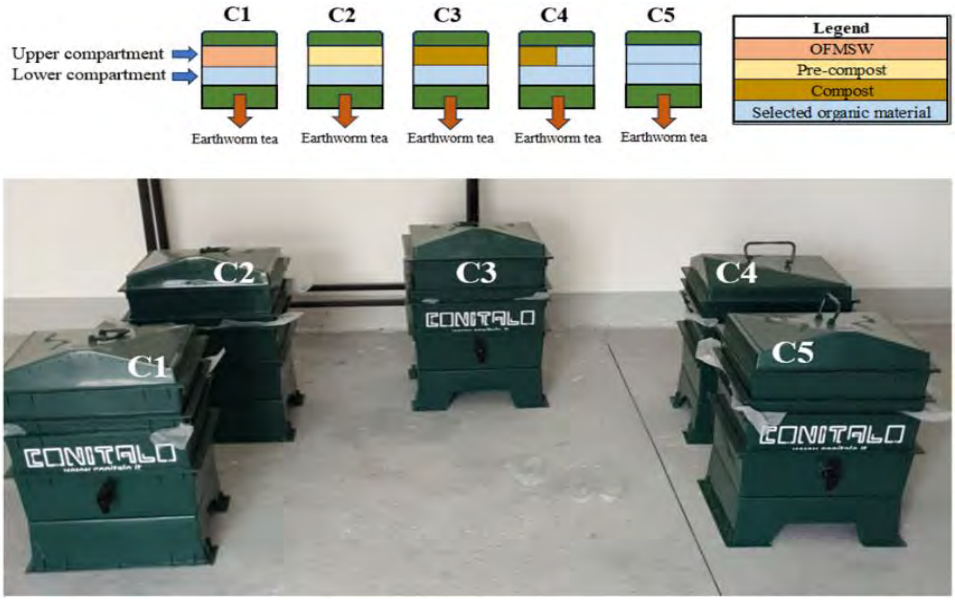

Figure 1. Vermicomposters experimental setup and details on filling of each reactor

The measurement of worm growth was comprehensively assessed only at the end of the experimentation (t=180 days), when watermelon scraps were placed inside the vermicomposters in separate compartments (above the one containing the transformed matrices). On the other hand, intermediate analyses at 15 and 90 days were conducted on 5 statistically significant samples taken from the center and the 4 corners of both trays. For the assessment of worm's metal bioaccumulation, approximately 50 g of worms from each significant compartment (C1-C5) were selected and after 24 hours and a washing phase, the content of heavy metals was analyzed using ICP spectrometry.

The results obtained, showed a significant decrease in C/N ratio after 180 days of biological process in all the tests conducted. Vermicomposting reduced the O.C./N ratio by 69.1% for C5, 60.8% for C4, 59.9% for C1, 52.1% for C3, and 43.5% for C2. In absolute terms, the O.C./N ratio was found to be below of 14 in all tests, with lower values observed for matrices from FORSU and the composting plant (≤ 11). Suthar **[7]** had previously reported that a C/N ratio <20 indicates acceptable maturity in finished compost, but a ratio of 15 is preferred for agricultural applications. At the end of the experiment, the total worm mass increased in all tests, even if some matrices were very "complex" and unsuitable for the ordinary growth scenario; consequently, in t=15 days the majority of the worms "died" with exception of C5. As expected, the most significant increase was achieved for C5, where the matrix obtained from selected organic material was investigated. Moreover, heavy metals content analysis showed that earthworms can potentially accumulate a certain amount of toxic substances, such as metals, in their tissues and inevitably introduce these toxic substances into terrestrial food chains.

The study confirmed that it's possible to obtain vermicompost from different organic fractions of municipal waste, whether raw or pre-treated. In Figure 2 it is easy to deduce the complete biological transformation of the organic matrix in stabilized material. In general, the achievable vermicompost could potentially have better nutritive properties compared to compost and initial blends, thanks to enhanced mineralization and humification. The availability of heavy metals in vermicompost is lower compared to the starting matrices and the compost obtained from a facility (the highest concentrations of heavy metals were still below the threshold values permitted for compost), as shown in Figure 3.

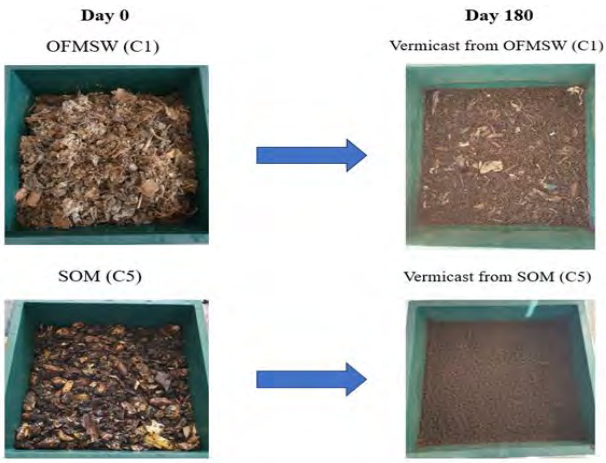

Figure 2. Transformation of organic matrices into soil improver after 180 days (C1-C5)

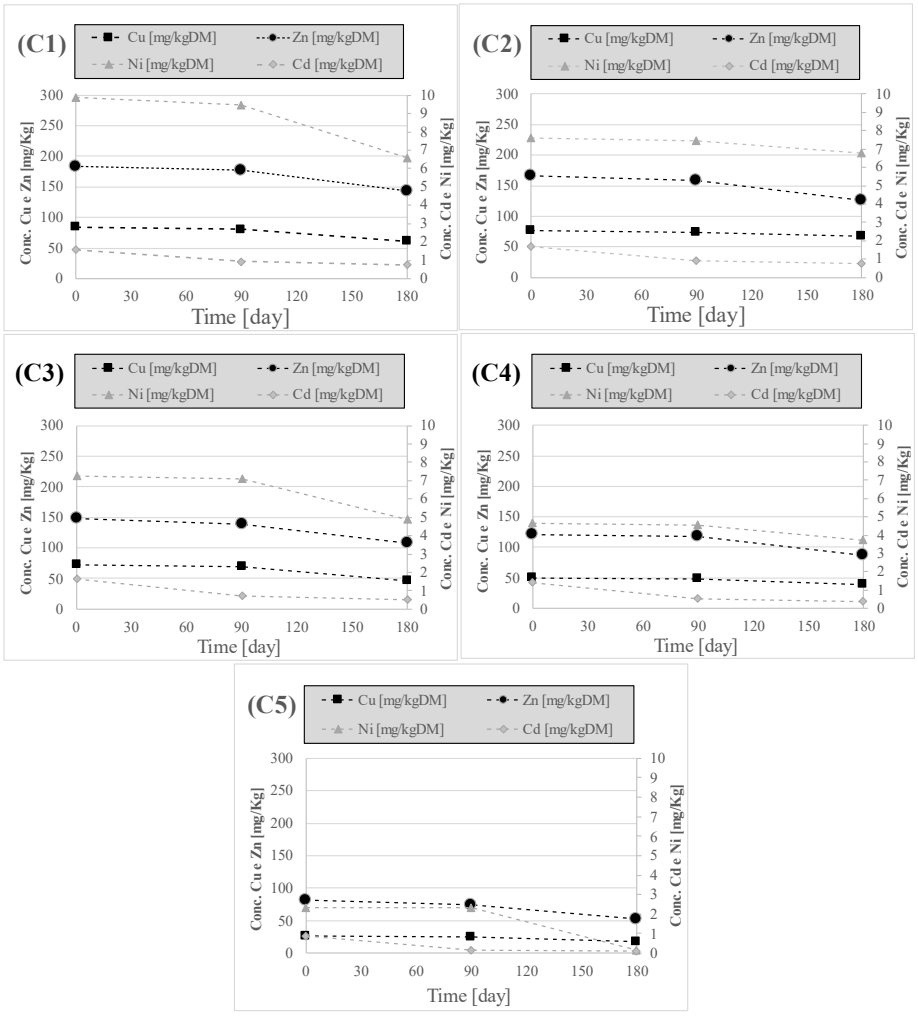

Figure 3. Evolution of the heavy metal content in the solid matrices of each reactor during the experimental period

Therefore, vermicomposting process could enhance nutrient quality compared to traditional compost (making the end product potentially a more effective soil amendment) and has the potential to mitigate the environmental risk of heavy metals from the disposal of solid organic waste, thanks to the worms activity that facilitate metals transformation into an unavailable fraction through bioaccumulation and stabilization associated with humus.

References

[1] Kumar V.V., Shanmugaprakash M., Aravind J., Namasivayam S.K.R. (2012). Pilot scale study of efficient vermicomposting of agro-industrial wastes. Environ. Technol. 33, 975-981. doi: 10.1080/09593330.2011.604856.
[2] Lim S.L., Lee L.H., Wu T.Y. (2016). Sustainability of using composting and vermicomposting technologies for organic solid waste biotransformation: recent overview, greenhouse gases emissions and economic analysis. J. Clean. Prod. 111, 262-278. https://doi.org/10.1016/j.jclepro.2015.08.083
[3] Rupani P.F., Embrandiri A., Ibrahim M.H., Shahadat M., Hansen S.B., Mansor N.N.A. (2017). Bioremediation of palm industry wastes using vermicomposting technology: its environmental application as green fertilizer. 3 Biotech 7, 155. https://doi.org/10.1007%2Fs13205-017-0770-1
[4] Pigatin L.B.F., Atoloye I.A., Obikoya O.A., Borsato A.V., Rezende M.O.O. (2016). Chemical study of vermicomposted agroindustrial wastes. Int. J. Recycl. Org. Waste Agric. 5, 55-63. https://doi.org/10.1007/s40093-016-0117-7
[5] Edwards C.A., Norman Q.A., Sherman R. (2011). Vermiculture Technology, Earthworms, Organic Waste and Environmental Management. CRC Press, 17-19. https://doi.org/10.1201/b10453
[6] Ducasse, V., Capowiez, Y. & Peigné, J. Vermicomposting of municipal solid waste as a possible lever for the development of sustainable agriculture. A review. *Agron. Sustain. Dev.* 42, 89 (2022). https://doi.org/10.1007/s13593-022-00819-y
[7] Suthar S., 2010. Recycling of agro-industrial sludge through vermitechnology. Ecol. Eng. 36, 1028–1036. https://doi.org/10.1016/j.ecoleng.2010.04.015
[8] Hait S., Tare V. (2012). Transformation and availability of nutrients and heavy metals during integrated composting–vermicomposting of sewage sludges. Ecotoxicol. Environ. Saf. 79, 214–224. doi: 10.1016/j.ecoenv.2012.01.004.
[9] Gupta R., Garg V. (2008). Stabilization of primary sewage sludge during vermicomposting. J. Hazard. Mater. 153, 1023–1030. https://doi.org/10.1016/j.jhazmat.2007.09.055
[10] Corsino S.F., Torregrossa M., Viviani G. (2021). Biomethane production from anaerobic co-digestion of selected organic fraction of municipal solid waste (Ofmsw) with sewage sludge: Effect of the inoculum to substrate ratio (isr) and mixture composition on process performances. International Journal of Environmental Research and Public Health, Volume 18, Issue 24, Article number 13048. https://doi.org/10.3390/ijerph182413048

Title: Evaluation of the leaching behaviour of different types of recycled aggregates from Construction and Demolition (C&D) waste for potential utilization

Authors: Luigi Acampora*[1], Giulia Costa[1], Francesco Lombardi[1], Andrea Paina[2], Nicolò Tonolo[1], Iason Verginelli[1]

[1]Department of Civil Engineering and Computer Science Engineering, University of Rome "Tor Vergata", Rome, 00133, Italy
[2] ISPRA, Institute for Environmental Protection and Research, Rome, 00144, Italy

Keywords: construction and demolition waste, leaching tests, End-of-Waste

Abstract

The waste produced from the construction and demolition of buildings and infrastructure account for more than one third of all the waste generated in the EU, reaching 374 million tonnes in EU-28 countries in 2016, excluding excavated soil [1]. This waste stream is highly heterogeneous, containing a variety of materials such as concrete, bricks, wood, glass, metals, asphalt, and plastics [2]. Its composition varies significantly based on factors such as the type of building or infrastructure involved, construction methods and materials used, as well as regional differences in demolition practices.
In EU countries, the management of Construction and Demolition (C&D) waste has seen notable progress in the past decade, aligning with circular economy principles. Recovery rates have increased, especially due to the need of meeting the 70% recovery target set by the 2008 Waste Framework Directive. Despite this positive trend, the European Environment Agency (EEA) highlights that much of the recovery efforts for construction and demolition waste heavily rely on methods such as backfilling or utilizing recycled aggregates from the mineral fraction of C&D waste, notably in applications like road sub-base construction [1]. In Italy non-hazardous C&D waste generation exceeded 50 million tons in 2022, with the majority (39 million tons) being successfully recovered [3]. Mechanical treatment processes, such as crushing and particle size classification, are common, with the resulting materials employed as recycled aggregates in various construction applications such as concrete, asphalt mixtures, or road sub-base construction [4]. The technical requirements of the obtained recycled aggregates are defined by specific norms that depend on the type of utilization strategy considered, whereas the evaluation of the environmental compatibility focuses on the total content of pollutants and how they are released at the native pH of the material, regardless of the intended use.
A recent Italian Decree (n.152 of September 27th, 2022) introduced End-of-Waste (EoW) criteria for recycled aggregates derived from non-hazardous C&D waste, addressing limits on total content of asbestos and organic contaminant levels, including polycyclic aromatic hydrocarbons (PAHs) and BTEX, among others. Additionally, it requires compliance to the results of the EN 12457-2 leaching test at the native pH of the material, focusing on the release of inorganic contaminants such as metals, metalloids, anions and pH values. The main potential environmental and health risks posed by the use of these materials, particularly in road sub-base construction, is the release of elements of potential environmental concern into percolating rainwater. These elements can subsequently migrate and contaminate soil, groundwater, and surface water, potentially affecting the quality of drinking water. Due to the diverse nature of C&D waste and the various potential applications of recycled aggregates, it is crucial to evaluate their characteristics and their leaching behaviour in conditions relevant to their

utilization applications [2]. Factors like pH changes due to weathering reactions or the different amount of water they can be exposed to upon use, are critical. During their use, these materials may exhibit pH conditions differing significantly from those observed in lab tests conducted at the native pH of the aggregates. For example, carbonation reactions occurring dure to the reaction of atmospheric carbon dioxide can gradually reduce alkalinity over time, leading to changes in the leaching behaviour [5].
In this study we investigated the leaching behaviour of five different types of recycled aggregates from treated non-hazardous C&D waste, characterized by different compositions and particle size distributions. Specifically, standardized column percolation tests (EN 14405 method) and different types of batch leaching tests performed at the native pH of the material (EN 12457-1 and EN 12457-2 methods) and as a function of pH (CEN/TS 14429 method), were carried out. For the pH-dependence leaching test, according to CEN/TS 14429, parallel batch tests were performed on the samples at a Liquid-to-Solid (L/S) ratio of 10 L/kg. Percolation column tests were carried out using 30-cm tall Plexiglas columns with a 5-cm inner diameter, according to the standard method CEN/TS 14405, and seven distinct leachates were collected at cumulative L/S ratios (0.1, 0.2, 0.5, 1, 2, 5, and 10 L/kg). The collected leachates underwent chemical analysis for major and trace inorganic elements, anions, total hydrocarbons, and polycyclic aromatic hydrocarbons (PAH). Based on the results obtained from the different tests, the leaching behaviour was analysed to identify release mechanisms for the different contaminants of interest (i.e.: solubility or availability control).
Overall, the three types of tests performed showed high reproducibility for all the constituents analysed, as the trends observed in the replicates carried out on the same sample matched closely in many cases. Instead, a notable difference was observed among the samples, particularly between the first three (01, 02, and 03) and the last two samples (04 and 05), both in terms of the amount and the mechanisms of release for the various constituents analysed. These differences can be attributed to the different composition of the samples. Samples 01, 02, and 03 mainly consisted of bricks and tiles mixed with other mineral residues, while samples 04 and 05 originated mainly from concrete demolition.
Specifically, with regard to the pH dependence test, differences in the leaching behaviour of the two categories of samples were observed for elements such as Ba, Ca, Cr, Fe, K, Mg, Ni, and V (see Figure 1 reporting the release curves resulting for Ba and V as a function of pH).

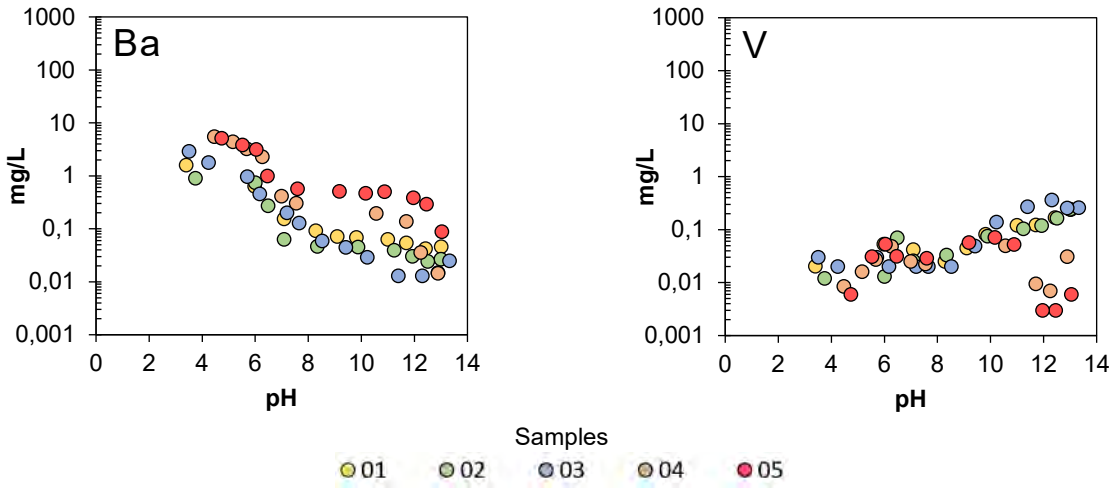

Figure 1 - Results of the pH dependence leaching test as a function of pH obtained for the five samples.

In the percolation column tests, significant differences were observed for Al, Mg, V, fluorides, and sulphates leaching, mainly as a result of the different chemical composition of the samples, which affects both pH and release trends. Specifically, the pH of the leachates of samples 04 and 05 exhibited a variable behaviour as a function of the L/S ratio, while that of the other three samples presented a consistently lower and quite constant pH value (Figure 2).

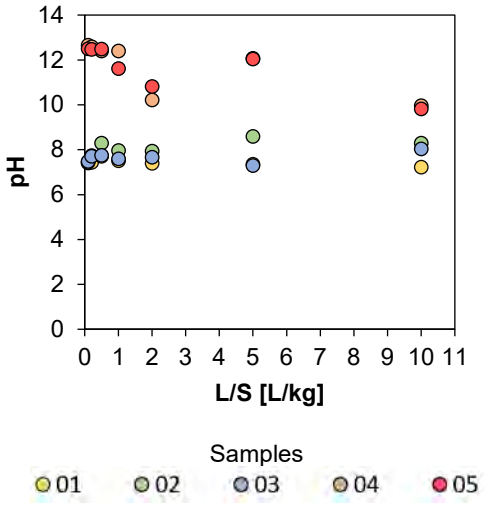

Figure 2 - pH measured in the leachates of the percolation column tests as a function of the L/S ratio for the five samples.

Furthermore, the results were compared with the Italian EoW regulation and other existing European EoW criteria for similar materials. The comparison allowed to highlight the constituents that may prove critical for the utilization of each type of sample on the basis of this approach, i.e. sulphates release for samples 1,2 and 3 and pH for samples 4 and 5.
The results of these tests are currently being integrated into a risk analysis procedure aimed at evaluating the environmental compatibility of these materials for specific utilization scenarios.

References

[1] EEA, European Environment Agency, “Construction and demolition waste: challenges and opportunities in a circular economy”, Briefing no. 14/2019, PDF TH-AM-19-016-EN-N, doi: 10.2800/07321, (2019)
[2] Butera S., Christensen T. H., Astrup T. F., “Composition and leaching of construction and demolition waste: Inorganic elements and organic compounds”, Journal of Hazardous Materials, Volume 276, 302-311, (2014).
[3] ISPRA, Institute for Environmental Protection and Research, “Report on special waste, 2022 edition, in Italian”. ISPRA Report n. 368/2022 ISBN 978-88-448-1117-4, (2022)
[4] Gálvez-Martos, J. L., Styles, D., Schoenberger, H., & Zeschmar-Lahl, B., “Construction and demolition waste best management practice in Europe”, Resources, conservation and recycling, 136, 166-178, (2018)
[5] Butera S., J. Hyks, Christensen T. H., Astrup T. F., “Construction and demolition waste: Comparison of standard up-flow column and down-flow lysimeter leaching tests”, Waste Management, Volume 43, 386-397, (2015)

Title: FISH DISCARD VALORISATION INTO LOW CARBON BIOCHAR-COMPOST COMPOSITE

Author(s): Salman Nisar*[1], Josué González-Camejo[1], Anna Laura Eusebi[1], Francesco Fatone[1]

1SIMAU, Department of Science and Engineering of Materials, Environment and Urban Planning-SIMAU, Marche Polytechnic University, 60131, Ancona, Italy

s.nisar@pm.univpm.it, j.gonzalez@univpm.it, a.l.eusebu@univpm.it, f.fatone@univpm.it

Keyword(s): compost, biochar, fish waste, nutrients recovery, circular economy

Abstract

Fish discard (FD) production is increasing continuously due to the higher demand for seafood worldwide. These by-products mostly consist of viscera, head, fin, etc. highly putrescible, and require proper stabilisation strategies to avoid environmental impacts. Normally, a discarding fee is paid by fish processing companies for disposing of these by-products. In the case of a company based in Ancona (Italy), whose annual discards account for 26 $t.y^{-1}$, they imply management costs amounting to 5720 €. y^{-1} (220 €. ton^{-1}). Alternatively, these by-products are rich in valuable nutrients and can be recovered using sustainable circular economy approach, like composting to recover nutrients for agricultural purposes. The environmental impacts of aerobic composting can be reduced by adding biochar, which is novel approach. This study aimed to recover composite biochar compost as a low-carbon, sustainable soil improver. Results showed that biochar addition resulted in low GHG emissions during composting process and preserved high nitrogen content in the final product compared to control compost.

Introduction

Worldwide production of fish from both capture and aquaculture was around 178.5 million tonnes (Mt) in 2018 and is projected to reach around 204 Mt by 2030 [1] due to increasing consumption demands, leading to massive generation of by-products volume which can account for 30–70% of original fish, depending on processing requirements [2]. Being highly putrescible, these by-products pose a global concern and require urgent stabilisation to avoid environmental impacts, and companies pay discarding fee for these by-products. Depending on the processing capacity, these amounts to considerable costs. Common stabilisation strategies include landfill, incineration, composting, anaerobic digestion, and pyrolysis. However, composting offers an economical and environmentally friendly approach by recycling nutrients into soil, promoting sustainability and circular economy [3]. Composting is biological decomposition of organic substrates, under conditions allowing development of thermophilic temperatures by biologically produced heat, producing a stable product, free from pathogens and plant seeds, which can be beneficially applied to land as soil improver or growth medium to enhance soil texture, water holding capacity, reduce synthetic fertilisers use and carbon storage [4].

FD is highly moist and has a low carbon-to-nitrogen (C/N) ratio. Thus, co-composted with a suitable renewable bulking agent (BA) to achieve optimal composting parameters is necessary. However, during composting process precious nutrients such as nitrogen (N) can be lost due to ammonia (NH_3) volatilisation and leachate formation, thus lowering the positive effects of the final product. Ammonia is produced in composting by rapid degradation of organic matter at thermophilic temperatures (>45℃) and higher pH (9) [5]. Similarly, emissions of GHG gases (CH_4, CO_2, N_2O) are also a downside of composting. To address these, biochar, a carbonaceous material obtained from pyrolysis in an oxygen-limited atmosphere, is added as amendment to composting feedstock. Biochar has high C/N ratio with recalcitrant carbon and porous structure offering favourable conditions for microorganisms' habitat by retaining nutrients and moisture and improving aeration and buffering pH, and nutrient absorption in the

final product [6]. However, the effects of biochar addition to the composting process of fish discards are scarcely understood.
The study aimed to evaluate the effects of adding biochar to the FD-based composting process to obtain low-carbon, sustainable biochar compost composite products. Specifically, the potential reduction of GHG emissions and nutrient preservation will be evaluated.

Materials and Methods

The active composting phase was carried out in a 30-L pilot composting reactor [Figure 1]. Fish discards, i.e., the substrate (S) was mixed with renewable BA comprised of recycled pruning waste and sawdust (1:1 w/w). The ratio of substrate to bulking agent (S: BA, w/w) was 1:3.5 to attain a target C/N of 20. Two different tests were conducted: one using the aforementioned mixture and another one incorporating biochar (10% by dry weight of feedstock) produced commercially from wood chips. Water was added to accomplish optimal humidity range of 40-60% for aerobic composting in both tests. To ensure aerobic conditions for microorganisms, an initial air flux of 20.4 L·h-1 (0.2L/kgDM/min)) was set in composting reactor, along with an aeration control (oxygen set point of 15-17%) based on oxygen concentration of the exhaust. Temperature and oxygen were monitored every 10 minutes by a datalogger, and NH_3 emissions in the exhaust gas were analysed daily by entrapping in boric acid, while GHG was monitored 3-5 times a week. Furthermore, feedstock was manually turned in each week to homogenise the mixture, weekly weighed for tracking weight losses and adjusted for humidity if required. During this procedure, samples were taken for analysis of humidity, dry and volatile matter concentrations, total Kjeldahl nitrogen, pH and Electrical Conductivity, biological stability (OUR) and heavy metals. The active phase was stopped after three weeks, followed by the maturation phase lasting until day 100. 65% compost was recovered from both final feedstocks by passing through a 6-mm sieve, while 35% BA agents were recovered and could be recycled.

Figure 1. 30L Pilot scale composter

Results and Discussion

Results confirmed that GHG emissions from the composting process could be reduced by adding biochar to the FD-based substrate. In fact, composite biochar compost emitted 6.5% less NH_3 and 23% less N_2O than the control (without biochar). During the composting period, cumulative 0.46 $gNH3.d^{-1}$ emitted from CoBC, while 0.49 $gNH3.d^{-1}$ was lost from control test. 5.7 gNH_3. $KgFD^{-1}$ volatilised from composite biochar compost, whereas 6.1 $gNH_3.kgFD^{-1}$ was lost from the control feedstock. In comparison with Awasthi et al. [7], our results were comparable for daily cumulative NH3 emissions (0.68 $gNH3.d^{-1}$ from 8% and 0.42 $gHN3.d^{-1}$ from 12% biochar by d.wt). However, cumulative NH3 reduction (6.5%) is lower than 43-59% reduction reported by Awasthi et al. for sewage sludge

composting with wheat straw BA. This low NH3 reduction may indicate that biochar amount was not enough to result significant NH3 reduction in FD composting, by adsorption of ammonia on biochar by its porous structure. This could also possibly be the effect of sawdust as BA, absorbing moisture and nutrients, reducing NH3 emission rates from control. These hypotheses will be addressed in future studies.

Regarding CH_4 emissions, the differences were even more relevant, accounting for 33% lower emissions than the control. This suggests that adding biochar can decrease greenhouse gas emissions, probably by enhancing the aeration conditions for feedstock, inhibiting the growth of methanogens, and promoting methanotroph bacteria as reported by Awasthi et al [8]. Concerning compost quality, pH, conductivity, and heavy metals concentrations of both composts were within the allowed limits of Italian legislation (D.Lgs. 75/2010) and EU regulation (EU 2019/1009) [Table 1]. Also, no leachate phenomena were observed in the tests, thus avoiding nutrient losses in this liquid residue, and can be attributed to nutrient absorption by sawdust, thus preserving nutrient in final product. Similarly, the C/N ratio of both composts was less than 20 within 10 days of the maturation phase, indicating a mature compost.

However, the thermophilic temperature for the required duration set by legislation was not met in both cases. In future tests, a high S: BA ratio and high biochar value will be tested to understand the temperature trends.

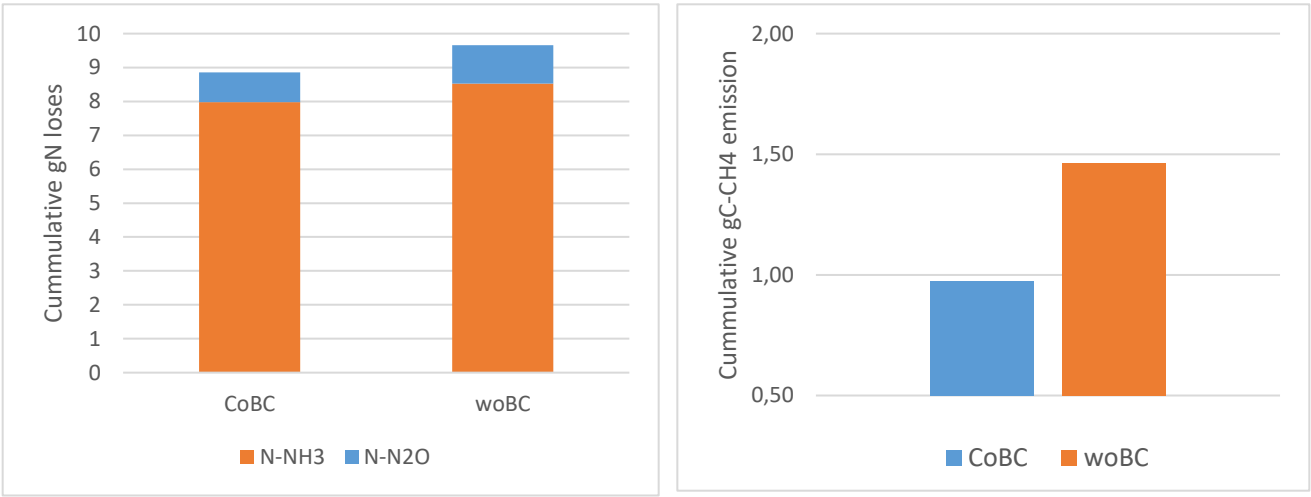

Figure 2 Cumulative losses during active composting period, (a) nitrogen losses, C-CH_4 emission (b), CoBC: composite biochar compost test, woBC: control test

Table 1 Comparison of heavy metals concentration with Italian and EU regulation

Parameter	Unit	D.Lgs. 75/2010	Reg. EU 2019/1009	CoBC	woBC
pH	-	4-12	-	6.27	6.50
EC	ms/m	≤1000	-	150.60	174.20

Humidity	%	≥20	-	58.28	63.44
Corg	%	Class 1: >=60	7.5-50	43.61	45.72
Cd	mg/kg DM	< 1.5	2	<0.12	<0.13
Hg	mg/kg DM	< 1.5	1	n.d.	n.d.
Ni	mg/kg DM	< 100	50	9.80 ± 1.84	8.95 ± 0.39
Pb	mg/kg DM	< 140	120	<7.34	<8.35
As	mg/kg DM	-	40	n.d.	n.d.
Cu	mg/kg DM	< 230	300	34.28 ± 0.01	74.04 ± 1.86
Zn	mg/kg DM	< 500	800	78.78 ± 6.63	114.01 ± 14.54

Conclusions

The study aimed to evaluate the effects of adding biochar to the FD-based composting process to obtain low-carbon, sustainable biochar compost composite products. Results obtained were promising as GHG (33% CH_4 and 23% N_2O) were reduced when comparing to the control. In addition, both the compost and composite accomplished legal requirements in terms of pH, conductivity, and heavy metals concentrations.

Acknowledgements

The authors acknowledge the European Union's Horizon 2020 research and innovation programme for its support to fund the "SEA2LAND" project under grant agreement 101000402. The authors also acknowledge CO.PE.MO and Ittica del Conero companies to provide the seafood residuals for characterisation.

References

[1] FAO, The State of World Fisheries and Aquaculture 2020. FAO, 2020. doi: https://doi.org/10.4060/ca9229en.
[2] I. Ahuja, E. Dauksas, J. F. Remme, R. Richardsen, and A.-K. Løes, "Fish and fish waste-based fertilizers in organic farming – With status in Norway: A review," Waste Management, vol. 115, pp. 95–112, Sep. 2020, doi: https://doi.org/10.1016/j.wasman.2020.07.025.
[3] M. Xu et al., "From waste to wealth: Innovations in organic solid waste composting," Environmental Research, vol. 229, pp. 115977–115977, Jul. 2023, doi: https://doi.org/10.1016/j.envres.2023.115977.
[4] R. T. Haug, "The Practical Handbook of Compost Engineering," in *Routledge eBooks*, 2018. [Online]. Available: https://doi.org/10.1201/9780203736234
[5] D. Janczak, K. Malińska, W. Czekała, R. Cáceres, A. Lewicki, and J. Dach, "Biochar to reduce ammonia emissions in gaseous and liquid phase during composting of poultry manure with wheat straw," Waste Management, vol. 66, pp. 36-45, Apr. 2017.
[6] M. K. Awasthi et al., "Role of biochar amendment in mitigation of nitrogen loss and greenhouse gas emission during sewage sludge composting," Bioresource Technology, vol. 219, pp. 270–280, Nov. 2016, doi: https://doi.org/10.1016/j.biortech.2016.07.128.
[7] Mukesh Kumar Awasthi et al., "Heterogeneity of biochar amendment to improve the carbon and nitrogen sequestration through reduce the greenhouse gases emissions during sewage sludge composting," Bioresource Technology, vol. 224, pp. 428–438, Jan. 2017, doi: https://doi.org/10.1016/j.biortech.2016.11.014.
[8] M. K. Awasthi, Y. Duan, S. K. Awasthi, T. Liu, and Z. Zhang, "Influence of bamboo biochar on mitigating greenhouse gas emissions and nitrogen loss during poultry manure composting," Bioresource Technology, vol. 303, p. 122952, May 2020, doi: https://doi.org/10.1016/j.biortech.2020.122952.

Title: Biocoal production and phosphorous recovery from stabilized sewage sludge and aerobic granular sludge by the integration of slow pyrolysis, hydrothermal carbonization, and chemical leaching

Author(s): Marta Di Bianca*[1,2,3], Andrea Salimbeni[2], Tommaso Lotti[1], Riccardo Campo[1], Hary Demey Cedeno[3], Geert Haarlemmer[3]

[1] *Department of Civil and Environmental Engineering, Università degli Studi di Firenze, 50139 Florence, Italy, marta.dibianca@unifi.it, tommaso.lotti@unifi.it, riccardo.campo@unifi.it*
[2] *Renewable Energy Consortium for Research and Demonstration (RE-CORD), 50038 Scarperia e San Piero, Italy, andrea.salimbeni@re-cord.org*
[3] *Université Grenoble Alpes, CEA LITEN, Laboratoire Réacteurs et Procedés (LRP), F-38000 Grenoble, France hary.demeycedeno@cea.fr, geert.haarlemmer@cea.fr*

Keyword(s): aerobic granular sludge, biocoal, chemical leaching, hydrothermal carbonization, phosphorous, recovery, sewage sludge, slow pyrolysis

Abstract

Context. Sewage sludge is the main by-product generated by wastewater treatment, and its disposal is an issue of shared concern. At present, the European Union (EU) produces around 10 million tonnes of sewage sludge dry matter per year, which are mainly destined to agriculture, incineration, composting and landfilling [1]. Although agricultural use and composting allow to take advantage of sewage sludge nutrients and organic matter, when sewage sludge quality is not compliant with the national regulations (in terms of heavy metals, organic pollutants, etc.) the only feasible solutions are incineration or landfilling, without materials recovery. However, in the framework of the EU transition to a circular economy, also promoted by the European Green Deal and by the Waste Framework Directive, finding strategies for sewage sludge reuse and recycling is crucial. The main potentialities for sewage sludge recovery are linked first to its carbon (C) content, typically around 22 to 33% [2], and most importantly to its phosphorus (P) content, usually in the range 1.5-4% [3]. The recovery of P is of particular interest in Europe, since the presence of phosphate rock and P was confirmed in the 2023 list of the critical raw materials for the EU [4], which includes the materials of high importance for the EU's economy but with a high risk associated to their supply. Apart from its environmental footprint, sewage sludge management has also an elevated economic impact, with an estimated cost of sewage sludge disposal in the order of hundreds of euros per ton of sewage sludge [1]. Moving towards the recovery of resources from sewage sludge, granular sludge is considered a promising technology, thanks to the potentialities for resources recovery (including P, bioplastics, and extracellular polymeric substances) held by aerobic granular sludge, and to the additional advantages of efficient biomass retention and more compact reactors compared to conventional activated sludge systems [5]. In fact, P storage in aerobic granules is attributed to P accumulating organisms (PAOs) that, thanks to their metabolism, accumulate P in the granules as poly-phosphate in aerobic or anoxic conditions. Thermochemical treatments are a possible way for sewage sludge management, as they allow sludge volume and pathogens reduction, and can offer some possibilities in the view of sewage sludge recycling. Many studies focused on the application of slow pyrolysis and hydrothermal carbonization of sewage sludge as a way to obtain spendable products [6][7]. HTC operates in subcritical water conditions in the absence of oxygen, at mild

temperatures (150-250 °C) and autogenic pressure (up to 10 MPa) and short retention times, leading to the production of a solid matrix (hydrochar), a liquid organic fraction and a gas phase (mainly composed by CO_2) [6]. Slow pyrolysis takes place in the absence of oxygen at higher temperatures (400-700 °C), low heating rates (0.5-10 °C/min) and long solids retention times (in the order of hours), producing a carbonaceous solid matrix (char) as main product, and a mixture of condensable gases (containing water, tar and other organic compounds) and permanent gases (CO, CO_2, H_2, CH_4) [8]. The main drawbacks of char and hydrochar from sewage sludge are related to their highly mineral nature, that often prevents their application in the energy sector (as fossil coal or peat substitutes), and to their inapplicability as soil improvers, forbidden in several EU countries by the EU fertilizers regulation (reg. EU 1009/2019) [9].

Objectives. This work aimed at studying the integration of chemical leaching with slow pyrolysis and hydrothermal carbonization as a strategy for the valorisation of sewage sludge. The processes integration targets the recovery of phosphorous, in the form of an inorganic precipitated salt to be spent for fertilizers production, and of a biocoal to be applied as a fossil coal substitute. After processing sewage sludge by slow pyrolysis or HTC, chemical leaching (a solid-liquid extraction process) was applied to the produced char from pyrolysis (pyrochar) and hydrochar aiming to reduce their ash content and improve their quality as fossil coal substitutes. Apart from biocoal production, the second advantage of the processes integration is the extraction of P (and other valuable compounds), recovered in the liquid phase from leaching, from the char. The two integrated processes were applied on two materials: (i) a municipal sewage sludge from the conventional activated sludge process (after stabilization) and (ii) a granular sludge from the aerobic granular sludge technology. The work aimed at assessing the efficacy of the two integrated processes on aerobic granular sludge with the purpose of resources recovery, in comparison with a conventional municipal sewage sludge.

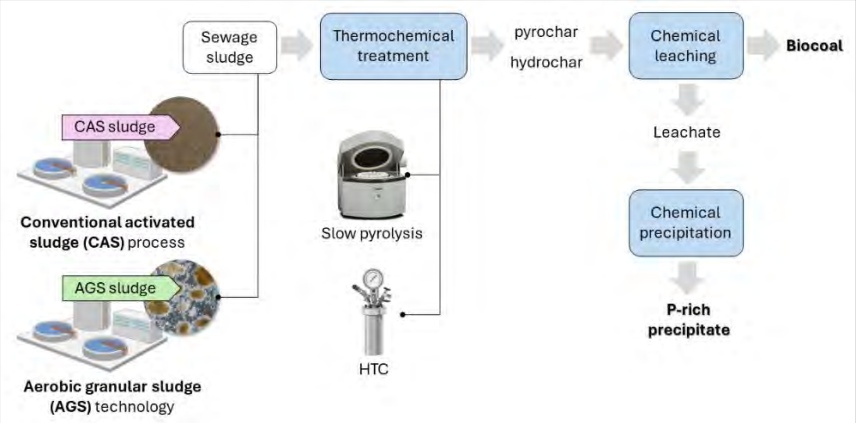

Figure 1. Schematic of the two assessed integrated processes.

Materials&methods. The sludge line of the WWTP originating the first sludge (CAS) includes anaerobic digestion – with a sludge retention time (SRT) of around 17 days –, thickening, dewatering, and drying (up to a 25% moisture content); in the sludge line, the waste sludge from the conventional activated sludge process of the WWTP biological section is processed, together with a contribution of sludge and liquid waste from other plants. The second material was an aerobic granular sludge (AGS) with a moisture content of 90%, coming from a full-scale plant, the hydraulic retention time (HRT) and the SRT of the process being 16 h and 30 days respectively. Before being processed, the two materials were irradiated for sterilization and oven dried at 105 °C until constant weight and then characterized. For the slow pyrolysis trials, the two sludges were dried and then separately processed by a thermo-gravimetric analyser (TgA, LECO TGA701) where up to 150 g dry sludge can be processed, at a temperature of

450-550 °C. HTC trials were performed on a 300 mL batch autoclave (PARR Mini Bench Top Reactor 4560), with induction heating at 210-270 °C. Prior to HTC tests, each dry sludge was mixed with deionised water to reach a 20% solid substance concentration. The produced pyrochars and hydrochars were characterized by proximate (moisture, ashes, volatiles content) and ultimate analysis (C, H, N and, S content), and by analysing their content in inorganic elements. The experimental setup of the chemical leaching trials included a heated plate equipped with a thermocouple, where the solid-liquid mixture of pyrochar or hydrochar and leaching solution was maintained in temperature and stirred by a magnetic agitator for a set contact time. For each trial, 50-100 mL of a 1 M HNO_3 solution were mixed with 5-10 g of solid and left stirring at 75 °C for 2 h. The solid (biocoal) was separated from the liquid phase (leachate) by vacuum filtration, then it was rinsed with demineralised water and vacuum filtered again, to be finally oven dried. To evaluate the performances of the leaching process, the degree of demineralization (DD, %) and the extraction efficiency (EE, %) of the inorganic elements of interest were adopted as performances indicators:

$$DD\ (\%) = \frac{\%ash,char - \%ash,biocoal}{\%ash,char} \cdot 100,\ EE(\%) = \frac{element,char - element,biocoal}{element,char} \cdot 100$$

Where %*ash,char* is the ash (% d.b.) in the processed hydro/pyrochar; a*sh,biocoal* is the ash (% d.b.) in the produced biocoal; *element,char* is the element mass (mg) in the processed hydro/pyrochar; *element,biocoal* is the element mass (mg) in the produced biocoal.
The biocoals were then characterized by proximate and ultimate analysis, content of inorganic elements, calorific value, and XRD. The quality of the biocoals was assessed by the Van Krevelen diagram, which classifies solid fuels according to their H/C and O/C atomic ratios. P and the other extracted inorganic compounds were recovered from the leachate by precipitation, dosing a KOH solution up to a pH >7. The composition of the precipitated salts in terms of P and other inorganic compounds was determined in laboratory and assessed according to the EU fertilizers regulation (reg. EU 1009/2019).

Results. Both sludges contained a relevant concentration of P (up to 3%), Ca and Fe. Due to the addition of chemicals in the CAS process, CAS sludge showed a higher Al concentration compared to AGS sludge, as well as a higher Si content. Therefore, CAS sludge showed a higher ash content. After pyrolysis, due to the loss of volatile matter, the ash content of all materials increased, reaching values up to 50% (AGS) and 70% (CAS), as well as the concentration of the inorganic compounds. The same trend was observed after the HTC trials, with a higher ash content obtained in CAS hydrochar (up to 55%). The DD of AGS pyrochar leaching appeared to be around two times the value of CAS pyrochar leaching: this may be attributed to the inefficacy of leaching (at the adopted operating conditions) on Si extraction (with EE values <20%) whose concentration in AGS pyrochar (<4%) was lower than CAS pyrochar (up to 9%). As a result, AGS biocoal from pyrochar showed an ash content around 20% and a C content around 55%, while, due to the higher ash content (around 50%), the CAS biocoal from pyrochar had a reduced C content (around 40%). In the case of CAS hydrochar leaching, values up to 50% of the DD were reached, with lower values compared to the DD of AGS hydrochar leaching. The leaching process applied to pyrochar and hydrochars showed to be effective on the extraction of P (up to 100% EE), Ca and Mg (up to 99% EE), but also Zn (up to 97%), with lower EE values reached for Al (up to 70%) and Fe (up to 90%). According to van Krevelen diagram, the biocoals from pyrochar are positioned in proximity of coal area, showing slightly lower H/C ratios; on the contrary, biocoals from hydrochar showed higher H/C ratios compared to coal (Figure 2). All precipitated solids showed a relevant P concentration (up to 6%), being promising NPK fertilisers or fertilizers precursors (e.g. phosphate rock substitutes). The concentration of heavy metals (Zn, Pb) in the precipitate from CAS was compliant with the EU fertilizers regulation, while Zn in the AGS precipitate exceeded the regulation limit.

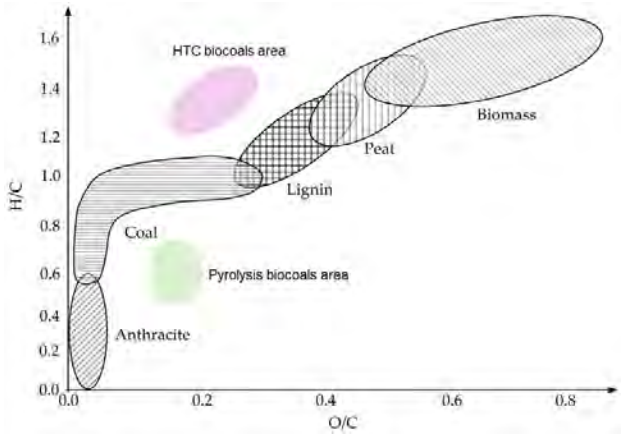

Figure 2. Classification of the produced biocoals in the Van Krevelen diagram (from [10]).

Conclusions. In conclusion, the integration of slow pyrolysis and leaching, and of HTC and leaching may be good strategies for CAS and AGS circular valorisation. In general, AGS biocoals (both from HTC and pyrolysis) showed a better quality in terms of C content compared to CAS biocoals, thanks to the lower content of inorganic compounds (Al, Si) in AGS sludge. Comparing HTC biocoals with pyrolysis biocoals, the first show a lower ash content and a higher volatiles content (due to the lower process temperatures applied). In addition, while HTC biocoals are located in the upper part region of the Van Krevelen diagram, pyrolysis biocolas are more comparable with a coal. The precipitated salts obtained from the leachate showed a high P content, with potentialities of application in the fertilizers industry.

References

[1] N. Anderson *et al.*, “Sewage sludge and the circular economy,” Copenhagen, May 2021. Accessed: May 29, 2024. [Online]. Available: https://forum.eionet.europa.eu/nrc-eionet-freshwater/library/urban-waste-water-treatment/sewage-sludge-and-circular-economy

[2] A. Callegari and A. G. Capodaglio, “Properties and beneficial uses of (bio)chars, with special attention to products from sewage sludge pyrolysis,” *Resources*, vol. 7, no. 1, 2018, doi: 10.3390/resources7010020.

[3] R. Canziani and R. Di Cosmo, “Stato dell’arte e potenzialità delle tecnologie di recupero del fosforo dai fanghi di depurazione,” *Ingegneria dell’ambiente*, vol. 5, no. 3/2018, 2018, doi: https://doi.org/10.32024/ida.v5i3.p01.

[4] European Commission, “Study on the Critical Raw Materials for the EU 2023 – Final Report,” 2023.

[5] C. Feng, T. Lotti, R. Canziani, Y. Lin, C. Tagliabue, and F. Malpei, “Extracellular biopolymers recovered as raw biomaterials from waste granular sludge and potential applications: A critical review,” *Science of the Total Environment*, vol. 753. Elsevier B.V., Jan. 20, 2021. doi: 10.1016/j.scitotenv.2020.142051.

[6] A. L. Tasca, M. Puccini, R. Gori, I. Corsi, A. M. R. Galletti, and S. Vitolo, “Hydrothermal carbonization of sewage sludge: A critical analysis of process severity, hydrochar properties and environmental implications,” *Waste Management*, vol. 93, pp. 1–13, 2019, doi: 10.1016/j.wasman.2019.05.027.

[7] J. Paz-Ferreiro, A. Nieto, A. Méndez, M. P. J. Askeland, and G. Gascó, “Biochar from biosolids pyrolysis: A review,” *Int J Environ Res Public Health*, vol. 15, no. 5, 2018, doi: 10.3390/ijerph15050956.

[8] M. C. Collivignarelli *et al.*, “Legislation for the reuse of biosolids on agricultural land in Europe: Overview,” *Sustainability (Switzerland)*, vol. 11, no. 21, pp. 1–22, 2019, doi: 10.3390/su11216015.

[9] “Regulation (EU) 2019/1009 of the European Parliament and of the Council of 5 June 2019” *Official Journal of the European Union*, vol. 2019, no. 2003, pp. 1–114, 2019, [Online]. Available: https://eur-lex.europa.eu/legal-content/EN/TXT/PDF/?uri=CELEX:32019R1009&from=EN

[10] J. M. C. Ribeiro, R. Godina, J. C. de O. Matias, and L. J. R. Nunes, “Future perspectives of biomass torrefaction: Review of the current state-of-the-art and research development,” *Sustainability (Switzerland)*, vol. 10, no. 7. MDPI, Jul. 05, 2018. doi: 10.3390/su10072323.

Abstract

Title: Pilot scale slow pyrolysis with vapours condensation for textile waste valorisation into coal and petrochemicals

Author(s): A. Salimbeni[1], L. Rosi[2], N. Pezzati*[1], B. Ciuffi[2], E. De Vita[1,2]

[1] Renewable Energy Consortium for Research and Development (RE-CORD), Scarperia e San Piero (Italy)
[2] Department of Chemistry "Ugo Schiff", University of Florence, Via della Lastruccia 3-13, I-50019, Sesto Fiorentino, Italy

Keyword(s): Slow pyrolysis, Textile waste, Benzoic Acid, Pilot-scale, Char valorization, Feedstock recycling

Introduction

In recent years, due to fast fashion trends, the textile industry has faced massive growth reaching around 62 Mt production. In Europe, estimated 11 kg of textile waste per capita are produced every year yielding a total of about 5.8 Mt/year [1, 2]. Several serious ecological threats are posed by the linear economic model that has been adopted so far due to low recycling rate (<1%), high disposal of in landfills (>69%), low bulk density, slow degradation rates, microplastic release from synthetic fibers and huge water consumption and soil contamination associated with cotton crops [1, 3, 4]. Thus, the transition to a circular model is needed that encourages reuse and recycling following the guidelines issued by the European Commission within the *EU Strategy for Sustainable and Circular Textiles* that aims to promote sustainable growth of the European textile sector that counts about 171˙000 companies. The textile hub of Tuscany (Italy) comprises well-established companies operating in the sector.

Materials and methods

Textile waste produced in the industrial textile hub of Tuscany (Italy) is considered in this study. The feedstock was initially characterised in laboratory to determine CHN, Ash, HHV, and heavy metals.

Table 1: Ultimate analysis after palettization of textile waste feedstock processed.

Parameter	Value	Unit
C	48.6 ± 1.1	wt.%
H	5.9 ± 0.2	wt.%
N	0.29 ± 0.04	wt.%
S	0.14 ± 0.01	wt.%
O	44.9 ± 1.1	wt.%

The material was firstly grinded with the aim of a knife-mill Meccanoplastica 800 BL and later it was compacted using Smartwood PLT-100 pelletizer. In order to achieve pellets with good mechanical strenght the textile waste was blended with a glue starch:water 1:15.

Figure 1: Pelletized textile waste.

The pellets then were converted via slow pyrolysis at 500°C using a 3 kg/h auger type pilot scale reactor unit operated at 0.44 rpm with 1h residence time.

The solid fraction was recovered in the form of char characterized in its proximate and ultimate composition. Concurrently the vapor phase produced during thermochemical conversion was condensed using a fractionate condensation unit (FCU). While permanent gases mainly comprising CO_2, CO, H_2 and C_1-C_3 hydrocarbons were monitored on-line with a micro-GC system and removed as flue gases, on the other hand condensates have been recovered and analyzed using GC/MS-FID with Shimadzu GC-2010 coupled with Shimadzu GCMS QP-2010. Both an organic and an aqueous phase were recovered from the FCU. Both phases have been analysed.

Figure 2: pilot scale pyrolysis unit integrated with the FCU.

Results

The pyrolysis test performance was assessed through a mass balance that gave the following distribution of the products: 24.6 wt% solid phase (i.e. char), 44.7 wt% vapours and 30.6 wt% permanent gases. The condensable fraction comprised 39.4 wt% aqueous phase and 5.1 wt% organic phase.
The char was characterised in its ultimate and proximate composition (see **Table 2**). The solid product

resulted in a carbonaceous substrate with 82 wt% fixed C, following close to the boundaries of coal and anthracite-like material according to Van Krevelen diagram. Its gross calorific value resulted 73% higher compared to the unprocessed feedstock. High porosity structure of the solid coal-like product can be enhanced by further activation by thermal post-treatment and the material can be leveraged as an adsorbent for removal of contaminants from industrial flue gases.

Table 2: Characterisation of pyrolysis derived char from textile waste

Parameter	Value	Unit
Moisture	1.3 ± 0.1	wt.%
Volatile matter	13.0 ± 0.4	wt.%
Ashes @550°C	3.3 ± 0.1	wt.%
Fixed C	82.4 ± 0.4	wt.%
C	85.7 ± 1.5	wt.%
H	2.62 ± 0.04	wt.%
N	0.8 ± 0.1	wt.%
S	0.17 ± 0.04	wt.%
O	10.9 ± 1.5	wt.%
HHV	32.7 ± 1.2	MJ/kg

Figure 3: Char from slow pyrolysis of textile waste pellets.

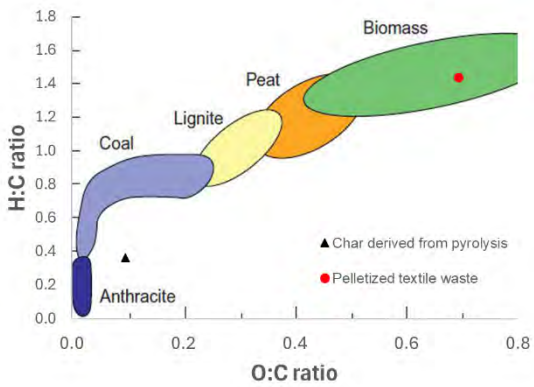

Figure 4: Processed textile waste and slow pyrolysis derived char positions within the Van Krevelen diagram.

As concern the condensation products benzoic acid, acetic acid, phenol, acetophenone, benzaldehyde, HMF and other compounds were identified as major components in the organic and aqueous phases. Roughly 7.3 g/L and 1.6 g/L benzoic acid was found respectively in the aqueous and in the organic phase. Also 4.4 g/L acetic acid was found in the aqueous phase.

Conclusions

The tests were carried out in order to validate the possibility of industrial scale up of a pyrolysis plant for the treatment of waste material from textile industries. It was possible to estimate mass balance of the slow pyrolysis process and assessing the vapours to be main share of the output. The char product was thoroughly characterised highlighting good chemical and physical properties in order to be used as an added value material for industrial applications (e.g. adsorbent, catalysis support,

etc…). The composition of the condensates which resulted particularly rich in benzoic acid leaves enough wiggle room for further investigation for isolation of the product. The recovery and isolation of petrochemicals such as benzoic acid can guarantee the creation of a supply chain for feedstock recycling within the textile sector itself being the benzoic acid a precursor of ε-caprolactam according to the Snia process mechanism. ε-Caprolactam can further be repolymerized to give PA-6 (nylon-6) that represents one of the main polymeric synthetic fibres used in textile sector. In the follow-up of the activity the scouting for off-takers of the produced benzoic acid might foster the development of the process within the scope of a feedstock recycling approach.

References

[1] Directorate-General for Environment, «EU strategy for sustainable and circular textiles,» 30 03 2022. [Online]. Available: https://environment.ec.europa.eu/publications/textiles-strategy_en. [Consultato il giorno 20 03 2024].

[2] European Environment Agency, «Textiles in Europe's circular economy,» 19 11 2019. [Online]. Available: https://www.eea.europa.eu/publications/textiles-in-europes-circular-economy. [Consultato il giorno 04 2024].

[3] D. Damayanti, L. Wulandari, A. Bagaskoro, A. Rianjanu e H.-S. Wu, «Possibility Routes for Textile Recycling Technology,» Polymers, vol. 13, p. 3834, 2021.

[4] B. Ruiz, E. Fuente, A. Pérez, L. Taboada-Ruiz, J. M. Sanz, L. F. Calvo e S. Paniagua, «Employment of conventional and flash pyrolysis for biomass wastes from the textile industry with sustainable prospects,» Journal of Analytical and Applied Pyrolysis, vol. 169, p. 105864, 2023.

Title: $Mg(OH)_2$ recovery from Mg^{2+}-rich brines

Authors: Giuseppe Battaglia*[1], Michela Cardella[1], Fabrizio Vassallo[1], Alessandro Tamburini[1], Andrea Cipollina[1], Giorgio Micale[1]

[1] Dipartimento di Ingegneria, Università degli studi di Palermo, Palermo, Italy, Viale delle Scienze, 90128.
**Speaker: Giuseppe Battaglia, giuseppe.battaglia03@unipa.it*

Keyword(s): mineral recovery; magnesium hydroxide; critical raw material; RO brine; saltworks bitterns.

Abstract

Desalination plants and saltworks are widely adopted to produce fresh water and table salt. However, these plants produce waste saline solutions that have been mainly handled following the linear economy approach. In the present study, the possible exploitation of waste saline streams is investigated aiming at producing highly pure magnesium hydroxide compounds, thus, turning waste into valuable products as well as reducing the environmental impact of these saline solutions.

Introduction

The increasing living standards and the continuous world population growth have been causing a reckless use of land resources and water. So far, the industrial production of goods has been based on the concept of the linear economy: raw materials are used for the manufacture of new products that, at the end of their life, are directly (or after a treatment) discharged into the environment or in landfills. This is the case of saline solutions produced by the desalination industry or the table salt production in saltworks. Waste solutions of the desalination industry are called brines, while bitterns are the waste streams of saltworks. Seawater contains all the elements in the periodic table. Sodium, chlorine, magnesium, calcium, and sulphate ions are the most abundant species. Among them, magnesium has been classified as a Critical Raw material (CRM) for its supply risk and importance for the social development of the European Union [1]. Mg^{2+} concentration in seawater is about ~1.3 g/L (~0.054 mol/L). It almost doubles in desalination brines, ~2.6 g/L (~0.100 mol/L), while it can be up to 60 times in saltworks bitterns. The high concentration of salts in saline solutions poses environmental concerns for their disposal. The valorisation of these streams is thus an appealing opportunity to produce magnesium-based goods by reusing industrial waste as well as a crucial chance to reduce the environmental impact of desalination industries. In this context, the Italian-funded CARMEn project aims at developing a novel circular approach to recover critical raw materials and energy from spent seawater brines [2]. In addition, the European-funded REWAISE project aims at creating a new smart water ecosystem to embrace the true value of water, reducing freshwater and energy use, and demonstrating innovative recovery of raw materials and minerals from water desalination [3]. In the present work, the recovery of Mg^{2+} from real saline solutions for the synthesis of magnesium hydroxide, $Mg(OH)_2$, compounds was investigated. Magnesium hydroxide is a chemical compound widely employed as a flame-retardant agent, an antibacterial agent, a neutralization reagent of acidic liquid waste, an environmentally friendly material for reducing the water pollution of heavy metals, a paper preservative and a precursor for magnesium oxide preparation [4]. In the present study, $Mg(OH)_2$ powders were synthesized by adopting a laboratory scale continuous stirred reactor treating three different saline solutions, namely (i) a waste brine outcoming from the reverse osmosis (RO) plant located in

Lampedusa (Italy), (ii) a more concentrated brine solution resulting from a concentration step of the RO brine through a nanofiltration (NF) unit; (iii) a waste bittern collected from the Margi saltworks located in Trapani, Italy. Synthetic sodium hydroxide, NaOH, solutions were employed as the alkaline reactant.

Materials and methods

Magnesium hydroxide precipitation tests were carried out using a laboratory continuous stirred tank reactor (CSTR) set-up, as shown in Figure 1.

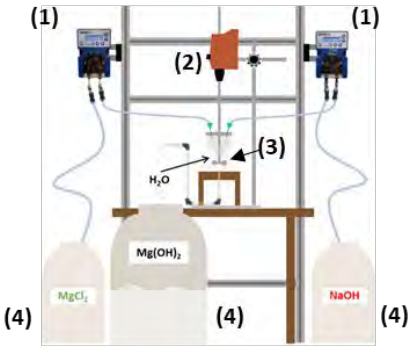

Figure 1. A schematic representation of the CSTR laboratory set-up: (1) peristaltic pumps (Kronos, 50), (2) a stirrer motor (LLG LABWARE), (3) a 1 L plexiglass reactor; (4) containers for feed and product solutions.

The reactor had a diameter of 10 cm and a height of 15 cm. A six blade Rushton turbine of 5 cm diameter was used to stir the solutions/suspensions at 400 rpm. Tests were conducted complying with standard geometry parameters; thus, the reactor was filled up to 750 mL, leading to a height of the liquid of ~10 cm. Reagents were pumped by two peristaltic pumps (Kronos, 50), conversely the product was collected through a plexiglass tube adequately positioned to maintain the desired fluid height in the reactor. Three real saline solutions were studied: (i) a RO waste brine from the RO plant in Lampedusa, Italy; (ii) a more concentrated brine obtained after treating the RO solution in a NF step; (iii) a waste bittern collected from the Margi saltworks, Trapani, Italy. Synthetic NaOH solutions were prepared by dissolving NaOH flakes (Inovyn, purity grade > 99%) of technical grade in ultra-pure water. The concentration of the magnesium and calcium ions was measured by complexometric titration with ethylenediaminetetraacetic acid, while the concentration of NaOH solutions was measured via acid-base titration. The reactor was filled with 750 mL of ultrapure water at the beginning of each test. Table 1 reports brine and NaOH solution concentrations and the adopted operating conditions for all tests.

Table 1. Brine and NaOH solution concentrations, operating conditions for all tests.

	RO pH 10.6	RO pH 12.5	RO+NF pH 10.6	RO+NF pH 12.5	Bittern pH 10.6	Bittern pH 12.5
Mg^{2+} [mol/L]	0.086	0.086	0.155	0.155	0.980	0.980
Ca^{2+} [mol/L]	0.018	0.018	0.027	0.027	0.002	0.002
OH [mol/L]	0.172	0.251	0.31	0.437	1.000	1.000
Brine flow rate [mL/min]	40	40	40	40	40	40
NaOH flow rate [mL/min]	40	40	40	40	40	104
Final pH	10.6	12.5	10.6	12.5	10.6	12.5

For each test, the pH was measured using a pH-meter (WTW 8830). Two final pH values were investigated: (i) the stoichiometric reaction pH value, 10.6, following the reaction $Mg^{2+} + 2 \cdot OH^{-} = Mg(OH)_2$, and (ii) a hydroxide ions excess condition, i.e. pH of 12.5.

The residual magnesium (C_{Mg}^{final}) and calcium (C_{Ca}^{final}) concentrations, after reaction, were assessed in clarified solutions, after $Mg(OH)_2$ particles thickening, by complexometric titration. The recovery of magnesium (Rec_{Mg}) and calcium (Rec_{Ca}) was then computed as follows:

$$Rec_{Mg} = \frac{\frac{C_{Mg}^{in}}{DF} - C_{Mg}^{final}}{\frac{C_{Mg}^{in}}{DF}} * 100 \qquad Rec_{Ca} = \frac{\frac{C_{Ca}^{in}}{DF} - C_{ca}^{final}}{\frac{C_{Ca}^{in}}{DF}} * 100 \qquad (1\text{-}2)$$

where C_i^{in} [mol/L] is the initial molar concentration of magnesium or calcium ions, and DF [-] is the dilution factor (equal to the ratio between the outlet flow rate and that of the brine one).

The purity of synthesized $Mg(OH)_2$ powders was assessed by dissolving ~150 mg of solids in 0.10 mol/L ultrapure hydrochloric acid (Honeywell-Fluka;>30% for trace analysis) and then measuring the concentration of cations species by Ion Chromatography (IC, Metrohm model 882 compact IC plus). Cationic purity was then calculated as the ratio between the Mg^{2+} concentration and the sum of the concentration of all cations.

Results

Figure 2 reports the Mg^{2+} and Ca^{2+} recoveries evaluated for all tests.

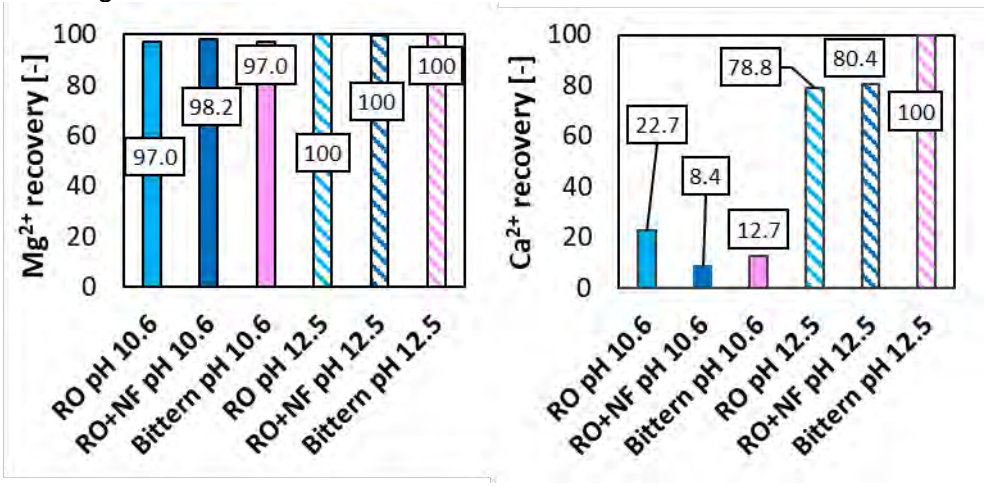

Figure 2. Mg^{2+} (a) and Ca^{2+} (b) recoveries from RO, RO+NF and saltworks bittern solutions at two final pH values of 10.6 and 12.5.

Magnesium ions recovery was always higher than 95 %, being 97.0, 98.2 and 97.0 for the RO, RO+NF and bittern solutions at the pH value of 10.6. At the higher pH of 12.5, a total Mg^{2+} recovery was achieved thanks to the higher availability of OH^- ions that ensured the total consumption of Mg^{2+} ones. Ca^{2+} recovery was 22.7, 8.4 and 12.7 %, for the three brines, at the pH value of 10.6, while recoveries were 78.8, 80.4 and 100 %, respectively, at the pH value of 12.5. The more basic environment favoured the co-precipitation of carbonate compounds. Ca^{2+} is expected to precipitate as calcium carbonate, from a pH value of 9, as a consequence of the presence of carbonate in the brines, or calcium hydroxide, from a pH value of 12.8. However, the precipitation of calcium compounds is not desired as it affects the purity of the synthesized $Mg(OH)_2$ powders [5]. The cationic purity of the synthesized powders is shown

in **Figure 3.**

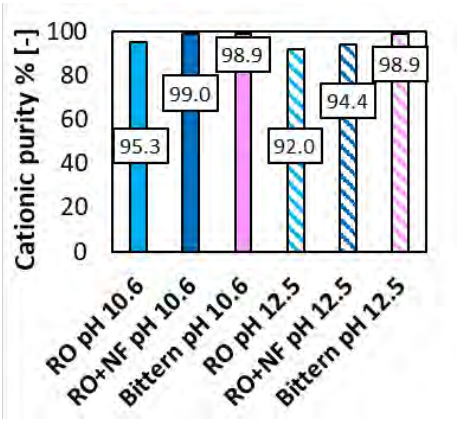

Figure 3. Cationic purity of $Mg(OH)_2$ powders synthesized from RO, RO+NF and saltworks bittern solutions at pH values of 10.6 and 12.5.

$Mg(OH)_2$ powders produced from bitterns had always a cationic purity >99%. Note that, in the calculation the Limit of Quantification for Na^+ and Ca^{2+} were always considered (3 mg/g and 1.3 mg/g, respectively). The high purity of the powders can be related to the low calcium content in the bittern, which precipitates in the saltworks through several evaporation ponds. The purity of the powders produced from the RO brine decreased from 95.3 to 92.0 increasing the final pH of the suspension, due to the co-precipitation of $CaCO_3$. The purity of $Mg(OH)_2$ powders produced from NF+RO solutions was 99 % at pH 10.6, while it decreased down to 94.4 % at the pH value of 12.5 due to the co-precipitation of $CaCO_3$. $Mg(OH)_2$ solids produced from the RO+NF brines was always higher than that of solids synthesized from the RO one. This can be attributed to a pre-acidification stage of the RO brine before the NF treatment. The acidification decreased the concentration of equivalent carbonates in the brine by more than 70 %, thus reducing the co-precipitation of $CaCO_3$ solids.

Conclusions

The recovery of $Mg(OH)_2$ compounds from real Mg^{2+}-rich solutions was investigated. The use of saltworks bitterns, thanks to the very low Ca^{2+} content, led to the precipitation of highly pure $Mg(OH)_2$ compounds with a Mg^{2+} recovery >99 %. Mg^{2+} recovery was always >95 % using RO brines, however, a pre-treatment is required to reduce their carbonate concentration to inhibit the co-precipitation of $CaCO_3$ impurities, as demonstrated by the higher purity of solids synthesized by an acidified RO brine.

Acknowledgements

The Authors would like to thank the European Union and the Horizon 2020 Research and Innovation Framework Programme for funding this research under the project REWAISE grant agreement No. 869496. The Authors would like to thank the Made in Italy Circolare e Sostenibile (MICS) project.

References

[1] Battaglia G., Ventimiglia L., Vicari F., Tamburini A., Cipollina A., Micale G., “Characterization of Mg(OH)2 powders produced from real saltworks bitterns at a pilot scale,” Powder Technol., Vol. 443, (2024).
[2] “CARMEn Project.” Available: https://www.mics.tech/en/projects/5-06-a-novel-circular-approach-to-recover-critical-raw-materials-and-energy-from-spent-seawater-brines-carmen/. [Accessed: 04-Jun-2024].
[3] “REWAISE Project.” Available: https://rewaise.eu/the-project/. [Accessed: 04-Jun-2024].
[4] Balducci G., Bravo Diaz L., Gregory D. H., “Recent progress in the synthesis of nanostructured magnesium hydroxide,” CrystEngComm, Vol. 19, pp. 6067–6084, (2017).
[5] Gong M. H., Johns M., Fridjonsson E., Heckley P., “Magnesium Recovery from Desalination Brine,” CEED Semin. Proc., pp. 49–54, (2018).

PARALLEL SESSION: A3

Wastewater treatment

Innovative approaches for monitoring and operating plants towards sustainability

Towards sustainable municipal wastewater treatment: an analysis of energy and greenhouse gases in Apulia

Author(s): Sarah Gregorio*[1], Gianfranco D'Onghia[1], Luigi Lopopolo[1], Ezio Ranieri[1]

[1] *Università degli Studi di Bari, Dipartimento di Bioscienze, Biotecnologie e Ambiente Bari, Italy*

Keyword(s): Keywords: Wastewater, Electric Energy; Nitrous Oxide, Carbon Dioxide, Methane, GHG

A study on energy consumption and greenhouse gas emissions has been conducted on the Apulian wastewater treatment plants. In Apulia, there are 183 conventional activated sludge plants managed by Italian water management companies –Acquedotto Pugliese S.p.a. (AQP) of which 140 have aerobic digestion sludge and 83 plants equipped with anaerobic digestion of the sludge. The typical configuration includes preliminary treatments, primary sedimentation (occasionally in the anaerobic plants), and secondary treatment represented by conventional activated sludge. The water line is followed by a sludge line constituted by a thickener, aerobic or anaerobic digester and dewatering unit.

The average equivalent population of an Apulian WWTP is equal to 60,336 PE with an average capacity of 8476 m^3 /d. Table 1 reports the principal operational data of the Anaerobic and Aerobic WWTPs in Apulia (average values that refer to five years of investigation from 2018 to 2022).

Table 1. Characteristics of Apulian wastewater treatment plants.

	PE	kWh/d	Inflow (Q) m^3/d	CODin (mg/l)	COD out (mg/l)	N in (mg/l)	N out (mg/l)
Anaerobic digestion	3,346,321	263,511	470,985	887	55	75	14
Aerobic digestion	1,517,781	237,684	210,853	798	48	78	13

In Italy, the electricity consumption in WWTPs is about 3,250 GWh/ year [1], corresponding to about 0.5 billion Euros per year. In addition, an increase of 12% in energy required by AQP WWTPs has been shown from 2013 to 2018, reaching a total value of approximately 182 GWh/year. This is due to the increasingly stringent environmental requirements and the need to enhance the plants' capacity, which has led to the upgrading of the main treatment stations, also the installation of new, more powerful and efficient electromechanical equipment [2].

The comparison between energetic consumptions in conventional WWTPs adopting Aerobic Digestion (AD) and Anaerobic Digestion (AnD) gives useful information to designers or water management companies about which technology should be used to reduce the electrical cost and have a high degree of sludge stabilisation.

The data analysis has been evaluated through specific energy demand indicators: kWh/m^3 and kWh/PE*year (Figure 1 e 2).

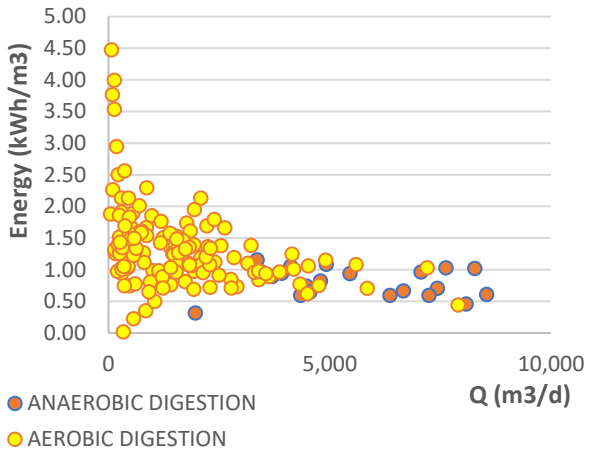

Fig 1. Energy consumption correlated with flow rates in the aerobic and anaerobic WWTPs of AQP.

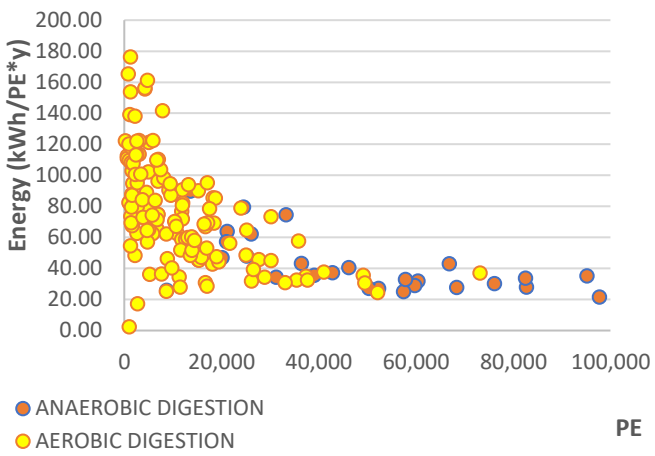

Fig 2. Energy consumption correlated with population equivalent in the aerobic and anaerobic WWTPs of AQP.

Overall, the energy consumed (kWh/m^3) decreases exponentially as a function of the daily flow rate in the plants. This situation is visible for both plant types but the one for aerobic digestion plants decreases faster than the others.

Literature reports aerobic plants are usually the most energy-intensive [3]; indeed, also aerobic Apulian plants require about 1.13 kWh/m^3 than anaerobic plants request 0.53 kWh/m^3, due to the smaller size of the aerobic WWTPs.

The same condition can be seen in the correlation between energy consumption and PE, the specific energy consumption tends to decrease with the increase of the number of PE, with greater evidence for anaerobic plants.

It follows that a larger plant capable of accommodating and treating higher incoming flow rates is advantageous from an environmental point of view only for plants with AnD treatment,

Therefore, the energy consumption per year is equal to 26,09 kWh/PE*y for anaerobic plants and 57,63 kWh/PE*y for aerobic plants (higher than double).

The investigation has been deepened by estimating the reduction in electricity consumption that would be achieved if anaerobic treatment were adopted on all the plants for which it is advantageous compared to the total of the plants considered.

Thus, if all the Apulian AD plants with a capacity higher than 10,000 PE were converted to anaerobic digestion, an energy saving, calculated on all plants, of about 16% would be achieved [4].

Considering that the use of anaerobic sludge treatment is more convenient in terms of electricity consumption, then it should also be in terms of GHG emissions.

All phases of treatment of Apulian plants are open tanks (except the anaerobic digester) and are considered a source of emissions. Anyway, wastewater treatment is a global source of greenhouse gases (GHGs), particularly, carbon dioxide (CO_2), nitrous oxide (N_2O) and methane (CH_4) [5], [6].

WWTPs in Apulia serve about 4,81 million PE (Population Equivalent), yielding approximately 600,000-ton equivalent CO_2 per annum.

It has been estimated the global warming potential (GWP) of Apulian WWTPs both their total GHGs and singular GHGs released from each unit of treatments, differentiated between aerobic and anaerobic plants [7].

The approach has considered the distinction between indirect emissions (CO_2 from fossil fuels), hence those released by electric energy consumption which used aerobic and anaerobic processes and direct emissions (CO_2 biogenic, N_2O, CH_4) examining all sources addressed by the IPCC guidelines [8], [9].
Following a wide survey of emission factors used in the other studies, and considering the influent average characteristics and the specific functioning data, in terms of typology and extension of the aeration basin and of the leakage in the biogas capture and storage systems in the WWTPs, the following conversion factor to estimate the total GHG emissions have been considered [7].

- N_2O: 0.035 kg N–N_2O per kg N removed
- CH_4: 0.035 kg CH_4 per kg COD removed
- CO_2 Biogenic: 0.73 kg CO_2 per kg COD removed
- CO_2 Fossil: 0.403 kgCO_2eq per kWh consumed [10].

Thus, the contributions of GHG emissions are shown in Figure 3.

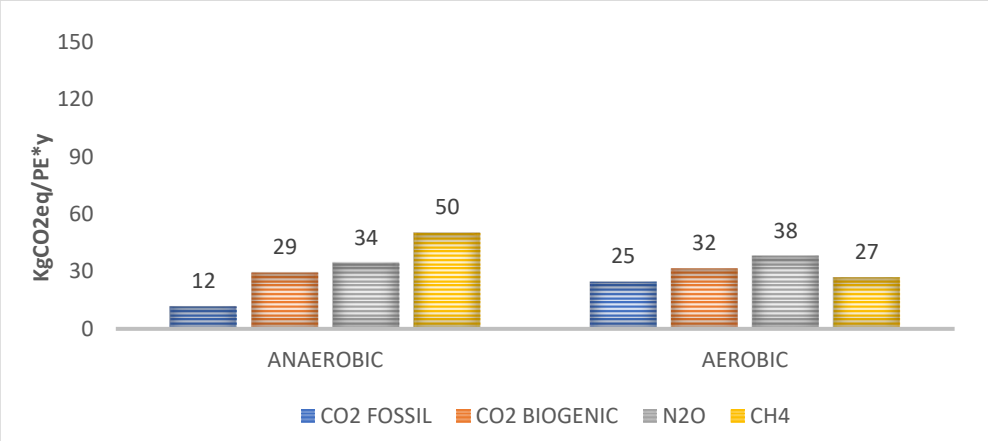

Fig 3. a Total kgCO_2/(PE·y) calculated for the 183 aerobic and anaerobic Apulian WWTPs [7].

The total GHG production per Person Equivalent per year is about 103 kgCO_2eq/(PE·y) for aerobic WWTPs and about 134.6 kgCO_2eq/(PE·y) for anaerobic WWTPs.
The anaerobic WWTPs, compared with the aerobic WWTPs, emit higher quantities of GHGs on a per PE per year basis, as shown in Figure 3. CH_4 represents their highest contribution to the total CO_2 equivalent because mainly biogas produced in the anaerobic tank is not recovered but burned in the flare generating and not saving CO_2. Instead, the larger contribution of emissions for aerobic WWTPs is N_2O as a result of a lack of denitrification step in the secondary treatment.
The analysis was prolonged to estimate greenhouse gases from each unit of treatment within the wastewater treatment and asses their reduction emission rates following quantified compensative measures [11], as reported in Table 2.

Table 2 Emission balance in the Apulian wastewater treatments.

WATER LINE	PRELIMINARY TREATMENT	PRIMARY CLARIFICATION	AEROBIC OXIDATION	SECONDARY CLARIFICATION
CURRENT ESTIMATION	1.73 kg CO_2eq/PE*y 0.034 kg CO_2eq/m^3	0.31 kg CO_2eq/PE*y 0.006 kg CO_2eq/m^3	52.58 kg CO_2eq/PE*y 1.026 kg CO_2eq/m^3	0.58 kg CO_2eq/PE*y 0.011 kg CO_2eq/m^3
AFTER UPGRADE	1.58 kg CO_2eq/PE*y 0.031 kg CO_2eq/m^3	0.31 kg CO_2eq/PE*y 0.006 kg CO_2eq/m^3	45.95 kg CO_2eq/PE*y 0.896 kg CO_2eq/m^3	0.56 kg CO_2eq/PE*y 0.011 kg CO_2eq/m^3

SLUDGE LINE	SLUDGE THICKENER	AEROBIC + ANAEROBIC DIGESTER	DEWATERING	TOTAL EMISSIONS
CURRENT ESTIMATION	1.61 kg CO_2eq/PE*y 0.032 kg CO_2eq/m^3	24.02 kg CO_2eq/PE*y 0.469 kg CO_2eq/m^3	1.93 kg CO_2eq/PE*y 0.038 kg CO_2eq/m^3	83 kg CO_2eq/PE*y 1.62 kg CO_2eq/m^3
AFTER UPGRADE	1.46 kg CO_2eq/PE*y 0.029 kg CO_2eq/m^3	10.65 kg CO_2eq/PE*y 0.209 kg CO_2eq/m^3	1.78 kg CO_2eq/PE*y 0.035 kg CO_2eq/m^3	62 kg CO_2eq/PE*y 1.22 kg CO_2eq/m^3

The investigation has been carried out, based on the mass balance of carbon removal and N removal and respective coefficient emission to calculate the singular GHGs from each unit [11]. These were estimated in the current situation and compared, for the same WWTPs, to those emitted after assuming structural compensatory measures to mitigate them. Total GHG emissions in the current estimation have been estimated equal to 83 kg CO2eq/PE·y and equal to 62 kg CO2eq/PE·y after the upgrade. Moreover, some compensatory measures have been discussed to lower GHGs emissions: the recirculation of sludge thickened in treatment secondary; reduction of biogas systems leakage, aerobic digester and thickener coverage and a new system to recover biogas from anaerobic digester generating energy. All upgrade systems considered result in electrical energy reduction and significant GHG emissions reduction, especially for anaerobic digestion-based WWTPs [11].

References

[1] Campanelli, M., Foladori, P. & Vaccari, M. 2013 Analisi del consumo e del costo energetico nel servizio idrico integrato (Analysis of energy consumption and costs in water and wastewater services). In: Consumi Elettrici eds Efficienza Energetica nel Trattamento Delle Acque Reflue (Electricity Consumption and Energy Efficiency in Wastewater Treatment) (Campanelli, M., Foladori, P. & Vaccari, M. eds). Maggioli, Bologna, Italia, pp. 41–48 (in Italian).

[2] Acquedotto Pugliese Spa 2019 Bilancio Societario. Report integrato. Bari, Italy (in Italian)

[3] Daw, J., Hallett, K., Dewolfe, J. & Venner, I. 2012 Energy Efficiency Strategies for Municipal Wastewater Treatment Facilities. s.l.: National Renewable Energy Laboratory, Golden, CO, USA.

[4] Ranieri, E., Giuliano, S., & Ranieri, A. C. (2021). Energy consumption in anaerobic and aerobic based wastewater treatment plants in Italy. *Water Practice & Technology*, *16*(3), 851-863

[5] Ranieri, E., D'Onghia, G., Lopopolo, L., Gikas, P., Ranieri, F., Gika, E., Ranieri, A. C. (2024). Influence of climate change on wastewater treatment plants performances and energy costs in Apulia, south Italy. *Chemosphere*, *350*, 141087.

[6] Schneider, A.G., Townsend-Small, A., Rosso, D., 2014. Impact of direct greenhouse gas emissions on the carbon footprint of water reclamation processes employing nitrification-denitrification. Sci. Total Environ. (505), 1166–1173.

[7] Ranieri, E., D'Onghia, G., Lopopolo, L., Gikas, P., Ranieri, F., Gika, E., ... & Ranieri, A. C. (2023). Evaluation of greenhouse gas emissions from aerobic and anaerobic wastewater treatment plants in Southeast of Italy. *Journal of Environmental Management*, *337*, 117767.

[8] H.S. Eggleston, L. Buendia, K. Miwa, T. Ngara, K. Tanabe, IPCC Guidelines for National Greenhouse Gas Inventories, 2006 (2006).

[9] IPCC, Refinement to the 2006 IPCC Guidelines for National Greenhouse Gas Inventories, 2019.

[10] Acquedotto Pugliese (AQP), 2021. Bilancio Sociale.

[11] Ranieri, E., D'Onghia, G., Ranieri, F., Lopopolo, L., Gregorio, S., & Ranieri, A. C. (2024). Compensatory measures to reduce GHGs in wastewater treatment plants in Southern Italy. *Journal of Water Process Engineering*, *60*, 105128.

Glucose Production from Cellulosic Sludge: Innovating Wastewater Recovery

Federico Micolucci*[1], Nicola Frison[1]

[1] *Department of Biotechnology, Verona, Italy, federico.micolucci@univr.it, nicola.frison@univr.it*

Keywords: wastewater, assisted metabolism, bioproducts, cellulose

This paper presents the first work package of the REFRAME project (HORIZON-MSCA,10/23, *project duration 36 months*), a scientific initiative aimed at transforming wastewater treatment plants into Water Resource Recovery Facilities, in alignment with the objectives of the SIDISA XII. Spearheaded by the University of Verona, REFRAME is at the forefront of addressing pressing water challenges by revolutionizing wastewater management. The project facilitates the sieving of incoming wastewater to obtain cellulosic primary sludge (CPS). This reduces the organic load on the treatment plant and enables the use of CPS to produce bioproducts.
Efficient wastewater management is essential for achieving environmental goals. However, many existing treatment plants struggle with stricter emission standards, increased loads causing capacity constraints, and challenges posed by urban encroachment. Building on this need, once the CPS is obtained, the main output of REFRAME will be a novel hybrid biological system. This system uses an oxidation-reduction potential (ORP) based control to selectively produce targeted bio-based volatile fatty acids (VFAs) and polyhydroxyalkanoates (PHAs) from CPS. This project, illustrated in Figure 1, aims to create a platform for producing chemicals, precursors for bioplastics, and ingredients for animal feed that are market-ready.
The state of the art in cellulose recovery from wastewater treatment focuses on enhancing resource recovery, motivated by the shift towards circular economy models. The benefits include reduced energy requirements and the potential to create valuable by-products, aligning with broader goals of sustainability and resource efficiency. By reducing the organic load on wastewater treatment processes, less energy is required for aeration, one of the most energy-intensive aspects of wastewater treatment. While cutting-edge technologies show promise, their full-scale application often faces challenges such as high initial investments and the need for tailored solutions based on local conditions and wastewater characteristics.

The study presented delineates a novel method for wastewater pre-treatment. This approach involves an initial coarse cleansing and sand separation, followed by fine sieve filtration to isolate suspended matter, predominantly toilet paper and other organic substances. During this process, dissolved organic compounds within the wastewater permeate the filter, while the CPS is collected and treated under oxygen-deprived conditions to induce hydrolysis. This work package also explores the implementation of user-friendly technologies, including Rotating Belt Filters (RBFs) and rapid cellulose sludge hydrolysis methods. RBF is technology that has been identified as one of the most effective methods for cellulose recovery [1]. This first step not only intercepts solid waste but also significantly reduces the organic load, thereby decreasing energy consumption required for aeration. RBFs are appreciated for their simplicity,

effectiveness in retaining solids, and their ability to operate continuously without chemical additives.
This study examined the extraction of organic matter from wastewater prior to biological treatment, pinpointing fine sieves with pore sizes ranging from 350–500 µm as the most effective method for this purpose. A pilot-scale Salsnes rotary belt filter, which operates without chemicals for flocculation/precipitation, was employed as a pre-filtration mechanism. This filter was integrated into the incoming water system of an urban wastewater treatment plant in Källby, Sweden. The Salsnes system utilizes a diagonally oriented screen that efficiently transports sludge away from the untreated water, resulting in a dense sludge that is subsequently collected.
The next step was to utilize the recovered CPS as a raw material decreasing operational costs and create new revenue streams from waste products by hydrolysis pre-treatment.
Hydrolysis batch tests were conducted using 5L bottles under various conditions including temperatures of 20, 38, and 55 °C; pH levels of control (CTRL, pH non-modified), 4, and 12; and retention times of 24 and 48 hours. These tests aimed to optimize the conditions for breaking down cellulosic material into simpler compounds. The analytical method employed for cellulose analysis is a recognized standard for assessing the composition of plant-derived materials in environmental studies [2].

Figure 1. REFRAME process scheme.

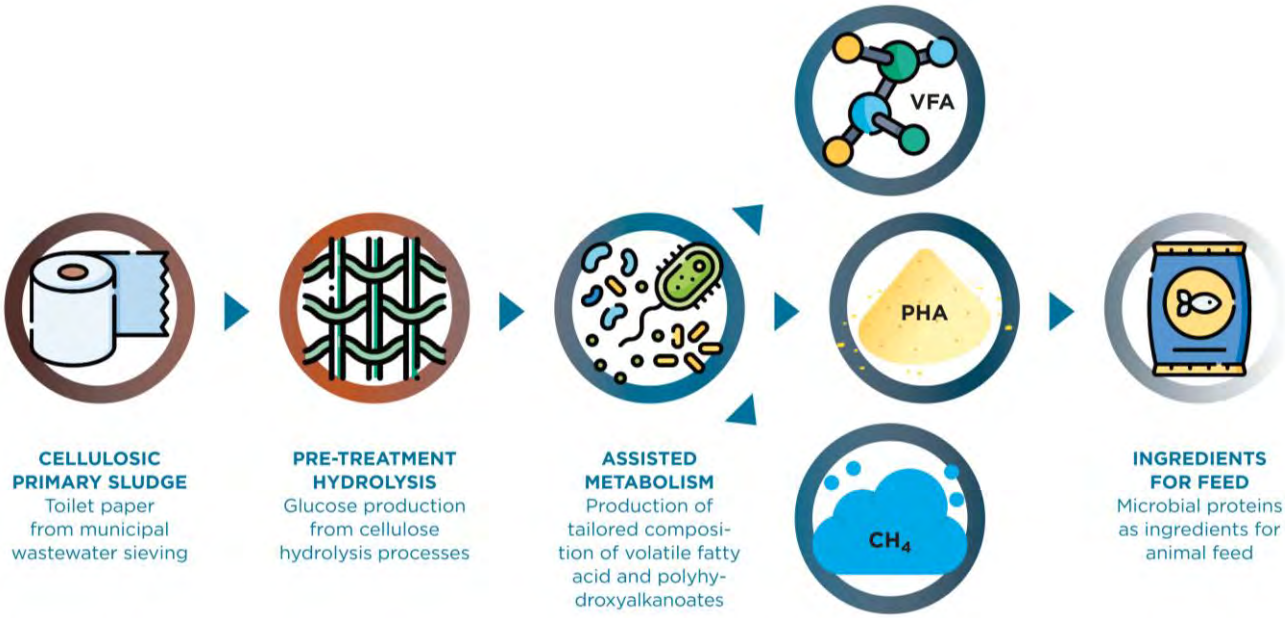

Our research indicates that approximately 48% (±3%) of the CPS is composed of cellulose (TS/TS).
Removing cellulose before biological treatment significantly reduces energy consumption, particularly in the aeration phase, by retaining approximately 60% of BOD through rotary belt filters. This process minimizes the load on subsequent treatment stages, enhancing plant efficiency and reducing operational costs. Net energy savings from this method range from 9% to 19% of the total water-line energy consumption, underscoring its effectiveness in optimizing overall performance and cost-effectiveness. Optimal pre-treatment hydrolysis conditions have demonstrated the ability to convert up to 50% of this cellulose into glucose and an addition of 2% converted into xylose. This conversion rate

was achieved using a pH of 4 and a temperature of 20°C over a 24-hour period. Furthermore, up to 42% of the cellulosic material can be hydrolyzed into soluble compounds (mainly glucose and ca. 4% xylose) in a batch environment with a pH of 12 at 38°C over the same duration.

Figure 2-3. Degradation of COD, total suspended solids and cellulose after the batch trials.

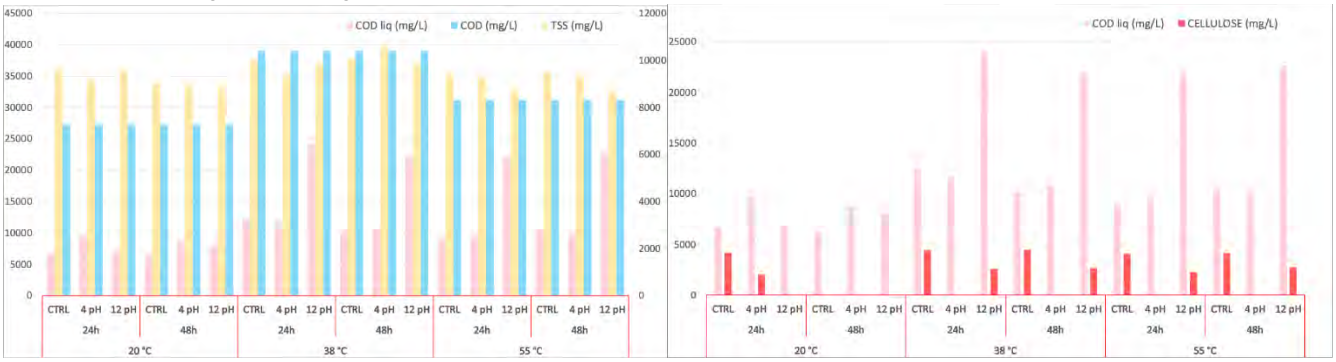

Furthermore, experimental observations indicate that hydrolysis at a pH of 4 effectively breaks down cellulose, albeit with a lower conversion of COD to SCOD in the liquid phase compared to batches processed at higher temperatures and basic pH levels. This suggests that cellulose hydrolysis into glucose (and to a lesser extent, xylose) is more efficient at an acidic pH, as demonstrated by a favorable SCOD/glucose ratio. Conversely, hydrolysis under alkaline conditions leads to a higher SCOD/glucose ratio. This does not necessarily indicate only a less efficient conversion of cellulose but rather points to a more effective degradation of other organic materials.

These hydrolyzed products, primarily glucose and other organic compounds, can be subsequently converted into volatile fatty acids (VFAs) with a yield of 340 mgCOD_{VFA}/gTVS at 38 °C [3].

Regarding the specific types of VFAs produced, acetic acid (C2) and propionic acid (C3) are the most prevalent, constituting 55% and 33% of the VFAs, respectively. The remaining fraction, approximately 12%, consists of butyric and valeric acids (C4 and C5). These findings underline the potential of optimized hydrolysis processes in enhancing the efficiency of bio-based product recovery from wastewater treatment processes, contributing significantly to the sustainable production of valuable biochemicals.

Considering that European population served by WWTP with a capacity higher than 150 000 PE (population equivalent) is around 100 million and the recovery yields reported in our previous work [4], REFRAME project will advance the state-of-the-art potential by the impact of the CPS to produce bio-based products (table 1). Currently, the EU bio-based production of a platform of chemicals is estimated at 181 kton/y, with a total EU production of 60791 kton/y [5]. The VFAs produced from CPS could potentially increase the annual production of bio-based acetic acid from 55 to 189 kton/y, so that the EU bio-based shares will be 3.4 higher compared with the current production. The annual global demand for propionic and butyric acid is estimated at 470 and 105 kton with a growing rate demand reported at 2.7 % and 15.1% CAGR [6]. Considering the same share EU bio-based share found for the platform of chemicals, the valorization of the CPS could completely cover the growing rate demand or partially replace the annual production of propionic and butyric acid from fossil to bio-based origin up to 70 and 14 kton. The valorization of the CPS will increase 1,4 times more the EU bio-based shares of polymer

for plastics, while the production of the sole PHAs will be increased from the current 2.3 kton/year to 104.3 kton by the project´s implementation, which are 45 times higher.

Table 1. Impact of the bio-based VFAs and PHAs production from CPS on the current production of EU bio-based platform of chemicals (*estimated considering 0.3% as current bio-based share).

Product category	Average Price (€/ton)	EU production (kton/y)	Current EU bio-based production (kton/y)	Total bio-based production with REFRAME (kton/y)
Chemical platform (EC-JRC, 2018)	1480	60791	181	315
Acetic acid	600	18500	55*	189
Propionic acid	2250	470	1.4*	70
Butyric acid	1575	105	0.3*	14
Polymer for plastics	2680	60000	268	372
PHA	5430	2.3	2.3	104

The consumption of toilet paper varies significantly around the globe, serving as a marker of a country's development and quality of life; for example, annual usage is 13 kg per person in Western Europe, 12.7 kg in the United States, 12.1 kg in Germany, 6.3 kg in Italy, 0.9 kg in Asia, and 0.7 kg in Africa. This disparity highlights a significant opportunity to recover and repurpose toilet paper from wastewater as a resource for manufacturing bio-based chemicals, particularly given that the European Union's contribution to global production of key bio-based chemicals is a mere 0.3%, indicating a substantial market gap. The substances hydrolyzed in these processes are then utilized as feedstock in oxidation-reduction potential-controlled fermentation processes to produce targeted VFAs. These VFAs are crucial building blocks for various bio-based products. Ongoing results from these investigations are currently being compiled and will be detailed in the final version of the paper.

References

[1] Liu, R., Li, Y., Zhang, M., Hao, X., & Liu, J. (2022). Review on the fate and recovery of cellulose in wastewater treatment. *Resources, Conservation and Recycling*, *184*, 106354.
[2] Sluiter, A., Hames, B., Ruiz, R., Scarlata, C., Sluiter, J., Templeton, D., & Crocker, D. L. A. P. (2008). Determination of structural carbohydrates and lignin in biomass. *Laboratory analytical procedure*, *1617*(1), 1-16.
[3] Crutchik, D., Frison, N., Eusebi, A. L., & Fatone, F. (2018). Biorefinery of cellulosic primary sludge towards targeted Short Chain Fatty Acids, phosphorus and methane recovery. *Water research*, *136*, 112-119.
[4] Botturi, A., Battista, F., Andreolli, M., Faccenda, F., Fusco, S., Bolzonella, D., ... & Frison, N. (2021). Polyhydroxyalkanoated-Rich Microbial Cells from Bio-Based Volatile Fatty Acids as Potential Ingredient for Aquaculture Feed. Energies, 14(1), 38.
[5] Report: Spekreijse, J., T. Lammens, C. Parisi, T. Ronzon, M. Vis (2019). Insights into the European market of bio-based chemicals. Analysis on then key products categories. JRC report.
[6] Research Grand View, 2018. Global Propionic Acid Market by Application (Animal Feed, Ca Na Propionate, Cellulose Acetate Propionate). San Francisco.

Title: Development of an innovative Laser Direct InfraRed (LDIR)-based methodology for monitoring microplastics in wastewater treatment plants

Author(s): Benedetta Pagliaccia*[1], Miriam Ascolese[2], Elena Vannini[1], Donatella Fibbi[3], Emiliano Carretti[4], Claudio Lubello[1], Riccardo Gori[1]

[1] Department of Civil and Environmental Engineering, University of Florence, Via di Santa Marta 3, 50139 Firenze, Italy, benedetta.pagliaccia@unifi.it, elena.vannini@unifi.it, claudio.lubello@unifi.it, riccardo.gori@unifi.it
[2] PIN, University of Florence, Piazza Giovanni Ciardi 25, 59100 Prato, Italy, miriam.ascolese@pin.unifi.it
[3] Gestione Impianti Depurazione Acque (GIDA) SpA, Via di Baciacavallo 36, 59100 Prato, Italy, d.fibbi@gida-spa.it
[4] Department of Chemistry "Ugo Schiff" and CSGI consortium, University of Florence, Via della Lastruccia 3, 50019 Sesto Fiorentino, Italy, emiliano.carretti@unifi.it

Keyword(s): microplastics; monitoring; wastewater; methodology; Laser Direct InfraRed.

Abstract

This contribution aims to explore the feasibility of applying the innovative Laser Direct InfraRed (LDIR) chemical imaging technique for the identification and characterization of microplastics (MPs) in wastewaters. The LDIR-oriented experimental and analytical methodologies were developed/validated by using standard MPs and then applied to influent and effluent samples coming from a wastewater treatment plant (WWTP) selected as case-study. The fine-tuned pretreatment protocol allowed a high MPs recovery rate without altering the characteristics of plastic particles. Both chemical and physical characterization methods were validated by comparing the LDIR data with those acquired by well-established techniques. A MPs removal efficiency of about 91% along the water line of the monitored WWTP was estimated. All these evidences confirmed the reliability and robustness of the proposed methodologies, thus highlighting the potential of LDIR-based methods for MPs monitoring purposes.

1. Introduction

The exponential rise in plastic consumption, combined to inadequate waste management practices, led to a massive dispersion of microplastics (MPs) in all environmental compartments, including soil and water bodies. MPs (defined as plastic particles in the size range 1 µm – 5 mm of primary or secondary origin [1]) became a contaminant of increasing concern due to their potential adverse impacts on ecosystems and organisms [2]. The heterogeneity of MPs in terms of chemical composition, size and shape represents a challenge for understanding their effects, behaviour and fate in the environment. The role of wastewater treatment plants (WWTPs) as potential sources of microplastic pollution in aquatic ecosystems was pointed out in the literature [3,4]. Although WWTPs proved to be effective in removing large quantities of MPs (up to 88–97%, depending on the process units employed), it was evidenced that many MPs could bypass the treatment chains, thus being discharged into the receiving water bodies [4]. Understanding the occurrence and fate of MPs in WWTPs is hence crucial for developing targeted solutions to minimize their release into the environment. To date, the lack of reference methodologies represents a bottleneck for MPs monitoring purposes, thus highlighting the need for effective detection, quantification, and characterization methods also in view of a regulatory framework development. In this perspective, this work aims to propose a robust method for monitoring MPs in WWTPs through the innovative Laser Direct InfraRed (LDIR) chemical imaging system. LDIR

allows a time-effective and automated analysis able to count and comprehensively characterize MPs in the samples under observation. By exploiting a quantum cascade laser (QCL) technology, coupled with rapidly scanning optics, this technique provides high-quality images and spectral data in the range 975–1800 cm^{-1} [1], enabling the real-time chemical identification and physical description of plastic particles.

2. Materials and methods

Since the LDIR technique is still poor investigated for its potential in detecting MPs in wastewaters, this work firstly aimed at fine-tuning both experimental and analytical procedures. To this aim, MPs produced by grinding common items in high-density polyethylene (HDPE), polyethylene terephthalate (PET) and acrylonitrile butadiene styrene (ABS) with an electric grater were used. The resulting plastic particles were sieved in the size range 38–106 µm and then dispersed in ultrapure water with concentrations of 10–30 mg MPs/L to obtain synthetic aqueous samples to be used as standards. Various pre-treatment methods were preliminary compared, leading to the following optimized protocol: (i) sample concentration by vacuum-filtration (5 µm mesh size) and subsequent recovery of the material retained on the filter via backwashing with ultrapure water; (ii) chemical digestion via Fenton reaction to remove organics [5]; (iii) density separation in 60 % (w/w) $ZnCl_2$ aqueous solution to remove inorganics (optional); (iv) MPs recovery by vacuum-filtration (5 µm mesh size) and backwashing of the filter with ethanol. The dispersions of MPs in ethanol thus obtained were analysed by Agilent 8700 LDIR. Chemical identification of MPs was carried out via real-time matching of the acquired IR spectra with the integrated libraries. Particles recognized as “cellulosic” were included in the MPs counting since LDIR workflow associates to this polymeric class both cellulose of natural origin and chemically modified/semi-synthetic cellulose (e.g. artificial textile fibers). Size and morphology characterization of the detected particles was performed based on the dimensional and geometric parameters given by the LDIR analysis (i.e. width, height, equivalent diameter, aspect ratio, circularity, etc.): MPs were hence classified into fibers (aspect ratio ≥ 3 or ≤ 0.33), spheres (circularity ≥ 0.9), pellets (0.6 ≤ circularity < 0.9) and fragments (0.33 < aspect ratio < 3; circularity < 0.6) [6], and a characteristic dimension was assigned to each of them (width/height for fibers and equivalent diameter for the other particle shapes). The analytical method was validated by comparing the acquired data with those obtained through well-established techniques: ATR-FTIR (IRAffinity-1S, Shimadzu) and size particle analyzer (Mastersizer 3000, with Hydro SM, Malvern Panalytical) for chemical and size characterizations, respectively. A WWTP located in Prato (Tuscany, Italy) managed by GIDA SpA and treating both municipal and industrial wastewaters (the latter partially collected to the plant by a separate sewer system) was selected as case-study to apply the above-described methodology. 24-hour composite samples were collected by autosamplers (200 mL sampled each 30 minutes) in the following sections: influent from separate industrial sewer ($IN_{Separate\ industrial\ sewer}$), inlet after union of flows from combined and separate sewers (IN) and effluent (OUT). Preliminary tests were carried out to identify the minimum sample volume to be treated and analyzed by LDIR. Blank control samples were processed to quantify (and subtract from the experimental sample data) the potential microplastic cross-contamination deriving from sampling and pretreatment phases.

3. Results and discussion

The described pretreatment protocol proved to be highly effective in extracting MPs from the targeted samples, evidencing a MPs recovery rate (96 ± 4 %) comparable or even higher than literature data [1,7]. No significant differences were found by comparing the ATR-FTIR spectra of the pristine and chemically digested MPs, thus suggesting that Fenton reaction did not cause chemical changes or structural degradation of plastic particles. The LDIR analysis confirmed the chemical nature of the tested MPs (ABS, PET and HDPE) with a quality index higher than 0.9, in line with the ATR-FTIR acquisitions. A MPs size distribution broader than expected from particle sieving in the size range 38–106 µm was obtained by LDIR (**Figure 1**) and confirmed through Mastersizer: this likely because particles in the form of fibers and/or elongated fragments (largely produced by grinding plastic items), thanks to their

morphology, can more easily pass through the sieve openings longitudinally even if characterized by a dimension higher than mesh size. However, the largest fraction of MPs was found in the range 38–106 µm (61%, 56% and 61% for ABS, PET and HDPE particles, respectively), thus suggesting the reliability of the LDIR analysis. All these evidences thus confirmed the robustness of the developed experimental and analytical methodologies, thus suggesting their applicability for MPs monitoring purposes.

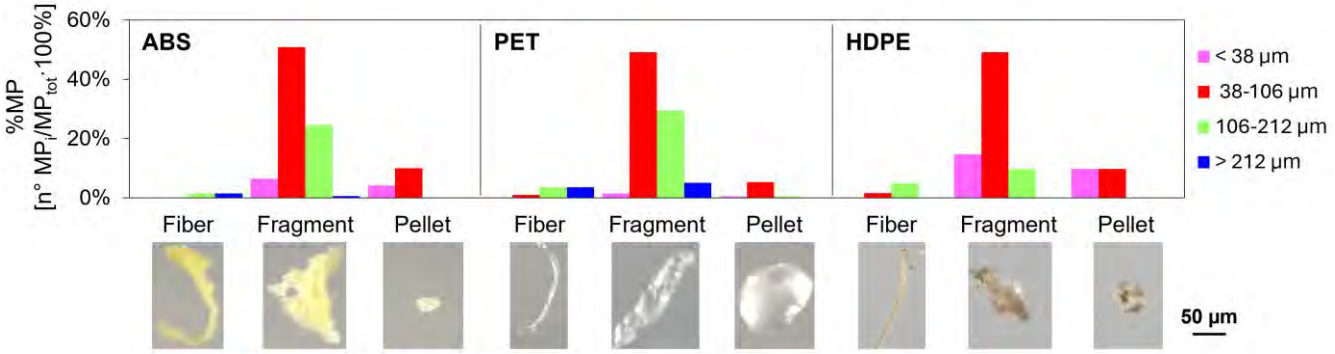

Figure 1. Size distribution obtained by LDIR analysis for ABS, PET and HDPE particles sieved in the size range 38–106 µm and their morphological classification into fibers, fragments and pellets. Examples of MPs for each category are shown as visible images acquired by LDIR–High magnification function.

Preliminary analyses indicated that the MPs concentrations in all treated samples from the monitored WWTP decreased with increasing the processed volume up to a achieve an almost constant value for the 1 L-treated aliquots. For summary constrains, only data related to 1 L-aliquots, judged as sufficiently representative, are hence presented. The overall concentrations of MPs estimated from the LDIR analysis were about $2.26 \cdot 10^5$ and $2.03 \cdot 10^4$ items/L for IN and OUT, respectively ($8.13 \cdot 10^4$ and $4.06 \cdot 10^3$ items/L for IN and OUT, respectively, without including cellulosic materials in the particle counting). According to these results, it was possible to predict a MPs removal efficiency of about 91% along the water line of the monitored WWTP (that increased up to around 95% if cellulosic particles are not considered), in line with literature data [4]. MPs concentrations (including cellulosic particles) in the range $1.67 \cdot 10^5$ – $2.26 \cdot 10^5$ items/L were observed for $IN_{Separate\ industrial\ sewer}$, thus suggesting that a large fraction of MPs entering the WWTP derived from the industrial discharges. The physical and chemical characterization of the detected MPs is summarized in **Figure 2**. No spheres were found in the processed samples, thus suggesting the secondary origin of the detected MPs. Particles of various origin (mainly in the form of fragments and pellets lower than 100 µm in size and fibers of 100–200 µm) were found in the influent, with a predominance of cellulose-derived materials (64%) followed by polytetrafluoroethylene (PTFE), polyethylene terephthalate (PET), polyurethane (PU) and acrylonitrile butadiene styrene (ABS). The separate sewer collected to the WWTP large quantities of polyamide (PA), cellulosic and polyurethane (PU) fibers (**Figure 2c**), that can be reasonably ascribed to the textile origin of the industrial wastewater. Only PU and cellulosic particles were detected in the effluent, thus indicating that MPs of various chemical compositions were removed along the wastewater treatment chain. The higher relative abundance of MPs in the size range 30–50 µm detected in OUT compared to IN samples (40 vs. 28%) would suggest that the monitored WWTP was less effective in removing this class of MPs. However, contrarily to what was expected, MPs lower that 30 µm in size were not found in OUT. In fact, according to literature data, the smallest plastic particles and fiber-like MPs are usually the most challenging to be removed in WWTPs, even in the presence of tertiary treatment units [4]. Large quantities of fibers in the size range 300–500 µm (40%) were also found in OUT. It is worth noting that the LDIR analysis allowed to acquire numerous parameters related to the MPs size and geometry that could be useful for modelling purposes (e.g. to study the MPs behavior in settling units in WWTPs), thus providing a powerful tool to support experimental campaigns. More details on these aspects as well as further methodological insights related to the unreported results will be presented at the Conference.

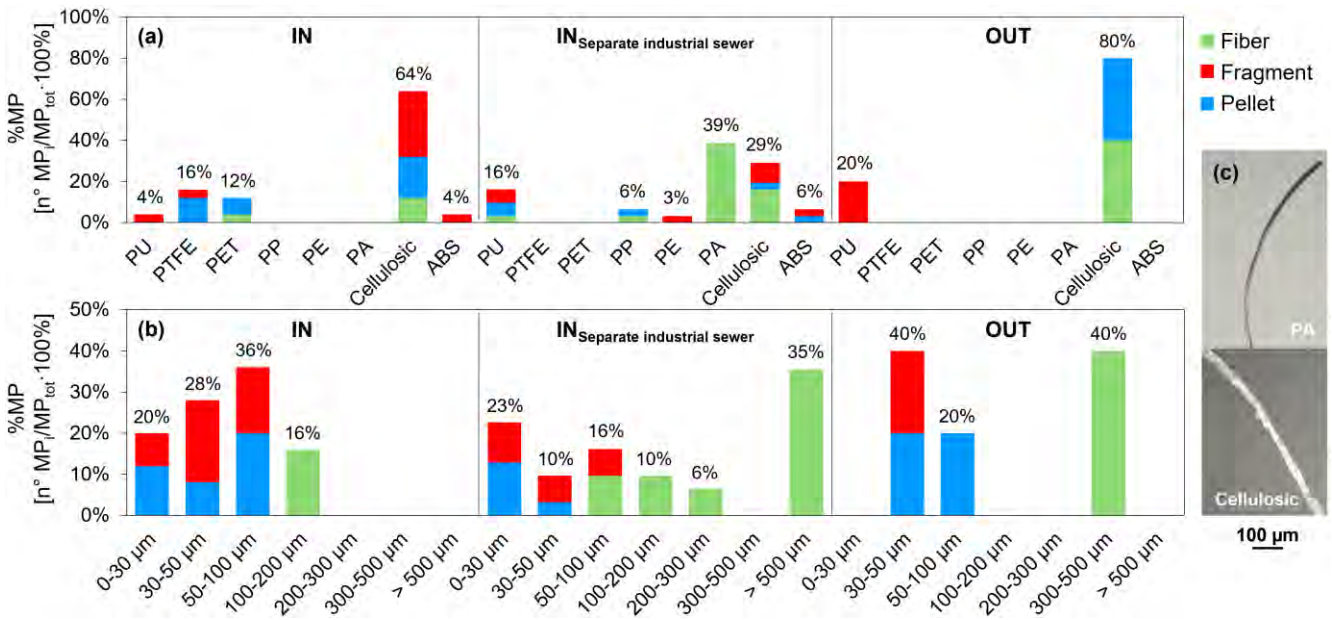

Figure 2. Chemical characterization **(a)** and size distribution **(b)** of MPs detected in IN, $IN_{Separate\ industrial\ sewer}$ and OUT. Example of fibers are shown as visible images acquired by LDIR–High magnification function **(c)**.

4. Conclusions

The developed LDIR-based methodology, combined to a rigorous pretreatment procedure having a high MPs recovery rate, proved to be time-effective, robust, and hence suitable for the detection and characterization of MPs in wastewaters. Coherent results were obtained for the monitored WWTP in terms of both estimated removal efficiency and type of plastic particles detected, which were consistent with the nature of treated wastewater, thus confirming the reliability of the proposed method.

Acknowledgements: This research was funded by the European Union - Next Generation EU. National Recovery and Resilience Plan (NRRP) - M4C2 Investment 1.3 - Research Programme PE_00000005 "RETURN" - CUP B83C22004820002. Views and opinions expressed are however those of the author(s) only and do not necessarily reflect those of the European Union or the European Commission. Neither the European Union nor the European Commission can be held responsible for them.

References

[1] Hildebrandt L., El Gareb F., Zimmermann T., Klein O., Kerstan A., Emeis K.C., Pröfrock, D., "Spatial distribution of microplastics in the tropical Indian Ocean based on laser direct infrared imaging and microwave-assisted matrix digestion", Environ. Pollut., 307, 119547 (2022).
[2] Koelmans A.A., Redondo-Hasselerharm P.E., Nor N.H.M., de Ruijter V.N., Mintenig S.M., Kooi M., "Risk assessment of microplastic particles", Nat. Rev. Mater., 7, 138–152 (2022).
[3] Alimi O.S., Farner Budarz J., Hernandez L.M., Tufenkji N., "Microplastics and Nanoplastics in Aquatic Environments: Aggregation, Deposition, and Enhanced Contaminant Transport", Environ. Sci. Technol., 52(4), 1704–1724 (2018).
[4] Sun J., Dai X., Wang Q., van Loosdrecht M.C.M., Ni B.J., "Microplastics in wastewater treatment plants: Detection, occurrence and removal", Water Res., 152, 21–37 (2019).
[5] Al-Azzawi M.S.M., Kefer S., Weißer J., Reichel J., Schwaller C., Glas K., Knoop O., Drewes J.E., "Validation of sample preparation methods for microplastic analysis in wastewater matrices–Reproducibility and standardization", Water, 12(9), 2445 (2020).
[6] Liu N., Cheng S., Wang X., Li Z., Zheng L., Lyu Y., Ao X., Wu H., "Characterization of microplastics in the septic tank via laser direct infrared spectroscopy", Water Res., 226, 119293 (2022).
[7] Bäuerlein P.S., Hofman-Caris R.C.H.M., Pieke E.N., ter Laak T.L., "Fate of microplastics in the drinking water production", Water Res., 221, 118790 (2022).

Title: VIT Safeguard - Establishment of a Microbiological and Process Engineering Monitoring System for Biological Wastewater Treatment Plants

Author(s): Jiri Snaidr*[1] and Claudia Beimfohr[1]

[1]*vermicon AG, Hallbergmoos, Germany, snaidr@vermicon.com*

Keyword(s): biological wastewater treatment, microbial processes, pollutant elimination, wastewater composition, microbial monitoring, vit gene probe technology, fluorescence in situ hybridization, FISH, amplicon sequence analysis, 16s rrna gene, process engineering, biocenosis, vit safeguard system

Abstract

Introduction
Biological wastewater treatment plants are a central element in wastewater treatment, as they are based on microbial processes that break down organic substances and eliminate pollutants. However, due to the sensitivity of these microbiological processes, wastewater treatment plants are susceptible to malfunctions. These disturbances can be caused by internal factors, such as changes in process management, or external factors, such as changing wastewater compositions and industrial dischargers. Inadequate treatment performance can lead to increased discharge values, environmental pollution, and legal consequences. Continuous monitoring and precise control of these microbiological processes are therefore crucial for stable and efficient operational management.

A biological wastewater treatment plant is ultimately a symbiosis of process engineering and microbiological processes. The process engineering processes are used to control and optimise the microbiological processes. This includes the regulation of conditions such as oxygen content, pH value, and nutrient supply to create the optimum environment for the microbial communities that are responsible for the degradation of pollutants. This close integration of both disciplines ensures stable and efficient wastewater treatment. It is, therefore, essential to monitor the microbiological processes to establish stable, efficient, and sustainable process management.

Methods of microbial monitoring
In this study, a multi-stage microbial monitoring system was implemented and used in industrial wastewater treatment plants. Two main technologies were used: VIT gene probe technology and Amplicon sequence analysis.

1) VIT gene probe technology:
The VIT gene probe technology is based on fluorescence in situ hybridization (FISH) [1], [2], [3]. Specific, dye-labeled oligonucleotide probes bind to the ribosomal RNA (rRNA) in the ribosomes of living bacterial cells. This enables the direct detection of specific microorganisms or groups of microorganisms based on their phylogenetic affiliation [6]. This technology is used to analyze the microbial population at defined sampling times and to identify lead bacteria. Leading organisms are specific bacterial species or groups that serve as indicators for the overall dynamics of the respective microbial community. The main group

analysis is carried out every three months, while the lead bacteria analysis is carried out every fortnight in order to obtain an up-to-date picture of the state of the biocenosis.

2) Amplicon sequence analysis
Amplicon sequence analysis is a molecular biological method for investigating the composition and diversity of microbial communities. Specific gene regions, such as the 16S rRNA gene in bacteria, are amplified using polymerase chain reaction (PCR) and analyzed by high-throughput sequencing. The sequences obtained are grouped using bioinformatic methods and assigned taxonomically to determine the diversity of microorganisms in a sample. This analysis is carried out once every six months and provides a detailed picture of microbial diversity and its changes over time.

Combination of technologies
The combination of VIT gene probe technology and Amplicon sequence analysis enables a comprehensive characterization of microbial communities in wastewater treatment plants. While the VIT gene probe technology provides fast and specific information on the identity of the microorganisms present in the wastewater [4], [5], the amplicon sequence analysis offers a deeper insight into the overall microbial diversity. The needs of the individual bacteria can be determined, which provides important information for process control. This combined data is crucial to understanding the dynamic changes within the biocenosis and to react to them in a targeted manner.

Process engineering integration
VIT Safeguard integrates microbiological data with process engineering parameters of the wastewater treatment plant. This includes the monitoring and control of parameters such as oxygen content, pH value, temperature, flow rates, and nutrient concentrations. The integration of this data makes it possible to recognize microbiological changes at an early stage and make specific adjustments to the process control. For example, changes can be made to the oxygen input in the aeration tanks, adjustments to the sludge recirculation rate or modification of the nutrient dosage to ensure optimum conditions for microbial activity.

Importance of combining microbiology with process engineering
Combining microbiological and process engineering data provides a holistic approach to monitoring and optimizing biological wastewater treatment plants. Microbiological analyses alone are insufficient to fully understand and control the complex processes within the wastewater treatment plant. Only through integration with process engineering parameters can a comprehensive picture of the plant dynamics be obtained, and targeted measures for process optimization can be taken.

Microbiological data provide insights into the structure and function of the microbial communities responsible for the degradation processes in the wastewater treatment plant. This information is crucial for recognizing changes in biocenosis that may be caused by external influences or internal process changes. Process engineering parameters, on the other hand, provide information about the physical and chemical conditions that influence microbial activity. By combining both data sets, anomalies can be identified and their causes determined more precisely.

VIT Safeguard system
The VIT Safeguard system distinguishes between three phases for prevention of disruptions: adaptation/calibration, observation, and modulation. In the adaptation/calibration phase, the system is initially calibrated and adapted to the specific conditions of the wastewater treatment plant. This phase includes setting the optimum operating parameters and baseline measurement of the microbial and

process engineering data. The observation phase comprises continuous monitoring and data analysis to assess the condition of the biocenosis and the process engineering parameters. In this phase, regular sampling and analyses are carried out to detect changes at an early stage. The modulation phase involves adjusting the process control based on the collected data and analyses to ensure the stability and efficiency of the treatment process. Intervention and disruption management only occur in an emergency, where specific measures are taken to resolve serious malfunctions (figure 1).

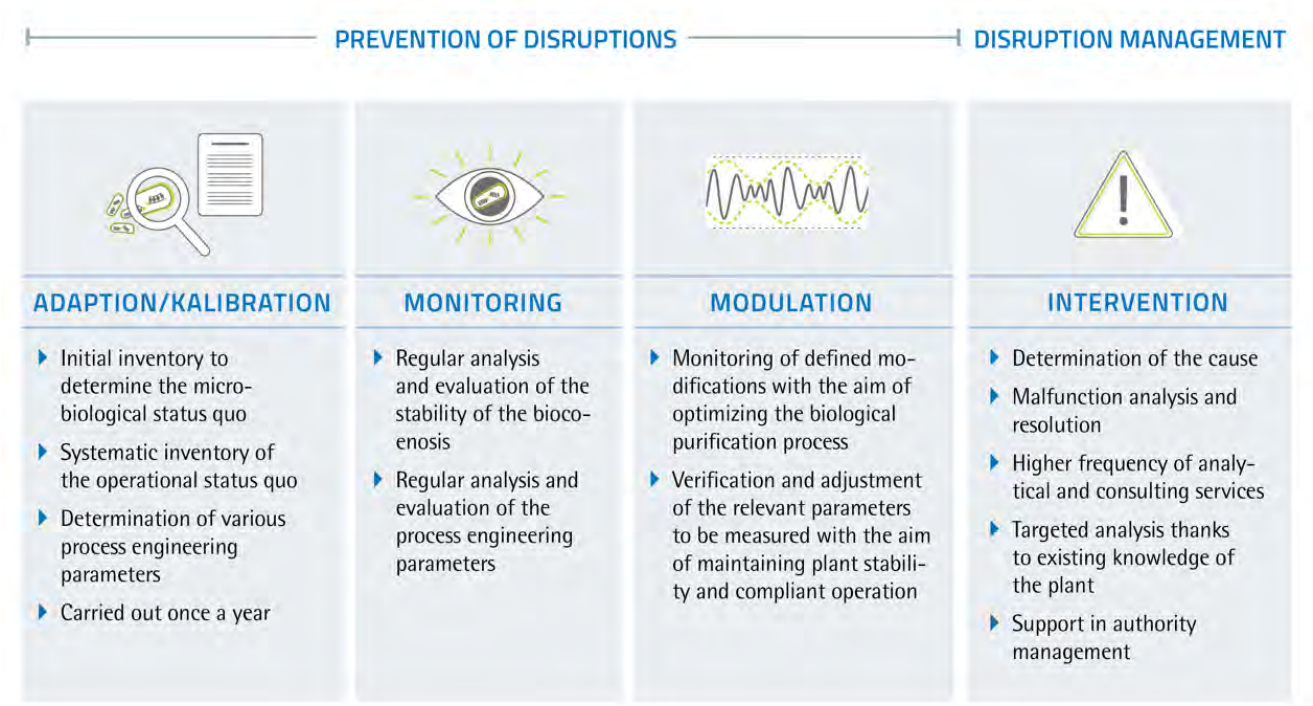

Figure 1. The different phases of the VIT Safeguard system

The wastewater treatment plant operators are supported by a VIT Safeguard software dashboard, which shows the most important microbiological changes over time.

Applications and results

Various applications demonstrate the use of VIT Safeguard for monitoring and optimizing wastewater treatment plants. The regular analysis and evaluation of microbiological and process engineering data make it possible to react to changes at an early stage and take appropriate measures. For example, the early identification of a decrease in certain microorganisms made it possible to adjust the aeration rate and thus the temperature in good time to ensure a stable and efficient cleaning performance. Another example shows how the analysis of filamentous bacteria enabled the optimization of the chemical dosage. These results show the usefulness of the VIT Safeguard approach.

Conclusion

The VIT Safeguard microbiological and process monitoring system is an innovative solution to ensure the stability and efficiency of biological wastewater treatment plants. Through the combination of VIT gene probe technology and Amplicon sequence analysis, specific microbiological changes can be

detected at an early stage, and appropriate measures can be initiated. Integrating microbiological data with process engineering parameters enables precise control and optimization of wastewater treatment plant processes, leading to a sustainable improvement in operational safety and treatment performance. The importance of combining microbiology and process engineering in wastewater treatment cannot be overemphasized. Microbial activity is the core of the biological degradation process, and process engineering provides the framework conditions under which these processes can run optimally. Stable and efficient operation of wastewater treatment plants can only be ensured through synergetic interaction between the two disciplines. The VIT Safeguard system offers a comprehensive and integrated solution for this, which makes it possible to react flexibly and efficiently to the dynamic challenges in wastewater treatment.

References

[1] Amann R, Ludwig W, Schleifer K, “Phylogenetic identification and in situ detection of individual microbial cells without cultivation,” Microbiological Reviews, 59, 143–169, (1995).

[2] Amann R, Snaidr J, Wagner M, et al, “In situ visualization of high genetic diversity in a natural microbial community,” Journal of Bacteriology, 178, 3496–3500, (1996).

[3] Snaidr J, Amann R, Huber I, et al, “Phylogenetic analysis and in situ identification of bacteria in activated sludge,” Applied and Environmental Microbiology, 63, 2884–2896, (1997).

[4] Snaidr J, Beimfohr C, Levantesi C, et al, “Phylogenetic analysis and in situ identification of ‘Nostocoida limicola’-like filamentous bacteria in activated sludge from industrial wastewater treatment plants,” Water Science and Technology: A Journal of the International Association on Water Pollution Research, 46, 99–104, (2002).

[5] Snaidr J, Fuchs B, Wallner G, et al, “Phylogeny and in situ identification of a morphologically conspicuous bacterium, Candidatus Magnospira bakii, present at very low frequency in activated sludge,” Environmental Microbiology, 1, 125–135, (1999).

[6] Woese CR, “Bacterial evolution,” Microbiol Rev, 51, 221–271, (1987).

Title: A model-based approach for estimating PAO activity in aerobic granular sludge

Author(s): Giacomo Rizzardi*[1], Arianna Catenacci[1], Roberto Canziani[1], Andrea Turolla[1]

[1] *Department of Civil and Environmental Engineering (DICA), Politecnico di Milano, Piazza Leonardo Da Vinci 32, 20133 Milano, IT, Italy (giacomo.rizzardi@polimi.it; arianna.catenacci@polimi.it; roberto.canziani@polimi.it; andrea.turolla@polimi.it)*

Keyword(s): Activated sludge models (ASM), aerobic granular systems, biochemical reactor engineering, biological nutrient removal, model calibration and testing

Abstract

Enhanced biological phosphorus removal (EBPR) systems offer a technological solution for high phosphorus (P) recovery with reduced resource consumption. These systems promote the selection of polyphosphate accumulating organisms (PAOs) by recirculating sludge through sequential anaerobic and aerobic conditions and thus favouring those organisms capable of exploiting feast-famine phases. Among EBPRs, aerobic granular sludge (AGS) systems are currently spreading worldwide. However, the use of mathematical models to optimize and control process performances remains underdeveloped due to both the complexity of process modelling and the difficulty to easily and accurately identify the kinetic parameters featuring the different microbial groups involved. With a specific focus on P fate, this study is aimed at the development of a model-based methodology to properly select operating test conditions for lab-scale batch activity assays targeted at accurately estimating PAOs kinetic parameters.

Introduction

Historical data on phosphorus (P) production and consumption, along with future trends, highlight the need for enhanced P recovery systems to meet the growing agricultural demand. Technologies for P removal from wastewater, aimed at limiting environmental damages resulting from nutrient spread, offer interesting opportunities for P recovery and recycling [1]. In the past decades, a great number of enhanced biological P removal (EBPR) systems emerged as enabling technological solution to achieve high P recovery with reduced resource consumption [2].

EBPR processes involve sludge recirculation through anaerobic and aerobic conditions to select for polyphosphate-accumulating organisms (PAOs). These microorganisms are essential in aerobic granular sludge (AGS) systems, an innovative biological treatment that is quickly spreading worldwide, based on microbial aggregation into dense and spherical structured biofilm [3]. In non-continuous AGS systems, the formation of granular sludge is promoted by specific environmental conditions and operational parameters, including cyclic feast-famine phases coupled with alternate anaerobic/aerobic conditions, favoring the growth of PAOs within the biofilm [2].

However, despite AGS systems spreading, involved processes are still scarcely interpreted by available mathematical models, particularly regarding P removal. Indeed, the fate of P in AGS systems may be affected not only by biological but also by physico-chemical (ion pairing and solid precipitation) removal mechanisms [4]. In addition, due to the complex model structure, accurate parameters estimation with datasets available from full-scale facilities is significantly challenging without falling into the risk of overfitting (i.e., a model with more parameters than can be estimated from datasets).

In this study, data collected from a field pilot-scale plant were compared with predictions from an AGS model, which includes a one-dimensional (1D) description of granules and uses default kinetic parameters from the literature. Despite achieving a satisfactory fit for soluble COD, ammonium ($N\text{-}NH_4^+$), and nitrate ($N\text{-}NO_3^-$) concentrations, significant deviations from the measured P concentrations were detected. To address the challenge of properly describing P concentration in AGS systems, the objective of this study is to improve the predictive ability of models through the development of batch activity assays for the accurate estimation of PAOs kinetic parameters that can serve as a support tool for the robust application of modelling tools. In detail, following the development of an AGS modelling framework, a methodology based on sensitivity analysis was defined for the detection of the best operating test conditions to be applied to maximize parameters identifiability. The obtained outcomes can be used to set up batch activity tests at the lab-scale, whose estimated parameters can be later applied to calibrate the AGS system model of a pilot-scale plant facility.

Materials and methods

Pilot-scale

A Nereda® field pilot-scale plant (1.45 m^3 volume) was used as reference case study, being operated for six months by a water utility in the north of Italy in collaboration with Royal HaskoningDHV. The volume exchange ratio was 0.69 and the cycle time 4 hours, consisting of a simultaneous anaerobic feeding and effluent withdrawal period (1 h), a reaction period (2 + 0.5 h, aerobic with about 2 mg DO/L + anoxic with less than 0.5 mg DO/L), and a settling/sludge withdrawal/idle period (0.5 h). The reactor was equipped with five sampling ports over its height, spaced 1-m apart and samples at the end of the aerobic phase and during the anaerobic feeding phase were collected at different heights and characterized for soluble components, among which phosphate ($P\text{-}PO_4^{3-}$).

Modelling framework

A 1D granule model was developed based on [5] and [6]. The granule model was then implemented in a Sequency Batch Reactor model for the comparison of data collected at the pilot-scale facility with model predictions. Such model was then applied to simulate batch activity tests at the lab-scale and then subjected to a sensitivity analysis (relative-relative sensitivity index, equation 1), which was carried out on different parameters at varying operating test conditions, in order to identify the most suitable settings capable of maximising the magnitude of $rrSI$ and minimizing the correlations of parameters sensitivities.

$$rrSI = \frac{\partial y_i}{\partial \theta_j} \cdot \frac{\theta_{j,0}}{y_{i,0}} \qquad \text{eq. 1}$$

where y_i is the *i-th* state variable ($y_{i,0}$ its nominal value) and θ_j is the *j-th* analyzed parameter ($\theta_{j,0}$ its nominal value).

Batch activity tests

Based on [7], preliminary batch activity tests were carried out using approximately 2-3 g VSS collected from the pilot reactor, and pretreated to completely remove from PAOs or saturate them with $P\text{-}PO_4^{3-}$ for aerobic and anaerobic tests, respectively. To assess P release under anaerobic condition, dissolved O_2 was removed by sparging N_2 gas into the nutrient solution. Subsequently, the bottle was sealed, and a concentrated solution of sodium acetate was injected into the bottle to have an initial concentration of 400 mg sCOD/L. Conversely, to evaluate the aerobic P uptake, a dissolved oxygen concentration of 2.5 mg O_2/L was maintained with intermittent aeration. At the test onset, a concentrated solution of K_2HPO_4 and KH_2PO_4 was injected to achieve an initial concentration of 8 mg $P\text{-}PO_4^{3-}$/L. Both tests lasted 150

minutes and liquid samples were regularly collected every 30 minutes to measure the P and soluble COD concentrations. The results from the sensitivity analysis may prompt modifications to the test settings and procedures of future experiments, with the aim of enhancing the identifiability of kinetic parameters.

Results and discussion

The distribution of microbial groups within the granules was determined by fitting model predictions at steady state with the measured effluent concentrations outlined in Table 1. Predicted microbial group distributions and concentrations of soluble components are shown in Figure 1, where S_{PO4} is predicted with concentrations of about 70 mg P-PO_4^{3-}/L at the external layer in contact with the bulk volume.

Table 1. Influent and effluent concentrations provided as average values with, in brackets, the standard deviation.

Parameter	Unit	Case study B
TSS concentration in the reactor	g TSS·L^{-1}	7.0 (±0.7) (81% VSS/TSS)
Influent / Effluent bCOD	mg COD·L^{-1}	300 (± 28) / 26 (± 2.9)
Influent / Effluent P-PO_4^{3-}	mg P·L^{-1}	2.3 (± 0.75) / 0.84 (± 2.7)
Influent / Effluent N-NH_4^+	mg N·L^{-1}	31 (± 11) / 0.68 (± 0.47)
Influent / Effluent N-NO_3^-	mg N·L^{-1}	0.32 (± 0.03) / 2.66 (± 2.5)

The concentrations of soluble compounds at the end of simulated aerobic phase are comparable those measured at the pilot-scale plant. In contrast, the concentrations measured at all heights at the end of the feeding phase (Fig. 2c) were poorly predicted by the model, which failed to accurately reproduce P release and COD uptake.

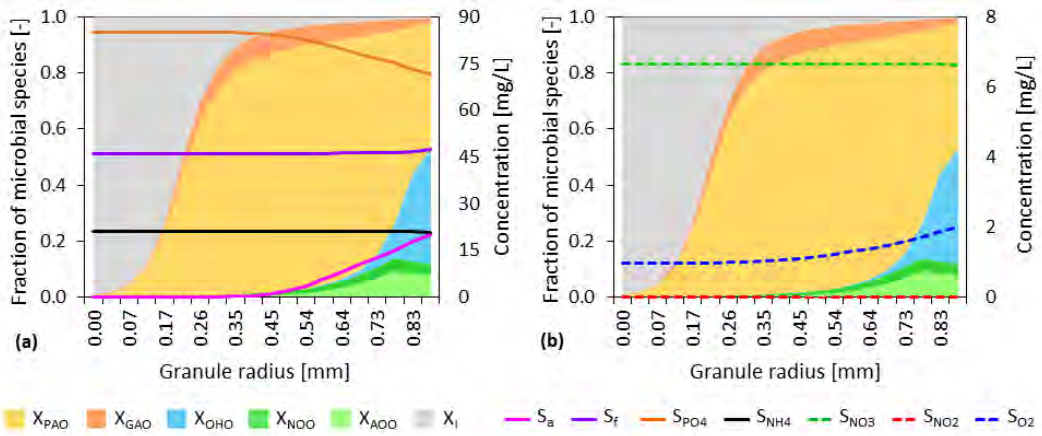

Figure 1. Relative distribution of active microbial groups at steady state as a function of distance from the granule centre. Overlaid lines represent concentrations of soluble components, predicted at the end of the anaerobic (a), and aerobic (b) phases.

In view of this, the AGS model requires further calibration and refinements specific to P dynamics. This could involve adjusting kinetic parameters related to phosphorus or incorporating additional processes or mechanisms that influence phosphorus behaviour in the system. To address the first aspect, highly informative batch activity tests can be carried out by selecting proper substrates and biomass concentrations. Regarding the second, the deviations in P concentrations might suggest that certain

biological or chemical processes affecting phosphorus were not fully captured in the model [4].

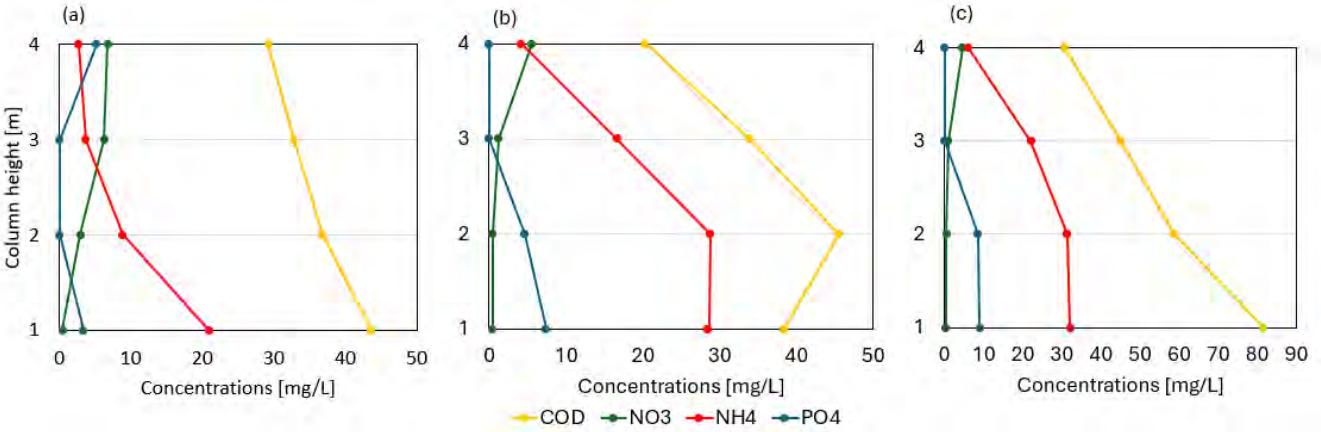

Figure 2. Concentration gradients of CODs, N-NO_3^-, N-NH_4^+ and P-PO_4^- along the column's height during the feed phase after (a) 20 minutes, (b) 40 minutes, and (c) 60 minutes.

Expected conclusions

- Enhance the robustness and predictive accuracy of the AGS model regarding phosphorus fate, enabling its use for optimizing the process;
- Integrate the 1D granule model with a batch reactor model to simulate batch activity tests;
- Incorporating vertical concentration gradients during the anaerobic phase as in a plug flow reactor;
- Provide guidance on setting up batch activity tests to estimate PAO kinetic parameters through modelling and sensitivity analysis of batch lab-scale tests;
- Integrate the processes of P precipitation and ion pairing, following the approach outlined by Batstone and Flores-Alsina [8].

References

[1] Carey D. E., Yang Y., McNamara P. J., & Mayer B. K., "Recovery of agricultural nutrients from biorefineries", Bioresource Technology, 215, 186-198, (2016).
[2] Izadi P., Izadi P., & Eldyasti A., "Design, operation and technology configurations for enhanced biological phosphorus removal (EBPR) process: a review", Reviews in Environmental Science and Bio/Technology, 19, 561-593 (2020).
[3] Oehmen A., Lemos P. C., Carvalho G., Yuan Z., Keller J., Blackall L. L., & Reis M. A., "Advances in enhanced biological phosphorus removal: from micro to macro scale", Water research, 41(11), 2271-2300, (2007).
[4] Baeten J.E., van Loosdrecht M.C.M., & Volcke E.I.P., "Modelling aerobic granular sludge reactors through apparent half-saturation coefficients", Water Research 146, 134–145, (2018).
[5] Wanner, O., Gujer, W., "A multispecies biofilm mode", Biotechnology and bioengineering. 28, 314–328, (1986)
[6] Wanner, O., Reichert, P., "Mathematical modeling of mixed-culture biofilms", Biotechnology and bioengineering, 49(2), 172-184, (1996).
[7] van Loosdrecht M. C., Nielsen P. H., Lopez-Vazquez C. M., & Brdjanovic D., "Experimental methods in wastewater treatment", IWA Publishing, (2016).
[8] Batstone D., & Flores-Alsina, X. (Eds.), "Generalised Physicochemical Model No. 1 (PCM1) for Water and Wastewater Treatment", IWA Publishing, (2022).

PARALLEL SESSION: B3

Biorefineries

Biopolymers recovery

Microbial protein from volatile fatty acids obtained through acidogenic co-fermentation of hemp and cheese whey

Carlo Moscariello*[1], Silvio Matassa[2], Giovanni Esposito[3], Francesco Pirozzi[4], Stefano Papirio[5]

[1] *Department of Civil, Architectural and Environmental Engineering, University of Naples Federico II, Naples, Italy, carlo.moscariello2@unina.it*
[2] *Department of Civil, Architectural and Environmental Engineering, University of Naples Federico II, Naples, Italy, silvio.matassa@unina.it*
[3] *Department of Civil, Architectural and Environmental Engineering, University of Naples Federico II, Naples, Italy, gioespos@unina.it*
[4] *Department of Civil, Architectural and Environmental Engineering, University of Naples Federico II, Naples, Italy, francesco.pirozzi@unina.it*
[5] *Department of Civil, Architectural and Environmental Engineering, University of Naples Federico II, Naples, Italy, stefano.papirio@unina.it*

Keywords: Volatile fatty acids; hemp biomass residues; microbial protein

Abstract

The sustainable synthesis of value-added products such as microbial protein (MP) using lignocellulosic materials stands out as one of the main emerging routes in the circular bioeconomy transition. In this view, this study aimed at valorising hemp biomass residues (HBRs) through a co-acidogenic fermentation (co-AF) process with cheese whey (CW) to maximise the volatile fatty acids (VFAs) production. A VFA production up to 3115 mg HAc/L was obtained with a HBRs:CW ratio of 4:1 (g VS/g VS). Moreover, the growth of the biomass under aerobic conditions was tested by changing the pH or the carbon to nitrogen (C/N) ratio of the VFA-rich fermentate, focusing on MP production. The best experimental condition tested identified involved 2 days of aerobic microbial fermentation with a C/N ratio of 5.0 and a pH of 9.0, reaching a biomass concentration of 2.40 g TSS/L with the 42% of protein (g protein/g TSS).

Introduction

Global population will reach about 10 billion people in 2050 [1], requiring a 70% increase of food production as compared to 2006 and highlighting the necessity to find alternative and reliable solutions to safeguard future food supply while minimizing the impact on global sustainability. In this view, an emerging approach is the biological capture of carbon and upgrading of nutrients from biowaste obtained by combining anaerobic bioprocesses and aerobic microbial fermentation to produce second-generation, high-quality protein-based products such as microbial protein (MP) [2,3]. The use of lignocellulosic biomass (*e.g.*, agricultural residues) in second-generation biorefineries is a promising approach due to its abundance and low supply cost. Among the many available lignocellulosic substrates, this study focused on industrial hemp (*Cannabis sativa* L.) biomass residues (HBRs), *i.e.*, hemp hurds (HH), leaves and discarded inflorescences [4].
This study proposes a potential biorefinery scheme implementing semi-continuous acidogenic co-fermentation (co-AF) of HBRs with another abundant organic waste such as cheese whey (CW) to increase the overall AF potential and recover carbon from the hemp biomass. The VFA production and composition was the main parameter evaluated for this phase. Moreover, aerobic fermentation batch

tests on the VFA-rich liquid fermentate were carried out to investigate the ability of the biomass used in the AF process to grow under aerobic conditions and produce MP at different carbon to nitrogen (C/N) ratios and pH.

Materials and Methods

The investigation of the semi-continuous co-AF process lasted 137 days, aiming at the concomitant valorisation of both HH and a mix of leaves and inflorescences (Mix) with CW into VFAs. The co-AF process was performed in a 2.2 L (working volume) borosilicate glass reactor under mesophilic conditions (*i.e.*, T = 37 ± 2°C). The hydraulic (HRT) and solid (SRT) retention times were set at 4 days. Different process conditions were tested by removing CW or by increasing the HBRs amount in terms of VS (*i.e.*, 2 and 4 times) to evaluate the performance of co-AF (Table 1).
The aerobic fermentation batch tests were performed in 250 mL Schott bottles filled with 150 mL of the VFA-rich liquid fermentate. The tests were performed by changing the pH of the fermentate (*i.e.*, Test 1 and Test 2) or by modifying C/N (*i.e.*, Test 3 and Test 4) in order to find the best condition for biomass growth and nitrogen assimilation.

Table 1. Experimental conditions tested during the semi-continuous co-AF. g VS: gram of volatile solids of HBRs and CW added; OLR: organic loading rate of HBRs and CW; g VS L^{-1}: gram of volatile solids added per litre of influent

Periods	Days	HBRs		CW
		(g VS)	OLR (g VS/L/d)	OLR (g VS/L/d)
I	1–24			3.06
II	25–50	12.24	0.79	n.a.*
III	51–66			
IV	67–107	24.48	1.85	3.06
V	108–137	48.96	6.35	

*n.a.: not available.

Results and Discussion

The results shown in Figure 1 highlighted how the presence of CW positively affected the VFA production rather than the lactic acid (LA) accumulation.

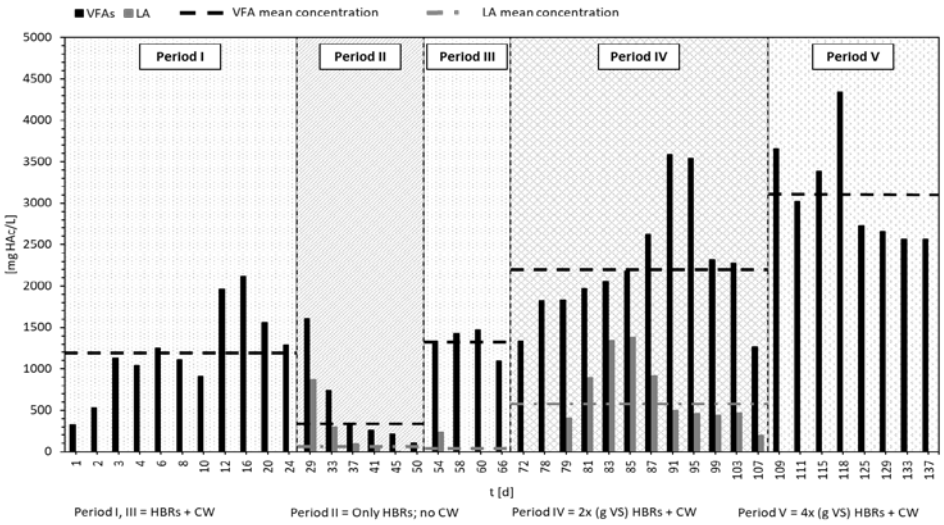

Figure 1. Evolution of the net VFA and LA productions obtained during the 137 days of semi-continuous co-AF of HBRs (*i.e.*, HH and Mix) and CW. VFA and LA productions are expressed as concentrations of acetic acid equivalent (mg HAc/L) and were obtained by subtracting to the effluent the VFAs and the LA of the influent for each day. Also, the mean of the net VFA and LA productions for the corresponding period is reported.

During period I, a mean VFA production of 1202 mg HAc/L was obtained with no LA accumulation, due to a possible conversion of LA into VFAs by heterolactic pathway. In period II, when CW was not supplemented, the lack of carbon (*e.g.*, lactose) and microorganisms (naturally present in CW) continuously entering the system led to a decrease in the mean VFA production (*i.e.*, 332 mg HAc/L), 72% lower than in period I, and a partial accumulation of LA (*i.e.*, 89 mg HAc/L). Probably, in period II, a different metabolic pathway such as the homolactic one stopped the conversion of LA into VFAs, leading to its accumulation.

The reintroduction of CW in the influent in period III improved the mean VFA production (*i.e.*, 1332 mg HAc/L), which was 11% higher than that obtained in period I (*i.e.*, 1202 mg HAc/L) and four times higher than that of period II (*i.e.*, 332 mg HAc/L).

The investigation about the possible synergistic effect in the VFA production between CW and HBRs was repeated in the last two periods (*i.e.*, IV and V), by increasing the amount of VS from HBRs, respectively 2 and 4 times in period IV and period V, while maintaining constant that of CW. As shown in Figure 1, the mean VFA production increased with the increase of the HBRs amount. Particularly, a mean production of 2235 mg HAc/L was reached in period IV, being 68% higher than the production of period III (*i.e.*, 1332 mg HAc/L). The further increase of the HBRs in period V led to an increase of VFA production (*i.e.*, 3115 mg HAc/L), which was 39% higher than in period IV.
Thus, with the increase in the VS amount from HBRs in period IV and V (*i.e.*, 2 and 4 times the VS of CW), the experimental VFA production observed in the same periods (*i.e.*, 2235 and 3115 mg HAc/L for period IV and V, respectively) was 40 and 38% higher than the productions theoretically obtainable from HBRs and CW alone, proving a synergistic effect on the VFA production.

In Figure 2, the growth of the microbial biomass (Panel A) and the VFA consumption (Panel B) during

the aerobic fermentation tests on the VFA-rich liquid fermentate are shown.

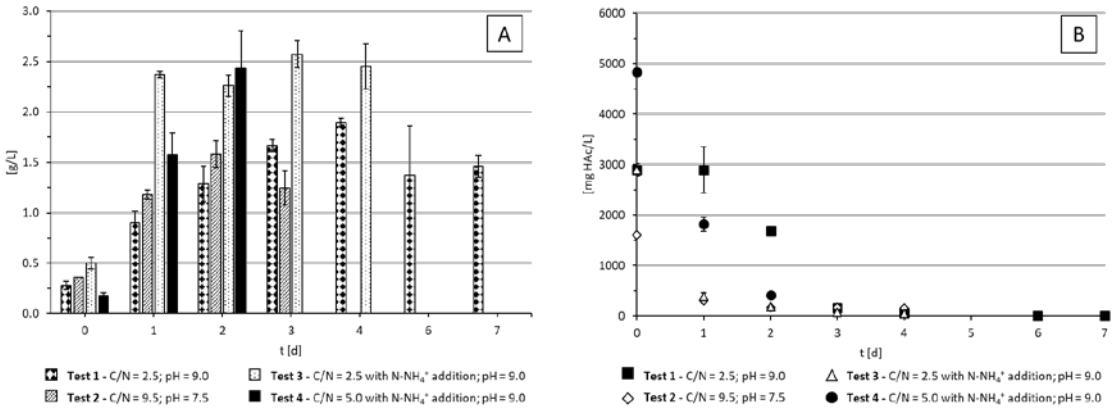

Figure 2. Evolution of the biomass growth in terms of total suspended solids (TSS) (Panel A) and VFA consumption (Panel B) during the four aerobic fermentation tests. Bars represent the standard deviation on three replicates.

Test 1 and Test 2 proved how the different pH did not affect the biomass growth (Figure 2 A), which reached the highest concentration (*i.e.*, 1.90 g TSS/L) in four days for Test 1. This trend reflects the one of VFAs (Figure 2 B), which were almost completely consumed in both tests (*i.e.*, - 98% and – 90% on day 4 for Test 1 and Test 2, respectively).
Test 3 and Test 4 were performed by adding nitrogen as ammonia nitrogen ($N\text{-}NH_4^+$) to reach a C/N ratio of 2.5 and 5.0, respectively. The results show that Test 4 resulted in the highest biomass concentration (*i.e.*, 2.40 g TSS/L) after only two days of aerobic fermentation, that was only 5% lower than the highest biomass concentration obtained from Test 3 in three days (*i.e.*, 2.60 g TSS/L). In both Tests, VFAs were completely consumed as already observed for the previous conditions tested (*i.e.,* Test 1 and Test 2) (Figure 2 B). Moreover, Test 4 showed also the highest protein content (*i.e.*, 42% g protein/g TSS) on day 2, that was 10% higher than the value for Test 3 on the same day (*i.e.*, 38%).

This study proved how the use of cheese whey in co-AF with the HBRs was necessary to achieve a high VFA concentration of up to 3115 mg HAc/L with a HBRs:CW ratio of 4:1 g VS/g VS. Moreover, the same biomass was able to grow under aerobic conditions reaching up to 2.40 g TSS/L in two days with a 42% protein content, thereby assimilating the carbon recovered as VFA into high-value MP.

References

[1] A.C. Ezeh, J. Bongaarts, B. Mberu, "Global population trends and policy options", Lancet 380,142–148, (2012).
[2] S. Matassa, S. Papirio, I. Pikaar, T. Hülsen, E. Leijenhorst, G. Esposito, F. Pirozzi, W. Verstraete, "Upcycling of biowaste carbon and nutrients in line with consumer confidence: The “full gas” route to single cell protein", Green Chem. 22, 4912–4929, (2020).
[3] S. Singha, M. Mahmutovic, C. Zamalloa, L. Stragier, W. Verstraete, A.J. Svagan, O. Das, M.S. Hedenqvist, "Novel Bioplastic from Single Cell Protein as a Potential Packaging Material", ACS Sustain. Chem. Eng. 9, 6337–6346, (2021).
[4] C. Moscariello, S. Matassa, G. Esposito, S. Papirio, "From residue to resource: The multifaceted environmental and bioeconomy potential of industrial hemp (*Cannabis sativa* L.)", Resour. Conserv. Recycl. 175, 105864, (2021).

Assessing the microbial and enzymatic degradation of bioplastic products

Marica Falzarano*, Alessandra Polettini, Raffaella Pomi, Andreina Rossi, Tatiana Zonfa

Department of Civil, Constructional and Environmental Engineering, Sapienza University of Rome, Rome, Italy
marica.falzarano@uniroma1.it

Keyword(s): bioplastics, biodegradation, anaerobic degradation, polylactic acid, enzymatic degradation

Abstract

Biodegradable plastics are currently replacing commodity plastics in various applications, especially after Europe adopted some measures for the phasing out of specific traditional plastic items [1]. Some of the most successful applications for bioplastics are disposable tableware, food and non-food packaging. The main advantage of biodegradable plastics is the possibility to treat them along with the organic fraction of municipal solid waste (OFMSW) in the existing composting or anaerobic digestion (AD) facilities [2]. When used with food, their presence can enhance food waste collection by allowing consumers to dispose of them together [3]. In particular, treating bioplastics in an anaerobic digester would mean having the possibility to recover both materials and energy from them [4].

However, a comprehensive understanding of bioplastics' behaviour under a variety of environmental conditions is currently missing and the efficiency of the co-digestion with OFMSW is still under examination [5, 6]. Full-scale digesters may need technical improvements to treat bioplastics and OFMSW while maintaining the quality of the final digestate [7].
One of the main aspects of concern is the potential generation of byproducts (including micro-bioplastics) during the biodegradation process [8], which could persist in the digestate and be released into the environment upon soil application [9]. This may create potential risks to vegetation and crops, in turn with further potential risks to human health along the food chain [10, 11].

New solutions for bioplastic waste disposal and treatment are needed, and for such purpose it is first necessary to assess their behaviour under different environmental conditions. The correlations among the biodegradation kinetics and yields, the operating parameters and the chemo-physical characteristics of the polymeric blend need to be identified. Bioplastic products can display many different compositions with their own biodegradation profile [8, 12]. For instance, PLA (polylactic acid) is one of the most used biopolymers, but due to its brittle behaviour it is usually blended with additives or other polymers to improve its mechanical and physical properties. Poly(1,4- butylene adipate-co-terephthalate) (PBAT) and poly(butylene succinate) (PBS) are commonly used for this purpose, but they are generally more recalcitrant to degradation. An efficient bioplastic degradation process should consider the different biodegradation kinetics of all the components, which generally require processing times beyond typical procedures even under thermophilic conditions.

In the present study, four biodegradable plastic products were selected: cups (CU), plates (PL), coffee capsules (CA), packing chips (CH) and shoppers (SH). The items were all compliant with the EN 13432 and the main characterization of the products is shown in Table1. All items were manually cut into 2 ×

2 cm^2 pieces. Anaerobic inoculum was collected at a full-scale mesophilic anaerobic digestion plant treating a mixture of organic residues from food industries. The sludge was sieved at 0.84 mm to remove the coarser fraction (fibers and inorganic particles) and stored at −15 °C until use. Cellulose was used as reference material to ensure test validity. Chemo-physical characterization of bioplastics was carried out using SEM, TGA and FT-IR.

Table 1. Main characterization parameters of bioplastic products in terms of total solids (TS), volatile solids (VS) and total organic carbon (TOC)

Product	TS [%ww]	VS [%ww]	TOC [gC/kg]
Plate	99.6	97	484.4 ± 0.2
Coffee pod	100 ± 0.1	100 ± 0.8	439.6 ± 0.8
Packing chips	100 ± 0.1	80.9 ± 0.1	413.9 ± 0.1
Cups	99.6 ± 0.1	99.6 ± 0.1	
Shopper	100 ± 0.2	98.2 ± 1.3	530.4 ± 28

The products were tested under anaerobic conditions and at different sets of time to assess the biodegradation degree and kinetics along the process.
The degree of biodegradation was calculated using equation (1):

$$Biodegradation\ (t) = \frac{P_{net}(t)+P_{IC}(t)}{P_{th}} \quad (1)$$

where $P_{net}(t)$ is the actual cumulative biogas production (net of blank) at time t, $P_{IC}(t)$ is the dissolved inorganic carbon (IC) (net of blank), and P_{th} is the theoretical biogas production calculated according to the Buswell equation [15] from the elemental composition of the investigated materials.

To assess the bioplastics mass loss, final digestates were sieved at 0.84 mm and the retained bioplastic fragments were carefully rinsed with deionized water. The fragments were then dried at 30 °C until constant weight. Mass loss was calculated according to equation 2:

$$ML\ (\%) = \frac{W_0-W_t}{W_0} \quad (2)$$

where W_0 is the initial weight of the bioplastic sample and W_t is the retrieved sample weight at time t.

Preliminary results of the anaerobic degradation are shown in Figure 1.

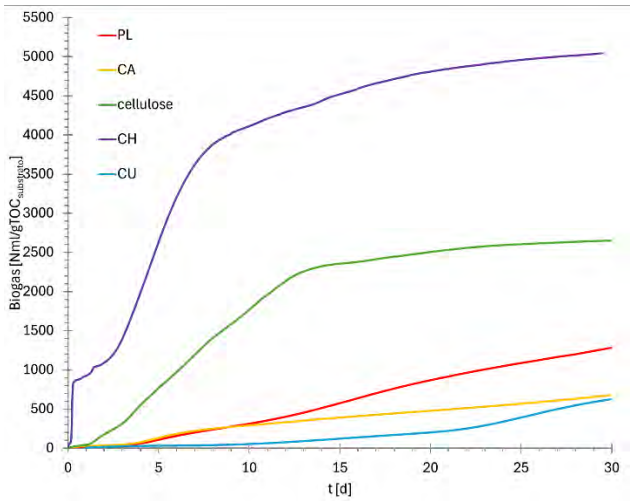

Figure 1. Biogas evolution for the experimental runs

In addition, PLA cups were powdered (<0.1 cm) and tested to assess the enzymatic degradation. Lipase from *Candida Rugosa* was used setting two different concentrations in the TrisHCl buffer 0.5 M (2 mg/ml and 10 mg/ml). The tests were carried out for two weeks and the production of lactic acid was monitored in time. A blank test was carried out for comparison using bioplastics and TrisHCl buffer only. Enzymatic treatment was effective in increasing the bioplastics' hydrolysis kinetics. Further experiments are required to test the actual potential of enzymatic degradation as a pre-treatment prior to anaerobic digestion, which could represent an innovative treatment strategy for bioplastic products.

References

[1] European Council, "Directive (Eu) 2019/904 of the European Parliament and of the Council of 5 June 2019 on the reduction of the impact of certain plastic products on the environment," 2019.

[2] V. Bátori, D. Åkesson, A. Zamani, M. J. Taherzadeh, and I. Sárvári Horváth, "Anaerobic degradation of bioplastics: A review," *Waste Manag.*, 2018, doi: 10.1016/j.wasman.2018.09.040.

[3] European Commission, "EU policy framework on biobased, biodegradable and compostable plastics," 2022.

[4] M. Cucina, G. Soggia, P. De Nisi, A. Giordano, and F. Adani, "Assessing the anaerobic degradability and the potential recovery of biomethane from different biodegradable bioplastics in a full-scale approach," *Bioresour. Technol.*, vol. 354, p. 127224, Jun. 2022, doi: 10.1016/J.BIORTECH.2022.127224.

[5] G. Cazaudehore *et al.*, "Can anaerobic digestion be a suitable end-of-life scenario for biodegradable plastics? A critical review of the current situation, hurdles, and challenges," *Biotechnol. Adv.*, vol. 56, p. 107916, May 2022, doi: 10.1016/J.BIOTECHADV.2022.107916.

[6] M. Falzarano, A. Polettini, R. Pomi, A. Rossi, and T. Zonfa, "Anaerobic Biodegradability of Commercial Bioplastic Products: Systematic Bibliographic Analysis and Critical Assessment of the Latest Advances," *Mater. 2023, Vol. 16, Page 2216*, vol. 16, no. 6, p. 2216, Mar. 2023, doi: 10.3390/MA16062216.

[7] P. S. Calabrò and M. Grosso, "Bioplastics and waste management," *Waste Management*, vol. 78. Elsevier Ltd, pp. 800–801, 2018, doi: 10.1016/j.wasman.2018.06.054.

[8] M. P. Bracciale *et al.*, "Disposable Mater-Bi® bioplastic tableware: Characterization and assessment of anaerobic biodegradability," *Fuel*, vol. 355, no. August 2023, pp. 1–12, 2024, doi: 10.1016/j.fuel.2023.129361.

[9] J. Fojt, J. David, R. Přikryl, V. Řezáčová, and J. Kučerík, "A critical review of the overlooked challenge of determining micro-bioplastics in soil," *Science of the Total Environment*, vol. 745. Elsevier B.V., p. 140975, Nov. 25, 2020, doi: 10.1016/j.scitotenv.2020.140975.

[10] E. Huerta-Lwanga, J. Mendoza-Vega, O. Ribeiro, H. Gertsen, P. Peters, and V. Geissen, “Is the polylactic acid fiber in Green compost a risk for lumbricus terrestris and triticum aestivum?,” *Polymers (Basel).*, vol. 13, no. 5, pp. 1–10, 2021, doi: 10.3390/polym13050703.
[11] Y. Qi *et al.*, “Macro- and micro- plastics in soil-plant system: Effects of plastic mulch film residues on wheat (Triticum aestivum) growth,” *Sci. Total Environ.*, vol. 645, pp. 1048–1056, 2018, doi: 10.1016/j.scitotenv.2018.07.229.
[12] M. P. Bracciale *et al.*, “Anaerobic biodegradation of disposable PLA-based products : Assessing the correlation with physical, chemical and microstructural properties,” *J. Hazard. Mater.*, vol. 452, no. January, 2023, doi: 10.1016/j.jhazmat.2023.131244.
[13] A. N. Mistry *et al.*, “Bioaugmentation with a defined bacterial consortium: A key to degrade high molecular weight polylactic acid during traditional composting,” *Bioresour. Technol.*, vol. 367, no. September 2022, p. 128237, 2023, doi: 10.1016/j.biortech.2022.128237.
[14] M. W. Myburgh, W. H. van Zyl, M. Modesti, M. Viljoen-Bloom, and L. Favaro, “Enzymatic hydrolysis of single-use bioplastic items by improved recombinant yeast strains,” *Bioresour. Technol.*, vol. 390, no. October, p. 129908, 2023, doi: 10.1016/j.biortech.2023.129908.
[15] A. M. Buswell and H. F. Mueller, “Mechanism of Methane Fermentation,” *Ind. Eng. Chem.*, vol. 44, no. 3, pp. 550–552, Mar. 1952.

Title: Enhancing lactic acid generation from mixed food waste as an electron donor in lactic acid-mediated chain elongation for medium-chain fatty acids synthesis

Author(s): Samuel Gyebi Arhin*[1], Alessandra Cesaro[1], Francesco Di Capua[2], Giovanni Esposito[1]

[1] *Department of Civil, Architectural and Environmental Engineering, University of Naples Federico II, Via Claudio 21, 80125, Naples, Italy, Email address (samuelgyebi.arhin@unina,it; alessandra.cesaro@unina.it; gioespos@unina.it)*
[2] *School of Engineering, University of Basilicata, via dell'Ateneo Lucano 10, 85100, Potenza, Italy, Email address (francesco.dicapua@unibas.it)*

Keyword(s): Biowaste valorization, Carboxylates platform, Circular economy, Heterolactic fermentation, pH, temperature

Abstract

The growing human population and rapid socioeconomic transformations have resulted in a substantial increase in the quantity of food waste (FW) produced globally. This presents a challenge and an opportunity to design environmental systems to harness the resource potential of FW streams effectively and efficiently within the context of a circular economy. Due to its relatively low capital and operating costs compared to pure culture fermentation, anaerobic mixed-culture fermentation has gained enormous scientific interest for FW valorization. Lactic acid is one potential high-value product from anaerobic fermentation of FW that has numerous industrial applications, including the food and beverage industries, pharmaceuticals, and in the synthesis of biodegradable plastics. The utility of lactic acid depends greatly on its nature and selectivity, which is influenced by the metabolic pathway assumed by the fermenting microbiome. Typically, the homo-lactic fermentation route is desirable during lactic acid fermentation because this pathway produces only lactic acid, precluding antagonistic pathways that may lead to the synthesis of volatile fatty acids (VFAs) or ethanol. Yet, the wide and complex spectrum of anaerobic microbiomes makes it challenging to steer fermentation reactions towards homo-lactic synthesis.

Recently, the utilization of FW-derived lactic acid as an electron donor in chain elongation reactions to generate medium-chain fatty acids (MCFAs) is increasingly gaining attention as an economically viable alternative route [1]. MCFAs are platform chemicals consisting of aliphatic straight chain monocarboxylates with 6-12 carbons (e.g., caproic, heptylic, and caprylic acid) and have numerous industrial applications, including aviation fuels, plasticizers, agrochemicals, fragrances, etc [2]. Their increased hydrophobicity resulting from their higher carbon-to-oxygen ratios grants them better separability than lactic acid. In the lactic acid-driven chain elongation pathway, lactate dehydrogenase catalyses lactic acid conversion into pyruvate followed by pyruvate oxidation into acetyl-coenzyme A (acetyl-CoA). The 2-carbon acetyl-CoA molecule is then added to an electron acceptor (e.g., VFAs) via the cyclic reverse β-oxidation (RBO) or fatty acids biosynthesis (FAB) pathway, elongating the carbon length of the electron acceptor with two carbons (C2) per cycle. Because by-products such as VFAs and ethanol generated alongside lactic acid via hetero-lactic fermentation are also vital intermediates in MCFAs production, hetero-lactic fermentation could be tolerated when lactic acid is to be used for MCFAs production, guaranteeing operational flexibility during lactic acid fermentation.

Although MCFAs could be generated from FW via a single-stage chain elongation, the two-stage

approach whereby a lactic acid-rich broth is generated in the first stage bioreactor followed by chain elongation in the second stage bioreactor has been demonstrated to outperform single-stage setups as the operational conditions for the two main functional groups (i.e., acidogenic bacteria and chain elongators) could be optimized separately [3]. Nonetheless, limited information exists on the systematic optimization of two-stage chain elongation, especially operational parameters for enhancing lactic acid yield via the hetero-lactic pathway for subsequent MCFAs synthesis. A key approach to control and influence the metabolic pathway during lactic acid fermentation is by manipulating environmental conditions such as temperature, pH, and organic loading. Therefore, the study aimed to maximize lactic acid production from mixed FW for subsequently utilization for MCFAs production by exploring the influence of various environmental conditions, including pH, temperature, and organic loading on lactic acid synthesis.

The experiments were conducted in three stages. In the first stage, the operational pH was varied from 5 to 8 under a mesophilic temperature of 35 ± 1°C and food-to-microorganisms (F/M) ratio of 1 g VS/g VS. Under these conditions, the highest lactic acid yield of 385 ± 53 mg COD/g VS was obtained at pH 5 (denoted as pH5M, **Table 1**). Lactic acid produced in the first 2 d of fermentation at pH 6, 7, and 8 was quickly consumed to generate VFAs, leading to lactic acid yield below 10 mg COD/g VS at the end of fermentation on day 7. In the second stage of experiments, the temperature was changed to a thermophilic condition (50 ± 1°C) while maintaining the pH of 5 to 8 and F/M ratio of 1 g VS/g VS. As shown in **Table 1**, lactic acid bacteria outperformed the VFA-producers under thermophilic settings, leading to high lactic acid yield. Overall, the highest lactic acid yield was observed at pH 6 under thermophilic conditions (684 ± 31 mg COD/g VS) with only 20 % of the recovered chemical energy (in the form of chemical oxygen demand, COD) converted to VFAs, ethanol, and H_2. Following these results, the F/M ratio was increased from 1 to 6 g VS/g VS at pH 6 under thermophilic settings in the third stage of the experiments to evaluate the impact of organic loading on lactic acid yield. Comparable lactic acid yields ($p > 0.05$) were observed at F/M ratio of 1 to 3 g VS/g VS. However, beyond F/M ratio of 3 g VS/g VS, the lactic acid yield decreased ($p < 0.05$). The low lactic acid yield at F/M ratio of 4 to 6 g VS/g VS may be due to the possibility thermophilic fermentation lowered the diversity and abundance of the microbial community thus, the highest F/M ratio that could be applied to convert the FW to lactic acid was 3 g VS/g VS.

After the lactic acid optimization process, preliminary chain elongation experiments were conducted to convert the FW-derived lactic acid into MCFAs. As depicted in **Fig. 1**, high-rate chain elongation was achieved with the lactic acid-rich FW effluent and about 238 ± 26 mM (1578 ± 170 mMC) of MCFAs could be generated without the supplementation of exogenous reactants such as ethanol. Heptylic acid was the dominant MCFAs, reaching a high concentration of 151 ± 15 mM (1060 ± 102 mMC). These results depict that by optimizing lactic acid generation in the first stage, high-rate MCFAs production could be achieved in the second stage during two-stage chain elongation processes, paving a sustainable way to generate high-value MCFAs from FW streams. The findings provide useful insights into a sustainable FW management approach and could serve as a platform for the synthesis of green chemicals within the context of a circular economy.

Table 1. Lactic acid, VFAs, H_2, and ethanol yield at the end of the fermentation experiments under different operational conditions. The final chemical energy in the form of COD recovered as lactic acid, VFAs, H_2, and ethanol is expressed as mg COD/g VS. ΔE_1 and ΔE_2 show the amount of chemical energy recovered as H_2 and ethanol in comparison with that obtained as carboxylic acids, respectively. ∑CA represent the total amount of chemical energy recovered as carboxylic acids and ∑COD represent the total amount of chemical energy recovered as carboxylic acids, H_2, and ethanol.

Test groups	Label	Lactic acid yield (mg COD/ g VS)	VFAs yield (mg COD/g VS)	∑CA (mg CA-COD/ g VS) [a]	H_2 yield (mg H_2-COD/ g VS) [a]	Ethanol yield (mg COD/g VS) [a]	ΔE_1 (mg H_2-COD /mg CA-COD) [b]	ΔE_2 (mg EtOH-COD/mg CA-COD) [c]	∑COD (mg COD/g VS)
Stage 1	pH5M	385 ± 53	39 ± 17	424 ± 36	99 ± 12	0 ± 0	23.3 %	0.0 %	523
	pH6M	0 ± 0	719 ± 94	719 ± 94	180 ± 13	4 ± 4	25.0 %	0.6 %	903
	pH7M	4 ± 3	699 ± 46	703 ± 48	120 ± 30	0 ± 0	17.1 %	0.0 %	823
	pH8M	9 ± 16	687 ± 147	696 ± 131	53 ± 11	0 ± 0	7.6 %	0.0 %	748
Stage 2	pH5T	577 ± 36	0 ± 0	577 ± 36	20 ± 16	0 ± 0	3.5 %	0.0 %	597
	pH6T	684 ± 31	78 ± 44	758 ± 81	27 ± 17	69 ± 11	3.6 %	9.1 %	854
	pH7T	401 ± 44	93 ± 48	494 ± 110	36 ± 15	0 ± 0	7.2 %	0.0 %	530
	pH8T	252 ± 75	118 ± 66	371 ± 141	14 ± 9	0 ± 0	3.8 %	0.0 %	385
Stage 3	F/M1T	684 ± 31	78 ± 44	758 ± 18	27 ± 17	69 ± 11	3.6 %	9.1 %	854
	F/M2T	532 ± 126	238 ± 116	771 ± 62	98 ± 10	4 ± 1	12.7 %	0.5 %	873
	F/M3T	583 ± 56	47 ± 39	640 ± 29	21 ± 11	9 ± 4	3.3 %	1.4 %	670
	F/M4T	494 ± 40	72 ± 0	572 ± 39	15 ± 3	6 ± 1	2.6 %	1.0 %	593
	F/M5T	399 ± 20	103 ± 8	502 ± 27	34 ± 11	16 ± 1	6.8 %	3.2 %	552
	F/M6T	497 ± 1	31 ± 2	531 ± 3	12 ± 1	14 ± 0	2.3 %	2.6 %	557

[a] Calculated based on the theoritical COD equivalents of the metabolites.
[b] CA= carboxylic acids.
[c] EtOH = ethanol.
[d] N/A = not applicable.

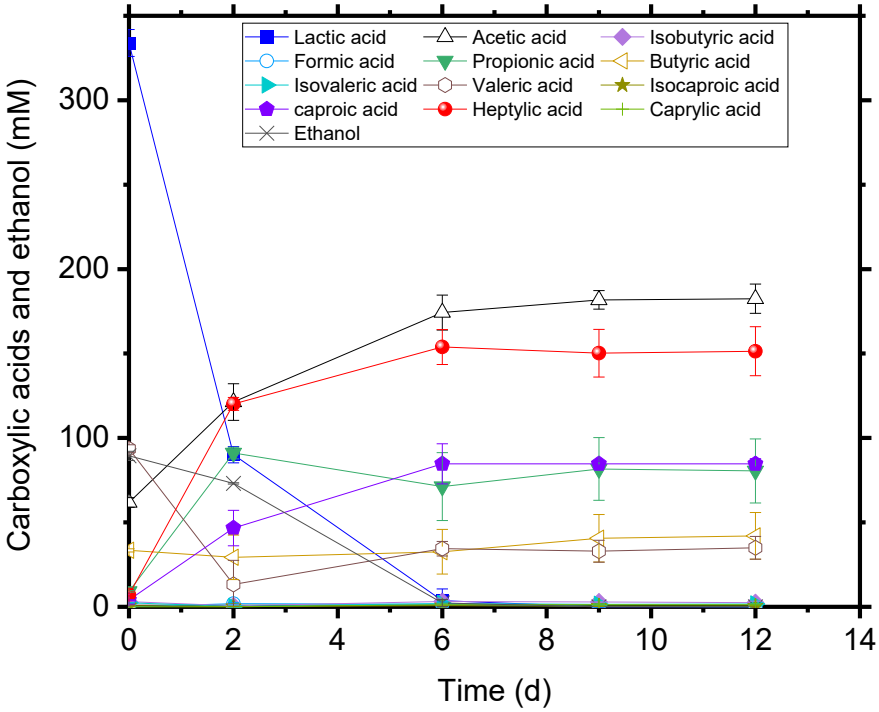

Fig. 1. Carboxylic acids and ethanol concentration during chain elongation with FW-derived lactic acid-rich effluent.

References

[1] Contreras-Dávila C.A., Carrión V.J., Vonk V.R., Buisman C.N.J., Strik D.P.B.T.B., "Consecutive lactate formation and chain elongation to reduce exogenous chemicals input in repeated-batch food waste fermentation", Water Res 169 (2020). https://doi.org/10.1016/j.watres.2019.115215.

[2] Arhin S.G., Cesaro A., Capua F. Di, Esposito G., "Recent progress and challenges in biotechnological valorization of lignocellulosic materials: Towards sustainable biofuels and platform chemicals synthesis", Science of the Total Environment 857 (2023). https://doi.org/10.1016/j.scitotenv.2022.159333.

[3] Zhang W., Wang S., Yin F., Cao Q., Lian T., Zhang H., Zhu Z., Dong H., "Medium-chain carboxylates production from co-fermentation of swine manure and corn stalk silage via lactic acid: Without external electron donors", Chemical Engineering Journal 439 (2022). https://doi.org/10.1016/j.cej.2022.135751.

Title: Recovery of structural extracellular polymeric substances (sEPS) from aerobic granular sludge as valuable biomaterials for the treatment of heavy metal-contaminated wastewaters

Author(s): Benedetta Pagliaccia*[1], Riccardo Campo[1], Mirko Severi[2], Claudio Lubello[1], Tommaso Lotti[1]

[1] Department of Civil and Environmental Engineering, University of Florence, Via di Santa Marta 3, 50139 Firenze (FI), Italy, benedetta.pagliaccia@unifi.it, riccardo.campo@unifi.it, claudio.lubello@unifi.it, tommaso.lotti@unifi.it
[2] Department of Chemistry "Ugo Schiff", University of Florence, Via della Lastruccia 3, 50019 Sesto Fiorentino (FI), Italy, mirko.severi@unifi.it

Keyword(s): extracellular polymeric substances; aerobic granular sludge; resource recovery; biosorption; heavy metals.

Abstract

The urge for high-effectiveness, low-impact and economically sustainable water treatment technologies is orienting research efforts towards resource recovery-based solutions. This contribution aims to address the potential of structural extracellular polymeric substances (sEPS) recovered from aerobic granular sludge (AGS) for the treatment of heavy metal-contaminated aqueous systems. Equilibrium adsorption studies were carried out by treating synthetic single- and multi-metal solutions with the recovered sEPS. High metal binding capacities were evidenced for sEPS both in the forms of aqueous suspensions and hydrogel beads, and guidelines for a large-scale development were suggested.

1. Introduction

The growing environmental concern related to water pollution (e.g. by heavy metals, emerging contaminants, etc.) is driving scientific community and water treatment stakeholders to design highly performing and low-impact remediation technologies [1]. Adsorption is recognized as a viable strategy for this kind of water purification purposes thanks to its advantages in terms of easy operation, cost-effectiveness, and efficiency [2]. These benefits are emphasized if bio-based and waste-derived adsorbent media are used. To this aim, value-added biomaterials can be recovered by re-thinking wastewater treatment chains according to circular economy logics. A high potential for resource recovery (e.g. biopolymers) is associated to aerobic granular sludge (AGS) processes for biological wastewater treatment [3]. In AGS, microorganisms produce large quantities of extracellular polymeric substances (EPS) to form a hydrogel matrix in which they are self-immobilized [4,5]. The structural properties of AGS are provided by the so-called structural EPS (sEPS), a subset of total EPS that can form hydrogels with peculiar physical-chemical features [5]. The recovery of sEPS from excess sludge and their conversion into valuable products is expected to play a crucial role in the transition towards a circular economy-based wastewater sector [3]. In this regard, this research aims to evaluate the feasibility of exploiting AGS-derived sEPS for the treatment of heavy metal-contaminated wastewaters. Equilibrium adsorption tests were carried out comparing the performance of sEPS aqueous suspensions and sEPS hydrogel beads in removing Cu^{2+}. The applicability of cross-linked sEPS in the presence of more complex aqueous systems (Cu^{2+}+Pb^{2+}+Ni^{2+}+sodium acetate) was then further investigated.

2. Materials and methods

The extraction of sEPS from AGS was carried out according to a physical-chemical method providing a thermo-alkaline solubilization of EPS (80 °C, Na_2CO_3, pH=11.3) followed by an acidic precipitation of

sEPS (HCl, pH=2.2). The sEPS acidic pellet recovered after centrifugation was re-suspended by adding NaOH until a pH=8.5–9 [5]. The extraction yield was calculated on a volatile solids (VS) basis as mass ratio of extracted sEPS to initial AGS. The hydrogel-formation was carried out via ionic cross-linking by applying an extrusion method: the sEPS aqueous suspension (Na^+-sEPS) was added dropwise into a 2.5 % (w/w) $CaCl_2$ solution and then left overnight to stabilize. The gelation threshold (i.e. minimum sEPS concentration enabling sol-gel transition) was determined by testing various sEPS concentrations (in terms of total solids to wet weight ratio, wt%=TS/WW·100%). Both Na^+-sEPS and sEPS hydrogel beads were analysed by Inductively Coupled Plasma–Atomic Emission spectroscopy (ICP–AES). The sEPS hydrogel beads were cut into smaller fragments and freeze-dried to use them in biosorption tests. The equilibrium adsorption studies were carried out at a controlled temperature of 20±0.5 °C by using both Na^+-sEPS and sEPS hydrogel beads to treat aqueous solutions containing increasing concentrations of $CuCl_2 \cdot 2H_2O$ (C_0=7–759 mg Cu^{2+}/L). Na^+-sEPS (in the form of aqueous suspensions at 2 wt% concentration) and freeze-dried hydrogel beads (formed from 5 wt% Na^+-sEPS aqueous suspensions) were kept in contact under stirred conditions with the targeted metal solutions overnight at pH=5. After centrifugation/settling, the supernatants were 0.45 µm-filtered and analysed by ICP-AES to measure the residual metal concentrations at equilibrium (C_e, mg/L). In both cases, an adsorbent dose (i.e. Na^+-sEPS or hydrogel beads) of 6.5 g TS/L was used. The freeze-dried sEPS hydrogel beads were also tested in muti-metal adsorption experiments to treat aqueous solutions containing increasing concentrations of $CuCl_2 \cdot 2H_2O$, $Pb(NO_3)_2$ and $NiCl_2 \cdot 6H_2O$ (C_0 = 6–389 mg Cu^{2+}/L+ 6–401 mg Pb^{2+}/L + 14–1024 mg Ni^{2+}/L) and from 0 to 100 mg/L of soluble COD (as sodium acetate). The adsorption capacity (Q_e, mg/g TS) and removal efficiency (%Removal, %) were determined through Eqs. 1 and 2, respectively, where m (g TS) is the adsorbent mass and V (L) is the solution volume. The experimental Q_e vs. C_e profiles were fitted by Langmuir and Freundlich models using Eqs. 3 and 4, respectively, where Q_m (mg/g) is the maximum adsorption capacity, b (L/mg) is the Langmuir constant, K_F (mg$^{1-(1/n)}$·L$^{1/n}$/g) and n (-) are the Freundlich constants related to adsorption capacity and intensity, respectively [2].

$$Q_e = \frac{(C_0 - C_e) \cdot V}{m} \quad (1) \qquad \%Removal = \frac{(C_0 - C_e)}{C_0} \cdot 100\% \quad (2) \qquad Q_e = \frac{b \cdot Q_m \cdot C_e}{1 + b \cdot C_e} \quad (3) \qquad Q_e = K_F \cdot {C_e}^{1/n} \quad (4)$$

3. Results and discussion

The applied extraction method yielded an average amount of sEPS of 257 mg VS_{sEPS}/g VS_{AGS} (898 mg VS_{sEPS}/g TS_{sEPS}), in line with literature data [5]. sEPS were able to form ionically cross-linked hydrogels storing up to 99 wt% of water into their 3D structure. The ICP-AES results confirmed the inclusion of large quantities of Ca^{2+} into the polymeric matrix during the cross-linking reaction (5 vs. 63 mg Ca^{2+}/g TS in Na^+-sEPS and hydrogel beads, respectively). As shown in **Figure 1**, the extrusion method allowed to obtain sEPS hydrogel beads stable and homogeneous in shape and size (equivalent diameter = 5.2 ± 0.7 mm), thus suggesting promising opportunities for a large-scale development.

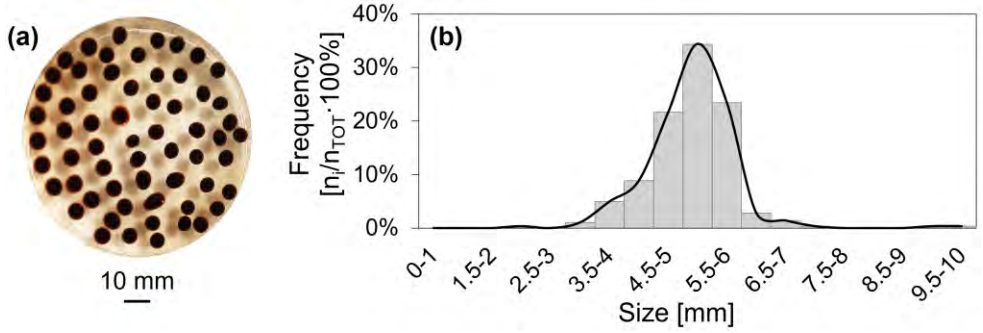

Figure 1. sEPS hydrogel beads formed by extrusion in a $CaCl_2$ solution **(a)** and their size distribution **(b)**.

For both Na^+-sEPS and sEPS hydrogel beads a decrease in removal efficiency and an increase in Q_e was observed with increasing C_0 (**Figure 2a**). The progressively higher driving force provided by

increasing C_0 reasonably made available an increasing number of binding sites for further Cu^{2+} adsorption. Some differences between Na^+-sEPS and sEPS hydrogel beads can be pointed out, although both showed adsorption capacities comparable or even higher than those reported for other adsorbent media (e.g. eucalyptus bark-derived activated carbon: Q_e=29 mg Cu^{2+}/g at C_0=635 mg Cu^{2+}/L [6]). In the case of sEPS hydrogel beads, a portion of binding sites is expected to be unavailable due to the cross-linking with Ca^{2+}. However, a significant Cu^{2+} uptake might be reasonably enabled by the 3D porous hydrogel structure that likely promoted Cu^{2+} diffusion into the polymeric network upon swelling: once penetrated into the whole hydrogel matrix, Cu^{2+} may hence largely adsorbed through multifaceted mechanisms (e.g. ion exchange, precipitation on the hydrogel surface/inner porosity, complexation, etc.). To be noticed that the structural integrity of sEPS hydrogel beads was preserved along the entire experiment: Cu^{2+} adsorption likely contributed to enhance the strength of the 3D network, increasing its cross-linking density and hence its chemical and mechanical stability over time. The beneficial effect due to the 3D polymer chain arrangement, and hence to the physical structure of the adsorbent medium, is emphasized in the case of low C_0 (in the order of a few mg/L), where Na^+-sEPS did not evidence a significant Cu^{2+} uptake. Na^+-sEPS showed slightly higher Q_e for the highest C_0, where flocculation and sEPS/Cu^{2+} co-precipitation phenomena (likely caused by multiple-bridging complexations [7]) were noted. From a technological standpoint, the use of sEPS hydrogel beads instead of Na^+-sEPS aqueous suspensions has advantages in terms of adsorbent storage/transport (powder vs. liquid forms) and post-treatment separation (gravity vs. filtration). Na^+-sEPS could be a viable alternative in the pre-treatment of highly concentrated heavy metal-contaminated wastewaters due to the co-precipitation of sEPS and M^{2+} composite aggregates that can be easily separated from the clarified effluent by gravity.

With increasing the Pb^{2+} and Ni^{2+} concentrations in the targeted solution (20–1425 mg Pb^{2+}+Ni^{2+}/L; 0 mg COD/L), sEPS hydrogel beads showed a decrease in Q_e towards Cu^{2+} with respect to that achievable in single-metal systems: in multi-metal adsorption, competition among different ionic species for the available binding sites can hence affect the Cu^{2+} binding capacity, especially for the highest C_0. Different mechanistic hypotheses were inferred by fitting the Q_e vs. C_e experimental profiles through Langmuir and Freundlich models (**Figure 2b**). Langmuir equation better modelled the Cu^{2+} uptake process promoted by Na^+-sEPS (R^2=0.973), thus suggesting a mono-layer sorption on a homogeneous surface (with all binding sites having a similar energy and affinity for the adsorbate) [2,7]. Conversely, the Q_e vs. C_e data of sEPS hydrogel beads both in single- and multi-metal aqueous systems were better simulated by Freundlich model (R^2=0.984), thus indicating a heterogeneous multi-layer adsorption [2,7].

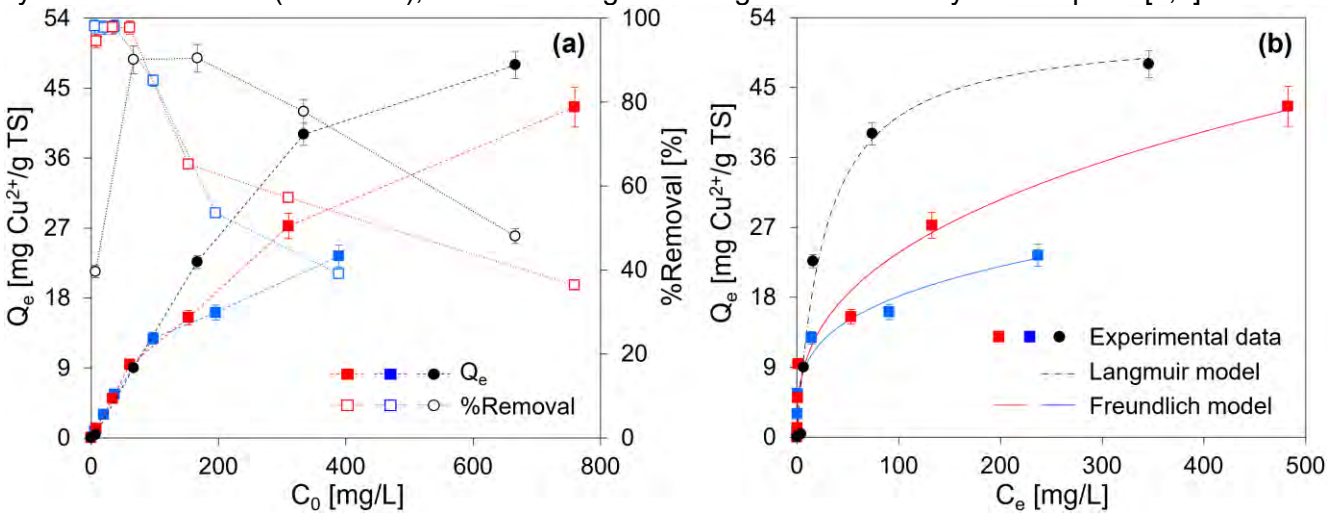

Figure 2. %Removal vs. C_0 and Q_e vs. C_0 plots **(a)**, and Q_e vs. C_e profiles with their fitting by Langmuir and Freundlich models **(b)** for Na^+-sEPS and sEPS hydrogel beads in single-metal systems (in **black** and **red**, respectively) and sEPS hydrogel beads in multi-metal systems not containing sodium acetate (in **blue**).

In multi-metal aqueous systems not containing sodium acetate (0 mg COD/L), the highest Q_e was found for Pb^{2+} followed by Cu^{2+} and Ni^{2+} (even if Ni^{2+} was initially present with a significantly higher C_0) (**Figure 3**). This trend, that reasonably reflected the affinity of the cross-linked sEPS towards the targeted M^{2+}, agreed with literature data on EPS of different origin [7]. In the presence of 100 mg/L of soluble biodegradable COD in the aqueous solution, Q_e increased, especially for Ni^{2+} (**Figure 3**): a potential reason could be the formation of complexes/co-precipitates more easily adsorbable into the 3D network of the hydrogel beads. Although further studies are surely encouraged to shed light on the effect of different kinds of organics and/or other heavy metals, these proof-of-concept results would suggest the applicability of sEPS hydrogel beads for the treatment of complex wastewaters where inorganic and organic contaminants are simultaneously present. Further results related to the modelling of all targeted M^{2+} uptake processes, not reported due to summary constrains, will be presented at the Conference.

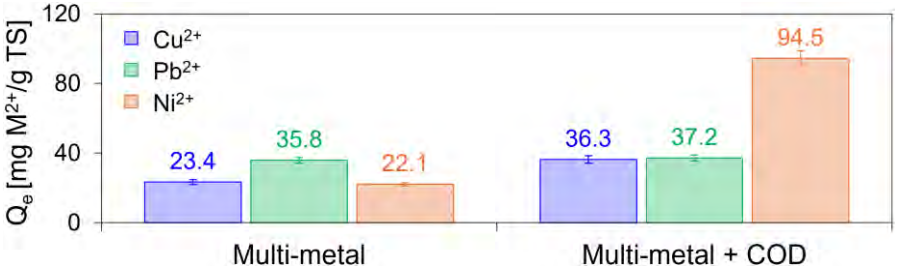

Figure 3. Influence of soluble COD (as sodium acetate) in the multi-metal solution on the adsorption capacity of sEPS hydrogel beads towards the targeted M^{2+} (C_0 = 389 mg Cu^{2+}/L + 401 mg Pb^{2+}/L + 1024 mg Ni^{2+}/L).

4. Conclusions

In summary, this study suggested that AGS-derived sEPS can be valorised in water remediation technologies, with environmental and economic benefits in waste sludge handling/disposal. Both in their not cross-linked and cross-linked forms (i.e. Na^+-sEPS aqueous suspensions vs. hydrogel beads), sEPS proved to be promising biomaterials for heavy metal biosorption thanks to their cost-effective production, stability over the treatment and high performance. The choice between the two adsorbent media should be driven by the expected level of heavy metal contamination, with sEPS hydrogel beads more efficient in terms of post-treatment separation and easier operation for a wider range of C_0.

Acknowledgements: This research was funded by POR FESR Toscana 2014–2020 (IDRO.SMART project, CUP: 3647.04032020.157000040).

References

[1] Morin-Crini N., Lichtfouse E., Fourmentin M., Ribeiro A.R.L., Noutsopoulos C., Mapelli F., Fenyvesi É., Vieira M.G.A., Picos-Corrales L.A., Moreno-Piraján J.C., Giraldo L., Sohajda T., Huq M.M., Soltan J., Torri G., Magureanu M., Bradu C., Crini G., "Removal of emerging contaminants from wastewater using advanced treatments. A review", Environ. Chem. Lett., 20, 1333–1375 (2022).
[2] Touihri M., Guesmi F., Hannachi C., Hamrouni B., Sellaoui L., Badawi M., Poch J., Fiol N., "Single and simultaneous adsorption of Cr(VI) and Cu(II) on a novel Fe_3O_4/pine cones gel beads nanocomposite: Experiments, characterization and isotherms modeling", Chem. Eng. J., 416, 129101 (2021).
[3] Kehrein P., van Loosdrecht M.C.M., Osseweijer P., Garfí M., Dewulf J., Posada J., "A critical review of resource recovery from municipal wastewater treatment plants – market supply potentials, technologies and bottlenecks", Environ. Sci.: Water Res. Technol., 6(4), 877–910 (2020).
[4] Flemming H.C., Wingender J., "The biofilm matrix", Nat. Rev. Microbiol., 8, 623–633 (2010).
[5] Felz S. Al-Zuhairy S., Aarstad O.A., van Loosdrecht M.C.M., Lin Y., "Extraction of structural extracellular polymeric substances from aerobic granular sludge", J. Vis. Exp., 115, e54534 (2016).
[6] Kongsuwan A., Patnukao P., Pavasant P., "Binary component sorption of Cu(II) and Pb(II) with activated carbon from *Eucalyptus camaldulensis Dehn bark*", J. Ind. Eng. Chem., 15, 465–470 (2009).
[7] Pagliaccia B., Carretti E., Severi M., Berti D., Lubello C., Lotti T., "Heavy metal biosorption by Extracellular Polymeric Substances (EPS) recovered from anammox granular sludge", J. Hazard. Mater., 424, 126661 (2022).

Title: Potential of the lactate-driven polyhydroxyalkanoates (PHA) production via mixed microbial culture

Author(s): Fabiano Asunis*[1], Luca Attene[1], Giorgia De Gioannis[1,2], Aldo Muntoni[1,2]

[1] Department of Civil, Environmental Engineering and Architecture (DICAAR), University of Cagliari, Cagliari, Italy, fabiano.asunis@unica.it – lucaattene18@gmail.com – degioan@unica.it – amuntoni@unica.it
[2] National Research Council of Italy (CNR), Institute of Environmental Geology and Geoengineering (IGAG), Cagliari, Italy

Keyword(s): Biopolymers PHA, lactic acid utilization, waste biorefineries, resource recovery

Abstract

The study investigates polyhydroxyalkanoates (PHA) production from lactic acid-rich substrates via mixed microbial cultures (MMC) using lactic acid rather than traditional volatile fatty acids (VFAs) as precursors. A MMC capable of producing PHA directly from a synthetic lactic acid solution was selected through the feast and famine approach by applying an organic loading rate (OLR) of 1.2 g_C L^{-1} and an uncoupled strategy for nutrient feeding. Preliminary accumulation tests showed that the selected biomass was able to reach up to 50% of PHAs accumulation by dry weight, primarily as hydroxybutyrate (HB). These findings underscore the potential of using lactic acid, potentially derived from dark fermentation of lactose-containing agro-industrial residues like cheese whey, for cost-effective and sustainable PHA production.

Introduction

The quest for sustainable alternatives to fossil-based plastics has intensified in the wake of escalating environmental concerns. PHA, biodegradable polymers synthesized by microorganisms, have emerged as a promising solution, offering a path towards mitigating pollution and reducing reliance on non-renewable resources [1]. As the research and market interest grows, a wide range of PHA-based applications are emerging, showcasing the versatility and potential of these biopolymers in various production activities, spanning from the packaging to the biomedical sector [2]. In this context, the production of PHA from biowaste is consistent with environmental sustainability goals, and represents an economically viable option as it is based on low-cost substrates, such as kitchen waste, cheese whey, confectionary wastes, etc. The production costs issue is further addressed by using mixed microbial cultures (MMC) instead of pure cultures.

The process for the production of PHA via MMC is based on a three-stage approach: the first stage involves the fermentation of an organic substrate (a biowaste, eventually) which is broken down to form volatile fatty acids (VFA) as PHA precursors. In the second stage, the PHA precursors are supplied to select a PHA-accumulating culture; specific microbial strains capable of efficient PHA synthesis are enriched under suitable conditions (feast and famine regime). The third stage aims at PHA accumulation by the selected culture that is fed with the same PHA precursors used for the selection step; the accumulation process is performed under nutrient-limiting conditions to promote PHA storage inside the microbial cells. Although this approach has been extensively studied, it needs further optimization. As far as the production of PHA precursors through dark fermentation is concerned, typical challenges may include long retention times and carbon losses in form of carbon dioxide emissions. Additionally, yielding

a mixture of PHA precursors characterised by steady VFA composition is difficult and strongly influenced by the type of fed biowaste and adopted process parameters. Performance stability, in particular, is critical for full-scale process development; therefore, it is of interest to study process modifications that address this aspect.

In this respect, we have documented in previous studies that the pH-controlled fermentation of cheese whey by indigenous biomass unfolds according to two-steps. During the first 24-48 hours, lactose is converted into lactic acid without production of typical gaseous metabolites of fermentation such as H_2 and CO_2. The lactic acid is then consumed to yield a pool of VFA consisting of butyric, propionic, acetic acid, and H_2 and CO_2 as gaseous metabolites [3]. It has been observed that the process can extend up to 7 days for the complete conversion of lactic acid into VFA, with approximately 20% of the initial carbon being converted into CO_2, thus lost in terms of conversion into useful products.

In light of the above and considering that lactic acid was reported to be a possible fermentation product also for other organic substrate such as bagasse and sugarcane [4, 5], it is of interest to evaluate whether lactic acid can be used as a direct precursor in the production of PHA, avoiding its conversion to VFA. In this way, the quest for stable performance would benefit from the use of a single, thus homogeneous, PHA precursor, and carbon losses in the form of CO_2 would be avoided.

Despite the extensive body of research on PHA production from biowaste via MMC, the direct use of lactic acid as substrate is largely underexplored. A study demonstrated that a MMC can accumulate PHB up to 77% of the cell dry weight from lactic acid, confirming the potential inherent in this approach [6]. Other studies have reported effective PHA synthesis from agricultural waste-derived, lactic acid-rich fermentation broth, further emphasizing the feasibility of lactic acid as feedstock [7, 8]. More precisely, it has been demonstrated the viability of significant PHA production based on confectionary industry wastewater fermentation; the fermentation broth consisting of 60–90% lactic acid was used to select a MMC capable of PHA accumulations up to 59% by dry weight despite the potential inhibitory effects related to the presence of ethanol [9]. Notably, although also other studies have mentioned lactic acid as main fermentation metabolite, its significant role as a PHA precursor was not extensively emphasized, nor to the best of our knowledge any systematic study has been performed so far [10].

In this framework, the present study aimed at exploring the potential of PHA production based on the use of a lactic acid solution as precursor instead of the usual mixture of VFA. A MMC capable of producing PHA directly from a synthetic lactic acid solution was obtained through the feast and famine approach and by applying an uncoupled strategy for nutrient feeding to further enhance the selection of the PHA accumulating biomass. The synthetic lactic acid solution was then used also in preliminary tests aimed at estimating the accumulation capacity of the previously selected biomass.

Materials and methods

The selection of the PHA-producing bacteria was conducted in a 4 L working volume managed as sequencing batch reactor (SBR). The reactor, inoculated with activated sludge (8 g_{VSS} L^{-1}) from municipal wastewater treatment, was operated under a feast-famine regime. According to such strategy, the microbial culture is exposed to alternate short periods of carbon availability (feast) followed by prolonged periods of carbon unavailability (famine). The feast and famine conditions impose selective pressure in form of competition for the organic substrate, favouring PHA-storing over non-storing microorganisms. Both the hydraulic retention time (HRT) and sludge retention time (SRT) were set at 1 day, and the temperature and organic loading rate (OLR) were 25 °C and 1.2 g_C L^{-1} d^{-1}, respectively. The operating pH was controlled within the range 7.5-9 through automatic additions of acid when necessary. Aeration provided oxygen to the microorganisms, and the dissolved oxygen (DO) was monitored over time with a polarographic probe. A synthetic lactic acid solution (1.5 g L^{-1}) was used as single carbon source for the selection and accumulation phases. A solution of nitrogen and phosphorus

was supplied to the SBR at the beginning of the famine phase and used to adjust the C/N and C/P ratios to 15 g_N/g_C and 36 g_P/g_C, respectively.

The PHA accumulation tests were conducted in a 1 L, continuous stirred fed-batch reactor, initially fed with 500 mL of enriched culture from the SBR. Lactic acid was used as single carbon source and avoiding any addition of nitrogen and phosphorus. The tests were performed at 25°C and continuous aeration was provided; pH was adjusted when necessary. Each accumulation test lasted 6 hours and it was performed in triplicate.

Results and discussion

The feasibility of selecting a PHA-storing MMC using lactic acid as single substrate was confirmed, consistently with the results of previous studies [6, 7, 8, 9]. The SBR reactor was operated for 100 days, and stable operation was achieved after 21 days, with a biomass concentration of 0.65 ± 0.14 g_{VSS} L^{-1}. The observed feast-to-famine (F/F) ratio was 0.34 ± 0.10, suitable for the selection of mixed cultures capable of storing PHA. It is worth to underline that the implementation of the uncoupled strategy in combination with the use of lactic acid as single carbon source is a novelty and proved to be successful. The uncoupling strategy, where feeding of carbon and nitrogen are separated, seems to provide an additional competitive advantage to the PHA-storing bacteria. In fact, delaying the nitrogen supply until the famine phase (2 hours after the beginning of the cycle) ensures that the biomass primarily utilizes the stored polymer, rather than external carbon, for growth. This approach is fundamental when nutrient-deficient feedstocks are used [11, 12]. Process monitoring confirmed that the lactic acid was completely depleted, and PHA accumulation occurred during the feast phase in the form of a copolymer of HB-HV that contains 10% hydroxyvalerate (HV).

Lactic acid proved to be a feasible substrate also for the accumulation phase. The maximum PHA content reached 50% of the cell dry weight with a maximum storage yield (Y_{PHA}) of 0.44 $g_{C\text{-}PHA}$ $g_{C\text{-}Lactic\ acid}^{-1}$, consistent with results from other studies [8, 9]; notably, these studies refer to tests where lactic acid was provided with other carbon sources such as butyrate or acetate that, indeed, were considered the main precursors for PHA production [13]. The confirmed 10% HV content underlines the lactic acid's role in producing a copolymer, a feature that deserves careful consideration depending on the application's specific requirement.

The attained preliminary results suggest that production of PHA from lactic acid is feasible, promising, and worth of further investigation. This approach is particularly intriguing when considering biowastes that yield substantial lactic acid streams through dark fermentation. For instance, homolactic fermentation of cheese whey may account for an impressive yield of 0.99 $g_{C\text{-}Lactic\ acid}$ $g_{C\text{-}Whey}^{-1}$, as compared to 0.75 $g_{C\text{-}VFA}$ $g_{C\text{-}Whey}^{-1}$ during mixed dark fermentation [12]. In light of the optimised conversion of organic carbon into PHA, the results of the present study support the inherent potential of lactic acid as a primary substrate for PHA production.

Conclusions

The study confirms the potential of using lactic acid as single carbon source for PHA production via mixed microbial cultures, representing a promising approach to simplify the process, improve performance stability, and avoid carbon losses in the form of CO_2, especially in the case of biowastes that produce lactic acid via dark fermentation

Acknowledgement

We acknowledge financial support under the National Recovery and Resilience Plan (NRRP), Mission 4 Component 2 Investment 1.5 - Call for tender No.3277 published on December 30, 2021 by the Italian Ministry of University and Research (MUR) funded by the European Union – NextGenerationEU. Project Code ECS0000038 – Project Title eINS Ecosystem of Innovation for Next Generation Sardinia – CUP F53C22000430001- Grant Assignment Decree No. 1056 adopted on June 23, 2022 by the Italian Ministry of Ministry of University and Research (MUR).

References

[1] Mukherjee A., Koller M., “Microbial PolyHydroxyAlkanoate (PHA) Biopolymers—Intrinsically Natural”, Bioengineering, Vol 10, 855, (2023).
[2] Palmeiro-Sánchez T., O’Flaherty V., Lens P.N.L., “Polyhydroxyalkanoate bio-production and its rise as biomaterial of the future”, Journal of Biotechnology, Vol 348, 10-25, (2022).
[3] Asunis F., De Gioannis G., Isipato M., Muntoni A., Polettini A., Pomi R., Rossi A., Spiga D., “Control of fermentation duration and pH to orient biochemicals and biofuels production from cheese whey”, Bioresource Technology, Vol 289, 121722, (2019).
[4] Aranda-Jaramillo B., León-Becerril E., Aguilar-Juárez O., Castro-Muñoz R., García-Depraect O., “Feasibility Study of Biohydrogen Production from Acid Cheese Whey via Lactate-Driven Dark Fermentation”, Fermentation, Vol 9, 644, (2023).
[5] García-Depraect O., Muñoz R., Rodríguez E., Rene E.R., León-Becerril E., “Microbial ecology of a lactate-driven dark fermentation process producing hydrogen under carbohydrate-limiting conditions”, International Journal of Hydrogen Energy, Vol 46, Issue 20, 11284-11296, (2021).
[6] Jiang Y., Marang L., Kleerebezem R., Muyzer G., van Loosdrecht M.C.M., “Polyhydroxybutyrate production from lactate using a mixed microbial culture” ,Biotechnol. Bioeng., Vol 108, 2022-2035, (2011).
[7] Zhou T., Wang S., Zhang W., Yin F., Cao Q., Lian T., Dong H., “Comparison of different aerobic sludge on enriching polyhydroxyalkanoate mixed microbial culture using lactic acid fermentation broth of agricultural wastes”, Chemical Engineering Journal, Vol 475, 146000, (2023).
[8] Zhou T., Wang S., Zhang W., Yin F., Cao Q., Lian T., Dong H., “Polyhydroxyalkanoates production from lactic acid fermentation broth of agricultural waste without extra purification: The effect of concentrations”, Environmental Technology & Innovation, Vol 32, 103311, (2023).
[9] Rangel C., Carvalho G., Oehmen A., Frison N., Lourenço N.D., Reis M.A.M., “Polyhydroxyalkanoates production from ethanol- and lactate-rich fermentate of confectionary industry effluents”, International Journal of Biological Macromolecules, Vol 229, 713-723, (2023).
[10] Gouveia A.R., Freitas E.B., Galinha C.F., Carvalho G., Duque A.F., Reis M.A., "Dynamic change of pH in acidogenic fermentation of cheese whey towards polyhydroxyalkanoates production: Impact on performance and microbial population", New Biotechnology., Vol 37, Pt A, 108-116, (2017).
[11] Oliveira CS, Silva CE, Carvalho G, Reis MA. "Strategies for efficiently selecting PHA producing mixed microbial cultures using complex feedstocks: Feast and famine regime and uncoupled carbon and nitrogen availabilities." New Biotechnoly. 2017 Jul 25;37(Pt A):69-79.
[12] Silva F, Campanari S, Matteo S, Valentino F, Majone M, Villano M. "Impact of nitrogen feeding regulation on polyhydroxyalkanoates production by mixed microbial cultures." New Biotechnoly. 2017
[13] Pardelha F, Albuquerque MG, Reis MA, Oliveira R, Dias JM. “Dynamic metabolic modelling of volatile fatty acids conversion to polyhydroxyalkanoates by a mixed microbial culture”. New Biotechnoly. 2014
[14] Asunis F., Carucci A., De Gioannis G., Farru G., Muntoni A., Polettini A., Pomi R., Rossi A., Spiga D., “Combined biohydrogen and polyhydroxyalkanoates production from sheep cheese whey by a mixed microbial culture,” Journal of Environmental Management, Vol 322, 116149, (2022).

PARALLEL SESSION: C3

Flash

Advanced treatment technologies in water and wastewater sectors

Title: Sludge Treatment & Advanced Recycling (STAR): complete synergy between mesophilic and thermophilic processes

Author(s): Maria Cristina Collivignarelli[1,2], Alessandro Abbà[3], Stefano Bellazzi[1], Gianluca Guido[1], Roberta Pedrazzani[4], Giorgio Bertanza[3]

1 *Department of Civil Engineering and Architecture, University of Pavia, Via Ferrata 3, 27100 Pavia, Italy*

2 *Interdepartmental Centre for Water Research, University of Pavia, Pavia, Via Ferrata 3, 27100 Pavia, Italy*

3 *Department of Civil, Environmental, Architectural Engineering and Mathematics, University of Brescia, Via Branze 43, 25123 Brescia, Italy*

4 *Department of Mechanical and Industrial Engineering, University of Brescia*

Keyword(s): Thermophilic/mesophilic processes; sludge minimization; circular economy; advanced respirometric test.

Abstract

In this research, a novel integrated sludge treatment scheme including the activated sludge process (Sludge Treatment & Advanced Recycling - STAR), is proposed.
The studied configuration combines a Conventional Activated Sludge (CAS) process and the Thermophilic Aerobic-Anaerobic Membrane Reactor (TAMR) for the treatment of thickened sludge.
The TAMR is a thermophilic fluidized bed biological reactor operated with pure oxygen coupled with an ultra-filtration membrane unit. TAMR has been introduced in a true to life plant in Lombardy. The structure has a volume of 200 m^3 and deals with a sludge flowrate of 20 m^3d^{-1} (Figure 1). The strengths of the proposed system, due to the introduction of the TAMR unit, may be summarized as follows:

(i) Strong reduction of the excess activated sludge (with a goal around 90%in terms of Volatile Solids).

(ii) Production of residues which can be recirculated as an external carbon source to improve the performance of the traditional mesophilic plant.

The experimental work was divided into two phases:

1. TAMR MONITORING: The objective was to quantify and optimize sludge minimization performance by evaluating the reduction of VSS, with average removal yields confirmed to be 90% over the 6 months studied. To assess the vitality of the biomass, respiratory measurements were carried out in a thermophilic field. Finally, to evaluate the variation in the mechanics of the fluid, the rheological properties of the mixed liquor in the biological reactor were studied.
2. ASSESSMENT OF THE RECIRCULATED RESIDUES: the aim was to verify and quantify the process improvements achievable by recirculating the TAMR effluents (liquid - permeate - and sludge) into the mesophilic unit; the nitrification and denitrification kinetics were measured, and specific tests were carried out to evaluate possible medium-term inhibitory effects (tests carried out lasting more than 90 hours).

The application of this new concept of activated sludge systems (STAR), thanks to the total synergy

between the mesophilic and thermophilic systems, allows to obtain zero-sludge production and, at the same time, to be able to recirculate the water effluent, rich in organic substance, as a nutrient in the denitrification tank, measured denitrification kinetics (using liquid permeate) are comparable to kinetics measured using a synthetic carbonaceous substrate (methanol), 4.4 mgN-NO_3^-/gSSV*h using synthetic methanol vs 4.0 mgN-NO_3^-/gSSV*h using liquid residue. The inert solid residue, composed mainly of silicon dioxide (SiO_2), represents 20% of the solid quantity treated by the system and is expelled from the plant following physical and mechanical dehydration treatment.

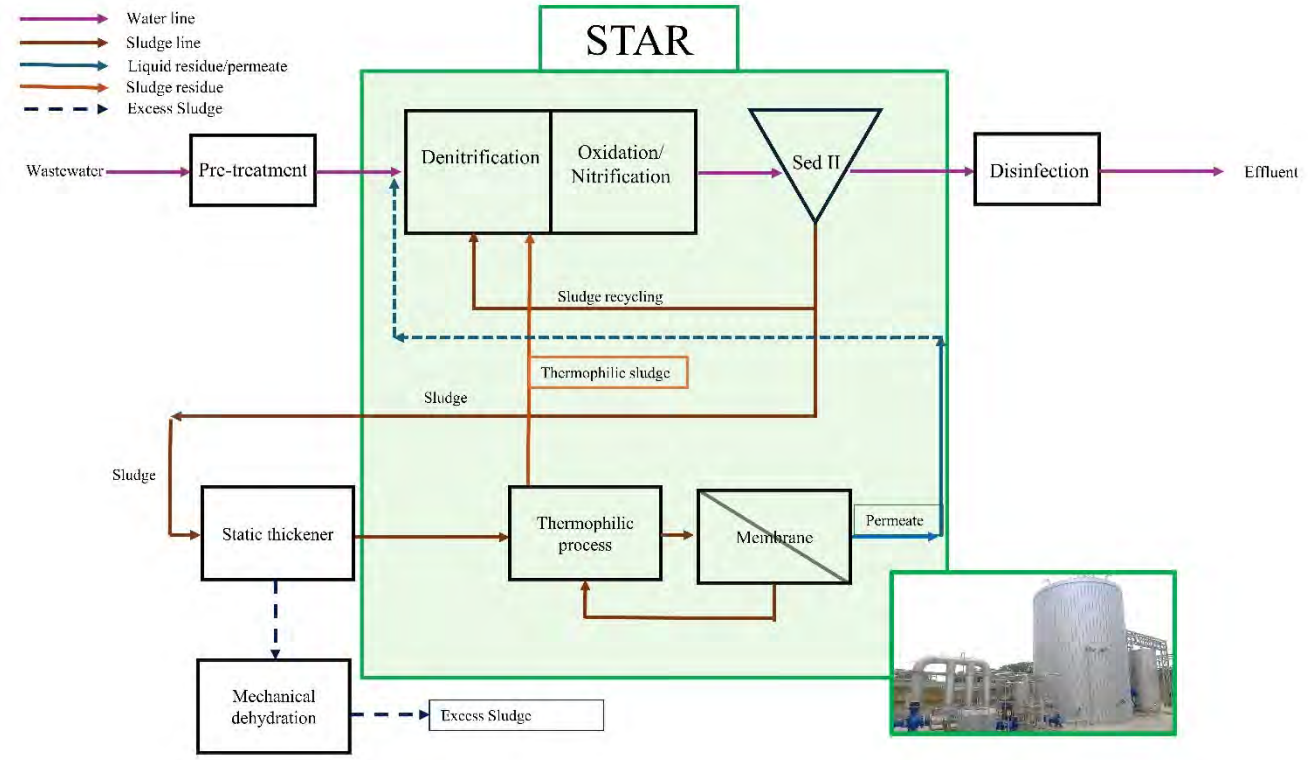

Figure1. Block diagram of the treatment platform designed for the application of the STAR system.

Title: Enhancing the adsorption potential of multi-layered graphene obtained from thermo-plasma expanded graphite for the removal of volatile organic compounds and dyes from water

Author(s): Francesco Di Capua*[1], Marco Cuccarese[1], Alireza Faraji[1], Ignazio Marcello Mancini[1], Donatella Caniani[1], Salvatore Masi[1]

[1] *School of Engineering, University of Basilicata, Potenza, Italy*

**Presenting author. Email address: francesco.dicapua@unibas.it*

Keyword(s): Adsorption, Graphene, BTEX, Methylene blue, Water decontamination.

Abstract

Introduction. Graphene, an allotrope of carbon, has been attracting an enormous interest due its excellent mechanical, thermal, electrical, and physicochemical properties such as its exceptionally high tensile strength, electrical conductivity, transparency, and being the thinnest 2-dimensional material in the world [1]. Recently, the adsorption capacity of multi-layer graphene (MG) produced via thermo-plasma expansion of natural graphite (TPEG) followed by exfoliation in water has been investigated. This material is composed by stacked sheets of graphene (>5), as shown by solid-phase characterization [2]. The extreme lightweight and volatility of MG, which eases transportation, limits its application in packed filters as it can be easily suspended in the flowing wastewater and considerable loss in the environment can occur during handling operations.

Volatile organic compounds and dyes are among the most common contaminants that can pollute drinking water sources such as aquifers and superficial bodies due to infiltration in the ground and discharge of contaminated streams. One of the most dangerous sources of contamination is the leakage from underground storage tanks, which are used in gas stations and several industries. Once this release occurs, liquids such as gasoline and diesel, which are mixtures of volatile and semi-volatile hydrocarbons including benzene, toluene, ethylbenzene, and xylene (BTEX), contaminate the soil and can move towards ground and surface waters [3]. The Environmental Protection Agency of the United States has classified BTEX as pollutants of primary importance and whose concentration must be significantly reduced both in wastewater and soil. According to the guidelines of the World Health Organization, the maximum permissible concentrations of benzene, toluene, ethylbenzene, and xylene in drinking water are respectively 0.01, 0.7, 0.3 and 0.5 mg L^{-1}. Among the different contaminants that must be removed from industrial wastewaters before discharge in sewers, cationic dyes such as methylene blue (MB) represent one of the most largely used especially in the textile industry [4] and, if enters the human body, can generate diverse diseases in humans [5]. Furthermore, MB can adsorb other pollutants, such as heavy metals or suspended solids. The adsorption process results to be one of the most applied methods to remove MB due its inexpensive maintenance, design and process simplicity, insensitivity to toxic pollutants, and limited release of potentially harmful substances [6]. The present study investigates the adsorption capacity of MG both as it is and in granular (granular MG, GMG) form embedded in alginate to remove BTEX and MB from water. Adsorption kinetics, isotherms, the effects of pH, temperature, initial contaminant concentration as well as adsorbent regeneration was investigated.

Materials and methods

Graphene-based materials. MG was produced by Innograf s.r.l. (Potenza, Italy) from natural graphite intercalated with chemical compounds and treated via thermal plasma expansion. This process ensures the exfoliation of graphite, with a volume expansion of up to 300 units, compared to an average of 200 units obtainable by other standard methods. For the experiments on BTEX adsorption, ultrasonication (35 kHz for 50 h) was applied to reduce the particle dimension of MG and enhance its solubility in water. MG was also granulated though embedding in sodium alginate at two different MG/alginate ratios (5%, 20%) to compare the adsorption capacity of MG and MG-alginate granules towards MB.
Design of adsorption tests. Batch adsorption tests were performed in 50 mL vials mixed on a rotary shaker. Different volumes of BTEX or MB stock solutions were added to the vials. Samples were collected at different time intervals and stored at 5°C before analysis.
Kinetic studies. Adsorption kinetics were studied by evaluating the adsorption capacity at different times according to *Eq. 1*:

$$q = \frac{(C_i - C_f) \times V}{g\ adsorbent} \quad \text{(Eq. 1)}$$

where C_i and C_f and the initial and final concentrations of the contaminants, *g adsorbent* is the mass of the adsorbent, and *V* is the volume of the solution used for the test. The following kinetic models were considered: 1) pseudo-first order, 2) pseudo-second order, 3) Elovich, 4) liquid film diffusion, and 5) intraparticle diffusion.
Adsorption isotherms. The adsorption isotherms of the process were evaluated for each compound at 20°C. For BTEX, a contact time of 6 h was used and the initial concentration of each pollutant was varied into the range of 2.5-180 mg L^{-1}. For MB, contact time was 2 h and the concentration was varied between 10 and 100 mg L^{-1}. The following isotherm models were considered: Langmuir, Freundlich, Temkin, and Dubinin-Radushkevich.
Tests at different operating conditions. The effect of different initial pHs (3-11), temperatures (5-60°C), and initial concentrations was evaluated on BTEX and/or MB adsorption.
Regeneration tests. The regeneration of graphene-based materials after use was investigated through chemical (with HCl) and thermal (105-200°C) treatment. Adsorption with regenerated materials was investigated up to 5 reuse cycles.
Analytical methods. BTEX concentration was evaluated by static headspace extraction coupled to gas chromatography with a barrier ionization discharge detector (GC-BID) (Shimadzu, Japan). MB concentration was evaluated with a 7600 UV-Vis spectrophotometer (WTW, Germany). pH was measured with a PC 7 Vio multiparameter (XS, Italy).

Results and Discussion

Adsorption capacity. Figure 1 illustrates the adsorption capacity of hydro-soluble MG and GMG towards BTEX and MB, respectively. Regarding BTEX adsorption, the adsorption capacity of hydro-soluble MG ranged between 16.5 and 22.4 mg g^{-1} when each compound (20 mg L^{-1}) was adsorbed alone. The presence of multiple BTEX led to a reduction of the adsorption capacity for ethylbenzene, an increase for toluene and o-xylene, and no significant variation for *m,p*-xylenes. The kinetics of toluene (at 20 mg L^{-1}) is faster compared to the other compounds; therefore, the molecules of toluene are bonded to TPEG surface for first and ethylbenzene molecules can find some active site occupied. For MB adsorption, different carbon materials were screened as adsorbent, resulting in GMG 5% as the one with the highest adsorption capacity (183±4 mg g^{-1}). Therefore, GMG 5% was used for subsequent tests.
Kinetic behavior. At 20 mg L^{-1}, toluene, ethylbenzene, and xylenes adsorption on hydro-soluble MG best fitted the intraparticle diffusion and pseudo-second order models. MB (50 mg L^{-1}) adsorption onto GMC 5% perfectly fitted a pseudo-second order kinetic model (R^2 = 0.9997) indicating that the slowest step of the adsorption process is the chemical/physical interaction between pollutants and adsorbent material

surface.

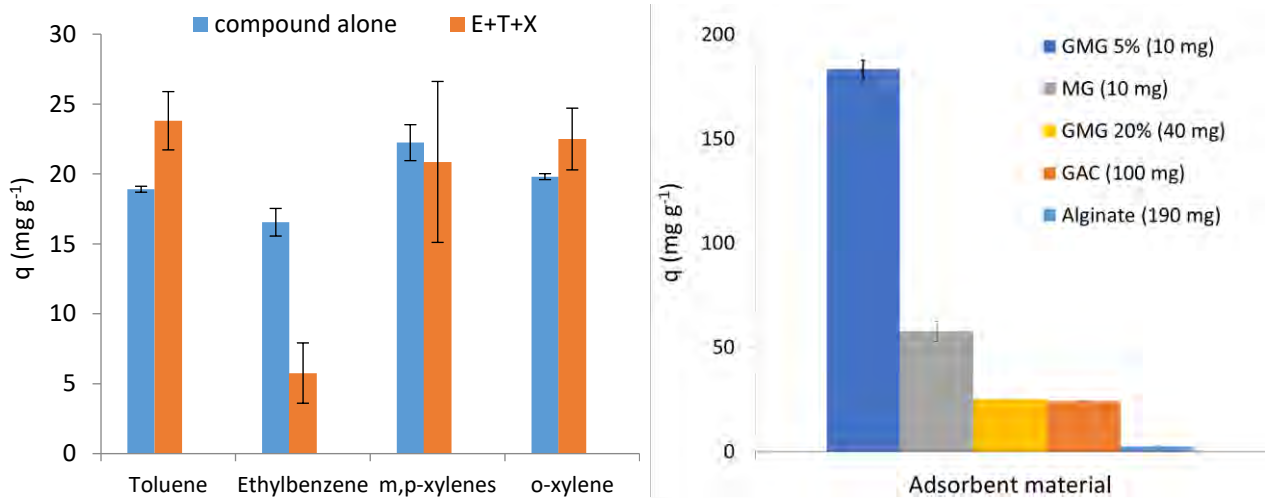

Fig. 1 – Adsorption capacity of hydro-soluble MG (left) and GMG (right) for the removal of BTEX (left) and MB (right) from water.

Isotherm model. MB adsorption onto GMG 5% followed the Freundlich model (R^2=0.97), indicating that multilayer adsorption occurs on GMG surface. Similarly, multilayer adsorption was observed for ethylbenzene and xylenes on hydro-soluble MG (R^2=0.86-0.96), while toluene best fitted Langmuir and Temkin models (R^2=0.94) suggesting mono-layer adsorption.
Effect of pH and temperature. Circumneutral pH (7.65) was best for BTEX adsorption on hydro-soluble MB. pH increase to 9.9 only slightly affected adsorption capacity, while a significant reduction was observed at the acidic pH 3.78 (Figure 2). MB adsorption on GMG 5% was not significantly affected by pH in the range of 3-11. Similarly, little variation was observed at temperatures ranging from 5 to 40 °C at 2 h, while the adsorption capacity was nearly halved when temperature was increased to 60 °C.

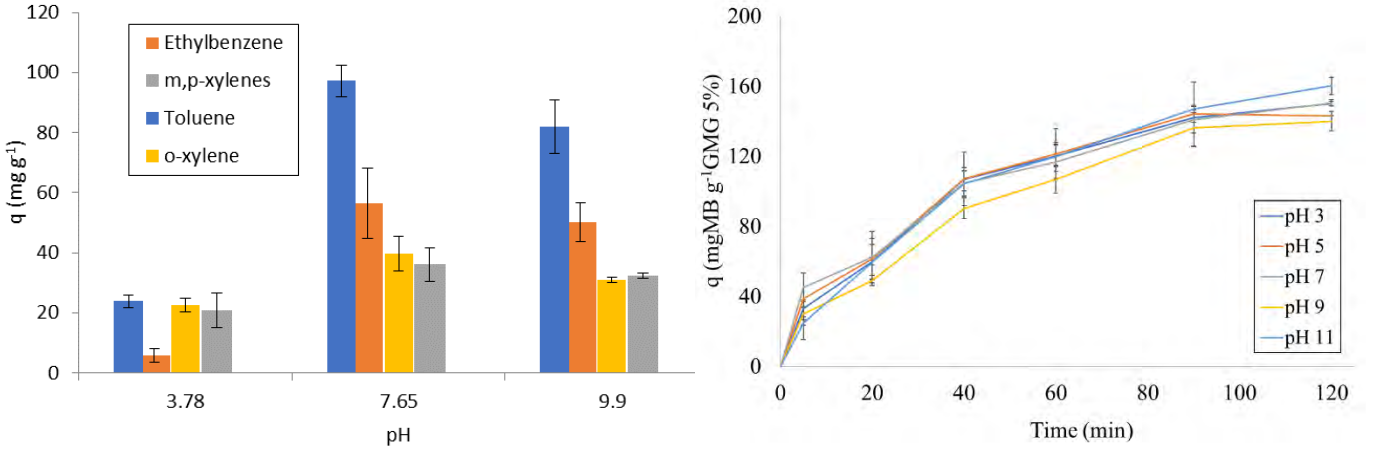

Fig. 2 – Effect of initial pH on the adsorption of BTEX and MB adsorption respectively on MG (left) and GMG (right).

Adsorbent regeneration. Acid washing with HCl 1M increased the adsorption capacity of GMG 5% by 24-38% up to the 5th reuse (Figure 3). This was likely due to the increased negative charge on GMG surface following acid washing, resulting in a stronger electrostatic interaction with MB in water. Thermal regeneration was not suitable for GMG as it degraded the alginate-MG structure.

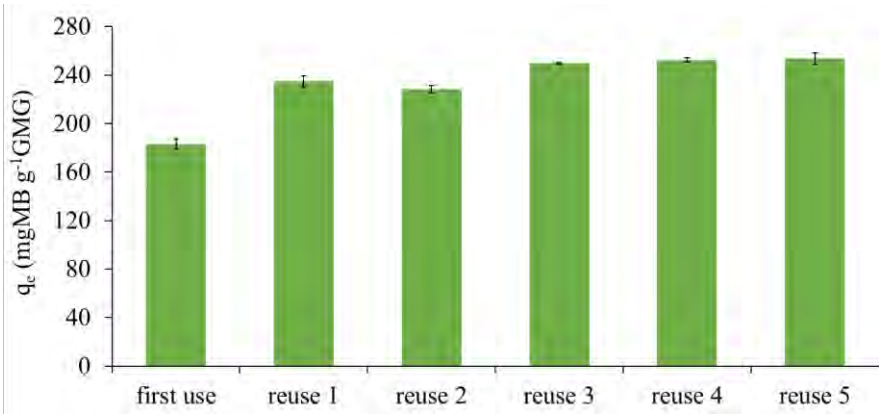

Fig. 3 – Reuse of chemically-regenerated GMG for MB adsorption.

Conclusions

The graphene-based materials examined in this study showed promising adsorption capacities and applicability for real-scale remediation of natural and industrial waters contaminated by BTEX and dyes such as MB. Granulation also enables easier utilization of MG in adsorption filters.

References

[1] V. Shanmugam, R.A. Mensah, K. Babu, S. Gawusu, A. Chanda, Y. Tu, R.E. Neisiany, M. Försth, G. Sas, O. Das, V. Shanmugam, R.A. Mensah, M. Försth, G. Sas, O. Das, K. Babu, S. Gawusu, Y. Tu, R.E. Neisiany, A Review of the Synthesis, Properties, and Applications of 2D Materials, Particle & Particle Systems Characterization 39 (2022) 2200031.

[2] M. Cuccarese, S. Brutti, A. De Bonis, R. Teghil, I.M. Mancini, S. Masi, D. Caniani, Removal of diclofenac from aqueous solutions by adsorption on thermo-plasma expanded graphite, Scientific Reports 2021 11:1 11 (2021) 1–15. https://doi.org/10.1038/s41598-021-83117-z.

[3] A.A.M. Daifullah, B.S. Girgis, Impact of surface characteristics of activated carbon on adsorption of BTEX, Colloids Surf A Physicochem Eng Asp 214 (2003) 181–193.

[4] I. Khan, K. Saeed, I. Zekker, B. Zhang, A.H. Hendi, A. Ahmad, S. Ahmad, N. Zada, H. Ahmad, L.A. Shah, T. Shah, I. Khan, Review on Methylene Blue: Its Properties, Uses, Toxicity and Photodegradation, Water 2022, Vol. 14, Page 242 14 (2022) 242.

[5] R. Al-Tohamy, S.S. Ali, F. Li, K.M. Okasha, Y.A.G. Mahmoud, T. Elsamahy, H. Jiao, Y. Fu, J. Sun, A critical review on the treatment of dye-containing wastewater: Ecotoxicological and health concerns of textile dyes and possible remediation approaches for environmental safety, Ecotoxicol Environ Saf 231 (2022) 113160.

[6] M. Cuccarese, S. Brutti, A. De Bonis, R. Teghil, F. Di Capua, I.M. Mancini, S. Masi, D. Caniani, Sustainable Adsorbent Material Prepared by Soft Alkaline Activation of Spent Coffee Grounds: Characterisation and Adsorption Mechanism of Methylene Blue from Aqueous Solutions, Sustainability 2023, Vol. 15, Page 2454 15 (2023) 2454.

Title: Removal of recalcitrant COD from secondary tannery effluent at neutral pH by electrochemical peroxidation technology

Author(s): Erika Pasciucco[1], Francesco Pasciucco[1], Renato Iannelli[1], Isabella Pecorini[1]

[1] Department of Energy, Systems, Territory and Construction Engineering, Via C.F. Gabba 22, Tuscany, University of Pisa, Pisa, 56122, Italy, Isabella.pecorini@unipi.it

Keyword(s): Wastewater treatment; tannery effluent; electrochemical process; COD; iron precipitation

Abstract

The Italian tannery industry is an undisputed international leader for the production of high-quality leather, accounting for 23% of world production [1]. However, the raw skin manufacturing process generates effluents with a high polluting load, impacting the environment [2]. Generally, biological processes are recommended for treating industrial effluents instead of chemical ones to remove organic content due to their cost-effectiveness and environmental sustainability, but they are unable to remove pollutants with low biodegradability, for which an advanced chemical process is required [3]. Furthermore, the high osmotic pressure of salinity wastewater prevents microbial growth, making the application of biological processes challenging [4]. In particular, the common processes of pickling and chrome tanning are primarily responsible for the high level of chlorides in the effluent [5]. The discharge of wastewater with a high concentration of chlorides into the environment represents a crucial bottleneck, as it involves a modification of the ionic composition of the water and limits its use for irrigation purposes [6]. Traditional technologies to remove chlorides, such as reverse osmosis, electro-osmosis and ion exchange are difficult to apply due to the presence of organic pollutants in tannery effluent.

Electrochemical advanced oxidation processes (EAOPs), such as electro-Fenton (EF), represent a promising approach against refractory and hazardous substances due to their high removal efficacy [7]. However, the EF process involves the addition of iron salts ($FeSO_4$ and $FeCl_2$) as source of iron, resulting in an increase in the total content of chlorides or sulphates. As an alternative, the electrochemical peroxidation process (ECP) uses a sacrificial iron anode to produce Fe^{2+} ions in the solution, avoiding the use of chlorine or sulphate-based chemicals.

In this study, the performance of the ECP process in the removal of recalcitrant COD from real secondary tannery effluent with high concentrations of chlorides and sulphates was investigated for the first time, so as to exploit the Fenton process without changing the initial pH.

The experiments were conducted in a cylindrical glass reactor with a working volume of 300 mL. Both anode and cathode were iron plates (99.5 % purity) with an area of 25 cm^2 and a thickness of 3 mm. A DC power generator was connected to the electrodes, which were installed in parallel at a distance of 3.5 cm from one another. Before electrolysis (60 minutes), 1.5 mL of H_2O_2 was added into the reactor. All experiments were conducted at a temperature of 25 °C under vigorous mixing.

The effect of electrical current (250, 500 and 750 mA) on COD and color removal efficiency was evaluated. In this case, COD and color removal increased as a function of electrical current from 60% to 69% and 91% to 97%, respectively (Figure 1).

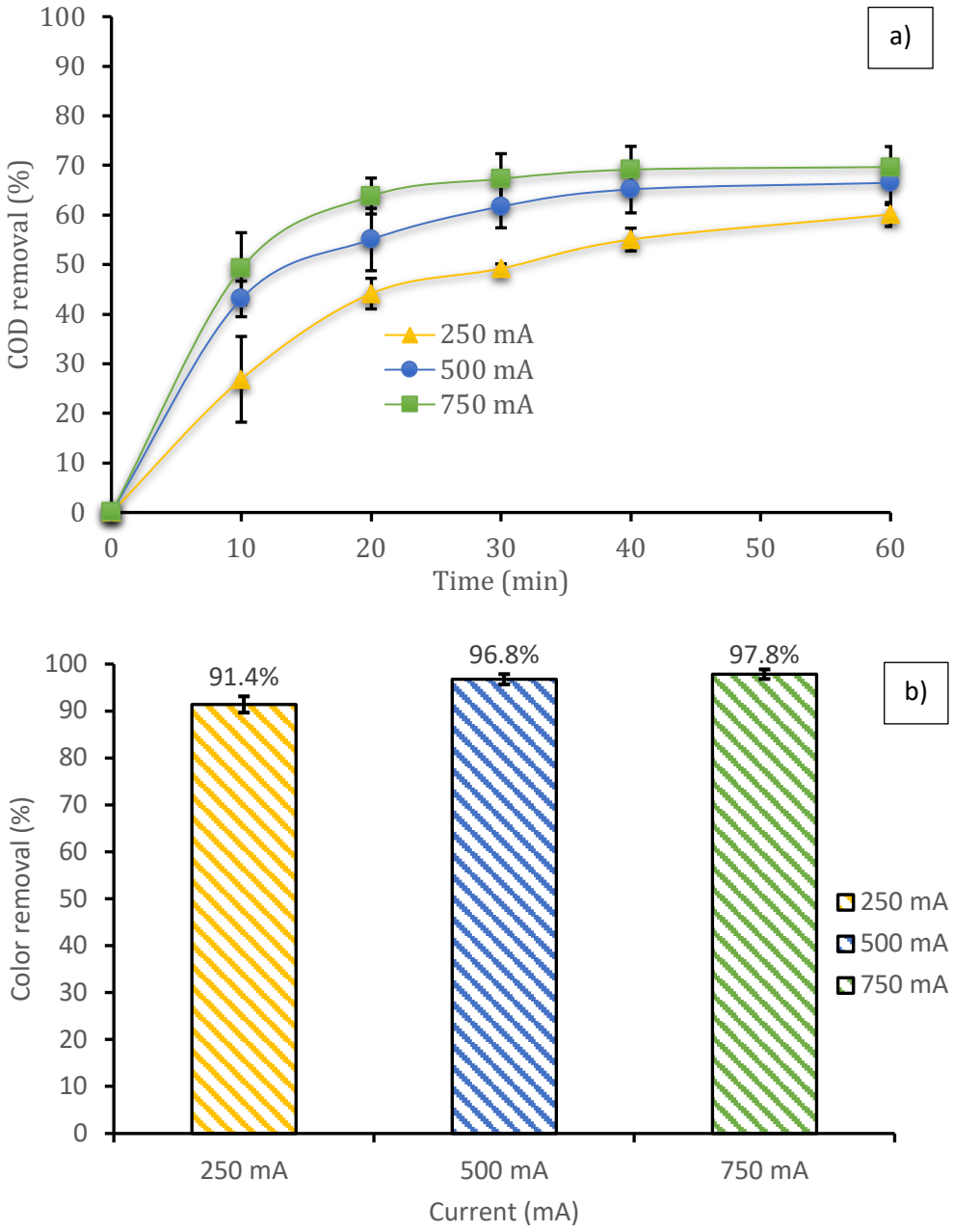

Figure 1: Effect of current on COD (a) and color (b) removal.

This could be explained by the fact that higher electrical currents increased the release of Fe^{2+} ions from the sacrificial iron anode, promoting the formation of hydroxyl radicals via the Fenton reaction and the precipitation of iron as hydroxides at neutral pH. Thus, pollutants were removed both by oxidation and electrocoagulation. Interesting, while Fenton-based technologies performed better at low pH levels [8], a COD removal of at least 60% was reached under alkaline conditions in this study. According to other authors, the high removal yield at neutral pH was mainly due to the formation of insoluble iron hydroxydes, as they acted both as coagulants and heterogeneous catalysts [9]. This allowed for the removal of organic and inorganic compounds via adsorption and the activation of H_2O_2 even in an alkaline environment, increasing removal efficiency over a wider pH range. At the same time, the increase in COD and color removal efficiency at higher currents corresponded to a greater amount of precipitated iron, meaning that the formation of iron hydroxides played a key role in both the removal of dyes and recalcitrant compounds.
The one-way ANOVA statistical analysis followed by a post-hoc Tukey test was performed to identify significant differences between the data, showing that the results obtained at 250 and 750 mA were statistically different ($p<0.05$). However, a value of 500 mA could be considered the best compromise between high removal efficiency and lower energy consumption.
The current intensity influences both the amount and morphology of the precipitate; therefore, XRD, SEM and FTIR analysis were conducted to characterize the produced sludge. According to SEM analysis, the structure of the precipitates changed as the electric current increased, resulting in smaller particle sizes. Furthermore, XRD analysis showed that the precipitate collected was mainly composed of iron oxides (e.g., Fe_2O_3 and Fe_3O_4). This was consistent with the FTIR analysis, where two characteristic bands were observed between 634 and 440 cm^{-1}, corresponding to the vibration of iron oxides. Furthermore, the absence of heavy metals such as chromium increased the potential reuse options of tannery sludge.

In conclusion, the ECP process represents a promising alternative for the tertiary treatment of tanning wastewater, meeting the standards required by Italian law for discharge. Future research in this field should focus on avoiding the consumption of chemical agents and encouraging the use of renewable energy sources and sustainable electrode materials to improve the environmental and economic sustainability of the ECP process.

References

[1] «UNIC, Sustenability Report», 2021. [Online]. Disponibile su: https://unic.it/storage/2021-Sustainability_Report_UNIC.pdf.
[2] S. Korpe e P. V. Rao, «Application of advanced oxidation processes and cavitation techniques for treatment of tannery wastewater—A review», *J. Environ. Chem. Eng.*, vol. 9, fasc. 3, p. 105234, giu. 2021, doi: 10.1016/j.jece.2021.105234.
[3] G. Lofrano, S. Meriç, G. E. Zengin, e D. Orhon, «Chemical and biological treatment technologies for leather tannery chemicals and wastewaters: A review», *Sci. Total Environ.*, vol. 461–462, pp. 265–281, set. 2013, doi: 10.1016/j.scitotenv.2013.05.004.
[4] H. Bao, M. Wu, X. Meng, H. Han, C. Zhang, e W. Sun, «Application of electrochemical oxidation technology in treating high-salinity organic ammonia-nitrogen wastewater», *J. Environ. Chem. Eng.*, vol. 11, fasc. 5, p. 110608, ott. 2023, doi: 10.1016/j.jece.2023.110608.
[5] K. J., R. C. Panda, e V. K. M., «Trends and advancements in sustainable leather processing: Future directions and challenges—A review», *J. Environ. Chem. Eng.*, vol. 8, fasc. 5, p. 104379, ott. 2020, doi: 10.1016/j.jece.2020.104379.
[6] Md. M. Uddin *et al.*, «A cleaner goatskin preservation with leaf paste and powder: An approach for salinity remediation in tannery wastewater», *Clean. Eng. Technol.*, vol. 6, p. 100357, feb. 2022, doi: 10.1016/j.clet.2021.100357.
[7] E. Isarain-Chávez, C. De La Rosa, L. A. Godínez, E. Brillas, e J. M. Peralta-Hernández, «Comparative study of electrochemical water treatment processes for a tannery wastewater effluent», *J. Electroanal. Chem.*, vol. 713, pp. 62–69, gen. 2014, doi: 10.1016/j.jelechem.2013.11.016.
[8] E. Brillas, «A review on the photoelectro-Fenton process as efficient electrochemical advanced oxidation for wastewater remediation. Treatment with UV light, sunlight, and coupling with conventional and other photo-assisted advanced technologies», *Chemosphere*, vol. 250, p. 126198, lug. 2020, doi: 10.1016/j.chemosphere.2020.126198.
[9] W. Lu, S. Lei, N. Chen, e C. Feng, «Research on two-step advanced treatment of old landfill leachate by sequential electrochemical peroxidation-electro-Fenton process», *Chem. Eng. J.*, vol. 451, p. 138746, gen. 2023, doi: 10.1016/j.cej.2022.138746.

Title: Unveiling the suitability of fluorescence indexes as surrogates for the *in situ* monitoring of contaminants of emerging concern removal through advanced oxidation processes designed for wastewater reuse

Authors: Filippo Fazzino*, Paolo Roccaro

Department of Civil Engineering and Architecture, University of Catania, Viale A. Doria, 6, Catania, Italy

Keywords: Contaminants of emerging concern; Advanced oxidation processes; Fluorescence spectroscopy; *In situ* monitoring.

Abstract

Contaminants of emerging concern (CEC) have been documented to be ubiquitously present in aquatic environments at trace concentrations (ng/L to µg/L) and discovered/suspected to be harmful to ecosystems and/or human health. CEC include pharmaceuticals, personal care products, biocides, poly- and perfluoroalkyl substances (PFAS), surfactants, disinfection by-products (DBPs), and others [1]. In this context, development of convenient strategies for CEC monitoring and investigation of effective processes for CEC removal are two crucial challenges currently tackled by extensive research.
Concentration of CEC in water is conventionally measured through analytical methods (e.g., HPLC, MS, LC-MS) requiring samples' pretreatments, complex procedures, high costs, and long-term calculations. Alternatively, fluorescence spectroscopy has gained particular attention for CEC 'indirect' determination. It allows to characterize the dissolved organic matter (DOM) in aquatic environments through molecule excitation by incident light. Fluorescence is the radiation (at various wavelengths) emitted by the excited molecule (fluorophore) [2]. As a result, aqueous samples can be characterized by distinct signatures (i.e., excitation/emission matrixes, EEMs) depending on DOM quality and quantity.In order to decode information present in EEMs, different methods have been developed: peak picking (PP) measures the intensity of fluorescence at specific pairs of excitation/emission (ex/em) coordinates, fluorescence regional integration (FRI) divides EEMs into five regions as a function of DOM type, and parallel factor analysis (PARAFAC) mathematically deconvolutes EEMs into independent components so that separating the contribution of different fluorophores. Implementation of these methods results in generation of various fluorescence indexes (*inter alia*, peaks intensities, EEM zones, PARAFAC components, total fluorescence, TF) to characterize DOM in a wide range of water matrixes as reported in previous studies [3,4]. Researchers discovered significant correlations between some of the aforementioned indexes and concentrations of CEC in aqueous samples, especially in effluents of advanced wastewater treatment processes [4,5].
Even though fluorescence spectroscopy has been observed to be more convenient in terms of cost and time compared to conventional detection techniques, however, the recording of the full EEM and the subsequent analysis to decode information on DOM composition unavoidably increase the overall duration and computational complexity of this approach. In this context, the use of fluorescence-based sensors would represent a further step towards advanced CEC monitoring. Portable devices are usually submersible and water-resistant (or otherwise cuvette-based) so that being installed directly on site (e.g., in natural water reservoirs or in pipelines of water treatment units) which implies actual real-time determination of a specific fluorescence feature of studied (waste)water DOM. Moreover, sensors can run continuously so that allowing to monitor especially performance of wastewater treatment processes.

However, to date, portable devices are able to determine only single pairs of ex/em coordinates thus providing limited information on DOM characteristics [6]. Therefore, in a perspective of real-time CEC monitoring in wastewater treatment processes, the most urgent issue to address is the selection of the most appropriate fluorescence indexes viable for sensor implementation that adequately correlate with target CEC occurrence.

It is widely accepted that advanced oxidation processes (AOPs) are the most suitable treatment technologies to remove CEC from wastewater. Ozonation is the most used one as witnessed by its development at full-scale level in wastewater and drinking water treatment plants. Moreover, the recent tendency is to adopt a multi-barrier approach, namely the combination of different processes to ensure an adequate level of CEC abatement especially for effluents used in wastewater reuse practices [7]. In this context, CEC estimation performed directly onsite through fluorescence-based sensors would allow to promptly adjust process conditions (e.g., oxidant dose, treatment time) to optimize CEC removal and concurrently save energy and materials (chemicals).

Taking all information into account, the present study aims at showing the suitability of fluorescence indexes, poorly or never considered in literature so far, for the estimation of CEC removal by AOPs. AOPs have been carried out in a pilot-scale apparatus (Wedeco, Xylem) installed at the end of the treatment train of a full-scale WWTP. The 6 tested AOPs were O_3, O_3/UV, H_2O_2/UV, H_2O_2/O_3/UV, Cl_2/O_3/UV, and Cl_2/UV performed at different doses of UV (i.e., 191-1622 mJ/cm^2), O_3 (i.e., 1.5-9.0 mg/L), H_2O_2 (i.e., 10 mg/L), and Cl_2 (i.e., 3 mg/L). The 19 target CEC included PFBA, PFBS, naproxen, diclofenac, ibuprofen, gemfibrozil, acetaminophen, trimethoprim, primidone, sulfamethoxazole, carbamazepine, fluoxetine, triclocarban, triclosan, hydrocortisone, DEET, caffeine, bisphenol A, and TCEP. Their contents were determined through SPE liquid chromatography coupled to mass spectrometry (Agilent Technologies). Spectroscopic measurements were performed through Shimadzu UV-1800 spectrophotometer and Shimadzu RF-5301PC spectrofluorophotometer for the determination of 11 fluorescence indexes, namely total fluorescence (TF), intensities of 5 fluorescence zones (FZi, i=1-5, determined through the FRI method), and 5 pairs of ex/em coordinates (I_i, i=1-5).

With the aim of showing the suitability of fluorescence indexes for estimation of CEC removal, Table 1 reports the number of CEC (out of the total of 19) that were strongly linearly correlated ($R^2 \geq 0.85$) with the 11 investigated indexes per each of the 6 performed AOPs.

Table 1. Number of times that each spectroscopic index strongly linearly correlated (with $R^2 \geq 0.85$) with individual CEC removal per each AOP

Fluorescence index/AOP	O_3	O_3/UV	H_2O_2/UV	H_2O_2/O_3/UV	Cl_2/O_3/UV	Cl_2/UV	*Sum*
TF (220-450/250-580 nm)	7	11	14	8	6	4	*50*
FZ1 (220-250/280-320 nm)	6	8	14	8	6	4	*46*
FZ2 (220-250/325-390 nm)	6	9	14	7	5	4	*45*
FZ3 (220-300/395-580 nm)	7	11	14	8	5	4	*49*
FZ4 (255-300/280-390 nm)	7	9	14	8	5	4	*47*
FZ5 (305-450/280-580 nm)	10	12	14	8	6	4	*54*
I_1 (225/290 nm)	6	8	14	8	6	1	*43*
I_2 (225/340 nm)	6	9	14	6	5	4	*44*
I_3 (245/440 nm)	7	11	14	8	6	4	*50*
I_4 (275/345 nm)	7	9	14	6	5	4	*45*
I_5 (345/440 nm)	10	12	14	7	6	4	*53*
Sum	*172*	*256*	*320*	*184*	*147*	*92*	

Previously, some PARAFAC components have been proven to provide reliable estimation of CEC removal by tested AOPs [5]. Specifically, O_3, O_3/UV, H_2O_2/UV, and Cl_2/O_3/UV processes have been observed to be successfully monitored (in terms of 6 pharmaceutical abatement) through variation in fluorescence intensity of protein-/tryptophan-like component (peak at 280/350 nm); whereas microbial humic-like (<250, 315/400 nm) and humic-like (<250, 350/440 nm) components were the most suitable indexes to monitor H_2O_2/O_3/UV and Cl_2/UV, respectively. Such results were consistent with extensive literature [8]. As a result of the present study, also TF confirmed to be suitable surrogate parameter to predict some CEC removal as previously reported [4]. In fact, TF variations have been observed to strongly linearly correlate (R^2≥0.85) with individual CEC removal for a total of 50 times across the 6 tested AOPs (Table 1). Similarly, variations in fluorescence intensities of five different zones of the EEM (FZi, i=1-5, determined with FRI method) showed remarkable numbers of strong correlations with CEC removals over all the tested AOPs (46, 45, 49, 47, and 54 for zone 1, 2, 3, 4, and 5, respectively, Table 1). However, PARAFAC components, TF, and FZi are the results of integration of the volumes under the EEM surfaces comprising the corresponding zones. This feature made those indexes not viable for *in situ* monitoring through miniaturized devices.

I_5 was the index with the highest number of strong correlations with CEC removals (53 times over all tested AOPs, Table 1). This evidence is consistent with the recent tendency to test humic-like-equipped fluorescent sensors. The peak centred at 280/440 nm, determined by a prototype LED UV/fluorescence sensor, showed promising results in terms of DBPs (trihalomethanes, haloacetic acids and bromate) monitoring and several CEC (same of this study) removals by ozonation [9,10]. What emerges from the present study is that another peak of the humic-like zone 5 (I_5 at 345/440 nm) could be successfully implemented for CEC removal prediction through *in situ* measurements.

Protein-like peak of zone 4 (285/350 nm) was previously tested as surrogate parameter in *in situ* tests through commercially available submersible fluorometer for the monitoring of the fate of spiked CEC (diesel, gasoline, ibuprofen, caffeine, lopinavir, and isoxathion) in creek water and after O_3 or UV treatments [11]. Results from the present study foster such investigation since I_4 at 275/345 nm was observed to strong correlate with ibuprofen removal during O_3/UV and UV/H_2O_2 and with caffeine removal during O_3 and O_3/UV/H_2O_2 (data not showed).

To the best of authors' knowledge, peaks of the other three zones (i.e., I_1, I_2, and I_3) have not been yet investigated as surrogate parameters for CEC monitoring through portable sensors. Fluorescence intensity at ex/em coordinates of 225/290 nm (I_1) is related to aromatic proteins and tyrosine-like fluorescence. It resulted the less strongly correlated index (43 times, Table 1) over the five zone peaks (I_i, i=1-5). Peaks I_2 and I_3 (225/340 nm, tryptophan-like substances, and 245/440 nm, fulvic- and humic-like substances, respectively) strong correlated with CEC removals 44 and 50 times, respectively, over all the tested AOPs. The latter was previously investigated in Spiliotopoulou et al. (2021) [12] as surrogate to predict pharmaceutical removal by ozonation. In the present study, I_3 was able to strong correlate with all the considered pharmaceuticals, except for acetaminophen and hydrocortisone, during UV/H_2O_2. Also for I_1, I_2, and I_3, excellent results in terms of correlations with several CEC removal would suggest the possibility of using such indexes as surrogate parameters for the online monitoring.

To sum up, what clearly emerges from the results reported in the present study is that CEC removal by AOPs could be effectively monitored through fluorescence indexes alternative to PARAFAC components and TF previously thoroughly investigated and validated. Indeed, for some CEC and AOPs, analyzing the complete but complex information contained in the full EEM could not have significant advantage compared to measuring fluorescence intensity in narrow ranges of wavelengths' values. As a practical implication of that, results reported in this study encourage the implementation and

investigation of commercially available or custom-made portable fluorometers able to generate excitations and record emissions peculiar of the tested I_i indexes for monitoring CEC removal by AOPs. Indeed, whilst I_4 and I_5 have been previously (still little) explored as surrogate parameters for *in situ* measurements, I_1, I_2, and I_3 have to unlock their potential on this regard. The advantage of online sensors implementation is the possibility of real-time monitoring of AOPs so that adjusting process conditions to optimize CEC removal in a perspective of wastewater reuse practices coupled with energy efficiency of future engineered water systems.

Acknowledgements
This work has been partially funded by European Union (NextGeneration EU), through the MUR-PNRR project SAMOTHRACE (ECS00000022).

References

[1] Yadav D, Rangabhashiyam S, Verma P, Singh P, Devi P, Kumar P, et al. Environmental and health impacts of contaminants of emerging concerns: Recent treatment challenges and approaches. Chemosphere 2021;272:129492. https://doi.org/10.1016/j.chemosphere.2020.129492.
[2] Lakowicz JR, editor. Instrumentation for Fluorescence Spectroscopy. Principles of Fluorescence Spectroscopy, Boston, MA: Springer US; 2006, p. 27–61. https://doi.org/10.1007/978-0-387-46312-4_2.
[3] Korshin GV, Sgroi M, Ratnaweera H. Spectroscopic surrogates for real time monitoring of water quality in wastewater treatment and water reuse. Current Opinion in Environmental Science & Health 2018;2:12–9. https://doi.org/10.1016/j.coesh.2017.11.003.
[4] Song Z-M, Xu Y-L, Liang J-K, Peng L, Zhang X-Y, Du Y, et al. Surrogates for on-line monitoring of the attenuation of trace organic contaminants during advanced oxidation processes for water reuse. Water Research 2021;190:116733. https://doi.org/10.1016/j.watres.2020.116733.
[5] Sgroi M, Anumol T, Vagliasindi FGA, Snyder SA, Roccaro P. Comparison of the new Cl2/O3/UV process with different ozone- and UV-based AOPs for wastewater treatment at pilot scale: Removal of pharmaceuticals and changes in fluorescing organic matter. Science of The Total Environment 2021;765:142720. https://doi.org/10.1016/j.scitotenv.2020.142720.
[6] Shin Y-H, Gutierrez-Wing MT, Choi J-W. Review—Recent Progress in Portable Fluorescence Sensors. J Electrochem Soc 2021;168:017502. https://doi.org/10.1149/1945-7111/abd494.
[7] Voulvoulis N. Water reuse from a circular economy perspective and potential risks from an unregulated approach. Current Opinion in Environmental Science & Health 2018;2:32–45. https://doi.org/10.1016/j.coesh.2018.01.005.
[8] Sciscenko I, Arques A, Micó P, Mora M, García-Ballesteros S. Emerging applications of EEM-PARAFAC for water treatment: a concise review. Chemical Engineering Journal Advances 2022;10:100286. https://doi.org/10.1016/j.ceja.2022.100286.
[9] Li W-T, Majewsky M, Abbt-Braun G, Horn H, Jin J, Li Q, et al. Application of portable online LED UV fluorescence sensor to predict the degradation of dissolved organic matter and trace organic contaminants during ozonation. Water Research 2016;101:262–71. https://doi.org/10.1016/j.watres.2016.05.090.
[10] Li W-T, Jin J, Li Q, Wu C-F, Lu H, Zhou Q, et al. Developing LED UV fluorescence sensors for online monitoring DOM and predicting DBPs formation potential during water treatment. Water Research 2016;93:1–9. https://doi.org/10.1016/j.watres.2016.01.005.
[11] Wasswa J, Mladenov N, Pearce W. Assessing the potential of fluorescence spectroscopy to monitor contaminants in source waters and water reuse systems. Environ Sci: Water Res Technol 2019;5:370–82. https://doi.org/10.1039/C8EW00472B.
[12] Spiliotopoulou A, Antoniou MG, Andersen HR. Natural fluorescence emission – an indirect measurement of applied ozone dosages to remove pharmaceuticals in biologically treated wastewater. Environmental Technology 2021;42:584–96. https://doi.org/10.1080/09593330.2019.1639827.

Title: Treatment of real pharmaceutical effluents through the homogeneous Fenton process

Author(s): Carlo Limonti*, Tiziana Andreoli, Giulia Maria Curcio, Elvis Gribaldo Aucancela Riveira and Alessio Siciliano

Laboratory of Sanitary Environmental Engineering, Department of Environmental Engineering (DIAm), University of Calabria, Rende 87036, Italy
**Corresponding: carlo.limonti@unical.it*

Keyword(s): catalytic chemical oxidation, Fenton process, hydrogen peroxide, pharmaceutical wastewater

Abstract

In the present paper an experimental investigation was conducted by treating effluents of pharmaceutical origin through the homogeneous Fenton process. The influence of Fe^{2+} and hydrogen peroxide dosage and of temperature was assessed through several batch tests. The results proved that the investigated parameters all together affect the performance of the process. In particular, the catalyst and hydrogen peroxide favour the COD removal up to a threshold value resulted equal to 0.4 g Fe^{2+}/gCOD and 2 gH_2O_2/gCOD, respectively. Temperature also improves the process and the value of 40°C was found to be the most favourable. With the optimal identified operating conditions, a COD removal of approximately 70% was achieved. Moreover, an increase of about 30% in the fraction of biodegradable organic matter was detected.

1. Introduction

Pharmaceutical industries produce hazardous wastewater that can represent serious sources of pollution for the environment [1]. These effluents result from the chemical synthesis and formulation of drugs. Therefore, their chemical composition depends on the pharmaceutical compounds produced and the manufacturing processes adopted. The produced effluents generally contain large amounts of both organic pollutants (solvents, unreacted reagents, by-products, etc.) and ionic species (chemicals, acids, bases, etc.) resulting in high levels of chemical oxygen demand (COD) with a low biodegradability, which makes difficult the treatment through biological processes [1]. Therefore, there is the need to apply adequate chemical-physical techniques able to efficiently reduce the polluting strength of these complex effluents. In a rational approach, chemical-physical processes could be exploited as pretreatments before a further biological process. Among the available techniques, advanced oxidation processes (AOPs) are recognized as a suitable option for the purification of low biodegradable and recalcitrant wastewater. AOPs include several techniques such as Fenton-related processes, ozone-based processes, electro-oxidation etc. Fenton and Fenton-like treatments are among the most applied processes to remove a wide range of refractory organic compounds. In the conventional process, Fe^{2+} ions are employed as catalysts which are maintained solubilized (homogeneous Fenton) during the reaction by working in an acidic environment (pH 2-4) [2]. After the treatment, the catalyst is removed from the solution and recovered by raising the pH to induce precipitation in the form of iron hydroxides [2]. Several modifications of the Fenton process such as heterogeneous Fenton, photo-Fenton, electro-Fenton (EF), ultrasound and microwave assisted Fenton, etc. have been investigated [3]. However, compared to the conventional Fenton method, these processes require more complex devices and installations and are often more energy expensive. Moreover, in homogeneous Fenton the removal of the catalyst after oxidation occurs through coagulation-precipitation which contributes to the removal of

pollutants. Therefore, this process can also be exploited to substitute the primary sedimentation treatment prior to the biological phase in the wastewater treatment plants [4]. Based on these considerations, the homogeneous Fenton appears to be more suitable in field applications for the pretreatment of pharmaceutical wastewaters. Despite this, only very few works have focused on the treatment of real pharmaceutical wastewater. In this regard, the present paper aimed to investigate the homogeneous Fenton process using Fe^{2+} as a catalyst for the treatment of raw effluents of a pharmaceutical industry. Several experiments were conducted to identify the most suitable operating conditions. The performance of the process was evaluated in terms of oxidation of organic matter and increase in biodegradability.

2. Materials and methods

2.1 Materials

The experimental activity was carried out on raw wastewater of a pharmaceutical industry that produces antitumoral active ingredients. Samples were stored in 25 L HDPE containers at 4°C to avoid alterations. Oxidations tests were conducted using $FeSO_4$ as the catalyst source and hydrogen peroxide with a concentration of 35 % (w/v). H_2SO_4 (98% w/v) and NaOH (6N) were exploited for pH corrections. All reagents were analytical grade and supplied by Sigma Aldrich.

2.2 Oxidation tests

Several experiments were conducted by changing the dosages of catalysts and hydrogen peroxide and at different temperatures. In particular, dosages of Fe^{2+} (Iron/COD ratio (R_{IC})) equal to 0.2, 0.4 and 0.6 gFe^{2+}/gCOD, doses of H_2O_2 (H_2O_2/COD ratio (R_{HC})) between 0.5 and 5 gH_2O_2/gCOD, and temperature of 20, 40 and 60°C were tested. Since the Fenton process with Fe^{2+} requires pH values between 2 and 4, the tests were executed a pH 3. The experiments were carried out in batch mode at atmospheric pressure in beakers of 250 mL capacity. The system was thermostated by means of a mixing hotplate controlled by a settable immersion thermostat. In each test, 100 mL of raw wastewater were placed in the beaker and the temperature and pH were adjusted to the established values. Subsequently, catalyst and hydrogen peroxide were added to set R_{IC} and R_{HC} ratios and the resulting solution was stirred at 300 rpm for 3 hours. After this period, the pH was raised to around 9 with NaOH (6N) and the solution was stirred for 5 minutes to allow effective formation of insoluble catalyst compounds. The mixer was then turned off and the produced sludge was left settling for 30 minutes. The supernatant was withdrawn and characterized to evaluate the performance of the treatment.

2.3 Analytical methods

Conductivity and pH were measured by means of benchtop analysers. Total COD was measured through digestion with potassium dichromate and volumetric titration with ammonium iron sulphate [5]. The soluble COD was determined after a coagulation treatment with zinc sulphate. The overall biodegradable COD (BCOD) was assessed by the respirometric procedure. H_2O_2 was measured by the iodometric titration method [5]. On the treated samples, the positive interference in COD estimation due to the presence of eventual residual H_2O_2 concentration was accounted by means of the procedure proposed by Mantzavinos [6]. The amount of Fe was determined through atomic absorption spectrophometry [5].

3. Results and discussion

3.1 Wastewater characteristics

The wastewater sample used in this work was characterized by a high COD of approximately 3.38 g/L. Since the wastewater mainly contained the reagents used in the production processes, the organic content was nearly totally composed of soluble compounds, as proved by the value of the COD_{SOL} which amounted to about 90% of the total COD. Moreover, the respirometric analysis revealed a biodegradable COD (BCOD) fraction of just around 27%. This value indicates a poor biodegradability which makes the biological processes not applicable without a suitable chemical-physical pretreatment able to improve the wastewater characteristics.

3.2 Oxidation tests

The first series of oxidation tests was conducted at T=20°C with a catalyst dose of 0.2 gFe^{2+}/gCOD, and testing peroxide amounts (R_{HC}) from 0.5 to 5 gH_2O_2/gCOD. As shown in Figure 1a, in this set of experiments unsatisfactory removal efficiencies were detected. Indeed, although the peroxide dosage produced a progressive increase in the COD removal, a maximum abatement of just about 24% was reached with the highest H_2O_2 addition of 5 gH_2O_2/gCOD. Dosages of this order allowed to obtain much higher efficiencies in previous studies conducted treating pharmaceutical compounds [7]. Therefore, the poor abatements recorded during the first set of experiments suggest that the operating conditions in terms of temperature and catalyst dosage were inadequate to effectively oxidize the wastewater organic load. Based on these considerations, subsequent tests were executed with Fe^{2+} doses of 0.4 and 0.6 gFe^{2+}/gCOD. In these experiments, as expected, higher efficiencies were monitored compared to those detected with a Fe^{2+} dose of 0.2 gFe^{2+}/gCOD. However, for each peroxide addition, the main improvement in process performance was observed when the catalyst dose was raised from 0.2 to 0.4 gFe^{2+}/gCOD, while a further increase to 0.6 gFe^{2+}/gCOD produced just a slight enhancement in COD abatement (Figure 1a). Therefore, values higher than 0.4 gFe^{2+}/gCOD are useless for inducing a more effective decomposition of hydrogen peroxide. Furthermore, it can be observed that for both Fe^{2+} ratios of 0.4 and 0.6 gFe^{2+}/gCOD, the COD abatements followed asymptotic trends in response to the H_2O_2 dose, suggesting that the amount of H_2O_2 is beneficial until reaching a threshold value. These outcomes may find a motivation in the numerous mechanisms that occur in the typical Fenton process.

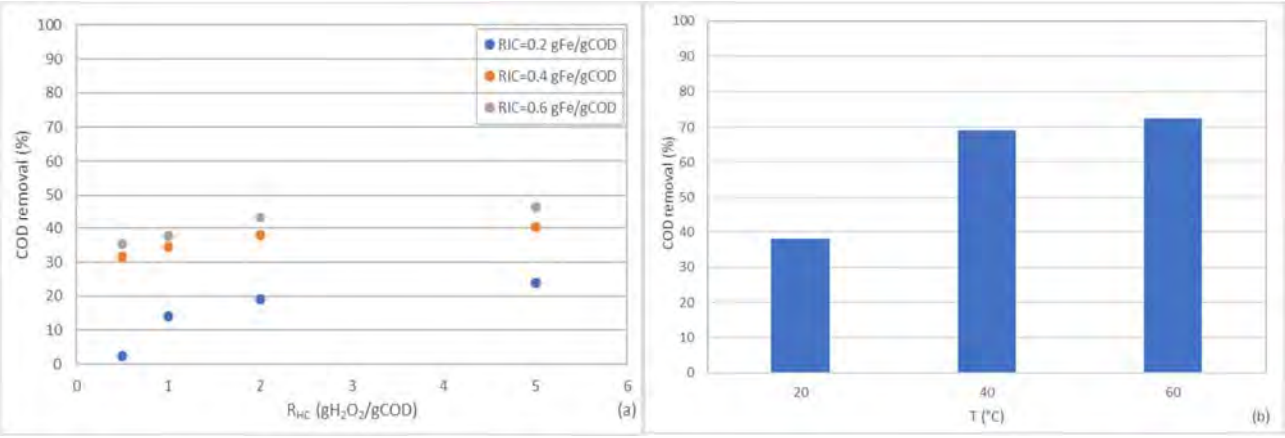

Figure 1. COD removal in the tests (a) conducted at T=20°C changing peroxide (R_{HC}) and catalyst (R_{IC}) dosage, (b) with R_{HC}=2 gH_2O_2/gCOD and 0.4 gFe^{2+}/gCOD at different temperatures.

As it is well known, the catalytic interaction between Fe^{2+} and H_2O_2 causes the formation of hydroxyl radicals which are the main responsible for the pollutant load removal. However, when dosed in excessive amount, hydrogen peroxide can act as an OH· scavenger with the formation of other less reactive radical species [8]. The depletion of hydroxyl radicals with the mutual H_2O_2 consumption is detrimental to the process performance causing a marked slowdown in the removal of organic

pollutants, despite a progressive increase in the addition of peroxide. As shown in Figure 1a, in our tests this condition was found at a dosage approximately of 2 $gH_2O_2/gCOD$. Consequently, this dose was applied to perform the next tests at 40 and 60 °C since higher additions of H_2O_2 are not suitable to substantially improve the COD removal efficiency. The trend depicted in Figure 1b confirms that the temperature has a beneficial effect on the processes. Indeed, the increase of temperature accelerates the reaction rate between ferrous ions and H_2O_2, which causes the generation of additional hydroxyl radicals [7]. However, the results of our experiments, in agreement with the literature statements, indicate that by conducting the reaction at a temperature higher than 40 °C the yields attenuate. This is imputable to the possible decomposition of H_2O_2 into water and oxygen at high temperatures, which compromises the process performance. Under optimal operating conditions, the process was able to remove approximately 70% of the COD concentration and to increase the fraction of biodegradable organic matter (BCOD) of about 30% compared to the value of untreated raw wastewater.

4. Conclusions

The present study aimed to investigate the applicability of the homogeneous Fenton process to real pharmaceutical wastewater treatment. The results of conducted experiments proved that the addition of Fe^{2+} up to a dose of 0.4 $gFe^{2+}/gCOD$ is useful for the process by promoting the radical decomposition of H_2O_2. The addition of hydrogen peroxide also enhances the strength in removing the organic load until a threshold of about 2 $gH_2O_2/gCOD$ is reached. Beyond this value the further increase of H_2O_2 is useless causing the elimination of hydroxyl radicals. With the dosages of Fe^{2+} and H_2O_2 indicated above, an efficiency close to 70% was obtained with a temperature value of 40°C, identified as optimal for the treatment. The detected outcomes support the applicability of the Fenton process as a suitable pretreatment of effluents of pharmaceutical origin. In any case, additional research could further optimize the performance of the process. In this regard, it would be interesting to test gradual additions of H_2O_2 and the recovery and reuse of produced sludge.

References

[1] Pérez, J.F.; Llanos, J.; Sáez, C.; López, C.; Cañizares, P.; Rodrigo, M.A. Treatment of real effluents from the pharmaceutical industry: A comparison between Fenton oxidation and conductive-diamond electro-oxidation. Journal of Environmental Management 2017, 195, 216-223.
[2] Mahtab, M.S.; Farooqi, I.H.; Khursheed, A. Sustainable approaches to the Fenton process for wastewater treatment: A review. Materials Today: Proceedings 2021, 47, 1480-1484.
[3] Monteagudo, J.M.; Durán, A.; San Martín, I. Mineralization of wastewater from the pharmaceutical industry containing chloride ions by UV photolysis of H_2O_2/Fe(II) and ultrasonic irradiation. Journal of Environmental Management. 2014, 141, 61-69.
[4] Changotra, R.; Rajput, H.; Dhir, A. Treatment of real pharmaceutical wastewater using combined approach of Fenton applications and aerobic biological treatment. Journal of Photochemistry & Photobiology A: Chemistry 2919, 376, 175-184.
[5] APHA. Standard methods for the examination of water and wastewater. 20th ed. Washington (D.C.): American Public Health; 1998.
[6] Mantzavinos, D. Romoval of benxoic acid derivatives from aqueous effluents by the catalytic decomposition of hydrogen peroxide. Trans IChemE 2003, 81B, 99-106.
[7] Mirzaei, A.; Chen, Z.; Haghighat, F.; Yerushalmi, L. Removal of pharmaceuticals from water by homo/heterogonous Fenton-type processes e A review. Chemosphere 2017, 174, 665-688.
[8] Dong, W.; Jin, Y.; Zhou, K.; Sun, S-P.; Li, Y.; Dong Chen, X. Efficient degradation of pharmaceutical micropollutants in water and wastewater by FeIII-NTA-catalyzed neutral photo-Fenton process. Science of the Total Environment 2019, 688, 513-520.

Assessment of the removal of micrometer-scale plastics in the stages of wastewater treatment plants using flow cytometry

Author(s): Paola Foladori[1], Alessia Torboli*[2] , Laura Bruni[3]

[1] *Department of Civil, Environmental and Mechanical Engineering, University of Trento, via Mesiano 77, 38123 Trento, Italy, paola.foladori@unitn.it*
[2] *C3A Center Agriculture Food Environment, University of Trento, Via Edmund Mach 1, 38098 TN, Italy, alessia.torboli@unitn.it*
[3] *ADEP, Agenzia per la Depurazione (Wastewater Treatment Agency), Autonomous Province of Trento, via Gilli 3, 38121 Trento, Italy, laura.bruni@provincia.tn.it*

Keyword(s): flow cytometry; microplastics; municipal wastewater; secondary treatment, tertiary treatment.

1. Introduction: need for research on micrometer-scale MPs in WWTPs

Microplastics are discharged in the sewer where undergo degradation into smaller pieces as a result of physical factors (i.e., abrasion), chemical factors (i.e., corrosion) or microbial biodegradation, leading to highly variable concentrations of these particles in municipal wastewater. The small micro- and nanoplastics with dimensions of 1 µm (called MNPs) are able to accumulate in biological cells and tissues and therefore have a much greater environmental impact and may affect human health, with largely unknown consequences [1]. For this reason, increasing attention is now being paid to the capacity of wastewater treatment plants (WWTPs) to remove particles in the micrometer range [2].

MNPs entering WWTPs undergo physico-chemical and biological processes, but knowledge on the fate of MNPs in WWTPs is currently limited. Further studies are needed to gain a better understanding of: (i) removal efficiency of MNPs in primary and secondary treatments, (ii) mechanisms involved, (iii) need of tertiary/quaternary treatments to improve MNP removal; (iv) MNP concentrations in treated effluents that spread into surface water bodies with potential concerns for the environmental and wastewater reuse.

The present study was carried out with 1-µm MNPs spiked in municipal wastewater and activated sludge in order to investigate their removal in the main processes involved in municipal WWTPs. In particular, the following processes were considered: (i) primary sedimentation; (ii) chemical precipitation with alum; (iii) secondary treatment with conventional activated sludge; (iv) tertiary treatment with 1-µm membrane filtration and (v) sand bed filtration.

The use of spiked 1-µm MNPs is advantageous due to the technical challenges involved in determining naturally occurring micrometer-scale MNPs in municipal wastewater and along the WWTP: (i) difficult detection using existing methods in complex matrices such as wastewater and sludge, (ii) methods requiring strong chemical pretreatments to eliminate interferences, (iii) time-consuming enumeration, (iv) not very repeatable and of poor quality results, (v) highly variable concentrations over time due to for example rainfall, (vi) uncertainties in calculating the maximum log-removal efficiency. Instead, the use of traceable spiked MNPs coupled with high-throughput flow cytometry (FCM) analysis enables the rapid and accurate identification and quantification of 1-µm MNPs, facilitating precise calculation of removal rates.

To our knowledge, this paper is one of the few studies on the fate of such small 1-µm MNPs across the various stages of a WWTP, contributing to the advancement of knowledge in this field.

2. Materials and methods

WWTP configuration - The WWTP layout (Figure 1) includes mechanical pre-treatments (screening and degritting) and primary settling (hydraulic retention time, HRT = 3 h). Pre-settled wastewater is treated in conventional activated sludge (CAS) stage followed by secondary sedimentation (total HRT = 17 h). Tertiary/quaternary treatment includes either membrane filtration or sand bed filtration.

Wastewater and activated sludge - Samples used for lab and pilot tests were collected in the following points (see Figure 1) along the wastewater line: (W1) influent raw wastewater collected after fine screening; (W2) pre-settled wastewater collected after the primary settling; (W3) activated sludge from the CAS stage; (W4) effluent after secondary sedimentation.

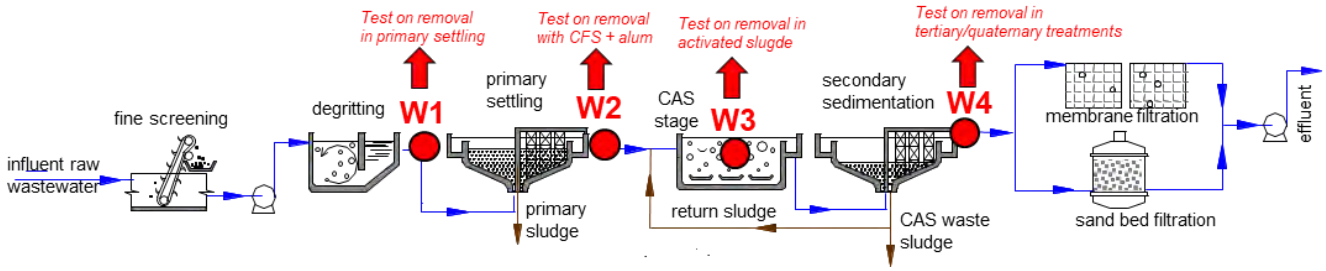

Figure 1. WWTP layout and sampling points of wastewater and activated sludge used in the removal tests.

1-µm MNPs – Polystyrene 1-µm MNPs (Fluoro Max G0100, ThermoFisher, USA) were used. MNPs emit green fluorescence with emission peak at 508 nm, that can be easily detected by FCM. Working suspension was prepared to achieve a concentration of 100 mg/L, corresponding to 1.8E+11 particles/L. Then it was diluted to obtain suitable initial concentrations for the lab- and pilot tests.

CFS jar tests with alum - Commercial stock of aluminum sulphate (30% w/w) was diluted to obtain concentrations of 3-30 mg Al^{3+}/L and then added to pre-settled wastewater (150-mL beakers). Jar tests were performed to investigate the coagulation-flocculation-sedimentation (CFS) process, involving 1-2 min of rapid mixing, 15 min of flocculation and 2 h of sedimentation.

Membrane filtration – Flat mesh membrane with a nominal cut-off of 1 µm (microfiltration, quaternary treatment) and a filtration area of 0.02 m^2 was used in a dead-end filtration apparatus (Sartorius).

Sand bed filter - Secondary-treated wastewater was fed in a pilot-scale sand filtration column (tertiary treatment) filled with 60 cm washed sand (2-4 mm), 10 cm gravel at the bottom, 5 cm gravel at the top and saturated with water. An average inlet concentration of 144 MNPs/µL was fed for a period of 10 d, during which effluent samples were collected over time to monitor the release of MNPs.

Flow cytometry – For FCM analyses, Attune NxT (ThermoFisher) was used and signals of scattering and fluorescences were collected for each MNP (Figure 2). Over 20,000 MNPs were counted for each sample to ensure statistically significant data. LOQ was established at 0.1 counts/µL.

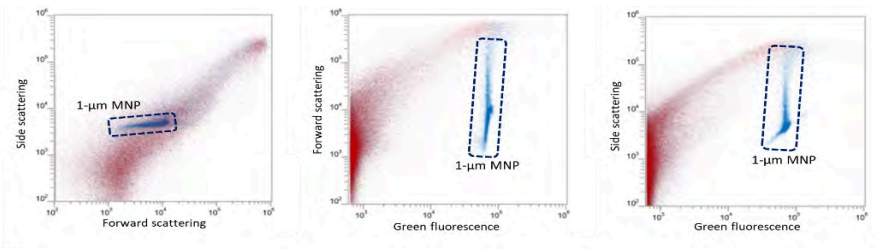

Figure 2. Cytograms of 1-µm MNPs in pre-settled wastewater (axes are expressed in arbitrary units).

3. Results

3.1. Removal of 1-µm MNPs in primary settling

Although primary sedimentation removed an average of 76% of TSS from raw wastewater (reducing from 338 ± 144 to 82 ± 44 mg TSS/L), spontaneous sedimentation of 1-µm MNPs after 2 h was poorly effective, with a removal efficiency of only 2.1 ± 1.4%. This result highlights that sedimentation alone cannot significantly contribute to the removal of 1-µm MNP from wastewater. Indeed, the density of polystyrene is 1.05 g/cm^3, similar to that of other plastic polymers, which makes MNPs highly stable in water and unable to settle. Furthermore, MNPs are negatively charged, resulting in electrostatic repulsion between particles. Bayarkhuu and Byun [3] observed high stability of polystyrene particles < 10 µm in deionized water, while better sedimentation occurred for particles > 50 µm.

3.2. Removal of 1-µm MNPs with CFS and alum

Aluminium sulphate, widely used in full-scale WWTPs for the chemical precipitation of phosphorus, can help separate MNPs from pre-settled wastewater. Adding alum at commonly applied dosages for P removal generates Al^{3+} cations that destabilize the negatively charged 1-µm MNPs, weakening the interparticle repulsive force, promoting attraction and floc formation, and thus enhancing precipitation by gravity.

At dosages of 0.3 - 3 mg Al^{3+}/L in pre-settled wastewater, the removal efficiency of 1-µm MNPs was 17.0 ± 7.0%. The initial MNP concentration of 1337 ± 18 MNP/µL decreased to 1107 ± 100 MNP/µL after CFS. With these dosages, the primary mechanism was the reduction of negative charges, while flocculation was not visually appreciable.

At a dosage > 3 mg Al^{3+}/L, the removal efficiency of 1-µm MNPs gradually increased. At dosages ranging from 12 to 30 mg Al^{3+}/L, the removal efficiency reached a maximum plateau of 98 ± 1.0%. With these dosages, floc formation occurred, improving the adsorption of MNPs onto the flocs.

3.3. Removal of 1-µm MNPs in activated sludge

The most significant reduction of 1-µm MNP concentrations occurred in the biological stages. The activated sludge showed an extremely high removal efficiency of 97.3 ± 0.9% due to the large and dense flocs that are particularly effective in capturing these MNPs with small volume and water-like density. The mechanisms involve enhanced adsorption, bioflocculation, entrapment and subsequent separation in the secondary clarifier. Activated sludge contains microbial extracellular polymeric substances (EPS), which play a role in the adsorption and flocculation of MNPs. Considering that the EPS content in activated sludge can vary depending on the carbon sources [4], behavior may differ between sludges. Additionally, the size and shape of the flocs affect the distribution of forces surrounding the particles, ultimately impacting flocculation on activated sludge.

3.4. Removal of 1-µm MNPs with filtration in tertiary/quaternary treatment

Membrane filtration – Dead-end filtration using membrane with a mesh of 1 µm was applied at lab-scale for the removal of 2.9-µm MNPs from secondary-treated wastewater. A removal efficiency of 22% was observed. The membrane's limited retention capacity was likely attributed to the unstable geometries and deformation of the fabric meshes when pressure was applied in the dead-end filtration, resulting in the enlargement and wrinkling of pores. In response to the deformed mesh, larger cavities formed, allowing 1-µm MNPs to escape into the effluent.

Sand bed filter – The capacity of the sand to progressively accumulate 2.9-µm MNPs was estimated to be at least 0.8 mg MNPs/kg of sand, equivalent to 6.7E+7 MNPs/kg of sand. Considering an average applied concentration of 144 MNPs/µL over a period of 10 days, the effluent concentration from the sand filter consistently remained below 2 MNPs/µL, resulting in a removal efficiency of 99%.

4. Comparison of removal in the main stages of WWTP

The results in Table 1 compare the removal of 1-μm MNPs across different stages of the WWTP.

The remarkable difference in removal efficiency between primary sedimentation of raw wastewater (2.1 ± 1.4%) and conventional activated sludge (97 ± 1%) underscores the substantial impact of solids concentration on 1-μm MNP removal. Indeed, the solids concentration varies by an order of magnitude: 5800 mg TSS/L in activated sludge compared to 338 mg TSS/L in raw wastewater. However, the 97% removal in activated sludge results in accumulation within the excess sludge produced by the plant [5], posing potential environmental risks during subsequent sludge disposal.

Table 1. Comparison of 1-μm MNPs removal efficiency across different stages of a WWTP (avg ± st.dev.). (*) result obtained with 2.9-μm MNPs.

WWTP stage	Details	1-μm MNP removal efficiency
Primary sedimentation	HRT = 2 h	2.1 ± 1.4%
CFS in pre-settled wastewater	0.3-3 mg Al^{3+}/L	17 ± 7%
CFS in pre-settled wastewater	12-30 mg Al^{3+}/L	98 ± 1%
Conventional activated sludge	6800 gTSS/L	97 ± 1%
Dead-end membrane filtration	1-μm mesh	22% (*)
Sand bed filtration	0.60 m depth	99%(*)

The application of the CFS process to wastewater significantly enhances the removal rate of 1-μm MNPs compared to gravity sedimentation alone. At dosages < 3 mg Al^{3+}/L, the CFS process achieves a removal rate of only 17 ± 7%, as the formed flocs are small in size and insufficiently efficient to capture and separate the MNPs during sedimentation. These flocs formed in wastewater during CFS are looser compared to those in activated sludge, resulting in lower efficiency than activated sludge. Indeed, when aggregates are too loose, their ability to adsorb and trap microplastics is reduced. Conversely, a greater quantity of dense flocs present in activated sludge or induced with coagulants at higher dosages of 12 - 30 mg Al^{3+}/L proves to be considerably advantageous for the removal of 1-μm MNPs.

References

[1] Tse, Y.-T., Lo, H.-S., Tsang, C.-W., Han, J., Fang, J.K.-H., Chan, S.M.-N., Sze, E.T.-P., 2023. Quantitative analysis and risk assessment to full-size microplastics pollution in the coastal marine waters of Hong Kong. Science of The Total Environment, 879, 163006, https://doi.org/10.1016/j.scitotenv.2023.163006.
[2] Caputo, F., Vogel, R., Savage, J., Vella, G., Law, A., Della Camera, G., Hannon, G., Peacock, B., Mehn, D., Ponti, J., Geiss, O., Aubert, D., Prina-Mello, A., Calzolai, L., 2021. Measuring particle size distribution and mass concentration of nanoplastics and microplastics: addressing some analytical challenges in the sub-micron size range. J. Colloid Interface Sci. 588, 401–417. https://doi.org/10.1016/j.jcis.2020.12.039.
[3] Bayarkhuu, B., Byun, J., 2022. Optimization of coagulation and sedimentation conditions by turbidity measurement for nano- and microplastic removal. Chemosphere 306, 135572. https://doi.org/10.1016/j.chemosphere.2022.135572.
[4] Wang, H., Qiu, C., Bian, S., Zheng, L., Chen, Y., Song, Y., Fang, C., 2023. The effects of microplastics and nanoplastics on nitrogen removal, extracellular polymeric substances and microbial community in sequencing batch reactor. Bioresour. Technol. 379, 129001. https://doi.org/10.1016/j.biortech.2023.129001.
[5] Gies, E.A., LeNoble, J.L., Noël, M., Etemadifar, A., Bishay, F., Hall, E.R., Ross, P.S., 2018. Retention of microplastics in a major secondary wastewater treatment plant in Vancouver, Canada. Mar. Pollut. Bull. 133, 553–561. https://doi.org/10.1016/j.marpolbul.2018.06.006.

Title: Evaluation of natural and industrial rejection streams on the performance of chloralkaline electrolyzers

Author(s): Iñaki Requena*, Mahmoud M. Gomaa, Rafael Granados, Carmen M. Fernández, Justo Lobato, Manuel A. Rodrigo

Department of Chemical Engineering, Faculty of Chemical Sciences and Technologies, University of Castilla-La Mancha, Ciudad Real, España, Inaki.Requena@uclm.es

Keyword(s): Waste valorization, chloralkaline electrolyzer, renewable energy, seawater, porewater, rejection water, desalination

Abstract

Nowadays, electrolysers are at TRL 8-9 which make this kind of technology competitive. Proton Exchange Membranes (PEM) electrolysers are based on the use of perfluoro sulfonic acid as main compound of the membrane, that allows the transport of the protons through its structure [1]. For these electrolysers, the main reactions that take place are:

$$\text{Anode side: } 2\ H_2O \rightarrow 2\ H^+ + 2\ OH^- + 2\ e^-$$
$$\text{Cathode side: } H^+ + 2\ e^- \rightarrow H_2$$

On the other hand, there are other type of electrolysers, called “Alkaline Water Electrolysers”, that are based on the use of anionic membranes to carry out the process properly. In contrast to PEM electrolysers, these ones allow the transport of anions, such as OH^-, through its structure [2]. Their reactions are slightly different from the PEM ones, and are the following:

$$\text{Anode side: } 2\ OH^- \rightarrow H_2O + 0.5\ O_2 + 2\ e^-$$
$$\text{Cathode side: } 2\ H_2O + 2\ e^- \rightarrow H_2 + OH^-$$

Besides of the differences of them, both require water of an extremely high purity to prevent damages of the membrane during performance. However, they can reach high efficiencies and the robustness of PEM electrolysers is very high. Conversely, for alkaline electrolysers robustness is their main drawback, as well as the need to supply high purity water to ensure proper performance.

In both cases, water undergoes different treatments, typically ending up with reversal osmosis. The rejection stream of these processes is an important issue for the technology, specially in the inlands of drought environments, where they can contribute to the salinization of groundwater reservoirs.

An alternative to these processes is the chlor-alkali electrolysis. It can work properly with low purity waters, and even the rejection streams of reversal osmosis can be used to make the system function in a correct way. So, the possibility of combining PEM electrolysis, which has a high TRL, with the chlor-alkali process, arises, so that the advantages of both techniques can be combined in one: operating the system with conventional aqueous streams while maintaining an optimal level of efficiency and

robustness [3]. The reactions occurring in a chlor-alkali electrolyzer are shown below:

Anode side: $2\ Cl^- \rightarrow Cl_2 + 2\ e^-$
Cathode side: $2\ H_2O + 2\ e^- \rightarrow H_2 + OH^-$

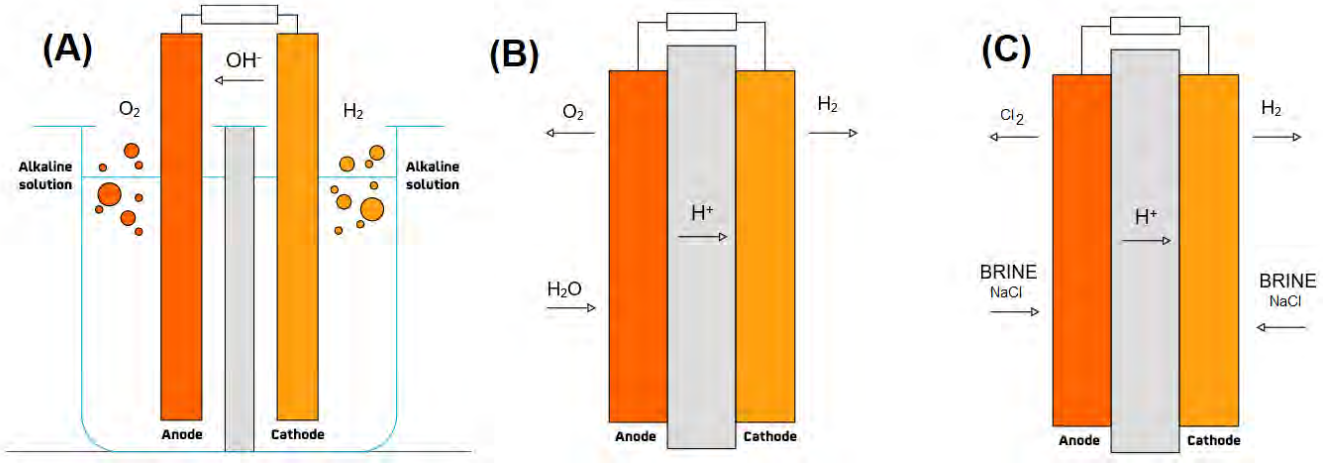

Figure 1. Different types of electrolysers. (A) Alkaline electrolyser; (B) PEM electrolyser; (C) Chlor-alkali electrolyser

This work is focused on the development of a chlor-alkali PEM electrolyzer, fed with synthetic laboratory-made brine solutions like those obtained in industrial desalination processes via reversal osmosis, to verify the feasibility of the combination of both electrolysis techniques and its potential for implementation and scaling.

A chlor-alkali laboratory made electrolyser was used in the system, paired with a 30 V power source and a multichannel peristaltic pump. The electrolyser was equipped with a commercial DSA as anode, with a titanium plate as cathode, both with 1 cm^2 area. A laboratory made PFSA membrane was casted to run the experiments. To contain both brine solutions and to store the gases generated (Cl_2 in the anode side and H_2 in the cathode one), two laboratory made gasometers were used [4].

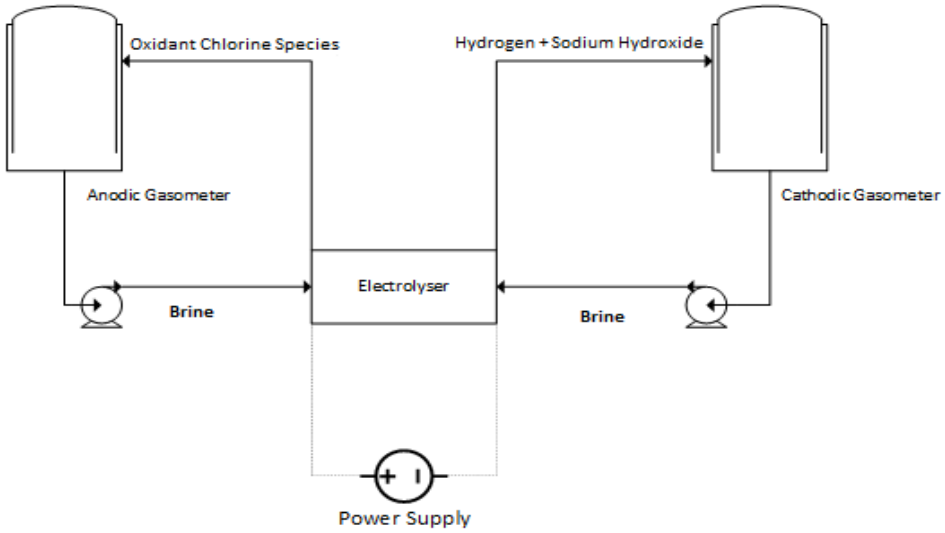

Figure 2. Scheme of the facility used to carry out the experiments.

The synthetic brine solutions were made using high purity sodium chloride, preparing three different concentrations: 60, 120 and 180 mg·L^{-1}. These solutions were fed to the electrolyser, and 200 mA·cm^{-2} was applied to it during 60 minutes at flowrate 300 mL·min^{-1}. The gases were collected in the gasometers and measured, to calculate the experimental efficiency of the system for hydrogen and chlorine species production.

Table 1 shows the hydrogen production efficiency for the different brine concentrations studied. In all cases, the efficiencies were higher than 85 % and a relationship between the concentration and the efficiency can not be obtained. Nevertheless, these values are similar to other ones obtained for a similar process [5].

Table 1. Efficiency values obtained for hydrogen after 60 minutes of operation.

Brine Solution (mg·L-1)	Theoretical H_2 (mg)	Measured H2 (mg)	Efficiency (%)
60	9	8.6	95
120	9.2	7.9	86
180	8.65	8.65	100

On the other hand, Table 2 collects the values of efficiency related with oxidant chlorine species (chlorine plus hypochlorous acid). It can be observed that, the mean efficiency to produce chlorine species is around 60-65 %, being superior to the ones obtained in industrial chlor-alkali process, where it's around 40 % [6].

Table 2. Efficiency values obtained for Oxidant Chlorine Species (OCS) after 60 minutes of operation.

Brine Solution (mg·L-1)	Theoretical OCS (mg)	Measured OCS (mg)	Efficiency (%)
60	315	208	65
120	324	194	60
180	304	230	75

This implies that this type of process can be scaled up to verify that efficiency remains higher than in industrial chlor-alkali processes, thereby improving the technology and granting it application on larger scales. Furthermore, having achieved such high yields, it is particularly interesting to use natural waters, such as from rivers, seas, or aquifers, as well as reverse osmosis reject streams water, since using water of purities lower than those required for a conventional PEM electrolyzer has not posed a subsequent problem.

Acknowledgements

The authors acknowledge the support from the Junta de Comunidades de Castilla-La Mancha and the EU-FEDER for financial support through the SER4WINE Project (SBPLY/21/180501/000075), the Government of Spain through the TED2021-131630B-I00 Project funded by the MCIN/AEI, and the Internal Research Fund from UCLM (Ref. 2022-GRIN-34344).

References

[1] Wang, T., Cao, X., & Jiao, L. (n.d.). PEM water electrolysis for hydrogen production: fundamentals, advances, and prospects. https://doi.org/10.1007/s43979-022-00022-8

[2] Van Haersma Buma, B. N. D., Peretto, M., Matar, Z. M., & Van De Kaa, G. (2023). Towards renewable hydrogen-based electrolysis: Alkaline vs Proton Exchange Membrane ☆. Heliyon, 9, 2405–8440. https://doi.org/10.1016/j.heliyon.2023.e17999

[3] Hubbard, D. O. (1952). The Chlor-Alkali Industry, 1902–52. Volume 99, Issue 11, Pages 307C - 309C, 99(11), 307C. https://doi.org/10.1149/1.2779621

[4] Kuhnert, E., Heidinger, M., Sandu, D., Hacker, V., & Bodner, M. (348 C.E.). Analysis of PEM Water Electrolyzer Failure Due to Induced Hydrogen Crossover in Catalyst-Coated PFSA Membranes. Volume 13, Issue 3, 13(3). https://doi.org/10.3390/membranes13030348

[5] Erden, M., & Karakilcik, M. (2024). Experimental investigation of hydrogen production performance of various salts with a chlor-alkali method. International Journal of Hydrogen Energy, 52, 546–560. https://doi.org/10.1016/J.IJHYDENE.2023.08.049

[6] Requena-Leal, I., Carvela, M., Fernández-Marchante, C. M., Lobato, J., & Rodrigo, M. A. (2024). On the use of chlor-alkali technology to power environmental electrochemical treatment technologies. https://doi.org/10.1016/j.coelec.2024.101461

Title: From Aerobic Granular Sludge (AGS) to Partial Nitritation Granular Sludge (PN-GS)

Author(s): Jan Pietro Czellnik*[1,2], Julio Pérez [2], Tommaso Lotti [1]

[1]*Department of Civil and Environmental Engineering, University of Florence, Florence, Italy, janpietro.czellnik@unifi.it, tommaso.lotti@unifi.it*
[2]*Department of Chemical, Biological and Environmental Engineering, Engineering School, Universitat Autònoma de Barcelona, Barcelona, Spain, Julio.Perez@uab.cat*

Keyword(s): Partial Nitritation (PN), Granular Sludge (GS), Autotrophic Nitrogen removal, biorefineries

Abstract

In this study, the possibility of converting conventional Aerobic Granular Sludge (AGS) biomass into autotrophic Partial Nitritation-Granular Sludge (PN-GS) was investigated. The ultimate goal of the research is to achieve a stable partial nitritation system for mainstream conditions (Cin=50 mg NH4-N/L) by combining the numerous advantages of granular biomass (compactness of systems, higher biomass concentrations, and enhanced removal rates [1]) with those of autotrophic biomass for nutrient removal (no need of organic carbon for denitrification, low sludge production and oxygen savings [2]). The experimentation lasted 27 weeks showing a successful startup of a PN-GS process using AGS as inoculum. Following the removal of COD from the influent, a reduction in granule size was observed, accompanied by the loss of 79% of the system total solids in the whole period, but remarkably maintaining the granular structure of the biomass. After an initial period of adaptation to the PN process, an effluent with NO2-N/NH4-N ratio of 1.02±0.2 g/g was achieved, thus suitable for subsequent anaerobic ammonia oxidation (anammox) treatment. The activity of Nitrite Oxidizing Bacteria (NOB) was successfully repressed resulting in effluent nitrate concentrations of 2.3±1.0mg N/L.

Introduction

In recent years, the pursuit of energy self-sufficiency in wastewater treatment has emerged as a pressing concern. Historically, achieving this objective seemed unattainable due to the large use of influent organic carbon in the denitrification processes. The discovery of Anammox microorganisms has transformed this landscape, providing an autotrophic pathway for N removal and enabling the maximization of organic carbon capture for energy recovery. Although extensively utilized for the side-stream treatment of digestate supernatant, characterized by high ammonium concentrations and temperatures, the adoption of the autotrophic combined process Partial Nitritation-Anammox (PN-A) in mainstream conditions faces challenges due to the proliferation of NOB during long-term operation [3]. To address this problem, granular morphology offers a competitive advantage over flocs in outcompeting NOB, allowing the establishment of oxygen and substrates gradients, which enhances the stratification of AOB over NOB [3]. However, forming such granular biofilms from a conventional active sludge is time-consuming and present many drawbacks, posing a challenge to research and full-scale system development. In this study, we address this challenge by utilizing AGS as inoculum. AGS, being widely applied in full-scale systems, ensures the availability of an inoculum to speed up PN-GS formation.

Materials and methods

The experimentation was carried out within a laboratory-scale Granular Sequencing Batch Reactor (GSBR) with a 5L useful volume, operated at a 50% Volumetric Exchange Ratio (VER), equipped with mechanical mixing, pH, and Dissolved Oxygen (DO) probes. Operative temperature was 19.8±0.9°C throughout the test. The experimental activity comprised three distinct phases:
i) Aerobic granular sludge phase (AGS): lasted 10 weeks. During this phase, the biomass was cultivated as conventional AGS aimed at removing organic carbon, nitrogen, and phosphorus. However, the primary aim was biomass growth for subsequent experimental phases. Cycle time = 6 h, Hydraulic Retention Time (HRT) = 12 h, Organic Loading Rate (OLR) = 0.8 gCOD/L*d, Nitrogen Loading Rate (NLR) = 0.1 gN/L*d, and Phosphorus Loading Rate (PLR) = 0.014 gP/L*d, DO<1ppm, pH=6.84±0.15.
ii) Transitionary partial nitritation phase (PN.1): lasted 10 weeks. Started with the complete removal of COD from the influent, to promote the decay of the heterotrophic fraction and the enrichment of Ammonium Oxidizing Bacteria (AOB). During this phase, reactor parameters were gradually adjusted to achieve a NH4/NO2 ratio of one in the effluent. The system's response was closely observed, and once stabilized for 2 weeks, we proceeded to the next phase. Cycle time 3h, HRT=6h, NLR= 0.4gN/L*d, Cin=100 mg NH4-N/L, DO=4-0.6ppm, pH=6.5-7.3 (or 6.82 ± 0.16).
iii) Stabilized partial nitritation (PN.2): lasted 7 weeks. In this phase, the inlet ammonium concentration and cycle duration were halved to mimic mainstream conditions. Cycle time 1.5h, HRT=3h, NLR=0.4 gN/L*d, Cin=50 mg NH4-N/L, DO<1 ppm, pH= 6.8-7.2 (or 6.9 ± 0.13).
The analyses were performed using commercial Hach LCK kits (314, 303, 348, 350) and the Dionex Integrion HPIC anionic chromatograph by Thermo Fisher. TSS and VSS concentrations were determined according to APHA 1998 standard procedure while granulometric analyses were conducted using Image Pro Plus software.

Results and discussion

In this section the performance of the biological process during the distinct operative phases are reported, followed by a focus on the evolution of biomass characteristics.

Overall reactor performance

During the AGS phase, organic matter (data not shown), phosphorus, and all forms of nitrogen were successfully removed (see a monitored cycle in Figure 1). Interestingly, nitrate accumulation in the bulk was not detected during the aerobic phase, indicating a probable nitrite-driven denitrification, resulting in carbon and oxygen savings. Moreover, this result indicates a relatively higher abundance of AOB compared to undesirable NOB, which is likely a key factor for the results obtained in subsequent phases.

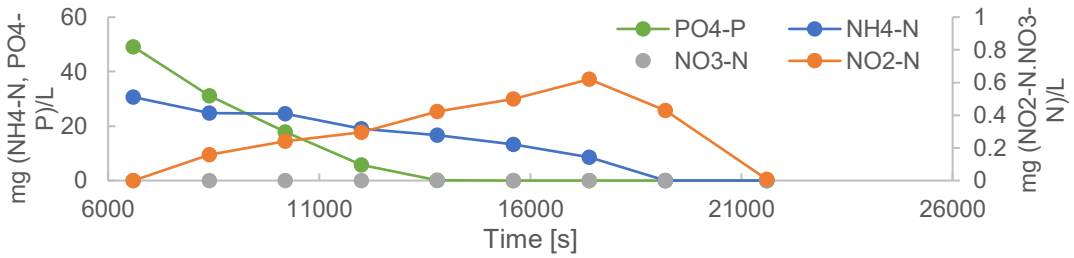

Figure 1: Nutrient concentrations in the bulk during a typical aerobic phase of an AGS cycle

Partial Nitritation was targeted after suppression of the organic matter from the effluent, the results obtained (Figure 2 and Table 1) indicate that during Phase PN.1 NOB repression was not fully achieved, which resulted in significant fluctuations during the initial weeks, and lower concentrations of total

nitrogen in the effluent were observed, likely attributed to heterotrophic denitrification processes using the COD resulting from the progressive decay of the heterotrophic fraction of biomass as e-donor.
As expected, higher rates of ammonium conversion to nitrite are associated with higher concentrations of nitrate in the effluent, as the selective pressure on NOB decreases (i.e., reduced ammonium concentrations limit AOB activity, allowing more oxygen availability to NOB, and increased nitrite concentrations provide more substrate for NOB). Past 8 weeks progressively adjusting parameters, the system was successfully stabilized. After an additional 2 weeks, transition to the PN.2 phase was made simply by halving the inlet concentrations and doubling the hydraulic load to maintain a constant NLR (0.4gNH4-N/L*d). A notable improvement in the reactor performance during the PN.2 phase was observed (Fig. 2), with stable operation and a consistently constant ratio of NO2-N to NH4-N in the effluent. During this phase, characterized by low DO concentrations and a nearly constant effluent ammonium concentration, it was possible to repress the metabolism of Nitrite Oxidizing Bacteria (NOB), as indicated by the extremely low concentrations of nitrate in the effluent (2.3 ± 1.0 mg NO_3^--N/L). This achievement addresses one of the most critical objectives for this type of experimentation and for PN systems in general.

Table 1: Effluent Nitrogen compounds summary for Transitionary PN (PN.1) and Stabilized PN (PN.2)

	Total N	NH4-N	NO2-N	NO3-N	N. samples	NO2-N/NH4-N
	Concentration ± Standard deviation (mg N/L)				//	dimensionless
PN.1	86.7 ± 5.2	37.6 ± 10.9	41.9 ± 10.5	7.2 ± 2.9	27	1.27 ± 0.6
PN.2	47.4 ± 1.6	22.5 ± 2.4	22.5 ± 1.9	2.3 ± 1.0	20	1.02 ± 0.2

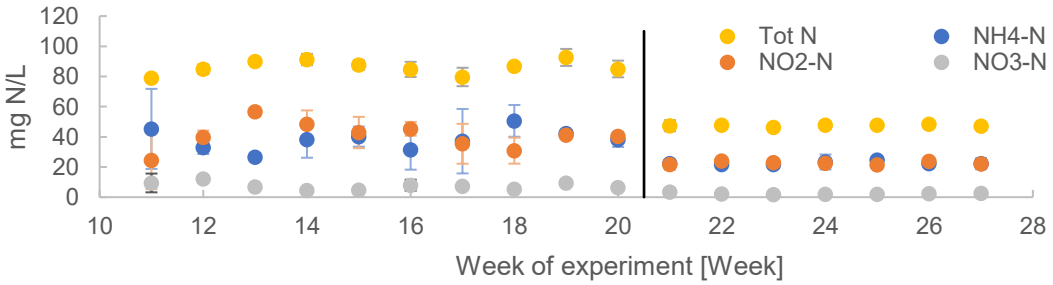

Figure 2: Weekly effluent quality for phase PN.1 and PN.2

Biomass evolution: total solids and morphological properties

The phase-specific total solids trends in biomass evolution are reported in Figure 3. In the AGS phase, a rapid biomass increase is evident, reflected by a rise in solids concentrations from 1.63 to 8.81 gTSS/L over 10 weeks. Moving to PN.1, the removal of organic carbon triggers a significant decay in the heterotrophic fraction, resulting in an approximate loss of 77% of total solids. Transitioning to PN.2, after 10 weeks, the system stabilizes with solids concentration setting slightly below 2 gTSS/L. Additionally, during the AGS phase, the ratio of volatile solids to total solids was found to be 89.0±1.6 % gVSS/gTSS (data not shown). After transitioning to partial nitritation, this value increased even further, reaching 97.5±0.6 % gVSS/gTSS. This can be attributed to the disappearance of heterotrophic accumulating microorganisms and their internal reserves of inorganic polymers, such as polyphosphate chains for Phosphorus Accumulating Organisms (PAO), which typically represent a significant portion of the total cell solids and the dissolution of phosphate-rich minerals usually precipitating in PAO-enriched

biomass[4].

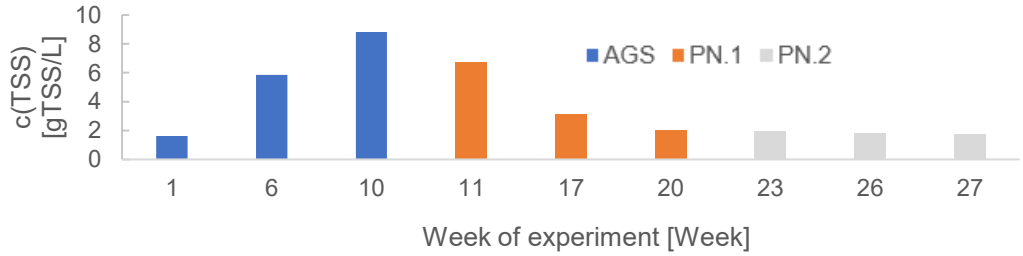

Figure 3: Concentration of total solids over time, data expressed in weeks for an easier comparison.

Regarding the morphological changes of the biomass during the experimentation, Figure 4 shows two comparative photos of the biomass before the transition and at the end of the experiment. A reduction in granule size is visible to the naked eye, with a decrease in the average diameter from 1067µm on week 10 to 763µm on week 25. Despite the reduction in granule size, the sedimentation properties of the biomass remained good, with the following values in terms of Sludge Volume Index (SVI) during PN.2 phase: SVI5=48±9 mL/gTSS, SVI30=49.6±9.1 mL/gTSS, and SVI5/SVI30=96.8±0.7%.
Additionally, moving from AGS to PN, a shift in color towards orange tones was observed, typical color of sludges enriched in AOB, suggesting a significant change in the microbial composition of the biomass. Biomass for metagenomic analysis was sampled periodically during the experiment. However, bioinformatics analysis is still ongoing, and results will be presented at the conference.

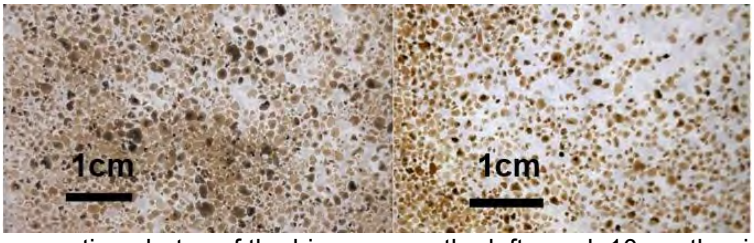

Figure 4: Comparative photos of the biomass: on the left, week 10; on the right, week 27

In summary, this study underscores the potential of converting conventional AGS into PN-GS, offering a promising approach for faster and more effective startup in the context of full-scale wastewater treatment. By preserving the granular structure during the transition to an autotrophic medium and achieving a favourable nitrite to ammonium ratio in the effluent, this method demonstrates promise for implementation in a PN-A system for complete autotrophic nitrogen removal from municipal wastewater. Furthermore, the widespread availability of AGS from full-scale treatment plants makes the entire procedure easily applicable, providing a practical advantage for future research and potential industrial application and facilitates the scalability and adoption of PN-GS technology, paving the way for sustainable and efficient wastewater treatment practices on a larger scale.

This research was funded by EU-PNRR as PRIN 2022 (N4En project, CUP: B53D23005590006)

References

[1] M. K. De Kreuk, J. J. Heijnen, and M. C. M. Van Loosdrecht, “Simultaneous COD, nitrogen, and phosphate removal by aerobic granular sludge,” *Biotechnol Bioeng*, vol. 90, no. 6, pp. 761–769, (2005).
[2] Z. Hu, T. Lotti, M. van Loosdrecht, and B. Kartal, “Nitrogen removal with the anaerobic ammonium oxidation process,” *Biotechnology Letters*, vol. 35, no. 8. pp. 1145–1154, (2013).
[3] X. Juan-Díaz, J. Carrera, and J. Pérez, “Ammonium oxidation activity promotes stable nitritation and granulation of ammonium oxidizing bacteria,” *Journal of Water Process Engineering*, vol. 45, (2022).
[4] C. Tarayre *et al.*, “Characterisation of phosphate accumulatingorganisms and techniques for polyphosphatedetection: A review,” *Sensors (Switzerland)*, vol. 16, no. 6. MDPI AG, (2016).

Title: An overview of the available strategies for the start-up process of a MABR

Author(s): Nicolas Hernandez-Alcayaga*[1], Giuseppe Campo *[1], Alberto Cerutti *[1], Mariachiara Zanetti *[1], Barbara Ruffino *[1]

[1] *Department of Environment, Land and Infrastructure Engineering, Politecnico di Torino, Torino, Italy, nicolas.hernandez@polito.it*

Keyword(s): Membrane, Biofilm, Nitrogen removal, Nitrification.

Introduction

Traditional wastewater treatment processes such as Conventional Activated Sludge (CAS) are characterized by their substantial energy requirements, primarily for aeration, and the generation of pollutants such as nitrous oxide (N2O) [1]. Given the current need for both economic and environmental efficiency, underscored by the impact of energy generation and greenhouse gas emissions on climate change, there exists a compelling necessity to explore alternatives for enhancing wastewater treatment processes.
Membrane Aerated Biofilm Reactor (MABRs), although is not a recent technology, has recently elicited considerable interest owing to its ability to augment energy efficiency in biological wastewater treatment and mitigate N2O emissions. Within MABRs, membranes serve to facilitate the transfer of oxygen essential for the oxidation of ammonium (NH4) within the biofilm adhered to the membrane surface. This biofilm engenders a partition, establishing distinct aerobic (membrane-biofilm) and anaerobic (biofilm-bulk liquid) sections, the latter capable of supporting denitrification of nitrate (NO3) to N2, for which an anoxic medium is necessary. Therefore, due the effect of using the membrane together with the biofilm, concentration of pollutants such as NH4 and Chemical Oxygen Demand (COD) in the biofilm decrease in an opposite direction than O2, generating what is called a counter-diffusion system [2].
Thanks to its enhanced oxygen transfer rate, MABR can achieve a noteworthy reduction, up to 90%, in aeration energy compared to conventional wastewater treatment methodologies [3]. The bubbleless aeration facilitated by the membrane enables the attainment of removal efficiencies of NH4 approaching 100% and COD nearing 95% [4]. Moreover, wastewater is responsible of 1.3% of the global emissions of greenhouse gases [5] and some common technologies such as CAS can release 0.01–90.75 % of the nitrogen load of the wastewater in the form of N2O [6]. It is important to consider that N2O global warming potential is 298 kg CO2e/ kg N2O [7].
Despite the growing interest in MABR, as evidenced by an increase in publications in recent years, there is still a lack of consensus and not clear information regarding diverse strategies for the start-up phase. This is particularly relevant due that the start-up phase is pivotal in establishing optimal conditions for biofilm development and can take a long time to complete. Consequently, this study aims to be a comprehensive overview of prevailing strategies pertinent to the initiation and optimization of MABRs.

Key parameters affecting a MABR process

The cultivation of biofilm on the membrane of a MABR necessitates careful consideration of optimal growth conditions for both Aerobic Oxidizing Bacteria (AOB) and Anaerobic Oxidizing Bacteria (AnOB). Extensive investigations have elucidated that the pH range capable of supporting nitrifying bacteria (AOB) growth falls within 6.5 to 8.5, whereas denitrifying bacteria (AnOB) thrive within a narrower pH range of 7.0 to 8.0 [8]. The temperature can also affect the microbial community structure changing the amount of detached biofilm or lead to out-competition of NOB, AOB and

AnOB [9]. The density of biofilm also plays a critical role in MABR system performance and is influenced by the Carbon/Nitrogen (C/N) ratio [10, 11]. Imbalances in DO levels within the biofilm ecosystem can significantly impact bacterial composition of biofilm and subsequent bioremediation processes. Prior studies have established the ideal dissolved oxygen (DO) concentrations for nitrifying and denitrifying bacteria to be 0.3–4.0 mg/L and 0.5–1.0 mg/L, respectively [8].

Strategies for start-up

The start-up phase of a MABR is critical for its proper functioning, yet it remains an area with limited information and studies despite extensive research on MABR operation at both laboratory and pilot scales. This phase is pivotal in establishing the optimal conditions for biofilm development and ensuring efficient pollutant removal. Various strategies have been explored to expedite and optimize the start-up phase, each offering unique insights into enhancing reactor performance. Nevertheless, the parameters reported by the various studies examined in this paper are not consistent, making it difficult to compare both the design processes and the initial operations of the reactors (Table 1).

Table 1. Different strategies for the start-up phase with the reported parameters and start-up time.

Strategy	Parameters reported	Start-up time reported	Source
MABR (SND)	C/N, NH4, COD and TN removal	57 days	[10]
SNPDR	NH4, TIN, TP and COD removal	110 days	[12]
H-MABR (SND)	COD, TN, NH4 and NO3 removal	45 days	[11]
MLE-MABR	NR, OTE, OTR	21 days	[13]
Anammox	N-Species concentration	120 days	[14]
SNAP	NLR and TN removal	Over 80 days	[15]

The study realized by Zhong et al. (2023), used return-activated sludge and after a 7-day period, the reactor transitioned to continuous feeding mode for 30 days to facilitate biofilm formation. After 20 additional days, the reactor achieved stable operation, exhibiting total nitrogen removal exceeding 60% and COD removal over 90% [10]. The study by He et al. (2022), focused on Simultaneous Nitrification, Denitrification, and Phosphorus Removal (SNDPR) using anaerobic/oxic/anoxic (A/O/A) mode. They operated the reactor on a 6-hour cycle comprising 120 minutes of anaerobic phase, 90 minutes of aerobic phase, 120 minutes of anoxic phase, and 30 minutes of settling phase. The operation process was divided into two stages based on NH4+-N removal efficiencies. The initial start-up stage (day 1–15) witnessed fluctuating effluent NH4+-N levels, indicating microbial adaption and enrichment. In contrast, the subsequent stable stage (day 16–110, phase II) demonstrated consistent and high removal rates for NH4 reaching up to 98% [12]. That study underscores the effectiveness of the A/O/A mode for SNDPR, highlighting the importance of microbial adaption during the start-up phase for achieving stable and efficient nutrient removal in wastewater treatment systems.

A study using Hybrid MABR (H-MABR) and employing a two-stage simultaneous nitrification-denitrification (SND) process involved intermittent water inflow during the initial phase (days 1-17) followed by continuous inflow and outflow (days 18-25). After optimizing the COD/N ratio, the reactor achieved significant removal efficiencies: TN% = 71.87, COD% = 79.92, and NH4% = 93.79 during the optimization phase (days 26-45) [11]. In a pilot plant comprising two reactors which utilize the Modified Ludzack-Ettinger–Membrane Aerated Biofilm Reactor (MLE-MABR) configuration and sludge was employed as the seed material. The first reactor operated with a High C/N ratio, while

the second reactor maintained a low C/N ratio and it was observed that a nitrifying biofilm developed within just three weeks after seeding the MABR with municipal nitrifying sludge [13].
There are different studies that employ Anammox according to different configurations and treatment processes. This leads to variations in operational performance and challenges, primarily because this method avoids the use of COD and relies solely on inorganic means to oxidize ammonium. The study by Sun et al. (2009), explored nitrification-denitrification followed by Anammox, employing two inoculation strategies (continuous Anammox inoculation strategy and sequential Anammox inoculation strategy), to assess their efficacy in achieving nitrogen removal. Challenges such as nitrite competition were identified, influencing the observed nitrogen removal efficiencies that did not exceed the 20% after 120 days [14]. Using Single-stage Nitrogen Removal using Anammox and Partial Nitritation (SNAP) method there was observed a gradual stabilization over 80 days in the first period using a Nitrogen Loading Rate (NLR) = 50 g/m3d and obtaining a total nitrogen removal of 78% [15].

Conclusion and future perspectives

The start-up phase of MABRs remains a critical yet understudied aspect despite extensive research on MABR operation. This phase is pivotal in establishing optimal conditions for biofilm development and efficient pollutant removal. Various strategies, such as those involving return-activated sludge seeding, SNDPR using A/O/A mode, and H-MABR employing SND processes, have been explored to enhance reactor performance during start-up indicating that start-up is possible in less than 50 days. Studies employing Anammox reveal diverse operational performances and challenges encountered, including nitrite competition and limitations in COD removal efficiency.
The advancement of MABR technology in wastewater treatment is based on continued research, collaboration, and the standardization of methodologies. Refining start-up protocols is crucial to unlocking the full potential of MABRs in pollutant removal and process optimization. Standardized methodologies will facilitate accurate comparisons between studies, enabling researchers to identify best practices and further enhance MABR performance. Regarding reactor design, parameters such as NLR and Organic Loading Rate OLR provide essential information and could be crucial for making appropriate comparisons between different reactor designs. Additionally, to evaluate and compare the efficiency of various strategies, Oxygen Transference Efficiency (OTE) and Oxygen Transference Rate (OTR) are suitable for understanding the oxygen consumption of the system, being a good basis for studying energy consumption or bacterial activity. Finally, NH4 and COD removal efficiencies are essential to compare the removal potential of a MABR.

References

[1] Martin, K. J., & Nerenberg, R., “The membrane biofilm reactor (MBfR) for water and wastewater treatment: Principles, applications, and recent developments.”, *Bioresource Technology, 122*, 83–94, (2012).
[2] Nerenberg, R., “The membrane-biofilm reactor (MBfR) as a counter-diffusional biofilm process.” *Current Opinion in Biotechnology,* 38, 131–136, (2016).
[3] Werkneh, A. A., “Application of membrane-aerated biofilm reactor in removing water and wastewater pollutants: Current advances, knowledge gaps and research needs - A review.”, *Environmental Challenges, 8,* (2022).
[4] Li, M., Li, Y., Wang, N., Li, T., Guo, H., Wu, Z., Zhang, P., Wang, B., & Li, B., “Achieving efficient nitrogen removal in a single-stage partial nitrification-anammox-partial denitrification (PN/A/PD) membrane aerated biofilm reactor (MABR).”, *Journal of Water Process Engineering*, 49, (2022).
[5] Gu, Y., Li, Y., Yuan, F., & Yang, Q., “Optimization and control strategies of aeration in WWTPs: A review.”, *Journal of Cleaner Production*, 418, (2023).
[6] Yang, R., & Yuan, L.,”Generation, emission reduction/utilization, and challenges of greenhouse gas nitrous oxide in wastewater treatment plants – A review.”, *Journal of Water Process Engineering,* 53, (2023).
[7] Parravicini, V., Svardal, K., & Krampe, J., “Greenhouse Gas Emissions from Wastewater Treatment Plants.”, Energy *Procedia*, *97*, 246–253, (2016).
[8] Li, X., Bao, D., Zhang, Y., Xu, W., Zhang, C., Yang, H., Ru, Q., Wang, Y. F., Ma, H., Zhu, E., Dong, L., Li, L., Li, X., Qiu, X., Tian, J., & Zheng, X. “Development and Application of Membrane Aerated Biofilm Reactor (MABR)—A Review.”, *Water (Switzerland),* 15, 3, (2023).

[9] Clements, E., Nahum, Y., Pérez-Calleja, P., Kim, B., & Nerenberg, R., "Effects of temperature on nitrifying membrane-aerated biofilms: An experimental and modeling study.", *Water Research*, *253,* (2024).
[10] Zhong, H., Dong, L., Tang, Y., Qi, L., & Wang, M. "The C/N Ratio's Effect on a Membrane-Aerated Biofilm Reactor (MABR): COD and Nitrogen Removal, Biofilm Characteristics, and Microbial Community Structure.", Water *(Switzerland)*, *15,* 24, (2023).
[11] Liu, H., Li, L., Ye, W., Ru, L., Liu, G., Peng, X., & Wang, X., "Nitrogen removal from low COD/N interflow using a hybrid activated sludge membrane-aerated biofilm reactor (H-MABR).", *Bioresource Technology*, *362,* (2022).
[12] He, Q., Yan, X., Fu, Z., Zhang, Y., Bi, P., Mo, X., Xu, P., & Ma, J., "Rapid start-up and stable operation of an aerobic/oxic/anoxic simultaneous nitrification, denitrification, and phosphorus removal reactor with no sludge discharge.", *Bioresource Technology,* 362, (2022).
[13] Silveira, I. T., Cadee, K., & Bagg, W. "Startup and initial operation of an MLE-MABR treating municipal wastewater.", *Water Science and Technology*, *85*(4), 1155–1166, (2022).
[14] Sun, S-P., Pellicer i Nàcher, C., Terada, A., Lackner, S., & Smets, B. F. "Start-up strategies of membrane-aerated biofilm reactor (MABR) for completely autotrophic nitrogen removal.", Proceedings of the 2nd IWA Specialized Conference on Nutrient Management in Wastewater Treatment Processes, 633-639, (2009).
[15] Augusto, M. R., Camiloti, P. R., & Souza, T. S. O., "Fast start-up of the single-stage nitrogen removal using anammox and partial nitritation (SNAP) from conventional activated sludge in a membrane-aerated biofilm reactor.", Bioresource *Technology*, *266*, 151–157, (2018).

Title: Removal of BTEX from water using KOH activated hydrochar produced by hydrothermal carbonization of municipal solid waste

Author(s): C. Caretti[1], I. Ducci[1], R. Campo[1], B. Charnnok[2], M. Puccini[3], F. Barontini[3], S. Dugheri[4], R. Gori[1]

[1] Department of Civil and Environmental Engineering, University of Florence, Via di Santa Marta 3, 50139 Florence, Italy, cecilia.caretti@unifi.it, iacopo.ducci@unifi.it, riccardo.campo@unifi.it, riccardo.gori@unifi.it
[2] Department of Interdisciplinary Engineering, Faculty of Engineering, Prince of Songkla University, Hat Yai District, Hat Yai, Songkhla 90110, Thailand, boonya.c@psu.ac.th
[3] Department of Civil and Industrial Engineering, University of Pisa, Largo Lucio Lazzarino, Pisa, Italy, monica.puccini@unipi.it, federica.barontini@unipi.it
[4] Experimental and Clinical Medicine Department, University of Florence, Largo Brambilla 3, 50134, Florence, Italy, stefano.dugheri@unifi.it

Keyword(s): Activated hydrochar, Adsorption, BTEX, Chemical activation, Hydrothermal carbonization, Municipal solid waste

Abstract

Activated carbon, widely available in the market, is predominantly derived from coal feedstock. However, with concerns over coal resource depletion and environmental impacts, there is a notable shift towards utilizing biomass or waste feedstock. Residual waste obtained from mechanical treatment (MT) comprises carbon-rich materials like paper, wood, plastic, and textile. This has become an increasingly attractive option as it offers a potentially cost-effective feedstock for activated carbon production. Moreover, utilizing this residual waste can substantially reduce the volume destined for landfill disposal or incineration. Thermochemical techniques play a crucial role in converting carbon feedstock into renewable materials and fuels, with hydrothermal carbonization (HTC) gaining increasing attention in recent years [1, 2].
This paper shows the results of an experimental study aimed at converting municipal solid waste under-screen fraction into porous carbon through integrative process of HTC and chemical activation of hydrochar with KOH. The activated hydrochar (AHC) was then applied as an adsorbent for Benzene, Toluene, Ethylbenzene, and Xylenes (BTEX) removal [3]. The optimum conditions of hydrochar activation for BTEX removal were investigated using Response Surface Methodology (RSM).
The solid waste sample was taken from the under screen of the MT located at Scapigliato (Rosignano Marittimo, Livorno). The HTC experiments were performed using 5% solid to liquid ratio (wt/wt), at 190 °C for 60 min (pressure 11.5 bar) in the Parr 4566 300 ml High Pressure SS Stirred Reactor. After the reaction, the hydrochar was separated through filtration and dried at 105 °C for 12 h. The activation of hydrochar with KOH impregnation was performed to enhance the adsorption of BTEX [4, 5].
The trials were performed according to the design of experiment (DoE) method based on central composite design following RSM approach [6]. AHC carbon content, surface area and BTEX adsorption capacity were used as the evaluation indexes, while the activation temperature (500°C; 600°C; 700°C) and KOH:HC impregnation ratio (0.5; 1; 1.5) were taken as the influencing factors (see Table 1).

Table 1. Design matrix for hydrochar activation

Run	Activation temperature (°C)	KOH: HC impregnation ratio
1	500	0.5
2	700	1.5
3	700	1.0
4	700	0.5
5	600	0.5
6	600	1.0
7	600	1.5
8	600	1.0
9	500	1.5
10	500	1.0

The activation was performed in a fixed-bed reactor, kept under inert atmosphere heated up to the designed temperature (500°C; 600°C; 700°C) by 10°C/min. The samples were kept at the designed temperature for 60 min. The reactor was then cooled down and the samples were washed before being subjected to adsorption test and physicochemical characterization.
The hydrochar (HC) and the activated hydrochar (AHC) were used and compared as adsorbents. A commercial activated carbon (CAC) (-20+40 mesh, CAS: 7440-44-0, Thermo Scientific) was used for the validation of the adsorption test method.
The chemical compositions of hydrochar and activated hydrochar were quantified by Thermogravimetric analysis (TGA Q 500 TA Instruments, USA), and HC and AHC carbon content was determined by a CHN analyzer (TruSpec CHN, Leco). The total specific surface area, external surface area (STSA), pore volume and micropore surface area of hydrochar, activated hydrochar and commercial activated carbon wern,e determined using the Brunauer Emmett Teller isotherm (BET) method. The functional groups present in the HC and AHC were identified using Fourier Transform Infrared Spectroscopy (FTIR), using FTIR spectrometer (FT/IR-4100, JASCO). The surface morphology of the HC and AHC was characterized using scanning electron microscopy (SEM) (Quanta FEG 450, FEI).
Batch adsorption experiments were carried out by adding 0.5 μL of BTEX stock solution to a 5 mL tap water volume in a 20-mL glass vial, resulting in initial concentrations of 21.75 mg/L for benzene (B), 21.50 mg/L for toluene (T), 21.50 mg/L for ethylbenzene (E), and 21.75 mg/L for xylene (X). The set initial concentration of the adsorbent was 4000 mg/L. All experiments were conducted at least in duplicates, and average values were reported. The glass vials were placed in a shaker at 23 °C and 300 rpm for 48 hours. Subsequently, the BTEX concentrations were measured using a gas chromatograph mass spectrometer (GC-MS).
According to the chemical characterization the average value of AHC yield and carbon content are respectively 28.92% (ranging from 17.02% to 35.78%) and 15.68% (ranging from 7.52% to 24.32%).
The change in the structure of the hydrochar is highlighted by the surface area after the HC activation (see Table 2).

Table 2. Physical characteristics of hydrochar and activated hydrochar

Sample	BET surface area (m^2/g)	Pore volume (cm^3/g)	STSA (m^2/g)	Micropore surface area* (m^2/g)
CAC	724.8±0.7	0.72	395.6	329.1

HC	2.2±0.2	0.25	-	-
AHC-1	228.7±0.5	0.24	140.5	88.2
AHC-2	587.3±1.1	0.52	213.8	373.6
AHC-3	479.9±0.6	0.43	126.5	353.4
AHC-4	383.6±0.5	0.37	104.9	278.7
AHC-5	236.9±0.1	0.25	78.3	158.6
AHC-6	324.6±0.3	0.30	100.5	224.1
AHC-7	432.2±0.4	0.35	115.3	316.9
AHC-8	440.7±0.4	0.36	76.8	363.9
AHC-9	208.2±0.2	0.25	65.3	142.9
AHC-10	146.4±0.5	0.23	74.6	71.8

*The micropore surface area, estimated by the difference of the total and the external surface area, is:
S micropore =S BET - STSA

The change in the structure is also evident from the FTIR analysis (Figures 1). The increase in porosity was well highlighted by the SEM analysis. As an example, Figure 2 shows the SEM photograph of the AHC-Run 8 (8000 x).

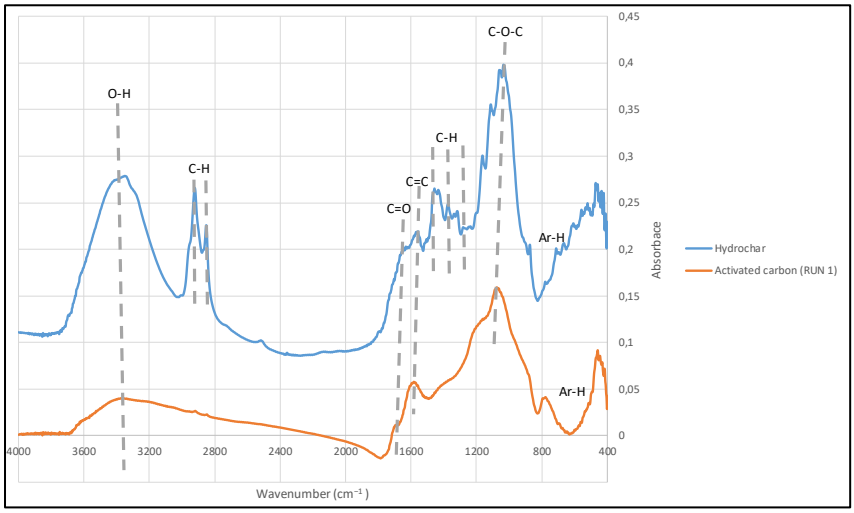

Figure 1. FTIR spectra of hydrochar and activated hydrochar obtained at 500°C and KOH/HC ratio of 0.5

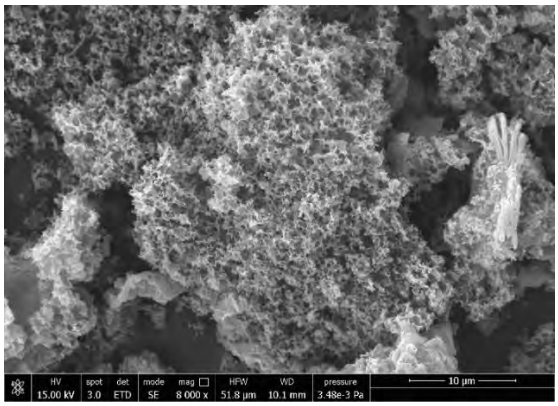

Figure 2. Scanning electron microscopy of the AHC-Run 8 (8000 x)

The following table shows the average values of the BTEX removal efficiency obtained with HC and with the different AHCs. The removal guaranteed by non-activated HC was less than 10%. The results highlighted the great removal efficiency increase due to the activation process. The AHCs showed a very high BTEX removal capacity, up to values of approximately 85% (AHC-Run 8) (see Table 3). According to experimental results, the BTEX removal increases with the value of the BET surface area.

Table 3. Adsorption of BTEX

Sample	Activation temperature (°C)	KOH: HC impregnation ratio	BTEX removal (%)
HC	-	-	8.8
AHC-Run 1	500	0.5	47.7
AHC-Run 2	700	1.5	69.0
AHC-Run 3	700	1.0	65.0
AHC-Run 4	700	0.5	65.7
AHC-Run 5	600	0.5	69.6
AHC-Run 6	600	1.0	76.0
AHC-Run 7	600	1.5	77.9
AHC-Run 8	600	1.0	84.7
AHC-Run 9	500	1.5	31.6
AHC-Run 10	500	1.0	33.3

The analysis for the optimal activation conditions assessment carried out with the Response Surface Methodology is underway and the results will be presented at the conference.
Thanks to the HTC process, the residual waste obtained from MT currently used for landfill cover can be recovered as a secondary raw material to produce activated carbons derived from hydrochar. The adsorption capacity of these activated carbons on emerging compounds such as BTEX makes their utilization particularly interesting, especially in relation to the prescriptions of the upcoming European Directive on wastewater concerning emerging contaminants.

References

[1] Zhang, Z., Yang, J., Qian, J., Zhao, Y., Wang, T., Zhai, Y., 2021. Biowaste hydrothermal carbonization for hydrochar valorization: Skeleton structure, conversion pathways and clean biofuel applications. Bioresour Technol. https://doi.org/10.1016/j.biortech.2021.124686
[2] Tasca, A.L., Puccini, M., Stefanelli, E., Gori, R., Galletti, A.M.R., Vitolo, S., 2020. Investigating the activation of hydrochar from sewage sludge for the removal of terbuthylazine from aqueous solutions. J Mater Cycles Waste Manag 22, 1539–1551. https://doi.org/10.1007/s10163-020-01045-y
[3] Yu, B., Yuan, Z., Yu, Z., Xue-song, F., 2022. BTEX in the environment: An update on sources, fate, distribution, pretreatment, analysis, and removal techniques. Chemical Engineering Journal. https://doi.org/10.1016/j.cej.2022.134825
[4] Yu, X., Liu, S., Lin, G., Yang, Y., Zhang, S., Zhao, H., Zheng, C., Gao, X., 2020. KOH-activated hydrochar with engineered porosity as sustainable adsorbent for volatile organic compounds. Colloids Surf A Physicochem Eng Asp 588, 124372. https://doi.org/https://doi.org/10.1016/j.colsurfa.2019.124372
[5] Yu, X., Liu, S., Lin, G., Yang, Y., Zhang, S., Zhao, H., Zheng, C., Gao, X., 2019. Promotion effect of KOH surface etching on sucrose-based hydrochar for acetone adsorption. Appl Surf Sci 496. https://doi.org/10.1016/j.apsusc.2019.143617
[6] Stefanelli, E., Vitolo, S., Di Fidio, N., & Puccini, M. (2023). Tailoring the porosity of chemically activated carbons derived from the HTC treatment of sewage sludge for the removal of pollutants from gaseous and aqueous phases. Journal of Environmental Management, 345, 118887

PARALLEL SESSION: D3

Flash

Waste treatment and valorization

Title: Full-scale anaerobic digestion of source-separated blackwater in UASB at RecoLab, Helsingborg, Sweden

Author(s): Saleh Abuzir*[1], Marta Domini[1], Giorgio Bertanza[1], Åsa Davidsson[2], Hamse Kjerstadius[3]

[1] *Department of Civil, Environmental, Architectural Engineering and Mathematics, University of Brescia, Brescia, Italy, saleh.abuzir@unibs.it, marta.domini@unibs.it, giorgio.bertanza@unibs.it*
[2] *Division of Chemical Engineering, Lund University, Lund, Sweden, asa.davidsson@ple.lth.se*
[3] *Nordvästra Skånes Vatten och Avlopp AB (NSVA), Helsingborg, Sweden, hamse.kjerstadius@nsva.se*

Keyword(s): UASB reactor, anaerobic digestion, anaerobic treatment, wastewater, blackwater, biogas, source separation

Abstract

This study is focused on evaluating the performance of a full-scale (50m^3) UASB reactor treating Blackwater (BW) (Figure 1) in order to determine whether the real-life implementation of anaerobic digestion (AD) of BW is in line with earlier lab-scale results of De Graaff [1] and Roeleveld [2,3]. The UASB treats source-separated BW from a new city district of Oceanhamnen in Helsingborg, Sweden, where all domestic and commercial buildings have vacuum toilets for the collection of BW using 1L per flush. The BW is treated in a local treatment facility (RecoLab) built especially for the new city district to evaluate the source-separation system (Greywater and BW) of the district. BW contains a high load of organic matter and is rich in nutrients, therefore, it is considered a good source for biogas production using AD [4,5]. De Graaff [1] and Roeleveld [2,3] successfully treated BW in lab-scale UASB and UASB-septic tank reactors, at temperatures of 15℃ and 25℃ (Table 1). The objectives of this study were: to determine the feasibility of digesting BW in a larger-scale UASB, to operate a large-scale UASB at 35℃, and to determine whether large-scale results align with previous lab-scale results.

Table 1. Operational parameters applied to UASB treating Blackwater.

	Unit	Full-scale UASB (this study)		Lab-scale UASB [1]		Lab-scale UASB-septic tank [2,3]	
		Phase 1	Phase 2	Before dilution	After dilution	$UASB_{st}1$	$UASB_{st}2$
Operating weeks	[Weeks]	56	74	74	62	52	52
Reactor volume	[L]	50,000	50,000	50	50	200	200
Temperature	[℃]	35	35	25	25	15	25
HRT	[d]	9.54±1.4	5.7±0.9	8.7±0.96	8.7±0.96	27-29	27-29
SRT	[d]	75	75	254	254	>365	>365
OLR	[kgCOD/m^3 d]	<1.5	1.5	1.0	1.0	0.33-0.42	0.33-0.42

Figure 1. Pilot-scale UASB treating Blackwater at RecoLab, Helsingborg.

The UASB in this study was operated continuously for 130 weeks at an operating temperature of 35℃. Chemical analysis of chemical oxygen demand (COD) was performed weekly. The UASB was fed intermittently. The sludge volume index (SVI) of different heights of the digester was measured once a week. Biogas flow was continuously measured using a drum-type flow meter (Ritter TG20-5), and the gas analysis was measured online using INCA4003 with sensors to measure methane and hydrogen sulfide (H_2S). The biomass used in the UASB was flocculant. Sludge was removed from the lowest part of the UASB twice a week. The UASB was operated in two phases (Table 1), characterised by two different organic loading rates (OLR) (Table 1). The OLR was changing in the first phase due to the increase in the flow rate which was a result of the continuous construction of new buildings in the district and was less than 1.5 kgCOD/m3 d (Figure 2). The total influent COD was 8.59±1.85 gCOD/L and was comparable with the previous studies of De Graaff [1] and Roeleveld [2,3] (9.8±2.6 and 9.5±6.46 gCOD/L, respectively). The OLR in this study was higher than in the previous studies of De Graaff [1] and Roeleveld [2,3] (1 and 0.33-0.42 kgCOD/m3 d, respectively). The total effluent COD in the first phase (1.05±0.18 gCOD/L) and in the second phase (2.24±1.2 gCOD/L) was lower than the total effluent COD obtained in the previous lab-scale results of De Graaff [1] and Roeleveld [2,3] (Table 2). However, in the second phase, there were more variations in the effluent total COD concentration (Table 2). The variations of the effluent COD concentrations in the second phase caused the COD removal to vary from an average value of 87.8% in the first phase to an average value of 73.9% in the second phase. The varying effluent concentration in the second phase (i.e., higher standard variation) was likely due to sludge floatation indicated by SVI at 5 meter height (Figure 3). The values of the daily biogas production obtained in this study (15.8±0.8 Nm^3/d in the first phase and 24.7±5.5 Nm^3/d in the second phase) were higher than the previous studies (Table 2). The biogas yield in the first phase was 0.11N $m^3/kgCOD_{in}$, and it increased in the second phase to a value of 0.32 $Nm^3/kgCOD_{in}$ (Figure 4).

Table 2. Performance results of blackwater anaerobic digestion.

	Unit	Full-scale UASB (this study)		Lab-scale UASB [1]		Lab-scale UASB-septic tank [2,3]	
		Phase 1	Phase 2	Before dilution	After dilution	$UASB_{st}1$	$UASB_{st}2$
$COD_{total\ effluent}$	[gCOD/L]	1.05±0.18	2.24±1.15	2.4±0.84	1.2±0.34	3.7±0.46	2.73±0.49
Biogas production	[m^3/d]	16.2±1.3	25.3±5.6	0.01	0.01	0.0064	0.0083
Methane production	[m^3CH_4/ m^3BW]	2.6±0.2	2.7±0.5	1.8	1.8	2.0	2.0

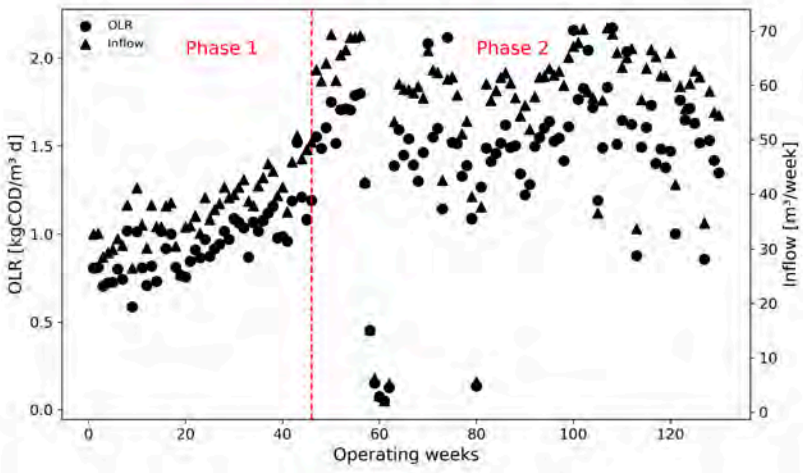

Figure 2. Variations in the organic loading rate and the inflow.

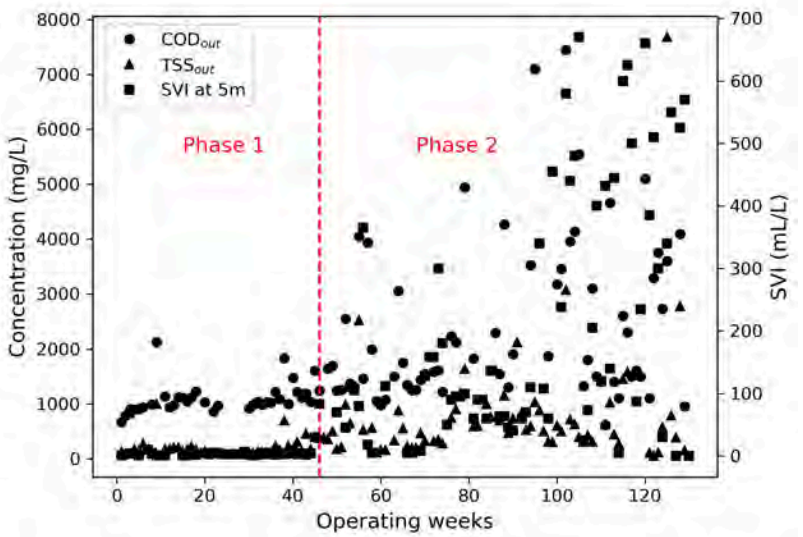

Figure 3. Effluent concentrations of COD and TSS, and SVI at 5 meters of the full-scale UASB.

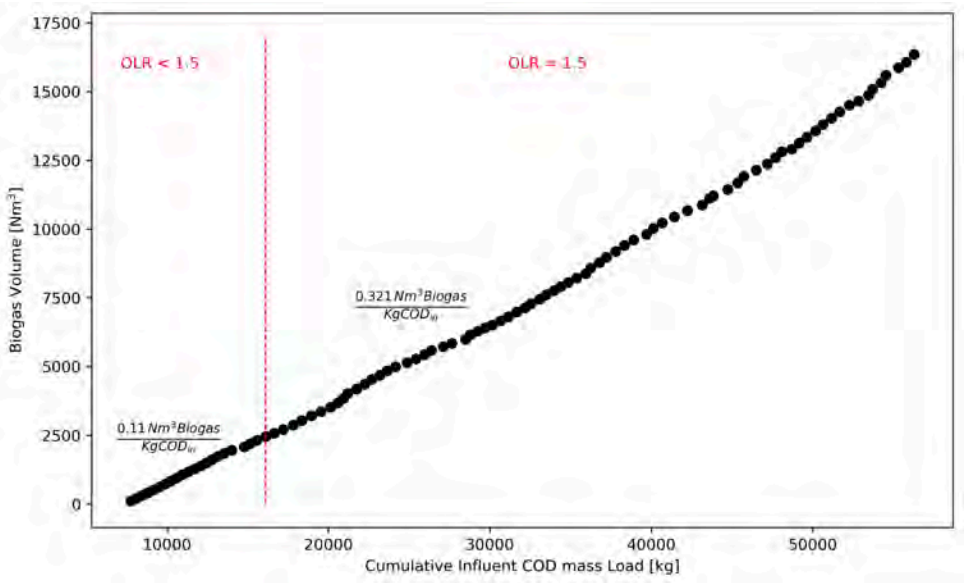

Figure 4. Biogas yield of the full-scale UASB.

Overall, the UASB in this study showed a stable performance in terms of biogas production. Additionally, it showed a stable performance for the COD removal at 87.8% especially in the first phase, while in the second phase, it dropped to 73.9%, due to sludge floatation. Daily biogas production was higher than the previous lab-scale UASBs [1,2,3] and was not affected by sludge floatation. Although sludge floatation occurred when higher OLR was targeted (i.e. 1.5 kgCOD/m^3 d), the effluent concentrations of COD were lower than the previous studies of lab-scale UASBs [1,2,3]. Higher OLR resulted in higher biogas yield per influent COD mass load. The causes of sludge floatation in the UASB remain elusive and require further investigation, but could be attributed to the higher OLR. Overall, the results showed higher removal of COD and higher biogas production compared to previous lab-scale results. High COD removal and biogas production conclude that the large-scale BW UASB system reached better results than previous lab-scale results when it was operated at 35℃. The results are promising for the further spread of source-separated sanitation systems with blackwater vacuum systems.

References

[1] De Graaff MS, Temmink H, Zeeman G, Buisman CJN. "Anaerobic Treatment of Concentrated Black Water in a UASB Reactor at a Short HRT," Water, vol. 2, pp. 101-119, (2010).
[2] Kujawa-Roeleveld, K.; Elmitwalli, T.; Zeeman, G. Enhanced primary treatment of concentrated black water and kitchen residues within DESAR concept using two types of anaerobic digesters. Water Sci. Technol, 53, 159-168 (2006).
[3] Kujawa-Roeleveld, K.; Fernandes, T.; Wiryawan, Y.; Tawfik, A.; Visser, M.; Zeeman, G. Performance of UASB septic tank for treatment of concentrated black water within DESAR concept. Water Sci. Technol. 52, 307-313 (2005).
[4] Otterpohl, R.; Albold, A.; Oldenburg, M. "Source control in urban sanitation and waste management: ten systems with reuse of resources" in Water Science and Technology, vol. 39, pp. 153-160, (1999).
[5] Kujawa-Roeleveld, K.; Zeeman, G. "Anaerobic treatment in decentralised and source-separation based sanitation concepts" in Reviews in Environmental Science and Bio/Technology, vol. 5, pp. 115-139, (2006).

Minimizing Sludge Production in Wastewater Treatment Plants: S^{4}WAT solutions and new strategies for digestion improvement

Author(s): Nicola Di Costanzo[1], Salvatore Masi[1], Donatella Caniani[1], Alessandra Cesaro[2], Giovanni Esposito[2], Francesco Di Capua[1,*]

[1] *School of Engineering, University of Basilicata, via dell'Ateneo Lucano 10, Potenza, Italy*
[2] *Department of Civil, Architectural, and Environmental Engineering, University of Naples Federico II, via Claudio 21, Naples, Italy*
*Corresponding author

Keywords: Sewage sludge minimization, municipal wastewater treatment, anaerobic digestion, static magnetic field

Abstract

Introduction. Sewage sludge (SS) production is an inevitable consequence of municipal wastewater treatment processes (MWWTPs) [1]. The most widely used method in these plants is the conventional activated sludge (CAS) process, which is primarily responsible for generating SS [2]. Globally, MWWTPs produce approximately 45 million tons of dried total solids (TS) per year, with European production rates ranging between 14.5 and 29.5 kg TS per person annually [3]. The amount of SS produced is influenced by several factors, including national regulations, population habits, urbanization levels, and the specific wastewater treatment cycles and sludge handling practices used. The interplay of these factors makes it challenging to precisely determine their impact on SS generation. Furthermore, SS production is expected to increase due to the establishment of new MWWTPs and the imposition of stricter discharge regulations [4]. Managing and disposing of this large volume of sludge is a significant challenge, often complicated by inadequate infrastructure, which can result in high costs that constitute up to 60% of the total operating expenses of MWWTPs.
To address the challenges associated with SS management, recent research has focused on strategies to reduce sludge volumes produced in MWWTPs. These strategies can be categorized into interventions along the water line and interventions along the sludge line. Water line interventions target the biological processes in mainstream wastewater treatment to reduce sludge yields by modifying bacterial metabolism or increasing decay rates. Sludge line interventions, on the other hand, are typically combined with anaerobic digestion (AD) processes and aim to enhance total solids (TS) reduction efficiency and improve the amount of produced biogas and the quality of the digestate [5].
One significant approach along the water line is the implementation of the Oxic-Settling-Anaerobic (OSA) process [6], which involves introducing an anoxic/anaerobic sludge holding tank (SHT) along the recycle line, allowing sludge to be retained before returning to the aeration tank. Studies have demonstrated that the OSA system can reduce sludge production by up to 80% through mechanisms such as uncoupling metabolism, cell lysis, cryptic growth, and the selection of slow-growing bacteria. Recent research has shown that when the OSA approach is combined with the integrated fixed-film activated sludge (IFAS) system, which merges suspended and attached-growth biomass, sludge production can be minimized to values close to 0 and nitrification is enhanced [7]. Further research is required for complete carbon and nitrogen removal in the IFAS system integrated within the OSA cycle.
On the sludge line, to enhance the efficiency of AD, several pretreatment methods have been proposed to boost the biodegradability and dewaterability of sewage sludge, thereby augmenting biogas output [8]. However, the use of static magnetic fields (SMF) in this context has received limited attention. Traditionally, this technology has been applied for calcium carbonate precipitation in water [9] and, more

recently, it has been proposed in combination with aerobic biological processes [10]. The application of a SMF to sewage sludge destined to AD is expected to impact both the generation of methane [11] and the quality of the digestate [12], leading to the possible precipitation of compounds that may enhance the fertilizing properties of sewage sludge.
This study focuses on the start-up of a novel integrated biological system combining simultaneous nitrification-denitrification (SND) in the IFAS to the OSA system with the aim to obtain a complete one-stage carbon and nutrients removal while minimizing sludge generation, being objectives the of PRIN PNRR 2022 project *"Smart Sustainable Saving Solutions for Water and wastewater Treatment (S^4WAT)"*. The evolution of carbon, nitrogen, and phosphorus concentrations was monitored during the study to provide a complete preview of this technology towards full-scale application. Moreover, the study evaluates the effects of sewage sludge exposure to SMF on AD performance, specifically focusing on biomethane production. Using a medium-intensity SMF of 50 mT, two different exposure conditions - limited and prolonged - were tested to determine their impact on AD in terms of methane production. The experimental results were analysed to explore the potential integration of this innovative SMF pretreatment technology into existing AD processes, assessing how different conditions of magnetic exposure can influence the efficiency of biomethane production.

Materials and methods. The start-up of the IFAS-OSA system was organized into three phases: cultivation of the attached biomass under anoxic conditions and suspended nitrifying biomass (Phase I), batch and continuous reactor start-up (Phase II), and full implementation of the IFAS-OSA configuration (Phase III). A 4-liter glass reactor vessel was inoculated with 10% (v/v) recycled sludge from the municipal wastewater treatment plant in Nola, Italy. Kaldness K1 carriers (Veolia, France) were added to the reactor at a 40% filling ratio along with the synthetic influent described earlier. Nitrifiers were cultivated in a continuously stirred tank reactor under SRT, temperature, and ammonium concentrations favoring nitritation over nitratation. Mixing in the bioreactors was provided by a magnetic stirrer. In Phase II, the anoxic bioreactor was initially operated in batch mode and then continuously at intermitting aeration as a moving bed biofilm reactor (MBBR) to encourage further growth of the biofilm on the carriers' surfaces. In Phase III, the IFAS-OSA system was completed by integrating the OSA configuration into the IFAS system. The system is being optimized in terms of DO range and air flow, while sludge production is under evaluation. For AD improvement, the magnetic pretreatment was explored under two conditions: limited exposure (0.1 L/min flow rate with 1 magnetization cycle) and prolonged exposure (10 L/min flow rate with 10 magnetization cycles). AD experiments were conducted in triplicate at 37±1 °C using 250 mL serum bottles with 100 mL working volume, ensuring anaerobic conditions by flushing with argon gas. Control tests with untreated sludge were also performed. Results were statistically analyzed using one-way ANOVA in Minitab 17, with significant differences identified at p-values less than 0.05.

Results and Discussion. The start-up of the intermittently aerated IFAS-OSA system was successful. Partial SND, consisting in no NO_3^- generation and NO_2^- accumulation in the aerobic tank, was maintained quite well due to biomass cultivation and DO regimes in the continuous system. In the first 2 month of operation, the system could achieve average COD removal of 94% and average TN removal close to 60%. TP removal was quite fluctuating but could reach values >60% under certain operational conditions.
Figure 1 shows the specific biomethane production after 38 days of AD tests. At the end of the test, the untreated sludge showed a maximum specific biomethane production of 336 L_{CH4}/kg_{VS}. The medium-intensity pretreatment, under limited exposure (Test A) increased the methane production by 6.4% (p<0.05) compared to control test, reaching a value of 359 L_{CH4}/kg_{VS}. On the other hand, the use of a prolonged exposure (Test B) resulted in a comparable methane production to the control test, reaching

340 L_{CH4}/kg_{VS}. This result is in line with those outlined in a previous work, where prolonged exposure to SMF was not beneficial for the specific biomethane production as it was 24% lower than that of the untreated sludge.

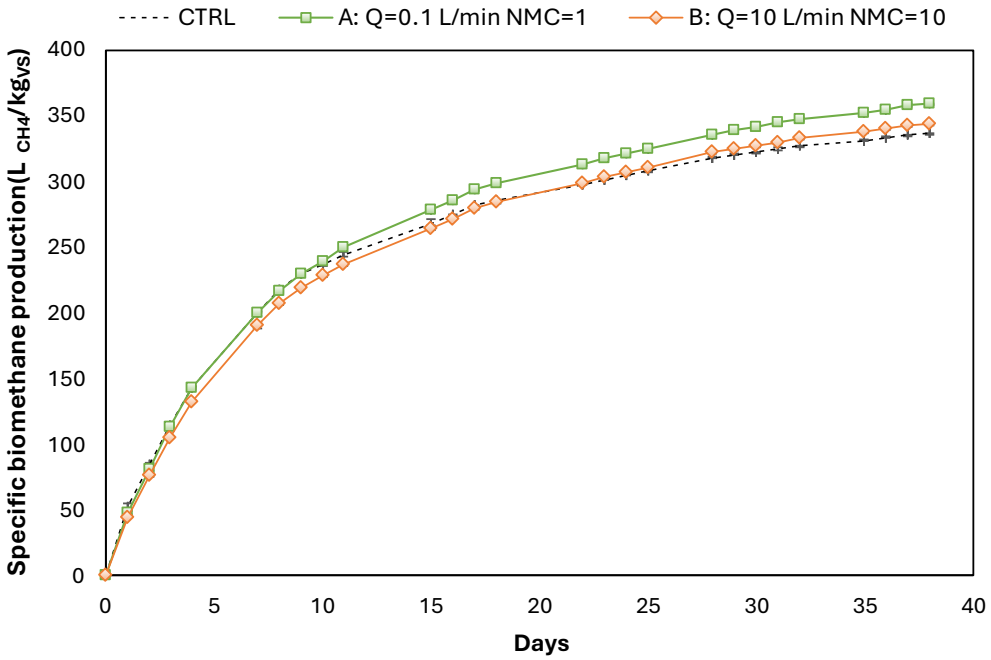

Figure 1. Specific biomethane production in AD tests.

Our study reveals that limited exposure to medium-intensity SMF pretreatment can effectively enhance AD performance, achieving a 6.4% increase (p<0.05) in methane production compared to untreated sewage sludge. Conversely, extensive exposure appears to adversely affect biomethane production. The underlying causes of these results may be attributed to alterations in metabolic pathways, enzyme activities, or changes in the relative abundance of microorganisms directly involved in biomethane generation. Furthermore, the improvements observed under limited SMF exposure might also be linked to an enhanced hydrolytic phase of anaerobic digestion. By potentially accelerating the breakdown of complex organic substrates into simpler monomers, SMF pretreatment could facilitate a more efficient microbial assimilation and subsequent methanogenesis. These findings suggest that the modulation of microbial activity by SMF exposure levels could play a critical role in optimizing methane yields from AD processes. In addition to its technological benefits, magnetic pretreatment also stands out for its economic potential. This pretreatment method requires no additional energy input, making it cost-effective. Moreover, its seamless integration into existing facilities highlights its practicality and adaptability.

Looking forward, our research opens new avenues for optimizing sewage sludge management. The implementation of the IFAS-OSA system can significantly minimize sludge production in the water treatment line by enhancing biomass retention and improving overall treatment efficiency. This system's ability to reduce excess sludge not only decreases the volume of sludge requiring disposal but also lowers the associated costs and environmental impacts.

Concurrently, magnetic pretreatment of sludge before anaerobic digestion (AD) shows promise in further reducing sludge volume and enhancing methane production. By fine-tuning magnetic field intensities and exposure durations, this method can be optimized for different sludge types, leading to more efficient breakdown and higher biogas yields. This dual approach, minimizing sludge in the water

treatment line with IFAS-OSA and enhancing sludge reduction in AD with magnetic pretreatment, offers a comprehensive strategy for maximizing both environmental and economic benefits. These innovations support a circular economy perspective, promoting sustainable wastewater management and resource recovery.

References

[1] N. Di Costanzo, A. Cesaro, F. Di Capua, G. Esposito, Exploiting the nutrient potential of anaerobically digested sewage sludge: A review, Energies. 14 (2021) 1–25. https://doi.org/10.3390/en14238149.
[2] F. Di Capua, M.C. Mascolo, F. Pirozzi, G. Esposito, Simultaneous denitrification, phosphorus recovery and low sulfate production in a recirculated pyrite-packed biofilter (RPPB), Chemosphere. 255 (2020) 126977. https://doi.org/10.1016/j.chemosphere.2020.126977.
[3] R. Morello, F. Di Capua, G. Esposito, F. Pirozzi, U. Fratino, D. Spasiano, Sludge minimization in mainstream wastewater treatment: Mechanisms, strategies, technologies, and current development, J. Environ. Manage. 319 (2022) 115756. https://doi.org/10.1016/j.jenvman.2022.115756.
[4] R. Morello, F. Di Capua, A. Cesaro, G. Esposito, F. Pirozzi, U. Fratino, D. Spasiano, Solutions for solid minimization in the sludge streamline of municipal wastewater treatment plants: Current state and recent developments, J. Water Process Eng. 64 (2024) 105725. https://doi.org/10.1016/j.jwpe.2024.105725.
[5] N. Di Costanzo, F. Di Capua, A. Cesaro, F. Carraturo, M. Salamone, M. Guida, G. Esposito, A. Giordano, Headspace micro-oxygenation as a strategy for efficient biogas desulfurization and biomethane generation in a centralized sewage sludge digestion plant, Biomass and Bioenergy. 183 (2024) 107151. https://doi.org/10.1016/j.biombioe.2024.107151.
[6] R. Morello, F. Di Capua, Ç. Kalkan Aktan, T. Yilmaz, G. Esposito, F. Pirozzi, U. Fratino, D. Spasiano, E. Sahinkaya, Unravelling the impact of oxic-settling-anaerobic cycle implementation and solid retention time on sludge generation, membrane operation, and contaminant removal in membrane bioreactors, Chem. Eng. J. 496 (2024). https://doi.org/10.1016/j.cej.2024.153800.
[7] R. Morello, F. Di Capua, E. Sahinkaya, G. Esposito, F. Pirozzi, U. Fratino, D. Spasiano, Operational strategies enhancing sewage sludge minimization in a combined integrated fixed-film activated sludge – oxic settling anaerobic system, J. Environ. Manage. 345 (2023) 118808. https://doi.org/10.1016/j.jenvman.2023.118808.
[8] N. Di Costanzo, F. Di Capua, A. Cesaro, M.C. Mascolo, F. Pirozzi, G. Esposito, Impact of High-Intensity Static Magnetic Field on Chemical Properties and Anaerobic Digestion of Sewage Sludge, Waste and Biomass Valorization. 14 (2023) 2469–2479. https://doi.org/10.1007/s12649-022-01891-x.
[9] M.C. Mascolo, Effect of magnetic field on calcium carbonate precipitated in natural waters with prevalent temporary hardness, J. Water Process Eng. 41 (2021) 102087. https://doi.org/10.1016/j.jwpe.2021.102087.
[10] H. Wang, W. Lyu, Q. Song, D. Zhou, X. Hu, B. Wang, R. Chen, Role of weak magnetic strength in the operation of aerobic granular reactor for wastewater treatment containing ammonia nitrogen concentration gradient, Bioresour. Technol. 322 (2021) 124570. https://doi.org/10.1016/j.biortech.2020.124570.
[11] N. Di Costanzo, A. Cesaro, F. Di Capua, M.C. Mascolo, G. Esposito, Exploring the effects of static magnetic fields for the enhanced valorization of sewage sludge by anaerobic digestion, Int. Conf. Environ. Sci. Technol. Proc. 18 (2023) 18–21. https://doi.org/10.30955/gnc2023.00090.
[12] N. Di Costanzo, A. Cesaro, F. Di Capua, M.C. Mascolo, G. Esposito, Application of high-intensity static magnetic field as a strategy to enhance the fertilizing potential of sewage sludge digestate, Waste Manag. 170 (2023) 122–130. https://doi.org/10.1016/j.wasman.2023.08.005.

Title: LarWaR Process – BSF LARVAE FOR WASTEWATER TREATMENT AND RESOURCE RECOVERY: state of art and recent developments

Author(s): Valentina Grossule*, Raffaello Cossu

DICEA, Department of Civil, Architectural and Environmental Engineering, University of Padova. Via Marzolo 9, 35131 Padova, Italy

Keyword(s): wastewater treatment, high organic content wastewater, resource recovery, Hermetia Illucens, Black Soldier Fly, Circular economy

Abstract

The biological process based on the use of BSF larvae has proven to be a highly promising alternative for the treatment of high organic content wastewater, capable of coupling high removal efficiencies with recovery of resources from waste, in compliance with the concept of Circular Economy. BSF larvae are able to metabolize, and stabilize large amounts of organics and nutrients, converting them into a valuable biomass suitable for direct use as animal food (i.a. [1]) or for processing to platform chemicals (e.g. protein, lipids, chitin, chitosan, etc.) and use in biorefineries in the manufacture of a range of products, including biodiesel, lubricants, antimicrobial peptides and other biomedical materials [1] [2] [3] [4] [5] [6].

While this important feature of BSF larvae metabolism (recovery of resources) has been successfully exploited in the treatment of putrescible solid waste (e.g., food residues), the application to wastewater has been hindered by the fact that larvae are terrestrial organisms and fail to survive in a liquid environment. Using very small (20mL) batch reactors, early observations revealed the ability of larvae to metabolize liquid substrates [7], whilst showing no evidence of the issue of larvae mortality in a liquid environment. This problem only emerged clearly at a later stage, when [8] tested the process on a larger scale. These authors confirmed that BSF larvae are able to feed on liquid substrate producing a high-quality prepupal biomass but evidenced the drowning of a high percentage of larvae [8] [9].

To overcome this critical issue, Grossule and Cossu (2021) have proposed and patented a technical solution (Italian Patent n. 102021000016700; PCT/IB2022/055888; priority 25/06/2021) based on the adoption of a porous material to be installed in the reactor to support larval mobility. The porous material, saturated with the targeted wastewater, allows larvae to dive for eating and to re-emerge for breathing [10].

The patented solution mentioned above paved the way to the development of a wastewater treatment process based on use of BSF larvae (shortened in the acronym LarWaR =Larvae for Wastewater treatment and Resource recovery) as an innovative and realistic perspective for a full-scale technology, although several aspects still require further investigation.

Subsequently, Grossule et al. (2022) investigated the influence of wastewater organic quality on process and removal kinetics, which yielded three-fold higher values compared to conventional activated sludge [11]. Grossule et al. (2023) investigated the role of concentration and load of wastewater organic substances on the larval metabolic process, concluding that concentration influences the conversion of substrate into new biomass, while substrate removal rate is only influenced by organic load. A minimum concentration in the feed (approx. 800-1000 mg TOC/L, depending on the quality of organics) was observed to be necessary to ensure optimal process performance, while higher concentrations

enhanced performance, thus indicating the suitability of LarWaR for use in pre-treating high organic content wastewater [12].

Key issues to be investigated with a view to optimizing the process and advancing towards technical application, include characteristics (shape, porosity, structure, etc.) of the supporting material and optimal larval density. The plastic granules (Valox) used to date in the aforementioned studies display very low porosity (35%), with 65% of the reactor volume being occupied by the granules, thus rendering the material impracticable for real-scale applications. With regard to larval density, Parra Paz et al. (2015) suggested an optimum density of 1.2 larvae/cm² for solid substrates, with a maximum tolerated density of 5 larvae/cm², although no data have yet been made available for liquid substrates [13].

The present study aimed to advance the understanding of these two issues. The optimum supporting material should maximise porosity (i.e. active working volume of the reactor) without compromising the ability of larvae to move and survive. Optimum larval density should maximize removal efficiencies without compromising survival rate (i.e. avoiding larval starvation and competition for breathing).

Three different plastic products (granules, Pall rings and geomat) were tested as supporting material at four different larval densities (4, 8, 16 and 32 larvae/cm^2). An artificial wastewater was used under constant feeding organic loads.

The artificial wastewater was prepared by diluting low-fat milk with tap water (1:10), resulting in a rapid and easily replicable wastewater. Total Organic Carbon (TOC), Biochemical Oxygen Demand (BOD) and Chemical Oxygen Demand (COD) of the artificial wastewater were 2740 mgC/L, 13800 mgO_2/L and 15300 mgO_2/L, respectively.

Process performance was compared in terms of larval growth and removal efficiency.

Figure 1 illustrates the variation of the specific substrate consumption rate (v_S, S=TOC). For all supporting materials the results obtained confirmed the absence of negative impact on larval performance, up to a larval density of 16 larvae/cm2, with v_S values increasing from initial approx. 0.125 mgTOC/larva/d to final approx. 0.14 mgTOC/larva/d, with the usual exception for G16, where v_S started from approx. 0.10 mgTOC/larva/d and slowly increased during the test up to a final value of approx. 0.13mgC/larva/d. The negative impact of the highest larval density was again also confirmed by v_S values.

Based on the results obtained, the following conclusive remarks can be drawn:

a) An increase in larval density only impairs process performance, in terms of overall biomass generation and removal efficiencies, once threshold density is exceeded.
b) The threshold depends on the supporting material used: threshold is lower in the presence of low porosity (8 larvae/cm2 in case of G) compared to higher porosity materials (16 larvae/cm2 with R and M). As a result, higher porosity materials allow the use of higher larval densities, and therefore higher organic loads, ultimately resulting in beneficial reduced reactor volumes. Suggested values are in any case higher than those suggested by literature (optimum 1.2 larvae/cm² for solid substrates, with a maximum tolerated density of 5 larvae/cm², [13]).
c) Optimum conditions were observed at a larval density of 16 larvae/cm^2 with R as supporting material, featuring a porosity of 75% (liquid volume/reactor volume filled with supporting material).
d) As the performance of Pall rings may be deemed comparable to that achieved with geomat, the former supporting material represents a valid alternative, particularly due to its very high porosity (0.92) that promotes an additional increase in liquid volume per unit of reactor volume.

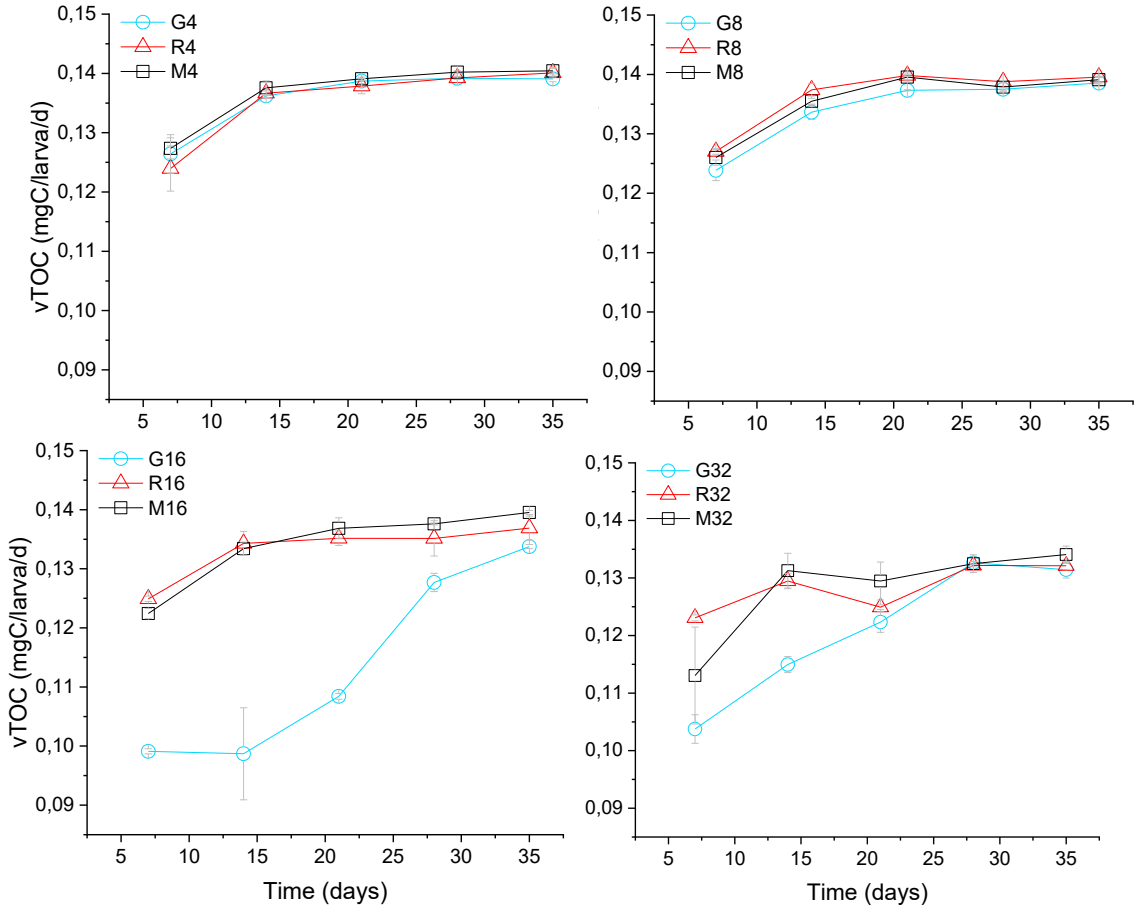

Figure 1. Table title (centered)

Figure 1. Variation of the specific substrate consumption rate (v_S, S=TOC) over time under reactor settings with different plastic supporting materials and different larval densities. (Supporting materials: G= Granules, R= Pall Rings, M= Geomat; Larvae Densities: 4, 8, 16, 32 larvae/cm2).

Acknowledgment

Funded by the European Union
NextGenerationEU

And by STARS@UNIPD programme – LarWaR-basics Project: Use of Black Soldier Fly Larvae for innovative Wastewater treatment and Resource recovery

References

[1] Allegretti, G., Talamini, E., Schmidt, V., Bogorni, P.C., Ortega, E., 2018. Insect as feed: An emergy assessment of insect meal as a sustainable protein source for the Brazilian poultry industry. J. Clean. Prod. 171, 403–412. https://doi.org/10.1016/j.jclepro.2017.09.244
[2] Di Somma, A., Moretta, A., Cané, C., Scieuzo, C., Salvia, R., Falabella, P., Duilio, A., 2022. Structural and functional characterization of a novel recombinant antimicrobial peptide from hermetia illucens. Curr. Issues Mol. Biol. 44, 1–13. https://doi.org/10.3390/cimb44010001
[3] Franco, A., Scieuzo, C., Salvia, R., Petrone, A.M., Tafi, E., Moretta, A., Schmitt, E., Falabella, P., 2021. Lipids from hermetia illucens, an innovative and sustainable source. Sustain. 13. https://doi.org/10.3390/su131810198
[4] Leong, S.Y., Kutty, S.R.M., Malakahmad, A., Tan, C.K., 2016. Feasibility study of biodiesel production using lipids of Hermetia illucens larva fed with organic waste. Waste Manag. 47, 84–90. https://doi.org/10.1016/j.wasman.2015.03.030
[5] Triunfo, M., Tafi, E., Guarnieri, A., Salvia, R., Scieuzo, C., Hahn, T., Zibek, S., Gagliardini, A., Panariello, L., Coltelli, M.B., De Bonis, A., Falabella, P., 2022. Characterization of chitin and chitosan derived from Hermetia illucens, a further step in a circular economy process. Sci. Rep. 12, 1–17. https://doi.org/10.1038/s41598-022-10423-5
[6] Xiong, J., Mao, J., Wang, T., Feng, W., Wang, W., Yang, C., Miao, X., Wang, C., 2020. Refining and Sulfurization of Oil from Black Soldier Fly and Its Application as Biodegradable Lubricant Additive. JAOCS, J. Am. Oil Chem. Soc. 97, 1243–1251. https://doi.org/10.1002/aocs.12403
[7] Popa, R., Green, T.R., 2012. Using black soldier fly larvae for processing organic leachates. J. Econ. Entomol. 105, 374–378. https://doi.org/10.1603/EC11192
[8] Grossule, V., Lavagnolo, M.C., 2020. The treatment of leachate using Black Soldier Fly (BSF) larvae: Adaptability and resource recovery testing. J. Environ. Manage. 253, 109707. https://doi.org/10.1016/j.jenvman.2019.109707
[9] Grossule, V., Vanin, S., Lavagnolo, M.C., 2020. Potential treatment of leachate by Hermetia illucens (Diptera, Stratyomyidae) larvae: Performance under different feeding conditions. Waste Manag. Res. 38, 537–545. https://doi.org/10.1177/0734242X19894625
[10] Grossule and Cossu 2021. IT patent 102021000016700, deposited on 25th June 2021.
[11] Grossule, V., Fang, D., Yue, D., Lavagnolo, M.C., 2022. Treatment of wastewater using black soldier fly larvae, under different degrees of biodegradability and oxidation of organic content. J. Environ. Manage. 319, 115734. https://doi.org/10.1016/j.jenvman.2022.115734
[12] Grossule, V., Fang, D., Lavagnolo, M.C., 2023. Treatment of wastewater using Black Soldier Fly larvae: Effect of organic concentration and load. J. Environ. Manage. 338, 117775. https://doi.org/10.1016/j.jenvman.2023.117775
[13] Parra Paz, A.S., Carrejo, N.S., Gómez Rodríguez, C.H., 2015. Effects of Larval Density and Feeding Rates on the Bioconversion of Vegetable Waste Using Black Soldier Fly Larvae Hermetia illucens (L.), (Diptera: Stratiomyidae). Waste and Biomass Valorization 6, 1059–1065. https://doi.org/10.1007/s12649-015-9418-8

Title: Influence of carbon to nitrogen ratio and dilution rate on microbial protein production from cheese whey

Author(s): Antonella Scotto di Uccio*[1], Silvio Matassa[1], Alessandra Cesaro[1], Giovanni Esposito[1], Stefano Papirio[1]

[1] *Department of Civil, Architectural and Environmental Engineering, University of Naples Federico II, Naples, Italy,* antonella.scottodiuccio@unina.it, silvio.matassa@unina.it, alessandra.cesaro@unina.it, giovanni.esposito1@unina.it, stefano.papirio@unina.it.

Keyword(s): Microbial protein; cheese whey permeate; mixed cultures; resource recovery; circular bioeconomy.

Abstract

INTRODUCTION: Global population is projected to reach 9 billion people by 2050, and to further exceed 10 billion by 2100 [1]. Such a growing anthropogenic pressure will entail the need to rapidly increase the current feed and food production potential, especially in terms of protein supply [2]. The highly sustainable and circular protein production potential offered by microbial protein (MP) could benefit from strategically important agrifood sectors such as that of the dairy industry. Indeed, the production of 1 kg of cheese generates up to 9 kg of cheese whey (CW), a yellowish liquid that is formed by coagulation of the milk after the curd phase. CW mainly consists of water (~ 94%), lactose (4.5%), proteins (1%), fats and minerals [3, 4] and about half of the 180 million tons generated each year is treated as wastewater [5]. Some microorganisms, including yeasts and lactobacilli, are capable of directly metabolizing lactose-rich dairy residues such as cheese whey permeate (CWP) to produce MP [4]. Using CWP for MP production could thus lead to the co-production, along with the recovered whey protein, of an alternative protein source characterized by high levels of vitamins, carotenoids and carbohydrates [6]. The present study investigated the use of CWP as a substrate for the production of MP through a mixed culture of yeast and bacteria. The experimental work involved the production of MP in a continuously stirred tank reactor (CSTR) fed with a synthetic CWP. The influence of different carbon to nitrogen (C/N) ratios and dilution (D) rates were evaluated with respect to key process performance indicators, such as biomass yield and biomass productivities, soluble chemical oxygen demand (sCOD) removal and nitrogen assimilation efficiencies, as well as biomass and microbial community composition for the evaluation of the final MP product.

MATERIALS AND METHODS: A synthetic solution of lactose and other macro- and micro-nutrients, adapted from Dubois Frigon [7], was used to simulate an organic substrate for MP production based on CWP. A lyophilized culture of yeasts and bacteria was used as source of microorganisms. The experimental set up consisted of a 1.5 L (working volume) CSTR initially seeded with 0.5 L of the activated microbial inoculum. Dissolved oxygen levels above 2 $mg \cdot L^{-1}$ were guaranteed by regulating aeration (1-4 $L \cdot min^{-1}$) and mechanical stirring (600-800 rpm) in the system. The process was maintained at a constant temperature of 30 °C while pH was automatically controlled at 4.5 ± 0.1 by addition of 1 M of NaOH or HCl solutions. The experimental work, as reported in Table 1, was divided into seven experimental periods in order to test the effect of varying C/N ratios and increasing dilution rates.

RESULTS AND DISCUSSION:

Effect of carbon to nitrogen ratio and dilution rate on aerobic fermentation performances

The time-dependent trends of total suspended solids (TSS), sCOD and NH_4^+-N concentration observed during the experimentation are shown in Figure 1. The biomass concentration values were strongly dependent on the dilution rate rather than on the C/N ratio. The average biomass concentrations obtained when D was equal to 0.33 d^{-1} were 9.0, 8.5, 8.1 and 6.1 g TSS·L^{-1} in period I, II, III and IV, respectively, while increased when D was raised from 0.50 to 0.67 to 1.00 d^{-1} reaching average values of 14.4, 15.7 and 10.6 g TSS·L^{-1} in period V, VI and VII, respectively. As reported in Table 1, the sCOD removal efficiency was constantly above 84% throughout the study, regardless of the value of D and C/N ratio. These sCOD removal efficiencies are slightly higher than those reported in the literature for similar processes obtained with real cheese whey. Clearly, the simpler composition of the synthetic CWP with respect to that of real cheese whey substrates, led to an overall more complete degradation of the organic substrate, resulting into slightly greater sCOD removal efficiencies. Conversely, the N-assimilation efficiency was strongly dependent on both D and C/N ratio, with higher values up to 100% (period VII) obtained at increasing D and C/N ratio of 15. The maximum average biomass productivity (P) achieved with a dilution rate of 0.33 d^{-1} was equal to 3.50 g TSS·L^{-1}·d^{-1} (period I). When higher dilution rates were applied, also the average biomass productivity increased substantially up to value of 11.31 g TSS·L^{-1}·d^{-1} (period VI). Such high productivities were also matched by an almost complete N-assimilation efficiency during period VI, highlighting how the process reached optimal conditions for biomass production and N-substrate utilization.

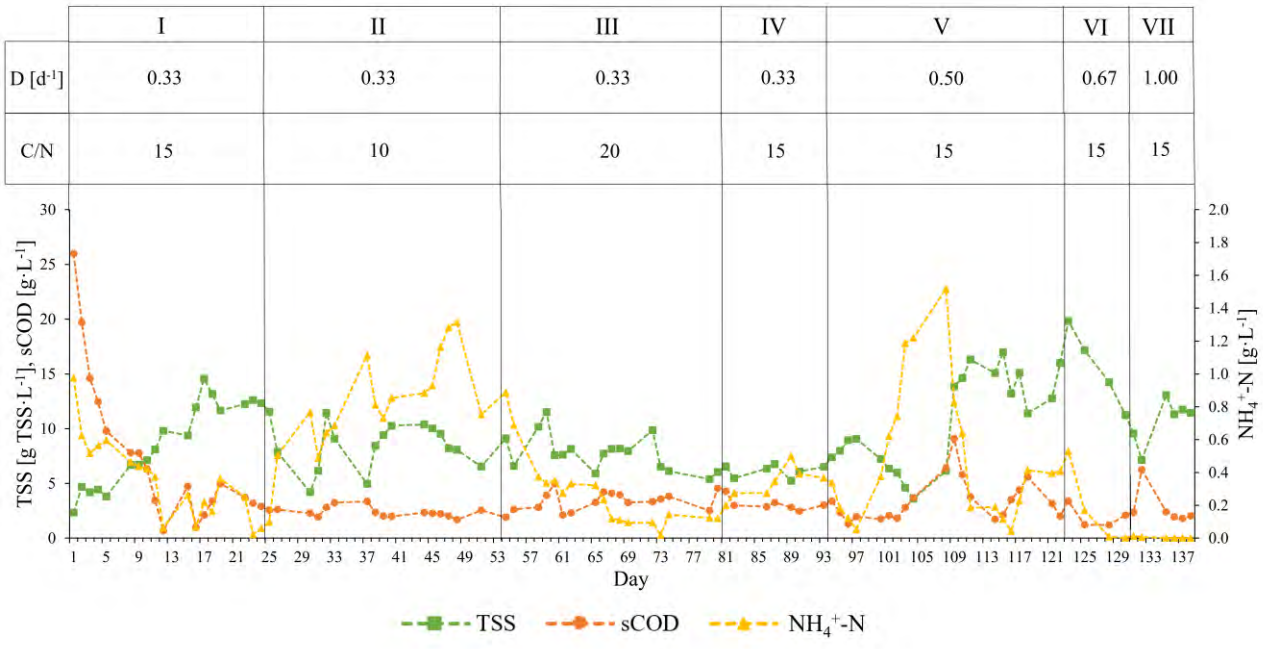

Figure 1. Performances of the aerobic fermentation process during the seven experimental periods in terms of TSS, sCOD and NH_4^+-N concentrations.

Table 1. Summary of the performances observed during the different experimental period in terms of sCOD removal efficiency, N-assimilation efficiency, biomass yield (Y) and biomass productivity (P). The values are reported as the average ± standard deviation for each experimental period.

Period	D (d^{-1})	C/N (mol/mol)	sCOD removal efficiency (%)	N-assimilation efficiency (%)	Y $\left(\frac{g_{TSS}}{g_{COD}}\right)$	P $\left(\frac{g_{TSS}}{L \cdot d}\right)$
I	0.33	15	84.3 ± 9.5	78.4 ± 12.5	0.24 ± 0.12	3.50 ± 1.62
II	0.33	10	92.9 ± 1.3	69.0 ± 11.6	0.25 ± 0.14	3.42 ± 1.87
III	0.33	20	91.9 ± 2.1	73.8 ± 10.6	0.22 ± 0.14	3.04 ± 1.83
IV	0.33	15	92.4 ± 1.3	78.6 ± 5.8	0.17 ± 0.06	2.10 ± 0.90
V	0.50	15	89.3 ± 5.2	78.5 ± 11.5	0.38 ± 0.16	7.46 ± 2.85
VI	0.67	15	95.1 ± 1.9	85.8 ± 13.6	0.42 ± 0.12	11.31 ± 2.66
VII	1.00	15	92.1 ± 4.3	99.7 ± 0.3	0.29 ± 0.03	10.36 ± 3.29

Effect of carbon to nitrogen ratio and dilution rate on microbial protein composition

As shown in Figure 2, protein was the main macromolecular component of the produced biomass, constituting about at least half (> 48%) of its dry weight. The remaining part of the biomass was made up of carbohydrates and, in smaller quantities, lipids and ashes. The highest protein contents were observed when the aerobic fermentation process was operated with a dilution rate of 0.33 d^{-1} regardless of C/N value. Under these conditions the produced MP biomass was characterized by an average protein content always above 70%. The protein levels observed in this study were generally higher than the average values found in other studies. However, when the dilution rate was gradually increased from 0.33 to 1 d^{-1} across experimental periods V, VI and VII, the protein content of the MP biomass decreased from 72.9 to 52.7%, leading to the increment of carbohydrates and lipids up of 23.5 and 17.7%, respectively.

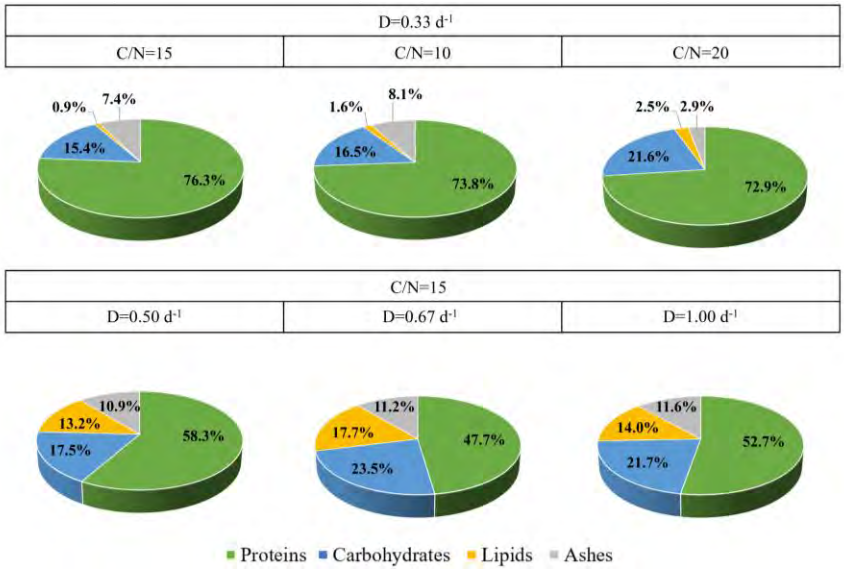

Figure 2. Overall compositions of biomass in terms of proteins, carbohydrates, lipids and ashes under the different conditions tested. The values were obtained by averaging the results of the analyses performed on at least half of the samples collected within each experimental period.

Effect of dilution rate on microbial community composition and MP quality

Among the tested experimental variables, the dilution rate is known to exert the highest selective pressure on the composition and the stability of mixed microbial cultures, especially under chemostat configurations. Therefore, microbiological analyses were carried out on samples collected at the end of the experimental periods characterized by the same D of 0.33 d^{-1} (end of period IV) and at the end of period VII, when D was 1.00 d^{-1}. At the end of period IV, after more than 90 days of continuous reactor operation at a dilution rate of 0.33 d^{-1}, the microbial community composition appeared rather balanced between yeasts (57%) and bacteria (43%).

Conversely, after having gradually increased D up to 1.00 d^{-1} at the end of the experimentation (period VII), yeasts constituted 71% of the microbial population, while the absolute abundance of bacteria decreased to 29%. These results could allow to better explain the variation in macromolecular composition of the produced MP. As a matter of fact, being characterized by a lower protein content than bacteria, the greater abundance of yeasts (71%) at the end of the experimentation could be linked to the lower protein content of the MP biomass produced in periods V, VI and VII with respect to that of periods I, II and III.

CONCLUSIONS:

A stable and well-performing mixed culture dominated by food-fermenting microorganisms was established during synthetic CWP treatment and valorisation into MP. Process performances were strongly influenced by D rather than the C/N ratio. Under a D higher than 0.33 d^{-1}, a maximum average productivity of up to 11.31 g $TSS \cdot L^{-1} \cdot d^{-1}$, together with sCOD removal efficiencies of up to 95% and an almost complete N-assimilation were achieved. With a D of 0.33 d^{-1}, the highest protein content of 73-76% was observed. Conversely, by increasing D, the abundance of yeasts also increased, thereby reducing the protein (48%) and increasing the lipid content (18%).

References

[1] Verstraete W., Clauwaert P., Vlaeminck S. E., “Used water and nutrients: Recovery perspectives in a ‘panta rhei’ context”. Bioresource Technology 215, 199–208, (2016).
[2] Charles H., Godfray J., Beddington J. R., Crute I. R., Haddad L., Lawrence D., Muir J. F., Pretty J., Robinson S., Thomas S. M., Toulmin C., “Food Security: The Challenge of Feeding 9 Billion People”, (2010).
[3] Prazeres A. R., Carvalho F., Rivas J., “Cheese whey management: A review”, Journal of Environmental Management 110 ,48–68, (2012).
[4] Yadav J. S. S., Yan S., Pilli S., Kumar L., Tyagi R. D., Surampalli R. Y., “Cheese whey: A potential resource to transform into bioprotein, functional/nutritional proteins and bioactive peptides”, Biotechnology Advances 33(6), 756–774, (2015).
[5] Baldasso C., Barros T. C., Tessaro I. C., “Concentration and purification of whey proteins by ultrafiltration”, Desalination 278, 381–386, (2011).
[6] Tiwari S., Bhimrao B., Arora N., Singh D. P., Upadhyaya S., Arora N. K, “Microbial Protein: A Valuable Component for Future Food Security”, (2016).
[7] Dubois Frigon M., “Acid whey treatment and conversion to single cell protein via aerobic yeast activated sludge”, Water Pract Technol 15, 494–505, (2020).

Title: Valorization of organic-rich waste through membrane-based technologies for volatile fatty acids recovery within the circular economy and sustainability goals

Author(s): Stefano Cairone*[1,2], Amir Mahboubi[2], Tiziano Zarra[1], Vincenzo Belgiorno[1], Mohammad J. Taherzadeh[2], Vincenzo Naddeo[1]

[1] Sanitary Environmental Engineering Division (SEED), Department of Civil Engineering, University of Salerno, Via Giovanni Paolo II #132, 84084 Fisciano, SA, Italy, {scairone, tzarra, v.belgiorno, vnaddeo}@unisa.it
[2] Swedish Centre for Resource Recovery, University of Borås, 501 90 Borås, Sweden, {stefano.cairone, mohammad.taherzadeh, amir.mahboubi_soufiani}@hb.se

Keyword(s): Resource recovery, biorefinery, anaerobic digestion, anaerobic membrane bioreactor, nanofiltration, volatile fatty acids

Abstract

The escalating depletion of natural resources, mainly due to global population growth, industrialization, and unsustainable consumption practices, presents a grave threat to the environment, exacerbating climate change and biodiversity decline [1, 2, 3]. Simultaneously, a surge in global waste production is recorded, underscoring the urgent need for efficacious waste management strategies [4].
The valorization of waste through sustainable resource recovery stands as a promising approach within the framework of the circular economy and sustainable development [5, 6, 7]. Anaerobic digestion (AD) processes, widely employed in waste treatment plants, conventionally yield biogas, recognized as a "green fuel" due to its high methane content [8, 9]. Additionally, AD presents a viable pathway for recovering volatile fatty acids (VFAs), considered more economically advantageous than biogas production [10]. By inhibiting the methanogenic phase, mixed VFAs, produced during fermentative stages, namely acidogenesis and acetogenesis, can be extracted.
Volatile fatty acids (VFAs) are short-chain aliphatic mono-carboxylate compounds containing two to six carbon atoms, encompassing acetic, propionic, isobutyric, butyric, isovaleric, valeric, and caproic acids, [11]. In the context of the circular bioeconomy, biologically-derived VFAs emerge as a sustainable alternative to petroleum-based VFAs, traditionally produced through thermochemical processes [12].
While pure single VFAs find application across various industrial sectors [13], mixed VFAs derived from AD hold promise in biodegradable polymer synthesis, bioenergy and biofuel production, biological nutrient removal from wastewater, and animal feed production [14, 15, 16]. However, challenges obstructing their widespread adoption include the relatively low VFAs concentration and the presence of other soluble compounds in AD effluent, necessitating post-treatment for concentration, separation, and purification. Membrane filtration technologies, particularly pressure-driven membrane processes, offer advantageous solutions to address these challenges [17, 18, 19, 20, 21].
Among pressure-driven membrane filtration processes, nanofiltration (NF) surpasses microfiltration (MF) and ultrafiltration (UF) in selectively separating low molecular weight compounds like VFAs. NF also demonstrates superior cost-effectiveness, energy efficiency, and suitability compared to reverse osmosis (RO), which indiscriminately rejects compounds other than water, hindering the selective separation of target compounds [22, 23, 24]. However, membrane fouling remains a primary challenge in membrane filtration processes. In fact, membrane fouling and other phenomena like concentration polarization effect impact permeate flux during filtration [25, 26, 27, 28].

This study explores the application of a membrane-based system, integrating an anaerobic membrane bioreactor (AnMBR) with a nanofiltration (NF) process (referred to as AnMBR+NF system), for recovering highly concentrated VFAs from organic-rich waste. A microfiltration (MF) membrane was immersed in the anaerobic reactor constituting the AnMBR system, described in our previous study [15]. Agro-industrial residues (apple pomace, thin stillage, and potato protein liquor) were used as feed for the AnMBR. The AnMBR effluent served as feed for NF, aimed at concentrating solubilized VFAs. The AnMBR, operated under the conditions described in our previous work [15], ensured VFAs production and the pre-treatment of the effluent, due to the installed MF membrane, with benefits for the subsequent NF process. A commercial laboratory-scale crossflow filtration unit (LABCELL CF-1, Koch Membrane System, United Kingdom) was employed to carry out the NF experiments. A commercial NF flat-sheet membrane ("NF270", Dow Filmtec) was used in the NF experiments.
Operating conditions of the NF process were optimized in our previous studies (not yet published) to achieve high VFAs concentration while ensuring substantial permeate flux. NF experiments were conducted under constant pressure (30 bar) and controlled temperature (40 °C), with feed pH adjusted to 9 using 2M NaOH to enhance VFAs rejection. Prior to initiating the NF experiments, the membranes underwent an initial phase of filtration using Milli-Q water as the feed to attain a state of steady flux [29]. Subsequently, after pH adjustment, 250 ml of the VFA effluent was introduced into the filtration unit and filtered under defined operating conditions. NF experiments continued until 200 ml of permeate (the target value) was collected, representing a 5x reduction in the initial feed volume. Samples of both permeate and retentate were collected at the conclusion of each filtration. Gas chromatograph (GC) (Clarus® 590, PerkinElmer, Norwalk, CT, USA) was employed for measuring VFAs concentrations in samples. VFAs concentrations in the feed (C_{feed}) and retentate (C_{ret}) are reported in **Table 1.** To compare the effect of the filtration process on the different VFAs contained in the AnMBR effluent in terms of concentration, the "VFA concentration factors" were calculated using Eq. (1):

$$R_{VFAs,retentate} = C_{ret}/C_{feed} \quad \text{(Eq. 1)}$$

Table 1. VFAs concentrations in the feed and retentate

Acid	Feed concentration	Retentate concentration	VFA concentration factor
Acetic	1,83 ± 0,03	4,88 ± 0,01	2,67
Propionic	0,51 ± 0,01	1,40 ± 0,01	2,75
Isobutyric	1,21 ± 0,02	3,97 ± 0,03	3,29
Butyric	1,87 ± 0,02	5,93 ± 0,05	3,17
Isovaleric	0,11 ± 0,00	0,19 ± 0,00	1,84
Valeric	0,46 ± 0,01	1,38 ± 0,02	2,99
Caproic	2,08 ± 0,03	6,47 ± 0,06	3,11
Total VFAs	8,06 ± 0,12	24,22 ± 0,16	3,01

Cyclic NF experiments were conducted, filtering fresh AnMBR effluent after the end of the previous filtration cycle. Five filtration cycles were performed reusing the same NF membrane. The study demonstrates stable VFAs concentration in retentate and permeate collected across the different filtration cycles. However, the membrane performance declined in terms of permeate flux. This is attributed to inevitable membrane fouling that causes higher filtration resistance and consequently lower permeate flux.

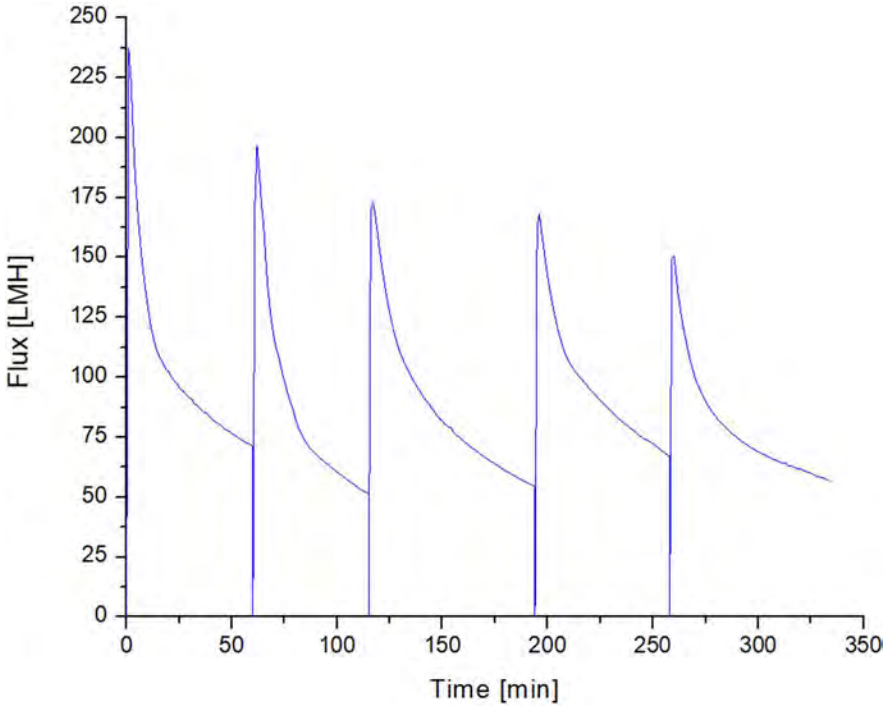

Figure 1. Flux graphs (NF270 membrane; feed pH = 9; T = 40 °C; p = 30 bar)

The results of this study indicate that employing the integrated AnMBR+NF system shows promise in both producing and concentrating waste-derived VFAs.
The outcomes of this research aim to offer valuable insights and establish a groundwork for future studies focused on optimizing and intensifying VFAs recovery processes. These pursuits are aligned with the overarching goal of advancing sustainable practices within the circular bioeconomy framework.

References

[1] Dubey B., Narayanan A.S., ”Modelling effects of industrialization, population and pollution on a renewable Resource”, Nonlinear Analysis: Real World Applications 11, 2833–2848 (2010).
[2] Huo J., Peng C., “Depletion of natural resources and environmental quality: Prospects of energy use, energy imports, and economic growth hindrances”, Resources Policy 86, 104049 (2023).
[3] Wang J., Azam W., “Natural resource scarcity, fossil fuel energy consumption, and total greenhouse gas emissions in top emitting countries” Geoscience Frontiers 15, 101757 (2024).
[4] Voukkali I., Papamichael I., Economou F., Loizia P., Klontza E., Lekkas D.F., Naddeo V., Zorpas A.A., “Factors affecting social attitude and behavior for the transition towards a circular economy”, Sustainable Chemistry and Pharmacy 36, 101276 (2023).
[5] Awasthi M.K., Ganeshan P., Gohil N., Kumar V., Singh V., Rajendran K., Harirchi S., Solanki M.K., Sindhu R., Binod P., Zhang Z., Taherzadeh M.J., “ Advanced approaches for resource recovery from wastewater and activated sludge: A review”, Bioresource Technology 384, 129250 (2023).
[6] Naddeo V., Korshin G., “Water, energy and waste: The great European deal for the environment”, Science of The Total Environment 764, 142911 (2021).
[7] Naddeo V., Taherzadeh M.J., “Biomass valorization and bioenergy in the blue circular economy”, Biomass and Bioenergy 149, 106069 (2021).
[8] Archana K., Visckram A.S., Senthil Kumar P., Manikandan S., Saravanan A., Natrayan L., ”A review on recent technological breakthroughs in anaerobic digestion of organic biowaste for biogas generation: Challenges towards sustainable development goals”. Fuel 358, 130298 (2024).

[9] Bhatt A.H., Tao L., ”Economic Perspectives of Biogas Production via Anaerobic Digestion”, Bioengineering (Basel) 7, 74 (2020).
[10] Liu He, Han P., Liu Hongbo, Zhou G., Fu B., Zheng Z., “Full-scale production of VFAs from sewage sludge by anaerobic alkaline fermentation to improve biological nutrients removal in domestic wastewater”, Bioresource Technology 260, 105–114 (2018).
[11] Njokweni S.G., Steyn A., Botes M., Viljoen-Bloom M., van Zyl W.H., ”Potential Valorization of Organic Waste Streams to Valuable Organic Acids through Microbial Conversion: A South African Case Study”, Catalysts 11, 964 (2021).
[12] Huang Y.L., Wu Z., Zhang L., Ming Cheung C., Yang S.-T., “Production of carboxylic acids from hydrolyzed corn meal by immobilized cell fermentation in a fibrous-bed bioreactor”, Bioresource Technology 82, 51–59 (2002).
[13] Agnihotri S., Yin D.-M., Mahboubi A., Sapmaz T., Varjani S., Qiao W., Koseoglu-Imer D.Y., Taherzadeh M.J., “A Glimpse of the World of Volatile Fatty Acids Production and Application: A review”, Bioengineered 13, 1249–1275 (2022).
[14] Mahboubi A., Agnihotri S., Uwineza C., Jomnonkhaow U., Taherzadeh M.J., “Chapter 18 - Waste-derived volatile fatty acids for sustainable ruminant feed supplementation”, in: Varjani S., Pandey A., Taherzadeh M.J., Ngo H.H., Tyagi R.D. (Eds.), Biomass, Biofuels, Biochemicals. Elsevier, pp. 407–430 (2022).
[15] Parchami M., Uwineza C., Ibeabuchi O.H., Rustas B.-O., Taherzadeh M.J., Mahboubi A., “Membrane bioreactor assisted volatile fatty acids production from agro-industrial residues for ruminant feed application”, Waste Management 170, 62–74 (2023).
[16] Sapmaz T., Manafi R., Mahboubi A., Lorick D., Koseoglu-Imer D.Y., Taherzadeh M.J., “Potential of food waste-derived volatile fatty acids as alternative carbon source for denitrifying moving bed biofilm reactors”, Bioresource Technology 364, 128046 (2022).
[17] Domingos J.M.B., Martinez G.A., Morselli E., Bandini S., Bertin L., “Reverse osmosis and nanofiltration opportunities to concentrate multicomponent mixtures of volatile fatty acids”, Separation and Purification Technology 290, 120840 (2022).
[18] Pervez Md. N., Mahboubi A., Uwineza C., Sapmaz T., Zarra T., Belgiorno V., Naddeo V., Taherzadeh M.J., “Feasibility of nanofiltration process for high efficient recovery and concentrations of food waste-derived volatile fatty acids”, Journal of Water Process Engineering 48, 102933 (2022).
[19] Pervez Md. N., Mahboubi A., Uwineza C., Zarra T., Belgiorno V., Naddeo V., Taherzadeh M.J., “Factors influencing pressure-driven membrane-assisted volatile fatty acids recovery and purification-A review”, Science of The Total Environment 817, 152993 (2022).
[20] Zacharof M.-P., Lovitt R.W., “Recovery of volatile fatty acids (VFA) from complex waste effluents using membranes”, Water Science and Technology 69, 495–503 (2013).
[21] Zacharof M.-P., Mandale S.J., Williams P.M., Lovitt R.W., “Nanofiltration of treated digested agricultural wastewater for recovery of carboxylic acids”, Journal of Cleaner Production 112, 4749–4761 (2016).
[22] Chowdhury T., Chowdhury H., Miskat M.I., Rahman M.S., Hossain N., “Chapter 19 - Membrane-based technologies for industrial wastewater treatment and resource recovery”, in: Shah M.P., Rodriguez-Couto S. (Eds.), Membrane-Based Hybrid Processes for Wastewater Treatment. Elsevier, pp. 403–421 (2021).
[23] Teow Y.H., Sum J.Y., Ho K.C., Mohammad A.W., “3 - Principles of nanofiltration membrane processes”, in: Hilal N., Ismail A.F., Khayet M., Johnson D. (Eds.), Osmosis Engineering. Elsevier, pp. 53–95 (2021).
[24] Zhang H., He Q., Luo J., Wan Y., Darling S.B., “Sharpening Nanofiltration: Strategies for Enhanced Membrane Selectivity”, ACS Appl. Mater. Interfaces 12, 39948–39966 (2020).
[25] Abdel-Fatah M.A., “Nanofiltration systems and applications in wastewater treatment: Review article”, Ain Shams Engineering Journal 9, 3077–3092 (2018).
[26] Contreras A.E., Kim A., Li Q., “Combined fouling of nanofiltration membranes: Mechanisms and effect of organic matter”, Journal of Membrane Science 327, 87–95 (2009).
[27] Giacobbo A., Moura Bernardes A., Filipe Rosa M.J., De Pinho M.N., “Concentration Polarization in Ultrafiltration/Nanofiltration for the Recovery of Polyphenols from Winery Wastewaters”, Membranes 8, 46 (2018).
[28] Winter J., Barbeau B., Bérubé P., “Nanofiltration and Tight Ultrafiltration Membranes for Natural Organic Matter Removal-Contribution of Fouling and Concentration Polarization to Filtration Resistance”, Membranes (Basel) 7, 34 (2017).
[29] Cho Y.H., Lee H.D., Park H.B., “Integrated Membrane Processes for Separation and Purification of Organic Acid from a Biomass Fermentation Process”, Ind. Eng. Chem. Res. 51, 10207–10219 (2012).

Review of the perspectives for the valorization of orange peel wastes

Author(s): Ilaria Orlandella, Silvia Fiore

DIATI, Department of Engineering for Environment, Land and Infrastructure, Politecnico di Torino, Italy

Keyword(s): *citrus, orange, biorefineries, waste, footprint*

Abstract

To preserve the environment, a shift toward a Circular Economy is crucial. The use of waste as an input material is compliant with the recommendations of the European Commission for the implementation of the waste management hierarchy. This hierarchy establishes a priority order that gives top priority to prevention, followed by preparation for re-use, recycling, energy recovery, and lastly, landfill disposal [1]. Given the volume produced annually in Europe (over 58 million tonnes), food waste and food processing waste need special attention [2]. Italy is the second producer (after France) in the EU 27 of agricultural products with a market of 38.4 billion of euros and a 13.7% increase in the national agricultural income indicator [3]. It's also important to observe how climate change is affecting agricultural output within individual nations. In 2022, Italy experienced a 6.8% increase in the volume of fruit crops, despite a significant decrease in other crop production. In spite of the increase in volume, the price has seen an increase, which for citrus is equal to 14.7%[3]. Specifically considering the production of orange juice, about 55 million tonnes per year of inedible orange peel waste (OPW, a mix of pulp, seeds, and peel) are created worldwide [4]. In overall, the juice corresponds to 35-45%wt of the fresh citrus and OPW up to 60%wt [5], and some factories [4] manufacture hundreds of tonnes of orange peel waste every week. OPW is usually managed through biological and thermochemical processes [6], and literature also explored active components extraction [7] and the conversion into animal feed [8]. These approaches are often considered unsatisfactory due to various drawbacks, such as high levels of energy consumption and limited local market demand [9].

The main objective of the present review study is an evaluation encompassing environmental and technical aspects of a range of technologies employed in OPW management. A literature research was performed on Scopus database, adopting the keywords “Orange waste”, “Footprint” or “LCA”. This provided 46 references. Anaerobic digestion emerged as the most applied technology (36% of the selected references), followed by incineration (29% of the references), pyrolysis (14% of the references), and composting and production of animal feed (14% of the references). About the recovery of active compounds (7% of the references) such as polyphenols, essential oils, and other bioactive substances, various methods were explored (e.g., steam distillation, enzymatic hydrolysis, and ethanol extraction) [7]. Also, biorefinery systems have been analysed to produce a wide range of commercially viable products and minimize the consumption of fossil fuels as energy source[7].

Concerning the applied tool, Life Cycle Assessment (LCA) was the prevalent choice (75% of the references) followed by Carbon Footprint (25% of the references). Moreover, LCA was frequently employed to show the reduction of environmental impacts through the use of OPW as substitutes for raw materials [10]. The choice of the functional unit mostly involved process inputs as OPW [4], [7], [9] (40% of the references) and OPW included in a mix of food waste(7% of the references) [11]; or outputs as electricity[12] heat [7], [13], (30% of the references), and orange juice [6], biofuel, digestate, and limonene [12] (23% of the references).

Anaerobic digestion demonstrates particular efficacy in the valorization of OPW, as biogas matches the energy demand of the plant, and digestate is applied as a fertilizer for orange crops; as a result of this integrated approach, the Global Warming Potential impact is reduced [6]. The presence of process inhibitors such as D-limonene must be prevented, either extracting them before the digestion of OPW as single substrate, or applying co-digestion [9]. When OPW undergoes pyrolysis, usually at temperatures between 400 and 800°C, many options are available for the valorization of the outputs (bio-oil, bio-char, and condensables), as biodiesel production, power generation, soil improvement, and carbon sequestration. When biochar derived from orange waste is used as biofuel the Global Warming Potential impact is 79% lower compared to fossil oil [10]. Furthermore, the production of biochar derived from OPW exhibits the lowest environmental impact compared to other agricultural waste materials, with a reduction of 16% compared to olive tree trimmings [13].
When considering the possibility of converting OPW into animal feed, it's important to remember that it can be easily dried and then pelletized to produce the final end product [9]. As an alternative, biorefinery processes may be applied, as microwave extraction of essential oil followed by a solid-state fermentation with recovery of citric acid from the liquid fraction and animal feed obtained from the solid fraction. In terms of feed recipients, it has been observed that ruminant animals exhibit a clear preference for a high fiber content, with exceptional palatability and suitability for consumption by sheep of feed derived from OPW [8]. In terms of CO_2 eq emissions, the conversion of OPW into animal feed demonstrated prominent performance (–302 kg CO_2 eq t^{-1} OPW) compared to the production of conventional crops (soybeans and maize) and the resulting effects on land-use change [9].
The emissions, in terms of CO_2 eq, deriving from the Krill Design bio-polymer production process are lower (around 30%) than the emissions from the production of plastics such as PVC, HDPE, PET.

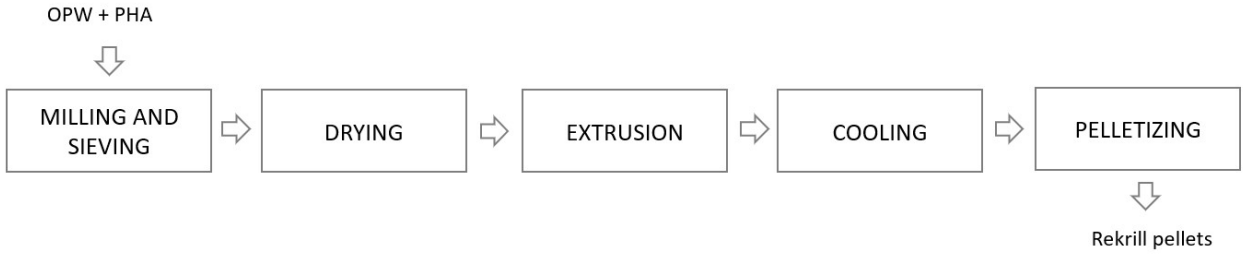

Figure 1: Steps of the production process of bio-composite material(OPW: orange peel waste, PHA: polyhydroxyalkanoate) .

Additionally, the Italian textile and fashion industries showed a special interest for cellulose fibers derived from OPW. In 2012, a start-up called Orange Fiber (https://orangefiber.it) was founded in Sicily, and in 2017 released its first collection of clothing made from waste oranges. This method's distinguishing feature is that cellulose is extracted chemically, without the use of chlorine, and that basic requirements are met when treating the citrus fruit raw materials with hydrogen peroxide. The Orange Fiber process exhibits reduced environmental impacts compared to the production of natural cellulose cotton fiber, as -90% water [15].
Regarding paper manufacture, an Italian company, Favini srl, has been producing paper (“Orange Crush Agrumi”) from agri-food transformation for many years. Agri-food residues (peels, shells, or pits) are ground into a flour and dried at a specific temperature before being mixed with paper pulp [16].
In conclusion, it is important to mention that some of the considered technologies, such as pyrolysis or incineration, can be defined “short loop” compared to others that are “large loop” (i.e. based on numerous consequent phases), such as anaerobic digestion in conjunction with steam extraction, or

even for the extraction of active compounds, such as microwave extraction prior to the production of animal feed, which required even more steps. It is crucial to consider the economic viability of each technology, which is closely tied to the local market where the plant is situated and the products sold [4]. In this study, the best management strategy for OPW in terms of mitigating the effects of global warming and resource depletion appears to be co-digestion with manure for biogas and biofertilizer production [9]. In Italy, incineration without heat recovery for district heating is not financially feasible due to high capital and operational costs (€115 per ton of OPW), which are not offset by electricity sales (€20 t^{-1} OPW) [9]. Anaerobic mono-digestion has lower capital and operational costs, but despite this, the net value, considering costs and revenues, is considerably lower (€11 t^{-1} OPW) compared to incineration (€95 t^{-1} OPW). Upgrading biogas to transportation fuel leads to higher income than converting it to electricity. Limonene extraction is the most attractive scenario, while using orange waste as animal feed is environmentally sustainable but not financially feasible when assuming OPW is in pellet form [9].

Acknowledgements

This study was carried out within the Agritech National Research Center and received funding from the European Union Next-GenerationEU (PIANO NAZIONALE DI RIPRESA E RESILIENZA (PNRR) – MISSIONE 4 COMPONENTE 2, INVESTIMENTO 1.4 – D.D. 1032 17/06/2022, CN00000022).

References

[1] EU, “EU action plan for the Circular Economy.” Accessed: Mar. 19, 2024. [Online]. Available: https://eur-lex.europa.eu/legal-content/EN/TXT/HTML/?uri=CELEX:52015DC0614

[2] European Commission, “Food Waste.” Accessed: Mar. 27, 2024. [Online]. Available: https://food.ec.europa.eu/safety/food-waste_en

[3] ISTAT, “STIMA PRELIMINARE DEI CONTI ECONOMICI DELL’AGRICOLTURA | ANNO 2022,” Jan. 2023. Accessed: Mar. 19, 2024. [Online]. Available: https://www.istat.it/it/files//2023/01/Report_Stima_prelim_andamento_economia_agricola_2022_30012023.pdf

[4] D. A. Teigiserova, L. Hamelin, L. Tiruta-Barna, A. Ahmadi, and M. Thomsen, “Circular bioeconomy: Life cycle assessment of scaled-up cascading production from orange peel waste under current and future electricity mixes,” *Science of The Total Environment*, vol. 812, p. 152574, Mar. 2022, doi: 10.1016/J.SCITOTENV.2021.152574.

[5] A. Ferrari, P. Morone, and V. E. Tartiu, “Tackling uncertainty through business plan analysis—A case study on citrus waste valorisation in the south of Italy,” *Agriculture (Switzerland)*, vol. 6, no. 1, Mar. 2016, doi: 10.3390/agriculture6010005.

[6] D. L. Ortiz, E. Batuecas, C. E. Orrego, L. J. Rodríguez, E. Camelin, and D. Fino, “Sustainable management of peel waste in the small-scale orange juice industries: A Colombian case study,” *J Clean Prod*, vol. 265, Aug. 2020, doi: 10.1016/j.jclepro.2020.121587.

[7] M. Ortiz-Sanchez, J. C. Solarte-Toro, P. J. Inocencio-García, and C. A. Cardona Alzate, "Sustainability analysis of orange peel biorefineries," *Enzyme Microb Technol*, vol. 172, p. 110327, Jan. 2024, doi: 10.1016/J.ENZMICTEC.2023.110327.

[8] V. A. Bampidis and P. H. Robinson, "Citrus by-products as ruminant feeds: A review," *Anim Feed Sci Technol*, vol. 128, no. 3–4, pp. 175–217, Jun. 2006, doi: 10.1016/J.ANIFEEDSCI.2005.12.002.

[9] V. Negro, B. Ruggeri, D. Fino, and D. Tonini, "Life cycle assessment of orange peel waste management," *Resour Conserv Recycl*, vol. 127, pp. 148–158, Dec. 2017, doi: 10.1016/J.RESCONREC.2017.08.014.

[10] E. Martinez-Hernandez *et al.*, "Energy-water nexus strategies for the energetic valorization of orange peels based on techno-economic and environmental impact assessment," *Food and Bioproducts Processing*, vol. 117, pp. 380–387, Sep. 2019, doi: 10.1016/J.FBP.2019.08.002.

[11] M. Eriksson and J. Spångberg, "Carbon footprint and energy use of food waste management options for fresh fruit and vegetables from supermarkets," *Waste Management*, vol. 60, pp. 786–799, Feb. 2017, doi: 10.1016/J.WASMAN.2017.01.008.

[12] M. Pourbafrani, J. McKechnie, H. L. Maclean, and B. A. Saville, "Life cycle greenhouse gas impacts of ethanol, biomethane and limonene production from citrus waste," *Environmental Research Letters*, vol. 8, no. 1, 2013, doi: 10.1088/1748-9326/8/1/015007.

[13] M. A. Cusenza *et al.*, "Environmental assessment of a waste-to-energy practice: The pyrolysis of agro-industrial biomass residues," *Sustain Prod Consum*, vol. 28, pp. 866–876, Oct. 2021, doi: 10.1016/J.SPC.2021.07.015.

[14] J. J. Ortega-Gras, M. V. Bueno-Delgado, G. Cañavate-Cruzado, and J. Garrido-Lova, "Twin transition through the implementation of industry 4.0 technologies: Desk-research analysis and practical use cases in europe," *Sustainability (Switzerland)*, vol. 13, no. 24, Dec. 2021, doi: 10.3390/SU132413601.

[15] E. D'Itria and C. Colombi, "Biobased Innovation as a Fashion and Textile Design Must: A European Perspective," *Sustainability (Switzerland)*, vol. 14, no. 1, Jan. 2022, doi: 10.3390/su14010570.

[16] E. Overturf, S. Pezzutto, M. Boschiero, N. Ravasio, and A. Monegato, "The circo (Circular coffee) project: A case study on valorization of coffee silverskin in the context of circular economy in Italy," *Sustainability (Switzerland)*, vol. 13, no. 16, Aug. 2021, doi: 10.3390/su13169069.

Title: Hydrometallurgical recycling of cobalt, manganese, and nickel from lithium-ion batteries: effects of microwave carbothermal reduction on the leaching efficiency

Author(s): Martina Bruno[1], Alessandra Zanoletti[2], Elza Bontempi[2], Silvia Fiore[1]

[1] Dipartimento di Ingegneria per l'Ambiente, il Territorio e le Infrastrutture, Politecnico di Torino, Corso Duca degli Abruzzi 24, 10129 Torino (TO), Italy, {martina.bruno, silvia.fiore}@polito.it
[2]INSTM and Chemistry for Technologies Laboratory, University of Brescia, 25123 Brescia, Italy, {alessandra.zanoletti, elza.bontempi}@unibs.it

Keyword(s): lithium-ion batteries, recycling, critical raw materials, organic acid

Abstract

Lithium-ion batteries (LIBs) find a wide range of applications, hence the demand for lithium, cobalt, manganese, and nickel for LIBs manufacturing has significantly increased over the years. In 2022, 125 kt of lithium, 183 kt of cobalt and 3,000 kt of nickel were required worldwide for LIBs manufacturing [1]. Ensuring sustainability, resilience, and safety of the LIBs' supply chain requires reducing the dependence on virgin minerals, particularly for critical raw materials. One way to achieve this is through the optimization of recycling processes, which enables to recovery of secondary materials as precursors to produce new batteries.

State of the art LIBs' recycling relies on pyrometallurgical and hydrometallurgical processes. Pyrometallurgy is a mature technology to recover metal alloys of cobalt, nickel, and manganese. However, its main drawbacks are the high energy demand, the generation of gaseous pollutants and the limited lithium recovery [2]. Hydrometallurgy instead is a chemical process to recover individual metals, including lithium, through leaching and separation steps. Hydrometallurgical processes conventionally employ inorganic acids, e.g. sulfuric, chloridic and nitric, often combined with hydrogen peroxide as a reducing agent to leach metals [3]. Inorganic acids exhibit high leaching efficiencies, but their application poses the risk of generating toxic gasses, such as Cl_2, SO_3 and NO_x and the need for specific operations because of the low pH [4]. Organic acids have been recently proposed to limit the environmental impact associated with hydrometallurgical processes, due to their good leaching performances, easy degradation, and recyclability [5-13]. Nonetheless, the long leaching kinetics of organic acids and their high cost, limit the scalability of LIBs' recycling. Acetic acid, which holds a limited production cost (0.48 €/kg [5]), represents a suitable alternative to overcome the economic drawbacks of organic acid leaching. Previous studies reported leaching efficiencies between 73%-99% for Co, 92%-99% for Mn and 93%-99% for Ni with acetic acid aided by reducing agents. The most common reducing agent used alongside acetic acid is hydrogen peroxide, with a concentration ranging from 4%vol. [6] to 7.5%vol. [7]. Besides, ascorbic [8], formic [9] and tannic [10] acids have been combined with acetic acid to increase leaching efficiency. These reduce high valence metals to increase their solubility in acidic solutions [11,12] and accelerate leaching kinetics [6]. However, their use increases the cost of the overall recycling process [13].

Pyrometallurgical treatments based on carbothermal reduction have been explored to reduce metals' valence state and increase their recovery [14]. A great focus has been given to the recovery of lithium, overlooking other metals and, since these processes require temperatures above 700°C for 90 minutes [15], this still poses an obstacle to the economic feasibility of the scale up. A novel thermal process has been recently proposed for the carbothermal reduction of spent black mass via microwave technology [16], which can decrease the energy demand by two orders of magnitude compared with conventional

thermal processes. This work aims to study the effect of this carbothermal reduction process on the leaching efficiency of acetic acid on Co, Mn, and Ni from two different black mass samples, without additional reducing agents. Two black mass samples, supplied by industrial recycling facilities, with different chemistries have been involved in this study. In detail, a nickel-based black mass (here on referred to as "Ni-BM") and a cobalt-based black mass (here on referred to as "Co-BM"). The BM samples have been characterized through X-Ray Fluorescence (XRF) spectroscopy, obtaining the compositions: 8.4%wt. Ni, 3.5%wt. Mn, 2.8%wt. Co, 1.1%wt. Al and 0.8%wt. Cu for Ni-BM, and 5.3%wt. Ni, 4.1%wt. Mn, 13.5%wt. Co, 1.9%wt. Al and 1.1%wt. Cu for Co-BM. The BM samples underwent the microwave carbothermal reduction process [16]. The composition of the microwave-treated samples, here on referred to as "Ni-BM-MW" and "Co-BM-MW", has been determined through XRF spectroscopy: 20.8%wt. Ni, 7.3%wt. Mn, 6.9%wt. Co, 1.9%wt. Al and 2.2%wt. Cu for Ni-BM-MW and 8.3%wt. Ni, 5.4%wt. Mn, 20.9%wt. Co, 3.4%wt. Al, and 1.8%wt. for Co-BM-MW. Material losses due to the microwave carbothermal reduction were 27%wt for Ni-BM and 1%wt for the Co-BM sample. The lower material loss in Co-BM can be attributed to a stronger thermal process performed by the treatment plant providing that sample.
Leaching with acetic acid has then been applied to the four BM and BM-MW samples. The operative conditions (acid concentration, solid/liquid ratio, temperature, and leaching time) were selected according to the average conditions applied in previous studies (Table 1). The leaching tests applied 2 M acetic acid, a solid/liquid ratio of 30 g/L for 45 minutes at 70°C. The leaching residues have been separated through centrifugation, rinsed with deionized water, and dried at 70°C, before characterization with XRF spectroscopy. The results of the leaching tests are reported in Figure 1.

Table 1. Literature overview of operative conditions (acid concentration, solid/liquid ratio, temperature, and leaching time) for acetic acid leaching

Acetic acid concentration (M)	S/L ratio (g/L)	Temperature (°C)	Time (min)	Reducing agent	References
3	100	90	60	oxalic acid (from molasses)	[17]
2.5	40	80	20	ascorbic acid	[8]
0.5	20	50	40	ascorbic acid and bagasse pith	[11]
1	20	80	240	tannic acid	[10]
3	20	70	40	hydrogen peroxide	[7]
1	20	70	60	hydrogen peroxide	[13]
3.5	40	60	60	hydrogen peroxide	[6]
2	20	70	30	hydrogen peroxide	[18]
2		60		hydrogen peroxide	[19]
2.8	10			hydrogen peroxide	[12]
2	30	70	45	none	this study

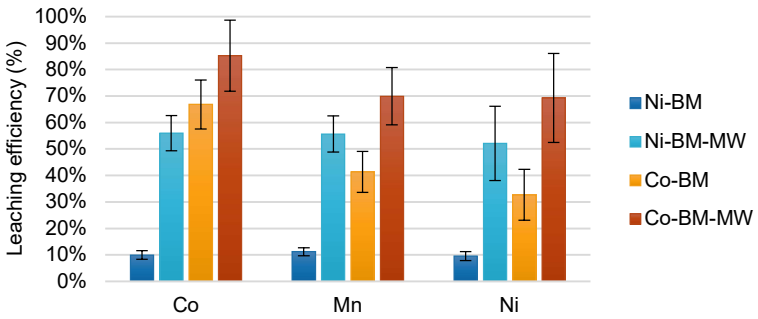

Figure 1. Leaching efficiency with acetic acid

Leaching efficiencies of Co, Mn and Ni from Co-BM are higher compared to Ni-BM, before and after microwave carbothermal reduction. The leaching efficiencies of the initial samples are 10±2% for Co, 11±2% for Mn and 10±2% for Ni in the Ni-BM sample and 67±14% for Co, 41±7% for Mn and 33±7% for Ni in the Co-BM sample. These values are scarce, but consistent with previous results obtained by acetic acid without additional reducing agents, due to the absence of a reducing agent or of the reducing effect of microwave carbothermal reduction. Indeed, previous studies reported leaching efficiencies of 17-20% for Co [12], 29-32% for Mn and 26-36% for Ni [17].
The samples treated with microwave carbothermal reduction exhibited higher leaching efficiencies: 56±10% for Co, 56±8% for Mn and 52±9% for Ni from the Ni-BM-BM sample and 85±17% for Co, 70±11% for Mn and 69±13% for Ni from the Co-BM-MW sample. Increased leaching efficiency after microwave carbothermal reduction has been observed also for other metals contained in the black mass. Indeed, Al leaching efficiency increased from 29±1% to 54±1% in the Ni-BM sample and from 48±2% to 82±1% in the Co-BM sample, and Cu leaching efficiency increased from 39±1% to 87±1% and from 51±1% to 85±1%, respectively. Thereby, microwave carbothermal reduction proved to be effective in increasing metals' leaching from the black mass. These results could be attributed both to the reduction of these metals and to the partial elimination of graphite from the black mass, which increased the concentration of the target metals (Co, Mn, and Ni) in the samples.
In conclusion, this work presents the benefits of microwave carbothermal reduction treatment to improve the leaching efficiency of acetic acid, without the need for additional reducing agents in the leaching process and reducing operational costs. Nonetheless, previous studies reported acetic acid leaching efficiency equal to 73%-99% for Co, 92%-97% for Mn and 93%-99% for Ni with the addition of hydrogen peroxide [6,7,13,18,19]; to 95%-98% for Co, 98% for Mn and Ni with the addition of ascorbic acid [8,11]. The leaching efficiency reached in this study after microwave carbothermal reduction is lower than the results obtained by previous studies applying reducing agents during leaching, therefore further research should focus on the optimization of leaching parameters to increase the efficiency of acetic acid leaching after microwave thermal reduction.

Acknowledgments

This study was carried out within the MICS (Made in Italy – Circular and Sustainable) Extended Partnership and received funding from Next-GenerationEU (Italian PNRR – M4 C2, Invest 1.3 – D.D. 1551.11-10-2022, PE00000004) and and MITO Technology.

References

[1] International Energy Agency, Global EV Outlook 2023, IEA. (2023) 9–10. www.iea.org/reports/global-ev-outlook-2023.
[2] A. Zanoletti, E. Carena, C. Ferrara, E. Bontempi, A Review of Lithium-Ion Battery Recycling: Technologies, Sustainability, and Open Issues, Batteries. 10 (2024). https://doi.org/10.3390/batteries10010038.
[3] G. Mishra, R. Jha, A. Meshram, K.K. Singh, A review on recycling of lithium-ion batteries to recover critical metals, J. Environ. Chem. Eng. 10 (2022) 108534. https://doi.org/10.1016/j.jece.2022.108534.
[4] Y. Yao, M. Zhu, Z. Zhao, B. Tong, Y. Fan, Z. Hua, Hydrometallurgical Processes for Recycling Spent Lithium-Ion Batteries: A Critical Review, ACS Sustain. Chem. Eng. 6 (2018) 13611–13627. https://doi.org/10.1021/acssuschemeng.8b03545.
[5] Ecoinvent, ecoinvent v3.8 - ecoinvent, (n.d.).
[6] W. Gao, J. Song, H. Cao, X. Lin, X. Zhang, X. Zheng, Y. Zhang, Z. Sun, Selective recovery of valuable metals from spent lithium-ion batteries – Process development and kinetics evaluation, J. Clean. Prod. 178 (2018) 833–845. https://doi.org/10.1016/j.jclepro.2018.01.040.
[7] S. Natarajan, A.B. Boricha, H.C. Bajaj, Recovery of value-added products from cathode and anode material of spent lithium-ion batteries, Waste Manag. 77 (2018) 455–465. https://doi.org/10.1016/j.wasman.2018.04.032.
[8] J. Zhang, X. Hu, T. He, X. Yuan, X. Li, H. Shi, L. Yang, P. Shao, C. Wang, X. Luo, Rapid extraction of valuable metals from spent LiNixCoyMn1-x-yO2 cathodes based on synergistic effects between organic acids, Waste Manag. 165 (2023) 19–26. https://doi.org/10.1016/j.wasman.2023.04.020.
[9] J. Zhang, Y. Ding, H. Shi, P. Shao, X. Yuan, X. Hu, Q. Zhang, H. Zhang, D. Luo, C. Wang, L. Yang, X. Luo, Selective recycling of lithium from spent LiNixCoyMn1-x-yO2 cathode via constructing a synergistic leaching environment, J. Environ. Manage. 352 (2024) 120021. https://doi.org/10.1016/j.jenvman.2024.120021.
[10] E. Prasetyo, W.A. Muryanta, A.G. Anggraini, S. Sudibyo, M. Amin, M. Al Muttaqii, Tannic acid as a novel and green leaching reagent for cobalt and lithium recycling from spent lithium-ion batteries, J. Mater. Cycles Waste Manag. 24 (2022) 927–938. https://doi.org/10.1007/s10163-022-01368-y.
[11] S. Yan, C. Sun, T. Zhou, R. Gao, H. Xie, Ultrasonic-assisted leaching of valuable metals from spent lithium-ion batteries using organic additives, Sep. Purif. Technol. 257 (2021) 117930. https://doi.org/10.1016/j.seppur.2020.117930.
[12] H. Setiawan, H.T.B.M. Petrus, I. Perdana, Reaction kinetics modeling for lithium and cobalt recovery from spent lithium-ion batteries using acetic acid, Int. J. Miner. Metall. Mater. 26 (2019) 98–107. https://doi.org/10.1007/s12613-019-1713-0.
[13] L. Li, Y. Bian, X. Zhang, Q. Xue, E. Fan, F. Wu, R. Chen, Economical recycling process for spent lithium-ion batteries and macro- and micro-scale mechanistic study, J. Power Sources. 377 (2018) 70–79. https://doi.org/10.1016/j.jpowsour.2017.12.006.
[14] J. You, Z. Qin, G. Wang, M. Rao, J. Luo, Z. Peng, S. Zou, G. Li, Recycling valuable metals from spent lithium-ion battery cathode materials based on microwave-assisted hydrogen reduction followed by grind-leaching and magnetic separation, J. Clean. Prod. 428 (2023) 139488. https://doi.org/10.1016/j.jclepro.2023.139488.
[15] Q. Yuan, J. Zeng, Q. Sui, Z. Wang, S. Xu, S. Mao, H. Wen, T. Xiao, Y. Wu, B. Yuan, J. Liu, Thermodynamic and experimental analysis of lithium selectively recovery from spent lithium-ion batteries by in-situ carbothermal reduction, J. Environ. Chem. Eng. 11 (2023) 111029. https://doi.org/10.1016/j.jece.2023.111029.
[16] A. Fahimi, I. Alessandri, A. Cornelio, P. Frontera, A. Malara, E. Mousa, G. Ye, B. Valentim, E. Bontempi, A microwave-enhanced method able to substitute traditional pyrometallurgy for the future of metals supply from spent lithium-ion batteries, Resour. Conserv. Recycl. 194 (2023) 106989. https://doi.org/10.1016/j.resconrec.2023.106989.
[17] D. Amalia, P. Singh, W. Zhang, A.N. Nikoloski, The Effect of a Molasses Reductant on Acetic Acid Leaching of Black Mass from Mechanically Treated Spent Lithium-Ion Cylindrical Batteries, Sustain. 15 (2023). https://doi.org/10.3390/su151713171.
[18] K. Wang, G. Zhang, M. Luo, Recovery of Valuable Metals from Cathode—Anode Mixed Materials of Spent Lithium-Ion Batteries Using Organic Acids, Separations. 9 (2022). https://doi.org/10.3390/separations9090259.
[19] J. Yu, J. Li, S. Zhang, F. Wei, Y. Liu, J. Li, Mechanochemical upcycling of spent LiCoO2 to new LiNi0.80Co0.15Al0.05O2 battery: An atom economy strategy, Proc. Natl. Acad. Sci. U. S. A. 120 (2023). ~~https://doi.org/10.1073/pnas.2217698120~~. https://doi.org/10.1073/pnas.2217698120

Modelling the EU plastic value chain and assessing its environmental impacts: approaches, data sources and hotspots towards a circular plastic value chain

Authors: Andrea Martino Amadei[1,2], Lucia Rigamonti[1], Serenella Sala[2]

[1] *Politecnico di Milano, Piazza Leonardo da Vinci 32, Milano 20133, Italy*
[2] *European Commission - Joint Research Centre, Ispra (VA), Italy*

Keyword(s): *Material flow analysis, Plastic value chain, Recycled plastics, Plastic litter, Mismanaged waste, Plastic consumption, life cycle assessment, environmental impacts*

Abstract

Despite the increasing attention to the European Union (EU) plastic flows, there is a lack of studies focusing on comprehensive assessments of the plastics value chains, across various sectors and polymers, both at the level of mass flows and at the level of environmental impacts. This deficiency is especially evident in the lack of consideration given to certain specific plastic sectors or to certain specific plastic flows such as plastic losses, mismanaged waste plastics, or the fate of recycled plastics. The EU has striven to tackle the plastic challenge through several key policy initiatives such as the EU Plastic Strategy [1] (flagging how plastics are currently produced, used, and discarded in way that leads to severe environmental impacts) and the Circular Economy Action Plan [2] (aiming at further developing a circular economy also for the plastic sector). The prevention and reduction of plastics impacts, especially due to single-use-plastics, has also been at the forefront of the EU attention, as highlighted in the Single-Use Plastics (SUP) [3]. A specific focus on plastic has also been outlined in the EU Green Deal [4], which not only aims at reducing intentionally added microplastics and unintentional releases of plastics, but also at ensuring that all packaging in the European market is reusable or recyclable in an economically viable manner by 2030. Understanding the impact of plastic pollution, particularly marine plastic debris, has also been recognized as critical for achieving UN Sustainable Development Goal (SDG) 14, aimed at conserving and sustainably utilizing oceans, seas, and marine resources [5]. Achieving the ambitious goals set forth by these actions needs a profound understanding of the flow of plastic materials within the EU.

This study developed a comprehensive top-down Material Flow Analysis (MFA) covering the entire value chain across nine economic sectors and focusing on ten specific polymers within the EU27 in 2019. MFA has in fact been employed in the recent years as a key tool for assessing products flows and to unveil hotspots of value chains that could hinder circularity and sustainability [6], [7], [8]. Sector-specific MFAs were computed using sets of Transfer Coefficients (TCs) matrices at the level of sectors and polymers. TCs are defined for each input and output flows of a process along the value chain and serve the purpose of detailing the total amount of a substance that is transferred from a process to another one. The MFA was also linked to a Life Cycle Assessment (LCA) analysis, aimed at unveiling the environmental impacts of the whole value chain and at providing methodological guidance on linking LCA with MFA results.

During the initial phase of the project, a thorough literature review was conducted to gather pertinent data, with a focus on identifying key literature sources. Subsequently, data adjustments were made to adjust data to a common reference point (EU27 2019) and to adapt the information to suit the system boundaries of the abovementioned sectors-specific and polymers-specific value chains under exam.

Employing a tailor-made top-down approach, the total EU plastic demand was differentiated by sectors and polymers and the fate of each plastics flow was followed from manufacturing to the end-of-life. The findings from the sector-specific MFAs are displayed in Figure 1.

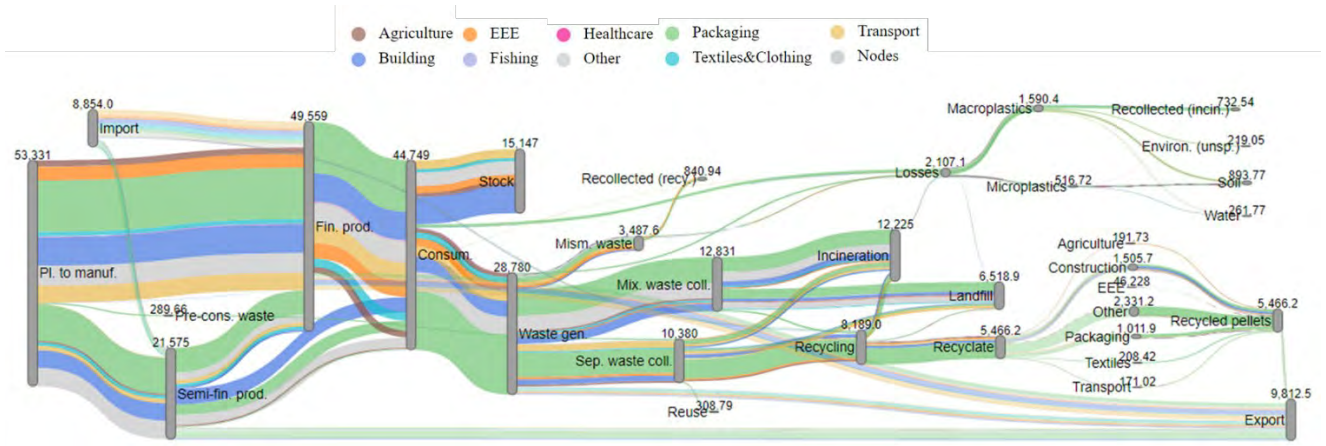

Figure 1. Overview of the EU27 2019 MFA for all the examined sectors. All data are expressed in ktonne.

The results emphasized the crucial role played by the packaging sector in the whole EU plastic value chain, as this sector amounted to 33% of the total plastic consumption, followed by the construction sector at 23%. Waste generated from consumption constituted 64% of total consumed plastics, with 34% ending up in “stock” and 2% lost during use. In the present study, the “stock” accumulation across all included sectors was determined by calculating as the amount of plastics balancing the total consumed amount and the total waste generated amount within each sector. Notably, the study revealed a gap of approximately 15 million tonnes between total consumed plastics and total waste generated in 2019 (gap which has been also recognized by other literature and report in the plastic field; e.g. [9]). A recent report by Material Economics and Agora Industry [10] indicates that this gap may be attributable to an underestimation, potentially as high as 45%, of the total mixed waste generated and collected.
Despite the significant amount of post-consumer waste generated in 2019 (28.8 million tonnes), only 38% was separately collected, and a notable fraction (13%) was mismanaged, particularly impacting the transport (44% of the total waste generated) and EEE (22% of the total waste generated) sectors. Plastic “mismanagement” was intended in this study as inadequately disposed waste - e.g., disposed in open dumps, unspecified landfills, unaccounted, etc. and/or treated/managed for example by unauthorized third parties - in ways that could create routes for potential losses and releases into the environment. Part of this waste could also be potentially recollected by waste pickers or informal collection systems and sent to recycling. Plastic mismanagement was recognized by the present study as a key hotspot in the EU plastic value chain, leading to an overall loss of valuable plastic fractions that could otherwise be directed to proper end-of-life management.

When looking at recycling, 70% of the plastic waste entering recycling facilities (being equal to a total of 8 million tonnes) originated from the packaging sector. Overall, 5.47 million tonnes of recyclates (i.e., secondary recycled plastics) were produced in the EU27 in 2019, with 4.46 million tonnes consumed domestically (considering 18% exported).
Despite uncertainty and data limitations in modelling the fate/destination of recyclates, the construction sector emerged as the primary destination for secondary plastics, followed by the packaging sector. The EU27 end-of-life recycling rate averaged to 19% (16.6% when trade effects are considered).

A significant amount (2.11 million tonnes) of microplastics and macroplastics losses in the entire value chain occurred during the use phase (39% due to e.g. emissions caused by tyre abrasion or washing of synthetic textiles). Losses of waste plastics could also occur (amounting to 37% of the total losses and including 20% due to plastic waste littered and 17% due to mismanaged waste not recollected). Lastly, 2.5% of plastics is lost during pre-consumption phases and 21.5% from incineration and landfill (11.6% and 9.90%, respectively).

Despite these findings, the estimated 4.46 million tonnes of recyclates used in the EU27 in 2019 would not meet the EU [1] target of 8.8 million tonnes to be recycled and consumed within the Union by 2025[1]. A series of scenarios were therefore developed to assess how the 2019 sector-specific MFAs could change for the year 2025, with the aim of aligning such changes with expected trends in the plastic value chain also as a consequence of EU plastic policies targets. These scenarios were crafted based on anticipated developments in the plastic value chain, considering key EU policies [11], [12], [4], international initiatives such as China's ban on waste imports [13], and insights from significant literature sources [14]. These potential improvements were reflected in alterations to the TCs, thereby representing hypothetical future changes in the value chain. The scenarios encompassed various aspects including for instance "reduced waste export", "improved waste collection", "improved recycling performance", etc. or scenarios combining multiple interventions along with variations in plastic production (e.g., +10%/-10% compared to the 2019 base results).
When combined with variations in plastic production, the EU target could be surpassed by 2025: notably, assuming a +10% production increase, a total recyclates consumption of 11.13 million tonnes could be realized by 2025. Considering trends in plastic packaging production, which suggest a yearly increase of around 4-5%, coupled with the impacts of events like the COVID-19 outbreak and the Ukraine war, a reduction in plastic production could be foreseeable. Even in the case of scenarios considering a 10% reduction in plastic production instead of a 10% increase, a total recyclates consumption of 9.11 million tonnes is achievable, meeting the EU target [1].

This study underscores the necessity for significant efforts to enhance the granularity and detail of plastic flow overviews in the EU to meet EU ambitions and industry targets like the EU target [1]. While packaging undoubtedly holds a central role in the EU plastic value chain, there is a pressing need to refine and bolster the analysis of less-explored sectors in the coming years. This is especially relevant for sectors like synthetic textiles, fishing, and healthcare, which remain largely unexplored in current literature. Despite challenges, such as data aggregation and sector-specific information gaps, concerted efforts are needed to enhance plastic flow monitoring frameworks and realistic assessments of future plastic flows to realize the untapped potential for additional and improved recycling in the plastic value chain. In conclusion, addressing plastic flows in the EU requires multisectorial approaches, with particular attention to improving plastic waste collection and considering alternative recycling processes. Despite uncertainties, achieving EU targets could be feasible with dedicated efforts and up-to-date knowledge not only of the plastic value chain's key flows but also less-explored ones.

In a second phase of the work, a LCA of the EU plastic value chain was performed. In fact, to date, few studies have tried to combine MFA to LCA in view of providing a complete overview of flows and impacts of the plastic value chain in Europe. The LCA aims at assessing the total emissions of the EU plastic value chain from raw materials manufacturing to end-of-life waste management and recycling, covering

[1] *To enable a fair comparison with the results of the present study, the EU target of 10Mt for EU27+UK was corrected to EU27 considering: (i) the ratio between the plastic demand in UK and the plastic demand in EU27+UK (equal to 7%), and that (ii) the amount of preconsumer PVC recyclates (approximately equal to 0.5Mt) from and used in construction sector is to be included in the 10Mt target.*

the 16 impact categories of the Product Environmental Footprint (PEF) [15]. The goal of the analysis is to assess the environmental impacts of all plastic flows modelled through the MFA, covering the impacts associated with each polymer in each sector and also covering the potential environmental pressures due to less-explored sectors (e.g., plastics in the healthcare and fishing sectors) and less-explored flows (e.g., plastics losses and plastic waste mismanagement). An overview of the methodological approach for assessing the life cycle impacts of the plastic value chain in accordance to the existing MFA plastic model will be provided, coupled with evidences related to the key drivers of the EU plastic value chain impacts and the key barriers to overcome for lowering its environmental pressures.

References

[1] EC (European Commission), Communication from the Commission to the European Parliament, the Council, the Economic and Social Committee and the Committee of the Regions, A European Strategy for Plastics in a Circular Economy, (2018).
[2] EC (European Commission), Communication from the Commission to the European Parliament, the Council, the Economic and Social Committee and the Committee of the Regions, A new Circular Economy Action Plan, For a cleaner and more competitive Europe, (2020).
[3] EC (European Commission), Directive 2008/56/EC DIRECTIVE 2008/56/EC of the European Parliament and of the Council of 5 June 2019 on the reduction of the impact of certain plastic products on the environment, (2019).
[4] EC (European Commission), Communication from the Commission to the European parliament, the European council, the Council, the European economic and Social Committee and the Committee of the regions. The European Green Deal, (2019).
[5] UNEP (United Nations Environment Program), Department of Economic and Social Affairs, Sustainable Development Goals, https://sdgs.un.org/goals, (2022).
[6] Chen W.Q., Ciacci L., Sun N.N., Yoshioka T., "Sustainable Cycles and Management of Plastics: A Brief Review of RCR Publications in 2019 and Early 2020", Resources, Conservation and Recycling, Vol. 159, p. 104822, (2020).
[7] Kawecki D., Scheeder P.R.W., Nowack B., "Probabilistic Material Flow Analysis of Seven Commodity Plastics in Europe", Environmental Science and Technology, Vol. 52, pp. 9874–9888, (2018).
[8] Hsu W.-T., Domenech T., McDowall W., "How Circular Are Plastics in the EU?: MFA of Plastics in the EU and Pathways to Circularity", Cleaner Environmental Systems, Vol. 2, p. 100004, (2021).
[9] PlasticsEurope, The Circular Economy for Plastics, A European Overview, https://plasticseurope.org/knowledge-hub/the-circular-economy-for-plastics-a-european-overview/, (2019).
[10] Material Economics, Europe's missing plastics, Agora Industry, Berlin, https://materialeconomics.com/publications/publication/europe-s-missing-plastics (2022).
[11] EC (European Commission), Council Directive 1999/31/EC of 29 April 1999 on the landfill of waste, (1999).
[12] EC (European Commission), Directive 2018/852 of the European Parliament and of the Council of 30 May 2018 amending Directive 94/62/EC on packaging and packaging waste, (2018).
[13] ECA (European Court of Auditors), Review No 4: EU action to tackle the issue of plastic waste, https://www.eca.europa.eu/Lists/ECADocuments/RW20_04/RW_Plastic_waste_EN.pdf, (2022).
[14] Systemiq, ReShaping Plastics, Pathways to a circular climate neutral plastics system in Europe, https://plasticseurope.org/wp-content/uploads/2022/04/SYSTEMIQ-ReShapingPlastics-April2022.pdf, (2022).
[15] EC (European Commission). Commission Recommendation (EU) 2021/2279 of 15 December 2021 on the use of the Environmental Footprint methods to measure and communicate the life cycle environmental performance of products and organisations, (2021).

Title: Valorisation of alkaline industrial residues through accelerated carbonation-based treatments

Author(s): Alessandra Masi*[1], Giulia Costa[1], Francesco Lombardi[1]

[1] *Department of Civil Engineering and Computer Science Engineering, University of Rome Tor Vergata, Rome 00133, Italy; masi@ing.uniroma2.it*

Keyword(s): accelerated carbonation, CO_2 storage, industrial residues, products

Abstract

Around 7 billion tonnes of residues are generated globally every year as by-products of different industrial activities [1]. Due to inadequate technical (e.g.: particle size, density or mechanical strength) and/or environmental properties (e.g.: alkaline pH and leaching of contaminants), these materials are generally employed only in low-grade applications or landfilled [2]. Accelerated carbonation has been proposed as a strategy to chemically stabilise alkaline residues via the reaction of Ca and Mg oxides-bearing phases with either pure or diluted CO_2 flows under controlled operating conditions. These reactions lead to the formation of Ca and/or Mg carbonates, therefore ensuring the permanent storage of carbon dioxide in a solid form [3]. Depending on the characteristics of the residues and on the reaction route selected, different types of products, which could be employed in various applications, may be obtained. With indirect process routes, by separating the dissolution of the reactive species from the carbonate precipitation phase, a fine relatively pure carbonate product can be obtained, while employing the direct route, products such as aggregates or binding materials may be manufactured [3], [4], [5]. It is important to underline that assessing the chemical, technical and environmental properties of the obtained products is a crucial step to determine their valorisation potential.

In this contribution we will describe the studies we have been carrying out in the framework of two different research projects with the aim of assessing the possibility of treating by accelerated carbonation-based processes different types of alkaline residues in order to produce valorisable products, following the circular economy paradigm.

The first one is the “BBCircle” research project, funded by the Lazio region, that aims at evaluating the implementability on a regional scale of a biorefinery for the production of biohydrogen employing different types of organic waste streams [6]. The specific function of the carbonation unit is to store part of the CO_2 content of the biogas generated employing different types of alkaline industrial waste streams produced within the Lazio Region. Three different industrial sectors were considered as potential sources for reactive materials for the carbonation process: construction and demolition activities, energy production from biomass and waste to energy (WtE) processes. All the nine samples tested in this study were collected from industrial sites operating within the region. Following a preliminary characterisation phase aimed at understanding the elemental and mineral composition of the residues, as well as their environmental behaviour, the materials presenting a higher carbonation potential were individuated, namely two samples of water-cooled and air-cooled bottom ash (BA_r1 and BA_r2) and one sample of fly ash from the electrostatic precipitator (FA_r) produced in a RDF-fed WtE plant and one sample of fly ash collected from the boiler of a biomass-fuelled power plant (FA_b). These samples underwent some preliminary carbonation tests under direct enhanced wet (L/S = 0.2 l/kg) and slurry (L/S = 5 l/kg) phase conditions [7] to assess their potential reactivity through the measurement of the achieved CO_2 uptake

by inorganic carbon analysis of the solid product. The average uptakes obtained for each sample were higher when slurry routes were applied and ranged from a maximum of 12%wt., for FA_r after slurry carbonation, to a minimum of 3%wt., for BA_r1 treated by wet carbonation.
The environmental behaviour of the carbonated products was then evaluated and compared to the results obtained in the characterisation phase of the initial materials to determine the effects of the tested treatments. Carbonation was effective in reducing the leachability of amphoteric constituents, such as Pb and Zn, but it led to a higher release of Sb; the effects on Cr and salts leaching, instead, could not be unequivocally determined.
Combining all the information obtained from the two previous steps, tailored carbonation-based processes were identified for each of the selected samples with the aim of obtaining products with suitable properties for the envisioned application. Specifically, for BA_r1 and BA_r2, owing to their significant content of reactive Ca in the form of silicates that showed a limited reactivity in the preliminary carbonation tests, the indirect route was tested employing several Ca extracting agents, selected on the basis of previous studies (e.g. [8] [9] [10]).
Figure 1a shows the Ca extraction efficiency as a function of the L/S ratio for the different reagents tested. Further extraction tests were then performed employing NH_4NO_3, HNO_3 or citric acid at different molarities and the liquid residue deriving from the biohydrogen production unit foreseen in the biorefinery scheme; the latter was tested both as received (IBES_tq) and re-acidified (IBES_a) (see Figure 1b). Carbonation tests were finally performed on the solutions obtained using the aforementioned reagents. 5M NaOH was used, if needed, to adjust the pH.

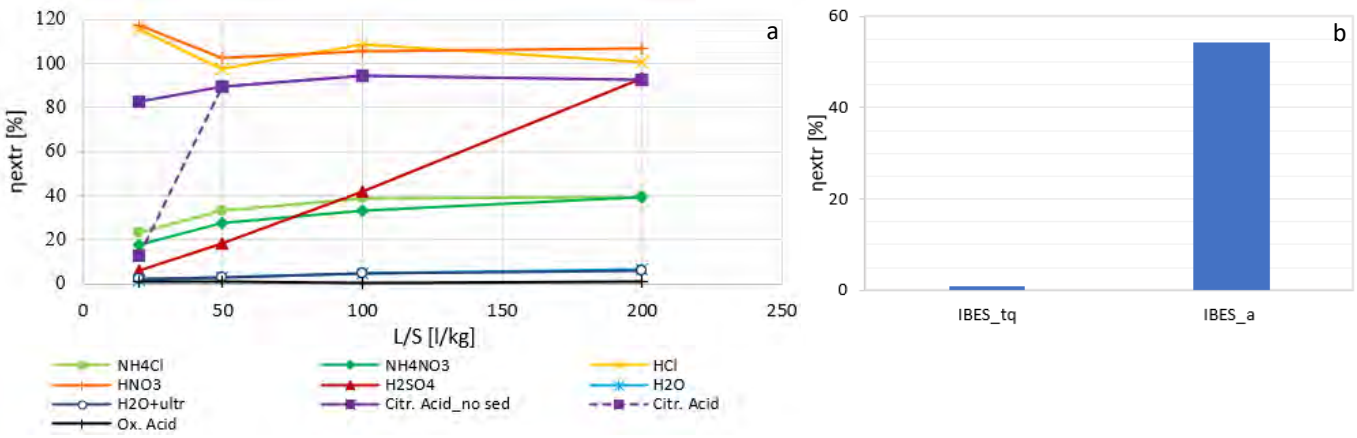

Figure 1: Effect of L/S ratio on Ca extraction efficiency from BA_r2 for different reagents (M ammonium salts = 1; M monoprotic acids = 1; M diprotic acids = 0.5; M triprotic acids = 0.33) (a); Comparison of IBES_tq and IBES_a Ca extraction efficiency from BA_r2 (b)

The carbonation efficiencies calculated were above 50% even considering short reaction times and the values never fell below 80% when the carbonation time was set to 30 min; Figure 2a shows the carbonation kinetics of the solution obtained after BA_r2 dissolution with HNO_3. From the XRD analysis of the precipitated products, calcite and vaterite were individuated as the main mineralogical phases (an example is provided in Figure 2b).

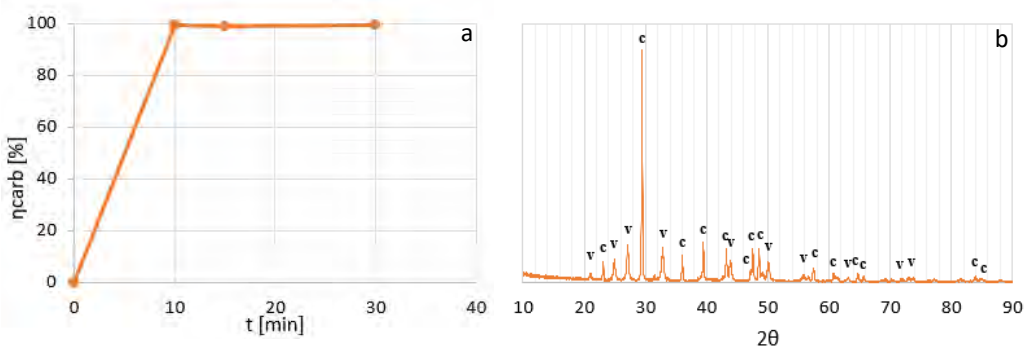

Figure 2: Carbonation kinetics of the solution obtained using 0.5M HNO_3 L/S = 50 l/kg as extracting agent (a); XRD analysis of the precipitated carbonate product obtained after 30 min carbonation (c = calcite, v = vaterite) (b).

FA_b and FA_r, instead, presenting a fine grain size distribution and Ca in the form of readily-reactive phases, were employed in direct aqueous carbonation tests performed at a low L/S, combined with a granulation process aimed at the formation of aggregates. The products obtained in the two configurations tested (carbonation with pre-granulation and carbonation with post-granulation) were characterised by a much larger particle size compared to those of the initial materials; an increase in the d_{50} of roughly two orders of magnitude was observed for all the tested conditions. The highest CO_2 uptake post curing, close to 5.6%wt., was obtained when pre-carbonation was applied for both samples. The aggregate crushing values (ACV) calculated for the aggregates from FA_r (those from FA_b could not be tested with this procedure due to their fragility) were never below 60% (reached when post carbonation was applied), indicating a limited mechanical strength of the products. As previously assessed after the preliminary carbonation tests, the implemented treatments showed to yield both positive and negative effects on the leachability of different constituents of the products, showing that critical aspects related to the environmental behaviour of these materials persist.
The second project we are currently working on is part of the “Rome Technopole” project, funded by the Italian National Recovery and Resilience Plan and aiming at developing a system, once again within the Lazio Region, in which universities, national research centres, institutions and business associations can work in a joint effort to tackle some critical and heavily-debated issues such as that of decarbonisation and circular economy [11].
Two streams deriving from the treatment of the residues of a steel manufacturing mill employing the Electric Arc Furnace technology were considered: a coarse fraction (slag), with dimensions ranging from 2 mm to 13 mm, and a fine fraction (filler), 80%wt. of which was characterised by particles that were below 0.06 mm in diameter. As in the previous case, the residues were first characterised from an elemental, mineralogical and environmental point of view, and then subjected to preliminary carbonation tests considering enhanced wet (L/S = 0.3 l/kg) and slurry (L/S = 5 l/kg) carbonation conditions, with the aim of understanding their reactivity with CO_2. Once again, it was observed that the increase in the L/S ratio had a positive effect on the uptake, that reached values of 18.6%wt. and 15%wt. for the coarse and fine fraction respectively when P = 10 bar was set during the tests. Several batch leaching tests were later performed on the materials obtained to assess the effects of the implemented processes on the environmental behaviour of the samples. As previously assessed for the other residues, carbonation proved to have both positive and negative effects: the release of Cr, Mo, and F^- from both the slag and the filler increased, while a reduction in Ba leachability from the filler was simultaneously observed. Further carbonation tests showed that the coarse sample only reacted if previously milled to reduce its initial dimensions to < 0.2mm, which was not considered a feasible option, given that it was proposed to reuse this material as a substitute for natural aggregate.

The fine sample, instead, presented interesting characteristics to be employed in further carbonation-based treatments considering both direct and especially indirect routes. For the direct route, we tested again carbonation/granulation processes to obtain aggregates; this time though, the effects of carbonation with pre-granulation and carbo-granulation (simultaneous application of the two processes) were compared. The aggregates were later characterised as described for the other residues. An increase in the d_{50} of more than two orders of magnitude with respect to the initial dimension of the filler was observed for both the aggregates obtained from the two implemented processes; the highest uptake (6%wt.) and the lowest ACV value (48%), hence the higher mechanical strength, were achieved when carbonation and granulation were performed simultaneously. Few critical aspects persist regarding the environmental behaviour of the products. Further studies are currently being carried out on the application of indirect processes on the fine fraction to precipitate pure $CaCO_3$.
In particular, the objective of this specific phase of the study will be that of testing, alongside with traditional pH-swing processes, more innovative treatments for both the Ca-extraction and the carbonation steps to reduce the use of reagents and improve the environmental sustainability of the treatment.

References

[1] P. Renforth, 'The negative emission potential of alkaline materials', *Nat Commun*, vol. 10, no. 1, p. 1401, Mar. 2019, doi: 10.1038/s41467-019-09475-5.
[2] H. I. Gomes, W. M. Mayes, M. Rogerson, D. I. Stewart, and I. T. Burke, 'Alkaline residues and the environment: a review of impacts, management practices and opportunities', *Journal of Cleaner Production*, vol. 112, pp. 3571–3582, Jan. 2016, doi: 10.1016/j.jclepro.2015.09.111.
[3] W. Liu, L. Teng, S. Rohani, Z. Quin, B. Zhao, C. C. Xu, S. Ren, Q. Liu, B. Liang, 'CO2 mineral carbonation using industrial solid wastes: A review of recent developments', *Chemical Engineering Journal*, vol. 416, p. 129093, Jul. 2021, doi: 10.1016/j.cej.2021.129093.
[4] A. Sanna, M. Uibu, G. Caramanna, R. Kuusik, and M. M. Maroto-Valer, 'A review of mineral carbonation technologies to sequester CO $_2$', *Chem. Soc. Rev.*, vol. 43, no. 23, pp. 8049–8080, 2014, doi: 10.1039/C4CS00035H.
[5] C. M. Woodall, N. McQueen, H. Pilorgé, and J. Wilcox, 'Utilization of mineral carbonation products: current state and potential', *Greenhouse Gases: Science and Technology*, vol. 9, no. 6, pp. 1096–1113, 2019, doi: 10.1002/ghg.1940.
[6] F. Minniti, F. Tatti, G. Farabegoli, G. Costa, L. Lombardi, A. Rossi, R. Pomi, A. Polettini, 'Biomaterials, Biofuels, CO2 reduction and circularity (BBCircle). Evaluation of biorefinery applicability in Lazio region' *Proceedings of SUM2022, 6th Symposium on Circular Economy and Municipal Mining, Capri (Italy) 18-20 may 2022*.
[7] R. Baciocchi, G. Costa, E. Di Bartolomeo, A. Polettini, and R. Pomi, 'Wet versus slurry carbonation of EAF steel slag', Greenhouse Gases, vol. 1, no. 4, pp. 312–319, Dec. 2011, doi: 10.1002/ghg.38.
[8] L. He, D. Yu, W. Lv, J. Wu, and M. Xu, 'A Novel Method for CO $_2$ Sequestration via Indirect Carbonation Coal Fly Ash', *Ind. Eng. Chem. Res.*, vol. 52, no. 43, pp. 15138–15145, Oct. 2013, doi: 10.1021/ie4023644.
[9] H.-J. Ho, A. Iizuka, E. Shibata, and T. Ojumu, 'Circular indirect carbonation of coal fly ash for carbon dioxide capture and utilization', *Journal of Environmental Chemical Engineering*, vol. 10, no. 5, p. 108269, Oct. 2022, doi: 10.1016/j.jece.2022.108269.
[10] A. Said, T. Laukkanen, and M. Järvinen, 'Pilot-scale experimental work on carbon dioxide sequestration using steelmaking slag', *Applied Energy*, vol. 177, pp. 602–611, Sep. 2016, doi: 10.1016/j.apenergy.2016.05.136.
[11] Fondazione Rome Technopole, retrieved 20th July 2024 from https://www.rometechnopole.it/

Title: THE CHARACTERISTICS OF RECYCLED AGGREGATES FROM C&D WASTE: RESULTS OF A MONITORING ACTIVITY FOLLOWING THE END-OF-WASTE REGULATION REQUIREMENTS

Author(s): Alessandro Abbà *[1], Sabrina Sorlini[1], Andrea Piccinali[2], Giovanni Plizzari[1]

[1] *Department of Civil, Environmental, Architectural Engineering and Mathematics, University of Brescia, via Branze 43, 25123 Brescia, Italy, alessandro.abba@unibs.it; sabrina.sorlini@unibs.it; giovanni.plizzari@unibs.it*
[2] *Ance Brescia, Via Ugo Foscolo 6, 25128, Brescia, Italy, andrea.piccinali@ancebrescia.it*

Keyword(s): construction and demolition (C&D) waste, End-of-Waste (EoW), total hydrocarbon, release of pollutants

Abstract

The building industry is one of the primary causes of the depletion of natural resources. One of the main waste streams produced in Italy and throughout Europe is construction and demolition (C&D) waste, which is included in Chapter 17 of the European Waste Code (EWC). Italy produced about 78 million tons of C&D waste in 2021 [1], placing it fourth in Europe behind Germany, France, and the United Kingdom [2].
Legambiente claims that although ISPRA data indicates that Italy has met the 70% target established by European Directive 2008/98/EC (and confirmed in 2018), the Italian data on the actual attainment of this objective are deemed untrustworthy because the official statistics only include companies of a specific size [3]
Preserving the depletion of natural resources can be achieved through the recovery of C&D waste to create recycled aggregate. The use of these materials has been more widely recognized, albeit it mainly concerns fillings and road underpasses; just 6% are now utilized to substitute natural aggregate in concrete. The introduction of Ministerial Decree (M.D.) 152 (EoW for inert waste) published on 27th September 2022 [4] may involve critical issues for the recovery of C&D waste mainly due to additional requirements. The Ministry of Environment and Energy Security, after the proposal to the European Union (in December 2023) of a draft for an update of M.D. 152/2022, with distinct requirements for different fields of use of the recycled aggregates (RAs), is now ready to issue the document.
Research carried out by Butera et al. (2014) [5] showed that the properties of the C&D waste have a significant impact on the chemical composition of that Ras produced by the recycling plants. Due to the great heterogeneity of C&D waste, which includes materials with varying origins (such as wood, masonry, plastic, metals, bricks, cement and plaster), RAs have different chemical compositions and may include various problems [6].
In this work, done in collaboration with ANCE (Associazione Nazionale Costruttori Edili), the features of the C&D waste and RAs generated by 10 recycling plants were examined to identify the critical issues for the implementation of the Italian EoW legislation. Leaching tests and chemical analyses were carried out in compliance with the updated version of M.D. 152/2022 regulation.
Table 1 shows the number of samples collected and tested for each recycling plant. The total samples are 79; the most of them are mixed C&D waste (EWC 17.09.04), followed by concrete C&D waste (EWC 17.01.01) – see **Table 2**.

The results obtained for the samples collected in the recycling plant #10 are excluded because the sensibility of the chemical analysis is not complying the requirements of the EoW regulation.

Table 1. Number of samples collected and tested for each recycling plant

Recycling Plant	Location Region (Province)	Number of samples	
		C&D waste	RA
#1	Veneto (Belluno)	4	4
#2	Veneto (Verona)	6	3
#3	Lazio (Roma)	2	2
#4	Lombardia (Bergamo)	4	4
#5	Emilia Romagna (Modena)	4	4
#6	Trentino Alto Adige (Bolzano)	8	8
#7	Toscana (Firenze)	4	6
#8	Piemonte (Cuneo)	7	3
#9	Lombardia (Brescia)	2	2
#10	Lombardia (Brescia)	2	0

Table 2. Number of samples of C&D waste and RA for different type of treated waste

C&D waste		RA	
Type of C&D waste treated (EWC)	Number of samples	Type of C&D waste treated (EWC)	Number of samples
17.09.04	20	100% - 17.09.04	16
17.01.01	10	100% - 17.01.01	9
17.01.07	7	Mix 17.01.07 - 17.09.04	5
17.03.02	3	100% - 17.01.07	2
17.05.04	1	100% - 17.03.02	2
Mix 17.01.01 - 17.01.07 - 17.09.04	2	Mix 17.01.01 - 17.01.07 – 17.09.04	2
Total	***43***	***Total***	***36***

The features of C&D wastes were also compared with the EoW standards, even though the requirements are exclusive to RAs. This was done to assess the C&D wastes' quality and investigate the impact of the recycling plants' treatments on their composition.
As far as the chemical composition is concerned, for ***C&D waste***:

- Heavy hydrocarbons (C>12) are the main critical parameters: they frequently exceed the more restrictive limit value set by EoW regulation for the environmental recoveries and filling applications (Table 2, column 1, draft revision of M.D. 152/2022) – see **Figure 1**. Other less critical parameters are Chromium VI (4 exceedances), Benzo(a)pyrene (4 exceedances), and Benzo(g,h,i)perylene (3 exceedances).
- Considering the less restrictive limit values provided for other applications (embankment, road sector, bituminous mixtures and concrete) – see the Table 2, column 2, draft revision of M.D. 152/2022) – the critical issues are strongly reduced: e.g. for heavy hydrocarbons (C>12) and Chromium VI only 2 exceedances occurs.

The same considerations can be made for ***RAs***, despite the critical issues seem to be slightly lower with respect C&D waste.
The content of heavy hydrocarbons (C>12) is measured not only in C&D waste like bituminous mixtures (EWC 17.03.02), but also in the mixed C&D waste (EWC 17.09.04). Instead, concrete C&D wastes

(EWC 17.01.01) present low content of heavy hydrocarbons (C>12), but not always below the more restrictive limit value set by EoW regulation.

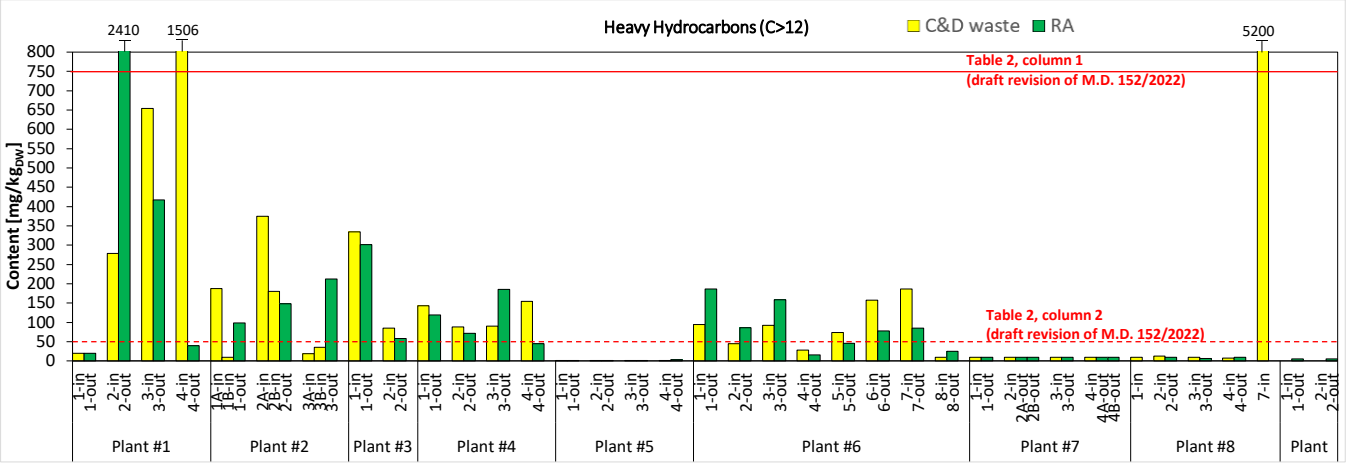

Figure 1. Content of heavy Hydrocarbons (C>12) on the C&D waste and RA samples.

As far as the results from leaching test are concerned, for ***C&D waste*** (also in this case the EoW requirements are provided only for RAs), the most critical pollutant is Total Chromium: 6 samples threshold the limit values. Other parameters such as COD (2 cases) and pH (1 case) exceed the limits. The release of pollutants in ***RAs*** is significantly reduced with respect the C&D waste. As example, it can be observed that the release of Total Chromium is always below the limit value. The high values are due to the treatment of the concrete fraction (EWC 17.01.01): in this case, the Chromium is present in the cement, that is a component of concrete.

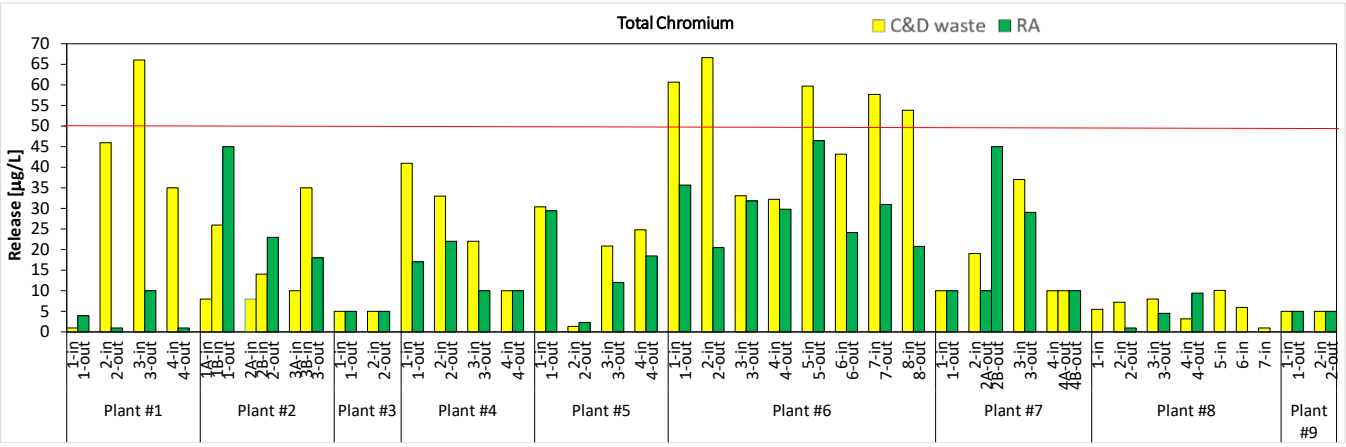

Figure 2. Release of Total Chromium from the C&D waste and RA samples.

References

[1] ISPRA, Rapporto Rifiuti Speciali – Edizione 2023, Rapporti 389/2023, Roma, ISBN 978-88-448-1169-3.
[2] Eurostat, Generation of Waste by Economic Activity, Available online at the following link: https://ec.europa.eu/eurostat/databrowser/view/ten00106/default/table?lang=en
[3] Legambiente, Rapporto Cave 2021 – La Transizione dell'economia circolare nel settore delle costruzioni, Roma, 2021.
[4] Ministerial Decree n. 152, September 27, 2022. Regulation governing the cessation of the waste status of inert construction and demolition waste and other inert waste of mineral origin, pursuant to article 184-ter, paragraph 2, of Legislative Decree April 3, 2006, n. 152. (22G00163) (Official Gazette General Series n.246, October 20, 2022) (in Italian).
[5] Butera S., Christensen T.H., Astrup T.F., "Composition and Leaching of Construction and Demolition Waste: Inorganic Elements and Organic Compounds", Journal of Hazardous Materials, 276, 302–311 (2014).
[6] Vázquez E., "Recycled Aggregates for Concrete: Problems and Possible Solutions". International Journal of Earth & Environmental Sciences, 1, 122 (2016).

Title: Polyolefins chemical recycling: experimental investigation of product yields in a semi-continuous pyrolysis of composting plant waste

Author(s): Davide Sorino*[1], Lorenzo Bartolucci[2], Stefano Cordiner[2], Francesco Lombardi[1], Vincenzo Mulone[2]

[1]Department of Civil Engineering and Computer Science Engineering, University of Rome "Tor Vergata", Rome, Italy, davide.sorino@uniroma2.it
[2]Department of Industrial Engineering, University of Rome "Tor Vergata", Rome, Italy, lorenzo.bartolucci@uniroma2.it
[2]Department of Industrial Engineering, University of Rome "Tor Vergata", Rome, Italy, cordiner@uniroma2.it
[1]Department of Civil Engineering and Computer Science Engineering, University of Rome "Tor Vergata", Rome, Italy, lombardi@ing.uniroma2.it
[2]Department of Industrial Engineering, University of Rome "Tor Vergata", Rome, Italy, mulone@uniroma2.it

Keyword(s): Pyrolysis, Mixed Contaminated Plastics, Waste to X, Characterization, Chemical recycling

Abstract

According to European statistical data [1], only 30% of the plastics produced each year are recycled, 40% are incinerated, and 30% end up in landfills, causing serious environmental problems. This is a significant loss of valuable chemical and/or highly energetic products [2] as Plastic Europe has evaluated that the global plastics production in 2022 amounted to 400.7 Mt, of which about 362.3 Mt were fossil-based [3]. In this context, an important issue that is less discussed is the treatment of plastic waste found in composting plants. The contamination of the organic waste fraction by microplastics reduces the compost quality and, therefore, requires that the plastic residues be separated and discarded through incineration or landfills. It is worth noting that a composting plant can discard more than 4% [4] of incoming wet-based waste, leading to high operating costs, especially when these plastic streams end up in landfills. Furthermore, with the European Directive 2018/850 on the landfill of waste, member states must ensure that by 2035, the amount of municipal waste landfilled is reduced to 10% by mass, or a lower percentage, of total municipal waste generated [5]. In this context, developing effective processes to recover the potential of these wasted plastics and pyrolysis seems to be a promising technique, as it allows for the recovery of precursors of processed plastics, together with high-value-added chemical compounds and fuels.

Pyrolysis is the thermal degradation of organic matter in the absence of oxygen yielding three distinct products type: solid, gaseous, and liquid [6]. The relative composition among three products categories depend on several process parameters such as temperature, residence time, heating rate, feedstock type, feedstock size, and others. The pyrolytic transformation of LDPE, HDPE, and PP starting from virgin products, before consumer use [7][3] is widely studied in the literature. However, post-consumer plastic wastes are contaminated by various impurities, prompting the need for research to ascertain the optimal conditions for its treatment.

For instance, Kusemberg et al. presented a detailed experimental analysis of the correlation between the polyolefin compositions present in packaging waste and the resultant pyrolysis oils. By conducting

experiments at 450°C, they managed to acquire liquid (wax) mass yields of 87% with PP, 85% with PE, and 89% with the mixture. However, in the context of post-consumer plastics, these results cannot be directly applied as this particular fraction is contaminated by other components. Notably, the levels of contaminants such as silicone, sodium, lead, and other impurities surpass the permissible thresholds for purification [8].

In this context, the possibility of an effective chemical recycling of waste plastics not only requires a deep understanding of the operating parameters that optimize the process as a function of the feedstock composition, but also the potential negative effects of the contaminants that may prevent the products from being used. In addition, it is also useful to analyze the relationships between the output products (not only gas, liquid, and solid, but also the type of hydrocarbon), the process parameters, and the mass fractions of the polymers that make up the feedstock.

The aim of this work is to investigate the application of pyrolysis to the plastic waste streams generated by an industrial composting plant. As in these streams there is a mix of different plastic, in the work, the interactions among them and the relation with process parameters like temperature and residence time is studied. Specifically, a composition analysis was performed on the sample (EER code 191912), which showed the following fractions: 72.18% of plastic, 26.79% of biomass, 0.38% of paper, and 0.65% of other materials. The plastic fraction was isolated and then dried at 40°C for three days. By chloroform testing, the percentage of bioplastic and traditional plastic was evaluated, and 100% traditional plastic was observed. Next, for polymer identification, a densiometric analysis was conducted. Two mixtures of distilled water and ethanol, one with a density of 915 kg/m³ and one with a density of 940 kg/m³, were prepared. Polymers (mainly plastic bags) were immersed in these solutions, which allowed the identification of three polymers: LDPE, HDPE, and PP, with mass percentages of 62.1%, 9.8%, and 28.1%, respectively.

A characterization of the feedstock by thermogravimetric analysis was performed before carrying out the pyrolysis tests, according to the ASTM E914, using the instrument TGA701 built by LECO Corp and evaluating the results according to the UNI EN ISO 18122:2016 and the ISO 18123:2015 standards. In addition to the thermogravimetric analysis, an elemental analysis was also carried out. Ultimate analysis tests were performed in accordance with international standard ISO 16948:2015 using a CHNOS Elementar Vario MACRO cube analyzer. The three polymers were then characterized by thermogravimetric analysis and elemental analysis. Characterization results are shown in Table 1 and Table 2.

Table 1. Termogravimetric analysis results

Sample	Moisture [wt.%]	Volatile matter [wt.%]	Ash [wt.%]	Fixed carbon [wt.%]
LDPE	1.88	87.16	9.45	1.51
HDPE	1.55	90.73	6.71	1.01
PP	0.88	91.24	6.73	1.15

Table 2. Elemental analysis results

Sample	N [wt.%]	C [wt.%]	H [wt.%]	S [wt.%]	Ash [wt.%]	O [wt.%]
HDPE	0.607	72.133	15.380	0.075	6.710	5.095
LDPE	0.470	71.797	14.123	0.163	9.450	3.997
PP	0.400	70.807	13.887	0.183	6.730	7.993

The high amount of ash and oxygen is due to the presence of organic residue on the surface of the identified plastics. After the characterization phase, the pyrolysis test campaign was carried out using a semi-continuous reactor. The tests were conducted by varying the temperature of the reaction chamber from 400 to 600°C. The samples tested included single polymers such as LDPE, HDPE, and PP, followed by a test with a mixture at different concentrations. The particle size used ranged from 850 to 2000 microns.

Each test was performed as follows: the sample (10 g) was placed on the flap valve and the temperature inside the reaction chamber was allowed to reach the set point. When this was achieved, the first valve was opened to allow the sample to fall onto the second valve, and the first valve was immediately closed. This created a chamber in which nitrogen was insufflated to remove the air that entered when the first valve was opened. The second valve was then opened to allow the sample to fall into the reaction chamber where the pyrolysis reaction took place. Nitrogen was also insufflated into this chamber at a flow rate of 0.5 Nl/min. The produced vapours were transferred to the condensation zone (at room temperature) for collection. The gas that did not condense was collected in impermeable bags.

Product yields related to tests carried out with the mixed feedstock in the temperature range of 400-550°C are shown in Figure 1.

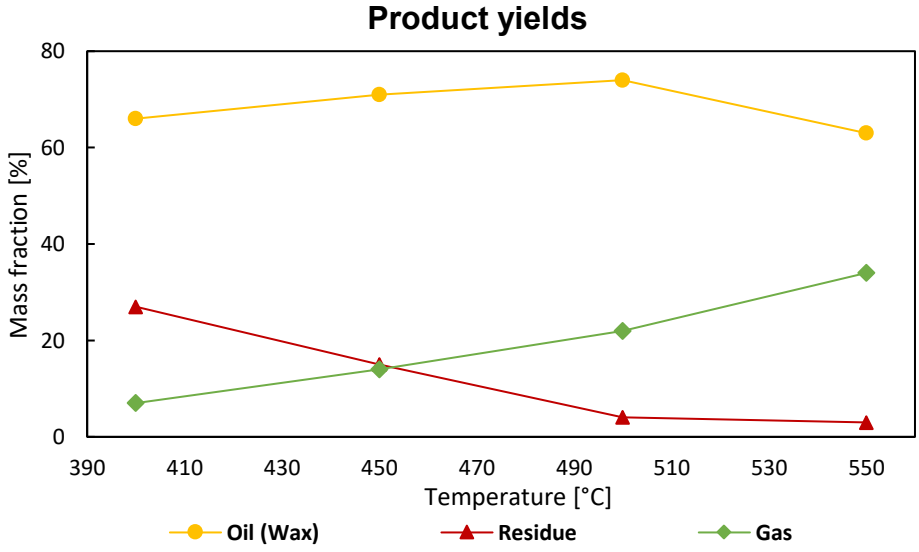

Figure 1. Product yields as function of the temperature

Looking at the three trends, to optimize oil/wax production, the temperature should not exceed 500°C. However, to increase gas production, it is necessary to use higher temperatures. Pyrolysis products will be analyzed to identify their chemical compounds, elemental compositions, and contaminants present.

References

[1] "The Circular Economy for Plastics A European Analysis," 2024.
[2] Y. Jaafar, L. Abdelouahed, R. El Hage, A. El Samrani, and B. Taouk, "Pyrolysis of common plastics and their mixtures to produce valuable petroleum-like products," *Polym Degrad Stab*, vol. 195, Jan. 2022, doi: 10.1016/j.polymdegradstab.2021.109770.
[31] "Plasticsthefastfacts2023-1. Accessed: Jan. 15, 2024. [Online]. Available: https://plasticseurope.org/knowledge-hub/plastics-the-fast-facts-2023/
[4] S. Bottausci, C. Magrini, G. A. Tuci, and A. Bonoli, "Plastic impurities in biowaste treatment: environmental and economic life cycle assessment of a composting plant," *Environmental Science and Pollution Research*, 2023, doi: 10.1007/s11356-023-28353-8.
[5] "Directive (EU) 2018/ of the European Parliament and of the Council of 30 May 2018 amending Directive 1999/31/EC on the landfill of waste," 2018.
[6] P. Basu, "Biomass Gasification and Pyrolysis: Practical Design and Theory."
[7] A. F. Anene, S. B. Fredriksen, K. A. Sætre, and L. A. Tokheim, "Experimental study of thermal and catalytic pyrolysis of plastic waste components," *Sustainability (Switzerland)*, vol. 10, no. 11, Oct. 2018, doi: 10.3390/su10113979.
[8] M. Kusenberg *et al.*, "A comprehensive experimental investigation of plastic waste pyrolysis oil quality and its dependence on the plastic waste composition," *Fuel Processing Technology*, vol. 227, Mar. 2022, doi: 10.1016/j.fuproc.2021.107090.

Co-digestion of agri-food and livestock wastes for boosting biomethane potential

Author(s): Daniele Ipsale*[1], Biagio Pecorino[2], Santo Fabio Corsino[3], Gaspare Viviani[4], Michele Torregrossa[5]

[1] *Università degli Studi di Palermo, Palermo, Italia, danieleipsale@yahoo.it*
[2] *Università degli Studi di Catania, Catania, Italia, pecorino@unict.it*
[3] *Università degli Studi di Palermo, Palermo, Italia, santofabio.corsino@unipa.it*
[4] *Università degli Studi di Palermo, Palermo, Italia, gaspare.viviani@unipa.it*
[5] *Università degli Studi di Palermo, Palermo, Italia, michele.torregrossa@unipa.it*

Keyword(s): Biomethane potential (BMP), Anaerobic digestion, Citrus pulp, Olive pomace, Opuntia cladodes, Livestock effluents

Abstract
This study explored the anaerobic digestion (AD) and co-digestion (Co-AD) of various organic matrices to produce biogas and biomethane, focusing on agricultural and agro-industrial by-products and livestock effluents from Sicily. The biochemical methane potential (BMP) of individual substrates and their mixtures was evaluated to identify synergistic or antagonistic effects on methane yield. Key findings indicated that meat poultry manure had the highest BMP, while co-digestion, such as olive pomace with poultry litter, can enhance biomethane production by 30%. However, certain mixtures exhibited inhibitory effects due to pH imbalances and slowly biodegradable components. The study underlined the importance of substrate selection and mixture ratios in optimizing biogas production, offering valuable insights for developing efficient and sustainable AD systems.

Introduction
Anaerobic digestion (AD) is a process through which organic matrices can be energetically valorised. In fact, AD of these matrices produces biogas, a gaseous mixture mainly composed of methane (CH_4) and carbon dioxide (CO_2) [1]. Biogas can be used as it is, as fuel in co-generators to produce electrical and thermal energy, or it can be further purified to obtain the so-called biomethane, which can be injected into the natural gas grid or used as biofuel in both compressed gaseous form (CNG) and liquid form (LNG) [2]. Among the organic matrices suitable for AD, livestock feedstocks, such as animal manure and bedding materials, are essential substrates for biogas production. Besides, agrifood wastes generated during the processing phase of the agri-food supply chain are commonly used for AD. These wastes include fruits and vegetables that do not meet the aesthetic standards set by retailers or consumers, residues from processing operations, and overproduction by farmers, among others [3]. Agri-food wastes are characterized by a high residual level of carbohydrates, proteins, and lipids, making them fermentable within a few days. The mono-digestion of a single substrate can present several drawbacks due to the specific properties of the substrate used. For example, some organic matrix has a low nitrogen content or high concentrations of slowly biodegradable organic material. This composition could lead to process concerns that could limit biogas productivity [4]. To overcome this issue, co-digestion (Co-AD) could be implemented. Co-digestion involves the anaerobic digestion of different substrates simultaneously, improving biogas production rates, methane yield, and the reduction of volatile solids. It enhances nutrient availability for microbial growth, dilutes toxic compounds, balances moisture, and compensates for seasonal fluctuations in organic waste. Co-digestion also boosts process efficiency, increases biodegradable components, enhances the microbial community, and stabilizes the process. Nevertheless, the right co-substrate balances should be carefully addressed to promote synergistic effects and avoid competitive reactions.
Within this framework, the aim of this study was to evaluate some possible solutions to produce biogas and biomethane from the anaerobic digestion and co-digestion of different organic matrices. Several of the main agricultural and agro-industrial by-products and the most prevalent livestock effluents in the

Sicilian territory were evaluated. More precisely, the study was aimed at assessing the biochemical methane potential (BMP) resulting from the anaerobic digestion of single substrates and their co-digestion in various mixtures to address possible synergistic or antagonistic effects useful for practical implementation.

Materials and methods

Different types of organic feedstock were studied, including laying hen manure, meat poultry manure, olive pomace, citrus paste, depectinized citrus paste, and opuntia cladodes. The feedstocks used in the experimental activity were collected from the biomethane production plant of Assoro Biometano srl, which produces bio-CNG and bio-LNG from livestock effluents and agro-industrial by-products. A solid digestate from the same plant was used as inoculum for BMPs assays. The experimental activity was divided into two phases: in the first phase, batch BMPs assays were conducted on the individual substrates, whereas in the second phase, BMPs were performed on various biphasic and triphasic mixtures of the substrates, simulating a co-digestion process. Glass bottles with a working volume of 600 mL were used for all the assays. The volume of the mixture between the organic matrices and inoculum added in each bottle was 500 mL, leaving a headspace volume of 100 mL. The inoculum/substrate ratio (ISR) was set at 2, based on the volatile solid (VS) content. In all samples, the percentage of total solids was maintained below 10% of total solids (TS) to simulate a wet anaerobic digestion process. The bottles were then sealed and connected to a Tedlar bag where the biogas was collected. The bottles were placed within a thermostatic chamber at a controlled temperature (39 °C) on a magnetic plate to ensure mixing. Every 2-3 days, the volume of methane accumulated in the bag was measured using a liquid-displacement method, with an alkaline solution (2% NaOH) as the barrier-liquid. The results from the BMP assays were expressed as the volume of methane per mass of VS added ($Nm^3/t\ VS_{added}$) or referred to the initial weigh of the feedstocks (Nm^3CH_4/t). Each test lasted until a steady methane production was obtained. Table 1 summarizes the main physical characteristics of each mixture, while Table 2 reports the composition of each reactor.

Table 1. Characterization of the feedstocks used for anaerobic co-digestion assays.

ID	Feedstock	TS (%)	U (%)	VS/TS (%)
A	Laying hen manure	35,35%	64,65%	74%
B	Meat poultry manure	50,46%	49,54%	86%
C	Olive pomace	10,82%	89,18%	89%
D	Citrus paste	16,41%	83,59%	95%
E	Inoculum digestate	7,03%	92,97%	62%
F	Opuntia cladodes	8,08%	91,92%	79%
G	Depectinized citrus paste	15,50%	84,50%	95%

Table 2. Composition of the BMP assays.

Reactor ID	Digestion feedstocks	Composition
A	Laying hen manure	100%
B	Meat poultry manure	100%
C	Olive pomace	100%
D	Citrus paste	100%
E	Inoculum digestate	100%
F	Opuntia cladodes	100%
G	Olive pomace + citrus paste	50%+50%
H	Olive pomace + meat poultry manure	50%+50%
I	Opuntia cladodes + depectinized citrus paste	50%+50%
L	Opuntia cladodes + laying hen manure	50%+50%
M	Opuntia cladodes + olive pomace	50%+50%

N	Opuntia cladodes + meat poultry manure	50%+50%
O	Laying hens manure + meat poultry manure + olive pomace	33%+33%+33%
P	Laying hens manure + meat poultry manure + citrus paste	33%+33%+33%
Q	Laying hens manure + meat poultry manure + olive pomace	50%+20%+30%

Results

The productivity of organic feedstocks in terms of biogas and biomethane depends closely on their volatile solids content, which represents their organic matter content. The percentage reduction of volatile solids, and thus the efficiency of the anaerobic digestion process in terms of volatile solids reduction, was found to be very high, mostly remaining above 85%. Regarding biomethane production, Table 3 presents the results related to the biomethane production potential, reported both in terms of the amount of volatile solids fed and the as-fed biomass quantity, for the tests conducted using individual substrates.

Table 3. Results of BMP assays on the sole organic feedstocks

Feedstock	BMP [Nm^3CH_4/tVS]	BMP [Nm^3CH_4/t]	VS reduction [%]
Laying hens manure	262,8	68,7	97.5
Meat poultry manure	370,6	160,0	97.8
Olive pomace	241,9	23,3	86.5
Citrus paste	178,7	27,9	92
Depectinized citrus paste	210.1	35.4	94
Opundia clatods	193.3	12.3	86.2

As reported in Table 3, the substrate with the highest specific production was the meat poultry manure, with a BMP of 370.6 Nm^3/t VS, followed by laying hen manure (262.8 Nm^3/t VS), olive pomace (241.9 Nm^3/t VS), depectinezed citrus paste (210.1 Nm^3/t VS), opuntia cladodes (193.3 Nm^3/t VS) and citrus paste containing residual of essential oils (178.7 Nm^3/t VS).

Based on the theoretical methane production obtainable from the mixture of the above feedstocks, it was possible to evaluate the occurrence of synergistic or competitive effects during co-digestion by comparing the theoretical value with the one observed (Fig. 1). A value lower than the real BMP indicated that the mixture had a competitive effect on the final methane production, whereas a higher value suggested that the mixture had a synergistic effect.

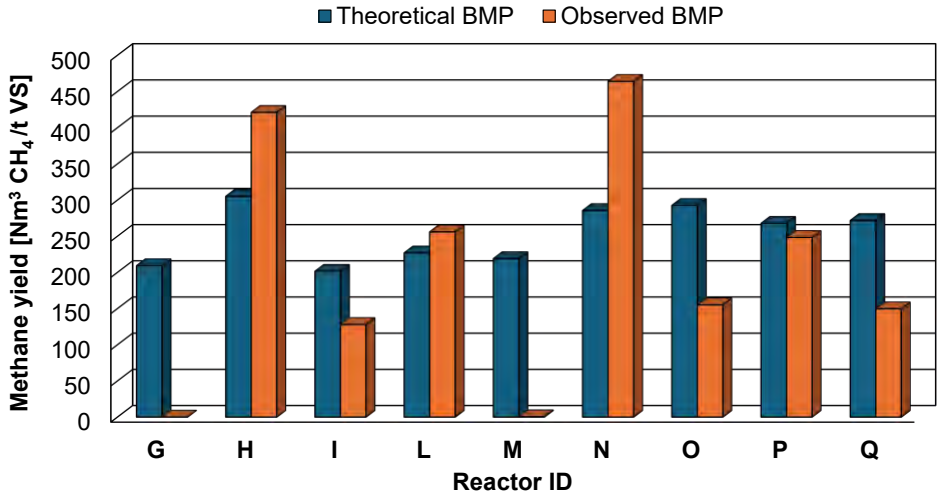

Figure 1: Theoretical and observed BMP from anaerobic co-digestion of different organic feedstocks.

It was noted that in the case of co-digestion between olive pomace and citrus paste (ID-G), there was an inhibitory effect, likely caused by a pH reduction and increased acidity, which likely inhibited methanogenic bacteria. Conversely, co-digestion of olive pomace and meat poultry manure (ID-H) showed a synergistic effect, leading to increased biomethane production (+30%) and production rate acceleration compared to anaerobic digestion of olive pomace alone. Conversely, co-digestion of opuntia cladodes and depectinized citrus paste (ID-I) showed a competitive effect, resulting in approximately 30% of BMP reduction, likely due to inhibition caused by the low pH of citrus paste.
Similarly, in the case of co-digestion between opuntia cladodes and olive pomace (ID-M), a completely inhibitory effect was observed, likely caused by both the high content of slowly degradable substances in olive pomace and the high content of fibrous material in opuntia cladodes, which slowed down the specific biomethane production rate. On the other hand, the anaerobic co-digestion process of opuntia cladodes with livestock effluents, pointed out that their mixing led to an increase in specific biomethane production. Specifically, co-digestion of opuntia cladodes with laying hen manure (ID-L) and with meat poultry manure (ID-N) determined a BMP improvement of 20% and 50%, respectively.
This increase was likely due to the high content of easily degradable proteinaceous material in the feedstock, which balanced the less easily degradable fibrous component present in opuntia cladodes. Furthermore, it was demonstrated that BMP of the three-phase mixture containing laying hen manure, meat poultry manure, and citrus paste did not show a significant decrease in methane production, thus indicating that no inhibitory effects occurred. On the other hand, while mixing laying hen manure, meat poultry manure and olive pomace, even with different ratios, competitive effects were noted, leading to a substantial decrease in BMP potential.

Conclusions

In conclusion, this study addressed the effectiveness of anaerobic digestion and co-digestion for converting various organic wastes into biogas and biomethane. It identified key agricultural and agro-industrial by-products, and livestock effluents from Sicily, highlighting optimal substrate mixtures for enhanced biogas production. Notably, co-digestion of olive pomace with meat poultry manure boosted biomethane production by 30%, while certain combinations, like olive pomace with citrus paste, showed inhibitory effects. Mixing opuntia cladodes with livestock effluents significantly improved BMP due to the balanced fibrous and proteinaceous materials. These findings emphasize the importance of selecting appropriate substrates and mixture ratios for optimizing biogas production, offering valuable insights for developing efficient and sustainable AD systems. Future research should delve deeper into Co-AD dynamics to further enhance biogas yields.

References

[1] F. Di Capua, D. Spasiano, A. Giordano, F. Adani, U. Fratino, F. Pirozzi, G. Esposito, High-solid anaerobic digestion of sewage sludge: challenges and opportunities, Appl. Energy 278 (2020) 115608. https://doi.org/10.1016/j.apenergy.2020.115608.
[2] A. Saravanakumar, M.R. Sudha, W.H. Chen, V. Pradeshwaran, V. Ashokkumar, A. Selvarajoo, Biomethane production as a green energy source from anaerobic digestion of municipal solid waste: A state-of-the-art review, Biocatal. Agric. Biotechnol. 53 (2023) 102866. https://doi.org/10.1016/j.bcab.2023.102866.
[3] E. Tamburini, M. Gaglio, G. Castaldelli, E.A. Fano, Biogas from agri-food and agricultural waste can appreciate agro-ecosystem services: The case study of Emilia Romagna region, Sustain. 12 (2020) 1–15. https://doi.org/10.3390/su12208392.
[4] W. Fang, X. Zhang, P. Zhang, J. Wan, H. Guo, D.S.M. Ghasimi, X.C. Morera, T. Zhang, Overview of key operation factors and strategies for improving fermentative volatile fatty acid production and product regulation from sewage sludge, J. Environ. Sci. (China) 87 (2020) 93–111. https://doi.org/10.1016/j.jes.2019.05.027.

Title: Potential Bio Hydrogen production: Co-digestion of mixed agricultural residues

Author(s): F. Illuminati*[1], R. Savio[1], M. C. Lavagnolo[1]

[1] DICEA, Department of Civil, Architectural and Environmental Engineering, University of Padova. Via Marzolo 9, 35131 Padova, Italy
** federico.illuminati@studenti.unipd.it*

Keyword(s): Dark fermentation, Agricultural residue, Anaerobic digestion, Bio Hydrogen

Abstract

Hydrogen has been explored as an alternative to fossil fuels, since its use for energy production does not result in pollutant emissions because only heat and water vapor are produced [1]. The two most common methods for producing hydrogen are steam-methane reforming and electrolysis [2]. However, it is necessary to explore also other pathways for hydrogen production from renewable resources, such as biomass. Nowadays, biomass-based hydrogen production technology mainly includes thermochemical, biological, and electrolysis methods [3] [4] [5]. Hydrogen can be produced biologically by bio-photolysis (direct and indirect), photo-fermentation and dark-fermentation or by a combination of these processes [6]. Dark-fermentation is the preferred biological methods for H2 production due to higher yields and lower operational costs [7] [8] [9]. The development of a profitable and environmentally sustainable bioenergy production must necessarily base on waste biomass, to decrease costs and produce marginal gains, and move toward advanced forms of biofuels, especially biomethane [10] [11]. The use of these biomasses, and in particular of agricultural and livestock by-products, does not conflict with food production, and allows for the exploitation of products that would otherwise have to be disposed of as waste, thus incurring additional costs. However, this system must consider the lower energy content of the by-products and their greater dispersion over land. Currently, several types of agricultural by-products can be used for energy pro-duction: straw [12], grass [13], pruning residues [14], and livestock manure [15] [16].
In the first part of the project a comprehensive review was conducted analysing selected papers to elucidate the hydrogen production potential of agricultural and livestock by-products.
Articles eligible for inclusion in the inventory must be scientific papers published between 2008 and 2023, including both articles and conference papers, written in either Italian or English. These papers should discuss the substrate utilized for hydrogen production through dark fermentation. In particular, target substrates of the research were defined consistently to the most common agricultural and livestock bioresources available in Europe [17] [18] [19], namely: agricultural harvesting by-products (especially for barley, beet, corn, oat, rapeseed, sorghum, sunflower, and wheat crops) and livestock manure from cattle, poultry, and swine farms. Those by-products are included in the list of raw materials suitable for producing advanced biofuel, according to Italian legislation [20]. A total of 5,973 documents were collected through the search. Following a two-stage literature screening process, 65 papers were identified for subsequent data extraction. The systematic review focused primarily on collecting data related to hydrogen yield (HY) during this phase. Additionally, information related to inoculum and substrate processing, general aspects, and experimental conditions was gathered. The data processing phase aimed to highlight current trends in hydrogen production through dark fermentation. Specifically, it involved analyzing data related to general aspects and experimental conditions. For the targeted

substrates, the goal was to establish a range of achievable hydrogen yields and provide insights into their variability. Furthermore, the review aimed to elucidate the impact of inoculum processing, substrate pre-treatment, and nutrient supplementation on hydrogen yield (HY).
The results of the review indicate that when both the inoculum and the substrate are treated, hydrogen production tends to be higher. Lower yields are observed when only the inoculum or only the substrate is processed. Additionally, the study suggest that inoculum processing is more effective than substrate processing in increasing hydrogen yield. Although the data for inoculum processing are somewhat, the average yield was around 44.5 ml/gVS, which is higher than the average yield for substrate processing at 32 Nml/gVS. Conversely, when both treatments are applied, the average yield reaches 81.4 ml/gVS, which is more than four times the average yield obtained without any processing.

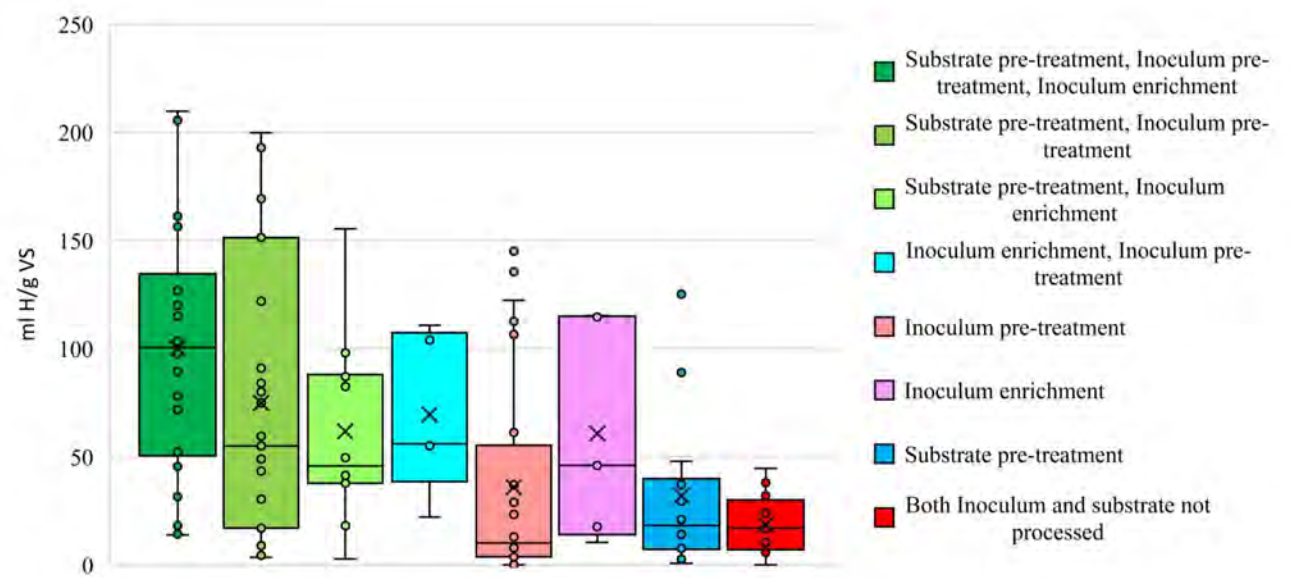

Figure 1. Box plot showing the synergies between inoculum and substrate processing under various treatments. Each box represents the interquartile range, with the median and mean indicated. Treatments include combinations of substrate pre-treatment, inoculum pre-treatment, and inoculum enrichment, with a control of no processing.

In the second part of the study, the hydrogen production potential of the most abundant agricultural and zootechnical by-products in the Veneto region through dark fermentation has been tested, both individually and in co-digestion scenarios. The implementation of single stage anaerobic digester to treat these kinds of residues is a common practice to stabilize the material and produce biogas rich in methane.
This laboratory test demonstrated that heat-treated granular sludge is highly effective as an inoculum for hydrogen production through dark fermentation. Agricultural residues showed promising hydrogen production, with corn residue achieving the highest yield at 17.81 Nml/gVS. In contrast, no hydrogen was produced from the fermentation of zootechnical effluents alone. However, co-digesting corn residue with zootechnical effluents resulted in a synergistic effect, leading to a higher hydrogen yield than the average yield of the individual substrates. The process's effectiveness appears to be influenced by the sludge pre-treatment duration. Heat-treating granular sludge at 100°C for 5 hours yielded slightly better results compared to a 4-hour treatment. Further research is needed to clarify this relationship and determine whether hydrogen production is linearly dependent on pre-treatment time. Notably, the corn

residue and co-digestion substrates were not pre-treated, yet they showed promising results. Pre-treatment of substrates could potentially increase hydrogen yield by up to 50 times. Future investigations should focus on identifying the optimal pre-treatment methods for substrates and evaluating their economic and energetic feasibility and sustainability.

Acknowledgements

This work was supported by the Interdepartmental Centre for Energy Economics and Technology "Giorgio Levi Cases", Padua, Italy, under the interdisciplinary project VASE (Valorisation of Agri-foodWastes for Sustainable Energy Production).

References

[1] Megia P. J., Vizcaíno A. J., Calles J. A., Carrero A. (2021) Hydrogen Production Technologies: From Fossil Fuels toward Renewable Sources. A Mini Review. Energy Fuels, 35, 16403-16415. https://doi.org/10.1021/acs.energyfuels.1c02501
[2] Production of hydrogen - U.S. Energy Information Administration (EIA)
[3] Cao L., Yu I. K. M., Xiong X., Tsang D. C. W., Zhang S., Clark J. H., Hu C., Hau Ng Y., Shang J., Sik Ok Y. (2020) Biorenewable hydrogen production through biomass gasification: A review and future prospects. Environmental Research, 186, https://doi.org/10.1016/j.envres.2020.109547
[4] Lin C Y., Nguyen T. M. L., Chu C. Y., Leu H. J., Lay C. H., (2018) Fermentative biohydrogen production and its byproducts: a mini review of current technology developments. Renewable and Sustainable Energy Reviews, 82, 4215-4220. https://doi.org/10.1016/j.rser.2017.11.001
[5] Ju H., Badwal S., Giddey S. (2018) A comprehensive review of carbon and hydrocarbon assisted water electrolysis for hydrogen production. Applied Energy, 231, 502-533. https://doi.org/10.1016/j.apenergy.2018.09.125
[6] Manish S., Banerjee R. (2008) Comparison of biohydrogen production processes. International Journal of Hydrogen Energy, 33. 279-286. https://doi.org/10.1016/j.ijhydene.2007.07.026
[7] Rafieenia R., Lavagnolo M. C., Pivato A. (2018) Pre-treatment technologies for dark fermentative hydrogen production: Current advances and future directions. Waste Management 71, 734-748. http://dx.doi.org/10.1016/j.wasman.2017.05.024
[8] Hallenbeck, P.C., Abo-Hashesh, M., Ghosh, D., 2012. Strategies for improving biological hydrogen production. Bioresour. Technol. 110, 1–9. http://dx.doi. org/10.1016/j.biortech.2012.01.103.
[9] Mathews, J., Wang, G., 2009. Metabolic pathway engineering for enhanced biohydrogen production. Int. J. Hydrogen Energy 34, 7404–7416. http://dx.doi. org/10.1016/j.ijhydene.2009.05.078.
[10] Chiumenti, A.; Pezzuolo, A.; Boscaro, D.; Da Borso, F. Exploitation of mowed grass from green areas by means of anaerobic digestion: Effects of grass conservation methods (drying and ensiling) on biogas and biomethane yield. Energies 2019, 12, doi:10.3390/en12173244.
[11] Statuto, D.; Frederiksen, P.; Picuno, P. Valorization of Agricultural By-Products Within the "Energyscapes": Renewable Energy as Driving Force in Modeling Rural Landscape. Nat. Resour. Res. 2019, 28, 111–124, doi:10.1007/s11053-018-9408-1.
[12] Brosowski, A.; Bill, R.; Thrän, D. Temporal and Spatial Availability of Cereal Straw in Germany Case Study: Biomethane for the Transport Sector. Energy Sustain. Soc. 2020, doi:10.21203/rs.3.rs-16344/v2.
[13] Mattioli, A.; Boscaro, D.; Dalla Venezia, F.; Correale Santacroce, F.; Pezzuolo, A.; Sartori, L.; Bolzonella, D. Biogas from Re-sidual Grass: A Territorial Approach for Sustainable Bioenergy Production. Waste Biomass Valorization 2017, 8, 2747–2756, doi:10.1007/s12649-017-0006-y.
[14] Pari, L.; Suardi, A.; Santangelo, E.; García-Galindo, D.; Scarfone, A.; Alfano, V. Current and innovative technologies for pruning harvesting: A review. Biomass Bioenergy 2017, 107, 398–410, doi:10.1016/j.biombioe.2017.09.014.
[15] Chiumenti, A.; Da Borso, F.; Pezzuolo, A.; Sartori, L.; Chiumenti, R. Ammonia and greenhouse gas emissions from slatted dairy barn floors cleaned by robotic scrapers. Res. Agric. Eng. 2018, 64, 26–33,

doi:10.17221/33/2017-RAE.
[16] Finzi, A.; Mattachini, G.; Lovarelli, D.; Riva, E.; Provolo, G. Technical, economic, and environmental assessment of a collec-tive integrated treatment system for energy recovery and nutrient removal from livestock manure. Sustainability 2020, 12, 2756, doi: 10.3390/su12072756.
[17] Scarlat et al, 2010; Assessment of the availability of agricultural crop residues in the European Union: Potential and limitations for bioenergy use; http://dx.doi.org/10.1016/j.wasman.2010.04.016
[18] Eurostat, 2020; https://ec.europa.eu/eurostat/statistics explained/index.php?title=Agricultural_production_-_crops.
[19] Scarlat et al, 2018; A spatial analysis of biogas potential from manure in Europe; https://doi.org/10.1016/j.rser.2018.06.035
[20] Ministero dello Sviluppo Economico, 2018; https://www.mise.gov.it/index.php/it/normativa/decreti-interministeriali/decreto-interministeriale-2-marzo-2018-promozione-dell-uso-del-biometano-nel-settore-dei-trasporti

PARALLEL SESSION: A4

Wastewater treatment

Emerging challenges in operation

Title: Improvement of Biomethane Production from Waste Activated Sludge through sonication pretreatment

Authors: Carlo Limonti*[1], Tiziana Andreoli[1], Giulia Maria Curcio[1], Elvis Gribaldo Aucancela Riveira[1], Adolfo Le Pera[2] and Alessio Siciliano[1]

[1] *Laboratory of Sanitary Environmental Engineering, Department of Environmental Engineering (DiAm), University of Calabria, Rende 87036, Italy*
[2] *Calabra Maceri SpA, Rende 87036, Italy*
**Corresponding:carlo.limonti@unical.it*

Keywords: anaerobic digestion, biomethane production, ultrasound pretreatment, waste activated sludge.

Abstract

The present work reports the results of an experimental investigation conducted with the aim to improve the anaerobic treatability of waste activated sludge through sonication pretreatment. Several batch experiments were conducted by varying the sonication power (80, 90 and 100 W), reaction time (90, 150, 300 and 600 seconds) and temperature (20, 40 and 60°C). The detected results showed a significant enhancement in the solubilization of organic matter when the power increased from 80 W to 100 W. Reaction time and temperature were also responsible for a substantial improvement in the process performance. The temperature of 20°C, reaction time of 600 s and sonication power of 100 W were defined as the optimal operating conditions which allowed an increase of dissolved VS by approximately of five times. During anaerobic batch tests, a biomethane yield of about 418 NmL_{CH4}/g_{VSIN} was reached with the pretreated WAS, which was of about 14 % higher than the production obtained on raw waste activated sludge.

1. Introduction

Activated sludge processes are the most widely used treatment for urban wastewater purification. This process produces treated effluent and waste activated sludge (WAS). The activated sludge is separated from the effluent in secondary settlers or through membrane filtration units. A large part of the separated sludge is recirculated upstream oxidation units while the excess fraction (WAS) is treated through aerobic or anaerobic stabilization processes [1]. Although aerobic processes provide quick sludge stabilization, they are high energy-intensive [2]. Anaerobic processes, on the other hand, allow proper sludge stabilization with the production of biogas characterized by a high energetic value [3]. Nonetheless, anaerobic digestion (AD) of WAS is severely slowed by the hydrolytic phase of particulate substrates [4]. Indeed, hydrolysis is the rate-limiting step because of the difficulty of converting the complex organic matter of WAS into simpler substances [5]. The slow hydrolytic phase leads to longer retention times, higher reactor volumes, and lower biogas yields [6]. Therefore, it is necessary to apply adequate pretreatments to improve the performance of anaerobic digestion of WAS by accelerating the hydrolytic phase [4]. In this regard, several technologies have been developed to improve the anaerobic degradability of WAS. These methods include thermal (low or high temperature), chemical (acid or alkali pretreatment), physical or mechanical (microwave irradiation, electro-kinetic disintegration, ultrasonication) pretreatments [7]. Among different pretreatment technologies, ultrasound (US) is a suitable option to improve the treatability of WAS [8]. Ultrasound induces cavitation in WAS causing lysis of cellular material. This phenomenon increases the amount of organic matter solubilized in the

liquid fraction, which can be more easily degraded during AD [9]. Recent studies confirmed that ultrasound (US) pretreatment can increase the biogas yields of the anaerobic digestion of WAS [9]. Anyhow, further research is needed to investigate the effect of sonication operating conditions on the characteristic of pretreated sludge and on the performance of the subsequent anaerobic digestion process. In this regard, the present study aimed to evaluate the influence of different sonication parameters on the improvement of WAS properties and AD evolution of pretreated sludge.

2. Materials and methods

2.1 Materials and analytical methods

Centrifugated WAS from the sludge treatment line of a conventional wastewater purification plant sited in Calabria Region (Italy), was used to perform the US tests. WAS sample was diluted 5 folds and stored in a 20 L tank at 4°C to avoid deterioration. A digestate sample from a waste anaerobic digestion plant treating the organic fraction of municipal solid waste (OFMSW) was used as an inoculum for the biomethane potential (BMP) tests.
Total solids (TS) and volatile solids (VS) were determined by gravimetric analysis after drying the samples at 105°C for 24 hours and 550°C for 1 hour, respectively [10].

2.2 Ultrasound tests

The effects of sonication power, sonication time, and temperature were investigated during the US tests. A first series of experiments was conducted at 20°C with a sonication time of 300 s, varying the sonication power between 80 and 100 W. Once the optimal US power was identified, further tests were performed by changing the sonication time between 90 and 600 s and the temperature from 20°C to 60°C. Each test was performed in batch mode at atmospheric pressure on a WAS volume of 50 mL, by working with a frequency of 30 kHz. The treated WAS samples were centrifuged at 4000 rpm for 10 minutes, and the supernatant fractions were characterized in terms of TS and VS content.

2.3 Biomethane potential tests

The biomethane potential (BMP) tests aimed to identify and compare the production yields detectable with raw and pretreated WAS. Two tests were conducted on mixtures prepared by mixing the raw and pretreated WAS samples with a small aliquot of inoculum consisting of OFMSW digestate. Another test was executed with digestate alone to account the methane production attributable to the inoculum. Table 1 shows the compositions of the mixtures. Tests were performed in batch mode at 37±2°C using the VELP Respirometric Sensor system (VELP Scientifica srl, Usmate, MB, Italy). The anaerobic process was monitored for 80 days.

Table 1. Mixtures composition

Mixture	Digestate	Treated WAS	Untreated WAS	Mixture weight
	[%]	[%]	[%]	[g]
Mix-0	100	-	-	100
Mix-1	10	90	-	180.2
Mix-2	10	-	90	180.6

3. Results and discussion

3.1 US tests

Through the ultrasound experiments, the best operating conditions to increase the dissolved VS in pretreated WAS were identified. In the first set of experiments, the influence of sonication power on the

release of organic matter in the supernatants at 20 °C and 300 s was evaluated. Specifically, with a sonication power of 80 W, the dissolved VS increased notably, reaching a concentration of approximately 5.8 g/kg (Figure 1a). Further moderate increases were observed when the sonication power was enhanced to 90 and 100 W. In particular, in the test carried out at the maximum power, the VS content in the liquid was three times higher compared to the concentration of raw WAS, achieving a value of about 6.6 g/kg. Based on these results, subsequent experiments were carried out by applying a sonication power of 100 W.

The second set of experiments evaluated the effects of different sonication times and temperatures. The increase in the reaction time produced a significant process improvement for each applied temperature (Figure 1b). In particular, in the tests performed at 20°C the VS was doubled by extending the treatment time from 90 s to 600 s. Even higher VS concentrations were observed at 40 and 60°C, which proved the positive influence of temperature on the dissolution of organic solids. In particular, the greatest impact of the temperature increase was detected with the shortest reaction time. At 40°C the solubilized VS increased almost linearly in response to the rise of reaction time. On the other hand, with a temperature of 60°C, a small variation in the VS concentration occurred for sonication times between 90 and 300 s, while the extension of the treatment to 600 s produced a marked increase in VS up to a concentration close to 12 g/kg. Although temperature allows for a general improvement in the process performance, its rise produces an increase in energy consumption and treatment costs. Therefore, a temperature of 20°C and a sonication time of 600 s were selected as operating conditions to pretreat the WAS sample for subsequent anaerobic digestion tests.

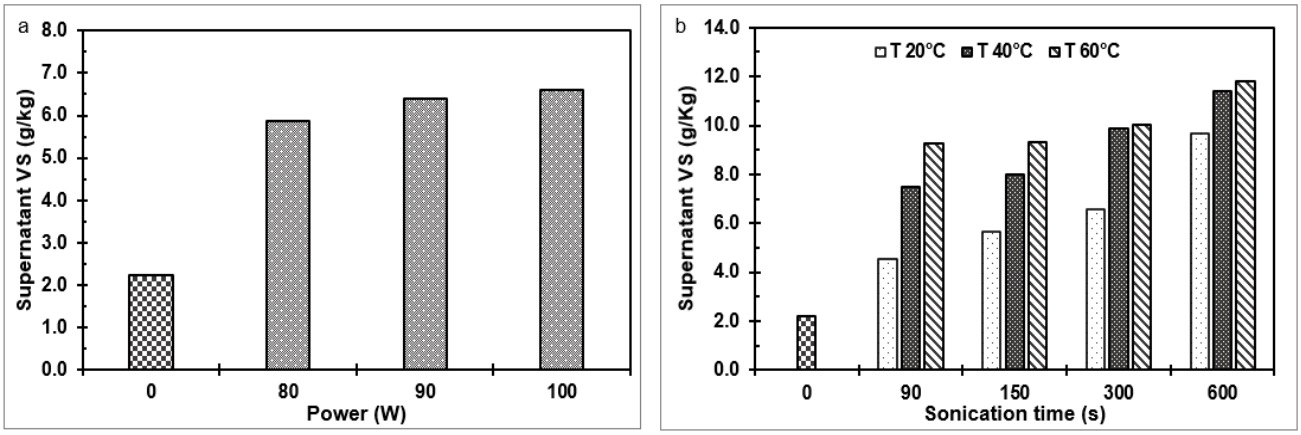

Figure 1. Dissolved VS (a) at different US power, (b) at different US sonication times and temperatures.

3.2 Biomethane potential tests

BMP tests were carried out on treated and raw WAS to assess the effect of sonication pretreatment on methane generation. A digestion test with the inoculum alone was also conducted. Cumulative methane productions were normalized to the initial VS content of the mixture and depicted in Figure 2. Some production was recorded with the inoculum, which indicates that the digestate had a significant residual amount of degradable organic matter. Notably higher productions were detected on mixtures with WAS samples. In particular, similar trends were found for the first 10 days, beyond which the productions had different behaviours and an overall increase in BMP of approximately 14 % was detected on the mixture with pretreated WAS (Mix-1), reaching a yield close to 418 NmL_{CH4}/g_{VSIN}. These results prove that the sonication pretreatment allows for an improvement in the WAS characteristic so as to achieve a superior methane production during the anaerobic digestion process.

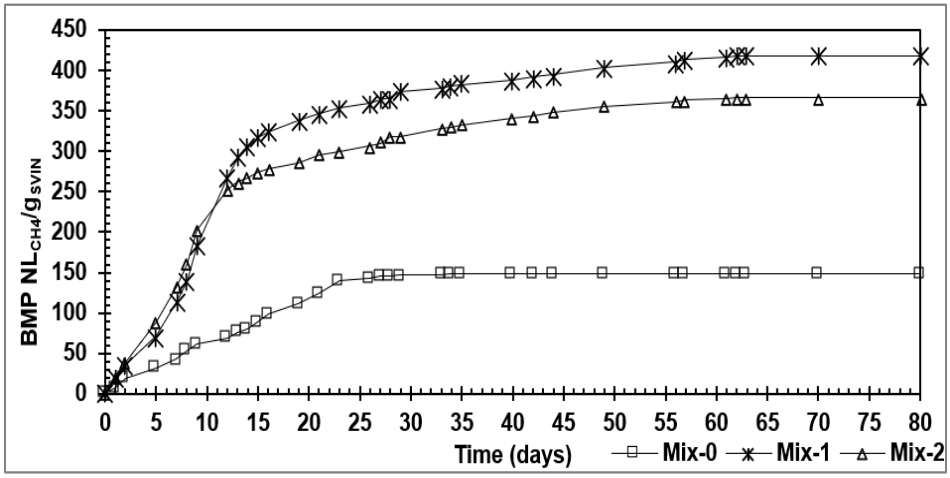

Figure 2. Normalized productions detected with inoculum (Mix-0), pretreated WAS (Mix-1) and untreated WAS (Mix-2)

4. Conclusions

In the present study, the sonication process was investigated as a pretreatment to improve the anaerobic treatability of waste activated sludge. Through a series of US tests carried out under different operating conditions, it was demonstrated that the sonication power, temperature and reaction time enhance the dissolution of organic solids in the liquid phase. At a temperature of 20°C, by treating the WAS for 600 s with a power of 100 W, the dissolved VS increased five times. The activated sludge pretreated with these operating conditions showed a rise of approximately 14 % in the biomethane production compared to the yield detected with raw WAS, reaching an overall value of 418 NmL_{CH4}/g_{VSIN}. These results, support the applicability of sonication to improve the methane yields detectable from waste activated sludge.

References

[1] Tchobanoglous, G.; Burton, F.L.; Stensel, H.D. Wastewater Engineering, Treatment and Reuse, 4th ed.; Metcalf & Eddy; McGraw-Hill: New York, NY, USA, 2003; ISBN 883866188-X.
[2] Pariente, M.I.; Segura, Y.; Molina, R.; Martínez, F. Wastewater treatment as a process and a resource. Wastewater Treat. Residues Resour. Biorefinery Prod. Biofuels 2020, 19–45.
[3] Khanal, S.K. Anaerobic Biotechnology for Bioenergy Production: Principles and Applications, 1st ed.; Wiley-Blackwell: Ames, IA, USA, 2008; ISBN 978-0-8138-2346-1.
[4] Calabrò, P.S.; Fazzino, F.; Limonti, C.; Siciliano, A. Enhancement of Anaerobic Digestion of Waste-Activated Sludge by Conductive Materials under High Volatile Fatty Acids-to-Alkalinity Ratios. Water 2021, 13, 391.
[5] Odnell, A.; Recktenwald, M.; Stensén, K.; Jonsson, B.-H.; Karlsson, M. Activity, lifetime and effect of hydrolytic enzymes for enhanced biogas production from sludge anaerobic digestion. Water Res. 2016, 103, 462–471.
[6] Elalami, D.; Carrere, H.; Monlau, F.; Abdelouahdi, K.; Oukarroum, A.; Barakat, A. Pretreatment and co-digestion of wastewater sludge for biogas production: Recent research advances and trends. Renew. Sustain. Energy Rev. 2019, 114, R713–R715.
[7] Nguyen, V. K., Chaudhary, D. K., Dahal, R. H., Trinh, N. H., Kim, J., Chang, S. W., & Nguyen, D. D. (2021). Review on pretreatment techniques to improve anaerobic digestion of sewage sludge. Fuel, 285, 119105.
[8] Pilli, S., Bhunia, P., Yan, S., LeBlanc, R. J., Tyagi, R. D., & Surampalli, R. Y. (2011). Ultrasonic pretreatment of sludge: a review. Ultrasonics sonochemistry, 18(1), 1-18.
[9] Y.K. Kim, M.S. Kwak, W.H. Lee, J.W. Choi, Ultrasonic pretreatment for thermophilic aerobic digestion in industrial waste activated sludge treatment, Biotechnol. Bioprocess Eng. 5 (2000) 469–474.
[10] APHA. Standard methods for the examination of water and wastewater. 20th ed. Washington (DC): American Public Health; 1998.

Title: Energy efficiency and class performance of WWTPs.

Author(s): Desara Malluta*[1], Erica Gagliano, Michela Gallo, Adriana Del Borghi

[1] *Department of Civil, Chemical and Environmental Engineering, University of Genova, Italy,*
*desara.malluta@edu.unige.it

Keyword(s): energy efficiency, benchmarking, wastewater treatment plants (WWTPs)

Introduction

Wastewater treatment plants (WWTPs) are significant electricity consumers, with their primary objective being the purification of wastewater from pollutants. Despite this clear aim, WWTPs are complex systems due to factors such as the characteristics of the incoming wastewater, treatment techniques, associated technologies, and external influences. Assessing energy efficiency is crucial for establishing operational standards and identifying areas of excessive energy consumption. Energy consumption in WWTPs depends on various factors such as treatment processes [1], the mass of pollutants removed [2], treated wastewater quality requirements (carbon, nutrients control, filtration, and disinfection), treated wastewater volume, design capacity of plant operating [1], plant aging [3], operation and maintenance.

Current regulations mandate energy efficiency audits for water utilities above a certain size, yet a standardized procedure for assessing energy performance in the wastewater sector is lacking. Benchmarking methods such as Key Performance Indicators (KPIs) offer the potential for evaluating energy efficiency and performance in WWTPs such as is described in the literature by Gallo et al.,[4]. This study introduces an applied methodology in the literature used by Di Fraia et al.,[5] to assess the energy efficiency of WWTPs by combining simple energy performance indicators (EPI) with pollution removal efficiency (η).

The objective of the research is to adapt the methodology of performance indicators and classification systems for existing WWTPs, aiming to provide more robust assessments of energy efficiency. To reach objectives in terms of assessing the energy performance of WWTPs through different methodologies is utilized as an instrument the benchmarking. Most of the methodologies of the energy benchmarking model are based on the identification of KPIs that reflect operational efficiency. The used KPIs are the ratio between the energy consumption in the plant and the amount of pollutants removed [3]. Many indicators have been proposed [6] and the most applied are built by considering the whole WWTP energy consumption to: plant size, influent and effluent quality, pollutant and volumetric loads [7]. The availability of the overall WWTPs energy consumption in this case is acquired directly from the point of delivery (P.O.D.) readings, allowing an easy calculation of the KPIs by relating the energy use to each parameter. The KPIs used are related to the total system energy consumption to the treated wastewater volume (KPI_V) and the plant size expressed as served (KPI_{PE}). The use of one single KPI is not sufficient when the aim is to obtain information on the overall efficiency of the plant of to take into account various aspects of the WWTP characteristics. Energy Performance Indicators (EPI) are obtained by comparing the value of each corresponding KPI for the parameters that we considered with its database distribution function. By coupling EPI with the removal efficiency (η) of that parameter allows us to introduce the

classes for evaluation of the energy performances of the plants. There are considered four classes of performances of the plants. It is proposed to be applied EPI_{BOD} which determines the overall electrical energy consumption per kg of inlet total amount of BOD (mg/l). This study aims to assess the energy efficiency and energy performance of the WWTPs. The plants are classified and calculated from the database analyzed of Italian WWTPs, and the removal efficiency of BOD is based on the D.Lgs.152/06 for the Italian normative.

Material and methods

A database of collected data on WWTPs was structured and utilized for the study research of statistical analysis. For each WWTP, the collected data were elaborated to calculate the KPIs yearly and daily basis. Firstly, it has been evaluated the linearity of two variables to estimate how certain factors affect the energy usage of WWTPs. We use the Pearson correlation coefficient, R^2, which quantifies the strength of the linear relationship between two variables.

Then the method adapted consists of defining new Energy Performance Indicators, (EPIs), that relate the overall energy consumption of the plant to a specific parameter represented in our case with BOD. Generally, there is no accepted procedure to assess the energy performance of wastewater treatment but a methodology of the current work is being adapted for a comprehensive assessment of treated wastewater quality that integrates performance indicators and performance indices. EPI_{BOD} is suitable since the biological stage is responsible for removing organic matter significantly increases the energy consumption of WWTPs. The removal efficiency is η_{BOD}, where BODin and BODout are the total amount of BOD in the inlet and the outlet, as expressed in the equations below:

$$\mathrm{EPIBOD} = \frac{\mathrm{EE}}{\mathrm{BODin}} \left[\frac{\mathrm{kWh}}{\mathrm{kgBODin}}\right]$$

$$\eta\mathrm{BOD} = \frac{\mathrm{BODin} - \mathrm{BODout}}{\mathrm{BODin}} [\%]$$

The group of data for the parameter of BOD is divided by using specific percentiles (10^{th}, 30^{th}, and 60^{th}) to identify several classes of energy performance and removal efficiency for BOD. In this case, it has been utilized different criteria for finding the limits of specific percentiles, such as percentiles of MS Excel, the percentiles of ranking and interpolation, and the third criterion is utilized Aggregate as a function of Excel taking into consideration Excel percentile and ignoring nothing since the plants with no data are not considered from both part for EPI and for removal efficiency for the parameter that has been considered. The table 1 shows the energy consumption referred to BOD.

Table 1. Classes of performances related to energy consumption and removal efficiency for BOD.

Class	η_{BOD} (%)	EPI_{BOD} (kWh/ kg BODin)
A	$\eta_{BOD} > 96.95\%$	$EPI_{BOD} < 2.15$
B	$96.95\% \geqslant \eta_{BOD} > 93.34\%$	$2.15 \leq EPI_{BOD} < 4.12$
C	$93.34\% \geqslant \eta_{BOD} > 80\%$	$4.12 \leq EPI_{BOD} < 9.70$
D	$\eta_{BOD} \leq 80\%$	$EPI_{BOD} \geqslant 9.70$

Results

Figure 1. shows relationships between energy consumption and several parameters that affect WWTPs operation. The higher the inlet flow rate of wastewater, the higher the electric energy consumption, the main limit of this indicator is that the influence of pollutant removal is not taken into account. When the

population served increases, energy consumption increases. The number of population served is also determined considering parameters that vary from country to country, sometimes calculated as influent of organic content.

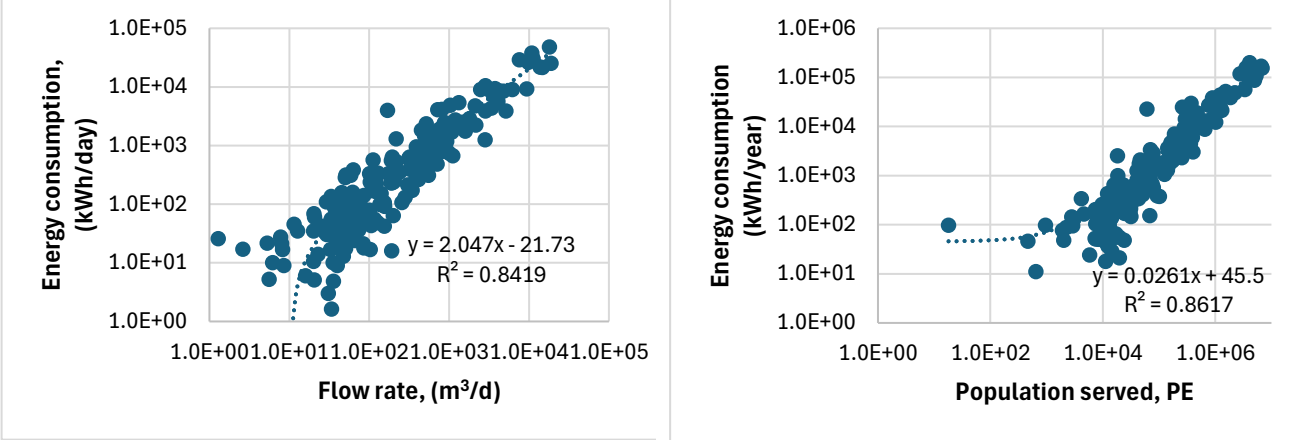

Figure 1. Energy consumption as a function of: a) daily flow rate (m^3/d); b) population served, PE.

The result of class performance for the parameter of BOD that we considered is such as in Figure 2. For the secondary and tertiary treatment, it can be seen that the WWTPs with tertiary treatment are concentrated more in classes of performance A, B, and C for the energy performance indicator and in classes A and B for the removal efficiency (η). The WWTPs with secondary treatment are more concentrated in classes C for removal efficiency and in classes A, B, and C of energy performance indicators.

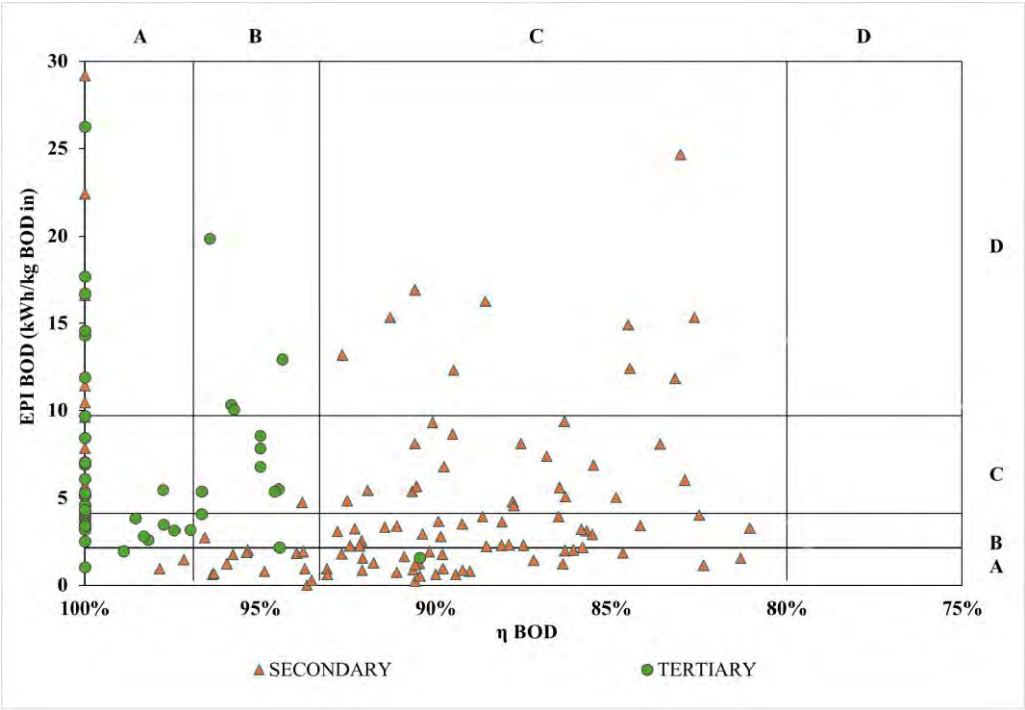

Figure 2. Classification of WWTPs according to EPI_{BOD} and removal efficiency (η).

The secondary and tertiary treatment plants meet the current Italian standards for removal efficiency. The secondary treatment requires further interventions to stabilize energy consumption and enhance overall plant performance. The tertiary treatment plant demonstrates the highet performance among the evaluated plants, serving as a benchmark.

Conclusions and future perspectives

Improving the energy efficiency of wastewater treatment plants (WWTPs) can also involve establishing performance standards and incentives for plant managers. Consequently, it becomes crucial to assess the energy performance of WWTPs. Various indicators have been suggested from the literature, linking energy consumption to key operational parameters of the process. These indicators have some limitations, such as KPI_V which assumes that inlet pollutant concentrations constantly neglect the concentration of organic matter, nutrients, and solids, and KPI_{PE} neglects the inlet pollutant concentration. Some other methods such as the Enerwater methodology is on-going to be applied to evaluate the energy performances of the WWTPs.

References

[1] Silva C., Rosa M. J., “Energy performance indicators of wastewater treatment: a field study with 17 Portuguese plants,” Water Science and Technology, vol. 72, no. 4, pp. 510–519, Aug. 2015, doi: 10.2166/wst.2015.189.
[2] Luo L., Dzakpasu M., Yang B., Zhang W., Yang Y., Wang X. C., “A novel index of total oxygen demand for the comprehensive evaluation of energy consumption for urban wastewater treatment,” Applied Energy, vol. 236, pp. 253–261, Feb. 2019, doi: 10.1016/j.apenergy.2018.11.101.
[3] Longo S., Antoni B. M., Bongards M., Chaparro A., Cronrath A., Fatone F., Lema J. M., Iglesias M. M., Soares A., Hospido A., “Monitoring and diagnosis of energy consumption in wastewater treatment plants. A state of the art and proposals for improvement,” Applied Energy, vol. 179, pp. 1251–1268, Oct. 2016, doi: 10.1016/j.apenergy.2016.07.043.
[4] Gallo M., Malluta D., Del Borghi A., Gagliano E., “A Critical Review on Methodologies for the Energy Benchmarking of Wastewater Treatment Plants,” Sustainability, vol. 16, no. 5, p. 1922, Feb. 2024, doi: 10.3390/su16051922.
[5] Di Fraia S., Massarotti N., Vanoli L., “A novel energy assessment of urban wastewater treatment plants,” Energy Conversion and Management, vol. 163, pp. 304–313, May 2018, doi: 10.1016/j.enconman.2018.02.058.
[6] Maktabifard M., Zaborowska E., Makinia J., “Achieving energy neutrality in wastewater treatment plants through energy savings and enhancing renewable energy production,” Reviews in Environmental Science and Bio/Technology, vol. 17, no. 4, pp. 655–689, Dec. 2018, doi: 10.1007/s11157-018-9478-x.
[7] Torregrossa D., Schutz G., Cornelissen A., Hernández-Sancho F., Hansen J., “Energy saving in WWTP: Daily benchmarking under uncertainty and data availability limitations,” Environmental Research, vol. 148, pp. 330–337, Jul. 2016, doi: 10.1016/j.envres.2016.04.010.

Title: Effective Sorbents from Waste Biomass for Emerging Pollutant Removal

Author(s): Martina Dlaskova*[1], Marketa Spacilova[1], Olga Solcova[1]

[1] *Institute of Chemical Process Fundamentals CAS, v.v.i., Rozvojova 135/1, 16500 Prague 6, Czech Republic, dlaskova@icpf.cas.cz*

Keyword(s): emerging pollutants, wastewater treatment, sorption, waste biomass, biochar

Abstract

Emerging pollutants (EP) and Contaminants of emerging concern (CEC) in wastewater treatment plant effluents present environmental and human health challenges. They are often persistent, resistant to degradation, and can remain in the environment for long periods of time with the potential to cause adverse health effects, including endocrine disruption, gene toxicity, genital disruption, antibiotic resistance, and many others [1, 2]. Regarding the fact that a large proportion of wastewater does not pass through the tertiary stage of treatment, these substances pass through the wastewater treatment plant into both surface and groundwater [3, 4]. Therefore, there is a need to find an effective but simple and cheap method of treating wastewater, which could be implemented not only in smaller decentralized on-site wastewater treatment plants as a tertiary water treatment stage.

In this study, a sorption technique is proposed as an additional stage of wastewater treatment. Sorption is a simple, effective and versatile method of removing a wide range of pollutants from water. As sorbents, various biochars were prepared by pyrolysis of different waste biomass. Although biochars appear considerably promising for removing pollutants from water, the pyrolysis conditions of the biomass feedstock are key to the effectiveness of biochar.

The sorption efficiency of prepared biochars was tested for the removal of three various pollutants commonly found in waters: acetaminophen - one of the most common analgesic and antipyretic drugs and the nonsteroidal anti-inflammatory drugs; naproxen and diclofenac. For better understanding of the sorption mechanism, the points of zero charge of sorbents were determined for all three types of biochar, as well as their texture properties and surface, by nitrogen adsorption, mercury porosimetry, and FTIR analysis. The effectiveness of biochar was compared with that of commonly used activated carbon.

Table 1. Textural properties of used sorbents

Sorbent	S_{BET} (m^2/g)	S_{meso} (m^2/g)	V_{tot} (mm^3_{liq}/g)	V_{micro} (mm^3_{liq}/g)
Biochar - microalgae	312	142	198	90
Biochar - macroalgae	304	71	162	112
Biochar - sunflower seed husks	243	74	132	87
Biochar – wood chip 1	416	114	265	147
Biochar – wood chip 2	282	62	151	112
Biochar – wood chip 3	465	147	288	153
Activated carbon Supersorbon	1 378	612	729	395

Acknowledgement:

The financial support from the Technology Agency of the Czech Republic project TN02000044 is gratefully acknowledged.

References

[1] Vasilachi I.C., Asiminicesei D.M., Fertu D.I., Gavrilescu M., “Occurrence and Fate of Emerging Pollutants in Water Environment and Options for Their Removal”, Water 13, 181, (2021). DOI: 10.3390/w13020181
[2] Calvo-Flores F.G., Isac García J., Dobado J.A., “Emerging Pollutants”, Wiley-VCH, (2018).
[3] Rathi B. S., Kumar P. S., "A review on sources, identification and treatment strategies for the removal of toxic Arsenic from water system", Journal of Hazardous Materials 418, (2021). https://doi.org/10.1016/j.jhazmat.2021.
[4] Narváez Valderrama J. F., García J. J., Gil R. D. H., Ríos S. R., Gonzalez J. D., Porras J., Agudelo E. D. M., “Adsorption of the emerging pollutants on Buena Vista landfill cover material and implications on regional aquatic pollution”, Groundwater for Sustainable Development 20, 100885, (2023). https://doi.org/10.1016/j.gsd.2022.100885

Title: What the flocs can still tell us: microfauna and filamentous bacteria examinations as invaluable tools in activated sludge operation

Author(s): Roberta Pedrazzani*

DIMI-Department of Mechanical and Industrial Engineering, University of Brescia, Brescia, Italy, roberta.pedrazzani@unibs.it

Keyword(s): biomass, ciliated protozoa, bulking, foaming, microscopy, sludge biotic index

Abstract

The activated sludge process was discovered and developed in 1913 by two British scientists, Edward Ardern and W.T. Lockett, while they were working at the Manchester Corporation Rivers Department in the United Kingdom. Their discovery was a result of experiments aimed at improving the treatment of sewage by using aeration techniques.
Ardern and Lockett's work focused on the observation that aerating sewage water allowed for the growth of a biological floc composed of bacteria and protozoa, which could efficiently break down organic matter. This biological floc, termed "activated sludge," could then be settled out of the treated water, with a portion being recycled to maintain a stable microbial population.

Their findings were first published in 1914 [1]. The development of the activated sludge process marked a significant advancement in wastewater treatment technology, leading to its widespread adoption and continuous improvement over the subsequent decades.
Since then, the interest in this process, which combined knowledge of hygiene, biology, chemistry and civil engineering, was the subject of researches, with the aim of better understanding the principles underlying wastewater purification and improving the efficiency of biodegradation reactions.
Some studies represented milestones in the knowledge of activated sludge: Ardern and Lockett (1936) themselves published an article in which, they already highlighted correlations between the quality of the effluent and the presence and abundance of some protozoa (with an approach similar to the criterion of saprobic indices) [2]. Baines et al. (1953) deepened their investigations, looking for correlations between the microfauna, rainfall, temperature and the concentration of dissolved oxygen [3].
Curds and Cockburn found relationships between sub-populations of ciliated protozoa, sludge load and effluent quality [4]. Klimowicz's studies shed new light on the influence of operating conditions and influent characteristics [5]. In the meantime, zoologists studied the ecology of ciliates and rotifers and revised their classification, working on individuals found in activated sludge plants [6] [7] [8]. Scientists gradually came to hypothesize the possibility of using the protozoa and metazoa of activated sludge as indicators of the efficiency of the purification process [9] [10] [11]. Madoni and Ghetti began to publish works on the activated sludge community in the 1980s, considering the oxidation tank as an artificial ecosystem, in which biodegradation occurred at extremely higher rates compared to natural conditions [12]. Knowledge increased, but observations always maintained a qualitative or at most semi-quantitative character [13] [14]. It was thanks to Madoni, in 1994, that finally a biotic index was introduced, which enabled an accurate and concise description of activated sludge quality, correlating the microfauna with the process efficiency [15].
Since then, the sludge biotic index, which was initially proposed only for conventional activated sludge

purification plants, has been applied more and more widely, even in plants with different process schemes. The studies involved systems with pre-denitrification, membrane systems, UASB reactors (up-flow anaerobic sludge blanket), moving bed biofilm reactors (MBBRs), and included also industrial wastewater [16] [17] [18] [19] [20].
Nowadays, the study of microfauna exploits also omics sciences, which, therefore, consolidate and confirm the robustness of the observations that have made this management approach ubiquitous. This work aims to illustrate the role that these analyses can still play and the challenges that arise, also considering climate change, as well as the different composition of wastewater, which has transformed drastically over the last few decades [21].
Similarly to the microfauna, this work intends to describe the stages that have led to the knowledge of bacterial populations not only for biodegradation, but also for the onset of some process dysfunctions, especially in the secondary sedimentation phase [21]. [22] [24] Even in the case of bacteria, new biomolecular techniques have made it possible to deepen studies and, above all, obtain results in much shorter times [25] [26] [27] [28]: FISH (Fluorescent In Situ Hybridization) technique, based on 16S rRNA gene, allows to visualize specific target bacteria directly in the flocs, thus seeing their location and estimating their abundance. Beside filamentous bacteria, also microorganisms responsible for nutrient removal have been searched for. DNA extraction and high-throughput sequencing (HTS) has been applied increasingly, in order to obtain a picture of the microbial diversity and correlate genera and families (sometimes even species) with environmental parameters and process efficiency. Metagenomics enables the identification of the trophic role and the physiology of bacteria and, together with the metabolomics profile (quantification of extracellular metabolites) allows to detect the populations responsible for the degradation of organic substances and to postulate metabolic pathways.
Finally, the need to obtain pure cultures of bacteria (for deeper biochemical investigations) urged the setup and definition of more efficient cultivation procedures, able to overcome the inherent criticalities of viable-but-not-culturable microorganisms. Therefore, omics sciences have met traditional biology, giving rise to the so-called culturomics. Matrix-assisted laser desorption ionization time-of-flight (MALDI-TOF) mass spectrometry (MS) couples with enrichment and cultivation protocols as well as with genome sequencing. This branch opens up countless possibilities, but, currently, needs to more feasible and automated.

Reference

[1] Ardern, E., & Lockett, W. T. (1914). "Experiments on the Oxidation of Sewage without the Aid of Filters". Journal of the Society of Chemical Industry, 33, 523-539.

[2] Ardern, E., and Lockett, W. T., "Laboratory Tests for Ascertaining the Condition of Activated Sludge. Jour. Inst. Sew. Purif.y 212 (1936).

[3] Baines, S., Hawkes, H. A., Hewitt, C. H., & Jenkins, S. H. (1953). Protozoa as indicators in activated sludge treatment. Sewage and industrial Wastes, 1023-1033.

4] Curds, C. R., & Cockburn, A. (1970). Protozoa in biological sewage-treatment processes—II. Protozoa as indicators in the activated-sludge process. Water Research, 4(3), 237-249.

[5] Klimowicz, H. 1973: Microfauna of activated sludge. Part 3. The effect of physico-chemical factors on the occurrence of microfauna in the annual cycle Acta Hydrobiologica (Krakow): 152: 167-188

[6] Reid, R. (1969). Fluctuations in populations of 3 Vorticella species from an activated-sludge sewage plant. The Journal of Protozoology, 16(1), 103-111.

[7] Sydenham, D. H. J. (1971). A re-assessment of the relative importance of ciliates, rhizopods and rotatorians in the ecology of activated sludge. Hydrobiologia, 38(3), 553-563.

[8] Sudo, R., & Aiba, S. (1972). Growth rate of Aspidiscidae isolated from activated sludge. *Water Research*, *6*(2), 137-144.

[9] Tokuz, R. Y., & Eckenfelder Jr, W. W. (1979). The effect of inorganic salts on the activated sludge process performance. *Water research*, *13*(1), 99-104.

[10] Booth, R., Henry, J. G., & Prasad, D. (1980). The role of protozoa in high rate wastewater treatment systems. Water Quality Research Journal, 15(2), 187-201.

[11] Curds, C. R. (1982). The ecology and role of protozoa in aerobic sewage treatment processes. *Annual Reviews in Microbiology*, *36*(1), 27-28.

[12] Madoni, P., & Ghetti, P. F. (1981). The structure of ciliated protozoa communities in biological sewage-treatment plants. Hydrobiologia, 83, 207-215.

[13] Al-Shahwani, S. M., & Horan, N. J. (1991). The use of protozoa to indicate changes in the performance of activated sludge plants. Water Research, 25(6), 633-638.

[14] Esteban, G., Téllez, C., & Bautista, L. M. (1991). Dynamics of ciliated protozoa communities in activated-sludge process. *Water Research*, *25*(8), 967-972.

[15] Madoni, P. (1994). A sludge biotic index (SBI) for the evaluation of the biological performance of activated sludge plants based on the microfauna analysis. Water Research, 28(1), 67-75.

[16] Siqueira-Castro, I. C. V., Greinert-Goulart, J. A., Rossetto, R., Guimarães, J. R., & Franco, R. M. B. (2016). Ciliated protozoa community of a combined UASB–activated sludge system in southeastern Brazil. Environmental Science and Pollution Research, 23, 23804-23814.

[17] Canals, O., Massana, R., Riera, J. L., Balagué, V., & Salvadó, H. (2018). Microeukaryote community in a partial nitritation reactor prior to anammox and an insight into the potential of ciliates as performance bioindicators. *New biotechnology*, *43*, 3-12.

[18] dos Santos, L. A., Ferreira, V., Pereira, M. O., & Nicolau, A. (2014). Relationship between protozoan and metazoan communities and operation and performance parameters in a textile sewage activated sludge system. European Journal of Protistology, 50(4), 319-328.

[19] Pedrazzani, R., Menoni, L., Nembrini, S., Manili, L., & Bertanza, G. (2016). Suitability of Sludge Biotic Index (SBI), Sludge Index (SI) and filamentous bacteria analysis for assessing activated sludge process performance: the case of piggery slaughterhouse wastewater. Journal of Industrial Microbiology and Biotechnology, 43(7), 953-964.

[20] Kepec, M., Matoničkin Kepčija, R., Vlaičević, B., Kepec, S., & Gulin, V. (2021). The applicability of the Sludge Biotic Index in a facility treating sugar refinery effluents and municipal wastewater. Water environment research, 93(7), 1087-1096.

[21] de Celis, M., Belda, I., Ortiz-Álvarez, R., Arregui, L., Marquina, D., Serrano, S., & Santos, A. (2020). Tuning up microbiome analysis to monitor WWTPs' biological reactors functioning. Scientific Reports, 10(1), 4079.

[22] Eikelboom, D. H. (1975). Filamentous organisms observed in activated sludge. *Water research*, *9*(4), 365-388.

[23] Strom, P. F., & Jenkins, D. (1984). Identification and significance of filamentous microorganisms in activated sludge. *Journal (Water Pollution Control Federation)*, 449-459.

[24] Jenkins, D., Richard, M. G., & Daigger, G. T. (2003). *Manual on the causes and control of activated sludge bulking, foaming, and other solids separation problems*. Crc Press.

[25] Abbà, A., Collivignarelli, M. C., Manenti, S., Pedrazzani, R., Todeschini, S., & Bertanza, G. (2017). Rheology

and microbiology of sludge from a thermophilic aerobic membrane reactor. *Journal of Chemistry*, *2017*.

[26] Wang, J., Ju, F., Yu, P., Lou, J., Jiang, M., Zhang, H., & Lu, H. (2024). Metabolomics-based estimation of activated sludge microbial composition and prediction of filamentous bulking. *Water Research*, 12180

[27] Bertanza, G., Menoni, L., Capoferri, G. U., & Pedrazzani, R. (2020). Promoting biological phosphorus removal in a full scale pre-denitrification wastewater treatment plant. *Journal of environmental management*, *254*, 109803.

[28] Zhang, Y., & Zhang, T. (2023). Culturing the uncultured microbial majority in activated sludge: a critical review. *Critical Reviews in Environmental Science and Technology*, *53*(5), 601-624.

Title: Experimental tests for acid flue gas emissions treatment in industrial applications.

Authors: Marco Ravina[1], Edoardo Marotta*[1], Giorgia Piccirillo[1], Alberto Cerutti[1], Giovanna Zanetti[1], Camila Mori de Oliveira[1], Barbara Ruffino[1], Deborah Panepinto[1], Paola Marini[1], Mariachiara Zanetti[1].

[1] Department of Environment, Land and Infrastructure Engineering, Politecnico di Torino, Corso Duca degli Abruzzi 24, 10129 Turin, Italy, edoardo.marotta@polito.it

Keyword(s): acid gas; alkaline sorbent; dry injection; gas scrubbing, hydrated lime; gas adsorption.

Abstract

Removal of acid gases from exhaust emissions of industrial applications (SO_x, HCl, HF) still represents a challenge for many sectors, in particular for waste-to-energy plants. New and existing installations must comply with even tighter emission requirements as new regulations are implemented. Typically, these industrial facilities employ wet or dry scrubbing technologies for compliance. In dry absorption processes, the solid reagent is injected counter-current to the gas in a reaction chamber that allows for optimal contact between the phases. Efficiency is influenced by the specific surface area of the solid (m^2 kg^{-1} reagent), by the degree to which it is mixed with the gas, the concentration of the gas to be adsorbed, the temperature and humidity of the flow and the concentration of the reagent, usually expressed in terms of stoichiometric ratio. In the case of carbonaceous sorbents (lime-based), the optimum operating temperature is around 140 - 150°C. As an alternative to using lime, sodium bicarbonate ($NaHCO_3$) can be used as an adsorbent agent. The optimum performance of this reagent is observed at temperatures around 170 - 180°C. Sodium bicarbonate has higher collection efficiency than lime, but it is more expensive.

After reacting, solid sorbents can be separated from the flue gas together with the dust particles via a fabric filter. The formation of a filter cake is necessary for the neutralization process, as it influences the retention time of the additive and, hence, the contact time of additive and pollutant in the flue gas. Recently, new formulation of calcium and sodium-based sorbents have been investigated. Hence, the design and development of accurate systems for the experimental characterization of these material is needed.

The object of this study was the characterization of solid sorbents for hydrochloric acid neutralization. The characterisation consisted in experimental tests for 1) the characterization of the sorbents, and 2) the calculation of adsorption capacity. Four different samples were considered, two of hydrated lime (samples C1 and C2) and two of sodium bicarbonate (samples C3 and C4). All samples were provided by industrial partners, except for C4 that was commercial sodium bicarbonate.

Adsorption tests were carried out using an experimental test bench, designed in the laboratory, with the aim of simulating the temperature, pressure and flue gas velocity conditions found in a Duct Sorbent Injection (DSI) configuration (Figure 1) [1]. Sorbent samples were put in contact with a mixture of nitrogen and hydrochloric acid (500 ppm), and measuring the concentration of chlorides dissolved in a downstream absorber using an ion chromatograph. The amount of chlorine retained by the sample, i.e. the adsorption capacity, was calculated assuming a plug-flow system model. Adsorption capacities were tested at 150°C. These tests showed that sodium-based sorbents showed up to 15% higher sorption capacity than lime-based sorbents. Important differences were also found among samples of the same type (e.g. C1 vs. C2).

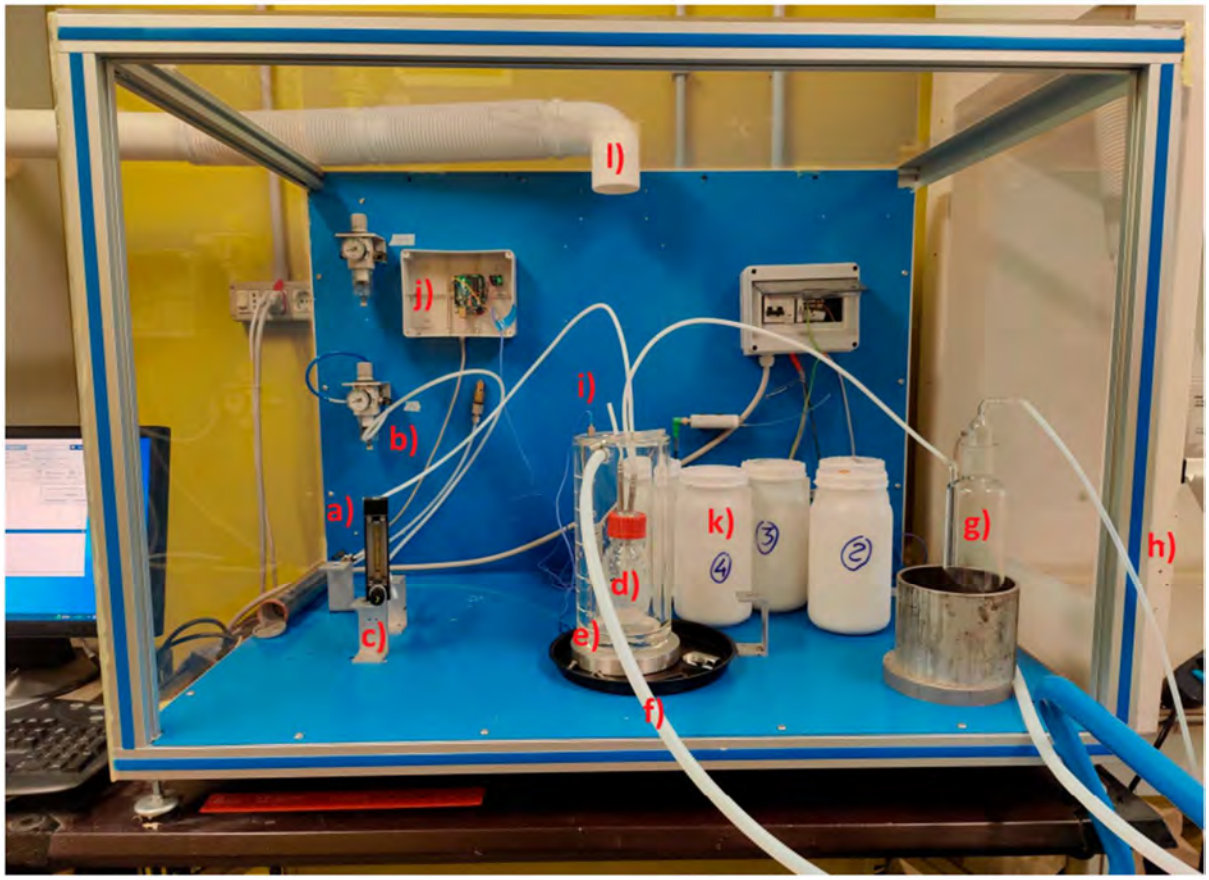

Figure 1. Photo of the experimental system: (a) HCl input line; (b) N2 input line; (c) Flowmeter; (d) Reactor, (e) jacketed beaker; (f) Thermo-conditioning circuit; (g) Water absorber; (h) vent line; (i) thermocouple; (j) Arduino device; (k) sorbent samples; (l) air extraction to ventilated hood [1].

Sorbent materials were also subjected to additional tests for their chemical-physical characterisation, i.e. analyses with scanning electron microscope (SEM, Figure 2), X-ray diffraction (XRD), inductively coupled plasma mass spectrometry (ICP-MS) and BET analyses with a porosimeter. SEM analyses identified hydrated lime samples composed of coarse elements, an intermediate fraction and a fine fraction, which were distributed homogeneously in space. The bicarbonate samples visually revealed the presence of coarse and intermediate elements (no fine fraction), which appeared more heterogeneously arranged in space.
X-ray diffraction analyses enabled a quantitative or semi-quantitative analysis of the composition of the samples (Rietveld method). XRD analyses showed that both lime samples consisted mainly of calcium hydroxide ($Ca(OH)_2$). In addition, calcium carbonate ($CaCO_3$) was found in C1 and C2, to an amount of 10% and 18% w/w respectively. This component probably represents the portion not converted during the calcination process. In sample C2, the presence of dolomite ($CaCO_3 \cdot MgCO_3$) and magnesium oxide (MgO) was found. The presence of magnesium in the form of magnesium oxide or magnesium hydroxide ($Mg(OH)_2$) depends on the different hydration modes. C3 and C4 were found to be entirely composed of sodium bicarbonate ($NaHCO_3$).

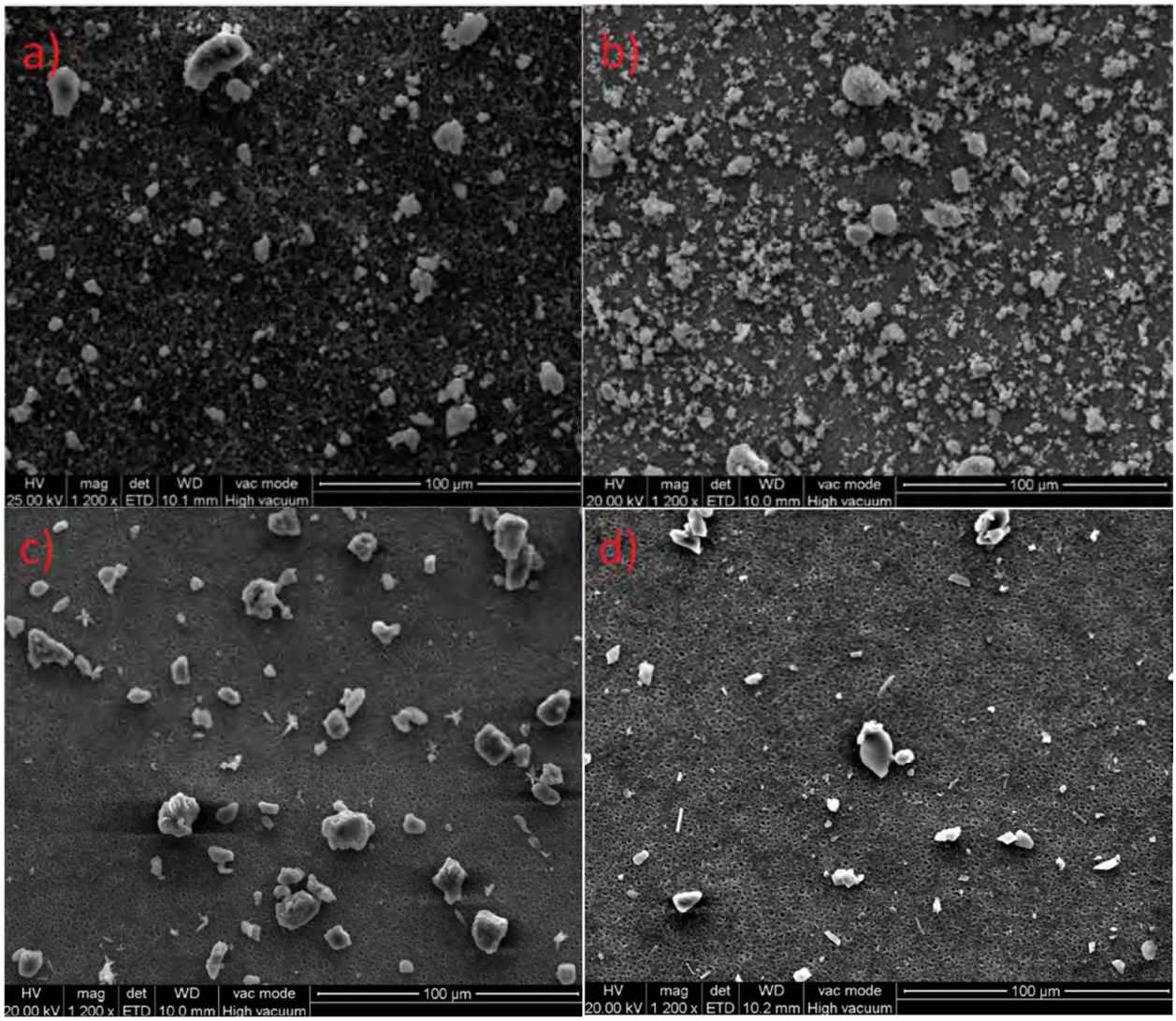

Figure 4. Scanning electronic microscopy (SEM) pictures of Sample C1 (a), Sample C2 (b), Sample C3 (c), and Sample C4 (d).

ICP-MS analyses provided a quantitative composition of single elements contained in the samples. Lime-based samples showed dominating percentages of calcium. Sample C2 also contained around 8% of magnesium. The composition of samples C3 and C4 was confirmed to be mostly sodium.
BET analysis was conducted with a porosimeter and allowed determining the specific surface area and porosity values of each sample. Sample C1 showed specific surface area and porosity values approximately four times higher than other samples.
Finally, tests were conducted on the sorbent samples after the reaction, to investigate the reaction products. An amount of 1 g of reacted sample was dissolved in ultrapure water during prolonged stirring, then the concentration of chlorides was measured. These tests showed that, except for C4, the measured chlorine mass values were lower than the expected. This is probably due to an incomplete dissolution of the reacted chlorine.
The results of the present study showed that a combination of properties, i.e. specific surface area, reactivity, favourable thermodynamic conditions, particle size, affect the adsorption capacity of solid

sorbents with respect to acid components in the flue gas. The good adsorption capacity of C1 is probably due to its high specific surface area, whereas that of C3 is more related to the higher reactivity. In order to achieve better abatement efficiencies, it would be necessary to ensure more uniform grain sizes and avoid undesired components (e.g. the presence of unreacted carbonates). Conversely, agglomeration of fine particles may have adversely affected the performance of sorbents.

References

[1] Ravina, M.; Marotta, E.; Cerutti, A.; Zanetti, G.; Ruffino, B.; Panepinto, D.; Zanetti, M. Evaluation of Ca-Based Sorbents for Gaseous HCl Emissions Adsorption. Sustainability 2023, 15, 10882, doi:10.3390/su151410882.

Title: Integration of electrochemical processes with the algae-activated sludge living membrane bioreactor for wastewater treatment

Author(s): Mary Vermi Aizza Corpuz*[1], Vincenzo Belgiorno[1], Kwang-ho Choo[2], Vincenzo Naddeo[1]

[1] *Sanitary and Environmental Engineering Division (SEED), Department of Civil Engineering, University of Salerno, Fisciano 84084(SA), Italy*
[2] *Department of Environmental Engineering, Kyungpook National University, 80 Daehak-ro, Buk-gu, Daegu 41566, Republic of Korea*

Keyword(s): algae for wastewater treatment, membrane fouling, electrochemical

Abstract
This study aimed to evaluate the efficiency of an electrochemically enhanced algae-activated sludge living membrane bioreactor (e-AAS-LMBR) in terms of wastewater treatment and membrane fouling alleviation. In this electro bioreactor, the biofilm layer, formed due to the of deposition of substances from the wastewater, serves as the membrane material. This biological layer, called Living Membrane® (LM), is encased between two coarse pore size support materials. The study also aimed to determine the effect of the application of electric field to the formation of the LM layer, which is composed of substances from the activated sludge and from the algae. The reactor's performance was compared to that of the algae-activated sludge LMBR (AAS-LMBR) (without applied electric field). The intermittent application of 0.5 mA/cm^2 in the e-AAS-LMBR led to the formation of a more stable LM layer compared to that of the AAS-LMBR, as seen in the lower permeate turbidity values. Significant increases in nitrogen and phosphorus removals in the e-AAS-LMBR were observed, which may be attributed to the synergistic effects of the algae's nutrient uptake, and the electrochemical removal mechanisms. The application of electric current also aided the e-AAS-LMBR to achieve lower fouling precursors concentrations and lower fouling rates (average *dTMP/dt* in e-AAS-LMBR: 0.05 kPa/day; AAS-LMBR 1.01 kPa/day). The membrane fouling rate reduction coincided with the remarkable decrease in the concentration of transparent exopolymer particles (TEP), one of the fouling substances produced both by the activated sludge bacteria and the algae.

1. Introduction

The symbiotic relationship between algae and bacteria has been proven useful for wastewater treatment [1]. The activated sludge bacteria break down the organic matter in wastewater, resulting in nutrients and CO_2 as byproducts, which are then consumed by the algae for photosynthesis. The algae produce O_2 for the bacteria to use in the decomposition of organic matter in wastewater [2], [3]. The study of combined algae and activated sludge in membrane bioreactors (MBRs) for wastewater treatment has been shown to potentially reduce fouling [4], [5]. However, its application in self-forming dynamic membrane bioreactors, which utilize biofilms/fouling layer as membrane filter, is yet to be explored. In this study, the Living Membrane® (LM), which utilizes a biological layer that is enclosed between two coarse-size mesh [6], is investigated using the combined activated sludge and algae as biomass. This study aimed to evaluate the efficiency of the algae-activated sludge living membrane bioreactor (AAS-LMBR) in terms of wastewater treatment and membrane fouling alleviation. In addition, it aimed to probe the effect of application of electric field using the electrochemically enhanced algae-activated sludge living membrane bioreactor (e-AAS-LMBR).

2. Materials and Methods

The e-AAS-LMBR made use of a poly (methyl methacrylate) (PMMA) cylindrical tank, with a working volume of 19 L, and a LM module installed in the tank's center. The LM module utilized two 30 µm polyester (Dacron®) mesh (Saati SpA), which served as an internal chamber for the LM to form in and had an effective membrane filtration area of 0.021 m^2. Side and bottom diffusers were mounted to

provide aeration. Perforated concentric cylindrical stainless steel (SS) cathode (positioned around the module) and aluminum anode (nearer the tank walls) were placed 6 cm from each other and were connected to an external CPX400S 420 W DC power supply (Aim-TTI Instruments, UK). External cold white LED lights were placed outside the tank, with a photosynthetic photon flux density (PPFD) of 120 μmol/m^2·s. A 12 – 12h dark-light cycle was employed based on the natural circadian rhythm of algae [7].The AAS-LMBR was set-up similarly as the e-AAS-LMBR, without supplying power to the electrodes. The inoculum biomass was a combination of algae dispersion and activated sludge, with mixed liquor total suspended solids (ML-TSS) ratio of 1:5, based on previously reported investigations [4]. The activated sludge inoculum was collected from the recirculation line of the secondary clarifier of a municipal wastewater treatment plant in Salerno. *Chlorella vulgaris* (strain CCAP 211/11B) microalgae were pre-cultured according to the procedure of a former study [8]. Synthetic municipal wastewater was continuously fed at 6.4 mL/min to the reactors. Intermittent permeate extraction was applied according to the following cycle: 9 minutes filtration, and 1 minute backwashing. The permeate flux was kept constant at 30 L/m^2 h. A low current density of 0.5 mA/cm^2 was applied in the e-AAS-LMBR using the following cycle: 5 min ON/ 20 min OFF. Samples from the influent, mixed liquor, and effluent of the reactor were obtained to monitor the pollutant removal: chemical oxygen demand (COD), ammonium-nitrogen (NH_4-N), nitrate-nitrogen (NO_3-N), phosphate-phosphorus (PO_4-P) [9]. Mixed liquor samples were analyzed for *chlorophyll-a* content [10], total suspended solids (TSS), and volatile suspended solids (VSS) according to standard methods [9]. Transmembrane pressure was monitored using a pressure transducer (PX409-0-15VI, Omega, USA) connected to a datalogger (34972A LXI, Agilent, USA) and a computer. Permeate turbidity was monitored using a turbidimeter (Hach 2100N).

3. Results and Discussion

3.1 Biomass Growth and Formation of Living Membrane

The chlorophyll-a in the AAS-LMBR increased over time during the operation period (

Figure *1*). The lower relative chlorophyll-a and higher VSS in the e-AAS-LMBR implied that the growth of non-algae biomass was favored. On the other hand, the application of electric field maintained the chlorophyll-a content relatively constant in the e-AAS-LMBR.

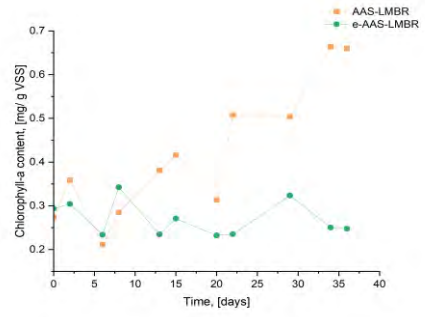

Figure 1. Monitoring of biomass growth in the AAS-LMBR and e-AAS-LMBR.

Since the reactors were operated at constant permeate flux, the turbidity values were used to determine the LM formation time. Turbidity of the e-AAS-LMBR reached below 5 NTU after 1 day of operation, which was faster than that observed in the AAS-LMBR (after 2 days). The application of electric field led to faster formation of the LM, due to larger flocs which could readily deposit on the mesh support. After this initial stage of LM formation, the average turbidity value in the e-AAS-LMBR was maintained at 0.34 ± 0.17 NTU, which was lower than the value obtained in the AAS-LMBR (1.17

± 0.47 NTU). The consistent low permeate turbidity implied that the application of the low current density resulted in a more stable LM layer in the e-AAS-LMBR throughout the operation.

3.2 Contaminant Removal Efficiencies.

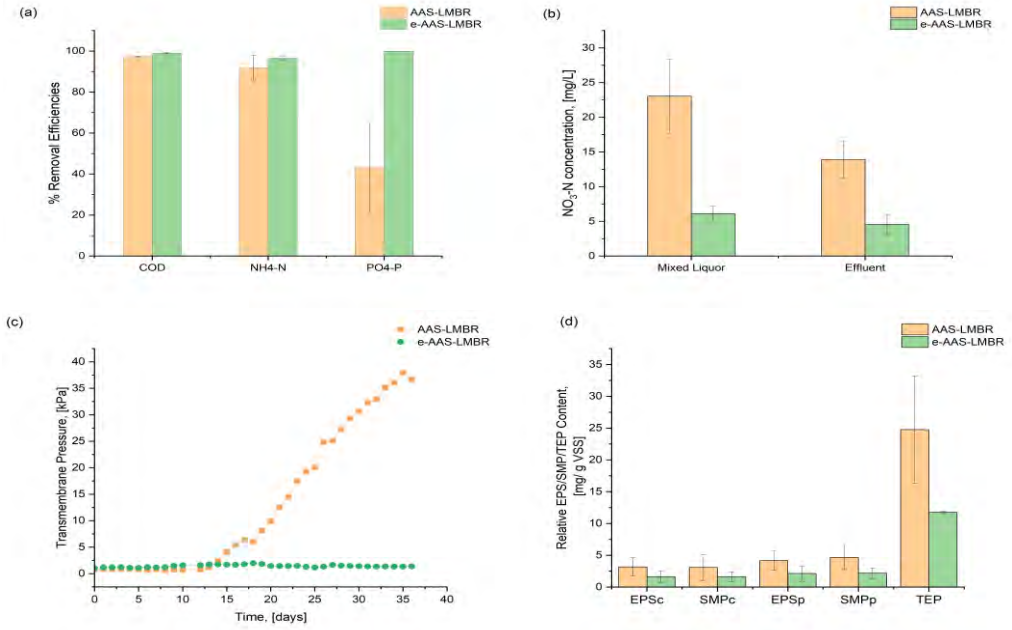

Figure 2. Mean chemical oxygen demand, ammonium-nitrogen, and phosphate-phosphorus removal efficiencies in the AAS-LMBR and e-AAS-LMBR, (b) nitrate-nitrogen concentrations in the reactor and effluent of the AAS-LMBR and e-AAS-LMBR, (c) profiles of the transmembrane pressure in the AAS-LMBR and e-AAS-LMBR, and (d) normalized concentrations of fouling precursors: carbohydrates content of EPS and SMP (EPSc, SMPc), protein content of EPS and SMP (ESPp, SMPp), and transparent exopolymer particles (TEP).

The mean %COD removal obtained in the e-AAS-LMBR was higher than that obtained in the AAS-LMBR by 1.42% (Figure 2a). The mean % removal of NH_4-N in the e-AAS-LMBR was higher by 4.65% than that achieved in the AAS-LMBR. In addition to the algae uptake of ammonium, the intermittent application of 0.5 mA/cm^2 in the e-AAS-LMBR may have potentially enhanced the oxygen uptake rate of ammonium oxidizing bacteria, as reported in previous studies [11], [12].Notably, mean concentrations of NO_3-N were lower by 73.53% in the mixed liquor and by 67.24% in the effluent of e-AAS-LMBR compared to those in the AAS-LMBR. This showed the improvement of removal of NO_3-N by the application of electric field in the e-AAS-LMBR. It is seen in Figure 2a that in the e-AAS-LMBR, the mean phosphorus removal (100%) from wastewater was higher than that obtained in the AAS-LMBR. In addition to the algae's phosphorus uptake [3] are the following removal mechanisms due to the applied electric current: *i)* enhanced activity of polyphosphate accumulating microorganisms, *ii)* precipitation of PO_4^{3-} with the electrogenerated Al^{3+} [13], and *iii)* adsorption of phosphorus to the Al $(OH)_3$ flocs, which were generated *in-situ.*

3.4 Membrane Fouling Control

The fouling rate in the e-AAS-LMBR was 0.05 kPa/day (average *dTMP/dt*), which was lower than that in the AAS-LMBR (1.01 kPa/day) (Figure 2c). This implied that the electric field has enhanced membrane fouling mitigation in the e-AAS-LMBR. Reduction of the concentrations of all the examined membrane fouling substances in the e-AAS-LMBR compared to that in the AAS-LMBR was observed (see Figure 2d). Different mechanisms also contributed to the reduction of fouling rate, notably electrocoagulation, electroosmosis, electrophoresis, and electrooxidation. The effect of quorum

quenching may also have been enhanced by the application of electric field. The very high EPSp in the AAS-LMBR may have contributed to faster increase in TMP in the AAS-LMBR vs e-AAS-LMBR. Less TEP in the mixed liquor of e-AAS-LMBR may have resulted in less sticky material tightly attached to the surface of the mesh, resulting in a lower fouling rate.

Conclusions

The synergistic effects of the algae's nutrient uptake, and the electrochemical processes resulted in enhanced NH_4-N, and PO_4-P removals. Higher TEP values, which were both produced by the activated sludge bacteria and algae, led to higher TMP values and fouling rates in the AAS-LMBR. The application of electric field reduced the TEP concentration in the e-AAS-LMBR, and consequently reduced fouling rates. A more stable LM layer (composed of algae and activated sludge) was produced by the application of electric current. These highlight the potential of e-AAS-LMBR as a sustainable wastewater treatment technology.

References

[1] X. Chen, Z. Hu, Y. Qi, C. Song, and G. Chen, "The interactions of algae-activated sludge symbiotic system and its effects on wastewater treatment and lipid accumulation," *Bioresour Technol*, vol. 292, no. 92, 2019, doi: 10.1016/j.biortech.2019.122017.

[2] H. J. Choi and S. M. Lee, "Effects of microalgae on the removal of nutrients from wastewater: Various concentrations of Chlorella vulgaris," *Environmental Engineering Research*, vol. 17, no. S1, pp. 3–8, 2012, doi: 10.4491/eer.2012.17.S1.S3.

[3] T. T. D. Nguyen *et al.*, "Co-culture of microalgae-activated sludge for wastewater treatment and biomass production: Exploring their role under different inoculation ratios," *Bioresour Technol*, vol. 314, no. April, 2020, doi: 10.1016/j.biortech.2020.123754.

[4] L. Sun, Y. Tian, J. Zhang, H. Li, C. Tang, and J. Li, "Wastewater treatment and membrane fouling with algal-activated sludge culture in a novel membrane bioreactor: Influence of inoculation ratios," *Chemical Engineering Journal*, vol. 343, pp. 455–459, Jul. 2018, doi: 10.1016/j.cej.2018.03.022.

[5] M. V. A. Corpuz *et al.*, "Wastewater treatment and fouling control in an electro algae-activated sludge membrane bioreactor," *Science of the Total Environment*, vol. 786, p. 147475, May 2021, doi: 10.1016/j.scitotenv.2021.147475.

[6] F. Castrogiovanni *et al.*, "Innovative encapsulated self-forming dynamic bio-membrane bioreactor (ESFDMBR) for efficient wastewater treatment and fouling control," *Science of the Total Environment*, vol. 805, p. 150296, May 2022, doi: 10.1016/j.scitotenv.2021.150296.

[7] C. S. Lee, S. A. Lee, S. R. Ko, H. M. Oh, and C. Y. Ahn, "Effects of photoperiod on nutrient removal, biomass production, and algal-bacterial population dynamics in lab-scale photobioreactors treating municipal wastewater," *Water Res*, vol. 68, pp. 680–691, 2015, doi: 10.1016/j.watres.2014.10.029.

[8] V. Senatore *et al.*, "Innovative membrane photobioreactor for sustainable CO2 capture and utilization," *Chemosphere*, vol. 273, Jun. 2021, doi: 10.1016/j.chemosphere.2021.129682.

[9] APAT and CNR-IRSA, "Metodi analitici per le acque. Manuali e Linee Guida 29/2003," 2003, *APAT Manuali e Linee Guida 29/2003*.

[10] APHA, AWWA, and WEF, "10200H. Chlorophyll," 2017, *American Public Helath Association, American Water Works Association and Water Environment Federation*.

[11] A. A. Battistelli *et al.*, "Application of low-density electric current to performance improvement of membrane bioreactor treating raw municipal wastewater," *International Journal of Environmental Science and Technology*, vol. 16, no. 8, pp. 3949–3960, 2019, doi: 10.1007/s13762-018-1949-7.

[12] T. J. Belli, A. A. Battistelli, R. E. Costa, C. M. S. Vidal, A. E. Schlegel, and F. R. Lapolli, "Evaluating the performance and membrane fouling of an electro-membrane bioreactor treating textile industrial wastewater," *International Journal of Environmental Science and Technology*, vol. 16, no. 11, pp. 6817–6826, May 2019, doi: 10.1007/s13762-019-02245-2.

[13] K. Bani-Melhem and E. Smith, "Grey water treatment by a continuous process of an electrocoagulation unit and a submerged membrane bioreactor system," *Chemical Engineering Journal*, vol. 198–199, pp. 201–210, May 2012, doi: 10.1016/j.cej.2012.05.065.

PARALLEL SESSION: B4

Wastewater treatment

Removal and control of emerging contaminants

Title: Fluorescence sensor enabled real-time monitoring of Contaminants of Emerging Concern (CEC) in reclaimed wastewater during Advanced Oxidation Processes (AOPs)

Author(s): Luigi Marino*[1], Erica Gagliano[2], Domenico Santoro[3], Paolo Roccaro[1]

[1] *Department of Civil Engineering and Architecture, University of Catania, Catania, Italy, luigi.marino@phd.unict.it, paolo.roccaro@unict.it*
[2] *Department of Civil, Chemical and Environmental Engineering, University of Genoa, Genoa, Italy, erica.gagliano@unige.it*
[3] *Department of Chemical and Biochemical Engineering, University of Western Ontario, London, Canada, dsantor@uwo.ca*

Keyword(s): real-time monitoring; fluorescence; wastewater reuse; contaminants of emerging concern; advanced oxidation processes;

Abstract

Contaminants of emerging concern (CEC) is a broad class of compounds that includes poly-perfluoroalkyl substances (PFAS), disinfection by-products (DBPs), pharmaceuticals, personal care products and more that has garnered more attention in recent years [1]. Indeed, numerous studies have demonstrated that CEC have high persistence in the environment, as well as negative impacts on both human health and wildlife [2], [3]. CEC are broadly detected at trace level (µg/L or ng/L) in many water matrices including surface water, groundwater, wastewater and drinking water, as shown by several studies. Wastewater effluents have been documented to be a significant source of CEC in the environment, since wastewater treatment plants (WWTPs) are generally designed for the removal of organic matter and suspended solids to meet regulation limits [4]. Therefore, there is the need to employ further advanced treatment stages to efficiently remove persistent contaminants [3]. Ozone and UV based AOPs have been recognized as effective technologies for the rapid degradation of CEC from water due to the production of highly reactive species, also in full-scale facilities [5], [6]. The lack of real-time monitoring systems of CEC in advanced treatment plants is a current key issue despite it is becoming crucial due to the introduction of new strict CEC requirements [7]. Typical analytical methods for CEC detection are expensive, time-consuming and do not allow the real-time control during the treatment process. Fluorescence spectroscopy emerged as an innovative surrogate parameter for CEC monitoring due to its cost-effectiveness and sensitivity [8]. However, real-time control may be still challenging to accomplish if samples are collected and then analyzed in lab. Moreover, acquisition and elaboration of excitation/emission matrices (EEMs) can take a long time. Improvements in technology have led to the development of an increasing number of sensors, allowing the online acquisition of fluorescence [9]. Several authors have reported promising applications of fluorescence sensors for monitoring DBPs, fecal contamination, dissolved organic matter in drinking water and wastewater as well [10], [11]. However, for the authors knowledge, there is still a lack of studies on the use of fluorescence sensors for in-situ and real-time monitoring of CEC during advanced treatments. Thus, the aim of this research was to employ a microbial/tryptophan-like fluorescence sensor to investigate the possibility of real-time monitoring of CEC at naturally occurring concentrations during UV and ozone based AOPs at pilot scale. Thus, the aim of this research was to employ a microbial/tryptophan-like fluorescence sensor to investigate the possibility of real-time monitoring of CEC at naturally occurring concentrations during UV and ozone based AOPs at pilot scale.

The AOP pilot plant operated downstream of two conventional WWTPs in a continuous-flow system having a capacity of 6 m^3/h. WW-1 and WW-2 are tertiary wastewater effluents used for agriculture reuse or aquifer recharge and were the inlet of the AOP pilot system. The treatment line consisted of an UV reactor and an oxidation with in-situ produced ozone. Hydrogen peroxide was dosed from a 35% (w/w) stock solution through a peristaltic pump. The following AOPs were investigated: O_3, O_3/H_2O_2 and UV/H_2O_2. Flowrates ranged from 0.3 to 6 m^3/h. A constant dose of H_2O_2 equal to 9 mg/L and 4 mg/L was used in WW-1 and WW-2 respectively. UV doses ranged from $\sim 150\ mJ/cm^2$ and $\sim 1600\ mJ/cm^2$, while ozone doses ranged from 2 to 9 mg/L. Samples of untreated and treated wastewater were taken in dark glass bottles with sodium thiosulfate for quenching the residual oxidant. Detailed information on CEC analysis are available in previously published literature [12]. Typical water quality parameter were obtained in situ. A Shimadzu UV-1800 spectrophotometer was used to obtain ultraviolet light absorbance. Fluorescence excitation/emission matrices (EEMs) were obtained with a Shimadzu RF-5301PC spectrophotometer and produced in Raman Units (RU) following the standardized procedure reported in previous work [13]. The peak-picking method was performed for the interpretation of EEMs. The fluorescence sensor was installed downstream of the system, being able to detect the fluorescence of both AOP influent and treated water, respectively before and after the dosing of reagents. The fluorescence sensor worked in conjunction with a Photometric Transmitter (PT) through a fiber optic cable, in turn connected to a computer for real-time data transfer of a log-file. Before starting the AOP tests an offline calibration of the sensor was performed on reference wastewater samples. Before starting the AOP tests an offline calibration of the sensor was performed on reference wastewater samples.
The real-time fluorescence data obtained with the sensor were validate by high correlations ($R^2 > 0.9$) with lab-scale fluorescence data. The online sensor showed excellent sensitivity to detect in real-time the fast degradation of microbial/tryptophan fluorescence caused by the release of •OH during the AOPs, despite high reactivity and short lifetime of •OH. Figure 1 shows as example the real-time monitoring of the O_3-AOPs in WW-2 through the microbial/tryptophan-like fluorescence sensor.

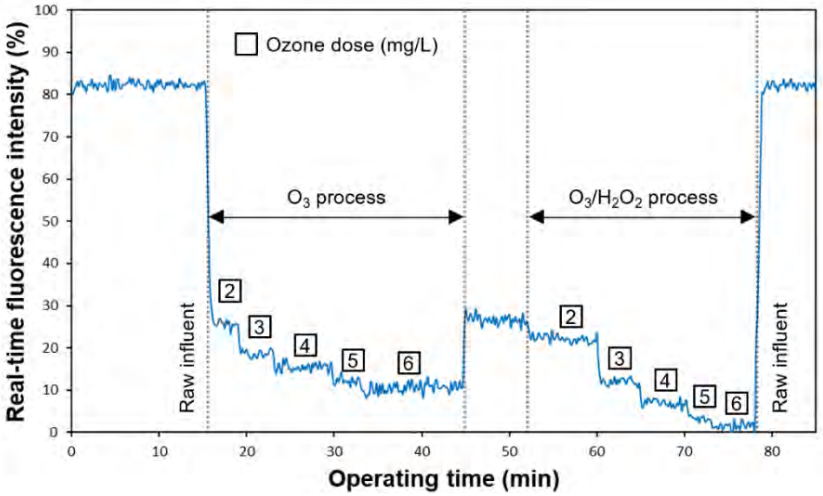

Figure 1. Real-time fluorescence trends recorded by the fluorescence sensor during O_3-AOPs in WW-2.

About 30 CEC were detected both in WW-1 and WW-2 samples, including pharmaceuticals (e.g., carbamazepine, diclofenac) and industrial compounds (e.g., BPA, PFAS). CEC removal occurred according to their reactivity with O_3 and •OH, oxidant doses and photo-susceptibility with UV. Removal efficiencies (REs) during ozonation in WW-1 ranged from 0% to 100%. In WW-2, ozonation resulted

slightly more efficient in reducing CEC (15%<RE<100%). O_3/H_2O_2 process did not really improved the CEC REs in WW-1, while it showed higher REs in WW-2 compared to ozonation. A higher •OH scavenging mechanism in WW-1 may be the cause of the differences in REs between WW-1 and WW-2. Indeed, the EEMs revealed the notable differences in effluent organic matter (EfOM) between the two wastewaters.

Assuming that CEC oxidation takes place simultaneously with microbial/tryptophan-like EfOM fraction, the removal of CEC was correlated with real-time fluorescence removal obtained with the online sensor. In general, high correlations were found between real-time fluorescence and CEC removals, developing linear models for UV/H_2O_2 process, linear and non-linear models for O_3-based AOPs. The real-time fluorescence was very accurate in predicting the removal of CEC having naturally occurring concentrations, different origin, different photo-susceptibility and reactivities with hydroxyl radical and ozone, in different wastewaters: $R^2 = 0.93$ for both O_3-AOPs in WW-1, $R^2 = 0.98$ and $R^2 = 0.84$ for O_3 and O_3/H_2O_2 processes respectively in WW-2, $R^2 = 0.90$ for UV/H_2O_2 in WW-1. As an example, in Figure 2 are showed the measured vs predicted CEC removals during O_3/H_2O_2 and UV/H_2O_2 processes in WW-1 using real-time fluorescence as surrogate parameter.

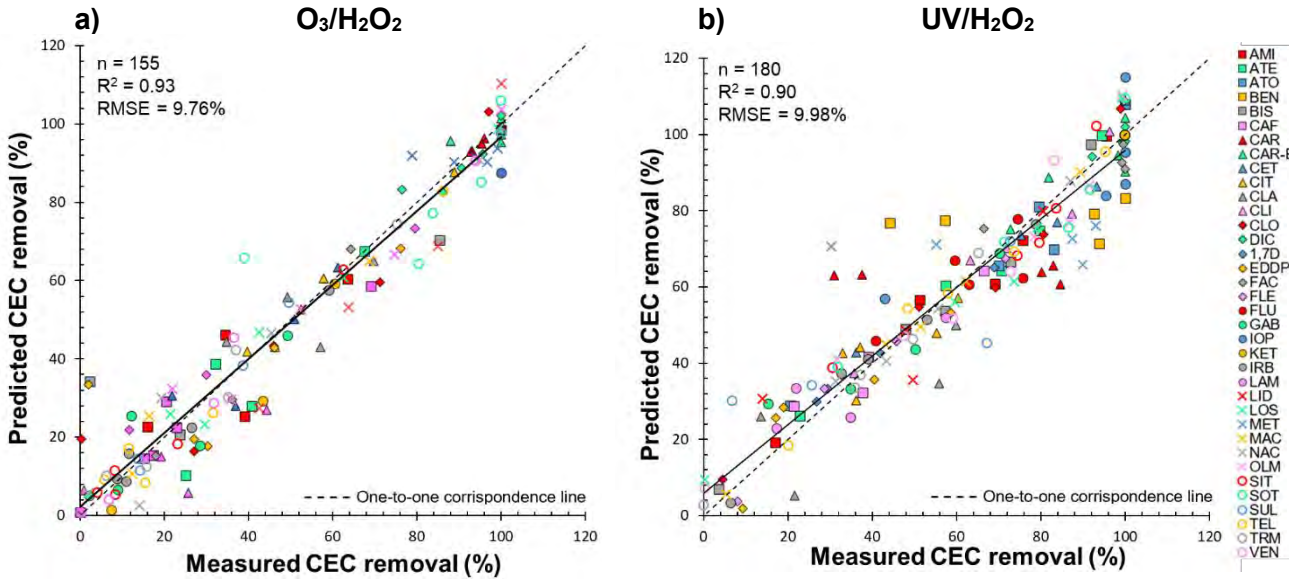

Figure 2. Measured versus predicted CEC removal during O_3/H_2O_2 (a) and UV/H_2O_2 (b) process through real-time fluorescence data.

From the results obtained in this study, the following conclusions can be summarized:

- In WW-1 and WW-2, the ozone-AOPs demonstrated high removal efficiencies for micropollutants. Moreover, in WW-1, the UV/H_2O_2 process showed higher removal efficiencies than ozone-AOPs. According to these results, these AOPs are strongly advised for reducing a broad range of CEC in wastewater effluents;
- Although processes involving •OH are very fast, the fluorescence detected in real-time showed higher sensitivity than lab-scale fluorescence, highlighting the importance of the online and in-situ monitoring of AOPs;
- Predictive models of CEC removal based on real-time fluorescence data resulted very accurate for all AOPs and wastewaters tested in this study, suggesting that real-time fluorescence spectroscopy could provide an excellent tool to monitor a wide class of different CEC in different

water matrices.

Acknowledgement - This study was partially supported by the European Union (NextGeneration EU), through the MUR-PNRR project SAMOTHRACE (ECS00000022).

References

[1] J. C. G. Sousa, A. R. Ribeiro, M. O. Barbosa, M. F. R. Pereira, and A. M. T. Silva, "A review on environmental monitoring of water organic pollutants identified by EU guidelines," *Journal of Hazardous Materials*, vol. 344, pp. 146–162, Feb. 2018, doi: 10.1016/j.jhazmat.2017.09.058.

[2] H. Brunn, G. Arnold, W. Körner, G. Rippen, K. G. Steinhäuser, and I. Valentin, "PFAS: forever chemicals—persistent, bioaccumulative and mobile. Reviewing the status and the need for their phase out and remediation of contaminated sites," *Environmental Sciences Europe 2023 35:1*, vol. 35, no. 1, pp. 1–50, Mar. 2023, doi: 10.1186/S12302-023-00721-8.

[3] Y. Yang, Y. S. Ok, K. H. Kim, E. E. Kwon, and Y. F. Tsang, "Occurrences and removal of pharmaceuticals and personal care products (PPCPs) in drinking water and water/sewage treatment plants: A review," *Science of the Total Environment*, vol. 596–597, pp. 303–320, Oct. 2017, doi: 10.1016/J.SCITOTENV.2017.04.102.

[4] E. Ben Mordechay, V. Mordehay, J. Tarchitzky, and B. Chefetz, "Fate of contaminants of emerging concern in the reclaimed wastewater-soil-plant continuum," *Science of The Total Environment*, vol. 822, p. 153574, May 2022, doi: 10.1016/j.scitotenv.2022.153574.

[5] C. Dong, W. Fang, Q. Yi, and J. Zhang, "A comprehensive review on reactive oxygen species (ROS) in advanced oxidation processes (AOPs)," *Chemosphere*, pp. 136205–136205, Dec. 2022, doi: 10.1016/j.chemosphere.2022.136205.

[6] D. B. Miklos, C. Remy, M. Jekel, K. G. Linden, J. E. Drewes, and U. Hübner, "Evaluation of advanced oxidation processes for water and wastewater treatment – A critical review," *Water Research*, vol. 139, pp. 118–131, Aug. 2018, doi: 10.1016/J.WATRES.2018.03.042.

[7] E. Deniere *et al.*, "Status and needs for online control of tertiary ozone-based water treatment: use of surrogate correlation models for removal of trace organic contaminants," *Reviews in Environmental Science and Bio/Technology 2021 20:2*, vol. 20, no. 2, pp. 297–331, Apr. 2021, doi: 10.1007/S11157-021-09574-0.

[8] G. V. Korshin, M. Sgroi, and H. Ratnaweera, "Spectroscopic surrogates for real time monitoring of water quality in wastewater treatment and water reuse," *Current Opinion in Environmental Science and Health*, vol. 2, pp. 12–19, Apr. 2018, doi: 10.1016/j.coesh.2017.11.003.

[9] E. M. Carstea, C. L. Popa, A. Baker, and J. Bridgeman, "In situ fluorescence measurements of dissolved organic matter: A review," *Science of The Total Environment*, vol. 699, pp. 134361–134361, Jan. 2020, doi: 10.1016/J.SCITOTENV.2019.134361.

[10] E. Bedell, O. Harmon, K. Fankhauser, Z. Shivers, and E. Thomas, "A continuous, in-situ, near-time fluorescence sensor coupled with a machine learning model for detection of fecal contamination risk in drinking water: Design, characterization and field validation," *Water Research*, vol. 220, Jul. 2022, doi: 10.1016/J.WATRES.2022.118644.

[11] K. Khamis, C. Bradley, H. J. Gunter, G. Basevi, R. Stevens, and D. M. Hannah, "Calibration of an in-situ fluorescence-based sensor platform for reliable BOD5 measurement in wastewater," *Water Science and Technology*, vol. 83, no. 12, pp. 3075–3091, Jun. 2021, doi: 10.2166/WST.2021.197.

[12] M. Sgroi, T. Anumol, P. Roccaro, F. G. A. Vagliasindi, and S. A. Snyder, "Modeling emerging contaminants breakthrough in packed bed adsorption columns by UV absorbance and fluorescing components of dissolved organic matter," *Water Research*, vol. 145, pp. 667–677, Nov. 2018, doi: 10.1016/j.watres.2018.09.018.

[13] M. Sgroi *et al.*, "Use of fluorescence EEM to monitor the removal of emerging contaminants in full scale wastewater treatment plants," *Journal of Hazardous Materials*, vol. 323, pp. 367–376, Feb. 2017, doi: 10.1016/j.jhazmat.2016.05.035.

Title: Spent Coffee Ground Biochar for enhanced removal of very small microplastics (1-5 µm) from polluted water: a quaternary treatment approach

Author(s): Alessia Torboli*[1], Paola Foladori[2]

[1] *C3A Center Agriculture Food Environment, University of Trento, Via Edmund Mach 1, 38098 TN, Italy, alessia.torboli@unitn.it*
[2] *Department of Civil, Environmental and Mechanical Engineering, University of Trento, via Mesiano 77, 38123 Trento, Italy, paola.foladori@unitn.it*

Keyword(s): biochar-based materials; microplastics removal; waste upcycle; wastewater treatment.

1. Introduction

Incessant production of plastics in modern times have led to the accumulation, fragmentation, and subsequent transformation of these synthetic polymers into microplastic waste. Microplastics (MP) (5 mm - 1 µm) are commonly present in municipal wastewater [1] where they enter through various sources connected to the sewage network and can be subsequently discharged to receiving surface water bodies if not properly removed, eventually entering the aquatic systems [2]. The effective control of microplastic pollution is contingent upon the development of versatile and sustainable removal technologies that can be applied on a large scale. Various technologies have been employed to remove microplastics from polluted waters, including but not limited to filtration, coagulation, and adsorption. Among these, adsorption has recently aroused great interest in pollutant removal, with biochar derived from renewable biomass emerging as one of the most promising adsorbents. Biochar is regarded as a low-cost and eco-friendly substitute for activated carbon, serving as a valuable by-product for the safe disposal of various feedstock materials, and its unique porous structure and active vacant sites offer extensive potential for the immobilisation of microplastic spheres [3].
The present study investigates a new, promising and sustainable approach for the remediation of MPs from polluted water using biochar derived from spent coffee grounds (SCG). A column filled with SCG biochar underwent filtration tests with short contact time, ideally suited as a quaternary treatment of wastewater. To assess the efficacy of biochar in removing MPs, the influence of various factors was investigated, including MP size, presence of solids in the aqueous matrix, and capacity for accumulation over time. Micrometric scale polystyrene particles ranging from 1-5 µm were used in the experimental tests as they represent the very small size range that tends to escape conventional wastewater treatments at full-scale, primarily due to limited settleability and surface interactions. To overcome the difficulties of detecting small MPs with size around 1 µm naturally present in polluted water, traceable microspheres were spiked into water and secondary-treated sewage effluent, and subsequently enumerated with flow cytometry (FCM).

2. Characterisation of SCG biochar

Spent coffee grounds underwent pyrolysis in a N_2-purged vertical furnace across a temperature range of 300-550°C, with a 1-h holding time. These grounds, inherently characterised by high purity, demonstrated a high potential for the production of biochar, yielding an average of 30%. Microscopically, the surface of SCGs granules appears coarse and homogeneous (Figure 1A), showcasing a uniform and well-graded structure. Instead, the SCG-derived biochar displayed a sponge-like morphology with enhanced porosity (Figure 1B). Active sites of the porous structure form via the rapid release of volatile substances from the initial biomass, with higher pyrolysis temperatures consequently enhancing carbon content, aromaticity, and surface area.

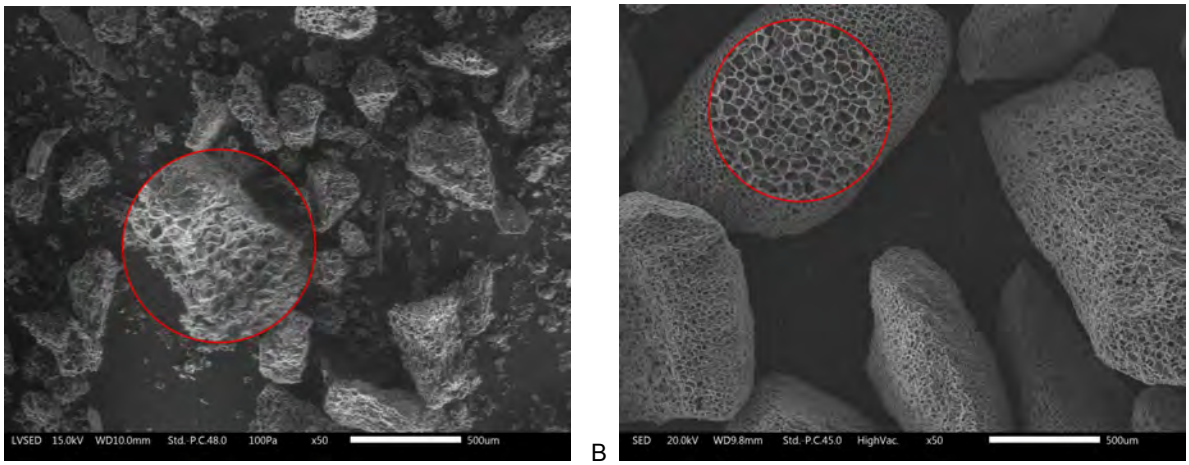

Figure 1. SED images of (A) unheated SCG at 50x magnification and (B) SCG biochar (450°C, N_2) at 50x.

3. *Filtration column tests* with SCG biochar

A layer of biochar with depth of 40 mm was packed into a cylindrical column measuring 80 mm in length and 18 mm in diameter. Biochar was positioned between two 20 mm-layers of sand to avoid loss of biochar, which has a grain size larger than 125 µm. To account for sand interference, a second column made up of 80 mm of sand was used in parallel as a control. At the end of the tests, biochar was extracted from the column and samples underwent scanning electron microscope (SEM) imaging.

3.1. Influence of MP size

Working suspensions of polystyrene microspheres (Fluoro Max microplastics, 1% solid, Thermo Fisher, USA) ranging in size from 1 to 5 µm in deionized water were prepared (Table 1). Aliquots of these suspensions were systematically injected into both biochar and sand filtration columns. Effluents were collected over time and MPs were subsequently enumerated by FCM.

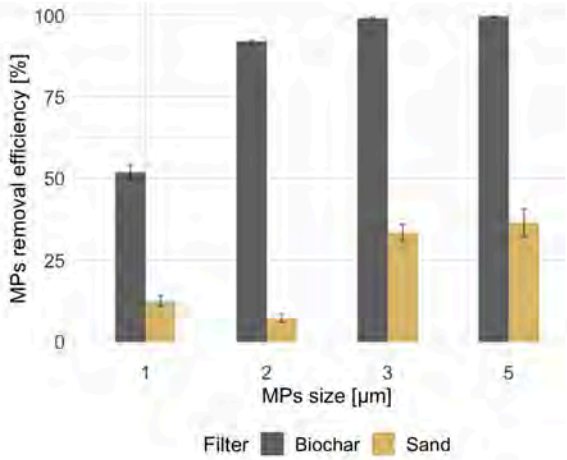

Table 1. MP concentrations in effluents from biochar and sand filter as a function of MP size

MP size	MPs applied	MPs in the effluent	
		Biochar filter	Sand filter
[µm]	[No. part/µL]	[No. part/µL]	[No. part/µL]
1	2488	1197 ± 59	2174 ± 42
2	1967	156 ± 2.6	1826 ± 24
3	546	4.5 ± 0.4	364 ± 13
5	264	0.9 ± 0.1	191 ± 35

Figure 2. Removal efficiency of MPs in biochar and sand filtration columns as a function of MP size (1, 2, 3, 5 µm).

SCG biochar demonstrates notably greater effectiveness in removing MPs compared to the sand filter (Figure 2). Larger MPs are easily trapped within the biochar pores, leading to a high removal capacity (92.1%, 99.2% e 99.7% for MPs sized at 2, 3, 5 µm, respectively). Conversely, 1 µm-sized MPs prove more demanding to remove (51.2% efficiency), posing significant challenges to filtration systems.

3.2. 1-µm MP removal from secondary-treated effluent

The most challenging MPs with a fixed size of 1 µm were suspended in both deionized water (DW) and secondary-treated wastewater (WW) at a constant concentration of 2500 particles/µL. The two filters (biochar and sand filters) were subjected to repeated application of these MP suspensions to assess their efficacy in retaining 1-µm MPs in complex water matrices. Remarkably, the biochar filter demonstrated a slight enhancement in filtration capacity when exposed to treated wastewater (Figure 3). This can be attributed to aggregation, wherein the 1-µm MPs tend to adhere or be entrapped on other solids present in the matrix. This aggregation facilitates the removal of MPs, thereby improving overall filtration efficiency.

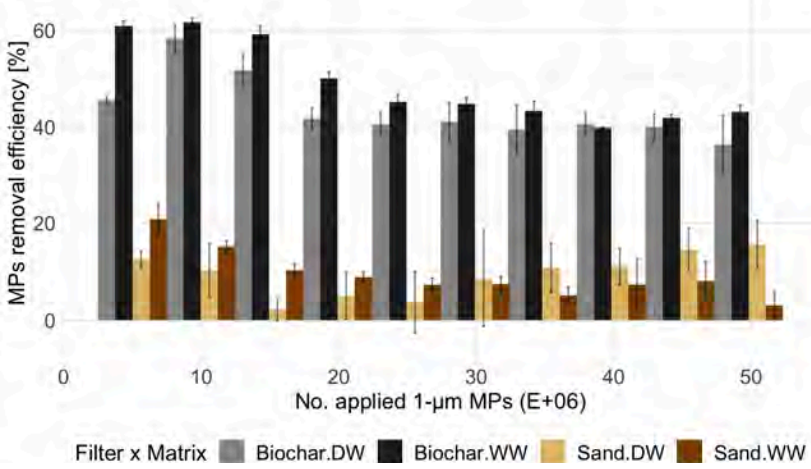

Figure 3. 1-µm MPs removal efficiency of biochar and sand filter as a function of the water matrix.

3.3. 1-µm MP cumulative retention

The assessment of cumulative 1-µm MPs retention by biochar and sand filtration columns bridges lab findings to real-scale applications. The accumulation capacity per gram of biochar rises steadily with applied particles (Figure 4), showing no plateau or saturation, and most importantly, no MP desorption over time. Notably, the sharper slope in the latter segment of the biochar curve indicates enhanced efficacy of the biochar filter in trapping MPs in presence of the wastewater matrix, underscoring its promising applicability in wastewater remediation.

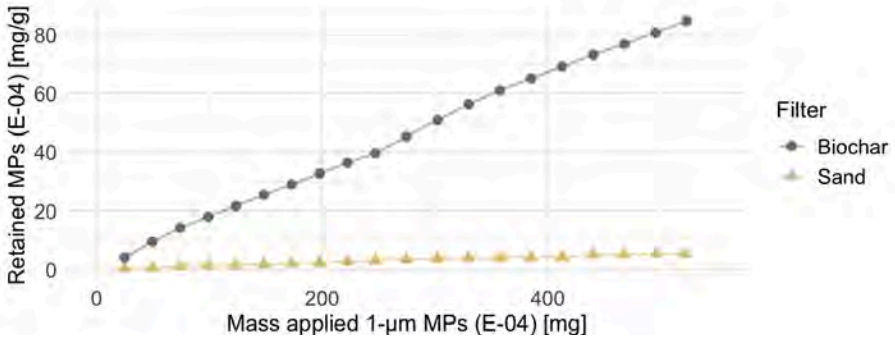

Figure 4. 1-µm MPs cumulative retention per gram of biochar and per gram of sand.

4. Microscopic observation of the adsorbed MPs

MPs were found to be both trapped within the porous structure of biochar (Figure 5A), entangled by flaky biochar particles which exhibited colloidal properties (Figure 5B) and stuck in the gaps between the filter particles (Figure 5C, D), further contributing to their immobilisation.

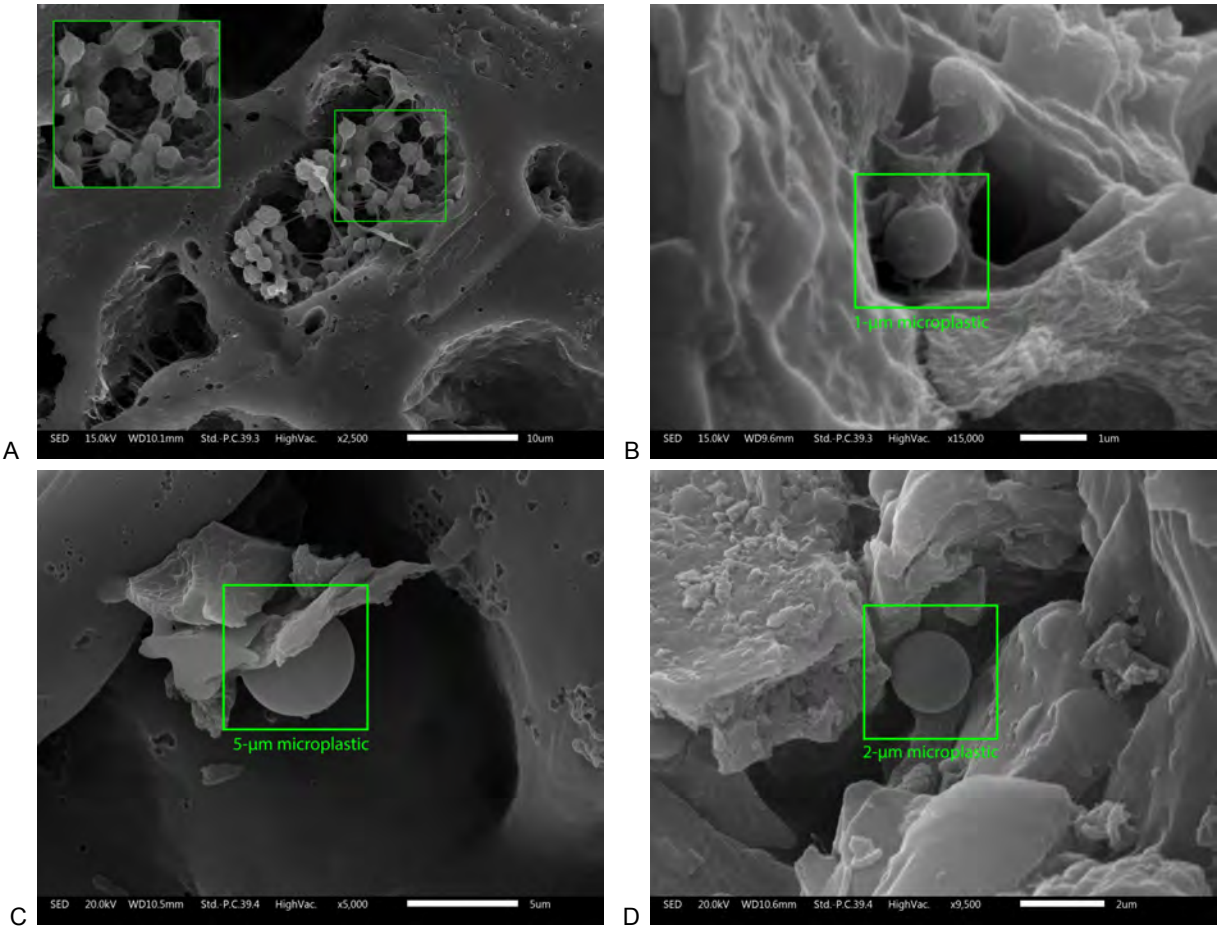

Figure 5. SED images of SCG biochar with microplastics (A) trapped, (B) entangled and (C,D) stuck.

5. Conclusions

The substantial accumulation capacity of MPs per gram of biochar highlights its potential for large-scale application in quaternary treatment of wastewater. Presently, there is limited research on MP concentration in influent and effluent wastewater, especially in the 1–10 µm range, which shows extremely large variation compared to MPs with size from 10 µm to 1 mm [4]. In this study, biochar demonstrated its ability to accumulate at least 8.5 mg MPs/kg biochar, equivalent to 1E+10 1-µm particles. These findings collectively highlight the potential of SCG biochar as a sustainable, cost-effective technology for remediating small microplastics from wastewater.

References

[1] Monira S., Roychand R., Hai F.I., Bhuiyan M., Dhar B.R., Pramanik B.K., (2023b). Nano and microplastics occurrence in wastewater treatment plants: A comprehensive understanding of microplastics fragmentation and their removal. Chemosphere 334, 139011.
[2] Zhao H., Huang X., Wang L., Zhao X., Yan F., Yang Y., Li G., Gao P., Ji P., (2022). Removal of polystyrene nanoplastics from aqueous solutions using a novel magnetic material: Adsorbability, mechanism, and reusability. Chem. Eng. J. 430, 133122.
[3] Wang Z., Sedighi M., & Lea-Langton A. (2020). Filtration of microplastic spheres by biochar: Removal efficiency and immobilisation mechanisms. Water Research, 184, 116165.
[4] Koutnik V. S., Alkidim S., Leonard J., DePrima F., Cao S., Hoek E. M. V., & Mohanty S. K. (2021). Unaccounted Microplastics in Wastewater Sludge: Where Do They Go? ACS ES&T Water, 1, 5.

Title: Lagoons: Quaternary Treatment of Micropollutants in WWTPs - Case Study of UWWTD Compliance of Cabezo Beaza WWTP

Authors: Lissette Díaz-Gamboa[1], Sofía Martínez-López[2], Luis Miguel Ayuso-García[2], Agustín Lahora[3] and Isabel Martínez-Alcalá*[1]

[1] Research Department, Universidad Católica de Murcia (UCAM), Av. de los Jerónimos, 135, 30107 Murcia, Spain pldiaz@ucam.edu; immartinezalcala@ucam.edu
[2] Environmental Department, National Technological Centre for the Food and Canning Industry (CTNC), C. Concordia, S/N, 30500 Murcia, Spain; sofiamartinez@ctnc.es; ayuso@ctnc.eu
[3] Regional Entity for Sanitation and Wastewater Treatment in the Region of Murcia (ESAMUR), C. Santiago Navarro, 4, 30100 Murcia, Spain agustin.lahora@esamur.com

Keywords: wastewater treatment; emerging pollutants; quaternary treatment; UWWTD, 91/271/EEC.

Abstract

The utilization of reclaimed water for agricultural purposes represents a sustainable approach to addressing water scarcity, particularly in arid and semi-arid regions. However, it is of paramount importance to ensure compliance with the stringent water quality standards in place to safeguard public health and the environment [1]. Advanced wastewater treatment processes in wastewater treatment plants (WWTPs) play a crucial role in meeting these standards. The increasing detection of micropollutants such as pharmaceuticals and pesticides in treated effluent is raising environmental and health concerns. European regulations, such as the new Urban Wastewater Treatment Directive (UWWTD), which was updated in 2024 from Directive 91/271/EEC, requires an 80% reduction in micropollutants, necessitating the implementation of quaternary treatment processes [2]. Moreover, the UWWTD specifies the rigorous monitoring of twelve pivotal substances (amisulpride, carbamazepine, citalopram, clarithromycin, diclofenac, hydrochlorothiazide, metoprolol, venlafaxine, benzotriazole, candesartan, irbesartan and methylbenzotriazole, including 4-methylbenzotriazole and 5-methylbenzotriazole). This assessment requires analysis of at least six of these substances and the calculation of their average removal percentages to confirm adherence to the minimum required reduction threshold of 80% [2]. Consequently, this study aims to evaluate the implementation of storage lagoons as a quaternary treatment method at the Cabezo Beaza WWTP, with the purpose of assessing effluent quality to ensure compliance with the current regulatory standards. The Cabezo Beaza WWTP (Figure 1) situated in a water-stressed region (Murcia, Spain), serves as an exemplary case study due to its established treatment processes and integration of storage lagoons. Natural attenuation systems, like lagoons, lakes, and ponds, play a crucial role in reducing micropollutant concentrations through various physical, chemical, and biological processes. Grasping these mechanisms is essential for efficient micropollutant management within ecosystems [3], [4].

This study assessed micropollutants before and after the storage lagoon stage at Cabezo Beaza WWTP. This facility has a secondary treatment process employing conventional double-stage activated sludge. Following secondary treatment, the effluent is directed to two parallel-operating lagoons, with an average hydraulic retention time of 34 days. Subsequently, chlorination disinfection is applied to the lagoon effluents before its use in agricultural irrigation (Figure 1). Micropollutants were analysed using high-performance liquid chromatography and mass spectrometric detection (HPLC-MS/MS or -HRMS),

adhering to the German standard methods DIN 38407-47:2017-07 for water and wastewater analysis. Finally, removal efficiency (RE) in the WWTP was calculated by comparing micropollutant concentrations in influent and effluent waters.

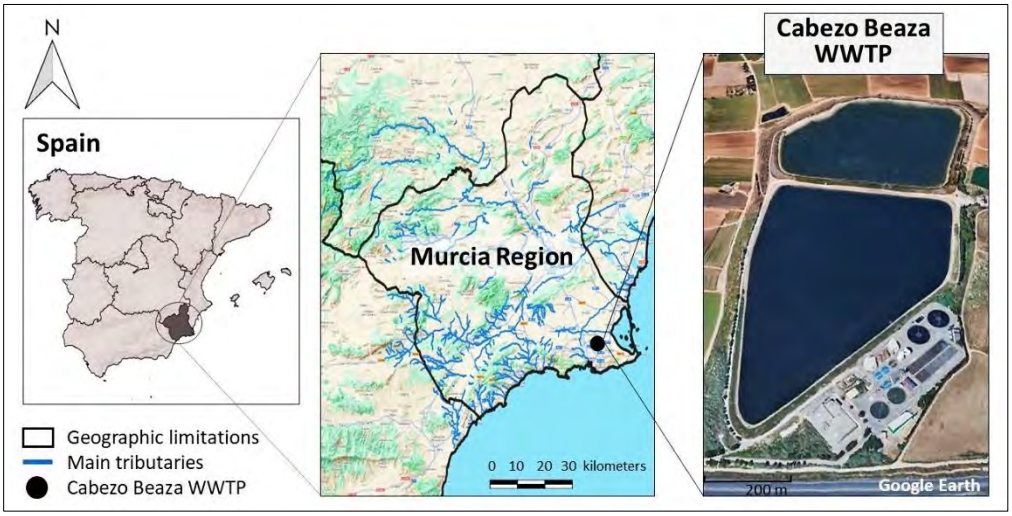

Figure 1. Location and image of the WWTP used in the study.

This study highlights the dynamic removal of twelve targeted micropollutants at the Cabezo Beaza WWTP. Micropollutants included pharmaceuticals such as antihypertensives (candesartan, irbesartan, metoprolol and hydrochlorothiazide), psychiatric pharmaceuticals (amisulpride, citalopram, venlafaxine, carbamazepine), an anti-inflammatory (diclofenac), an antibiotic (clarithromycin), and industrial chemicals (benzotriazole and methylbenzotriazole). It is noteworthy that the highest influent concentrations included benzotriazole (5.94 µg/L), irbesartan (3.22 µg/L) and hydrochlorothiazide (3.00 µg/L) (Table 1). It is notable that these compounds despite having the highest initial concentrations, demonstrates substantial removal improvements in the lagoon phase (>75%).

Table 1. Mean concentrations ± standard deviations of all micropollutants at different stages of wastewater treatment in the Cabezo Beaza WWTP.

Parameters	Influent	Secondary treatment effluent	Lagoons effluent
Amisulpride	0.10 ± 0.01	0.04 ± 0.03	0.01 ± 0.01
Carbamazepine	0.22 ± 0.13	0.14 ± 0.03	0.13 ± 0.06
Citalopram	0.41 ± 0.36	0.17 ± 0.07	0.11 ± 0.04
Clarithromycin	0.17 ± 0.06	0.06 ± 0.06	0.02 ± 0.02
Diclofenac	0.87 ± 0.22	0.75 ± 0.30	0.16 ± 0.11
Hydrochlorothiazide	3.00 ± 0.53	3.76 ± 0.90	0.38 ± 0.18
Metoprolol	0.09 ± 0.07	0.03 ± 0.02	0.01 ± 0.01
Venlafaxine	0.75 ± 0.16	0.45 ± 0.22	0.36 ± 0.28
Benzotriazole	5.94 ± 2.24	2.72 ± 1.13	1.56 ± 0.78
Candesartan	1.54 ± 0.22	1.44 ± 0.74	1.66 ± 0.35
Irbesartan	3.22 ± 0.43	3.24 ± 0.57	0.76 ± 0.70
Methylbenzotriazole	0.34 ± 0.13	0.36 ± 0.12	0.36 ± 0.13

Carbamazepine, and citalopram exhibited concentrations of 0.22 µg/L and 0.41 µg/L in the influent, respectively. In the secondary treatment of the WWTP, both substances showed low removal efficiencies, with percentages around 50%. However, in the lagoon treatment, the removal efficiency for

citalopram was significantly higher, achieving values greater than 70%. The study further revealed that while secondary treatment generally achieved lower removal efficiencies (around 60%), the subsequent lagoon treatment consistently reached higher efficiencies, often surpassing 85% (Figure 2). Moreover, this study at the Cabezo Beaza WWTP identifies significant challenges in measuring the removal efficiencies of certain micropollutants, notably candesartan, irbesartan, and methylbenzotriazole, which showed increased concentrations post-treatment, indicating negative removal rates (Figure 2). Such outcomes are likely exacerbated by factors including low detection limits and the complex nature of the influent matrix, which can increase the likelihood of discrepancies due to matrix effects [5]. Additionally, the phenomena of reversion, where human or microbiological metabolites revert to their parent compounds during treatment, contribute further to the recording of negative efficiencies [6]. The resistance of these compounds to degradation highlights their recalcitrant nature, underscoring the need for advanced techniques to better manage wastewater treatment processes.

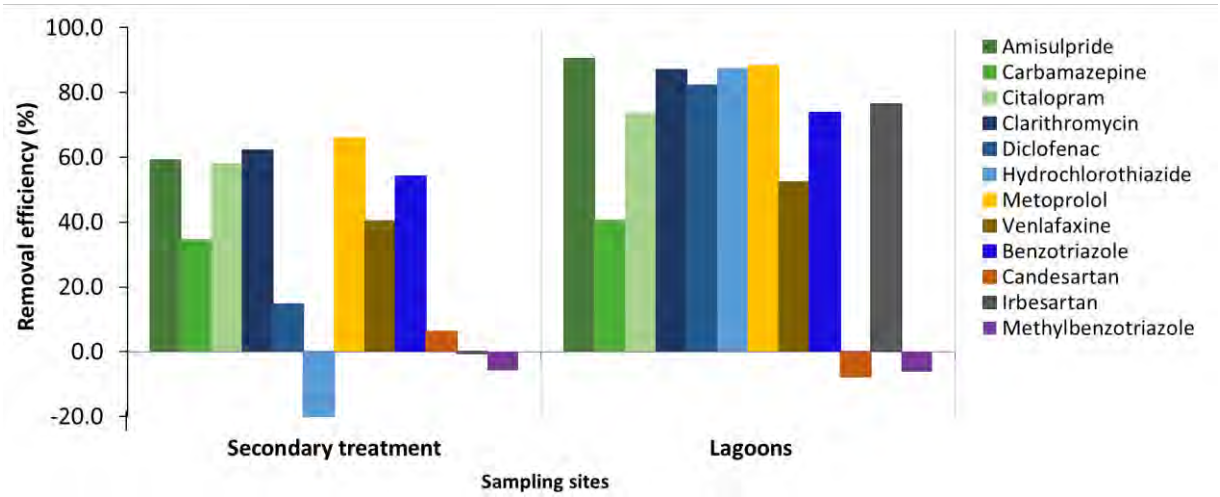

Figure 2. Removal percentages of twelve micropollutants after the WWTP secondary treatment and lagoon treatment.

The removal efficiencies for the six micropollutants are significantly improved in both treatment methods. In particular, the lagoon treatment successfully meets the 80% removal target set by the Directive, in stark contrast to the secondary treatment, which fails to meet this threshold. However, when evaluating twelve micropollutants, neither method consistently meets the 80% removal benchmark (Figure 3).

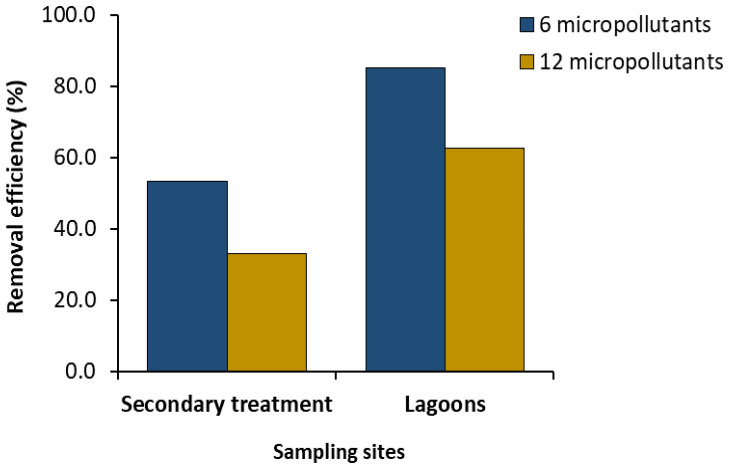

Figure 3. Average removal percentages of six and twelve micropollutants after the WWTP secondary treatment and lagoon treatment.

This variability underscores the complexity of using a standardized set of twelve micropollutants to assess treatment efficacy across different WWTPs. The assumption that pollutant removal is uniform across various conditions is limited, given that the effectiveness of the treatment is influenced by the specific characteristics and operational settings of the plant. While detecting all evaluated micropollutants underscores their role as indicators but also reveals the limitations of using a fixed set of six substances to fully assess treatment efficacy.

Lagoons represent a sustainable alternative to conventional quaternary wastewater treatment methods, utilising both biotic and abiotic mechanisms for the degradation of contaminants [7]. These natural systems retain nutrients and create an environment conducive to diverse microbial activities, which are crucial for the effective breakdown of micropollutants. Key processes include the biodegradation activities of autotrophic ammonium-oxidising bacteria and various algae, which transform pollutants into less harmful substances [7], [8]. Abiotic factors like solar radiation, water temperature, and oxygen availability significantly contribute to contaminant degradation [4], [9]. For instance, UV light and high temperatures accelerate chemical reactions that degrade pollutants, while sedimentation acts as a filter, trapping chemical contaminants [3], [4]. Moreover, Cabezo Beaza lagoons serve as vital ecosystems that support biodiversity by providing essential habitats for a variety of waterbirds, contributing to ecological conservation [10]. This multifunctional role underscores lagoons as an eco-friendly and effective water treatment solution that combines pollutant management with ecological benefits. In conclusion, the findings demonstrate the emerging role of artificial wetlands or lagooning as a sustainable quaternary treatment that combines high efficiency with environmental benefits, such as lower energy use and minimal waste generation. These systems have shown potential in significantly reducing micropollutant levels in aquatic environments and could represent a new era in sustainable water management strategies. However, further research is needed to confirm these findings and to explore the adaptability and scalability of lagooning in various ecological and geographical contexts. This ongoing research is crucial not only for validating the effectiveness of lagooning but also for establishing it as a recognised quaternary treatment method that complies with current standards.

References

[1] Foglia A., González-Camejo J., Radini S., Sgroi M., Li K., Eusebi A. L., and Fatone F., “Transforming wastewater treatment plants into reclaimed water facilities in water-unbalanced regions. An overview of

possibilities and recommendations focusing on the Italian case," J. Clean. Prod., vol. 410, p. 137264, (2023).
[2] Council of the European Union, Proposal for a Directive of the European Parliament and of the Council concerning urban wastewater treatment (recast). Letter to the Chair of the European Parliament Committee on the Environment, Public Health and Food Safety (ENVI). Brussels, p.1–148, (2024).
[3] Wang K., Li K.-Z., Zhou,Y.-Y., Liu Z.-H., Xue G., and Gao P., "Adsorption characteristics of typical PPCPs onto river sediments and its influencing factors," Huan jing ke xue, vol. 36, p. 847–854, (2015).
[4] Kavitha V., "Global prevalence and visible light mediated photodegradation of pharmaceuticals and personal care products (PPCPs)-a review," Results Eng., vol. 14, p. 100469, (2022)
[5] Blair B., Nikolaus A., Hedman C., Klaper,R., and Grundl T., "Evaluating the degradation, sorption, and negative mass balances of pharmaceuticals and personal care products during wastewater treatment," Chemosphere, vol. 134, p. 395–401, (2015)
[6] Angeles L. F., Mullen R. A., Huang I. J., Wilson C., Khunjar W., Sirotkin H. I., McElroy A. E., and Aga D. S, "Assessing pharmaceutical removal and reduction in toxicity provided by advanced wastewater treatment systems," Environ. Sci. Water Res. Technol., vol. 6, p. 62–77, (2019).
[7] Bilal M., Adeel M., Rasheed T., Zhao Y., and Iqbal H. M. N., "Emerging contaminants of high concern and their enzyme-assisted biodegradation – A review," Environ. Int., vol. 124, p. 336–353, (2019).
[8] Men Y., Achermann S., Helbling D. E., Johnson D. R., and Fenner K., "Relative contribution of ammonia oxidizing bacteria and other members of nitrifying activated sludge communities to micropollutant biotransformation," Water Res., vol. 109, p. 217–226, (2017).
[9] Southwell R. V., Hilton S. L., Pearson, J. M., Hand L. H., and Bending G. D., "Water flow plays a key role in determining chemical biodegradation in water-sediment systems," Sci. Total Environ., vol. 880, p. 163282, (2023).
[10] ANSE, "Conservación de las Lagunas de Beaza - ANSE - Asociación de Naturalistas del Sureste", (n.d).

Title: Landfill leachate treatment by NF/RO pilot plant for PFAS removal

Author(s): Ali Hydar*[1], Elisa Blumenthal[1], Massimiliano Sgroi[1], Marco Lazzazzara[2], Alessandro Frugis[2], Giancarlo Cecchini[2,3], Paolo Crocetti[3], Maria Grazia Asci[3], Anna Laura Eusebi[1], Francesco Fatone[1]

[1]Department of Science and Engineering of Materials, Environment and Urban Planning-SIMAU, Marche Polytechnic University (UNIVPM), Via Brecce Bianche, 12, 60131 Ancona, Italy (e-mail: a.hydar@staff.univpm.it)
[2]Acea Infrastructure, gruppo Acea S.p.A., Via Vitorchiano, 165, 00189 Roma, Italy
[3]SIMAM S.p.A., gruppo Acea S.p.A., Via Giovanni Cimabue, 11/2, 60019 Senigallia, Italy

Keyword(s): PFAS, Nanofiltration, Reverse Osmosis, Landfill leachate, Circular Economy

Abstract

This study addresses the persistent issue of per- and poly-fluoroalkyl substances (PFAS) in landfill leachate, a significant source of environmental contamination. PFAS, known for their persistence, mobility, and potential toxicity, pose challenges to environmental and human health. The research focuses on a pilot plant in Italy designed to mitigate PFAS contamination in landfill leachate before it enters wastewater treatment plants (WWTPs). Employing a two-stage filtration system consisting of Nanofiltration/Reverse Osmosis (NF/RO), the pilot plant effectively removes and concentrates PFAS from the leachate. Results indicate high removal efficiencies, with NF achieving around 96.5% removal for 30 measured PFAS and RO achieving complete removal. Additionally, the study evaluates operational parameters and energy consumption, crucial for assessing the feasibility and sustainability of such treatment technologies. This research contributes to understanding PFAS mitigation strategies, aligning with the objectives of the European Green Deal and Circular Economy Action Plan by promoting resource circularity and pollution prevention.

Introduction

Per- and poly-fluoroalkyl substances (PFAS) are a family of compounds used in many commercial and industrial application. Consumer goods like carpets, fabrics, clothing, packaging, food wrappers, and even cleaning and personal care products that are stain- and water-resistant contain PFAS [1,2].

The short and long-chain PFAS are defined as persistent, mobile, and potentially toxic (PM(T)) substances. In landfills, PFAS precursors such as fluorotelomer-based coatings on carpet, clothing and food packaging are biologically transformed into stable and more mobile PFAS [3]. Globally, landfills are considered to be one of the major sources of PFAS contamination to the environment. In landfills, PFAS-based products can release these compounds into leachate and even into the air [4]. Wei et al., (2019) carried out a review on the presence of PFAS in several landfills worldwide, and they found that in Europe PFAS concentrations in landfill leachates generally range from 0.005 to 18 µg/L [5]. Masoner et al. (2020) pointed out that disposal of treated leachate into wastewater treatment plants (WWTPs) can contribute substantially to the increase of PFAS concentrations in the wastewater influents [6]. Helmer et al., (2022) found out that leachate from young landfills tends to have a higher presence of short-chain PFAS than older landfills, due to industrial bans on long-chain PFAS in the recent years [7]. Short-chain PFAS have higher solubility and lower sorptivity than long-chain PFAS. It is common practice to discharge landfill leachate, after some treatment, to municipal WWTPs. Conventional WWTPs have demonstrated to be ineffective at removing PFAS and the presence of precursors in the influent may lead to an increase of PFAS concentrations in the effluent after biological transformation [8]. Thus, PFAS from landfill leachate may be released to the aquatic environment via WWTP effluents but can also be

adsorbed into municipal sewage sludge limiting its agronomic reutilization [9].

In this respect, H2020-PROMISCES project (www.promisces.eu) will identify how industrial pollution prevents the deployment of the circular economy in the EU and which strategies help overcome key bottlenecks to deliver the ambitions of the European Green Deal and Circular Economy Action Plan. In fact, the control of PFAS will increase the circularity of the resources, contributing, moreover, to the zero-pollution ambition and improving human health protection on the path to acceptance and sustainability of the circular economy.

Materials and methods

This study considers a pilot plant for the removal of PFAS from the effluent of a Landfill Leachate Treatment Plant (LLTP) in Italy, before entering the wastewater treatment plant (WWTP).

The pilot consists of a 2-stage filtration system: Nanofiltration/ Reverse Osmosis (NF/RO). The NF/RO pilot is removing and concentrating the PFAS from the stream, and the resulting concentrate should be treated later to destroy PFAS or be disposed of according to the national laws. A block flow diagram of the pilot is given in Figure 1. The pilot is composed of two identical containers (Figure 2) with different filtration systems, one for the RO system and the other for the NF system (Figure 3).

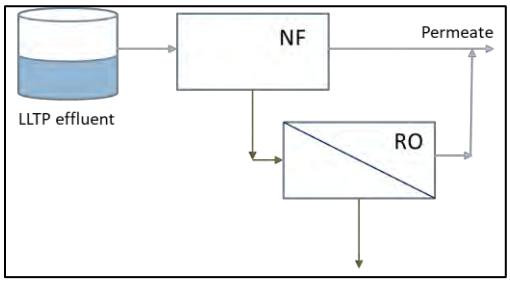

Figure 1 – NF/RO Pilot plant Configuration

The effluent of LLTP is treated in the NF system and then it produces NF Permeate and NF Concentrate.

NF Concentrate is sent into the RO system to be treated again and produces RO permeate and RO Concentrate.

The permeate from both systems is sent to the head of the WWTP or collected for reuse and recovery.

The RO concentrate is collected to be treated later or to be disposed in a safe way due to its high concentration of PFAS, heavy metals and other pollutants.

Through the work of the pilot plant, several parameters have been monitored for both NF and RO systems. These data will be used to evaluate the effectiveness of the system and for Life Cycle Assessment (LCA) and Life Cycle Costing (LCC).

The main monitored parameters are the Flow of each stream, Conductivity, Pressure, pH, and Energy Consumption.

Moreover, the analysis for 30 PFAS and other conventional laboratory tests has been performed.

Figure 2 – NF/RO Pilot Plant

Figure 3 – NF System

Results and Discussion

Several sampling campaigns were performed for about one month and the related results are shown in Table 1, Table 2, Figure 4. A good permeate flow and recovery rate were reached using operation pressure around 20 bar for NF and 50 bar for RO, with energy consumption almost doubled in the case of RO. The results of some conventional parameters (COD, TKN, pH, Conductivity) are also shown in Table 2 and a good removal of the NF system with 95% removal for COD and more than 97% for TKN was obtained. On the other hand, almost a full removal of more than 99% in the RO system for both COD and TKN was observed. As for the conductivity, NF had an acceptable decrease of 35% and RO had a higher decrease of more than 99%.

A decrease in the permeate production for both NF and RO systems can be noticed after several days of running due to the fouling of the membranes (Figure 4).

Table 1 – Parameters of the NF/RO Pilot Plant

Parameters	NF	RO
Permeate Flow (m^3/h)	0.76	0.52
Concentrate Flow (m3/h)	1.28	1.51
Operation Pressure (bar)	21.97	48.40
Recovery (%)	37.16%	25.67%
Energy Consumption (kWh/m^3)	2.7	5.4

Table 2 – COD and TKN analysis for several Campaigns

Samples	COD (mg/l)	TKN (mg/l)	pH	Cond. (µS/cm)
NF Influent	2211.4	56.2	6.9	8197
NF Permeate	116.0	1.5	7.0	5347
NF Concentrate	3317.1	91.9	6.8	9863
RO Permeate	5.9	0.5	5.7	23
RO Concentrate	5105.7	129.6	6.3	12517

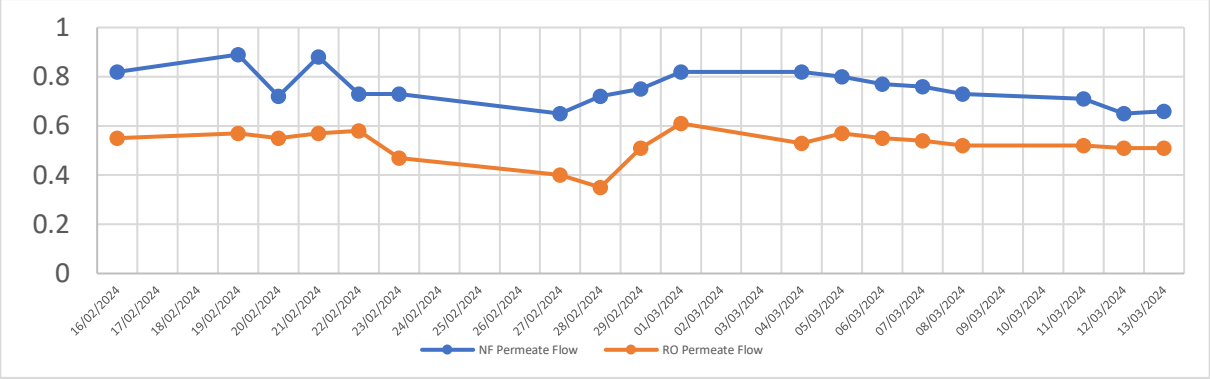

Figure 4 – Permeate production decrease over time for both NF and RO systems

As for the PFAS measurements, Table 3 shows the average results of PFAS concentrations in the performed campaigns. The measurements have been done for 30 PFAS. Nevertheless, only 6 have been detected, and all the other 24 were below the detection limits (1000 ng/l for influent and concentrate and 20 ng/l for permeate). Both NF and RO systems were able to remove PFAS with a high efficiency reaching more than 96% for NF and more than 99% for RO (calculated on the basis of the sum of PFAS).

A similar behaviour of removal efficiency can be seen even considering each single type of PFAS.

Conclusion

- RO was able to completely remove PFAS from the Leachate.

- NF on the other hand was not able to remove all the PFAS, but it had a good Removal Efficiency of almost 96.5% at lower energy consumption and lower concentrate production.

Table 3 – PFAS Concentration and removal efficiency in the NF/RO pilot

Name	NF Influent*	NF Permeate**	NF Concentrate*	RO Permeate**	RO Concentrate*	NF Rejection	RO Rejection
PFBA (ng/l)	1133	33	2200	<	3033	97.06%	> 99.09%
PFPeA (ng/l)	<	30	1367	<	1933	-	> 98.54%
PFHxA (ng/l)	1400	23	2633	<	3733	98.33%	> 99.24%
PFBS (ng/l)	4900	230	8400	<	11700	95.31%	> 99.76%
PFHpA (ng/l)	<	<	<	<	1000	-	> 98.00%
PFOA (ng/l)	3267	57	7533	<	10233	98.27%	> 99.73%
Σ PFAS (ng/l)	**10700**	**373**	**22133**	**-**	**30967**	**96.51%**	**> 99.91%**

Only 6 PFAS has been detected out of 30 measured ones. All other 24 PFAS were below the LOQ. 4-2 FTS, GENX, C6O4, PFPeS, NaDONA, 6-2 FTS, PFHxS, PFNA, 8-2 FTS, PFHpS, PFDA, N-MeFOSAA, PFOS, N-EtFOSAA, PFUdA, PFNS, PFDoA, PFDS, FOSA, PFTrDA, PFUdS, PFTeDA, PFDoS, PFTrS *** LOQ is 1000 (ng/l)** **** LOQ is 20 (ng/l)**

References

[1] Hamid H, Li LY, Grace JR. Review of the fate and transformation of per- and polyfluoroalkyl substances (PFASs) in landfills. Environ Pollut 2018;235:74–84. https://doi.org/10.1016/j.envpol.2017.12.030.

[2] Prevedouros K, Cousins IT, Buck RC, Korzeniowski SH. Sources, Fate and Transport of Perfluorocarboxylates. Environ Sci Technol 2006;40:32–44. https://doi.org/10.1021/es0512475.

[3] Hamid H, Li LY, Grace JR. Aerobic biotransformation of fluorotelomer compounds in landfill leachate-sediment. Sci Total Environ 2020;713:136547. https://doi.org/10.1016/j.scitotenv.2020.136547.

[4] ITRC. PFAS — Per- and Polyfluoroalkyl Substances 2023. https://pfas-1.itrcweb.org/ (accessed May 2, 2024).

[5] Wei Z, Xu T, Zhao D. Treatment of per- and polyfluoroalkyl substances in landfill leachate: status, chemistry and prospects. Environ Sci Water Res Technol 2019;5:1814–35. https://doi.org/10.1039/C9EW00645A.

[6] Masoner JR, Kolpin DW, Cozzarelli IM, Smalling KL, Bolyard SC, Field JA, et al. Landfill leachate contributes per-/poly-fluoroalkyl substances (PFAS) and pharmaceuticals to municipal wastewater. Environ Sci Water Res Technol 2020;6:1300–11. https://doi.org/10.1039/D0EW00045K.

[7] Helmer RW, Reeves DM, Cassidy DP. Per- and Polyfluorinated Alkyl Substances (PFAS) cycling within Michigan: Contaminated sites, landfills and wastewater treatment plants. Water Res 2022;210:117983. https://doi.org/10.1016/j.watres.2021.117983.

[8] Lenka SP, Kah M, Padhye LP. A review of the occurrence, transformation, and removal of poly- and perfluoroalkyl substances (PFAS) in wastewater treatment plants. Water Res 2021;199:117187. https://doi.org/10.1016/j.watres.2021.117187.

[9] Fredriksson F, Eriksson U, Kärrman A, Yeung LWY. Per- and polyfluoroalkyl substances (PFAS) in sludge from wastewater treatment plants in Sweden — First findings of novel fluorinated copolymers in Europe including temporal analysis. Sci Total Environ 2022;846:157406. https://doi.org/10.1016/j.scitotenv.2022.157406.

Acknowledgment

The PROMISCES project has received funding from the European Union's Horizon 2020 research and innovation programme under Grant Agreement No 101036449

Microplastics in municipal wastewaters: Efficiency of different purification processes, main removal mechanisms, and emission factors into the environment

Author(s): Simone Cavazzoli*[1], Francesca Murari[1], Massimo Donegà[2], Werner Tirler[2], Karl Mair[3], Gianni Andreottola[1]

[1] *Department of Civil, Environmental and Mechanical Engineering (DICAM), University of Trento, Via Mesiano, 77 – 38123, Trento (TN), Italy, simone.cavazzoli@unitn.it, gianni.andreottola@unitn.it;*
[2] *Eco Research, Via Luigi Negrelli, 13 - 39100 Bolzano (BZ), Italy, m.donega@eco-research.it, w.tirler@eco-research.it;*
[3] *Eco Center S.p.A., Lungo Isarco Destro, 21 -39100 Bolzano (BZ), Italy, k.mair@eco-center.it.*

Keywords: Emerging contaminants; analytical method; mass spectrometry; environmental remediation.

Abstract

Over the past 70 years, global plastic production has surged from two million to over 450 million tons annually, leading to widespread environmental contamination resulting from mismanagement of plastic waste [1]. Microplastics (MPs), particles with size dimension between 5 mm and 1 µm, are a concerning consequence of plastic pollution, arising from both primary manufacturing and secondary breakdown of larger plastics. MPs pose health risks to humans, including cardiovascular issues, and environmental hazards such as transporting contaminants and altering soil structure [2]. An important entry route of MPs into aquatic systems is sewage discharge, with wastewater treatment plants (WWTPs) serving as crucial interception points [3]. While WWTPs remove a substantial portion of MPs, by accumulating these and other pollutants in the sewage sludges, their effluents still contribute to environmental contamination. In fact, although the concentration of MPs in the effluent is typically a few particles per litre of outgoing water, considering the daily flows emitted by a medium-sized WWTP, the emission factors attributable to the WWTP can be significant [4]. It should also be considered that MPs leaving a WWTP may carry various hazardous contaminants (e.g., priority and emerging pollutants), increasing the negative impact on ecosystems [5].

Despite acknowledging the issue, there's a lack of regulatory directives for MP emissions, with ongoing research focusing on standardized analysis methods. Complexities in analysing MPs in WWTPs stem from the challenge to collect a representative sample, and from rich organic and inorganic content of wastewater, necessitating appropriate purification and analytical procedures [6]. Common analytical methods include FTIR and Raman spectroscopy for particle counting and characterization. Thermal desorption coupled with gas chromatography-mass spectrometry (TD-GC/MS) is a widely used analytical method for different types of organic contaminants, but not yet for the analysis of microplastics [7]. This instrumental analysis, downstream of an appropriate optimisation of the analytical method and a rigorous calibration to the polymers to be investigated, makes it possible to identify the chemical nature of MPs contained in the sample, and to quantify their total mass.

This study aims to identify and quantify different MP polymers, in the size fraction between 5000 to 2 µm, suspended in the influent and effluent of different WWTPs. The purpose is to assess the mass removal of MPs following a specific wastewater treatment process (conventional, tertiary filtrations, MBR, MBBR), explaining in detail the main mechanisms determining such removal and highlighting the

most effective removal technologies. The acquired data are used to estimate emission factors attributable to WWTPs.

Figure 1 - System for wastewater collection and filtration. 1) 400 L stainless steel tank for effluent 24 h accumulation, b) peristaltic pump for tank loading, c) centrifuge pump for rapid filtration, d) stainless-steel filter cartridges (300-10-2 µm) for solids capturing.

Table 1 - Wastewater treatment plants investigated and related volumes of influent, pre-tertiary filtration module, and effluent sampled over 24 h. For effluent and pre-filtration, the maximum volume collected most often coincides with the clogging of one of the 300-10-2 µm cartridge filters (except for MBR and pilot tertiary filter, where all the volume in the stainless-steel tank was filtered without clogging). [a] = conventional line without primary sedimentation; [b] = membrane bioreactor line; c = full scale tertiary filtration system; d = pilot scale filtration system.

#	Treatment technology	Influent Sampled Volume [L]	Pre-Tertiary Filter Sampled Volume [L]	Effluent Sampled Volume [L]
1	Conventional	2	-	200
2	MBBR	2	-	160
3	Conventional + MBR	2	-	80 [a] 395 [b]
4	Tertiary Pile Cloth Filter	2	160	200
5	Tertiary Stainless-Steel Filter	2	12	40 [c] 390 [d]

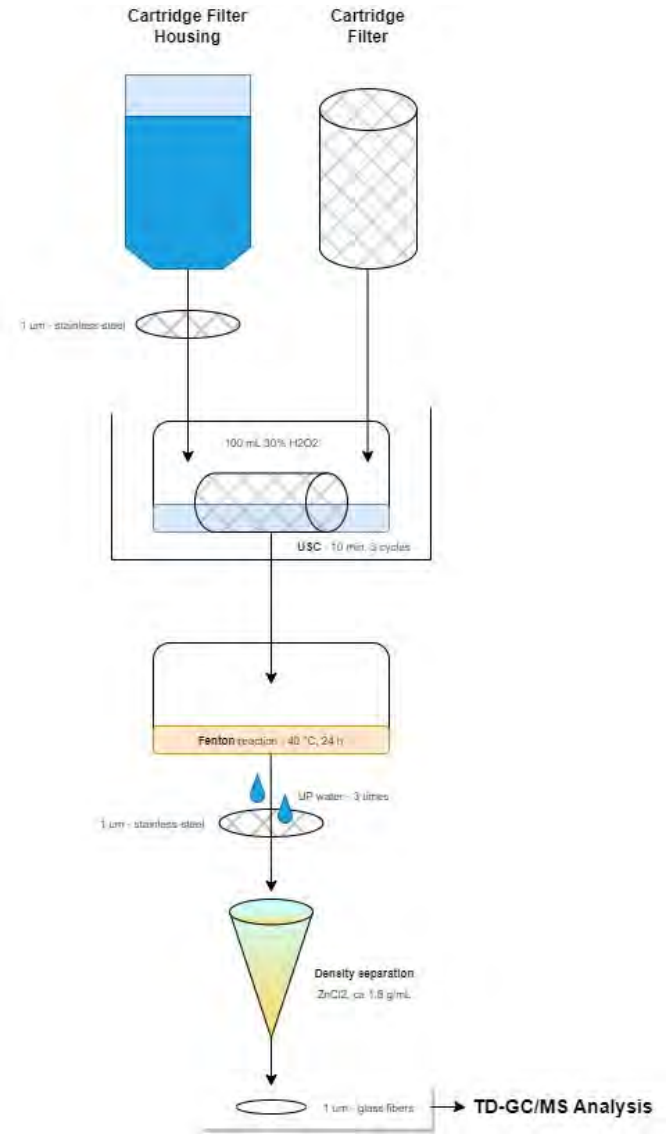

Figure 2 - Representative diagram of the sample preparation method prior analysis by thermal desorption gas chromatography mass spectrometry. Steps for separating microplastics include cartridge filter cleaning in ultrasonic cleaner, Fenton reaction to remove organic matter, and densiometric separation to remove inorganic material.

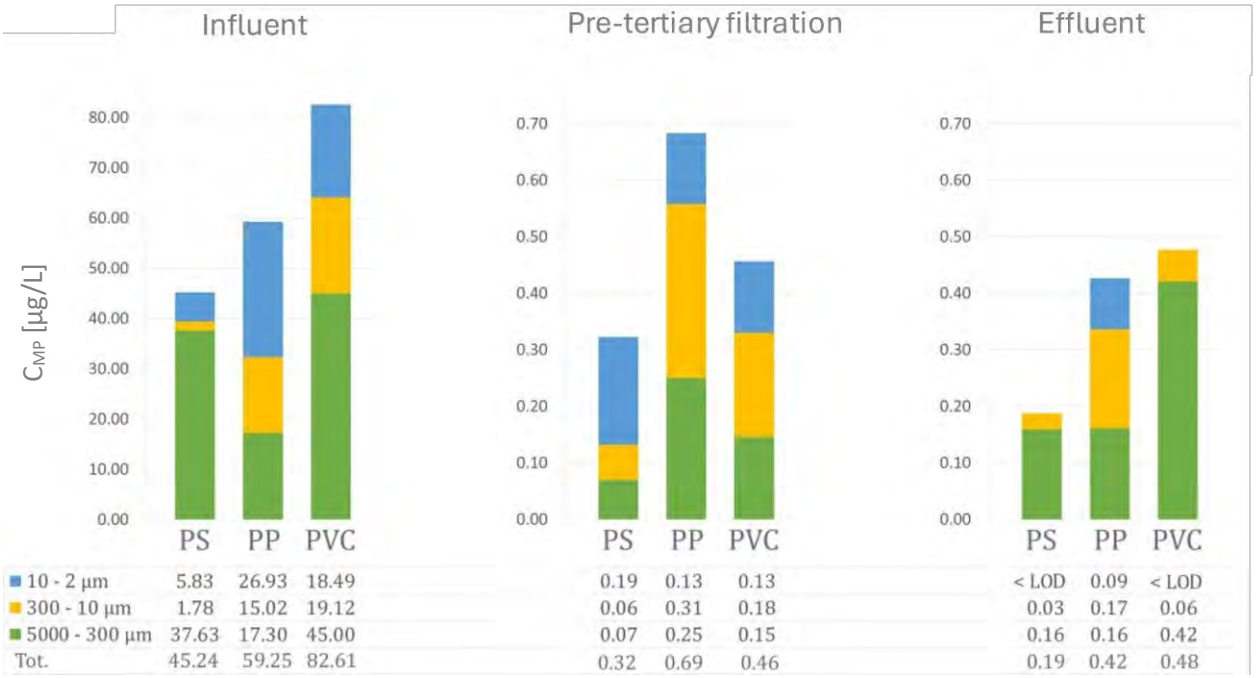

Figure 3 - Mass concentrations of PS, PP and PVC measured in samples collected at the WWTP #4. Results are expressed in µg/L. The measured concentrations are assigned to the relevant analysed size fractions, i.e., >300, 300-10, 10-2 µm.

Table 2 - Partial and total MP removal percentages in WWTP #4 (in brackets the removal percentages of the individual polymers PS, PP and PVC), and environmental emission calculated considering average wastewater flow treated per day in the same plant.

	Partial MP Removal	Total MP Removal	Environmental Emissions
Influent	-	-	-
Pre-tertiary filtration	99.22% (99.29%, 98.85%, 99.45%)	99.22% (99.29%, 98.85%, 99.45%)	-
Effluent	25.39% (41.87%, 37.56%, Increase.)	99.42% (99.59%, 99.68%, 99.77%)	1.09 µg/L, 6.13 g/day

References

[1] https://ourworldindata.org/plastic-pollution
[2] Rachel R. Hurley, Luca Nizzetto, Fate and occurrence of micro(nano)plastics in soils: Knowledge gaps and possible risks, Current Opinion in Environmental Science & Health, Volume 1, 2018, Pages 6-11, ISSN 2468-5844, https://doi.org/10.1016/j.coesh.2017.10.006.
[3] Imran Ali, Tengda Ding, Changsheng Peng, Iffat Naz, Huibin Sun, Juying Li, Jingfu Liu, Micro- and nanoplastics in wastewater treatment plants: Occurrence, removal, fate, impacts and remediation technologies – A critical review, Chemical Engineering Journal, Volume 423, 2021, 130205, ISSN 1385-8947, https://doi.org/10.1016/j.cej.2021.130205.
[4] Rachid Dris, Johnny Gasperi, Vincent Rocher, Mohammed Saad, Nicolas Renault, et al. Microplastic contamination in an urban area: a case study in Greater Paris. Environmental Chemistry, CSIRO Publishing, 2015, pp.2015. https://doi.org/10.1071/EN14167.
[5] Hui He, Hui-Ping Wen, Ji-Peng Liu, Chen-Chou Wu, Lei Mai, Eddy Y. Zeng, Hydrophobic organic contaminants affiliated with polymer-specific microplastics in urban river tributaries and estuaries, Science of The Total Environment, Volume 899, 2023, 166415, ISSN 0048-9697, https://doi.org/10.1016/j.scitotenv.2023.166415.
[6] Cavazzoli, S., Ferrentino, R., Scopetani, C. et al. Analysis of micro- and nanoplastics in wastewater treatment plants: key steps and environmental risk considerations. Environ Monit Assess 195, 1483 (2023). https://doi.org/10.1007/s10661-023-12030-x.
[7] Jonathan W. Leff, Noah Fierer, Volatile organic compound (VOC) emissions from soil and litter samples, Soil Biology and Biochemistry, Volume 40, Issue 7, 2008, Pages 1629-1636, ISSN 0038-0717, https://doi.org/10.1016/j.soilbio.2008.01.018.

Title: Endocrine and metabolic disruptor effects of wastewater treatment plant effluents from conventional and membrane biological reactor systems: first results

Author(s): Francesco CIMINO[1], Antonino Nazareno VIRGA[2,3], Maria Sofia MOLONIA[1], Michele TORREGROSSA[4]

[1] Department of Chemical, Biological, Pharmaceutical and Environmental Sciences, University of Messina, Messina, Italy, fcimino@unime.it;
[2] Department of Agricultural, Food and Forestry Sciences, University of Palermo, Italy, antoninonazareno.virga@unipa.it
[3] Meat and Agribusinnes Chain Research Consortium, Messina, Italy;
[4] Department of Engineering, University of Palermo, Palermo, Italy, michele.torregrossa@unipa.it

Keyword(s): wastewater treatments, endocrine disruptors compounds, obesogens, in vitro toxicity assays.

Abstract

Effluents from municipal wastewater treatment plants (WWTPs) constitute a very complex matrix that can include numerous known and unknown emerging contaminants. To date, the treatment units that make up the plants are not designed to treat most of these contaminants and among these the so-called endocrine disruptors compounds (EDCs), which are natural or artificial chemical compounds (industrial chemicals, veterinary drugs, pesticides and food additives) capable of influencing the correct functioning of the endocrine system in humans as well as in animals (Thacharodi et al., 2023). EDCs interact with nuclear receptors that regulate various physiological processes such as cell development, differentiation, proliferation and metabolism. Furthermore, EDCs combinations can produce additive/synergistic effects, even when each chemical is present at low doses that individually do not induce observable effects. This study aimed to analyze the toxicological characteristics of treated wastewater by comparing the differences between effluents from plants using conventional activated sludge biological technology and advanced membrane treatment effluents (MBR), using a battery of biological tests. For this purpose, the raw influent and treated effluents of four WWTPs operating in the Sicilian territory were sampled, two conventional plants serving the municipalities of Carini and Ribera, the first with nitrification and denitrification treatments for the removal of nitrogen, the second only with organic substance removal treatment, and two MBR plants, serving the municipalities of Riesi and Sciacca, both with nitrification and denitrification treatments for nitrogen removal. Bioanalysis tools, in addition to the physicochemical assessment of water quality, can provide further information on the toxic effects of pollutants present in wastewater discharges by considering the entire mixture of contaminants (cocktail effect) (Shrivastava et al., 2017; Biasiotto et al., 2016). The influent samples (INF), taken downstream of the screening unit, and the treated wastewater samples (EFF), taken downstream of the biological treatment, were extracted and concentrated using solid phase extraction (SPE - Oasis HLB Glass Cartridge). Extracts (with 3x higher concentration factor) were analyzed for endocrine disrupting and metabolic bioactivity using two cell culture assays for estrogenic and obesogenic activity. The results of the analyzes, reported in Figures 1 and 2, showed that all extracts of the influent sewage samples led to an increase in the proliferation rate of estrogen-sensitive MCF-7 breast cancer cells, while no effect was observed for the extracts of treated effluents. Furthermore, no effect was observed in estrogen-negative MDA-MD-231 breast cancer cells confirming the estrogen receptor role in the

effects observed in MCF-7 cell line. This highlights that cleansing treatments, both conventional and advanced, appear effective in withdrawing estrogen-mimicking agents.

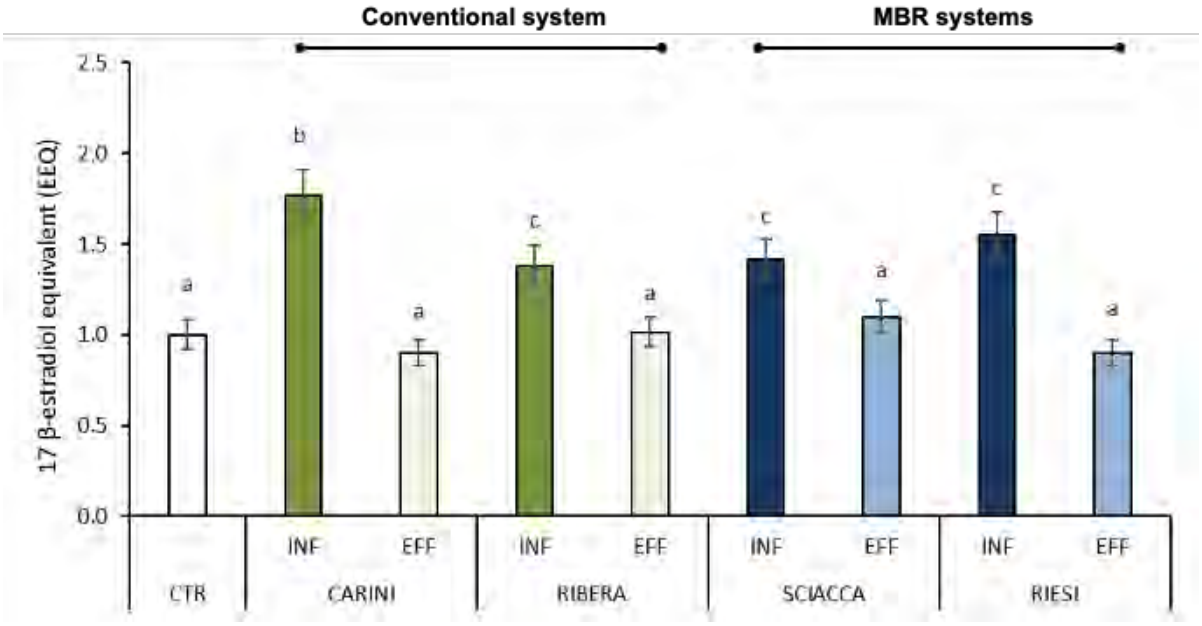

Figure 1 – Estrogenic activity (E-assay) of wastewater extracts on MCF-7 (breast cancer cell line estrogen-responsive). CTR represents a distilled water sample extracted in the same conditions of wastewaters. Means with the same letter are not significantly different from each other ($p > 0.05$)

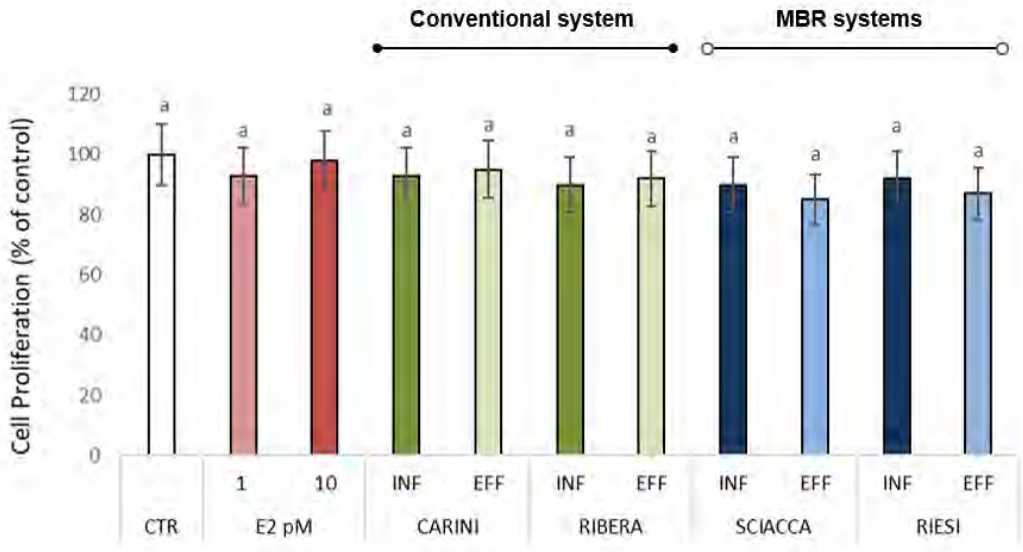

Figure 2 – Effects of wastewaters extracts on MDA-MB-231 breast cancer cell line estrogen-negative. CTR represents a distilled water sample extracted in the same conditions of wastewaters. 17β-estradiol (E2) was used to confirm the lack of estrogen receptor. Means with the same letter are not significantly different from each other ($p > 0.05$)

Exposure to EDCs has been causally linked with obesity in model organisms and associated with obesity occurrence in humans. We then evaluated the effects of wastewaters extracts to promote *in vitro* adipogenesis and lipid accumulation (obesogen effect). At this aim, using an experimental model of preadipocytes differentiation we studied the *in vitro* effects of the wastewater samples to elicit a predisposition to obesity. As showed in figure 3 all extracts from influent samples were able to induce lipid accumulation in 3T3-L1 murine adipocytes and this effect was associated to the presence of compounds with obesogen activity. Finally, the test results highlighted that, while the extracts of the treated effluents taken downstream of plants with conventional treatments showed partial effects, although not significant, on the induction of preadipocytes differentiation (Fig. 3), this was not observed for the effluent extracts from the MBR systems (Fig. 3). This circumstance appears significant as it is symptomatic of a good efficiency of removal of metabolic interfering compounds.

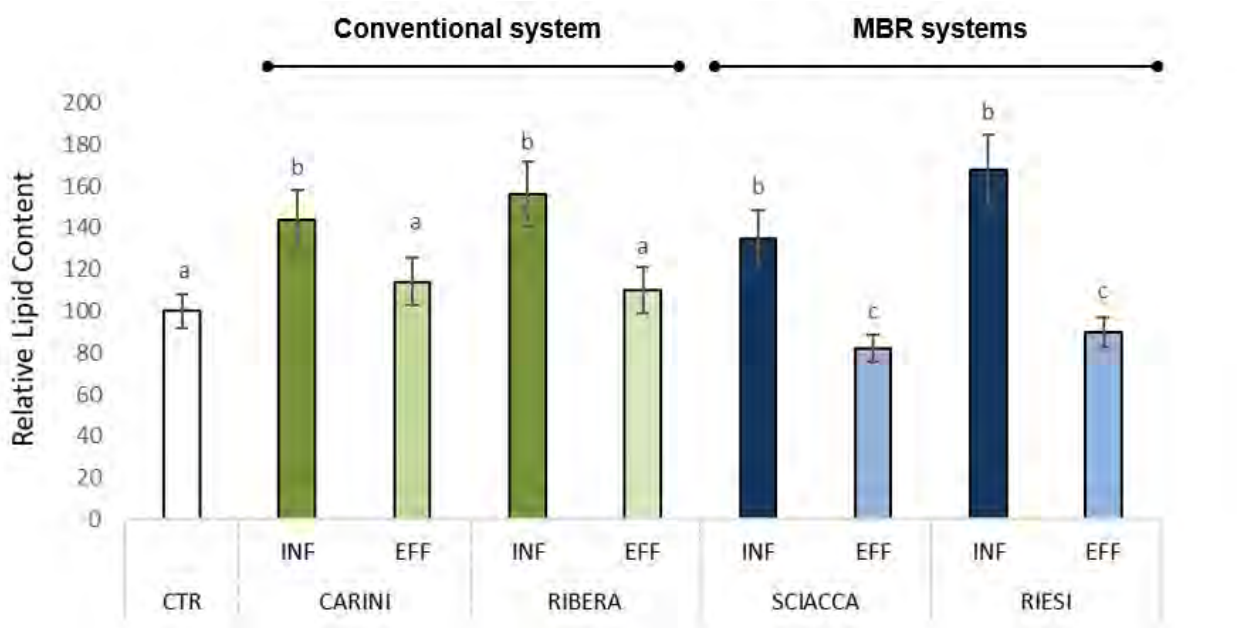

Figure 3 – Intracellular lipid content measured by Oil Red O staining. The lipid droplets accumulated in mature differentiated 3T3-L1 cells were quantified at 490 nm using a microplate reader. Means with the same letter are not significantly different from each other ($p > 0.05$).

However, morphometric analysis of lipid vacuoles dimension (Figure 4), revealed increased vacuoles size for all the influent samples confirming inducing effects on adipocytes fat accumulation. Wastewaters treatments reduced the effects on lipid accumulation even if MBR systems (Figure 4b) showed values similar to CTR. These results further confirmed improved efficacy of contaminant removal exerted by treatments with advanced MBR system.

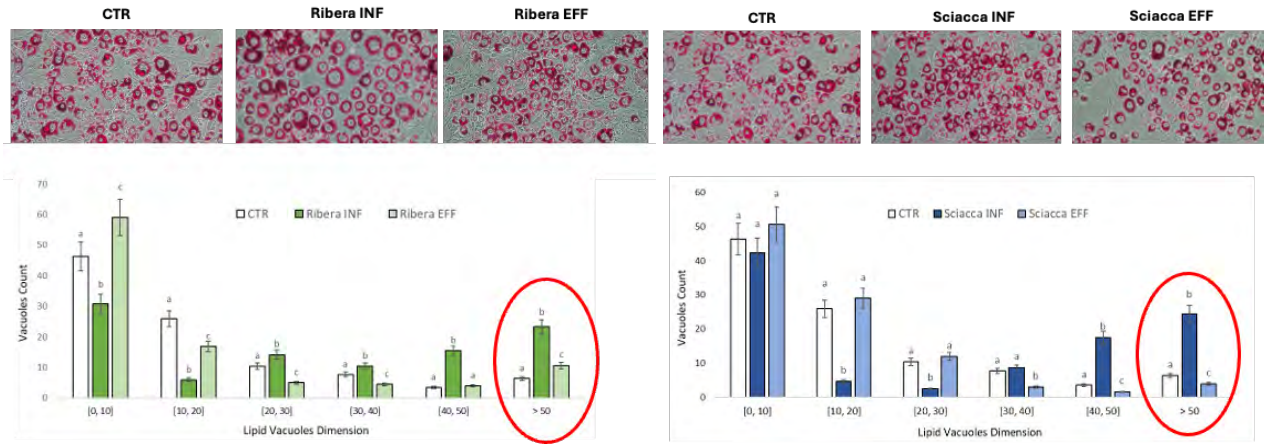

a) Conventional WWTP b) MBR WWTP

Figure 4 – morphometric lipid vacuole size analysis in 3T3-L1 mature adipocytes performed with ImageJ. The cells were photographed using an optical microscope (magnification 40X). Means with the same letter are not significantly different from each other ($p > 0.05$).

The results of the investigations carried out confirm that, in general, wastewater treatments reduce agents that disrupt the endocrine system and metabolism, although to varying degrees. In particular, MBR technology shows a removal efficiency even on EDCs compounds greater than that obtainable with conventional treatments.

References

Biasiotto G, Zanella I , Masserdotti A, Pedrazzani R , Papa M, Caimi L, Di Lorenzo D. (2016), *Municipal wastewater affects adipose deposition in male mice and increases 3T3-L1 cell differentiation*,Toxicol Appl Pharmacol. Apr 15; 297: 32-40. doi: 10.1016/j.taap.2016.02.023

Shrivastava P, Naoghare P K, Gandhi D, Saravana Devi S, Krishnamurthi K, Bafana A, Kashyap S M b, Chakrabarti T (2017) *Application of cell-based assays for toxicity characterization of complex wastewater matrices: Possible applications in wastewater recycle and reuse*, Ecotoxicol Environ Saf.; 142: 555-566. doi: 10.1016/j.ecoenv.2017.04.023

Thacharodi A, Hassan S, Hegde T A, Dilip Thacharodi D, Brindhadevi K, Pugazhendhi A (2023) *Water a major source of endocrine-disrupting chemicals: An overview on the occurrence, implications on human health and bioremediation strategies*. Environ Res., 15; 231:116097. doi: 10.1016/j.envres.2023.116097

PARALLEL SESSION: C4

Biorefineries

Biorefinery andvanced methods and processes

Title: Selection of a mixed microbial culture for PHA production through phosphate limitation: insight into the selection process and the main kinetic parameters

Author(s): Alessio Castagnoli*[1], Sitihaya Malibo[1,2], Giulio Petroni[3], Prawit Kongjan[4], Renato Iannelli[1] Isabella Pecorini[1],

[1] *Department of Energy, Systems, Territory and Construction Engineering (DESTEC), University of Pisa, 56122 Pisa, Italy*
[2] *Energy technology program, Faculty of Engineering, Prince of Songkla University, Hatyai 90110, Thailand*
[3] *Department of Biology, University of Pisa, 56126 Pisa, Italy*
[4] *Department of Science, Faculty of Science and Technology, Prince of Songkla University, Pattani, 94000, Thailand*

Keyword(s): Polyhydroxyalkanoates, Mixed Microbial Cultures, Biorefineries, Circular Economy

Abstract

Introduction

The utilization of waste streams as feedstock for manufacturing polyhydroxyalkanoates (PHAs) is increasingly recognized, offering an effective approach for resource recovery through the production of biodegradable plastics [1]. Recent research has emphasized the production of PHAs from volatile fatty acid (VFA)-rich streams, which are commonly derived from the fermentation of food waste or wastewater sludge. Presently, industrial-scale PHA production via biological methods predominantly relies on pure cultures; however, the high associated costs render PHAs less competitive compared to other biopolymers [2]. To mitigate these costs, the exploitation of mixed microbial cultures (MMCs) has emerged as a promising strategy. MMCs are developed through a selection process that involves dynamic feast and famine conditions applied to an inoculum sourced from activated sludge plants [3]. The selection reactor, supplied with VFA-rich streams and optimized nutrient concentrations, promotes the predominance of the accumulation process over direct microbial replication on VFAs, thereby selecting for an MMC capable of subsequently converting VFAs into PHB/V in another reactor [4]. Nutrient limitation plays a crucial role, as it promotes PHA accumulation over cellular growth, thereby favouring PHA-accumulating microorganisms over conventional heterotrophs.

Materials and methods

A feast-and-famine regime and limiting nutrient conditions were induced in a sequencing batch reactor (SBR) inoculated with activated sludge to select a mixed microbial culture capable of PHA accumulation. The biomass was selected using sludge from the secondary settler of the Viareggio wastewater treatment plant as inoculum. This was aerated overnight to remove fats, oils, and residual COD, then characterized and introduced into the SBR reactor. Before the feeding, the Total Suspended Solids (TSS) and Volatile Suspended Solids (VSS) concentrations were 6.56 ± 0.27 g/L and 5.57 ± 0.14 g/L, respectively.

The SBR reactor cycle lasted 12 hours, comprising the following phases: feeding (6 min, 2.3 L), reactive phase (659 min), settling (30 min), supernatant purging (15 min, 1.74 L), sludge purging (5 min, 0.52 L), and idle (5 min). The reactor was fed with organic waste containing a dark fermentative composition [5].

Ammonium and phosphate were reduced to achieve nutrient-limiting conditions, resulting in a C:N:P ratio of 100:8:1.5, which was identified as limiting for this inoculum in previous experiments. Micronutrient supply was ensured as described by Castagnoli et al. (2024) [6]. The pH of the solution was adjusted with NaOH, calculated stoichiometrically to balance the free protons from VFAs in their dissociated states. An Organic Loading Rate (OLR) of 3 gCOD/L/d was applied, achieving a feast/famine (F/F) ratio of less than 0.33, providing appropriate selective pressure. The sedimentation phase allowed for supernatant separation, yielding a Hydraulic Retention Time (HRT) of 1 day and a Solids Retention Time (SRT) of 3 days. Except during sedimentation and supernatant separation, the reactor was continuously mixed and oxygenated, with aeration provided by a centrifugal pump at a rate of 0.8 L/L/min. The temperature was controlled at 25 ± 1 °C. Dissolved oxygen and pH were continuously monitored and recorded. During working days, the end of the famine phase was characterized by measuring concentrations of COD, NH_4^+, and PO_4^{3-}. A full cycle analysis was conducted weekly to detect changes in substrate trends and calculate VFA and nutrient uptake rates. Additionally, TSS and VSS were monitored weekly for biomass at the end of the feast period and for supernatants removed in the morning, with analyses conducted in triplicate. COD, NH_4^+, and PO_4^{3-} were measured using spectrophotometric methods, with all samples filtered through 0.45 µm filters. VSS and TSS were determined by filtering specific volumes (10 mL for sludge, 30 mL for supernatants) through 0.45 µm filters, then drying at 105°C for 24 hours followed by muffling at 550°C for 4 hours.

Results and Discussions

Since reactor startup, pseudo-stationary conditions have been observed starting from the 32nd cycle. This cycle was characterized by a maximum pH of 8.70 and an F/F ratio of 0.19. Subsequently, these conditions remained relatively stable, with a maximum pH of 8.75 ± 0.13 and an F/F ratio of 0.17 ± 0.03. The fluctuations in these conditions are primarily due to the progressive fouling of the probes and reactor walls. Table 1 presents the solid characterization of the reactor at the end of the feast phase. The biomass concentration, expressed as VSS, decreases in cycle 42 in both the reactor and supernatant.

Table 1. Solids characterization of the reactor and the supernatants for the 16th cycle 16 and 42nd cycle.

	TSS [g/L]	SD TSS [g/L]	VSS [g/L]	SD VSS [g/L]	VSS/TSS [%]	SD VSS/TSS [%]
Biomass - cycle 16	3.33	0.08	3.01	0.06	90%	0.32%
Biomass - cycle 42	2.57	0.07	2.31	0.05	90%	0.33%
Supernatant - cycle 16	0.40	0.01	0.34	0.01	86%	1.86%
Supernatant - cycle 42	0.13	0.00	0.11	0.00	82%	1.97%

Figures 1 and 2 report the cycle analysis conducted in the 16th and 42nd cycles.
Figure 1A depicts a very short feast cycle of approximately 90 minutes, with nutrient consumption following a similar slope. Ammonium concentration reaches its minimum at around 250 minutes, while phosphate concentration remains constant thereafter. Phosphate uptake shows a nonlinear trend, as

noted by Castagnoli et al. (2024) [6]. Initially, it is primarily assimilated by the bacteria and subsequently utilized for replication, as indicated by the prolonged ammonium uptake.

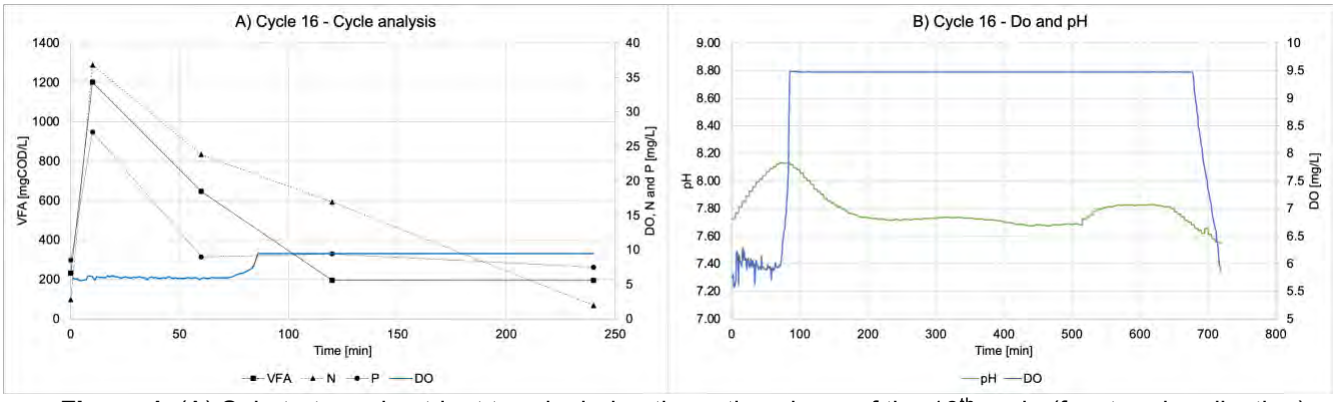

Figure 1. (A) Substrate and nutrient trends during the active phase of the 16th cycle (feast and replication); (B) DO and pH variation during the whole 16th cycle.

Figure 1B indicates that the pH peak at the end of the feast phase signifies the point of potential maximum PHB accumulation. After this peak, the pH decreases due to the growth, which consumes ammonium, releasing CO_2 within the reactor and thus reducing the pH. The pH stabilizes, with an increase occurring only at minute 520 due to the prevalence of CO_2 stripping once growth is complete.

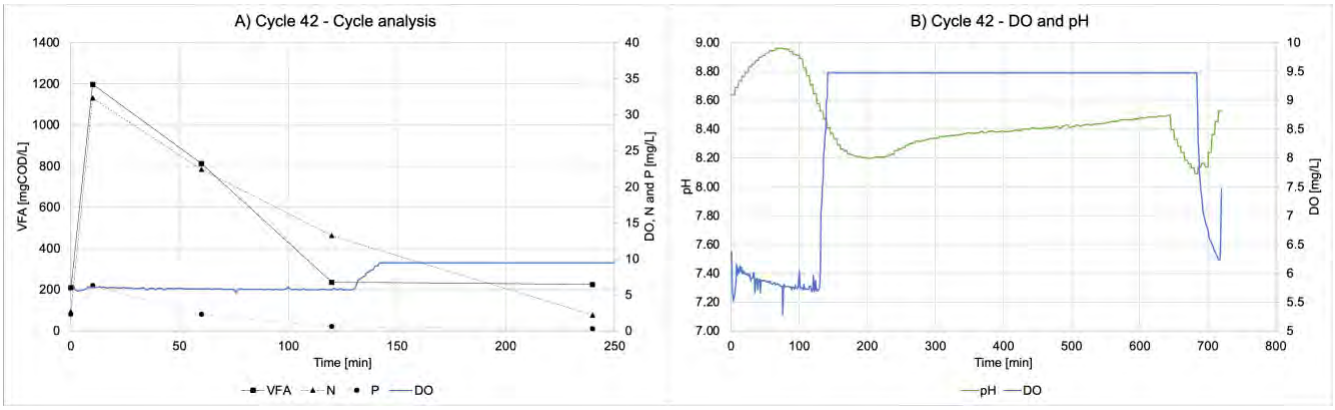

Figure 2. (A) Substrate and nutrient trends during the active phase of the 42nd cycle (feast and replication); (B) DO and pH variation during the whole 42nd cycle.

Cycle 42 is characterized by a longer feast phase (Figure 3A), despite identical aeration, as indicated by the minimum dissolved oxygen (DO) levels. This is attributed to slower VFA consumption as the biomass undergoes selective pressure, gradually favouring PHA-accumulating bacteria. Ammonium again reaches its minimum within 250 minutes, while phosphate is completely consumed within 120 minutes. Figure 2B shows a different pH trend. It starts at a higher level and reaches a value close to 9, which is identified in the literature as typical for a steady-state process. This is followed by a sharp decrease with a steeper slope than previously observed, which stabilizes around minute 200. Subsequently, the CO_2 stripping begins to dominate, indicating the end of the growth. This behaviour suggests a higher concentration of PHA-accumulating bacteria even if VSS concentration is reduced.

Table 2 presents the kinetic values for the two cycles. The VFA rates reflect the DO trends, indicating a longer feast duration. NH_4^+ is consumed quicker in the first hour of cycle 16, likely due to the PO_4^{3-} concentration. Lower nutrient consumption rates in the first hour and higher rates in the second hour suggest that in cycle 42 VFAs are allocated more towards PHA accumulation rather than direct growth.

Table 2. VFA, ammonia and phosphate consumption rates expressed in $mgL^{-1}h^{-1}$.

	Cycle 16			**Cycle 42**		
	VFA	N	P	VFA	N	P
1st hour rate	666.0	15.6	21.7	460.8	11.9	4.8
2nd hour rate	450.0	6.9	-0.4	577.0	9.2	1.7
Feast rate	548.2	10.8	9.7	524.2	10.4	3.1
After feast rate	0.5	7.5	1.0	5.5	5.5	0.2

Conclusions

Preliminary results indicate that the selected biomass is capable of accumulating PHA. The PHB/V results sampled during cycle 42 will validate the observations regarding pH and ammonium kinetics. Future investigations will focus on analyzing additional limiting conditions to determine how varying phosphorus limitations influence biomass selection. This will explore whether a specific concentration causes the reactor to shift towards a storage reactor. Further data will also aim to establish a correlation between pH, PHA concentration, and nutrient levels, facilitating the development of a method to monitor the process using DO and pH, thereby reducing operational costs.

References

[1] M. Gottardo *et al.*, 'Producing volatile fatty acids and polyhydroxyalkanoates from foods by-products and waste: A review', *Bioresour. Technol.*, vol. 361, p. 127716, Oct. 2022, doi: 10.1016/j.biortech.2022.127716.
[2] E. Touloupakis, A. Chatziathanasiou, D. F. Ghanotakis, P. Carlozzi, and I. Pecorini, 'Poly(3-hydroxybutyrate) production by Rhodopseudomonas sp. S16-VOGS3 cells grown in digested sludge', *Environ. Technol. Innov.*, vol. 30, p. 103058, May 2023, doi: 10.1016/j.eti.2023.103058.
[3] G. Papa, T. Pepè Sciarria, A. Carrara, B. Scaglia, G. D'Imporzano, and F. Adani, 'Implementing polyhydroxyalkanoates production to anaerobic digestion of organic fraction of municipal solid waste to diversify products and increase total energy recovery', *Bioresour. Technol.*, vol. 318, p. 124270, Dec. 2020, doi: 10.1016/j.biortech.2020.124270.
[4] G. Moretto, I. Russo, D. Bolzonella, P. Pavan, M. Majone, and F. Valentino, 'An urban biorefinery for food waste and biological sludge conversion into polyhydroxyalkanoates and biogas', *Water Res.*, vol. 170, p. 115371, Mar. 2020, doi: 10.1016/j.watres.2019.115371.
[5] E. Albini, I. Pecorini, and G. Ferrara, 'Improvement of Digestate Stability Using Dark Fermentation and Anaerobic Digestion Processes', *Energies*, vol. 12, no. 18, p. 3552, Sep. 2019, doi: 10.3390/en12183552.
[6] A. Castagnoli *et al.*, 'Influence of Aeration Rate on Uncoupled Fed Mixed Microbial Cultures for Polyhydroxybutyrate Production', *Sustainability*, vol. 16, no. 7, p. 2961, Apr. 2024, doi: 10.3390/su16072961.

Title: Life cycle assessment of passenger cars fed with a blend of LPG, bio-LGP, and renewable DME, and comparison with conventional and electric passenger cars

Author(s): Stefano Puricelli*[1], Michelle Eid[1], Simone Casadei[2], Mario Grosso[1], Giovanni Lonati[1], Lucia Rigamonti[1], Stefano Cernuschi[1]

[1] *Department of Civil and Environmental Engineering, Politecnico di Milano, Milano, Italy, stefano.puricelli@polimi.it, stefano.cernuschi@polimi.it, michelle.eid@polimi.it, mario.grosso@polimi.it, giovanni.lonati@polimi.it, lucia.rigamonti@polimi.it*
[2] *Sustainable Mobility Team, Innovhub – Stazioni Sperimentali per l'Industria, Milano, Italy, simone.casadei@mi.camcom.it*

Keyword(s): LCA, transport, biofuels, e-fuels, LPG, DME, electric car, petrol

Abstract

The Life Cycle Assessment (LCA) methodology was applied to comparatively assess the environmental impacts of passenger cars (from both segments B and C) with spark-ignition (SI) engine and with electric motor. The SI cars complied with the Euro 6d emission standard and were fuelled with petrol or a mixture of liquefied petroleum gas (LPG) (60% m/m), bio-LPG (20% m/m), and renewable dimethyl ether (20% m/m). The Life Cycle Assessment (LCA) methodology was applied for evaluating comparatively the environmental impacts of two passenger cars (of B and C segments) powered by:

- a SI engine fuelled by petrol;
- a SI engine fuelled by a mixture of LPG (60% m/m), bio-LPG (20% m/m), and renewable dimethyl ether (20% m/m);
- an electric motor.

Three types of dimethyl ether (DME) were tested in the evaluation: the biofuel (bio-DME), the e-fuel (e-DME), and the recycled carbon fuel (RC-DME). The fuels for SI engine cars were analysed and tested by Innovhub-SSI on a chassis dynamometer laboratory test bench, using two B-segment cars and one C-segment car. The results for the two B-segment cars were averaged. All the passenger cars belonged to the category of Sport Utility Vehicles (SUV). Moreover, two battery electric cars, those modelled in [1], were considered. The functional unit was defined as "traveling 1 km in Italy with a passenger car". The total mileage covered by the cars was set at 190,000 km for the B segment and 210,000 km for the C segment [2]. The system boundaries include the entire life cycle of the car (production, use, maintenance, end of life) and the energy carriers that power it, as well as the construction and end of life of the road. Multifunctionality issues in the foreground system were solved following the hierarchy recommended by [3], although in some cases it was preferred to deviate from it. For instance, for modelling processes involving waste treatment activities or the use of waste streams as feedstock, the "polluter pays" approach was adopted: impacts occurring until the waste has a negative market price are attributed to the system that generated the waste. The geographical horizon of the LCA is Italy and the time horizon is the year 2023. The modelling of the foreground system was primarily based on secondary data from literature or specific websites, while for the background system it was based on secondary data acquired from the ecoinvent database version 3.9.1 (cut-off system model) [4]. The analysis was conducted using SimaPro 9.5 software. The evaluation considered the 16 impact

categories suggested in [5]. Carbon neutrality was assumed for CO_2 emissions from the biofuel combustion. CO_2 captured from a cement plant, incorporated into a renewable fuel and subsequently combusted, was also considered neutral.

It was assumed that petrol production takes place in Italy, as it accounts for 97% of the petrol consumed locally [6], [7]. To model the production chain of LPG, a questionnaire was prepared and sent to four Italian LPG-selling companies, for a total of 508,000 t sold in 2022. Based on the information gathered from the questionnaires, 27% of LPG is produced in Italy and 73% is imported. Bio-LPG (also referred to as biopropane) was modelled as a by-product of the hydrotreatment process called Hydroprocessed Esters and Fatty Acids (HEFA), yielding HEFA-diesel as primary product. The assessed scenario refers to the future configuration of the "Porto Marghera" biorefinery (Venice, Italy), detailed in the IPPC permit documentation [8]–[11]. In this analysis, the most used raw material in Italy for HEFA production, namely used cooking oil (UCO), was considered. According to 2018 data [12], the UCO used in the European Union (EU) to produce conventional biodiesel (FAME) and HEFA-diesel comes for 42% from EU countries, 21% from China, 11% from Indonesia, and the remaining 26% from other non-European countries. After a series of pretreatments for reducing the contaminants inside the UCO, this feedstock is treated with hydrogen (produced from natural gas) and the final products of the process are HEFA-diesel, bionaphtha, bio-jet fuel, and bio-LPG. The production of bio-DME was modelled according to [13] and involves two stages: the first one is the dry reforming of methane and CO_2 (captured) into syngas, the second one is the direct synthesis of DME. The CO_2 capture process was added to the model of [13] by using data retrieved in [14]. For this study, fossil methane was replaced with its biogenic counterpart, biomethane, which comes from the organic fraction of municipal solid waste and is the most used raw material in Italy to produce biomethane for automotive use [15]. To model the production of e-DME, data retrieved in [16] were used. In this theoretical model, methanol is firstly produced by CO_2 hydrogenation, with CO_2 captured from the exhaust gases of a cement plant; e-DME is then obtained through methanol dehydration. The electricity required for electrolysis was modelled using the Italian hydropower production mix [17], as this was the highest consumed one (39.1%) among renewable sources used in Italy in 2021 [18]. The production process of RC-DME was modelled by using data from a study on methanol production from waste plastics (50% polypropylene and 50% polyethylene) [19]. The plastics, after being transported to the plant, are crushed to 5 mm and fed into the gasification reactor. The resulting syngas undergoes a series of purification stages and is then subjected to steam reforming. Methanol with a purity of 99.8% is synthesised from the resulting syngas. The final conversion into DME was based on data from [16].

Exhaust emissions and fuel consumptions from the SI cars were obtained from measurements conducted in the laboratory of Innovhub-SSI. Driving tests were conducted according to the WLTC (Worldwide harmonized Light vehicle Test Cycle). Measurements included regulated pollutants (CO, total hydrocarbons [THC], non-methane hydrocarbons [NMHC], NOx, particulate matter [PM], and solid particle number [PN]) as well as other conventional and trace compounds of significance for traffic environmental evaluations (CO_2, CH_4, PM soot, total PN (via EEPS), NH_3, N_2O, 1,3-butadiene, formaldehyde, and benzene). To complete the exhaust emissions inventory of SI cars with evaporative emissions and other trace compounds unmeasured in laboratory and coming from the combustion of fuels and lubricant oil, data available in [20] were used. Electric car consumptions were calculated by a weighted mean of WLTC consumptions of the B- and C-segment SUVs models mostly registered in Italy in the first nine months of 2023 [21], [22]. Production and distribution of electricity refer to the Italian electricity mix of 2019. The demand for materials for the domestic charging column of the electric car was also included in the inventory [23]. Emissions due to tyre, brake, and road surface wear were estimated using emission factors available in [20]. For electric cars, emissions from brake wear were

decreased by correcting the corresponding SI cars' emission factors with specific scaling coefficients derived from [20]. This is because of the presence of regenerative braking, which significantly reduces the use of conventional braking systems. Evaporative emissions were estimated only for the petrol cars, for which an emission factor was available in [20]. The production, maintenance, and end-of-life phases of the vehicles' life cycle were modelled based on the datasets retrieved from [1].

Table 1 shows the percentage differences in environmental impacts compared to the petrol car. Red and bold digits highlight variations greater than +10%, whilst green and italic digits highlight variations greater than -10%. Due to the inherent uncertainty in every LCA, variations below 10 percentage points were not considered significant (black digits). The type of renewable DME did not significantly influence the results, due to its low content in the blend (20% by mass), except for the water use impact category. For this reason, it was preferred to calculate and report in Table 1 an average of the results of the three rDME blends.

Table 1. Percentage differences in impacts compared to the petrol car scenario.

Impact category	SI engine with LPG + bio-LPG + rDME* (B segment)	Electric motor (B segment)	SI engine with LPG + bio-LPG + rDME* (C segment)	Electric motor (C segment)
Acidification	+5%	**+55%**	**+10%**	**+50%**
Climate change	*-21%*	*-36%*	*-16%*	*-38%*
Ecotoxicity, freshwater	*-36%*	*-27%*	*-34%*	*-29%*
Particulate matter	-5%	-1%	-3%	-4%
Eutrophication, marine	+8%	**+45%**	**+17%**	**+39%**
Eutrophication, freshwater	**+13%**	**+122%**	**+14%**	**+113%**
Eutrophication, terrestrial	+8%	**+31%**	**+19%**	**+26%**
Human toxicity, cancer	+1%	**+44%**	+3%	**+40%**
Human toxicity, non-cancer	+2%	**+141%**	+3%	**+135%**
Ionising radiation	+8%	**+170%**	+9%	**+155%**
Land use	-0.5%	**+31%**	+0.4%	**+25%**
Ozone depletion	*-27%*	*-32%*	*-24%*	*-35%*
Photochemical ozone formation	*-33%*	*-37%*	*-23%*	*-33%*
Resource use, fossils	*-18%*	*-31%*	*-13%*	*-33%*
Resource use, minerals and metals	+7%	**+134%**	+8%	**+120%**
Water use	**+372%**	**+236%**	**+394%**	**+219%**

* The results of the sub-scenarios involving the use of the three different types of rDME have been averaged.

As easily predictable, an increase in absolute impacts is observed across all categories when transitioning from the B-segment to the C-segment car. The use of the innovative blends shows improvement over petrol in five impact categories, including climate change, for both segments, with reductions ranging from 13% to 36%. The use of electric cars, for both segments, also shows improvement over petrol in five impact categories but deterioration in ten, especially for water use, ionising radiation, non-carcinogenic human toxicity, and freshwater eutrophication. All the alternatives, when compared to petrol, require a relevant increase in water use. Comparing the estimated percentage differences for SI and electric cars, the former would offer better environmental performance in 11 of the 16 impact categories for the B-segment and in 10 out of 16 for the C-segment, but not for the particularly significant one of climate change. More specifically, for this impact category, the innovative blend of GPL, bio-GPL, and rDME reduces impacts on average by 21% in B-segment cars and 16% in C-segment car, whilst the electric car lowers impacts by 36% in B-segment cars and 38% in C-segment car. The impact on climate change is primarily due to fossil CO_2 and CH_4 emissions from petrol and LPG

combustion, and to the activities related to the production of energy carriers and cars. In the case of petrol cars, more than half of the impact is due to exhaust emissions, with the corresponding reduction resulting for the innovative blend originated by the inclusion of biofuels. The electric car emerges as the best option for climate change because the absence of exhaust emissions is more than capable to offset the higher impacts associated with car production and with battery recharging.

References

[1] Sacchi R., Bauer C., “Life-cycle inventories for on-road vehicles”, (2023). https://doi.org/10.5281/zenodo.5156043
[2] Weymar E., Finkbeiner M., “Statistical analysis of empirical lifetime mileage data for automotive LCA”, Int. J. Life Cycle Assess., vol. 21, no. 2, pp. 215–223, (2016).
[3] ISO, “ISO 14044:2006/Amd 2:2020 Environmental management - Life cycle assessment - Requirements and guidelines”, (2020). https://www.iso.org/standard/76122.html
[4] Wernet G., Bauer C., Steubing C., Reinhard J., Moreno-Ruiz E., Weidema B., “The ecoinvent database version 3 (part I): overview and methodology”, Int. J. Life Cycle Assess., vol. 21, no. 9, pp. 1218–1230, (2016). doi: 10.1007/s11367-016-1087-8.
[5] European Commission, “Commission Recommendation (EU) 2021/2279”, Off. J. Eur. Union, vol. 471, (2021).
[6] Unem, “Produzione delle raffinerie (volumi)”, (2021). https://www.unem.it/i-numeri-dellenergia/italia/
[7] Unem, “Importazioni di benzine, gasoli e olio combustibile per Paesi di provenienza”, (2022). https://www.unem.it/i-numeri-dellenergia/italia/
[8] Eni S.p.A., “Raffineria di Venezia - Dichiarazione Ambientale 2020-2022 - Edizione 2021”, (2021). https://www.eni.com/assets/documents/ita/attivita/mid-downstream/Dichiarazione-Ambientale-Venezia-2021.pdf
[9] Eni S.p.A., “Progetto ‘Steam Reforming’”, (2022). https://va.mite.gov.it/it-IT/Oggetti/Documentazione/8802/12947
[10] Eni S.p.A., “Riesame AIA - Scheda A: Allegati”, (2020). https://va.minambiente.it/en-GB
[11] Eni S.p.A., “Riesame AIA - Scheda B: Dati e notizie sull’impianto attuale”, (2019). https://va.minambiente.it/en-GB
[12] European Commission, “COM(2020) 952 final”, (2020). https://eur-lex.europa.eu/legal-content/GA/TXT/?uri=CELEX:52020DC0952
[13] Fernández-Dacosta C., Shen L., Schakel W., Ramirez A., Kramer G.J., “Potential and challenges of low-carbon energy options: Comparative assessment of alternative fuels for the transport sector”, Appl. Energy, vol. 236, pp. 590–606, (2019). doi: 10.1016/j.apenergy.2018.11.055.
[14] Meunier N., Chauvy R., Mouhoubi S., Thomas D., De Weireld G., “Alternative production of methanol from industrial CO2”, Renew. Energy, vol. 146, pp. 1192–1203 (2020). doi: 10.1016/j.renene.2019.07.010.
[15] GSE S.p.A., “Energia nel settore dei trasporti 2005-2021”, (2022). https://www.gse.it/documenti_site/Documenti GSE/Rapporti statistici/Energia nel settore Trasporti 2005-2021.pdf
[16] Galusnyak S.C., Petrescu L., Chisalita D.A., Cormos C-C., “Life cycle assessment of methanol production and conversion into various chemical intermediates and products”, Energy, vol. 259, p. 124784, (2022).
[17] Terna S.p.A., “Produzione 2022”, (2023). https://www.terna.it/it/sistema-elettrico/statistiche/pubblicazioni-statistiche
[18] Terna S.p.A., “Dati statistici sull’energia elettrica in Italia - 2021”, (2022). https://www.terna.it/it/sistema-elettrico/statistiche/pubblicazioni-statistiche
[19] Afzal S., Singh A., Nicholson S.R., Uekert T., DesVeaux J.S., Tan E.C.D., Dutta A., Carpenter A.C., Baldwin R.M., Beckham G.T., “Techno-economic analysis and life cycle assessment of mixed plastic waste gasification for production of methanol and hydrogen”, Green Chem., vol. 25, no. 13, pp. 5068–5085, (2023).
[20] EEA, “EMEP/EEA air pollutant emission inventory guidebook 2023”, (2023). https://www.eea.europa.eu/publications/emep-eea-guidebook-2023
[21] UNRAE, “Immatricolazioni autovetture e fuoristrada BEV - 9 mesi 2023”, (2023). https://unrae.it/dati-statistici/immatricolazioni/6436/immatricolazioni-bev-per-modello-settembre-2023
[22] Quattroruote, “Listino Nuovo”, (2023). https://www.quattroruote.it/listino/
[23] Lucas A., Alexandra Silva C., Costa Neto R., “Life cycle analysis of energy supply infrastructure for conventional and electric vehicles”, Energy Policy, vol. 41, pp. 537–547, (2012).

Title: Sulfide-rich biogas conversion into microbial protein and S-amino acids through a mixed culture-based fermentation process

Author(s): Marica Areniello*[1], Silvio Matassa[2], Giovanni Esposito[3], Piet N.L. Lens[4]

[1] *Department of Microbiology, University of Galway, Galway, Ireland, m.areniello1@universityofgalway.ie*
[2] *Department of Civil, Architectural and Environmental Engineering, University of Naples Federico II, Naples, Italy, silvio.matassa@unina.it*
[3] *Department of Civil, Architectural and Environmental Engineering, University of Naples Federico II, Naples, Italy, gioespos@unina.it*
[4] *Department of Microbiology, University of Galway, Galway, Ireland, piet.lens@universityofgalway.ie*

Keyword(s): Single cell protein; sulfide-rich biogas; sulfur amino acids; methane oxidizing bacteria; sulfur oxidizing bacteria.

Introduction

The traditional linear economy approach of extraction, production, use and disposal of resources is nowadays becoming unsustainable in the face of global population growth leading to increasing energy and feedstocks demands as well as high waste generation and environmental damages. Such pressing challenges are urgently calling for a more sustainable circular management of resources [1].
In this framework, microbial fermentation technologies can potentially enable the recovery of untapped carbon, energy and nutrients from organic waste and residues towards the production of valuable bio-based products, such as microbial protein (MP), having applications in the feed/food market and beyond [2]. The treatment of organic waste through biological processes such as anaerobic digestion (AD), can represent an efficient strategy to produce clean carbon and energy substrates for gas-based microbial fermentation. Indeed, besides its mere conventional energetical valorization, biogas produced through the AD of organic waste (containing CH_4, CO_2 and other trace gases, such as H_2S or NH_3) is suitable for the biological conversion into high-quality MP [3].
Importantly, the suitability of biogas for biological processes is potentially limited by the presence of trace gases, in particular of H_2S, which can potentially inhibit the microbial conversion operated by methane oxidizing bacteria (MOB). To overcome this hurdle, the possibility to use a mixed culture-based fermentation process by coupling MOB with sulfur oxidizing bacteria (SOB) has already been demonstrated in preliminary batch screening studies [4].
The present study investigated the process of sulfide-rich biogas conversion into MP in two bubble column bioreactors, focusing on process performance in terms of volumetric productivity, biomass yield and protein content. Specifically, the effect of simulated and raw biogas, with different composition and increasing sulfide levels, on the overall process performances as well as on the amino acids profile of the produced MP were evaluated.

Material and Methods

Two 1.05 L bubble column reactors with a working volume of 1 L were operated under the same conditions as biological replicates. The inoculum, consisting of a MOB-SOB mixed culture enriched with synthetic biomethane and sulfide as described by Areniello et al. [4], was cultured in an ammonium mineral salts (AMS) medium. The first 80 days of experiments were aimed at the optimization of the process performance and, once the optimal operating conditions in terms of HRT, mineral medium composition and buffer capacity were reached, the subsequent experimental phases (lasting from days 80 to 187) were aimed at testing the influence of several experimental parameters on the process (Table 1).
Until day 69, during the initial optimization phase, the reactors were run in a fed-batch mode. Subsequently, and until the end of the experiments (day 187), they were operated in continuous mode by setting a liquid influent and effluent flow of 400 mL/d, thereby setting a hydraulic retention time of 2.5 days. The supply of the gas to the reactors was constantly guaranteed through a flow rate of 10 L/d of a mixture of oxygen, CH_4 (synthetic biomethane) and CO_2 (synthetic biogas), or of oxygen and real biogas collected from an anaerobic digestion plant (Green generation Ltd, Kildare, Ireland). When synthetic biogas was used, sulfides were provided as sodium sulfide ($Na_2S{\cdot}9H_2O$) dissolved in the liquid medium as proposed by Xu et al. [5], to simulate the presence of H_2S in the gas phase.

Table 1. Overview of the operating conditions tested from day 80, after the optimization phase.

Phase	Duration (days)	Liquid medium	Gas substrates	Gas composition	H_2S concentration
1	80-93	AMS medium	Synthetic biomethane (CH_4), O_2	CH_4:O_2 = 2:3	1500 ppm (equivalent)
2	93-106		Synthetic biogas (CH_4, CO_2), O_2	CH_4:CO_2 = 70:30 CH_4:O_2 = 2:3	1500 ppm (equivalent)
3	106-123			CH_4:CO_2 = 50:50 CH_4:O_2 = 2:3	1500 ppm (equivalent)
4	123-137			CH_4:CO_2 = 70:30 CH_4:O_2 = 2:3	3000 ppm (equivalent)
5	137-148			CH_4:CO_2 = 70:30 CH_4:O_2 = 2:3	4000 ppm (equivalent)
6	148-162		Real biogas, O_2	CH_4:CO_2 = 50:50 CH_4:O_2 = 2:3	2000 ppm
7	162-169	AMS medium without sulfates		CH_4:CO_2 = 50:50 CH_4:O_2 = 2:3	2000 ppm
8	169-176	AMS medium	Synthetic biogas (CH_4, CO_2), O_2	CH_4:CO_2 = 50:50 CH_4:O_2 = 2:3	2000 ppm (equivalent)
9	176-187			CH_4:CO_2 = 50:50 CH_4:O_2 = 2:3	0 ppm

Results and Conclusions

Table 2 summarizes the main results arising from the experimental activities. Concerning the influence of the biogas composition, the higher methane content in the synthetic biogas was more effective in terms of biomass growth as the biomass concentration decreased by 13.6% when moving from a CH_4:CO_2 ratio of 70:30 to a ratio of 50:50 (from phases 2 to 3). Moreover, the simulation of increasing sulfide levels in the synthetic biogas had detrimental effects on the biomass growth as the biomass concentration decreased of 29.6% and 42.1% when moving from 1500 ppm of equivalent H_2S to 3000 and 4000 ppm, respectively (from phase 2 to 4 and 5, respectively). The decreased biomass concentration in the presence of higher sulfide concentrations was coupled with a lower biomass productivity and yield, the latter being 21.8% and 32.2% lower in phase 4 and 5, respectively, than in phase 2.
The utilization of real biogas in phase 6 led to an increase of the biomass content of 20.0% then in the previous phase, probably due to the lower presence of sulfides (Table 1.1), which also led to increases of both volumetric productivities and biomass yields of 16.1% and 31.2%, respectively. Moreover, even biomass concentration and yield increased, by reaching values close to the ones of previous phases with synthetic biogas and more similar sulfide levels (phases 3 and 4).
Overall, the process worked with encouraging performances with quite high sulfide levels despite similar studies demonstrated the inhibition of methanotrophs even with lower H_2S concentrations, e.g. 200-500 ppm [6,7]. The absence of sulfides (phase 7) instead had detrimental effects on all the key parameters of the process.

Table 2. Overview of the operating conditions tested from day 80, after the optimization phase.

Phase	Biomass concentration (mg VSS/L)	Protein (g/g VSS)	Methane consumption (%)	Volumetric productivity (mg VSS/L*d)	Biomass yield (g VSS/L*d*g CH_4-COD)
1	677.8	56%	61	271.2	0.050
2	559.9	57%	64	224.8	0.042
3	483.5	59%	52	195.7	0.049
4	394.2	57%	60	160.1	0.033
5	324.1	55%	59	131.9	0.028
6	389.0	58%	55	153.2	0.037
7	397.2	58%	58	162.6	0.039
8	385.4	58%	49	151.8	0.041
9	301.3	52%	54	125.1	0.032

Interestingly, the different operating conditions seemed not to have any significant effect on the biomass protein content throughout all the experiments, with protein concentrations within a range of 49-64% g protein/g VSS. Nevertheless, particularly relevant results came from the analysis of the amino acids (AA) profile of the biomass which was various and abundant, including a wide range of essential AA (Figure 1). Interestingly, according to Soda et al. [8] that predicted the stimulating effects of H_2S on the S-amino acids production, the increasing sulfide concentrations enhanced the production of sulfur-containing essential AA, *i.e.*, cysteine and methionine, which have a crucial role in view of the applications of the extracted biomass in the feed/food industry. Indeed, methionine and cysteine were

3.7 and 2.0 times higher, respectively, in the presence of 4000 ppm of H_2S than in the absence of sulfides in the biogas.

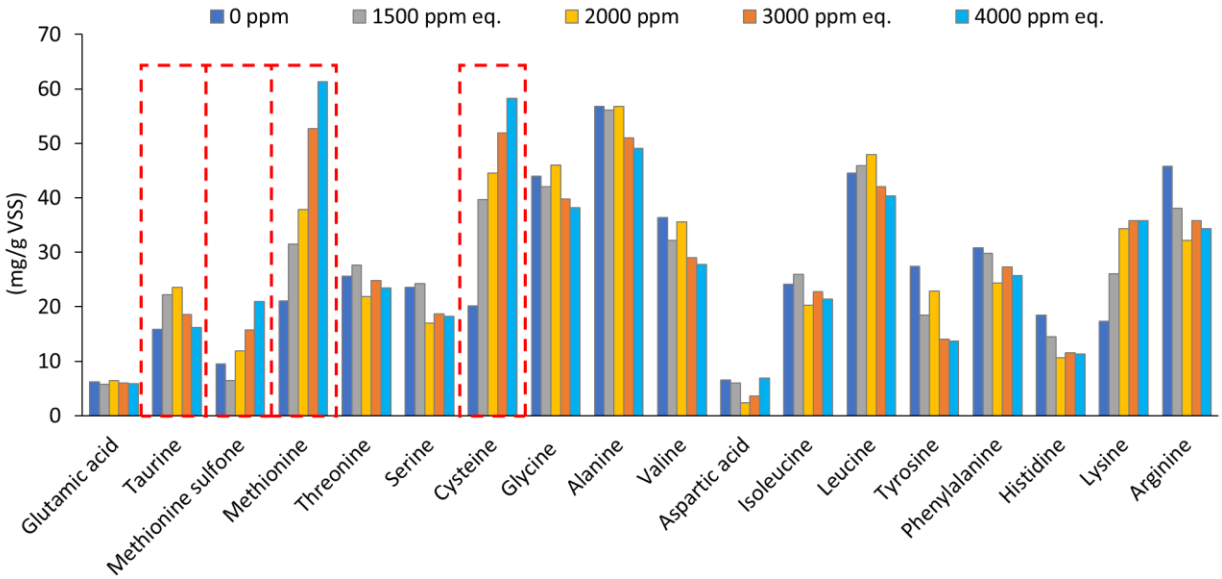

Figure 1. Amino acids profile of the biomass in presence of 1500 ppm of equivalent H_2S, 3000 ppm of equivalent H_2S, 4000 ppm of equivalent H_2S, 2000 ppm of H_2S, and 0 ppm of H_2S. The red dashed line indicates the S-amino acids positively affected by the sulfide presence.

In conclusion, the feasibility of the process of sulfide-rich biogas conversion into MP through a mixed culture of MOB and SOB has been demonstrated in this study, paving the way for the raw biogas conversion into high-value products, potentially rich in S-amino acids.

References

[1] S. Venkata Mohan, S. Dahiya, K. Amulya, R. Katakojwala, T.K. Vanitha, Can circular bioeconomy be fueled by waste biorefineries — A closer look, Bioresour. Technol. Reports 7 (2019) 100277. https://doi.org/10.1016/j.biteb.2019.100277.
[2] K. Spalvins, L. Zihare, D. Blumberga, Single cell protein production from waste biomass: Comparison of various industrial by-products, Energy Procedia 147 (2018) 409–418. https://doi.org/10.1016/j.egypro.2018.07.111.
[3] M. Areniello, S. Matassa, G. Esposito, P.N.L. Lens, Biowaste upcycling into second-generation microbial protein through mixed-culture fermentation, Trends Biotechnol. 41 (2023) 197–213. https://doi.org/10.1016/j.tibtech.2022.07.008.
[4] M. Areniello, S. Matassa, G. Esposito, P.N.L. Lens, Microbial protein production from sulfide-rich biogas through an enrichment of methane- and sulfur-oxidizing bacteria, Bioresour. Technol. 383 (2023) 129237. https://doi.org/10.1016/j.biortech.2023.129237.
[5] M. Xu, H. Zhou, X. Yang, I. Angelidaki, Y. Zhang, Sulfide restrains the growth of Methylocapsa acidiphila converting renewable biogas to single cell protein, Water Res. 184 (2020) 116138. https://doi.org/10.1016/j.watres.2020.116138.
[6] M. Càceres, J.C. Gentina, G. Aroca, Oxidation of methane by Methylomicrobium album and Methylocystis sp . in the presence of H2S and NH3, Biotechnol. Lett. 36 (2014) 69–74. https://doi.org/10.1007/s10529-013-1339-7.
[7] W. Zhang, X. Ge, Y.-F. Li, Z. Yu, Y. Li, Isolation of a methanotroph from a hydrogen sulfide-rich anaerobic digester for methanol production from biogas, Process Biochem. 51 (2016) 838–844. https://doi.org/10.1016/j.procbio.2016.04.003.
[8] K. Soda, Microbial Sulfur Amino Acids: An Overview, Methods Enzymol. 143 (1987) 453–459. https://doi.org/10.1016/0076-6879(87)43080-2.

Title: Recovery of carboxylic acids by employing sequential cation and anion exchange resins: studies using an actual effluent at semi pilot scale

Author(s): Gonzalo A. Martinez*, Andrea Negroni, Maurizio Mancini, Fabio Fava, Lorenzo Bertin

[1] *Department of Civil, Chemical, Environmental and Materials Engineering (DICAM), University of Bologna, via Terracini, 28, I-40131 Bologna, Italy City, Country, gonzalo.martinez3@unibo.it*

Keyword(s): volatile fatty acid; bioprocess; ion exchange resin; agro-industrial side-stream valorisation; carboxylate platform; extraction; ammonia; phosphate

Abstract

Introduction

The valorisation of agro-industrial and urban biowaste (UBWs, e.g. municipal surplus activated sludge and organic fraction of solid waste) through the production of carboxylic acids (CAs) has been intensively studied during the last years. [1–3] The interest in this subject lies in the possibility of exploiting CAs as the precursors of many products referring to several industrial fields (e.g. pharmaceutical, food, energy and materials, among others) with a robust and economic technology such as the open mixed cultured anaerobic fermentation. However, the low obtained CAs' titer streams (*ca.* 30 g L^{-1}), which make it difficult to feed consecutive target units (*e.g.*, esterification or fed-batch fermentation) with such CAs-rich stream ($UBWs_{\_Acid}$). In this framework, various promising technologies were reported for recovering CAs from fermentation broths, e.g.: nanofiltration/reverse osmosis [4], electrodialysis [5], spontaneous separation by acidification [6] or liquid-liquid extraction [7]. The most appropriate operation depends on the final purpose, e.g.: obtainment of single highly purified VFAs as fine chemicals or the esterification of the produced CAs that requires their separation from the aqueous fermentation broth since water is a byproduct of esterification reaction, CA recovery in an organic solvent (e.g. ethanol) would unbalance the esterification equilibrium to products, resulting in improved reaction yields [3].

To this purpose, the application of an anionic resin to recover CAs from an actual effluent was first reported by *Rebecchi et al.* with adsorption yield of ca. 30% [8]. However, higher performances are required in the perspective of developing an economically feasible process. As a whole, the proposed strategy is affected by the fact that CA-rich broths are usually close to neutral pH ($5 < pH < 7$), this meaning that each mole of carboxylate is paired with a cation (e.g. Na^+) arising from the base (e.g. NaOH) added during the fermentation to adjust the pH level. Thus, carboxylates are less available for ionic adsorption due to the formation of ion pairs in the solution ($R\text{-}COO^- Na^+$) [9]. This is in accordance with the fact that a NaOH solution is usually applied for desorbing the anions from the resin in an almost stoichiometric relation [8]. Besides, also the inorganic anions (e.g. Cl^-, PO_4^{x-}) interfere on CAs adsorption.

Notarfrancesco et al. demonstrated that the reason of the low adsorption yields are those competitive ion-interactions by performing several experiments -at flask scale- aiming to determine the CAs adsorption isotherms. To this aim, four different actual broths were pretreated with a cation exchange resin for removing Na^+ at different levels (final pH 1.5-2.4). Thereafter, anion adsorption isotherms were determined using the four decationised broths. Besides confirming anions competition for resin exchange sites, results also evidenced that Na^+ competed with the anionic resin exchange sites for binding the CAs, while other organic compounds else than CAs (COD_{Other}) exerted a negligible

competition for CA adsorption. A homogeneous mass action ideal model, that also considers Na^+ competition, was calibrated using the collected data. It shows a very good capability to predict adsorption isotherms despite very dissimilar broths were used.[10]
Despite the mentioned evidences, the assessment using cationic and anionic adsorption columns is needed in order to confirm the ions competition mechanisms by means of a different experiment, i.e. breakthrough tests. This would also allow to obtain accurate and representative breakthrough (BT) curves data useful for analysing the process scale-up at its maximal potentiality. To these aims, a small pilot plant was set-up for studying the recovery process (**Figure 1**). Specifically, BT tests were carried out at different feeding rate as to determine the optimal condition.

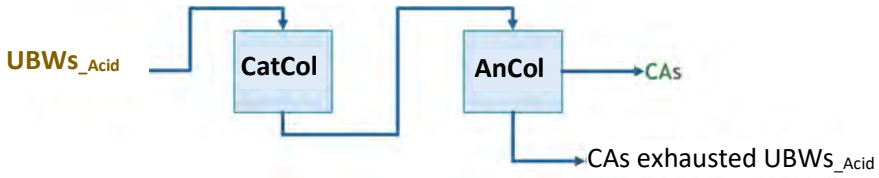

Figure 1: Process scheme for recovering CAs from acidified effluents (e.g. $UBWs_{\_Acid}$) by sequentially employing cationic (CatCol, for diminishing the pH) and anionic columns (AnCol, for adsorbing CAs).

Results and Discussions
The generation of the homogenous stock of decationised UBW-broth (to be used later in the anions adsorption studies) was obtained during the CatCol process optimization assessment. Hence, the breakthrough (BT) assessment at different feeding rates were carried out using the cationic column (CatCol) in the conventional operating mode, i.e. the orthodox packed bed mode. **Figure 2** shows an example of the obtained BT-curves at different feeding rates. Besides the feasibility of extracting Na^+/NH_4^+ and the optimisation of the feeding rates, it was demonstrated that the COD_{Other} (neither the fraction behaving as cations) do not interfere with Na^+/NH_4^+ adsorption (data not shown). Thereafter, the expanded bed mode was assessed as well since it could represent a condition not requiring an exhaustive filtration for removing the fine suspended solids, i.e. the hydraulic classification with the bottom-up flow would allow retaining the resin while the small solids pass through the column. Due to final project goal, this was tested by using a lab prepared solution which simulated the actual broth (data

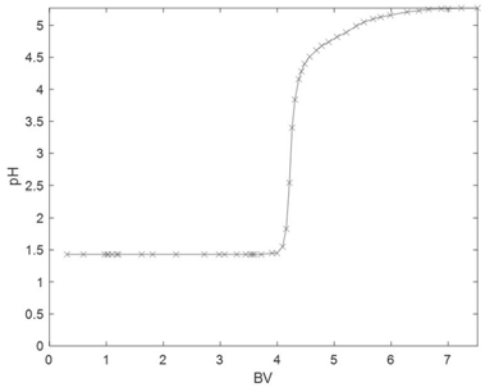

Figure 2: CatCol BT test carried out in packed bed mode by feeding the UBW-broth at 5.1 cm/min. Outlet profile of pH levels.

not shown). Briefly, owing to less axial dispersion effects, the obtained BT-curves were also S shape but steeper than those acquired in packed bed mode and the breaking points were much closer to τ = 1.

While pre-treating the $UBWs_{\_Acid}$ with the CatCol, first experiments in the AnCol were carried out using a lab prepared solution which simulated the decationised broth. This allowed to assess the differences between packed and expanded bed mode. Considering the obtained results, CAs recovery from the actual broth (already decationised) was carried out in expanded bed mode which allowed to use almost the entire installed capacity, **Figure 3** shows an example of a BT test. Importantly, obtained results confirmed that it is possible to recover 100% of the CAs occurring (data not shown) without needing to optimise the broth's pH but by previously decationising the broth. The same BT tests showed also that the COD_{Other} resulted weaker than CAs. Only the inorganic anions compete with CAs for an adsorption site, which suggest two options: 1) to operate the AnCol -as in this work- until the BT point for total anions; or 2) to install two AnCols, the first one for inorganic anions and the second one for the CAs.

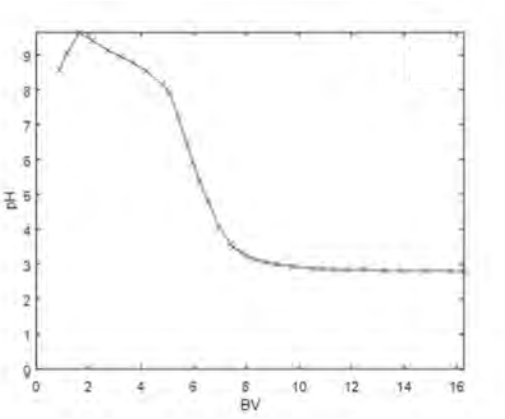

Figure 3: AnCol breakthrough test carried out in expanded bed mode and by feeding the decationised UBW-broth at 6 cm/min. Outlet profiles of pH levels.

Importantly, preliminary tests indicated that CAs can be desorbed from weak anionic resins by using CO_2-expanded ethanol, this allowing to avoid salts by-product generation. Such strategy was previously reported by *Cabrera et al* [11] for desorbing CAs from strong anionic resin. Yet, this work still represents an improvement with respect to that since the direct application of a strong anion exchange resin (without decationisation pretreatment) still suffer from inorganic cation interferences which results in prompt breakthrough and from the low CAs titer in the desorption eluent. Finally, a very preliminary economic analyses indicate overall costs could be potentially competitive depending on the process set-up.

References

[1] EU Project-RES URBIS, Resources from Urban Biowaste, EU H2020. (2020). https://www.resurbis.eu/ (accessed March 18, 2020).

[2] G. Moretto, I. Russo, D. Bolzonella, P. Pavan, M. Majone, F. Valentino, An urban biorefinery for food waste and biological sludge conversion into polyhydroxyalkanoates and biogas, Water Res. 170 (2020) 115371. doi:https://doi.org/10.1016/j.watres.2019.115371.

[3] L. di Bitonto, S. Menegatti, C. Pastore, Process intensification for the production of the ethyl esters of

volatile fatty acids using aluminium chloride hexahydrate as a catalyst, J. Clean. Prod. 239 (2019) 118122. doi:https://doi.org/10.1016/j.jclepro.2019.118122.

[4] J.M.B. Domingos, G.A. Martinez, E. Morselli, S. Bandini, L. Bertin, Reverse osmosis and nanofiltration opportunities to concentrate multicomponent mixtures of volatile fatty acids, Sep. Purif. Technol. 290 (2022) 120840. doi:10.1016/J.SEPPUR.2022.120840.

[5] J.M.B. Domingos, S. Puccio, G.A. Martinez, N. Amaral, M.A.M. Reis, S. Bandini, F. Fava, L. Bertin, Cheese whey integrated valorisation: Production, concentration and exploitation of carboxylic acids for the production of polyhydroxyalkanoates by a fed-batch culture, Chem. Eng. J. 336 (2018) 47–53. doi:10.1016/j.cej.2017.11.024.

[6] G.A. Martinez, S. Puccio, J.M.B. Domingos, E. Morselli, C. Gioia, P. Marchese, A.M. Raspolli Galletti, A. Celli, F. Fava, L. Bertin, Upgrading grape pomace contained ethanol into hexanoic acid, fuel additives and a sticky polyhydroxyalkanoate: an effective alternative to ethanol distillation, Green Chem. 24 (2022) 2882–2892. doi:10.1039/D2GC00044J.

[7] M. Atasoy, I. Owusu-Agyeman, E. Plaza, Z. Cetecioglu, Bio-based volatile fatty acid production and recovery from waste streams: Current status and future challenges, Bioresour. Technol. (2018). doi:10.1016/J.BIORTECH.2018.07.042.

[8] S. Rebecchi, D. Pinelli, L. Bertin, F. Zama, F. Fava, D. Frascari, Volatile fatty acids recovery from the effluent of an acidogenic digestion process fed with grape pomace by adsorption on ion exchange resins, Chem. Eng. J. 306 (2016) 629–639. doi:10.1016/J.CEJ.2016.07.101.

[9] M.A. Mehablia, D.C. Shallcross, G.W. Stevens, Prediction of multicomponent ion exchange equilibria, Chem. Eng. Sci. 49 (1994) 2277–2286. doi:https://doi.org/10.1016/0009-2509(94)E0041-N.

[10] S. Notarfrancesco, E. Morselli, G.A. Martinez, W. Harasimiuk, J.M.B. Domingos, A. Negroni, F. Fava, L. Bertin, Improved recovery of carboxylic acids using sequential cationic-anionic adsorption steps: A highly competitive ion-equilibrium model, Sep. Purif. Technol. 261 (2021) 118253. doi:10.1016/j.seppur.2020.118253.

[11] C.I. Cabrera-Rodríguez, L. Paltrinieri, L.C.P.M. De Smet, L.A.M. Van Der Wielen, A.J.J. Straathof, Recovery and esterification of aqueous carboxylates by using CO2-expanded alcohols with anion exchange, Green Chem. 19 (2017) 729–738. doi:10.1039/c6gc01391k.

Electrocatalytic acid reduction of carboxylic acids by using Cu electrode.

Rainy Alves de Sousa*[1], Suelya da Silva Mendonça de Paiva[1], Carlos Alberto Martínez-Huitle[1], Elisama Vieira dos Santos[1], Justo Lobato[2], Manuel A. Rodrigo-Rodrigo[2], Raúl García-Cervilla[2]

[1] *Renewable Energies and Environmental Sustainability Research Group, Institute of Chemistry, Federal University of Rio Grande do Norte, Natal, Brazil*
[2] *Department of Chemical Engineering, Universidad de Castilla La Mancha, Ciudad Real, Spain*

Keyword(s): Electrocatalytic reduction, Carboxylic acid, PEM, Cell design, Biorrefinery.

Abstract

1. Introduction

The development of effective wastewater treatment solutions will have a beneficial impact on the achievement of the sustainable development goals, which are currently being discussed by global governments. In light of these considerations, the development of new treatment processes is of paramount importance. Electrochemical-based processes demonstrate considerable potential for environmental remediation, largely due to the advent of innovative materials and reactors. These methods are emerging as reliable alternatives to more conventional biological and physicochemical methods, as well as to classic advanced oxidation processes such as ozonation, heterogeneous photocatalysis, or the Fenton process. Additionally, they can be combined with renewable energy sources [1].
In the initial stages of development, the primary objective of electrochemical technologies was the complete mineralization of organic compounds. This approach aimed to minimize the impact of discharging treated waste into the environment by completely destroying the organics. Nevertheless, numerous investigations have documented challenges in achieving complete oxidation of organic pollutants in diverse water matrices through various electrochemical methods. Based on the existing literature, the oxidation of various organics primarily results in the formation of various by-products, which can be aromatic or non-aromatic [2]. Carboxylic acids represent the latter category, and these have diverse applications in the chemical industry and can be utilized as raw materials to obtain a range of valuable chemical products, including sustainable synthetic fuels, aldehydes, and others.
The reduction of carboxylic acids and their derivatives represents a highly relevant transformation in the field of synthetic organic chemistry. The reduction of carboxylic acids is expected to result in the formation of aldehydes, alcohols, or even hydrocarbons.
In light of the aforementioned considerations, the present study aims to employ the electrocatalytic reduction of a range of carboxylic acids derived from the electrochemical degradation of wastewater generated by the wine industry. This process is intended to facilitate the conversion of these acids into value-added compounds, including sustainable fuels.

2. Material and Methods

The cell where the experiments were carried out was designed in Fusion 360® and printed in resin on a printer (formlabs 3B). A schematic of the cell assembly can be seen in the Figure 1. A 25x25 mm pure Cu sheet was used as cathode and a RuO_2 dimensionally stable anode (DSA) was used as anode. The anolyte chamber and the catholyte were separated by a proton exchange membrane (PEM) (Nafion™).

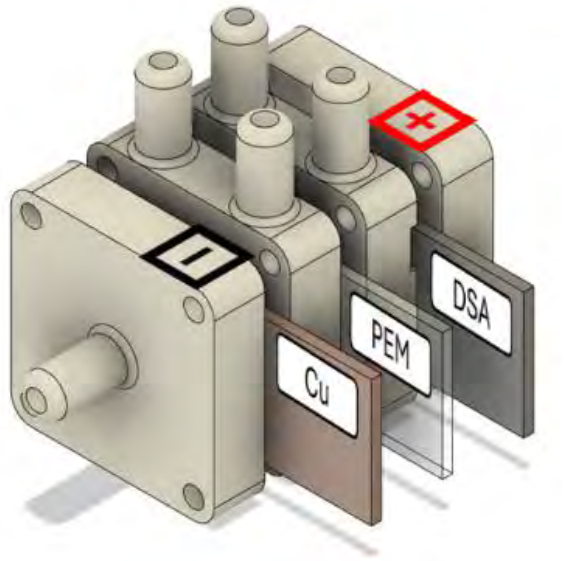

Figure 1. Schematic of the cell assembly used in the carboxylic acid reduction experiments.

In anode was added an aqueous solution with H_2SO_4 at 500 mM. In cathode was added different concentrations (50 - 100 mM) of oxalic, acetic, and formic acid in aqueous solution at acid (by adding H_2SO_4) and alkaline (by adding KOH) pH. Three of the most common acids as by-products in the oxidation of organic matter in wastewater [3]. Electroreduction of acids was carried out at different current densities, J_A, (0-400 mA·cm^2). Solutions was always prepared in milliQ water. The reaction time used in the experiments was 2 - 8 h.

3. Results

Experiments at alkaline pH (pH > 10) showed zero conversion of the acids used (oxalic, acetic and formic acid). This can be explained by an electrostatic repulsion between the Cu electrode (negatively charged) and the carboxylate generated by the alkaline medium.

Experiments at acid pH were always carried out at pH values significantly lower than the pK_a of the respective carboxylic acid. In Figure 2, can be seen the conversion obtained in the experiment under acid pH conditions for oxalic acid. As can be seen, the experiment at 2 h of reaction time was not observed effect of the current density in the conversion of oxalic acid. However, in experiment at 8 h of reaction time was observed an increase of the conversion of oxalic acid with the current density applied.

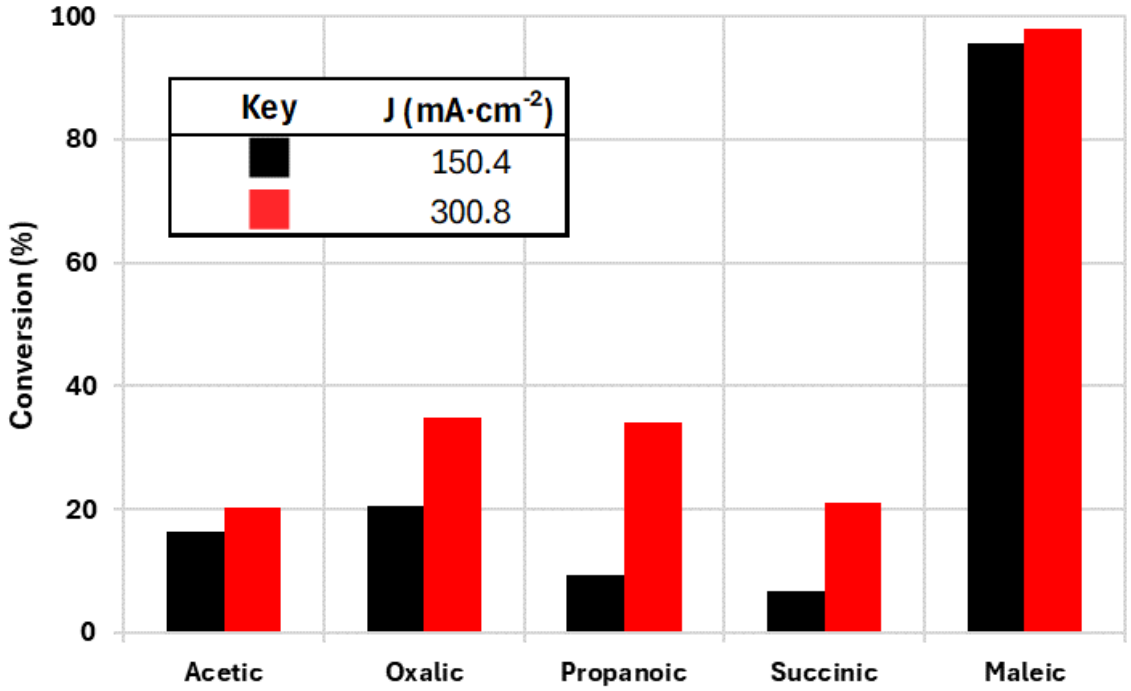

Figure 2. Conversion of carboxylic acids after electroreduction with Cu cathode under acid conditions (pH = 0.95-1.00).

This increase of the conversion under acid conditions could be explained by a higher electrophilicity of the acid molecule. The acidity of the carboxyl group almost always interferes with the reactions to be carried out in an alkaline medium, since it neutralizes the base and prevents them from taking place. Therefore, the nucleophilic attack on the carbonyl carbon should be carried out in an acidic medium. The reactions of carboxylic acids are carried out in mineral or Lewis acid medium. In this way the interference of the acidity of the OH group is avoided and the electrophilicity of the carbon is increased by partial protonation of the carbonyl group, which has basic properties [4]. The mechanism is shown in Figure 3.

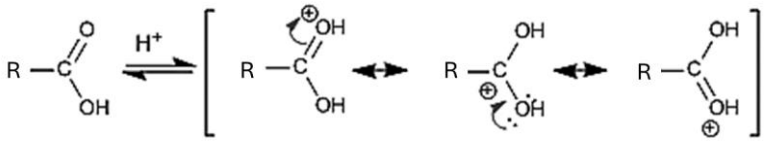

Figure 3. Mechanism that by protonation of carbonyl oxygen activates carboxylic acid.

TOC of the samples was analysed, and no was observed a considerable loss of C, that can be explained by volatilization of the samples during the experiments. Experiment with acetic and formic acid was observed an increase of the conversion.

4. Conclusions

In this work was confirmed the electroreduction of three of the main acids that could be produced by oxidation of wastewater with organic contaminants by using acid conditions. This fact is of extraordinary relevance since a great difficulty in the electroreduction of carboxylic acids has been found in the

literature [5, 6]. However, the results obtained are far from optimal, and deeper investigation of the process is needed.

5. Acknowledgments

This work was supported by Spanish Ministry of Science, Innovation and Universities through the ElectroRefin4O project (PID2022-138401OB-I00). Rainy Sousa and Suelya Paiva are acknowledged by for the financial support given by CNPq as fellowships and projects (403008/2022-0 and 408110/2022-8). Raúl García Cervilla is acknowledged for the Spanish Juan de la Cierva postdoctoral grant. (JDC2022-049619-I).

References

[1] C. A. Martinez-Huitle, M. A. Rodrigo, I. Sires, and O. Scialdone, "A critical review on latest innovations and future challenges of electrochemical technology for the abatement of organics in water," *Applied Catalysis B-Environmental,* Review vol. 328, Jul 5 2023, Art no. 122430, doi: 10.1016/j.apcatb.2023.122430.

[2] E. V. dos Santos, C. A. Martinez-Huitle, and M. A. Rodrigo, "The electro-refinery in organics: A new arising concept for valorization of wastes," *Current Opinion in Electrochemistry,* Review vol. 39, Jun 2023, Art no. 101267, doi: 10.1016/j.coelec.2023.101267.

[3] J. Agbaba *et al.*, "Oxidation of natural organic matter with processes involving O3, H2, O2 and UV light: formation of oxidation and disinfection by-products," *Rsc Advances,* Article vol. 6, no. 89, pp. 86212-86219, 2016 2016, doi: 10.1039/c6ra18072h.

[4] J. McMurry and E. Simanek, *Fundamentals of organic chemistry*. Brooks/Cole Belmont, CA, 2011.

[5] E. Bertheussen, T. V. Hogg, Y. Abghoui, A. K. Engstfeld, I. Chorkendorff, and I. E. L. Stephens, "Electroreduction of CO on Polycrystalline Copper at Low Overpotentials," *Acs Energy Letters,* Article vol. 3, no. 3, pp. 634-640, Mar 2018, doi: 10.1021/acsenergylett.8b00092.

[6] S. Ikeda, T. Ito, K. Azuma, K. Ito, and H. Noda, "ELECTROCHEMICAL MASS REDUCTION OF CARBON-DIOXIDE USING CU-LOADED GAS-DIFFUSION ELECTRODES .1. PREPARATION OF ELECTRODE AND REDUCTION PRODUCTS," *Denki Kagaku,* Article vol. 63, no. 4, pp. 303-309, Apr 1995, doi: 10.5796/kogyobutsurikagaku.63.303.

Title: Innovative design and analysis of a flat panel photobioreactor featuring a customizable LED lighting system.

Author(s): Michele Carone[1], Graziano Frungieri[2], Mariachiara Zanetti[1], Marco Vanni[2], Vincenzo A. Riggio[1*]

[1] *Department of Environment, Land and Infrastructure Engineering, Politecnico di Torino, Corso Duca degli Abruzzi 24, 10129 Torino, Italy*
[2] *Department of Applied Science and Technology, Institute of Chemical Engineering, Politecnico di Torino, Corso Duca degli Abruzzi 24, 10129 Torino, Italy*

Keyword(s): Flat Panel Photobioreactor, CFD simulation, Numerical tracer experiment, LED lighting, *Acutodesmus obliquus*, *Galdieria sulphuraria*.

Abstract

Microalgae-based biorefinery processes are gaining particular importance to produce high-quality biomass and energy feedstock for several industrial markets. However, there are still several factors that contribute to poor yields of microalgae growth in current technologies. These include inadequate light management, inefficient gas exchange, limited control over temperature and pH, and susceptibility to contamination. Additionally, challenges associated with scalability and high operational costs of photobioreactors (PBR) further hinder the achievement of optimal yields in microalgae cultivation. This work presents a detailed characterization of a novel flat-panel PBR equipped with a tuneable LED lighting system (Fig. 1).

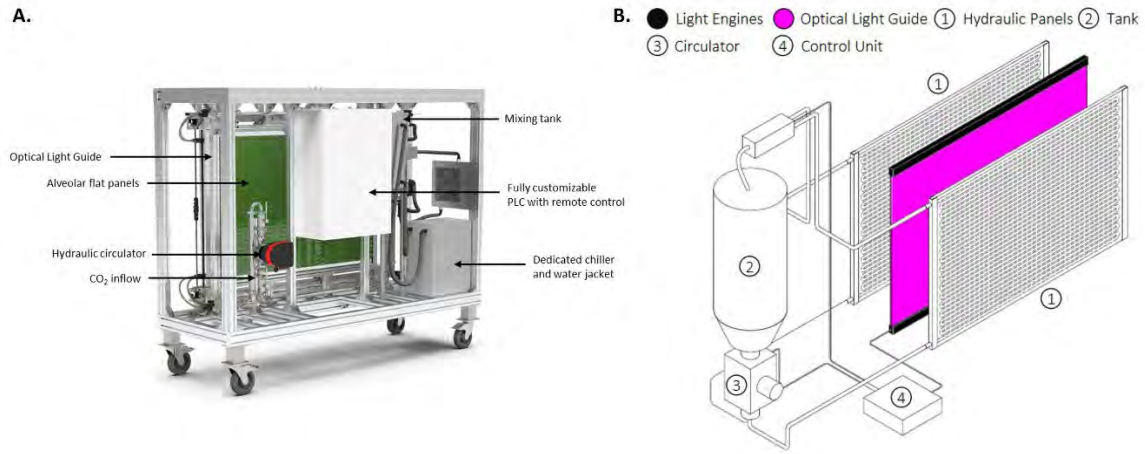

Figure 1: The alveolar flat-panel PBR. A. 3D isometric representation of the PBR. B. Schematic representation of the lighting engine. PLC: Programmable Logic Controller.

A computational fluid dynamics (CFD) study was conducted to characterize in detail the equipment from the hydrodynamics point of view. CFD results showed that the flow field has several peculiar features, such as vortices and a by-pass current, that can be expected to affect the light absorbance statistics, and the microalgae and nutrients spatial distributions. Considerations for both the system

optimization and the modelling of its behaviour during the operation were drawn. it has been observed that the system hydrodynamics has several peculiar features which must be expected to determine the statistics of light and flow field sampling by the microalgae. In the mixing tank (Fig. 2), two main regions of interest were observed: a vortex occupying almost completely the bulk of the tank, and a rather large lateral by-pass current traveling directly from the inlet to the outlet, counting for approximately 30% of the inlet flow and having a short residence time compared to what is obtained under perfectly mixed conditions.

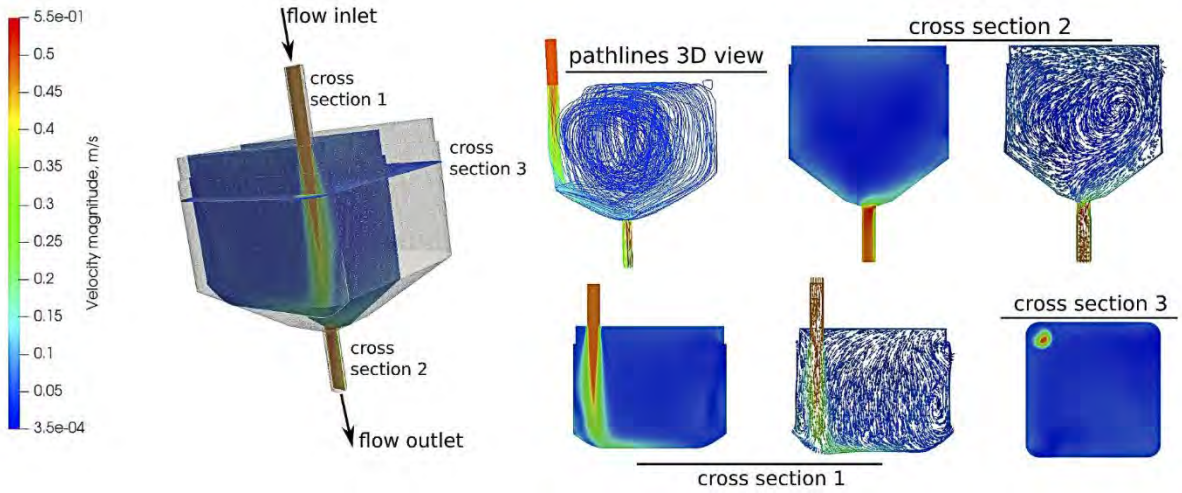

Figure 2: Visualization of the flow field in the mixing tank, by a contour plot representation of the velocity magnitude field and by fluid path lines. Three cross-sections are reported together with a 3D representation.

Also, the flat panel was seen to have a peculiar feature: close to the passage hole between two subsequent channels, the fluid was accelerated and two vortical regions were observed, causing the axial dispersion of the particles and a distinctive behaviour of the distribution of the residence times. Overall, the CFD analysis returned several useful indications for the technical optimization of the system and put the basis for a few further studies. Among these, the use of internal baffles or deflectors of the fluid flow will be considered, as these can improve the mixing and mass transfer performance of the equipment.

Additionally, two different microalgae strains, namely the green microalga *Acutodesmus obliquus* and the red extremophile *Galdieria sulphuraria*, each with specific growth parameters and spectra irradiation requirements (Fig. 3), were successfully cultivated using tailored light spectra. The biomass concentrations and yields achieved (yields on light of 0.58 and 0.45 g molph-1 for *A. obliquus* and *G. sulphuraria*, respectively) were consistent with currently reported productivities for both the species, highlighting the effectiveness of the adopted strategy for light management and the PBR overall design. The PBR has been equipped with a peculiar LED system capable of unpacking the entire visible spectrum. The possibility to dynamically change the light spectrum and intensity allows a high degree of customization of the cultivation process. This has been demonstrated by cultivating two completely different microalgae strains characterized by different growth parameters and spectral requirements. The biomass concentrations and yields achieved with both the strains, for which specific spectra were built, were perfectly in line with the data reported in the literature. These highlight the effectiveness of the adopted strategy for light management, which includes precise control of the light intensity and wavelength, and showcase the high efficiencies achieved by the PBR, with still ample room for improvement also considering the low light intensities applied.

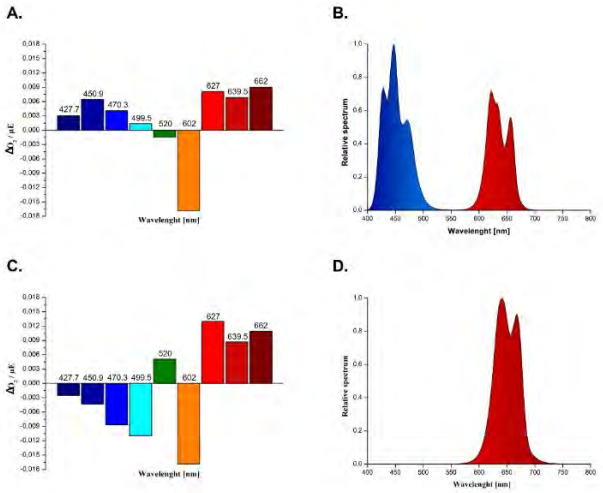

Figure 3: Light spectra customization. A. Wavelength-specific normalized oxygen evolution response (ΔO2 [mg L-1] / µE [µmolph m-2 s-1]) of A. obliquus. B. Resultant final spectrum employed for A. obliquus. C. Wavelength-specific normalized oxygen evolution response of G. sulphuraria. D. Resultant final spectrum employed for G. sulphuraria. (Kindly refer to section [2.4]). Graphs were produced with the software OriginPro8.5®.

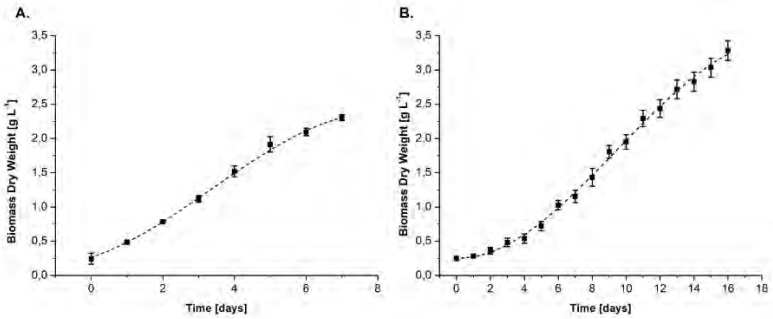

Figure 4: Photoautotrophic batches. A. Biomass concentration of Acutodesmus obliquus in the flat panel photobioreactor. B. Biomass concentration of Galdieria sulphuraria in the flat panel photobioreactor. Squares represent the dry weight measurements ± standard deviation (n = 2 A. obliquus, n = 3 G. sulphuraria). The dotted lines represent the third-degree polynomial interpolation (R2 = 0.999 A. obliquus, R2 = 0.997 G. sulphuraria) obtained with the software OriginPro8.5®.

The peculiar light management features would also open the investigation of wavelength-specific effects on biomass composition at a pilot scale. The PBR's hardware components, equipped with the multi-probes system – transductor - integrated PLC connections, make this prototype already suitable for remote monitoring and control of cultivation parameters to incorporate the Internet of Things (IoT). This aspect is becoming relevant as both academic research and industry are gradually moving towards process automation and remote operation. In this study, the behaviour of PBR's fluid dynamics as well as the influence of the composed spectra on the biomass productivity of the two different microalgae (*A. obliquus, G. sulphuraria*) was investigated [1]. After 7 days of cultivation, the *A. obliquus* cells reached a final concentration of 2.305 g L-1 (Fig. 4A.). The analysis of the growth curves showed a mean daily volumetric productivity (Px) of 0.295 g L-1 d-1 ± 0.03 (n = 3). The biomass yield on light energy was found to be on average 0.58 g molph-1 during the exponential phase, a value between the highest found in the literature for several green microalgae [2,3], although continuous experiments should be performed to address consistent estimations of this value. Nevertheless, to the authors' opinion, there is ample room for improvement, especially considering that in this work the batch experiments were

conducted with a relatively low averaged light intensity (150 µmolph m-2 s-1). Overall, the results obtained in this work are slightly higher than what was found in the previous study conducted with fluorescent lights, where the average light intensity on the panels' surface was found to be 120 µmolph m-2 s-1. This confirms the suitability of using the composed optimized spectrum for *A. obliquus*. In this work, it has been also decided to assess the photoautotrophic growth of *G. sulphuraria* strain 074W, one of the most performant autotrophic strains [4], to show the versatility of the presented PBR to investigate and achieve high biomass growth even with extremophiles, far from common green microalgae. After 16 days of cultivation, the cells reached a final concentration of 3.28 g L-1 (Fig. 4B.). The analysis of the growth curves showed a mean daily volumetric productivity Px of 0.22 g L-1 d-1 ± 0.03 (n = 3). Although the observed Px may seem quite low compared to other reported autotrophic batches [5,6], it is noteworthy pinpoint that the light intensity used is relatively low as well as, to the authors' knowledge, this work is one of the few studies where *G. sulphuraria* growth was conducted at real scale. Indeed, the biomass yield on light energy was found to be on average 0.45 g molph-1 during the exponential phase, a value in accordance with what has been found by Canelli and co-authors [7] in a 17 L annular column PBR (G. sulphuraria strains ACUF 064 and SAG 108.79), and close to the highest (0.5 – 0.65 g molph-1) reported for *G. sulphuraria* (ACUF 064 and 074G) grown in autotrophic conditions at lab-scale [5,8,9]. Taken together, the results obtained show the potential of the presented PBR prototype to achieve relatively high biomass concentrations, at a real scale, with more microalgae belonging to different phyla. Furthermore, the adopted strategy for the wavelength-specific spectra composition turned out to effectively achieve comparable yields on light obtained at the lab scale, especially considering *G. sulphuraria*.

References

[1] Carone, M.; Alpe, D.; Costantino, V.; Derossi, C.; Occhipinti, A.; Zanetti, M.; Riggio, V. A. Design and Characterization of a New Pressurized Flat Panel Photobioreactor for Microalgae Cultivation and CO2 Bio-Fixation. Chemosphere 2022, 307. https://doi.org/10.1016/j.chemosphere.2022.135755.
[2] Kliphuis, A. M. J.; de Winter, L.; Vejrazka, C.; Martens, D. E.; Janssen, M.; Wijffels, R. H. Photosynthetic Efficiency of Chlorella Sorokiniana in a Turbulently Mixed Short Light-Path Photobioreactor. Biotechnol Prog 2010, 26 (3), 687–696. https://doi.org/10.1002/btpr.379.
[3] Li, J.; Stamato, M.; Velliou, E.; Jeffryes, C.; Agathos, S. N. Design and Characterization of a Scalable Airlift Flat Panel Photobioreactor for Microalgae Cultivation. J Appl Phycol 2015, 27 (1), 75–86. https://doi.org/10.1007/s10811-014-0335-1.
[4] Graziani, G.; Schiavo, S.; Nicolai, M. A.; Buono, S.; Fogliano, V.; Pinto, G.; Pollio, A. Microalgae as Human Food: Chemical and Nutritional Characteristics of the Thermo-Acidophilic Microalga Galdieria Sulphuraria. Food Funct 2013, 4 (1), 144–152. https://doi.org/10.1039/c2fo30198a.
[5] Abiusi, F.; Trompetter, E.; Hoenink, H.; Wijffels, R. H.; Janssen, M. Autotrophic and Mixotrophic Biomass Production of the Acidophilic Galdieria Sulphuraria ACUF 64. Algal Res 2021, 60. https://doi.org/10.1016/j.algal.2021.102513.
[6] Wan, M.; Wang, Z.; Zhang, Z.; Wang, J.; Li, S.; Yu, A.; Li, Y. A Novel Paradigm for the High-Efficient Production of Phycocyanin from Galdieria Sulphuraria. Bioresour Technol 2016, 218, 272–278. https://doi.org/10.1016/j.biortech.2016.06.045.
[7] Canelli, G.; Abiusi, F.; Vidal Garcia, A.; Canziani, S.; Mathys, A. Amino Acid Profile and Protein Bioaccessibility of Two Galdieria Sulphuraria Strains Cultivated Autotrophically and Mixotrophically in Pilot-Scale Photobioreactors. Innovative Food Science and Emerging Technologies 2023, 84. https://doi.org/10.1016/j.ifset.2023.103287.
[8] Abiusi, F.; Moñino Fernández, P.; Canziani, S.; Janssen, M.; Wijffels, R. H.; Barbosa, M. Mixotrophic Cultivation of Galdieria Sulphuraria for C-Phycocyanin and Protein Production. Algal Res 2022, 61. https://doi.org/10.1016/j.algal.2021.102603.
[9] Wan, M.; Wang, Z.; Zhang, Z.; Wang, J.; Li, S.; Yu, A.; Li, Y. A Novel Paradigm for the High-Efficient Production of Phycocyanin from Galdieria Sulphuraria. Bioresour Technol 2016, 218, 272–278.

https://doi.org/10.1016/j.biortech.2016.06.045.

PARALLEL SESSION: D4

Contaminated sites

Advanced sustainable remediation processes

Title: Lab tests for in situ bioelectrochemical remediation of Cr(VI) plumes in groundwater

Author(s): Gabriele Beretta*[1], Elena Sezenna[1], Anna Espinoza Tofalos[2,3], Andrea Franzetti[2], Sabrina Saponaro[1]

[1]*Department of Civil and Environmental Engineering, Politecnico di Milano, Milano, Italy, gabriele.beretta@polimi.it*

[2]*Department of Earth and Environmental Sciences, University of Milano-Bicocca, Milano, Italy*

[3]*Environmental Research and Innovation (ERIN) Department, Institute of Science and Technology (LIST), Luxembourg, Luxembourg*

Keyword(s): Bioelectrochemical process, Groundwater, Hexavalent chromium, In situ remediation

Introduction

Hexavalent chromium (Cr(VI)) contamination poses significant risks to environmental and human health due to its toxicity and carcinogenic properties. Various abiotic and biotic approaches for the removal of Cr(VI) contamination have been developed, including bioremediation [1]. Bioremediation is a promising strategy to remove Cr(VI) from groundwater as it is cost-effective, sustainable, and has a low impact on the environment. Among biological methods, bioelectrochemical systems (BESs) have emerged as a promising option, harnessing the power of electroactive bacteria to reduce Cr(VI) to the less toxic and stable trivalent species [2].

Potentiostatically-controlled or externally powered biocathodes have shown high efficiency in Cr(VI) reduction in groundwater without the addition of any organic substrate or in co-contamination with chlorinated solvents [2, 3]. However, most of the literature has focused on ex situ treatments of groundwater, without investigating the potential effects of the solid phase of the aquifer. This paper presents the results of lab soil column experiments aimed at investigating the performance of bioelectrochemical systems for in situ remediation of Cr(VI) plumes in groundwater.

Materials and Methods

Three identical transparent vertical plastic columns, 260 mL internal volume each, 3.8 cm internal diameter and 25.5 cm long, were employed for setting up three water-saturated continuous flow systems: i) a bioelectrochemical system, ii) an open circuit control, and iii) an abiotic control (Fig. 1).

Both the bioelectrochemical system (BE) and the open circuit control (OCC) were filled at the bottom and at the top with a layer of glass spheres (3 mm in diameter) and clean quartz sand, to ensure uniform flow distribution. The abiotic control (AC) was set up by using only glass spheres to fill up the space between the electrodes and the column inlet and outlet sections.

All the electrodes were prepared using circular graphite felts (3.8 cm in diameter), stainless steel mesh, and titanium wire. In each system, the anode and the cathode were buried in a layer of Cr(VI)-contaminated sandy loam, at a distance of about 11 cm.

In BE and AC, a constant voltage gradient of 0.6 V was applied between the anode and cathode, based on previous experiences in heavy metal bioelectrochemical treatments from the literature, to avoid water electrolysis (above 1.2 V) and side effects related to hydrogen and oxygen produced at the electrodes.

Two tests were conducted using different initial concentrations of Cr(VI) in the feeding solution (20 and 50 mg/L added to tap water). The contaminated solution was continuously circulated up-flow through each column at a controlled flow rate, corresponding to a seepage velocity of 5.8 m/d, as in a real sandy aquifer (≈ 1-10 m/d). Outflowing samples were periodically collected to assess Cr(VI) concentration over time. During the systems set up and at the end of the test soil and outflowing water samples were collected for microbiological communities' characterization.

The circulating current in the BE system was monitored during the test by using a recording digital multimeter (Iso-Tech IDM-8344, with UT61E Interface Program Ver 4.01 software tool), which measured the voltage drop across a 10 Ω resistance between the cathode and the power supply. The voltage drop was converted to current values by the first Ohm's law.

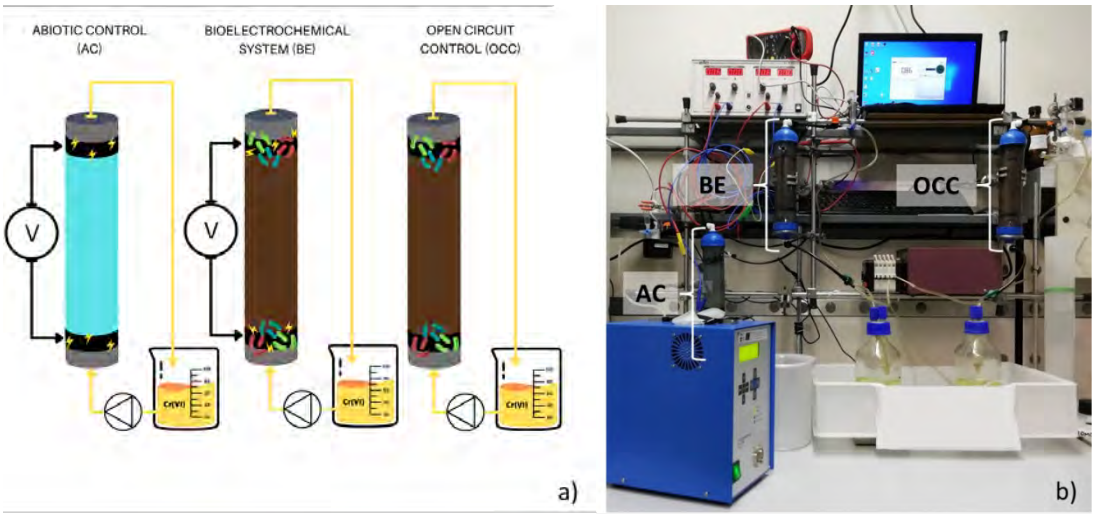

Figure 1. Experimental setup.

Under the hypotheses that dichromate ion was the only reducible species and the sole electron acceptor in the reactors, based on the calculated currents and the measured Cr(VI) concentrations in the effluent from the BE system, the Coulombic Efficiency (CE) of Cr(VI) bioelectrochemical removal (i.e., the fraction of the electrons circulating in the system compared to the electrons theoretically required for the reduction of dissolved Cr(VI)) was calculated according to:

$$CE = \frac{(M\ I\ \Delta t)}{(F\ b\ \Delta Cr\ V)} \qquad (1)$$

where M (245.99 g mol^{-1}) is the mole weight of Cr_2O7^{-2}, I (A) is the circulating current during the time interval Δt (s), F is the Faraday constant (96485.3 C mol^{-1} of electrons), b is the stoichiometric factor for dichromate reduction (i.e., 6 moles of electrons per mole of dichromate), ΔCr is the variation in Cr(VI) concentration over time Δt (g L^{-1}) based on two successive monitoring events, and V (L) is the volume of the BE system.

Results

At 20 mg Cr(VI)/L as the initial concentration, all the systems exhibited reduction in Cr(VI) concentrations over 20 days, with dissolved residual Cr(VI) concentrations at the end of the tests of 2.66 ± 0.13, 1.37 ± 0.07, and 0.10 ± 0.01 mg/L, corresponding to removals of 86.7%, 93.2%, 99.5% in the abiotic control (AC), in the open circuit control (OCC) and in the bioelectrochemical system (BE), respectively (Fig. 2a).

At 50 mg/L Cr(VI) as the initial concentration (Fig. 2b), the abiotic system AC showed fast but short-lasting Cr(VI) electrochemical reduction up to about 34%, whereas both BE and OCC showed over 90% Cr(VI) reduction after about 70 days, with lower concentrations in the bioelectrochemical system compared to OCC in the following period (70 – 150 days). In fact, at the end of the experiment BE achieved >99.9% reduction, with a residual concentration of about 30 µg/l, two orders of magnitude lower than in OCC.

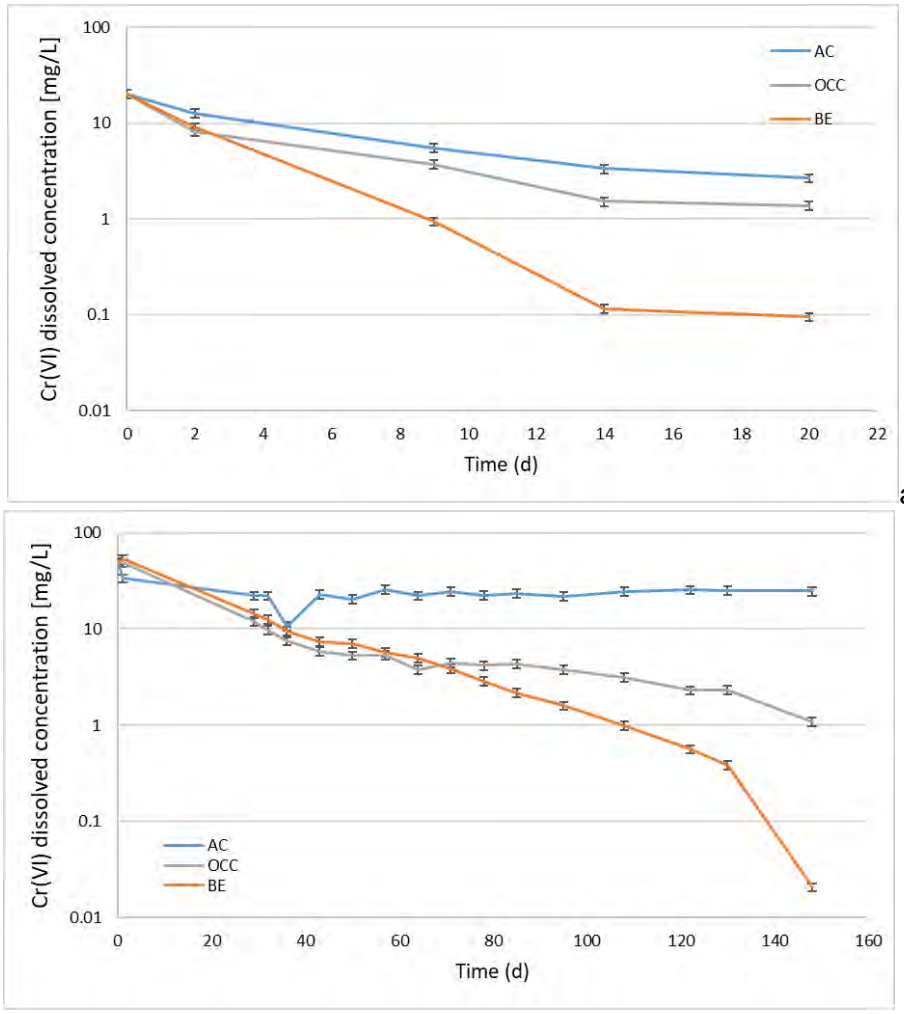

Figure 2. Cr(VI) concentration in the effluent of AC (blue line), OCC (grey line), and BE (orange line) systems with time: a) 20 mg Cr(VI)/L as the initial concentration; b) 50 mg Cr(VI)/L as the initial concentration.

In the BE test, with 50 mg Cr(VI)/L as the initial concentration, the calculated CE showed an increase with time, from 29% in the first month of testing up to above 100% after day 108 (Fig. 3). Therefore Cr(VI) reduction rate and CE showed to be somehow inversely related.
The declining rate in Cr(VI) reduction correlates with the progressive decrease in dissolved Cr(VI) concentration in the BE system. Conversely, the rising CE suggests that a portion of the cathodic electrons has been diverted toward different processes. CE values of 80-100% may indicate electrochemical or bioelectrochemical activities beyond Cr(VI) reduction alone.

As Cr(VI) concentration declines over time, the inhibitory impact on sensitive bacteria likely declines as well. Consequently, electroactive bacteria, may no longer face growth constraints, potentially leveraging electrodes as the electron donors/acceptors to enhance their metabolic functions.
Microbial communities in soil and water samples from different reactor systems showed distinct compositions, with soil samples containing bacteria belonging to the *Solirubrobacteriales*, *Gaiellales*, and *Bacillales* orders, while water samples had higher abundances of *Burkholderiales* and *Mycobacteriales*. This highlights the influence of environmental niches on microbial diversity, reflecting specific adaptations and roles of electroactive bacteria.

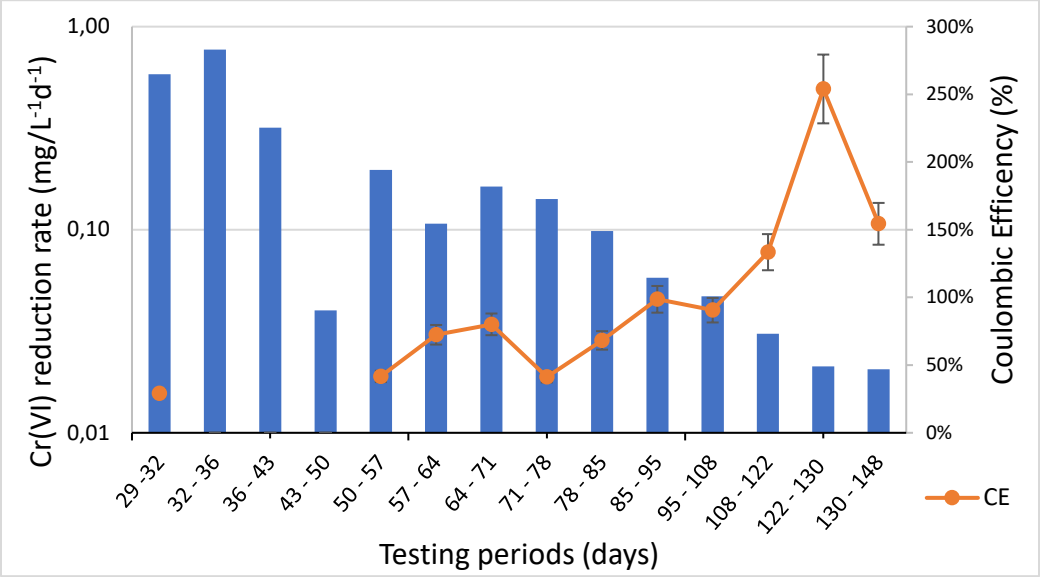

Figure 3. Cr(VI) reduction rate (blue bars) and Coulombic Efficiency CE (orange dots and line) in BE (50 mg Cr(VI)/L as the initial concentration).

Conclusions

At the lab scale, the bioelectrochemical system showed higher efficiency in Cr(VI) reduction compared to abiotic and open circuit controls. This result highlights the potential of BESs for in situ effective remediation of Cr(VI) contamination in groundwater and underlines the importance of further research to understand the mechanisms involved in Cr(VI) reduction and to optimize system performance.

References

[1] Barrera-Díaz, C.E., Lugo, V., Bilyeu, B. (2012), A review of chemical, electrochemical and biological methods for aqueous Cr(VI) reduction, Journal of Hazardous Materials, Volumes 223–224, 1-12, https://doi.org/10.1016/j.jhazmat.2012.04.054
[2] Beretta, G., Daghio, M., Espinoza Tofalos, A., Franzetti, A., Mastorgio, A. F., Saponaro, S., Sezenna, E. (2019). Progress towards bioelectrochemical remediation of hexavalent chromium. Water, 11(11), 2336. https://doi.org/10.3390/w11112336
[3] Beretta, G., Daghio, M., Espinoza Tofalos, A., Franzetti, A., Mastorgio, A. F., Saponaro, S., Sezenna, E. (2020). Microbial Assisted Hexavalent Chromium Removal in Bioelectrochemical Systems. WATER, 12(2), 1–16. https://doi.org/10.3390/w12020466
[4] Matturro, B., Zeppilli, M., Lai, A., Majone, M., & Rossetti, S. (2022). Corrigendum: Metagenomic Analysis Reveals Microbial Interactions at the Biocathode of a Bioelectrochemical System Capable of Simultaneous Trichloroethylene and Cr(VI) Reduction. Frontiers in Microbiology, 13, 879964. https://doi.org/10.3389/fmicb.2022.879964

"Multispectral Techniques for Environmental Situational Awareness: Monitoring Soil and Water Pollution in EIA"

M. Lega

Department of Engineering, University of Naples Parthenope (Italy)
email: massimiliano.lega@uniparthenope.it

Keyword(s): Environmental impact assessment, Environmental Characterization, Environmental Monitoring, Situational Awareness, Multispectral Techniques, Bioindicators

Abstract

In recent decades, a growing global consciousness has emphasized the critical importance of maintaining a healthy environment to safeguard human well-being and promote sustainable development. This heightened awareness has underscored the pivotal role of environmental impact assessment activities in all realms of project development and broader initiatives related to sustainability.

The scientific community is actively engaged in advancing strategies for more effectively characterizing, monitoring, and modelling contaminated soil and water resources. Given the intricate and interconnected nature of environmental systems, addressing these challenges requires an interdisciplinary approach that integrates diverse procedures and technologies to optimize information workflows.

In response to these needs, our research group has pioneered an innovative integrated approach that combines traditional on-site and laboratory surveys, sampling, and analyses with advanced techniques, including remote and proximal multispectral analyses, alongside the use of bioindicators [1-4].

This advanced methodology is designed to elevate environmental situational awareness, aligning with established environmental models (source-path-target), and providing insights into the complex dynamics of pollution phenomena.

The key elements of this methodology are:

1. developing interdisciplinary procedures to address complex systems, incorporating various forms of applied intelligence and specialized IT tools to continually enhance situational awareness;
2. exploring the added value of remote and proximal sensing, using satellites, aircraft, rotorcraft, and drones with customized payloads to characterize the environment and study pollution phenomena;
3. integrating nature as an advanced sensor, with case techniques and technologies focused on bio-tracking, bio-monitoring, and bio-magnification using specific bio-indicators.

This work showcases the outcomes of several case studies that validate our approach, with a focused examination on two specific types: 1) the interface between solid waste landfills and surrounding areas, and 2) the behaviour of pollutants originating from wastewater that enter coastal water bodies.

Through these case studies, we illustrate a comprehensive and systematic workflow that underscores the effectiveness of our integrated approach in addressing pressing environmental challenges.

Finally, this methodology highlights the value of Environmental Forensics, an emerging field that combines scientific principles with investigative techniques to identify, analyze, and understand environmental issues, thereby supporting informed decision-making and effective resource allocation.

Our proposed approach innovates not only through the techniques and technologies utilized, but also through the representations of the scenarios under examination and related phenomena. This enables sanitary environmental engineering to serve as a bridge connecting diverse domains, fostering enhanced value through an interdisciplinary approach, and facilitating improved dialogue with communities and governmental bodies responsible for implementing solutions.

Acknowledgments:

The authors' activities were also supported by the project 'STOPP - Strumenti e Tecniche di Osservazione della Terra in Prossimità e Persistenza' (STOPP - Tools and Techniques for Earth Observation in Proximity and Persistence), managed by the Italian Space Agency (ASI) and involving several Italian universities, institutions, and research centres.

Figure 1: Graphical Abstract.

References

[1] Lega, M., Casazza, M., Teta, R., & Zappa, C. J., Environmental impact assessment: A multi-level, multi-parametric framework for coastal waters, International Journal of Sustainable Development and Planning, 13(8), 1041-1049, (2018). https://doi.org/10.2495/SDP-V13-N8-1041-1049.

[2] Esposito, G., Teta, R., Marrone, R., De Sterlich, C., Casazza, M., Anastasio, A., ... & Costantino, V., A Fast Detection Strategy for Cyanobacterial blooms and associated cyanotoxins (FDSCC) reveals the occurrence of lyngbyatoxin A in Campania (South Italy). Chemosphere, 225, 342-351, (2019). https://doi.org/10.1016/j.chemosphere.2019.02.201.

[3] Esposito, G., Glukhov, E., Gerwick, W. H., Medio, G., Teta, R., Lega, M., & Costantino, V., Lake Avernus Has Turned Red: Bioindicator Monitoring Unveils the Secrets of “Gates of Hades”. Toxins, 15(12), 698, (2023). https://doi.org/10.3390/toxins15120698.

[4] Lega, M., & Endreny, T., Quantifying the environmental impact of pollutant plumes from coastal rivers with remote sensing and river basin modelling, International Journal of Sustainable Development and Planning, 11(5), 651-662, (2016). https://doi.org/10.2495/SDP-V11-N5-651-662.

Title: Application of Low Temperature Thermal Desorption of marine sediments: operational and management assessment

Author(s): Enrico Licitra*[1], Maria Gabriella Giustra[1], Maurizio Volpe[1], Daniele Di Trapani[2], Antonio Messineo[1], Gaetano Di Bella*[1]

[1]*Department of Engineering and Architecture, University of Enna "Kore", Cittadella Universitaria, 94100 Enna, Italy, enrico.licitra@unikore.it mariagabriella.giustra@unikore.it maurizio.volpe@unikore.it antonio.messineo@unikore.it gaetano.dibella@unikore.it*
[2]*Department of Engineering, University of Palermo, Viale delle Scienze, 90128, Palermo, Italy, daniele.ditrapani@unipa.it*

Keyword(s): Sediments; Dredging; Thermal Desorption; Hydrocarbons; Energy consumption

Abstract

Sediments represent an important component of marine ecosystems. They serve both as a final receptor for pollutants (toxic and persistent) originating from anthropogenic activities as well as a source of exchange with the aquatic environment and its organisms. Specifically, among chemical contaminants, heavy metals and petroleum hydrocarbons pose a significant threat due to their capacity for bioaccumulation in aquatic ecosystems. The management of marine sediments may therefore be necessary not only for remediation of contaminated sites but also after periodic dredging operations in port areas [1,2]. Indeed, the participations of dredging can have the twofold objective of the fruition of the marine-coastal areas for navigation and the maintenance of the environmental quality. In these areas, there is no doubt about the need for verification and evaluation of the possible effects (physical, chemical, biological and ecotoxicological) on the environment that can be traced back to the execution of such activities, especially when environmental concerns are recognized that may cause direct or indirect contamination of both sediment and water column [3].

Nationwide, the management of contaminated sediments dredged from marine and port areas is often based on landfill disposal and/or confined disposal in containment basins. However, these strategies have several disadvantages, mainly due to the limited availability of space and low environmental sustainability; in addition, Italian environmental regulation and guidelines (such as Legislative Decree 152/2006 and Ministerial Decree 173/2016), as well as international literature, consider sediments as a resource and their reuse as a suitable and preferable solution, provided that contamination levels comply with regulatory standards [4].

Therefore, the evaluation of remediation strategies to be applied for contaminated sediments must necessarily consider the possibility of re-using the matrix as a result of appropriate treatments. Among the remediation techniques of contaminated marine sediments, with off-site application, thermal desorption is an effective treatment for the removal of volatile and semi-volatile organic pollutants, despite the disadvantages that can be traced back to the high energy consumption, strictly related to the process temperature to be reached, and the need for specific management systems of pollutants desorbed from sediment. However, Low Temperature Indirect Thermal Desorption (LTITD) can be considered as a 'sustainable' remediation technology, thanks to energy savings (due to low temperature), the maintenance of physic and chemical proprieties and rapid recolonization of microbial communities in thermally treated soils and sediments [5,6,7].

Thus, with the aim of assessing the capacity of this thermal technique for the remediation of sediments contaminated by *total petroleum hydrocarbons* (TPH), thermal desorption was applied using laboratory scale pilot plant. The experimental work was carried out in the *Laboratory of Energy and Environment* and the *Laboratory of Environmental Sanitary Engineering* of the University of Enna. Several experimental tests were conducted to identify the optimal process parameters (maximum process temperature and contact time heat source/solid matrix) for the reclamation of marine sediments with different levels of artificial diesel contamination. The surveys were also carried out to assess the energy consumption required in the different tests carried out and to assess the potential application of adsorbent materials with similar properties to those of activated carbon, usually used for the management of contaminants downstream of heat treatments and to prevent air pollution.

The chemical characterization of the contaminated matrix was carried out using in particular the EPA method 3545A (Pressurized fluid extraction) with subsequent analysis with GC/FID. To assess the concentration of organic contaminants, reference was made to the TPH parameter which returns a "global" measurement of organic carbon from petroleum compounds.

The experimental plant used to simulate thermal desorption (showed in Figure 1) consisted of a tubular furnace (Split Furnace) with heating elements "SAFTherm SANTE FURNACE", equipped with a quartz tube of 60 mm diameter and 800 mm length, closed at the ends by sealed stainless steel flanges for the control of the internal atmosphere and the flushing of specific gas carriers (typically inert gas such as nitrogen). The sample of polluted sediment (approx. 20 grams and grain size < 2mm) was placed in the middle of the tube inside a quartz vessel. From one end of the quartz tube the carrier gas (nitrogen) was flushed with a constant flow rate of 1.5 l/min in order to render the atmosphere inside the tube inert, thus preventing any oxidative phenomena. The opposite end of the quartz tube was connected to a pollutants recovery system. The experimental work was organized in three phases (Table 1): the first two with the aim of identifying the best process parameters by varying the extent of sediment TPH contamination and evaluating at the same time energy consumption (using a digital wattmeter); the third phase with the aim of evaluating the potential application of biochars, in particular waste materials (coarse grain size for biochar 1 and fine grain size for biochar 2) resulting from pyrolytic treatments on tree essences (pine and eucalyptus). Figure 2 shows a graphical diagram of the experimental tests carried out in the three phases.

Figure 1. SAFTherm SANTE FURNACE experimental setup containing quartz tube

Table 1. Operating conditions during the three experimental phases

Experimental phase	Sediment mass	Max Temperature	Contact time	Management system
Phase 1	20 grams	200 °C	20 mins	traps
		350 °C		
		500 °C		
Phase 2	20 grams	200 °C	10 mins	traps
			15 mins	
			20 mins	
Phase 3	20 grams	200 °C	15 mins	GAC + trap
				BIOCHAR 1 + trap
				BIOCHAR 2 + trap

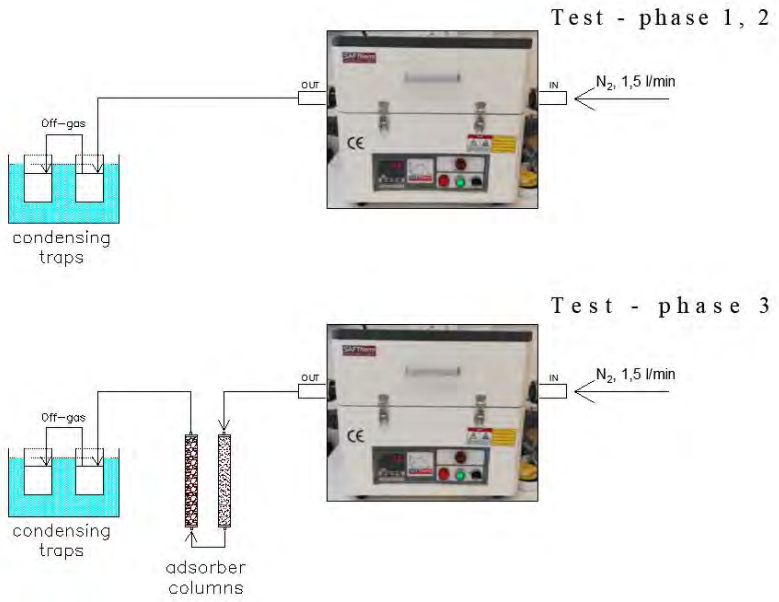

Figure 2. Representative graphic diagram of the pilot plant downstream linked with contaminants management system for the three phases

Thus, the maximum treatment temperatures investigated in the first phase were 200ºC, 350ºC and 500ºC with a contact time of 20 minutes (initial TPH concentration of about 1300 mg_{TPH}/kg_{DM}). In the second phase, the contact time was changed to 10, 15 and 20 minutes using a maximum heating temperature of 200 ºC (initial TPH concentration of about 35000 mg_{TPH}/kg_{DM}). Finally, in the third phase, the process parameters used were maximum heating temperature of 200 ºC and a contact time of 15 minutes (initial TPH concentration of about 13000 mg_{TPH}/kg_{DM}).

From the results of the artificial contamination of sediments, it has emerged a pollution of all the sediments artificially contaminated, with exceedances of the limits provided by the Italian legislation for residential sites, with extremely higher values for sediment used in the third experimental phase.

The results obtained following the experimental tests showed the high efficiency of thermal desorption for the removal of organic pollutants such as TPH from marine sediments, even at high concentrations and at low treatment temperatures, achieving yields removal between 98,7% and 100% in the different tests and obtain potentially reusable sediments according to national regulation. Energy consumption evaluation showed a significant reduction for tests conducted at a temperature of 200 ºC, with further maximum reduction to be considered by varying contact time from 20 minutes to 10 minutes (table 2).

Nevertheless, the residual concentrations of TPH in marine sediment following heat treatment, compared with the regulatory limits, have allowed to claim that the optimal process parameters are represented by the temperature of 200 ºC and the contact time of 15 minutes.

Table 2. a) energy consumption varying process temperature; b) energy consumption varying contact time at 200 ºC

a) Energy consumption varying T [%], 20 mins			b) Energy consumption varyin contact time [%],		
Tmax [°C]	EC [kWh/kg]	ΔEC [%]	tc [min]	EC [kWh/kg]	ΔEC [%]
500	3,75	-	20	1,59	-
350	2,67	28,75	15	1,37	14,20
200	1,59	57,46	10	1,16	27,14

With regard to the contaminants management system and in particular the adsorbent materials tested, potentially promising results were obtained. In fact, biochar 1 adsorbed about 78% of the pollutants, with efficiencies similar to those obtained from the active carbon used for comparison (83%). These results showed the convenience of the application of Thermal Desorption technology by using low temperatures that, with high efficiencies even if slightly lower than those obtained at high temperatures (350 and 500 ºC), ensure a reduction in energy consumption of 40-70% compared to applications at medium-high temperatures. In particular, considering the average cost of energy (for industrial applications) at the time of the survey (0,23 €/Kwh + VAT), it is possible to consider the treatment of sediments contaminated with LTITD at 200°C that varies between 325 and 383 €/tons with a process conducted at 10 or 15 minutes of contact time, respectively, against more than 1000 €/tons for TD conducted at 500°C (and 20 minutes contact time).
Finally, considering the initial contamination status of the sediments as an additional element of assessment, it was found that the heat treatment is fast and effective even for high initial contamination in marine sediments, contrary to what characterize their biological treatments although they are much cheaper. The possibility of using recycled materials for the management of contaminants downstream of heating treatment also allows to consider a further reduction of the necessary costs, avoiding the use of commercial materials obviously more expensive than a waste material.

Acknowledgements

This study was carried out within the RETURN Extended Partnership and received funding from the European Union Next-GenerationEU (National Recovery and Resilience Plan – NRRP, Mission 4, Component 2, Investment 1.3 – D.D. 1243 2/8/2022, PE0000005).

References

[1] Dell'Anno A., Beolchini F., Corinaldesi C., Amato A., Becci A., Rastelli E., Hekeu M., Regoli F., Astarita E., Greco F., Musco L., Danovaro R. (2020). *Assessing the efficiency and eco-sustainability of bioremediation strategies for the reclamation of highly contaminated marine sediments*. Marine Environenmental Research, Elsevier.
[2] E. García, I. Giráldez, M. Ruiz Montoya, E. Morales (2020). *Determination of booster biocides in sediments by focused ultrasound-assisted extraction and stir bar sorptive extraction–thermal desorption–gas chromatography–mass spectrometry*, Microchemical Journal, Volume 152, 2020, 104445, ISSN 0026-265X, https://doi.org/10.1016/j.microc.2019.104445.
[3] Lumia L., Di Bella G., Harbottle M.J. (2020). *Remediation of contaminated marine sediments – case study on the sediments of Augusta Bay*. Thesis for the achievement of the PhD. University of Enna "Kore", Faculty of Engineering and Architecture.
[4] Falciglia, P. P., Lumia, L., Giustra, M. G., Gagliano, E., Roccaro, P., Vagliasindi, F. G. A., & di Bella, G. (2020).

Remediation of petrol hydrocarbon-contaminated marine sediments by thermal desorption. *Chemosphere*, *260*. https://doi.org/10.1016/j.chemosphere.2020.127576
[5] Yimin Sang, Wang Yu, Liao He, Zhefeng Wang, Fujun Ma, Wentao Jiao, Qingbao Gu (2021), *Sustainable remediation of lube oil-contaminated soil by low temperature indirect thermal desorption: Removal behaviors of contaminants, physicochemical properties change and microbial community recolonization in soils*, Environmental Pollution, Volume 287, 117599, ISSN 0269-7491, https://doi.org/10.1016/j.envpol.2021.117599
[6] Yuying Zhang, Claudia Labianca, Liang Chen, Sabino De Gisi, Michele Notarnicola, Binglin Guo, Jian Sun, Shiming Ding, Lei Wang, *Sustainable ex-situ remediation of contaminated sediment: A review*, Environmental Pollution, Volume 287, 2021, 117333, ISSN 0269-7491, https://doi.org/10.1016/j.envpol.2021.117333.
[7] Cheng Zhao, Yan Dong, Yupeng Feng, Yuzhong Li, Yong Dong (2019), *Thermal desorption for remediation of contaminated soil: A review*, Chemosphere (2019), doi: 10.1016/j. chemosphere.2019.01.079

Title: Facing the challenge of copper polluted olive groves by electrokinetic remediation.

Author(s): Cristina Navas-Higuero[1*], Ismael F. Mena[1], Engracia Lacasa[1], A. Manzaneda[2], Manuel A. Rodrigo[1], Cristina Sáez[1].

[1] Departamento de Ingeniería Química, Universidad de Castilla-La Mancha. Av. Camilo José Cela n 12, Edificio Enrique Costa Novella, Ciudad Real (13071) España.
[2] Departamento de Biología animal, biología vegetal y ecología, Universidad de Jaén. Campus Las Lagunillas. Edificio Ciencias Experimentales y de la Salud (B3). Av. De la Universidad n 9 Jaén (23009) España.

Keyword(s): Electrokinetic transport, copper, fungicide, soil remediation.

Abstract

Olive cultivation holds substantial global significance from economic, cultural, and environmental perspectives. The presence of copper in olive orchards has become a critical issue in agricultural practices, with far-reaching implications across environmental, agricultural, and public health domains [1]. Copper, often introduced via anthropogenic activities such as pesticide and fungicide applications, irrigation practices, and soil amendments, accumulates in olive orchards. This accumulation poses risks of soil degradation, diminished crop yields, and contamination of groundwater and adjacent ecosystems. Despite their effectiveness in pest management, these chemicals persist in the soil over time due to slow degradation rates [2]. Additionally, the bioaccumulation of copper in olives raises concerns about food safety, impacting consumer health [3]. Copper exhibits varying behavior in soils, influenced by factors like soil pH, organic matter content, and mineral composition. In acidic soils, copper tends to be more soluble and mobile, increasing the risk of leaching into groundwater and surface water bodies. Conversely, in alkaline soils, copper may form insoluble complexes, limiting its bioavailability to plants [4].

To solve this, electrokinetic remediation (EKR) appears as an alternative to remediate copper-polluted sites. EKR is based on the application of an electric field among electrodes sited in the soil to induce different transport mechanisms such as electroosmosis, electromigration or electrophoresis. Additionally, the electrolysis of water can take place on the electrolyte wells, leading to the generation of acid and basic fronts which may cause side processes such as redissolution or precipitation of species, as well as fixation or liberation of species by ionic exchange.

This work aims to assess the effectiveness of electrochemically assisted soil remediation technology ito mitigate chemical risks associated with the use of copper-fungicides in olive groves. In a first step, the sampling and chemical characterization of soils of olives groves located in different countries of the Mediterranean basin were carried out. In each orchard, 5 sampling points were selected and divided in two horizons: 0-10 cm and 10-20 cm. In total, 500 samples from 5 different countries (Spain, Italy, Greece, Portugal, Morocco) have been processed. The quantification of copper in solid samples has been done according to ISO STANDARD 11466 and a conventional extraction procedure without digestion step was also carried out for comparison purpose. After extraction, the liquid phase (centrifuged and filtered) was measured by Atomic Absorption Spectrometer SpectrAA 220 FS.

The results of this diagnosis step indicate that a portion of the copper is strongly retained or fixed in the soil, and copper pollution levels range from 5 to 200 mg/kg. Generally, copper accumulation in the 0-10 cm soil horizon is higher than in the 10-20 cm horizon. The collected data were arbitrarily classified into five copper concentration ranges. Table 1 displays the percentage of samples within each interval for different countries. Notably, there is significant variability among countries, with the order being Spain, Greece > Italy > Morocco > Portugal. Additionally, the type of orchard (traditional, organic, intensive) appears to play a relevant role (data not shown).

Table 1. Classification of copper-concentration ranges and percentage of samples per country.

% samples	SPAIN	ITALY	MOROCCO	GREECE	PORTUGAL
0-15 mg/kg	5.1	15.2	11.4	6.7	16.0
15-30 mg/kg	11.5	15.2	31.4	41.3	24.0
30-50 mg/kg	34.6	6.1	37.1	24.0	60.0
50-150 mg/kg	37.2	57.6	17.1	21.3	0.0
+150 mg/kg	11.5	6.1	2.9	6.7	0.0
Number of samples	*79*	*33*	*35*	*75*	*25*

Then, the evaluation of copper remediation in real olive grove soils was evaluated by soil washing and, after that, by electrokinetic remediation (EKR). Soil washing was carried out in stirred tanks and allowed to evaluate the most suitable washing agent (water, chelating agents solutions or acid solutions). EKR tests were carried out at lab scale using a mock-up system with a capacity of 400 g of soil, and in which graphite electrodes were inserted in electrolyte wells, as shown in Figure 1. For comparison purpose, tests were also carried out with silt and clay soil polluted with copper sulfate. The influence of the applied electric fields (1-1.6 V/cm) and the type and concentration of flushing fluid (citric or nitric acid, and EDTA [5]) were evaluated over a period of 33-days. Daily monitoring included measurements of current intensity, pH and copper concentration in the electrolyte wells. Finally, a detailed post-mortem analysis of the soil was carried out.

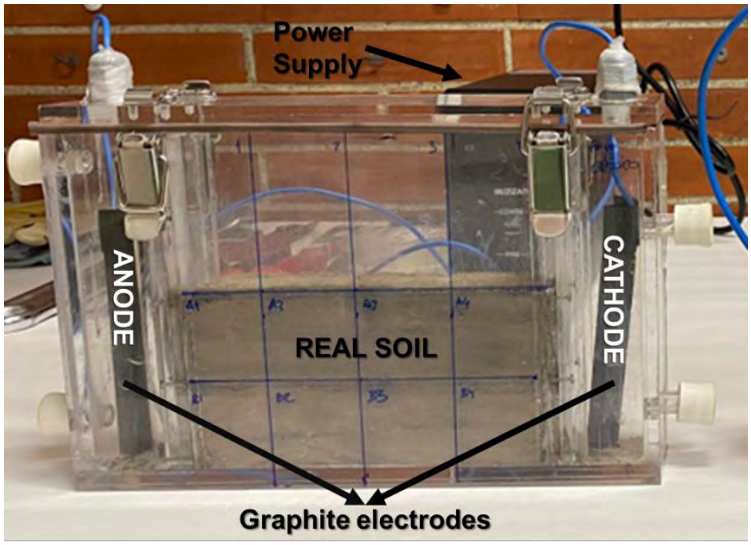

Figure 1. Electrokinetic soil remediation set up.

Results of soil washing tests show that due to the high alkalinity of the soil, it presents a relevant buffering capacity. Additionally, there is a limited solubility of copper accumulated in the soil. Then, it is strongly fixed in the soil, and it is very difficult to extract with water. The use of EDTA solutions as washing fluids allows to attain up to 50% of copper contained in the soil.

Regarding EKR results, preliminary tests with synthetic soils spiked with copper sulfate show that ionic copper is transported to electrolyte wells by electrokinetic fluxes. At alkaline pH, ionic copper remains insoluble as Cu (OH)2. Additionally, the transport of copper through the soil is greater in sandy soils than in soils rich in clay or organic matter because ionic copper can bind in soil to organic matter particles, clay, and metal hydroxides. Results also show that ionic copper transported to the cathodic well can be also deposited on the cathodic surface.

In the tests with real soil, the experimental behavior strongly differs. As expected, new copper-biocides formulations are more persistent, and they prevent the mobility of copper in the soil. The percentage of copper recovered was slightly lower in the case of using water or acid solutions as flushing fluid. On the contrary, the addition of chelating agents is highly recommended. Figure 2 shows the trend of current intensity and the amount of copper transported by electrokinetic fluxes to electrolyte wells during EKR tests carried out at 1 and 1.6 V cm^{-1} (test 1 and test 2) and using citric acid as flushing fluid. As can be observed, the intensity increases in the first hours of treatment, then it decreases until 0.01A, approximately. Regarding copper, the amount of copper transported depends on the cell voltage applied. Additionally, it was observed the precipitation of citrate in the nearness of the cathodic well.

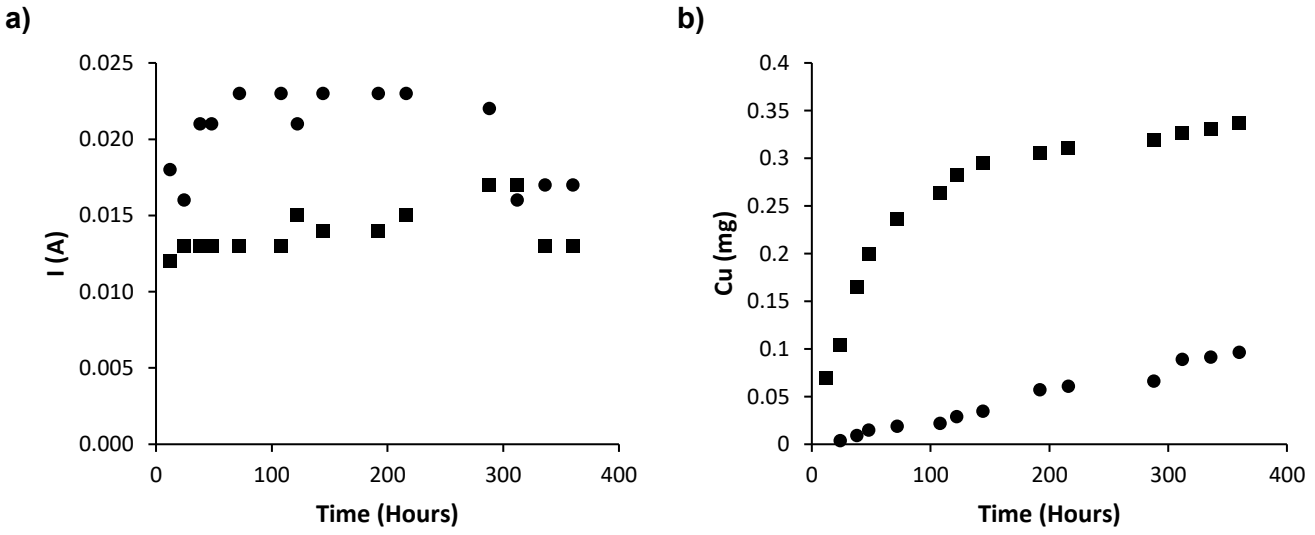

Figure 2. Variation of intensity and copper mobilized using citric acid as flushing fluid at 1 (■) and 1.6 (●) V cm^{-1}

As conclusion, it can be stated that ionic copper can be effectively mobilized through electrokinetic mechanisms. However, the retention of actual copper-fungicides in the soil required the addition of chelator solutions. Moreover, this study demonstrates the potential of electrochemically assisted soil remediation for managing copper contamination in olive groves. The findings emphasize the importance of tailoring remediation strategies based on specific soil characteristics and contaminants.

Acknowledgment

This work was carried out within the framework of the SOIL O-LIVE project. This Project has received funding from European Union's Horizon research and innovation programme under grant agreement No. 101091255.

References

[1] Miloš, B., & Bensa, A. (2021). The Copper Content in Soil of Olive Orchards from Dalmatia, Croatia. *Eurasian Soil Science*, *54*(6), 865-874. https://doi.org/10.1134/s1064229321060119

[2] Karthick, A., Roy, B., & Chattopadhyay, P. (2019). A review on the application of chemical surfactant and surfactant foam for remediation of petroleum oil contaminated soil. *Journal Of Environmental Management*, *243*, 187-205. https://doi.org/10.1016/j.jenvman.2019.04.092

[3] Wilson, B., & Pyatt, F. B. (2007). Heavy metal bioaccumulation by the important food plant, Olea europaea L., in an ancient metalliferous polluted area of Cyprus. *Bulletin of environmental contamination and toxicology*, *78*(5), 390–394. https://doi.org/10.1007/s00128-007-9162-2

[4] Whalen, J. K., Chang, C. J., Clayton, G. W., & Carefoot, J. P. (2000). Cattle Manure Amendments Can Increase the pH of Acid Soils. *Soil Science Society Of America Journal*, *64*(3), 962 966. https://doi.org/10.2136/sssaj2000.643962x

[5] Gluhar, S., Kaurin, A., & Leštan, D. (2020). Soil washing with biodegradable chelating agents and EDTA: Technological feasibility, remediation efficiency and environmental sustainability. *Chemosphere*, *257*, 127226. https://doi.org/10.1016/j.chemosphere.2020.127226

Title: Advanced nanoremediation processes for the effective removal of complex mixtures of persistent pollutants from groundwater

Author(s): Carlo Bianco*[1], Serena Barbero[2] and Rajandrea Sethi[3]

[1] *Department of Environment, Land and Infrastructure Engineering, Politecnico di Torino, Turin, Italy, carlo.bianco@polito.it*
[2] *Department of Environment, Land and Infrastructure Engineering, Politecnico di Torino, Turin, Italy, serena.barbero@polito.it*
[3] *Department of Environment, Land and Infrastructure Engineering, Politecnico di Torino, Turin, Italy, rajandrea.sethi@polito.it*

Keyword(s): nanoremediation, environmental nanotechnology, groundwater remediation, persistant pollutants, nZVI, zerovalent iron

Abstract

Groundwater contamination poses a pervasive threat to human health and ecosystems, necessitating effective remediation strategies. In this context, zerovalent iron microparticles (mZVI) and nanoparticles (nZVI) have emerged as a powerful solution, offering unprecedented opportunities for in situ groundwater cleanup [1,2]. Their efficacy is attributed to their nanoscale size, which endows them with a high surface area-to-volume ratio, enhancing their reactivity with a range of contaminants [2,3,4]. This quality makes nZVI particles particularly effective in reducing contaminants through both chemical reduction and sorption processes. The unique reactivity of these nanoparticles is further augmented by their ability to be injected in aqueous slurries directly into contaminated aquifers, thus enabling targeted source treatment and plume remediation (Figure 1).

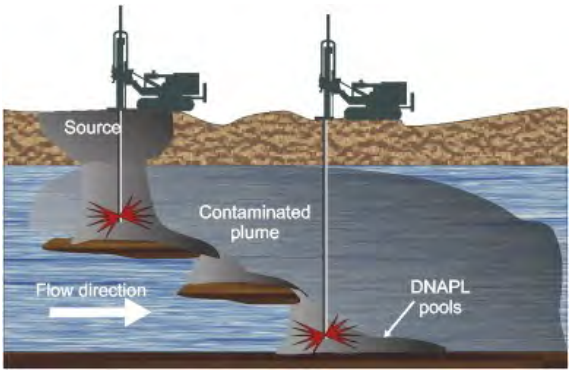

Figure 1. Remediation of a DNAPL-contaminated aquifer through injection of a suspension of nZVI/mZVI directly in proximity of the source of contamination [2].

nZVI-based treatments are increasingly applied for in-situ groundwater remediation as they allow for effective removal of various contaminants including chlorinated solvents, metal ions, PAH, PCBs, and pesticides [3] (Figure 2). However, some widespread contaminants, such as 1,2-dichloroethane (1,2-DCA) and 1,2-dichloropropane (1,2-DCP), are known to be resistant to this treatment [4], thus posing

significant challenges for in situ remediation of aquifer systems contaminated with complex contaminant mixtures.

From a practical perspective, optimizing the reactivity of zero-valent iron and carefully managing particle injection are critical for implementing this technology on a large scale. Depending on the unique characteristics of the site being treated, micro and nanoparticles can be used as-is or modified to enhance their effectiveness in the aquifer. Common modifications include:

- Addition of biodegradable stabilizing agents to improve suspension stability and distribution during injection. These agents also alter the fluid's viscosity, preventing particle aggregation and sedimentation while facilitating injection.
- Surface functionalization with trace catalysts to enhance electron exchange, speeding up reaction kinetics and broadening the range of treatable contaminants.
- Sulfidation by formation of an inorganic sulfur-based layer on particle surfaces, to increase reactivity towards specific contaminants (e.g. tetrachloroethylene and trichloroethylene) and prolong the iron's lifespan in the aquifer by partial inhibition of corrosion reactions in contact with water.

In this study, different types of nZVI particles were tested through laboratory experiments to evaluate the applicability of nanoremediation for the treatment of site contaminated with a complex mixture of persistent chlorinated solvents. Specifically, the study area is affected by groundwater contamination by chlorinated organic compounds at concentrations of thousands of µg/L. The contamination includes both compounds effectively treatable with zerovalent iron, such as PCE, TCE, and PCM, and pollutants highly resistant to nZVI treatment (e.g., 1,2-DCA and 1,2-DCP).

Materials and methods

Laboratory batch tests (Figure 2) were performed to compare the effectiveness of nZVI-based products for the decontamination of groundwater samples collected at the study site. The tested products included standard zero-valent iron nanoparticles (nZVI), i.e. in absence of any surface modification, sulfidated nZVI (nZVI-S), as well as IronGel Plus (DeltaNova), an innovative nZVI-based reactant containing catalysed nanoparticles. IronGel Plus (Figure 2) consists of a viscoelastic biopolymeric gel containing reactive nanoscale zero-valent iron particles (d50 < 100 nm) [5], functionalized by addition of a food-grade metallic catalyst to enhance their reactivity and effectiveness against contaminants.
The effectiveness of the tested reagents in reducing the target contaminants over time was evaluated by determining the degradation kinetics of different compounds in contact with the reactive materials.

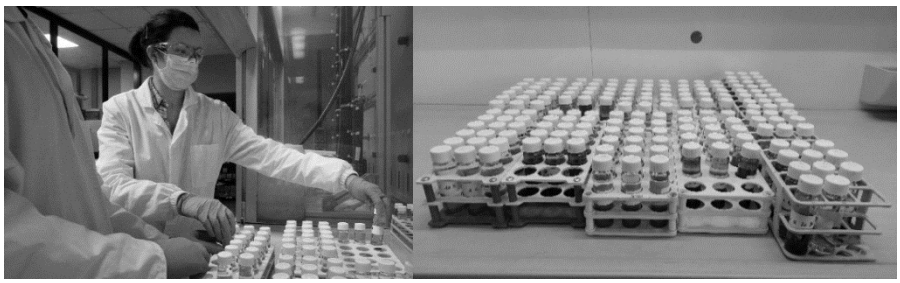

Figure 2. Preparation of samples for reactivity batch tests.

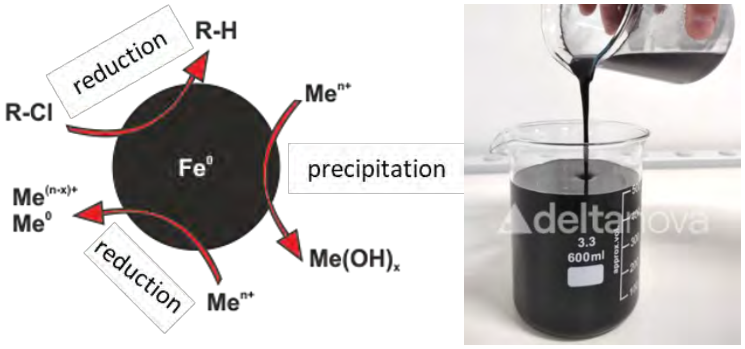

Figure 3. Contaminant removal processes in contact with zero-valent iron particles (left) and colloidal nZVI suspension prepared with IronGEL Plus.

Results

Experimental results (Figure 4) demonstrated the effectiveness of standard nZVI in removing most chlorinated organic compounds, except for 1,2-DCP and 1,2-DCA. In particular, very fast degradation of chlorinated ethenes was observed, including cis-1,2-DCE and vinyl chloride. On the other hand, the experiments confirmed the inability of nZVI in the dehalogenation of 1,2-DCA and 1,2-DCP. Sulfidated iron (nZVI-S) showed comparable results with unmodified nZVI for PCE and TCE, whereas no relevant degradation was observed for cis-1,2-DCE and VC, as well as for 1,2-DCA and 1,2-DCP. With both nZVI and nZVI-S, partial and temporary formation of dichloromethane was observed as a result of the degradation of PCM and TCM. Finally, complete removal of all chlorinated solvents, including those resistant to treatment with zero-valent iron, was instead observed in the presence of IronGel plus. Importantly, unlike the other nZVI-based products tested, no formation of other intermediates or by-products was observed when the catalysed iron was applied.

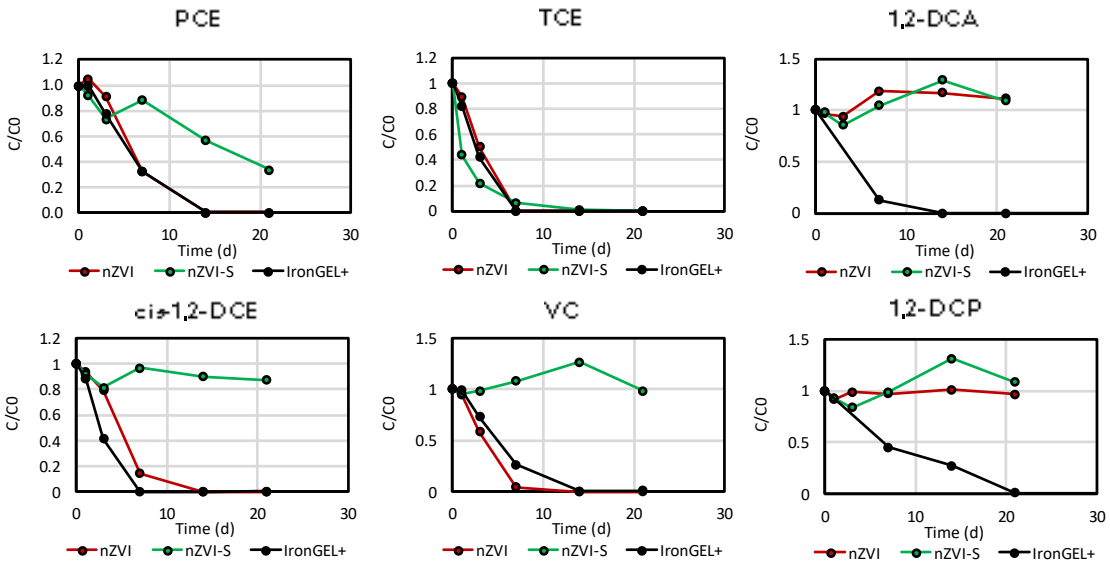

Figure 4. Results of batch degradation tests for tetrachloroethylene (PCE), trichloroethylene (TCE), cis-1,2-dichloroethylene (cis-1,2-DCE), vinyl chloride (VC), 1,2-dichloroethane (1,2-DCA) and 1,2-dichloropropane (1,2-DCP) in presence of nZVI, sulfidated nZVI and IronGel Plus.

Conclusions

The results of this study confirmed that nZVI is a powerful reducing agent for reductive dechlorination of most chlorinated solvents and highlighted the importance of surface modification as a relevant factor to tune the nanoparticle reactivity. In particular, for the specific site investigated in this study, IronGEL Plus proved to be the most effective reagent for the dechlorination of all contaminants present in groundwater, including 1,2-DCA and 1,2-DCP (removal > 99%).
This study also indicated that the selection of the most suitable surface modification to be applied in a specific case should come from a meticulous analysis of the site-specific contamination, especially in the presence of complex mixtures of persistent pollutants. In fact, despite unmodified nZVI particles can be very effective towards chlorinated ethylenes, it is almost ineffective for 1,2-DCA removal and can lead to transitory formation of undesired intermediates in the presence of chlorinated methanes. Similarly, nZVI-S can be a viable solution only when vinyl chloride and cis-1,2-DCE are not the main target contaminants of the remediation process.
To confirm results obtained at laboratory scale, the effectiveness of IronGEL Plus for the remediation of the investigated site will be further evaluated in an upcoming pilot test in the field.

References

[1] Sethi, R., Di Molfetta, A, “Groundwater Engineering. A Technical Approach to Hydrogeology, Contaminant Transport and Groundwater Remediation”, Springer Tracts in Civil Engineering (2019).
[2] Tosco T., Petrangeli Papini M., Cruz Viggi C., Sethi R. “Nanoscale zerovalent iron particles for groundwater remediation: a review”, Journal of Cleaner Production, 77, 10-21, ISSN 0959-6526 (2014)
[3] Arnold, W.A., Roberts, A.L., “Pathways and kinetics of chlorinated ethylene and chlorinated acetylene reaction with Fe(0) particles.” Environmental Science and Technology, 34 (9), pp. 1794-1805 (2000).
[4] Tobiszewski M., Namieśnik J. “Abiotic degradation of chlorinated ethanes and ethenes in water”, Environ Sci Pollut Res 19:1994–2006 (2012).
[5] Bianco, C.; Mondino, F.; Casasso, A. “Improved Delivery of Nanoscale Zero-Valent Iron Particles and Simplified Design Tools for Effective Aquifer Nanoremediation.”, Water, 15, 2303 (2023)

The role of the duration of remediation procedures in reducing land consumption and brownfield regeneration

Federico Pinzin*[1], Silvia Sbaffoni[2], Emanuela Demarco[2], Federico Araneo[3], Eugenia Bartolucci[3], Fabio Pascarella[3], Mentore Vaccari[1]

[1] *Department of Civil, Environmental, Architectural Engineering and Mathematics, University of Brescia, Brescia, Lombardy, Italy*
[2] *ENEA, Sustainability Department, Resource Valorisation Lab, Casaccia Research Center, Via Anguillarese 301, Rome, 00123, Italy*
[3]*Department for the Geological Survey of Italy, Italian Institute for Environmental Protection and Research, 00144 Rome, Italy*
Keywords: contaminated sites; land use; brownfield; sustainable remediation

Introduction

Soil is a fundamental resource for essential functions such as food production, fibre cultivation, energy generation, climate moderation, and water provision [1]. Despite its main role, many businesses overlook the critical link between soil health and economic performance. An alarming trend is the excessive consumption of soil, in Italy, following a recent study conducted by ISPRA, land consumption affected 76.8 km^2 in 2022. In the past year alone, this equates to consuming more than 21 hectares of land every day [2]. This uncontrolled urbanization is dangerous for biodiversity and natural resources and represents a significant threat to the environment and humans. These considerations underscore the urgent need for sustainable land-use planning strategies aimed at preserving environmental resources.

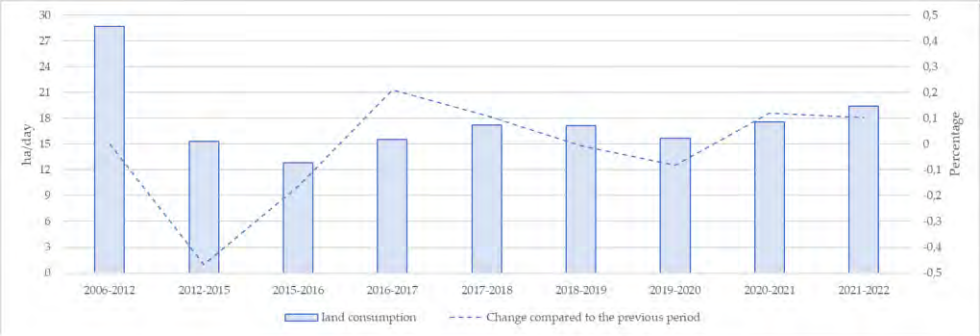

Figure 1. Rate of net daily land consumption (2006-2022). The dotted line represents the change compared to the previous period.

A primary role in limiting land-consumption is played by initiatives whose common orientation is the reuse of what is underused or unused, as regenerating abandoned areas and reusing abandoned buildings [3]. Crucially in this respect, the EPA launched the *Brownfields Economic Redevelopment Initiative* in 1994 to address contamination in abandoned industrial and commercial sites. The initiative aimed to rejuvenate these sites, known as brownfields, by mitigating environmental risks and fostering economic growth through job creation and housing development, benefiting communities of all sizes. The strategic redevelopment of brownfields has emerged as a promising approach for achieving mutually beneficial outcomes for both the economy and the environment. Reviving neglected areas allows communities to regain valuable land, foster sustainable development, enhance quality of life, and protect environmental well-being. Central to tackling these issues is the notion of reclamation sustainability, which primarily focuses on two crucial aspects: assessing resource efficiency and balancing the value of the resource slated for restoration with the environmental effort required to

achieve it [4]. The reuse of land and the regeneration of brownfields are currently slowed down by numerous obstacles, mainly of a regulatory, procedural, and economic nature. These can be overcome with targeted interventions [3]. An example in this sense was the introduction of simplified procedures for reclamation operations, reducing times compared to the ordinary procedure [5]. Effective and timely remediation is essential for reducing threats, managing liabilities, controlling expenses, and enhancing property values [6]. In this regard, the European Commission proposed a new soil-monitoring law in 2023 to promote sustainable soil management and restoration, setting the EU on a path towards healthy soil by 2050 [7]. Italian legislation on Contaminated Sites Management was introduced with Ministerial Decree n. 471/99 (DM 471/99) and was significantly modified by Legislative Decree 152/06 (D.Lgs. 152/06), which is still in force. DM 471/99 sets concentration limit values (CLA) for soil/subsoil and groundwater, and if these values are exceeded, the site is defined as contaminated [48,49]. Legislative Decree n. 152/06 sets screening values (CSCs) for soil/subsoil and groundwater; if the CSC is exceeded, the site is identified as potentially contaminated. This study aims to identify the main factors slowing down the regeneration of brownfields by a thorough examination of the timeframes associated with managing contaminated sites, including those that have been completed as well as those currently in progress.

Methodology

The evaluation at the national level was conducted utilizing the national register of contaminated sites in Italy, MOSAICO. The dataset was assessed concerning several key factors: (i) the management stage in which closure occurred (notification, conceptual model, intervention); (ii) the type of procedure (previous or current legislation, and, for the latter, ordinary or simplified procedures). The study identified the number of procedures conducted under Ministerial Decree 471/99 legislation before 2006, and those conducted under Legislative Decree 152/2006 legislation after 2006. A statistical analysis was conducted on the dataset comprising 8023 completed procedures documented in MOSAICO, categorized into various classes, as detailed below in the Result section.

Results

The first statistical analysis was performed on the complete dataset extracted from MOSAICO (8023 procedures) clustered into three classes according to the procedure closure mode: Procedure Closure after Notification (PCN); Procedure Closure after Conceptual Model (PCCM); Procedure Closure after Intervention (PCI). The PCN, PCCM, and PCI distributions are shown in Figure 2. Box plots represent the 25th and 75th percentiles (bottom and top of the box), while the inner line represents the median. The upper and lower whiskers of a box plot represent the interquartile range (IQR) multiplied by 1.5 above and below the 75th and 25th percentiles, respectively. The analysis indicates that procedures concluded after notification are generally the quickest on average. Additionally, there doesn't seem to be a significant time difference between procedures closed after the conceptual model and those closed after intervention.

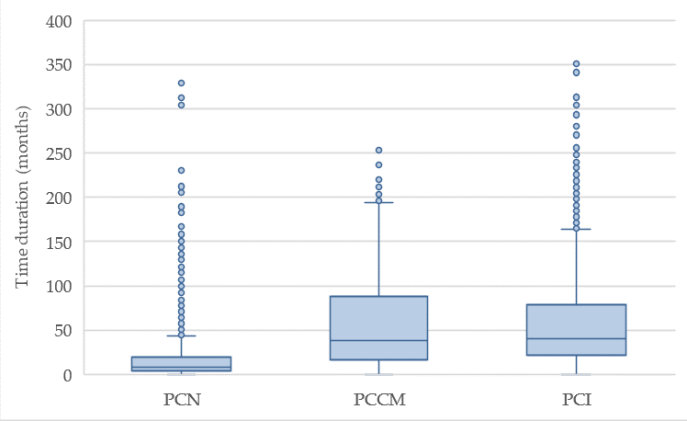

Figure 2. Time duration for completed procedures in Italy according to closure modality: (PCN), (PCCM), (PCI).

A second statistical analysis was performed on PCI alone, divided into two classes: Procedure Closure after Intervention by Remediation (PCIR, 1749 sites) and Procedure Closure after Intervention by Other Management Processes (PCIOMP, 1200 sites). We applied the same statistical tests mentioned above, and, as above, the obtained results showed no normal distributions and the absence of outliers. The PCIR and PCIOMP medians are statistically different (p-value less than 0.05) at the 95% confidence level; the difference is even more significant when comparing the 75th percentile (66.0 and 95.5 months). The PCIR duration distribution (percentiles) is systematically lower than PCIOMP.

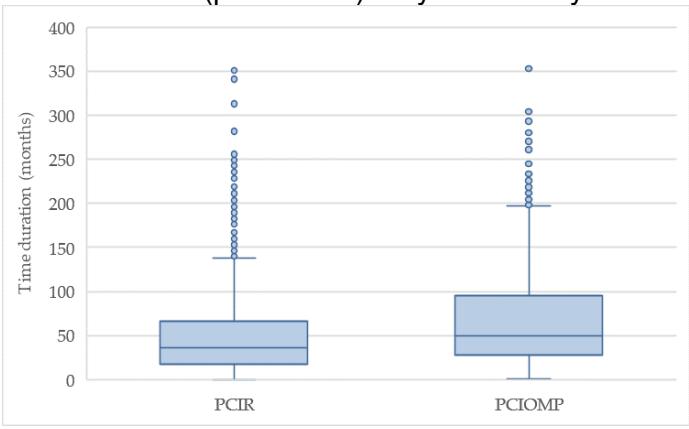

Figure 3. Time for completed procedures with intervention according to intervention type: (PCIR), (PCIOMP).

A third statistical analysis was performed on PCI, considering the relevant legislation: Procedure Closure after Intervention under DM 471/99 (PCI471); Procedure Closure after Intervention under D.Lgs. 152/06—ordinary procedures (PCIO152); Procedure Closure after Intervention under D.Lgs. 152/06—simplified procedures (PCIS152). Non-parametric distributions describe the PCIO152 and PCI471 duration, while the PCIS152 data are found to be lognormal. To compare the three groups, we performed non-parametric statistical tests. The distributions are significantly different (p-value less than 0.05 at the 95% confidence level). As shown in Figure 4, the timing median follows the order of PCIO152 (48.7 months) > PCI471 (37.1 months) > PCIS152 (23.5 months)

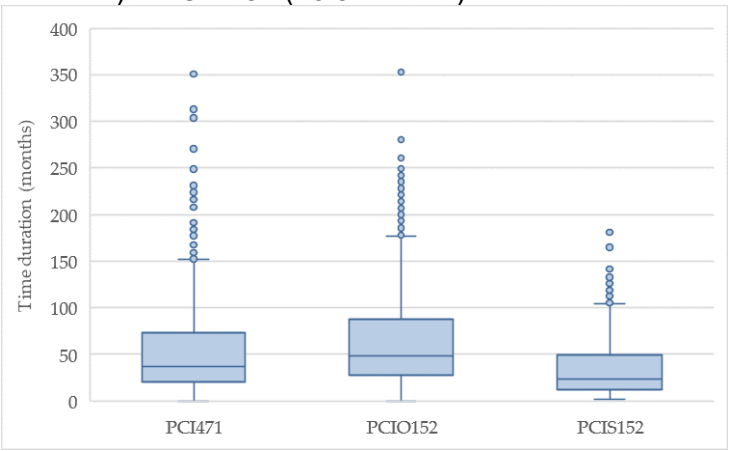

Figure 4. Time duration for completed procedures with intervention in Italy according to procedure type: DM471/99 (PCI471), DLgs152/06-ordinary procedures (PCIO152), DLgs152/06-simplified procedures (PCIS152).

Conclusion

The timing of contaminated site remediation procedures holds paramount importance, as it impacts various critical aspects such as environmental and health considerations, effectiveness, adherence to legal requirements, land restoration, community involvement, and long-term environmental implications. This study fills a gap in the scientific literature by investigating the timing of contaminated site remediation in the context of the Italian scenario, utilizing the MOSAICO database and referencing Italian legislation. Through statistical analysis, we have uncovered significant heterogeneity in the duration of administrative management procedures, influenced by various factors and stages of the remediation process. The causes of the lengthening of remediation process times are multiple and require solutions of various kinds, such as regulatory, procedural, and technical. For example, a procedure must be defined that clarifies times, methods, and responsibilities when sites of national interest are downgraded to sites of local interest. Additionally, regional task forces should be formed to assist officials from smaller municipalities lacking specialized expertise in this area. Lastly, competent authorities could develop and release guidelines that meticulously specify the required data and technical standards for project documentation. It appears necessary to introduce simplified procedures for the redevelopment of abandoned industrial sites. As observed with the procedure governed by Article 242bis, there are noticeable reductions in the time required. It is necessary to identify incentive mechanisms for the reuse of anthropized areas for the location of new investments, giving priority to reclaimed sites and abandoned industrial areas, or partially abandoned or in the process of conversion. the declaration of public utility must be extended to degraded and abandoned areas for the purposes of unlocking/accelerating recovery activities.
Future research is needed to comprehensively evaluate the remediation costs associated with contaminated sites and their correlation with time. Analysing expenses at different stages and understanding this relationship will facilitate cost-effective decision making and resource optimization for successful site cleanup in Italy.

References

[1] Doula, M.K.; Sarris, A. Soil Environment. In Environment and Development; Elsevier: Amsterdam, The Netherlands, 2016; pp. 213–286.
[2] SNPA (2023a). *Consumo di suolo, dinamiche territoriali e servizi ecosistemici. Edizione 2023.* Report SNPA 37/23, ISBN 978-88-448-1178-5
[3] CeRAR (2020). *Proposte per favorire le bonifiche di siti contaminati in Italia*. Documento elaborato dal CeRAR – Centro di Ricerca "Risanamento ambientale e recupero di aree degradate e siti contaminati" dell'Università degli Studi di Brescia. Foroeuropa, n. 3, vol. 2020, ISSN 2038-5161. Disponibile sul sito
[4] Vaccari M., Villani I. (2021). *Sostenibilità e benefici generati dagli interventi di risanamento e recupero di siti contaminati: analisi di un caso studio*. In "Siti contaminati. Esperienze negli interventi di risanamento", a cura di M.R. Boni, C. Collivignarelli, F.G.A. Vagliasindi, Ed. CSISA, Catania, febbraio 2021, pp.301-307, ISBN 88-7850-025-9
[5] Araneo, F.; Bartolucci, E.; Pascarella, F.; Pinzin, F.; Illankoon, W.A.M.A.N.; Vaccari, M. The Role of Procedure Duration in the Sustainability Assessment of Contaminated Site Management in Italy. *Sustainability* **2024**, *16*, 2329. https://doi.org/10.3390/su16062329
[6] Sousa, C.D. Contaminated Sites: The Canadian Situation in an International Context. J. Environ. Manag. 2001, 62, 131–154. https://doi.org/10.1006/jema.2001.0431.
[7] Stankovics, P.; Montanarella, L.; Kassai, P.; Tóth, G.; Tóth, Z. The Interrelations of Land Ownership, Soil Protection and Privileges of Capital in the Aspect of Land Take. Land Use Policy 2020, 99, 105071. https://doi.org/10.1016/j.landusepol.2020.105071.
[8] Cecchi, G.; Marescotti, P.; Di Piazza, S.; Zappatore, S.; Zotti, M. Fungal Richness in the Extreme Environments of the Libiola Mine (Eastern Liguria, Italy): Correlations among Microfungi, Lithology, Mineralogy, and Contaminants. Environ. Earth Sci 2019, 78, 541. https://doi.org/10.1007/s12665-019-8553-0.

PARALLEL SESSION: A5

Wastewater treatment

Advanced biological wastewater treatments

Title: Salinity effects on the Purple non-sulfur bacteria biomass production

Author(s): Anuska Mosquera-Corral, Miguel Bouzas, José Ramón Lorenzo-Llarena, Ángeles Val, Alba Pedrouso

[1] Department of Chemical Engineering, CRETUS Institute, Universidade de Santiago de Compostela, Spain, anuska.mosquera@usc.es; miguel.bouzas.fernandez@usc.es; joseramon.lorenzo.llarena@usc.es; mangeles.val@usc.es; alba.pedrouso@usc.es.

Keyword(s): growth, polyhydroxyalkanoates, PPB, wastewater

Abstract

Purple phototrophic bacteria (PPB) based processes are under study as candidates to improve the circularity of wastewater treatment. PPBs are characterized by their great versatility in terms of the transformations that they develop, such as organic matter oxidation (aerobically or anaerobically), production of protein-rich biomass, polyhydroxyalkanoates (PHA), H_2, etc. [1].

Therefore, PPBs are studied to develop either processes for wastewater treatment and/or valorisation. Among the possible valorisation processes are those devoted to the production of material products, as the PPB biomass itself outstands while simultaneously removing pollutants from wastewater. Both processes have been extensively studied in systems operating with pure cultures [2], but more research is needed to understand the effect of compounds present in wastewater, like for example salts.

In the present research work, the performance of PPB-based processes under saline conditions to produce protein-rich biomass and remove organic matter and nitrogen are studied.

Materials and methods

A mixed culture enriched on PPB was inoculated in a hermetically closed 2-L glass reactor operated in discontinuous mode as a Sequencing Batch Reactor (SBR). Its operation was controlled by a Programmable Logic Controller (PLC). The feeding and discharge of the reactor were performed with two peristaltic pumps, and the reactor was provided with a mechanical stirrer (90 rpm) to guarantee the complete mixture. Operational cycles were defined with a duration of 3.5 days (2 cycles per week). The duration of the cycles was chosen to ensure that enough time was available for the complete removal of the chemical oxygen demand (COD) fed and biomass production regardless of the potential decrease in activity caused by the increasing salinities tested. The operational cycles comprised 3 stages: feeding of 1.52 L (8 min), reaction (3.5 days) and effluent withdrawal of 1.52 L (9 min). The volume exchange ratio was set at 76 %. The reactor was covered with an *ecolours+ e299* selector filter that favoured the passage of infrared light between 805 and 1035 nm. An incandescent type of lamp (100 W), continuously switched on, was located 20 cm from the reactor surface. The feeding was a synthetic solution of 0.467 mg CH_3COOH/L, 0.405 mg NH_4Cl/L, and other macro and micronutrients and adjusted to a pH of 6.5, according to Ormerod et al. [3]. Four NaCl concentrations were tested: 0, 5, 10, and 20 g/L. The biomass concentration at the beginning of each cycle ranged from 60 to 80 mg VSS/L. After the acclimation to

each different salt concentration that lasted 4 operation cycles (two weeks), single operational cycles were monitored.

The maximum COD consumption rate was estimated as the maximum slope of the curve described by the evolution of the concentration of acetic acid expressed as COD at the beginning of the monitored cycles (first day). The COD content of the biomass used for the calculations was estimated as 1.43 g COD/g VSS from the elemental analysis of a biomass sample, which provided the following stoichiometry: $C_5H_{9.8}O_{2.26}N_{1.13}S_{0.04}$. The total amount of biomass (VSS) produced in each cycle was estimated from the ammonia nitrogen consumption and according to the previous stoichiometry. Volatile suspended solids (VSS) were also determined analytically for suspended biomass. Samples for the VSS were always taken from the same height in the reactor to minimize the error of possible stratification when comparing different operational periods.

Results and discussion

The COD consumption as acetic acid took place, for all salinities studied, on the first day of the cycle (Figure 1a). Associated biomass growth was observed during this period, although the biomass concentration measured as suspended solids decreased significantly with increasing salinity (Figure 2a). The pH value slightly increased from 6.5 to 7.1 (Figure 1b) in all experiments during due to the acetic acid consumption. Then, the pH remained stable during the rest of the cycle. Salinity also affected the physical properties of the biomass, which partially lost its characteristic purple colour, while its tendency to adhere, first to the reactor wall (5 and 10 g NaCl/L) and later forming aggregates (20 g NaCl/L), led to biomass stratification remaining at the bottom of the reactor. The amount of attached biomass was higher with the increment in saline concentrations (Figure 2b).

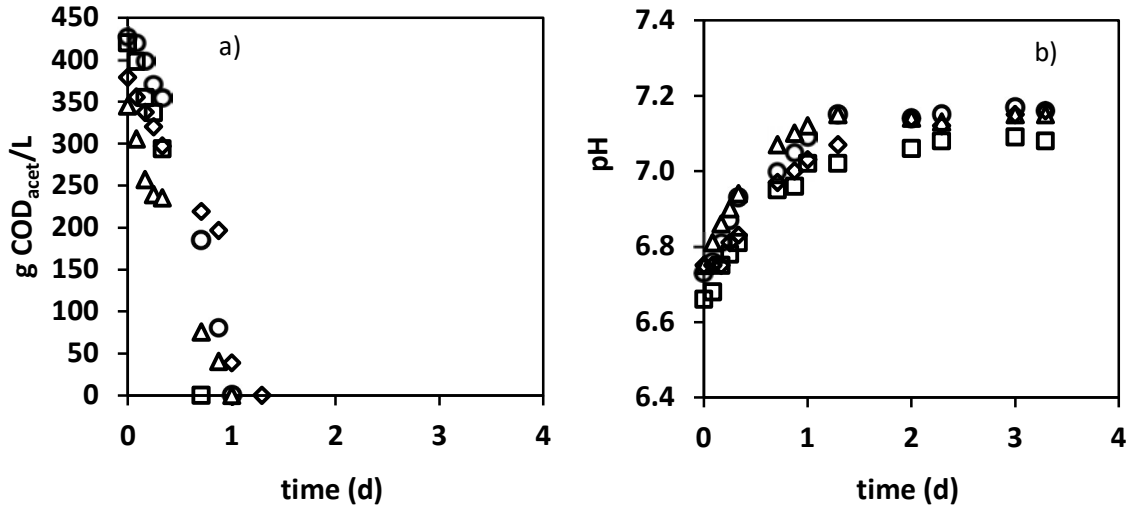

Figure 1. Evolution of acetic acid concentration as COD (g COD_{acet}/L) (a) and pH (b) throughout the monitored cycles performed at concentrations of 0 (○), 5 (△), 10 (□), and 20 (◇) g NaCl/L.

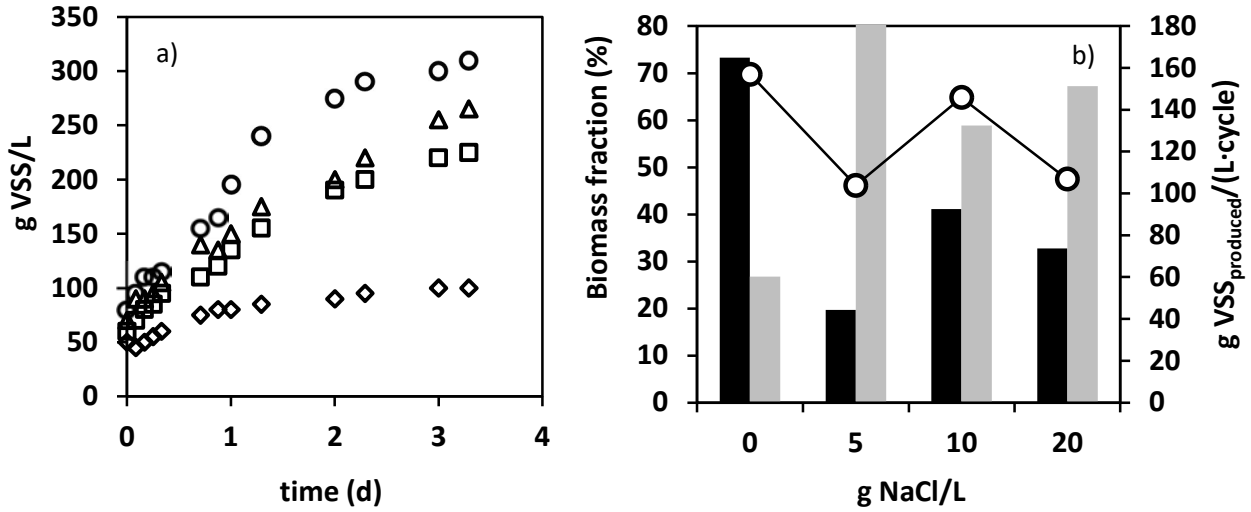

Figure 2. a) Evolution of biomass concentration throughout the monitored cycles performed at concentrations of 0 (○), 5 (△), 10 (□), and 20 (◇) g NaCl/L. b) Percentage of biomass suspended (■); and attached to the reactor wall and/or settled as granules (■), and total amount of biomass production estimated in a cycle (○).

Regarding the effect of salinity on biomass activity a stimulatory effect in the case of adapted biomass is frequent at relatively low salt concentrations of 5 and 10 g NaCl/L, while inhibition takes place at 20 g NaCl/L [4]. In the present study, although a similar effect on COD removal rate is observed (Figure 3), it cannot be directly attributed to stimulatory or inhibitory effects. In this way, if the biomass concentration is considered, the maximum specific COD removal rates (Table 1), measured on the first day of the cycle, remain at values similar to those obtained by other authors [2] independently of the saline conditions.

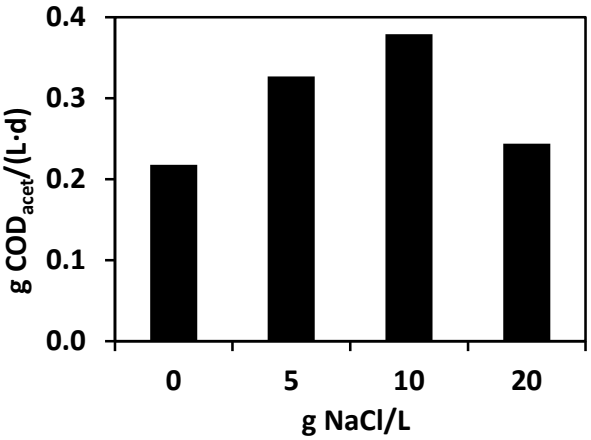

Figure 3. Maximum COD consumption rate measured in the cycles performed at different salt concentrations.

Regarding the organic matter and nitrogen removal efficiencies the fed acetate was completely removed in the reactor on the first day of operation, while nitrogen removal corresponded to the ammonia assimilation for biomass growth throughout the whole cycle (Table 1).

Table 1. Removal efficiencies of COD and nitrogen fed.

g NaCl/L	$COD_{acetate}$ removal (%)	NH_4^+-N removal (%)	g $COD_{acet,rem}$/(g VSS·d)
0	100	31.0	1.37
5	100	41.4	0.89
10	100	23.1	1.85
20	100	17.5	1.96

Conclusions

Salinity affects the physical properties of the biomass by enhancing its attachment capacity and aggregation which facilitates its separation from the effluent and its retention inside the reactor if needed. The maximum specific COD removal activity is not affected by salinity and remains above 0.8 g COD/(g VSS·d) in all experiments. Ammonia nitrogen was removed only for biomass growth. Concerning the biomass production, it varied in a range from 106 to 150 g VSS/(L·cycle) but no clear relationship was observed between these values and the salinity of the experiments.

Acknowledgments

This research was supported by the Spanish Government (AEI) through the ECOPOLYVER project (PID2020-112550RB-C21). Alba Pedrouso also acknowledges the Xunta de Galicia (Spain) for her postdoctoral fellowship (ED481B-2021-041). Likewise, José Ramón Lorenzo Llarena thanks the Ministry of Science, Innovation and Universities (Spain) for the FPU Grant 021/05797. The authors belong to a Galician Competitive Research Group (GRC ED431C 2021/37).

References

[1] Capson-Tojo G., Batstone D.J., Grassino M., Vlaeminck S.E., Puyol D., Verstraete W., Kleerebezem R., Oehmen A., Ghimire E., Pikaar I., Lema J.M., Hülsen T., "Purple phototrophic bacteria for resource recovery: Challenges and opportunities", Biotechnology Advances, 43, 107567, (2020).

[2] Cerrutti, M., Stevens B., Ebrahimi S., Alloul A. Vlaeminck S.E., Weissbrodt D.G., "Enrichment and aggregation of purple non-sulfur bacteria in a mixed-culture sequencing-batch photobioreactor for biological nutrient removal from wastewater", Frontiers in Bioengineering and Biotechnology, 8, 557234, (2020).

[3] Ormerod, J.G, Ormerod K.S., Gest H., "Ligth-dependent utilization of organic compounds and photoproduction of molecular hydrogen by photosynthetic bacteria; relationships with nitrogen metabolism", Archives of Biochemistry and Biophysics, 94, 449-463. (1961).

[4] Dapena-Mora A., Vázquez-Padín J.R., Campos J.L., Mosquera-Corral A., Jetten M.S.M. and Méndez R. "Monitoring the stability of an Anammox reactor under high salinity conditions", Biochemical Engineering Journal, 51, 167-171. (2010).

Title: Autochthonous microalgae for the treatment of urban wastewaters

Authors: Serena Lima*[1,2], Alessandro Cosenza[1,2], Franco Grisafi[1], Giuseppe Caputo[1], Francesca Scargiali[1].

[1] *Dipartimento di Ingegneria, Università degli Studi di Palermo, Palermo, Italy, dipartimento.ingegneria@unipa.it.*
[2] *National Biodiversity Future Center (NBFC), Palermo, Italy, hub@nbfc.it.*

Keywords: Indigenous microalgae, Microalgal wastewater treatment, Civil wastewaters, Kinetic model, Growth modeling.

Abstract

The rapid increase in human population over the last few centuries, alongside concurrent industrialization, has exerted a profound impact on the environment, characterized by a substantial surge in waste generation. Considering these critical global challenges, the remediation and responsible management of wastewater have become of critical importance in environmental science, policy development, and public awareness. Biological purification mainly occurs through consortia of microorganisms, typically heterotrophic bacteria that utilize carbon sources present in sewage, in presence of oxygen, for their growth and energy needs. In this context, microalgae may play an important role in the remediation of wastewaters, moreover, a microalgal biomass valorization perfectly centre the circular economy purposes. Microalgae, in fact, represent a diverse array of photosynthetic microorganisms, spanning a wide range of species across different phyla. They also possess the remarkable ability to thrive in diverse types of wastewaters and efficiently remove nitrogen and phosphorus from these environments [1]. This feature makes them a promising option for integration into traditional wastewater treatment plants. Microalgae find application in wastewater treatment processes for several reasons: i) decreasing nitrate and phosphate concentrations; ii) reducing aeration costs due to oxygenation resulting from photosynthesis; iii) producing biomass that can be utilized in various sectors and contains high-value biomolecules [2].
The biomass of microalgae, including that grown in wastewater treatment tanks, can be used in various sectors, such as biofuel production or the production of carbohydrates and lipids for food and nutraceutical purposes. Furthermore, they are exploited for their content of high-value biomolecules (such as carotenoids and omega-3 fatty acids), and research over the years has proposed several strategies to optimize the production of these biomolecules [3].
The effectiveness of the autochthonous microalga Chlorella sp. CW2 in treating urban wastewater has been analyzed in the present work. In particular, the kinetic growth parameters of this microalga specie were found, through batch experiments. To comprehend and forecast the wastewater treatment process, as well as to operate it under the desired conditions, kinetic models serve as a valuable tool. Critical kinetic parameters are required for the design and proper sizing of raceway reactors, including the maximum specific growth rate (μmax) and the substrate constant (Ks). Typically, these parameters are obtained from batch experiments in which microalgae are introduced into a photobioreactor containing a known initial quantity of nutrients. During these experiments, the cellular concentration increases over time while the nutrient concentration decreases. By analyzing the cellular growth rate for each batch culture in relation to the initial substrate concentration, valuable information about kinetic parameters can be derived.

The microalgae strain, previously isolated and characterized [4], was cultured in a synthetic wastewater with the composition detailed in Table 1.

Table 1. Synthetic wastewater composition

Component	Concentration [mg L^{-1}]
Glucose	221.7
NH_4Cl	153.0
$NaNO_3$	160.0
$CaCl_2 \cdot (2H_2O)$	165.0
Na_2SO_4	63.37
K_2HPO_4	56.37
$NaHCO_3$	200.0
EDTA (Na_2 salt)	6.37
$FeCl_3 \cdot (6\ H_2O)$	4.85
$CuSO_4 \cdot (5\ H_2O)$	0.02
$ZnSO_4 \cdot (7\ H_2O)$	0.03
$CoCl_2 \cdot (6\ H_2O)$	0.02
$MnCl_2\ (4\ H_2O)$	0.28
$Na_2MoO_4\ (2\ H_2O)$	0.01

Once the cells reached the late exponential phase (typically after approximately 8 days of cultivation), 10 mL of the cell suspension were transferred to inoculate the main culture in the sewage medium. Cultures were grown in 250 mL Erlenmeyer flasks containing 150 mL of culture, placed in an oscillating incubator (Corning Lse) under a photon flux of 200 µmol m^{-2} s^{-1} at 27°C. To acquire the kinetic parameters, microalgae were cultured in biological triplicates using 250 mL Erlenmeyer flasks. The growth medium utilized was derived from the original synthetic wastewater formula, with varying concentrations of glucose ranging from 2.2 mg L^{-1} to 300.0 mg L^{-1} (GLUC series), phosphate from 0.6 mg L^{-1} to 56.4 mg L^{-1} (PO_4^- series), and ammonium from 9.6 mg L^{-1} to 153 mg L^{-1} (NH_4^+ series). Additionally, another set of cultivations was conducted by growing the microalgae in diluted media. This dilution process was implemented gradually, starting from the original 100% concentration of limiting nutrients and progressively reducing it to 0.5% (STD series). Through these cultivations, the objective was to investigate the impact of nutrient limitation on microalgae growth and to analyze how their growth behavior adapts to varying levels of nutrient availability.
Throughout the 3-day cultivation period, the concentration of the microalgal suspension was regularly monitored at least twice daily by measuring the absorbance of the culture at 750 nm using a spectrophotometer (Cary 60 UV–Vis, Agilent Technologies).
The specific growth rate µ can be represented by the Monod equation:

$$\mu = \frac{\mu_{max}\, S}{K_s + S}$$

where S is the nutrient concentration, and μ_{max} and Ks are the kinetic parameters. This equation describes the relationship between the concentration of the limiting substrate and the specific growth rate µ. The specific growth rate µ was determined during the exponential phase of cell growth using the following formula:

$$\mu = \frac{\ln X - \ln X_0}{t - t_0}$$

where X_0 is the biomass concentration at time t_0, and X is the biomass concentration at time t.
The kinetic parameters were estimated through a Langmuir Plot. To obtain the kinetic parameters, μ_{max} and Ks, Equation (2) can be rearranged according to Langmuir as:

$$\frac{S}{\mu} = \frac{1}{\mu_{max}} S + \frac{K_s}{\mu_{max}}$$

A Langmuir plot of S/μ versus S should yield a linear relationship, from which the kinetic parameters can be derived from the slope ($1/\mu_{max}$) and intercept (Ks/μ_{max}).
Figure 2 illustrates the growth pattern of the microalgae Chlorella sp. CW2. The temporal progression displays characteristic growth curves, featuring an exponential growth phase followed, in certain instances, by a lag phase. A discernible trend is evident from the figure, emphasizing the impact of fluctuating nutrient concentrations on the growth dynamics.

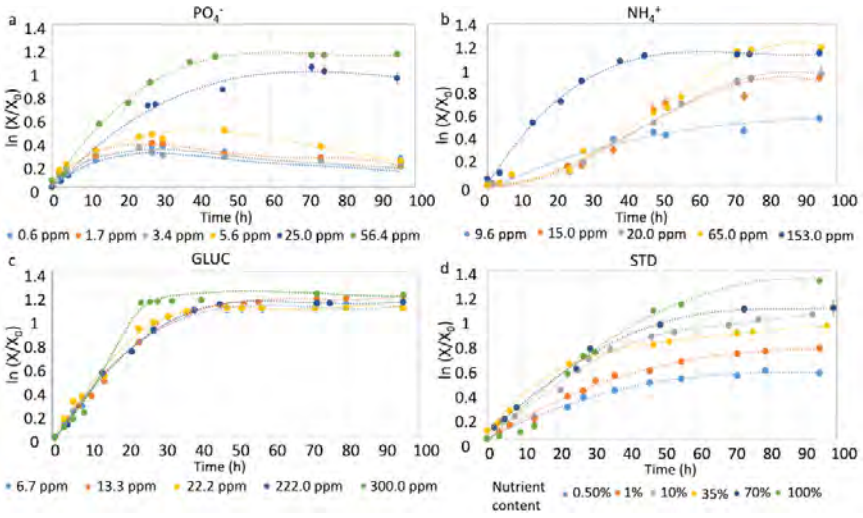

Figure 1. Growth of microalga Chlorella sp. CW2 in different limiting nutrients concentrations.

By employing the computed growth rate from each cultivation, a Langmuir plot was generated for every cultivation series. This approach facilitated the calculation of the kinetic parameters, including the maximum growth rate (μ_{max}) and half-saturation constant (Ks), for each limiting nutrient. These parameters are depicted alongside the measured growth rates (μ) for each cultivation series, as shown in the example in Figure 2 for the PO_4^{3-} case.

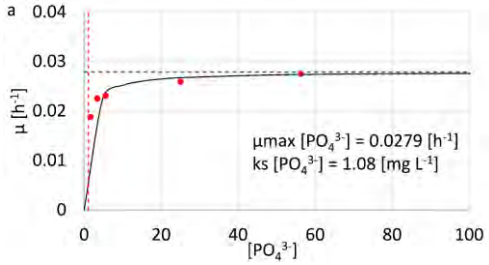

Figure 2. Specific growth rate versus different limiting nutrient concentrations of the microalga Chlorella sp CW2. Red circles indicates the experimental data, while the line represents the Monod equation.

The obtained kinetic parameters were used to model and predict the biomass growth both in Erlenmeyer flasks and in a lab-scale raceway photobioreactor.
Cell concentration modeling involved tracking the concentration of individual nutrients at discrete time

intervals. This process utilized a specific growth factor μ, computed for each interval using the Equation:

$$\mu = \frac{1}{3}\left(\frac{\mu_{maxNH_4^+}}{K_{maxNH_4^+} S_{NH_4^+}} + \frac{\mu_{maxPO_4^{3-}}}{K_{PO_4^{3-}} S_{PO_4^{3-}}} + \frac{\mu_{maxgluc}}{K_{gluc} S_{gluc}}\right)$$

which incorporated the kinetic parameters specific to each nutrient. This modeling approach was applied to both the batch growth in the raceway reactor and the batch growth in Erlenmeyer flasks, using the standard formulation of synthetic sewage. The outcomes of the Equation:

$$X = X_i e^{(\mu - kd)\Delta T}$$

(where X_i represents the initial cell concentration for the specific time interval, μ is the growth factor at the prevailing nutrient concentration of that time interval [h^{-1}], k_d is the death factor and ΔT is the duration of the time interval [h]) and the fitting of the experimental data are depicted in Figure 3, together with the experimental data.

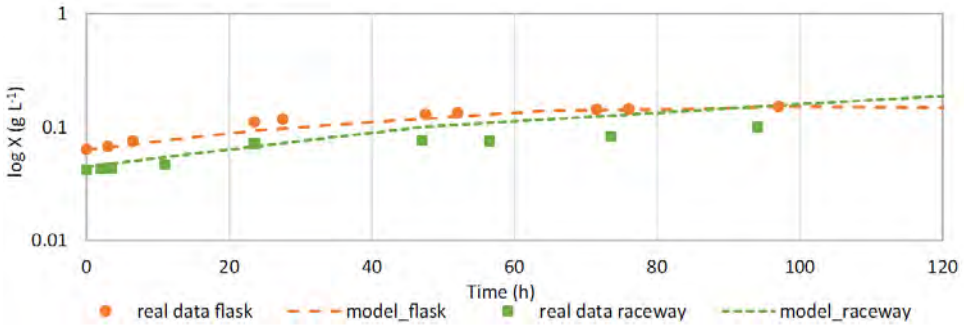

Figure 3. Comparison between model prediction (with k_d = 0.3 μ_{max}) and experimental data of Chlorella sp. CW2 growth curves in batch raceway reactor and shaking flask: "orange" shaking flask, "green" raceway photobioreactor. Dotted lines, model predictions; symbols, experimental data.

This study illustrates the potential of employing microalgae, particularly indigenous strains, for municipal wastewater treatment. Additionally, a straightforward approach, featuring a novel kinetic model, for tackling wastewater treatment utilizing microalgae was proposed.

References

[1] Molinuevo-Salces B., Riaño B., Hernández D., Cruz García-González M., Microalgae and Wastewater Treatment: Advantages and Disadvantages, in: Md.A. Alam, Z. Wang (Eds.), Microalgae Biotechnology for Development of Biofuel and Wastewater Treatment, Springer Singapore, Singapore, 2019: pp. 505–533. https://doi.org/10.1007/978-981-13-2264-8_20.
[2] Lima S., Schulze P.S.C., Schüler L.M., Rautenberger R., Morales-Sánchez D., Santos T.F, Pereira H., Varela J.C.S., Scargiali F., Wijffels R.H., Kiron V., Flashing light emitting diodes (LEDs) induce proteins, polyunsaturated fatty acids and pigments in three microalgae, J Biotechnol 325 (2021) 15–24. https://doi.org/10.1016/j.jbiotec.2020.11.019.
[3] Lima S., Villanova V., Grisafi F., Caputo G., Brucato A., Scargiali F., Autochthonous microalgae grown in municipal wastewaters as a tool for effectively removing nitrogen and phosphorous, Journal of Water Process Engineering 38 (2020). https://doi.org/10.1016/j.jwpe.2020.101647.
[4] Lima S., Brucato A., Caputo G., Grisafi F., Scargiali F., Inoculum of indigenous microalgae/activated sludge for optimal treatment of municipal wastewaters and biochemical composition of residual biomass for potential applications, Journal of Water Process Engineering 49 (2022) 103142. https://doi.org/10.1016/j.jwpe.2022.103142.

Title: Development of aerobic granular sludge from activated sludge in a pilot scale sequencing batch reactor treating municipal wastewater

Author(s): Caterina Senesi*[1], Riccardo Campo[2], Simone Caffaz[3], Claudio Lubello[4], Tommaso Lotti[5].

[1,2,4,5]Department of Civil and Environmental Engineering, University of Florence, Florence, Italy, caterina.senesi@unifi.it[1]; riccardo.campo@unifi.it[2]; claudio.lubello@unifi.it[4]; tommaso.lotti@unifi.it[5];
[3] Publiacqua S.p.A., Florence, Italy, s.caffaz@publiacqua.it

Keyword(s): aerobic granular sludge, low influent C/N ratio, phosphate removal, COD anaerobic uptake, pilot scale demonstration, granulation process.

Abstract

This work reports on the formation of aerobic granular sludge (AGS), starting from an activated sludge inoculum, that was obtained in a pilot plant sequencing batch reactor (SBR) treating low strength municipal wastewater. Feast/famine regime, together with the application of increasing hydraulic selective pressure (HSP) and the increase in organic loading rate (OLR) resulted key for the development of an almost full granular system (flocculant sludge mass fraction <10%) with chemical oxygen demand (COD) and phosphate (PO_4-P) removal efficiencies of 88% and 100%, respectively, within three months.

Introduction

AGS is an innovative and promising technology for biological wastewater treatment. Compared to conventional activated sludge (CAS) systems, AGS technology shows multiple advantages: (i) lower footprint (25-75%), (ii) savings in term of energy (20-50%); (iii) faster sludge settleability and higher biomass retention allowing smaller reactor size [1-3]. AGS is a particular type of biofilm consisting in self-aggregated microbial structures with high density and a multilayered conformation with different redox potential conditions due to e-donors and e-acceptors radial concentration gradients [1]. The layered structure facilitates the co-existence of aerobic nitrifying microorganism in the outer layers of the granules and denitrifying (phosphate, glycogen) accumulating organisms (dPAOs, dGAOs) in the anoxic core [1].Therefore, this technology is ideal for simultaneous removal of COD, nitrogen (N) and phosphorus (P) [1,4]. AGS technology was firstly scaled-up for high strength industrial and municipal wastewater treatment under the trade name Nereda® [5]. Recently, there is a growing interest in extending the AGS application also to low strength municipal wastewater.

In the Italian case, municipal wastewaters are often characterised by low carbon to nitrogen (C/N) ratios [3]. This is due to the widespread presence of wastewater pretreatment by septic tanks prior its release in sewerage systems. Moreover, most of sewerage systems are combined and wastewater is diluted by meteoric precipitations as well as by infiltrations and inlets of extraneous waters [3]. Low C/N wastewater treatments often imply hight costs for the dosage of exogenous COD, since most of the N removal technologies rely on heterotrophic denitrifying organisms [6]. The application of AGS to the treatment of low C/N wastewater will reduce these costs and furthermore would allow the recovery of organics' chemical energy (e.g. methane production) and/or mass (e.g. PHA, C-commodities) in the case of high C/N ratio wastewater [6].

In a previous study conducted by the same research group, AGS resulted in a long-term successful

treatment of low C/N ratio (3.8 g/g) real wastewater in a lab scale granular SBR (G-SBR), obtaining simultaneous removal of COD, PO_4-P and N with efficiencies of 84%, 96% and 71% respectively [4]. The aim of this project is demonstrating in a pilot scale G-SBR the results previously achieved at lab-scale [4] and providing an operational strategy for quick start-up. In this abstract, the granulation process of the activated sludge used as inoculum is presented.

Materials and methods

A pilot scale SBR, with an operative volume of 2 m^3 and height/diameter ratio of 1.18, was inoculated with 1.5 m^3 of activated sludge taken from a full scale SBR treating municipal wastewater. From that moment on, the pilot plant was fed with real municipal wastewater for 95 days with the aim to obtain granulation through the application of metabolic selection and HSP, as suggested by many authors [1-5]. The set up of the pilot plant is schematized in Figure 1. The G-SBR cycle structure was composed of 6 phases: anaerobic phases of (i) feeding and (ii) mixing; (iii) an aerobic phase with external air supply; (iv) a mixed anoxic phase; (v) settling and consequent (vi) withdrawal of the effluent. The operational cycle length was 6 hours. The volume exchange ratio (VER) was 43%.
The operative period of the pilot plant was divided into two phases. During operational Phase I (days 0-37), concentrated acetic acid (~900 gCOD/L) was added to the influent, raising the dosage in three steps up to 150 mgCOD/L, in order to increase OLR and accelerate the granulation process [2]. Furthermore, a stepwise increase of HSP was applied by reducing settling time from 39 min to 11 min (corresponding to minimum settling velocities of 1.6 m/h and 5.6 m/h, respectively, having discarded the first minute of settling phase due to inertial movements). In Phase II (days 38-95), settling time of 11 min and the addition of 150 mgCOD/L in the influent were maintained constant.

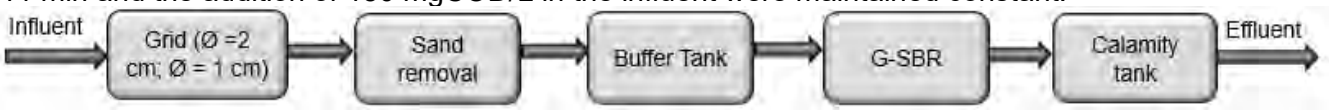

Figure 1. Schematic representation of the setup of the pilot plant.

Total suspended solids (TSS), volatile suspended solids (VSS), sludge volume index after 30 (SVI30) and 5 (SVI5) minutes were measured according to the Standard Methods [7]. Total COD (tCOD), ammonia–nitrogen (NH_4-N), nitrite (NO_2-N), nitrate (NO_3-N) and PO_4-P were measured through kits HACH Lange®. Soluble COD (sCOD) was determined after filtration at 0.45 µm. Total inorganic nitrogen (TIN) was calculated as the sum of NH_4-N, NO_2-N and NO_3-N. The particle size distribution (PSD) of granules was measured according to [4]. Mass fraction of flocculent biomass over granular biomass was determined by sieving mixing liquor through a 0.2 mm screen according to [1].

Results

At the day of the inoculum, TSS concentration in the reactor, SVI30/SVI5 ratio and SVI30 were 2.5 gTSS/L, 0.49 and 85 mL/gTSS, respectively. Due to the application of increasing HSP, in Phase I, TSS concentration decreased until 1.4 gTSS/L. During Phase II, the indicators of granulation performance started improving. SVI30/SVI5 ratio rose from 0.5 at the beginning of phase II up to 0.8 in last 2 weeks of monitoring, indicating the formation of a system dominated by granules. SVI 30 decreased from 80 mL/gTSS (day 42) to about 42 mL/gTSS (days 86-93), in accordance with AGS typical values [2]. TSS concentration increased up to 4.8 gTSS/L on day 93. In Figure 2, TSS concentration in the reactor and SVI30/SVI5 ratio for Phase II are reported. Results are expressed as the average value obtained during the weekly analysis, except for the last week of operations, when only one monitoring was performed. PSD analysis revealed that the D50 grew from 0.138 mm to 0.251 mm after 23 days of operation, denoting the formation of granular aggregates. After 51 days of operation, the D10, D50, D90 were 0.226 mm, 0.370 mm, 1.084 mm, respectively, and the mass fraction of flocs counted less than 10% [gTSS/gTSS], thus indicating an almost completely granular

mixed liquor. From this point on, the granular aggregates became more stable and mature, and the PSD analysis showed that on day 93 the most populated size-classes were 0.2-0.3 mm and 0.3-0.4 mm (Figure 3).

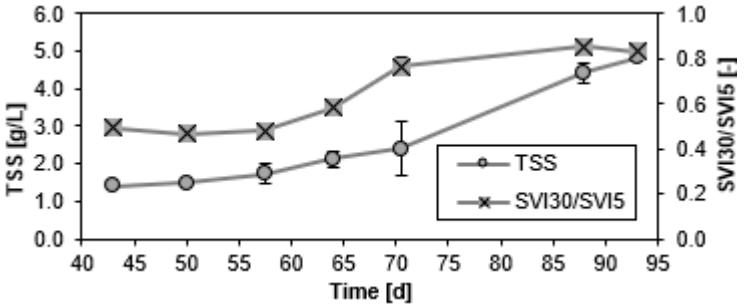

Figure 2. TSS concentration in the G-SBR and SVI30/SVI5 ratio trends in phase II. Error bars represent standard deviations.

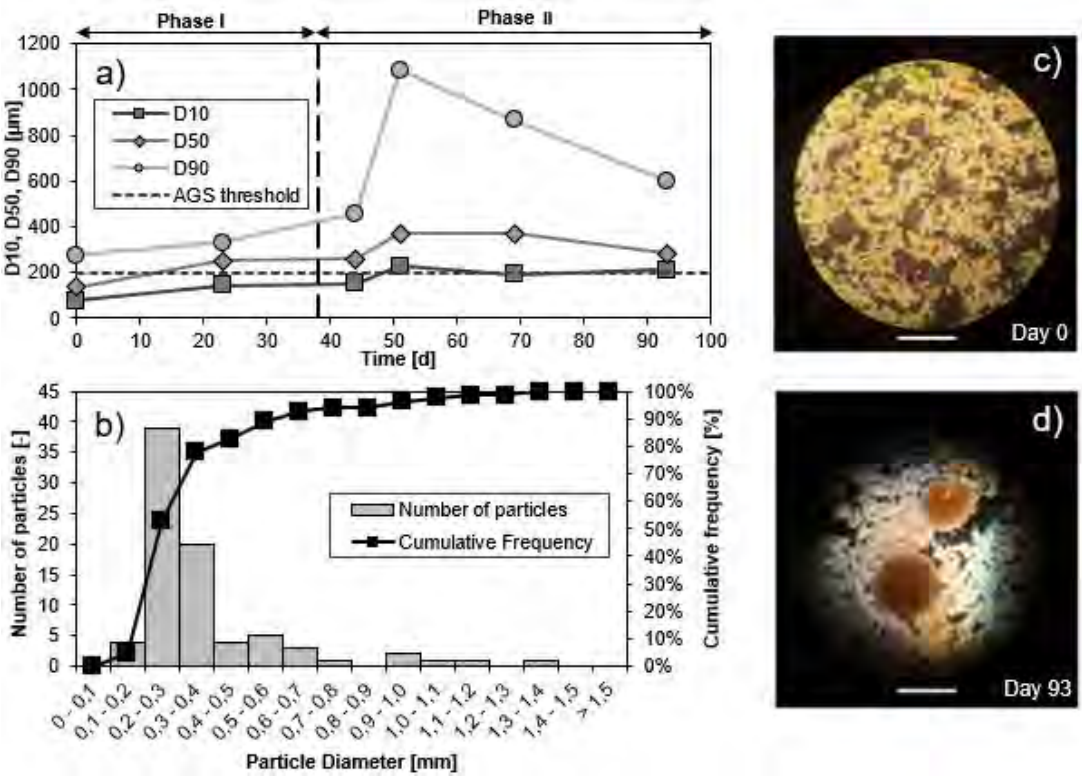

Figure 3. (a) Changes in granulometric distribution during the experimental period; (b) granulometric distribution of day 93; visual images of biomass on (c) day 0 and on (d) day 93.

In this experimental period the raw influent was characterized by average tCOD, sCOD, NH_4-N and PO_4-P concentrations of 135.8±56.3 mg/L, 69.6±17.4 mg/l, 30.2±9.9 mg/L and 3.0±1.0 mg/L respectively (4.5 g tCOD/g N; 2.3 g sCOD/g N).

As can be seen in Table 1, in both phases, sCOD was almost entirely removed anaerobically, with average removal efficiencies near 85%, confirming previous lab-scale results [4]. In Phase II, such an efficient anaerobic sCOD-uptake is proved by the negligible difference in sCOD concentration at the end of the anaerobic (36.6±4.9 mg/L) and aerobic phases (34.8±4.1 mg/L), showing the successful selection of a microbial community enriched in PAOs and GAOs. P removal efficiency was on average

over 83% in the Phase I and reached almost 100% in the Phase II, demonstrating even a better performance than the one reported at lab-scale by [4]. During the period of granulation described in this abstract, nitrification and TIN removal were intentionally not optimized to speed up the granulation process.

Table 1. Average and standard deviation of removal efficiencies in phases I and II.

	Phase I (days 0-37)	Phase II (days 38-95)
sCOD removal efficiency during the cycle [%]	84.1±6.4	86.0±1.8
sCOD removal efficiency in anaerobic phase [%]	81.8±4.6	83.7±1.5
PO_4-P removal efficiency [%]	83.5±32.6	100.0±0.1
NH_4-N removal efficiency [%]	59.2±21.8	52.2±15.7
TIN removal efficiency [%]	41.1±24.0	48.1±17.5

The adopted strategy consists on limiting the accumulation of electron acceptors (nitrite and nitrate) at the end of a cycle with a double aim in view of the beginning of the next cycle: i) providing the ideal redox conditions for anaerobic COD uptake by PAOs and GAOs, ii) avoiding the competition for COD by ordinary heterotrophic organisms (OHOs) that would favour the growth of flocculant/filamentous aggregates [4]. Nitrification and simultaneous denitrification will be then optimized once the layered granular structures, and therefore sufficient anoxic biofilm volume, are obtained.

Conclusions

Granulation to AGS from an activated sludge inoculum was achieved in three months in a pilot scale SBR fed with low-strength municipal wastewater supplied with exogeneous COD. At the end of the investigated period, TSS concentration of 4.8 gTSS/L, SVI 30/SVI5 ratio of 0.83, SVI 30 of 41.4 mL/gTSS, and P and sCOD removal efficiencies of 100% and 88%, respectively, were obtained. During these 3 months of granulation, nitrification and nitrogen removal were intentionally not optimized. The further research activities will focus on the optimization of nitrification and TIN removal.

Acknowledgements

The EU-PNRR - PRIN 2022 (N4En project. CUP: B53D23005590006) and the POR FESR Toscana 2014–2020 (IDRO.SMART project, CUP: 3647.04032020.157000040) are kindly acknowledged for financial support.

References

[1] Winkler M. H., Meunier C., Henriet O., Mahillon J., Suárez-Ojeda M. E., Del Moro G., De Sanctis M., Di Iaconi C., Weissbrodt D. G., “An integrative review of granular sludge for the biological removal of nutrients and recalcitrant organic matter from wastewater”, Chemical Engineering Journal, vol. 336, page 489-502, (2018).
[2] Sepúlveda-Mardones M., Campos J. L., Magrí A. , Vidal G., “Moving forward in the use of aerobic granular sludge for municipal wastewater treatment: an overview”, Reviews in Environmental Science and Bio/Technology, vol. 18, page 741-769, (2019).
[3] Sguanci S., Lubello C., Caffaz S., Lotti T., “Long-term stability of aerobic granular sludge for the treatment of very low-strength real domestic wastewater”, Journal of Cleaner Production, vol. 222, pp. 882-890, (2019).
[4] Campo R., Sguanci S., Caffaz S., Mazzoli L., Ramazzotti M., Lubello C., Lotti T., “Efficient carbon, nitrogen and phosphorus removal from low C/N real domestic wastewater with aerobic granular sludge”, Bioresource Technology, vol. 305, (2020).
[5] Pronk M., van Dijk E. J.H., van Loosdrecht M. C.M, Biological Wastewater Treatment: Principles, Modelling and Design – 2nd edition, IWA Publishing, London (2023).
[6] Kartal B., Kuenen J. G., van Loosdrecht M. C. M., “Sewage Treatment with Anammox”, Science, vol. 328, n. 5979, page 702-703, (2010).
[7] APHA/AWWA/WEF, “Standard Methods for the Examination of Water and Wastewater, 23rd ed.”, American Public Health Association, Washington DC, USA, (2017).

Title: Effect of Membrane on Chromium Removal Efficiency in photobioreactor (PBR) containing *chlorella vulgaris*

Author(s): Hadis Saeedikia[1], Salar Helchi[1], Mir Mehrshad Emamshoushtari[1,2], Omid Tavakoli[3], Geoffroy Lesage [4*], Marc Heran [4], Farshid Pajoum Shariati[1,4*]

[1] Department of Chemical Engineering, Science and Research Branch, Islamic Azad University, Tehran, Iran.(h.saeedikia.hs@gmail.com; salar.helchi1@gmail.com)
[2] Institute of Chemical, Environmental & Bioscience Engineering, TU Wien, Getreidemarkt 9/166, 1060 Vienna, Austria (mehrshad.emamshoushtaro@tuwien.ac.at)
[3] College of Chemical Engineering, University of Tehran, Tehran, Iran (otavakoli@ut.ac.ir)
[4] Institut Européen des Membranes (IEM), Université de Montpellier, CNRS, ENSCM, 34090, Montpellier, France (geoffroy.lesage@umontpellier.fr; marc.heran@umontpellier.fr; farshid.pajoumshariati@umontpellier.fr)

Keyword(s): Chromium removal; photobioreactor; *chlorella vulgaris*; heavy metal

Abstract

The increasing concern regarding heavy metal pollution in water and wastewater has led to the investigation of novel and effective methods for removing or reducing these environmental contaminants [1, 2]. Among the most harmful heavy metals, chromium is highly toxic to humans and the environment [3]. Bioremediation through Chlorella vulgaris microalgae represents a promising eco-friendly technology for heavy metal removal from aqueous media and wastewater, providing a suitable alternative to conventional methods [4, 5]. This study aimed to investigate the effect of integrating membrane technology in the photobioreactor (PBR) on the removal efficiency of Cr(III) from tannery synthetic wastewater. All experiments were conducted with a microalgae dry weight of 1.5 $g.L^{-1}$, pH of 7–8, and Cr(III) concentration of 1000 $mg.L^{-1}$. Firstly, the experiments were carried out by only *Chlorella vulgaris* microalgae within a flat-plate PBR. For comparison, the effect of the membrane on the same synthetic tannery wastewater was carried out in a flat-plate membrane bioreactor (MPBR) with a working volume of 5 Liters. Figure 1 demonstrates a comparison between the flat plate PBR and the MPBR for the removal efficiency of chromium during different times. The error percentage of these experiments were 3% and each experiment was repeated 3 times. The results demonstrated that the maximum removal efficiency of the PBR reached 74.64%, indicating that the removal efficiency increase rate was negligible beyond this point. This may be attributed to the filamentation of active sites of the microalgal cells. Although the utilization of the membrane further enhanced the removal efficiency of Cr(III), the trend remained similar, reaching 82.15% after 5 minutes. The results demonstrated that using the membrane in the PBR increased the removal rate by more than 8% and allowed a continuous Cr removal wastewater treatment.

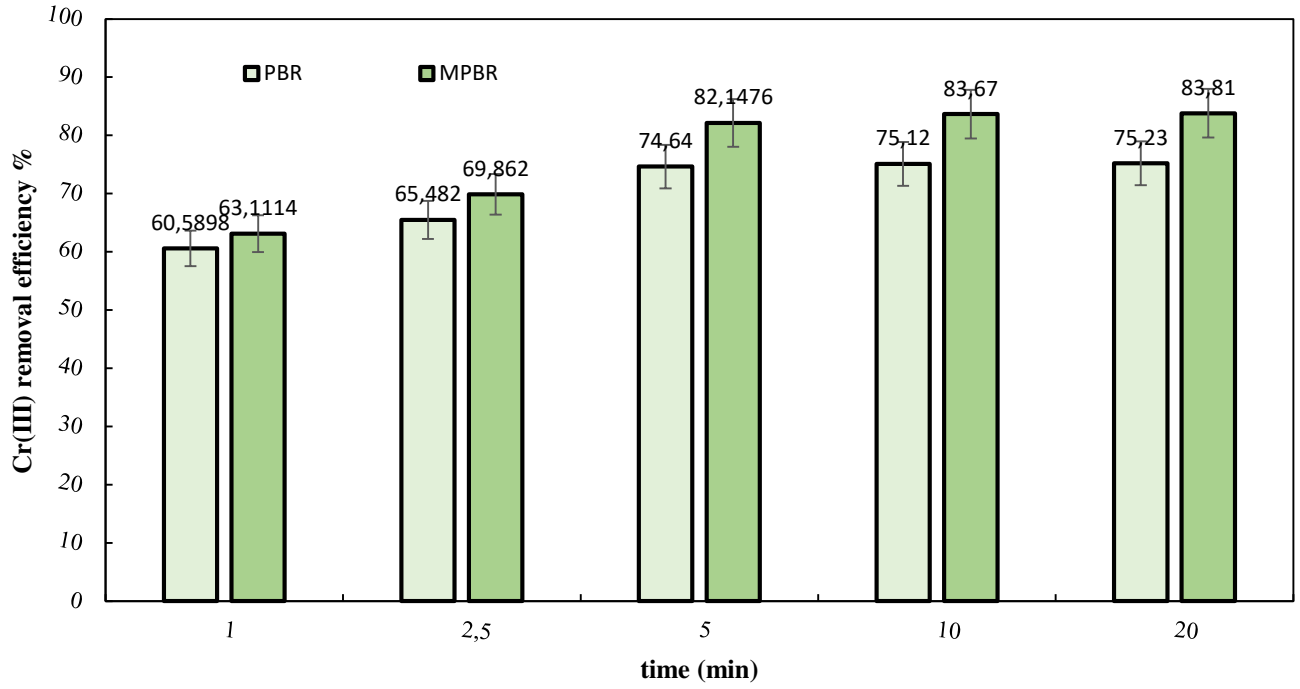

Figure 1- A comparison of flat plate PBR and MPBR chromium removal efficiency during time

References:

[1] Abdelfattah, A., Ali, S. S., Ramadan, H., El-Aswar, E. I., Eltawab, R., Ho, S. H., Elsamahy, T., Li, S., El-Sheekh, M. M., Schagerl, M., Kornaros, M., & Sun, J., "Microalgae-based wastewater treatment: Mechanisms, challenges, recent advances, and future prospects", *International Environmental Science and Ecotechnology*,13, 1-3, (2023).
[2] Blanco-Vieites, M., Suárez-Montes, D., Delgado, F., Álvarez-Gil, M., Battez, A. H., & Rodríguez, E., "Removal of heavy metals and hydrocarbons by microalgae from wastewater in the steel industry". *Algal Research*, 64, 663–672, (2022).
[3] Singh, D. V., Bhat, R. A., Upadhyay, A. K., Singh, R., & Singh, D. P., "Microalgae in aquatic environs: A sustainable approach for remediation of heavy metals and emerging contaminants". *Environ Technol Innov,* 21, 8-12, (2021).
[4] Manzoor, F., Karbassi, A., & Golzary, A., "Removal of Heavy Metal Contaminants from Wastewater by Using Chlorella vulgaris Beijerinck: A Review", *Current Environmental Management*, *6*(3), 174–187, (2019).
[5] Rajalakshmi, A. M., Silambarasan, T., & Dhandapani, R., "Small scale photobioreactor treatment of tannery wastewater, heavy metal biosorption and CO2 sequestration using microalga Chlorella sp.: a biodegradation approach". *Appl Water Sci*, 11(7), 1-3, (2021).

PARALLEL SESSION: B5

Air quality and treatment

Air quality monitoring and impacts

Title: Long term air quality monitoring of trace toxic pollutants in the area surrounding a WtE plant.

Author(s): Giovanni Lonati[1], Stefano Cernuschi[*1], Elena Sezenna[1]

[1] *Department of Civil and Environmental Engineering, Politecnico di Milano, Milano, Italy, giovanni.lonati@polimi.it, stefano.cernuschi@polimi.it, elena.sezenna@polimi.it*

Keyword(s): urban waste, incineration, trace toxics, air emissions, air quality impacts

Abstract

Despite strict regulations progressively adopted for their emissions control, particularly for stack flue gases, trace toxic compounds, including inorganic heavy metals and organic POPs (PCDD/F, PCBs, PAHs) are still one of the most significant issues related to the potential impact of waste to energy (WtE) plants on the surrounding environment, strongly affecting both the siting procedures of new installations than the operation of existing units. Long term measurements of these compounds addressed to evaluating their levels in the surrounding area of the incinerator may be usefully utilised for observing any effects expected from stack plant emissions, as well as to analyze their variations over extended time periods that could reflect either any corresponding modifications with time in the input waste and/or the general plant design than potential accumulation effects of the pollutants considered [1].
In order to evaluate some of these aspects, monitoring investigations were performed over a yearly period for measuring atmospheric levels of the most significant toxic trace compounds of waste incineration interest, including both heavy metals (As, Cd, Hg, Ni, Pb) and organic substances (PCDD/Fs, PAH). Sampling was performed at three sites, located in the surrounding area of a WtE plant and selected in order to be representative of different exposure situations to its emissions: higher expected source impact (R1), industrial contribution from an area aside the eastern boundary of the plant (R2) and a reasonable background condition (R3) identified in a residential urban at nearly 8 km from the plant, along a direction not affected by prevailing winds for most of the year.
Plant design configuration includes three separate moving grate furnaces, for a total feed capacity of 232 t/day of residual residential waste from separate collection, with a small fraction of hospital waste (less than 5%). Energy recovery is performed with a steam cycle for electricity production, whilst flue gas treatment is conducted with single lines equipped with electrostatic precipitation, dry sorption reactor with sodium bicarbonate and activated carbon addition, fabric filtration, and final catalytic $DeNO_x$ unit. Treated flue gas is released from the plant through two 40 m height stacks.
Measurements were conducted for two weeks at each site during two different seasonal periods of the same year (winter and summer), following standard procedures included in current regulations of interest for all the cases [2]. Daily PM samples were collected for As, Cd, Ni, Pb and PAHs evaluation, whilst for PCDD/Fs a single sample for every biweekly period was collected. Hg was evaluated for its gaseous form (TGM) through a semicontinuous automated system (Mercury Ultratracer UT-3000) that combines a gold trap amalgamation module with an atomic absorption spectroscopy detector for mercury vapor.
Concentrations results during winter and summer campaigns are reported in Table 1 for daily values in terms of overall averages and minimum-maximum range during the whole campaigns.

Table 1. Air concentrations (ng/m^3) of pollutants measured during the campaigns (average, min and max values)

Pollutant	Winter campaign			Summer campaign		
	R1	R2	R3	R1	R2	R3
As	0.3 (<0.5-0.6)	0.6 (<0.5-0.9)	0.8 (<0.5-1.9)	< 0.5	0.3 (<0.5-0.5)	0.4 (<0.5-0.7)
Cd	<0.5	<0.5	<0.5	< 0.5	<0.5	<0.5
Ni	3.6 (1-13.1)	5.8 (1.1-21.7)	1.3 (0.3-3.2)	1.1 (0.3-2.3)	2.8 (1.2-5.8)	2.7 (1.7-3.9)
Hg	1.4 (0.9-1.9)	1.1 (0.8-1.3)	0.7 (0.3-1)	1.9 (1.2-3)	0.74 (0.7-1)	1.7 (1-2.3)
Pb	5.9 (1.8-14.6)	7.1 (3.9-11.8)	6.1 (2.3-14.7)	1.9 (0.9-3.3)	2.6 (1.2-3.7)	3.1 (1.6-4.8)
Benzo(a)pyrene	0.3 (0.1-0.9)	0.1 (0.01-0.3)	0.2 (0.04-0.3)	<0.02	<0.02	<0.02
PCDD/F ($fg_{I\text{-}TEQ}$/m^3)	17.7	22.5	19.4	<5	<5	<5

For all metals, concentrations are largely located around low range of values. Cd was never found in any sample at levels higher than its detection limit (0.5 ng/m^3); similar results apply also for As, whose presence is frequently overlapped with detection capabilities of 0.5 ng/m^3. Despite still remaining at comparable small magnitudes, Ni and Pb show more observable levels, with some variations especially between campaigns, less pronounced for the different sites. During colder winter season, As average concentrations are included in the range 0.3-0.8 ng/m^3, with the highest recordings at background (R3) and minimum values observed at expected observable plant impact site (R1), where the majority of the measurements are below the detection limit. For Ni, included between 1.3 and 5.8 ng/m^3, the most significant values are observed at the industrial background site (R2), with intermediate results detected at plant impact site and the lower ones at background location (R3). For Pb the data, between 5.9 and 7.1 ng/m^3, show greater homogeneity, with slightly higher values recorded at industrial background site. Hg results located on average around 1 ng/m^3, with slightly higher values at plant impact site (R1) with respect both to industrial background (R2) and to general background (R3), also in terms of the hourly recorded data. Time fluctuations of average daily concentrations are very limited, whilst more appreciable variations result for hourly data, with different behaviors at single sites: peaks in afternoon periods are recorded at general background whilst for plant expected impact and industrial background locations measurements result almost uniform in the morning and throughout the night, with 30-40% lower levels during the afternoon.
For warmer summer campaigns, comparable when not still lower values with respect to winter situation are generally recorded without significant differences between sites. As concentrations are always lower than the detection limit of 0.5 ng/^{3} at expected plant impact site (R1) and only during a single day exceed it at background industrial position (R2); the greatest variability is observed at background site R3, with daily averages lower than the detection limit in three days and values up to 0.75 ng/m^3. For Ni, whole average daily values are generally located between 1.1 and 2.8 ng/m^3, with more observable levels at background industrial site (R2) and general background (R3) and lower recordings at plant impact site (R1), where during three days concentrations result below detection limits. For Pb, whole average data are included between 1.9 and 3.1 ng/m^3, with slightly higher values recorded at general background (R3) compared to industrial background (R2) and plant impact site (R1). Hg results present average values at comparable levels with those during winter conditions and included in the range 0.7-1.9 ng/m^3, with lower values at industrial background (R2) and slightly higher and comparable measurements at general background (R3, average of 1.7 ng/m^3) and at plant impact site (R1, average 1.9) and a trend towards a reduction during the last days of the campaigns for general background and plant impact sites. Same comparative considerations between sites arise also from hourly data, with most significant peaks measured at plant impact and general background locations. Any recognizable and/or repeatable time pattern of average daily values is observed in all sites; hourly data result in relatively more appreciable variations, particularly for general background site, with less fluctuations at plant impact site

and almost constant and more contained values at industrial background.
PAHs results were analyzed in terms of benzo(a)pyrene, the most toxic component of the whole mixture and normally considered in air quality regulations. During winter samplings, whole average weekly data result in similar levels for the sites, with measurements range included between 0.1 ng/m^3 at the industrial background site and 0.3 ng/m^3 at the plant impact site, whose results are significantly influenced by the highest single daily measurements of 0.6 ng/m^3 and 0.9 ng/m^3 for the whole sampling period recorded for two days. Time pattern of daily averages is essentially qualitatively the same for all sites and for all the PAHs species measured beyond benzo(a)pyrene. For summer samplings, all sites and daily measurement values are non-detectable at the analytical limit of 0.02 ng/m^3. The difference observed in monitoring results, in terms of the higher pattern of winter levels with respect to not non-detectable values recorded during summer campaigns, has already been considered to be typical for similar areas, where residential heating with small wood combustion appliances is extensively utilized.
For PCDD/F family of pollutants, evaluated in terms of a single biweekly sample, winter season values are located at the lower fg$_{I\text{-}TEQ}$/m^3 levels, within the range around 18 to 23 fg$_{I\text{-}TEQ}$/m^3 and with any significant and relevant difference between sites, included in the normal fluctuations expected for measurements located at the same level, when not lower to, the detection limit. Toxic congeners distribution profiles have an essentially overlying pattern, with high degree chlorinated compounds (OCDD and OCDF) largely prevailing and tetra- to hexa-substituted congeners constantly below the detection limit of 0.005 pg/m^3. For summer samplings, all the congeners were always nondetectable at all sites.
Overall results for all the investigated pollutants are well below the air quality regulatory limits established in terms of average yearly values (Table 2, [2]). Mercury and dioxins limits are still not included in EU regulations. For the former, concentration levels remain far lower than the yearly average value of 1000 ng/m^3 proposed as a reference by the Guidelines of the World Health Organization [3]. PCDD/Fs assessment might rely on estimated atmospheric levels of 100 fg$_{I\text{-}TEQ}$/m^3 for urban environments reported by the World Health Organization [3], on the target value of 150 fg$_{I\text{-}TEQ}$/m^3 (including the contribution of toxicity from PCBs) adopted by the federal committee for the control of air pollution in Germany [4], and the standard of 600 fg$_{I\text{-}TEQ}$/m^3 established in Japan for air quality by Ministry of Environment [5].

Table 2. EU air quality standards for the pollutants investigated.

Pollutant	Regulatory limit (ng/m^3, average yearly basis)
As	6
Cd	5
Ni	20
Hg	1000 (suggested WHO)
Pb	500
Benzo(a)pyrene	1
PCDD/F (fg$_{I\text{-}TEQ}$/m^3)	100 (WHO), 150 (Germany), 600 (Japan)

Additional considerations related to WtE plant impacts are obtained through the comparative examination of actual investigation results with similar periodic monitoring exercises, conducted previously in the area for same or similar sites. Available data cover a relatively long-term period, with the first campaigns conducted almost 15 years ago and mostly with the same sampling and analysis approach. Despite all the possible effects over time associated with analytical methodology and meteorological conditions, yearly variations of the pollutants measured are restrained in a relatively narrow range, with the latest actual investigation measurements frequently located near the lower range of available data. Some illustrative examples are illustrated in Fig. 1, where average data time patterns along the years for some representative conditions are reported.
Concluding remarks arising from the investigations indicate firstly levels of the WtE pollutants of interest

essentially expected from the emissions source pattern of the area, characterized by diffuse home heating residential and industrial activities settlements and with an extended road network including some major communication routes with significant shares of heavy traffic. For both summer and winter conditions, average measurement levels pattern observed during long time periodically sampling periods, obtained by similar investigation methodologies, seem not characterized by clearly identifiable variations, beyond their intrinsic fluctuations due to the meteorological conditions present during the time of measurements. This confirms the absence of particular exposures in the area to specific sources of one site compared to others as well as that of systematic actions of local sources on some of them, both in general terms than from the WtE plant investigated. The absence of particular trends towards long-term variations in the main trace pollutants associated with waste-to-energy activity should be finally considered an important complementary element for evaluating the lack of a systematic contribution of the plant to air quality.

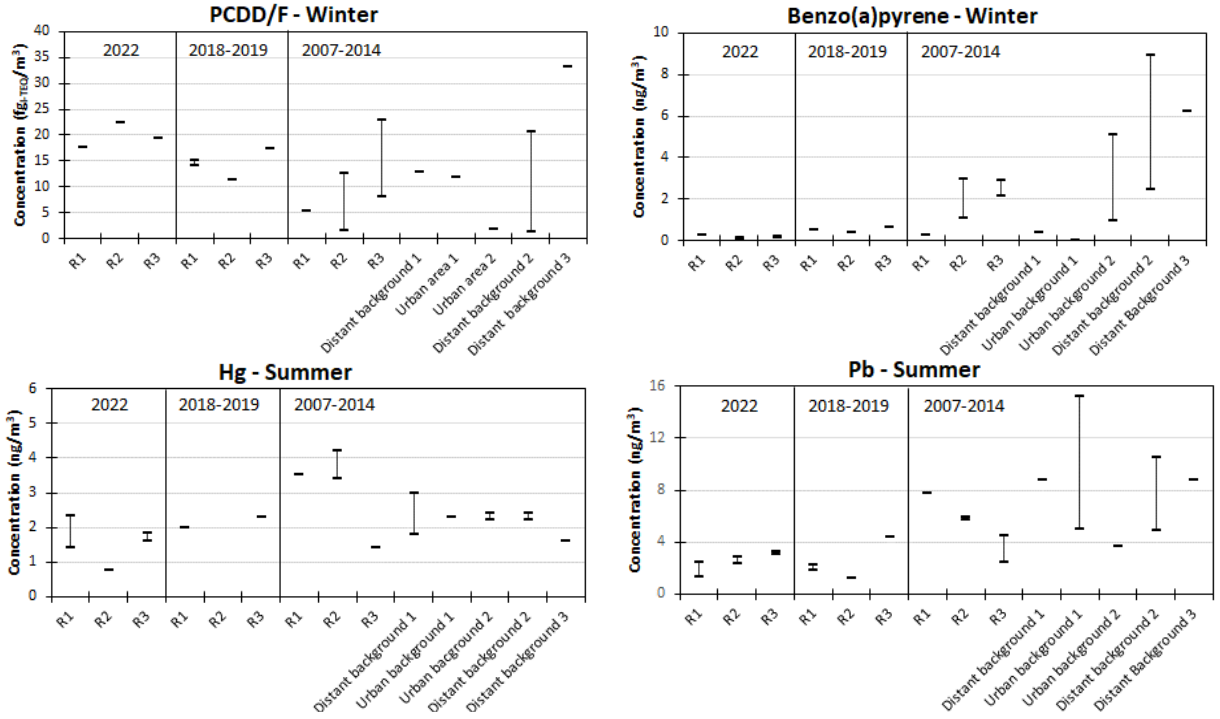

Figure 1. Long term average time pattern of selected pollutants measured in the area during summer and winter campaigns

References

[1] Schumacher M., Domingo J., "Long-term study of environmental levels of dioxins and furans in the vicinity of a municipal solid waste incinerator", Environment International, vol. 32, page 397, 2006.
[2] D.L. 155. Attuazione della direttiva 2008/50/CE relativa alla qualità dell'aria ambiente e per un'aria più pulita in Europa. G.Uff. n. 216, suppl. ordinario, 15/9/2010.
[3] WHO, Air Quality Guidelines for Europe - 2nd ed. World Health Organization, Regional Office for Europe, Copenhagen, 2001.
[4] LAI (National Committee for Immission Control), Report "Assessment of pollutants" for which no immission values have been set. 21 September 2004.
[5] Environmental Quality Standards in Japan - Air Quality, Ministry of the Environment, Government of Japan. Available at https://www.env.go.jp/en/air/aq/aq.html, accessed 12/02/2024.

Title: Gaseous ethanol removal by homemade dielectric barrier discharge plasma reactor

Author(s): Nacer BELKESSA*[1], Abdelkrim BOUZAZA[1], Aymen Amine ASSADI [1,2], Abdelatif AMRANE[1]

[1] Univ Rennes, École Nationale Supérieure de Chimie de Rennes, CNRS, ISCR (Institut des Sciences Chimiques de Rennes) – UMR 6226, F-35000 Rennes, France
[2] College of Engineering, Imam Mohammad Ibn Saud Islamic University, IMSIU, Riyadh, 11432, Saudi Arabia

Keyword(s): VOCs, Plasma, Dielectric barrier discharges, Ethanol, Ozone, Gas Flowrate, Humidity, Energy, Chemical degradation

Abstract

Volatile organic compounds (VOCs) are known as a carbon-based compounds which are characterized by their low boiling point (<250 C°) at atmospheric pressure[1]. Managing and controlling their emission is attracting a great deal of interest from researchers because of their devastating effects on humans and the environment[2]. Nowadays, several technologies are used to control VOCs emissions based on the recovery and destruction methods[3]. In last decade, non-thermal plasma (NTP) process is used as an attractive technology to remove a wide range of VOCs from air due to its ability to operate under normal temperature and pressure without the need of toxic chemicals[4]. Furthermore, it has also demonstrated good efficiency toward a wide range of pollutants. Nevertheless, application of high voltages to generate discharges and the production of non-suitable by-products such as ozone and NOx at the reactor outlet are its main drawbacks[5]. Among NTP plasma technologies, dielectric barrier discharge plasma (DBD) is mostly used thanks to its simple installation, high stability and reproducibility[6]. It is generated by applying high voltage between two electrodes separated by a dielectric material. Electrons are accelerated in the electric filed to reach 1-10 eV , which are involved in neutral gases ionisation and generation of highly reactive species[7]. Herein, gaseous ethanol decomposition was studied in a homemade dielectric barrier discharge reactor as shown in the figure 1. Ethanol is mainly released from daily life products used for cleaning, well-being and in building materials[8]. It was established that the long-term exposure to gaseous ethanol can cause several diseases as cancers and kidney failure[8]. For this purpose, ethanol was chosen as a model pollutant in this work.

The effect of experimental parameters such as inlet concentration (10-60 mg/m^3), flow rates (0.25-1m^3/h), Plasma injected energy (0.29-11.7 J/L) and water vapor composition (5-62.6%) on the degradation efficiency were investigated. The results showed that, increasing ethanol concentration from 10 mg/m^3 to 60 mg/m^3 leads to a significant diminution of the removal efficiency from 44 % to 11 % at a flow rate of 1m^3/h and plasma energy of 11.7 J/L. It was also demonstrated that for a fixed concentration at 25 mg/m^3 and applied voltage of 18kV, ethanol decomposition decreases drastically as the flow rate increase (from 91% to 39%), which can be explained by the decrease of the residence time of pollutant inside the reactor. Additionally, the study of the effect of plasma energy showed an increasing trend in ethanol degradation efficiency as the injected energy increased (from 3% to 39% at 0.3J/L and 11.7 J/L, respectively. At a constant concentration of 25.5 mg/m^3 and a flow rate of 1m^3/h), energy increase is related to the increase of reactive species densities at high plasma power. Moreover, relative humidity (RH) has a significant impact on the evolution of the degradation yield.

Indeed, the results of this work highlighted the presence of an optimal water vapor composition at RH of 35 %. The amount of the generated ozone in the discharge quantified and a concentration of 53 ppm was reached at 11.7 J/L at a relative humidity of 5%.
According to the literature, ethanol degradation mechanism occurs mainly through the attack of OH^* radicals and atomic oxygen species and energetic electrons generated by the discharge.
Further investigations dealing with the by-products of ethanol decomposition are underway in order to establish the plausible degradation mechanism.

Figure 1. Homemade DBD plasma reactor

Figure 2. Effect of the Ethanol inlet concentration on degradation efficiency under: RH=5%, Q=1m^3/h, SED=11.7J/L.

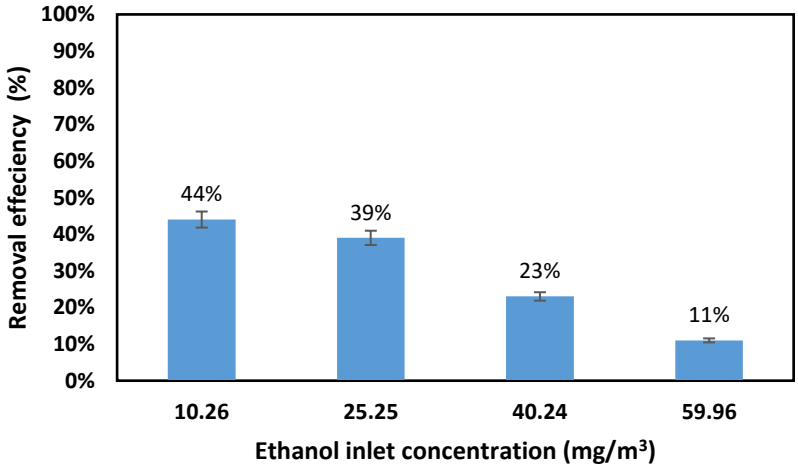

Figure 3. Effect of the flowrate on the degradation efficiency under: RH=5%, C=25.25 mg/m^3, V_{app}=18kV

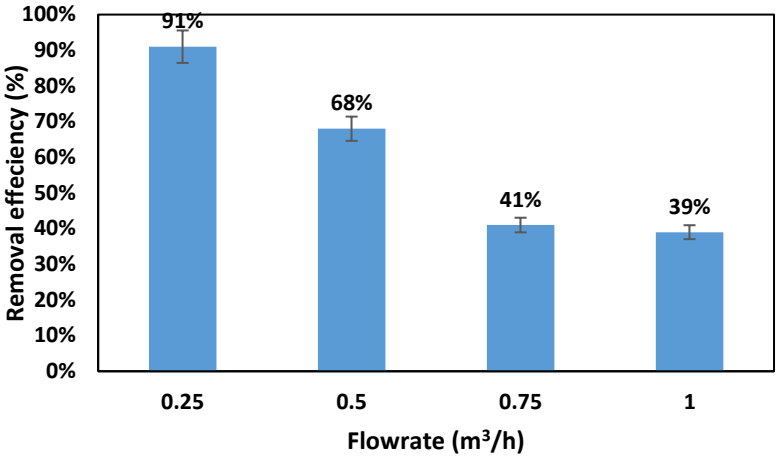

Figure 4. Effect of the injected energy on the degradation efficiency under: RH=5%, C=25.25 mg/m^3, Q=1m^3/h

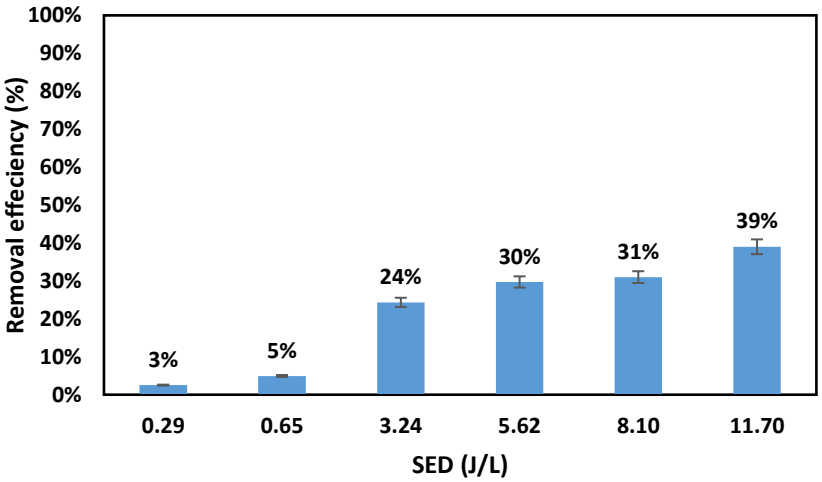

Figure 5. Effect of the relative humidity on the degradation efficiency under: C=25.25 mg/m^3, Q=1m^3/h, SED=11.7J/L

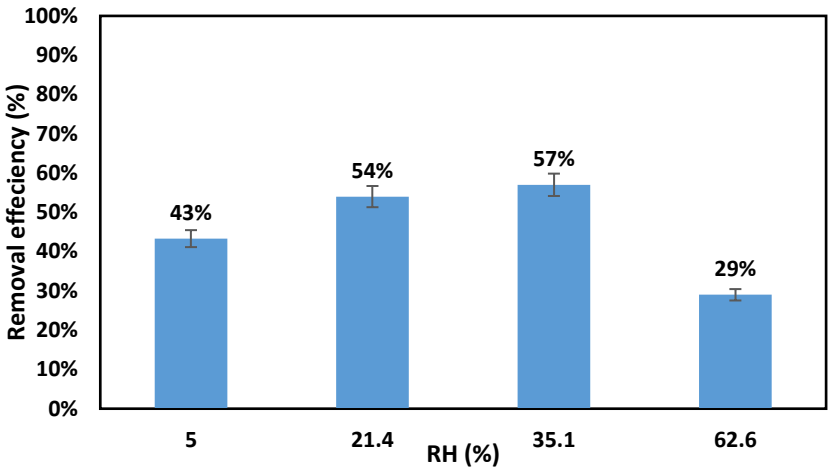

References

[1] T. Chang, Y. Wang, Y. Wang, Z. Zhao, Z. Shen, Y. Huang, S.K.P. Veerapandian, N. De Geyter, C. Wang, Q. Chen, R. Morent, A critical review on plasma-catalytic removal of VOCs: Catalyst development, process parameters and synergetic reaction mechanism, Sci. Total Environ. 828 (2022) 154290. https://doi.org/10.1016/j.scitotenv.2022.154290.

[2] Y.F. Guo, D.Q. Ye, K.F. Chen, J.C. He, W.L. Chen, Toluene decomposition using a wire-plate dielectric barrier discharge reactor with manganese oxide catalyst in situ, J. Mol. Catal. A Chem. 245 (2006) 93–100. https://doi.org/10.1016/j.molcata.2005.09.013.

[3] S. Li, X. Dang, X. Yu, R. Yu, G. Abbasd, Q. Zhang, High energy efficient degradation of toluene using a novel double dielectric barrier discharge reactor, J. Hazard. Mater. 400 (2020) 123259. https://doi.org/10.1016/j.jhazmat.2020.123259.

[4] F. Saleem, A.H. Khoja, J. Umer, F. Ahmad, S.Z. Abbas, K. Zhang, A. Harvey, Removal of benzene as a tar model compound from a gas mixture using non-thermal plasma dielectric barrier discharge reactor, J. Energy Inst. 96 (2021) 97–105. https://doi.org/10.1016/j.joei.2021.02.008.

[5] M. Qu, Z. Cheng, Z. Sun, D. Chen, J. Yu, J. Chen, Non-thermal plasma coupled with catalysis for VOCs abatement: A review, Process Saf. Environ. Prot. 153 (2021) 139–158. https://doi.org/10.1016/j.psep.2021.06.028.

[6] W. Abou Saoud, A.A. Assadi, M. Guiza, A. Bouzaza, W. Aboussaoud, I. Soutrel, A. Ouederni, D. Wolbert, S. Rtimi, Abatement of ammonia and butyraldehyde under non-thermal plasma and photocatalysis: Oxidation processes for the removal of mixture pollutants at pilot scale, Chem. Eng. J. 344 (2018) 165–172. https://doi.org/10.1016/j.cej.2018.03.068.

[7] D. Ray, C. Subrahmanyam, CO2 decomposition in a packed DBD plasma reactor: Influence of packing materials, RSC Adv. 6 (2016) 39492–39499. https://doi.org/10.1039/c5ra27085e.

[8] A. Ranjbari, K. Demeestere, C. Walgraeve, K.H. Kim, P.M. Heynderickx, Novel kinetic modeling of photocatalytic degradation of ethanol and acetaldehyde in air by commercial and reduced ZnO: Effect of oxygen vacancies and humidity, Chemosphere. 358 (2024) 142118. https://doi.org/10.1016/j.chemosphere.2024.142118.

Title: The importance of reducing $PM_{2.5}$ in the prevention of neuro-degenerative diseases. An *in vitro* study

Author(s): Antonio Cristaldi[*1], Rosalia Pellitteri[2], Paola Dell'Albani[2], Valentina La Cognata[2], Maria Fiore[1], Eloise Pulvirenti[1], Gea Oliveri Conti[1], Margherita Ferrante[1].

[1] *LIAA – Food and Environmental Hygiene Laboratory, Department of Medical Sciences, Surgical and Advanced Technologies "G.F. Ingrassia", University of Catania, Italy.*

[2] *Institute for Biomedical Research and Innovation, National Research Council, Catania, Italy.*

Keyword(s): environmental pollution, $PM_{2.5}$, public health, neurodegenerative diseases.

Abstract

Air pollution is one of the main environmental risks for human health, and specifically, air quality can be altered by vehicular traffic, agricultural and industrial practices, domestic heating, activities that favor the release into the atmosphere of SO_x, NO_x, CO_x, CH_4, PM_x [1]. $PM_{2.5}$ has attracted the attention of stakeholders, due to its size, it is able to cross the blood-alveolar barrier and even the blood-brain barrier (BBB) [2]. Therefore, high levels of $PM_{2.5}$ in the atmosphere can favor the onset and/or worsening of respiratory, cardiovascular and neurodegenerative diseases. Several studies [3,4] have shown that the olfactory mucosa is involved in $PM_{2.5}$ translocation to the brain, and the identification of more susceptible cell types could be the key to understanding how olfactory mucosa alterations may be linked to neurodegenerative processes induced by particulate matter. Therefore, we considered Olfactory Ensheathing Cells (OECs), and also SH-SY5Y cells since they are often used as *in vitro* models of neuronal function and differentiation as well as in studies on Parkinson's and neurogenesis disease.

The $PM_{2.5}$ sampling was carried out in a high-traffic area of the city of Catania, as reported by the UNI EN ISO 12341:2014 regulation. The instrumentation used consisted of a Zambelli Explorer suction pump with relative chimney with fractionator with sampling heads for $PM_{2.5}$, sampling flow set to 38 L/min for 24 hours, for a total of 55 m^3 of aspirated air. After that, we performed gravimetric determination and chemical-physical characterization of $PM_{2.5}$ samples collected in the metropolitan area of Catania. Both cell lines were exposed *in vitro* to $PM_{2.5}$ extracts to test their viability, mitochondrial damage, cytoskeletal modifications and induction of apoptosis by MTT assay, MitoHealth test, Tunel test, and expression of vimentin and caspase 3, respectively. Furthermore, the dimensional and surface morphological detection of $PM_{2.5}$ was carried out using scanning electron microscopy analysis.

We have found an average annual value of $PM_{2.5}$= 16.9 µg/m^3 and a maximum value of $PM_{2.5}$= 27.6 µg/m^3 during the winter season. $PM_{2.5}$ samples collected during the winter season also showed higher concentrations of PAHs and heavy metals. The MTT viability assay showed a reduction in cell viability for both OECs (44%, 62% and 64%) and SH-SY5Y (16%, 17% and 28%) after 24, 48 and 72 hours of exposure, for both cell lines. Furthermore, the samples exposed for 72 hours showed a greater mitotoxicity effect, alteration of the vimentin functionality and the presence of effector caspases, starting the apoptotic process. These events are involved in

neurodegenerative processes, and could be triggered not only by the concentration and time of exposure to $PM_{2.5}$, but also by the presence of inorganic elements, such as trace elements, and organic elements, such as PAHs, on the PM substrate.

The identification of more sensitive cell lines, therefore, could be the key to understand how $PM_{2.5}$ exposure can contribute to the onset of neurodegenerative processes. The results obtained provide a first indication of the possible effects of $PM_{2.5}$ and related molecules on OEC and SH-SY5Y cells. This highlights the need to reduce fine particulate matter emissions to protect the environment and public health. Finally, the evidence obtained in this study can represent a starting point for further investigations in the attempt to clarify the mechanisms that cells activate as self-defense and in neurodegenerative processes.

References

1. Cristaldi, A., Fiore, M., Oliveri Conti, G., Pulvirenti, E., Favara, C., Grasso, A., Copat C., Ferrante, M., 2022. Possible association between $PM_{2.5}$ and neurodegenerative diseases: A systematic review. Environmental Research 208 (2022)112581. https://doi.org/10.1016/j.envres.2021.112581
2. Wang, Y., Zhang, M., Li, Z., Yue, J., Xu, M., Zhang, Y., Yung, K.K.L., Li, R., 2019. Fine particulate matter induces mitochondrial dysfunction and oxidative stress in human SH-SY5Y cells. Chemosphere 218, 577–588. https://doi.org/10.1016/j. chemosphere.2018.11.149.
3. Kanninen K.M., Lampinen R., Rantanen L.M., Odendaal L., Jalava P., Chewa S., White A.R., 2020. Olfactory cell cultures to investigate health effects of air pollution exposure: Implications for neurodegeneration. Neurochemistry International 136 (2020) 104729. https://doi.org/10.1016/j.neuint.2020.104729
4. Zhang, M., Wang, Y., Wong, R.M.S., Yung, K.K.L., Li, R., 2022. Fine particulate matter induces endoplasmic reticulum stress-mediated apoptosis in human SH-SY5Y cells. Neurotoxicology 88, 187–195. https://doi.org/10.1016/j.neuro.2021.11.012.

Title: Impact assessment of mercury emissions from a waste-to-energy plant on local air quality

Authors: Stefano Cernuschi[1], Maria Sansone[2], Giovanni Lonati*[1]

[1]*Department of Civil and Environmental Engineering, Politecnico di Milano, Milano, Italy, stefano.cernuschi@polimi.it, giovanni.lonati@polimi.it*
[2] *Environmental Agency of Veneto region (ARPA Veneto, Dipartimento Regionale per la Sicurezza del Territorio - Unità Meteorologia e Climatologia), maria.sansone@arpaveneto.it*

Keyword(s): Air quality, Total gaseous mercury, Waste incineration, Dispersion modelling

Introduction

The reduction in the application of mercury and the introduction of effective separate collection systems, particularly for batteries, has resulted in the progressive reduction of its presence in waste. Nevertheless, waste combustion is still considered a major source of anthropogenic emissions of mercury into the atmosphere [1, 2] because in the incineration process it evaporates almost entirely from the waste and is transferred into the flue gas as elemental mercury and mercury chlorides. In waste incineration plants, the commonly adopted techniques to meet the emission limit of 0.05 mg/m^3 as an 8-hour average concentration [3] are wet scrubbing and adsorption on activated carbon [4]. These techniques are indicated as best available techniques (BAT) to reduce mercury emissions to air (including emission peaks) from waste incineration in the EU Decision 2019/2010, that establishes the BAT conclusions for waste incineration [5]. Studies investigating the actual impact on local air quality of mercury emissions from waste combustion plants are still rather limited. This work presents results of atmospheric dispersion modeling for mercury emissions from a municipal waste-to-energy (WtE) plant in northern Italy and their comparison with values observed in the atmosphere around the plant. The work adopts the methodological approach of a previous study conducted for the same plant in 2018-2019 [6] and provides new elements of knowledge on the impact of the WtE plant on local air quality.

Materials and methods

Air quality data

Ambient air measurements of total gaseous mercury (TGM) were performed by means of an automated system (Mercury Ultratracer UT-3000) that combines a gold trap amalgamation module with an atomic absorption spectroscopy detector for mercury vapour. Mercury in filtered sampled air is first captured, retained and accumulated on the gold surface of the gold trap. Then, it is suddenly released to a clean air stream through thermal desorption induced by the fast heating of the gold trap and finally swept into the optical cell, where the absorption of 253.7 nm UV beam is measured by means of solid state UV detectors. TGM concentration data were obtained at 15-minute time resolution in the 0.1-1000 ng/m^3 range. TGM is operationally defined as the gaseous fraction of atmospheric mercury, mainly composed of elemental Hg vapor (Hg^0) with minor fractions of other volatile species such as $HgCl_2$. At urban and remote locations, TGM makes up almost entirely (> 99%) the total mercury concentration in air [7], with concentrations levels usually in the range of few ng m^{-3}, but up to 10-12 ng m^{-3} at sites heavily impacted by anthropogenic emission sources.
TGM measurements were carried out at three sites, located in the surrounding area of the WtE plant

and selected in order to be representative of different exposure situations to its emissions. Site R1 is the downwind sensitive receptor (permanently inhabited location) closest to the plan (about 1 km as crow fly distance to the South), and thus suitable for assessing the impact of the plant; conversely, site R2 is representative of the industrial area aside the eastern boundary of plant, and site R3, located in a residential area, may reasonably be considered as background situation, since it is not significantly affected by the emissions of the plant due to its location and distance (about 8 km to the North-East, direction not affected by prevailing winds for most of the year). Cold and warm season monitoring campaigns were performed in 2018-2019 (September 10th-26th, 2018 and February 17th-March 4th, 2019) and 2022 (February 2nd-March 15th and June 14th-July 25th for 2022). In 2018-2019 campaign, measurements were taken at sites R1 and R3 for about one week, whilst in 2022 campaign monitoring activities were extended to two weeks at each site and included also site R2. Summary statistics of hourly TGM concentrations measured at the three monitoring sites are summarized in Table 1.

Table 1. Summary statistics of hourly Hg concentrations (ng/m^3) at the three monitoring sites.

	2018-2019 campaign*						2022 campaign					
	Cold season			Warm season			Cold season			Warm season		
	R1	R2	R3	R1	R2	R3	R1	R2	R3	R1	R2	R3
Mean	1.1	-	0.9	2.3	-	2.0	1.3	1.1	0.7	1.9	0.7	1.8
Standard deviation	0.4	-	0.6	0.6	-	0.6	0.4	0.3	0.4	0.7	0.1	0.5
Median	1.1	-	0.9	2.2	-	1.9	1.3	1.1	0.6	1.7	0.7	1.7
1st quartile	0.8	-	0.6	1.9	-	1.8	1.1	0.9	0.4	1.3	0.6	1.4
3rd quartile	1.4	-	1.2	2.6	-	2.1	1.6	1.3	1.0	2.3	0.8	2.1

*Measurements not performed at Site R2

Seasonal average concentrations did not show significant inter-site variability, but showed a common temporal variability, with higher values in the warm season: cold season levels were in the 0.9-1.3 ng/m^3 range, whereas warm season levels were about twice as high, in the 1.8-2.3 ng/m^3 range except for the industrial site R2, monitored only in 2022, where the observed levels (0.7 ng/m^3) were comparable with those at site R3 in the cold season. Observed values were in reasonable agreement both with data reported in literature, typically less than 10 ng m^{-3}, and with respect to the results, included between 1.4 and 5.2 ng m^{-3}, of previous monitoring campaigns conducted in the same area. Even though concentration levels at site R1 were always slightly higher than at the other two sites, observed values resulted very similar, regardless for the distance and location of the monitoring sites from the plant. This suggests that TGM ambient levels were determined by a rather uniform background source, apparently without an appreciable impact on air quality attributable to the emissions from any single source.

WtE Plant emission data

WtE plant design configuration includes three separate moving grate furnaces, for a total feed capacity of 232 t/day of residual residential waste from separate collection, with a small fraction (less than 5%) of hospital waste. Energy recovery is performed with a steam cycle for electricity production, whilst flue gas treatment is conducted with single lines equipped with electrostatic precipitation, dry sorption reactor with sodium bicarbonate and activated carbon addition, fabric filtration, and final catalytic DeNOx unit. Treated flue gas is released from the plant through two 40-m tall stacks, one serving Line 1 and 2 (combined throughput of 132 tons/day), the other Line 3 (100 ton/day). Each line is equipped with Continuous Emission Monitoring (CEM) system, collecting hourly-resolved data for gas flow rate, gas stack temperature, mercury concentration. Summary statistics of hourly Hg concentrations for the three

combustion lines registered by the CEM systems during the periods when air quality monitoring campaigns and model simulations were performed are reported in Table 2.

Table 2. Summary statistics of hourly Hg concentrations (μg/m^3 dry gas @ 0° C, 101,3 kPa, 11% O_2) for the three combustion lines.

	2018-2019 campaign*						2022 campaign**					
	Cold season			Warm season			Cold season			Warm season		
	Line 1	Line 2	Line 3	Line 1	Line 2	Line 3	Line 1	Line 2	Line 3	Line 1	Line 2	Line 3
Mean	0.4	5.1	0.7	4.2	4.4	3.5	1.8	2.6	-	2.2	2.5	3.1
Standard deviation	0.5	15.2	0.5	10.4	4.6	8.0	4.2	4.0	-	4.5	6.2	13.5
Median	0.3	1.9	0.6	2.5	2.8	1.7	0.9	2.0	-	0.9	1.4	0.9
1st quartile	0.2	1.3	0.4	1.0	2.0	0.9	0.5	1.6	-	0.5	1.1	0.6
3rd quartile	0.5	3.4	0.7	4.0	4.8	3.1	1.7	2.6	-	2.0	2.2	1.5

*One-week data. **Two-week data (Line 3 not active during the cold season period).

Except for the lower values observed for Line 1 and Line 3 in the cold season of the 2018-2019 campaign (0.4 and 0.7 μg/m^3, respectively), all the measured stack-gas concentrations were essentially of the same order, ranging between 1.8 μg/m^3 and 5.1 μg/m^3, in substantial agreement with data (4.0 ± 2.7 μg/m^3) reported for municipal solid waste plants [8-10]; however, average, median, and 3rd quartile values were generally lower in 2022 campaign. Mean concentrations were all within the range (1-10 μg/m^3) of the BAT-associated emission levels (BAT-AELs) for long-term averaging period indicated in the EU Decision 2019/2010 [5]. Hourly concentration peaks were recorded on all the lines, as outlined by some large values of data standard deviation, likely due to unusually mercury-rich waste batches. However, all the measured concentrations were within the 5-20 μg/m^3 range indicated as BAT-AELs for the daily averaging period.

Model simulations

Atmospheric dispersion modelling was performed by means of the CALMET-CALPUFF modelling system, based on hourly-resolved data measured by the CEM systems of the plant. Model simulations were performed over a 20 x 20 km^2 computational domain centered on the plant location with a grid step of 125 m for the periods corresponding to the monitoring campaigns for air quality. The hourly meteorological input data to the CALPUFF model were obtained from a simulation with the CALMET pre-processor based on data from the local meteorological monitoring network. The generated data set, which included the 3-dimensional fields of atmospheric temperature, wind speed and direction for ten vertical layers up to an altitude of 3000 m, as well as the descriptive parameters of atmospheric stability, mixed layer height and precipitation intensity, was available with a spatial resolution of 1 km in the computational domain. The analysis of seasonal data highlighted similar meteorological conditions in the monitoring periods, in particular for the direction and speed of the wind and for the absence of significant rainfall events that could cause wash out of the atmosphere. It also confirmed that site R1 was the most exposed, being fairly aligned with the plant along the direction of the prevailing winds (north west-south east) and downwind of the plant during the night and early morning hours.

Results and conclusions

In accordance with the more exposed location of site R1, model simulations resulted in a higher contribution of plant emissions to ambient levels at this site than at sites R2 and R3. (Table 3). At site R1, period averaged contributions were estimated in the orders of 6-10 pg/m^3 in the cold season and 27-59 pg/m^3 in the warm season; at sites R2 and R3 estimated contributions were one order of

magnitude lower, in the 0.2-0.7 pg/m^3 in the cold season and 4-8 pg/m^3 in the warm season, neglecting the 0.1 pg/m^3 contribution estimated for site R3 in the 2018-2019 campaign. With respect to the observed ambient levels, the average contributions estimated for the two cold season periods at site R1 and R3 were in reasonable agreement (0.31%-0.45% at site R1, 0.02%-0.04% at site R3), whereas for the warm seasons they showed a different behaviour with a higher value in 2018-2019 at site R1 (2.2% vs. 1.4%) and the opposite at site R3 (0.2% vs. 0.01%).

Table 3. Hourly mean concentration (pg/m^3) and mean relative contribution (%) of plant emission to Hg ambient levels measured at the three monitoring sites.

	2018-2019 campaign*						2022 campaign					
	Cold season			Warm season			Cold season			Warm season		
	R1	R2	R3	R1	R2	R3	R1	R2	R3	R1	R2	R3
Mean	10.3	-	0.3	20.5	-	0.1	5.6	0.5	0.2	5.7	0.4	1.1
Mean relative contribution	0.94%	-	0.04%	1.26%	-	0.01%	0.45%	0.05%	0.02%	0.32%	0.06%	0.06%

*Measurements not performed at Site R2

Despite these differences, the estimated contributions of the plant emissions during air quality monitoring campaigns were included at most around few tens of pg/m^3, whereas ambient levels resulted in the ng/m^3 orders. Daily time patterns obtained from model simulations showed that hourly peak events might occasionally occur in the surroundings of the plant, due to fumigation conditions on morning hours at the break-up of the nocturnal lapse rate inversion, generating highest hourly concentration peaks reaching up to about 1 ng/m^3, still with low appreciable impacts on measured air levels.

References

[1] Hu Y., Cheng H., Tao S. (2018). The growing importance of waste-to-energy (WTE) incineration in China's anthropogenic mercury emissions: emission inventories and reduction strategies, Renewable and Sustainable Energy Reviews, 97, 119-137
[2] Pirrone N., Cinnirella S., Feng X., Finkelman R.B., Friedli H.R., Leaner J. et al. (2010). Global mercury emissions to the atmosphere from anthropogenic and natural sources. Atmospheric Chemistry and Physics, 10, 5951-5964.
[3] Directive 2010/75/EU of the European parliament and of the Council of 24 November 2010 on industrial emissions (integrated pollution prevention and control), Official Journal of the European Union, L 334/17
[4] Li G., Wu Q., Wang S., Duan Z., Su H., Zhang L., Li Z., Tang Y., Zhao M., Chen L., Liu K., Zhang Y. (2018), Improving Flue Gas Mercury Removal in Waste Incinerators by Optimization of Carbon Injection Rate, Environmental Science & Technology, 52, 1940-1945
[5] Commission implementing decision (EU) 2019/2010 of 12 November 2019 establishing the best available techniques (BAT) conclusions, under Directive 2010/75/EU of the European Parliament and of the Council, for waste incineration, Official Journal of the European Union, L 312/55
[6] Lonati G., Cernuschi S., Piccoli A. (2021). Impact assessment of mercury emissions from a WtE plant: dispersion modelling vs. field measurements, Proceedings SIDISA 2020 – XI International symposium on environmental engineering, Torino, 29 giugno – 2 luglio 2021.
[7] European Commission (2001), Ambient air pollution by mercury – Position paper. ISBN 92-894-4260-3
[8] Takahashi F., Shimaoka T., Kida A. (2012). Atmospheric mercury emissions from waste combustions measured by continuous monitoring devices, Journal of the Air & Waste Management Association, 62, 686-695
[9] Chen L., Liu M., Fan R., Ma S., Xu Z., Ren M., He Q. (2013). Mercury speciation and emission from municipal solid waste incinerators in the Pearl River Delta, South China, Science of the Total Environment, 447, 396-402
[10] Bourtsalas A.C., Themelis N.J. (2019). Major sources of mercury emissions to the atmosphere: The U.S. case, Waste Management, 85, 90-94

PARALLEL SESSION: C5

One health and environmental safety

Emerging contaminants

Title: Effects of Natural Organic Matter interaction with Bisphenol-A on toxicity in the seawater

Authors: Giulia Paolella*[1, 2], Massimiliano Fabbricino[1], Annamaria Locascio[2], Ludovico Pontoni[1], Maria Sirakov[2]

[1] Department of Civil, Architectural and Environmental Engineering, University of Naples Federico II, via Claudio 21, 80125 Naples (Na), Italy (giulia.paolella, massimiliano.fabbricino, ludovico.pontoni)@unina.it
[2] Department of Biology and Evolution of Marine Organisms, Stazione Zoologica Anton Dohrn, Villa comunale 1, 80121 Naples (Na), Italy (giulia.paolella, annamaria.locascio, maria.sirakov)@unina.it

Keywords: Natural Organic Matter (NOM), Bisphenol-A (BPA), marine organisms, aquatic environment, complexes/interactions

Abstract

Natural organic matter (NOM), ubiquitous in inland and marine water, is a complex matrix of organic materials and a key component into the environment. For a long time the NOM was considered inert in the ecosystem and unable to induce any direct chemical/molecular effect on the organisms, however recent studies indicate that this is not the case. Therefore, it can induce reactive oxygen species accumulation, reduced antioxidant capacity, production of stress proteins and DNA damage in cells [1]. Due to its chemical structure, once in water, NOM closes in on itself, encapsulating both natural and anthropogenic contaminants, carrying them into the environment and making them undetectable by classical measurements. Unfortunately, it is not known if the complexation increases or decreases the bioavailability of the contaminants, and therefore increases or decreases their toxicity.

The always increasing use of disposable and plastic-made materials has inevitably allowed the spread in each compartment of the environment of “new” toxic contaminants: among them Bisphenol-A (BPA) is a widely used plasticizer, which is known to be an endocrine disruptor [2].

Many researches pointed out the ecological consequences of BPA, both on the environment and in aquatic wildlife [3, 4]. But until now, its real speciation in natural waters and its environmental consequences remain largely elusive. In other words, it is not known how the BPA is complexed with the NOM to form “invisible” entities, potentially very dangerous. For this reason, this research aims to analyze and define the chemical interactions between NOM and BPA to understand the behaviour of these complexes in aquatic environments.

In particular, the fate and effects of BPA complexes in the sea are studied in the mussel *Mytilus galloprovincialis*. These organisms are excellent indicators of aquatic pollution due to their filtration

capacity and sedentary lifestyle. Accordingly, they can offer the opportunity to highlight the extent and nature of the biological effects of BPA alone and in complexation with NOM under acute or chronic conditions.

From a biological point of view, subjecting these marine organisms to different concentrations of BPA and BPA/NOM complexes, different effects were observed in their mantles compared to the untreated controls.

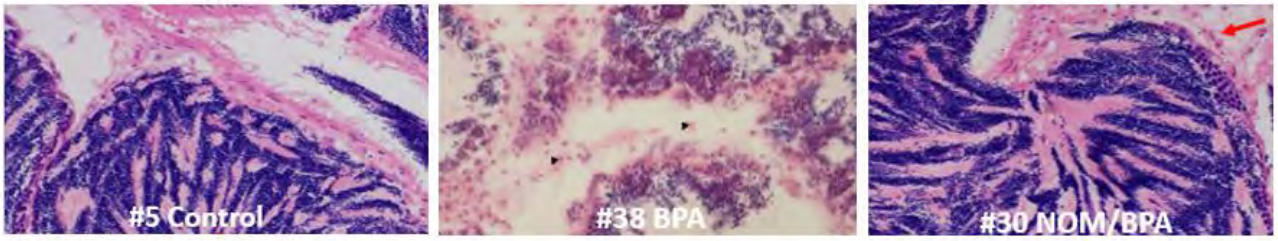

Figure 1. Images of mantles of Mytilus galloprovincialis after 96 hours of treatment. Scale bar is 20 μm

Thus, it is essential to define the chemical interaction between BPA and NOM and then investigate its negative and positive effects on marine organisms.

References

[1] Steinberg C.E.W., "NOM as Natural Xenobiotics", ACS Symposium Series, 115–144, (2014).
[2] Rubin B.S., "Bisphenol A: An endocrine disruptor with widespread exposure and multiple effects", The Journal of Steroid Biochemistry and Molecular Biology", 127, 27–34, (2011).
[3] Hermabessiere L., Dehaut A., Paul-Pont I., Lacroix C., Jezequel R., Soudant P., Duflos G., "Occurrence and effects of plastic additives on marine environments and organisms: A review", Chemosphere, 182, 781–793, (2017).
[4] Liu J., Zhang L., Lu G., Jiang R., Yan Z., Li Y., "Occurrence, toxicity and ecological risk of Bisphenol A analogues in aquatic environment – A review", Ecotoxicology and Environment Safety, 208 (2021).

Title: Monitoring contaminants of emerging concern and bacterial communities in surface water impacted by wastewater discharge

Authors: Filippo Fazzino*[1], Massimiliano Sgroi[2], Andrea Franzetti[3], Federico Vagliasindi[1], Gregory Korshin[4], Paolo Roccaro[1]

[1] *Department of Civil Engineering and Architecture, University of Catania, Viale Santa Sofia, 64, Catania, Italy*
[2] *Department of Science and Engineering of Materials, Environment and Urban Planning, Marche Polytechnic University, Ancona, 60131, Italy*
[3] *Department of Earth and Environmental Sciences, University of Milano-Bicocca, Milano, 20126, Italy*
[4] *Department of Civil and Environmental Engineering, University of Washington, Box 352700, Seattle, 98195-2700, WA, United States*

Keywords: Surface water; Wastewater discharge; Microbial community; Contaminants of emerging concern; Linear regression; Principal component analysis.

Abstract

Surface water quality has been progressively deteriorating by anthropogenic activities (municipal, industrial, and agriculture discharges, consumption of water resources) and natural events (precipitations, erosion, seepage of groundwater) thus sometimes compromising its ecological status and its drinking, industrial, and agricultural uses [1]. Furthermore, contaminants of emerging concern (CEC) have been ubiquitously detected in the aquatic environment at trace levels (ng/L to µg/L). CEC comprise a wide variety of compounds with different origins and characteristics (e.g., pharmaceuticals and personal care products, biocides) proved or suspected to exert adverse effects (e.g., endocrine disruption) on environment/human health [2]. What emerges from this context is that monitoring of surface water (to mitigate its deterioration) requires the collection and analysis of comprehensive water quality information (biological, physical, and chemical properties).

This study aimed to investigate i) the variations of the microbial communities along the length of rivers (likely driven by wastewater treatment plant, WWTP, discharges), ii) possible correlations among spectroscopic features of water samples, as described by several relevant indexes, individual CEC, and individual bacterial orders. For this purpose, results of the monitoring of two rivers located in the East Coast Region of Sicily (Italy) close to the city of Catania are presented. A series of samples were collected from 22 and 12 sampling points along, respectively, the Simeto and San Leonardo Rivers. The sampling points included effluents of 6 WWTPs discharging in the rivers and tributaries (Figure 1).

The performed analyses are summarized in Table 1. Shannon indexes (i.e., H and E, Table 1) define the biodiversity of a population by measuring the relative abundance of a single species. Particularly, E (i.e., normalized H) ranges from 0 (dominant species) to 1 (uniformly distributed species). Based on that, the samples from Simeto River were observed to exhibit higher values of biodiversity indexes compared to San Leonardo (data not shown), as demonstrated by the more heterogeneous distribution depicted in Figure 2.

In the most impacted points, *Pseudomonadales* was the predominant order of bacteria. Since large biodiversity is commonly associated with good quality surface water, what emerges from microbial analyses is that the San Leonardo River is generally more impacted than the Simeto River. Such evidence is corroborated by the measurements of CEC concentrations (data not shown). Indeed, concentrations of representative CEC were far larger in most of the sampling points in the San Leonardo transect than that of the Simeto River. Among WWTPs discharging into the Simeto River, the highest CEC concentrations were detected in effluents of WWTPs 1 and 4 (Figure 1). In general, caffeine and sucralose were the most detected CEC. The former is considered an indicator of untreated (or poorly treated) wastewater since it is known to be susceptible to biodegradation thus it should be partially or totally removed by conventional WWTPs. Conversely, the latter, being recalcitrant to biological removal, acts as a marker of WWTP discharges. Combined that information with microbial community analyses, two groups of orders of bacteria were established based on water quality. Specifically, 20 different orders of bacteria were mostly detected in the least impacted points of the rivers whereas 12 orders were selected as markers of untreated (or poorly treated) wastewater.

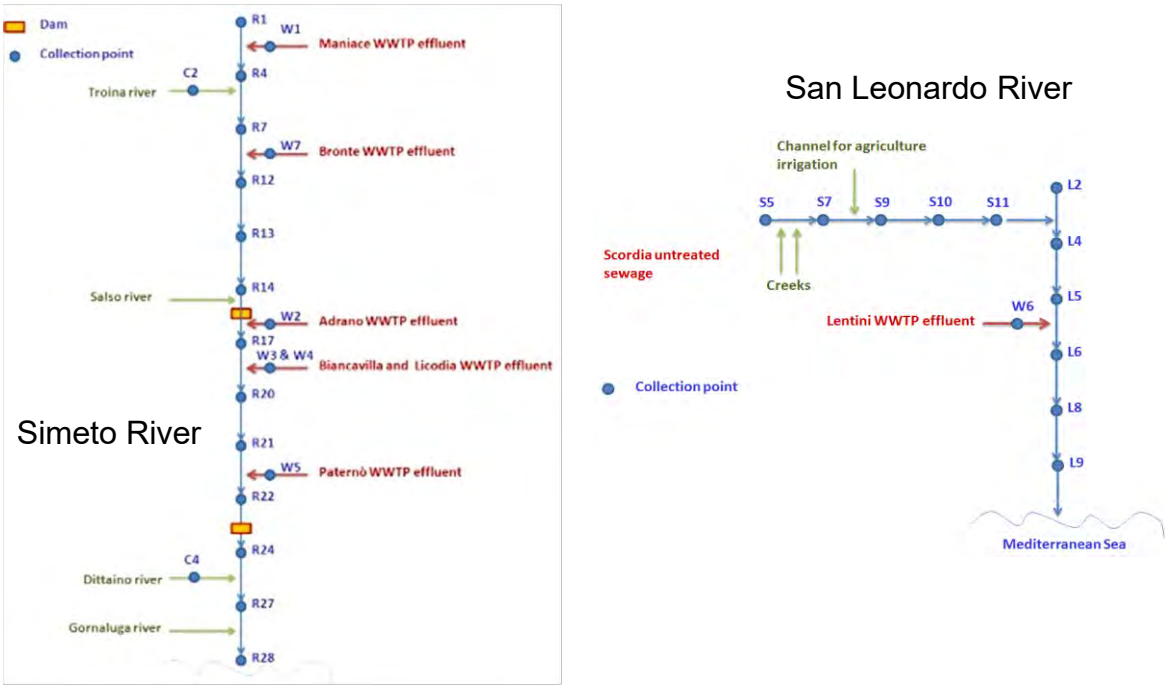

Figure 1. Sampling points along Simeto (a) and San Leonardo (b) Rivers

Table 1. List of analyses carried out on samples collected from Simeto and San Leonardo Rivers

Analysis	Parameters/indexes
Microbial community in terms of orders (confidence > 0.8) and abundance	Shannon and normalized Shannon indexes (H and E, respectively)
Physical-chemical properties	Dissolved oxygen, temperature, conductivity, pH, COD, NH_4^+-N, NO_3^--N
CEC concentrations through HPLC-MS	Caffeine, carbamazepine, DEET, sucralose, sulfamethoxazole, TCEP, trimethoprim, diclofenac, ibuprofen, iopromide

Absorbance and fluorescence	UVA_{254}, total fluorescence (TF), peak picking indexes Ii and PARAFAC components Ci (i=1-5)
Correlation	Linear regression (R^2) and principal component analysis (PCA)

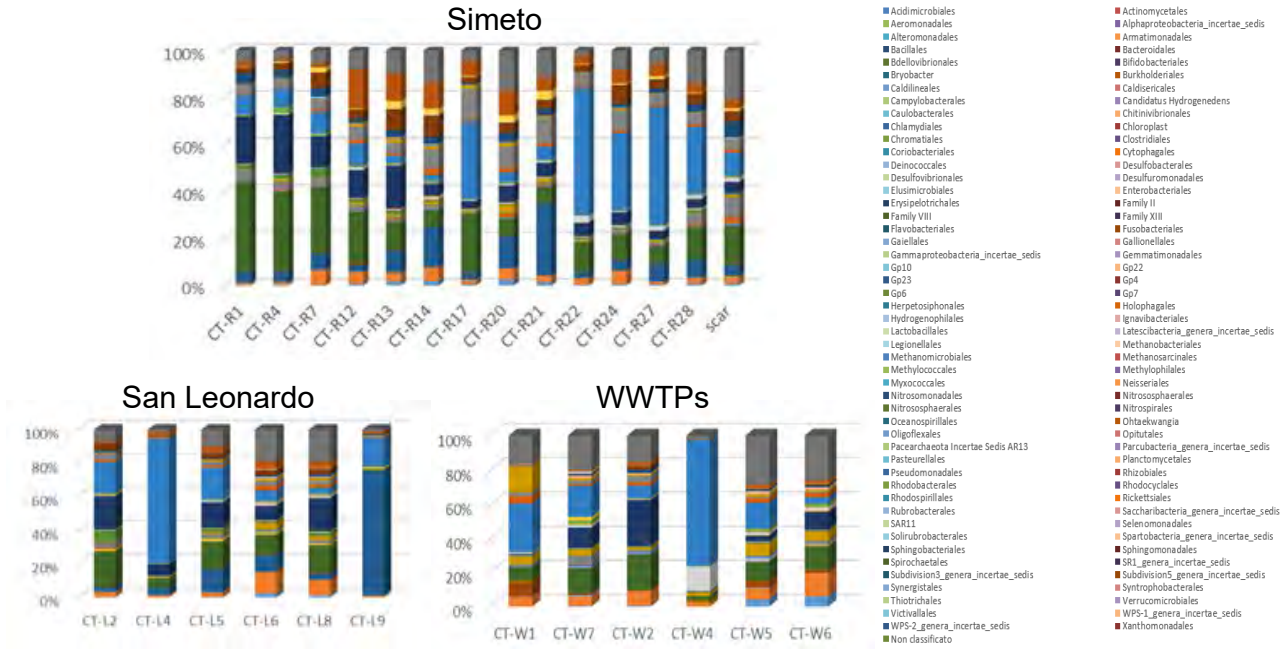

Figure 2. Microbial communities at order level in some sampling points of Simeto and San Leonardo Rivers and in WWTP effluents

A prior study demonstrated the applicability of fluorescence indexes as surrogate parameters to monitor the behaviour of CEC in the Simeto and San Leonardo Rivers [4]. In the present study, a similar approach was used to investigate possible correlations between bacteria and CEC and the chemical properties of the water. Specifically, along Simeto River, *Bacteroidales*, *Planctomyceales*, and *Spingobacteriales* correlated with TCEP, *Actinomycetales* correlated with ibuprofen, *Thiotrichales* correlated with diclofenac, *Methanosarcinales* and *Caldilineales* correlated with COD and *Ignavibacteria* correlated with I5 (345/440 nm) and C2 (250, 380/475 nm). On the other hand, water samples collected from the San Leonardo River exhibited a greater number of strong correlations compared to the Simeto case. For instance, carbamazepine, sucralose, and sulfamethoxazole well correlated with a wide variety of microbial orders; moreover, *Bdellovibrionales*, *Bifidobacteriales*, *Caldilineales*, *Methanosarcinales*, and *Thiotrichales* were observed to concomitantly correlate with several parameters.

Finally, in effluents of WWTPs, the greatest number of correlations between bacteria and spectroscopic indexes were determined. Specifically, the abundance of *Bifidobacteriales* was well correlated with all considered indexes except for C5 (with R^2 values ranging from 0.73 to 0.93), *Legionellales* correlated with I2, I4, TF, C3, and C5 (R^2=0.77-0.80), while that *Xanthomonadales* was correlated with I2, I3, I4, I5, TF, UVA_{254}, C1, C2, C3, and C4 (R^2=0.77-0.93).

Principal component analysis (PCA) of the effluents of WWTPs and San Leonardo stretch impacted by discharge of raw wastewater (Figure 3) showed that *Pseudomonadales*, ibuprofen, caffeine, ammonia

and COD can be considered as good indicators of untreated (or poorly treated) wastewater. Indeed, Figure 3 shows that *Pseudomonadales* is in the left part of the PCA biplot along with the most impacted sampling points, namely S5, S7, S9, S10, and S11 (in which raw wastewater was discharged, see Figure 1) and WWTPs 1 and 4 (in which highest CEC concentrations were detected). Similarly, especially ibuprofen and caffeine (Figure 3 b) and ammonia and COD (Figure 3 c) values were linked to the most impacted points.

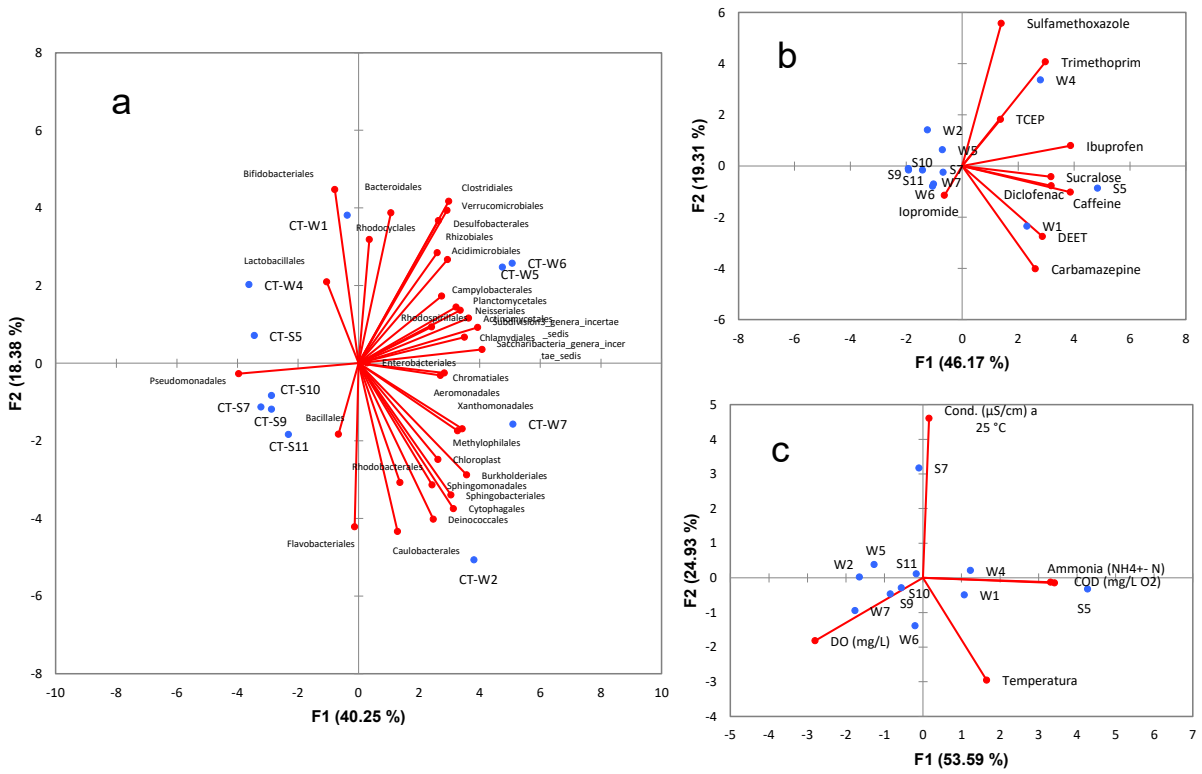

Figure 3. Biplots of PCA on effluents of WWTPs and San Leonardo stretch impacted by discharge of raw wastewater; a) orders of bacteria, b) CEC, c) physical and chemical parameters

Acknowledgements
This work has been partially funded by European Union (NextGeneration EU), through the MUR-PNRR project SAMOTHRACE (ECS00000022).

References
[1] Sgroi M, Vagliasindi FGA, Roccaro P. Feasibility, sustainability and circular economy concepts in water reuse. Current Opinion in Environmental Science & Health 2018;2:20–5. https://doi.org/10.1016/j.coesh.2018.01.004.
[2] Yadav D, Rangabhashiyam S, Verma P, Singh P, Devi P, Kumar P, et al. Environmental and health impacts of contaminants of emerging concerns: Recent treatment challenges and approaches. Chemosphere 2021;272:129492. https://doi.org/10.1016/j.chemosphere.2020.129492.
[3] Uddin MdG, Nash S, Olbert AI. A review of water quality index models and their use for assessing surface water quality. Ecological Indicators 2021;122:107218. https://doi.org/10.1016/j.ecolind.2020.107218.
[4] Sgroi M, Roccaro P, Korshin GV, Vagliasindi FGA. Monitoring the Behavior of Emerging Contaminants in Wastewater-Impacted Rivers Based on the Use of Fluorescence Excitation Emission Matrixes (EEM). Environ Sci Technol 2017;51:4306–16. https://doi.org/10.1021/acs.est.6b05785.

Title: An integrated comparison among organic matrices intended for agricultural reuse: final results of the SLURP project

Author(s): Giorgio Bertanza *[1,2], Alessandro Abbà [1], Carlotta Alias [3], Achille Amatucci [1], Andrea Binelli [4], Sara Castiglioni [5], Marco Fossati[5], Catarina Cruzeiro [6], Camilla Della Torre [4], Marta Domini [1], Donatella Feretti [3,2], Gianni Gilioli [1], Stefano Magni [4], Giovanna Mazzoleni [7,2], Michele Menghini [8], Roberta Pedrazzani [8,2], Peter Schroeder [6], Anna Simonetto [1], Nathalie Steimberg [7], Vera Ventura [1], Simona Vezzoli [8], Ilaria Zerbini [3]

[1] *Dipartimento di Ingegneria Civile, Architettura, Territorio e Ambiente e di Matematica, Università degli Studi di Brescia. Via Branze 43, I-25123 Brescia, Italy*
[2] *MISTRAL, Centro Interuniversitario di Ricerca, Università di Brescia, Milano Bicocca e Verona "Modelli Integrati di Studio per la Tutela della Salute e la Prevenzione negli Ambienti di Vita e di Lavoro", Italy*
[3] *Dipartimento di Specialità Medico-Chirurgiche, Scienze Radiologiche e Sanità Pubblica, Università degli Studi di Brescia. Viale Europa 11, I-25123 Brescia, Italy*
[4] *Dipartimento di Bioscienze, Università degli Studi di Milano, Via Celoria 26, I-20133 Milano, Italy*
[5] *Dipartimento Ambiente e Salute, Istituto di Ricerche Farmacologiche Mario Negri, IRCCS. Via Mario Negri 2, I-20156 Milano, Italy*
[6] *Helmholtz Zentrum München – Deutsches Forschungszentrum für Gesundheit und Umwelt (GmbH), Ingolstädter Landstraße 1, D-85764 Neuherberg, Germany*
[7] *Dipartimento di Scienze Cliniche e Sperimentali, Università degli Studi di Brescia. Viale Europa 11, I-25123 Brescia, Italy*
[8] *Dipartimento di Ingegneria Meccanica e Industriale, Università degli Studi di Brescia. Via Branze 38, I-25123 Brescia, Italy*

Keyword(s): Bioassays, compost, digestate, manure, sewage sludge, emerging contaminants

Abstract

Several organic residues, such as sewage sludge, compost, and manure, can be used in agriculture, as valuable source of organic carbon and nutrients. In principle, their use represents an ideal solution in terms of waste management priorities and circular economy, improving soil properties, such as texture and water holding capacity, and reducing the use of synthetic fertilizers. Moreover, phosphorus is included in the list of critical raw materials [1].
However, potential negative effects due to the presence of pollutants have to be considered and deeply investigated. As a matter of fact, it is not possible to measure all the chemicals which are contained in a matrix, nor the concentration of different compounds can be directly associated with the overall toxicity exerted by their mixture [2]. Notwithstanding this, current regulations, worldwide, set limitations on the reuse of organic residues in agriculture based on maximum allowable thresholds for a few physical-chemical and microbiological indicators.
Despite the advantages of reusing sludge, manure, digestate/compost, biochar and other matrices in agriculture, it is still debated whether these matrices represent a risk for environmental and human health. Approaches based on theoretical risk assessment models have been proposed, however their use encounters difficulties related to the lack of data [3].
On the other hand, powerful bioassays are nowadays available to directly assess the toxicity of organic matrices, theoretically avoiding the need for a physical-chemical characterization, as shown by several

recent studies ([4], [5], [6]). Using a multilevel characterization protocol based on toxicity tests might play a role to reliably assess the suitability of organic residues as substitutes for synthetic fertilizers and soil improvers. This is the central idea behind the SLURP [7] and the more recently funded 3D-WWTP-TOX [8] projects.
During the SLURP project, four types of residues were investigated: sewage sludge, liming materials, livestock manure, and soil improver, for a total of nine samples. They were compared by conducting a battery of analyses and tests, using several biological models representative of the soil and aquatic ecosystem as listed below:

- physical-chemical and microbiological characterisation according to legal requirements;
- nitrogen and carbon agronomic characterization;
- trace organic pollutants: about 40 emerging contaminants selected among pharmaceuticals, antibiotics, personal care products and perfluorinated compounds were quantified;
- plastics;
- biogas production potential;
- microbiome;
- assessment of the non-specific modes of action (baseline toxicity tests) on plant and animal organisms with increasing evolutionary complexity and with different trophic roles;
- assessment of the specific modes of action (e.g. endocrine disruption);
- reactive modes of action (biomarkers detection, Ames test, detection of Chromosomal aberrations etc.).

Bioassays, depending on the type of test, were conducted on the fresh matrices and/or aqueous extracts and/or organic extracts.
Finally, a big effort was made to homogeneously evaluate/interpret experimental results, through statistical analysis and “contextualization”, i.e. a normalization process aimed at estimating toxicity values under field conditions (the real dilution of substrates obtained during the application on land).
A detailed description of the whole protocol is published in [9].

As for physical-chemical characterization, the investigations showed different profiles of contamination in the different substrates investigated, with the prevalence of fluoroquinolones, antibiotics for human use, in sewage sludge and veterinary antibiotics in manure. Nevertheless, considering the real land application dosages, which were calculated based on composition, crops need and legislative limitations, it emerged that: a) metals accumulation on soil achieved by sewage sludge spreading is the highest among the tested matrices (about one order of magnitude greater than manure); b) the same rank also occurs for measured organic chemicals; nevertheless, their contribution is one order of magnitude (or even more) lower than the load of active principles of pesticides c) as for plastics, the greatest contribution originates from compost, followed by sludge, then manure and digestate [10].
A detailed comparison of results of the whole battery of bioassays was conducted considering all the types of matrices (either fresh or extracts) and the three families of tests (aimed at assessing either the baseline toxicity or specific modes of action or reactive modes of action).
Some tests evidenced toxicity on some or all the samples; others did not show any effect neither at the highest dosages. For instance, the aqueous and organic extracts were tested on *Allium cepa*, *Cucumis sativus*, *Lepidium sativum*, *Salmonella typhimurium* and human hepatoma cell line (HepG2) to assess toxicity (as seed germination, root elongation, proliferation), mutagenicity and genotoxicity (as primary DNA damage, chromosomal aberrations). All samples caused toxic or genotoxic effects in plant or human cells. Some samples caused toxic and genotoxic effects in all the tested organisms. None of the extracts induced mutagenic effects in *S. typhimurium*. *Latuca sativa* tests demonstrated comparable yields to those observed under control conditions (synthetic fertilizer). Similarly, tests on earthworms (*Lumbricus terrestris*) did not show significant differences among substrates (as for mortality and

reproduction), and also the comet assay, performed for evaluating DNA damage, as well as the oxidative stress response did not show appreciable differences. The embryotoxicity test conducted on zebrafish embryos showed the induction of developmental defects upon exposure to elutriates of all matrices, with EC50 higher in manures with respect to other matrices. The tested matrices also induced oxygen consumption and maximal respiration rate in embryos, suggesting an increase of metabolic demand to cope with stressful conditions. Conversely, no oxidative stress and neurotoxicity were observed in embryos exposed to all matrices.
By considering all the results of bioassays and focusing on those obtained with the dosages which reproduced as closely as possible the field application conditions, a unique toxicity ranking of the tested matrices was not evidenced. This means that, despite the different composition and presence of contaminants (as shown by the physical-chemical characterization), the whole battery of bioassays did not show clear differences among the substrates. This can be explained considering that the detected pollutants do not exert significant effects at the measured concentrations and/or that other pollutants than those analysed may contribute to the overall biological effect, which were in some cases detected also in matrices that should be considered safe from an environmental point of view (compost, manures and digestate). In any case, bioassays did not reveal differences among the matrices considered at their actual dosages on the field.
A survey was also conducted among students of the University of Brescia from different courses to evaluate the public acceptance of sewage sludge reuse in agriculture. The final sample comprised of 507 respondents. Findings suggest that the use of synthetic fertilizers raises greater concerns compared to organic matrices. Additionally, results show that the development of a certification protocol by a research institution enhances the social acceptability of sewage sludge reuse in agriculture. This observation is consistent with earlier research in the biosolids field [11].
Future developments of this research will be addressed to increase the number of samples and matrices to test according to the proposed protocol as well as to select a limited number of reliable and low-cost bioassays, for achieving a sound integrated physical-chemical-biological characterization for reusing organic substrates in agriculture, fostering a “safe” circular economy.

Acknowledgements

This work was funded by the CARIPLO Foundation (Milan, Italy) under the call “Circular Economy 2020”. The funded project’s title is: “SLURP - SLUdge Recovery in agriculture: environment and health Protection”. Grant number: 2020-1029. https://sites.unimi.it/slurp_project/en/home_en/

References

[1] European Commission (2020). Study on the EU’s list of Critical Raw Materials. Available online: http://europa.eu/rapid/press-release_MEMO-14-377_en.htm (accessed on 22 August 2023)
[2] R. Pedrazzani, G. Bertanza, I. Brnardić, Z. Cetecioglu, J. Dries, J. Dvarionienė, A.J. García-Fernández, A. Langenhoff, G. Libralato, G. Lofrano, B. Škrbić, E. Martínez-López, S. Meriç, D. Mutavdžić Pavlović, M. Papa, P. Schröder, K.P. Tsagarakis, C. Vogelsang (2019). Opinion paper about organic trace pollutants in wastewater: Toxicity assessment in a European perspective. Science of the Total Environment, 651, 3202-3221. doi: https://doi.org/10.1016/j.scitotenv.2018.10.027
[3] Huygens D., García-Gutierrez P., Orveillon G., Schillaci C., Delre A., Orgiazzi A., Wojda P., Tonini D., Egle L., Jones A., Pistocchi A. & Lugato E, (2022). Screening risk assessment of organic pollutants and environmental impacts from sewage sludge management - Study to support policy development on the Sewage Sludge Directive (86/278/EEC), Publications Office of the European Union, Luxembourg, https://doi.org/10.2760/541579
[4] B.I. Escher, M. Allinson, R. Altenburger, P.A. Bain, P. Balaguer, W. Busch, J. Crago, N.D. Denslow, E. Dopp, K. Hilscherova, A.R. Humpage, A. Kumar, M. Grimaldi, B.S. Jayasinghe, B. Jarosova, A. Jia, S. Makarov, K.A. Maruya, A. Medvedev, A.C. Mehinto, J.E. Mendez, A. Poulsen, E. Prochazka, J. Richard, A. Schifferli, D. Schlenk,

S. Scholz, F. Shiraishi, S. Snyder, G. Su, J.Y.M. Tang, B. van der Burg, S.C. van der Linden, I. Werner, S.D. Westerheide, C.K.C. Wong, M. Yang, B.H.Y. Yeung, X. Zhang, F.D.L. Leusch, Benchmarking Organic Micropollutants in Wastewater, Recycled Water and Drinking Water with In Vitro Bioassays, Environ. Sci. Technol. 48 (2014) 1940–1956. doi: https://doi.org/10.1021/es403899t.
[5] R. Pedrazzani, E. Ziliani, I. Cavallotti, E. Bollati, M. Ferreri, G. Bertanza (2019) Use of ecotoxicology tools within the environmental footprint evaluation protocols: the case of wastewater treatment plant. Desalination and Water Treatment 172, 2-14. doi: https://doi.org/10.5004/dwt.2019.24344
[6] G. Bertanza, N. Steimberg, R. Pedrazzani, J. Boniotti, E. Ceretti, G. Mazzoleni, M. Menghini, C. Urani, I. Zerbini, D. Feretti (2022). Wastewater toxicity removal: Integrated chemical and effect-based monitoring of full-scale conventional activated sludge and membrane bioreactor plants - Science of The Total Environment, 851, 158071, ISSN 0048-9697. DOI: https://doi.org/10.1016/j.scitotenv.2022.158071
[7] https://sites.unimi.it/slurp_project/
[8] https://3d-wwtp-tox.unibs.it/
[9] G. Bertanza, A. Abbà, C. Alias, A. Amatucci, A. Binelli, S. Castiglioni, M. Fossati, C. Cruzeiro, C. Della Torre, M. Domini, D. Feretti, G. Gilioli, S. Magni, G. Mazzoleni, M. Menghini, R. Pedrazzani, P. Schroeder, A. Simonetto, N. Steimberg, V. Ventura, S. Vezzoli, I. Zerbini (2024): “To spread or not to spread? Assessing the suitability of sewage sludge and other biogenic wastes for agriculture reuse” – MethodsX, 12 (2024) 102599. https://doi.org/10.1016/j.mex.2024.102599
[10] S. Magni, M. Fossati, R. Pedrazzani, A. Abbà, M. Domini, M. Menghini, S. Castiglioni, G. Bertanza, A. Binelli, C. Della Torre (2024) “Plastics in biogenic matrices intended for reuse in agriculture and the potential contribution to soil accumulation” - Environmental Pollution, 349, 123986. DOI: https://doi.org/10.1016/j.envpol.2024.123986
[11] M. Hébert (2007) “Public acceptance and independent certification of biosolids in Canada” - Water Practice and Technology, 2(4). https://doi.org/10.2166/wpt.2007.084

Title: How to deal with PFAS in urban water systems? A combination of removal strategies, fate modelling and risk assessment

Author(s): Jessica Ianes, Mattia Stefanoni, Beatrice Cantoni, Manuela Antonelli*

Politecnico di Milano, Department of Civil and Environmental Engineering (DICA), Piazza Leonardo da Vinci 32, 20133 Milan, Italy
** Corresponding Author: Manuela Antonelli, email: manuela.antonelli@polimi.it*

Keyword(s): *Adsorption, Drinking Water, Ozonation, PFAS, Risk Assessment, Wastewater.*

Introduction

Per- and polyfluoroalkyl substances (PFAS) represent a class of emerging contaminants that raised a significant concern for the environment and human health due to their widespread use, persistence, and potential adverse effects. Therefore, understanding the nature of PFAS contamination is crucial for shaping effective management strategies.
Industrial and municipal wastewater treatment plants (WWTP) discharges are considered the primary point sources of PFAS entering the environment. The increasing presence of PFAS in wastewater (WW), and inevitably also in surface water and drinking water (DW) poses a significant challenge in managing water quality within integrated urban water systems. Moreover, other anthropic sources can play an important role, such as stormwater (SW) runoff and cross-contamination with contaminated groundwater infiltration or direct discharge. Given the diverse sources, pathways, and receptors involved, it is essential to identify primary sources through specific monitoring campaigns, to adopt modelling strategies to predict PFAS fate, and to plan mitigation strategies based on their effective contribution to the reduction of human health and environmental risks.
While PFAS are not explicitly addressed in the proposed revision of the Urban Wastewater Treatment Directive (UWWTD), significant emphasis is placed on producers' responsibility. The industrial sector is phasing out the use of long-chain PFAS, which pose greater health risks, in favour of short-chain compounds, that are less hazardous, but more challenging to be removed due to their hydrophilic nature. In addition, increasingly stringent limits are being imposed on PFAS concentrations in surface water and DW (DW Directive 2021). As a result, water utilities must upgrade or manage their treatment processes to meet these new challenges.
Adsorption is the most promising process for PFAS removal. Ozonation, while not directly degrading PFAS, is useful in this context as a pre-treatment aimed at reducing the organic content in the real water matrices, since it has a competing effect on PFAS adsorption, but this is still not fully evaluated. Moreover, in a risk perspective, for drinking water treatment no procedures are available to optimize the adsorption process with regards to the health risk due to the mixture of PFAS, having both different affinity towards activated carbon and toxicity.
In this context, our study aims to investigate and optimize the removal of PFAS using advanced processes in both WWTP and drinking water treatment plants (DWTP) through lab-scale and pilot-scale testing, and full-scale monitoring, developing also a risk assessment framework to investigate the effectiveness of the various mitigation scenarios, comprising both treatment and preventive actions.

Materials and Methods

The water cycle has been conceptualized as shown in Figure 1, to describe the fate and transport of PFAS through: (i) discharges to surface water of groundwater used for heat pumps (GHP),

municipal/industrial WWTP effluents, and stormwater (SW) during rainy periods exceeding the capacity of the sewer and the WWTP; (ii) use of surface water for crop irrigation; (iii) supply for DW production; (vi) human consumption. Four case studies have been identified whose boundaries are reported in Figure 1.

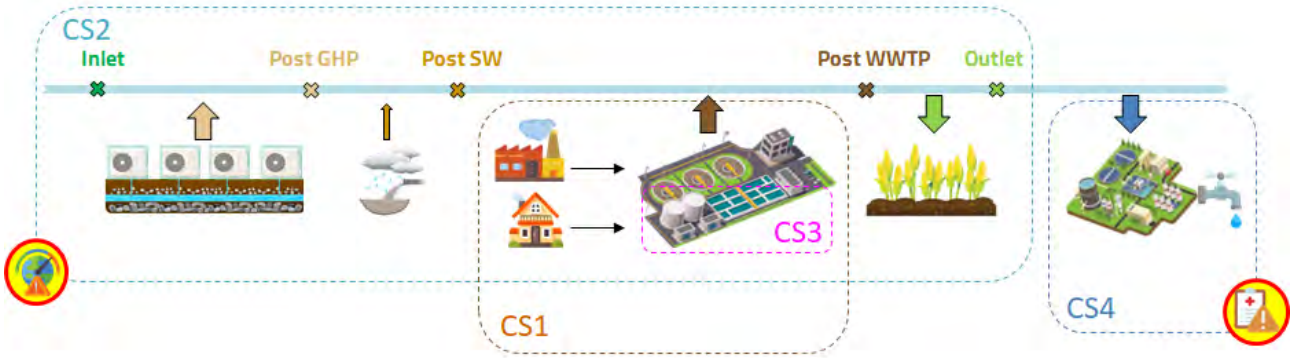

Figure 1. Conceptual scheme of the integrated urban water system, indicating PFAS sources, transport and risk receptors. Boundaries of the investigated case studies are also highlighted.

In detail, Case Study 1 (CS1) is a textile district in Como province (Italy), where mixed wastewater (textile and urban) is collected to a municipal WWTP (25-40% of the inlet COD load and 34% of inlet flowrate of industrial origin), comprising pre-treatments, activated sludge, coagulation-flocculation followed by a lamella clarifier, and ozonation. Eleven campaigns have been performed collecting 7 samples: the WWTP inlet, the biological process outlet, the ozonation inlet, the WWTP effluent, the biological sludge, the chemical sludge from the lamella clarifier, and the final dewatered sludge. A total of 14 PFAS (with chain lengths C4-C12) have been analysed.
In Case study 2 (CS2), a modelling framework was developed to simulate the input sources discharging in a waterway, including transport and degradation processes. Different scenarios of water management were investigated: use of GHP considering the interest towards a green energy transition, separation of the sewer system (SS) to limit pollution discharge during wet weather, wastewater effluent indirect reuse. The focus was on PFOA and PFOS, being the most present in the input sources of the case study.
In Case Studies 3 and 4, activated carbon removal was investigated in wastewater and drinking water, respectively. Real water matrices were tested, both collected upstream and downstream of full-scale ozonation: wastewater was sampled in the WWTP in CS1, while drinking water was sampled in a DWTP fed on surface water. Experiments were structured in two steps: (i) lab-scale batch isotherm tests and (ii) column tests. Four activated carbons (AC) characterized by different porosity and surface charge were used. The removal of natural organic matter (NOM), in terms of absorbance and fluorescence, and 14 different PFAS (C4-C12) were evaluated. Two types of column tests were performed to determine the breakthrough curves of PFAS and NOM in granular activated carbon (GAC) filters: (i) Rapid Small-Scale Column Test (RSSCT), and (ii) Field Adsorption Pilot Plant (FAPP). For RSSCT, tests were conducted in both single-column and in series (lead-lag) configurations.

Results

In the WWTP influent in CS1, 7 out of 14 PFAS were detected with a mean concentration of 0.44 µg/L. Urban wastewater contained more long-chain PFAS (21.6%) than textile wastewater (8.3%). Concentration showed high variability due to textile discharge fluctuations. Some PFAS, especially short-chain ones, were found at higher concentrations in the effluent compared to the influent. The average PFAS concentration and its variability mainly increased during the biological process.

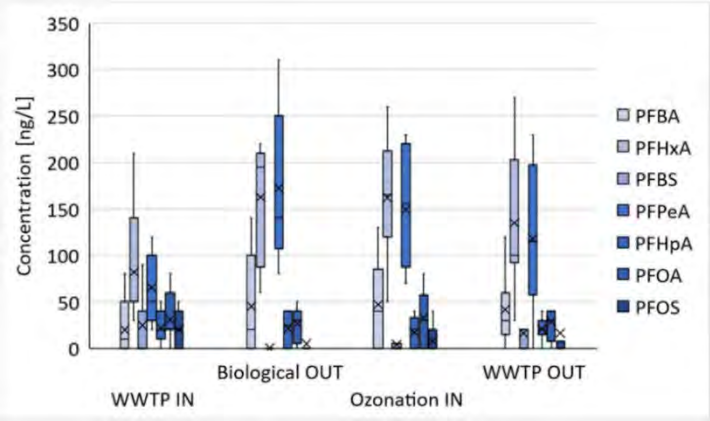

Figure 2. PFAS concentrations fate along the WWTP in CS1 (data derived from FANGHI project).

As for CS2, PFOA and PFOS concentrations were modelled along the waterway and their risks assessed over a year. Results are summarised in Figure 3. No acute environmental risk was detected. However, chronic environmental risk exceeded acceptable levels after WWTP effluent discharge already in the Baseline scenario, representing the main source. For this scenario, the predicted result was compared with the measurements at the OUTLET monitoring point, obtaining concentrations equal to 13.2±1.25 ng/L for PFOA and 3.6±1.00 ng/L for PFOS, while the measurements are equal to 15.0±6.2 ng/L for PFOA and 6.0±3.2 ng/L for PFOS. Higher chronic risk was found in scenarios involving GHP discharge, that significantly increases the risk level (risk quotient values from <1 to 10), mitigated by WWTP effluent dilution effect. Risk variability was influenced by seasonal GHP usage and storm water discharges, characterized by lower concentrations, and thus reducing the risk for dilution.

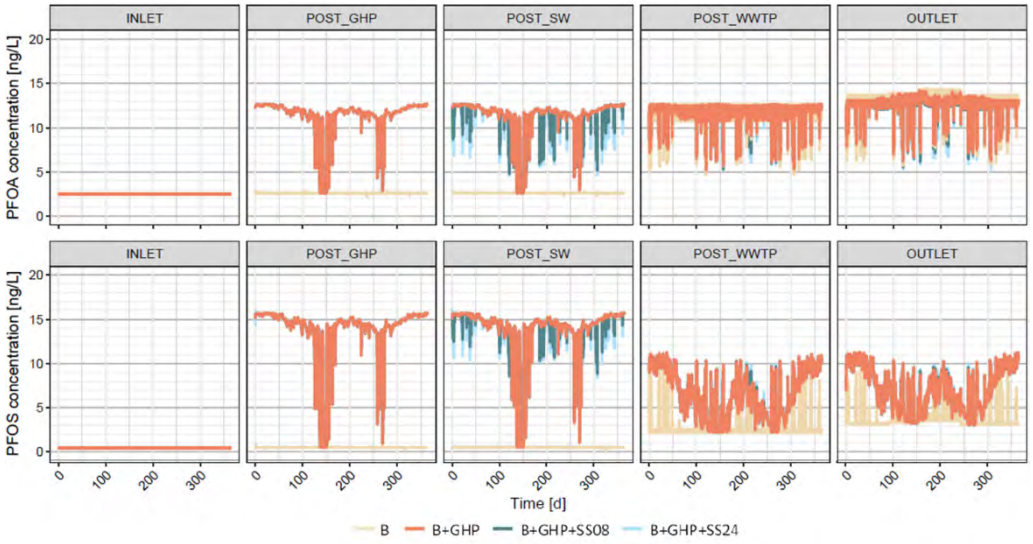

Figure 3. PFOA and PFOS concentrations in different points of the waterway under different scenarios of water management. B represents the baseline scenario, without GHP and with a combined sewer system.

In CS3 and CS4, isotherm tests showed that PFAS removal efficiencies depend on the intrinsic nature of these compounds. For short-chain hydrophobic PFAS, removal efficiencies were low, and no significant differences among the various tested carbons were observed. However, for long-chain hydrophobic PFAS, removal efficiencies were found to be higher when increasing the porosity.

Similarly, in RSSCT and FAPP column tests, we observed that PFAS breakthrough slows down with increasing pore size and hydrophobicity in both wastewater and drinking water (Figure 4).
In the lead-lag configuration for wastewater, macroporous carbon was selected as the "lead" to reduce competition effects related to organic matter and hydrophobic PFAS, while microporous and mesoporous carbons were tested as "lag" to assess the enhancement of their performance, especially on hydrophilic PFAS. However, it was observed that the ozone pretreatment effect is far more effective in improving adsorption performance than the lead-lag configuration and mitigates the chromatographic effect of short-chain PFAS. Finally, a potential correlation was observed between PFAS removal and NOM removal (across all various experimental scales tested), enabling the use of rapid and cost-effective NOM measurements (such as UV254 and fluorescence) as proxy variables to estimate PFAS breakthrough.

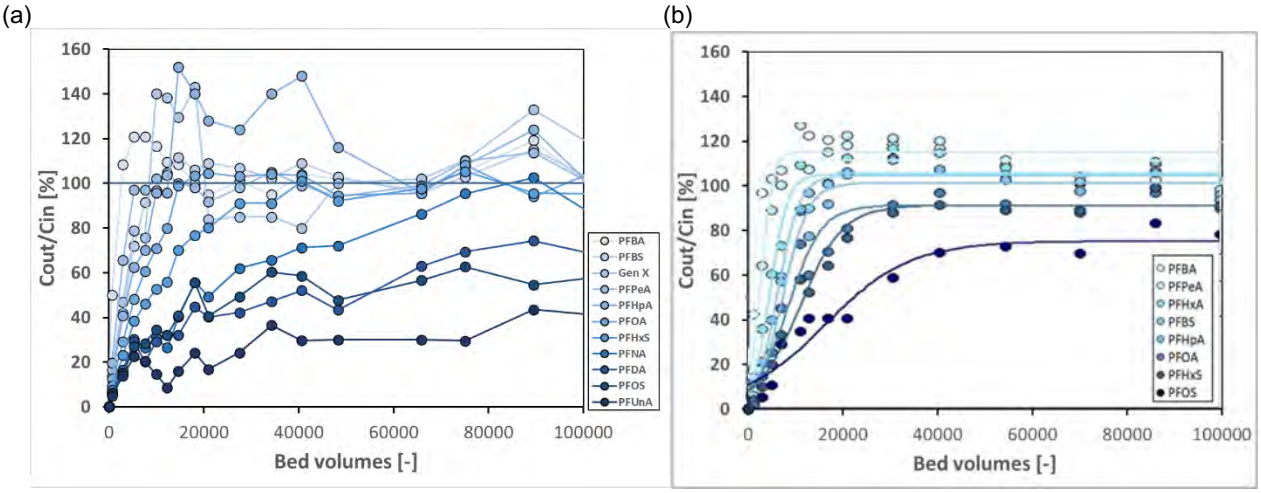

Figure 4. RSCCT breakthrough curves for tested PFAS in (a) wastewater sampled in CS1 and (b) drinking water sampled in CS4. Line colours were chosen based on PFAS octanol-water partition coefficient (Log D_{OW}), with lighter colours representing PFAS with lower Log D_{OW} values.

Conclusions

Prevention and removal strategies should be implemented to avoid PFAS spread in the environment, reducing the environmental risk on receiving surface water. Our study provides insights for the optimization of PFAS removal in both DWTP and WWTP, contributing to the sustainable management of water resources.

References

[1] Cantoni, B., Bergna, G., Baldini, E., Malpei, F., Antonelli, M., 2024. PFAS in textile wastewater: An integrated scenario analysis for interventions prioritization to reduce environmental risk. Process Safety and Environmental Protection 183, 437-445.
[2] Cantoni, B., Ianes, J., Bertolo, B., Ziccardi, S., Maffini, F., & Antonelli, M. (2024). Adsorption on activated carbon combined with ozonation for the removal of contaminants of emerging concern in drinking water. Journal of Environmental Management, 350.
[3] Cantoni B., Turolla, A., Wellmitz J., Ruhl A.S., Antonelli, M., 2021. Perfluoroalkyl substances (PFAS) adsorption in drinking water by granular activated carbon: Influence of activated carbon and PFAS characteristics. Science of the Total Environment 795, 148821.

PARALLEL SESSION: D5

Biorefineries

Bioproducts obtained from microalgae cultivation

SINGLE CELL PROTEIN PRODUCTION FROM CARBON DIOXIDE THROUGH A CONSORTIUM OF MICROALGAE AND HYDROGEN-OXIDIZING BACTERIA

Author(s): Raffaele Manzo*[1], Stefano Papirio[1], Giovanni Esposito[1], Silvio Matassa[1].

[1] Department of Civil, Architectural and Environmental Engineering, University of Naples Federico II, via Claudio 21, 80125, Naples, Italy. Email: raffaele.manzo@unina.it (Raffaele Manzo); stefano.papirio@unina.it (Stefano Papirio); giovanni.esposito1@unina.it (Giovanni Esposito); silvio.matassa@unina.it (Silvio Matassa).

Keyword(s): Single Cell Protein, Carbon Capture and Utilization, Hydrogen-Oxidizing Bacteria, Microalgae

Abstract

INTRODUCTION

Global population is bound to reach more than 9 billion people in 2050 [1]. In view of this, the global supply of protein poses severe concerns, since a more intensive production of conventional animal and plant protein would exacerbate the already high pressure on the environment through, for instance, greenhouse gas (GHG) emissions, freshwater consumption and land use. GHG emissions are particularly concerning, considering that livestock rearing alone contributes to 14.5% of the anthropogenic global GHG emissions [2]. An interesting and potentially more sustainable alternative for protein production is constituted by single cell protein (SCP), which represents the dried and protein-rich microbial cells of microalgae, yeasts, bacteria, and fungi. Thanks to the high content of protein, together with lipids, carbohydrates, vitamins, and essential amino acids, SCP have been proposed as potential feed and food additives [3].

The present study aims to produce SCP through a microbial consortium composed of microalgae and hydrogen-oxidizing bacteria (HOB). Thanks to their ability to fix carbon dioxide (CO_2) during their growth [4], these two groups of microorganisms could potentially allow capturing and valorising CO_2. While microalgae and HOB have been widely studied separately for SCP production, to the best of the authors' knowledge their combination has never been evaluated so far. Combining microalgae and HOB could help addressing some of the main limitations of the two microbial groups and could result in potential unexpected synergies. As a matter of fact, one of the main bottlenecks linked to HOB cultivation, relying on the use of hydrogen (H_2), oxygen (O_2) and CO_2, is the flammability hazard of the gas mixture [5]. Microalgae, on their side, are capable of O_2 production through photosynthesis, which would be directly available and consumed by HOB without the need of supplying or accumulating a potentially explosive gas mixture. Furthermore, microalgae could benefit from the consumption of O_2 and the presence of H_2, which could stimulate further CO_2 fixation through the metabolic pathway of photoreduction carried out by the hydrogenase enzyme, a bidirectional enzyme susceptible to the presence of O_2 [6].

In view of the above, the experimental work here presented investigated the growth of a HOB-microalgae consortium through a series of batch tests under different conditions, aiming at evaluating the performances of the process and the composition of the produced microbial biomass. The tested conditions involved different gas mixtures in terms of O_2, CO_2 and H_2 content, and the benchmarking of the HOB-microalgae consortium with microalgae and HOB alone.

MATERIALS AND METHODS

The batch tests were carried out in serum bottles of 250 mL with a working volume of 25 mL. The headspace was filled with a gas mixture composed of H_2, O_2 and CO_2 at different concentrations depending on the tested condition, while argon (Ar) was used as inert gas to replace H_2 in the control conditions aiming at assessing the growth of microalgae alone (Table 1). The tests were carried out in

a thermostatic bath at a constant temperature of 30 °C and at a neutral pH of 7. The thermostatic bath was set on a shaker at 70 RPM to improve H_2 solubilization in the liquid phase. LED lights were used as light source for the growth of microalgae. For the control conditions aimed at assessing the growth of HOB alone, light penetration was avoided by means of an aluminium foil cover. All tests were conducted in triplicate. The growth of the microorganisms was monitored through the measurement of suspended COD (COD) concentration, which was further converted into volatile suspended solids (VSS) concentration by using a conversion factor of 1.42 g COD/g VSS. The sCOD was calculated as the difference between the total (tCOD) and soluble COD (sCOD) concentration. The latter two parameters were analysed according to the APHA standard method [7]. Ammonium (NH_4^+) concentration in the liquid phase was measured through the indophenol-blue method [8]. Gas composition was measured through gas chromatography. Pressure and pH were also monitored. Furthermore, to gather information about the carbohydrates and protein fractions composing the SCP biomass, the DuBois [9] and Lowry [10] protocols were applied, respectively.

Table 1. Overview of the tested conditions in terms of gas composition, light time exposure, and favoured culture.

Test	Condition	Gas composition [%v/v]				Light time exposure	Favoured culture
		Ar	H_2	O_2	CO_2		
1	1.1	0	65	20	15	12 h of light/12 h of dark	HOB-microalgae (test)
	1.2	65	0	20	15	12 h of light/12 h of dark	Microalgae (control)
	1.3	0	65	20	15	24 h of dark	HOB (control)
2	2.1	0	50	20	30	12 h of light/12 h of dark	HOB-microalgae (test)
	2.2	50	0	20	30	12 h of light/12 h of dark	Microalgae (control)
	2.3	0	50	20	30	24 h of dark	HOB (control)
3	3.1	0	85	0	15	12 h of light/12 h of dark	HOB-Microalgae (test)
	3.2	85	0	0	15	12 h of light/12 h of dark	Microalgae (control)
4	4.1	0	68	3.4*	16	12 h of light/12 h of dark	HOB-microalgae (test)
	4.2	68	0	3.4*	16	12 h of light/12 h of dark	Microalgae (control)

*O_2 injected as air, present at 16%v/v

RESULTS AND DISCUSSION

The results concerning biomass growth (VSS), nitrogen consumption (NH_4^+) and pressure trends obtained with the HOB-microalgae consortium are reported in Figure 1 and compared to those obtained with the HOB and microalgae alone in Table 2. The tests showed promising results regarding the growth of the microalgae-HOB microbial consortium, constantly reaching VSS values higher than the respective controls of microalgae or HOB alone. Test 1, which evaluated the growth of the microbial consortium when provided with the optimal gas mixture according to the stoichiometry of HOB growth, showed a maximum VSS concentration of 4.7 g/L, and a complete consumption of NH_4^+ after 14 days (condition 1.1), thereby indicating that further growth could have been supported by supplying additional nitrogen. At the end of the test, condition 1.2 and 1.3 reached around half (2.7 g/L) and a third (1.4 g/L) of the VSS concentration value displayed by condition 1.1, respectively, while NH_4^+ was consumed up to around 50% of the initial value in both conditions. Test 2, which was characterized by an increase in CO_2 concentration from 15 to 30% (v/v), was meant to evaluate the growth of the HOB-microalgae consortium under conditions that are usually unfavourable to microalgae alone. Within this test, condition 2.1 showed a similar VSS concentration trend to condition 1.1, even though stabilising around a slightly lower values, closer to 4 g/L. Ammonium consumption was also slower, never reaching its full depletion. The control represented by condition 2.2 showed similar trends for both VSS and NH_4^+

concentrations to condition 2.1. On the other hand, the HOB culture grown in condition 2.3 showed a final VSS concentration of only 0.4 g/L and consumed only 17% of the initial value of NH_4^+. These results might point out that the HOB were those mainly affected by the change in the gas composition, which would explain the similarities between condition 2.1 and 2.2. Test 3 and 4 were designed to study the growth of the microbial consortium in a condition characterized by the absence of O_2 or by the presence of O_2 in an atmosphere of H_2 below the lower flammability limit, respectively, therefore evaluating whether or not the microalgae could support the HOB growth through O_2 production while minimising the flammability hazard. In condition 3.1, the microbial consortium failed to reach the same concentrations of VSS as condition 1.1 and 2.1, stabilising at a VSS concentration of around 2.5 g/L after the first week and then showing only a slight increase during the last days of the test. The same conditions also showed an incomplete consumption of ammonium. Condition 3.2 showed the same trends as condition 3.1 in terms of both VSS and NH_4^+ concentration. The cause of such lower growth might be linked with the low levels of O_2 provided, which might indicate that the microalgae could not provide enough O_2 through photosynthesis to satisfy the demand of HOB. This could have undermined the growth potential of the HOB in condition 3.1, possibly explaining the similarity between condition 3.1 and condition 3.2. On the other hand, condition 4.1 showed the highest growth of biomass, up to a value of 5.5 g/L of VSS, together with a complete consumption of NH_4^+. The results from condition 4.2 showed a similar VSS concentration trend to condition 4.1, reaching its highest value of 4.7 g/L at the end of the third week. Pressure measurement was particularly important to gather information about the activity of the HOB. Since the majority of the headspace was filled with H_2, a lowering in pressure also meant an active consumption of H_2 by the HOB. The conditions in which the pressure lowered the most were condition 1.1 and 1.3, with a variation of pressure of 1.0 and 1.1 bar respectively. This is coherent with test 1 having the optimal gas composition for the growth of HOB. Interestingly, the headspace pressure in condition 4.1 did not lower further after the first week, and yet H_2 was detected only in small residual quantities while O_2 was being accumulated in the headspace. It might thus be that the production of O_2 kept the pressure stable even though H_2 was being constantly consumed. Regarding the macromolecular composition of the SCP obtained with the microalgae-HOB consortium, a similar protein content was found in all tests, with the highest value of 52.6% of protein in condition 1.1. The same observation can be made in relation to carbohydrates. Condition 3.1 is the one that performed the worst both in terms of carbohydrates and protein content, being also the one that yielded the lower biomass, according to the measured VSS concentration values. The overall results are summarised in Table 2.

This study showed overall promising results in relation to the performances of the HOB-microalgae consortium, which reached biomass concentrations systematically higher than the respective controls, demonstrating that growing microalgae and HOB together offers potential benefits. The average protein content was also comparable to that reported in literature for microalgae and HOB [11]. The performances of the HOB-microalgae in the microbial consortium were particularly remarkable under conditions 4.1, where the highest VSS concentration was reached under operating conditions that allow to minimize the flammability hazard. Of further interest to this study is also the information given by the nitrogen consumption, since in condition 1.1, 2.1, and 4.1 the availability of NH_4^+ acted limited the growth of the consortium, meaning that it could be possible to reach even higher concentrations of VSS, which are not common to microalgae grown only with light.

Table 2. Summary of the process performances and SCP composition obtained in the different tests.

Condition	Highest VSS value [g/L]	Highest NH_4^+ consumption [%]	ΔP^*_{max} [bar]	ΔP^*_{min} [bar]	Final protein content [% Protein/VSS]	Final carbohydrates content [% Carbohydrates/VSS]
1.1 - test	4.7	100	1.000	0.600	52.6	28.82
1.2 - control	2.7	51	0.040	-0.016	57.6	27.15
1.3 - control	1.4	40	1.100	0.700	42.1	28.56
2.1 - test	4.2	92	0.770	0.250	43.6	30.17

2.2 - control	3.8	97	0.061	-0.035	59.4	14.01
2.3 - control	0.4	17	0.600	0.180	36.6	21.71
3.1 - test	3.3	85	0.720	0.200	36.7	15.30
3.2 - control	2.9	94	0.110	-0.021	39.1	18.80
4.1 - test	5.5	100	0.450	0.074	40.3	28.49
4.2 - control	4.6	100	0.016	-0.040	39.8	31.64

* Pressure reduction

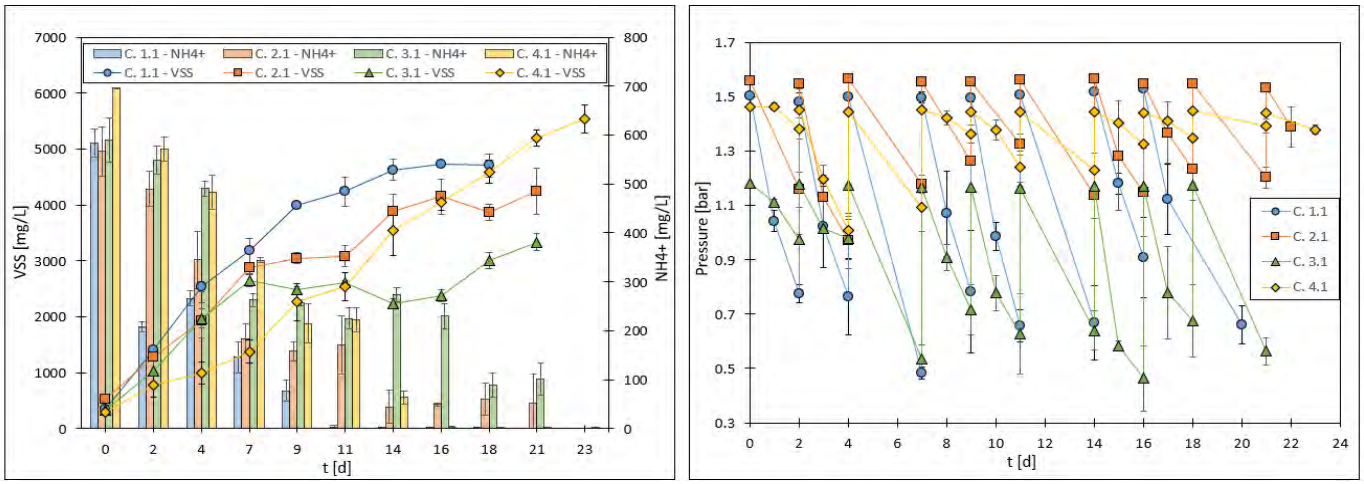

Figure 1. VSS and NH_4^+ concentration trends and pressure trend measured in Condition (C.) 1.1, 2.1, 3.1, and 4.1.

References

[1] R. Lee, "The outlook for population growth," Science, vol. 333, no. 6042. pp. 569–573, Jul. 29, 2011.doi: 10.1126/science.1208859.
[2] M. M. Rojas-Downing, A. P. Nejadhashemi, T. Harrigan, and S. A. Woznicki, "Climate change and livestock: Impacts, adaptation, and mitigation," Clim Risk Manag, vol. 16, pp. 145–163, Jan. 2017, doi: 10.1016/J.CRM.2017.02.001.
[3] S. Matassa, N. Boon, I. Pikaar, and W. Verstraete, "Microbial protein: future sustainable food supply route with low environmental footprint," Microb Biotechnol, vol. 9, no. 5, pp. 568–575, Sep. 2016, doi: 10.1111/1751-7915.12369.
[4] T. G. Volova and V. A. Barashkov, "Characteristics of proteins synthesized by hydrogen-oxidizing microorganisms," Appl. Biochem. Microbiol., vol. 46, no. 6, pp. 574–579, Nov. 2010, doi: 10.1134/S0003683810060037.
[5] X. Hu, Q. Xie, J. Zhang, Q. Yu, H. Liu, and Y. Sun, "Experimental study of the lower flammability limits of H2/O2/CO2 mixture," Int J Hydrogen Energy, vol. 45, no. 51, pp. 27837–27845, Oct. 2020, doi: 10.1016/J.IJHYDENE.2020.07.033.
[6] D. C. Howarth and G. A. Codd, "The Uptake and Production of Molecular Hydrogen by Unicellular Cy anobacteria," J Gen Microbiol, vol. 131, no. 7, pp. 1561–1562, 1985.
[7] APHA, Standard Methods for the Examination of Water and Wastewater. 2007.
[8] A. Aminot, D. S. Kirkwood, and R. Kcrouel, "Determination of ammonia in seawater by the indophenol-blue method: Evaluation of the ICES NUTS I/C 5 questionnaire," 1997.
[9] M. DuBois, K. A. Gilles, J. K. Hamilton, P. A. Rebers, and F. Smith, "Colorimetric Method for Determination of Sugars and Related Substances," Anal Chem, vol. 28, no. 3, pp. 350–356, 1956, doi: https://doi.org/10.1021/ac60111a017.
[10] O. H. Lowry, N. J. Rosebrough, A. L. Farr, and R. J. Randall, "Protein measurement with the folin phenol reagent," Journal of Biological Chemistry, vol. 193, no. 1, pp. 265–275, 1951.
[11] A. Ritala, S. T. Häkkinen, M. Toivari, and M. G. Wiebe, "Single cell protein-state-of-the-art, industrial landscape and patents 2001-2016," *Frontiers in Microbiology*, vol. 8, no. OCT. Frontiers Media S.A., Oct. 13, 2017. doi: 10.3389/fmicb.2017.02009.

Microalgae CO_2 capture a new way to electro-refinery.

Author(s): Sandra Maldonado[2], Raúl García-Cervilla[2], Gabriela Roa-Morales[1], Reyna Natividad[1], Justo Lobato[2], Manuel A. Rodrigo-Rodrigo[2]

[1] Joint Research Centre in Sustainable Chemistry (CCIQS)UAEM-UNAM, highway Km. 14.5, Unit San Cayetano, Toluca - Atlacomulco, 50200 Toluca de Lerdo, Méx., Mexico; sandra.maldom@gmail.com
[2] Department of Chemical Engineering, University of Castilla-La Mancha, Ciudad Real, Spain,

Keyword(s): CO_2 capture, Microalgae, Electrolysis, Carboxylic acids, Electrodialysis

Abstract

1- Introduction

During latest years CO_2 levels are increased considerably with the consequent effects on the climate and the environment [1]. For this reason, CO_2 capture technologies have attracted increasing interest. Algae are being considered a great alternative not only to reduce CO_2 levels and purify the air [2], but also to produce some byproducts that could be used as fuels after the process. This versatility of algae, which allows them to be an important resource in electro-refinery, has been demonstrated in several studies such as the one carried out by Y. Liang et al. [3]. Y. Liang et al., used the algae as organic matter in process to obtain biomass that is able to produce biofuels or only to capture CO_2.

In this work *chlorella vulgaris* was employed as raw material, inasmuch as this specie is a great option for its great capacity to reach high photosynthetic efficiencies, therefore more CO_2 consumption, and high growth rates [4]. The first stage of the processes consisted in create an algae laboratory scale farm able to capture CO_2 as feed from environment considering that CO_2 is captured by the microalgae and invested in the growth of organic matter. Once algae density is enough the second stage consist in treating a volume of 500 mL of algae solution in a parallel electrolysis cell with an BDD anode and stainless-steal cathode with the main purpose of hydrolyse algae and produce different carboxylic acids. The carboxylic acids are able to vary according to current density, these can be formic acid, acetic acid, oxalic acid, oxamic acid, malonic acid, among others. On this way organic matter is then degraded in an electrochemical cell.

Continuously, the third stage consist in electrodialysis cell employing an anionic membrane, where cathodic chamber was fed with algae solution, meanwhile, anodic chamber was fed with a solution 0.05M NaOH as electrolyte, with the purpose of obtain carboxylates in the cationic chamber and increase the concentration of them during the process and decrease the concentration of carboxylic acids in the anionic chamber.

Considering that, the research of carboxylic acids production employing algae it's relatively a new process, therefore the energetic analysis and comparing the efficiency of this method to obtain these compounds will be conducted in subsequent research. In addition to this, it is intended to implement the use of solar cells to supply the energy needed to carry out the process and the scaling up of the system.

2- Materials ant methods

For this research *chlorella vulgaris* (supplied by *el Banco Español de Algas*) was cultivated in specific conditions of 20°C (controlled temperature), controlling light/dark cycles, constant agitation (till 250ml) and bubbling (from volumes of 500 mL till 2 L) for the purpose of supplying CO_2 from the environment and covered with filter lid as axenic strain. The scale up of microalgae production was conducted in proportion of 1/10 in a staggered manner.

Algae characterization was carried out by spectrophotometry (UV-vis) (0-800 nm). Total organic carbon, chemical oxygen demand and total suspended solids were also analyzed. Carboxylic acids were quantified by HPLC-DAD from AGILENT (Hi-Plex H column, λ = 210nm, mobile phase H_2SO_4 100 mM at 0.6 mL-min^{-1}, temperature 50 ºC).

The electrochemical tests were conducted in a double electrochemical cell employing boron dopped diamond (BDD) anode and stainless-steel cathode (total area of 50 cm^2). For this experiments a specific electrolyte was not necessary, considering the conductivity between 4.4-5 mS cm^{-1} as result of algae medium feed (Table 1). Different current densities were used, taking samples at 0, 5, 15, 30, 60, 120, 180, 240 and 300 minutes in order to observe if the variation of the current density influences the formation of the different carboxylic acids.
On the other hand, electrodialysis tests were conducted in a cell, employing a DSA anode for anionic chamber and stainless-steel cathode for cationic chamber and these compartments were separated with an anionic membrane. Figure 1 shows the diagram configuration system employed in these tests.

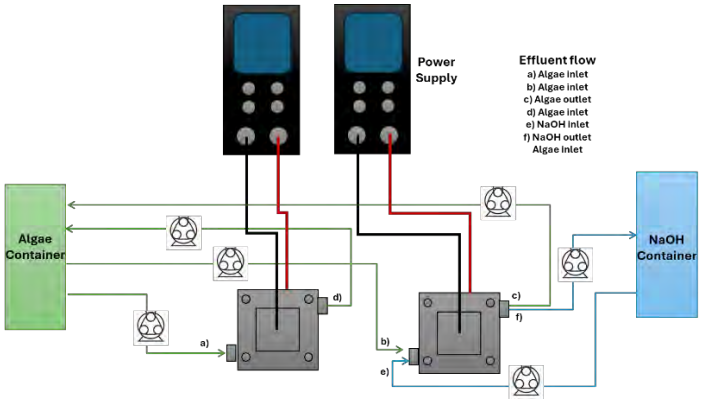

Figure 1. System configuration of electrochemical cell, electrodialysis cell and effluent flow

Table 1. The Modified Bold's Basal composition, algae cultivation media [5]

Compound	Concentration (g·L^{-1})	Compound	Concentration (g·L^{-1})
$NaNO_3$	0.220	EDTA	0.050
$MgSO_4$	0.075	NaCl	0.025
K_2HPO_4	0.175	KOH	0.031
$NaNO_3$	0.125	H_3CO_3	0.010
NH_4Cl	0.125	$FeSO_4$	0.005
KH_2PO_4	0.075	$ZnSO_4$	0.009
$CaCl_2$	0.025	$MnCl_2$	0.002

3- Results and discussion

The figure 2 shows the algae after 5 hours of electrochemical process. Chlorophyll present in algae was degraded during the experiment, because by adding an electric current, the algae died, reducing the characteristic green colour of the chlorophyll and generating a greater amount of organic matter.

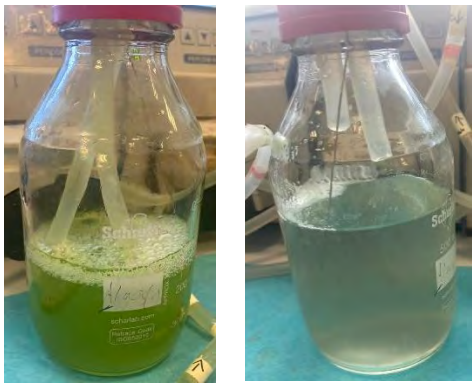

Figure 2. Appearance of the chlorella vulgaris microalgae solution before the beginning of the experiment (left) and after 5 h of treatment at 245 mA (right).

Figure 3 shows the carboxylic acids produced during the experiment. Can be seen how oxalic acid started to increase slowly. On their side oxamic acid was also increased quickly, however reached a plateau value with the time. Formic acid increased dramatically and subsequently decrease slowly. Although this experiment shows a clear disappearance of the typical chlorophyll coloration, the reduction of the organic matter present in the sample is negligible. Therefore, the extension of the reaction times and the applied current density are carefully studied to avoid the elimination of the carboxylic acids and to achieve the complete conversion of the organic matter present in the sample. While, figure 4 show the main carboxylic acids obtained during the electrolysis process. Oxalic acid concentration increases during all the treatment, in the same way formic acid concentration increases slightly in comparison with oxalic acid. Furthermore, acetic acid is obtained after 240 minutes of treatment.

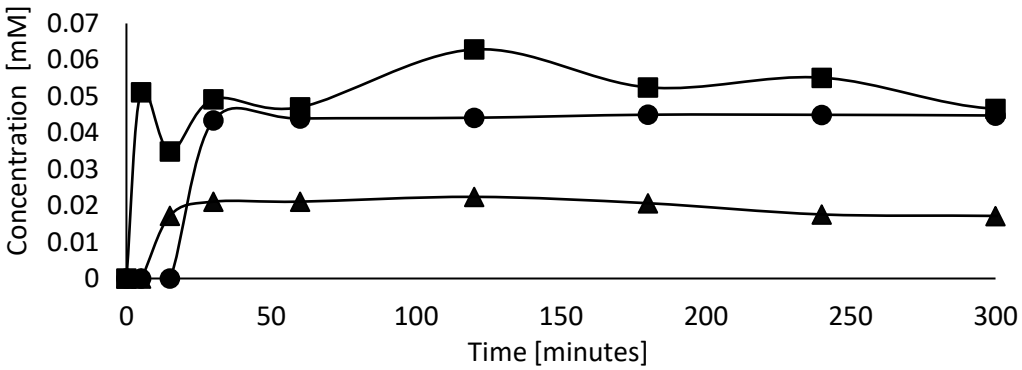

Figure 2. Carboxylic acids (▲oxalic acid , ■formic acid and ●oxamic acid) produced in the electrocatalytic cell, employing BDD anode and stainless-steal cathode at 245 mA.

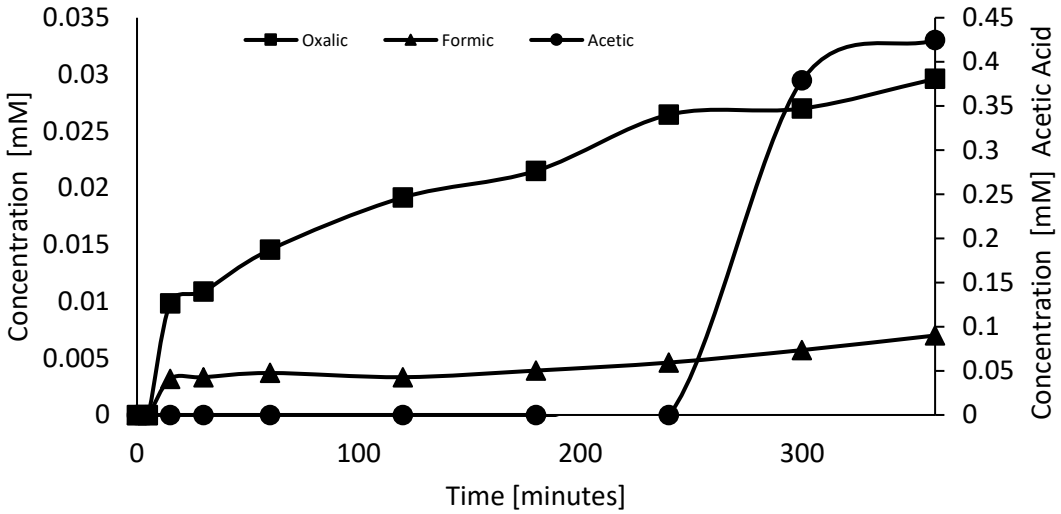

Figure 4. Carboxylic acids obtained employing an anionic membrane (▲formic acid,, ■ oxalic acid and ●acetic acid) in the electrodialysis cell, employing DSA anode and stainless-steal cathode at 245 mA.

4- Conclusions

CO_2 is an environmental pollutant that affects human health and the environment. However, following the principles of biorefinery, it is become in an important resource to produce value-added compounds. In this study, CO_2 capture its achieved employing microalgae, in addition to their production and its subsequent electrochemical oxidation to produce carboxylic acids and purification through electrodialysis cell. This process has shown promise, although it requires further study and optimization.

Acknowledgements

This work was supported by CONACYT project (320965) for financial support from Mexican government. This work was supported by Spanish Ministry of Science, Innovation and Universities through the ElectroRefin4O project (PID2022-138401OB-I00). Raúl García Cervilla is acknowledged for the Spanish Juan de la Cierva postdoctoral grant. (JDC2022-049619-I).

References

[1] I. Hernandez-Mireles, R. Van Der Stel, and E. Goetheer, “New methodologies for integrating algae with CO2 capture,” *Energy Procedia*, vol. 63, pp. 7954–7958, 2014, doi: 10.1016/j.egypro.2014.11.830.

[2] D. Moreira and J. C. M. Pires, “Atmospheric CO2 capture by algae: Negative carbon dioxide emission path,” *Bioresour. Technol.*, vol. 215, no. 2016, pp. 371–379, 2016, doi: 10.1016/j.biortech.2016.03.060.

[3] Y. Liang *et al.*, *Algal Biorefineries*. Elsevier B.V., 2015. doi: 10.1016/B978-0-444-63453-5.00002-1.

[4] A. H. Alami, S. Alasad, M. Ali, and M. Alshamsi, “Investigating algae for CO2 capture and accumulation and simultaneous production of biomass for biodiesel production,” *Sci. Total Environ.*, vol. 759, 2021, doi: 10.1016/j.scitotenv.2020.143529.

[5] K. Santhoshkumar, S. Prasanthkumar, and J. George Ray, “Biomass Productivity and Fatty Acid Composition of Chlorella lobophora V M Andreyeva, a Potential Feed Stock for Biodiesel Production,” *Am. J. Plant Sci.*, vol. 06, no. 15, pp. 2453–2460, 2015, doi: 10.4236/ajps.2015.615247.

SIDISA 2024
XII International Symposium on Environmental Engineering
Palermo, Italy, October 1 – 4, 2024

Harnessing the Power of Microalgae: Phenolic Compounds for Health, Sustainability, and Biorefinery Applications

Carmen Sica[1*], Chiara Copat[1], Claudia Favara[1], Maria Dolores Torres Perez[4], Sheyma Inoubli[3,4], Luciano Falqui[2], Gea Oliveri Conti[1], Herminia Gonzalez Dominguez[4], Ferrante Margherita[1]

(1) Department of Medical, Surgical and Advanced Technologies "G.F. Ingrassia", University of Catania, Italy.
(2) PLASTICA ALFA, S.p.A, Caltagirone, Italy
(3) Faculty of sciences of Bizerte, Carthage University, Tunisia
(4) Department of Chemical Engineering, Universidad de Vigo, Campus de Ourense

E-mail contact: carmensica@phd.unict.it
Keywords: phenolic, green, spirulina

Microalgae represent an excellent example of dualism in the field of environmental sustainability and biotechnological innovation, primarily for two reasons: their ability to fix CO_2 and their role in extracting bioactive molecules (1). The species Chlorella Vulgaris has become essential in biorefinery for applications in sectors such as biofuels, cosmetics, nutraceuticals, and pharmaceuticals, thanks to its natural properties that offer sustainable alternatives to synthetic products (2). This study is based on an experiment of green extraction of phenolic compounds, which have demonstrated significant antioxidant and anti-inflammatory properties (3).
Spirulina was cultivated in photobioreactors at the Plastica Alfa S.p.A. facility. Total phenols were quantified after freeze-drying the sample,and we are put the sample in microwave for 10 minute but a different temperature (4). Phenolic compounds were subsequently determined using the Folin-Ciocalteu method.
The results obtained it was observed that the temperature is directly proportional to the growth, in percentage, of total phenolic compounds, with a variation ranging from 5400 µg/g to 7000 µg/g.
In summary, phenolic compounds from microalgae not only provide significant health benefits but also support environmental sustainability, making them ideal for use in creating eco-friendly pharmaceutical products and supplements.

References

(1)Wright, C.Y., Godfrey, L., Armiento, G., Haywood, L.K., Inglesi-Lotz, R., Lyne, K., Schwerdtle, P.N., 2019. Circular economy and environmental health in low- and middle-income countries. Glob. Health 15, 65. https://doi.org/10.1186/s12992-019-0501-y

(2)Abdel-Daim, M.M., Farouk, S.M., Madkour, F.F., Azab, S.S., 2015. Anti-inflammatory and immunomodulatory effects of Spirulina platensis in comparison to Dunaliella salina in acetic acid-induced rat experimental colitis. Immunopharmacol. Immunotoxicol. 37, 126–139. https://doi.org/10.3109/08923973.2014.998368

(3)Machado, A.R., Silva, P.M.P., Vicente, A.A., Souza-Soares, L.A., Pinheiro, A.C., Cerqueira, M.A., 2022. Alginate Particles for Encapsulation of Phenolic Extract from Spirulina sp. LEB-18: Physicochemical Characterization and Assessment of In Vitro Gastrointestinal Behavior. Polymers 14, 4759. https://doi.org/10.3390/polym14214759

(4)Kapoore, R.V., Butler, T.O., Pandhal, J., Vaidyanathan, S., 2018. Microwave-Assisted Extraction for Microalgae: From Biofuels to Biorefinery. Biology 7, 18. https://doi.org/10.3390/biology7010018

Title: Microalgae to Biodiesel: A Leap Forward in Optimized Biomass Valorisation with Biorefinery Perspectives

Author(s): Giuseppina Oliva*[1], Antonio Buonerba[2], Vincenzo Belgiorno[1], Tiziano Zarra[1], Vincenzo Naddeo[1]

[1]*Sanitary Environmental Engineering Division (SEED), Department of Civil Engineering, University of Salerno, via Giovanni Paolo II 132, 84084 Fisciano (SA), Italy*

[2] *Department of Chemistry and Biology "Adolfo Zambelli", University of Salerno, via Giovanni Paolo II 132, 84084 Fisciano (SA), Italy*

Keyword(s): Algal biomass, Lipid extraction, Gaseous emission treatment, Integrated algal biotechnology, Bio-based fuels

Abstract

Biotechnologies are an effective platform to attain green transition objectives, especially when synergically integrated to promote health and environmental protection. In this context, microalgae-based biotechnologies are considered among the most effective tools for treating gaseous effluents and simultaneously capturing carbon sources for further biomass valorisation. A systematic comparison of two systems operated in parallel for biological carbon capture and utilization (bCCU) was implemented. The performances of a conventional photo-bioreactor (PBR) were compared to those of a similar photo-bioreactor with a submerged membrane (membrane photo-bioreactor, mPBR). A newly designed living membrane (LM) was used to promote synergistically the harvesting and cultivation phases. Lipids accumulation mechanisms were mainly attributed to the increased photons availability in mPBR. The integration of LM in mPBR enhanced biomass recovery and lipid accumulation. The cultivated biomass was treated with a newly designed method to extract lipids simultaneously transesterificated in fatty acid methyl esters (FAME) via In Situ Transesterification (IST) with a Kumagawa-type extractor. The results of this study demonstrated the potential application of the optimised method to overcome the gap to green transition. Using hexane-methanol (v/v = 19:1) mixture in the presence KOH in Kumagawa extractor lipids were extracted and converted in fatty acid methyl esters. The process showed the enhanced extraction of lipids converted in bio-sourced fuels with circular economy approach, broadening the applicability of biotechnologies as sustainable tools for energy source diversification.

Introduction

The population growth resulted in increasing environmental pressures which needs to be faced with new approaches of green technology [1]. In this context, bioeconomy has been recognized as the paramount platform to boost the transition from linear to circular economy with algal technologies among the main drivers of this change [2]. Biological Carbon Capture and Utilization (bCCU) process, promoted by microalgae, can convert carbon dioxide in valuable biomass, for retrieving food and animal feed [3], cosmetics, pigments, biofuel and bioplastics [4]. Even if bCCU technologies have been demonstrated as effective for capturing CO2, their wider application is still hindered by the high costs of the harvesting and materials recovery phases [5–7]. Cost-effective biomass harvesting is essential to channel the

cultivation stage toward enhanced downstream applications [8–11]. To meet the need of defining more sustainable solutions for promoting algal bCCU applications, the present study focuses the attention on the technological optimization of the cultivation phase using a Living Membrane Module ® (LMM), a newly designed technology patented by the SEED group. LMM is an innovative application of self-forming dynamic membrane (SFDM), in which the living membrane is progressively formed between two layers of polyester supports. The performance evaluation was implemented by comparing carbon dioxide biofixation, conversion rate in microalgae biomass, harvested biomass and lipids recovery of two identical system (PBR, mPBR) operated in parallel, which differ only for the presence of the LMM in mPBR. For further increasing the recovery potential of the investigated system, it was operated a systematic optimization of the process for lipid recovery and conversion in fatty methyl esters (FAME).The results demonstrated that the LM served as a crucial tool in promoting the economic and technical feasibility of algal bCCU for carbon sequestration and biodiesel production.

Materials and methods

Culture Collection of Algae and Protozoa (CCAP) used was Chlorella vulgaris strain CCAP 211/11B [12]. The two systems (PBR and mPBR) are operated in parallel. The experimental set-up of mPBR is reported in Figure 1. PBR and mPBR are different only in the presence of a submerged Living Membrane Module (LMM) in mPBR. The LMM was submerged in the cylindrical photo-bioreactor, with filtering area (A) of 0.02 m^2. CO_2 concentrations were daily measured day by analyzing inlet and outlet gaseous samples of both reactors with a GC equipped with a Thermal-Conductivity Detector (TCD) (TRACETM 1300 Gas Chromatograph, Thermo Fisher). Three Stages were implemented and from Stage I to Stage III the Liquid/Gas ration (L/G) was increased from 5 to 20.

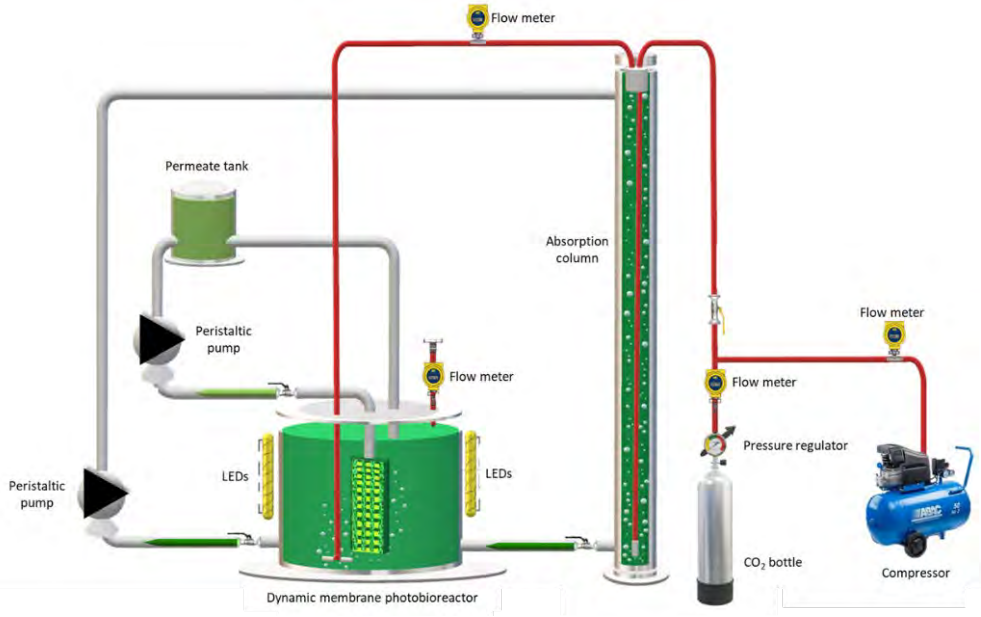

Figure 1. mPBR experimental set-up

Results

The increasing in L/G from Stage I to III enhanced the contact between gas and liquid phases and, consequently, the mass transfer rate. For this reason, it was observed an higher removal of CO2 in algal

biomass by increasing L/G ratio for both system [13]. However, the presence of LM did not determine a significant increase in CO2 removal since the two systems supported similar removal yields. The main effect of LM was indeed linked to the lipids accumulation mechanisms supported by the enhanced lights penetration and photons utilization for the generation of new algal cells. This result was confirmed by the higher consumption of nutrients recorded in mPBR, as displayed in Figure 2, along with the significant increase in terms of harvested biomass and total lipid production.

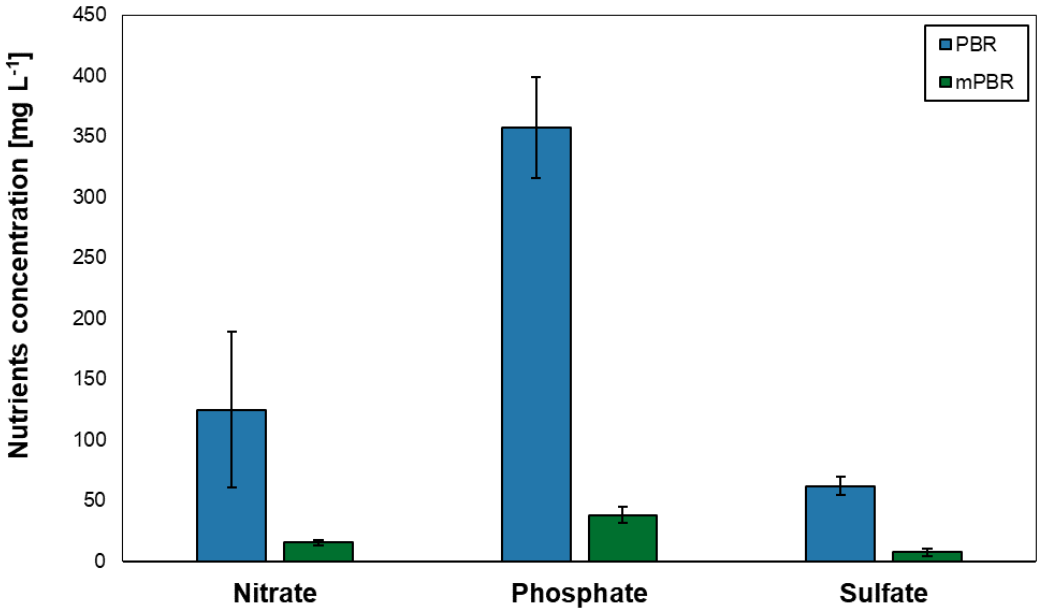

Figure 2. Nutrients concentration in PBR and mPBR

The higher lipid content in mPBR was achieved thanks to the balance between the production of new algal cells and the availability of nutrients, which allowed to implement nutrient starvation condition without negatively affecting the biomass production. The cultivated biomass was then processed with a newly designed process to extract lipids simultaneously transesterificated in fatty acid methyl esters (FAME) via In Situ Transesterification (IST) with a Kumagawa-type extractor. The produced lipids are converted in biodiesel with 96.5% of the oil transformed to esters during transesterification [14]. The quantitative formation of the FAMEs was demonstrated by analysing the extract obtained at the end of the extraction process, which revealed the characteristic signals of triglycerides and the absence of glyceride signals [15].

Conclusions

The research results have been discussed to evaluate the performances of an innovative configuration of photo-bioreactor in which was submerged a LM to synergistically implement the cultivation and harvesting of valuable algal biomass. The mPBR supported similar performances in terms of CO2 capture with a significant enhancement in terms of biomass production and lipid accumulation. The extraction of lipids has been optimised and the in-situ transesterification to fatty acid methyl esters was successfully carried out for the direct production of biodiesel. The results demonstrated the potential application of the optimised method to overcome the gap to green transition.LM can thus represent a cutting-edge tool for improving harvesting in microalgae valorisation, offering an integrated solution for algal biorefinery.

References

[1] J.V. Henderson, B.Y. Jang, A. Storeygard, D.N. Weil, Climate Change, Population Growth, and Population Pressure, SSRN Electron. J. (2024). https://doi.org/10.2139/ssrn.4731054.
[2] A.V. Shah, A. Singh, S. Sabyasachi Mohanty, V. Kumar Srivastava, S. Varjani, Organic solid waste: Biorefinery approach as a sustainable strategy in circular bioeconomy, Bioresour. Technol. 349 (2022) 126835. https://doi.org/10.1016/j.biortech.2022.126835.
[3] I. Haoujar, M. Haoujar, A. B. Altemimi, A. Essafi, F. Cacciola, Nutritional, sustainable source of aqua feed and food from microalgae: a mini review, Int. Aquat. Res. 14 (2022). https://doi.org/10.22034/iar.2022.1958713.1278.
[4] A.K. Patel, F.P.J.B. Albarico, P.K. Perumal, A.P. Vadrale, C.T. Nian, H.T.B. Chau, C. Anwar, H.M. ud din Wani, A. Pal, R. Saini, L.H. Ha, B. Senthilkumar, Y.-S. Tsang, C.-W. Chen, C.-D. Dong, R.R. Singhania, Algae as an emerging source of bioactive pigments, Bioresour. Technol. 351 (2022) 126910. https://doi.org/10.1016/j.biortech.2022.126910.
[5] A. Pandey, V.V. Pathak, R. Kothari, P.N. Black, V.V. Tyagi, Experimental studies on zeta potential of flocculants for harvesting of algae, J. Environ. Manage. 231 (2019) 562–569. https://doi.org/10.1016/j.jenvman.2018.09.096.
[6] G. Oliva, R.R. Pahunang, G. Vigliotta, T. Zarra, F.C. Ballesteros, A. Mariniello, A. Buonerba, V. Belgiorno, V. Naddeo, Advanced treatment of toluene emissions with a cutting-edge algal bacterial photo-bioreactor: Performance assessment in a circular economy perspective, Sci. Total Environ. 878 (2023) 163005. https://doi.org/10.1016/j.scitotenv.2023.163005.
[7] G. Oliva, M.G. Galang, A. Buonerba, S.W. Hasan, V. Belgiorno, V. Naddeo, T. Zarra, Carbon capture and utilization in waste to energy approach by leading-edge algal photo-bioreactors: The influence of the illumination wavelength, Case Stud. Chem. Environ. Eng. 7 (2023) 100348. https://doi.org/10.1016/j.cscee.2023.100348.
[8] V. Ananthi, P. Balaji, R. Sindhu, S.-H. Kim, A. Pugazhendhi, A. Arun, A critical review on different harvesting techniques for algal based biodiesel production, Sci. Total Environ. 780 (2021) 146467. https://doi.org/10.1016/j.scitotenv.2021.146467.
[9] A. Khanra, S. Vasistha, M.P. Rai, W.Y. Cheah, K.S. Khoo, K.W. Chew, L.F. Chuah, P.L. Show, Green bioprocessing and applications of microalgae-derived biopolymers as a renewable feedstock: Circular bioeconomy approach, Environ. Technol. Innov. 28 (2022) 102872. https://doi.org/10.1016/j.eti.2022.102872.
[10] V. Senatore, G. Oliva, A. Buonerba, T. Zarra, L. Borea, S.W. Hasan, V. Belgiorno, V. Naddeo, An integrated algal membrane photobioreactor as a green-transition technology for the carbon capture and utilization, J. Environ. Chem. Eng. 10 (2022) 107344. https://doi.org/10.1016/j.jece.2022.107344.
[11] V. Senatore, A. Buonerba, T. Zarra, G. Oliva, V. Belgiorno, J. Boguniewicz-Zablocka, V. Naddeo, Innovative membrane photobioreactor for sustainable CO2 capture and utilization, Chemosphere 273 (2021) 129682. https://doi.org/10.1016/j.chemosphere.2021.129682.
[12] F. Pasquarelli, G. Oliva, A. Mariniello, A. Buonerba, C.-W. Li, V. Belgiorno, V. Naddeo, T. Zarra, Carbon neutrality in wastewater treatment plants: An integrated biotechnological-based solution for nutrients recovery, odour abatement and CO2 conversion in alternative energy drivers, Chemosphere 354 (2024) 141700. https://doi.org/10.1016/j.chemosphere.2024.141700.
[13] Q. Fu, H.-X. Chang, Y. Huang, Q. Liao, X. Zhu, A. Xia, Y.-H. Sun, A novel self-adaptive microalgae photobioreactor using anion exchange membranes for continuous supply of nutrients, Bioresour. Technol. 214 (2016) 629–636. https://doi.org/10.1016/j.biortech.2016.04.081.
[14] V. Makareviciene, E. Sendzikiene, M. Gumbyte, Application of Simultaneous Oil Extraction and Transesterification in Biodiesel Fuel Synthesis: A Review, Energies 13 (2020) 2204. https://doi.org/10.3390/en13092204.
[15] G. Oliva, A. Buonerba, A. Grassi, S.W. Hasan, G.V. Korshin, A.A. Zorpas, V. Belgiorno, V. Naddeo, T. Zarra, Microalgae to biodiesel: A novel green conversion method for high-quality lipids recovery and in-situ transesterification to fatty acid methyl esters, J. Environ. Manage. 357 (2024) 120830. https://doi.org/10.1016/j.jenvman.2024.120830.

PARALLEL SESSION: A6

Wastewater treatment

Physical-chemical treatments

Continuous bioelectrochemical treatment of nitrate-containing wastewater in a double-chamber bioelectrochemical system

Anna Lanzetta*[1], Reka Hajdu-Rahkama[2], Francesco Di Capua[3], Marika Kokko[2], Giovanni Esposito[1], Francesco Pirozzi[1] and Stefano Papirio[1]

[1] *Department of Civil, Architectural and Environmental Engineering, University of Naples Federico II, Via Claudio 21, 80125 Naples, Italy*
[2] *Tampere University, Faculty of Engineering and Natural Sciences, PO Box 589, FI-33014 Tampere, Finland*
[3] *School of Engineering, University of Basilicata, via dell'Ateneo Lucano 10, 85100 Potenza, Italy*

Keyword(s): bioelectrochemical system, nitrate; wastewater, heterotrophic and autotrophic denitrification.

Abstract

Nitrate (NO_3^-) is one of the most common water pollutants in the world, leading to eutrophication of surface waters, increased risk of nitrate/nitrite-related diseases even at low concentrations (>10 $mg \cdot L^{-1}$), and disruption of aquatic ecosystems threatening biodiversity [1]. Anthropogenic activities such as the intensive use of agricultural fertilizers and nitrogen-based chemicals in chemical, pharmaceutical, food processing, and petroleum refining industries are the major sources of NO_3^- pollution in aquatic environments [2]. Currently, to reduce the impact of NO_3^- contamination on drinking water quality and human health, the EU regulation (Directive 2020/2184) and the World Health Organization (WHO) set the acceptable threshold of nitrate concentration in groundwater at 50 mg $NO_3^- \cdot L^{-1}$ as nitrate [3]. Recently, NO_3^- removal has also been accomplished in denitrifying bioelectrochemical systems (BESs) [4] through autotrophic or heterotrophic denitrification or with both simultaneously [5]. In BES, electrons and protons are generated at the anode, for example, by the degradation of organic substrates, and are then transferred to the cathode via an external circuit containing a power supply and an ion exchange membrane, respectively [6]. At the cathode, reduction reactions take place, which may include the H_2 evolution reaction [7] or direct electron transfer by microorganisms capable of transferring metabolic electrons through the cell envelope to extracellular electron acceptors [8]. In addition, recent studies have focused on the development of BESs as an alternative to conventional wastewater treatment [9] or their integration into wastewater and sludge treatment [10]. Combining BES with existing technologies could not only reduce the overall costs but also improve the efficiency of wastewater treatment and the reliability of the combined system [11]. For this purpose, this study aimed to investigate the potential use of BES as an integrated treatment to improve the removal of residual NO_3^- deriving from a previous biological treatment consisting of simultaneous carbon and nitrogen removal in a continuous-upflow (micro)aerobic granular sludge blanket reactor (UAGSB) [12].
The experiments were carried out in two-chamber flow-through BES reactor, reactor 1 (R1), consisting of anode and cathode chambers (33 mL each) hydraulically connected to each other and separated by a cation-exchange membrane (CEM, CMI-7000, Membranes International, USA). Both the anode and cathode chambers were filled using graphite granules (EC-100, Graphite Sales, USA) as electrodes and biofilm carriers. Graphite rods (l=75 mm, d=6 mm, 99.995% trace metals basis, Sigma-Aldrich) were then inserted into each anodic and cathodic chamber as current collectors. A potentiostat (BioLogic VMP3, France) was used to maintain the cathode potential at −0.650 V vs. standard hydrogen electrode (SHE). Prior to the experiments, the anode and cathode electrodes were separately enriched for electroactive microorganisms responsible for CH_3COOH oxidation and autotrophic denitrification,

respectively.
R1 was operated in continuous mode for 63 days divided into 7 experimental periods as reported in **Table 1**, using a cathode potential of -650 mV vs. an Ag/AgCl reference electrode. A synthetic wastewater containing (mg·L^{-1}) KNO_3 (217), NH_4Cl (6), KH_2PO_4 (25), $NaHCO_3$ (95.4), $NaNO_2$ (5), CH_3COONa (150), and TES [13] was used as feed to reactor to mimic the UAGSB reactor effluent characterized by a N-NO_3^- concentration of 31.1 ± 4.1 mg N·L^{-1} [12]. In addition, 1 g·L^{-1} BESA was added to the influent solution to R1 to inhibit the growth of methanogens [14].

Table 1. Operating conditions and duration of each experimental period during the continuous operation of the two-chamber flow-through bioelectrochemical system (Reactor 1 (R1))

Period	Duration (days)	Feeding	Potential (mV)
I	0-9	Anode	-650 at the cathode
II	10-15	Anode	-650 at the cathode
III	16-22	Cathode	-650 at the cathode
IV	23-36	Cathode	-650 at the cathode
V	37-46	Cathode	-650 at the cathode
VI	47-58	Cathode	-650 at the cathode
VII	59-63	Cathode	No current

The temporal profiles of N-NO_3^-, N-NO_2^- and CH_3COOH concentrations in the influent and effluent of anode and cathode during the continuous operation of R1 in **Fig. 1**. Anodic feeding during periods I and II resulted in average NOx and CH_3COOH removal efficiencies at the anode of 99 ± 2 and 98 ± 4 %. These results indicate that heterotrophic denitrification with acetate as the electron donor occurred. The average influent CH_3COOH concentration in these periods was equal to 116 ± 30 mg·L^{-1}. Considering the stoichiometry of the denitrification reaction using CH_3COOH as an electron donor [15], the estimated effluent Nox removed by heterotrophic denitrification ($Nox_{Rem,het}$) at the anode accounted for 100% in period I and for 83% in period II. However, when the anode effluent was further fed to the cathode chamber, a significant cathodic production of CH_3COOH occurred during periods I and II (p<0.05), being 75 ± 55 mg·L^{-1}(**Fig. 1**), which could indicate the presence of homoacetogenic bacteria in the cathode biofilm. The reversal of influent feed resulted in a stable (p>0.05) Nox removal efficiency of 100 ± 0 %. In R1, an average cathodic N-NO_2^- accumulation of 0.5 ± 0.4 mg N·L^{-1} was observed, which was then followed by complete denitrification at the anode. Additionally, a CH_3COOH removal efficiency of 100 ± 0 % was achieved at the cathode with no acetate production at the anode. The estimated $Nox_{Rem,het}$ accounted for 90 %.
In period IV, the HRT was further reduced to 4 h. This resulted in effluent Nox and CH_3COOH removal efficiencies of 100 ± 1 and 100 ± 0 %. Additionally, the percentage of $Nox_{Rem,het}$ reached 100 %. An HRT reduction to 2 h (period V) had little impact on the effluent Nox and CH_3COOH removal efficiencies, which were 96 ± 11 % and 100 ± 0 % in R1. Also, an average N-NO_2^- accumulation of 1.3 ± 0.6 mg N·L^{-1} occurred at the cathodes of R1. However, after biomass acclimation (day 37-43), the average effluent N-NO_2^- concentration was below the Italian standard (D. Lgs. 152/2006, Annex V, Part III) for industrial wastewater discharge into sewers (0.6 mg N-NO_2^-·L^{-1}). In Period VI, the share of autotrophic denitrification on NO_3^- removal was evaluated by eliminating the CH_3COOH in the influent. Only relying on the electron donors provided by the electrode at an HRT of 2 h resulted in Nox removal efficiencies of 65 ± 16 %. Nevertheless, after biomass acclimation (day 48-54) the effluent N-NO_3^- and N-NO_2^-

concentrations never exceeded the Italian standard (D. Lgs. 152/2006, Annex V, Part III) for the release of industrial wastewater into sewers (30 mg $N\text{-}NO_3^-\cdot L^{-1}$ and 0.6 mg $N\text{-}NO_2^-\cdot L^{-1}$). Period VII, on the other hand, was designed to study the effect of heterotrophic denitrification alone at open circuit conditions by feeding CH_3COOH with the influent medium and providing no cathodic potential. Although a high effluent NOx removal efficiency of 96 ± 1 % was achieved, a slight increase in $N\text{-}NO_2^-$ concentration of 1.3 ± 0.2 mg $N\cdot L^{-1}$ was observed in the effluent. The results indicate that both autotrophic and heterotrophic denitrification occurred in the system. Therefore, given the considerable variability in organic matter concentration in wastewater, integrating autotrophic and heterotrophic denitrification within the same system could ensure consistently high removal efficiencies. Additionally, a specific energy consumption of $1.8\cdot10^{-6}$ kWh·g $N_{removed}^{-1}$ was reported at an HRT of 2 h, demonstrating the feasibility of the method.

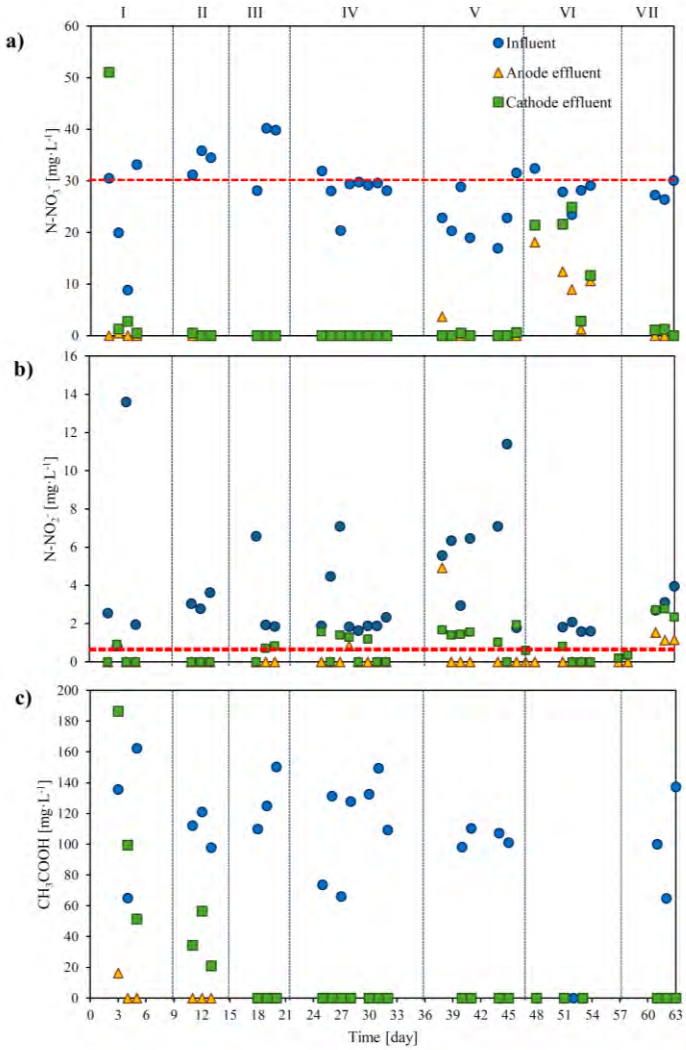

Figure 1. Temporal trends $N\text{-}NO_3^-$, $N\text{-}NO_2^-$, and CH_3COOH concentrations ($mg\cdot L^{-1}$) measured in the influent and in the anode and cathode effluent during the study in R1. The red line indicates the Italian standard for industrial effluent discharge to sewers.

References

[1] X. Zou, J. Xie, C. Wang, G. Jiang, K. Tang, C. Chen, Electrochemical nitrate reduction to produce ammonia integrated into wastewater treatment: Investigations and challenges, Chinese Chem. Lett. 34 (2023) 107908. https://doi.org/10.1016/j.cclet.2022.107908.
[2] F. Ortmeyer, B. Hansen, A. Banning, Groundwater nitrate problem and countermeasures in strongly affected EU countries—a comparison between Germany, Denmark and Ireland, Grundwasser. 28 (2023) 3–22. https://doi.org/10.1007/s00767-022-00530-5.
[3] B.H. Jacobsen, B. Hansen, J. Schullehner, Health-economic valuation of lowering nitrate standards in drinking water related to colorectal cancer in Denmark, Sci. Total Environ. 906 (2024). https://doi.org/10.1016/j.scitotenv.2023.167368.
[4] S.S. Gadegaonkar, Ü. Mander, M. Espenberg, A state-of-the-art review and guidelines for enhancing nitrate removal in bio-electrochemical systems (BES), J. Water Process Eng. 53 (2023). https://doi.org/10.1016/j.jwpe.2023.103788.
[5] D. Cecconet, S. Zou, A.G. Capodaglio, Z. He, Evaluation of energy consumption of treating nitrate-contaminated groundwater by bioelectrochemical systems, Sci. Total Environ. 636 (2018) 881–890. https://doi.org/10.1016/j.scitotenv.2018.04.336.
[6] W.T. Mook, M.K.T. Aroua, M.H. Chakrabarti, I.M. Noor, M.F. Irfan, C.T.J. Low, A review on the effect of bio-electrodes on denitrification and organic matter removal processes in bio-electrochemical systems, J. Ind. Eng. Chem. 19 (2013) 1–13. https://doi.org/10.1016/j.jiec.2012.07.004.
[7] A.W. Jeremiasse, H.V.M. Hamelers, C.J.N. Buisman, Microbial electrolysis cell with a microbial biocathode, Bioelectrochemistry. 78 (2010) 39–43. https://doi.org/10.1016/j.bioelechem.2009.05.005.
[8] M. Rosenbaum, F. Aulenta, M. Villano, L.T. Angenent, Cathodes as electron donors for microbial metabolism: Which extracellular electron transfer mechanisms are involved?, Bioresour. Technol. 102 (2011) 324–333. https://doi.org/10.1016/j.biortech.2010.07.008.
[9] L. Gil-Carrera, A. Escapa, P. Mehta, G. Santoyo, S.R. Guiot, A. Morán, B. Tartakovsky, Microbial electrolysis cell scale-up for combined wastewater treatment and hydrogen production, Bioresour. Technol. 130 (2013) 584–591. https://doi.org/10.1016/j.biortech.2012.12.062.
[10] U. Schröder, Bioelectrochemical Systems, 2023. https://doi.org/10.1039/bk9781849739757-00347.
[11] M.M. Ghangrekar, S. Das, B.R. Tiwari, Integration of bioelectrochemical systems with other existing wastewater treatment processes, INC, 2020. https://doi.org/10.1016/B978-0-12-817493-7.00011-4.
[12] A. Lanzetta, F. Di Capua, B. Panneerselvam, D. Mattioli, G. Esposito, S. Papirio, Impact of Influent Composition and Operating Conditions on Carbon and Nitrogen Removal from Urban Wastewater in a Blanket Reactor, (2023).
[13] K. Rabaey, W. Ossieur, M. Verhaege, W. Verstraete, Continuous microbial fuel cells convert carbohydrates to electricity, Water Sci. Technol. 52 (2005) 515–523. https://doi.org/10.2166/wst.2005.0561.
[14] P. Chatterjee, P. Dessì, M. Kokko, A.M. Lakaniemi, P. Lens, Selective enrichment of biocatalysts for bioelectrochemical systems: A critical review, Renew. Sustain. Energy Rev. 109 (2019) 10–23. https://doi.org/10.1016/j.rser.2019.04.012.
[15] F. Di Capua, F. Pirozzi, P.N.L. Lens, G. Esposito, Electron donors for autotrophic denitrification, Chem. Eng. J. 362 (2019) 922–937. https://doi.org/10.1016/j.cej.2019.01.069.

Title: Treatment of hospital effluents polluted with the cytotoxic carboplatin by electrochemical oxidation

Author(s): Ana Hayat*, Julio Ortiz-Montes, Jose L. da Silva Duarte, Carmen M. Domínguez, Aurora Santos, Salvador Cotillas

Department of Chemical and Materials Engineering, Complutense University of Madrid, Spain, anahayat@ucm.es

Keyword(s): carboplatin, electrochemical oxidation, diamond, hospital effluents

Abstract

In recent years, the presence of pharmaceuticals in aqueous effluents has increased, mainly due to the massive consumption of medicines by the human population. These drugs enter waterways via urine and/or faeces, either in their metabolized form or unchanged. Conventional water treatment systems in wastewater treatment plants struggle to remove these contaminants, leading to their uncontrolled release into the environment [1]. Additionally, the absence of specific regulations regarding the proper disposal of pharmaceuticals and the inappropriate disposal of expired medicines further exacerbates the prevalence of these pollutants in water, posing challenges to public health and aquatic ecosystems [2].

According to the World Health Organization (WHO), antibiotics in wastewater pose a significant threat to human, animal, plant, and environmental health as they contribute to the development of multi-resistant bacteria, often called the silent pandemic. Effluents generated in hospital facilities pose a particular risk because high doses of antibiotics are administered to hospitalized patients. However, other drugs, such as antineoplastics (cytostatic and cytotoxic) used to combat cancer cells, are also found in significant concentrations in these effluents. Such compounds significantly disrupt ecosystems due to their toxicity and low biodegradability. One of the most widely used antineoplastic drugs, carboplatin (CPT) ($C_6H_{12}N_2O_4Pt$), is the most nephrotoxic antineoplastic drug, directly impacting renal function. Hence, it is imperative to eliminate it from hospital effluents before they reach wastewater treatment plants to mitigate its hazardous effects.

Advanced Oxidation Processes (AOPs) present a promising alternative for treating wastewater from hospital facilities. These processes have demonstrated high efficiency in removing recalcitrant organic compounds by generating reactive species with potent oxidation capabilities. Compared to conventional treatment methods, AOPs offer several advantages, including reduced sludge generation, improved organoleptic characteristics of treated effluents, and generation of innocuous compounds during the process. These characteristics render AOPs particularly effective in various applications, such as converting refractory pollutants into biodegradable ones or treating contaminants at very low concentrations (as in the case of pharmaceuticals).

Among the most commonly used AOPs for eliminating organic compounds in aqueous effluents, electrochemical oxidation stands out for its ability to achieve high degradation efficiencies without requiring the addition of any reagents to the water, thereby preserving its original physicochemical

properties. This process involves the in-situ generation of reactive species, primarily hydroxyl radicals, through the electrolysis of water and naturally present ions in the treated effluents. The composition of the effluent and the anode material determine the types of oxidizing species produced, which may include hypochlorite or persulfate, formed from the oxidation of chloride and sulphate, respectively, thereby contributing to the efficiency of the degradation process.

With this background, this work focuses on removing carboplatin from synthetic hospital effluents by electrochemical oxidation. This process generates reactive species in situ from the electrolysis of water and the ions naturally contained in the effluents, which attack the pollutants until they are eliminated. The nature and concentration of reactive species depend mainly on the electrode material used and the applied current density. Boron-Doped Diamond (BDD) and Mixed Metal Oxides (MMO) were used as anode materials. The efficiencies obtained with both electrodes in the degradation of the target cytostatic drug were compared. The electrocatalytic properties of BDD anodes favour the generation of hydroxyl radicals and other oxidants, such as peroxocompounds, whereas MMO electrodes promote chlorine evolution [3].

The impact of electrolyte composition on CPT removal was initially investigated to assess the technical feasibility of the proposed technology. This preliminary study allows an initial understanding of how the nature of the ions present in the effluent can influence the generation of oxidants and, consequently, the degradation mechanism of the pollutant. Subsequently, CPT degradation was carried out in synthetic hospital wastewater to evaluate the efficiency of the process in a complex matrix that simulates actual effluent conditions. Figure 1 shows the conversion of CPT during the electrochemical oxidation of synthetic effluents polluted with 5 mg dm^{-3} CPT at a current density of 10 mA cm^{-2} using BDD anodes. The concentration of the electrolyte used was 1 g dm^{-3}.

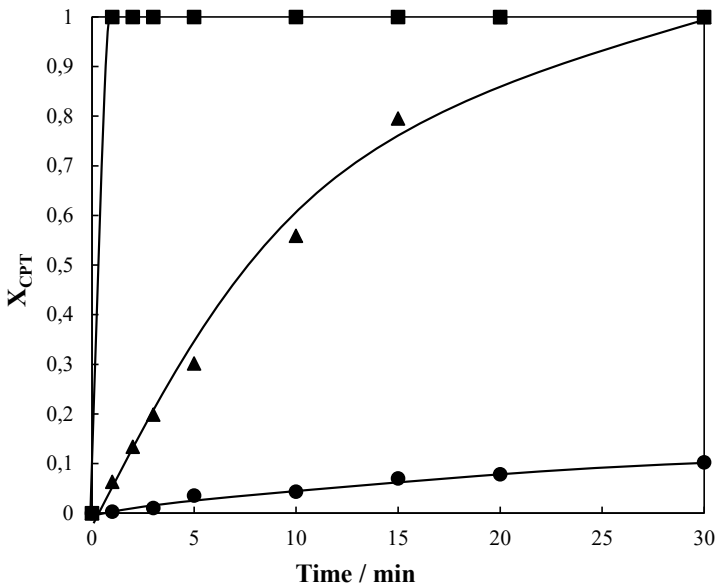

Figure 1. Effect of supporting electrolyte on carboplatin conversion during electrochemical oxidation in (■)1 g dm^{-3} NaCl; (▲) 1 g dm^{-3} Na_2SO_4; (●) 1 g dm^{-3} $HClO_4$; $[CPT]_0$: 5 mg dm^{-3}; anode: BDD; cathode: Stainless steel; j:10 mA cm^{-2}.

When working in a chloride media as an electrolyte, chlorine-based oxidants are expected to be generated. In contrast, peroxodisulfate is produced mainly as the primary electrogenerated oxidant in a sulphate media. Perchloric acid promotes direct oxidation mechanisms since only water can be oxidized to produce hydroxyl radicals (no anion can be oxidized to generate reactive species). As can be seen, the CPT conversion increases with the operating time regardless of the electrolyte used. However, the pollutant conversion occurs most rapidly in the chloride media, reaching complete elimination within one minute of the reaction, followed by the sulphate media and then the perchloric acid media. These results reveal that the nature of the electrogenerated oxidants significantly influences the conversion of carboplatin by electrochemical oxidation, with chlorinated species being the most effective in eliminating this type of drug.

After assessing the efficiency of the electrochemical oxidation process to degrade CPT in simple aqueous matrixes (sulphate, chloride and perchloric media), the degradation of this pollutant in synthetic hospital wastewater was investigated. Figure 2 shows the conversion of CPT with the operating time during the electrochemical oxidation of synthetic hospital effluents using BDD anodes at current densities ranging from 5 to 50 mA cm^{-2}. These low current densities were chosen to promote a selective oxidation process and minimize the degree of mineralization in the treated effluents.

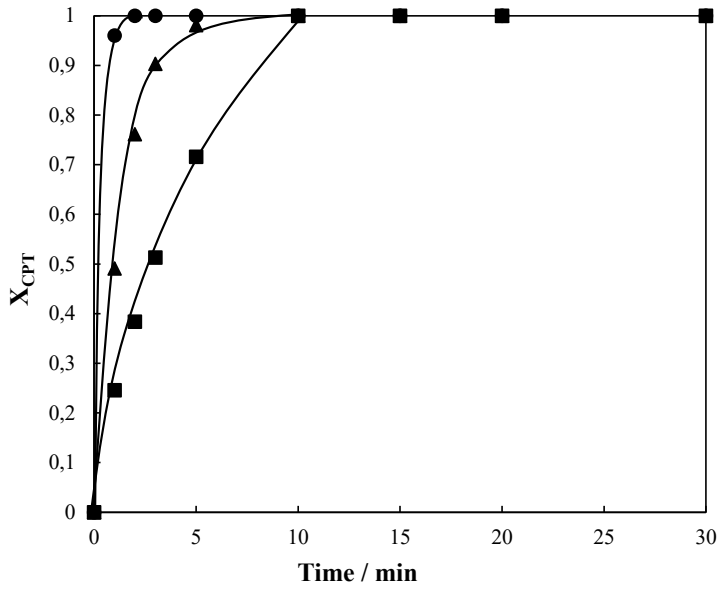

Figure 2. Evolution of carboplatin conversion with the operation time during electrochemical oxidation of synthetic hospital wastewater. (■) 5 mA cm^{-2}; (▲) 10 mA cm^{-2}; (●) 50 mA cm^{-2}; $[CPT]_0$: 5 mg dm^{-3}; anode: BDD; cathode: SS.

The CPT conversion increases with the operating time until complete contaminant removal is achieved, regardless of the current density applied. However, the time required to accomplish this complete conversion varies depending on the current density used. Specifically, 100 % conversion is achieved in 10 minutes when a current density of 5 mA cm^{-2} is applied, while this operating time is reduced to 6 and 3 minutes when the current density is increased to 10 and 50 mA cm^{-2}, respectively. Increasing the current density leads to a higher concentration of oxidants and, therefore, to a higher CPT removal rate in hospital wastewater. These results demonstrate the feasibility of electrochemical oxidation to remove

CPT (5 mg dm^{-3}) from hospital effluents using low current densities, which involves moderate energy consumption. CPT conversion is increased in synthetic hospital wastewater compared to the results obtained with pure electrolytes. This finding indicates that small concentrations of oxidants of different natures (oxidants cocktail) favour the removal of the pollutant.

Acknowledgements

The authors gratefully acknowledge the financial support through the grant CNS2022-135764 funded by MICIU/AEI/10.13039/501100011033 and by "European Union NextGenerationEU/PRTR". Ana Hayat acknowledges the CT19/23-INVM-44 grant funded by the INVESTIGO program of the Spanish Ministry of Labor and Social Economy. Jose L. da Silva Duarte also acknowledges the funding received through the Marie Skłodowska-Curie grant nº. 847635 from the H2020 program (UNA4CAREER) and the grant 2023-T1/ECO-29390 from the "Atracción de Talento César Nombela" program of the Community of Madrid.

References

[1] Jelic, A., Gros, M., Ginebreda, A., Cespedes-Sánchez, R., Ventura, F., Petrovic, M., & Barcelo, D.,"Occurrence, partition and removal of pharmaceuticals in sewage water and sludge during wastewater treatment", Water Research, 45(3), 1165-1176, (2011).
[2] Fekadu, S., Alemayehu, E., Dewil, R., & Van der Bruggen, B., "Pharmaceuticals in freshwater aquatic environments: A comparison of the African and European challenge", Science of the Total Environment, 654, 324-337, (2019).
[3] Cotillas, S., Lacasa, E., Herraiz, M., Sáez, C., Cañizares, P., & Rodrigo, M. A., "The Role of the Anode Material in Selective Penicillin G Oxidation in Urine". ChemElectroChem, 6(5), 1376-1384, (2019).

Title: Enhancing Winery Wastewater Treatment: The Synergistic Approach of Hydrodynamic Cavitation and the Fenton Process

Author(s): Karima Ayedi*[1], Nicolò Maria Ippolito[1], Valentina Innocenzi[1], Giuseppe Mazziotti di Celso[2] and Marina Prisciandaro[1]

[1] Department of Industrial and Information Engineering and Economics, University of L'Aquila, Piazzale Ernesto Pontieri 1, Monteluco di Roio, 67040, L'Aquila, Italy
[2] Faculty of Bioscience and Agro-food and Environmental Technology, University of Teramo, Via R. Balzarini 1, 64100 Teramo, Italy

Keyword(s): Hydrodynamic cavitation, winery wastewater treatment, Fenton process, Advanced oxidation process

Abstract

Among the leading sectors of the food industry is wine production. The wine industry produces a large amount of wastewater characterized by high strength in terms of organic pollution and large variability throughout the year. Wineries vary in size and winemaking processes, resulting in different amounts and quality of wastewater generated throughout the vinification process. Winery wastewaters include high COD, TSS, low pH, and fluctuating salinity and nutrient levels, posing an environmental risk [3,4] Most of the organic matter is soluble and quickly biodegradable. On the other hand, nitrogen and phosphorous are lacking. In some cases, biological processes alone fail to reduce the concentration of organics; for this reason, wastewater is often treated by advanced oxidation processes such as Fenton or, even more innovative, the hydrodynamic cavitation process (HC) [5,6]. In this paper, the preliminary results of the treatment of winery wastewater have been presented. The effluent has been treated by Fenton and HC to degrade the organic substances and reduce the COD values.

Introduction

The detection and analysis of common winery wastewater pollutants, as detailed in the literature, encompass a range of parameters crucial for assessing water quality. Among these parameters are Chemical Oxygen Demand (COD), Biochemical Oxygen Demand (BOD), Total Solids, Total Volatile Solids, Suspended Solids, pH, Total Nitrogen, Phosphorus, Potassium, and Sodium. COD, measured in milligrams per liter (mg/L), is indicative of the oxygen equivalent of organic materials present in the wastewater. For instance, the reported range for COD spans from 340 mg/L to 130,000 mg/L, reflecting varying levels of organic pollutants across different studies [7]. BOD also measured in mg/L, quantifies the oxygen consumption by microorganisms during the decomposition of organic matter in liquid

streams. The observed BOD values range from 125 mg/L to 8,024 mg/L, indicating the extent of organic material decomposition and microbial activity in the wastewater samples [4,8].

The Fenton process, a widely used technique in wastewater treatment, involves the combination of Fe2+ salts and hydrogen peroxide (H_2O_2), resulting in the generation of hydroxyl radicals. This process is valued for its ability to efficiently oxidize organic compounds, as illustrated by the chemical equations below:

$Fe^{2+} + H_2O_2 \rightarrow Fe^{3+} + OH^- + OH^{\cdot}$ (Equation 1)

$Fe^{3+} + H_2O_2 \rightarrow Fe^{2+} + HOO^{\cdot} + H^+$ (Equation 2)

The efficiency of the Fenton process hinges on the formation of potent hydroxyl radicals ($OH^{\cdot}$) and the oxidation of $Fe2^+$ to $Fe3^+$. Given that both ions act as coagulants, the Fenton process may exhibit a synergistic effect, combining oxidation and coagulation [9].

Materials and Methods

The effluent utilized in experimental activities was provided by a winery industry located in Teramo district (Abruzzo region, Italy). The research aimed to investigate the efficiency of the oxidation process of Fenton and hydrodynamic cavitation for the treatment of winery effluents. The Fenton operation was conducted under the following conditions: at room temperature and pH 3.5, utilizing 40 mL reactors agitated in an orbital shaker at 160 rpm. At first, the pH of the effluent was adjusted to 3 using a sulfuric acid solution. Specific dose of iron ($FeSO_4.7H_2O$) and H_2O_2 were added for the reactions. After an hour, sodium hydroxide was introduced to complete the process, facilitating the precipitation of iron hydroxides and the depletion of residual H_2O_2. Experiments were carried out at hydrogen peroxide concentrations ranging from 0.08 to 0.4 M. In addition to the Fenton process, combined treatment of Fenton and hydrodynamic cavitation has been studied.

Results

The TOC and COD analysers were used to determine total organic carbon (TOC) and chemical oxygen demand (COD). The chemicals utilized in the COD and TOC analyses were test cuvettes (LCK114 and LCK381, respectively). Total solids (TSS) have been determined by drying the effluent sample in an oven at 104 degrees Celsius (UF160) for 24 hours.
The cuvette-based spectrophotometric methods for detecting ammonium and nitrate chloride in real textile wastewater were evaluated. The methods detect wavelengths ranging from 340 to 900 nm in ready-to-use cuvettes (bar-coded reagent cuvettes). The results obtained are reported in Table 1shows the characteristics of the effluent. The most likely pollutants in the effluent are chlorinated compounds, Nitrogen, and sulfates.

.

Table 1: Characteristics of effluent.

Parameter	Range	Unit
pH	7	-

color	__	Abs
Total suspended solids ()	_-	mg/L
Chemical oxygen demand	1200	mg/L
Total Organic carbon TOC	42.4	mg/L
Biochemical oxygen demand	428.22	mg/L
Phenols	1	mg/L
Ammonium	0.15	mg/L
Chloride	12.9	mg/L
Nitrate	1.29	mg/L
Sulfates	36.7	mg/L
Total Nitrogen	5.46	mg/L

The study showed that a combination of Fenton's reagents used along with a subsequent addition of lime resulted in a significant 72% decrease in COD and 99%. Figure 1 shows how H_2O_2 concentration influences COD and phenols removal rates. Increasing H_2O_2 concentration had a positive impact on COD and phenols breakdown. COD is eliminated mostly at the start of the process. A similar pattern can be observed in phenol elimination. The amount of H_2O_2 used directly influences oxidation and, consequently, the removal of COD rates.

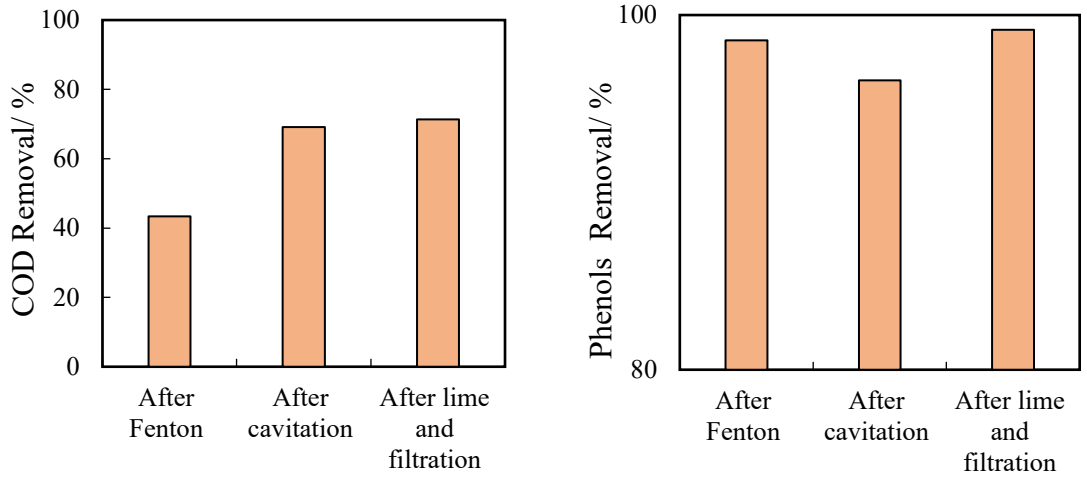

Figure 1. Extent of COD and Phenols reduction obtained for different approaches.

Acknowledgements

This research is part of the HYDROCAVI-TECH project “Sustainable Management strategies of liquid waste for transition to circular economy through hydrodynamic cavitation technology” funded by Italian Ministry for Universities and Research (MIUR), within PRIN 2022 (Research Projects of National Interest) Program.

References

[1] AHMADI, Leila et MERKLEY, Gary P. Wastewater reuse potential for irrigated agriculture. *Irrigation Science*, 2017, vol. 35, p. 275-285.
[2] DEVESA-REY, R., VECINO, X., VARELA-ALENDE, J. L., *et al.* Valorization of winery waste vs. the costs of not recycling. *Waste management*, 2011, vol. 31, no 11, p. 2327-2335.
[3] MOSSE, K. P. M., PATTI, A. F., CHRISTEN, Evan W., *et al.* Winery wastewater quality and treatment options in Australia. *Australian Journal of Grape and Wine Research*, 2011, vol. 17, no 2, p. 111-122).
[4] ILOMS, Eunice, OLOLADE, Olusola O., OGOLA, Henry JO, *et al.* Investigating industrial effluent impact on municipal wastewater treatment plant in Vaal, South Africa. *International journal of environmental research and public health*, 2020, vol. 17, no 3, p. 1096
[5]AYEDI, Karima, INNOCENZI, Valentina, et PRISCIANDARO, Marina. Application of hybrid oxidative processes based on cavitation for the treatment of methyl blue solutions. *Sustainable Water Resources Management*, 2024, vol. 10, no 2, p. 92.
[6]AYEDI, Karima, INNOCENZI, Valentina, et PRISCIANDARO, Marina. Combined Hydrodynamic Cavitation-based Processes as an Efficient Treatment Approach for Real Textile Industrial Wastewater. *Chemical Engineering Transactions*, 2023, vol. 100, p. 181-186.
[7] BUELOW, Maya C., STEENWERTH, Kerri, SILVA, Lucas CR, *et al.* Characterization of winery wastewater for reuse in California. *American Journal of Enology and Viticulture*, 2015, vol. 66, no 3, p. 302-310.
[8] HOWELL, C. L., MYBURGH, P. A., LATEGAN, E. L., *et al.* Seasonal variation in composition of winery wastewater in the breede River Valley with respect to classical water quality parameters. *South African Journal of Enology and Viticulture*, 2016, vol. 37, no 1, p. 31-38.
[9] IPPOLITO, N. M., ZUEVA, S. B., FERELLA, F., *et al.* Treatment of waste water from a winery with an advanced oxidation process (AOP). In : *IOP Conference Series: Earth and Environmental Science*. IOP Publishing, 2021. p. 062025

Title: Advanced oxidation of organic contaminants in water by persulfate and peroxymonosulfate activated with ZVI bimetals

Author(s): Giovanni Scaggiante[*1], Alicia Checa-Fernández[2], Daniela Zingaretti[1], Carmen Maria Dominguez[2], Aurora Santos[2], Renato Baciocchi[1]

[1] *Laboratorio di Ingegneria Sanitaria Ambientale, Dipartimento di Ingegneria Civile e Ingegneria Informatica, Università degli Studi di Roma "Tor Vergata", Via del Politecnico 1, 00133, Roma, Italia*
[2] *Dipartimento di Ingegneria Chimica e dei materiali, Facoltà di scienze chimiche, Università Complutense di Madrid, Ciudad Universitaria S/N. 28040, Madrid, Spagna*

scaggiante@ing.uniroma2.it

Keyword(s): advanced oxidation processes, persulfate, peroxymonosulfate, zero-valent iron, bimetallic particles

Abstract

Advanced oxidation processes (AOPs) demonstrated to be effective technologies for treating recalcitrant organic compounds from water, including emerging contaminants [1–3]. In this context, persulfate (PS) and peroxymonosulfate (PMS) are recognized as advanced oxidants because of their capacity to generate highly reactive species, such as sulfate radicals ($SO_4^{\bullet-}$), when activated [3,4]. Compared to hydroxyl radicals ($OH^{\bullet}$) that are typically produced by conventional AOPs based on hydrogen peroxide, $SO_4^{\bullet-}$ exhibit a longer half-life and higher selectivity towards organic contaminants [3,4]. Among the various activation techniques, those based on iron are promising due to their cost-effectiveness, environmental friendliness, and non-toxicity [3,5]. Zero-valent iron (Fe^0) has been already used as an activator for PS and PMS and showed to be superior to Fe^{2+} in limiting the generation of undesirable side reactions [5]. To achieve a higher reactivity and overcome some limitations of Fe^0, such as its potential surface passivation, iron-based bimetallic materials were recently tested and proved to enhance the oxidant activation, promoting electron transfer [5,6]. However, further investigation is needed to evaluate the performance of bimetallic materials in combination with PS and PMS and with respect to the most common activators. In this work, PS and PMS were investigated under the activation by zero-valent iron-copper (FeCu) bimetals for the chemical oxidation of organic contaminants in water and compared to the activation by other iron-based activators (i.e., Fe^0 and Fe^{2+}). 4-chlorophenol (4-CP) was chosen as model compound for its high stability and resistance to biological treatment [7]. FeCu bimetals were synthesized by disc milling, since this technique can avoid using harmful solvents that are typically required to produce bimetals by chemical methods. A comparative study was then carried out, using Fe^0 (particle size < 63 μm) and FeCu bimetals to activate both PS and PMS. Batch tests in lab-scale PTFE reactors were performed to select the best oxidation systems. Compared to Fe^0, FeCu bimetals showed to highly increase 4-CP degradation rates with both PS and PMS. However, FeCu showed a higher synergy with PMS rather than PS, allowing to achieve a higher contaminant removal. On the other hand, instead, when PS was used as oxidant a higher extent of 4-CP degradation was achieved with Fe^0 as activator even if the contaminant degradation rate was lower. Fe^{2+} exerted the lower effect among the tested activator for both PS and PMS. To better investigate the role of the bimetals in the activation of PS and PMS, the effect of the following operating parameters was also

studied: i) bimetals initial concentration, ii) weight percentages of Cu in the bimetals (1%, 5% and 50%), and iii) milling of bimetals. The effect of higher Cu content in the bimetal was evident with PMS, increasing 4-CP degradation and remarking the greater suitability of bimetals with PMS rather than Fe^0. Interestingly, PS showed better results when a lower dosage of FeCu bimetals was used, possibly due to a reduction in the unproductive consumption of oxidant. The concentrations of Fe and Cu in water were measured during the reaction to elucidate the activation mechanism, showing that bimetals significantly promoted the iron corrosion and the subsequent generation of reactive species. Thus, to investigate which reactive species are involved in the bimetallic systems, quenching tests were performed with both PS and PMS. Results showed the presence of both $SO_4^{\bullet-}$ and $OH^{\bullet}$ radicals and an additional contribution of non-radical species (e.g., $^1O_2$ or high valent metals). Overall, FeCu bimetals, especially with PMS, can be considered as promising activators for the treatment of recalcitrant organic contaminants in water, enhancing the oxidant activation and potentially aiming to reduce the use of chemical reagents in the field of AOPs.

References

[1] Lee J, Von Gunten U, Kim JH. Persulfate-Based Advanced Oxidation: Critical Assessment of Opportunities and Roadblocks. Environ Sci Technol 2020;54:3064–81. https://doi.org/10.1021/acs.est.9b07082.
[2] Wang J, Wang S. Reactive species in advanced oxidation processes: Formation, identification and reaction mechanism. Chemical Engineering Journal 2020;401:126158. https://doi.org/10.1016/j.cej.2020.126158.
[3] Zhou Z, Liu X, Sun K, Lin C, Ma J, He M, et al. Persulfate-based advanced oxidation processes (AOPs) for organic-contaminated soil remediation: A review. Chemical Engineering Journal 2019;372:836–51. https://doi.org/10.1016/J.CEJ.2019.04.213.
[4] Xiao S, Cheng M, Zhong H, Liu Z, Liu Y, Yang X, et al. Iron-mediated activation of persulfate and peroxymonosulfate in both homogeneous and heterogeneous ways: A review. Chemical Engineering Journal 2020;384:123265. https://doi.org/10.1016/j.cej.2019.123265.
[5] Wang J, Wang S. Activation of persulfate (PS) and peroxymonosulfate (PMS) and application for the degradation of emerging contaminants. Chemical Engineering Journal 2018;334:1502–17. https://doi.org/10.1016/j.cej.2017.11.059.
[6] Settimi C, Zingaretti D, Sanna S, Verginelli I, Luisetto I, Tebano A, et al. Synthesis and Characterization of Zero-Valent Fe-Cu and Fe-Ni Bimetals for the Dehalogenation of Trichloroethylene Vapors. Sustainability (Switzerland) 2022;14:na. https://doi.org/10.3390/su14137760.
[7] Barzegar G, Jorfi S, Zarezade V, Khatebasreh M, Mehdipour F, Ghanbari F. 4-Chlorophenol degradation using ultrasound/peroxymonosulfate/nanoscale zero valent iron: Reusability, identification of degradation intermediates and potential application for real wastewater. Chemosphere 2018;201:370–9. https://doi.org/10.1016/j.chemosphere.2018.02.143.

Title: Effect of pH on electrodialysis for selective separation and purification of carboxylic acids from wastewater.

Author(s): Maya Richa*[1], Justo Lobato[1], Manuel A. Rodrigo-Rodrigo[1], Raúl García-Cervilla[1].

[1] *Department of Chemical Engineering, Universidad de Castilla La Mancha, Ciudad Real, Spain*

Keyword(s): Electrodialysis, Purification, Separation, Carboxylic acid, Material recovery.

Initial Abstract

Oxidation is a common and expensive method used in wastewater treatment to mineralize organic contaminants. This study explores partial oxidation to produce valuable carboxylic acids like oxalic (OA) and acetic acid (AA). Using electrodialysis and pH adjustments based on the acids' pK_a values, these acids were successfully separated and purified. Although more optimization is required, the technique demonstrated excellent separation with potential for industrial applications.

Abstract

1. Introduction

Wastewater treatments for the removal of organic contaminants often involves oxidation. Whether by advanced oxidation processes (AOPs) or electrochemically, the main objective is the mineralization of the organic pollutant [1]. However, this always results in a cost without the possibility of obtaining a benefit from the remediation process. Moreover, this cost for the mineralization of the compound will strongly depend on the contaminant and the concentration in which it is found.

In order to obtain value-added products, some interest could be found in the partial oxidation of the pollutant to obtain carboxylic acids with a low number of carbon atoms (1-3). Acids such as oxalic (OA) or acetic acid (AA) are acids that are observed in the by-products of oxidation of organic matter and require more extreme conditions than most organic compounds for their mineralization. However, they are acids of industrial interest.

In this work the separation and purification of the different mixtures of the main acids observed in the real degradation of organic matter (OM) was studied. Separation of each acid was performed by electrodialysis. To achieve the desired degree of separation, the pH of the feed solution was adjusted according to the pK_a of the different acids present in the sample. In this way, streams with a single acid were obtained from a mixture of 2 - 4 different acids. The purification of each stream was performed by the same principle using a volume lower than the feed for the collection of the desired acid. This step was carried out simultaneously with the separation step.

2. Material and Methods

Cell configuration was performed as can be seen in the Figure 1. Anode was MMO of RuO_2 and cathode was stainless steel. Experiments were performed with and without cationic exchange membranes (CEM) (Fumasep FKS-50). In feed a solution with the concentration of carboxylic acid tested in each

experiment was recirculated. This unit was separated from concentrate by one anionic exchange membrane (Fumasep FAB-PK-130). In concentrate unit a concentration of the corresponding acid at low concentration (10 times lower than initial concentration in feed) was added. For mixtures with more than 2 acids (3-4) the concentrate unit was repeated to sequentially separate each of the different acids.

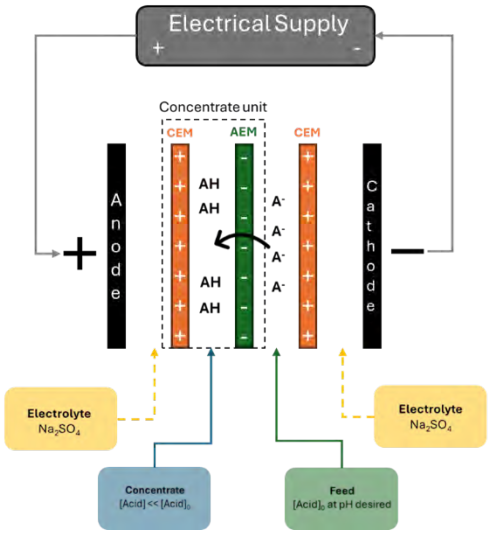

Figure 1. Scheme of the experimental setup for the separation of carboxylic acid mixtures.

3. Results

A binary mixture with oxalic acid (OA) and acetic acid (AA) was carried out at 0.5 molar fraction of each acid, similar to the one observed in bibliography after electrooxidation of OM [2]. The pH of feed was selected by studying the ionization of OA and AA at different pH. The Eq. (1) represent the ionic fraction of ionized acid [3]. In Figure 1 can be seen the prediction of ionic fraction and molar fraction of acids in the concentrate unit.

$$a_j = 1 - \left(\frac{1}{1 + antilog(pH - pK_a)}\right) \quad (1)$$

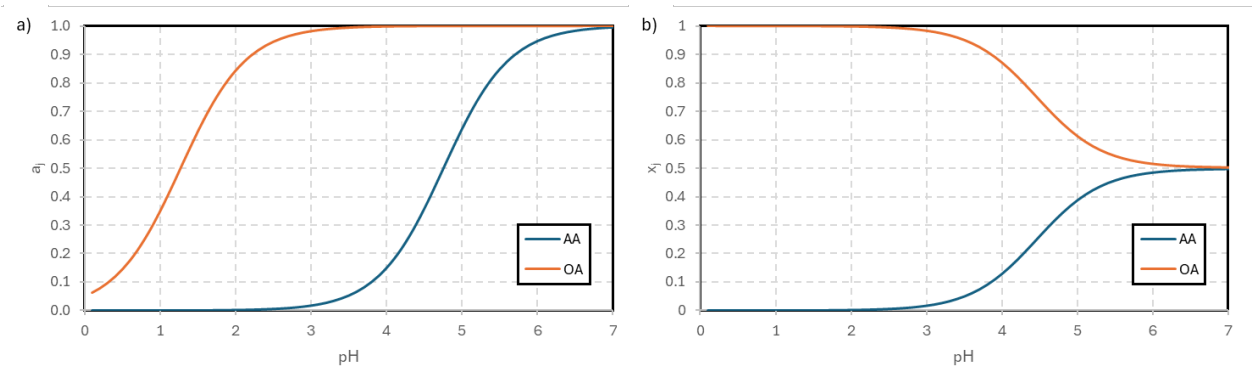

Figure 2. a) Estimated ionic fraction of acids in feed; b) estimated molar fraction of acids in concentrate.

The pH selected for experiments with OA/AA was 3, the limit where the ionization of AA starts. Because of this the separation of OA is the maximum in concentration. After 4 h at a current density of 12.8 $mA \cdot cm^{-2}$, in the concentrate a 1 and 0 molar fraction of oxalic and acetic acid respectively was obtained, Figure 3. The volume of concentrate was 5 times lower than feed, because of this the concentration in the concentrate unit was higher than initial concentration of OA in feed (50 mM). The OA was purified in the process of separation from AA. As can be seen in Figure 3 the configuration with CEM allowed to obtain a higher concentration of OA than without CEM.

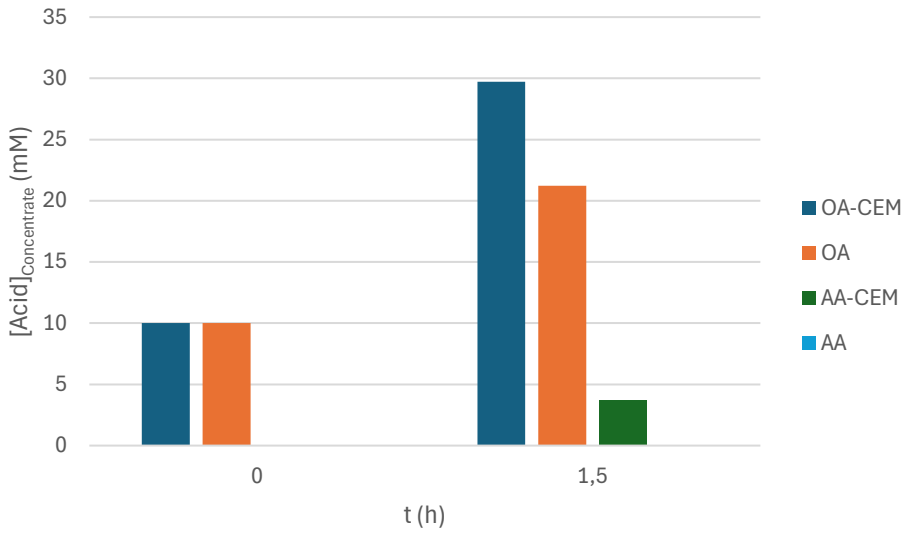

Figure 3. Evolution of the molar concentration of acids (configuration with and without CEM) in concentrate stream with time.

The variation of pH at times lower than 3 h was negligible. However, in experiments with longer times, higher concentration of acids or higher current densities the pH variation was considerable. These variations affected the ratio of separation of acids and a control of the pH was needed at different times by adding H_2SO_4/NaOH to achieve the complete separation of OA from mixture and purify. AA was purified after the separation by using a pH higher than pK_a of AA.

Excellent reproducibility was obtained using more complex mixtures with ratios similar to those observed in the literature (oxalic acid, acetic acid, formic acid, etc) [1]. However, the concentrations used were

higher than those observed in the literature since in the literature the objective of these processes is mineralization.

4. Conclusions

The main carboxylic acids obtained from oxidation of organic matter was selected and the ratios obtained in bibliography were replicated to carry out its separation and purification. The pH selective separation and purification by electrodialysis was carried out successfully at different pH selected by ionization prediction of the acid species. However, a more deeply study of the process is necessary. The bibliography of the partially degradation of organic contaminants to acid production does not exist (to the best of our knowledge) and variables as the kind of membranes, impurities or possible reactions during dialysis have not been studied.

5. Acknowledgments

This work was supported by Spanish Ministry of Science, Innovation and Universities through the ElectroRefin4O project (PID2022-138401OB-I00). Maya Richa Richa is acknowledged for the Spanish grant (PRE2022—000324). Raúl García Cervilla is acknowledged for the Spanish Juan de la Cierva postdoctoral grant. (JDC2022-049619-I).

References

[1] J. Agbaba et al., "Oxidation of natural organic matter with processes involving O3, H2, O2 and UV light: formation of oxidation and disinfection by-products," Rsc Advances, Article vol. 6, no. 89, pp. 86212-86219, 2016 2016, doi: 10.1039/c6ra18072h.

[2] S. Liu, J. Kim, and G. V. Korshin, "Comparison of the formation of aldehydes and carboxylic acids in ozonated and electrochemically treated surface water," Chemosphere, Article vol. 307, Nov 2022, Art no. 135664, doi: 10.1016/j.chemosphere.2022.135664.

[3] A. Chandra, J. G. D. Tadimeti, E. Bhuvanesh, D. Pathiwada, and S. Chattopadhyay, "Switching selectivity of carboxylic acids and associated physico-chemical changes with pH during electrodialysis of ternary mixtures," Separation and Purification Technology, Article vol. 193, pp. 327-344, Mar 20 2018, doi: 10.1016/j.seppur.2017.10.048.

Title: Pilot-scale monitoring of AOP processes by Fluorescence and UV Absorbance on-line Sensors

Author(s): Daniele Caterino*[1], Massimiliano Sgroi[1], Josué Gonzalez Camejo[1], Nicolò Ciuccoli[1], Chiara Giansanti[2], Camillo Palermo[2], Anna Laura Eusebi[1], Francesco Fatone[1]

[1] *Dipartimento di Scienze ed Ingegneria della Materia, dell'Ambiente ed Urbanistica*, *Facoltà di Ingegneria – Università Politecnica delle Marche, Ancona (AN), Italy*
[2] *Consorzio ARETUSA, Via Del Gazometro, 9 - 57122 Livorno, Italy*

Keyword(s): AOP, Pilot plant, Absorbance, Fluorescence

Abstract

This study, conducted within the framework of the H2020 project ULTIMATE, aims to monitor in real-time the removal of emerging organic contaminants through the UV/H2O2 AOP process. Using fluorescence and UV absorbance sensors, the work demonstrated the sensitivity and efficacy of the fluorescence sensor in monitoring changes in dissolved organic matter during UV/H2O2 treatment of effluents. Significant correlations were observed between fluorescence and the removal of emerging contaminants, suggesting the potential use of this approach for real-time environmental monitoring of wastewater treatment processes.

Introduction This work is framed within the H2020 project ULTIMATE which aims to facilitate the transition from a linear to a circular economy in the water sector and high water-consumption industries. This involves establishing closed-loop systems to minimize waste and optimize resource efficiency while recovering useful resources such as reclaimed water. One of the key technologies that enables the reuse of wastewater is represented by Advanced Oxidation Processes (AOPs). In particular, the UV-based AOP has become a focal point of scientific interest, given its effectiveness in addressing the removal of emerging pollutants from water [1] (Salimi et al., 2017), which is not possible with conventional wastewater treatments. AOPs are based on the in-situ generation of strong oxidants for the oxidation of organic compounds [2] (Miklos et al., 2018). Fluorescence is a fast and sensitive technique able to characterize bulk organic matter in natural and engineered aquatic systems. Fluorescence of natural water and wastewater tend to have distinct features with maxima located at characteristic combinations of excitation and emission wavelengths, and this spectroscopic technique has been shown to be very useful for discriminating between different source and components of DOM (Sgroi et al., 2020) [3]. Due to these facts, fluorescence has been also suggested as useful surrogate parameter to monitor emerging contaminant removal during wastewater treatment (Korshin et al., 2018) [4]. Objective of this work was the continuous monitoring of AOP treatment of a secondary wastewater effluent by the spectroscopic parameters fluorescence and UV absorbance carried out by a pilot plant. In particular, the monitoring system based on fluorescence and UV absorbance sensors was investigated to test its capability to monitor the removal of emerging contaminants AOP process during pilot scale experiments. The investigated Pilot plant is equipped with innovative sensors based on fluorescence and UV absorbance that provide a real-time characterization of organic content during UV/H_2O_2 treatment of a wastewater secondary effluent.

Materials and Methods The investigated pilot plant is located at the experimental platform of the "Università Politecnica delle Marche", which is located at the Wastewater Treatment Plant (WWTP) of Falconara Marittima (Ancona, Italia) (Figure 1). Using a pump, the treated secondary wastewater from the municipal WWTP is directed into the pilot plant, which is also equipped by sand and cartridge filters to reduce suspended solid concentration before the AOP process. Before the UV irradiation, hydrogen peroxide (10 – 30 mg/L) is mixed with the wastewater by a static mixer. By adjusting the flow rate, which can range from 0.2 to 3.6 m^3/h, it was possible to change the UV fluence used during the AOP process (180 – 400 mJ/cm^2). The pilot plant is equipped with advanced sensors based on fluorescence measurements (ex/em 375/345 nm), UV absorbance at 254 nm (UV_{254}), and conductivity measurements. This configuration enables real-time monitoring of these parameters, allowing for the continuous characterization of organic content of wastewater and potential correlations with the removal of emerging organic contaminants. Monitored emerging organic contaminants included atenolol, caffeine, carbamazepine, diclofenac, fluoxetine, primidone, naproxen, sulphametoxazole, which were selected according to their rate constants with hydroxil radicals.

Results A characterization of the investigated wastewater effluent is reported in Table 1.

Table 1 *Characterization of influent and effluent*

	pH	Absorbance [a.u.]	Fluorescence [a.u.]	Conductibility [µS/cm]	COD [mgO_2/L]
Influent	7.1±0.1	0.13±0.03	0.71±0.09	(20±7) ·10^2	(4±3) ·10
Effluent	7.1±0.1	0.12±0.02	0.5±0.1	(3±2) ·10^3	(3±1) ·10

Figure 1 *AOP Pilot plant equipped with on-line sensors.*

In Figure 2, signals collected during online monitoring of fluorescence are displayed, along with the respective values of fluorescence values observed during sampling. During the performed experiments, it was observed that fluorescence signal was much more sensitive than UV_{254} to monitor the effects of the AOP treatment on the wastewater, and the removal of the selected emerging contaminants. Particularly very good correlations were observed between fluorescence sensors removal and organic emerging contaminants by UV/H_2O_2 process.

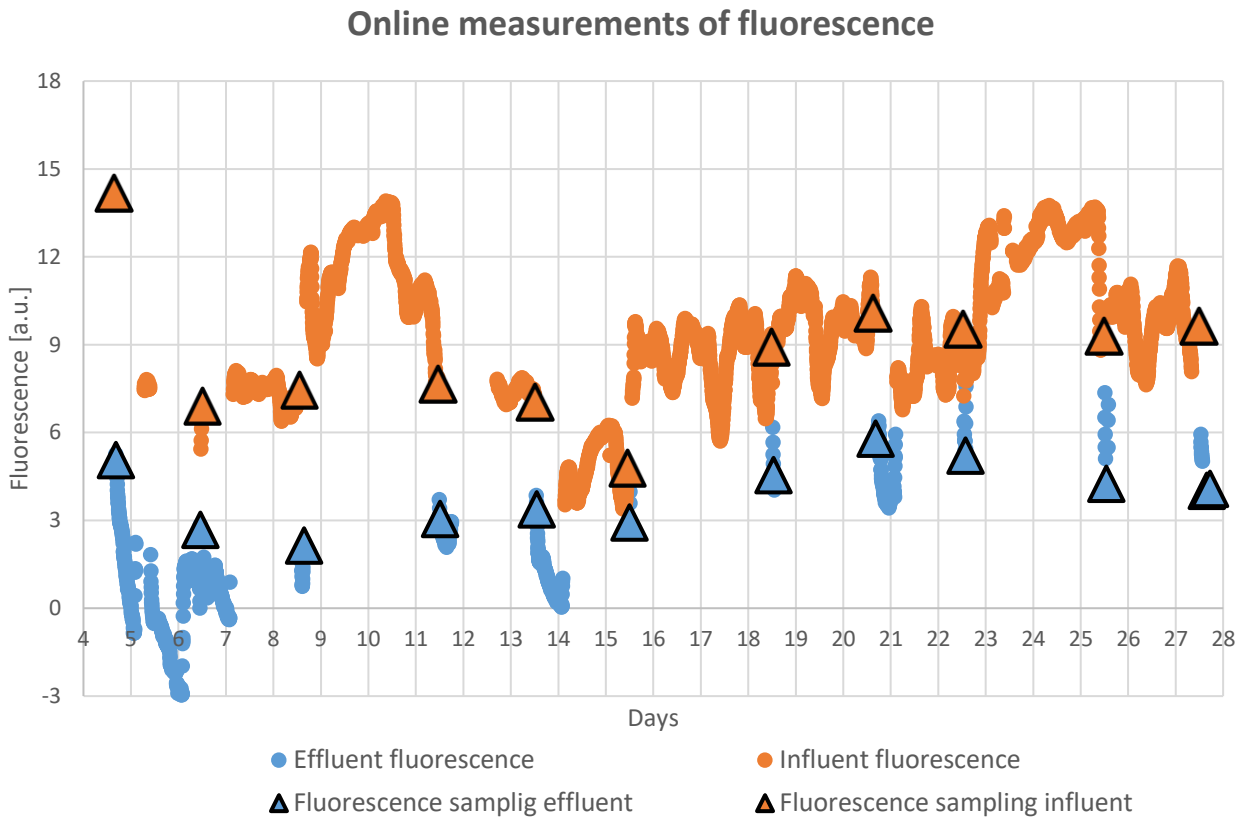

Figure 2 *Online measurements of fluorescence*

Furthermore, the reliability of the fluorescence sensors acquired on-line was validated by a strong correlation with fluorescence measurements obtained by using a laboratory instrument.

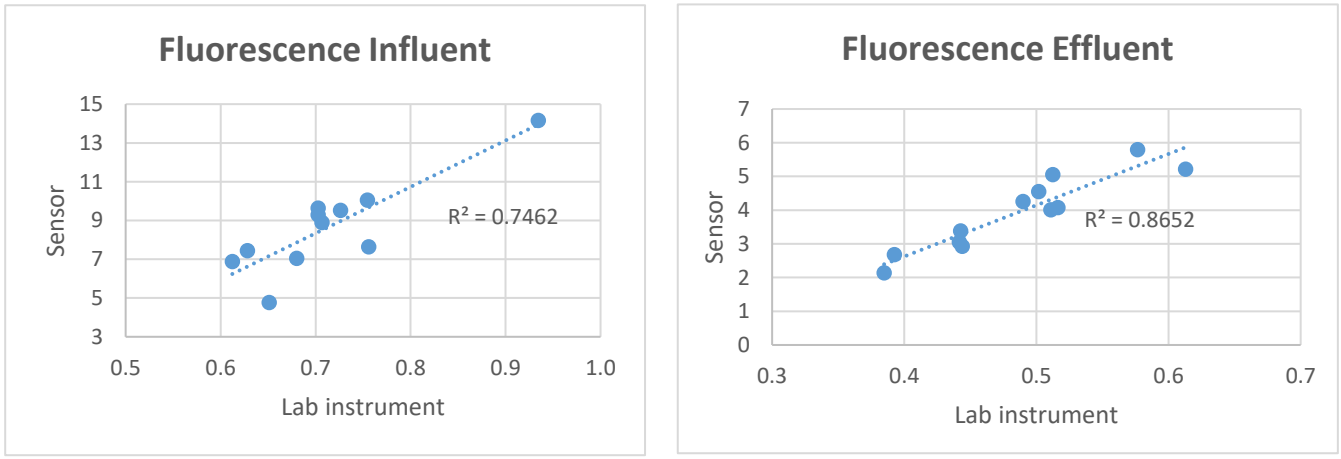

Figure 3 *Correlation between probe measurements and laboratory measurements*

Conclusion In this work, on-line fluorescence and UV absorbance sensors were investigated to monitor the removal of emerging organic contaminants by the AOP process UV/H_2O_2. For the scope an AOP pilot plant was equipped with a fluorescence sensor reading at ex/em wavelengths of 375/345 nm), an UV absorbance sensor that collect measurements at 254 nm. Obtained results showed that fluorescence sensor showed a much higher sensitivity to monitor change and modification of dissolved organic matter in wastewater after UV/H2O2 treatment. In addition, important correlations were observed between fluorescence and emerging contaminants removal.

Acknowledgement Authors would like to acknowledge the H2020 project ULTIMATE for funding the present work under Grant Agreement 869318.

References

[1] Salimi M, Esrafili A, Gholami M, Jonidi Jafari A, Rezaei Kalantary R, Farzadkia M, Kermani M, Sobhi HR. Contaminants of emerging concern: a review of new approach in AOP technologies. Environment Monitoring and Assessment. Volume 189, 414.2017.

[2] David B. Miklos, Rebecca Hartl, Philipp Michel, Karl G. Linden, Jörg E. Drewes, Uwe Hübner. UV/H2O2 process stability and pilot-scale validation for trace organic chemical removal from wastewater treatment plant effluents. Water Research. Volume 136, 169-179. 2018

[3] Sgroi, M., Gagliano, E., Vagliasindi, F.G.A., Roccaro, P. Absorbance and EEM fluorescence of wastewater: Effects of filters, storage conditions, and chlorination. Chemosphere. Volume 243, 125292. 2020

[4] Gregory V. Korshin, Massimiliano Sgroi, Harsha Ratnaweera. Spectroscopic surrogates for real time monitoring of water quality in wastewater treatment and water reuse, Current Opinion in Environmental Science & Health, Volume 2, 12-19. 2018

PARALLEL SESSION: B6

Green Economy and Smart Cities

Green Economy and Smart Cities

Title: CO_2 emissions and primary energy used in thermoplastic with flame retardant process production: a Life Cycle Assessment comparison between three compounds.

Author(s): Alberto Pietro Damiano Baltrocchi*[1], Davide Lotti[2], Marco Carnevale Miino[1], Lucrezia Maggi[1], Cristiana Morosini[3], Fabio Conti[1], Elena Cristina Rada[1], Vincenzo Torretta[1]

[1] *Department of Theoretical and Applied Sciences (DiSTA), University of Insubria, Via G.B. Vico 46, I-21100, Varese, Italy, apdbaltrocchi@uninsubria.it*
[2] *LATI Industria Termoplastici S.p.A., Via F. Baracca 7, I-21040, Vedano Olona, Italy*
[3] Department of Science and High Technology (DiSAT), University of Insubria, Via Valleggio 11, I-22100, Como, Italy

Keyword(s): Life Cycle Assessment, Climate change, Environmental impacts, Circular economy, Fit for 55, Flame retardant.

Abstract

Polyamide is an engineering thermoplastic characterised by high-performance segments of synthetic plastic materials well known for their important properties. Common thermoplastics include polyethylene, polypropylene, polystyrene, polyvinylchloride (PVC) and polyethylene terephthalate (PET). Polyamide is currently used in several processes in automotive, construction, building, and textile applications [1,2]. Polyamide 6,6 is, together with polyamide 6, one of the two significant types of polyamides currently produced, obtained by the condensation polymerisation of hexamethylene diamine with adipic acid. Most of the present polyamide production includes petroleum-based raw materials, which implies important and several negative environmental impacts [3], such as fossil resource depletion and difficulties in recycling and restoration processes [4]. Polyamides and thermoplastics have faced an intense and significant increase in application in electronic engineering [5]. In this specific sphere of interest, flame retardants are added to plastic to implement Fire Safety [6]. A significant impact of adding flame retardants to plastic is due to the interaction between potentially harmful chemicals and the human body [7]. Furthermore, due to a worldwide flame retardant use of 2.4 million metric tons in 2019, destined to grow around 3% per year [8], the need to find productive and disposal environmental-friendly systems is mandatory. Furthermore, thermoplastics with flame retardants must comply with the indication from CE and FIT for 55 [9]. In order to do so, this study analyses the Global Warming Potential (GWP) and Cumulative Energy Demand (CED) of the production process of three different polymers, based on polyamide 6,6 with glass fiber and added with three distinct flame retardants. In detail, the flame retardants are brominated polystyrene (BPS-at) in combination with antimony trioxide (density: 1.58 g cm^{-3}), aluminium diethylphosphinate (DEPAL) (density: 1.40 g cm^{-3}) and red phosphorus masterbatch (RFm) (density: 1.34 g cm^{-3}).

The analysis was carried out using the Life Cycle Assessment (LCA) approach; this methodology is well known for being a useful tool for understanding the environmental, social and economic impact of a product or process [10] according to ISO 14040 [11] and 14044 [12]. The analysis aimed to find the thermoplastic compound with lower CO_2 emissions and primary energy used. The LCA analysis was carried out with SimaPro v9 software [13], Ecoinvent database v3.9.1 [14], IPCC 2021 GWP100 v1.02

[15] and CED assessment v1.11 [16] impact methodologies. The scheme of the research followed the Product Category Rules (PCR) 2010:16 Plastics in primary forms v3.0.2 [17]; the functional unit (FU) considered was 1 kg of compound in granular form with cradle-to-gate system boundaries. The primary data was collected in a facility near Varese (Italy) that procured thermoplastics compound for engineering purposes and referred to 2023.

Figure 1 shows the environmental analysis results for 1 kg of compound. In terms of GWP, the compound with RFm has the highest emissions (6.95 kg CO_2 eq), followed by DEPAL (6.77 kg CO_2 eq) and BPS-ta (6.12 kg CO_2 eq) flame retardants. Regarding CED, the compound with RFm has the highest impact (115.48 MJ), followed by DEPAL (107.02 MJ) and BPS-ta (97.82 MJ).

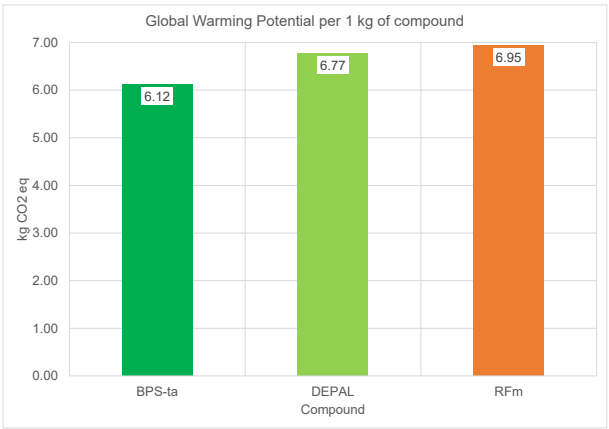

(a)

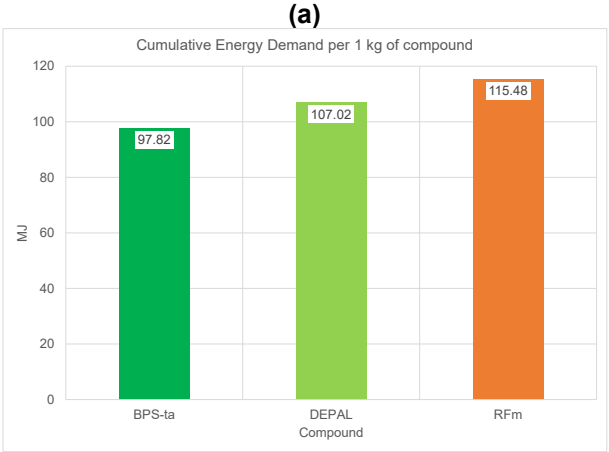

(b)

Figure 1. Results: (a) GWP and (b) CED per 1 kg of compound.

In addition, since flame retardants influence product density, it is crucial to report the results by considering the final density (Figure 2). On the one hand, as far as GWP is concerned, the results are the opposite of GWP per kg. The compound that has the most significant impact is BPS-ta (9.66 kg CO_2 eq), followed by DEPAL (9.48 kg CO_2 eq) and RFm (9.311 kg CO_2 eq). On the other hand, for CED, the compound with RFm (154.74 MJ) is slightly higher than the BPS-ta (154.56 MJ) and, lastly, the DEPAL (149.83 MJ).

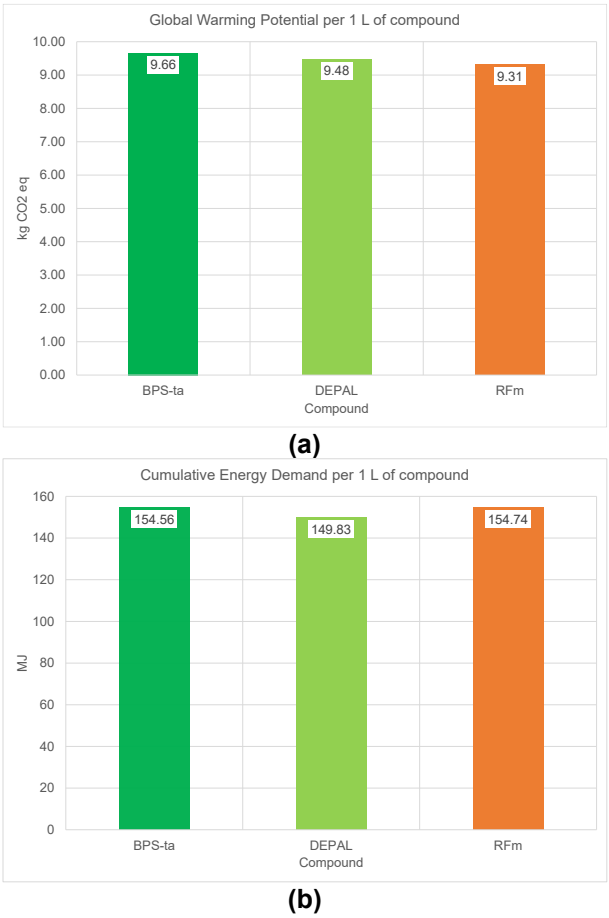

Figure 2. Results: (a) GWP and (b) CED per 1 L of compound.

In conclusion, the environmental analysis of the considered compounds shows ~~significant~~ that the impact variations depending on the flame retardant and density. Initially, when evaluating GWP per kg, compounds with flame retardants RFm, DEPAL and BPS-ta report a decreasing order of emissions. However, the hierarchy has changed when considering the overall impact based on density. In this case, BPS-ta, despite initially being in third place in terms of emissions per kg, turns out to be the compound with the highest GWP due to its density. These results highlight the importance of considering the characteristics of compounds, such as density, when accurately evaluating their environmental analysis. Therefore, in environmental decision-making processes related to compound selection, it is mandatory to consider emissions per kg and their influence on product density.

Acknowledgements

This research has been supported by the collaborative partnership between LATI Industria Termoplastici S.p.A Research and Development Department (R&D) and the Department of Theoretical and Applied Sciences (DiSTA) at the University of Insubria. LATI is involved in co-financing PhD program of M.sc Alberto Pietro Damiano Baltrocchi at the University of Insubria.

References

[1] Li M., Cui H., Li Q., Zhang Q., Thermally Conductive and Flame-Retardant Polyamide 6 Composites. Journal of reinforced plastics and composites, 35, 435–444, doi:10.1177/0731684415618538, (2016).
[2] Choi M., Byun J., Kang D., Jeong K., Lee J., Kim S.M., Han J.H., Environmental Analysis of Nylon 6,6 Production from Gamma-Valerolactone Derived from Kenaf. Industrial Crops and Products, 204, doi:10.1016/j.indcrop.2023.117365, (2023).
[3] Bhushan S., Jayakrishnan U., Shree B., Bhatt P., Eshkabilov S., Simsek H., Biological Pretreatment for Algal Biomass Feedstock for Biofuel Production. Journal of Environmental Chemical Engineering, 11, doi:10.1016/j.jece.2023.109870, (2023).
[4] You P., Zhang P., Chen P., Xie R., Chen L., Xiong Y., Strong Self-Healing and Flame-Retardant Elastomer Composite Based on Epoxidised Natural Rubber, Polylactic Acid, Chitosan and Guanidine Phosphate. Journal of Polymer Research, 31, doi:10.1007/s10965-024-03886-9, (2024).
[5] Maga, D.; Aryan, V.; Beard, A. Toward Sustainable Fire Safety: Life Cycle Assessment of Phosphinate-Based and Brominated Flame Retardants in E-Mobility and Electronic Devices. ACS Sustain Chem Eng 2024, 12, 3652–3658, doi:10.1021/acssuschemeng.3c07096
[6] Nayanathara Thathsarani Pilapitiya P.G.C., Ratnayak, A.S., The World of Plastic Waste: A Review. Cleaner Materials, 11, doi:10.1016/j.clema.2024.100220, (2024).
[7] Peña C., Civit B., Gallego-Schmid A., Druckman A., Caldeira-Pires A., Weidema B., Mieras E., Wang F., Fava J., Canals L.M., et al. Using Life Cycle Assessment to Achieve a Circular Economy. International Journal of Life Cycle Assessment, 26, 215–220, doi:10.1007/s11367-020-01856-z, (2021).
[8] S&P Global. Flame Retardants: Specialty Chemicals Update Program, (2019). Available online: https://qa.www.spglobal.com/commodityinsights/en/ci/products/chemical-flame-retardants-scup.html [access at 22/03/2024].
[9] Commission welcomes completion of key “Fit for 55” legislation, putting EU on track to exceed 2030 targets. Available online: https://ec.europa.eu/commission/presscorner/detail/en/IP_23_4754 [access at 25/03/2024].
[10] Ferronato N., Baltrocchi A.P.D., Romagnoli F., Calle Mendoza I.J., Gorritty Portillo M.A., Torretta V., Environmental Life Cycle Assessment of Biomass and Cardboard Waste-Based Briquettes Production and Consumption in Andean Areas. Energy for Sustainable Development, 72, 139–150, doi:10.1016/j.esd.2022.12.005, (2023).
[11] ISO 14040:2006: Environmental Management-Life Cycle Assessment-Principles and framework, (2006).
[12] ISO 14044:2006/Amd 2:2020 Environmental management. Life Cycle Assessment. Requirements and guidelines, (2006).
[13] PRé Sustainability, SimaPro database manual, methods library, (2020). Available online: https://simapro.com/wp-content/uploads/2020/10/DatabaseManualMethods.pdf [access at 15/03/2024].
[14] The ecoinvent Database: Overview and Methodological Framework. The International Journal of Life Cycle Assessment, 10(1), 3-9, doi:10.1065/lca2004.10.181.1, (2004).
[15] Climate Change 2021: The Physical Science Basis. Contribution of Working Group I to the Sixth Assessment Report of the Intergovernmental Panel on Climate Change Cambridge University Press, (2021). Available online: https://www.ipcc.ch/report/sixth-assessment-report-working-group-i/ [access at 22/03/2024].
[16] Frischknecht R., Jungbluth N., et.al, Implementation of Life Cycle Impact Assessment Methods. Final report ecoinvent 2000, Swiss Centre for LCI. Duebendorf, CH, (2003).
[17] PCR 2010:16 Plastics in primary forms v3.0.2. Available online: https://environdec.com/pcr-library/with-documents [access at 16/03/2024].

Title: Life Cycle Assessment as a decision support tool for the implementation of circular economy and decarbonization strategies in the steel industry

Author(s): Monia Niero*[1,2], Federico Rossi[1,2], Francesca Albano[2], Fabio Iraldo[2,1], Marco Frey[1,2]

[1] Sant'Anna School of Advanced Studies, Sustainability and Climate Interdisciplinary Center, Piazza Martiri della Libertà 33, Pisa, Italy, corresponding author: monia.niero@santannapisa.it
[2] Sant'Anna School of Advanced Studies, Institute of Management, SUM (Sustainability Management) Lab, Piazza Martiri della Libertà 24, Pisa, Italy

Keyword(s): LCA, secondary steel, slags, scrap, circularity

Abstract

The assessment of environmental sustainability in the steel sector is attracting an increasing interest in European policies [1], as well as research projects and initiatives [2]. One of the most widely used methodologies to quantify the potential environmental impacts of the steelmaking industry is Life Cycle Assessment (LCA), which has a long history of application in the sector, e.g. [3, 4, 5]. More recently, the LCA methodology has also been used to support the investigation of circular economy (CE) and decarbonization strategies in steel production and recycling, see [6] and [7], respectively.
According to Rieger et al. [8], there are three main options to implement CE strategies in the steel sector: i) enhancing steel recycling, ii) valorising steelmaking residues (e.g. dust, slags, foundry sands, and flue gases), and iii) using secondary sources from non-steel sectors (e.g. carbon sources, reducing agents). In relation to the first option (enhancing steel recycling), steel and iron scraps can be used to produce secondary steel in electric arc furnaces (EAFs) as a more environmentally friendly alternative to primary steelmaking plants like blast furnaces (BF) and basic oxygen furnaces (BOF) [9]. In relation to the second option, several steelmaking residues such as dust and slags contain valuable metals (e.g. zinc) to be recovered and reintegrated into the metallurgical industry thus avoiding the environmental impacts of further virgin materials extraction and processes [10]. Finally, some of these residues (e.g. slags and foundry sands) are also suitable to be used in other industrial sectors, e.g. for the production of construction materials like cement or asphalt, therefore supporting industrial symbiosis practices [11].
According to Suer et al. [7] breakthrough technologies for a decarbonized steel production are available, but as interim scenarios, modifications of the BF related steel production route should be used, like hydrogen injection into the BF or use of pre-reduced iron ores in the BF. However, the decarbonization cannot be fulfilled completely within the BF route, therefore the steel production via direct reduction (DR) plants is also promising. Moreover, DR plants in combination with electrical melting offer the opportunity to minimize GHG (Greenhouse Gases) emissions.
It is acknowledged that there is an increasing interest in the steelmaking industry in outlining the potential of LCA as a useful tool for the evaluation of the environmental performances of alternative CE and decarbonization strategies, as highlighted by a recent review of the application of LCA to CE in steelmaking industry [12]. In this context, the aim of this contribution is to show how the LCA methodology can be actively used to guide the decision-making process toward the implementation of the most effective CE and decarbonization strategies for future steel production targeting reduced environmental impacts, in relation to two real-world research projects funded by the European Union in the context of the Horizon Europe program, namely ALCHIMIA and GreenHeatEAF.

ALCHIMIA project

ALCHIMIA "Data and decentralized Artificial intelligence for a competitive and green European metallurgy industry" is a European project funded by the Horizon Europe program. The project aims to develop methodologies for the environmental optimization of steelmaking processes through the application of digital technologies based on Artificial Intelligence techniques (https://alchimia-project.eu/). In three of the case studies considered in the ALCHIMIA project, LCA is used to optimize the scraps mix and the energy consumption flows based on 3 EAF steelmaking plants owned by CELSA Group [13]. The fourth case study refers to the optimization of the production of automotive components in an Italian foundry that is engaged in the improvement of the resource efficiency of the production line (Fonderia di Torbole, FdT) [14]. A list of the case studies considered in the ALCHIMIA project and key aspects of the LCA methodology (functional unit and type of technology used in the plant) are listed in Table 1.

Table 1. List of case studies considered in ALCHIMIA and GreenHeatEAF projects and use of LCA methodology

Project	Case study n#	Company	Geography	Functional unit	Baseline technology
ALCHIMIA	1	CELSA	France	1 ton of steel	EAF
ALCHIMIA	2	CELSA	Spain	1 ton of steel	EAF
ALCHIMIA	3	CELSA	Poland	1 ton of steel	EAF
ALCHIMIA	4	FdT	Italy	1 ton of steel components	Cupola furnace
GreenHeatEAF	1	SSAB	Sweden	1 ton of steel	BOF-BF
GreenHeatEAF	2	Sidenor	Spain	1 ton of special steel	EAF - scrap route batch EAF
GreenHeatEAF	3	CELSA Nordic	Poland	1 ton of steel	EAF - Scrap route Consteel
GreenHeatEAF	4	Hoganas	Sweden	1 ton of iron powder	EAF - Scrap route batch EAF

A graphical illustration of the use of LCA to support the implementation of CE strategies and the steelmaking residues valorization practices in CELSA France case study is presented in Figure 1.

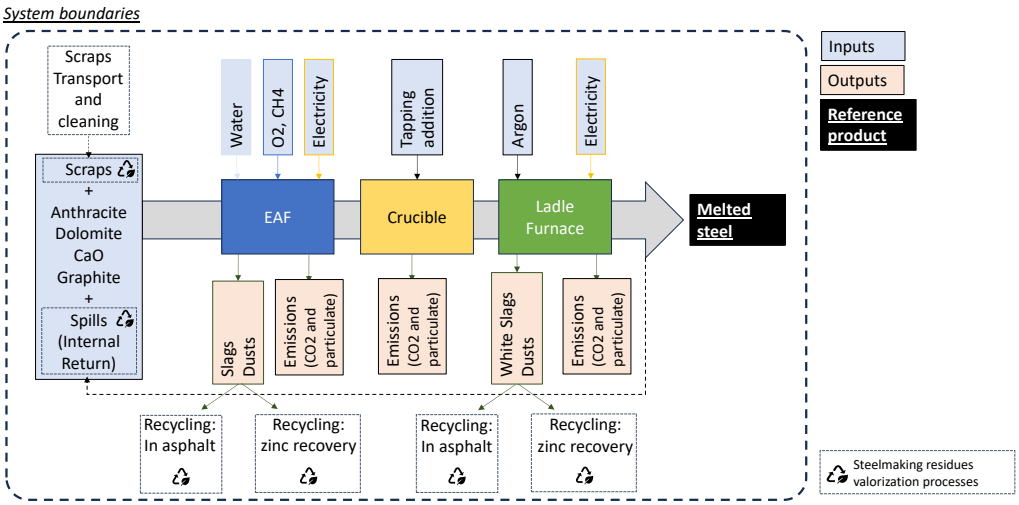

Figure 1. System boundaries of the CELSA France case study with indication of main steelmaking residues valorization practices investigated.

The focus in the ALCHIMIA project is primarily on the production of secondary steel from scraps. Therefore, a key aspect to be analysed is related to steel quality issues. Indeed, cleaning scraps operations during pre-treatment allows an increase in the quality of scraps and it overall reduces the energy consumption of steel foundries by 45% [9]. Moreover, the recovery of valuable materials from slags and dust represents another effective CE strategy, since relevant environmental benefits can be obtained through the recovery of chromium [10] and zinc [15]. On the other side, steel slags are also suitable to produce high-quality direct reduction iron [16]. To optimize the input of materials and energy consumption a mathematic optimization tool is expected to be developed within the ALCHIMIA project.

GreenHeatEAF project

The EU-funded project entitled “Gradual Integration of REnewable carbon and alternative non-carbon Energy sources and modular HEATling technologies in EAF for progressive CO2 decrease” (GreenHeatEAF) aims at investigating the replacement of natural gas and other fossil energy sources with hydrogen or renewable carbon sources (e.g. biochar) in EAF. In addition, technologies to re-optimise the heating management with maximum heat recovery from off-gas and slag are explored. Coupling pilot tests with digital applications constitutes the strength of GreenHeatEAF (https://www.estep.eu/clean-steel-partnership/list-of-csp-projects/greenheateaf/project-overview/).

LCA and Life Cycle Costing (LCC) methods are used in the GreenHeatEAF project to assess the environmental and economic performance of the melting process to evaluate the impact after the implementation of developed scenarios (integration of non-carbon gases, renewable C-sources and modular heating technologies in steelworks) and to be compared to a baseline scenario.

Three main decarbonization strategies are investigated within the GreenHeatEAF project:

- Integration of non-fossil gases flows, which test the use of hydrogen in different blends, thanks to the development of the hydrogen CoJet, manufactured by Linde;
- Fossil C-sources replacement with biomass/biochar;
- Modular and alternative heat recovery, through off-gas or slags.

A schematization of the concept implemented in the GreenHeatEAF project is presented in Figure 2.

Figure 2. Overview of key elements in the GreenHeatEAF. Source: https://www.estep.eu/clean-steel-partnership/list-of-csp-projects/greenheateaf/project-overview/

Acknowledgements

This study was funded by the European Union (Project 101070046 – ALCHIMIA and Project 101092328 - GreenHeatEAF). Views and opinions expressed are however those of the author(s) only and do not necessarily reflect those of the European Union or the European Commission. Neither the European Union nor the granting authority can be held responsible for them.

References

[1] European Steel Technology Platform (ESTEP) “Clean Steel Partnership Roadmap. 2020”. Available online: https://www.estep.eu/assets/Uploads/200715-CSP-Roadmap-version-public-consultation.pdf (accessed on 8 April 2024) (2020)
[2] Andreotti M., Brondi C., Micillo D., Zevenhoven R., Rieger J., Jo A., Hettinger A.L., Bollen J., Malfa E., Trevisan C., Peters K., Snaet D., Ballarino A., “SDGs in the EU Steel Sector: A Critical Review of Sustainability Initiatives and Approaches”. Sustainability (Switzerland) 15, 7521 (2023)
[3] Andersson G., Ponzio A., Gauffin A., Axelsson H., Nilson G., “Sustainable steel production–Swedish initiative to ‘close the loop.’ Transactions of the Institutions of Mining and Metallurgy”, Section C: Mineral Processing and Extractive Metallurgy 126, 81–88, (2017)
[4] Renzulli P.A., Notarnicola B., Tassielli G., Arcese G., Di Capua R., “Life cycle assessment of steel produced in an Italian integrated steel mill”. Sustainability (Switzerland), 8, 719., (2016)
[5] Mitterpach J., Hroncová E., Ladomerský J., Balco K., “Environmental analysis of waste foundry sand via life cycle assessment”. Environmental Science and Pollution Research 24, 3153–3162., (2017)
[6] Colla V., Branca T.A., Pietruck R., Wölfelschneider S., Morillon A., Algermissen D., Rosendahl S., Granbom H., Martin, U., Snaet D., “Future Research and Developments on Reuse and Recycling of Steelmaking By-Products”. Metals (Basel), 13, 676., (2023)
[7] Suer J., Traverso M., Jäger N., “Review of Life Cycle Assessments for Steel and Environmental Analysis of Future Steel Production Scenarios”. Sustainability (Switzerland), 14, 14131., (2022)
[8] Rieger J., Colla V., Matino I., Branca T.A., Stubbe G., Panizza A., Brondi C., Falsafi M., Hage J., Wang X., Voraberger B., Fenzl T., Masaguer V., Faraci E.L., Di Sante,L., Cirilli F., Loose F., Thaler C., Soto A., Frittella P., Foglio G., Di Cecca C., Tellaroli M., Corbella M., Guzzon M., Malfa E., Morillon A., Algermissen D., Peters K., Snaet D., “Residue valorization in the iron and steel industries: Sustainable solutions for a cleaner and more competitive future Europe.” Metals (Basel), 11, 1202., (2021)
[9] Haupt M., Vadenbo C., Zeltner C., Hellweg S.,”Influence of Input-Scrap Quality on the Environmental Impact of Secondary Steel Production” Journal of Industrial Ecology 21, 391–401. (2017)
[10] Buyle M., Maes B., Van Passel S., Boonen K., Vercalsteren A., Audenaert A., ”Ex-ante LCA of emerging carbon steel slag treatment technologies: Fast forwarding lab observations to industrial-scale production.” Journal of Cleaner Production 313, 127921., (2021)
[11] Di Maria A., Salman M., Dubois M., Van Acker K., “Life cycle assessment to evaluate the environmental performance of new construction material from stainless steel slag”. International Journal of Life Cycle Assessment 23, 2091–2109., (2018)
[12] Rossi F, Niero M., Frey, M, “Application of LCA to circular economy strategies in steelmaking industry: state-of-the-art and recommendations. In Proceedings of XVIII Convegno dell’Associazione Rete Italiana LCA “LIFE CYCLE THINKING A SUPPORTO DI MODELLI DI PRODUZIONE E DI CONSUMO SOSTENIBILI” 3-7 July 2024 Pescara, Italy (under review)
[13] CELSA Group, “Sustainability Report”, viewed 11 Mar 2024, https://www.celsagroup.com/en/sustainability-report-celsa-group/ (2022)
[14] EF Group, 2021. “The Founderia di Torbole Sustainability Report”, viewed 11 Mar 2024, https://www.ef-group.it/en/the-fonderia-di-torbole-sustainability-report (2021)
[15] Ng K.S., Head I., Premier G.C., Scott K., Yu E., Lloyd J., Sadhukhan J., “A multilevel sustainability analysis of zinc recovery from wastes”. Resources Conservation and Recyclyng 113, 88–105. (2016)
[16] Nurdiawati A., Zaini I.N., Wei W., Gyllenram R., Yang W., Samuelsson P., “Towards fossil-free steel: Life cycle assessment of biosyngas-based direct reduced iron (DRI) production process “. J Cleaner Production 393. (2023)

Preliminary Results of Laboratory Tests on Hydrogen Production from Slag and Surplus Heat in Steel Plants

Authors: Giuseppe Campo[1]*, Giovanna Zanetti[1] and Mariachiara Zanetti[1]

[1] *DIATI, Department Environmental, Land and Infrastructure Engineering, Politecnico di Torino – Corso Duca degli Abruzzi 29, Torino (To), 10129, Italy*

Keywords: Industrial waste, Energy Valorisation, Steelmaking Slag, Hydrogen Production, Laboratory tests-

Abstract

The iron and steel manufacturing industries play a fundamental role in the economies of many countries, providing essential materials for the development and upkeep of infrastructures, vehicles, buildings, industrial facilities, and various other daily necessities. In 2016, it was reported 1666.2 million tonnes of crude steel were produced [1].

Apart from energy consumption and CO_2 emissions, the steel industry contributes significantly to industrial solid waste generation, predominantly in the form of steel slag. Liu and Wang [2] reported that global steel slag production is estimated to exceed 1600 million tons annually.

The objective of the study is to evaluate the feasibility of producing hydrogen from the residues generated by steelmaking activities. In the steelmaking industry, "slag" refers to the by-product that is created during the process of refining metal ores. It is a mixture of the impurities removed from the metal and various fluxes used to aid the process. Slag is usually a molten material that floats on the surface of the molten metal and can be skimmed off.

Nevertheless, the potential to generate hydrogen from metallic iron has been recognized for an extended period, there are few published experimental results on this topic. The steam-iron process, which utilizes iron as an oxygen carrier material, is one of the earliest methods for hydrogen production. In the early 20th century, the Messerschmitt-process and the Lane-process were commercialized for hydrogen generation. Lustenberger et al. (2022) and Plescia et al (2010) report that many steel slags have the capacity to produce hydrogen when chemically activated in an alkaline or acidic environment [3], [4]. TATA Industries filed a patent in 2009 that employs freshly exited, high-temperature steel slags to produce hydrogen [5]. The process involves wetting the semi-molten slags with water; in the presence of reducing agents (primarily coal and metallic iron), this results in the splitting into hydrogen and oxygen [4]. For the wide application of this potential hydrogen energy carrier, suitable storage hydrogen solutions are required. One storage solution is the thermochemical reduction/oxidation of metal oxides (MnOm)/metals.

Moreover, the thermochemical oxidation of iron/or other metals is the main mechanism for producing hydrogen from waste steel slags [6]. The general reaction for the oxidation of metals is shown in Equation (1).

$$nM + mH_2O \leftrightarrow MnOm + mH_2 \qquad (1)$$

In order to maximize hydrogen production from residues generated by steelmaking activities, the thermodynamic conditions and kinetics of the process(es) need to be carefully considered and studied. This work presents the outcomes of a preliminary study aimed at assessing the feasibility of producing hydrogen using byproducts from hydrogen production and thermal waste generated by the same industrial activities.

The two slag samples used for the tests were obtained from an Italian steel plant. The first of the two samples is a Basic Oxygen furnace Slag (BOS) while the second one is Steelmaking Slag (SMS). Before undergoing treatment, the two samples were subjected to comminution. The initial comminution process involved crushing, and additionally, a portion of the crushed samples were milled. Consequently, the number of samples studied to evaluate the hydrogen production was four: Crushed Basic Oxygen furnace Slag (C BOS), milled Basic Oxygen furnace Slag (M BOS), crushed Steelmaking Slag (C SMS) and milled Steelmaking Slag (M SMS). Table 2 provides the composition of the utilized steel slags.

Figure 1. Steelmaking Plants and Slag production

The tests conducted to evaluate hydrogen production were performed at the laboratory scale, with all experiments carried out at a temperature of 100°C and ambient pressure.

Figure 2 illustrates the equipment used for these experiments. The setup comprised a 1.2 L bottle serving as the test reactor, another bottle functioning as a gasometer, and an open water container. The reactor and gasometer were connected by a tube, while the gasometer and open water container were linked by additional piping. Initially, the gasometer was completely filled with distilled water.

The reactor was heated using a heating plate, and mixing within the reactor was achieved with a magnetic stirrer. Each test involved introducing 5 g of the sample and 1 L of distilled water into the reactor. Prior to each test, nitrogen gas was flowed for 10 minutes to purge oxygen from the reactor's headspace.

As each test commenced, the gas inside the reactor expanded due to the temperature increase, partially filling the gasometer and causing some of the water in the gasometer to transfer to the third container. Water that evaporated from the reactor during the tests condensed in the gasometer. The tests were terminated when all the water initially present in the reactor had evaporated. After completing the tests,

the reactor was cooled to room temperature.
The gas volumes from both the reactor and the gasometer were then collected in a 5-L Tedlar® bag. Finally, the gas volume in the 5-L bag was measured using the headspace displacement method and the gas quality was assessed with a micro gas chromatograph. The room temperature during the experiments was recorded, and the produced gas volumes were referenced to Standard Conditions (275.15 K at 1 bar).

Figure 2. Lab tests equipment

Table 1 shows the main results of experimental tests. The maximum Specific Hydrogen Production (SHP) was recorded after testing the M-BOS sample. The SHP (M-BOS) is 12.41 Sm^3/ton, this value is two orders of magnitude higher than the SHP of C-BOS sample. The same behaviour was observed in the SMS samples. The SHP of the M-SMS sample was 3.29 Sm^3/ton, while that of the C-SMS was only 0.05 Sm^3/ton.As easily understandable, milling has a positive effect on hydrogen production. Therefore, the hydrogen production per unit mass also increases with an increase in specific surface area.

Table 1. Specific Hydrogen Production- Laboratory tests preliminary results

Sample	Specific Hydrogen Production $Sm^{3(*)}$ H_2/ton
C-BOS	0.18
M-BOS	12.41
C-SMS	3.29
M-SMS	0.05

(*) Standard Temperature-Pressure Conditions (S) were defined as a temperature of 273.15 K (0 °C, 32 °F) and an absolute pressure (100 kPa, 1 bar).

Comments

Unlike the TATA patent [5], which involves contacting water with molten slag, this research demonstrated that hydrogen can be produced through the oxidation of reduced metals in slag at low temperatures (100 °C) and atmospheric pressure. Preliminary lab test results show that using milled BOS yields an SHP of 12.41 Sm^3 H_2/ton. The results presented in this work are preliminary to a more comprehensive future study. In order to enhance the outcomes: all tests will be conducted in triplicate; all samples used will be analyzed before and after the experimental test, the samples should undergo

tests that determine the oxidation state of the metals present both before and after the procedures. The same sample will undergo treatment multiple times until the SHP becomes negligible; process kinetics will be evaluated through continuous analysis of the produced gases; additional process conditions will be studied by increasing pressure and temperature.
Furthermore, the electrical energy required for the comminution (crushing and milling) of the treated slags will also be assessed.

References

[1] Naidu, T. S., Sheridan, C. M., & van Dyk, L. D. “Basic oxygen furnace slag: Review of current and potential uses” . Minerals Engineering, 149, 106234. (2020).
[2] Liu, J., & Wang, D. “Influence of steel slag-silica fume composite mineral admixture on the properties of concrete”. Powder technology, 320, 230-238 (2017).
[3] Lustenberger, U. B. (2022). Steam-iron based seasonal energy and hydrogen storage (Doctoral dissertation, ETH Zurich).
[4] P. Plescia, M. Tocino, S. Papeschi, M. Pinna and E. Barbarese, “il processo hysteel per le scorie siderurgiche” Vols. pp 69-75, May, (2010).
[5] Mukherjee, Tridibesh, and Debashish Bhattacharjee. "Method for Producing Hydrogen and/or Other Gases from Steel Plant Wastes and Waste Heat." U.S. Patent Application No. 12/088,579. (2009)
[6] Gamisch, B., Huber, L., Gaderer, M., & Dawoud, B. (2022). “On the Kinetic Mechanisms of the Reduction and Oxidation Reactions of Iron Oxide/Iron Pellets for a Hydrogen Storage Process” . Energies, 15(21), 8322.(2022).

Title: RESILISTORM - Resilience Framework and Tool for Urban Stormwater Services

Author(s): João Barreiro*[1], Filipa Ferreira*[1] and José Saldanha Matos*[1].

[1] *CERIS, Instituto Superior Técnico, Universidade de Lisboa, Av. Rovisco Pais 1, 1049-001, Lisboa, Portugal, joao.barreiro@tecnico.ulisboa.pt, filipamferreira@tecnico.ulisboa.pt, jose.saldanha.matos@tecnico.ulisboa.pt*

Keyword(s): Urban Resilience, Urban Stormwater Management, Resilience Framework, 1D/2D Simulation Model

Abstract

The challenge of managing urban stormwater services (USS) has become increasingly complex. This is due, on the one hand, to the rising and rapid pressures from the effects of climate change on the urban water cycle [1] and, on the other hand, to growing urbanization and land occupation [2]. Innovative solutions are required to adequately manage intense precipitation events and actively mitigate their negative impacts on cities, services, and infrastructure. Additionally, conventional urban drainage systems have inherent limitations in their design [3] that are not easily resolvable, given the implications such interventions have on cities [4].

Urban resilience has increasingly been recognized as a new reference framework for flood risk management, helping to reduce the effects of disturbances by viewing them as opportunities for more sustainable city development, with implications on the operation of urban systems. Thus, resilience promotes a management paradigm shift from conventional "fail-safe," focused on resistance to shocks, to holistic "safe-to-fail" [5], focusing on flexibility and adaptation by anticipating and planning for failures in exceptional situations with varying degrees of predictability [6]. This concept has been widely studied, applied, and developed in various urban fields, especially since the second decade of the 21st century [7]. However, organizations, decision-makers, and urban managers are still not sufficiently familiar with urban resilience, compromising the effectiveness of implementing related approaches. Furthermore, methodologies found in the literature tend to distinguish between qualitative and quantitative approaches [8]. While each has distinct advantages, seeking complementarity between these approaches is essential.

As an urban service, USS are impact-driven as they are purposefully designed to deal with weather-related events (namely rainfalls) and minimize the consequences of rain on the population, goods, and services [9]. The current work focuses on providing managing entities, professionals, and researchers with a resilience framework for USS, aiming to enhance their integration into smart city management by incorporating resilience as an innovative and transformative factor. This framework, named RESILISTORM, includes an intrinsic evaluation component and serves as a roadmap for identifying crucial points that may compromise USS's response, adaptation, and transformation capabilities. RESILISTORM incorporates a temporal analysis that integrates past experiences and evaluates the capacity to face future adverse conditions, such as the effects of climate change, promoting continuous resilience assessment over time. This adaptability is essential for facing evolving challenges and incorporating refinements in resilience assessments. Additionally, attention is given to the spatial scale by evaluating interactions between USS and other urban infrastructures and services. Thus, RESILISTORM is a comprehensive methodology that emphasizes key properties of resilience, such as robustness, recovery, adaptation, flexibility, and the human capacity for transformation, and it enhances sustainable urban development through improved planning.

Following a hierarchical structure, a set of resilience objectives are defined for each dimension and detailed through criteria that cover different aspects to be considered in the evaluation. It incorporates a Strategic Dimension and a Performance Dimension, providing segmented and overall resilience ratings that enable utilities to identify critical aspects that may undermine the service's resilience (Figure 1). Each dimension or objective is rated through a weighted average of the respective sub-level, with the weights assigned according to the priorities established in the assessment, which are context-dependent. A global index, the Urban Stormwater Resilience Index (USRI), is also proposed, following the same calculation rationale. All indicators and consequent ratings are normalized between 0 (worst resilience) and 1 (great resilience).

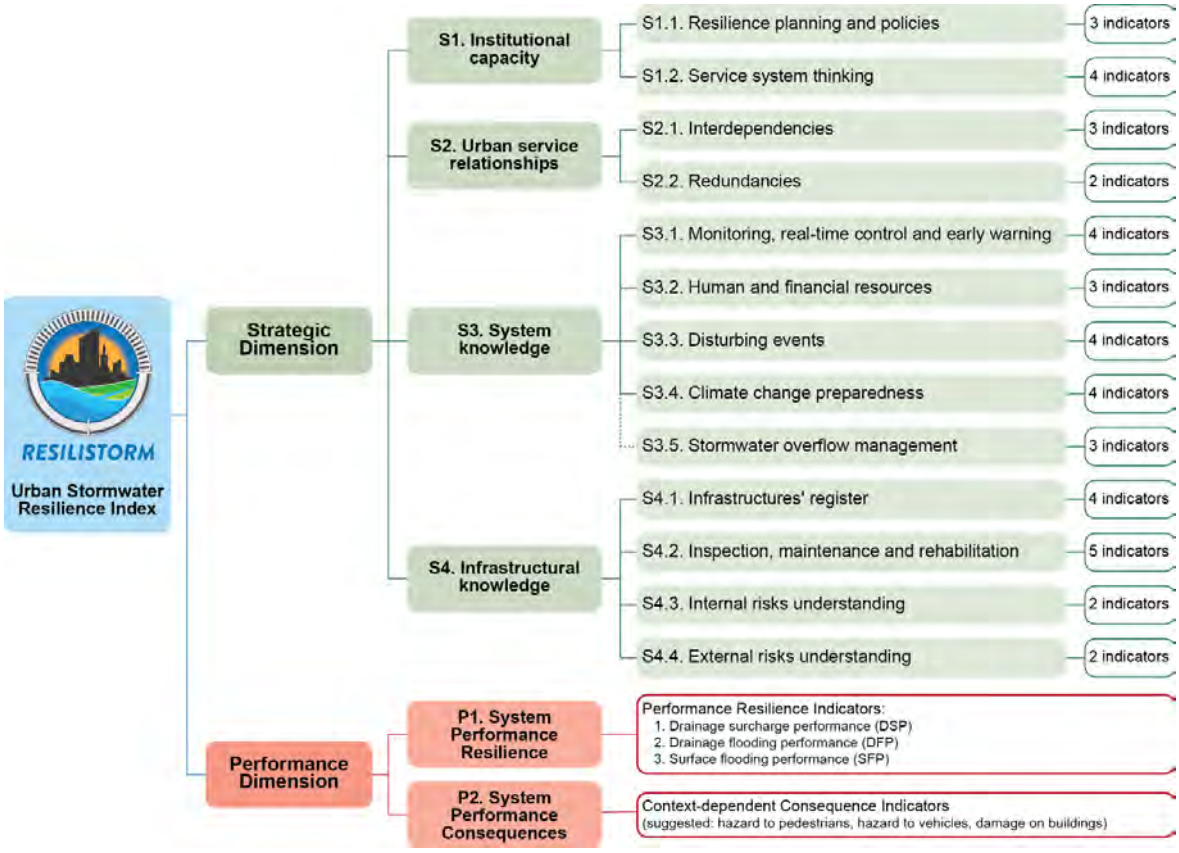

Figure 1. Resilience Framework for Urban Stormwater Systems: dimensions, objectives, and criteria.

The Strategic Dimension emphasizes the system's organizational and planning capacity to reach the desired resilience objectives. It evaluates 40 indicators based on the utilities' answers to a detailed questionnaire, which assesses various aspects of the system's management and planning procedures. In contrast, the Performance Dimension focuses on the service's ability to maintain core functions and minimize the impact of disturbances, namely urban flooding. This is achieved by evaluating context-dependent performance indicators based on 1D/2D hydrodynamic models, which assess the system's performance under different scenarios and conditions.

The concept of performance curve allows for analyzing the system's reaction during a disruptive event (Figure 2) and is indicated to assess the Performance Dimension indicators. The time variables are as follows: t_i is the initial time of the rainfall event; t_{ds} is the time where disruption of the system starts, i.e.,

performance values reach the admissible performance value (AP); t_{fs} is the time from which the system is in a failure state; t_{rs} is the recovering starting time; t_{ar} is the time where the system retrieves the admissible performance; and t_f is the final time of analysis.

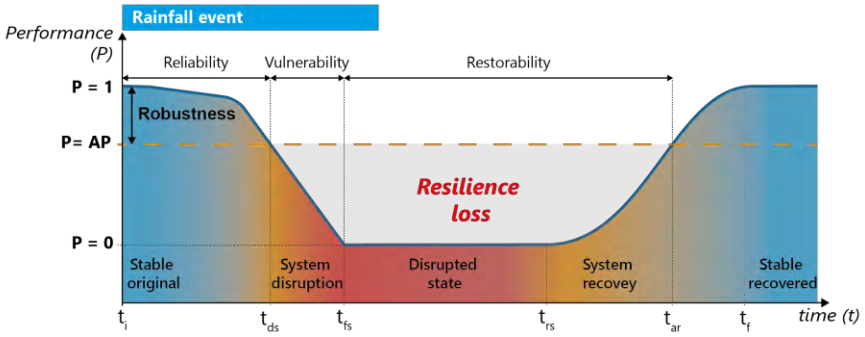

Figure 2. Theoretical generalized performance curve for stormwater systems.

The structure of the presented framework is designed to accommodate the inclusion of alternative objectives/criteria for stormwater service resilience evaluation. Similarly, performance indicators appropriate to diverse contexts and distinct urban consequences can be incorporated into specific applications of the framework and tool. The framework is valid for traditional grey stormwater systems based on underground infrastructure, nature-based blue and green systems, or hybrid systems that combine grey and blue-green solutions. To broaden the applicability and reach of this framework, the "RESILISTORM-tool" was developed, which is open-source and available in an online repository. This tool features a graphical user interface that facilitates answering qualitative Strategic Dimension indicators through a questionnaire and calculates Performance Dimension indicators based on the output files of EPA-SWMM (a 1D hydrodynamic model) and BASEMENT (a 2D hydrodynamic model). RESILISTORM-tool aggregates answers, calculates resilience indices and allows comparisons between scenarios through a resilience dashboard.

RESILISTORM was applied to two critical drainage catchments in the city of Lisbon, Portugal: the historic downtown catchment, crucial for its centrality in the city, and the Alcântara catchment, the largest in Lisbon's drainage system, with a focus on its lower area. These areas share challenges related to stormwater services' performance due to their limited capacity to react and respond to intense precipitation events. The evaluation of the Strategic Dimension enabled the identification of critical aspects that limit the capacity of Lisbon's Sewerage Department to become more resilient, being rated with 0,53 (insufficient resilience). Identified issues include the necessity to seek redundancies within the urban space that allow for the safe management of increased surface runoff and the need to improve the monitoring of the system to have real and continuous information regarding its performance in critical locations. Furthermore, from an environmental perspective, the service must enhance its ability to control and minimize the occurrence of stormwater overflows to limit receiving waters' pollution due to stormwater. The assessment of the Performance Dimension included present and future climate scenarios and system configurations - current situation (CS) and future situation (FS) (e.g., Figure 3). In the case of the Alcântara catchment, the performance indicators also proved helpful in comparing Adaptation Strategies (AS) in the light of a resilience perspective (e.g., Figure 4).

Applying RESILISTORM to these case studies demonstrates its potential for practical implementation and highlights the possibility of adaptation to specific and contextual objectives, thereby contributing to the definition of strategies that enhance the city's overall resilience. The application of the framework is

possible in other cases/locations, regardless of their level of maturity in resilience studies, as the framework itself guides the water utilities through this process, mainly via the Strategic Dimension. The Performance Dimension requires more resources to enable 1D or 1D/2D dynamic simulation of the system. Nonetheless, such assessment is an evolutionary process and indicates the capacity to study the system and its resilience.

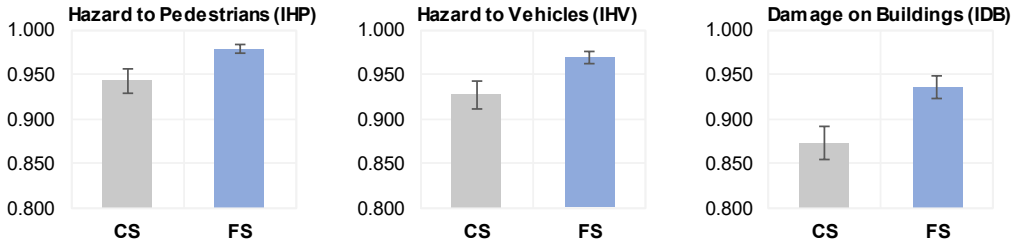

Figure 3. Example of results comparing the indicators of *Objective P2. System Consequences Resilience* for the Current (CS) and Future Situation (FS) in the Alcântara Catchment.

Figure 4. Example of results comparing the Indicator of Hazard to Pedestrians (IHP) with implementing Adaptation Strategy 1 (left) and Adaptation Strategy 2 (right) in the Alcântara catchment.

References

[1] IPCC. Summary for Policymakers. In: H.-O. Pörtner, D.C. Roberts, E.S. Poloczanska, K. Mintenbeck, M. Tignor, A. Alegría, et al., editors. Clim. Change 2022 Impacts Adapt. Vulnerability, Cambridge, UK and New York, NY, USA: Cambridge University Press; 2022, p. 3–33.
[2] Paul MJ, Meyer JL. Streams in the Urban Landscape. Annu Rev Ecol Syst 2001;3:333–65.
[3] Birgani YT, Yazdandoost F, Moghadam M. Role of Resilience in Sustainable Urban Stormwater Management. J Hydraul Struct 2013;1. https://doi.org/10.22055/jhs.2013.10074.
[4] Matos JS. Ambiente e Saneamento – Sistemas de Drenagem Urbana. Lisboa, Portugal: IST Press; 2006.
[5] Mugume SN, Diao K, Astaraie-Imani M, Fu G, Farmani R, Butler D. Enhancing resilience in urban water systems for future cities. Water Sci Technol Water Supply 2015;15:1343–52. https://doi.org/10.2166/ws.2015.098.
[6] Almeida M do C, Telhado MJ, Morais M, Barreiro J, Lopes R. Urban Resilience to Flooding: Triangulation of Methods for Hazard Identification in Urban Areas. Sustainability 2020;12:2227. https://doi.org/10.3390/su12062227.
[7] Nunes DM, Tomé A, Pinheiro MD. Urban-centric resilience in search of theoretical stabilisation? A phased thematic and conceptual review. J Environ Manage 2019;230:282–92. https://doi.org/10.1016/j.jenvman.2018.09.078.
[8] Blanco-Londoño SA, Torres-Lozada P, Galvis-Castaño A. Identification of resilience factors, variables and indicators for sustainable management of urban drainage systems. DYNA 2017;84:126–33. https://doi.org/10.15446/dyna.v84n203.58116.
[9] Evans B. Selection of methods for quantification of impacts of identified hazards. RESCCUE Project; 2017.

Title: Product Environmental Footprint assessment of smart technical clothing

Author(s): Michele Menghini*[1], Irma Cavallotti[2], Marta Ferreri[2], Edoardo Bollati[2], Roberta Pedrazzani[1], Claudio Di Iaconi[3], Giuseppe Mascolo[3]

[1] *DIMI-Department of Mechanical and Industrial Engineering, University of Brescia, Brescia, Italy,* michele.menghini@unibs.it; roberta.pedrazzani@unibs.it
[2] *ICA - Società di Ingegneria Chimica per l'Ambiente S.r.l., Kilometro Rosso innovation district, Bergamo,* Italy, irma.cavallotti@studioica.it, marta.ferreri@studioica.it, edoardo.bollati@studioica.it
[3] *Water Research Institute (IRSA), National Research Council (CNR), Bari, Italy,* giuseppe.mascolo@cnr.it; claudio.diiaconi@cnr.it

Keyword(s): LCA, LED, OLED, optoelectronics, sustainable materials, textile

Abstract

Smart clothing for workers is increasingly recognized as a critical innovation for enhancing occupational safety across various industries. These garments, embedded with sensors and connectivity technologies, provide real-time monitoring of physiological parameters such as heart rate, body temperature, and hydration levels, as well as environmental conditions like exposure to hazardous substances or extreme temperatures. By alerting both the worker and management to potential health risks and unsafe conditions, smart clothing facilitates timely interventions, thereby reducing the incidence of accidents and occupational illnesses. Furthermore, data collected from these wearable devices can be analyzed to identify patterns and implement proactive measures to prevent future incidents. The integration of smart clothing into workplace safety protocols not only augments traditional protective gear but also supports a more dynamic and responsive safety management system, ultimately fostering a safer and more productive work environment. Research has demonstrated that such technology can significantly lower the risk of injuries and improve overall worker well-being, underscoring its potential as a valuable asset in occupational health and safety strategies [1] [2] [3].

While smart clothing offers substantial benefits for worker safety, it also raises significant sustainability concerns, particularly regarding its CO_2 and water footprint. The production of these high-tech garments involves the use of advanced materials and electronic components, which contribute to considerable greenhouse gas emissions. The manufacturing processes for electronic textiles, including the extraction of raw materials, fabrication of sensors, and assembly of wearable devices, are energy-intensive and often rely on non-renewable energy sources. This results in a high CO_2 footprint, exacerbating climate change. Additionally, the production of textiles and electronic components consumes substantial amounts of water, particularly in the dyeing and finishing stages, which further strains freshwater resources. The challenge of electronic waste disposal also poses environmental risks, as improperly discarded smart clothing can lead to soil and water contamination from heavy metals and other toxic substances. To address these sustainability issues, it is crucial to develop more eco-friendly production techniques, utilize renewable energy sources, and implement efficient recycling programs to mitigate the environmental impact of smart clothing [4] [5] [6].

The Organizational Environmental Footprint (OEF) and Product Environmental Footprint (PEF) methodologies are invaluable tools for environmental impact assessment due to their comprehensive, standardized approaches to evaluating the environmental performance of products and organizations. These methodologies offer a robust framework that incorporates a wide range of environmental impact categories, from greenhouse gas emissions to water and resource use, providing a holistic view of environmental performance. The standardization inherent in OEF and PEF ensures consistency and comparability of results across different products and organizations, facilitating better-informed decision-making and policy development. Furthermore, the detailed life cycle perspective adopted by these methods helps identify critical stages in the product life cycle where interventions can most effectively reduce environmental impacts. By employing OEF/PEF, companies can not only improve their environmental transparency and accountability but also drive sustainable innovations and enhance their competitiveness in markets increasingly focused on sustainability.

This PEF study was developed to establish the optimal production processes (among three methods: printing, thermal evaporation, and an intermediate process that involves a mix of the previous techniques) of OLED (Organic Light-Emitting Device) and optoelectronic devices integrated into textiles. The study aims to: a) Identify the most relevant stages of the life cycle; b) Identify the most relevant processes; c) Identify data quality requirements. The goal was to quantify the impacts generated during the life cycle of the prototypes, including stages from raw material and energy production to the realization of the prototypes, including energy use during the use phase. The evaluation was developed according to Recommendation No. 2279 of 16/12/2021. This PEF study was developed based on existing and widely tested methods, aiming to define a common European methodology for calculating the environmental impacts of a product. This PEF study relates to prototypes for the production of OLED and optoelectronic devices integrated into textiles. By definition, the functional unit identifies the qualitative and quantitative aspects of the functions and/or services provided by the product under evaluation. This phase was particularly challenging, because these devices perform multiple functions and their entire life cycle is unknown. The system boundaries are cradle-to-gate, excluding downstream processes such as B2B distribution, further processing of textiles for finished consumer products, product distribution to final consumers, the use phase, and end-of-life treatments. In cradle-to-gate with option studies (from cradle to gate, including the use phase), end-of-life parameters (recyclability, energy recovery, disposal) were not considered. Distribution and end-of-life phases were excluded from the analysis. The use phase was included, considering expected operating hours, specifically 1,000 hours. System boundaries thus include all processes linked to the supply chain of the prototype relative to the unit of analysis [7] [8] [9] [10] [11].

All impact categories and related methods from Recommendation 2021/2279/EU were applied in the product environmental footprint impact assessment. The environmental footprint impact categories refer to the considered effect categories and constitute the environmental footprint impact assessment method. Characterization models quantify the environmental mechanism between LCI (life cycle inventory) inputs (resources and emissions associated with the product life cycle) and each EF impact category indicator. The overall objective of the project is to create a demonstrative system, define laboratory-scale manufacturing technology, and subsequently draft an engineering and industrialization study.

An inventory analysis of all material/energy flows and emissions to air, water, and soil for each phase of the product supply chain was conducted as a basis for PEF modeling, using specific directly collected data whenever possible. Once input data was determined, impact assessment proceeded with classification (assigning inventory data to respective environmental impact categories) and characterization (multiplying inventory values by characterization factors for each impact category), allowing estimation of 16 impact indicators. Environmental impact values were normalized, divided by a "reference value" or "normal effect" to establish the magnitude of each environmental effect relative to an average reference, typically annual per capita emission factors as per Recommendation 2021/2279/EU. Normalization establishes the relative significance of different indicators: the factors were taken from the updated document issued by the JRC [9].

Normalized environmental footprint results were multiplied by weighting factors [12] reflecting perceived importance of considered impact categories. Weighted results can be compared to assess relative importance and aggregated into a single overall impact indicator. However, caution is needed as this score does not reflect the detailed analysis necessary to interpret results across different indicators. Weighting determines the magnitude of each environmental issue and identifies significant impact categories representing 80% of overall environmental impact. One of the main objectives of a PEF study is to provide the basis for evaluating, monitoring, and attempting to improve the environmental performance of a product over time. The PEF study serves as a valuable support in identifying opportunities to improve the environmental performance of the product at different stages of its life cycle. It provides information that allows for strategic planning, helping to make choices based on objectively derived priorities, designing or redesigning products or processes, and selecting environmental performance indicators with related measurement techniques. From the normalization and weighting analysis, it emerges that the three most relevant impact categories for the analyzed devices are (in order of relevance): Climate Change (0.732 - 1.535 mPt), Resource Use-Fossil (0.532 - 1.058 mPt) and Resource Use - Mineral and Metals (0.351 – 1.463 mPt). Subsequently, an analysis was developed to highlight the life cycle stages, processes, and elementary flows with the greatest impact on the various categories (Hotspot Analysis). The value of each impact indicator was distributed among the various contributions and life cycle stages included in the analysis.

An opportunity to deepen the PEF study is represented by improving the inventory quality, as one of the study's limitations is the lack of databases for modeling some specific compounds for which proxy data were used, particularly concerning printed products.

In conclusion, the analysis has made it possible to highlight the most significant stages and processes in the life cycle of the products across the broad spectrum of analyzed environmental impacts. It is emphasized that the results refer to primary data collected in the context of laboratory experimental tests. The studied technology is still under development, and the engineering and industrialization phases have not yet begun. These phases, through optimization of energy consumption during both the production and usage phases of the device, would reduce the associated impacts.

Acknowledgements. The research has been realised and funded by the project PON R&I ECOTEC - Fibre e tessuti intelligenti ed ECOsostenibili per l'abbigliamento TECnico _ ARS01_00951 (ECO-

sustainable and intelligent fibers and fabrics for TEChnic clothing (ECOTEC)_ ARS01_00951).

References

[1] Podgorski, D., Majchrzycka, K., Dąbrowska, A., Gralewicz, G., & Okrasa, M. (2017). Towards a conceptual framework of OSH risk management in smart working environments based on smart PPE, ambient intelligence and the Internet of Things technologies. International Journal of Occupational Safety and Ergonomics, 23(1), 1-20.

[2] Chen, D., & Lawo, M. (2017). Smart textiles and smart personnel protective equipment. Smart Textiles: Fundamentals, Design, and Interaction, 333-357.

[3] Flor-Unda, O., Fuentes, M., Dávila, D., Rivera, M., Llano, G., Izurieta, C., & Acosta-Vargas, P. (2023). Innovative technologies for occupational health and safety: a scoping review. Safety, 9(2), 35..

[4] Blackburn, R. (Ed.). (2009). Sustainable textiles: life cycle and environmental impact. Elsevier.

[5] Li, Q., Xue, Z., Wu, Y., & Zeng, X. (2022). The status quo and prospect of sustainable development of smart clothing. Sustainability, 14(2), 990.

[6] Provin, A. P., de Aguiar Dutra, A. R., Machado, M. M., & Cubas, A. L. V. (2021). New materials for clothing: Rethinking possibilities through a sustainability approach-A review. Journal of cleaner production, 282, 124444.

[7] UNI EN ISO 14040:2021 - Gestione ambientale - Valutazione del ciclo di vita - Principi e quadro di riferimento

[8] UNI EN ISO 14044:2021 Gestione ambientale - Valutazione del ciclo di vita - Requisiti e linee guida

[9] Andreasi Bassi, S., Biganzoli, F., Ferrara, N., Amadei, A., Valente, A., Sala, S. and Ardente, F., Updated characterisation and normalisation factors for the Environmental Footprint 3.1 method, EUR 31414 EN, Publications Office of the European Union, Luxembourg, 2023, ISBN 978-92-76-99069-7, doi:10.2760/798894, JRC130796

[10] IPCC, 2021: Climate Change 2021: The Physical Science Basis. Contribution of Working Group I to the Sixth Assessment Report of the Intergovernmental Panel on Climate Change [Masson-Delmotte, V., P. Zhai, A. Pirani, S.L. Connors, C. Péan, S. Berger, N. Caud, Y. Chen, L. Goldfarb, M.I. Gomis, M. Huang, K. Leitzell, E. Lonnoy, J.B.R. Matthews, T.K. Maycock, T. Waterfield, O. Yelekçi, R. Yu, and B. Zhou (eds.)]. Cambridge University Press. In Press.

[11] information to the characterisation factors of recommended EF Life Cycle Impact Assessment method - New models and differences with ILCD (Fazio, S. Castellani, V. Sala, S. Schau, EM. Secchi, M. Zampori, L., Diaconu E. – 2018);

[12] Sala S, Cerutti AK, Pant R. (2018). Development of a weighting approach for Environmental Footprint. European Commission, Joint Research Centre, Publication Office of the European Union, Luxembourg. ISBN 978-92-79-68041-0.

Title: Economic valuation of ecosystem services in the waste management framework

Author(s): Maria Cristina Lavagnolo*, Giovanni Felici

DICEA, Department of Civil, Architectural and Environmental Engineering - DICEA, University of Padova - Lungargine Rovetta 8, 35127 Padova, Italy), mariacristina.lavagnolo@unipd.it; giovanni.felici@phd.unipd.it

Keyword(s): biodiversity, waste management, ecosystem service, decentralisation, circular economy

ABSTRACT

Ecosystem services represent the benefits that nature provides to humans, playing a pivotal role in supporting human well-being, economic development, and societal progress. These services encompass a wide range of functions, from regulating climate and purifying water to providing food, medicine, and recreation. Despite their recognized importance, quantifying the value of ecosystem services remains a complex and challenging endeavor. This complexity arises from the multifaceted nature of these services and the intricate interplay between ecological processes and human activities. The recognition of the integral relationship between ecosystem services and human well-being has led to an increasing emphasis on the need for their valuation. Valuation techniques aim to assign economic values to ecosystem services, thereby providing a tangible metric that can be used to inform decision-making processes. These valuation methods vary in complexity and applicability, ranging from market-based approaches that assess the direct market value of ecosystem goods and services to non-market valuation techniques that use indirect methods such as stated preference surveys, hedonic pricing, and cost-based methods. The overarching objective of this intervention is threefold. Firstly, it seeks to elucidate the pivotal role that ecosystem services play in shaping our society and economy, highlighting their contribution to economic growth, human well-being, and sustainable development. Secondly, it aims to explore the diverse methodologies employed for valuing ecosystem services, providing an overview of the strengths, limitations, and applications of various valuation techniques.

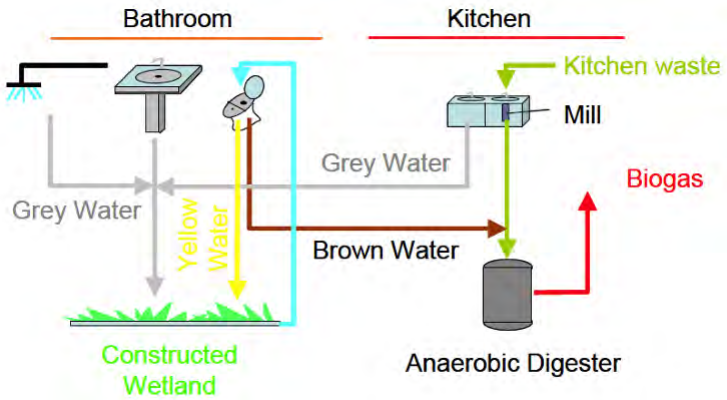

Figure 1. Conceptual scheme of Aquanova system

Lastly, the intervention focuses on a practical application of these valuation methods through a case study of waste management: the Acquanova project. The Acquanova project, which is a virtuous example of a decentralized waste management system, essentially provides two outputs: biogas production and phytoremediation. Therefore, the intervention will focus on how to determine the ecosystem services associated to biogas and phytoremediation and how to provide an economic value to them. The intervention will delve into the methodology employed to quantify the economic benefits derived from these ecosystem services, examining the costs, benefits, and trade-offs associated with their implementation. In conclusion, this intervention underscores the importance of understanding and valuing ecosystem services in fostering sustainable management practices and informed decision-making. By providing insights into the role of ecosystem services in our society, elucidating the methodologies for their economic valuation, and showcasing a practical application through the Acquanova project, this intervention aims to contribute to the ongoing dialogue on the sustainable utilization and conservation of our natural resources.
Aquanova System is an example of a decentralizes waste management system and it is based on the concept of waste separation directly at the source, in this way each waste flux can be treated with the proper technique in order to maximize the efficiency of the entire plant. The separation in this case is described as follow: yellow water (urine flow), brown water (fecal matter flow), grey water (soaped water), each one treated in different manners. Wastewater fluxes separation is made possible with the installation of an experimental toilet, characterized by the presence of a special mechanism that allows the division of the urine and the fecal flux. The Aquanova system is described with scheme in Figure 1.

Table 1. Ecosystem services related to biogas production.

ES type	ES benefit	Definition
Provisioning	Bioenergy	Energy production by means of biomass residues and waste anaerobic digestion (AD)
Regulating and Maintenance	Soil Quality	Regulation of nutrients in soil by reduction of organic load and spreading of digestate
	GHG savings	Regulation of global climate by reduction of GHG emissions

Table 2. Ecosystem services related to phytoremediation system.

ES type	ES benefit	Definition
Provisioning	Plants	Phytoremediation system is based on the fact that selected species of plants can reduce pollutants
Regulating and Maintenance	Soil Quality	Regulation of nutrients in soil by plants activities. In particular, regulation of N, P and K
	GHG savings	Regulation of global climate by reduction of GHG emissions

The Aquanova waste management system produces two outputs, which are object of this study: (i) biogas production derived form the anaerobic digestion and; (ii) phytoremediation derived from the

wastewater treatment. The aim of this study is therefore to identify the ecosystem services coming from these two outputs and providing an economic value to such services.

Based on the literature and on the Common International Classification of Ecosystem Services (CICES), the ESs linked to the biogas production and phytoremediation have been identified as in Table 1 and Table 2.

After identifying the different ecosystem services related to biogas production and phytoremediation, they need to be valued. To accomplish this, various economic valuation approaches have been chosen to better fit each ecosystem service. Methods such as cost-benefit analysis and the replacement-cost method will be utilized in this study.

The expected results will have a threefold purpose:

(i) They are expected to provide a detailed cost-benefit analysis of the "Aquanova" project. This analysis is particularly comprehensive as it incorporates the economic valuation of ecosystem services, thereby serving as a valuable example for the Natural Capital Accounting framework.

(ii) Furthermore, the findings from this study can contribute significantly to the growing literature on the economic valuation of ecosystem services by offering a practical example that showcases the application of various economic valuation methods in a real-world context.

(iii) Lastly, the results are poised to be beneficial for policymakers. They can offer an objective and tangible indication of the potential benefits that such technology can bring, aiding policymakers in making informed decisions regarding the adoption and promotion of sustainable technologies and practices.

PARALLEL SESSION: C6

Contaminated sites

Modelling, monitoring tools and risk assessment

Helianthus annuus assessment for nickel phytoremediation

Authors: Luigi Lopopolo[1*], Gianfranco D'Onghia[1], Sarah Gregorio[1], Ezio Ranieri[1]

[1] *Dipartimento di Bioscienze, Biotecnologie e Ambiente, Università degli studi di Bari, Bari, Italy.*

Keywords: Phytoextraction, Helianthus annuus, Nickel, Pollution

Abstract

Heavy metals (HMs) are distributed in various forms within the soil, including dissolved in the soil solution, adsorbed on soil constituents, and associated with organic matter (Shuman, 1991). HMs pose serious environmental threats due to their persistence and toxicity (Gu et al., 2018; Wang et al., 2020). They accumulate in soil and organisms through natural processes and human activities like mining, pesticide use, inadequate waste management, and industrial practices contribute significantly. (Brodin et al., 2017; Ferrey et al., 2018).
Exposure to heavy metals can lead to a range of health issues, including neurological disorders and organ damage. Lead, for example, can cause appetite loss and renal dysfunction, mercury toxicity results in neurological symptoms like tremors and cognitive loss, and organic mercury compounds pose health risks, nickel causes vomiting, nausea, headache, and, in more severe cases, gastric hemorrhage (Guzzi et al., 2020).
Therefore, it is important to develop remediation technologies for soils contaminated by heavy metals.
Phytoremediation is a technique that utilizes plants to absorb, transfer, or transform pollutants and emerges as a green and effective method for environmental cleanup. It addresses soil, water, and sediment contamination caused by heavy metals, organic pollutants, and even radioactive elements. The process involves absorption, volatilization, degradation, and stabilization by plants to eliminate or immobilize pollutants, offering promise for environmental purification (Lin et al., 2021; Singh et al., 2016). This technique encompasses various approaches categorized into phytoextraction, phytostabilization, phytovolatilization, phytofiltration, and phytotransformation. Phytoextraction involves plants accumulating heavy metals in their shoots without altering soil properties, enabling the removal of pollutants from polluted environments. (Al-Baldawi et al., 2018).

Several factors influence phytoremediation efficacy, including the choice of plant species, soil characteristics, rhizospheric microbial communities, climatic conditions, and heavy metal bioavailability. The bioavailability of heavy metals, affected by soil pH, moisture, organic matter, and oxygen levels, directly impacts phytoextraction efficiency. Heavy metals in soils are categorized into available, unavailable, and exchangeable fractions, with pH playing a crucial role in their dissolution. Alkaline pH reduces metal bioavailability due to low dissolution rates, highlighting the intricate interplay between soil chemistry and phytoremediation effectiveness (Ashraf et al., 2019; Javed et al., 2019; Wei et al., 2008).

In this study, the evaluation of Helianthus annuus's potential in phytoremediation has been assessed, considering two polluted pots irrigated with 80 mgCu/L and 40 mgCu/L in a continuous irrigation rate of 1.644 mm/day for 12 weeks.

The tolerance and phytoextraction capacity for nickel has been evaluated, and the overall phytoextraction potential has been evaluated considering bioaccumulation and translocation factors.

The Nickel tolerance test, depicted in Figure 1, shows Helianthus annuus' varying tolerance to Nickel concentrations. The difference in growth between the two pots is notably evident after the sixth week, with a considerable decrease observed in Pot 1, attributable to the high concentrations of Nickel. Tolerance to the pollutant constitutes a key factor in implementing phytoremediation interventions. Having approximate knowledge of the pollutant's limit concentrations allows for better evaluation of the species to be used for the remediation intervention.

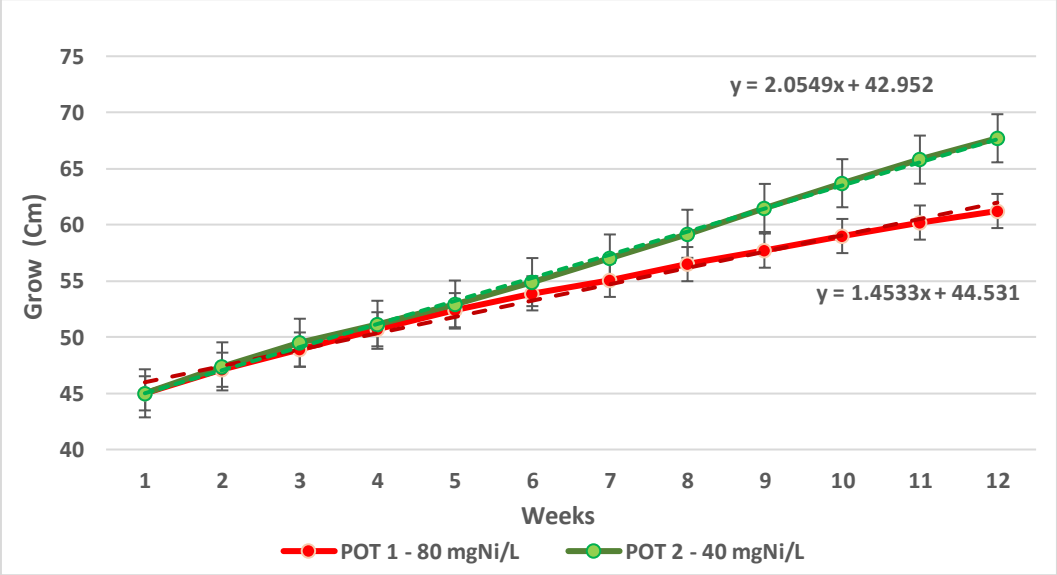

Figure 1. Tolerance test of Helianthus Annuus evaluated with 80 mgNi/L and 40 mgNi/L in contaminated water.

Figure 2 illustrates the nickel concentrations in underground tissues and aerial tissues after 12 weeks of phytoextraction test. The phytoextraction test aims to determine the concentrations of pollutants in the various plant tissues, thereby enabling proper assessment of the species' adaptability to the correct phytoremediation technology.
These data illustrate a direct correlation between environmental nickel concentration and its uptake and accumulation in plant tissues. Primarily acting as the main absorption site from the soil, roots exhibit the highest concentrations, followed by stems and leaves. These findings underscore Helianthus annuus's capability to accumulate nickel from its surroundings, particularly in roots, intensifying accumulation as the surrounding soil or water nickel concentrations elevate.

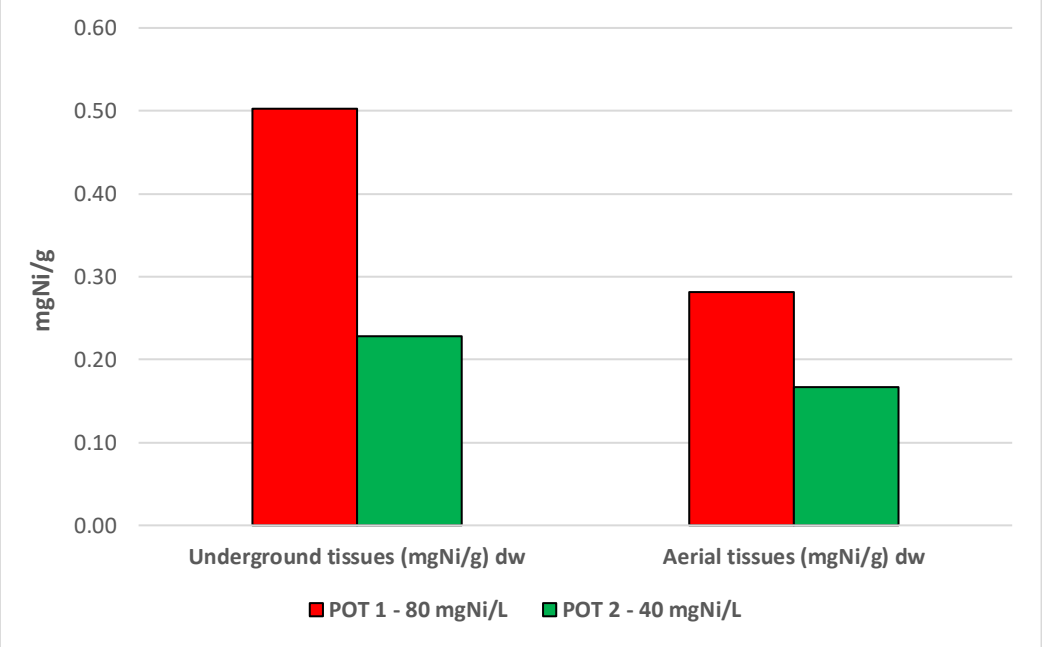

Figure 2. Phytoextraction test of Helianthus Annuus evaluated with 80 mgNi/L and 40 mgNi/L in contaminated water after 12 weeks.

To evaluate the phytoextraction capacity of Helianthus annuus the bioconcentration factor (BCF) and translocation factor (TF) have been determined. BCF of metals is an index of the ability of the plant to accumulate a particular metal concerning its concentration in the soil. TF represents the ratio of nickel concentration in the aboveground plant parts to the nickel concentration in the root and rhizome system (Buscaroli 2017).
At concentrations of 40 mg/L and 80 mg/L, the bioconcentration factors were found to be 1.03 and 0.86, respectively. Corresponding translocation factors were determined as 0.73 and 0.56, respectively. These results suggest that Helianthus annuus possesses a moderate ability to accumulate metals in its tissue compared to the concentration in the surrounding soil. However, it exhibits limitations in translocating metals from roots to aboveground parts. Helianthus annuus demonstrates varying levels of tolerance towards different concentrations of nickel, which has implications for its efficacy as a phytoremediation agent. The results suggest that as environmental nickel concentrations rise, so does the uptake and storage of nickel in plant tissues, particularly in the root system. In the tolerance assessments, a more pronounced correlation between nickel concentration and observed effects is evident only at 80 mg/L, indicating the existence of a tolerance threshold between 80 and 40 mg/L of nickel. Nonetheless, the plant's capacity to transport and store nickel diminishes at higher concentrations, indicating a limitation in its ability to remediate effectively.
From the results obtained, it can be stated that Helianthus annuus appears to be a good species for the remediation technology of phytoextraction in Apulian heavy metals polluted soils.

References

[1] Shuman, L. M.. Chemical forms of micronutrients in soils. In J. J. Mortvedt (ed.). Micronutrients in agriculture. Soil Soc. Soc. Amer. Book Series #4. Soil Sci. Soc. Amer., Inc., Madison, WI. 1991

[2] Gu, Y.-G., Ning, J.-J., Ke, C.-L., Huang, H.-H. Bioaccessibility and human health implications of heavy metals in different trophic level marine organisms: a case study of the South China Sea. Ecotoxicol. Environ. Saf. 163, 551–557. 2018

[3] Wang, N., Qiu, Y., Hu, K., Huang, C., Xiang, J., Li, H., Tang, J., Wang, J., Xiao, T. One-step synthesis of cake-like biosorbents from plant biomass for the effective removal and recovery heavy metals: effect of plant species and roles of xanthation. Chemosphere 129129, 2020.

[4] Brodin, M., Vallejos, M., Opedal, M.T., Area, M.C., Chinga-Carrasco, G.,. Lignocellulosics as sustainable resources for production of bioplastics–A review. J. Cleaner Prod. 162, 646–664. 2017.

[5] Ferrey, M.L.; Coreen Hamilton, M.; Backe, W.J.; Anderson, K.E. Pharmaceuticals and Other Anthropogenic Chemicals in Atmospheric Particulates and Precipitation. Science of The Total Environment, 612, 1488–1497, doi:10.1016/j.scitotenv.2017.06.201. 2018.

[6] Guzzi, G., Ronchi, A., Pigatto, P. Toxic effects of mercury in humans and mammals. Chemosphere 263, 127990. 2020.

[7] Li, Y.P., Xie, T.C., Zha, Y.D., Du, W.C., Yin, Y., Guo, H.Y.,. Urea-enhanced phytoremediation of cadmium with willow in pyrene and cadmium contaminated soil. J. Hazard Mater. 405, 124257. 2021.

[8] Singh, S., Fulzele, D.P., Kaushik, C.P. Potential of Vetiveria zizanoides L. Nash for phytoremediation of plutonium(239Pu): chelate assisted uptake and translocation. Ecotoxicol. Environ. Saf. 132, 140–144. 2016

[9] Al-Baldawi, I.A., Abdullah, S.R.S., Anuar, N., Hasan, H.A. Phytotransformation of methylene blue from water using aquatic plant (Azolla pinnata). Environ. Technol. Inno. 11, 15–22. 2018.

[10] Ashraf, S., Ali, Q., Zahir, Z.A., Ashraf, S., Asghar, H.N. Phytoremediation: environmentally sustainable way for reclamation of heavy metal polluted soils. Ecotoxicol. Environ. Saf. 174, 714–727. 2019.

[11] Javed, M.T., Tanwir, K., Akram, M.S., Shahid, M., Niazi, N.K., Lindberg, S., Chapter 20 - phytoremediation of cadmium-polluted water/sediment by aquatic macrophytes: role of plant-induced pH changes. In: Hasanuzzaman, M., Prasad, M.N. V., Fujita, M. (Eds.), Cadmium Toxicity and Tolerance in Plants. AcademicPress, pp. 495–529. 2019.

[12] Buscaroli, A. An Overview of Indexes to Evaluate Terrestrial Plants for Phytoremediation Purposes (Review). Ecological Indicators 2017, 82, 367–380, 2017.

[13] Alaboudi, K. A., Ahmed, B., & Brodie, G. Phytoremediation of Pb and Cd contaminated soils by using sunflower (Helianthus annuus) plant. Annals of agricultural sciences, 63(1), 123-127. 2018.

Title: Risk assessment approach for heavy metals contaminated sites of mining waste storage

Author(s): Rusalina Lupu*[1], Irina Aura Istrate[2], Florin Nenciu[3], Diana Mariana Cocârță[1,4]

[1] Department of Energy Production and Use, Splaiul Independentei No. 313, Faculty of Energy Engineering, University of Science and Technology POLITEHNICA of Bucharest, 006042 Bucharest, Romania, lupurusalina@gmail.com (R.L.), diana.cocarta@upb.ro (D.M.C.)
[2] Department of Biotechnical Systems, Splaiul Independentei No. 313, Faculty of Biotechnical Systems Engineering, University of Science and Technology POLITEHNICA of Bucharest, 006042 Bucharest, Romania
[3] National Institute of Research—Development for Machines and Installations Designed for Agriculture and Food Industry—INMA Bucharest, 013811 Bucharest, Romania
[4] Academy of Romanian Scientists, 030167 Bucharest, Romania

Keyword(s): Risk assessment, soil investigation, exposure modelling, heavy metals, tailing dams

Abstract

Contaminated soils containing toxic and persistent pollutants present diverse and significant risks to both the environment and humans' health. Therefore, to protect the environment and public health, it is critical to emphasise how important it is to include the assessment of the potential hazards in predictive models related to long-term exposure to the contaminants.

This study is focused on presenting the functionality of an environmental risk assessment tool, specifically focusing on quantitative risk posed by carcinogenic compounds (as heavy metals) derived from the tailing dams, aligning with the Romanian contaminated sites regulation in force, while comparing the output values with a validated software widely used in Italy. At national level, there is no recognised and authorized tool for assessing human health risk from contaminated sites. So, the proposed instrument developed by University of Science and Technology POLITEHNICA of Bucharest may become a viable and present interest to the public and private institutions.

Introduction

Soil pollution is the result of naturally present as well as artificially produced contaminants. In the last centuries, the environment has faced a growing exposure to both natural and synthetic harmful chemicals due to industrialization, the widespread manufacturing of artificial chemicals, rapid urban growth, and intensified agricultural practices [1]. In terms of soil pollution, the Romanian soils are highly affected by the past mining activities and the waste derived given by the tailing dams, thus directly affecting the soil properties and quality [2], [3].

As part of the Soil Strategy for 2030 (2021) at European Level, Law of Management of Contaminated and Potentially Contaminated sites (2019) and Methodology on Contaminated and Potentially Contaminated Sites in Romania (2020), the current study is focused on improving the knowledge in soil contamination area, and the negative effects on humans' health. In addition, the study suggests actions tailored to the needs of the region in order to restore soil health while integrating and highlighting the value of a software tool in environmental investigation activities [4][5].

Materials and Methods

The evaluation of humans' health risks from contaminated sites with carcinogenic substances is a crucial environmental concern to safeguard people's well-being. Hence, arising the need of immediate action from public and private institutions in identifying and limiting the soil contamination. Due to a considerable amount of data while quantifying the exposure to soil contaminants, different specialized

environmental tools for risk assessment from contaminated sites have been developed at European and international level [6], [7]. Some examples are: CSOIL [8] (in Netherlands), Risk.Net [9] (in Italy), CLEA [10] (in United Kingdom). In Romania, between 2015-2017 a software tool dedicated to risk assessment from contaminated soils have been developed by the POLITEHNICA Bucharest (REMPET v1.0).

Heavy metals soil contamination analyses and results

The case study in the current paper is focused on soil contamination by the tailing dams in Jiu Valley region, southwestern Transylvania, Romania, and the effects posed by the soil contamination to the humans' health. Large-scale mining wastes and their unproper handling were the cause of the pollution in the region. As a result, there were persistent pollution leak into the rivers, but also into atmosphere from the soil. Contaminants considered for the investigated site are heavy metals.

Soil sampling, collection and analytical tests were performed in accordance with the requirements of the soil quality standards (STAS 7184/1:1984). A total of 27 soil samples from a 2250 m^2 area were taken as part of the present study. The contamination degree was evaluated based on the Romanian regulation in force – Ministerial Order no 756/1997. Normal, Alert and Intervention thresholds were considered taking into account the industrial land use scenario [11]. With the aim of identifying heavy metals concentration in soil, the analytical procedure was performed according to the current standard methods: ISO 11464:2006 [12]. Soil samples were dried and passed through a sieve of 2 mm openings in width. Afterwards, was homogenized with another 20-30 g of fine soil. Preparation for digestion was done according to EPA 3051A [13] and the soil samples were analysed using ICP-OES.

The highest concentration values ($mg/kg_{d.w.}$) of the pollutants identified in the investigated soil area were determined as: Fe > Mn > Zn > Ba > Ni > Cu > Cr total > Co > Pb > Mo > Cd.

The assessment carried out was focused on identifying the presence of different metals in soil based on the Romanian Regulation (21 metals compounds), out of the total only 11 types were present in the soil samples, presented in the list above. In the case of human health risk assessment, analysed data was focused on heavy metals identified in soil with the highest toxicity risk and carcinogenic potential (Ni, Pb, Cd) belonging to group 1 and 2A of IARC carcinogenicity classification[14]. However, Cd concentration is below the limit of quantification and was considered N/A.

Risk assessment and human exposure modelling

Human health risk assessment has been investigated using one software tool: "REMPET v1.0" (POLITEHNICA of Bucharest), which was developed in the framework of the research project REMPET, accessing National Funds, between 2015-2017 (UEFISCDI, REMPET, PNII-RU-TE2014-4-2348/contract nr. 354/01.10.2015). The software tool has the capability to conduct a rapid and precise evaluation of human health hazards originating from contaminated areas [15]. The second software tool used in the assessment was Risk.Net, developed by the University of Rome "Tor Vergata"[9].

There are three primary stages to assessing the risk to humans' health: exposure assessment, toxicity assessment, and risk characterization. The phase of exposure assessment implies determining the exposure magnitude, frequency, and duration of the exposed/potentially exposed population. Toxicity assessment involves hazard identification and dose-response assessment. Risk characterisation estimates the cancer and non-cancer hazard [6]. A reference level of individual risk is 10^{-6} is established, as recommended by the World Health Organization, signifying that an incidence of cancer among one million exposed individuals is considered as acceptable [16].

Results and discussion

The degree of soil contamination considering the national regulation in force was firstly evaluated. REMPET and Risk.Net allowed the dose estimation and the assessment of the carcinogenic risk of the exposed population to the contaminated sites via two different exposure pathways (for the current

industrial scenario, dermal contact and accidental soil ingestion). The min and max individual risks generated by REMPET, identified in the investigated area were between 7.68 x 10^{-4} and 1.28 x 10^{-3}, as of Risk.net the risk values were between 1.19 x 10^{-5} and 2.05 x 10^{-5}. The different risk values generated by both tools is given by the toxicological parameters, namely Absorbtion Factor (or ABS) of the contaminants, parameter used within the dermal contact exposure route equation. The ABS integrated in REMPET for Ni and Pb is 2 and 3, while the ABS in Risk.Net is 0.01 for both.

The risk derived from the presence of Ni in soil, in both cases is bigger than the one derived from Pb presence due to main reasons: i) the first one is related to the level of concentration in soil (for Ni 115.30 mg/$kg_{d.w.}$, while for Pb 15.98 mg/$kg_{d.w.}$), while the second one ii) is given by the level of carcinogenicity of these two chemical compounds: Slope Factor for Ni is 9.1 x 10^{-1} (mg/kg day)$^{-1}$ and for Pb is 8.5 x 10^{-3} (mg/kg day)$^{-1}$.

On the second hand, the risk information generated by the REMPET tool in the investigated area considers soil contamination with Ni which contributes more than 99% to the identified risk. Regarding the exposure pathway contributing mainly to the evaluated risk, the highest concern is given by the exposure to Ni and Pb via the dermal contact exposure route. Consequently, the risk values obtained using Risk.net software display otherwise data, Ni is contributing 64% and Pb 36% to the identified risk and the highest concern is given by the ingestion exposure pathway. Minimum, average and maximum carcinogenic risk, using REMPET and Risk.Net tools, evaluated for the investigated area was compared to the acceptable individual level of risk 1 x 10^{-6} (Figure 1).

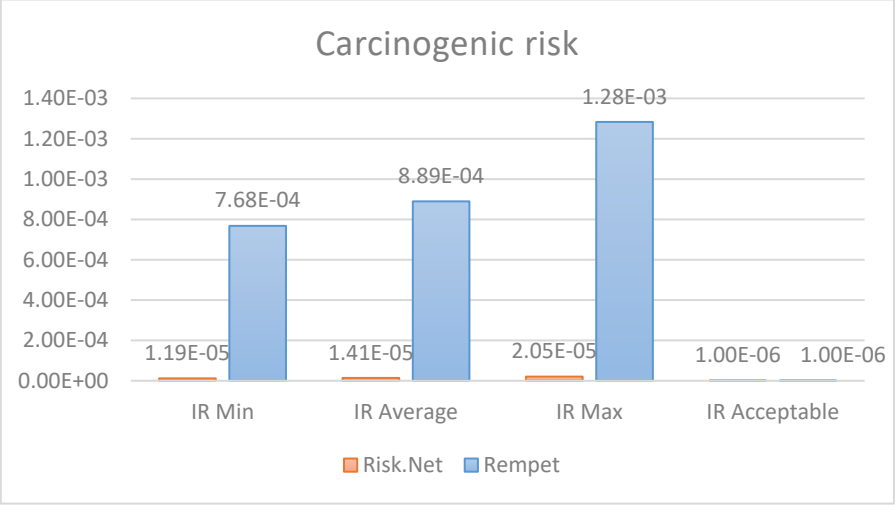

Figure 1. Minimum, average and maximum carcinogenic risk using Risk.net and REMPET

Conclusion

The evaluation of heavy metals in soil contaminated because of mining waste storage and their effects on human health have been studied. The study progressed the assessment of possible hazards to human health by employing a risk assessment software application (REMPET v1.0). Considering the human health risk values obtained in the current research, the mean carcinogenic risk using REMPET (8.89 x 10^{-4}) and Risk.Net (1.41 x 10^{-5}) is primarily determined by Ni (REMPET) and both Ni and Pb (Risk.Net), which in both cases is much higher comparable with the acceptable value recommended by WHO (10^{-6}). Herein, a higher attention must be paid to tailing dams soil contamination and the associated health effects which may endanger the proximity communities. The main findings showed that maintaining appropriate mining waste management practices and selecting the most suitable remediation technology are essential for restoring soil health. Soil pollution represents a big challenge

for the decision-makers, to protect public health and manage contaminated sites. Using an environmental software tool at a local level, such as REMPET, can really support the process on quantifying the data, reduce time on data management, and provide quality output information risks posed via different exposure pathways and health effects.

Acknowledgement

This research was supported by project Establishment and operationalization of a Competence Center for Soil Health and Food Safety – CeSoH, Contract no.: 760005/2022, specific project no.2, with the title: *Restoring soil health on unproductive land through biomass crops for sustainable energy - Soil- Bio mass- Sustainable*, Code 2, financed through PNRR-III-C9-2022 – I5 (PNRR-National Recovery and Resilience Plan, C9 Support for the private sector, research, development and innovation, I5, Establishment and operationalization of Competence Centers).

References

[1] FAO and UNEP, "Environmental, health and socio-economic impacts of soil pollution," in *Global assessment of soil pollution: Report*, FAO and UNEP, Ed. Rome, Italy: FAO and UNEP, 2021, p. 846.
[2] N. Walaszczyk and R. Jasiński, "Removal of Petroleum Derivative Pollutants from the Environment: Techniques and Methods," *Eng. Prot. Environ.*, vol. 21, no. 4, pp. 347–359, 2018, doi: 10.17512/ios.2018.4.3.
[3] M. Marinescu, M. Toti, V. Tanase, G. Plopeanu, I. Calciu, and M. Marinescu, "The Effects of Crude Oil Pollution on Physical and Chemical Characteristics of Soil," *Res. J. Agric. Sci.*, vol. 43, pp. 125–129, 2011.
[4] EU, "Thematic strategy for soil protection," *COD/2006/0086*, 2011. [Online]. Available: https://eur-lex.europa.eu/EN/legal-content/summary/thematic-strategy-for-soil-protection.html. [Accessed: 11-Apr-2024].
[5] A. ȘI P. MINISTERUL MEDIULUI and D. ȘI A. MINISTERUL LUCRĂRILOR PUBLICE, "METODOLOGIE de investigare a siturilor potențial contaminate și a celor contaminate," *MONITORUL OFICIAL nr. 823 bis din 8 septembrie 2020*, 2020. [Online]. Available: https://legislatie.just.ro/Public/DetaliiDocumentAfis/260085. [Accessed: 11-Apr-2024].
[6] D. M. Cocârţă, M. A. Stoian, and A. Karademir, "Crude oil contaminated sites: evaluation by using risk assessment approach," *Sustain.*, vol. 9, no. 8, p. 1365, 2017, doi: 10.3390/su9081365.
[7] D. M. Cocarta, E. C. Rada, M. Ragazzi, A. Badea, and T. Apostol, "Methodology for the Human Health Risk Assessment from the Thermoelectric Plants," *UPB Sci. Bull.*, vol. 70, no. Series C: Inginerie Electrica, No 1, pp. 41–50, 2008, doi: ISSN 1454-234x.
[8] P. Van Breemen, J. Quik, E. Brand, P. F. Otte, A. M. Wintersen, and F. Swartjes, "CSOIL 2020: Exposure model for human health risk assessment through contaminated soil. Technical description," *Rivm*, 2020.
[9] V. I., "Risk.Net - User Guide," no. September, pp. 1–126, 2019.
[10] DEFRA, "Contaminated land exposure assessment CLEA tool," *UK Government page*, 2015. [Online]. Available: https://www.gov.uk/government/publications/contaminated-land-exposure-assessment-tool.
[11] MINISTERUL APELOR PĂDURILOR ŞI PROTECŢIEI MEDIULUI, "ORDIN nr. 756 din 3 noiembrie 1997." MONITORUL OFICIAL nr. 303 bis din 6 noiembrie 1997, Romania, p. 1, 1997.
[12] "ISO 11464:2006 - Soil quality Pretreatment of samples for physico-chemical analysis," 2006.
[13] "EPA 3051A - MICROWAVE ASSISTED ACID DIGESTION OF SEDIMENTS, SLUDGES, SOILS, AND OILS." p. 2007.
[14] IARC, "Agents Classified by the IARC Monographs," *IARC*, 2023. [Online]. Available: https://monographs.iarc.who.int/agents-classified-by-the-iarc/. [Accessed: 24-Apr-2024].
[15] Cocârță D.M.; Stan C., *Riscuri pentru Sănătate în Industria Energetică - Indrumar Tehnic*. Bucharest: Editura Politehnica PRESS, 2017.
[16] C. . Dumitrescu, Cocârță, D.M.; Badea, and A., "An integrated modeling approach for risk assessment of heavy metals in soils.," *Sci. Bull. Ser. D*, vol. 74, pp. 217–228, 2012.

Title: Development of screening tools for the risk assessment applied to contaminated sites

Author: Iason Verginelli*

Laboratory of Environmental Engineering, Department of Civil Engineering and Computer Science Engineering, University of Rome Tor Vergata, Via del Politecnico, 1, 00133 Rome

verginelli@ing.uniroma2.it

Keywords: contaminated sites; human health; risk assessment; screening tools

Abstract

In recent decades, soil and groundwater contamination caused by abandoned waste disposal sites and industrial activities has become a critical environmental concern. Risks to human health because of toxic chemicals introduced into the environment are a matter of main concern to modern society, and the effective management of environmental contamination problems has become an important environmental priority of both national and European policies.

In this context, the management of contaminated sites often adopts a risk-based corrective action (RBCA) approach, wherein the actual pollution of a site is assessed based on the potential risk it poses to human health or the environment. When dealing with potentially contaminated sites, investigations typically begin with a preliminary screening phase, followed by a site-specific risk-based assessment [1]. This risk assessment is a valuable tool, providing a rational and objective foundation for setting priorities and making decisions [2]. Although using predetermined guideline values is straightforward and cost-effective compared to more complex site-specific assessment methods, exclusive reliance on such values can result in overly conservative cleanup actions due to a lack of site-specificity [3]. Therefore, a combined approach is generally recommended by employing predetermined screening values to streamline initial decision-making stages, followed by site-specific risk assessment to determine cleanup levels in later investigation phases [1]. The ASTM Risk-Based Corrective Action (RBCA) standards, notably ASTM E1739-95 for petroleum sites and ASTM E2081-00 for chemical release sites, serve as key technical references for the risk-assessment approach. These standards guide evaluating potential health effects on exposed receptors and the environment based on data collected during contaminated site investigations, determining whether remedial action is necessary and establishing specific risk-based remediation goals. The ASTM RBCA framework employs a tiered approach to risk and exposure assessment, where each tier represents a different level of complexity. Tier 1 involves contamination screening values employing simple analytical models and conservative default values. Tier 2, which aims to evaluate site-specific target levels, relies on site-specific input data while still utilizing analytical models for contaminant transport. Typically, risk analysis is conducted under Tier 2 conditions, balancing detailed site assessment needs and the practicality of using a straightforward management tool [3]. Tier 3, which involves more detailed contaminant transport descriptions through numerical models, is employed in specific circumstances where greater detail is required.

Over the years, significant advancements have been made in developing and refining risk analysis tools that allow overcoming some of the limitations of standard screening models while keeping the original simplicity and analytical form of the Tier 2 evaluations.

In this work, the following free screening tools developed by the Laboratory of Environmental Engineering at the University of Rome Tor Vergata over recent years will be presented:

- Risk-net: software for the application of risk assessment at contaminated sites (available at www.reconnet.net);
- Leach8: software for the application of risk assessment at landfill sites (available at www.reconnet.net);
- PVI2D: screening tool for the assessment of petroleum vapor intrusion (available at www.pvitoools.net);
- RemChem: software for the assessment and management of workers' risks during remediation activities (developed within a BRIC project of INAIL and available at isa.uniroma2.it);
- CVI2D: software for the assessment of vapor intrusion of chlorinated solvents (available at www.pvitoools.net).

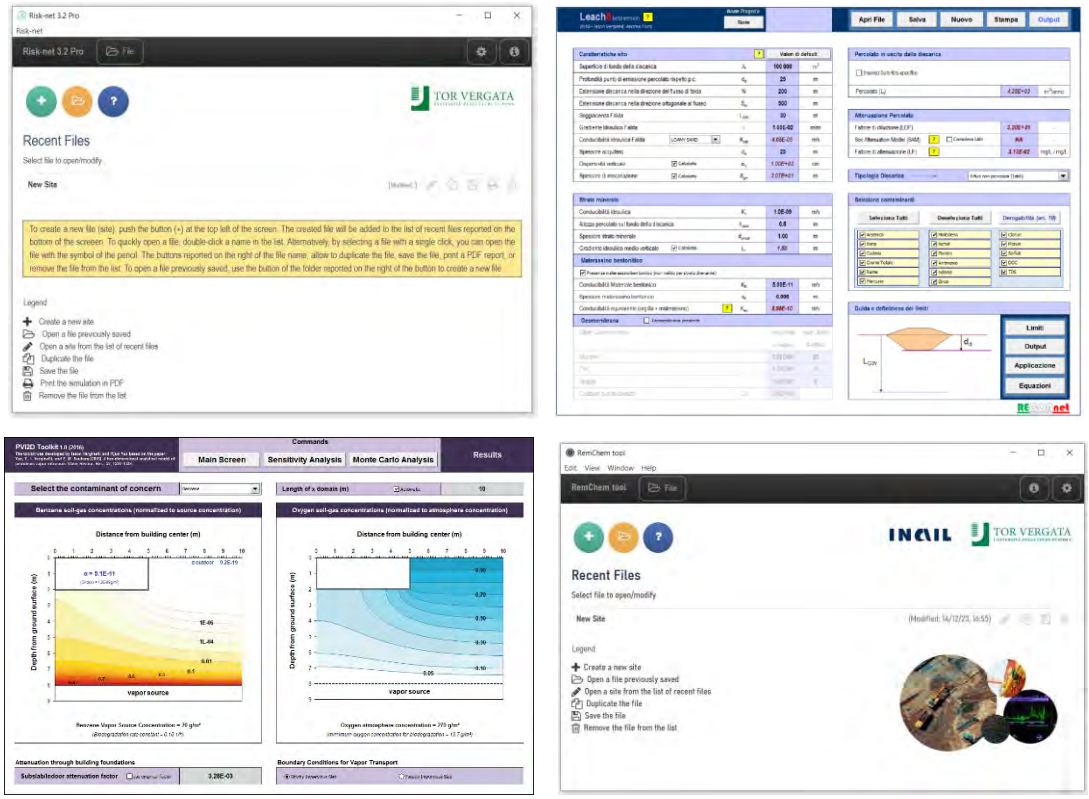

Figure 1. Examples of screening tools developed by the University of Rome Tor Vergata.

Table 1 reports the models and procedures implemented in the various developed tools. Before their official release, each tool underwent a detailed and rigorous verification and validation process to ensure the accuracy and reliability of the models and algorithms implemented. The testing phase comprised both internal assessments and external peer reviews. These steps were taken to detect and address any potential issues, thereby assuring that the tools satisfy the necessary quality and performance standards.

Table 1. Models and procedures implemented in the developed tools.

Tool	Models/procedures implemented in the software
Risk-net	ASTM (2000) [4]; ISPRA (2008) [5]
Leach8	ISPRA (2005, 2011) [6-7]
PVI2D	Yao et al. (2016a, 2016b) [8-9]; Verginelli et al. (2016) [10]
RemChem	ASTM (2000) [4]; U.S.EPA (1996; 2002; 2006) [11-13]; ISPRA (2008) [5]
CVI2D	Yao et al. (2017) [14]; Verginelli et al. (2019) [15]

References

[1] Provoost J., Cornelis C., Swartjes F., "Comparison of Soil Clean-up Standards for Trace Elements Between Countries: Why do they differ?". J. Soils Sediments 6, 173-181, (2006).

[2] Ferguson C., Darmendrail D., Freier K., Jensen B.K., Jensen J., Kasamas H., Urzelai A., Vegter J., "Risk Assessment for Contaminated Sites in Europe". Volume 1. Scientific Basis. LQM Press, Nottingham, (1998).

[3] Verginelli, I., Baciocchi, R., "Role of natural attenuation in modeling the leaching of contaminants in the risk analysis framework". Journal of environmental management, 114, 395-403, (2013).

[4] ASTM, "Standard Guide for Risk-Based Corrective Action". Designation: E-2081-00, (2000).

[5] ISPRA, "Criteri metodologici per l'applicazione dell'analisi assoluta di rischio ai siti contaminati". rev. 2, (2008).

[6] ISPRA, "Criteri metodologici per l'applicazione dell'analisi assoluta di rischio alle discariche". Agenzia per la Protezione dell'Ambiente e per i Servizi Tecnici, (2005).

[7] ISPRA, "Nota integrativa della nota ISPRA prot. n. 30237 del 16/09/2010, sull'applicazione della circolare del Ministero dell'ambiente della Tutela del Territorio e del Mare n. 0014963 del 30/06/2009". prot. ISPRA n. 36365 del 31/10/2011, (2011).

[8] Yao, Y., Verginelli, I., Suuberg, E. M., "A two-dimensional analytical model of petroleum vapor intrusion", (2016a).

[9] Yao, Y., Wang, Y., Verginelli, I., Suuberg, E. M., Ye, J., "Comparison between PVI2D and Abreu–Johnson's Model for Petroleum Vapor Intrusion Assessment". Vadose Zone Journal, 15(11), 1-11, (2016b).

[10] Verginelli, I., Yao, Y., Suuberg, E. M., "An excel®-based visualization tool of two-dimensional soil gas concentration profiles in petroleum vapor intrusion". Groundwater Monitoring & Remediation, 36(2), 94-100, (2016).

[11] U.S.EPA, "Soil Screening Guidance: Technical Background Document". Office of Solid Waste and Emergency Response Washington, DC, Pub. Num. EPA/540/R95/128, (1996).

[12] U.S.EPA, "Supplemental Guidance for Developing Soil Screening Levels for Superfund Sites". OSWER 9355.4-24, (2002).

[13] U.S.EPA, "AP-42: Compilation of Air Emissions Factors", (2006). Available at: https://www.epa.gov/air-emissions-factors-and-quantification/ap-42-compilation-air-emissions-factors

[14] Verginelli, I., Yao, Y., Suuberg, E. M., "Risk assessment tool for chlorinated vapor intrusion based on a two-dimensional analytical model involving vertical heterogeneity". Environmental Engineering Science, 36(8), 969-980, (2019).

[15] Yao, Y., Verginelli, I., Suuberg, E. M., "A two-dimensional analytical model of vapor intrusion involving vertical heterogeneity", (2017).

Title: Python-QGIS-based Model for Assessing and Mapping Subsurface Volatile Organic Compound (VOC) Emissions

Author(s): Marco Pitardi*[1], Sofia Costanzini[1], Nicolò Tonolo[2], Alessandra Cecconi[2], Sergio Teggi[1], Iason Verginelli[2], Simona Berardi[3]

[1] *University of Modena e Reggio Emilia, Via Università 4, 41125, Modena, Italy, marco.pitardi@unimore.it,*
[2] *University of Rome 'Tor Vergata', Via del Politecnico 1, 00133, Roma, Italy,*
[3] *INAIL, Department of Technological Innovations and Safety of Plants, Anthropic Products and Settlements, Via Ferruzzi 30/40 00143 Roma, Italy*

Keyword(s): Air Quality, Volatile Organic Compounds (VOC), Geographic Informative Systems (GIS), Contaminated sites.

Abstract

The migration of Volatile Organic Compounds (VOCs) in contaminated sites and the consequent emissions from the subsurface are critical factors in evaluating the impacts on indoor or outdoor air quality.
Understanding these processes is essential for assessing risks and ensuring compliance with safety regulations outlined in the Italian Legislative Decree 81/2008, particularly in commercial or industrial sites where high concentrations of contaminants may be present in the subsurface.
The present work is part of the project "Monitoring system of air concentrations and subsurface VOCs emissions at contaminated sites", an INAIL research project in collaboration with the University of Modena and Reggio Emilia, the University of Rome "Tor Vergata" and ATS of Milan.
Central to this project's objective is developing and validating an automated monitoring system employing flux chambers and air concentration devices equipped with Photoionization Detectors (PID) sensors. These sensors are well known for their affordability and facilitate real-time data collection, which is transmitted via a 4G/5G connection to a centralized server. The raw data are then cataloged within a PostgreSQL database, accessible through a QGIS platform.
Additionally, a Python-QGIS-based model was developed within this project to assess VOC emissions from the subsurface based on characterization data such as concentrations of contaminants in soil and groundwater, as well as other factors like lithology and meteorological conditions. Specifically, a pre-built database containing soil and pollutant parameters was included in a Python-based model, developed to simulate soil VOCs emissions into the atmosphere. The actual presence of multiple VOCs in the subsurface and their distribution among different phases, the potential saturation conditions that may be reached with the consequent formation of Light Non-Aqueous Phase Liquids (LNAPL), the diffusive gas transport in a moisture soil profile variable with depth are all issues simulated by the model.
The code created using Python will be integrated into a QGIS platform as a complete and functional toolbox. This toolbox is designed to allow even non-expert users of Python to run simulations and evaluate the presence of VOCs by using georeferenced maps of fluxes to identify the areas of potential major concern in terms of VOC emissions. These data can serve in the early stage as a supporting tool for designing monitoring soil gas plans. Furthermore, the tool will assist in interpreting collected field data as it also includes the capability to calculate expected concentrations within flux chambers. Comparing measured and predicted VOC fluxes will refine the conceptual model and, consequently, the

risk assessment. The tool will be integrated in an easy-to-use graphical interface (see an example in **Figure 1**).

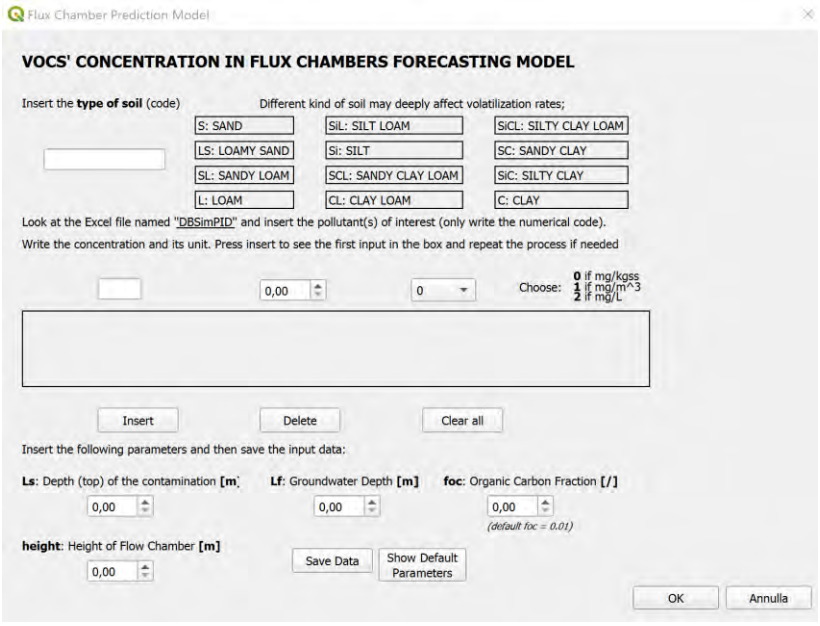

Figure 1. The graphical user interface of the QGIS toolbox

The concentrations modeled by the toolbox can also be utilized as an input for CAREA [1], an atmospheric Python-GIS-based Gaussian dispersion model for pollutants. The link between the two models could lead to the development of a unified model for investigating the migration of contaminants from the subsoil to the surface and their dispersion in the atmosphere through a QGIS platform.

The input data required by the tool is collected in a database that contains all the parameters requested by a monitoring system. This database includes information on the physical and chemical properties of various pollutants, such as solubility, molecular weight, and Henry's constant, sourced from the ISS INAIL 2018 database [2]. It also contains regulatory limits provided by Italian law for soil, subsoil, and groundwater [3], regulatory limits for air concentrations [4] and detection limits for PID sensors and response factors [5].
The processed output consists of the VOC flux emitted from the soil, which will be displayed at the end of the tool's run on QGIS.

The application presented in this study will undergo evaluation and experimentation in the coming months; therefore, modeling and its corresponding outputs will be assessed during future development phases.

References

[1] *Teggi, S., Costanzini, S., Ghermandi, G., Malagoli, C. and Vinceti, M. (2018). A GIS-based atmospheric dispersion model for pollutants emitted by complex source areas. Science of the total environment, 610, 175-190.*
[2] *ISS, INAIL (2018), Banca dati ISS INAIL per Analisi di Rischio Sanitario Ambientale.*
[3] *Tables 1,2, Attachment 5 to Parte 4 of the D.Lgs 152/2006 e ss.mm.ii. "Norme in materia ambientale", Parte Quarta, Titolo V "Bonifica dei siti Contaminati".*
[4] Attachments 38 and 43 to D.Lgs 81/2008 e ss.mm.ii. "Attuazione dell'articolo 1 della legge 3 agosto 2007, n. 123, in materia di tutela della salute e della sicurezza nei luoghi di lavoro".
[5] Alphasense (2009), "VOC Correction Factor, Application Note".

Title: Radon Gas Monitoring in the Headspace of Groundwater Wells for the Evaluation of Residual LNAPL Contamination

Authors: Alessandra Cecconi*[1], Iason Verginelli[1], Renato Baciocchi[1], Camilla Lanari[2], Federico Villani[2], Guido Bonfedi[2]

[1] *Department of Civil Engineering and Computer Science Engineering, University of Rome Tor Vergata, Via del Politecnico, 1, 00133 Rome, Italy*
[2] *Eni Rewind S.p.A., Piazza M. Boldrini 1, 20097 San Donato M.se (MI), Italy*

Keywords: Radon deficit technique, LNAPL delineation, Soil gas, Field test protocol, Groundwater monitoring wells

Abstract

The occurrence of light non-aqueous phase liquids (LNAPL) in hydrocarbon-contaminated sites is typically monitored by analyzing the apparent thickness of the free product in the piezometric network [1,2]. This approach, however, does not provide information on the distribution of LNAPL in residual form, which is essential for a proper design of remediation activities [3,4]. Among the possible alternatives, in recent decades, there has been growing interest in utilizing naturally occurring radon (Rn) as a method for detecting and quantifying LNAPL in the subsurface. Because of its preferential partitioning into oily phases, the natural activity concentrations of Rn in soil gas the subsurface can be influenced by LNAPL contamination [5]. Specifically, Rn concentrations in soil gas are expected to decrease in areas impacted by LNAPL compared to background values in uncontaminated zones, creating a measurable Rn deficit that can be used to identify and quantify LNAPL in the subsurface [6]. In the last few decades, the use of radon (Rn) has been proposed as an alternative approach. Due to its proven tendency to preferentially partition into oily phases, it is considered a natural tracer for the presence of LNAPL in the subsurface in both residual and mobile form [7,8]. It has been shown that in the areas contaminated by LNAPL, there is a local decrease of Rn concentration in the soil gas compared to the background value detected in the subsurface not impacted by LNAPL. By monitoring the Rn in the soil gas, it is possible to determine a Rn deficit between the two zones, which can be used for identifying and quantifying LNAPL in the subsurface.
In this paper, the feasibility of using Rn monitoring data in soil gas for this purpose is analyzed on a modelling and experimental level. To this end, an analytical model was developed to describe the expected Rn behavior in the presence of separate phases in the subsurface [9,10]. Using the developed solution, the vertical Rn concentration profiles in the soil gas expected above the source zone and in the area not impacted by LNAPL were evaluated under different conditions. Based on the simulations performed, it was observed that the parameter that most influences the effectiveness of the use of Rn as a tracer for LNAPL is the vertical distance of the soil gas probe from the source zone. In particular, at distances greater than 2 m, the method appears to be no longer sensitive to the presence of LNAPL. Therefore, using soil gas probes to apply the Rn-deficit technique for estimating LNAPL would only be applicable if the probes are installed in proximity of the source zone. As an alternative, Rn can be monitored in the headspace of groundwater monitoring wells, typically screened in the portion affected by the presence of LNAPL (saturated zone and capillary fringe) [11]. In order to verify the performance of the method, a series of tests were conducted at two gasoline stations owned by Eni, where the concentrations of Rn and other markers (O_2, CO_2, CH_4 e VOC) were analyzed using portable

instrumentation in the headspace of monitoring wells installed at the sites. In all the tests carried out, Rn concentrations in the hydrocarbon-impacted zones were lower than in the background areas, thus indicating that the method is applicable for the determination of the presence of residual phase in the unsaturated zone, which is not possible with the sole monitoring of the free product in monitoring wells or with water sampling. The method was also effective for estimating the expected concentrations in the investigated area, with results consistent with those available from the characterization phase. In the application of the method, some uncertainties were found related to the presence of heterogeneities in the subsurface (which may affect the estimation of the Rn deficit) and to the temporal variabilities (daily and seasonal) of Rn emissions from the subsurface, suggesting that in such cases these estimates should be considered semi-quantitative.

To address the daily variability of soil gas Rn concentrations, an alternative sampling mode was tested. Soil gas Rn measurements were still performed in groundwater monitoring wells but using passive Rn dosimeters. The devices were installed in the headspace of the wells for a few days to provide Rn activity data representative of the point under investigation. This approach potentially improves the performance of the method and overcomes some of the limitations encountered, by allowing Rn measurements to be performed at a depth close to the NAPL source zone and also ensuring that detected Rn deficits are independent of daily Rn variations.

Following the results obtained, it is believed that Rn monitoring in the well headspace is a rapid and minimally invasive method for the identification of mobile and residual phase LNAPL, which can prove additional information to that typically available from the piezometric network monitoring alone. Future efforts should be directed toward evaluating the accuracy of this method for a quantitative assessment of residual LNAPL saturations.

References

[1] US EPA. Ground Water Issue: Light Nonaqueous Phase Liquids; US EPA: Washington, DC, USA, 1995.
[2] CL:AIRE. An Illustrated Handbook of LNAPL Transport and Fate in the Subsurface; CL:AIRE: London, UK, 2014.
[3] ITRC. LNAPL Site Management: LCSM Evolution, Decision Process, and Remedial Technologies; ITRC: Washington, DC, USA, 2018.
[4] ITRC. Implementing Advanced Site Characterization Tools; ITRC:Washington, DC, USA, 2019.
[5] Nazaroff,W.W. Radon Transport from Soil to Air. Rev. Geophys. 1992, 30, 137‐160.
[6] ITRC. Dense Non-Anazaqueous Phase Liquids (DNAPLs): Review of Emerging Characterization and Remediation Technologies. Interstate Technology and Regulatory Cooperation Work Group, DNAPLs Chemical Oxidation Work Team, 2000.
[7] Semprini, L.; Hopkins, O.S.; Tasker, B.R. Laboratory, Field and Modeling Studies of Radon-222 as a Natural tracer for Monitoring NAPL Contamination. Transp. Porous Media 2000, 38, 223‐240.
[8] Schubert, M. Using Radon as Environmental Tracer for the Assessment of Subsurface Non-Aqueous Phase Liquid (NAPL) Contamination–A Review. Eur. Phys. J. Spec. Top. 2015, 224, 717‐730.
[9] Cecconi, A.; Verginelli, I.; Baciocchi, R. Modeling of Soil Gas Radon as an in Situ Partitioning Tracer for Quantifying LNAPL Contamination. Sci. Total Environ. 2022, 806, 150593.
[10] Cecconi, A.; Verginelli, I.; Barrio-Parra, F.; De Miguel, E.; Baciocchi, R. Influence of Advection on the Soil Gas Radon Deficit Technique for the Quantification of LNAPL. Sci. Total Environ. 2023, 875, 162619.
[11] Cecconi, A.; Verginelli, I.; Baciocchi, R.; Lanari, C.; Villani, F.; Bonfedi, G. Using Groundwater Monitoring Wells for Rapid Application of Soil Gas Radon Deficit Technique to Evaluate Residual LNAPL. J. Contam. Hydrol. 2023, 258, 104241.

Title: Numerical modeling of in situ thermal desorption for soil remediation: preliminary results

Authors: Filippo Fazzino[1]*, Antonio Gagliano[2], Federico Vagliasindi[1], Pietro Paolo Falciglia[1]

[1] *Department of Civil Engineering and Architecture, University of Catania, Viale Santa Sofia, 64, Catania, Italy*
[2] *Department of Electrical Electronic and Computer Engineering, University of Catania, Viale Santa Sofia, 64, Catania, Italy*

Keywords: In situ thermal desorption; organic pollutant remediation; numerical modelling; process optimization; thermal conductive heating.

Abstract

Thermal desorption is a process widely used to remediate volatile organic compounds (VOCs) and semi-volatile organic compounds (SVOCs) in soils. It based on soil heating, which results in the vaporization and, subsequently, desorption of organic pollutants [1].
Thermal Conductive Heating (TCH) is one of the most performing and effective *in situ* thermal technologies. Its implementation entails the insertion into the contaminated soil of cylindrical elements containing electrical resistances capable of reaching temperatures up to 1000°C (Joule effect). The transfer of generated heat to the surrounding soil occurs through mechanisms of conduction (i.e., exchange of thermal energy by direct contact) and convection (i.e., transport of thermal energy by motion of a fluid). Pollutants, reaching the respective vaporization temperatures, pass to the vapor state and are extracted by soil vapor extraction wells [2].
One of the TCH main limits to a widespread application is its considerable energy consumption, which is difficult to predict at a design stage due to its dependance on site specific conditions (i.e., pollutant properties, soil features) and TCH configuration (i.e., depth, arrangement, and spacing of the heating wells). Accordingly, preliminary characterization of both site and contamination state (in terms of pollutants and extension) is necessary in pilot-scale application planning, which, in turns, allows the definition of the optimum TCH configurations [2].
In this context, numerical modeling would represent an effective and rapid tool able to evaluate a large series of process conditions in order to reach this objective. By virtue of that, research recently started to investigate the suitability of COMSOL Multiphysics modeling software for such purpose [3,4].
In the present study, the heat transfer induced by the heating elements of an *in situ* TCH application to a contaminated soil have been investigated via numerical simulation through COMSOL Multiphysics. The study preliminary investigated the effects of some operating conditions (i.e.: pollutant concentration, temperature and spacing of heating elements) on the heat transfer process. The ultimate aim is to demonstrate the possibility of using modeling software at the design stage of TCH applications in order to select the system configuration that optimizes soil remediation.
COMSOL Multiphysics allows the study of various physical phenomena through the numerical solution of partial differential equations by using the finite element method. In particular, the physics module “Heat transfer in porous media” has been adopted for simulating a contaminated soil volume of 18 m^3 (area of 3 × 3 m and depth of contamination of 2 m). Sand has been chosen as soil constituting material, whereas bitumen as the organic pollutant. Their physical-chemical properties are reported in Table 1. Four scenarios of bitumen contamination have been considered (7.5, 12.1, 15.5, and 18.0% w/w) in addition to the uncontaminated soil option.

Table 1. Physical-chemical properties of materials used in the simulation

Property	Sand	Bitumen
Density [kg/m^3]	1560	1600
Thermal conductivity [W/m·K]	0.20	0.15
Specific heat [J/kg·K]	800	2000
Porosity	0.3	-

Four 1.8 m height heating elements with a radius of 9 cm have been arranged in proximity of the vertices of the soil volume with variable spacing distance (1.5 and 2 m). Constant TCH element temperatures of 750 and 900°C have been investigated and results are discussed as follow.
In the following, effects of bitumen concentration (Figures 1 and 2), operating temperature (Figure 3), and spacing of heating elements (Figure 4) are reported.

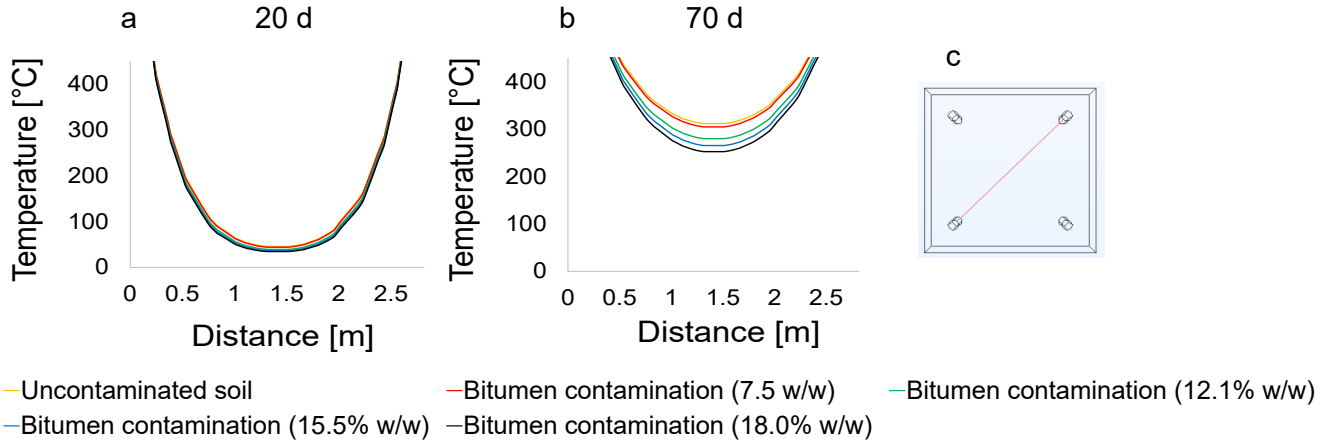

Figure 1. Comparison of soil temperature variations among the different contamination scenarios at 20 (a) and 70 (b) days of treatment (legend at bottom) at operating temperature of 750°C; (e) diagonal plane in which temperature variations were evaluated.

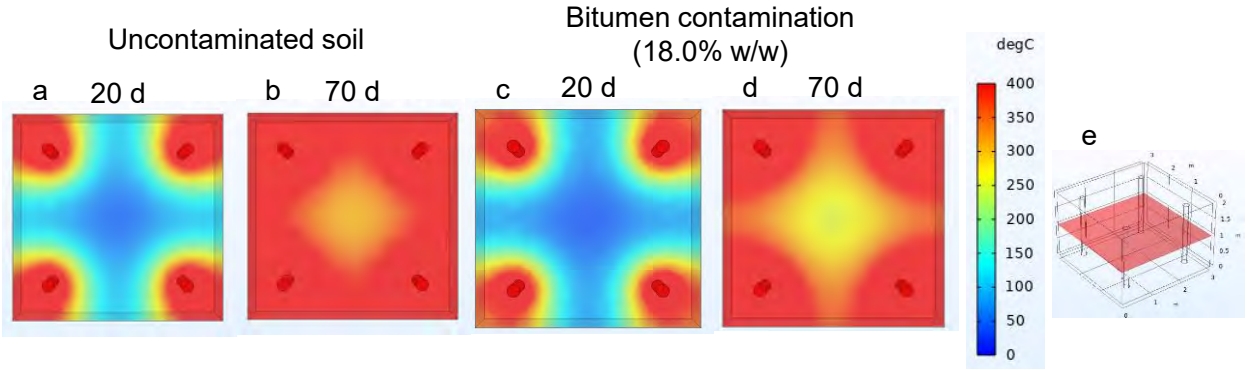

Figure 2. Soil temperature variation in the horizontal plane (e) for uncontaminated soil (a and b after 20 and 70 days, respectively) and bitumen contamination at 18.0% w/w (c and d after 20 and 70 days, respectively) at an operating temperature of 750°C.

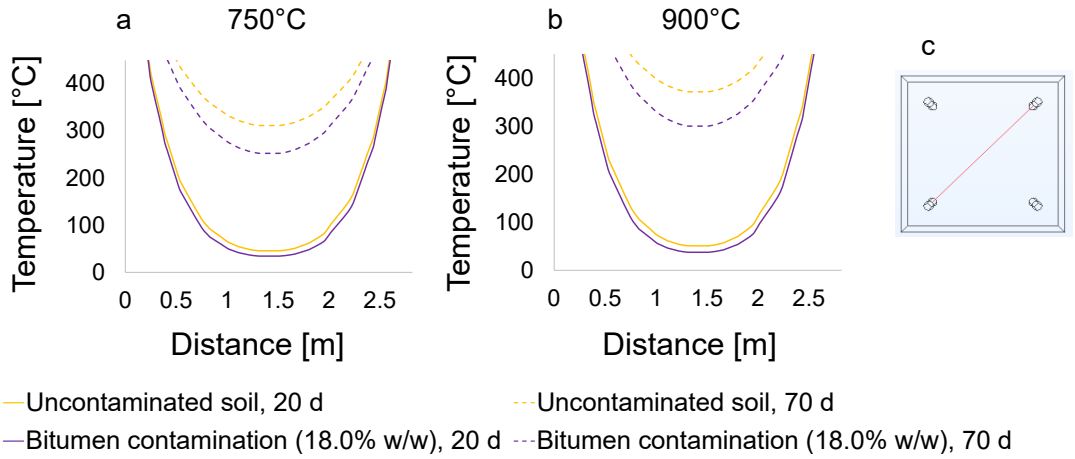

Figure 3. Effects of operating temperature (a, 750°C, b, 900°C) on heat transfer in uncontaminated and bitumen contaminated soil (18.0% w/w) at 20 and 70 days of treatment (legend at bottom); (c) diagonal plane in which temperature variations were evaluated.

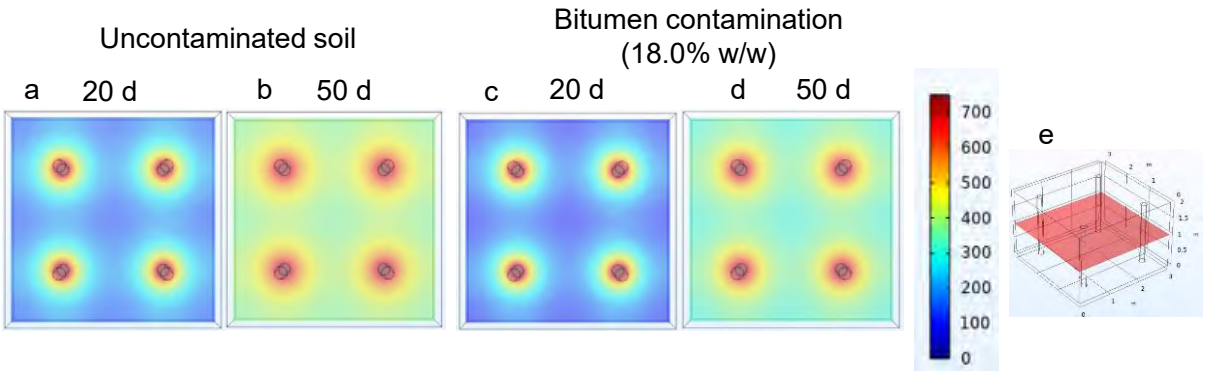

Figure 4.Effects of heating element spacing (1.5 m) on heat transfer (a and b after 20 and 50 days, respectively) and bitumen contamination at 18.0% w/w (c and d after 20 and 50 days, respectively); (e) horizontal plane in which temperature variations were evaluated.

What firstly emerges is that soil temperatures were higher around the heating elements and spread radially with minimum values in the central zone of the volume (Figures 1 and 2). Moreover, the more the concentration of bitumen the less the soil was prone to heat up (Figure 1 b). Such evidence is consistent with the heat transfer equation. Indeed, as the bitumen content increases, the specific heat (i.e. the amount of heat necessary to raise the temperature of 1 kg of material by 1 K) of the heterogeneous material sand-bitumen increases. Specifically from 800 J/kg·K (i.e., sand) to 922, 979, 1014, and 1048 J/kg·K, in cases of bitumen contamination at 7.5, 12.1, 15.5, and 18.0% (w/w), respectively. Similarly, thermal conductivity (i.e. the ability of a material to conduct heat) decreases as the presence of bitumen in the soil increases.

The target temperature has been set at 300°C, namely the temperature of bitumen vaporization. On the basis of this assumption, it can be noted that the mildest contamination scenario (i.e., bitumen at 7.5% w/w) corresponded to the fastest beginning of desorption process (i.e., 69 days to reach 300°C in the barycentric point, Figure 1 b), at the operating temperature of 750°C, versus 74, 78, and 81 days in cases of soil contamination with 12.1, 15.5, and 18.0% (w/w) of bitumen. Such delays entailed

corresponding increases of the specific energy consumption (necessary to start the vaporization process of the organic contaminant) of 120, 216, and 288 MWh, respectively, in the cases of bitumen contamination at 12.1, 15.5, and 18.0% (w/w) compared to the 7.5% (w/w) scenario. It is highlighted how the application of COMSOL Multiphysics software delivers results consistent with full-scale TCH applications since actual treatment times are known to be in the order of months [1].

The effects of a different treatment temperature (i.e., 900°C) and heating elements spacing (i.e., 1.5 m) have been also evaluated (Figures 3 and 4). With regard to the former, it has been expectedly observed that the more the operating temperature the less the time to reach 300°C. Particularly, with heating elements at 900°C, in the most severely contaminated scenario (i.e., bitumen at 18.0% w/w), the desorption process started after 70 days of treatment (Figure 3) versus 81 days at the operating temperature of 750°C.

Similarly, by reducing the spacing between the heating elements from 2 to 1.5 m at the operating temperature of 750°C, the heat transfer resulted even faster since the target temperature was reached in the barycentric point of the volume after 50 days of treatment in the case of bitumen contamination of 18.0% w/w (Figure 4 d). Moreover, regardless of the level of contamination, it is evident that heating elements closer to each other induced a more homogeneous heat transfer (Figure 4).

Although such preliminary results are promising, the numerical modeling approach requires further investigation. First of all, it would be advisable to make the simulation more realistic through the addition of the physics “Electric current” in order to determine the electrical supply needed to heat the elements. Secondly, the interaction between the water naturally present in the soil and the organic contaminant should be explored and the effects of that on heat transfer and pollutant desorption evaluated. Finally, the numerical simulation should be validated with data obtained from real full-scale *in situ* TCH applications.

To sum up, in light of the reported preliminary results, it can be concluded that the modeling approach is potentially applicable (in partial or total replacement of pilot-scale tests) for the optimization of process conditions, remediation times and energy consumption of *in situ* TCH application already at its design stage. In fact, through this tool, different possible process conditions and treatment configurations (such as contamination scenarios, operating temperatures, arrangements and spacing of heating elements) could be easily investigated in order to maximize the removal of organic pollutant(s) and optimize costs and times of the treatment.

References

[1] Ding D, Song X, Wei C, LaChance J. A review on the sustainability of thermal treatment for contaminated soils. Environmental Pollution 2019;253:449–63. https://doi.org/10.1016/j.envpol.2019.06.118.

[2] Sun X, Zhao L, Huang M, Hai J, Liang X, Chen D, et al. In-situ thermal conductive heating (TCH) for soil remediation: A review. Journal of Environmental Management 2024;351:119602. https://doi.org/10.1016/j.jenvman.2023.119602.

[3] Wang W, Li C, Li Y-Z, Yuan M, Li T. Numerical Analysis of Heat Transfer Performance of In Situ Thermal Remediation of Large Polluted Soil Areas. Energies 2019;12:4622. https://doi.org/10.3390/en12244622.

[4] Xu X-Y, Hu N, Wang Q, Fan L-W, Song X. A numerical study of optimizing the well spacing and heating power for in situ thermal remediation of organic-contaminated soil. Case Studies in Thermal Engineering 2022;33:101941. https://doi.org/10.1016/j.csite.2022.101941.

PARALLEL SESSION: D6

Biorefineries

Bioproducts from mixed civil and industrial wastewater

An innovative biorefinery approach for selective hexanoic acid production from wine lees

Authors: Paolo Dessì[1,2], Meritxell Romans-Casas[1], Elisabet Perona-VIco[3], Michele Tedesco[4], Hubertus V.M. Hamelers[5], Lluis Bañeras[3], M. Dolors Balaguer[1], Sebastià Puig[1]

[1] *LEQUiA, Institute of the Environment, University of Girona. Campus Montilivi, Carrer Maria Aurèlia Capmany 69, E-17003 Girona, Spain*
[2] *Department of Agricultural Sciences, University of Naples Federico II, Via Università 100, 80055 Portici, Italy*
[3] *Molecular Microbial Ecology Group, Institute of Aquatic Ecology, University of Girona, Maria Aurèlia Capmany 40, 17003 Girona, Spain*
[4] *TNO, Sustainable Process and Energy Systems, Lange Kleiweg 1D, 2288 GH Rijswijk, The Netherlands*
[5] *Wetsus, European Centre of Excellence for Sustainable Water Technology, Oostergoweg 9, 8911, MA, Leeuwarden, The Netherlands*

Corresponding author: Paolo Dessì. Email: paolo.dessi@unina.it.

Keyword(s): biochemical, caproic acid, chain elongation, fermentation, pertraction

Abstract

Chemical industry is expected to become the first global oil consumer by 2050, with a forecasted requirement of 2.4 billion L [1]. However, environmental concerns, resource depletion, market dynamics, and the increasing carbon pricing will make the business-as-usual model unsustainable. In this scenario, organic waste or industrial byproducts can progressively displace fossil fuels as a raw material for producing a wide array of chemicals, transforming chemical industries in so-called “biorefineries” [2].

The agri-food sector produces over one billion tons of organic waste per year worldwide, which will inevitably increase in the next years due to population growth, with increasing concerns on waste management. However, organic waste also represents a relevant business opportunity, as its production matches the scale of feedstock required by chemical industry. Thus, innovative technologies must be developed to exploit this hidden potential.

Several biorefinery models have been developed to convert carbohydrates, proteins and lipids from agricultural waste or byproducts into chemical products including short-chain carboxylic acids (SCCAs) and ethanol through fermentation [3]. However, the consolidation of these models at full scale is hindered by the low market value of those products (0.4-1.5 €/kg for SCCAs and 0.7-1.0 €/kg for ethanol). Furthermore, their separation and purification are technically difficult and expensive being such products water miscible.

Over one decade ago, it was observed that certain microorganisms, referred to as “chain elongators”, can produce middle chain carboxylic acids (MCCAs) in presence of SCCAs and an electron donor such as ethanol through a reaction called “reverse *β*-oxidation” [4]. The main product obtained through such reaction is hexanoic (or caproic) acid, a molecule with relatively high market value (2.5-3.5 €/kg) that finds industrial application as food additive, green pesticide, and lubricant, among others, besides being a building block to produce bioplastics and biofuels [5,6]. Notably, hexanoic acid is only partially soluble

in water, with a solubility of 10.8 g/L under standard conditions, which considerably facilitates downstream processing.

The relatively high value, wide applicability and ease of purification makes hexanoic acid an ideal target product in biorefineries. This attracted the attention of several research groups, that in a relatively brief time unrevealed the fundamentals and the biochemistry of the process, as well as developing and optimizing bioreactors to achieve relatively high production rates and selectivity [7]. The success of this research field is further demonstrated by the appearance of full-scale plants and start-ups, such as ChainCraft in The Netherlands and Capro-X in the US.

Despite the high promise, some drawbacks remain to be addressed. First, real waste substrates contain undesired microorganisms (such as methanogens or acetogens) whose metabolism could direct a share of the carbon flow away from hexanoic acid production, resulting in lower product yield and purity. Secondly, some feedstocks, such as cheese whey or wine lees, contain an excess of organic compounds requiring dilution to avoid inhibiting the chain elongating microorganisms. Finally, the reverse *β*-oxidation pathway requires specific feedstock characteristics, including precise ratios between electron donor (i.e., ethanol) and electron acceptors (i.e., SCCAs) that usually do not match with the characteristics of the substrate to be treated. Ethanol:SCCAs ratios of at least 3, but possibly of 5-6, are required for efficient hexanoic acid production [8]. However, most wastewaters or fermented organic waste contain, in proportion, more SCCAs than ethanol, requiring the addition of exogeneous ethanol, increasing the operation costs.

In this study, we have developed an innovative technology that solves at once the three challenges mentioned above. It consists of a hybrid bioreactor in which the substrates required for chain elongation (ethanol and SCCAs) are transferred from the feedstock to the fermentation broth containing the chain elongating microorganisms via passive (concentration-driven) diffusion through a selective membrane (Figure 1). More in details, the feedstock (ethanol and SCCAs containing wastewaters or fermentate) is recirculated in the inner part of a tubular membrane submerged in the fermenter. The membrane allows the diffusion of ethanol and SCCAs while preventing the cross-over of microorganisms and chemical contaminants such as metals. The membranes can be designed to dose the required amounts of substrates for chain elongation, avoiding over-feeding even in case of highly concentrated feedstock sources. Furthermore, the selectivity of the membrane towards ethanol or SCCAs can be adjusted based on the feedstock characteristics, allowing to achieve optimal ethanol:SCCAs ratios in the fermenter even from sub-optimal feedstock sources.

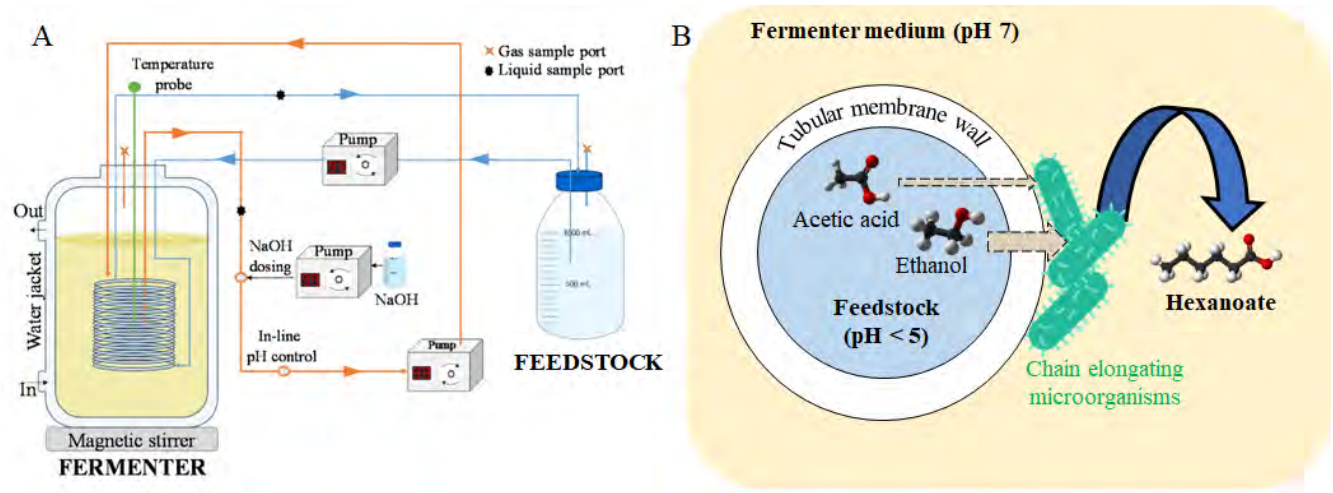

Figure 1. Bioreactor configuration used in this study (A); details of the process showing hexanoate production from ethanol and acetic acid diffusing through the tubular membrane (B).

Proof of concept experiments were performed in two replicate fermenters with a working volume of 1.4 L, operated at 35°C. The pH was controlled at 7 by automatic 3 M NaOH dosing. Firstly, a synthetic feedstock solution (containing ethanol and acetic acid, 1 M each) was recirculated in the inner part of the tubular membrane. Results confirmed that an ideal ethanol:acetic acid of 6:1 can be achieved by differential diffusion through the membrane, even from feedstocks with equimolar concentrations of ethanol and acetic acid. This promoted the development of a specialized microbial community, widely dominated by chain elongators from the *Clostridiaceae* and *Oscillospiraceae* families, that produced hexanoate at a sustained production rate of 3.1 g/(L·d) and up to 99% selectivity. The final hexanoate concentration achieved in the fermenter was 18.3 g/L. Since the fermenter was controlled at pH 7, >99% of the product was in its dissociated form (hexanoate), which is rejected by the membrane, allowing to concentrate the product in the fermenter avoiding its back-diffusion towards the feedstock stream.

Demonstration experiments confirmed that highly selective (93%, with peaks of 99%) hexanoate production can be achieved from a real feedstock (wine lees, WL). Such selectivity was higher than previously reported from similar substrates [9,10]. However, the production rate was limited to 1.0 g/(L·d) due to the lack of acetic acid in the WL feedstock. Although the reverse β-oxidation pathway can proceed from substrates containing only ethanol [11], the presence of acetic acid in the feedstock is necessary for optimizing the process. In fact, production rates of 2.7 g/(L·d), comparable to those achieved with the synthetic substrate, were achieved after amending the wine lees with acetic acid.

A simple downstream process was implemented to separate and recover the hexanoic acid from the fermentation broth. This included: (i) acidification of the fermentate to pH 3 to convert the hexanoate (dissociated) to hexanoic acid (undissociated); (ii) settling to naturally separate the insoluble hexanoic acid from the fermentation broth as an oily emulsion; and (iii) centrifugation to further separate the hexanoic acid from the water trapped in the emulsion. This procedure allowed to recover between 7 and 13 mL/L_{WL} of product containing up to 6.75 M (794 g/L) hexanoic acid, with 84% purity. The main contaminants detected were butyric acid (0.1 M) and hexanol (0.01 M), while, as confirmed by the extremely low conductivity (1-2 µS/cm), ions concentration was negligible. Dosage of chemicals (NaOH and HCl) was individuated as the main cost of the whole process, suggesting that alternative options, such as membrane electrolysis, must be considered to adjust pH.

In conclusion, this study introduces a membrane-based fermentation process to selectively produce hexanoate from concentrated substrates, such as wine lees. The properties of the membrane allowed to separately optimize the ethanol and SCCAs fluxes delivered towards the chain elongating microorganisms, allowing to adapt the process to the characteristics of the feedstock. Future work will focus on the development of high-rate bioreactors to increase the production rates and optimize the purification steps to achieve purities >98% that can make the process economically competitive.

Acknowledgements

This project has received funding from the European Union's Framework Programme for Research and Innovation Horizon 2020 (2014-2020) under the Marie Skłodowska-Curie, project ATMESPHERE, Grant Agreement No. 101029266, and from the Spanish Ministry of Innovation and Science, project PANGEA, Grant Agreement PID2021-126240OB-I00.

References

[1] P. Gabrielli, L. Rosa, M. Gazzani, R. Meys, A. Bardow, M. Mazzotti & G. Sansavini. "Net-zero emissions chemical industry in a world of limited resources", *One Earth, 6,* 682–704 (2023).

[2] T.M. Attard, J.H. Clark & C.R. McElroy. "Recent developments in key biorefinery areas", *Curr Opin Green Sustainable Chemistry, 21,* 64–74 (2020).

[3] L. Alibardi, T.F. Astrup, F. Asunis, W.P. Clarke, G. De Gioannis, P. Dessì, P.N.L. Lens, M.C. Lavagnolo, L. Lombardi, A. Muntoni, A. Pivato, A. Polettini, R. Pomi, A. Rossi, A. Spagni & D. Spiga. "Organic waste biorefineries: Looking towards implementation", *Waste Management, 114,* 274–286 (2020).

[4] M.T. Agler, C.M. Spirito, J.G. Usack, J.J. Werner & L.T. Angenent. "Chain elongation with reactor microbiomes: Upgrading dilute ethanol to medium-chain carboxylates", *Energy and Environmental Science, 5,* 8189–8192 (2012).

[5] D. Licursi, A.M. Raspolli Galletti, C. Antonetti, G.A. Martinez, E. Jones, L. Bertin, N. Di Fidio, S. Fulignati, G. Pasini & S. Frigo. "Tunable production of diesel bio-blendstock by rhenium-catalyzed hydrogenation of crude hexanoic acid from grape pomace fermentation", *Catalysts, 12,* 1550 (2022).

[6] F. Silva, M. Matos, B. Pereira, C. Ralo, D. Pequito, N. Marques, G. Carvalho & M.A.M. Reis. "An integrated process for mixed culture production of 3-hydroxyhexanoate-rich polyhydroxyalkanoates from fruit waste", *Chemical Engineering Journal, 427,* 131908 (2022).

[7] T.I.M. Grootscholten, K.J.J. Steinbusch, H.V.M. Hamelers & C.J.N. Buisman. "Improving medium chain fatty acid productivity using chain elongation by reducing the hydraulic retention time in an upflow anaerobic filter", *Bioresource Technology, 136,* 735–738 (2013).

[8] Q. Wu, W. Ren, W. Guo & N. Ren. "Effect of substrate structure on medium chain fatty acids production and reactor microbiome", *Environmental Research, 204,* 111947 (2022).

[9] G.A. Martinez, S. Puccio, J.M.B. Domingos, E. Morselli, C. Gioia, P. Marchese, A.M. Raspolli Galletti, A. Celli, F. Fava & L. Bertin. "Upgrading grape pomace contained ethanol into hexanoic acid, fuel additives and a sticky polyhydroxyalkanoate: an effective alternative to ethanol distillation", *Green Chemistry, 24*, 2882–2892 (2022).

[10] Q. Wu, X. Feng, W. Guo, X. Bao & N. Ren. "Long-term medium chain carboxylic acids production from liquor-making wastewater: Parameters optimization and toxicity mitigation", *Chemical Engineering Journal, 388,* 124218 (2020).

[11] C.M. Spirito, H. Richter, K. Rabaey, A.J.M. Stams & L.T. Angenent. "Chain elongation in anaerobic reactor microbiomes to recover resources from waste", *Current Opinion in Biotechnology, 27,* 115–122 (2014).

Title: Dark fermentation of winery by-products using indigenous microbial cultures

Authors: Grazia Policastro*[1], Marco Race[2], Massimiliano Fabbricino[3]

[1] Department of Engineering, Telematic University Pegaso, Centro Direzionale Isola F2, Naples, 80132, Italy
[2] Department of Civil and Mechanical Engineering, University of Cassino and Southern Lazio, Via Di Biasio 43, Cassino, 03043, Italy
[3] Department of Civil, Architectural and Environmental Engineering, University of Naples Federico II, Via Claudio 21, Naples, 80125, Italy
** Email address (grazia.policastro@unipegaso.it)*

Keywords: Aged wine, Biohydrogen, Bioethanol; Dark Fermentation, Grape pomace, Wine lees.

Abstract

Every year, approximately 260 million hectoliters of wine are produced worldwide [1]. The resulting by-products contain a high organic content, posing a potential contamination risk if not managed correctly [2]. However, they also present an opportunity for their sustainable utilization through biorefinery processes, such as Dark Fermentation (DF) [3]. DF is gaining increasing attention due to its ability to produce hydrogen (H_2) gas, a valuable alternative to fossil fuels [4]. By converting organic waste into energy, DF contributes to waste disposal in line with the Waste-to-Energy approach. However, for the DF to be competitive compared to traditional processes, it is necessary to study approaches simplifying the process operations and management. For example, the use of indigenous inocula would streamline the process from the operating point of view, since the utilized microbial cultures are already present in the waste substrate [5]. Moreover, some regulations prohibit the use of conventional inocula, such as sewage sludge, due to its classification as waste. Concerning the possibility of using indigenous inocula to conduct the DF of winery by-products, a recent study has found that bacteria capable of producing hydrogen are present in wine sediment [6]. Unfortunately, the valorization of wine by-products through dark fermentation using indigenous cultures is a underexplored field. Therefore, the operational conditions required to steer the process towards hydrogen production are not yet understood.

In this study, the operational conditions promoting hydrogen production from winery by-products and selection methods of indigenous cultures contained in the wine sediment via DF of winery by-product were investigated. Experiments were carried out in two phases: in the first phase, the effect of operational conditions on the selection of a hydrogen-producing indigenous inoculum was tested. Specifically, it was investigated the effect of heat shock pre-treatment (3 hours at 105°C), typically used when external inocula, such as digestate, are employed, as well as the effect of nutrients addition, by providing the medium reported by Toscano et al. (2014) [7]. Glucose was used as substrate for all first phase tests, calculating the glucose concentration according to the fixed F/M ratio. The effect of two different F/M ratios (i.e. 1 and 5 $gVS_{substrate}/gVS_{microorganisms}$ on the fermentation process was examined. In the second phase, the conditions promoting hydrogen production were applied to real substrates. Firstly, the effect of diluting the inoculum-substrate mixture with tap water (i.e. percentage of mixture of 25%, 50%, 75%, 100%) was investigated, using wine lees as substrate. Successively, the best condition was applied to further winery by-products, i.e., grape pomace and aged wine. Both phases were conducted using the solid fraction of wine lees (sediment) as inoculum. Figure 1 details the experimental plan.

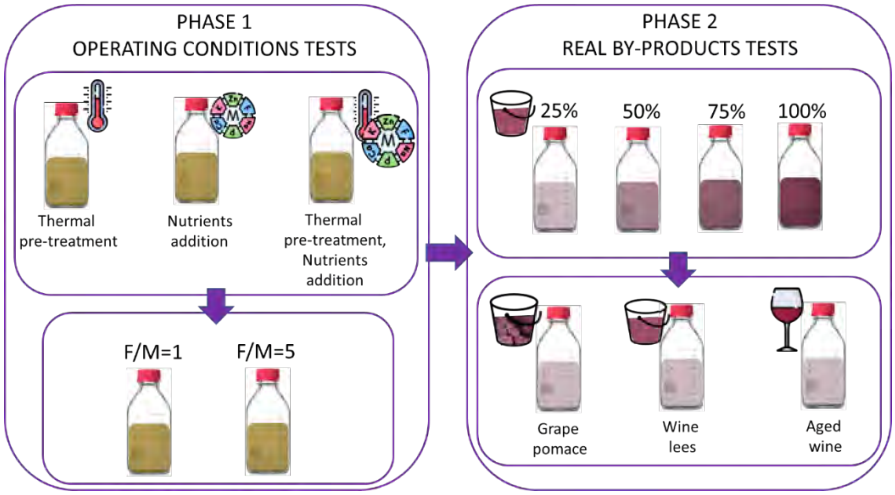

***Figure 1**. Operating conditions tested in the two phases of the experimental plan*

Transparent borosilicate glass bottles (Simax, Czech Republic) with a working volume of 400 mL were utilized for the experiments. Screw caps made of PVC were appropriately modified with tubing to facilitate gas and liquid extraction processes. DF reactors were placed in a water bath to maintain a temperature of 35±1°C. A batch feeding strategy was employed. Daily analysis of liquid and gas samples were conducted to measure the content of organic compounds and the quantity and composition of biogas. Biogas production was quantified using water displacement, following the method described in Policastro et al. (2022) [4]. Subsequently, gas chromatographic analysis was carried out to determine the hydrogen percentage. This analysis was performed using a Varian Star 3400 gas chromatograph equipped with a ShinCarbon ST 80/100 column and a thermal conductivity detector, with argon as the carrier gas. Liquid fermentation products were determined using a Dionex LC 25 Chromatography Oven equipped with a Metrohom Organic Acids column (Metrosep Organic Acids - 250/7.8) and two different detectors: a Dionex UVD 340U for volatile fatty acids (VFAs) and a Jasco RI-2031 for ethanol.

Figure 2 presents the results obtained during the first phase of the experimental plan, in terms of cumulative hydrogen production

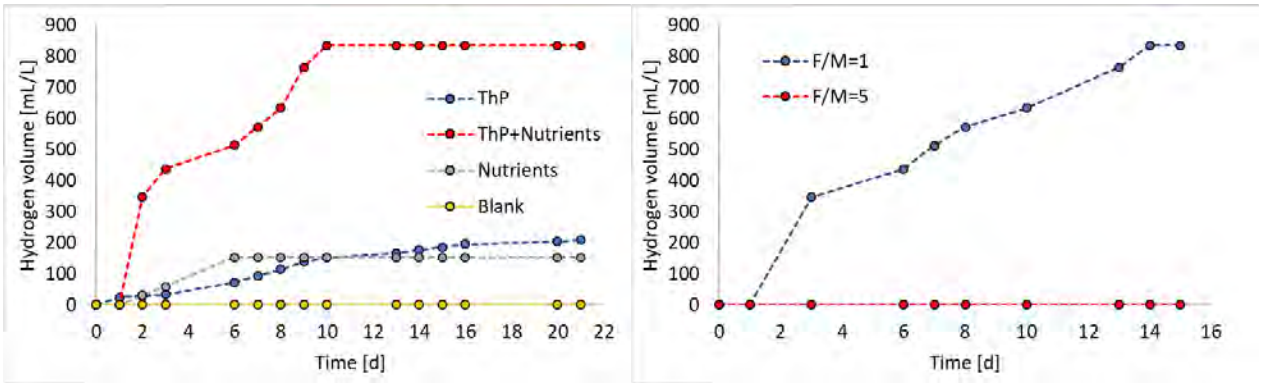

***Figure 2**. Impact of applying various operating conditions on the DF process, conducted with solid wine lees as inoculum and a synthetic glucose substrate, in terms of the cumulative hydrogen production. (a)*

effect of thermal pre-treatment (ThP) and Nutrients addition; (b) Effect of the Food to Microorganisms (F/M) ratio.

The fermentation process conducted without the addition of nutrients and without performing the thermal pre-treatment of the inoculum led to a null hydrogen production. Conversely, the sole addition of nutrients or sole thermal pre-treatment allowed for a similar cumulative production of 153 mL/L and 208 mL/L, respectively. These results highlights that the solid fraction of wine lees do not contain the necessary nutrients for the process development. This experiment was also repeated by replacing the glucose solution with other wine by-products, yielding the same result (data not shown). Furthermore, thermal pre-treatment was essential for enriching a hydrogen-producing consortium. As previously reported, winery deposits contain *Clostridium* spp., which can degrade sugars into hydrogen [6]. However, it is likely that other microorganisms, which were inhibited during the thermal pre-treatment, predominated over the Clostridia. Applying both strategies resulted in a synergistic effect, allowing to obtain the best production outcome. In this condition, the cumulative hydrogen production reached 834 mL/L. Regarding the effect of the F/M ratio (Figure 2 (b)), increasing this ratio from 1 to 5 led to a null hydrogen production. This result indicates that increasing this ratio promotes the establishment of different metabolic pathways compared to those leading to hydrogen production. The analysis of the liquid effluent indicated that employing an F/M ratio of 1 primarily led to the production of volatile fatty acids, typically observed when the bioconversion is directed towards hydrogen production [8]. Conversely, under the F/M=5 ratio, there was an increase in ethanol concentration, rising from 1.18 g/L to 7.73 g/L throughout the process. This result is in line with a recent study demonstrating the possibility of producing ethanol under dark fermentative conditions [4]. This result suggests that by modifying the F/M ratio, it is possible to select the desired process output. Ethanol, in particular, is another interesting product as it is the most common renewable fuel, primarily derived from corn grain and sugar cane, with anticipated constraints on the supply of these raw materials in the future [9].

Figure 3 shows the results obtained during the second phase of the experiments, where glucose was replaced with real winery by-products.

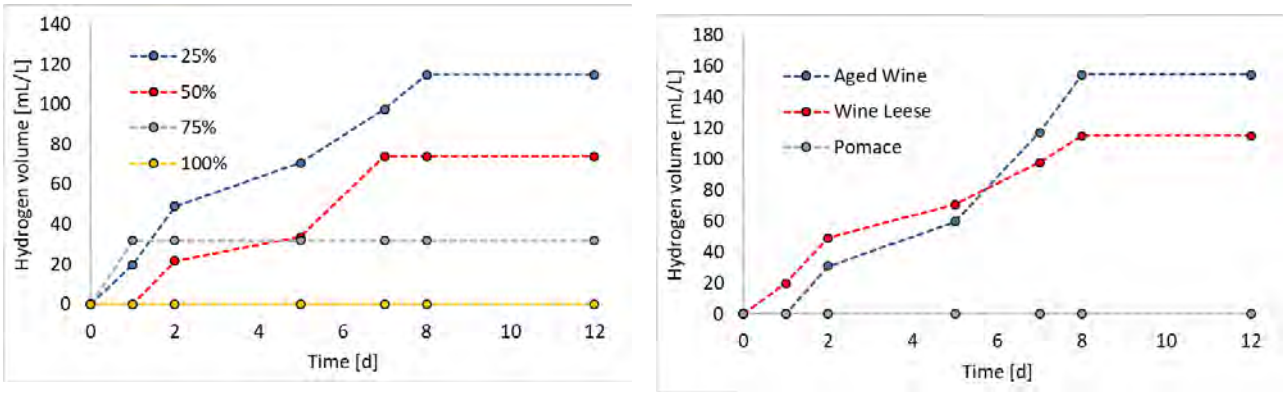

***Figure 3**. Cumulative hydrogen production obtained via the DF process of real winery by-products, using solid with wine lees as inoculum. (a) Effect of dilution on wine lees fermentation; (b) Effect of aged wine, wine lees and grape pomace as substrates.*

From Figure 3 (a) it can be observed that hydrogen production increases when transitioning from 100% substrate-inoculum mixture to 25%. Unlike the tests conducted during phase 1, the analysis of the liquid

effluent did not show a corresponding increase in ethanol with decreasing hydrogen production (data not shown). Therefore, in this case, the increase in hydrogen production with decreasing waste percentage may be attributed to the presence of phenolic compounds, known for their antimicrobial effect [10]. From Figure 3 (b), the analysis of hydrogen productivity from various winery by-products revealed that lees and aged wine are excellent substrates for DF. In contrast, grape pomace did not produce hydrogen. This could be due to the lignocellulosic nature of this waste, which would require pre-treatments before being used in the process.

In conclusion, the present study shows that it is possible to produce hydrogen from winery by-products using indigenous cultures contained in solid lees as inoculum. However, a thermal pre-treatment is necessary to enrich the hydrogen producing culture. Regarding the substrates to be used, aged wine and liquid lees can be employed without the need for other pre-treatments than those applied in this study, unlike grape pomace. On the other hand, there is a need for nutrient supplementation. Therefore, an interesting solution would be to conduct the process using two different substrates simultaneously to supplement the nutrients lacking in wine by-products with a second waste. Finally, further study is needed, including measuring the concentrations of polyphenols and thoroughly testing the effect of these compounds and their possible recovery to obtain both high-value-added chemicals and increased hydrogen production from wine by-products.

References

1. Freimann, A. Logistical challenges in the process of internationalization of internationalization of companies in the wine. Helena Štimac , PhD , Associate Professor Faculty of Economics Osijek Trg Ljudevita Gaja 7 , 31000 Osijek Anita Freimann , PhD , Associate Profes. **2022**.
2. Constantin, O.E.; Stoica, F.; Rațu, R.N.; Stănciuc, N.; Bahrim, G.E.; Râpeanu, G. Bioactive Components, Applications, Extractions, and Health Benefits of Winery By-Products from a Circular Bioeconomy Perspective: A Review. *Antioxidants* **2024**, *13*, doi:10.3390/antiox13010100.
3. Velidandi, A.; Kumar Gandam, P.; Latha Chinta, M.; Konakanchi, S.; reddy Bhavanam, A.; Raju Baadhe, R.; Sharma, M.; Gaffey, J.; Nguyen, Q.D.; Gupta, V.K. State-of-the-Art and Future Directions of Machine Learning for Biomass Characterization and for Sustainable Biorefinery. *J. Energy Chem.* **2023**, *81*, 42–63, doi:10.1016/j.jechem.2023.02.020.
4. Policastro, G.; Giugliano, M.; Luongo, V.; Napolitano, R.; Fabbricino, M. Enhancing Photo Fermentative Hydrogen Production Using Ethanol Rich Dark Fermentation Effluents. *Int. J. Hydrogen Energy* **2022**, *47*, 117–126, doi:10.1016/j.ijhydene.2021.10.028.
5. Dauptain, K.; Trably, E.; Santa-Catalina, G.; Bernet, N.; Carrere, H. Role of Indigenous Bacteria in Dark Fermentation of Organic Substrates. *Bioresour. Technol.* **2020**, *313*, 123665, doi:10.1016/j.biortech.2020.123665.
6. François, E.; Dumas, C.; Gougeon, R.D.; Alexandre, H.; Vuilleumier, S.; Ernst, B. Unexpected High Production of Biohydrogen from the Endogenous Fermentation of Grape Must Deposits. *Bioresour. Technol.* **2021**, *320*, doi:10.1016/j.biortech.2020.124334.
7. Toscano, G.; Zuccaro, G.; Ausiello, A.; Micoli, L.; Turco, M.; Pirozzi, D. Production of Hydrogen from Giant Reed by Dark Fermentation. *Chem. Eng. Trans.* **2014**, *37*, 331–336, doi:10.3303/CET1437056.
8. Ghimire, A.; Frunzo, L.; Pirozzi, F.; Trably, E.; Escudie, R.; Lens, P.N.L.; Esposito, G. A Review on Dark Fermentative Biohydrogen Production from Organic Biomass: Process Parameters and Use of by-Products. *Appl. Energy* **2015**, *144*, 73–95, doi:10.1016/j.apenergy.2015.01.045.
9. Gray, K.A.; Zhao, L.; Emptage, M. Bioethanol. *Curr. Opin. Chem. Biol.* **2006**, *10*, 141–146, doi:10.1016/j.cbpa.2006.02.035.
10. Tapia-Quirós, P.; Montenegro-Landívar, M.F.; Reig, M.; Vecino, X.; Cortina, J.L.; Saurina, J.; Granados, M. Recovery of Polyphenols from Agri-Food By-Products: The Olive Oil and Winery Industries Cases. *Foods* **2022**, *11*, 1–26, doi:10.3390/foods11030362.

Title: Investigation of low temperature thermal pretreatment on VFA production from the dark fermentation of organic waste

Author(s): Isabella Pecorini*[1], Francesco Pasciucco[2], Erika Pasciucco[3], Alessio Castagnoli[4], Roberta Palmieri[5], Antonio Panico[5], Renato Iannelli[7]

[1] *Department of Energy, Systems Territory and Construction Engineering, Via C.F. Gabba 22, Tuscany, University of Pisa, Pisa, 56122, Italy, isabella.pecorini@unipi.it*
[2] *Department of Energy, Systems Territory and Construction Engineering, Via C.F. Gabba 22, Tuscany, University of Pisa, Pisa, 56122, Italy, francesco.pasciucco@phd.unipi.it*
[3] *Department of Energy, Systems Territory and Construction Engineering, Via C.F. Gabba 22, Tuscany, University of Pisa, Pisa, 56122, Italy, erika.pasciucco@phd.unipi.it*
[4] *Department of Energy, Systems Territory and Construction Engineering, Via C.F. Gabba 22, Tuscany, University of Pisa, Pisa, 56122, Italy, alessio.castagnoli@phd.unipi.it*
[5]*Department of Engineering, University of Campania L. Vanvitelli, 81031, Aversa, Italy, roberta.palmieri@unicampania.it*
[6]*Department of Engineering, University of Campania L. Vanvitelli, 81031, Aversa, Italy, antonio.panico1@unicampania.it*
[7] *Department of Energy, Systems Territory and Construction Engineering, Via C.F. Gabba 22, Tuscany, University of Pisa, Pisa, 56122, Italy renato.iannelli@unipi.it*

Keyword(s): keywords list (Arial font – 11 point size)

Abstract

The following study is carried out within the research project “BIOpolymers from agri-food waste digestates for SMART release bioFERTilisers” (BIOSMARTFERT), PRIN 2022 5WLFFR, funded by the European Union - Next Generation.

In the circular economy approach, the BIOSMARTFERT project aims to define the production chain of a new generation of renewable biofertilisers with a modulated release, defined below as SMART release FERTilisers (SRF), derived from digestate of biowaste. First, the granule part of the SRF will be produced from an anaerobic biorefinery by treating agri-food wastes. Then they will be encapsulated and covered with degradable biopolymers such as polyhydroxyalkanoates (PHA), also produced by anaerobic biorefinery.

Fertilisers are one of the most critical elements to ensure global food security and safety requested by the growth of the human population. Moreover, fertilisers are indispensable to maintaining and recovering healthy soils. One of the flagship targets established in the EU Green Deal 2030 is to reduce the use of traditional fertilisers by at least 20% [1].

Digestate from dark fermentation of organic solid waste has been shown to have excellent fertiliser potential [2,3]. Furthermore, the application of digestate as fertiliser has proved to be safe [4] and closes the nutrient cycle and reduces the demand for mineral fertiliser, whose production requires non-renewable raw materials and high energy input production [5].

However, the application of digestate to soils can cause environmental problems, such as high levels of GHG emissions [6] and release of soluble N in the soil, and low levels of acceptance rate in the nearby communities.

Pelletising on the solid fraction of digestate has been proposed as a promising solution to reduce the volume of the raw material, increase the homogenisation of nutrients, improve fertilising properties and

decrease potential risks linked to nuisance problems. However, this practice can trigger relatively high climate-relevant GHG emissions when applied to soils [7,8].

The coated fertilisers can represent a technical advantage, which can mitigate these negative aspects. Innovative coated fertilisers were introduced to supply sufficient nutrients for plants at different growth stages. Slow-release fertilisers are fertilisers in a form that releases, or converts to a plant-available form, plant nutrients at a slower rate relative to an appropriate reference soluble product. Controlled-release fertilisers are engineered to provide nutrients over time under specific conditions [9].

The surface of granules of fertilisers can be coated with a natural or synthetic material to slow or control the nutrient release [10].

However, synthetic polymers (polyolefin polyurethane-like resins) have led to severe environmental concerns regarding the slow decomposition rate and the permanence of residues in soils. So, the adoption of biodegradable polymers, like polyhydroxyalkanoates (PHA), which can be easily degraded by soil microorganisms, for coatings fertilisers has been recently proposed, with encouraging results in supporting the growth of plants as well as soil microflora [11].

Using current renewable biomass sources to produce biodegradable polymers such as PHA can increasingly conflict with their traditional food use. However, this conflict can be overcome by promoting the use of other natural resources like photosynthetic microorganisms (PM).

To keep the production costs of PHA low and consequently make PHA-based bioplastics competitive with traditional fossil fuel-based plastics, organic wastes can be successfully used as feedstock for producing biologically solutions containing volatile fatty acids (VFA), which can be used as precursors of PHA [12], and several pretreatments can be used to enhance VFA production.

In view of the above, experimental tests were carried out on a laboratory scale, to evaluate the influence of thermal pretreatments on the production of VFA from the dark fermentation process of the organic fraction of municipal solid waste. Specifically, the influence of low temperature thermal pretreatments was investigated (generally below 100°C), as they are little addressed in the literature, also evaluating their influence on parameters such as COD, ammoniacal nitrogen, proteins and carbohydrates.

Based on a literature review on low temperature thermal pretreatments, the significant time and temperature ranges affecting the process were identified, and a dataset of experimental tests was developed using a central composite design (CCD) combined with response surface methodology (RSM) at three levels (-1, 0, +1) [13], resulting in 26 experimental tests aimed at identifying the optimal condition that maximize the production of VFA.

After that, representative samples (in the form of puree) of the organic fraction of municipal solid waste were made (figure 1) [14], while samples of excess sludge were taken from a wastewater treatment plant and used as an inoculum inside the reactors. Then, the experimentation was carried out as follows:

i) Shock of the inoculum (4 hours in oven at 105°C), in order to break down the methanogenic biomass that could disturb the dark fermentation process.

ii) Thermal pretreatment of the puree in the oven, following the exposure times and temperatures identified using the RSM methodology.

iii) Assembly of the dark fermentation reactors, according to the following steps: mixing the shocked inoculum and the pre-treated puree (food/microorganism ratio 2:1, based on volatile solids), adjusting of the initial pH value of the mixture obtained at 7$\pm$0.1 via buffer solution, hermetic closure of the reactors using caps equipped with ball valves to allow sampling of the gases produced during the process and injection of inert gas (N_2) into the reactors to create anaerobic conditions.

iv) Starting the dark fermentation process (figure 2): the reactors described in the previous point are incubated in a water bath at 37°C for 72 hours. Heating takes place inside beakers filled with water and positioned on stirrers, to guarantee complete mixing of the contents inside the reactors (300 rpm).

Figure 1. organic fraction puree.

Figure 2. dark fermentation process.

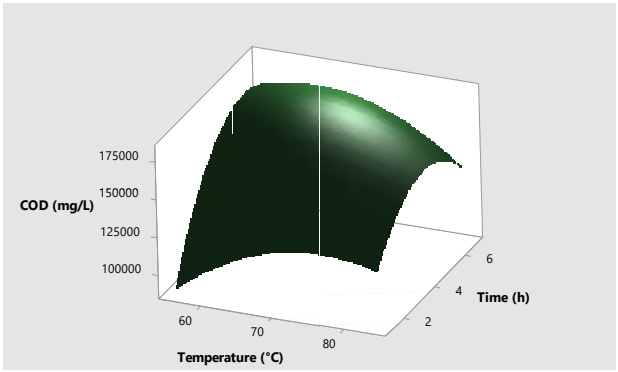

Figure 3. Surface of COD vs Temperature and time

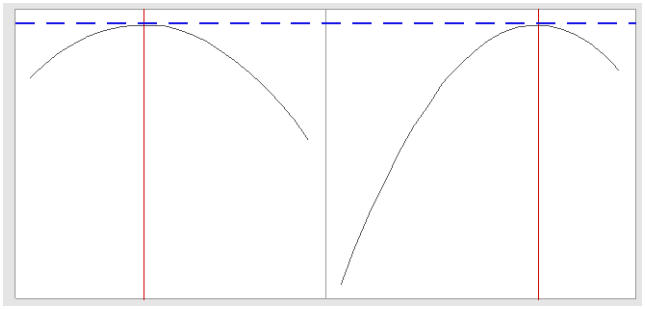

Max COD with Temperature = 67.3°C; time = 5.2 h

Figure 4. COD optimization of temperature and time.

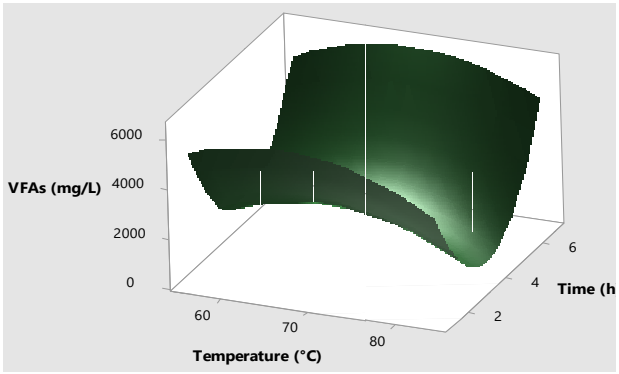

Figure 5. Surface of VFAs vs Temperature and time

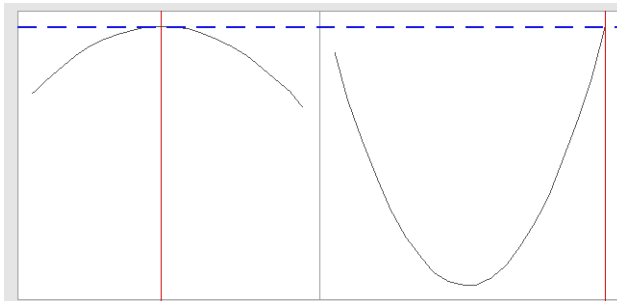

Max VFAs with Temperature = 69.3°C; time = 6.8 h

Figure 6. VFAs optimization of temperature and time

Experimental results were processed by RSM (minitab release 18) with the aim of studying the effects of temperature and time in COD solubilisation as well as VFAs production (figures 3-6). Both phenomena are temperature and time dependent. About temperature COD solubilisation and VFAs production showed a similar trend and the best values ranged between 67.3°C and 69.3°C, whereas the effect of time on both processes was contrasting: COD solubilisation was positively affected by the increase of time of exposure until reaching the maximum around 5.2 hours and then the effect from positive turned to be negative, whereas the trend of VFAs production was diametrically opposite, even if the best results are reached for time in the range of 5-6 h, the same range where the COD solubilisation was maximum.

About the trend of COD solubilisation with temperature and time, the maximum for the couple 67.3°C and 5.2 h is likely due to the volatilization process of organic compounds that is enhanced by temperature and time, whereas about the trend of VFAs, as they were already present in the sample after thermal pretreatment, and their concentration was the highest in sample pretreated for a shortest time (data not shown), the effect of time was firstly negative and then, after 4 hours of exposure, positive. As all the methanogenic archea were removed from the inoculum by thermal shock, VFAs were not consumed during dark fermentation process, therefore the final amount of VFAs from each reactor was the sum of VFAs already present in the sample and those produced from the biological conversion of soluble COD into VFAs and this production was maximum where the soluble COD was the highest. Therefore a minimum in VFAs concentration was found around 4 h of pretreatment, when the VFAs in the pretreated sample was low and when the conversion of soluble COD in VFAs was low as well, because the maximum VFAs concentration in the pretreated sample was achieved at the shortest time of pretreatment and the maximum concentration of soluble COD was reached around 5.2 hours.

In conclusion, it can be stated that thermal pretreatment can increase the production of VFA. Future research should be directed towards the perspective of scale-up, plant application and economic optimization of the process.

References

[1] EC COM (2020) 381 Final. A Farm to Fork Strategy for a Fair, Healthy and Environmentally-Friendly Food System.
[2] Yang J et al. Roles of calcium-containing alkali materials on dark fermentation and anaerobic digestion: A systematic review. Int J Hydrogen Energ. 2021.
[3] Soares JF et al. Dark fermentative biohydrogen production from lignocellulosic biomass: Technological challenges and future prospects. Renew Sustain Energy Rev. 2020.
[4] Carraturo F, Panico A, Giordano A, Libralato G, Aliberti F, Galdiero E, et al. Hygienic assessment of digestate from a high solids anaerobic co-digestion of sewage sludge with biowaste by testing Salmonella Typhimurium, Escherichia coli and SARS-CoV-2. Environ Res. 2022.
[5] Stürmer B et al. Legal requirements for digestate as fertilizer in Austria and the European Union compared to actual technical parameters. J Environ Manage. 2020.
[6] Pecorini I, Peruzzi E, Albini E, Doni S, Macci C, Masciandaro G, et al. Evaluation of MSW Compost and Digestate Mixtures for a Circular Economy Application. Sustainability-basel. 2020.
[7] Petrova IP et al. Pellets from Biogas Digestates: A Substantial Source of N2O Emissions. Waste Biomass Valori. 2020.
[8] Purnomo CW et al. Slow Release Fertilizer Production from Poultry Manure. Chemical Engineering Transactions 2017.
[9] Trenkel, M.E. Slow- and Controlled-Release and Stabilized Fertilizers: An Option for Enhancing Nutrient Use Efficiency in Agriculture; IFA. Paris, 2010.
[10] Dimkpa CO et al. Development of fertilizers for enhanced nitrogen use efficiency – Trends and perspectives. Sci Total Environ. 2020.
[11] Murugan P et al. Development and evaluation of controlled release fertilizer using P(3HB-co-3HHx) on oil palm plants (nursery stage) and soil microbes. Biocatal Agric Biotechnology. 2020.
[12] Pagliano G, Ventorino V, Panico A, Pepe O. Integrated systems for biopolymers and bioenergy production from organic waste and by-products: a review of microbial processes. Biotechnol Biofuels. 2017.
[13] Khuri, A. I., & Mukhopadhyay, S. (2010). Response surface methodology. Wiley interdisciplinary reviews: Computational statistics, 2(2), 128-149.
[14] Campuzano, R., & González-Martínez, S. (2016). Characteristics of the organic fraction of municipal solid waste and methane production: A review. Waste Management, 54, 3-12.

Title Enhancing material and energy recovery through WtE industrial symbiosis in South Europe regions

Author(s): Antonella Luciano*[1], Giuseppe Mancini[2], Lidia Lombardi[3], Paolo Viotti[4], Debora Fino[4]

[1] *ENEA – Italian National Agency for New Technologies, Energy and Sustainable Economic Development Department for Sustainability (SSPT), Casaccia Research Centre, Rome, Italy. antonella.luciano@enea.it*
[2] *Electric, Electronic and Computer Engineering (DIEEI), University of Catania, Catania, Italy, giuseppe.mancini@unict.it*
[3] *Niccolò Cusano University, Rome, Italy. lidia.lombardi@unicusano.it.it*
[4] *Department of Civil, Construction and Environmental Engineering (DICEA), Sapienza University of Rome, Rome , Italy. paolo.viotti@uniroma1.it*
[5] *Department of Applied Science and Technology (DISAT), Politecnico di Torino, Turin, Italy. debora.fino@polito.it*

Keyword(s): Industrial Symbiosis; Waste; Wastewater; Anaerobic digestion, Energy, heat

1. Introduction

Most of Mediterranean regions have disjointed approaches to the management of waste, wastewater and residual biomass. In many of these regions these “sole” approaches are also not fully sustainable as they entirely focus on material recovery (both from waste and from wastewater) while neglecting the energy issues so leading to unjustifiable energy waste and related direct/indirect impacts on the environment. Significant delay in the planning and construction of plants for the valorisation of recyclable material and -above all - for a sustainable and concurrent energy and material recovery from the residual waste (i.e. Waste to Energy (WtE) plants) and organic waste (i.e. Anaerobic Digestion (AD) plants) [1] is still detected in many of these regions [2] also due to the opposition of citizens which, in turns, affects political choices and planning. The immediate consequence of this scenario is still an abnormal resort to landfill not taking into account the approaching 10% landfill limit in 2035 as expected by the European Directives. Furthermore, despite the historical water scarcity in many of these areas [3], no effective actions for wastewater reuse are implemented [4,5] mostly because of the still too high costs of the reclaimed wastewater which make this marginal resource not competitive with the albeit limited natural water [6]. The disposal of sludge from wastewater treatment is likewise still problematic, both in land-based applications, composting and landfill routes.
An IS application, based on waste-water-energy nexus, was recently proposed to address the overmentioned issues and well-assessed through material end energy flow analysis [7]. The proposed symbiotic application is intended as a modern IS-based circular industrial district, able to self-provide electricity, heat, and biomethane to itself and the surrounding cities. The proposed scenario was also compared in term of environmental impact with other management scenarios [8,9].
In this works a further advance in the implementation of the proposed Industrial symbiosis application [10] is reported focusing on the symbiotic exploitation of thermal energy for different industrial processes whose main characteristics were identified in order to support stakeholders in planning the development of an efficient IS-based ecosphere as the one described in Figure 1.

2. IS -based waste/water energy nexus "ecosystem"

The proposed IS scenario includes three different treatment and recovery sections: 1) a wastewater treatment plant; 2) an anaerobic digestion section for the separate treatment of organic fraction from separate collection of municipal solid waste (OFMSW) and the WWT sludge (this last assumed to be already occuring in the WWTP AD reactor); 3) an incinerator with production of electricity and heat able to thermally valorize the residual waste (unsorted + scraps from selection). New industrial opportunities for existing and new companies in an industrial district can supported by the additional electric and -above all – thermal energy made available, at reduced cost, from the energy recovery exploitation of the residual waste - otherwise destined to be disposed of in landfill producing more relevant impacts. The assessment here presented refers to a metropolitan area involving 2 million inhabitants with a waste production per capita of about 511 kgd^{-1} inh^{-1}. The metropolitan area embraces a main large city and smaller surrounding towns with an overall mean separate collection efficiency that is assumed to be 70% in compliance with the 2030 EU target. The WWTP is assumed to treat only the wastewater produced by the citizens of the main city (545,000 inhabitants). Energy production in WtE plant and energy demands of the processes involved in the symbiotic exchanges are calculated according to [7]. Furthermore, an evaluation of exceeding thermal energy production (and related temperatures) is provided and compared with potential demands by different industrial sector in order to identify the most suitable industrial sectors, where residual thermal heat could be fruitfully used.

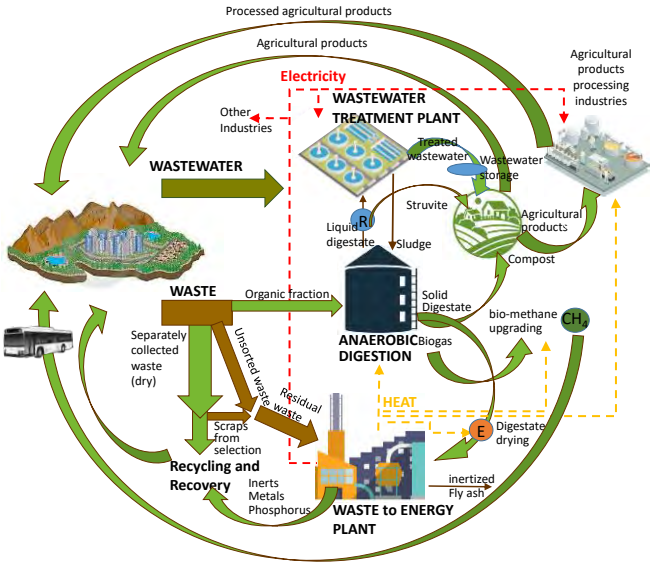

Figure 1. Industrial symbiosis ecosphere

3. Results

Electric and thermal energy production in WtE plant and energy demands of the processes involved in the symbiotic exchanges are represented in Figure 2.

3.1 Analysis of the heat requirement for other IS processes

The thermal treatment of 452383 tons of residual waste produces more than 453 GWhy^{-1} of electricity (230 kWh y^{-1} per capita) and 726 GWh y^{-1} of thermal energy (360 kWh y^{-1} per capita) - as hot vapor - respectively. The electricity produced is used (just few percentage units) to support the tertiary and quaternary treatment - essential to satisfy the reuse standards requirement - and to pump the treated wastewater to agricultural fields (generally located at a higher altitude). Specifically the energy demand for the enhanced treatment and pumping reclaimed wastewater to the agricultural areas is evaluated in 20 GWh per year. As a consequence of the additional energy supply, provided at competitive prices, the cost of treated wastewater could be reduced with respect to groundwater and superficial waters promoting its full reuse (a storage phase should be specifically designed) so to achieve the ZERO - discharge conditions into water bodies. This last result, favored by the energy recovered from residual waste, is of particular interest in islands and coastal areas for preserving touristic activities. In order to

furtherly reduce the cost of the treated wastewater also the energy for the oxidation phase in the WWTP - evaluated in 9,9 GWh per year (5 kWh y^{-1} pro capita) could be provided by the residual waste thermal treatment plant so achieving a net zero energy WWTPs. Part of the heat generated by the WtE process is also used to shift AD to thermophilic regime thus reducing digestion times and volumes and/or increasing the biogas production yield with respect to traditional mesophilic processes. The heat required is calculated in 19,4 GWh per year (10 kWh y^{-1} pro capita) and 14,2 GWh per year (7 kWh y^{-1} pro capita) for the AD of OF-MSW and WWTP sludge respectively. In the proposed scenario WWTP sludge is dehydrated - after mechanical dewatering by centrifugation - using the excess heat (29 GWh per year) produced by the WtE process. This option, is aimed not only to provide a robust solution to the severe issues of sludge management but also to recovery the phosphorus content from the deriving ash. Analogously the digestate from OFMSW is dehydrated using 112 GWh per year. The availability of extra thermal energy suggests to collect and treat also the sludge form other nearby towns.

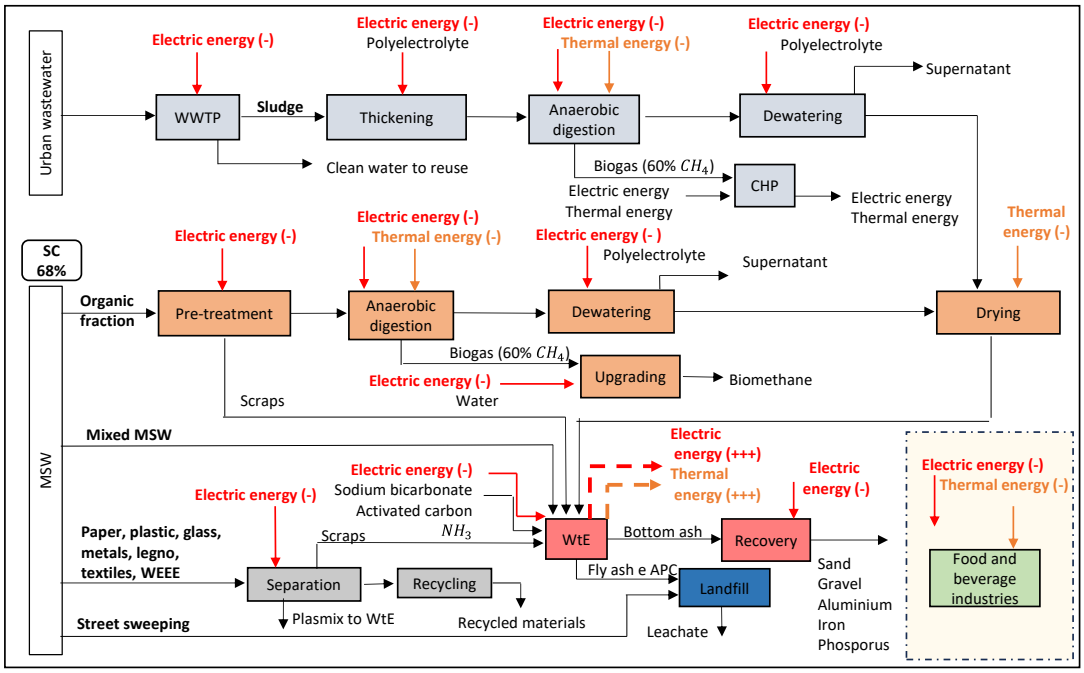

Figure 2. Energy-material flow analysis of the IS scenario.

3.2 Analysis of the heat requirement for other IS processes

After the proposed uses are satisfied still most of the heat produced from thermal treatment of the residual waste is available for further applications (552 GWh). This relevant amount of heat can support other companies by exploiting the hot vapor - provided at advantageous conditions - for their processes (e.g. agri-food process industry), in addition to any heating and cooling (i.e. trigeneration) needs, in a full perspective of industrial symbiosis and with a consequent reduction in CO_2 emissions from current fossil-fuel energy production. By considering the thermal energy required per tons of produced product in food and beverage sector [11] an evaluation of potential products supported by the residual thermal energy was developed and reported in Table 1.

Table 1. Amount of product produced with the residual thermal energy (552 GWh) in food and beverage sector

Production (10^3 t/y)	Backeries	Beverages	Dairy	Fruits / vegetable	Meat	Beer	Sugar	Slaughtering	Meat Processing
	414	1743	524	1204	1083	1481	728	3565	903

4. Conclusions

It is well assessed that to achieve the goal of reducing the landfill need to less than 5-10% - as required by 2035 from the EU, both material and energy recovery must be implemented. However in most of the countries where landfill has already achieved a really residual role this implementation has been carried out in a separate, additive way, mostly limiting thermal energy recovery to urban heating. Recovery of sludge has not been frequently placed in relation to the energy recovery from waste and even rarely with wastewater reuse, at least within an holist approach. This work has provided a wider perspective to be implemented also in those area where winter temperatures are less severe – so requiring limited urban heating - but water shortage is - or is rapidly becoming - a critical issue. The proposed Symbiotic approach allows a much higher circularity to the community, making possible the fruitful recovery of the energy from the residual waste treatment to supply the sustainable recovery of sludge and wastewater and the processing of agricultural products grown through the recovered wastewater and nutrients (i.e. phosphorus) from the sludge. A further not negligible advantage is the sensible reduction of pollution thanks to a minimized landfill role and the zero wastewater discharge to water bodies.

References

[1] Mancini G., Luciano A., Cutaia L., Pulvirenti G. (2017). Industrial symbiosis (is) in the energetic valorization of different organic fractions through the ad process. Proceedings of the first SUN Conference. Rome, 25 October 2017.
[2] Antonopoulos I, Faraca G, Tonini D. Recycling of post-consumer plastic packaging waste in the EU: recovery rates, material flows, and barriers. Waste Manag 2021; 126:694–705. 4–705.
[3] European Envoronmental Agency. Water resources across Europe — confronting water stress: an updated assessment. 2021. doi:10.2800/320975
[4] Fatta D, Alaton IA, Gokcay C, Rusan MM, Assobhei O, Mountadar M, Papadopoulos A. Wastewater Reuse: Problems and Challenges in Cyprus, Turkey, Jordan and Morocco. European Water 2015; 11/12: 63–9.
[5] Barceló D, Petrovic M. Waste Water Treatment and Reuse in the Mediterranean Region. Springer-Verlag Berlin Heidelberg; 2011.
[6] Canaj K, Mehmeti A, Berbel J. The Economics of Fruit and Vegetable Production Irrigated with Reclaimed Water Incorporating the Hidden Costs of Life Cycle Environmental Impacts. Resources 2021;10:90.
[7] Mancini, G., Luciano, A., Bolzonella, D., Fatone, F., Viotti, P., Fino, D., 2021. A water-waste-energy nexus approach to bridge the sustainability gap in landfill-based waste management regions. Renewable and Sustainable Energy Reviews 137, 110441.
[8] Mancini G., Lombardi L., Luciano A., Cutaia L., Fino D. (2022). Assessing environmental and social benefits of industrial symbiosis in urban residues management. Proceedings of 6th SUN Conference. Rimini, November 8th, 2022.
[9] Mancini G., Lombardi L., Luciano A., Bolzonella, D., Viotti, P., Fino, D. (2024). A reduction in global impacts through a waste-wastewater-energy nexus: A life cycle assessment. Energy, 289, 130020.
[10] Mancini G., Luciano A., Cutaia L., Lucchetti M.C., Fino D. (2021). A symbiotic approach for sustainable waste, wastewater and residual biomass management. Proceedings of 4th SUN Conference. Rimini, November 4th, 2020
[11] Steven Meyers, Bastian Schmitt, Mae Chester-Jones, Barbara Sturm, Energy efficiency, carbon emissions, and measures towards their improvement in the food and beverage sector for six European countries (2016) , Energy, 104: 266-283.

Title: Hydrogenotrophic methanogens activity batch tests: insights from an experimental and modelling approach

Author(s): Anna Santus[1], Irene Bonato[1], Arianna Catenacci[1], Francesca Malpei[1]

[1] *Department of Civil and Environmental Engineering, Politecnico di Milano, Milano, Italy*
francesca.malpei@polimi.it

Keyword(s): biomethanation, power-to-gas, hydrogenotrophic methanogenesis, activity batch test, hydrogen transfer

Abstract

1. Introduction

Climate change is a global emergency that requires immediate and substantial intervention in the energy system. In this context, Power-to-Gas (PtG) technologies are gaining interest due to their ability to connect renewable energy production with existing energy systems. Methanation of CO_2 with green H_2 can be catalysed chemically or biologically, by harnessing the metabolism of hydrogenotrophic methanogenic (HM) *Archaea* [1]. The biogenic way operates under milder operating conditions of temperature and pressure and can be more easily integrated with facilities where anaerobic digesters already exist, providing a source of biogenic CO_2 and where it is possible to exploit the oxygen released by water electrolysis fed with renewable energies in excess. This technology is now close to market, after several demo projects of *ex-situ* methanation have been developed in the last years [2].
An efficient management of biological CO_2 conversion to CH_4, however, relies on the ability to predict the growth of HM *Archaea* and the hydrogen consumption rates and, to elucidate the relation among these parameters and the hydrogen gas transfer rate. A method for measuring the activity of HM has been firstly set-up by [3]. Originally, specific hydrogenotrophic methanogenic activity (SHMA) assays were applied to elucidate biomass performance in conventional anaerobic digestion (AD). In recent years, the growing interest in *ex-situ* biomethanation as a PtG technology has led to an increased focus on SHMA measurement. The scientific literature recognizes two methods, developed by [4] and by [3]. In both cases, the main shortcoming of the methods proposed lies in the limited focus on gas-liquid mass transfer optimisation, which is crucial when dealing with the measurement of the uptake rate of a scarcely soluble gas such as H_2. Moreover, the *inoculum* used were always mixed culture from AD systems. Values found in literature ranges from 720 $mL_N\ CH_4 \cdot g\ VSS^{-1} \cdot d^{-1}$ for mixed culture [3] to 38'086 $mL_N\ CH_4 \cdot g\ VSS^{-1} \cdot d^{-1}$ for a pure strain of HM [4], clearly showing the magnitude of the differences in the activity rates of mixed or pure cultures of HM.
Based on a mechanistic interpretation of experimental data, this work investigates the role of operating conditions (working volume to total volume ratio, mixing speed and initial H_2 partial pressure) and their correlation with the activity rate of an enriched HM culture. The results obtained are expected to help improving the accuracy and reproducibility of SHMA measurements, ultimately expanding the application of this tool for full-scale process monitoring.

2. Material and Methods

2.1 SHMA test protocol

SHMA tests were conducted following the guidelines proposed by [3] and [5]. The MethanTUBE® (MT) equipment (Biological Care, IT) was used, including 4 reactors, each featuring a volume of 3.76 L (V_{tot}), a digital manometer recording pressure every five minutes, a temperature control system, and a lid

ensuring anaerobic conditions (Figure 2.1 a). A total of 42 trials was carried out, each of them including two blank bottles (tests performed with *inoculum* only) and two activity test bottles as replicates. The *inoculum* used was collected from a biological biogas upgrading *ex-situ* pilot plant after 300 days operation, and it can be regarded as an enriched HM culture. The *inoculum* concentration on a volatile solids basis (C_{VS}) was 1.52±0.26 g VS·L^{-1}. The reactors were fed with *inoculum* according to the desired working volume (V_{liq}, mL), while keeping fixed the *inoculum* concentration. Once the reactor reached the operating temperature (310±0.5 K), the headspace (V_{gas}, mL) was flushed with an H_2:CO_2 mixture (80:20 v/v) for 15 minutes to ensure total gas replacement and, finally, the desired overpressure was set. During the test, pressure was continuously recorded to estimate H_2 consumption and thus, CH_4 production rate.

2.2 Experimental plan

In order to elucidate the role of operating conditions on test results three parameters (values reported in Table 2.1) were varied during tests: the initial overpressure ($p_{gas,0}$, bar), the mixing speed (rpm), and the ratio working volume (V_{liq}, L) to total volume (V_{tot}). The combination of tested operating conditions was chosen according to a DOE methodology [6], applied considering the following extreme values of interest: $p_{gas,0}$ = 2.0 bar, V_{liq}/V_{tot} = 1/15, and mixing speed = 800 rpm[1].

Table 2.1 Operating conditions adopted for batch tests.

Operating condition	Unit	Values
$p_{gas,0}$	bar (absolute)	1.2 – 1.6 – 2.0
Mixing speed	rpm	0 – 400 – 800
V_{liq}/V_{tot}	-	1/15 – 1/10 – 1/5

2.3 Data analysis

The SHMA value, expressed as mL$_N$ CH_4·gVS^{-1}·d^{-1}, was computed from experimental data by selecting the maximum slope of the linear part of the curve before an elbow occurred (Figure 2.1 b):

$$SHMA = max\left(\frac{\Delta p}{\Delta t} \cdot \frac{V_M \cdot V_{gas} \cdot s}{R \cdot T_{op} \cdot VS}\right) \quad \text{Equation 2.1}$$

where: Δp (bar) is the pressure increase/decrease at a generic time interval Δt (d), V_M (22.414 L$_N$·mol^{-1}) is the gas molar volume at standard conditions, V_{gas} (mL) is the headspace volume of the test, VS (g VS) is the total mass of volatile solids, R (0.0083145 L$_N$·bar·mol^{-1}·K^{-1}) is the ideal gas constant, T_{op} (K) is the operating temperature of the test, and s (0.239 mol CH_4·mol H_2^{-1}) is the stoichiometric methane production derived from [7] metabolic pathway.

In order to understand if SHMA experimental results are influenced by the operating parameters, a multiple linear regression model has been developed where the independent variables are X_1 (V_{liq}/V_{tot}), X_2 (mixing speed) and, X_3 ($p_{gas,0}$). Therefore, the formulation of the model is:

$$\hat{Y} = \beta_0 + \beta_1 \cdot X_1 + \beta_2 \cdot X_2 + \beta_3 \cdot X_3 + \varepsilon_i \quad \text{Equation 2.2}$$

For model adequacy, four steps have been followed: **Step 1**) verify collinearity of the predicted variables (X_1, X_2 and X_3), analysing the linear correlation matrix; **Step 2**) verify the normality of residuals distribution using the Shapiro-Wilk test (α = 0.05) and verify homoscedasticity of residuals with the Durbin-Watson coefficient; **Step 3**) ANOVA F-test on the whole model (α = 0.05); **Step 4**) t-test (α = 0.05) to test the significance of every β_j of the regression. The regression model has been implemented with the standardised variables in order to obtain standardised β_j coefficients to understand which of the

[1] Part of this work was funded within PNRR project CN Agritech Spoke 8, WP 8.2, Task 8.2.3.

selected parameters have a higher impact respect to the expected $\hat{Y}$.

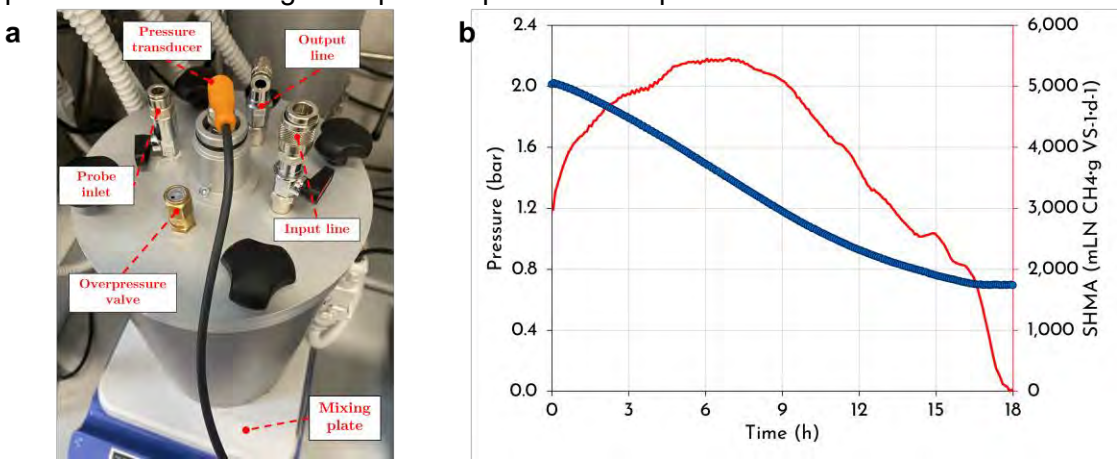

Figure 2.1 a) Laboratory set-up for SHMA tests. **b)** SHMA tests results: blue dots represent pressure values in the headspace, the red line is the instantaneous SHMA value calculated with Equation 2.1.

3. Results and discussion

3.1 The role of operating conditions

High variability of SHMA values was detected (more than an order of magnitude minimum-maximum range of variation (118 - 5'709 mL_N $CH_4 \cdot g$ $VS^{-1} \cdot d^{-1}$), combined with high dispersion of data around the average (1'622 ± 1'627 mL_N $CH_4 \cdot g$ $VS^{-1} \cdot d^{-1}$). High variability and dispersion are particularly associated to small liquid volumes and high mixing conditions, as depicted in Figure 3.1 through boxplots. Moreover, on average, low SHMA values were measured at increased liquid volume and reduced mixing speed and initial overpressure (except for $p_{gas,0}$ = 1.6 bar): it is evident that under such conditions the SHMA value is representative of the hydrogen gas-liquid mass transfer rate which is the rate-limiting process compared to the biological uptake rate by HM.

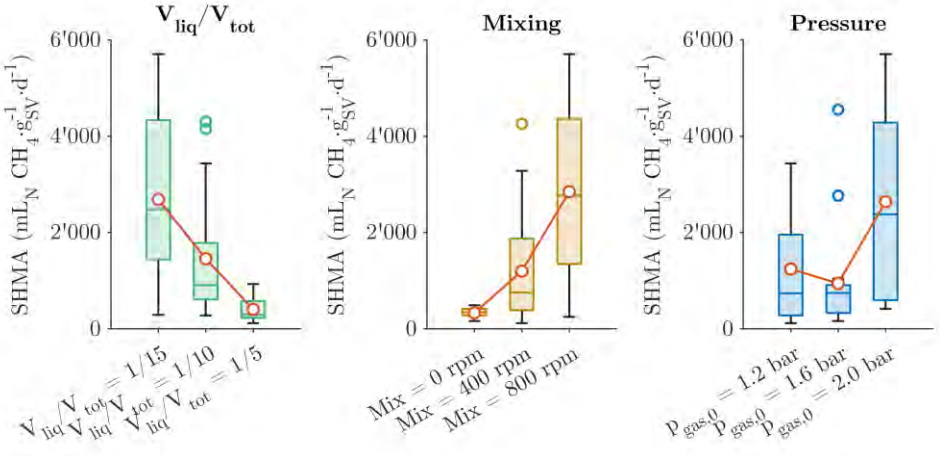

Figure 3.1. Results of activity batch tests aggregated in boxplots at varying of the selected operating conditions.

Normality of residuals has been verified through the Shapiro-Wilk test. Shapiro-Wilk test report a p-value of 0.3, higher than α = 0.05, meaning that hypothesis H_0 is accepted and confirming that residuals are normally distributed. Moreover, the Durbin-Watson coefficient result in DW = 1.69, meaning that there is absence of auto-correlation in the residuals. The statistic of the model (ANOVA) shows an R^2_{adj} = 0.71. Then, the p-value = $8.0 \cdot 10^{-10}$, lower than α = 0.05, means that H_0 is rejected, and thus at least one

β_j is different from zero, supporting the linear relation between X_i and $\hat{Y}$. Table 3.1 reports standardised coefficients of the regression model. The higher β_j is the one associated to the mixing speed (β_2 =0.55), meaning that mixing has the higher influence on the predicted variable and thus, on SHMA. Then V_{liq}/V_{tot} (β_1 = - 0.43), followed by initial pressure (β_3 = 0.24). Moreover, all the p-values are lower than α = 0.05, meaning that H_0 is rejected and thus, all β_j are not equal to zero, meaning that there is a linear relation between the predictors and the predicted variable.

Table 3.1. t-test results of the regression model.

	Estimate	p-value
β_0	$-2.5\cdot10^{-16}$	1
β_1	- 0.43	$4.83\cdot10^{-5}$
β_2	0.55	$8.98\cdot10^{-7}$
β_3	0.24	0.0135

The statistical analysis confirmed what was shown qualitatively by the experimental results. Increasing the whole H_2 gas-liquid mass transfer leads to higher measured SHMA.

4. Conclusions

This study demonstrates that SHMA measurements are significantly impacted by the H_2 transfer rate (k_La_{H2}) and by operational parameters that influences that rate. In order of relevance: mixing speed, which directly impacts the gas-liquid transfer process, and the V_{liq}/V_{tot} ratio. This outcome was further corroborated by a multiple linear regression. Whatever the goal and the application of this measure (testing a full scale system, optimizing the activity, selection of inoculum, research aims, etc.) the experimental device of SHMA and the operating parameters of the test should mimic as close as possible the conditions to investigate, and the measure of the gas transfer capacity should always be included. To improve the outcome of this work, new tests will be conducted at different biomass concentrations, and everything will be optimized and validated by using an existing mechanistic model.

References

[1] V. Corbellini *et al.*, 'Performance Analysis and Microbial Community Evolution of In Situ Biological Biogas Upgrading with Increasing H_2/CO_2 Ratio', *Archaea*, vol. 2021, pp. 1–15, Feb. 2021, doi: 10.1155/2021/8894455.

[2] M. Bailera, P. Lisbona, L. M. Romeo, and S. Espatolero, 'Power to Gas projects review: Lab, pilot and demo plants for storing renewable energy and CO_2', *Renewable and Sustainable Energy Reviews*, vol. 69, pp. 292–312, Mar. 2017, doi: 10.1016/j.rser.2016.11.130.

[3] J. D. Coates, M. F. Coughlan, and E. Colleran, 'Simple method for the measurement of the hydrogenotrophic methanogenic activity of anaerobic sludges', *Journal of Microbiological Methods*, vol. 26, no. 3, pp. 237–246, Aug. 1996, doi: 10.1016/0167-7012(96)00915-3.

[4] J. Dolfing and W. G. B. M. Bloeman, 'Acitivity measurements as a tool to characterize the microbial composition of methanogenic environments', *Journal of Microbiological Methods*, vol. 4, no. 1, pp. 1–12, Jun. 1985, doi: 10.1016/0167-7012(85)90002-8.

[5] E. Ripoll, I. López, and L. Borzacconi, 'Hydrogenotrophic activity: A tool to evaluate the kinetics of methanogens', *Journal of Environmental Management*, vol. 270, p. 110937, Sep. 2020, doi: 10.1016/j.jenvman.2020.110937.

[6] G. E. P. Box and D. W. Behnken, 'Some New Three Level Designs for the Study of Quantitative Variables', *Technometrics*, vol. 2, no. 4, Nov. 1960, [Online]. Available: https://www.stat.cmu.edu/technometrics/59-69/VOL-02-04/v0204455.pdf

[7] R. E. Speece, *Anaerobic biotechnology for industrial wastewaters*. Nashville, Tennessee: Archae Press, 1996.

Upcycling AD by-products to single-cell proteins: laboratory validation of two bioprocesses based on digestate and waste off-gas utilization

F. Di Benedetto*[1,2], S. Cantera[2], R. Muñoz[2], A. Turolla[1], E. Ficara[1]

[1] *Department of Civil and Environmental Engineering (DICA), Politecnico di Milano, P.zza L. da Vinci 32, 20133 Milano, Italy (E-mail: francesca.dibenedetto@polimi.it, andrea.turolla@polimi.it, elena.ficara@polimi.it)*
[2] *Institute of Sustainable Processes, University of Valladolid, Dr. Mergelina, s/n, 47011 Valladolid, Spain (E-mail: sara.cantera@uva.es, raul.munoz.torre@uva.es)*

Keywords: microbial proteins; digestate valorization; carbon and nutrient upcycling

Introduction

Digestate is the nutrient-rich (N, P, K) by-product of anaerobic digestion (AD), which has been used for years for direct application on farmland soils for fertilizing purposes [1], leading to several pollution issues [2]. As EU strictly regulated digestate application, effective and sustainable technological solutions are requested to exploit digestate valuable content [3]. A possible alternative method for digestate valorization consists in its utilization as a substrate to produce single-cell proteins (SCP). SCP are microbial dried cells, used as protein supplement in human foods or animal feeds [4], representing a promising alternative to partially replace the poorly sustainable conventional ones (soy, fish meal) and to support increasing nutritional needs [5]. While SCP are currently produced from fossil-based carbon sources, recent research frontiers are exploring novel bioprocesses based on waste feedstocks.
For upscale-oriented research, in this study a preliminary cost analysis of two bioprocesses for SCP production was carried out and after economic feasibility verification, these were subjected to technical comparison at lab-scale. For both processes, the nutrient-rich substrate was centrate from liquid digestate, while the two processes differed in the carbon sources to please autotrophic metabolism, respectively using carbon dioxide (CO_2) separated from biogas upgrading and syngas (35% H_2, 30%CO, 25% CO_2, 10% CH_4) from solid digestate gasification. Two aerobic microbial isolates (isolate-1 and isolate-2) and an anaerobic consortium were selected and preliminary tested in 1-L batch bioreactors on traditional liquid substrate to validate the capability of consuming the selected off-gases as carbon sources. Growing performances (doubling time and lag phase), protein/biomass production, and gas consumption rate were studied. Lately, agricultural liquid digestate has been characterized, studying N and P, solids, metal and pathogen content. As these contaminants could interfere with the microbial growth and compromise the final protein quality, different pre-treatments for digestate purification were compared and final centrate was analysed. The bacteria with shorter doubling time were selected for further implementation in 2-L batch bioreactors with centrate as liquid nutrient source. Final SCP production and gas consumption efficiency were compared for each bacterial isolate and growing condition. Optimal outcomes were identified in the view of process scale-up in continuous bioreactors for further process optimization. The final goal of this project is to identify the most promising technology trains capable of maximizing nutrient and carbon utilization from the AD plants, enhancing the overall process sustainability and cost-effectiveness.

Materials and Methods

Two aerobic isolates, isolate-1 and isolate-2, as well as an anaerobic consortium were selected for physiological cultivation (Task1 - **Figure 1**) and batch bioconversion in conventional nutrient sources (Task 2 - **Figure 1**). Additionally, the anaerobic consortium, capable of consuming the desired off-gases and to produced acetate, was cultivated. The acetate produced was intended to be fed as carbon substrate to a second bioreactor, where an acetate-consuming pure strain could grow in a two-step

process to enable efficient protein production.

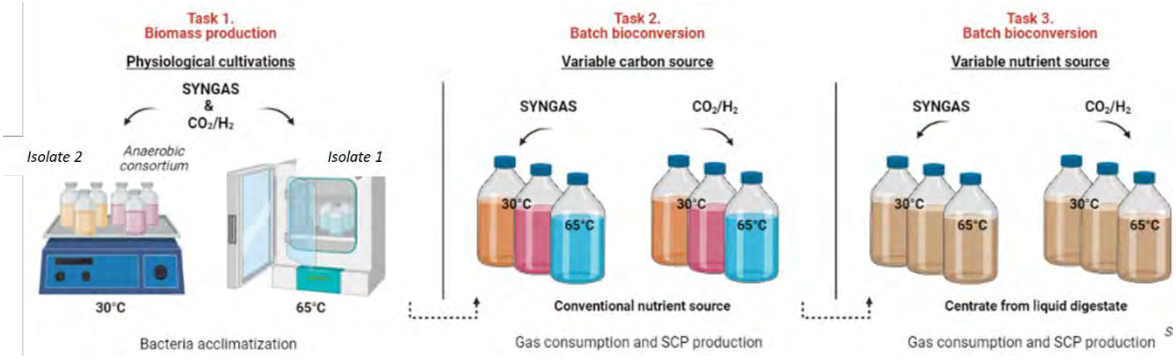

Figure 1. Experimental design of the selected processes.

The experimental design of this study and the main tasks are reported in **Figure 1**. The experimental procedure began with biomass enrichment and acclimatization to the medium (Task 1). Subsequently, both isolates and the consortium were tested in 1-L bioreactors using conventional Ammonium Mineral Salt (AMS) medium for the aerobic isolates and CP-medium for the anaerobic consortium to assess doubling time, maximum biomass and protein production, and the rate of carbon and energy substrate consumption (Task 2). A liquid-gas ratio of 25-75% and an agitation speed of 200 rpm were maintained to improve gas transfer to liquid phase, hence bacterial consumption.

For experiments in aerobic conditions, gas phase configurations were:

1. H_2-CO_2/air: (%v/v) 10% O_2, 40% N_2, 40% H_2, and 10% CO_2;
2. Syngas/air: (%v/v) 10% O_2, 40% N_2, 10% O_2, 17% H_2, 15% CO_2, 12.5% CO, and 5% CH_4.

For experiments in anaerobic conditions (O_2<2%v/v), gas compositions were:

1. H_2-CO_2: (%v/v) 80% H_2 and 20% CO_2
2. Syngas: (%v/v) 35% H_2, 30% CO, 25% CO_2, and 10% CH_4.

Isolate-1 is a thermophile and the experiment was carried out at its optimal growth temperature of 65 °C while isolate-2 was grown at 23 °C. The anaerobic consortium was tested both at 23 °C and 37 °C (optimal growth temperature). A pH of 7 was maintained for both isolates and consortium.

Liquid digestate characterization was carried out through conventional methods for total nitrogen, ammonium, TS-VS and phosphorus determination. Furthermore, metal content (Al, As, Cr, Cu, Fe, Mn, Ni, Pb, Zn, Mo) was determined through Atomic Spectroscopy ICP-MS and pathogens (*Escherichia choli, Clostridium perfinges, Listeria monocytogenes*, *Salmonella* spp. and *Campylobacter* spp.) were analysed through plate count and immunofluorescence.

Different liquid digestate pre-treatments were tested to obtain a purified centrate for SCP production and different liquid outputs were characterized and compared to select the best pre-treatment technologies. Preliminary centrifugation for solid removal and sequential membrane filtration (cascade pore-size of 0.7, 0.45 and 0.22 μm) for metal, pathogens and solids removal were performed. Stepwise filtration was operated both with and without inorganic coagulants to speed up the pre-treatment process. The tested coagulants were $Al_2(SO_4)_3 \cdot 18H_2O$ and $FeCl_3 \cdot 6H_2O$ at 2 g/L concentration. Jar test method ASTM D2035-08 was performed to select the optimal concentration of selected coagulant.

Once a suitable centrate was obtained and pre-treatment steps optimized, the bacterial isolates with shorter doubling time were selected for the subsequent validation phase in 2-L bioreactors using

digestate-based centrate as N source (Task 3).

Growing performances, protein production and gas consumption rate were investigated.

Results and Conclusions

Both the aerobic isolates and the anaerobic consortium were able to growth in conventional nutrient sources. While isolate-2 was able to grow at room temperature (23 °C), avoiding the need for external heating sources, the anaerobic consortium was only able to growth at 37 °C. To select the best isolates/consortium for further implementation, the doubling time of each isolate/consortium both for H_2-CO_2 condition and syngas condition were evaluated. The results are shown in **Table 1**. As the anaerobic consortium shown the longest lag phase, it was discarded for the following implementation in digestate.

Table 1. Doubling times for considered isolates and consortium at different tested conditions.

Isolates/consortium	Conditions	Doubling time (h)	Lag phase(h)
isolate-1	H_2-CO_2/AIR	9.16 ± 2.94	< 24
	SYNGAS/AIR	6.52 ± 0.65	< 24
isolate-2	H_2-CO_2/AIR	14.66 ± 2.32	48
	SYNGAS/AIR	29.45 ± 0.02	72
Anaerobic consortium	H_2-CO_2	93.06 ± 0.13	96
	SYNGAS	260.56 ± 0.11	192

For Task 3, a preliminary study for the best centrate production was carried out, testing the membrane filtration of Liquid Digestate (LD) without coagulants, and with $FeCl_3$ and $Al_2(SO4)_3$. Filtration rates of the three different configurations through a 0.7 μm pore-sized membrane are shown in **Table 2**.

Table 2. Filtration rates in 0.7μm pore-sized membrane.

Sample	Filtration rate (min/L)
LD	960
LD (treated with $FeCl_3$)	23
LD (treated with $Al_2(SO_4)_3$)	60

Finally, further filtration on 0.45 and 0.22 μm pore-sized membranes was performed. Total nitrogen, ammonium, phosphate, COD of untreated LD and centrate filtrated with 0.22 μm pore-sized membrane were characterized, also considering the dosage of with $FeCl_3$ and $Al_2(SO_4)_3$. The composition of the three samples is reported in **Table 3**.

Table 3. Total nitrogen, ammonium, phosphate, COD of LD, LD ($FeCl_3$) and LD ($Al_2(SO_4)_3$).

Sample	Ammonium (gN/L)	Total Nitrogen (gN/L)	COD (gO_2/L)	Phosphate (mg/L)
LD	0.91	1.02	1.37	UDL
LD (treated with $FeCl_3$)	0.86	0.89	0.98	UDL
LD (treated with $Al_2(SO_4)_3$)	0.88	0.88	0.95	UDL

UDL= under detection limit

These results show that the ammonium content in untreated LD and both filtrated centrate samples is very abundant, compared to the ammonium content of the AMS medium, which is 0.126 gN/L. As ammonium is the form of nitrogen assimilable by bacteria, these results confirmed the possibility to exploit digestate as growth medium. However, the phosphate content is very low so 1 g/L of KH_2PO_4 was added to the liquid centrate, contributing to pH reduction to 7.5 (optimum for bacterial growth), starting from a value of 8.7 of LD and guaranteeing the satisfaction of bacterial phosphate need.
Not a significative difference in solid, metal and pathogens content was observed between 0.45 and 0.22 μm membrane filtration as in both cases metal and pathogens were below the established limits for SCP production. So, the best pretreatment consisted in a preliminary step of centrifugation, addition of 2 g/L of $FeCl_3 \cdot 6H_2O$ coagulant, 0.45 μm pore-sized membrane filtration.

2-L bioreactors using centrate as liquid source of nutrient and the two different gaseous carbon sources were set up. So far, isolate-2 showed the capability of growing on digestate with CO_2 and H_2 as carbon and energy sources, at 23 °C producing a biomass three times more concentrated than the one obtained in conventional AMS medium experiments. Further experiments will aim at testing isolate-1 growth on digestate-based centrate as liquid source, using both CO_2-H_2/air and syngas/air configurations.

This study proves the possibility to produce SCP for animal feed starting from AD liquid and gaseous by-products, making value out of solid and liquid digestate and CO_2. The biotechnological route for off-gases and digestate valorisation studied will enhance the integration of innovative processes in AD plants, promoting the circular use of resources and lowering the environmental impact of biogas production chain.

References

[1] Kovačić, Đ., Lončarić, Z., Jović, J., Samac, D., Popović, B., & Tišma, M. (2022). Digestate Management and Processing Practices: A Review. In Applied Sciences (Switzerland) (Vol. 12, Issue 18). MDPI. https://doi.org/10.3390/app12189216
[2] Rizzioli, F., Bertasini, D., Bolzonella, D., Frison, N., & Battista, F. (2023). A critical review on the techno-economic feasibility of nutrients recovery from anaerobic digestate in the agricultural sector. In Separation and Purification Technology (Vol. 306). Elsevier B.V. https://doi.org/10.1016/j.seppur.2022.122690
[3] Hermann, L., Hermann, R., & Schoumans, O. F. (2019). Report on regulations governing anaerobic digesters and nutrient recovery and reuse in EU member states. https://doi.org/10.18174/476673
[4] Nasseri, A. T., Rasoul-Ami, S., Morowvat, M. H., & Ghasemi, Y. (2011). Single Cell Protein: Production and Process. American Journal of Food Technology, 6(2), 103–116. https://doi.org/10.3923/ajft.2011.103.116
[5] Zha, X., Tsapekos, P., Zhu, X., Khoshnevisan, B., Lu, X., & Angelidaki, I. (2021). Bioconversion of wastewater to single cell protein by methanotrophic bacteria. Bioresource Technology, 320, 124351. https://doi.org/10.1016/j.biortech.2020.124351

PARALLEL SESSION: A7

Flash

Process optimization and sustainability

Title: Life cycle assessment of a new approach for micro-PET recovery from domestic laundry wastewater and subsequent valorisation into amino acids

Author(s): Marco Carnevale Miino*[1], Alberto Pietro Damiano Baltrocchi[1], Fabio Conti[1], Elena Cristina Rada[1], Vincenzo Torretta[1]

[1] *Department of Theoretical and Applied Sciences, University of Insubria, Via J.H. Dunant 3, 21 100, Varese, Italy; marco.carnevalemiino@uninsubria.it*

Keyword(s): LCA; microplastics; polyethylene terephthalate; plastic pollution; circular economy

Abstract

Microplastics (MPs) represent an issue of concern due to their spread in the environment and bad implications on the health of wildlife and potentially humans [1,2]. They are generally defined as particles smaller than 5 mm but can have several shapes [3]. Among the many existent pathways of release of MPs in the environment, the household production of MPs and the consequent release in the sewer system represents one of the major ones [4].

WWTPs demonstrated to be effective in removing MPs from waters (up to 99%) but to date fail to act as a complete barrier against their spread in the environment [3,5,6]. In fact, residues produced during wastewater treatment (e.g., sewage sludge) can be a source of MPs when recycled/reused for other purposes [7,8]. In this sense, actions for limiting MPs' release at the source can be potentially more effective.

In a domestic environment, MPs can derive from the use of several products such as cosmetics that contain synthetic polymers, wipes flushed in toilets, and sponges made of plastic materials [9]. However, among these, laundry activities (washing and drying) seem to be a major source of release, especially for microfibres of polyethylene terephthalate (PET), a polyester, and one of the most used synthetic textile fibres [10]. Due to their properties such as high resistance to strain and deformation, this type of synthetic fabric is now widely used in clothing, carpets, and other materials [11]. To date, some studies pointed out that the release of synthetic microfibers during domestic laundry activities can be very high (up to 18 million microfibers released for a reference load of 6 kg of synthetic clothes) [12]. In most cases, these fibres are released in the sewer system but recently devices for filtering the discharges of domestic laundry have been tested for the separation of MPs [13-15].

However, to date, possible solutions for the valorisation of PET microfibers recovered from laundry wastewater are not clear and the MPs are generally disposed of through the solid waste management system. This work aims to evaluate the environmental sustainability of a new approach, currently under study in the project Protein from Plastic (ProPla), for the separation of micro-PET from wastewater and subsequent valorisation into amino acids thanks to an engineered *E. coli* strain [16].

The project has a very huge potential considering the high amount of micro-PET released yearly. Based on literature data, up to 65 mg of microfibres can be released per kg of washed clothes [17]. Considering that, on average, 20-30% of clothes' textile is represented by PET, it means that more than 15 mg of micro-PET per kg of textile washed can be potentially collect and recovered with this approach.

The Life Cycle Assessment (LCA) approach, according to ISO 14040 [18] and 14044 [19], has been used to solve the following questions: what is the most impactful process in the entire approach? Is the ProPla project more sustainable compared to other conventional systems for production?

To develop the analysis, SimaPro v9 software [20] with Ecoinvent v3.9.1 database [21] have been used and 1 g of the target amino acid has been considered as the functional unit. The system boundaries considered two main blocks of processes: (i) micro-PET extraction and pre-treatment, and (ii) micro-PET conversion and valorisation. The normalized results of the analysis carried out on primary data were compared with the conventional production of the target amino acid (secondary data collection). Avoided impacts due to micro-PET removal from the environment were also taken into account in terms of Ecosystem Quality (PDF m^2 y^{-1}) and Human Health (DALY) end-point categories.
The results that will be presented will be helpful to understand if the proposed approach is sustainable from an environmental point of view and what are the margins for improvement to reduce environmental impact.

Acknowledgments

This work was supported by the Fondazione Cariplo grant "ProPla: proteins from plastics" 2022-0631.

References

[1] Pauna V. H., Buonocore E., Renzi M., Russo G. F., Franzese P. P., The issue of microplastics in marine ecosystems: A bibliometric network analysis. Marine Pollution Bulletin, 149, 110612, (2019). https://doi.org/10.1016/j.marpolbul.2019.110612
[2] Nava V., Chandra S., Aherne J., Alfonso M.B., Antão-Geraldes A.M., Attermeyer K., Bao R., Bartrons M., Berger S.A., Biernaczyk M., Bissen R., Brookes J.D., Brown D., Cañedo-Argüelles M., Canle M., Capelli C., Carballeira R., Cereijo J.L., Chawchai S., Christensen S.T., Christoffersen K.S., de Eyto E., Delgado J., Dornan T.N., Doubek J.P., Dusaucy J., Erina O., Ersoy Z., Feuchtmayr H., Frezzotti M.L., Galafassi S., Gateuille D., Gonçalves V., Grossart H.-P., Hamilton D.P., Harris T.D., Kangur K., Kankılıç G.B., Kessler R., Kiel C., Krynak E.M., Leiva-Presa À., Lepori F., Matias M.G., Matsuzaki S.S., McElarney Y., Messyasz B., Mitchell M., Mlambo M.C., Motitsoe S.N., Nandini S., Orlandi V., Owens C., Özkundakci D., Pinnow S., Pociecha A., Raposeiro P.M., Rõõm E.-I., Rotta F., Salmaso N., Sarma S.S.S., Sartirana D., Scordo F., Sibomana C., Siewert D., Stepanowska K., Tavşanoğlu Ü.N., Tereshina M., Thompson J., Tolotti M., Valois A., Verburg P., Welsh B., Wesolek B., Weyhenmeyer G.A., Wu N., Zawisza E., Zink L., Leoni B., Plastic debris in lakes and reservoirs. Nature, 619, 317–322, (2023). https://doi.org/10.1038/s41586-023-06168-4
[3] Sun J., Dai X., Wang Q., Van Loosdrecht M. C., Ni B. J., Microplastics in wastewater treatment plants: Detection, occurrence and removal. Water research, 152, 21-37, (2019). https://doi.org/10.1016/j.watres.2018.12.050
[4] Wang T., Li B., Zou X., Wang Y., Li Y., Xu Y., Mao L., Zhang C., Yu W., Emission of primary microplastics in mainland China: Invisible but not negligible. Water research, 162, 214–224, (2019). https://doi.org/10.1016/j.watres.2019.06.042
[5] Collivignarelli M.C., Carnevale Miino M., Caccamo F.M., Milanese C., Microplastics in Sewage Sludge: A Known but Underrated Pathway in Wastewater Treatment Plants. Sustainability, 13, 12591, (2021). https://doi.org/10.3390/su132212591
[6] Galafassi S., Di Cesare A., Di Nardo L., Sabatino R., Valsesia A., Fumagalli F.S., Corno G., Volta P., Microplastic retention in small and medium municipal wastewater treatment plants and the role of the disinfection. Environmental Science and Pollution Research, 29, 10535–10546, (2022). https://doi.org/10.1007/s11356-021-16453-2
[7] Rolsky C., Kelkar V., Driver E., Halden R.U., Municipal sewage sludge as a source of microplastics in the environment. Current Opinion in Environmental Science & Health, 14, 16–22, (2020). https://doi.org/10.1016/j.coesh.2019.12.001
[8] van den Berg P., Huerta-Lwanga E., Corradini F., Geissen V., Sewage sludge application as a vehicle for microplastics in eastern Spanish agricultural soils. Environmental Pollution, 261, 114198, (2020). https://doi.org/10.1016/j.envpol.2020.114198
[9] Jessieleena A., Rathinavelu S., Velmaiel K.E., John A.A., Nambi I.M., Residential houses — a major point

source of microplastic pollution: insights on the various sources, their transport, transformation, and toxicity behaviour. Environmental Science and Pollution Research 30, 67919–67940, (2023). https://doi.org/10.1007/s11356-023-26918-1
[10] Tian Y., Chen Z., Zhang J., Wang Z., Zhu Y., Wang P., Zhang T., Pu J., Sun H., Wang L., An innovative evaluation method based on polymer mass detection to evaluate the contribution of microfibers from laundry process to municipal wastewater. Journal of Hazardous Materials, 407, 124861, (2021). https://doi.org/10.1016/j.jhazmat.2020.124861
[11] Napper I.E., Thompson R.C., Release of synthetic microplastic plastic fibres from domestic washing machines: Effects of fabric type and washing conditions. Marine Pollution Bulletin, 112, 39–45, (2016). https://doi.org/10.1016/j.marpolbul.2016.09.025
[12] Galvão A., Aleixo M., De Pablo H., Lopes C., Raimundo J., Microplastics in wastewater: microfiber emissions from common household laundry. Environmental Science and Pollution Research 27, 26643–26649, (2020). https://doi.org/10.1007/s11356-020-08765-6
[13] Belzagui F., Gutiérrez-Bouzán C., Carrillo-Navarrete F., López-Grimau V., Sustainable Filtering Systems to Reduce Microfiber Emissions from Textiles during Household Laundering. Polymers, 15, 3023, (2023). https://doi.org/10.3390/polym15143023
[14] Erdle L.M., Nouri Parto D., Sweetnam D., Rochman C.M., Washing Machine Filters Reduce Microfiber Emissions: Evidence From a Community-Scale Pilot in Parry Sound, Ontario. Frontiers in Marine Science, 8, (2021). https://doi.org/10.3389/fmars.2021.777865
[15] Le L.-T., Nguyen K.-Q.N., Nguyen P.-T., Duong H.C., Bui X.-T., Hoang N.B., Nghiem L.D., Microfibers in laundry wastewater: Problem and solution. Science of The Total Environment 852, 158412, (2022). https://doi.org/10.1016/j.scitotenv.2022.158412
[16] ProPla, Project “Proteins from Plastics”, (2023). Available online at: https://www.theproteinfactory2.it/propla
[17] Kelly M.R., Lant N.J., Kurr M., Burgess J.G. Importance of water-volume on the release of microplastic fibers from laundry. Environmental science & technology 53(20), 11735-11744, (2019). https://doi.org/10.1021/acs.est.9b03022
[18] ISO 14040:2006: Environmental Management-Life Cycle Assessment-Principles and framework, (2006).
[19] ISO 14044:2006/Amd 2:2020 Environmental management. Life Cycle Assessment. Requirements and guidelines, (2006).
[20] PRé Sustainability, SimaPro database manual, methods library, (2020). Available online: https://simapro.com/wp-content/uploads/2020/10/DatabaseManualMethods.pdf [access at 15/03/2024].
[21] The ecoinvent Database: Overview and Methodological Framework. The International Journal of Life Cycle Assessment, 10(1), 3-9 (2004). https://doi.org/10.1065/lca2004.10.181.1

Title: From dissipative to assimilative wastewater treatment: the potential of hydrogen-oxidizing bacteria to upcycle nitrogen and mitigate greenhouse gas emissions from wastewater.

Author(s): Manoj Kumar*[1], Silvio Matassa[1], Chiara Belloni[1], Francesco Pirozzi[1], Giovanni Esposito[1], Stefano Papirio[1]

[1]*Department of Civil, Architectural and Environmental Engineering, University of Napoli Federico II, via Claudio 21, 80125 Napoli (Italy), manoj.kumar@unina.it, silvio.matassa@unina.it, chiara.belloni@unina.it, francesco.pirozzi@unina.it, gioespos@unina.it, stefano.papirio@unina.it*

Keyword(s): Hydrogen-oxidizing bacteria; wastewater treatment; nitrogen assimilation, microbial protein, greenhouse gas.

Abstract

Wastewater treatment presents a dual challenge of efficiently eliminating pollutants such as nitrogen while minimizing environmental impacts such as greenhouse gas emissions [1]. This study proposes a novel approach to address these challenges through the utilization of H_2-driven assimilatory mixotrophic metabolism. By leveraging the metabolic capabilities of hydrogen-oxidizing bacteria (HOB), this approach aims to upcycle nitrogen in wastewater, while mitigating the release of greenhouse gases such as carbon dioxide (CO_2) and nitrous oxide (N_2O). HOB have demonstrated a remarkable efficiency in converting nitrogen into a protein-rich biomass, also known as microbial protein (MP). This versatile resource holds promise for a wide range of applications, including nutrition for both animals and humans, as well as the development of techno-functional polymers [2]. In the nitrogen assimilation process, HOB utilize hydrogen (H_2) as electron donor and oxygen (O_2) as electron acceptor to fix carbon dioxide (CO_2) and ammonium nitrogen ($N\text{-}NH_4^+$) [3].

For this purpose, a mixed culture of hydrogen-oxidizing bacteria (HOB) capable of mixotrophic growth was here assessed under batch and continuous systems for treating both synthetic and real wastewater across various carbon-to-nitrogen (C/N) ratios. The same mixed HOB culture was cultivated under heterotrophic conditions to compare treatment and process efficiencies, focusing on ammonium

nitrogen ($N\text{-}NH_4^+$) removal and assimilation, chemical oxygen demand (COD) removal, CO_2 emission, biomass concentration, yield, and protein content. Batch biological nitrogen assimilation experiments were performed using 250 mL serum bottles with a working volume of 25 mL. The bottles were incubated at 30 ± 1 ºC and placed on a shaker set at 85 rpm. The hydraulic retention time (HRT) and solid retention time (SRT) were set at 3.33 days by refreshing 15 out of 25 mL of medium every 48 h. Under mixotrophic conditions, the highest biomass concentration was 342.5 mg $VSS \cdot L^{-1}$, which was twice the amount obtained under heterotrophic conditions (161.2 mg $VSS \cdot L^{-1}$) in batch assays (Figure 1). Under mixotrophic conditions, the mixed HOB culture grew by utilizing acetate or the organic carbon present in the wastewater as both energy and carbon sources. Additionally, the introduction of H_2 enhanced the capture of all CO_2 generated during the oxidation of organic carbon, effectively mitigating potential greenhouse gas (GHG) emissions. Mixotrophic conditions not only met discharge limits for both COD and total N but also achieved nitrogen removal and assimilation into protein-rich biomass up to 99%. On the contrary, under heterotrophic conditions, the high content of residual nitrogen as nitrite (up to 26 $mg \cdot L^{-1}$ of $N\text{-}NO_2^-$) did not allow to meet discharge limits for total N. Under mixotrophic conditions, neither nitrite nor nitrate were detected, confirming the absence of nitrification-denitrification dynamics and, consequently, avoiding potential N_2O emissions. The mixed HOB culture exhibited promising results in terms of biomass yield (0.32 g $VSS \cdot g\ COD_{H2+acetate}^{-1}$) and protein content (up to 56% of VSS) when grown mixotrophically (Table 1). Under heterotrophic conditions, instead, the biomass yield (0.25 g $VSS \cdot g\ COD_{acetate}^{-1}$) and protein content (35%) were substantially lower.

For biological nitrogen assimilation under continuous mode, a reactor with a working volume of 700 mL was operated at room temperature, with a pH of 7 and a C/N ratio of 5, employing a mixed HOB culture under mixotrophic conditions. H_2 was supplied through a hydrophobic membrane, while O_2 was supplied via sparger. During continuous reactor operation, the biomass concentration reached its peak at 467.6 mg $VSS \cdot L^{-1}$ under mixotrophic conditions with a hydraulic retention time (HRT) of 5 days. The highest

protein content achieved under continuous operation was 58% of VSS (Table 1). Notably, no CO_2 or N_2O emissions were detected during continuous operation, indicating minimal greenhouse gas (GHG) emissions. However, a nitrate concentration of 14.5 $mg \cdot L^{-1}$ was detected. Figure 2 illustrates a potential scheme for integrating this process into an urban wastewater treatment plant (WWTP).

Overall, the integration of this process into wastewater treatment processes represents a promising avenue for achieving both environmental sustainability and resource recovery objectives. Further research and development efforts are needed to optimize this approach and enable its widespread implementation in wastewater treatment facilities worldwide.

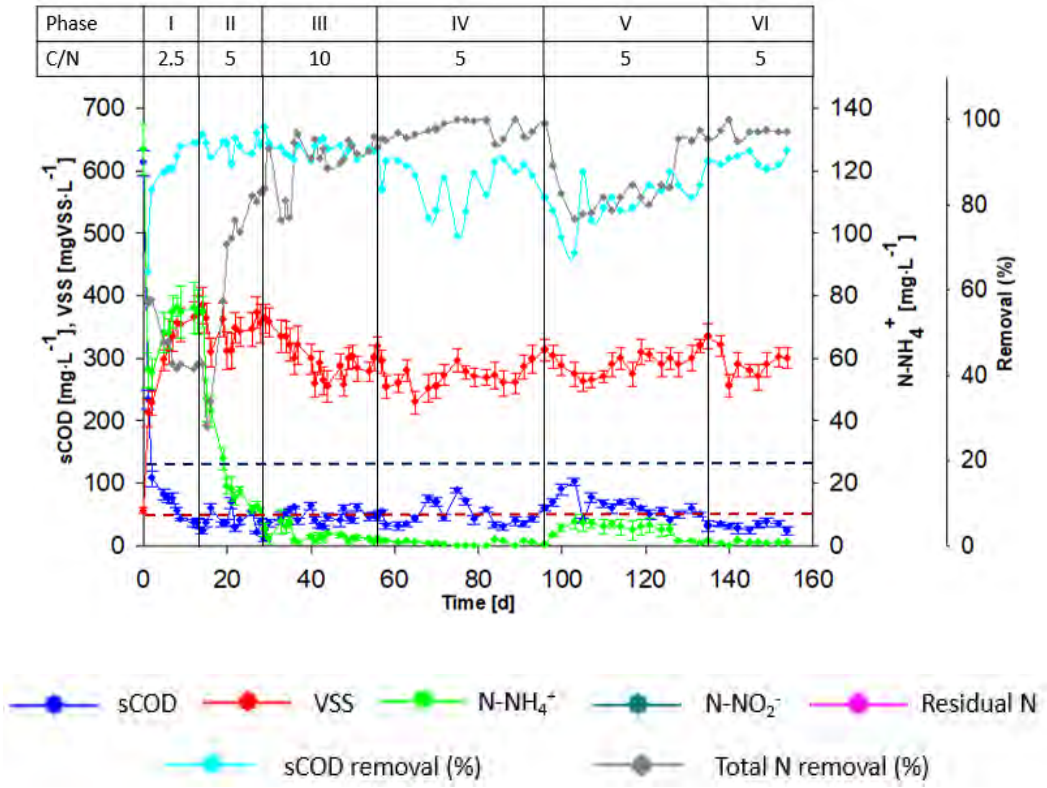

Figure 1. VSS, sCOD, ammonium ($N\text{-}NH_4^+$) and nitrite ($N\text{-}NO_2^-$) concentrations as well as sCOD and ammonium nitrogen removal efficiencies (%) under mixotrophic (H_2+acetate) conditions. Error bars refer to the standard deviation calculated from the triplicates of each test. Note: $N\text{-}NO_2^-$ was not reported in panel A since it was not detected in the experiments carried out mixotrophically. The blue and red dotted lines indicate the total N (10 $mg \cdot L^{-1}$) and COD (125 $mg \cdot L^{-1}$) discharge limits.

Table 1. Summery of batch and continuous reactor systems under mixotrophic mode

Mode	Highest biomass concentration (mg VSS·L^{-1})	Protein content (% of VSS)	Greenhouse gas emission	Nitrate and nitrite (mg·L^{-1})
Batch	342.5	56	No	0
Continuous	467.6	58	No	Nitrite = 0 Nitrate = 14.5

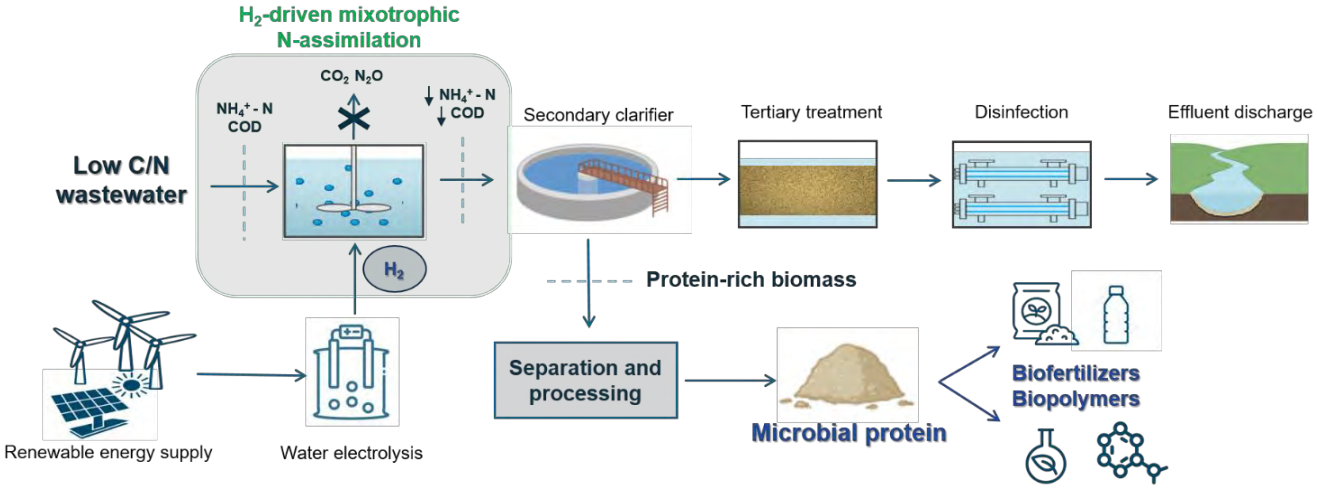

Figure 2. Potential process scheme for the implementation of the H_2-driven mixotrophic N- assimilation in WWTPs.

References

[1] S. Matassa, D.J. Batstone, T. Hülsen, J. Schnoor, W. Verstraete, "Can Direct Conversion of Used Nitrogen to New Feed and Protein Help Feed the World?" Environmental Science & Technology, 49, 5247–5254 (2015).
[2] M. Areniello, S. Matassa, G. Esposito, P.N.L. Lens, "Biowaste upcycling into second-generation microbial protein through mixed-culture fermentation" Trends in Biotechnology, 41, 197–213 (2023).
[3] S. Matassa, N. Boon, W. Verstraete, "Resource recovery from used water: The manufacturing abilities of hydrogen-oxidizing bacteria" Water Research, 68, 467–478 (2015).

Title: Sustainable Electrochemical Reduction of contaminants of emerging concern and Pathogens in WWTP effluent for Irrigation of Crops (SERPIC)

Author(s): M. Pilar. Castro[1]*, Ismael. F. Mena[1], Ángela Moratalla Tolosa[2], Paola Verlicchi[2], Carla S. Santos[3], Ana I. Gomes[3], Vítor J.P. Vilar[3], Alexander Wolf[4], Pawel Krzeminski[5], Marelize Botes[6], Jan Gäbler[7], Cristina Sáez[1], Manuel. A Rodrigo[1].

[1] Department of Chemical Engineering. Faculty of Chemical Sciences &Technologies. University of Castilla-La Mancha, Campus Universitario s/n, 13071 Ciudad Real, Spain.
[2] Department of Engineering, University of Ferrara, Vai Saragat 1, 44122 Ferrara, Italy.
[3] LSRE-LCM – Laboratory of Separation and Reaction Engineering - Laboratory of Catalysis and Materials, Faculty of Engineering, University of Porto, Rua Dr. Roberto Frias, 4200-465 Porto, Portugal
ALiCE – Associate Laboratory in Chemical Engineering, Faculty of Engineering, University of Porto, Rua Dr. Roberto Frias, 4200-465 Porto, Portugal
[4] SolarSpring GmbH. Christaweg 40, 79114 Freiburg, Germany
[5] Norwegian Institute for Water Research. Gaustadalléen 21, 0349, Oslo, Norway.
[6] Stellenbosch University, Stellenbosch Central, Stellenbosch, South Africa.
[7] Fraunhofer Institute for Surface Engineering and Thin Films IST, 38108 Braunschweig, Germany.

Keyword(s): Contaminants of Emerging Concern, SERPIC, wastewater, multi-barrier system, ozone, persulfate, nanofiltration, photoreactor.

Abstract

In recent years, the impact of climate change has manifested in major droughts and extreme temperatures, and, in numerous instances, our mismanagement of water has led to the depletion of global water resources. Consequently, there is a critical imperative to explore novel and alternative water sources. Reusing treated wastewater for irrigating crops has gained prominence among these alternatives. However, this approach is not without its drawbacks. The reclaimed water may contain contaminants of emerging concern (CECs), including pesticides and pharmaceuticals, among other substances, as well as antibiotic-resistant bacteria (ARB) and antibiotic-resistance genes (ARG). Most of them persist after undergoing conventional treatment processes in wastewater treatment plants (WWTPs), posing potential risks to human health and the environment [1]. To address this challenge, the European project “Sustainable Electrochemical Reduction of Contaminants of Emerging Concern and Pathogens in WWTP Effluent for Irrigation of Crops” (SERPIC, https://www.serpic-project.eu/) emerges as an alternative solution for treating such water. Figure 1 illustrates the urban water cycle, and where SERPIC technology would come in.

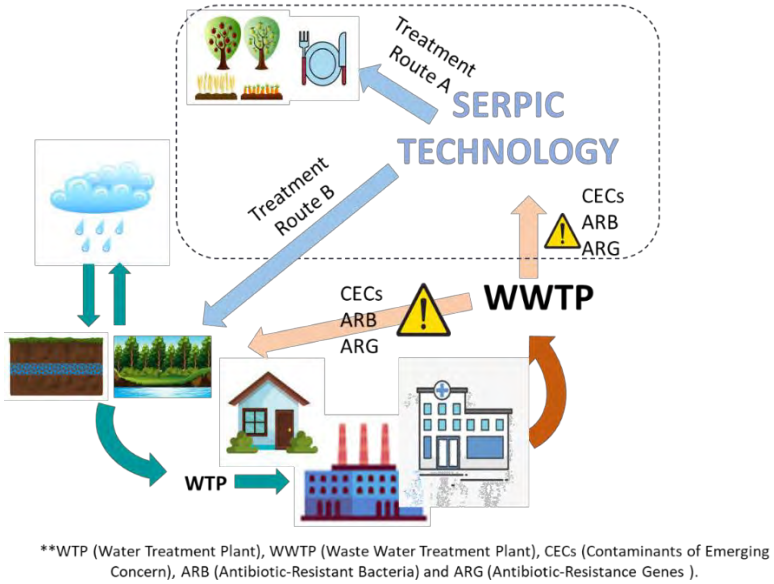

Figure 1. Schematics of the urban water cycle with the SERPIC technology.

The primary aim of the SERPIC project is to reduce the spread of CECs, ARB, and ARGs present in a secondary effluent intended for crop irrigation. To achieve this goal, the project proposes a multi-barrier treatment strategy that integrates membrane filtration processes with the electrochemical generation of powerful oxidants, activated by deep ultraviolet irradiation (UVC). This innovative approach aims to establish a highly dependable process for the decontamination and disinfection of wastewater with a treatment capacity of 960L/day while minimizing the production of hazardous by-products and ensuring cost-effectiveness. Figure 2 provides a simplified schematic of the SERPIC treatment plant. Each member of the project consortium contributed by designing a specific treatment unit, which was subsequently assembled and tested at the University of Castilla-La Mancha facilities in Ciudad Real, Spain.

In the SERPIC treatment facility, the feeding (the secondary effluent of the local municipal WWTP of Ciudad Real) was stored in a 10 m^3 tank. It was directed into a nanofiltration (NF) unit equipped with specific membranes (NANO7-XL-1812). Subsequently, two distinct treatment routes have been delineated: Route A, designed for the treatment of NF permeate, which exhibits negligible concentrations of CECs while retaining vital nutrients essential for plant growth; This treatment route includes a disinfection unit using gaseous ozone, electrogenerated within a Proton Exchange Membrane (PEM) cell. The cell features a commercial Membrane Electrode Assembly (MEA), a boron-doped diamond lattice (BDD) anode, and a cathode. Notably, the cell housing is custom designed through 3D printing, yielding an ozone gas output of 36 $mg \cdot h^{-1}$, figure 3a shows a picture of the ozone cell design [2]. The ozone contactor promotes the oxidation of residual contaminants and disinfection, and its final effluent can be destined for irrigation without concern. To evaluate its efficacy, potatoes and carrots were cultivated in 48 m^3 of soil, distributed across 6 pots (8 m^3 each). The study encompassed not only the liquid flow dynamics but also the soil properties and the vegetables irrigated using three distinct water sources: drinking tap water, WWTP secondary effluent, and the effluent of Route A.

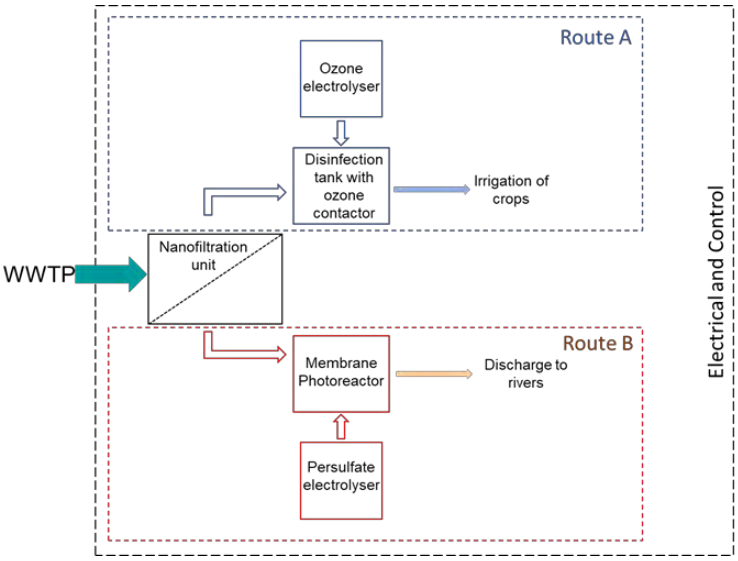

Figure 2. Simplified schematic of the SERPIC treatment plant.

On the other hand, route B, designed for the processing of NF concentrate, which is distinguished by notable levels of CECs, ARB, and ARG, involves a tubular membrane photoreactor. This technology comprises a tubular ceramic ultrafiltration membrane that provides uniform distribution of the oxidant, in this case, persulfate, through multiple dosing points along its entire length. The persulfate is electrogenerated within a parallel plate reactor, meticulously designed using 3D printing. The reactor features a boron-doped diamond anode and a stainless-steel cathode. The innovative aspect is based on the versatility afforded by 3D printing, enabling customized reactor designs and cost savings, figure 3b shows a picture of the design [3,4]. Upon exposure to ultraviolet light, it becomes activated, thereby enhancing its degradation capacity [5]. The treated water is subsequently discharged into rivers. Notably, the entire plant incorporates an automation and monitoring system, ensuring continuous operation—an appealing feature for its eventual industrial-scale implementation.

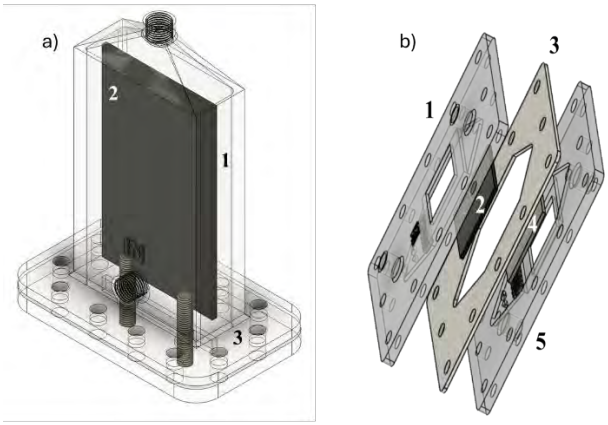

Application of diverse types of hydrogels as separators in microbial fuel cells

Author(s): Isabel Torrejón*[1,2], Carlos Martín[2], Rafael Granados[1], Alberto Rodríguez[1], M.A. Rodrigo[1], Ester Vázquez[2], C.M. Fernández[1]

*[1] Dept. of Chemical Engineering, Electrochemical and Environmental Engineering Lab., University of Castilla-La Mancha, Ave. Camilo José Cela, 12, 13005, Ciudad Real, Spain, *isabel.torrejon@uclm.es*
[2] Regional Institute for Applied Scientific Research (IRICA), University of Castilla-La Mancha, Ave. Camilo José Cela, 1, 13005, Ciudad Real, Spain, ester.vazquez@uclm.es

Keyword(s): *hydrogel, microbial fuel cell, 3D printing, air-breathing.*

Abstract

Currently, two of society's greatest concerns are developing alternative energy sources with less impact on the environment and searching for more efficient and sustainable waste treatment technologies. Carbon dioxide (CO_2), nitrous oxide (N_2O), and other volatile compounds are among the many greenhouse gases (GHGs) emitted into the atmosphere throughout the treatment process. An example of this would be the release of 0.9 kg of CO_2 emissions for every kWh of electricity produced, and 1500 tons of greenhouse gasses are released for every 1000 tons of wastewater treated. [1]

A transformative approach would be converting wastewater treatment plants (WWTPs) into energy-neutral or positive service providers. This approach may be possible by harnessing the chemical energy of organic compounds in wastewater. In this way, WWTPs would contribute to meeting the EU's commitment to reduce greenhouse gas emissions by 40% by 2030. In this context, innovative systems for simultaneous energy recovery and wastewater treatment have gained interest. Microbial fuel cells (MFCs) are one of the microbial electrochemical technologies (METs) used for wastewater treatment. Compared to anaerobic digesters, MFCs are a promising option because they do not require high temperatures and long retention times. They are also a unique, carbon-neutral technology that can treat wastewater while generating useful electricity. For this reason, research on MFCs has been promoted as a novel green energy technology [2].

These devices can convert chemical energy stored in organic and inorganic molecules directly into electricity, using microorganisms as biocatalysts. Microorganisms are important in energy production because they transfer electrons from their metabolic processes to the anode. They can be present as a biofilm on the anode surface, forming layers on the anode, in the material's pore, or suspended. Electrons are moved by physical contact between bacteria and the anode, through nanowires by extracellular electron transfer at a considerable distance from the electrode, and by diffusive redox species that promote electron transfer [3].

Microorganisms oxidize organic matter at the anode, producing electrons that move through an external electrical circuit to the cathode, where an electron acceptor is reduced, see Figure 1.

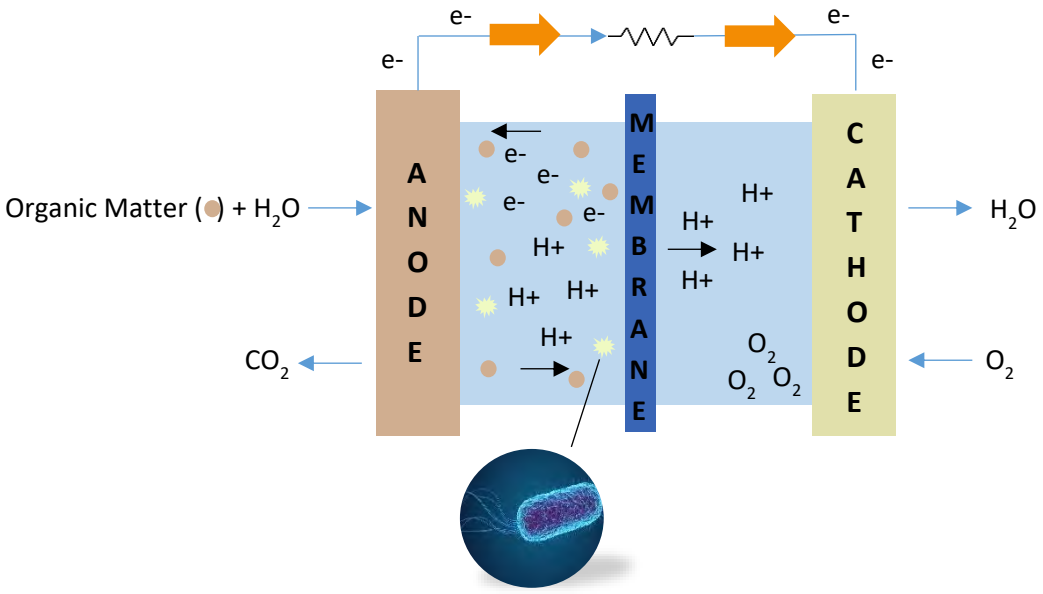

Figure 1. Scheme diagram of the performance of a microbial fuel cell.

Still, it is known that this technology's power output is insufficient for devices with higher energy demand. In recent years, numerous studies have been published to improve the configuration and materials used in these electrogenic systems [4]. In terms of design, small-scale devices are receiving increasing attention due to their ease of fabrication and the ability to manipulate fluid dynamic conditions precisely. Additive manufacturing (AM) or 3D printing allows the fabrication of unique and elaborate reactor designs that minimize assembly complexion, increasing the economic viability of MFCs [5,6].

The performance of batteries depends on several parameters, including operating conditions, reactor configuration, electrode material, or membrane type [7]. Most recent work has used carbon-based electrodes due to their high conductivity and adaptability to bacterial growth. In particular, carbon cloth is a flexible material with great porosity [8]. Concerning configuration, the use of membrane electrode assemblies, or MEAs, reduces internal resistance and minimizes the distance between electrodes, increasing the power output of the cell [9]. Air-breathing MFCs have been developed using oxygen as the electron acceptor, mainly due to its sustainability and availability. The slow kinetics of the oxygen reduction reaction have an impact on MFC performance, so catalysts are used to reduce the activation energy [10]. Moreover, Nafion solution has been mostly used as a catalyst binder, while the proton exchange membrane Nafion N117® has found wide application as a proton exchange membrane (PEM). However, it has drawbacks in its long-term application, in addition to its high economic [9][11].

On the other hand, hydrogels are a soft material with many advantages for use in METs, such as swelling behaviour, biocompatibility, non-toxicity, porous structure, and self-healing [12].

At an early stage, the compatibility of the microbial fuel cell technology with the hydrogel was investigated to assess the viability of the hydrogel as a separator element.

Current work tested eight types of hydrogels made from synthetic monomers and natural polymers in double-compartment cells, designed using 3D printing. This work aims to study the influence of different types of hydrogels on the power density of MFCs.

Regarding methodology and experimental procedure, the hydrogels were characterized by measuring their weight and size before and after the experiment. Carbon cloths were used as anionic and cationic electrodes, assembled with the soft material, setting an electrode-membrane-electrode assembly (MEA) configuration (Figure 2).

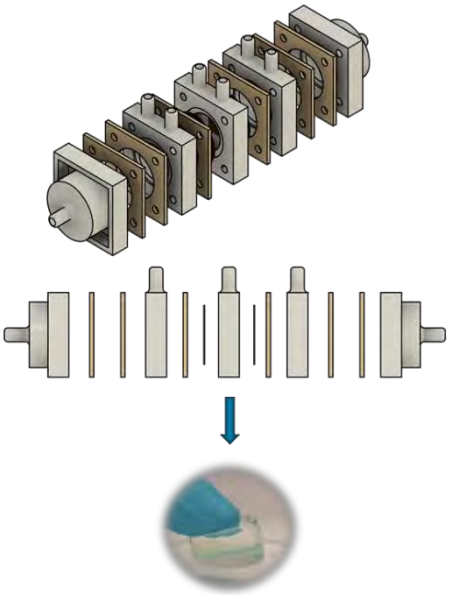

Figure 2. Configuration of the microbial fuel cell was used in the experiment.

Anaerobic activated sludge from the municipal WWTP of Ciudad Real (Spain) was introduced in a 1:2 ratio with a feed solution as the inoculum for the anodic compartment. An acidic HCl solution (pH=3) was added to the cathodic tank and renewed daily. An aquarium compressor supplied the oxygen at the cathode through a porous stone diffuser integrated into the tank. The anodic and cathodic flows were circulated by two peristaltic pumps.

After the first week of the microorganism's life in the system, they were re-inoculated with the same analyte as mentioned above, thus forcing the population already attached to the electrode to acclimatize. Afterwards, a feeding cycle was set in a continuous regime of three days of hydraulic retention time (HRT), to achieve the selection of an electrogenic population from a mixed culture.

During almost 70 days of the study, samples were collected for physicochemical measurement (pH, conductivity, and chemical oxygen demand (COD)). Anolyte samples were analysed to monitor the COD concentration of the influent and the effluent. This measure was evaluated to observe the COD consumption rates of different MFCs and the direct relationship between microbial organic matter oxidation and power generation. Table 1 shows the COD consumption rate determined from the effluent COD using a mass balance.

Table 1. Results of the COD consumption rate obtained from each cell.

MFCs	COD Consumption Rate (mg/d)
Hydrogel 1	28.05
Hydrogel 2	27.61
Hydrogel 3	20.68
Hydrogel 4	22.11
Hydrogel 5	19.25
Hydrogel 6	19.58
Hydrogel 7	20.46
Hydrogel 8	15.95

The electrodes were connected to an external 100 ohms resistance by stainless steel wires. Each cell was simultaneously attached to a potentiostat, which allowed for constant voltage monitoring. Electric current was calculated using Ohm's Law, shown in eq. 1.

$$V = I \cdot R \quad \text{(eq. 1)}$$

Where V is the voltage (V), I is the current (A) and R is the electric resistance (Ω). Current density ($mA \cdot m^{-2}$) was determined from the anode surface for all cells studied. The results show that the current density has a cyclic behaviour over time in all MFCs, associated with the feeding cycle (Figure 3).

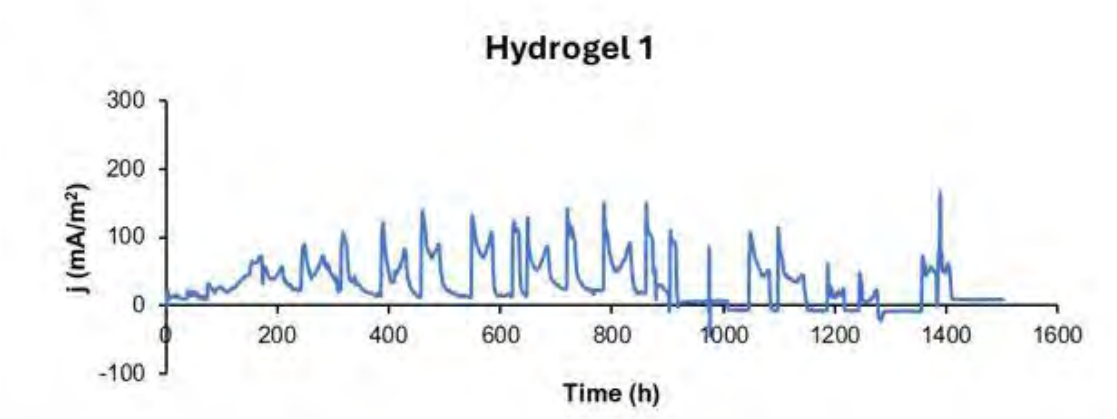

Figure 3. Evolution of current density over time of the MFC equipped with Hydrogel 1.

Acknowledgements

This study forms part of the Advanced Materials Program and was supported by MCIN with funding from European Union NextGenerationEU (PRTR-C17.I1) and Junta de Comunidades de Castilla-La Mancha.

References

[1] Gnaneswar, V., “Wastewater treatment in microbial fuel cells - an overview”, Journal of Cleaner Production, Vol. 122, 287-307, (2016).
[2] Mateo, S., Mascia M., Fernández-Morales, F.J., Rodrigo, M.A. & Di Lorenzo, M., “Assessing the impact of design factors on the performance of two miniature microbial fuel cells”, Electrochimica Acta, Vol. 297, 297-306, (2019).
[3] Mateo, S. Zamorano-López, N., Borras, L., Fernández-Morales, F.J., Cañizares, P., Seco, A. & Rodrigo, M.A., “Effect of sludge age on microbial consortia developed in MFCs”, Journal of Chemical Technology & Biotechnology, Vol. 93, 1290-1299, (2018).
[4] Penteado, E.D., Fernández-Marchante, C.M., Zaiat, M., González, E.R. & Rodrigo, M.A., “Optimization of the performance of a microbial fuel cell using the ratio electrode-surface area/anode-compartment volume”, Brazilian Journal of Chemical Engineering, Vol. 35, 141-146, (2018).
[5] Kim, A. & Simson, A., “Rapid optimization of 3D printed sediment microbial fuel cells”, International Journal of Energy and Environmental Engineering, Vol. 14, 243-255, (2023).
[6] Chung, T.H. & Dhar, B.R., “A mini-review on applications of 3D printing for microbial electrochemical technologies”, Frontiers in Energy Research, (2021).
[7] Penteado, E.D., Fernández-Marchante, C.M., Zaiat, M., Cañizares, P., González, E.R. & Rodrigo, M.A., “Influence of sludge age on the performance of MFC treating winery wastewater”, Chemosphere, Vol. 151, 163-170, (2016).
[8] Asensio, Y., Montes, I.B., Fernández-Marchante, C.M., Lobato, J., Cañizares, P. & Rodrigo, M.A., “Selection of cheap electrodes for two-compartment microbial fuel cells”, Journal of Electroanalytical Chemistry, Vol. 785, 235-240, (2017).
[9] Nandy, A., Kumar, V., Mondal, S., Dutta, K., Salah, M. & Kundu, P.P, “Performance evaluation of microbial fuel cells: effect of varying electrode configuration and presence of a membrane electrode assembly”, New Biotechnology, Vol. 32, 2, (2015).
[10] Penteado, E.D., Fernández-Marchante, C.M., Zaiat, M., González, E.R. & Rodrigo, M.A., “On the Effects of Ferricyanide as Cathodic Mediator on the Performance of Microbial Fuel Cells”, Electrocatalysis, Vol. 8, 59-66, (2017).
[11] Asensio, Y., Fernández-Marchante, C.M., Lobato, J., Cañizares, P. & Rodrigo, M.A., “Influence of the ion-exchange membrane on the performance of double-compartment microbial fuel cells”, Journal of Electroanalytical Chemistry, Vol. 808, 427-432, (2018).
[12] López-Díaz, A., Martín-Pacheco, A., Rodríguez, A.M., Herrero, M.A., Vázquez, A.S. & Vázquez, E., “Concentration Gradient-Based Soft Robotics: Hydrogels Out of Water”, Advanced Functional Materials, Vol. 30, 46, (2020).

Figure 3. Computer-aided assisted design of a) ozone electrogeneration cell [2] (1 housing, 2 MEA, 3 base) and b) persulfate electrogeneration cell [3,4] (1 and 5 clamping plates, 2 BDD, 3 SS, and 3 silicone gasket)

The research findings are encouraging, as the various treatment approaches yield high-quality water. Initially, the liquid flow dynamics were monitored. To this end, the bacteria and resistance genes present in the secondary-treated wastewater from the WWTP-of Ciudad Real, Spain, were specifically targeted. Additionally, four distinct types of emerging target compounds - namely, diclofenac, iopromide, sulfamethoxazole, and venlafaxine were monitored at the different treatment steps.
Regarding Route A treatment, the nanofiltration unit alone removes approximately 80% of the CECs and 25-38% of the targeted ARB and ARG (permeate). After the following ozonation step, the monitored contaminants reach a removal of at least 90%. Regarding Route B, the removal percentage depends on the concentration of persulfate supplied (specifically, at levels of 0.44, 0.99, and 1.6 mM). For Venlafaxine, the removal range is between 55-70%. Meanwhile, *sul*1 achieves and 68 - ≥99% removal. Remarkably, the remaining compounds and bacteria exhibit near-complete removal, regardless of the persulfate dosage.
In summary, the SERPIC treatment plant has demonstrated its efficacy in disinfecting and degrading CECs, ARB, and ARG. As such, it stands as a viable alternative for reusing this type of water in crop irrigation.

Acknowledgements
This work comprises the research project PCI2021-121963 granted by MCIN/ AEI/10.13039/501100011033/ and "Unión Europea NextGenerationEU/PRTR". The authors would like to thank the EU and Bundesministerium für Bildung und Forschung, Germany, Ministero dell'Università e della Ricerca, Italy, Agencia Estatal de Investigación, Spain, Fundação para a Ciência e a Tecnologia, Portugal, Norges forskningsråd, Norway, Water Research Commission, South Africa for funding, in the frame of the collaborative international consortium SERPIC financed under the ERA-NET AquaticPollutants Joint Transnational Call (GA Nº 869178). This ERA-NET is an integral part of the activities developed by the Water, Oceans and AMR Joint Programming Initiatives. This work was supported by national funds through FCT/MCTES (PIDDAC): LSRE-LCM, UIDB/50020/2020 (DOI: 10.54499/UIDB/50020/2020) and UIDP/50020/2020 (DOI: 10.54499/UIDP/50020/2020); and ALiCE, LA/P/0045/2020 (DOI: 10.54499/LA/P/0045/2020). C. S. Santos acknowledges her PhD scholarship funded by FCT (2022.10796.BD).

References

[1] P. Verlicchi, V. Grillini, E. Lacasa, E. Archer, P. Krzeminski, A.I. Gomes, V.J.P. Vilar, M.A. Rodrigo, J. Gäbler, L. Schäfer. "Selection of indicator contaminants of emerging concern when reusing reclaimed water for irrigation – A proposed methodology", Science of Total Environment, 873, 162359, (2023).
[2] Ismael F. Mena, Miguel A. Montiel, Cristina Sáez, Manuel A. Rodrigo., "Improving performance of proton-exchange membrane (PEM) electro-ozonizers using 3D printings", Chemical Engineering Journal, 464, 142688 (2023).
[3] M Pilar. Castro; M. A. Montiel; Ismael F. Mena; Jan Gäbler; Hunter King; Cristina Sáez; Manuel A. Rodrigo. "Outstanding productions of peroxymonosulfuric acid combining tailored electrode coating and 3D printing", Journal of Water Process Engineering, 53, 103902 (2023).
[4] M Pilar. Castro; Ismael F. Mena; M. A. Montiel; Jan Gäbler; L. Schäfer; Cristina Sáez; Manuel A. Rodrigo. "Optimization of the electrolytic production of Caro's acid. Towards industrial production using diamond electrodes", Separation and Purification Technology, 320, 124118 (2023).
[5] M. Martín-Sómer, J.Moreira, Carla Santos, Ana I. Gomes, J. Moreno-SanSegundo, Vítor J.P. Vilar, J. Marugán. "Reflector desing dor the optimization of photoactivated processes in tubular reactors for water treatment", Journal of Environmental Chemical Engineering",11, 110609, (2023).

Title: Testing low-cost materials for nutrients adsorption in wastewater.

Authors: Marco Ravina*[1], Edoardo Marotta[1], Mariachiara Zanetti[1].

[1] Department of Environment, Land and Infrastructure Engineering, Politecnico di Torino, Corso Duca degli Abruzzi 24, 10129 Turin, Italy, marco.ravina@polito.it

Keyword(s): wastewater treatment, adsorption, ammonium, phosphates, low-cost adsorbents.

Abstract

The following study was conducted on behalf project ‘’Supporting OWSSB in upgrading Capacity in Wastewater and faecal Sludge Management (SO-WOP)’’. The project aims to improve capacity of the Odisha Water Supply and Sewerage Board (India), to effectively manage wastewater treatment, to introduce low-cost technology, to carry out pilot interventions and explore the possibilities to reuse treated wastewater and sludge in a ‘’capacity development’’ approach. In this project, the Jatni septage treatment plant was selected as a benchmark case study. The plant is composed by a receiving chamber with screen, settler thickener, anaerobic baffled reactor, planted gravel filter (PGF), polishing pond, and sludge drying beds. After the technical assessment, the activity was focused on improving the removal of nutrients. With this regard, tests for the phosphates and ammonium adsorption by mean of low-cost adsorption media were conducted.

The first phase consisted in batch tests with the objective of characterizing the adsorption isotherms. Four adsorbents were evaluated: two types of active carbon, raw biochar and zeolites (clinoptilolite). Batch tests consisted in introducing a known mass of sample in a mixed reactor and, after the equilibrium time, measuring the contaminant equilibrium concentration. For each sample, 10 g of adsorbent were placed in test tubes. The tubes were filled with a solution of 50 ml of water and contaminant (ammonium or phosphate) at known concentration. The tubes were then mixed for 14 hours at 21°C. The contaminant concentrations in the liquid phase were finally measured.

The resulting isotherms of ammonium adsorption by clinoptilolite is reported in Figure 1. The adsorption capacity at equilibrium was also calculated according to:

$$Q = \frac{C_0 - C_{eq}}{m_{ad}} * V$$

where Q is the adsorption capacity [mg/g], C_{eq} is the contaminant concentration in the liquid phase [mg/l], C_o is the initial contaminant concentration [mg/l], V is the volume of solution [l], and m_{ad} is the mass of adsorbent [g].

The results of ammonium adsorption capacity of different materials are reported in Table 1. For phosphates, activated carbon showed higher adsorption capacity than zeolites. Adsorption capacity of biochar was found to be close to zero. This is in partial contrast with other scientific publications, which report adsorption capacity for biochar higher than zero.

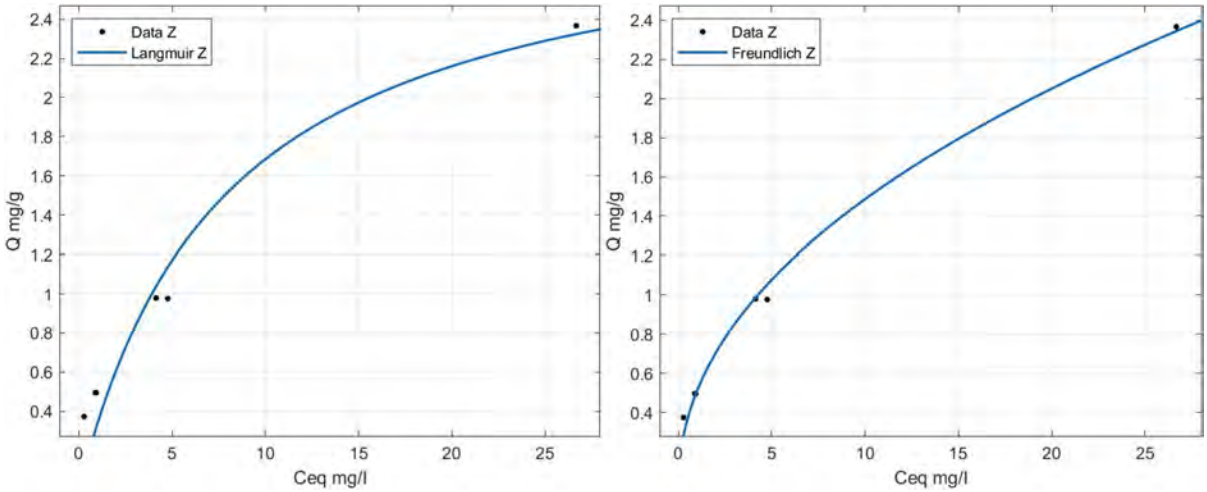

Figure 1 : Langmuir (left) and Freundlich (right) isotherm fitting for ammonium adsorption with zeolites at 21 °C.

Table 1. Ammonium adsorption capacity of different materials

	Ammonium Adsorption capacity (mg/g)		
	C_{eq} =1 mg/l	C_{eq} =3 mg/l	C_{eq} =4mg/l
Activated Carbon	0.015 - 0.019	0.027 - 0.038	0.037 - 0.055
Biochar	0.043 - 0.046	0.054 - 0.064	0.054 -0.072
Zeolite	0.495	0.786 - 0.818	0.976 - 0.979

After having completed the characterization of the materials, adsorption column tests were conducted. The instrumental set up is reported is Figure 2. These tests were preceded by a tracer test for the determination of the hydrodynamic dispersion coefficient of the column. In column adsorption tests, the adsorbent was introduced in the column and a solution of water and contaminant was pumped into the column at a flow Q_{in} = 0.28 ml/s. Samples were taken every 2 hours at different sampling ports located at different height of the column. Ammonium and phosphates concentration were measured with a spectrophotometer. The test was stopped when saturation of the material was reached. The breakthrough curve of the ammonium adsorption test with zeolites at a height of 0.22 m is reported in Figure 2. Experimental measurements were compared to a general adsorption model. The fitting yielded a retardation factor of around 1100, in accordance with other publications [1].
Additional column adsorption tests and evaluations of possible field applications are currently ongoing.

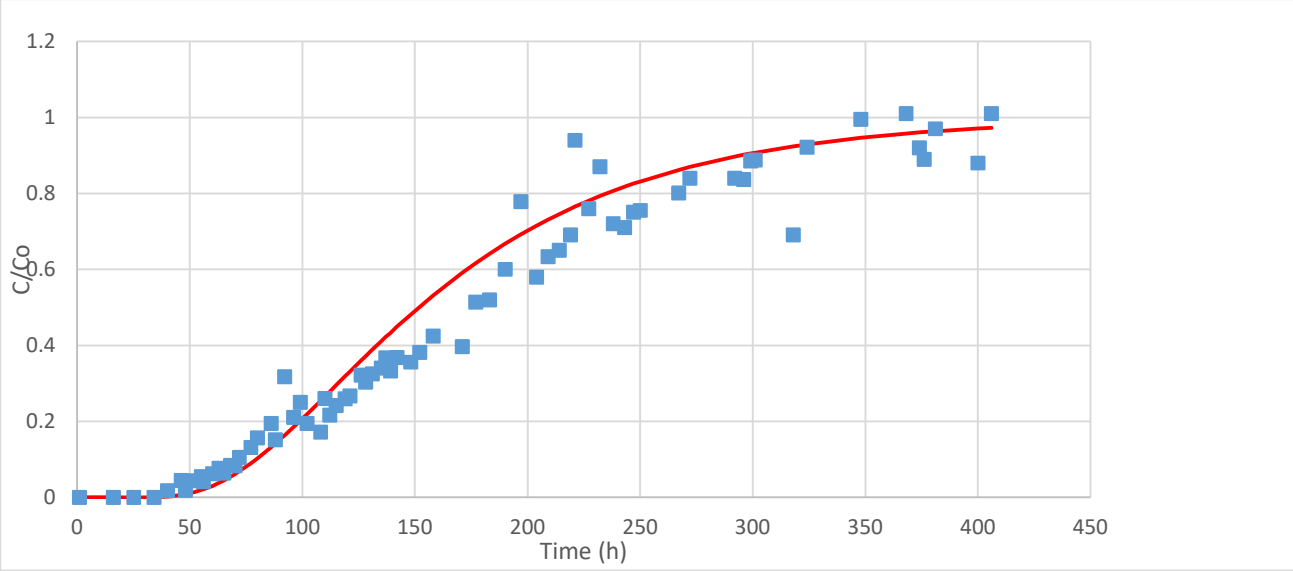

Figure 2 : Breakthrough curve of ammonium adsorption with zeolites at a column height of 0.22 m.

References

[1] Guida, S.; Potter, C.; Jefferson, B.; Soares, A. Preparation and Evaluation of Zeolites for Ammonium Removal from Municipal Wastewater through Ion Exchange Process. Sci Rep 2020, 10, 12426, doi:10.1038/s41598-020-69348-6.

Title: A chain for the treatment of oilfield produced waters: case study and experimental analysis

Author(s): Giovanni Campisi*, Alice Sorrenti, Alessandro Cosenza, Serena Randazzo, Santo Fabio Corsino, Marco Capodici, Alessandro Tamburini, Giorgio Micale

Dipartimento di Ingegneria, Università degli Studi di Palermo (UNIPA), Palermo, Italy, Viale delle Scienze Ed.6. 90128, giovanni.campisi02@unipa.it
Consorzio Interuniversitario Nazionale per la Scienza e Tecnologia dei Materiali (INSTM), Firenze, Italy, Via Giusti 9, 50121

Keyword(s): Produced Waters (PWs), Assisted- Reverse Electrodialysis (A-RED), Sequencing Batch Moving Bed Biofilm Reactor (SBMBBR), Experimental treatment chain.

Abstract

Produced water are salty and organic polluted waters that are drilled out during the extraction of oil. Typically, these waters are re-injected into the extraction well, without any treatment or valorisation. In this work, a more sustainable and environmental friendly solution is proposed consisting of an innovative PWs treatment scheme: Assisted Reverse Electrodialysis (ARED) is used to reduce the PWs salinity to make them compatible with the downstream Sequencing Batch Moving Bed Biofilm Reactor (SBMBBR), aimed at removing the organic content. To this purpose, a 20-cell pair ARED unit was continuously operated for 24 hours to desalinate PWs down to a target concentration of 20 g L^{-1} of NaCl. Then, the desalinated stream was treated in a 50 L bioreactor and an abatement up to 40 % of the Total Petroleum Hydrocarbon (TPH) was achieved.

Introduction

Due to the depth of the reservoir, the fluid pressure of the oil certainly helps the drilling techniques, but over time this pressure difference decreases, and water is used to enhance the oil recovery (waterflooding method). As a result, downstream separation processes are used to separate the water from the organic component. The latter, referred to as produced water (PW), is characterised by (i) high salinity due to contact with subsurface rocks and (ii) hydrocarbon compound contaminants [1]. Overall, PWs present a complex and variable composition depending on oil maturity, extraction methods, well depth and site morphology [2]. Due to all these variables, it is not possible to standardise the characteristics of PWs, and consequently, their treatment must be defined on a case-by-case basis through ad-hoc studies and experimental investigations. Their complex nature is further complicated by the large volumes involved. Estimates suggest an annual generation of 11.2 million of m^3, with production increasing progressively with the well age, generating at least 3 barrels of PWs for every barrel of oil produced [3]. The management of PWs usually consists of re-injection into the well, but due to increased public and legislative attention, this might not be longer possible. This would require to treat these PWs appropriately, with treatment chains leading to (i) the Minimum Liquid Discharge (MLD) target and to (ii) the reuse for potable or irrigation purpose [4].
Environmental awareness has increased in recent years, attracting the interest and efforts of the scientific community to propose new technologies and treatment chains capable of handling PWs. Typically, three main process categories are employed to treat PWs: physical treatment (e.g., evaporation, filtration), chemical processes (e.g., oxidants, electrochemistry), and biological remediation [5]. Physical and chemical treatments are the most efficient, but also the most expensive. Conversely,

biological treatments are among the most cost-effective and efficient technology to deal with wastewaters. Traditionally used for urban wastewaters, biological remediation has the main limit of the high salinity, i.e., PWs high salinity is detrimental for conventional bio-remediation treatment processes [6]. Since the direct dilution of wastewater is not allowed as regulated by D.Lgs 152/06 (Italian law), a low-cost pre-treatment for the salinity reduction represents an appealing way to economically manage this kind of wastewaters.

Plant proposal/ Treatment chain

Reverse Electrodialysis (RED) is a process exploiting the salinity gradient between two streams to move the salt ions from a concentrated solution to a diluted one, generating electric energy. The ions migrations can be boosted with ARED, by the application of an external electric field. In this new scheme, PWs are fed to the ARED unit for the salinity reduction, to make them compliant with the downstream biological section. The ARED stack is constituted by repetitive modules units as cell pairs, each comprising of two channels and two Ion Exchange Membranes (IEMs): an Anion Exchange Membrane (AEM) and a Cation Exchange Membrane (CEM). Spacers were placed between the membranes to create the channels where a concentrated solution (H) and a low-concentrated solution (L) are alternately fed. Electrode compartments are positioned at both ends of the stack. In these compartments an Electrode Rinse Solution (ERS) containing redox couples (Fe^{3+}/Fe^{2+}) continuously circulates, allowing the conversion of electric current into ionic current. After the dilution up to an equivalent NaCl concentration target of 20 g L^{-1} (see **Figure *1***), the PWs are sent to a biological section consisted of a biological reactor with IFAS (Integrated Fixed Film Activated Sludge) technology operating in a batch cycle, hereafter named SBMBBR (Sequencing Batch Moving Bed Biofilm Reactor). The latter has the purpose to reduce the organic content of PWs and make the PWs respectful of the legislative limit for discharge. In this preliminary analysis, the outgoing effluent is sent to discharge, however, it could be addressed to a valorisation section for a subsequent recovery of the high-value minerals present or mixed with the diluted solution (L_{out}) of ARED to produce freshwater by a reverse osmosis unit.

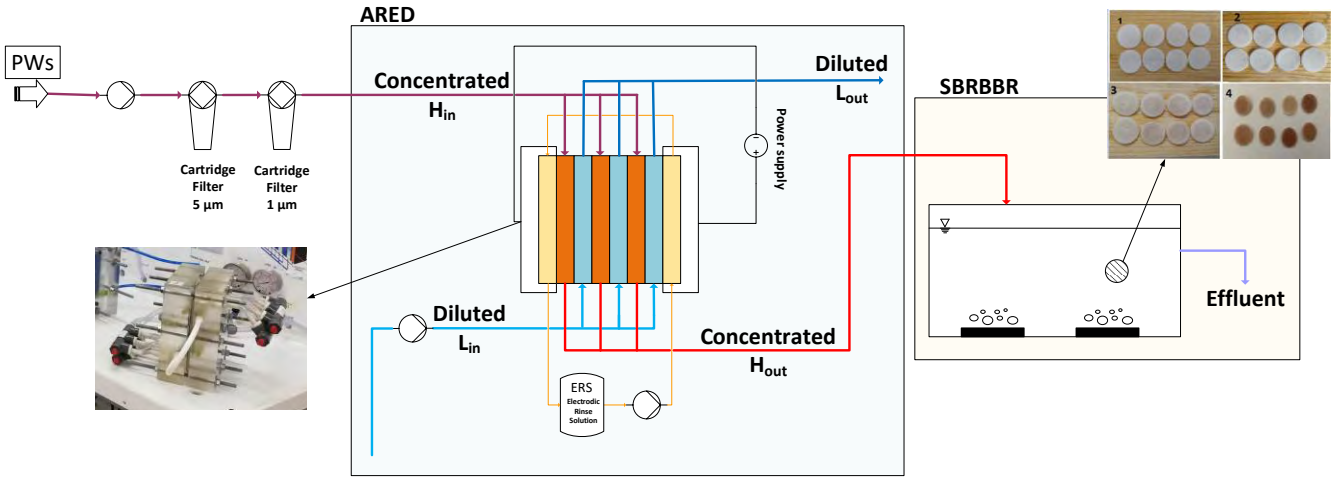

Figure 1. Scheme of the proposed treatment chain.

Methodology

The experimental tests were performed with real PW solutions by coupling the two units described in the previous section. PWs feed was firstly filtered in 2 cartridge filters in series (5 and 1 µm) to avoid clogging phenomena. The ARED unit has a 10x10 cm^2 active area constituted by 10 cell pairs, assembled with Fujifilm membranes Type 10 and separated by 300 µm woven spacers. PW presented a conductivity of 95 mS cm^{-1} and is recirculated in the stack to reduce its concentration to 20 g L^{-1}.

Recirculation is necessary due to the use of a laboratory unit that is not able to lead to the target concentration in a single pass. The diluted solution was also recirculated in a separated tank. Each load of PW had a volume of approximately 4 L, while the diluted solution had a volume of 50 L and a test lasted approximately 24 hours. The treated PW was then collected in a buffer reservoir and transferred to the biological reactor once the previous cycle was completed. The bioreactor (capacity of 20 L) started to operate without an active sludge inoculum to allow the development of autochthonous halophilic biomass present in the PWs on the carriers. The carriers used were the Mutag BioChipsal type (surface area of 5,500 m^2/m^3). The total volume of carriers used was 5 L, corresponding to approximately 5000 carriers. The reactor was equipped with a blower connected to two porous stone diffusers for air supply (flow rate of 5 L min^{-1}) and two peristaltic pumps for the PW feeding and effluent discharging. All the equipment were connected to a PLC for cycle phase management.
The biological reactor operated in continuous mode, by alternating cycles with a duration of 6 hour. The volumetric exchange ratio was set to 5 % to avoid organic overloading. Consequently, the treatment capacity of the plant was 4 L day^{-1}. Each cycle was divided into the following phases: a feeding phase lasting 1 hour; a reaction phase lasting 3 hours; a settling phase lasting 2 hours; and a discharge phase lasting 30 minutes. Biological performances were evaluated by measuring the total organic carbon (TOC) and total petroleum hydrocarbons (TPH) removal efficiencies. TOC was measured in surface water samples at the inlet and outlet of the ARED and the biological reactor using a Shimadzu TOC-V analyser. Additionally, total petroleum hydrocarbons (TPH) were also measured in samples taken upstream and downstream the units. Specifically, liquid/liquid extraction with hexane was performed, followed by measurement of C10-C40 hydrocarbons using a GC-FID (Gas Chromatography-Flame Ionization Detector).

Results and Discussions

Conductivity, TOC and TPH were monitored for each 4 L-charge of PW. The trend for one cycle of treatment is described in **Figure 2**, where it is possible to observe the inlet and the outlet values in each unit. The PW entered in the ARED unit with a conductivity of about 95 mS cm^{-1}, showing some variability, and after 24 hours of treatment, the outlet conductivity was always lower than 33 mS cm^{-1}, corresponding to a salinity concentration of 20 g L^{-1}. As stated before, this value was considered tolerable for the biomass and favourable for its growth. Inside the ARED unit the TOC concentration remained constant at the initial value of about 95 mg L^{-1}, meanwhile the TPH concentration decreased by about 15 % (value at the inlet of the integrated system was 34 mg L^{-1} on average), probably due to the adhesion of hydrocarbons on the ARED components due to continuous recirculation of PW. The total applied energy for the salinity reduction until the goal conductivity was of about 7.4 Wh (i.e., 1.84 kWh m^{-3}). The PW enters the SBMBBR for the biological treatment where an abatement of 80% was achieved (from 95 to 19 mg L^{-1}). This good result allows to consider the SBMBBR as a system capable of producing a consistently high-quality effluent even with varying organic load inputs, demonstrating excellent resilience to load fluctuations. This was likely due to both the low volumetric exchange ratio applied in the reactor and the predominant presence of attached biomass, which is more effective at withstanding load fluctuations compared to suspended biomass. As further evidence of the efficiency of the bioreactor, the gradual development of the biofilm on the carriers is shown in **Figure *1***. Overall, the bacterial mass per unit surface area was 38.17 g m^{-2}, after approximately 180 days from the start-up of the plant, indicating good development of the autochthonous halophilic biomass in the system. Additionally, the attached biomass exhibited a good biological activity measured as the consumption rate of dissolved oxygen, which averaged about 5 mgO_2 $L^{-1}{\cdot}h^{-1}$. In contrast, the concentration of suspended biomass was quite modest, averaging around 400-500 mgTSS L^{-1}. In the biological unit, the TPH concentration was reduced to an average of 18 mg L^{-1}, contributing to an additional reduction of about 30 %. SBMBR operated for more than 275 days, maintaining an average performance of 70%.

Overall, the integrated system could remove about 35-40 % of the TPH present in the produced water.

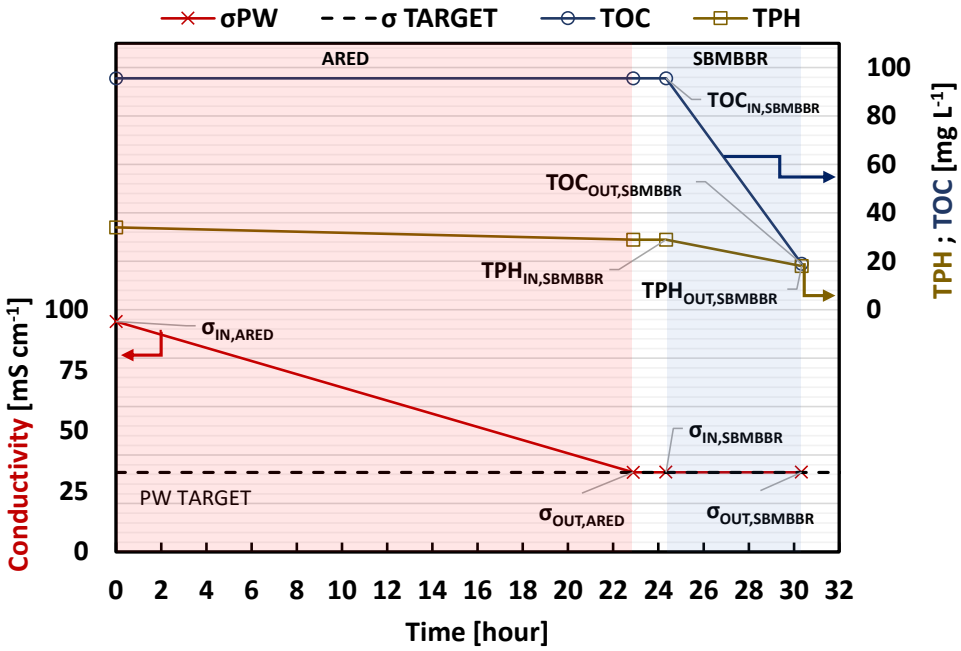

Figure 2. a) Conductivity (σ), Total Organic Carbon (TOC) and Total Petroleum Hydrocarbons (TPH) trends of a single PW load (4 L) in the A-RED unit and the SBMBBR reactor.

Conclusions

A novel treatment chain was developed and tested with real PW. The need for a preliminary desalination was effectively addressed using an ARED unit, able to reduce the salinity down to the concentration target of 20 g L^{-1}, established as a minimum requirement for the bacteria growth. The SBMBBR was identified as one of the most promising biological treatment for dealing with PWs, for which a TOC reduction of 80 % was observed. At the same time, also a reduction up to the 40 % of the TPH concentration was detected. These preliminary results on the coupling of ARED with SBMBRR show that the integrated proposed treatment is effective and efficient and a promising option for the future.

References

[1] S. Jiménez, M. M. Micó, M. Arnaldos, F. Medina, and S. Contreras, 'State of the art of produced water treatment', *Chemosphere*, vol. 192, pp. 186–208, Feb. 2018, doi: 10.1016/j.chemosphere.2017.10.139.
[2] M. Nasiri and I. Jafari, 'Produced Water from Oil-Gas Plants: A Short Review on Challenges and Opportunities', *Period. Polytech. Chem. Eng.*, 2016, doi: 10.3311/PPch.8786.
[3] M. A. Al-Ghouti, M. A. Al-Kaabi, M. Y. Ashfaq, and D. A. Da'na, 'Produced water characteristics, treatment and reuse: A review', *Journal of Water Process Engineering*, vol. 28, pp. 222–239, Apr. 2019, doi: 10.1016/j.jwpe.2019.02.001.
[4] A. Ruiz-Aguirre *et al.*, 'Diffusion dialysis for the treatment of H2SO4-CuSO4 solutions from electroplating plants: Ions membrane transport characterization and modelling', *Separation and Purification Technology*, vol. 266, p. 118215, Jul. 2021, doi: 10.1016/j.seppur.2020.118215.
[5] Y. Liu *et al.*, 'A review of treatment technologies for produced water in offshore oil and gas fields', Jun. 2021. Accessed: Feb. 10, 2023. [Online]. Available: https://linkinghub.elsevier.com/retrieve/pii/S0048969721005532
[6] J. Nie, Y. Chen, S. Cohen, B. D. Carter, and R. F. Boehm, 'Numerical and experimental study of three-dimensional fluid flow in the bipolar plate of a PEM electrolysis cell', *International Journal of Thermal Sciences*, vol. 48, no. 10, pp. 1914–1922, Oct. 2009, doi: 10.1016/j.ijthermalsci.2009.02.017.

Remanufacturing of off-road vehicles spare parts: process analysis and environmental assessment

Author(sd): Livia Nastasi, Silvia Fiore

Department of Environment, Land, and Infrastructure Engineering (DIATI), Politecnico di Torino, Corso Duca degli Abruzzi 24, 10129 Torino, Italy (livia.nastasi@polito.it; silvia.fiore@polito.it)

Keyword(s): remanufacturing process; off-road vehicles

Abstract

Nowadays, the world is facing global environmental issues, such as climate change, pollution and biodiversity loss [1]. In response to these challenges, as a part of the European Green Deal, the European Commission adopted the New Circular Economy Action Plan aiming to promote a transition towards a resource efficient and competitive economy, to achieve carbon neutrality by 2050 [2]. Within this framework, remanufacturing can be considered a key circular strategy to extend products' lifecycle by restoring a used product to at least its original performance and providing a warranty that is equivalent to or better than a newly manufactured product [3]. Remanufacturing can be applied to a wide range of industrial sectors [4], such as: aerospace, automotive, electrical and electronic equipment, furniture, heavy-duty and off-road equipment, machinery, marine, medical devices and rail. Focusing on vehicles, including both automotive and heavy-duty and off-road vehicles sector, remanufacturing plays a crucial role to extend the spare parts' lifecycle, such as engines, gearboxes, alternators, hydraulic pumps, radiators and air compressors [5]. The aim of this work was to investigate the remanufacturing process applied to spare parts of CNH Industrial's off-road vehicles, focusing specifically on electronic control units (ECUs) and aftertreatment systems (ATS). Subsequently, a gate-to-gate environmental assessment was conducted for the remanufacturing process of each chosen spare part. This research was carried out in partnership with CNH Industrial and two remanufacturing companies selected as case studies, both of which are suppliers to CNH Industrial.

The adopted methodology was represented in Figure 1.

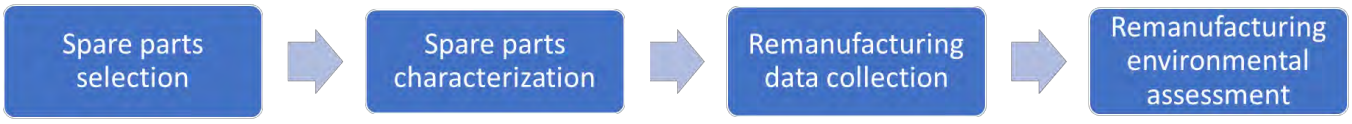

Figure 1. Methodology

At first, representative spare parts were selected for each category: engine control units, joysticks, displays, and De NOx modules were analyzed for ECUs; while for ATS, a comprehensive system including Diesel Oxidation Catalyst (DOC), Diesel Particulate Filter (DPF), Selective Catalytic Reduction and Ammonia Slip Catalyst (SCR-ASC) was considered. Afterwards, each chosen spare part was characterized through the analysis of technical drawings, disassembly, and the mass balance of individual components to provide a deeper understanding of the composition of the spare parts. At this point, remanufacturing processes performed by the two case study companies were analysed;

specifically, were gathered general information about key phases of the process, logistics and packaging of the cores through interviews and on-site investigations. Furthermore, Microsoft Excel spreadsheets were developed to gather the following information for each remanufacturing process: duration time of the different process stages; quantity of defective components; type and quantity of identified failures; type and quantity of materials and resources utilized; type and quantities of replaced components. These data were collected for a total of 20 repetitions/spare part to ensure the reliability of the results.
In conclusion, an environmental evaluation was conducted for each remanufacturing process. This involved performing a carbon footprint analysis following the guidelines of ISO 14064 [6] and the Greenhouse Gas (GHG) Protocol Product Standard [7]. The aim of this assessment was to quantify the GHG emissions associated with each type of spare part remanufacturing process, identifying the stages that contribute most to the Global Warming Potential, expressed as KgCO2eq/ECU. The evaluation adopted a 100-year Global Warming Potential time horizon.

The system boundaries (Figure 2) are gate-to-gate, encompassing the phases from the end-of-life spare part to the remanufactured item. This includes the transportation of the end-of-life spare part from the storage warehouse to the remanufacturing company, the remanufacturing processes, and the packaging operations conducted by the involved companies. Equipment production and disposal were excluded from the analysis. The chosen functional unit was the “single end-of-life spare part used in an off-road vehicle undergoing the remanufacturing process”.

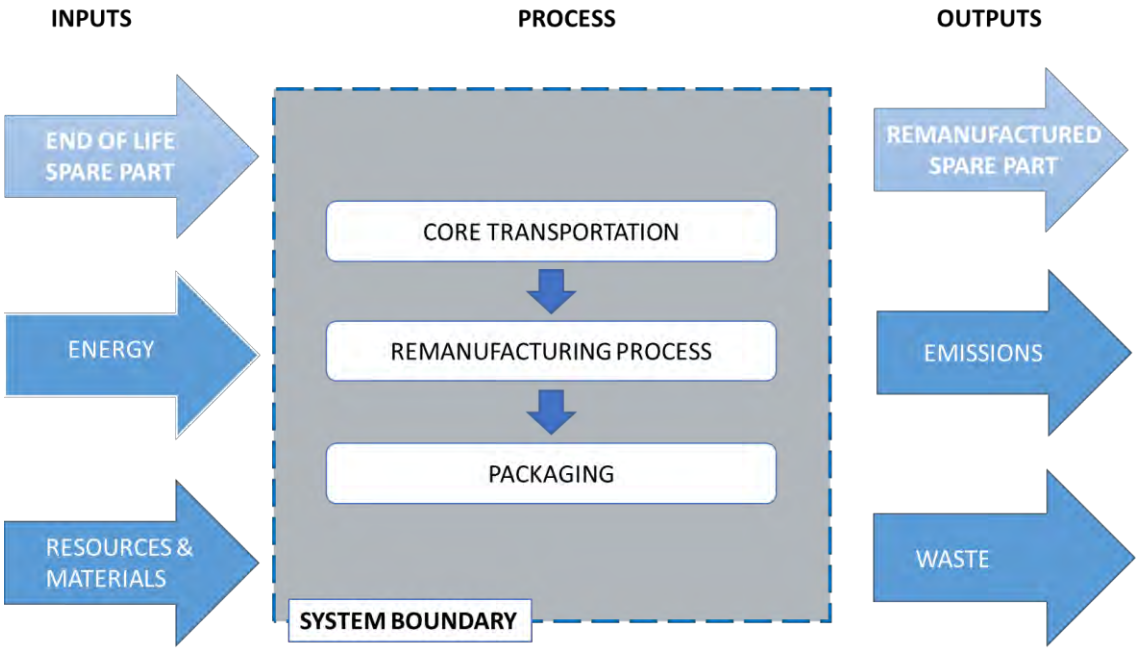

Figure 2. System boundary

The primary data necessary for conducting the carbon footprint analysis, including used resources and materials, energy consumption of the electronic equipment, waste generation and emissions, were collected from CNH Industrial and remanufacturing case study companies. Background data were gathered from Ecoinvent database [8], Product Environmental Footprint database [9] and relevant literature.

The carbon emissions related to each spare parts remanufacturing process was calculated according to the following equation (1):

$$CF\ [KgCO_{2eq}] = \sum_i A_i[unit] * EF_i \left[\frac{KgCO_{2eq}}{unit}\right] \quad (1)$$

where *i* represents the specific stage within the remanufacturing process under consideration, *EF* denotes the emission factor associated with the *i-th* stage, and *A* represents the activity data corresponding to the *i-th* stage [10].
In this study, the carbon footprint was evaluated considering the most frequent spare parts failures scenarios, basing on the previous data collection.

As a result, basing on the collected information, remanufacturing process varies depending on the type of spare parts being considered. Concerning ECU, the remanufacturing process generally consists of visual preliminary test, disassembly of the components, identification of failures, reverse engineering operations to identify a possible solution, components substitution and final diagnostic test. At the end, components are externally cleaned and then are packaged ready to be sent to the final customer. The total duration of the process is about 3.13 hours for engine control units, 1.3 hours for De NOx, 47 minutes for joysticks, 29 minutes for displays. The total retained mass is about 95.8%.
Regarding ATS, the system is initially disassembled and the single components (DOC, DPF, SCR-ASC) are inspected in order to determine whether the components are suitable for remanufacturing or if they need to be replaced with new ones. DOC and SCR-ASC are chemically analysed and, in most of cases, they must be substituted by new ones. On the other hand, DPF is often subjected to remanufacturing process, as follows: at first, a preliminary visual inspection is conducted, followed by pressure and flow testing. Then, chemical remediation is carried out, followed by thermal treatment at 700°C. Afterward, remaining ashes are removed using compressed air, and finally, a final pressure and flow test is performed. At the end, the external case is cleaned and all the components are reassembled. The process lasts about 14 hours and the total retained mass is about the 89.5%.

Concerning the Carbon Footprint results, it was obtained an average value of 3.7 KgCO2eq for engine control units, 0.339 KgCO2eq for joysticks and 15.3 KgCO2eq for displays. The final result is highly affected from the replaced component type and most of the contribution is due to the manufacturing of electronic components, such as logic and memory integrated circuits. As regards De NOx modules, the environmental impact will be lower due to the absence of electronic components. Focusing on aftertreatment systems, the total carbon footprint will be influenced by various factors such as manufacturing processes of not-repairable components, transportation, materials and energy consumption during operation, and end-of-life disposal of the different not repairable parts (DOC, SCR-ASC) and substances (such as chemicals). Most of the total GWP contribution will be due to the manufacturing of DOC and SCR-ASC and the energy consumption associated to thermal treatment.

Acknowledgments
This research activity was performed with the support of PON “Ricerca e Innovazione” 2014-2020, Asse IV “Istruzione e ricerca per il recupero” con riferimento all’Azione IV.4 “Dottorati e contratti di ricerca su tematiche dell'innovazione” e all’Azione IV.5 “Dottorati su tematiche green”. DM 1061/2021.

References

[1] European Commission, “COMMUNICATION FROM THE COMMISSION TO THE EUROPEAN PARLIAMENT, THE EUROPEAN COUNCIL, THE COUNCIL, THE EUROPEAN ECONOMIC AND SOCIAL COMMITTEE AND THE COMMITTEE OF THE REGIONS-The European Green Deal,” 2019. Accessed: Mar. 30, 2022. [Online]. Available: https://eur-lex.europa.eu/resource.html?uri=cellar:b828d165-1c22-11ea-8c1f-01aa75ed71a1.0002.02/DOC_1&format=PDF

[2] European Commission, “A new Circular Economy Action Plan,” 2020. Accessed: Mar. 30, 2022. [Online]. Available: https://eur-lex.europa.eu/resource.html?uri=cellar:9903b325-6388-11ea-b735-01aa75ed71a1.0017.02/DOC_1&format=PDF

[3] M. (VTT) Arnold *et al.*, “Contribution of remanufacturing to Circular Economy,” 2021. Accessed: Sep. 20, 2022. [Online]. Available: https://www.eionet.europa.eu/etcs/etc-wmge/products/etc-wmge-reports/contribution-of-remanufacturing-to-circular-economy

[4] D. Parker, K. Riley, S. Robinson, H. Symington, J. Tewson, and O. Hollins, “Remanufacturing Market Study,” 2015.

[5] M. Saidani, B. Yannou, Y. Leroy, and F. Cluzel, “Heavy vehicles on the road towards the circular economy: Analysis and comparison with the automotive industry,” *Resour Conserv Recycl*, vol. 135, pp. 108–122, Aug. 2018, doi: 10.1016/J.RESCONREC.2017.06.017.

[6] ISO, “UNI EN ISO 14064-1:2019 - UNI Ente Italiano di Normazione.” Accessed: Nov. 06, 2023. [Online]. Available: https://store.uni.com/uni-en-iso-14064-1-2019

[7] WRI and WBCSD, “Product Standard | GHG Protocol,” 2011. Accessed: Nov. 06, 2023. [Online]. Available: https://ghgprotocol.org/product-standard

[8] Ecoinvent 3.9.1, “Ecoinvent, Allocation, cut-off by classification, Ecoinvent database version 3.9.1 .” Accessed: Feb. 20, 2024. [Online]. Available: https://ecoinvent.org/

[9] European Commission, “Product Environmental Footprint database .” Accessed: Feb. 20, 2024. [Online]. Available: https://nexus.openlca.org/database/Environmental%20Footprints

[10] E. Bonamente, F. Scrucca, S. Rinaldi, M. C. Merico, F. Asdrubali, and L. Lamastra, “Environmental impact of an Italian wine bottle: Carbon and water footprint assessment,” *Science of The Total Environment*, vol. 560–561, pp. 274–283, Aug. 2016, doi: 10.1016/J.SCITOTENV.2016.04.026.

Title: Combining material flow analysis and life cycle assessment to support decision-making of municipal solid waste management: a case study in Catalonia

Author(s): Stefano Fiaschi[1,2], Claudio Lubello[1], Laura Talens Peiró[2]

[1] Department of Civil and Environmental Engineering, University of Florence, Via di Santa Marta 3, 50139 Firenze (FI), Italy, stefano.fiaschi@unifi.it, claudio.lubello@unifi.it
[2] Sostenipra Research Group (2021SGR 00734), Institut de Ciència i Tecnologia Ambientals (ICTA-UAB, 'Maria de Maeztu' unit of excellence CEX2019-000940-M), Universitat Autònoma de Barcelona, 08193 Cerdanyola del Vallès, Barcelona, Spain, laura.talens@uab.cat

Keyword(s): Municipal solid waste management, Recycling rate, Separate collection rate, Carbon footprint, Greenhouse gas emissions

Abstract

1. Introduction

The waste management sector in European countries has made significant strides in mitigating climate change, reducing greenhouse gas (GHG) emissions by 42% since 1990 [1]. This reduction has primarily been achieved by measures diverting municipal solid waste (MSW) from landfills to recycling or energy recovery [1]. Thus, the recycling objectives set by waste policies (i.e., Directive 2018/851/EC [2]) and the life cycle assessment (LCA) models used to analyze the environmental impact of MSW management (MSWM) are based on the assumption of a linear relationship between separate collection rates (SCR), recycling rates and GHG savings [3,4]. However, the environmental burdens of real collection and recycling schemes are likely to be a non-linear function of the collection rate [5]. For instance, high SCRs may cause lower purity of the collected waste fraction, with contaminants that cannot be easily sorted, resulting in more energy-intensive recycling processes [5]. Additionally, increasing the SCR requires more collection points and more recycling and sorting facilities, leading to higher transport distances, which results in increased fuel consumption and GHG emissions [5]. Houpt et al. (2018) highlighted the need to consider these non-linear effects when analysing MSWM systems. Furthermore, several modern waste treatment technologies are designed to offer recovered materials as secondary raw materials to the market, and/or generate energy resources. This requires close interaction with various other sectors, including manufacturing, agriculture, and energy production [5]. Numerous authors [3,6,7,8] have emphasized the importance of performing material flow analysis (MFA) to properly assess the flows and stocks of materials (raw materials, products, and waste) prior to conducting LCA. MFA is crucial for understanding the quantity and quality of flows and stocks, while LCA helps assess the potential environmental impact of their end-of-life management. For all these reasons, the combination of these methodologies is useful to support decision-making in MSWM, helping to analyse the growing complexity of modern integrated systems [6,9]. In this study, we propose to integrate the methodologies of MFA and LCA to evaluate the MSWM systems at two different scales in Catalonia. We aim to employ scenario analysis to compare the potential effects of diverse management strategies on the environmental performance of the systems, focusing on measures aimed at increasing the SCR for specific waste streams.

2. Case study areas

The areas under study are Catalonia (Northeast of Spain), and Vallès Occidental (VO), one of its counties. Catalonia is administratively divided into four regions, which are further divided into 42 counties and 947 municipalities. The territory has an extension of approximately 32,000 km^2 and a population of 8 million inhabitants (2023). The Waste Agency of Catalonia (Catalan acronym, ARC) is the public administrative entity responsible for MSWM. The primary waste fractions separately collected from households for recycling include organic waste, paper and cardboard, light packaging, and glass. Additionally, green waste (pruning), textile, WEEE, wood, bulky waste and other waste collected at drop-off centers are waste fractions considered in source-separated collection. VO is the second most populous county of Catalonia, with a population of approximately 940.000. It covers an area of 580 km^2 and includes 23 municipalities. The responsibility for managing the majority of the MSW was delegated by ARC to the Consortium for Waste Management of Vallès Occidental (CWMVO), which oversees the urban service in 16 municipalities. In the remaining 7 cities, MSW is managed by the Metropolitan Entity for Hydraulic Services and Waste Treatment (EMSHTR).

3. Methodology

The methodology proposed in this study is a combination of MFA and LCA. A static MFA, based on the mass conservation principle, is applied to illustrate the mass flows of each waste stream. Data visualization is conducted using the freely available online tool SankeyMATIC [11]. Subsequentially, MFA results are integrated in life cycle inventory (LCI) to quantify the related GHG emissions. The LCA is performed using the SimaPro software [12]. The Catalan MSWM system is illustrated in Figure 1. Compared to Catalonia, in the VO case study, there is no direct flows of Unsorted Waste (UW) to landfill or incineration. All the UW from this area is processed at a centralized Mechanical-Biological Treatment (MBT) plant located in Vacarisses before reaching its final disposal. Both case studies were analyzed using the management of 1 tonne of MSW in 2022 as the functional unit.

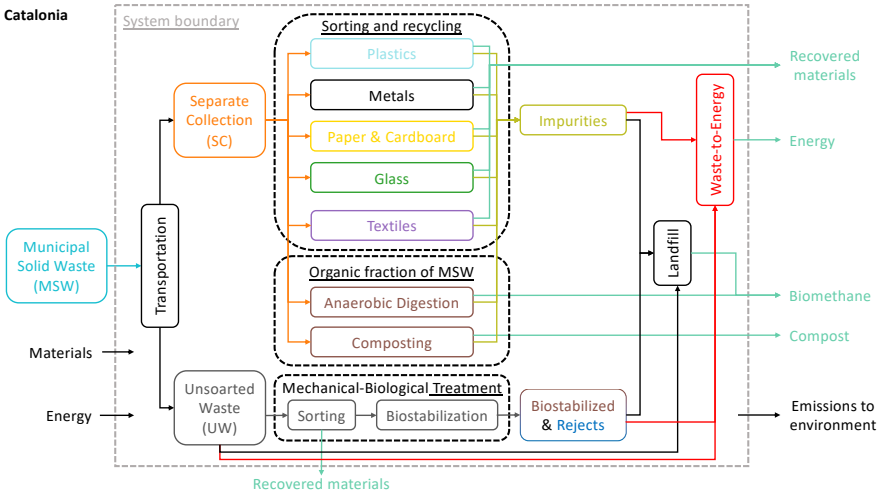

Figure 1: Description of the MSW management processes in Catalonia.

All MSW flows through the systems were modelled using publicly available waste data [13,14]. The basic management entity considered as the reference for data acquisition was the municipality. To calculate the total generation of MSW for a municipality, the following contributions were considered: (i) Waste from conventional selective collections (organic waste, paper and cardboard, glass, and light packaging); (ii) Waste collected at drop-off centers; (iii) Waste collected through other dedicated collection channels (textiles, pruning, bulky waste, etc.); and (iv) UW. Each waste flow undergoes tailored treatments to recover recyclable materials and minimize the environmental impacts associated

with final disposal. These processes were modeled based on literature [15]. The output flows considered in this study resulting from the treatment of waste from separate collections include both the removed foreign fractions and the quantities of materials sorted and reprocessed for recycling. “Impurities” or “foreign fractions” refer to materials that do not correspond to the target waste of a specific selective collection. Their quantities serve as indicators of the quality of selective collection. While data on the quality of the organic fraction are available at municipal level in the case study areas, the regional average values of impurities [13] were assumed for all municipalities for glass (2%), paper and carboard (6%), and light packaging (30.4%) fractions. For the selective collection of textile waste, the average percentages of material destined for recycling (81.9%), landfill (4.5%), energy recovery (3%), and stock (9%) were assumed based on [8]. All other quantities of selectively collected waste were aggregated under the category “Other.” This category includes bulky waste, green waste, and all other waste from drop-off centers. The presence of impurities in these categories and their distribution between recycling, landfill, and energy recovery are still under investigation. On the other hand, the treatment of UW aims to recover recyclable materials and stabilize organic matter. The residual material, traditionally defined “rejects”, is compacted into bales with a low percentage of biodegradable material. Output flows from the MBT of UW fraction were calculated based on a 2022 report by ARC on MBT plants in Catalonia. Additionally, mass balance data from the MBT plant of Vacarisses, provided by CWMVO, were used to calculate the output flows in VO.

4. Integration of MFA results for scenario analysis in LCA

The results of the MFA for the Catalonia case study are presented in Figure 2. In 2022, a total of 3,839 Gg of MSW was generated. 1,740 Gg (SCR 45.3%) was source separated for recycling. The overall recycling rate was estimated to be 33.4%, below the EU MSW recycling rate target of 55% by 2025 [2]. Analogously, in the VO the SCR was estimated to be 44.1% while the recycling rate was 30%. Short-term strategies to raise recycling rate seems to be in order to meet EU targets. As previously mentioned, enhancing SCRs does not necessarily imply an increase in recycling rates and GHG savings. The indicator we will employ to assess the performance of the separate collection system is the composition of UW.

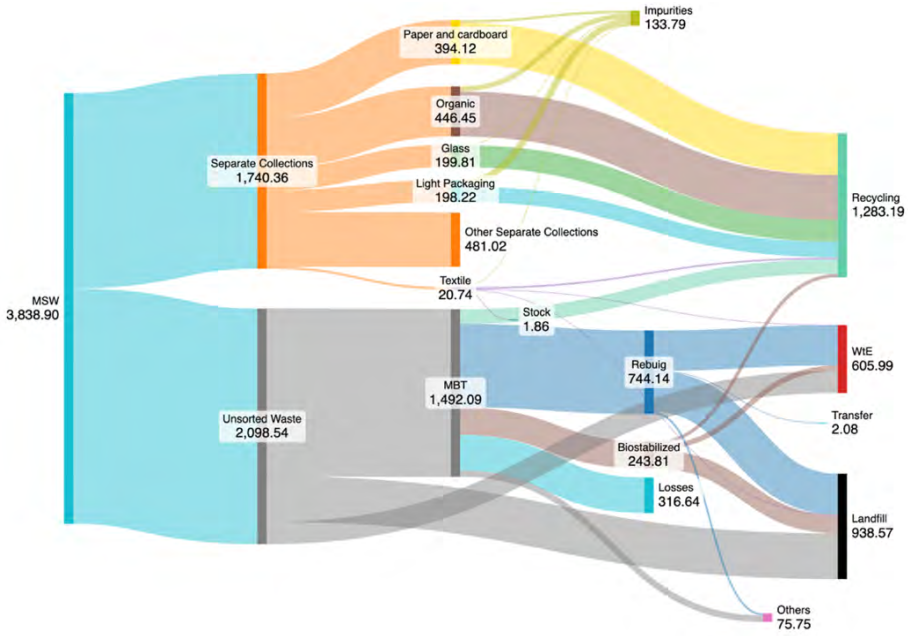

Figure 2: Material flow diagram for the MSWM system in Catalonia (all quantities expressed in Gigagrams, Gg).

We propose a comparison between two different scenarios based on varying the UW composition: (1) Current scenario (SCR of 45.3%): This scenario utilizes regional-level average composition data [16], representing the current MSWM framework in Catalonia; (2) Future scenario (SCR of 65%): This scenario utilizes the average composition of UW in 2022 from the Tuscany region (Italy) [unpublished data]. It has been chosen to assess how potential future outcomes of the LCA might change if MSWM strategies capable of raising the SCR were implemented. As the composition of UW and SCR vary, the quantities of impurities present in the different flows of separate collection also change. Another critical parameter influencing LCA outcomes in MSWM systems is the allocation of these residual fractions resulting from sorting treatments of recyclable materials. Consequently, we propose a sensitivity analysis based on potential variations in the allocation of impurities across three extreme configurations: (1) Equal Allocation**:** Residual fractions are evenly divided between landfill disposal and incineration; (2) Complete Landfill Disposal: All residual fractions are sent to landfill, assuming this is the most cost-effective and readily available option, despite its potential environmental consequences; (3) Complete Energy Recovery: All residual fractions are directed towards energy recovery processes, assuming waste-to-energy facilities can effectively convert waste into energy while minimizing GHG emissions. The next step is the use of the MFA results to generate a LCI framework and perform LCA to assess the environmental performance of the diverse scenarios.

References

[1] European Environmental Agency, “Capturing the climate change mitigation benefits of circular economy and waste sector policies and measures”, Briefing no. 25/2023, (2024).
[2] European Commission, “Directive (EU) 2018/851 of the European Parliament and of the Council of 30 May 2018 amending Directive 2008/98/EC on waste”, Official J. Eur. Union L 150, p. 109-140, (2018).
[3] Sevigné-Itoiz E., Gasol C.M., Rieradevall J., Gabarrell X., “Methodology of supporting decision-making of waste management with material flow analysis (MFA) and consequential life cycle assessment (CLCA): case study of waste paper recycling”, J. Clean. Prod., 105, p. 253–262, (2015).
[4] Haupt M., Waser E., Würmli J.C., Hellweg S., “Is there an environmentally optimal separate collection rate?”, Waste Management, 77, p. 220-224, (2018).
[5] Ekvall T., Assefa G., Björklund A., Eriksson O., Finnveden G., “What life-cycle assessment does and does not do in assessments of waste management”, Waste Management, 27 (8), p. 989-996, (2007).
[6] Turner D.A., Williams I.D., Kemp S., “Combined material flow analysis and life cycle assessment as a support tool for solid waste management decision making”, J. Clean. Prod., 129, p. 234–248, (2016).
[7] De Meester S., Nachtergaele P., Debaveye S., Vos P., Dewulf J., “Using material flow analysis and life cycle assessment in decision support: a case study on WEEE valorization in Belgium”, Resour. Conserv. Recycl., 142, p.1–9, (2019).
[8] Morell-Delgado G., Peiró L.T., Toboso-Chavero S., “Revealing the management of municipal textile waste and citizen practices: The case of Catalonia”, Science of The Total Environment, 907, Article 168093, (2024).
[9] Blengini G.A., Fantoni M., Busto M., Genon G., Zanetti M.C., “Participatory approach, acceptability and transparency of waste management LCAs: case studies of Torino and Cuneo”, Waste Management, 32, p. 1712–1721, (2012).
[10] Associacio de Municipis Catalans per a la Recollida Porta a Porta, Retrieved on March 13, 2024, from https://www.portaaporta.cat/en/municipis.php, (2022).
[11] SankeyMATIC (BETA): Build a diagram, [online] Available from: http://sankeymatic.com/build/.
[12] PRé Consultants B. V, SimaPro 9.2.0.2 Multi user, (2022).
[13] Agència de Residus de Catalunya, Estadístiques de Residus Municipals, http://estadistiques.arc.cat/ARC/#, (accessed 2.1.24).
[14] Consorci per a la Gestio de Residus del Vallès Occidental, Observatori de Residus del Vallès Occidental, Dades, https://observatori.residusvalles.cat/dades/consulta-totes-les-dades/ (accessed 2.2.24).
[15] Haupt M., Kägi T., Hellweg S., “Life cycle inventories of waste management processes”, Data Brief, 19, p. 1441–1457, (2018).
[16] Agència de Residus de Catalunya, “Petjada de carboni de la gestió i tractament dels residus municipals de Catalunya. Informe 2022”, Documents section, Available from: https://estadistiques.arc.cat/ARC/#, (2024).

Title: Indicators and parameters for the Life Cycle Sustainability Inventory of Municipal Solid Waste Management Systems

Author(s): Annachiara Ceraso*[1], Alessandra Cesaro[1]

[1] *Department of Civil, Architectural and Environmental Engineering, University of Naples Federico II, via Claudio 21, 80125 Naples, Italy, annachiara.ceraso@unina.it (Annachiara Ceraso); alessandra.cesaro@unina.it (Alessandra Cesaro)*

Keyword(s): Life Cycle Thinking; Sustainability; Circular Economy; Impact Assessment.

Abstract

1. Introduction

In recent years, the importance of Municipal Solid Waste Management Systems (MSWMSs) in industrialised countries has grown significantly, due to the increase in solid waste generation in urban areas, consistently with population growth and improved economic conditions. Therefore, identifying optimal solutions for MSWMSs has become an urgent concern, in line with the priority of encouraging Circular Economy (CE) practices and promoting sustainability [1]. For these reasons, there is a pressing need for tools to comprehensively assess the full spectrum of impacts of MSWMSs on the three pillars of sustainability, namely environment, economy, and society, especially when CE strategies are applied. In this regard, the Life Cycle Sustainability Assessment (LCSA) has been proposed as the most suitable approach, framed within the Life Cycle Thinking concept [2]. This method represents a holistic tool to evaluate the environmental, economic, and social impacts of MSWMSs, among other productive systems, even though it is often performed as the integration of three separate analyses, each focusing on a distinct sustainability pillar and conducted through the environmental Life Cycle Assessment (eLCA), the Life Cycle Cost (LCC), and the social Life Cycle Assessment (sLCA), which can lead to inefficiencies and time constraints [3]. Concerning the implementation of this method to circular MSWMSs, some limits must be overcome, starting from those linked to the initial phase of LCSA, namely the Life Cycle Sustainability Inventory (LCSI), during which all the indicators and parameters (i.e., representative measures of phenomena of interest [4]), relevant for a case study, are collected, as delineated by the ISO 14040 and ISO 14044 standards [5,6]. For instance, the commonly used approach for evaluating circular MSWMSs is the “grave to gate” approach, which considers only the indicators to evaluate the management of goods from the moment they become waste, until they are first reintroduced in the economy, without fully accounting for the impact of circular solutions. To this end, adopting a “grave to grave” approach would be more effective, because it would assess the impact of a product from the moment it becomes waste until it is dismissed in a landfill after having been reintegrated into the economy. To reach this goal it is necessary to identify and analyse the most pertinent indicators required to delineate input and output flows associated with the environmental, economic, and social impacts of MSWMSs, overcoming the double-counting issues, which can overestimate or conceal certain impacts [7]. This phenomenon is linked to the use of the same indicators for evaluating multiple impact categories, often related to different pillars of sustainability. Besides, it is also necessary to define additional and adequate parameters to characterise the relationship between sustainability and

circularity of waste management solutions. In this context, building on the first attempts to implement the LCSA of MSWMSs, the present research mainly aims at identifying additional indicators that can be used since the LCSI phase to establish the impacts caused by the implementation of circular solutions for waste management systems, to grant a better evaluation of their sustainability. Further research is, thus, necessary to overcome these issues and set a LCSA method that can comprehensively assess the overall sustainability of MSWMSs (Fig. 1).

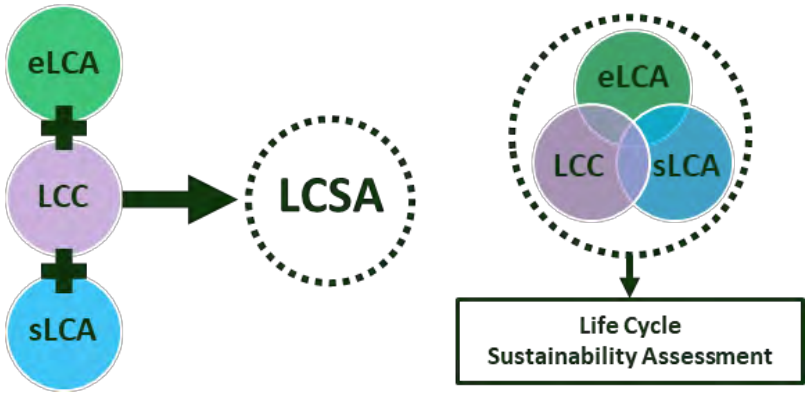

Figure 1. Life Cycle Sustainability Assessment development

2. Methodology

To this end, a systematic literature review was carried out to analyse the indicators and parameters adopted for the assessment of MSWMSs on either single or multiple sustainability pillars. Following the extensive analysis of the relevant scientific literature over the last 20 years, the present research allowed to identify some of the most relevant and problematic indicators used for the LCSA of MSWMSs, and to define some additional key parameters to evaluate the circularity of waste management solutions, delving into their applicability across different phases and treatments, their alignment with sustainability pillars, and their significance for various stakeholders.

3. Results and discussion

Notably, it was possible to highlight how certain indicators may be interconnected across sustainability pillars or vary in significance depending on the stakeholders involved in the assessment. These issues may limit the validity of LCSA studies on MSWMSs, as the indicators collected during the LCSI phase may lead to double-counting phenomena, as for health-related parameters, or economic indicators with a social relevance [8,9]. For example, the parameters used for quantifying different types of emissions may be used to assess the impacts on both environmental and social categories, overestimating the impact on human health. This is also the case for the parameters related to the labour costs, which include the costs for safety equipment, training, and the workers' salaries. The relevance of these parameters strongly depends on their perception from the affected stakeholders; indeed, the increase of these costs is generally considered beneficial by the workers, while it is assumed to be disadvantageous by the facilities owners. Therefore, to overcome this limit during the implementation of the LCSA for MSWMSs and other systems, it is necessary to properly define the pertinence and boundaries of the indicators relevant to the considered case studies, since the LCSI phase.

In addition, this research addresses the need for additional parameters to quantify the sustainability of CE solutions applied to MSWMSs [10]. As a result of the analysis of the state-of-the-art, new parameters

were proposed to address the LCSA studies of MSWMSs implementing circularity. More specifically, indicators that refer to the lost matter and energy that could have been recovered through management processes were developed to promote the set-up of a methodology for the effective LCSA of MSWMSs in a circular perspective, as well as parameters necessary to characterise the treated waste, and establish the revenues that can be obtained from its treatments and the associated social burdens.
Most of the proposed parameters are related to the characteristics of the treated waste flow, which depends on the served population and its economic conditions [11]. Indicators on the amount of treated waste can help evaluate whether waste prevention and collection strategies are efficient. Besides, proper knowledge of the qualities of treated waste is fundamental to establishing the amount of resources wasted during MSWM or the amount of energy that is not recovered during waste treatments, as in the case of the biogas produced from landfills, which is generally not destined for any energy generation process. These parameters are useful for assessing the lack of circularity of waste treatments and to help consider improvements for MSWMSs. In particular, a further distinction between the amount of recoverable resources and reusable materials present in a waste stream could help better assess the impact of material recovery, as the recycling of substances and materials can cause different burdens. Similarly, when quantifying the energy that could have been produced from MSWMSs but is instead lost, it would be beneficial for the LCSI of MSWMSs to distinguish between the energy that can be obtained in the form of biofuels and the energy directly produced from Waste-to-Energy systems. Besides, the economic value of the available resources, materials, or energy recoverable from waste also needs to be included in the LCSI, as LCSA studies often focus only on the economic value of the recovered resources, without considering the revenues that are wasted, due to the lack of employment of circular solutions. Then, regarding the social pillar, it has been observed that the commonly used indicators mainly focus on the well-being of workers, and only consider the impact of MSWMSs on the community in terms of disamenities due to the proximity to waste treatment plants. Instead, the present research also includes indicators to consider how circular and sustainable products are perceived by society, for example by including the parameters useful for quantifying the costs of products or energy obtained from recycled or reused waste, which can help evaluate their acceptance by the consumers. Finally, to better evaluate waste prevention strategies, such as deposit-refund systems (DRSs), it is necessary to gather all the indicators for quantifying the plausible economic revenues for the community, to establish whether a circular management of waste can be potentially adopted by society (Tab. 1).

Table 1. LCSA indicators for MSWMSs

Indicator	Unit of measure	Stakeholders	Sustainability pillar
Lost resources	kg	Community	Environment
Lost materials	kg	Community	Environment
Lost biofuels	m^3	Community	Environment
Lost energy	Joules	Community	Environment
Lost revenues	€	MSWMSs owners	Economy
Recycled product	€	Consumers	Social
Recovered energy	€	Consumers	Social
Recovered biofuels	€	Consumers	Social
DRSs revenues	€	Consumers	Social

4. Conclusions

The introduction of indicators addressing the impact of the lack of circularity in MSWMSs on the environment, economy, and society is essential to help identify proper sustainable solutions for waste management and to further improve their sustainability, by addressing the limits and the missed opportunities of waste management processes. In conclusion, the present research contributes to the enhancement of the LCSA methodology, which can support waste management promoters and policymakers in developing the most sustainable and circular solutions for MSWMSs. By considering the entire life cycle of waste, including its reintegration into the circular economy, this approach ensures comprehensive sustainability. The use of specific indicators to evaluate the impacts of flawed or incomplete circular solutions on the three pillars of sustainability can help identify superior options and improvements for MSWMSs.

References

[1] Van Fan Y., Klemeš J.J., Lee C.T., Tan R.R., “Demographic and socio-economic factors including sustainability related indexes in waste generation and recovery”, Energy Sources, Part A: Recovery, Utilization and Environmental Effects (2021).
[2] Valdivia S., Backes J.G., Traverso M., Sonnemann G., Cucurachi S., Guinée J.B., Schaubroeck T., Finkbeiner M., Leroy-Parmentier N., Ugaya C., Peña C., Zamagni A., Inaba A., Amaral M., Berger M., Dvarioniene J., Vakhitova T., Benoit-Norris C., Prox M., Foolmaun R., Goedkoop M., “Principles for the application of life cycle sustainability assessment”, International Journal of Life Cycle Assessment 26, 1900–1905, (2021).
[3] Valdivia S., Ugaya C.M.L., Hildenbrand J., Traverso M., Mazijn B., Sonnemann G., “A UNEP/SETAC approach towards a life cycle sustainability assessment - Our contribution to Rio+20”, International Journal of Life Cycle Assessment, 18, 1673–1685, (2013).
[4] Heink U., Kowarik I., “What are indicators? On the definition of indicators in ecology and environmental planning”, Ecol Indic, 10, 584–593, (2010).
[5] ISO, “ISO 14040 International Standard. Environmental management — Life cycle assessment — Principles and framework.”, International Organization for Standardization (ISO), Geneva, Switzerland, (2006).
[6] ISO, “ISO 14040 International Standard. Environmental management — Life cycle assessment — Requirements and guidelines Management environmental.”, International Organization for Standardization (ISO), Geneva, Switzerland, (2006).
[7] Finkbeiner M., Schau E.M., Lehmann A., Traverso M., Towards life cycle sustainability assessment, Sustainability, 2, 3309–3322, (2010).
[8] Woon K.S., Lo I.M.C., “An integrated life cycle costing and human health impact analysis of municipal solid waste management options in Hong Kong using modified eco-efficiency indicator”, Resour Conserv Recycl, 107, 104–114, (2016).
[9] Costa D., Quinteiro P., Dias A.C., “A systematic review of life cycle sustainability assessment: Current state, methodological challenges, and implementation issues”, Science of the Total Environment, 686, 774–787, (2019).
[10] Magrini C., Degli Esposti A., De Marco E., Bonoli A., “A framework for sustainability assessment and prioritisation of urban waste prevention measures”, Science of the Total Environment, 776, (2021).
[11] Ayodele T.R., Ogunjuyigbe A.S.O., Alao M.A., “Economic and environmental assessment of electricity generation using biogas from organic fraction of municipal solid waste for the city of Ibadan, Nigeria”, J Clean Prod, 203, 718–735, (2018).

Life cycle-based assessment of graphite recovery from spent Li-ion batteries

Dilshan Sandaruwan Prematilake*[1], W.A.M.A.N. Illankoon[1], Amilton Barbosa Botelho Junior[2], Denise Crocce Romano Espinosa[2], Mentore Vaccari[1]

[1]*Department of Civil, Environmental, International Cooperation and Mathematical Engineering, University of Brescia, Brescia, Italy, d.prematilake@unibs.it, a.wijepalaabeysi@unibs.it, mentore.vaccari@unibs.it*
[2] *Department of Chemical Engineering, University of Sao Paulo, Brazil, amilton.junior@usp.br, espinosa@usp.br*

Keyword(s): Li-ion battery recycling, graphite recycling, life cycle analysis, recycling method comparison

Abstract

There is a lack in recycling processes focus on graphite recovery from spent Li-ion batteries (LiB). In the current study, aiming to identify environemtnally sustainable graphite recovery methods, three different graphite recovery methods have been used to recycle graphite from spent LiBs. Chemical recycling demonstrated a higher recycling efficiency reaching 84%, while physical and combination reached lower efficiencies – 54% and 80%, respectively. Additionally, the physical method showed the lowest environmental impact (0.0407 kg CO_2 eq.), while the combination method showed the highest (2.75 kg CO_2 eq.) per 1kg of graphite recovery. The highest impact is attributed to electricity consumption followed by greenhouse gas emissions. Physical recovery of graphite emerges as the best compromise between extraction efficiency and environmental impacts.

Introduction

Recently, many authors have explicitly discussed the importance of graphite recycling from spent Li-ion batteres (LiB) [1], [2], [3]. Many of the materials categorized as critical to numerous countries are extensively used in LiB production. Despite the efforts by scholars and recyclers to identify methods for recovering most materials from spent LiBs, graphite has been largely overlooked for many years due to its lower economic importance than other battery materials [1]. Nevertheless, the significant increase in graphite usage across various industries and the rapid growth of the electric vehicle sector drives to an increasing demand of graphite from graphite ores. Furthermore, these factors contribute to the accumulation of waste graphite, which cannot be ignored in future [2]. Consequently, there is a pressing need to identify effective and environmentally friendly methods for graphite recycling. Hence, in the aim of identifying environemtnally sustainable graphite recovery methods, we developed three different methods for graphite recovery from spent LiBs. We performed an attributional life cycle assessment (LCA) to analyse and compare the impacts of the three methods in relation to the recovery efficiencies determined.

Methodology

Extraction of graphite: Fiat-Panda hybrid EV batteries (manufactured by Samsung in 2019) were supplied by RMB Spa, Brescia, Italy for the study. The battery packs were manually opened using wrenches and heavy tools, followed by cell disassembly under a fume hood. Subsequently, the aluminium (cathode) and copper (anode) current collectors were untangled and dried in a vacuum furnace for 24 hours at 40°C.

The dried anode (copper current collectors) was then used in the next part of the experiment. A sample from the dried anode was subjected to a reaction with concentrated nitric acid at a solid-to-liquid (S/L)

ratio of 1:5 to identify the maximum purity and yield of graphite that could be recovered from the anodic material.

$$3Cu + 8HNO_3 \rightarrow 3Cu(NO_3)_2 + 4H_2O + 2NO \text{-------- (1)}$$

Afterwards, three different methods were used to recover the graphite available in the anodic material: physical, chemical and combination. The methodology is described as follows.

50 g of dried anode material was ground using a blade cutter grinder (100 W laboratory grinder) for 2 minutes. The resulting powder was then sieved with a 200 µ sieve [3], and the finer fraction was selected for analysis.

50 g of dried anode material was scrapped into roughly 10 mm-sized pieces. These pieces were then mixed with a royal solution (1:3 of HNO_3:HCl molar ratio) at a S/L ratio of 1:5. The solution was stirred until all the anode material dissolved completely. The filtered residue from the mixture was washed with deionized (DI) water several times until the pH reached around a neutral value. Finally, the received slurry was dried at 105°C in a vacuum oven for 30 minutes.

In the combination method, first, 50 g of anodic materials were roughly scrapped into 10 mm-sized pieces. These pieces were then covered with CaO in a ratio of 1:3 (anode:CaO) in a crucible. The crucible was then heated at 250°C for 20 minutes. The heated material was washed thoroughly with DI water and allowed to dry at 105°C for 30 minutes. The washed material was then ground using the cutter grinder for 2 minutes and sieved with a 200 µ sieve. The finer fraction was selected for analysis. Graphite samples obtained from each recovery method were analyzed for their carbon content.

Life Cycle Assessment (LCA) was conducted using SimaPro software (PhD version) to evaluate three methods utilized for the extraction of graphite from spent LiBs. The life cycle boundary of the system was defined to include the recovery of graphite from anodic parts, while steps in the pretreatment were excluded from the study as they are common for all three methods [4]. The functional unit of the study is the recovery of 1 kg of graphite from anodic materials. Inventory calculations were performed for each method, considering the materials inputs and outputs required to recover 1 kg of graphite. Subsequently, an analysis was carried out to identify the most favourable method using the “ReCiPe 2016 Midpoint (H) V1.04/World (2010) H” calculation method.

Results and Discussion

Anode material is reacted with concentrated nitric acid dissolving the copper, and giving a residual of 38% (eq.1). The residual was found to have a carbon content of 96.6%, indicating that the total pure graphite availability in the anode to be 36.71 wt.% which is used as the basis for calculating the efficiency of each recovery method utilized.

In the physical recovery method of graphite, no chemicals were used. Instead, physical steps such as grinding and sieving were employed. Grinding the anode material effectively separates the graphite active material as the organic binders (PVDF) decay due to friction. However, copper in the anode material does not powderize as the metal itself is malleable and forms small lumps during grinding. Therefore, sieving (>200 µ) was utilized to separate the mixture. The method resulted in 30.50% of materials under 200 µ, with a carbon content of 64.80%, achieving a recovery of 53.83 wt.% of the total graphite available in the anode current collector.

In the chemical recovery method, the royal solution was used, as its environmental impact is lower than using the nitric acid according to the eco-invent 3.6 database. The total graphite recovery received with royal solution is less than that of nitric acid, though, both experiments carried out at similar solid-to-liquid (S/L) ratio. This could be due to the high oxidation capacity of nitric acid compared to the mild oxidation potential of royal solution, which contains hydrochloric acid. Nevertheless, the recovery is higher than the other two methods studied. The filtered material amounted to be 38 wt.% with a carbon content of 81%, resulting in a total recovery of 83.84 wt.% of graphite in the anode.

Finally, In the combination method, CaO was used to react with PVDF binders present in the anode material. The reaction between CaO and PVDF at 250°C forms CaF_2, which avoids the generation of HF, making the process environmentally healthy. Also, this allows more efficient liberation of graphite during the grinding as the organic binder disintergrated during the heating. However, wastewater is generated as water is required for washing the CaF_2 present in the mixture. The finer fraction after sieving was 40.22%, with a carbon content of 70.00%, resulting in a recovery of 80.46 wt.% graphite from the total graphite in the anode part.

For the LCA, gaseous emission content in each method utilized was calculated using stoichiometry. Wastewater content and waste acid content were calculated using mass balances of the process. Italian market values were used for energy and materials, and all inputs and outputs were taken from the Eco-invent 3.6 database. Preliminary results from the LCA show that the physical method causes a total of 0.0407 kg CO_2 eq. emissions, the chemical process: 2.26 kg CO_2 eq. and combination method: 2.75 kg CO_2 eq. for 1 kg of graphite recovery under global warming impact catagory. Hence, physical process showed the lowest impact despite the lower recovery values received. Figure 1 shows the comparative analysis of the environmental impact of the three methods utilized.

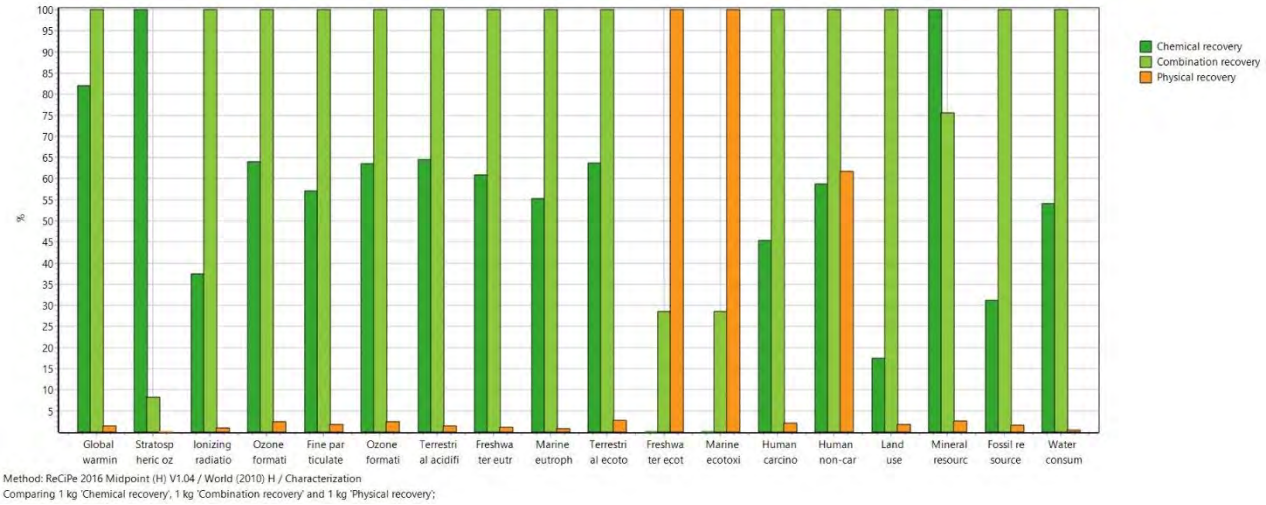

Figure 1. Relative impacts (in percentages) of the three recovery methods under different impact categories.

According to Figure 1, the impact generated from the combination method is the highest across many categories. The main reason for this is higher electricity utilization for the thermal treatment. Additionally, the combination process shows milder impacts, under “water toxicity categories” due to particle emissions resulting from further treatment of scrap copper derived from the process. Though relatively lower energy is consumed for chemical recovery, emissions of NO and HF cause the highest impact

across various categories. However, these impacts are relatively lower than that of the combination method. Overall impacts are lowest in the physical method, attributed to lower energy utilization compared to the other two methods. However, “water ecotoxicity categories” show higher impacts for physical recovery, mainly due to the high amount of unsorted scrap copper derived from the recovery. Also, the treatment of these scrap metals causes a high amount of particulate matter that can elevate the impact under the human non-carcinogenic category.

However, there is a possibility to further reduce the impacts of recovering graphite from End-of-Life (EoL) LiBs by combining two or more methods. Mainly, water toxicity and particulate matter impacts can be reduced if the output scrapped copper from the physical method is treated with mild acidic solvents. Hence, the copper can be extracted through electrowinning without causing impacts with copper processing. However, this might lead to other undesirable impacts as well.

Conclusion:

Physical separation mechanisms are better suited for graphite extraction from waste Li-ion batteries (LiBs) due to their lower environmental impacts (~0.0407 kg CO_2 eq.). Utilizing heat-based treatments like the use of CaO to break down PVDF significantly increases the impacts, making the recovery method undesirable. Although using chemicals provides relatively better recovery, gaseous emissions can increase the environmental impact associated with the method.

Acknowledgement: This work was supported in part by the Italian Ministry of Foreign Affairs and International Cooperation, grant number BR22GR09. The authors would like to acknowledge the Fundação de Amparo à Pesquisa do Estado de São Paulo and Capes (grants: 2019/11866-5 and 2020/00493-0 São Paulo Research Foundation) for their financial support.

References

[1] S. Natarajan and V. Aravindan, “An Urgent Call to Spent LIB Recycling: Whys and Wherefores for Graphite Recovery,” *Adv Energy Mater*, vol. 10, no. 37, Oct. 2020, doi: 10.1002/aenm.202002238.

[2] D. S. Premathilake, M. Vaccari, A. B. Botelho Junior, J. A. S. Tenório, D. C. R. Espinosa, and F. Colombi, “Valorization of waste graphite deriving from ‘End Of Life Lithium-Ion Battery recycling’ for a second use in wastewater treatment.,” in *18th International Conference on Environmental Science and Technology*, Athens, 2023. doi: 10.30955/gnc2023.00266.

[3] D. S. Premathilake, A. B. Botelho Junior, J. A. S. Tenório, D. C. R. Espinosa, and M. Vaccari, “Designing of a Decentralized Pretreatment Line for EOL-LIBs Based on Recent Literature of LIB Recycling for Black Mass,” *Metals (Basel)*, vol. 13, no. 2, p. 374, Feb. 2023, doi: 10.3390/met13020374.

[4] F. Duarte Castro, E. Mehner, L. Cutaia, and M. Vaccari, “Life cycle assessment of an innovative lithium-ion battery recycling route: A feasibility study,” *J Clean Prod*, vol. 368, p. 133130, Sep. 2022, doi: 10.1016/j.jclepro.2022.133130.

Title: Carbon Lifecycle Management Through Innovative Forest Land Management and Regulatory Frameworks

Authors: Isabel Martínez-Alcalá*[1], José Luis Durán-Sánchez[2], Rubén Martínez-Alpañez[2] and

Víctor Meseguer-Sánchez[2]

[1] *Vicerrectorado de Investigación, Universidad Católica de Murcia, Murcia, 30107, Spain, immartinezalcala@ucam.edu*
[2] *Social Responsibility and Innovation research group, Universidad Católica de Murcia, Murcia, 30107, Spain; jlduran@ucam.edu; rmartinez6@ucam.edu; jvmeseguer@ucam.edu*

Keywords: EU Green Deal, carbon lifecycle, forest management, sustainable practices, climate action, Eddy Covariance.

Abstract

Forest ecosystems play a pivotal role in the global carbon cycle, acting as significant carbon sinks that mitigate the accumulation of greenhouse gases in the atmosphere [1]. Despite their critical importance, the rate at which CO_2 is sequestered in these natural reservoirs is often undermined by deforestation, forest degradation, and mismanagement [2]. Addressing these challenges necessitates innovative approaches to forest management and carbon accounting.

The new LIFE TOKEN CO_2 project is at the forefront of addressing the pressing global challenge of climate change through innovative forest management and technology integration. It embodies the ambitious goals set forth in the European Green Deal, aiming for a carbon-neutral EU by 2050 by decoupling economic growth from resource use and aiming for no net emissions of greenhouse gases [3].

This study leverages the dual capabilities of advanced environmental science and cutting-edge blockchain technology to create a robust platform for managing the lifecycle of carbon—capturing data from emission to sequestration and compensation. Inspired by a profound understanding of forest carbon dynamics and bolstered by technological innovation, this project aims to revolutionize how carbon credits are quantified, issued, and traded globally.

The integration of blockchain technology with empirical scientific research to ensure that each carbon credit token is grounded in verifiable carbon sequestration data is the core of the project. This integration ensures a transparent, secure, and efficient marketplace for carbon credits, addressing common challenges in current carbon markets such as transparency and fraud [4]. By tokenizing carbon credits, the project ensures that each unit of sequestered carbon is accounted for and traded on a public blockchain, providing unprecedented traceability and security [5].

In order to start with the project, a comprehensive bibliometric analysis has been conducted to track the evolution of forest management research for carbon sequestration, examining changes in both volume and focus. Also, to identify key publications, leading researchers, and pivotal institutions that have significantly influenced the field. And finally, to identify gaps in the current research and predict emerging trends that could inform future studies and guide policy development.

The articles for the study were sourced from Scopus due to its extensive coverage of relevant journals and articles and following the methodological procedure showed in the figure 1 (Fig. 1). The search was refined to papers published between 1993 and 2022 to understand the evolution over a fixed period. In this context, Microsoft Excel was utilized for tracking publication trends, citation analysis, and temporal

keyword frequency. While VOSViewer offered insights into the relational dynamics among keywords, authors, and institutions, helping to visualize the intellectual structure and collaborative networks within the field.

Figure 1. Methodological procedure applied.

The data showed a marked increase in the number of publications, especially during 2005-2013, indicative of heightened interest and research activity in this area (Fig. 2). Studies often addressed how forest management could be adapted to mitigate climate change impacts. Research has robustly explored various silvicultural techniques and their effectiveness in enhancing the carbon storing capabilities of forests. Increasingly, studies are incorporating socio-economic evaluations of forest management practices, acknowledging the role of human activity in shaping forest landscapes.

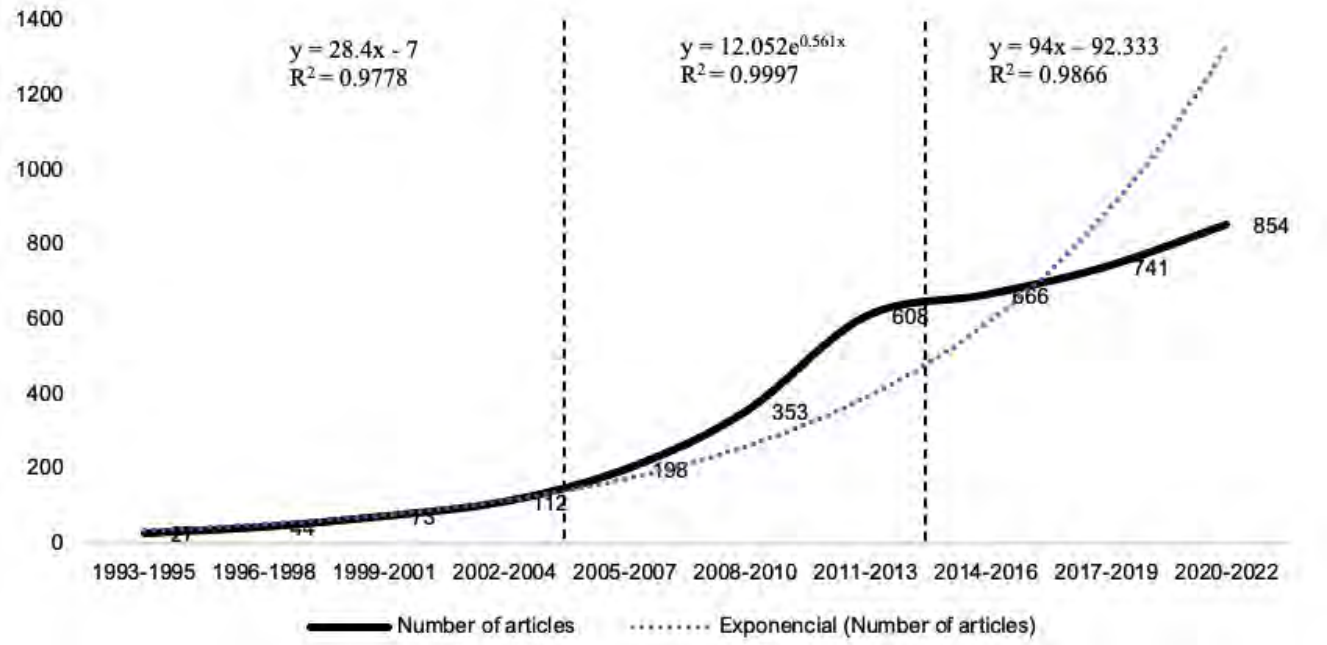

Figure 2. Number of documents published in each sub-period.

The leadership of the U.S. and China in this research area (Fig. 3) suggests significant national investments in climate mitigation strategies involving forest management. Moreover, collaboration patterns indicate a robust network of international research, underscoring the global importance of the issue.

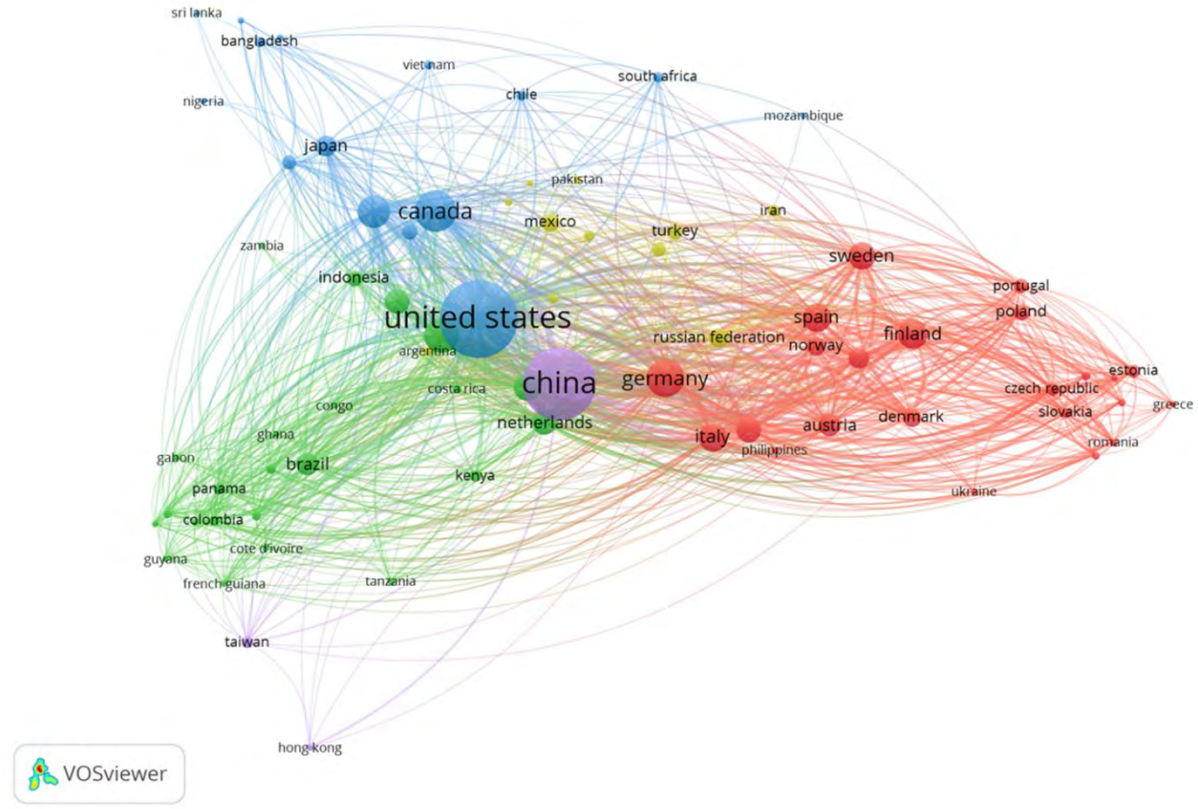

Figure 3. Countries' international cooperation network.

The integration of socio-economic factors and legal aspects into forest management research is a relatively new but rapidly growing focus. Understanding the economic benefits, alongside the ecological ones, can drive more comprehensive policy development. In this sense, effective forest management policies can serve as powerful tools for governments and organizations aiming to meet their carbon neutrality goals. Moreover, policies that incentivize sustainable forest management, protect old-growth forests, and promote reforestation are vital.

This bibliometric analysis underscores the pivotal role of forest management in global climate change mitigation efforts. The study not only charts the growth and focus shifts in the field over three decades but also highlights critical areas for future research and policy-making. Sustainable forest management is integral to global efforts to curb greenhouse gas emissions, and as such, requires concerted efforts from researchers, policymakers, and forest managers worldwide.

This project has been cofounded by the European union in the life call Nº 101074388

References

[1] Cui J., Zheng M., Bian Z., Pan N., Tian H., Zhang X., ... & Gu B. “Elevated CO_2 levels promote both carbon and nitrogen cycling in global forests”. Nature Climate Change, 1-7, (2024).

[2] FAO. “State of the World’s Forests 2020”. Rome, FAO. [online] Available at: http://www.fao.org/documents/card/en/c/ca8642en [Accessed 24 Sept. 2023].

[3] European Commission. “The European Green Deal” (2019). [online] Available at: https://ec.europa.eu/info/strategy/priorities-2019-2024/european-green-deal_en [Accessed 24 Sept. 2023].
[4] Mulligan C., Morsfield S., & Cheikosman E. “Blockchain for sustainability: A systematic literature review for policy impact”. Telecommunications Policy, 102676, (2023).

.

Title: Removal of pesticides from olive orchards through electrochemical generation of ozone and hydrogen peroxide

Author(s): Ismael F. Mena[1], Cristina Navas-Higuero[1]*, Engracia Lacasa[1], A.J. Manzaneda[2], Manuel A. Rodrigo[1], Cristina Sáez[1]

[1] Departamento de Ingeniería Química, Universidad de Castilla-La Mancha, Av. Camilo José Cela n 12, Edificio Enrique Costa Novella, Ciudad Real (13071) España. cristina.navas@uclm.es
[2] Departamento de Biología animal, biología vegetal y ecología, Universidad de Jaén. Campus Las Lagunillas. Edificio Ciencias Experimentales y de la Salud (B3). Av. De la Universidad n 9 Jaén (23009) España.

Keyword(s): ozone, hydrogen peroxide, AOPs, pesticides, soil treatment.

Abstract

A wide variety of pesticides had been used in the agricultural sector in recent decades due to the increase in food demand resulting from the growth in the population. These compounds are used to prevent diseases and plagues that can affect the plants. The problem related to their application is the low biodegradability and persistence in soils [1]. New treatment alternatives for the removal of these pollutants from soil need to be developed, with the aim of reducing ecotoxicity and improving soil quality.

The use of oxidant species such as ozone or hydrogen peroxide for the removal of organic pollutants has been widely studied in recent years, being pesticides efficiently removed from water and wastewater by advanced oxidation processes (AOPs) [2]. Among these, electrochemical AOPs (EAOPs) have emerged as an economical and effective alternative.

However, the treatment of polluted soils directly with EAOPs have been slightly studied for the complexity of their application. For this reason, a novel technology based on the addition of electrochemical generated oxidant species to soil has emerged. The oxidants can be produced and added directly on-site without the modifying the soil. Depending on the oxidant generated, the system can involve the application of a solution on the surface or the introduction of a gaseous stream into a well. Among oxidants, ozone is a gaseous compound considered as high selective and eco-friendly due to the low harmful intermediates produced [3], being the final products oxygen and carbon dioxide [4]. In the case of hydrogen peroxide, a large amount of hydroxyl radicals can be produced after its activation. One of the most studied activation methods is the Fenton reagent, which is based on the generation of hydroxyl radicals using Fe^{2+} as catalyst, and Fenton-like system, which use other metal as catalyst, such as Cu^{2+} or Al^{3+}, found in the olive soils.

In this work, we propose the treatment of spiked and real olive orchard soils polluted with different herbicides to study the on-site addition of oxidants (ozone and hydrogen peroxide) in soil for their remediation.

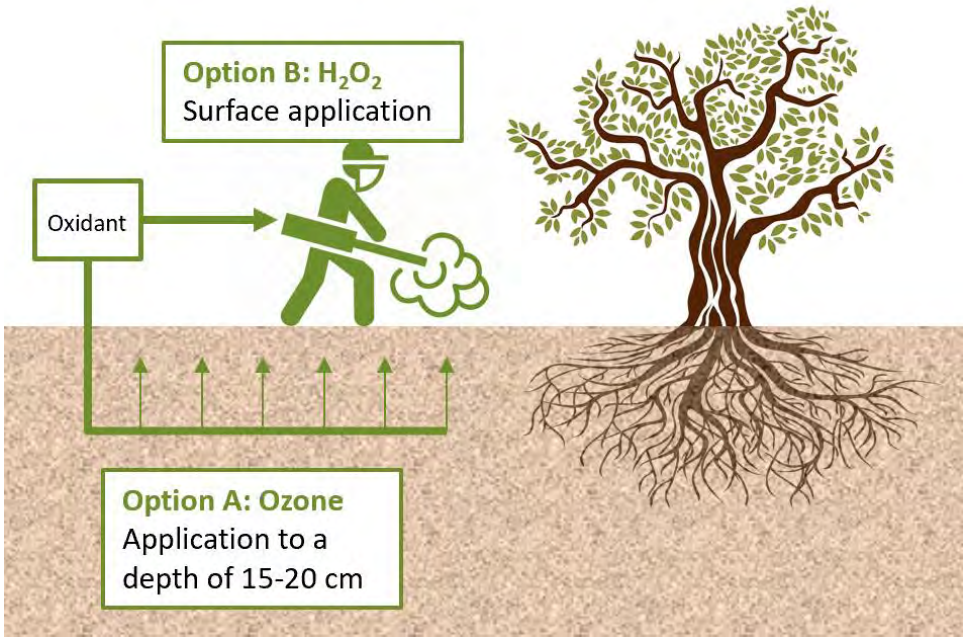

Figure 1. Representation of the oxidant dosage in real olive soils with ozone and hydrogen peroxide.

Oxyfluofen and Atrazine (pestanal grade, provided by Sigma-Aldrich) were selected as target compounds. Initially, clean soil was polluted with the pesticides using acetonitrile as solvent. The concentration in soil ranged between 100-1500 μg kg^{-1}, slightly higher than the concentrations found in real olive soils, to determine the efficiency of the process. The concentration of pesticide was analysed by means of high-performance liquid chromatography coupled with mass-Spectrometry (HPLC-MS) using a QuEChERS extraction from the soil.

Electrochemical production of ozone was carried out using a CabECO® cell (CONDIAS) with a Membrane Electrode Assembly (MEA) using Boron-Doped Diamond anodes and Proton Exchange Membrane (PEM) electrolysers. A solution of $HClO_4$ (1 mM, 500 mL) was continuously recirculated (30 L h^{-1}) using a current density of 170 mA cm^{-2}. The gaseous ozone production (together with oxygen and hydrogen) was vented out from the tank. Remediation experiments were conducted in a cylindrical mock-up (inner diameter: 3 cm, heigh: 18 cm) containing the contaminated soil (100-1500 μg kg^{-1}, heigh: 15 cm). The gaseous ozone was introduced continuously for 120 min through a well (diameter: 0.6 cm, heigh 14.5 cm) centrally located in the mock-up. Various sections of the soil were extracted (0-5 cm, 5-10 cm, and 10-15 cm depth) for post-mortem analysis. Figure 2 shows an image of the set up for the remediation of soil with O_3.

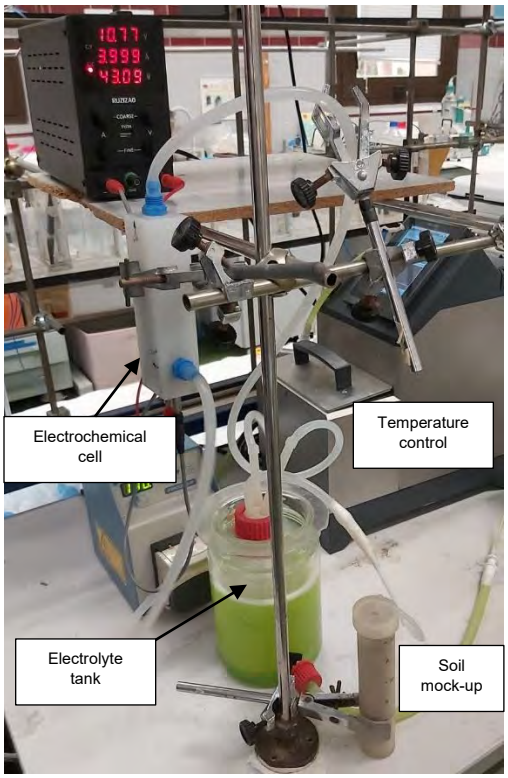

Figure 2. Set-up for remediation of soil with O_3.

Electrochemical production of hydrogen peroxide was carried out in a single compartment cell, using a Dimensional Stable Anode (DSA, Tianode) and a carbon paper gas-diffusion electrode (GDE, Freudenberg H23C8) as the cathode. A solution of $NaHCO_3$ (50 mM) was continuously passed through the cell (70 mL h^{-1}) using a current density of 5 mA cm^{-2}. The outlet effluent was introduced from the upper surface into a designed mock-up (inner diameter: 3 cm, heigh: 18 cm) containing the polluted soil (15 cm). The solution passed through the soil, and the permeate effluent was collected at the bottom of the mock-up. Different sections of the soil were then extracted (0-5 cm, 5-10 cm, and 10-15 cm depth) for post-mortem analysis.

The ozone cell was able to produce a continuous flow of 0.27 mg min^{-1} under the studied conditions, with a faradaic efficiency of around 2 %. This flow was directly introduced into soil polluted with oxyfluorfen and atrazine for 120 min (32.4 mg). In both cases, the highest degradation occurred in the deeper portion (10-15 cm), where the ozone effluent was introduced. Comparing the degradation of both compounds, oxyfluorfen was more effectively removed (27.3 µg of oxyfluorfen removed per mg of ozone for the soil polluted with 1500 µg kg^{-1}) than atrazine (19 µg of atrazine removed per mg of ozone for the soil polluted with 1500 µg kg^{-1}). Although both compounds achieved more than 65 % removal at a depth of 10-15 cm, the removal efficiency decreased as the depth decreased, achieving 37 and 12 % removal at a depth of 0-5 cm, respectively. When the amount of pesticide was reduced in the soil, the removal of oxyfluorfen was similar across all soil depths (around 85-88 %), whereas the efficiency in the removal of atrazine was reduced (ranging from 2-66 % depending on the depth).

In the case of hydrogen peroxide, the production achieved was around 7.8 mg h^{-1}, with a faradaic efficiency of 30-40 %. When the solution of H_2O_2 was introduced into the soil for 30 min (3.9 mg), two different behaviour were observed. For oxyfluorfen, most of the pollutant was retained in the soil,

achieving removals of around 10 and 45 % in soil polluted with 1500 and 100 µg kg^{-1}, respectively, with a slightly amount of oxyfluorfen appearing in the bottom effluent. The efficiency of this process is 34 µg per mg of hydrogen peroxide. For soil polluted with atrazine, removal percentages in the soil were up to 95-100 %. However, a high amount of atrazine appeared in the final effluent. This is related to the solubility of both compounds in water. Whereas oxyfluorfen is almost insoluble in water, atrazine is soluble and can be mobilized in soil by permeation. This can create a problem due to the mobility of the pollutants, that can appear in groundwater or surface water.

Comparing the results of both treatments, it can be seen that oxyfluorfen removal is higher when using ozone as oxidant, although the efficiency in terms of pollutant removed per mg of oxidant is lower. In the case of atrazine, ozone is less efficient than the hydrogen peroxide, but it is important to consider that atrazine can be solubilized in the effluent obtained from the bottom portion of the treated soil.

Regarding these efficiencies, comparing to another study of electrokinetic treatment (which achieved around 27 %) [5], using a higher amount of pollutant and soil (6 L of oxyfluorfen (24%) in 150 kg of soil), it can be concluded that the treatment using electrochemically generated oxidants results in higher pollutant removal, except in the case of oxyfluorfen with H_2O_2. Moreover, the treatment with ozone did not alter the soil pH and degraded the pollutant in-situ, whereas the electrokinetic produced pH gradients in soil and mobilized the pollutants.

In conclusion, both oxidants, ozone and hydrogen peroxide, are able to degrade herbicides in spiked soils at concentrations higher than those typically found in real olive soil. Removal percentages up to 80-95 % were achieved with both oxidants for the degradation of the studied pesticides, with ozone being more effective for oxyfluorfen removal, and hydrogen peroxide for the atrazine removal. However, special care should be taken with the use of hydrogen peroxide, as soluble compounds can appear in the final effluent.

Acknowledgments

This project has received funding from the European Union's Horizon Europe research and innovation program under grant agreement No 101091255.

References

[1] Sharma A., Kumar V., Shahzad B., Tanveer M., Sidhu G.P.S., Handa N., Kohli S.K., Yadav P., Bali A.S., Parihar R.D., Dar O.I., Singh K., Jasrotia S., Bakshi P., Ramakrishnan M., Kumar S., Bhardwaj R., Thukral A.K., "Worldwide pesticide usage and its impacts on ecosystem", SN Applied Sciences, vol. 1, 1446, (2019).
[2] Quiroz M.A., Bandala E.R., Martínez-Huitle C.A., "Advanced Oxidation Processes (AOPs) for Removal of Pesticides from Aqueous Media", in Pesticides - Formulations, Effects, Fate, M. Stoytcheva, Ed. IntechOpen, (2011).
[3] Rodríguez-Pena M., Barrios Pérez J.A., Llanos J., Saez C., Rodrigo M. A., Barrera-Díaz C.E., "New insights about the electrochemical production of ozone", Current Opinion in Electrochemistry, vol. 27, 100697, (2021).
[4] Rodríguez-Pena M., Barrios Pérez J.A., Llanos J., Saez C., Barrera-Díaz C.E., Rodrigo M. A., "Toward real applicability of electro-ozonizers: Paying attention to the gas phase using actual commercial PEM electrolyzers technology", Chemosphere, vol. 289, 133141, (2022).
[5] Risco C., Rodrigo S., López-Vizcaíno R., Yustres, A., Saez C., Cañizares, P., Navarro V., "Removal of oxyfluorfen from spiked soils using electrokinetic soil flushing with linear rows of electrodes", Chemical Engineering Journal, vol. 294, 65-72 (2016).

Title: Resource recovery hub for net zero carbon and climate change mitigation

Author(s): Daniele Di Trapani[1], Rosa Alduina[2], Luigi Badalucco[3], Marika Carnesi[1], Alida Cosenza[1], Ylenia Di Leto[3], Pedro Thomas Bulacio Fisher[3], Giuseppe Gallo[3], Vito Armando Laudicina[3], Antonio Mineo[1], Paulo Marcelo Bosco Mofatto[1], Sofia Maria Muscarella[3] and Giorgio Mannina*[1]

[1]*Department of Engineering, University of Palermo, Viale delle Scienze, 90128 Palermo, Italy* *giorgio.mannina@unipa.it
[2] *Department of Agricultural, Food and Forest Science, Palermo University, Viale delle Scienze, 90128 Palermo, Italy*
[3] *Department of Biological, Chemical and Pharmaceutical Sciences and Technologies, University of Palermo, Viale delle Scienze, 90128 Palermo, Italy;*

Keyword(s): circular economy; wastewater treatment; water resource; water smart solutions, climate change

Abstract

The wastewater treatment plants (WWTPs) must be transformed into Water Resource Recovery Facilities (WRRFs) in view of a more sustainable approach focusing on the circular economy concept. Different to WWTPs, the WRRFs have as a major goal not only the wastewater treatment to meet the legislation limits but also the recovery of resources such as: treated water for water reuse, carbon, nutrients, biopolymers etc.. According to the new Urban Wastewater Treatment Directive, prepared by the EU, greenhouse gas emissions must be minimized to achieve net zero carbon emissions. Despite the importance of WRRFs, several barriers hamper a straightforward application (namely, technical, administrative, legislative, social etc.). In view of boosting the WRRFs application in the real WWTs, a WRRF at Palermo University has been built within the EU project: Achieving Wider-Uptake of Water Smart Solutions. Insightful results were derived from such a system inspiring the application to the real WWTPs of Corleone and Marineo (Italy) by scaling-up the experience achieved at the pilot scale.

Introduction

Releasing inadequately treated wastewater into the environment poses significant health risks and ecosystem quality risks. Wastewater treatment plants (WWTPs) are tasked with generating treated effluent that meets regulatory standards, even though the characteristics of influent wastewater can vary greatly hourly, daily, and seasonal. Additionally, WWTPs need to address emerging challenges in wastewater treatment, such as removing contaminants of emerging concern (CECs) and reducing greenhouse gas (GHG) emissions. In this light, the recent paradigm is that WWTPs need to be transformed into Water Resource Recovery Facilities (WRRFs) to adopt a more sustainable approach that aligns with the principles of the circular economy. Unlike traditional WWTPs, WRRFs aim to treat wastewater to meet regulatory standards and recover valuable resources, such as treated water for reuse, carbon, nutrients, and biopolymers. The wastewater sector is evolving toward an integrated model that emphasizes resource recovery and achieving net-zero carbon emissions. This shift is further supported by the EU's new Urban Wastewater Treatment Directive, which mandates minimizing greenhouse gas emissions to meet net-zero targets. Despite the potential of WRRFs, various challenges, including technical, administrative, legislative, and social barriers, hinder their widespread implementation. To advance the adoption of WRRFs, a facility at Palermo University has been established as part of the EU project "Achieving a wider uptake of water-smart solutions". This initiative

aims to demonstrate the viability of transitioning to a more sustainable, circular approach and to promote the application of this model to real-world WWTPs, such as those in Corleone and Marineo, Italy, by scaling up the successful outcomes of the pilot project.

Material and methods

The Unipa WRRF was inaugurated in 2022 after a year of construction and is composed of four main elements (Figure 1):

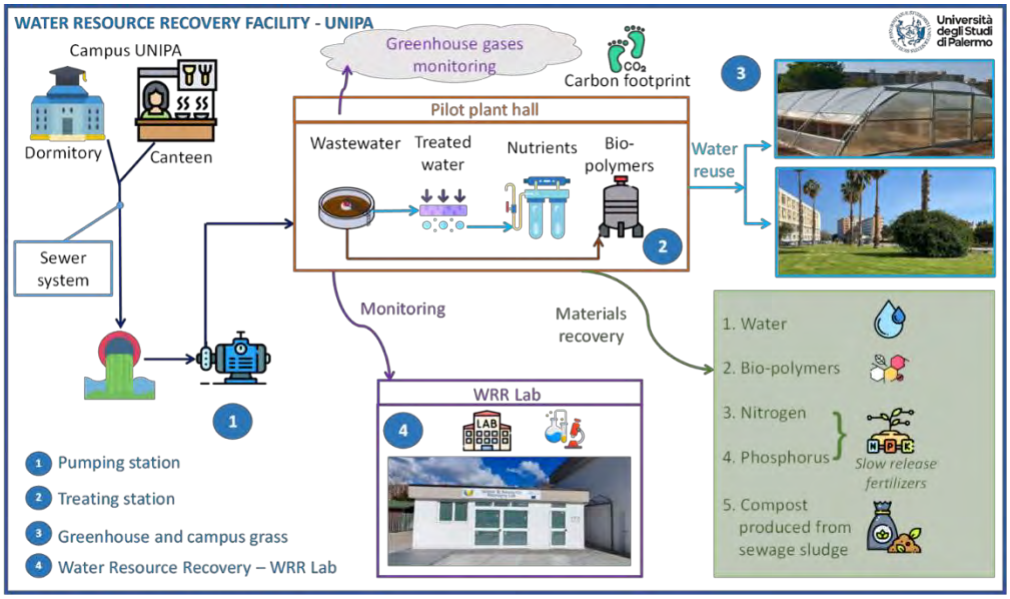

Figure 1. UNIPA WRRF conceptual scheme

I. An innovative pumping station (1500 m underground conduits d=800 mm) for collecting the wastewater produced by the university campus facilities;
II. A pilot plant hall composed of three treatment lines (0.7 m^3/day treatment capacity): nutrients recovery, biopolymer production and water reuse;
III. A greenhouse facility and an irrigation system for the green areas of the campus to study the water-soil-plant interaction;
IV. An innovative Water & Resource Recovery laboratory (around 100 m2) is used to perform chemical-physical analyses, greenhouse gas emissions monitoring and environmental impact evaluation.

The main goal of the WRRF – UNIPA is the recovery of the following resources from wastewater treatment:

1. Nutrients (nitrogen and phosphorus): adsorption/desorption columns filled with biochar and zeolite are used to recover the nutrients in view of reusing them in agricultures as slow-release fertilizers.
2. Biopolymers for bioplastic materials production: An innovative pilot plant aimed to transform sewage sludge into biopolymers, such as polyhydroxyalkanoates, used as bioplastic precursors. This process reduces the harmful wastes that require an economically and energetically expensive disposal treatment while producing a sustainable alternative to conventional petroleum-based plastic materials.
3. Water and excess sludge reduction: According to the new law 2020/741 EU, water

suitable for reuse in agriculture is produced by applying innovative and advanced wastewater treatment technologies with a low carbon footprint, also enabling the minimization of excess sludge production.

4. Sewage sludge composting: obtained through a pilot plant aimed to produce compost for reuse in agriculture.

Results and conclusions

1. Water reuse and excess sludge minimization: the wastewater from the University residence and the canteen was collected in a pumping station and pumped to the resource recovery laboratory of the WRRF. The pilot plant hall of the WRRF produced treated water, which, through a pipeline, reached the storage tanks. The aim of the main treatment line, based on Conventional Activated Sludge (CAS) and Membrane Bioreactor (MBR) technologies, was to study the feasibility of sludge reduction through oxic-settling-anaerobic (OSA) implementation and produce water suitable for reuse.

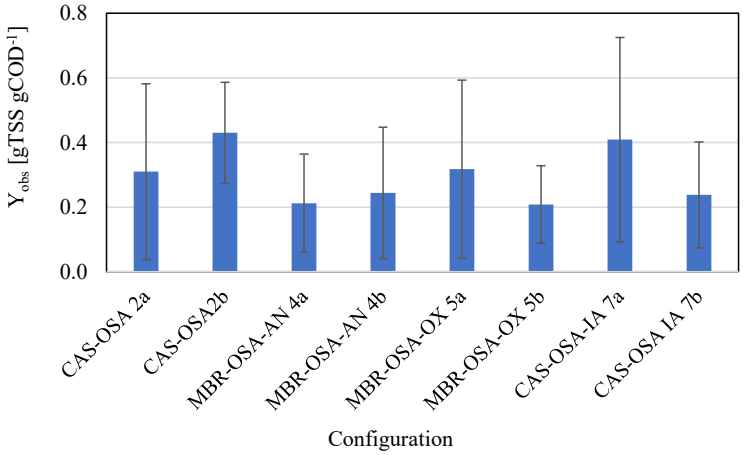

Figure 2. Different HRTs in the ASRR characterize average values of the yield coefficient for the Configurations.

The treated water irrigated green areas and an experimental field inside the University Campus. Several plant layouts were investigated, and different operational conditions were explored to assess the feasibility of excess sludge reduction. The average values of Yobs achieved under HRT variation in the ASRR for the different configurations studied are summarized in Figure 2. It was observed that the HRT increase in the ASRR compartment did not significantly influence sludge reduction. The findings suggest that, despite being effective, the OSA configuration can be significantly influenced by the plant's operational conditions, which mainly depend on raw wastewater characteristics. On the other hand, concerning plant removal efficiencies, it was observed that the increase of sludge retention under anaerobic conditions was detrimental regarding nitrification and nitrogen removal. The treated water was used to water crops at the greenhouse facility of the WRRF to study the water-soil-crop nexus. Figure 3 shows results related to tomato plant growth. Plants dry weight did not show significant differences among treatments, although plants irrigated with treated water showed a lower weight than those irrigated with tap water (Figure 3). TAP refers to control soil, irrigated with tap water; EB+EZ+TAP to soil amended with enriched biochar and enriched zeolite, irrigated with tap water; TWW to soil irrigated with TWW; EB+EZ+TWW to soil amended with enriched biochar and enriched zeolite, irrigated with TWW; NB+NZ+TWW to soil amended with natural biochar and natural zeolite, irrigated with treated wastewater.

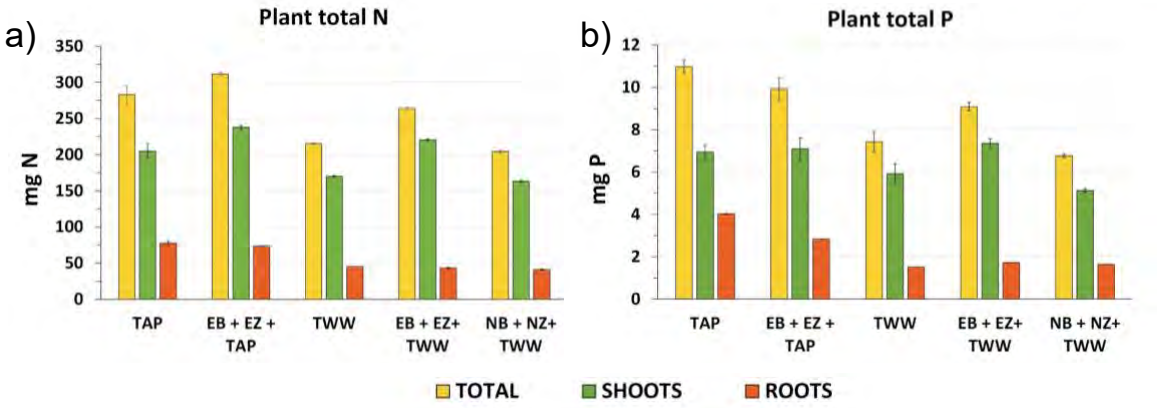

Figure 3. Total mass of (a) N and (b) P of plants at the end of experiments for the different tests.

Root weights of plants grown in soil irrigated with treated water and not amended with biochar and zeolite showed lower weight than all other treatments and were 39% lower than the control. Such results suggested a potential adverse effect of treated water on plant growth reasonably ascribed to the high electrical conductivity and soluble Na^+ concentration in treated water.

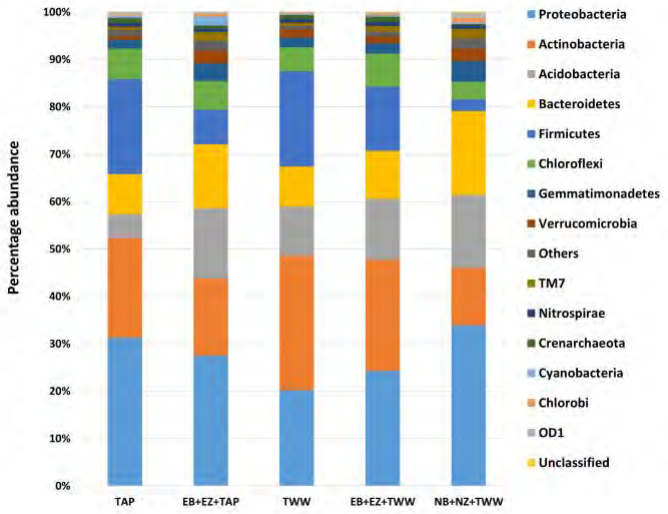

Figure 4. Relative abundance of the different bacterial strains at phyla level.

Metagenomic analysis was carried out to understand the relation between water-crop-soil better. Specifically, the composition of the prokaryotic microbiota in rhizospheric soil was analyzed using metataxonomic techniques. Next-generation sequencing (NGS) of DNA obtained after the amplification of the 16S rRNA gene using metagenomic DNA as a template was performed. This analysis led to bacterial identification and abundance (Figure 4). Different colours indicate different bacterial phyla.
It is notable that phyla involved in the nitrogen and phosphorus cycles having possible roles as PGPB according to scientific literature showed statistically significant variations in percentage abundance, as determined by one-way ANOVA with Bonferroni and Holm method. These phyla are Acidobacteria, Chloroflexi, Verrucomicrobia, and TM7, as depicted in Figure 4.

2. Nutrients recovery: The results of nutrient recovery experiments involving absorption columns filled with zeolite and biochar, used as an absorption medium to create slow-release fertilizers, are

shown in Figure 5. Specifically, Figure 5 reports the ammonium mass balance analysis by considering the inflow mass, outflow mass and the mass absorbed. The results indicated that an increase in flow rate resulted in more adsorbed ammonia into zeolite. The zeolites subjected to a flow rate of 2.36 L/h (C3 and C6) exhibited the highest adsorption, averaging 500-600 mg more NH_4^+ absorbed than other columns (Figure 2a). This might be attributed to the increased flow rate passing through the column, leading to more NH_4^+ encountering the zeolite per unit of time. Additionally, the zeolite with a diameter of 0.5-1 mm adsorbed approximately 60 mg more NH_4^+ in the case of column 3 (C3) compared to column 6 (C6), which utilized zeolite with a diameter of 2.5 mm (Figure 2b-c). The more excellent absorption by column 3 (C3) is attributed to the larger surface area of the zeolite, thus facilitating greater contact of the material with the flowing TWW in the column.

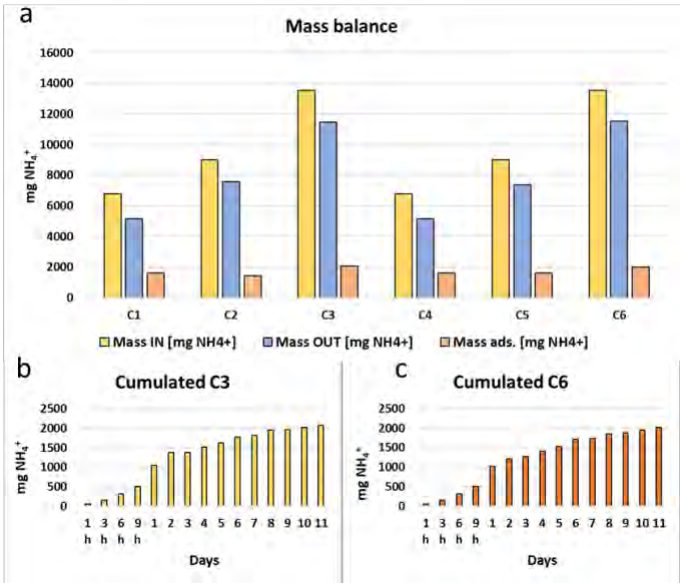

Figure 5. Mass balance was calculated for the six columns (a), and the cumulated mass of ammonium was calculated for C3 (b) and C6 (c).

3. Biopolymer production: as previously described, the PHA production pilot plant aimed to produce biopolymers from the water line's waste activated sludge (WAS). The pilot plant is based on the different process phases defined for the mixed microbial culture based PHA production [2]:

- ✓ WAS fermentation is controlled and stopped at the acidogenic step where volatile fatty acids (VFA) are produced.
- ✓ Biomass enrichment: microorganisms that produce the PHA are selected by feeding the VFA produced. The selection was performed on the abundance and deficiency (feast and famine) cycle of the substrate, which can be consumed aerobically (Aerobic Dynamic Feeding - ADF) or by mixing anoxic/aerobic conditions (Aerobic/Anoxic enrichment - AE/AN).
- ✓ PHA accumulation: once the PHA producers are selected, they are stressed to favour PHA production.

Implementing the ADF enrichment strategy increased the amount of PHA produced compared to the AE/AN enrichment, reaching up to 0.46 g PHA/g^{-1} VSS with a PHA yield of 0.65 gCODPHA/gCODVFA (Figure 6a) [3]. ADF also achieved the lowest carbon footprint (7.93 kg CO2/day), which was calculated by considering direct, indirect, and derived greenhouse gas (GHG) emissions (Figure 6b) [4]. The results

offer potential high-value insights towards a successful, efficient, environmentally friendly process application at the pilot and industrial levels. The WRRF within Palermo University can be a model for other systems' scale-up, providing valuable insights into achieving a sustainable resource recovery rate while limiting GHG emissions.

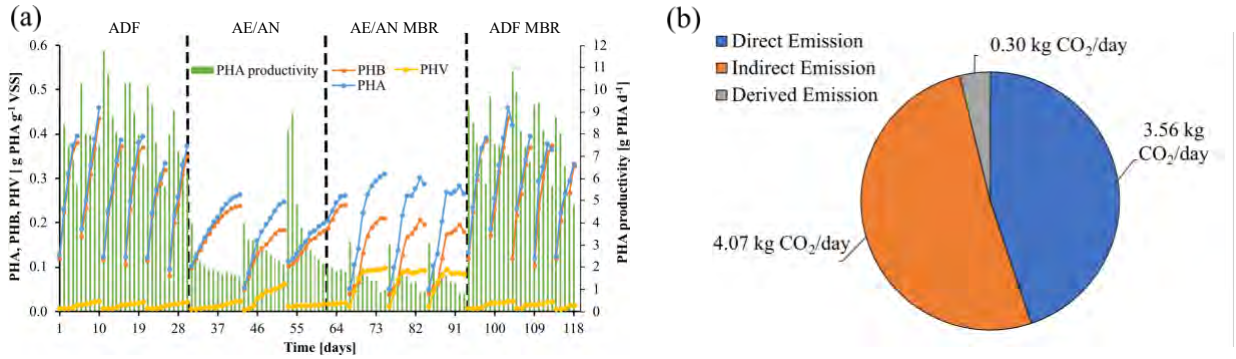

Figure 6. PHA accumulated for the four configurations studied (a) and the carbon footprint of the ADF strategy (b).

4. Sewage sludge composting: The waste activated sludge of the mainstream of the WRRF was used to produce compost in view of a circular economy perspective. The effects of compost and crops were studied by running different experiments. The pot experiment to test the effect of the three composts on sunflower growth lasted 81 days. According to the BBCH-scale [5], plants' phenological development stages are reported in Figure 7. The application of compost to the soil for sunflower cultivation affected both biomass partitioning and chemical plant parameters. Shoot dry weights were not significantly different among treatments. The increase of root and plant total biomass, but not of shoot biomass, following composts' addition suggests that they positively influenced plant growth and affected biomass partitioning of sunflower plants. Root biomass was the highest when composts with biochar and zeolite were applied. In general, the organic amendment stimulates plant growth because it provides favourable conditions for plant development in terms of soil structure improvement, water and nutrients retention and decreases soil density [6]. In this study, such a favourable condition may have been further improved in soil+CB and soil+CZ thanks to biochar and zeolite, two organic and inorganic soil amendments well-known for their positive effect on soil fertility [7,8].

Figure 7. Sequential growth stages of sunflower plant (*Helianthus annuus L.*) cultivated in soil amended with compost obtained by mixing pruning residues (woody and herbaceous) and sewage sludge (Soil + CC) with biochar (Soil+CB) or zeolite (Soil+CZ) as a bulking agent.

Acknowledgements

This work was funded by the project “Achieving wider uptake of water-smart solutions—WIDER UPTAKE” (grant agreement number: 869283) financed by the European Union’s Horizon 2020 Research and Innovation Programme, in which the last author of this paper, Giorgio Mannina, is the principal investigator for the University of Palermo.

References

[1] Pagilla KR. Pathways to water sector decarbonization, carbon capture and utilization. Pathways to water sect decarbonization. Carbon Capture Util 2022: 51–66. https://doi.org/10.2166/9781789061796.
[2] D. Puyol, D.J. Batstone, T. Hülsen, S. Astals, M. Peces, J.O. Krömer, Resource Recovery from Wastewater by Biological Technologies: Opportunities, Challenges, and Prospects, Front Microbiol 7 (2017). https://doi.org/10.3389/fmicb.2016.02106.
[3] G. Mannina, A. Mineo, Polyhydroxyalkanoate production from fermentation of domestic sewage sludge monitoring greenhouse gas emissions: A pilot plant case study at the WRRF of Palermo University (Italy), J Environ Manage 348 (2023) 119423. https://doi.org/10.1016/j.jenvman.2023.119423.
[4] G. Mannina, A. Mineo, A comprehensive comparison between two strategies to produce polyhydroxyalkanoates from domestic sewage sludge, J Clean Prod 468 (2024) 143052. https://doi.org/https://doi.org/10.1016/j.jclepro.2024.143052.
[5] Meier, U., 2001. Growth stages of mono-and dicotyledonous plants – BBCH monograph. Federal Biological Research Centre for Agriculture and Forestry. DOI: 10.5073/20180906-074619.
[6] Muscarella, S. M., Alduina, R., Badalucco, L., Capri, F. C., Di Leto, Y., Gallo, G., Laudicina, V. A., Paliaga, S., & Mannina, G. (2024). Water reuse of treated domestic wastewater in agriculture: Effects on tomato plants, soil nutrient availability and microbial community structure. Science of The Total Environment, 928, 172259. https://doi.org/10.1016/j.scitotenv.2024.172259
[7] Becker S., Thompson A., “The title of the paper” in Proceedings of Conference Title, where it took place, date of Ramesh, K., Reddy, D.D., 2011. Zeolites and their potential uses in agriculture. Advances in agronomy, 113, 219-241. DOI: 10.1016/B978-0-12-386473-4.00004-X.
[8] Kapoor, A., Sharma, R., Kumar, A., Sepehya, S., 2022. Biochar as a means to improve soil fertility and crop productivity: a review. J. Plant Nutr.45(15), 2380-2388. https://doi.org/10.1080/01904167.2022.2027980.

PARALLEL SESSION: B7

Flash

Emerging environmental risk and control

Characterization and control of particulate matter in ambient air: instruments, techniques and interferences.

Author(s): Lorenzo Raso[1], Vincenzo Marino[1], Maria Rosaria Della Rocca[2], Vincenzo Belgiorno[1], Vincenzo Naddeo[1], Tiziano Zarra[1]
[1] *Sanitary Environmental Engineering Division (SEED), Department of Civil Engineering, University of Salerno, via Giovanni Paolo II, Fisciano, SA, Italy*
[2] *Regione Campania, D.G. Difesa del Suolo e Ecosistema, UOD Sviluppo Sostenibile, Acustica, qualità dell'aria e radiazioni- criticità ambientali in rapporto alla salute umana, Via R. Bracco, 15/A - 80113 Napoli (NA), Italy*

Keyword(s): *air quality, gravimetric analysis, atmospheric pollution, sampling, EN12341:2023*

Abstract
Industrial activities and urban traffic are just a few of the many sources whose emissions contributes to worsening air quality and which represent an environmental risk factor for human health. Among the conventional gaseous pollutants, particulate matter has received special attention from the scientific community. Reduction and control measures, to be properly implemented and identified, require at first step the characterization, in order to provide reliable and repeatable measurements, minimizing sources and variables of uncertainty. The research aims to investigate the measurement uncertainties of the determination of the PM10 concentration according to the standard EN1234:2023.

1. Introduction

The demographic growth in urban centres corresponds to an increase in the demand for more infrastructure and service for citizen. Numerous research studies have been linked air quality deterioration and the expansion of city. The increase in vehicular traffic, land consumption, the opening of new industrial activities and the need to equip cities with sanitary and environmental treatments plants are some of the most relevant causes of air pollution [1]. Air pollution represents one of the most important challenges for our planet, that modern society needs to resolve. Currently, 91% of the global population still lives in areas with annual average of air pollutants concentrations above the maximum allowable levels [2]. The European Environment Agency (EEA) estimates that exposure to particulate matter is the thirteenth cause of human mortality globally. PM particles can be inhaled and deposited, inducing tissue damage and lung inflammation, impacting respiratory and cardiovascular health. [4] [3] Particulate matter represents the set of solid and liquid particles suspended in air. Its harmful and complex characteristics depend on the composition and size of the particles. [5] Commonly PM pollutant are classified based on their aerodynamic diameter and can by grouped into different categories (e.g.: PM10, PM2,5, PM1). Among these categories, PM10 represents the most used as indicator of air quality [6]. Their control is therefore a key aspect in order to avoid negative effects on the environment and for the exposed people. Strategies to control the concentration of this harmful pollutant in ambient air, must start from the characterization and measurement phase. The reference method for sampling and determination of the PM10 concentrations in ambient air is the gravimetric methods according to the official standard EN12341:2023. The gravimetric method is based on particle sampling on filters. The filters are appropriately weighed before and after the collection operations to determine the total mass of the selected particulate matter fraction. The mass is then used to calculate the concentration of PM10 in the air, relating it to the sampled air volume in the reference sampling time, equal to 24 hours. As it turns out, the determination of PM10 concentration in ambient air is complex because it includes a lot of actions that result in a potential significant level of measurement uncertainty. As far as the authors know, there has been no study on the identification of the variables and consequent integrated and exhaustive analysis on the measurement uncertainty linked to the determination of the concentration

of PM10 in ambient air. This study aims to fill the gap in the literature. The research presents and discusses the investigation and identification of the sources of uncertainty in the process of determining the concentration of PM10 in ambient air, with the aim of evaluating their contribution and proposing management and technical improvement actions, to guarantee the data reliability. The study is helpful for promoting accurate and reliable PM10 concentration measurement practices, providing control authorities and the scientific community with tools for a objective assessment of air quality and the associated risks of suspended particulate matter exposure.

2. Material and methods

2.1. Investigation methodology

To achieve the goal of the study a multicriterial methodology composed of four steps was identified. The first step of the methodology refers to the in depth study of the technical-scientific state of the art in order to to characterize and identify measurement chain of the determination of the PM10 concentration in ambient air through gravimetric analysis. The second step is based on the identification of the different sources and variables that can influence the accuracy of the measurement. In the third step, to investigate and quantify the contribution of the single identified variables of the sources at the different units of the measurement chain, exhaustive experimental activities were conducted. Finally, the quantification of uncertainty was carried out in the fourth step.

2.2. Experimental analysis

Figure 1 summarizes the measurement chain identified for determining the PM10 concentration. Five main phases have been identified.

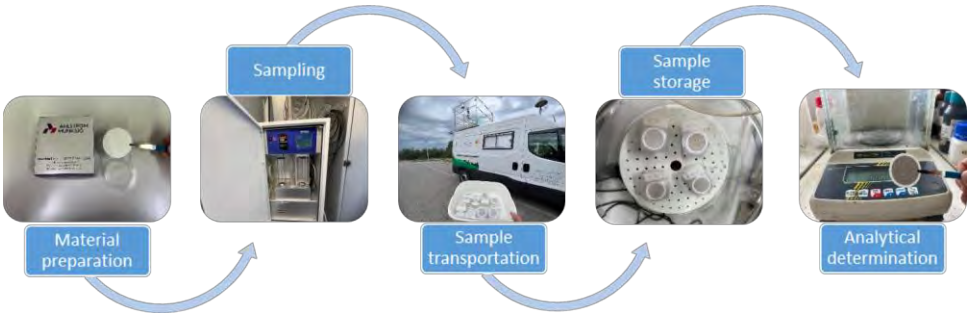

Fig. 1. Measurement chain for the determination of the PM10 concentration in ambient air

For each of the identified phases, environmental, instrumental and operational interferences have been identified. For each interference, the main variables were then searched and associated, such as: temperature, relative humidity and wind speed, for the environmental sources; filter material and withdrawal frequency and analysis of sampled filters, for the operational sources; different samplers and balance characteristics, for the instrumental sources. During the experimental activities multiple and simultaneously investigations were taken. In this research, the activities and results of the analysis of the variations in the frequency of sampling and analysis of the filters, following sampling, belonging to the sources of operational uncertainty are presented. Ten consecutive days of ambient air monitoring were conducted using two equal instruments, model Charlie Tecora (TCR Tecora srl, Italy), placed inside the *seedAIR* mobile Laboratory (Sanitary Environmental Engineering Division, Department of Civil Engineering, University of Salerno, Italy) located in a parking area inside the University Campus. Two different filter withdrawal frequencies were analysed: daily(D) and weekly (W). Glass fiber filter of the type Ahlstrom Munksjo, were used.

2.3. Uncertainty analysis

The quantification of the uncertainty was conducted through the comparative analysis of the different measurements, applying the formulas reported in equation 1.

$$m = \frac{C_D - C_W}{2}; \quad SD = \sqrt{\frac{(C_D - m)^2 + (C_W - m)^2}{2}}; \; S_{i\%} = \frac{|m - C_i|}{C_i} \qquad (1)$$

where: C_i (i = D, W) = PM10 concentrations determined with filters collected daily or weekly; m= mean value; SD = standard deviation; $S_{i\%}$ (i= D, W) = percent deviation determined with filters collected daily or weekly.

3. Results and discussion

Table 1 reports the concentration of PM10 collected and determined using daily withdrawal (C_D) and weekly withdrawal (C_W) filters respectively, overall, the experimental activities, together with the weight of PM deposited on the filter in 24 hours ($P_{PM,24h}$).

Table 1. Concentration of PM10

DAY	DAILY WITHDRAWAL		WEEKLY WITHDRAWAL	
	$P_{PM,24h}$ [g]	C_D[mg/m^3]	$P_{PM,24h}$ [g]	C_w[mg/m^3]
1	0,000207	3,75	0,000227	4,11
2	0,000323	5,86	0,000427	7,74
3	0,000490	8,89	0,000683	12,39
4	0,000600	10,88	0,000723	13,12
5	0,000867	15,71	0,001063	19,28
6	0,000670	12,15	0,000867	15,71
7	0,000750	13,60	0,001157	20,97
8	0,000527	9,55	0,000810	14,69
9	0,000377	6,83	0,000647	11,73
10	0,000673	12,21	0,000873	15,84

The results show that for the all investigations, the concentration of PM10 determined using filters withdrawal weekly (C_W) was higher than the same determined using filters withdrawal daily (C_D). The maximum PM10 concentration value, equal to 20,97 µg/m^3, was recorded using a filter collected weekly on day 7. While, the minimum PM10 concentration value, equal to 3,75 µg/m^3, was recorded using a filter collected daily on day 1.

Figure 2 shows the PM concentration values measured during the entire experimental analysis period, for the two investigated withdrawal frequencies, using a vertical bar diagram, also highlighting the standard deviation values. The result returns an average standard deviation value of 2.56 for the all investigations. While with reference to the different frequencies, it is possible to observe that the daily frequency has an average deviation of 18%, which is higher compared to that of weekly frequency, which is 13%.

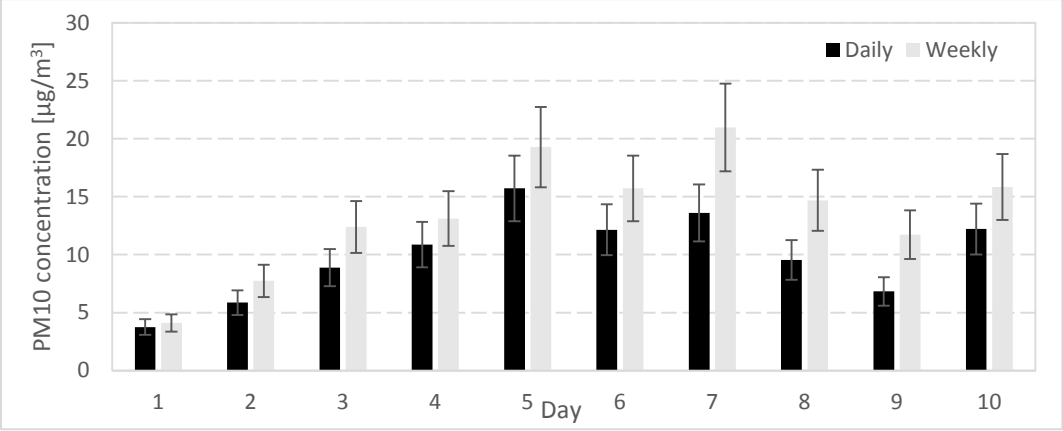

Figure 2. PM10 concentration and standard deviation values for the daily and weekly withdrawal investigation

4. Conclusions

To prevent and mitigate the negative impacts of air pollution, the monitoring of air quality is needed. Objective measurement methods and instruments are required in order to have reliable and repeatable data. The analyses conducted highlight the existence of uncertainties in the measurement of PM10, even when the indications outlined in the reference standard are followed. In detail, by comparing different filter withdrawal frequencies, after the sampling phase, it is observed that a weekly withdrawal could have greater deviation compared to the daily withdrawal. Assessing and reducing measurement uncertainty is crucial to guide mitigation actions aimed at better environmental protection and safeguarding public health.

5. Acknowledgement

This research is funded by the Agreement Program for the Protection of Air Quality MASE/Campania Region – Ricerca finanziata con i fondi dell'Accordo di Programma sulla Tutela della Qualità dell'aria MASE\Regione Campania.

6. References

[1] A. Fraiese, V. Naddeo, C. Uyguner Demirel, M. Prado, A. Cesaro, T. Zarra, H. Liu, V. Belgiorno, F. Ballesteros Jr, Removal of Emerging Contaminants in Wastewater by Sonolysis, Photocatalysis and Ozonation, Global Nest Journal 21 (2018). https://doi.org/10.30955/gnj.002625.

[2] I. Guseva Canu, P. Wild, T. Charreau, R. Freund, A. Toto, J. Pralong, K. Sakthithasan, Long-term exposure to PM10 and respiratory health among Parisian subway workers, International Journal of Hygiene and Environmental Health 256 (2024) 114316. https://doi.org/10.1016/j.ijheh.2023.114316.

[3] V. Naddeo, V. Belgiorno, T. Zarra, D. Scannapieco, Dynamic and embedded evaluation procedure for strategic environmental assessment, Land Use Policy 31 (2013) 605–612. https://doi.org/10.1016/j.landusepol.2012.09.007.

[4] N. Parasin, T. Amnuaylojaroen, S. Saokaew, Exposure to PM10, PM2.5, and NO2 and gross motor function in children: a systematic review and meta-analysis, Eur J Pediatr 182 (2023) 1495–1504. https://doi.org/10.1007/s00431-023-04834-

[5] Zarra, T., Naddeo, V., Giuliani, S., Belgiorno, V., 2010. Optimization of Field Inspection Method for Odour Impact Assessment. Chemical Engineering Transactions 23, 93–98. https://doi.org/10.3303/CET1123016.

[6] A. Barba-Lobo, I. Gutiérrez-Álvarez, J.A. Adame, J.P. Bolívar, A simple and precise methodology to determine particulate matter mass in atmospheric filters; validation and application cases, Environmental Research 214 (2022) 113817. https://doi.org/10.1016/j.envres.2022.113817.

Title: Pollutant reductions through Vegetative Environmental Buffers for livestock facilities: onsite surveys for two sites

Author(s): Luca Baccini*[1], Erin Cortus[2], Federico G.A. Vagliasindi[1]

[1] *Department of Civil Engineering and Architecture, University of Catania, Catania, Italy*
luca_baccini@outlook.it, federico.vagliasindi@unict.it
[2] *Department of Bioproducts and Biosystems Engineering, University of Minnesota – Twin Cities, Saint Paul, Minnesota (USA), ecortus@umn.edu*

Keyword(s): Vegetative Environmental Buffers, livestock facilities, monitoring, pollutant reductions

Abstract

Vegetative Environmental Buffers (VEBs) are vegetation systems that use trees and shrubs arranged in rows to redirect wind and reduce wind speeds, commonly planted around livestock facilities [1]. [2], [3], [4], and [5] were among the first authors who started investigating the use of VEBs as a control system for air pollution coming from livestock facilities. According to [1], VEB mitigation mechanisms are: i) dilution and dispersion, ii) filtration and trapping, iii) deposition, iv) adsorption into and onto plants' tissues. When the exhaust air intercepts the VEB a portion of it is displaced upward, some will move around, and part will flow through it. In the last 23 years several authors studied the effects of VEBs on improving ambient air quality surrounding livestock facilities. [2], [6], [7] reported high hydrogen sulphide (H_2S) concentration reductions ranging between 60-81%; [4], [8], [9], [10], [11], and [12] reported concentration data accounting for 46-92% ammonia (NH_3) reduction; [13], [14], [15], and [16] reported concentrations data accounting for 40-75% dust reduction; and finally [3], [5], and [17] reported odours and volatile organic compounds (VOCs) concentration reductions ranging between 6-93% and 38-69%, respectively. The variability in reduction could be attributed to the VEB and site characteristics (i.e., type of vegetation, VEB dimensions, weather, topography, source type, etc.), or the various monitoring methodologies used by the researchers. Indeed, there is no standardized survey protocol to evaluate the VEB efficiency for air pollution control. The lack of such protocols makes it difficult to compare publications' results. Considering the many parameters influencing the VEB monitoring, the data nowadays available to determine VEB effectiveness are not enough. Therefore, the aim of this research was to provide further data about VEB effects on pollutants gained through a monitoring campaign, as well as recommendations for future monitoring activities.

Downwind NH_3 and H_2S concentrations and Total Suspended Particles (TSP) count were recorded at two finishing pig barns with VEBs in Minnesota. The sites are referred to as Fairfax and Nicollet, characterized by mature and immature VEBs, respectively. Mature VEBs were fully developed in width and height and had no voids between plants making up the VEB. This configuration could increase the chances of pollutants interception compared to immature VEBs.The monitoring activity was done in September 2023 for two consecutive days at each site, when the wind blew from the south to the north (from the source to the northern VEB). The monitoring set-up consisted of three telescopic poles deployed as reported in Figure 1, and adjusted vertically to 2.3, 4.6 and 9.2 m above the ground every 20 minutes. This approach created a grid of nine sampling spots. Every day 2 to 4 sampling cycles lasting 1h each were done. At the top of each pole, air samples were drawn through Teflon tubing to 10 L Tedlar bags in vacuum boxes (for subsequent gas analyses) and superthane tubing for particulate analysis by a handheld Airborne Particle Counter (Aerotrak, Model 9306, TSI Incorporated, Shoreview, MN) at ground level. Only one particle counter was available, so it was transferred between Pole 1 and

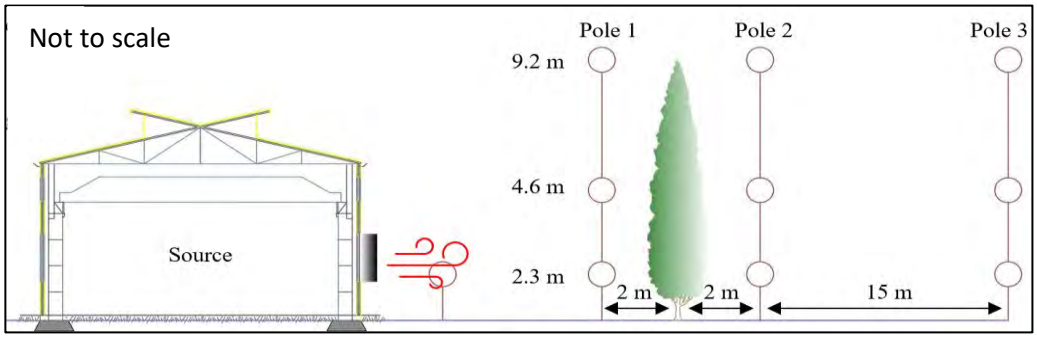

Figure 1. Representative scheme of the onsite set-up used for the monitoring activity.

Pole 2 at the end of each sampling cycle. At the source, two Single Point Monitor Gas Detectors (SPM) equipped with NH_3 and H_2S chemcassettes were used for gas sampling. The same SPMs were used to analyse the contents of the bag samples collected at the poles.

Statistical differences (p-values) were evaluated among the concentrations measured at each pole and among those recorded along each pole. The RStudio software (R version 4.3.2) was used. The appropriate statistical tests (e.g., One-Way ANOVA coupled with t-tests, Friedman test coupled with Wilcoxon test, …) were determined based on the normality and the homogeneity of each data groups. Calculated comparison p-values that fell below the 0.01 alpha value were considered significantly different. In this abstract it is shown whether the calculated p-values were above or below 0.01.

Figure 2 outlines that the highest concentration reductions occurred between source and Pole 1 for both gases, suggesting that natural attenuation occurred, most likely as dilution and deposition. In Fairfax between Pole 1 and Pole 2 was an 18 m distance; H_2S and NH_3 showed an average concentration reduction of 37% and 68% (p-value<0.01), respectively, while between Pole 2 and Pole 3 with 15 m distance the same pollutants' average concentrations varied between 16% and 17% (p-value>0.01), respectively. Therefore, along a similar distance a significantly high concentration reduction occurred right after the VEB, allowing speculating that the VEB could have played a key role in reducing the concentrations. In Nicollet, between Pole 1 and Pole 2 was a 30 m distance; H_2S and NH_3 showed an average concentration reduction of 68% and 74% (p-value<0.01), respectively; while between Pole 2 and Pole 3 with a 15m distance the same pollutants' average concentrations varied between 26% and 13% (p-value>0.01), respectively. Considering the distance between Pole1 and Pole 2 and the immature VEB, both the VEB effects and natural attenuation phenomena may have occurred.

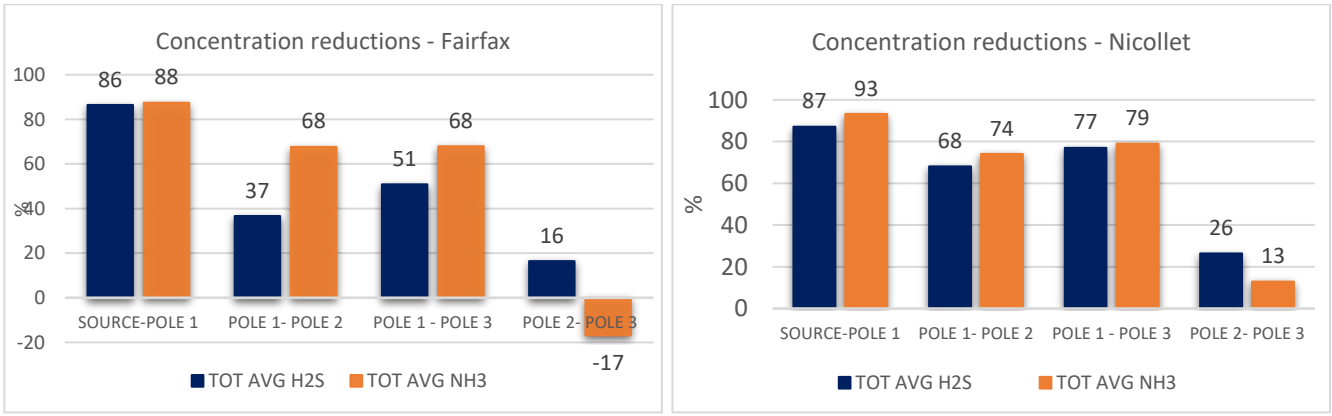

Figure 2. Average concentration reductions of NH_3 and H_2S recorded at Fairfax (left) and Nicollet (right).

Figure 3 shows two representative average gas concentration reductions calculated between each

couple of surveyed heights along each pole, at both sites. The results suggest that the average vertical concentration variations do not follow any trend and are frequently negative, probably because of the slight differences among each poles' concentrations. Indeed, calculated p-values were always above 0.01, suggesting no significant differences among the pollutants' concentrations along each pole.

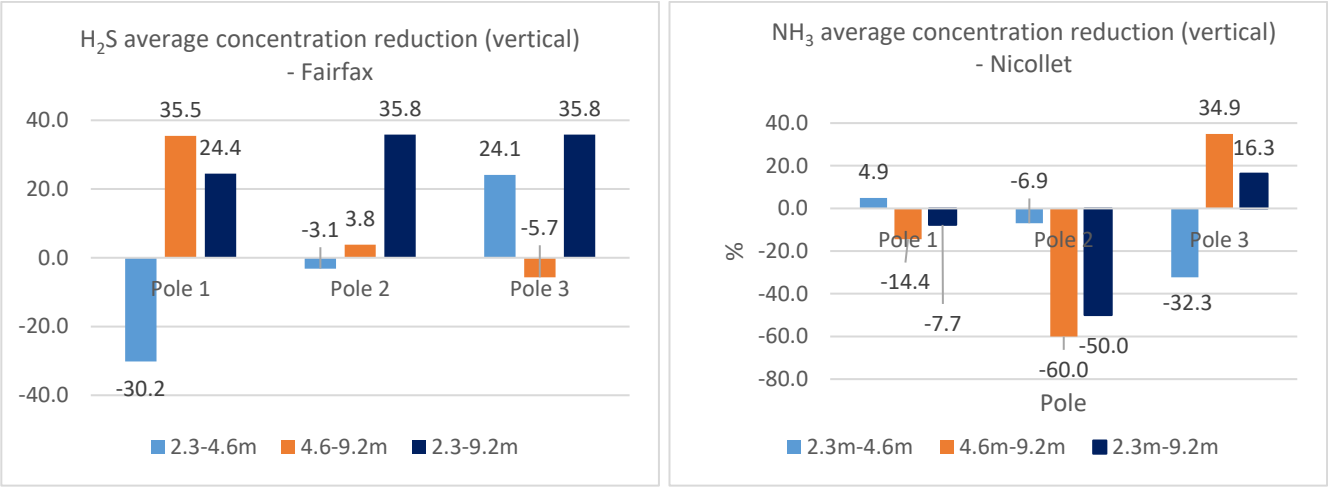

Figure 3. Average gas concentration variations along each pole.

TSP count did not show significant differences neither between Pole 1 and Pole 2 nor along each pole at both sites (p-values>0.01). TSP number reduction between Pole 1 and Pole 2 was 10% and 29%, while along each pole was -2.3% and -4.7% at the Fairfax and Nicollet sites, respectively. PM1 size accounted for almost the 98% of TSP, so probably such small particles were not intercepted by the VEBs or were easily resuspended once the wind hit the VEBs, entailing concentration increase on the VEBs' leeside. Finally, operating with just one particle counter, moved between Pole 1 and Pole 2 every hour, might have influenced the results obtained.

Based on the weaknesses and strengths of this study the following recommendations can be drawn for future monitoring activities:

- to deploy multiple sampling spots in the horizontal and vertical direction downwind the source and VEB could allow a better understanding of pollutant distributions,
- to add sampling spots on the vertical direction close to the source would allow evaluating the occurrence of buoyancy phenomena,
- to install instrumentation with data logging capabilities would allow remote control and real time monitoring,
- to continuously survey many close farms to make pollutant concentrations collected at different sites more comparable, since weather conditions could be considered similar.

From the results of this study the following conclusions can be summarized:

- average gas concentrations reduced more with the distance (between poles) than with the height (along the poles),
- average gas concentration reductions can be attributed both to natural attenuations, especially between the source and the VEB, and to the VEB itself. Though the outcomes obtained and the way the survey was shaped do not allow further speculation into the primary mode of mitigation,
- average particulate number did not diminish after the VEBs, most likely because of the dust's small size, that is, PM1.
- VEBs can be a useful and cost-effective pollutant control "technique", though further and appropriate monitoring activities need to be done to evaluate VEBs effectiveness.

Acknowledgement. The authors wish to acknowledge the cooperative farmers for making their farms available to do this research activity, and to the colleagues from University of Minnesota for the support during the monitoring campaigns. This study was financially supported by University of Minnesota.

References

[1] J. Tyndall e J. Colletti, «Mitigating swine odor with strategically designed shelterbelt systems: a review», Agroforest Syst, vol. 69, fasc. 1, pp. 45–65, gen. 2007, doi: 10.1007/s10457-006-9017-6.
[2] R. E. Nicolai, S. H. Pohl, R. Lefers, e A. Dittbenner, «Natural Windbreak Effect on Livestock Hydrogen Sulfide Reduction and Adapting an Odor Model to South Dakota Weather Conditions», 2004.
[3] J. Colletti, S. Hoff, J. Thompson, e J. Tyndall, «Vegetative Environmental Buffers to Mitigate Odor and Aerosol Pollutants Emitted from Poultry Production Sites», 2006.
[4] G. Malone, G. VanWicklen, S. Collier, D. Hansen, e C. Research, «Efficacy of Vegetative Environmental Buffers to Capture Emissions from Tunnel Ventilated Poultry Houses», 2006.
[5] X.-J. Lin, S. Barrington, J. Nicell, D. Choinière, e A. Vézina, «Influence of windbreaks on livestock odour dispersion plume in the field», Agriculture, Ecosystems & Environment, vol. 116, fasc. 3–4, pp. 263–272, set. 2006, doi: 10.1016/j.agee.2006.02.014.
[6] B. J. Hofer, «Effect of a shelterbelt on H_2S concentrations from swine barns», 2009.
[7] Y. Liu, Z. Liu, P. Murphy, R. Maghirang, e J. Derouchey, «Vegetative environmental buffers (VEBs) for mitigating multiple air pollutants emissions from a research swine barn», presented at American Society of Agricultural and Biological Engineers Annual International Meeting 2015, 2015, pp. 4422–4431.
[8] Adrizal et al., «The Potential for Plants to Trap Emissions from Farms with Laying Hens: 2. Ammonia and Dust», Journal of Applied Poultry Research, vol. 17, fasc. 3, pp. 398–411, ott. 2008, doi: 10.3382/japr.2007-00104.
[9] P. H. Patterson *et al.*, «The Potential for Plants to Trap Emissions from Farms with Laying Hens. 1. Ammonia», Journal of Applied Poultry Research, vol. 17, fasc. 1, pp. 54–63, mar. 2008, doi: 10.3382/japr.2007-00014.
[10] H. K. Burley *et al.*, «The potential of vegetative buffers to reduce dust and respiratory virus transmission from commercial poultry farms», Journal of Applied Poultry Research, vol. 20, fasc. 2, pp. 210–222, lug. 2011, doi: 10.3382/japr.2010-00298.
[11] K. Ro *et al.*, «Enhanced Dispersion and Removal of Ammonia Emitted from a Poultry House with a Vegetative Environmental Buffer», Agriculture, vol. 8, fasc. 4, p. 46, mar. 2018, doi: 10.3390/agriculture8040046.
[12] Z. Yang *et al.*, «Effectiveness and diurnal variations of vegetative environmental buffers (VEBs) for mitigating NH3 and PM emissions from poultry houses», Environmental Pollution, vol. 334, p. 122154, ott. 2023, doi: 10.1016/j.envpol.2023.122154.
[13] A. Adrizal *et al.*, «Vegetative buffers for fan emissions from poultry farms: 2. ammonia, dust and foliar nitrogen», Journal of Environmental Science and Health, Part B, vol. 43, fasc. 1, pp. 96–103, 2008, doi: 10.1080/03601230701735078.
[14] H. Guo, Y. Wang, e Y. Yuan, «Annual Variations of Odor Concentrations and Emissions from Swine Gestation, Farrowing, and Nursery Buildings», Journal of the Air & Waste Management Association, vol. 61, fasc. 12, pp. 1361–1368, dic. 2011, doi: 10.1080/10473289.2011.623636.
[15] G. Hernandez, S. Trabue, T. Sauer, R. Pfeiffer, e J. Tyndall, «Odor mitigation with tree buffers: Swine production case study», Agriculture, Ecosystems & Environment, vol. 149, pp. 154–163, mar. 2012, doi: 10.1016/j.agee.2011.12.002.
[16] W. B. Willis *et al.*, «Particulate capture efficiency of a vegetative environmental buffer surrounding an animal feeding operation», Agriculture, Ecosystems & Environment, vol. 240, pp. 101–108, mar. 2017, doi: 10.1016/j.agee.2017.02.006.
[17] D. B. Parker, G. W. Malone, e W. D. Walter, «Vegetative Environmental Buffers and Exhaust Fan Deflectors for Reducing Downwind Odor and VOCs from Tunnel-Ventilated Swine Barns», Transactions of the ASABE, vol. 55, fasc. 1, pp. 227–240, 2011, doi: 10.13031/2013.41250.

Continuous removal of VOCs and bacteria in a LED planar reactor: effect of operating parameters and kinetics modeling.

Mohamed Aziz Hajjaji[1,2*], Abdelkrim Bouzaza[2], Abdeltif Amrane[2], Anouar Hajjaji[1], Aymen Assadi[2]

[1]*Laboratoire de Photovoltaïque, Centre de Recherches et des Technologies de l'Energie, Technopole de Borj-Cédria, BP 95, 2050 Hammam-Lif, Tunisia*

[2]*Ecole Nationale Supérieure de Chimie de Rennes, University of Rennes, CNRS, ISCR—UMR6226, 35000 Rennes, France*

Keyword(s): Continuous reactor, Photocatalysis, Plasma DBD, VOCs, Bacteria.

Introduction

Indoor air quality is a paramount concern for human health, particularly due to the proliferation of volatile organic compounds (VOCs) and bacterial contaminants in enclosed environments. This study investigated the effect of different parameters, kinetics, and chemical degradation pathways of photocatalytic removal of Ethyl Acetate (EA) in a continuous reactor based on light-emitting-diode (LED). The VOC degradation was performed using TiO2 nanoparticle immobilized on a glass fiber tissue on a lab-scale continuous reactor. The performance of elaborated catalyst TiO2/GFT was studied by the control of different parameters such as EA inlet concentration (5, 10, 15, 20 mg/m3), flow rate (1, 2, 4 m3/h), relative humidity (5, 48, 92%), air gap (35, 50 mm) and LED intensities (16, 47,95 mW/m2). The exploitation of these parameters allows us to understand the performance of the catalyst, the different phenomena involved and the kinetics of the photocatalytic reaction [1].

Materials and methods

The study is carried out in a continuous reactor with a new configuration based on LED lighting as shown in **Figure 1**. The assembly allows air circulation inside a chamber containing two catalyst plates irradiated by LED lamps located in the middle. The LED lamps, emitting adjustable radiation which can reach a maximum power of 100 mW.cm-2, are installed in the middle so that the entire surface of the catalyst is illuminated with a perfect distribution.

The VOC is continuously injected into the air flow upstream of the reactor inlet using a syringe pump: this allows for a stable VOC concentration during the experiments.

Monitoring of the degradation of the pollutant is carried out using gas chromatography. The used device is a Focus gas chromatography (GC) device (oven: 30°C, injector: 180°C) with a flame ionization detector (FID).

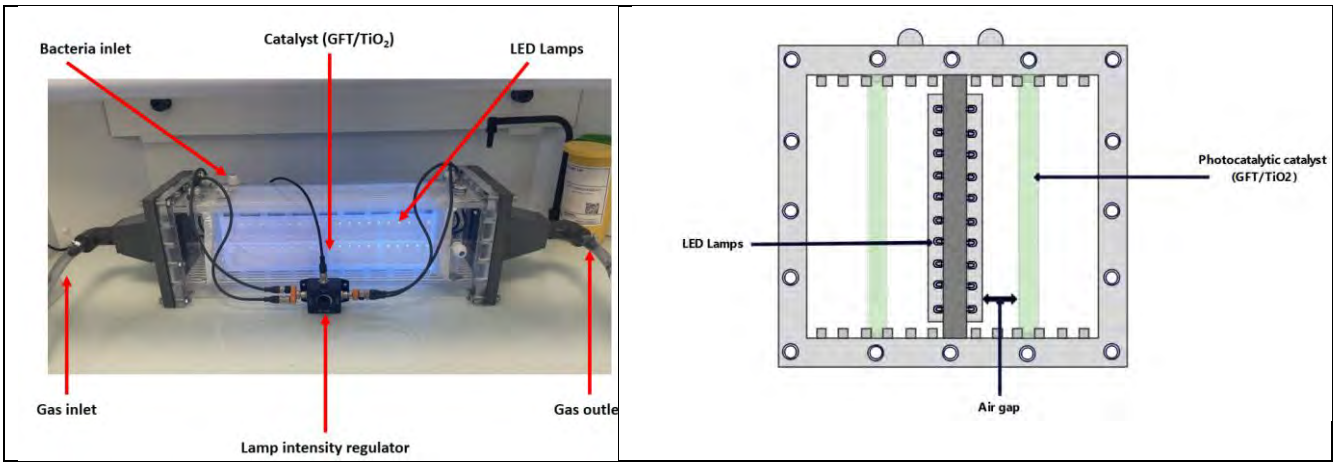

Figure 1. Schematic illustration of the continuous reactor: (a) planar reactor and (b) sectional drawing.

The variation of different parameters for monitoring the degradation of EA and E. Coli using photocatalysis and plasma DBD was summarized in **Table 1**:

Table 1. Experimental parameters

	Parameters	Values	Unit
Photocatalysis	EA inlet concentration	5, 10, 15, 20	mg/m^3
	Airflow rate	1, 2, 4	m^3/h
	Relative humidity	5, 48, 92	%
	Air gap	35, 50	mm
	LED intensity	16, 47,95	mW/m^2
Plasma DBD	Voltages	7.5, 12, 18	kV
	Frequency	50	Hz

Results and discussion

1. Catalyst characterization

SEM images displays the glass fibers with a diameter around 10 µm are disorderly dispersed on the tissue. It's clearly seen the deposit of Titanium dioxide nanoparticles onto the glass fibers. TiO_2 nanoparticles with a white colour are dispersed homogeneously on the tissue. Anatase TiO_2 nanoparticles with a spherical shape are perfectly observable in Figure 2. The nanoparticles size dispersion reveal different sizes for particles with a diameter between 50 and 160 nm.

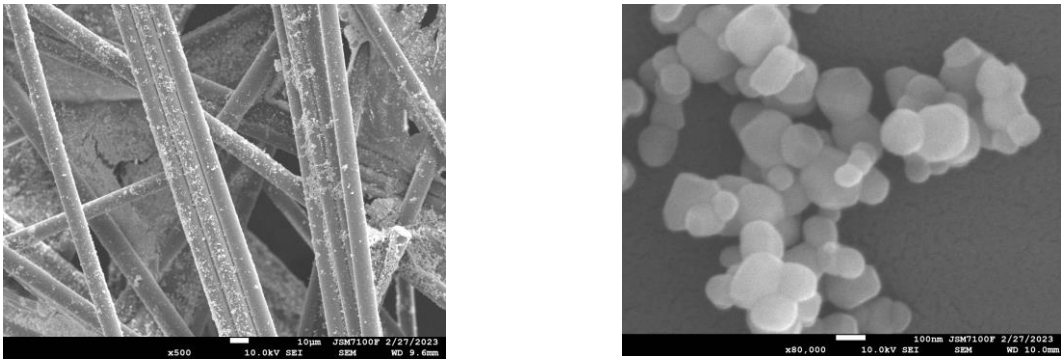

Figure 2. SEM images of catalyst GFT/TiO2 (a) magnification = 10 μm (b) magnification = 100 nm

2. Photocatalysis for EA removal

The airflow rate and the inlet concentration are key factors for the photodegradation of pollutants. In a constant airflow, we remark that increasing the initial concentration of the contaminant decreases the removal efficiency towards EA degradation. Generally, the photocatalytic degradation is more efficient for pollutants removal in low concentrations because of the limited number of active sites which affects the adsorption capacity of the catalyst.

Concerning the airflow rate effect, reducing the airflow improves the adsorption of pollutants on the surface of the catalyst by increasing the residence time. The increase in air flow reduces this residence time in the reactor, which affects the photocatalytic efficiency.

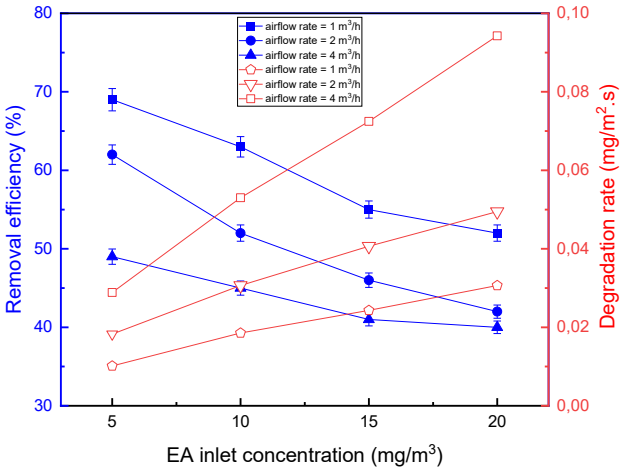

Figure 3. Variation of removal efficiency and the degradation rate with the flow rate at different values of Ethyl Acetate inlet concentration (RH = 48%, I = 95 mW/m^2, Air gap = 35 mm).

3. Photocatalysis for simultaneous removal (EA with bacteria)

In this part, a study on the simultaneous removal of pollutants was made. The purpose of this part is to ensure more realistic factors for indoor air that can contain several contaminants. **Figure 4** manifest a slight reduce in the removal efficiency of EA with the presence of bacteria, we deduce that the co-existence of E. coli disturb the photocatalytic degradation of VOC. This is explained by the degradation competition of pollutants molecules on the surface of catalyst. The photocatalytic degradation of VOCs and bacteria is driven by the generated ROS, which makes the photocatalytic efficiency limited by these oxidants species.

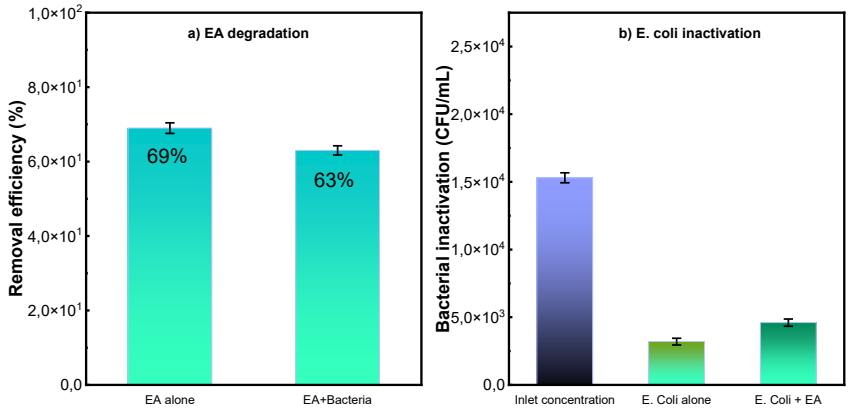

Figure 4: (a) variation of removal efficiency of EA alone and in presence of bacteria and (b) Bacterial inactivation of E. Coli alone and in presence of EA (Cin = 5 mg/m3 , Q = 1 m3/h).

Conclusions

In this present study, the photocatalytic degradation of Ethyl Acetate on a prepared TiO_2/GFT photocatalyst was performed. The results of the elaborated catalyst on the continuous reactor with a novel LED configuration seem better concerning previous works also the results of the simultaneous degradation of VOCs and bacteria are interesting. We successfully prepared a good and durable photocatalytic activity of the prepared catalyst toward VOCs and bacteria.

References

[1] A.A. Assadi, J. Palau, A. Bouzaza, D. Wolbert, Modeling of a continuous photocatalytic reactor for isovaleraldehyde oxidation: Effect of different operating parameters and chemical degradation pathway, Chem. Eng. Res. Des. 91 (2013) 1307–1316. https://doi.org/10.1016/j.cherd.2013.02.020.

[2] N. Belkessa, Y. Serhane, A. Bouzaza, L. Khezami, A.A. Assadi, Gaseous ethylbenzene removal by photocatalytic TiO2 nanoparticles immobilized on glass fiber tissue under real conditions: evaluation of reactive oxygen species contribution to the photocatalytic process, Environ. Sci. Pollut. Res. 30 (2022) 35745–35756. https://doi.org/10.1007/s11356-022-24636-8.

[3] M. Abidi, A. Hajjaji, A. Bouzaza, K. Trablesi, H. Makhlouf, S. Rtimi, A.A. Assadi, B. Bessais, Simultaneous removal of bacteria and volatile organic compounds on Cu2O-NPs decorated TiO2 nanotubes: Competition effect and kinetic studies, J. Photochem. Photobiol. A Chem. 400 (2020) 112722. https://doi.org/10.1016/j.jphotochem.2020.112722.

Title: Full-scale Application of a Combined In Situ Chemical Reduction and Enhanced Reductive Dechnlorination Technology for the treatment of an Aerobic Aquifer Impacted with Tetrachloromethane and Chloroform

Author(s): Alberto Leombruni*[1], Mike Mueller[2]

[1] *Evonik Operations GmbH, Hanau, Germany, alberto.leombruni@evonik.com*
[2] *Evonik Operations GmbH, Hanau, Germany, mike.mueller@evonik.com*

Keyword(s): **)**: Aquifer, Remediation, Injection, Tetrachloromethane, Chloroform, Hexavalent Chromium

Abstract

The site is in a highly industrialized area of northern Italy where groundwater is contaminated with tetrachloromethane (CT; >10 ppb), chloroform (CF; >10 ppb), hexavalent chromium and, to a lesser extent, PCE and TCE (<1 ppb). The applied technology deploys In Situ Chemical Reduction (ISCR) mechanisms along with Enhanced Reductive Dichlorination process for treatment of impacted groundwater [1]. It is comprised of two ingredients which are easily combined and diluted for injection: i) a controlled-release food-grade carbon in the form of lecithin (ELS™ Microemulsion), and ii) an organo-iron compound (EHC® Liquid Reagent Mix). The addition of organic carbon in a saturated zone is widely known to promote conventional enzymatic reductive dichlorination reactions [2]. As bacteria ferment the microemulsion component, they release a variety of volatile fatty acids (VFAs) such as lactic, propionic and butyric acids, which diffuse from the site of fermentation into the groundwater plume and serve as electron donors for other bacteria including dehalogenators [3]. Lecithin itself is primarily composed of phospholipids, with both hydrophilic and hydrophobic properties at different positions of the molecular structure. Further, phospholipids support remediation by providing essential nutrients (carbon, nitrogen, phosphorus) to bacteria [4]. Synergistically, the soluble organo-iron component is comprised of a ferrous iron (Fe^{2+}) that can form a variety of iron minerals (e.g. magnetite, pyrite) capable of reducing contaminants as they oxidize further to the ferric (Fe^{3+}) state via one electron transfer. The ferric ion can then be “recycled” back to ferrous, as long as other electrons from supplied carbon and indigenous carbon are available [5].

Standard Pump & Treat wells were located in the intervention areas and the respective downstream sectors, and were designed to accelerate the removal of various contaminants. However, the presence of active pumps near the technology injection zones could have compromised their effectiveness. This as a function of the increase in groundwater speed and potential removal of the injected emulsion. For this reason, a strategy was first modelled and implemented that adjusted the onsite well flow rates by reducing them to below threshold values, thus protecting effectiveness of the ERD treatment. Through use of mathematical modelling, optimal flow rates were defined to keep natural seepage velocity <300 m/year in the ERD treatment area, whilst still allowing P&T of groundwater in a wide downstream area, and effectively capturing flow from the injections area. Application of the remedial reagent was performed via direct injection through fixed Manchette tubes distributed in the source area. Less than 12 months after injection of the combined technology into the main source area and hot spots, concentrations of CT and CF contaminants were rapidly reduced up to 95% compared to pre-treatment

levels. Requisite remedial target values were reached in all main monitoring piezometers in the areas. Main field parameters in the treatment areas included: i) increase of Mn & Fe(II) in solution as anaerobic cometabolites, ii) decrease of DO (mg/L) and sulphate (mg/L) – competing electron acceptors pH stable in the neutral range, and iii) negative Redox around -150 mV.

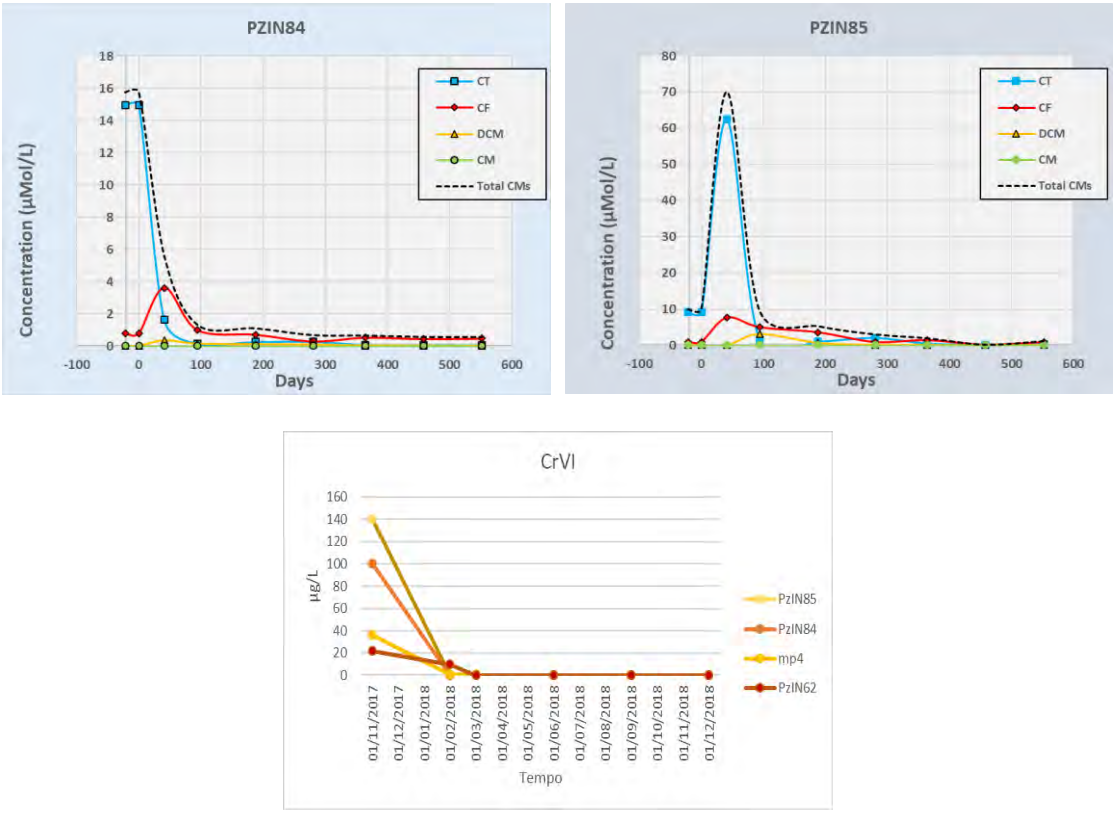

Figure 1. Post-application contaminant concentrations in the main monitoring points of the injection area

References

[1] Adamson DT, Parkin GF (1999) Biotransformation of mixtures of chlorinated aliphatic hydrocarbons by an acetate-grown methanogenic enrichment culture, Water Res 33: 1482–1494.

[2] Force, U. A. (2007) Protocol for in situ bioremediation of chlorinated solvents using edible oil.

[3] Harbaugh, A.W., Banta, E.R., Hill, M.C., and McDonald, M.G. (2000) MODFLOW-2000, The U.S. Geological Survey modular ground-water model—User guide to modularization concepts and the ground-water flow process, U.S. Geological Survey Open-File Report 00-92, 121 p.

[4] Lewis TA, Cortese MS, Sebat JL, Green TL, Lee CH, Crawford RL A Pseudomonas stutzeri gene cluster encoding the biosynthesis of the CCl4-dechlorination agent pyridine-2,6-bis (thiocarboxylic acid), Environ Microbiol. 2000 Aug;2(4):407-16.

[5] Penny C, Vuilleumier S, Bringel F. Microbial degradation of tetrachloromethane: mechanisms and perspectives for bioremediation, Departement Micro-organismes, Genomes, Environnement, Université de Strasbourg, UMR 7156 CNRS, Strasbourg, Fr.

Title: Remediation of sediments contaminated by microplastics: a first approach.

Author(s): Danilo Spasiano*[1], Maryam Soufizadeh[1,2], Raffaele Morello[1], Alberto Ferraro[1], Umberto Fratino[1]

[1] Dipartimento di Ingegneria Civile, Ambientale, del Territorio, Edile e di Chimica (DICATECh), Politecnico di Bari, via Orabona n°4, 70125, Bari (BA), Italy
[2] Scienze Agro Ambientali e Territoriali (DiSAAT), Università degli Studi di Bari "Aldo Moro", via Orabona n°4, 70125, Bari (BA), Italy

Keyword(s): treatment, flotation, density separation, sucrose,

Abstract

In recent years, many studies were focused on presence of microplastics (MPs) in marine sediments and the environmental risks associated with these pollutants [1-3]. Some of these studies were aimed to the quantification of MPs in the sediments through density separation using saturated solutions of inorganic salts, such as $ZnCl_2$, NaCl, and NaI [4-6]. Even if these practices are useful as analytical method for the estimation of MPs contamination, they cannot be used for the treatment contaminated sediments due to the costs associated with the management of the spent solutions. Consequently, an innovative treatment of MPs contaminated sediments, based on the adoption of a concentrated sucrose solution is proposed in this study. Indeed, since a saturated sucrose solution could reach a density of 1.4 g/cm^3, the flotation of many plastic materials, such as PP, HDPE, and PLA, occurs after the suspension of MPs contaminated sediments (figure 1). In addition, the spent sucrose solutions discarded from the separation tank could be diluted and used as feedstock for the biological production of polyhydroxyalkanoates (PHA) [7-9].
As reported in figure 1, the separation treatment could take place in a settlement-like tank eventually equipped with two hoppers: the first for the collection of sands and the second for the separate collection of slowly settling solids, supposedly rich in high density MPs. At the same time, the floating material, rich in low density MPs could be collected with a conventional skimmer.
As regard the dimension of the tank, it could be designed with an overflow rate (OFR) assumed to be equal to the floating velocity of a MP characterized by 1.0 mm diameter and a density of 1.3 g/cm^3. In laminar flow condition, this particle particle is characterized by a settling/flotation velocity (v_p) that can be expressed by the Stokes's law [10]:

$$v_p = \frac{g \cdot (\rho_p - \rho_s) \cdot d^2}{18 \cdot \mu} \qquad \text{(Eq.1)}$$

where g is gravity acceleration, ρ_p and ρ_s are the density of the particle and of the solution, respectively, d is the diameter of the particle, and μ is the viscosity of the solution.

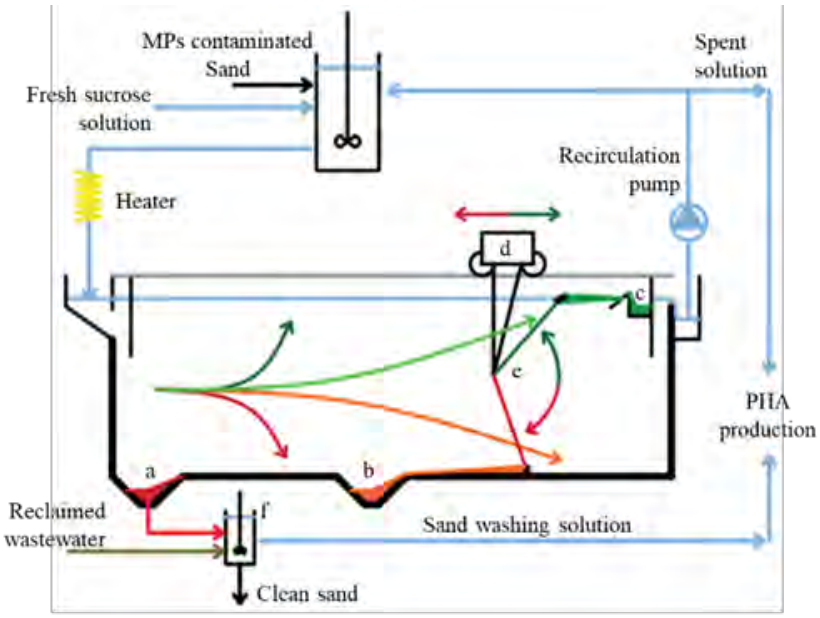

Figure 1. Separation process for the removal of MPs from contaminated sediments. a) hopper for the collection of rapidly settling solids; b) hopper for the collection of slowly settling solids; c) skimmer for the collection of floating solids; d) scraper bridge; e) scraper for handling suspended material (when raised and the cart moves to the right) and settled material (when lowered and the cart moves to the left); f) compartment for the sand washing.

Referring to an aqueous sucrose solution, both ρ_s and μ are dependent on temperature (T) and sucrose concentration. In particular, Barber [11] reported the following expression of the ρ_s as a function of the T (expressed in °C) and the mole fraction of sucrose (y):

$$\rho_{s\,T,y}\left[\frac{kg}{m^3}\right] = \frac{yMW_s + (1-y)MW_w}{y(C_1 + C_2T + C_3T^2) + (1-y)(A_1 + A_2T + A_3T^2)} \cdot 10^3 \qquad \text{(Eq.2)}$$

where MW_s and MW_w are the molecular weights of sucrose and water, respectively, and C_1, C_2, C_3, A_1, A_2, and A_3 are constants, which values are reported in table 2.

Table 2. Values of the constant used for the evaluation of the density of the sucrose aqueous solution at varying the temperature and the sucrose concentration.

	Values		
A_1	18.027525	C_1	212.57059
A_2	$4.8318329 \cdot 10^{-4}$	C_2	0.13371672
A_3	$7.7830857 \cdot 10^{-5}$	C_3	$-2.9276449 \cdot 10^{-4}$

The viscosity of an aqueous sucrose solution could be described as function of T sucrose and the sucrose weight fraction (Y) [12]:

$$\mu_{s\,T,Y}\left[\frac{kg}{m \cdot s}\right] = \mu_{s_{293\,K,Y}} \cdot \exp\left[\frac{E_a}{R}\left(\frac{1}{T} - \frac{1}{293.15\,K}\right)\right] \cdot 10^{-3} \qquad \text{(Eq.3)}$$

were R is the gas constant, $\mu_{s_{293\,K,Y}}$ is the fluid viscosity at 20 °C (293.15 K), and E_a is the activation energy, which may be been expressed as function of the solute volumetric molar fraction (φ):

$$E_a\left[\frac{J}{mol}\right] = E_{a0}\frac{(1+0.5\varphi)}{(1-\varphi)} \quad \text{(Eq.4)}$$

being E_{a0} an adjustment constant equal to $15.08 \cdot 10^3$ J/mol. The φ was estimated as function of the solute free volumetric fraction (φ_{sf}) (Eq.5), which, in turn, was calculated as a function of Y (Eq.6):

$$\varphi = \frac{\varphi_{sf}}{(1+\varphi_{sf})} \quad \text{(Eq.5)}$$

$$\varphi_{sf} = \frac{Y}{(1-Y)}\frac{MW_w}{MW_s}\frac{V_s}{V_w} \quad \text{(Eq.6)}$$

where V_s and V_w are the Van der Waals molar volumes of sucrose and water, respectively.
In this way, it has been possible to evaluate the temperature and sucrose concentration that maximize the floating velocity of the target particle. Indeed, as reported in figure 2, a 70%$_{w/w}$ sucrose aqueous solution maintained at 50 °C guarantees a floating velocity of 1 m/h, which correspond to an overflow rate generally adopted for secondary settlement tanks.

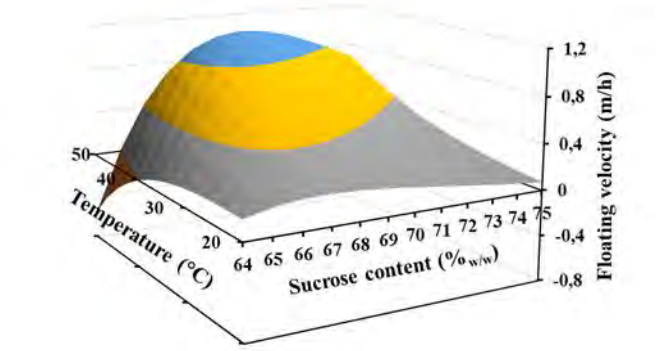

Figure 2. Floating velocities of a 1.0 mm spherical MPs with fixed density of 1.3 g/cm3 at different sucrose solution concentration and temperature.

To this purpose, some preliminary experimental runs were carried out to evaluate the effectiveness of the proposed treatment. All the experiments were carried out with commercial silica sand (Bassanetti, Italy), characterized by particle size in the range 0.3-1.0 mm, and PP, HDPE, PLA, and PVC. The PLA-MPs were obtained from the cutting of a PLA Ingeo 850 filament (Eolas Print, Spain) with a diameter of 1.75 mm. The other MPs were obtained from wastes and were reduced to 1-2 mm size with a cutter.
In each test, the sand involved was artificially contaminated by MPs at a concentration of 8 particles (2 for each MPs typology) per 1.0 g of sand (Table 3). Then, the separation experiments were carried out in 50 mL conical test tubes by mixing through a vortex different amount of MPs contaminated sand with 40 mL of 70% sucrose solution in order to investigate the effect of various S/L ration on the process effectiveness. After the mixing, the suspension was left still for 2 h at 50 °C.
In the following experimental phase, density separation tests were performed with different solid to liquid (S/L) ratio to further identify proper amount sand load for an efficient treatment. Results, reported in figure 3, showed that all the HDPE and PLA particles floated regardless of the sand amount. This outcome was expected since the densities values of HDPE and PLA were both lower than the 70% sucrose solution one. Instead for PP, high sand concentration values affected the particles floating and recoveries rate of 96% and 90% were observed for tests at S/L equal to 100 and 125 kg/m^3, respectively. In this case, it is possible that the higher S/L ratio values negatively affected the PP separation due to the triggering of a hindered sedimentation phenomenon causing the MP particles entrapment within the sand matrix and consequent limiting the flotation process. It is also worth highlighting the behavior of some PVC particles for which flotation was observed instead of settlement phenomena. In particular, highest number of PCV particles was found on the sucrose solution surface for the test carried out at

S/L equal to 75 kg/m^3. For this experiment, considering its replicates, the PVC particles floating were between 4 and 5 out of 6 for a mean separation percentage of 77.8%. Nonetheless, it is also noticeable that lowest results reproducibility was displayed for PVC in different density separation tests. Probably, the presence of air bubble retained on the PVC surface could significantly affect the separation process resulting in significant differences of the results obtained from each replicate.

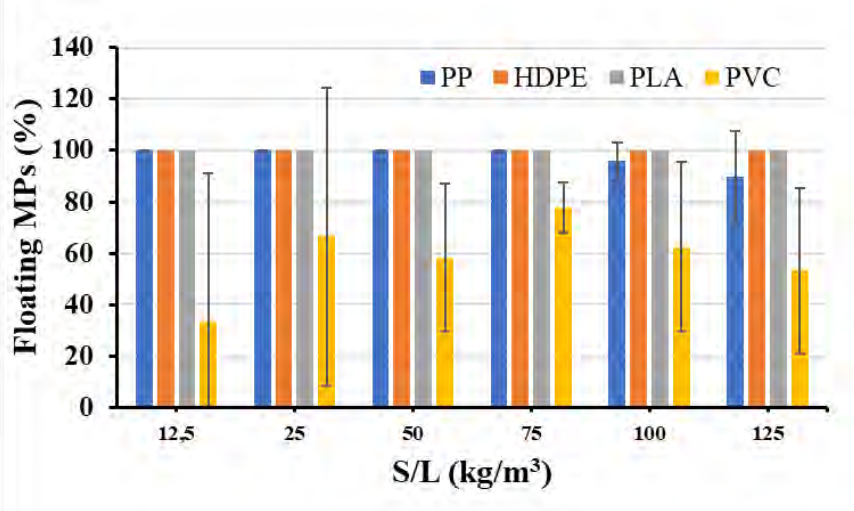

Figure 3. Effect of the S/L ratio on the separation efficiency of tested MPs in a 70% sucrose aqueous solution at 50 °C.

References

[1] Harris, P. T. (2020). The fate of microplastic in marine sedimentary environments: a review and synthesis. Marine pollution bulletin, 158, 111398.
[2] Phuong, N. N., Fauvelle, V., Grenz, C., Ourgaud, M., Schmidt, N., Strady, E., & Sempéré, R. (2021). Highlights from a review of microplastics in marine sediments. Science of the Total Environment, 777, 146225.
[3] Perumal, K., & Muthuramalingam, S. (2022). Global sources, abundance, size, and distribution of microplastics in marine sediments-A critical review. Estuarine, Coastal and Shelf Science, 264, 107702.
[4] Bäuerlein, P. S., Erich, M. W., van Loon, W. M., Mintenig, S. M., & Koelmans, A. A. (2023). A monitoring and data analysis method for microplastics in marine sediments. Marine Environmental Research, 183, 105804.
[5] Cashman, M. A., Ho, K. T., Boving, T. B., Russo, S., Robinson, S., & Burgess, R. M. (2020). Comparison of microplastic isolation and extraction procedures from marine sediments. Marine pollution bulletin, 159, 111507.
[6] Mattsson, K., Ekstrand, E., Granberg, M., Hassellöv, M., & Magnusson, K. (2022). Comparison of pre-treatment methods and heavy density liquids to optimize microplastic extraction from natural marine sediments. Scientific Reports, 12(1), 15459.
[7] Sohn, Y. J., Kim, H. T., Baritugo, K. A., Song, H. M., Ryu, M. H., Kang, K. H., ... & Park, S. J. (2020). Biosynthesis of polyhydroxyalkanoates from sucrose by metabolically engineered Escherichia coli strains. International journal of biological macromolecules, 149, 593-599.
[8] Geethu, M., Chandrashekar, H. R., & Divyashree, M. S. (2021). Statistical optimisation of polyhydroxyalkanoate production in Bacillus endophyticus using sucrose as sole source of carbon. Archives of Microbiology, 203, 5993-6005.
[9] Wang, J., Liu, S., Huang, J., Cui, R., Xu, Y., & Song, Z. (2023). Genetic engineering strategies for sustainable polyhydroxyalkanoate (PHA) production from carbon-rich wastes. Environmental technology & innovation, 30, 103069.
[10] Metcalf, E., Eddy, S. (1991). Wastewater engineering: treatment, disposal, and reuse, 3rd ed., McGraw-Hill, New York.
[11] Barber, E. J. (1966). Calculation of density and viscosity of sucrose solutions as a function of concentration and temperature. National Cancer Institute Monograph, 21, 219-239.
[12] Telis, V. R. N., Telis-Romero, J., Mazzotti, H. B., & Gabas, A. L. (2007). Viscosity of aqueous carbohydrate solutions at different temperatures and concentrations. International Journal of food properties, 10(1), 185-195.

Title: Towards integrated plant-surface-subsurface hydrological modelling of bioreactive solute transport

Author(s): Daniele la Cecilia*[1], Claire Lauvernet[2], Claudio Paniconi[3], Matteo Camporese[4]

[1] Department of Civil, Environmental and Architectural Engineering, University of Padua, Padua, Italy, daniele.lacecilia@unipd.it
[2] UR RiverLy, INRAE, Lyon, France, claire.lauvernet@inrae.fr
[3] INRS-ETE, Université du Québec, Quebec City, Canada, claudio.paniconi@inrs.ca
[4] Department of Civil, Environmental and Architectural Engineering, University of Padua, Padua, Italy, matteo.camporese@unipd.it

Keyword(s): CATHY, bioreactive transport, Michaelis-Menten-Monod, soil-plant continuum

Abstract

The number of synthetic chemicals found in terrestrial and aquatic ecosystems is increasing given that about 300,000 such chemicals are approved for urban, industrial and agricultural applications. In the environment, these chemicals can biodegrade into their corresponding transformation products. Microbial metabolic strategies and the occurrence of promoting/inhibiting substances affect biodegradation effectiveness. In addition, there is a growing interest in the exploitation of nature-based solutions, like phytoremediation, to improve soil and water quality given that vegetation effortlessly contributes to the removal of known - and unknown - contaminants through absorption and degradation. Water flow and solute bioreactive transport models are nowadays crucial tools to evaluate environmental remediation opportunities at large spatial scales. However, these models typically (1) enforce first-order degradation kinetics, thus neglecting microbial metabolic strategies, which can be described by means of Michaelis-Menten-Monod (MMM) kinetics and (2) disregard the mechanistic understanding of the transformation of dissolved chemicals within the plant system.

As part of the European Union-funded projects REWATERING (MSCA-PF) and AQUIGROW (Water4All), we are (1) implementing the MMM framework for modelling substrate consumption, (2) coupling a dynamic, mechanistic, multi-compartment plant model describing bioreactive transport processes among and within roots, stem, leaves and fruits and (3) accounting for any number of biochemical species within an integrated, surface-subsurface, flow-transport hydrological model. The hydrological model (CATchment HYdrology or CATHY) already simulates water fluxes accounting for the interactions among surface water, groundwater and vegetation, including the vegetation stress response based on root zone abiotic conditions. The coupled model will serve in this study to explore the effectiveness of bio- and phyto-remediation in relation with local conditions by means of synthetic scenarios.

Introduction

The large use of synthetic chemical substances in urban, industrial and agricultural applications may expose terrestrial and aquatic ecosystems to hazardous chemical concentration levels. These chemicals, and their transformation products should the parent compounds undergo biochemical reactions, are transferred within and across environmental spheres. While there is a large consensus on the fundamental processes that govern contaminant transport, the mathematical representation of

bioreactive processes splits the scientific community in two major groups. Most modellers assume first order degradation rates. However, first order decay neglects the natural processes underlying biochemical reactions [1]. A more suitable framework would assume Michaelis-Menten-Monod (MMM) equations [1,2,3], as shown in [4], which are widely used in wastewater engineering but only little in other disciplines such as catchment scale contaminant hydrology. The MMM framework allows for describing the microbial strategies to degrade contaminants (EQs 1 and 2):

$$\frac{dS}{dt} = -\frac{\mu B}{Y}\frac{S}{S+K} \quad \text{EQ 1}$$

$$\frac{dB}{dt} = -Y\frac{dS}{dt} - \delta B \quad \text{EQ 2}$$

where S is the concentration (mol/l) of a compound, t is time (s), μ is the reaction rate constant (1/s), B is the wet microbial biomass concentration (mg/l), Y is the yield coefficient (mg/mol) and K is the half saturation constant (mol/l). One type of microorganism (μ-strategists) has evolved to rapidly consume a suitable substrate present at high concentrations. The other type of microorganism (K-strategists) has adapted to consume substrates present at low concentrations faster than μ-strategists. Therefore, the complete degradation of such chemicals depends on the presence in-situ of both the μ- and K-strategists, as was numerically simulated for the biodegradation in a soil column of the herbicide glyphosate [5].

While this is not often the case, models that take into account feedback loops among chemicals can mechanistically explain why some reactions are fast under certain conditions. These feedbacks are well understood in remediation, whereby carbon sources are sometimes added to co-metabolize a persistent contaminant or increase the biomass of microorganisms able to degrade the contaminant (biostimulation). Moreover, selected bacteria can be inoculated to make a reaction happen or proceed faster (bioaugmentation). For example, in the presence of both the microbial functional groups able to biodegrade the herbicide glyphosate, additional carbon sources can speed up one biodegradation pathway as well as biodegrade the persistent transformation product AMPA [5]. Conversely, some reactions may be slowed down in the presence of inhibitory compounds. Using again glyphosate as the example, the pathway leading to the biodegradation of glyphosate along the cleaner pathway – not producing AMPA – as well as the AMPA biodegradation pathway are inhibited by inorganic phosphate.

In addition to soil microorganism-mediated biodegradation, plants may absorb and degrade contaminants. Multi-compartment (roots, xylem, leaves, fruits) dynamic plant uptake models, which account for differentiated multiple metabolization pathways in the plant continuum, have been used to simulate the fate of plant protection products after uptake [6]. This phenomenon was shown to bring about advantages and disadvantages. On the plus side, contaminants are removed from the soil and water matrix [7]. On the minus side, a mass fraction of the contaminant may remain in the plant's compartments susceptible to re-entering the environment. For example, contaminants in the plant's edible parts would pose a risk to humans and any other feeding organism and pollinators. Moreover, contaminated leaves along streams may fall in the water and become the source of food for invertebrates, eventually causing a threat to these organisms and the food chain [8].

Considering the importance of the MMM framework and the dynamic plant models for the more robust simulation of contaminant fate in the soil-water-plant continuum, we will implement such coupling within the widely used CATchment HYdrology (CATHY) model [9]. We will prepare synthetic scenarios that

contribute to a better understanding of optimization and trade-offs of nature based solutions designed for environmental bioremediation.

Materials and Methods

The CATHY model is a physics-based integrated surface-subsurface flow and transport hydrological model (ISSHM) [9]. It solves the interactions among surface water, groundwater and vegetation from the plot to the catchment scale at any required temporal scale (seconds to decades). Water flow on the surface is described by the diffusion wave approximation of the shallow water equations and solved with an explicit finite difference scheme. The subsurface flow is described according to the 3D Richards equation for variably saturated porous media and solved with a finite element method. Finally, the CATHY model may reduce the prescribed actual EvapoTranspiration (ETa) based on the vegetation response to the water stress function according to the Feddes approach [10]. Currently, the kinetics solver can simulate the first-order degradation of one solute per simulation. We will thus add the possibility to solve the kinetics with the classical MMM framework. At the same time, we will expand the MMM framework to include any number of chemical and biological species, competitive and inhibitory terms, as proposed in EQs 3 and 4:

$$\frac{dS_i}{dt} = -\frac{\mu_i B_j}{Y_i} \prod_l \frac{S_l}{S_l + K_l\left(1 + \sum_m \frac{S_m}{K_m}\right)} \prod_n \frac{K_n}{S_n + K_n} \qquad \text{EQ 3}$$

$$\frac{dB_j}{dt} = -\sum_i Y_i \frac{dS_i}{dt} - \delta_j B_j \qquad \text{EQ 4}$$

where the subscripts *i*, *j*, *l*, *m* and *n* respectively refer to the *i*-th chemical species, *j*-th biological species, *l*-th (co-)metabolic term, *m*-th competitive term and *n*-th inhibitory term.

The multi-compartment (roots, xylem, leaves, fruits) dynamic plant uptake model proposed by [7] after [6], which accounts for differentiated multiple metabolization pathways in the plant continuum, will be used to represent the fate of neutral compounds in the plant system. Under this condition, chemicals are taken up by the roots with the transpiration flow and undergo advection-diffusion-sorption to the stem, leaves and fruits. Chemicals can volatilize from/deposit to the stem, leaves, and fruits. Dilution may be included in all compartments following plant growth. Compounds undergo phytodegradation in all compartments according to first-order or MMM kinetics.

Two synthetic scenarios are planned to explore the knowledge that can be achieved upon integrating advanced hydrological models and comprehensive plant uptake models:

1) The fate of a systemic contaminant that undergoes advection-sorption-degradation from a contaminated soil to a nearby stream passing through a vegetated buffer strip. Our interest is to reveal to what extent contaminants transported in the subsurface are taken up by plants and returned to the nearby streams through the loss of leaves. This scenario will consider a hypothetical parcel of 100 m × 100 m × 5 m (length×width×depth) decreasing in altitude along its width from an upland crop to a lowland buffer strip, before a stream to prevent its contamination from the upland runoff. We will generate a pulse of contaminant in the topsoil of the crop at the beginning of the year and expose it to given atmospheric conditions taken from a time-series of the Veneto Region to have realistic boundary conditions for one year to capture seasonality effects.

2) The potential of vegetation to reduce the load of naturally present inhibitory compounds on the effectiveness of Soil Aquifer Treatment for artificial groundwater aquifer recharge. Particularly for the reclamation of agricultural runoff, it is important to remove inorganic phosphate from water because it is a powerful biodegradation inhibitor of organophosphorus compounds [11] like glyphosate and its transformation product AMPA. This scenario will simulate a control volume (100 m × 100 m × 5 m) of a hypothetical gently sloped unconfined permeable aquifer. The water source will contain solutes found after wastewater treatment. The water source will be intermittently infiltrated through an infiltration basin.

Expected results

In this work, we will couple a catchment scale flow-transport hydrological model with a dynamic plant uptake model. The comprehensive modelling along the soil-plant continuum is foreseen to be extremely beneficial to reveal environmental trade-offs of nature-based solutions for environmental clean-up applications and comprehensive contaminant risk assessment. Moreover, the implementation of the Michaelis-Menten-Monod framework in the bioreactive solver is fundamental to account for natural strategies affecting contaminant biodegradation.

Acknowledgements

This project has received funding from the European Union's Horizon Europe research and innovation programme under the Marie Skłodowska-Curie grant agreement No. 101062255 and support by the project AQUIGROW (Water4All-2022-00110), funded by the Water4All partnership within the Water4All 2022 Joint Transnational Call

References

[1] Bekins B., Warren E., Godsy E., "A comparison of zero-order, first-order and Monod biotransformation models", Ground Water, 36, 261–268, (1998)
[2] Belser L.W., "Population ecology of nitrifying bacteria", Annu. Rev. Microbiol., 33, 309–333, (1989)
[3] Monod J., "The growth of bacterial cultures", Annu. Rev. Microbiol., 3, 371–394, (1949)
[4] Cheyns K., Mertens J., Diels J., Smolders E., Springael D., "Monod kinetics rather than a first-order degradation model explains atrazine fate in soil mini-columns: Implications for pesticide fate modelling", Environmental Pollution, 158, 1405-1411, (2010)
[5] la Cecilia D., Tang F.H.M., Coleman N.V., Conoley C., Vervoort R.W., Maggi F., "Glyphosate dispersion, degradation, and aquifer contamination in vineyards and wheat fields in the Po Valley, Italy", Water Research, 146, 37-54, (2018)
[6] Trapp S., "Fruit tree model for uptake of organic compounds from soil and air", SAR and QSAR in Environmental Research, 18, 367–387, (2007)
[7] Brunetti G., Kodešová R., Šimůnek J., "Modeling the translocation and transformation of chemicals in the soil-plant continuum: A dynamic plant uptake module for the hydrus model", Water Resources Research, 55, 8967–8989, (2019)
[8] Englert D., Zubrod J.P., Link M., Mertins S., Schulz R., Bundschuh M., "Does Waterborne Exposure Explain Effects Caused by Neonicotinoid-Contaminated Plant Material in Aquatic Systems?" Environ. Sci. Technol., 51, 5793−5802, (2017)
[9] Camporese M., Paniconi C., Putti M., Orlandini S., "Surfacesubsurface flow modeling with path-based runoff routing, boundary condition-based coupling, and assimilation of multisource observation data", Water Resources Research, 46, W02512, (2010)
[10] Camporese M., Daly E., Paniconi C., "Catchment-scale Richards equation-based modeling of evapotranspiration via boundary condition switching and root water uptake schemes", Water Resources Research, 51, 5756–5771, (2015)
[11] McGrath J.W., Chin J.P., Quinn J.P., "Organophosphonates revealed: new insights into the microbial metabolism of ancient molecules", Nat. Rev. Microbiol, 11, 412-419, (2013).

Title: Surfactant enhanced remediation of marine sediments using anionic, non-ionic and mixed surfactants: role of operational conditions

Authors: Manuela Russo Tiesi[1,*], Gaetano Di Bella[2], Enrico Licitra[2], Giovanni Vinti[1], Gaspare Viviani[1], Daniele Di Trapani[1]

[1] *Department of Engineering, University of Palermo, Palermo, Italy, *manuela.russotiesi@unipa, giovanni.vinti@unipa.it, gaspare.viviani@unipa.it, daniele.ditrapani@unipa.it*
[2] *Facoltà di Ingegneria e Architettura, Università Kore di Enna, Cittadella Universitaria, Enna, Italy, gaetano.dibella@unikore.it, enrico.licitra@unikore.it*

Keywords: anionic surfactant; non-ionic surfactant; mixed surfactant; sediment washing; batch test

Abstract

Chemical pollution represents a global threat caused by deliberate or unintentional release of pollutants into the environment, estimated to be between 120,000 and 220,000 million tonnes per year [1]. Prüss-Ustün et al. [2] evaluated that 12.6 million deaths globally, representing 23% of all deaths, were attributable to environmental factors, including air, water and soil pollution.
Sediment is one of the environmental matrices that can be affected by chemical pollution. It consists of materials that accumulate at the bottom of water bodies by sedimentation. Due to the close interplay between sediment and the aquatic environment, contaminants can be absorbed or released by sediment, making it both a sink and a source of pollutants [3].
Among chemical pollutants, total petroleum hydrocarbon (TPH) plays a crucial role since oil leakage is common. Noteworthy, TPH may pose risks to human health and the environment and, over the years, it has been associated with significant contamination [4].
Therefore, remediation techniques are pivotal to reducing such risks by removing environmental contaminants. Among the proposed technologies, sediment washing represents a promising ex-situ treatment, where pollutants are extracted from sediments by means of a washing solution, eventually augmented with chemicals. Therefore, contaminants are transferred from the sediment to the solution and subsequently removed [5]. Referring to petroleum hydrocarbons, literature studies revealed that surfactants play a crucial role since they can enhance the mobilization and dissolution of oil contaminants into water through the reduction of air/water surface tension, oil/water interfacial tension, and micellar solubilisation [4,6]. Sediment washing can achieve high removal efficiencies, limiting the deterioration of physical-chemical properties of sediment and microbial activity while leading to reduced operating costs [5]. Surfactants are amphiphilic molecules composed of a hydrophilic head and hydrophobic tail; they can have natural origins, e.g. derived from plants or microorganisms, or can be artificially synthesized. When surfactant molecules are at low concentrations, they are dispersed in solution as monomers. As the concentration of surfactant increases, they begin to aggregate into micelles, driven by the mutual attraction of hydrophobic groups. The concentration threshold at and beyond which micelles form is the critical micelle concentration (CMC), which varies for each surfactant. Generally, the solubilisation of oil contaminants is not effective until the CMC is exceeded [4]. CMC varies among surfactants, and a lower value indicates that more micelles will form at the same surfactant concentration.
Over the last years, Tween 80 and Sodium dodecylbenzene sulfonate (SDBS) are among the

surfactants that have aroused significant interest in removing petroleum hydrocarbons. In particular, Tween 80 is a non-ionic surfactant. Non-ionic surfactants are not ionized and do not have charge; noteworthy, the monomers of non-ionic surfactants aggregate more easily to form micelles thanks to the absence of a repulsive effect between monomers. Thus, they usually have a lower CMC than other surfactant categories, such as anionic and cationic. SDBS is an anionic surfactant. Compared to non-ionic surfactants, electrostatic repulsion makes the aggregation of monomers into micelles more difficult; thus, CMC is typically higher than non-ionic ones. Furthermore, the combination of anionic and non-ionic surfactants has shown promising synergistic effects in previous studies [4]. This is because non-ionic surfactants, being uncharged, are highly compatible with both non-ionic and ionic surfactants. However, the CMC of mixed anionic/non-ionic surfactants cannot be estimated with the ideal solution theory because of the mentioned synergistic effect making the CMC smaller [7]. Noteworthy, previous research investigated the effectiveness of SDBS and Tween 80 in removing petroleum hydrocarbons both alone [4] and as mixed surfactants [8], with promising results. However, further research is necessary, considering the influence of operational conditions. Additionally, little is known about their effectiveness in dealing with contaminated sediment, whose properties can significantly differ from soils [9]. Indeed, to the best of our knowledge, Tween 80 has only been studied for the remediation of petroleum hydrocarbon-contaminated sediments in Italy but as an enhancing agent in combination with other treatments [10]. In contrast, SDBS was solely studied for washing contaminated sediment from a Taiwanese industrial harbour [6]. Thus, additional investigations are essential.
Therefore, the aim of the present study was to ensure a comprehensive understanding of the removal efficiency of TPH from marine sediments through a sediment washing treatment using two surfactants, Tween 80 and SDBS, both individually and to form mixed surfactants.
The investigations were conducted through batch washing tests. The marine sediments used for the washing tests were obtained from Augusta Bay (Italy), a contaminated site of national interest. An artificial contamination procedure further increased the TPH concentration by adding a known volume of diesel oil (Figure 1). The sample was manually mixed for 15 days to allow for the volatilization of the most volatile components, to ensure better homogenization of the sample and to foster air-drying outdoors. Then, the sediment was dried in an oven at 40°C for 72 hours. The dried sample was then crushed using a mortar and sieved with a first sieve having a mesh size of 2 mm and, subsequently, with a sieve having a mesh size of 0.63 µm. The crushing and subsequent sieving of the sediments allowed working with samples consisting of particles with a diameter smaller than 2 mm. Indeed, the concentration of hydrocarbons adsorbed to the solid matrix is prone to increase with the specific surface area [11] and focusing on the washing efficiency on this fraction appeared of higher interest.

Figure 1. a) 1.5 kg of sediments; b) 150 ml of diesel oil; c) Mixing.

The experimental campaign lasted about three months, during which several washing tests were carried out. Preliminary, washing tests were carried out with distilled water only as blank control (test A).

Additionally, 3 sets of washing tests (B, C, and D) were conducted at different surfactant concentrations. All tests were conducted with a sediment-water (S:W) ratio 1:4 (w/v). Furthermore, all measurements were performed in duplicate to ensure data reliability. Table 1 reports the tests and the various concentrations (w/w) of Tween 80 and SDBS. Surfactant concentration was always above the CMC of SDBS and Tween 80. Indeed, CMC of SDBS and Tween 80 is 0.612 mM (212.57 mgL^{-1}) and 0.012 mM (13.1 mg L^{-1}) at 25 ºC, respectively [12].

Table 1. Summary of the experimental tests carried out

Test A H_2O	**Test B** Tween80	**Test C** SDBS	**Test D** SDBS + Tween80
S:W =1:4	C_1 :0.2%	C_1 :0.2%	S:T = 1:1 (0.2%:0.2%)
	C_2:0.4%	C_2:0.4%	S:T = 1:2 (0.2%:0.4%)
	C_3:0.6%	C_3:0.6%	S:T = 2:1 (0.4%:0.2%)

Each test involved the contact between a sediment sample and a washing solution with different surfactant concentrations. In particular, each Pyrex glass bottle contained 10 g of sediment sample and 40 mL of washing solution. The bottles were subject to mixing for 24 hours at 100 rpm using an orbital shaker (Figure 2).

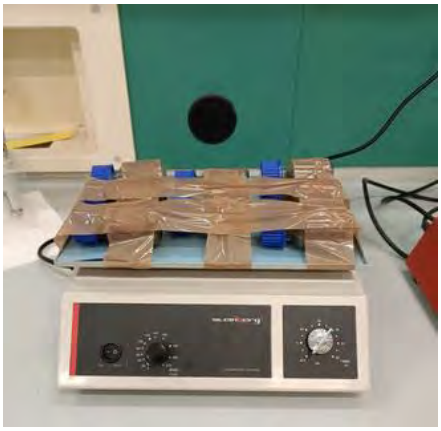

Figure 2. Panoramic view of the orbital shaker during experiments

After the agitation phase, the samples were allowed to settle for 2 hours and then air-dried for at least 96 hours, depending on the external temperatures. The TPH measurement in the solid phase was carried out according to the procedure proposed by ISPRA [13]. A dried sediment sample of 10 g was used for the extraction procedure. The sample was placed in a Pyrex glass bottle, and 20 ml of acetone ($(CH_3)_2CO$) was added. After manual agitation, 10 ml of RTW solution was added. Subsequently, the bottle was immersed for half an hour in a VWR ultrasonic bath to facilitate the separation of the organic phase, allowing its extraction from the sediment. After extraction and purification on Florisil, the procedure involves analysis by GC-FID [12]. In detail, the TPH concentration was determined by headspace gas-chromatographic analysis using a gas-chromatograph (Agilent 6890 N Network GC System) equipped with a Flame Ionization Detector (FID) and the column Agilent 7683 Series. Once the

filtration phase was completed, the purified fraction was stored at 4 °C, and then transferred to a 2 ml vial for subsequent analysis by GC-FID.

The results obtained from the washing tests showed that the TPH extraction yields significantly improved when the two surfactants were used, both individually and as mixed surfactants, compared to the washing test with only water. In addition, the removal rates of hydrocarbons improved as the surfactant concentration increased.

Acknowledgements

This study was carried out within the RETURN Extended Partnership and received funding from the European Union Next-GenerationEU (National Recovery and Resilience Plan – NRRP, Mission 4, Component 2, Investment 1.3 – D.D. 1243 2/8/2022, PE0000005).

References

1. Naidu, R.; Biswas, B.; Willett, I.R.; Cribb, J.; Kumar Singh, B.; Paul Nathanail, C.; Coulon, F.; Semple, K.T.; Jones, K.C.; Barclay, A.; et al. Chemical Pollution: A Growing Peril and Potential Catastrophic Risk to Humanity. *Environ. Int.* **2021**, *156*, 106616.
2. Prüss-Üstün, A.; Wolf, J.; Corvalán, C.; Bos, R.; Neira, M. *Preventing Disease through Healthy Environments: A Global Assessment of the Environmental Burden of Disease*; World Health Organization (WHO), 2016; Vol. 259; ISBN 978924156519 6.
3. Zhang, Y.; Labianca, C.; Chen, L.; De Gisi, S.; Notarnicola, M.; Guo, B.; Sun, J.; Ding, S.; Wang, L. Sustainable Ex-Situ Remediation of Contaminated Sediment: A Review. *Environ. Pollut.* **2021**, *287*, 117333.
4. Liu, J.W.; Wei, K.H.; Xu, S.W.; Cui, J.; Ma, J.; Xiao, X.L.; Xi, B.D.; He, X.S. Surfactant-Enhanced Remediation of Oil-Contaminated Soil and Groundwater: A Review. *Sci. Total Environ.* **2021**, *756*.
5. Lumia, L.; Giustra, M.G.; Viviani, G.; Di Bella, G. Washing Batch Test of Contaminated Sediment: The Case of Augusta Bay (SR, Italy). *Appl. Sci.* **2020**, *10*, 473.
6. Shih, Y.J.; Wu, P.C.; Chen, C.W.; Chen, C.F.; Dong, C. Di Nonionic and Anionic Surfactant-Washing of Polycyclic Aromatic Hydrocarbons in Estuarine Sediments around an Industrial Harbor in Southern Taiwan. *Chemosphere* **2020**, *256*, 127044.
7. Zhou, W.; Zhu, L. Solubilization of Polycyclic Aromatic Hydrocarbons by Anionic–Nonionic Mixed Surfactant. *Colloids Surfaces A Physicochem. Eng. Asp.* **2005**, *255*, 145–152.
8. Zhang, M.; Zhu, L. Effect of SDBS-Tween 80 Mixed Surfactants on the Distribution of Polycyclic Aromatic Hydrocarbons in Soil-Water System. *J. Soils Sediments* **2010**, *10*, 1123–1130.
9. Chiou, C.T.; Mcgroddy, S.E.; Kile, D.E. Partition Characteristics of Polycyclic Aromatic Hydrocarbons on Soils and Sediments. *Environ. Sci. Technol.* **1998**, *32*, 264–269.
10. Falciglia, P.; Catalfo, A.; Finocchiaro, G.; Vagliasindi, F.; Romano, S.; De Guidi, G. Microwave Heating Coupled with UV-A Irradiation for PAH Removal from Highly Contaminated Marine Sediments and Subsequent Photo-Degradation of the Generated Vaporized Organic Compounds. *Chem. Eng. J.* **2018**, *334*, 172–183.
11. Falciglia, P.P.; Giustra, M.G.; Vagliasindi, F.G.A. Low-Temperature Thermal Desorption of Diesel Polluted Soil: Influence of Temperature and Soil Texture on Contaminant Removal Kinetics. *J. Hazard. Mater.* **2011**, *185*, 392–400.
12. Di Trapani, D.; De Marines, F.; Greco Lucchina, P.; Viviani, G. Surfactant-Enhanced Mobilization of Hydrocarbons from Soil: Comparison between Anionic and Nonionic Surfactants in Terms of Remediation Efficiency and Residual Phytotoxicity. *Process Saf. Environ. Prot.* **2023**, *180*, 1–9.
13. ISPRA *Procedure for the Analysis of Hydrocarbons > C12 in Contaminated Soils (in Italian)*; Rome, Italy, 2011.

Title: Assessing the Impact of Climate Change on Water Quality Parameters in the Brescia Water Supply System

Author(s): Hoan Thi Kim Tran*, Arici Silvia**, Sabrina Sorlini*

*Department of Civil Engineering, Architecture, Land and Environment and Mathematics, University of Brescia, Brescia, Italy, Email: sabrina.sorlini@unibs.it, h.tranthikim@unibs.it;

**A2A Ciclo Idrico – Brescia, email: silvia.arici@a2a.eu

Keyword(s): Drinking water Supply System, Climate change, water treatment

Abstract

Climate change, as per the latest IPCC report, profoundly impacts water supply, crucial for human survival and recognized as a basic human right [3]. Safeguarding water quantity, quality, and availability demands global resource management and consumption policies [2] . Water treatment plants, essential for safe drinking water, face challenges intensified by severe weather events, altering water's characteristics and treatment costs [1]. Certain climate-affected parameters, like turbidity, pH, microbiology can influence water source safety management. Floods, as in Emilia-Romagna in 2023, underscore adaptation needs for water quality maintenance [4]. Although climate change affects water treatment processes, transformative solutions remain elusive, with proposed strategies mostly short-term. Despite documented impacts, drinking water utilities' resilience to climate change remains uncertain. This study aims to examine how water quality variations correlate with climate change in Brescia, analysing physical, chemical, and microbiological properties alongside meteorological parameters. Monitoring will focus on key locations: the source, within utility, and in the distribution network.

Figure 1: Public water distribution system of the city of Brescia and supply sources (Source: A2A Ciclo Idrico di Brescia (2022)).

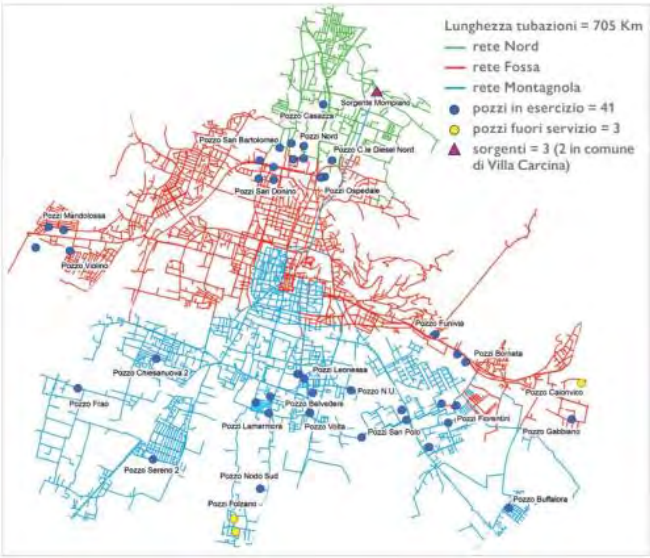

Brescia, a city situated at the foot of the Alps, in proximity to Lake Garda and Lake Iseo, has a population exceeding 200,000 within the city limits, while the urban area encompasses 672,822 residents. The water supply network of the city of Brescia extends for approximately 705 kilometers and is equipped with numerous storage and reserve tanks, with a total volume of around 29,000 cubic meters. The primary source of water for Brescia's water supply system is groundwater.

The supply is ensured by 41 wells scattered throughout the territory, which extract water from deep aquifers, in addition to the aforementioned natural sources of Mompiano and Cogozzo (two sources located in the municipality of Villa Carcina in the North of Brescia). The network comprises three interconnected sub-networks that provide potable water to three distinct areas of the city: the North Network, the Fossa Network, and the Montagnola Network. The waters of Mompiano supply 73 continuous jet public fountains. The deep wells have treatment systems with activated carbon for the removal of chlorinated solvents. Regarding the treatment system applied in Mompiano source, it solely consists of disinfection using chlorine dioxide (ClO_2), commonly used in all the plants.

Methodology:

The methodology employed in this study involves the collection and analysis of historical data pertaining to temperature and precipitation records from the ARPA (Environmental Protection Regional Agency).[4] These data will be utilized to investigate potential correlations between changes in water quality at the source and the influence of climate change. This approach aims to evaluate whether climatic factors contribute to observable trends or shifts in specific water quality parameters. Within the utilities, the Mompiano source and the associated control system monitor various critical parameters through a programmable logic controller (PLC) network. These parameters include turbidity, electrical conductivity, redox potential (oxidation-reduction potential), chlorine levels, pH, and temperature. On the occasion of significant meteorological events that result in an increase in turbidity, when the Lange instrument reaches a value of 1 NTU, the PLC activates the "High Turbidity" alarm. If the exceedance of this value persists after 10 minutes, the water source is not used and it is directly discharged in surface water stream. Such probes carry out continuous measurements on the incoming water: the first is a Lange probe, capable of carrying out measurements of turbidity, pH, conductivity and redox, while the second is an Isoil multiparametric probe which carries out a measurement of turbidity, nitrates and a spectral fingerprint.

Results and discussion:

Correlation of climate change with raw water quality: case study in Mompiano plant

Turbidity

Based on the graph 1, we can provide the following observations and analysis:

1. The most significant variation occurred on February 15th 2022, the day after the precipitation peak event on February 14th. This is evident from the sharp spike in the "Precipitation" parameter on that date.

2. Other parameters like turbidity, conductivity, and nitrate also show elevated levels on February 15th or 16th, suggesting an increase in suspended solids, dissolved ions, and nitrogen compounds, respectively, following the precipitation event.

3. The "Flow rate Q" parameter exhibits a peak on February 16th, one day after the precipitation event, indicating a potential increase in water flow due to the additional water input.

4. The air temperature ("T air") appears to have a slight dip around February 15th, which could be related to the weather conditions associated with the precipitation event.

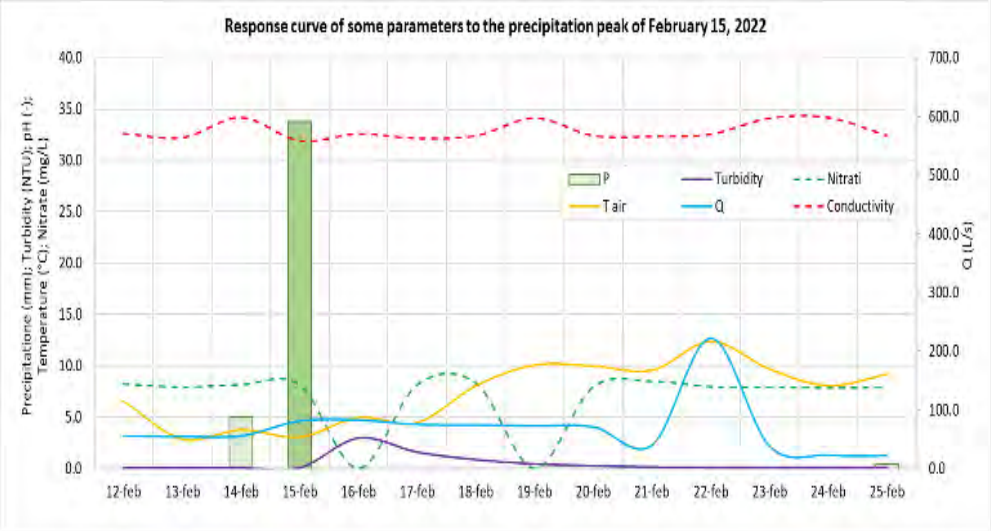

Graph 1: Repose curve of some parameters to the precipitation peal of Feb 2022.

The graph shows that the water quality parameters returned to their pre-event levels within a few days after the precipitation peak, suggesting a relatively short-term impact on the monitored water body. It's important to note that without specific information about the measurement units and the water body being monitored, it's difficult to provide a more detailed quantitative analysis of the observed trends.

Overall, the graph clearly illustrates the impact of the precipitation event on various water quality parameters, with the most significant changes occurring within one or two days after the event, followed by a return to pre-event levels within a few days.

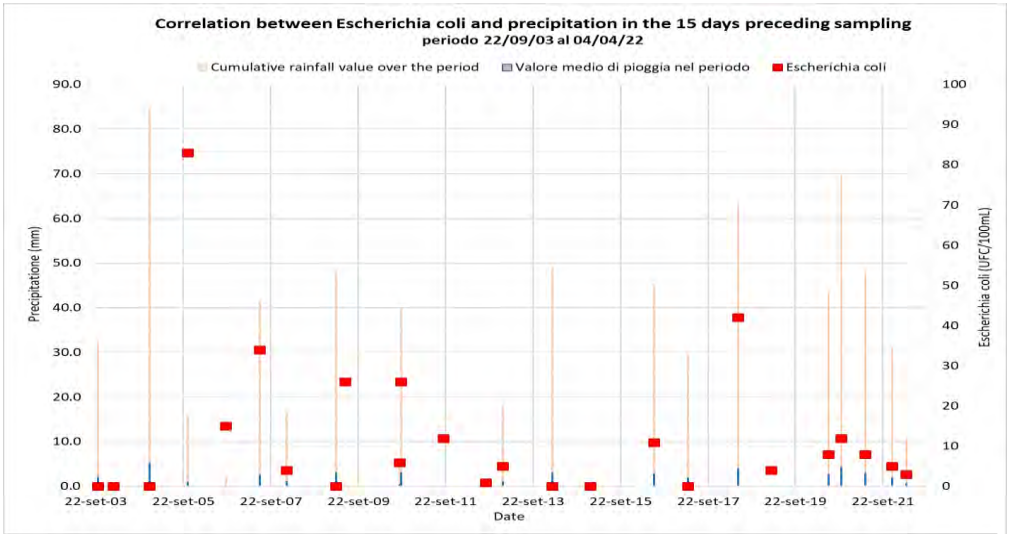

Graph 2: Correlation between Escherichia Coli and Precipitation in the 15 days preceding sampling period 2003-2022

The data points in Graph 2 suggest that higher levels of precipitation tend to be associated with higher counts of Escherichia coli, which is a common pattern observed in water quality monitoring. However, there are also some instances where high precipitation levels do not correspond to elevated Escherichia coli counts.

Conclusion

The water arriving at the Mompiano source is subject to critical conditions due to the presence of microbiological contamination, turbidity, and increases in parameter values resulting from isolated significant events. Moreover, a safety measure has been implemented, which states that if the turbidity exceeds 1 NTU (Nephelometric Turbidity Unit), the source will be immediately excluded from the distribution network. These actions aim to ensure the water quality supplied to consumers by implementing advanced monitoring techniques, adhering to updated regulations, and establishing strict criteria for removing contaminated sources from the distribution system, thereby safeguarding public health and maintaining high standards of water quality. The future work will involve an in-depth analysis of the water distribution system, extending the study to other water sources in the Brescia area, and enhancing the infrastructure through an upgrading process. This upgrading aims to introduce a specific treatment system tailored to address turbidity challenges, as the current infrastructure was not originally designed for this purpose. These developments will contribute to a more comprehensive understanding and improvement of the overall water supply system, ensuring better water quality and operational efficiency.

Reference:

[1]Sheng Wang, Shuang Wang, Sheng Wang, Xin Qian, Bo-Ping Han, Liancong Luo, Lian-Cong Luo, Rui Ye, and Wen Xiong. 2013. Effects of different operational modes on the flood-induced turbidity current of a canyon-shaped reservoir: case study on Liuxihe Reservoir, South China. *Hydrological Processes* 27, 26 (December 2013), 4004–4016. https://doi.org/10.1002/hyp.9534

[2]1984. *World Health Organization (WHO), Guidelines for drinking-water quality, 1a edizione, Vol. 1.*

[3]2023. *IPCC, The Intergovernmental Panel on Climate Change*. Retrieved from https://www.ipcc.ch/, 2023

[4]2023. Health System Response to the 2023 Floods in Emilia-Romagna, Italy: A Field Report. Retrieved from https://www.cambridge.org/core/journals/prehospital-and-disaster-medicine/article/health-system-response-to-the-2023-floods-in-emiliaromagna-italy-a-field-report/923FB238255C4AA5BA9EBDFF100A8FFF

[5]ARPALombardia,2023. Retrieved from https://www.arpalombardia.it/Pages/Meteorologia/Richiesta-dati-misurati.aspx. 2.Circolare del Ministero della Salute 13400 del 01.04.2021 con parere dell'Istituto

Title: Vulnerability Scenario Characterization using a Natech Indicator and a Territorial Multi-hazard Approach.

Author(s): Maria Castiglione*[1], Santo Fabio Corsino[1], Michele Torregrossa[1].

[1] *Department of Engineering, University of Palermo, Palermo, Italy, maria.castiglione01@unipa.it*

Keyword(s): Climate change, critical infrastructures, GIS, Natech, wastewater treatment plants.

Abstract

Climate change accelerates and intensifies the water cycle influencing the spatial and temporal distribution of precipitation and in general progressively modifying magnitude and recurrence of natural events. Their increasing frequency raised a concern about the possible interference of these natural hazards with some critical infrastructures. This contribution aims to illustrate the evaluation methodology that allows to identify in a spatially explicit manner the quadrants of the territory most vulnerable to a given set of hazards according to a multi-hazard approach in response to new regulations concerning the resilience of critical infrastructures.
In particular, the vulnerability of wastewater treatment and drinking water plants is assessed according to a multi-hazard approach.

Introduction

According to the fifth assessment report of the Intergovernmental Panel on Climate Change (IPCC), the existing climatic models forecast increases in the number and intensity of extreme events for this century [1]. In this framework, critical infrastructures are under threat for the impacts of climate change. Considering their crucial role for the development and sustenance of a functional society, their response and adaptation ability to climate change need to be carefully addressed [2].
Nevertheless, lacking attention is paid to the risk assessment related to accidents triggered by natural events (Natech - Natural Hazard Triggering Technological Disasters). In this scenario, the European Commission issued the Directive 2022/2557, addressing the resilience of critical entities. Specifically, it defines 'critical infrastructure' as an asset, a facility, equipment, a network or a system, which is necessary for the provision of an essential service. More in detail, Directive 2022/2557 aims to enhance the resilience and protection of critical infrastructure against various threats, including natural and man-made hazards, and to ensure the continuity of essential services that are vital for the functioning of society and the economy within the European Union. Member States are required to identify and assess their risks, emphasizing the influence of all relevant natural and man-made hazards that might result in accidents.
Wastewater treatment plants are a recognised critical section within industrial plants, belonging to the major hazards industries (MHIs). Wastewater infrastructures are essential to ensure the public health of many communities [3]. Climate change and natural disasters could significantly impact WWTPs in several ways. These include flooding, sea level rise, severe storms, earthquakes, etc. To mitigate these impacts, a throughout knowledge of the combined effects of such events is an essential first step to improve WWTPs resilience. However, literature concerning the adaptation of critical infrastructures to climate change and natural disasters is just emerging and it is also still far from a full understanding of

the potential interrelationships (cause/effect) between the different hazards and the related effects and potential impacts [4]. Moreover, most of hazard assessment and risk management protocols focus on individual hazards and their combined effect is not addressed. In this scenario, a multi-hazard approach could be a new concept to apply in risk minimization plans as it allows to consider the combined effect of all the potential risks, in contrast to the classical approach of considering each hazard and its potential impacts separately.
Considering this, this study was aimed at generating a multi-hazard map within the Sicilian region territory that included earthquake, geomorphological, coastal and hydraulic hazards, in order to evaluate the combined risk for WWTPs located in the same territory.

Materials and methods

The methodology framework to assess territorial vulnerability considered four types of natural hazards: earthquake, hydraulic, geomorphological, and coastal.
Considering the high number of WWTPs on a national scale (17897) (data referred to 2015 from ISTAT), it was decided to carry out the study on a regional scale, specifically on the Sicilian territory.
Spatial analyses were developed using data on wastewater treatment plants provided by the Sicilian Region and integrated water service bodies, as well as hazard maps from the PAI and civil protection agencies.
Space-dependent analysis was developed using geographical information systems (GIS). From the provided information, firstly, the WWTPs were represented as point infrastructures, distinguishing between existing, abandoned and expected.
Secondly, the natural hazards in the area of interest (hydraulic, geomorphological, seismic and coastal) were identified. Each hazard map was standardised so that P1 corresponded to the lowest hazard and P4 corresponded to the highest. Then, a score was assigned to each hazard class: 0.25 for P1; 0.50 for P2; 0.75 for P3; 1.00 for P4.
Third, a multi-hazard GIS-analysis was applied at the municipal scale with a focus on the wastewater treatment plants. The aim was to characterize vulnerability scenarios considering the bidirectional interaction between industry and territory [5]
The municipality of Cefalù was considered as a case study. The territory was divided into a grid with 200m x 200m cells.
A multi-hazard index (MHI) was evaluated for each cell calculated as the sum of the individual indicators of each hazard (HI_j) by assuming an equal weight for each of them.

$$\boldsymbol{MHI = HI_s + HI_g + HH_I + CH_I}$$

HI_s seismic hazard indicator
HI_g geological hazard indicator
HI_h hydraulic hazard indicator
HI_c coastal hazard indicator

The value of systemic individual hazard indicator HI (0-1) for each cell has been calculated as the weighted sum of the products of each specific hazard class score in the cell for each weight.
More precisely, each weight was calculated by dividing the area of each hazard portion by the total area of the cell, according to the hazard class to which it belongs.

$$\boldsymbol{HI_j = \Sigma \sum_{i=1}^{n} H_i y_i}$$

$$y_i = \frac{\sum A_i}{A_{tot}}$$

H_i is the value of the score that was assigned to each element belonging to the i-th hazard class 0,25 for P1; 0.50 for P2; 0.75 for P3; 1.00 for P4.
y_i is the weight of each element belonging to the i-th hazard class.
n number of hazard class (1 ÷ 4)
A_i represents the area of the portion of the i-th Hazard (respectively P1, P2, P3, P4) falling within the cell.
A_{tot} represents the total area of the single cell (40000 m²)

Finally, a multi-hazard map was created. This mapping was carried out at the municipal level, focusing on the two existing wastewater treatment plants "Presidiana S. Antonio Treatment Plant" and "Sant'Ambrogio Treatment Plant".
Then, to assess possible consequences following plant failure due to natural phenomena, two analyses were carried out: the population failing in service as a result of a breakdown and the environmental compartments concerned. Finally, a Natech indicator, previously validated in an industrial context [6], was implemented for the case study.

Results

The synthesis of the principal results is represented in Figure 1.
Focusing on the two wastewater treatment plants in the area, it is observed that both are located in zones where the multi-hazard index is high. However, for the Presidiana Sant'Antonio WWTP, the predominant hazard is seismic, followed by geomorphological. Conversely, for the Sant'Ambrogio plant, the predominant hazard is geomorphological, followed by seismic This analysis reveals that the measures for hazard prediction and protection that need to be implemented differ between the two plants. A specific analysis for each plant allows for the identification of the most at-risk units and the assessment of the appropriate mitigation actions to be taken.

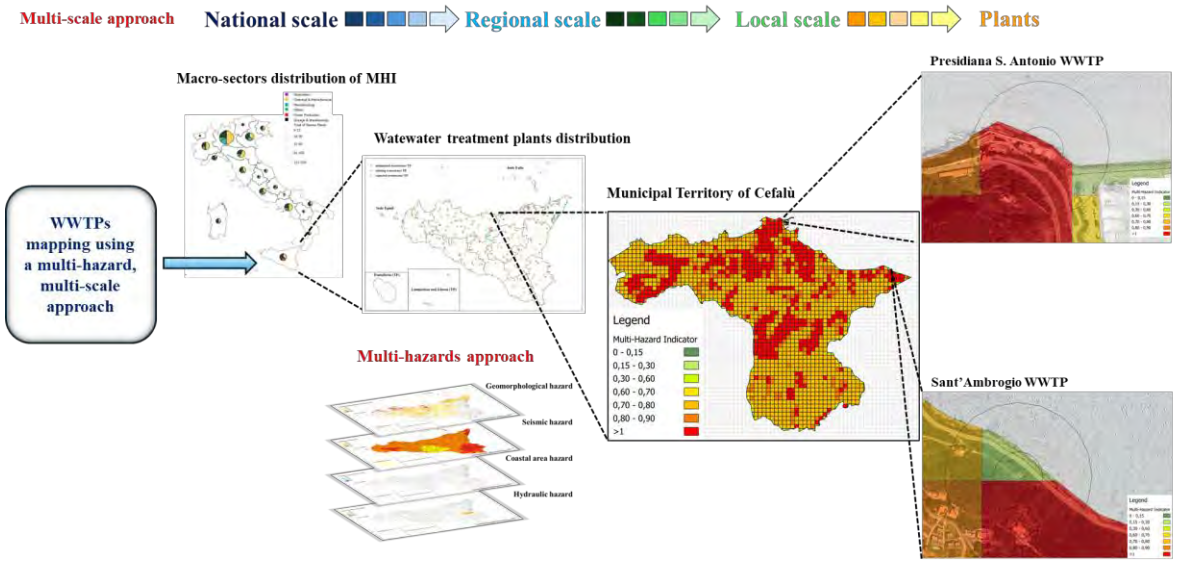

Figure 1. *Results from the multi-hazard, multi-scale approach depicting vulnerability between Industry and Territory.*

Conclusions

The subsequent identification of possible equipment failures triggered by a natural event, and its potential consequences, can suggest to WWTP managers the correct measures to adopt in order to increase the resilience of the infrastructure. This tool contributes to increase awareness of territorial vulnerability based on spatial analysis. Moreover, it allows considering the combined effect of different hazards to be analysed according to a holistic approach, so as many hazards can be added. The analysis carried out in the municipality of Cefalù will be extended to all municipalities in the province of Palermo and subsequently to Sicily. To conclude, the innovative aspect is that the tool is not configured as an index on a municipal basis to compare territories but ensures the visualization of variations in the index within the territory itself.

Acknowledgments

This study was carried out within the RETURN Extended Partnership and received funding from the European Union Next-GenerationEU (National Recovery and Resilience Plan – NRRP, Mission 4, Component 2, Investment 1.3 – D.D. 1243 2/8/2022, PE0000005 - Spoke TS2).

References

[1] S. R. Kovats *et al.*, "IPCC - Climate Change 2014. Impacts, Adaptation, and Vulnerability. Part B: Regional Aspects," *Cambridge University press*. Meriwether Wilson, pp. 1267–1326, 2014.

[2] L. M. Shakou, J. L. Wybo, G. Reniers, and G. Boustras, "Developing an innovative framework for enhancing the resilience of critical infrastructure to climate change," *Saf Sci*, vol. 118, pp. 364–378, Oct. 2019, doi: 10.1016/j.ssci.2019.05.019.

[3] J. Hughes, K. Cowper-Heays, E. Olesson, R. Bell, and A. Stroombergen, "Impacts and implications of climate change on wastewater systems: A New Zealand perspective," *Climate Risk Management*, vol. 31. Elsevier B.V., Jan. 01, 2021. doi: 10.1016/j.crm.2020.100262.

[4] M. López-Saavedra and J. Martí, "Reviewing the multi-hazard concept. Application to volcanic islands," *Earth-Science Reviews*, vol. 236. Elsevier B.V., Jan. 01, 2023. doi: 10.1016/j.earscirev.2022.104286.

[5] D. J. Castro Rodriguez, S. Beltramino, M. Scalas, E. Pilone, and M. Demichela, "Territorial Representation of a Vulnerability Associated with the Seveso Installations in a Nord Italian Case Study," Research Publishing Services, Aug. 2022, pp. 1463–1470. doi: 10.3850/978-981-18-5183-4_r25-02-574-cd.

[6] D. J. Castro Rodriguez *et al.*, "Vulnerability Scenario Characterization in an Industrial Context using a Natech Indicator and a Territorial Multi-risk Approach," 2023, doi: 10.3850/981-973-0000-00-0.

Title: Water reuse from wastewater treatment: comparison between MBR and tertiary filtration processes

Author(s): Marika Carnesi[1], Alida Cosenza[1], Daniele Di Trapani[1], Antonio Mineo[1], Paulo Marcelo Bosco Mofatto*[1], Giorgio Mannina[1]
[1]*Engineering Department, Palermo University, Viale delle Scienze, Ed. 8, 90128 Palermo, Italy*

Keyword(s): water reuse, carbon footprint, advanced technology, membrane

Abstract

Resource recovery from wastewater must become a common practice for a sustainable environment. In view of this need, advanced wastewater treatments, such as Membrane Bioreactors (MBR), Integrated fixed film activated sludge (IFAS), intermitted aeration, etc., can be employed. Greenhouse gas (GHG) emissions must be monitored and reduced. Different treatment trains and technologies can be used to achieve the above needs. An experiment study was carried out in the Water Resource Recovery Facility of Palermo University to gain insights about the best solutions to be employed. Specifically, a comparison between two pilot plant configurations, operated in parallel, was carried out: MBR: Line I and CAS-Ultrafiltration: Line II. Two periods were monitored: intermittent aeration (Period I) and continuous aeration (Period II). Removal efficiencies of carbon and nutrients were monitored. GHG emissions, membrane fouling and respirometry analysis were carried out, and water quality was assessed in view of water reuse according to European Regulation 2020/741. The study demonstrates that continuous aeration had higher removal efficiency for carbon and nitrogen, and Line II registered higher removal performance than Line I. The high continuous aeration performance was also confirmed in the carbon footprint, which was lower than in intermittent aeration.

1. Introduction

Water demand will be 64% higher than global water availability by the next five years [1]. By 2030, 1.6 billion people will not have access to safely managed drinking water [2]. Freshwater withdrawals for human scopes increased from 500 km^3/year in 1900 to 4000 km^3/year in 2018 [3]. Around 70% is consumed by the agricultural sector. Therefore, it is important to consider alternative sources besides natural ones. Adopting treated wastewater can be considered an alternative approach to reducing the amount of natural water for irrigation. Wastewater treatment plants (WWTPs) are now becoming resource recovery facilities, extracting water, energy, nutrients (phosphorus and nitrogen), and biosolids. With this regard, the European Union (EU) have proposed the EU 2020/741 regulation to facilitate water reuse for agricultural scopes, imposing limits for four parameters (total suspended solids- TSS, turbidity, biological oxygen demand- BOD5, Escherichia coli- E. coli) according to four classes of reclaimed water quality (namely, A – D). Regardless of the class, secondary treatment and disinfection are mandatory for each class. To be classified as class A, reclaimed water must meet specific criteria such as BOD_5 and TSS concentrations below 10 mg/L, turbidity below 5 NTU, and an E. coli count below 10 cfu/100 mL [4].

To achieve this, the tertiary treatment following the secondary treatment of wastewater is required. The adoption of ultrafiltration as a membrane bioreactor (MBR) and tertiary treatment has spread during the last decade. However, adopting UF membrane filtration, both as MBR and tertiary treatment, has some drawbacks mainly related to the high energy consumption and operation costs primarily due to membrane aeration to keep it clean, for pumping sludge from the biological reactor to the membranes and for pumping the permeate for extraction and backwashing. Intermittent Aeration (IA) has been demonstrated to be most promising for reducing energy consumption and operational costs [5].
This study compares the performance of two pilot plant configurations operated in parallel: Period I (with intermittent aeration) and Period II (with continuous aeration). Specifically, the UF membrane was operated as MBR (Line I) and tertiary treatment after a CAS system (Line II). A comparison was made between both wastewater treatment performance and permeate quality according to the EU 741/2020 regulation. Nitrous oxide (N_2O) emission was measured. Further, the carbon footprint and operational costs have been quantified.

2. Material and methods

Two pilot plant configurations were assembled parallelly (Figure 1) at the Water Resource Recovery Facility (WRRF) of Palermo University [6]. Both configurations were connected by a Fixed Film Activated Sludge (IFAS) reactor devoted to carbon and nitrogen removal from an influent flow rate (Qin) of 36 L h^{-1}. During Period I, the IFAS reactor worked in intermittent aeration with 40 minutes of aeration on and 20 minutes off, while in Period II, the biological reactor worked in continuous aeration. Inside the IFAS reactor were 40 liters of carriers, which guaranteed the combination of suspended and attached biomass. After the IFAS reactor, the pilot plant was divided into two Lines with the same inlet flow rate.

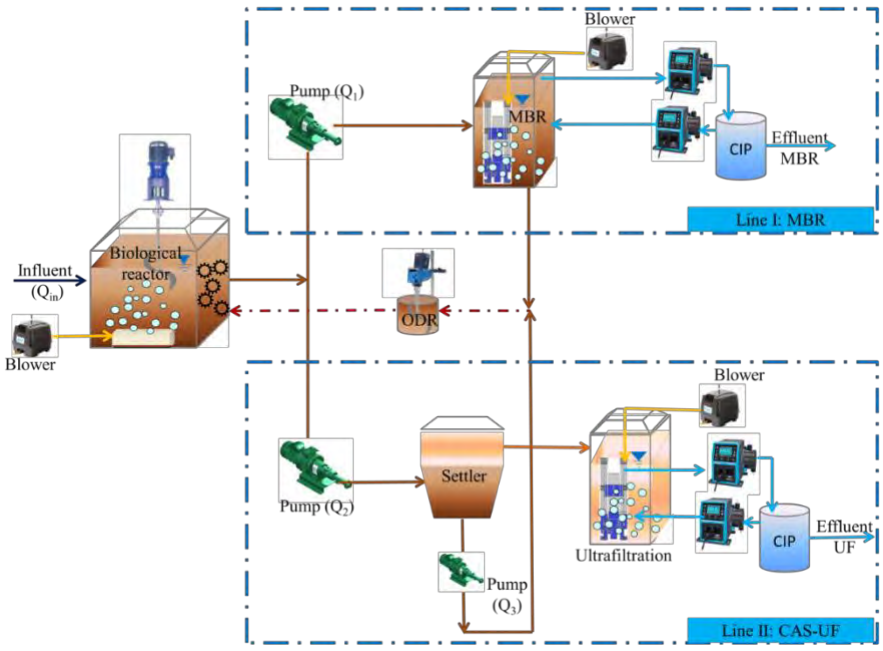

Figure 1, Representation of pilot plant

For Line I, the solid/liquid separation occurred using a membrane bioreactor (MBR) with a hollow fiber ultrafiltration membrane module (0.03µm porosity and 1.4 m^2 surface). From the top of MBR, the mixed

liquor was recirculated back to the IFAS through the Oxygen Depletion Reactor (ODR) to reduce the oxygen mass.
For Line II, a vertical settler was devoted to the solid/liquid separation, followed by a tertiary unit equipped with a hollow fiber ultrafiltration membrane module. From the bottom of the settler, 63L h^{-1} of recirculated activated sludge was pumped back to the biological reactor through the ODR. The permeate flow rate from both Lines was equal to 18 L h^{-1}. The hollow fiber ultrafiltration membrane module had the same features for both configurations. The membranes were operated under filtration cycles (9 minutes of filtration and 1 minute of backwashing) using peristaltic pumps. The membrane reactors had a clean-in-place (CIP) tank for ordinary backwashing.
During the experimental campaign, Chemical oxygen demand (COD), ammonia nitrogen (NH4+-N), nitrate nitrogen (NO^{3+}-N), nitrite nitrogen (NO^{2+}-N), orthophosphate (PO_3^{4-}-P), total suspended solid (TSS) and volatile suspended solid (VSS) concentrations, biological oxygen demand (BOD) and Total Nitrogen (TN) were measured according to Standard Methods [7]. Moreover, the sludge settling features were calculated by measuring the sludge volume index (SVI). Extracellular polymeric substances (EPS) and soluble microbial products (SMP) were extracted and measured according to the literature [8]. Dissolved and gaseous N_2O concentrations were measured using a Gas Chromatograph (GC). Further, the carbon footprint quantification was performed considering both direct (due to energy consumption) and indirect (due to energy consumption) emissions, according to the literature (2023). The membrane fouling was quantified by monitoring the transmembrane pressure (TMP) (kPa) and the permeate flux (J) (m^3 m^{-2} s^{-1}) every day to calculate the total membrane resistance (R_T) according to the general form of Darcy's Law. Moreover, in view to assess the type of membrane fouling, the resistance in series (RIS) model has been used by using the procedure according to Di Bella et al. (2019)

3. Result and discussion

During Period I, the average TCOD removal efficiency of Line I was 90% and was slightly increased to 92% for Line II. During Period 2, the TCOD removal efficiency was equal to 97% and 98% for Lines I and II, respectively. In terms of biological removal efficiency, during Period I, the average COD biological removal performance was equal to 26% and 17% for Lines 1 and 2, but during Period II, the biological performance of both Line I and Line II highly increased till 74% of COD biological removal for both lines. These results were attributed to the higher oxygen diffusion within the biofilm, favouring the biomass growth during Period II (Figure 2a, b).
Regarding nitrogen removal efficiency, no significant difference in biological activity between Line I and Line 2 in Period I were registered rather than the total removal efficiency in which Line II removal performance was slightly higher than Line I (29% Line I, 40% Line II). During Period II, nitrogen removal efficiency was higher than in Period I both for biological (72% and 78%, Line I and II, respectively) and total (84% 80% Line I and II, respectively) (Figure 2c, d).

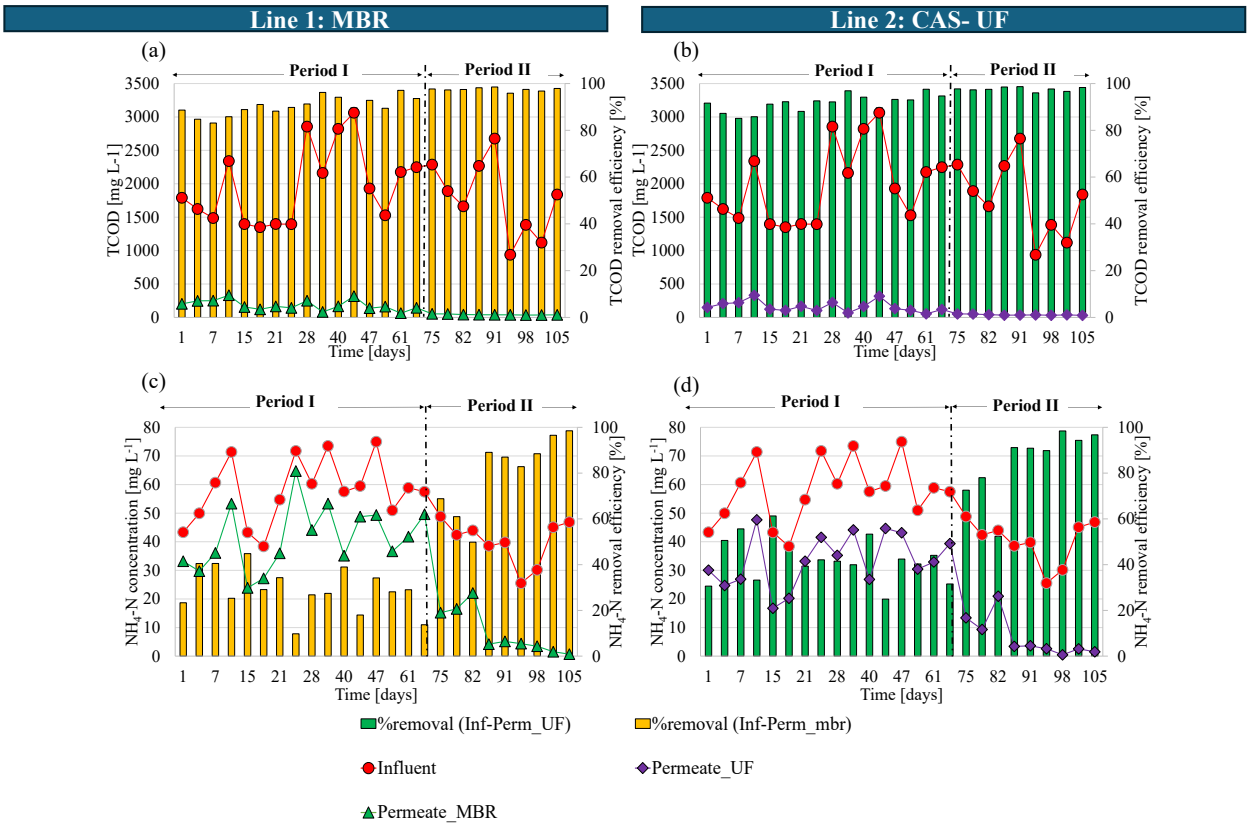

Figure 2: Total removal efficiency for total COD in Lines I (a) and II (b). Removal efficiency of NH_4 in Line I (c) and Line II (d)

N_2O emissions were registered as higher in Line II, and this could be because of the incomplete nitrification pathway compared to Line 1 (Figure 3a, b). Moreover, it measured a lower carbon footprint despite Period I. In particular, Line II achieved a slightly higher carbon footprint than Line I (2.2 and 2.6 kgCO2 day^{-1}, respectively). The main difference is the indirect emission contribution, which suffers from using one pump more than Line I.

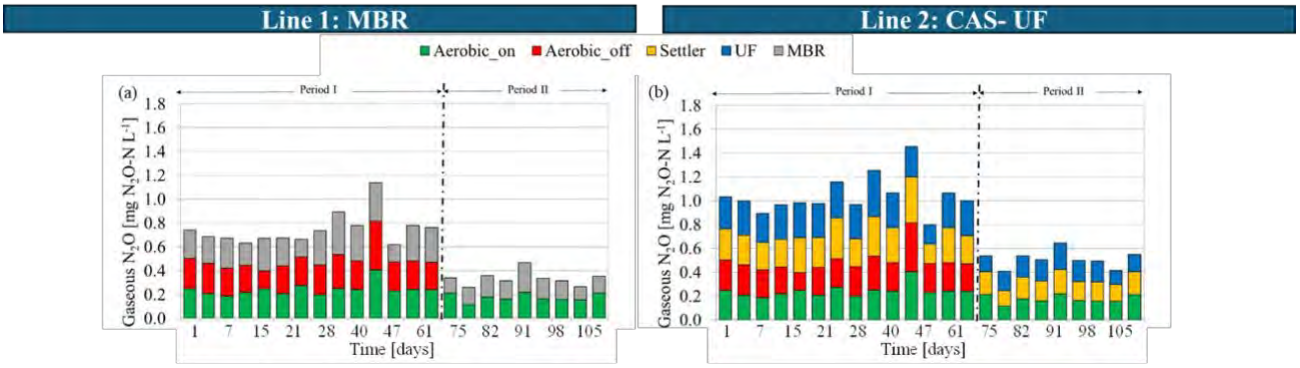

Figure 3: N_2O emission in Line I (a) and in Line II (b)

Regarding membrane fouling, the results obtained regarding the RIS model application corroborated the hypothesis of the increasing stable cake layer. Indeed, in Line II, the fraction of Rc, IRR was almost 10% higher than that of Line I. Also, in Period I, the membrane cleanings were more frequent due to the high TMP in both membranes. This result can be attributed to the higher concentration of SMP (both carbohydrates and proteins) measured in the biological reactor sludge samples and the MBR (Figure 4).

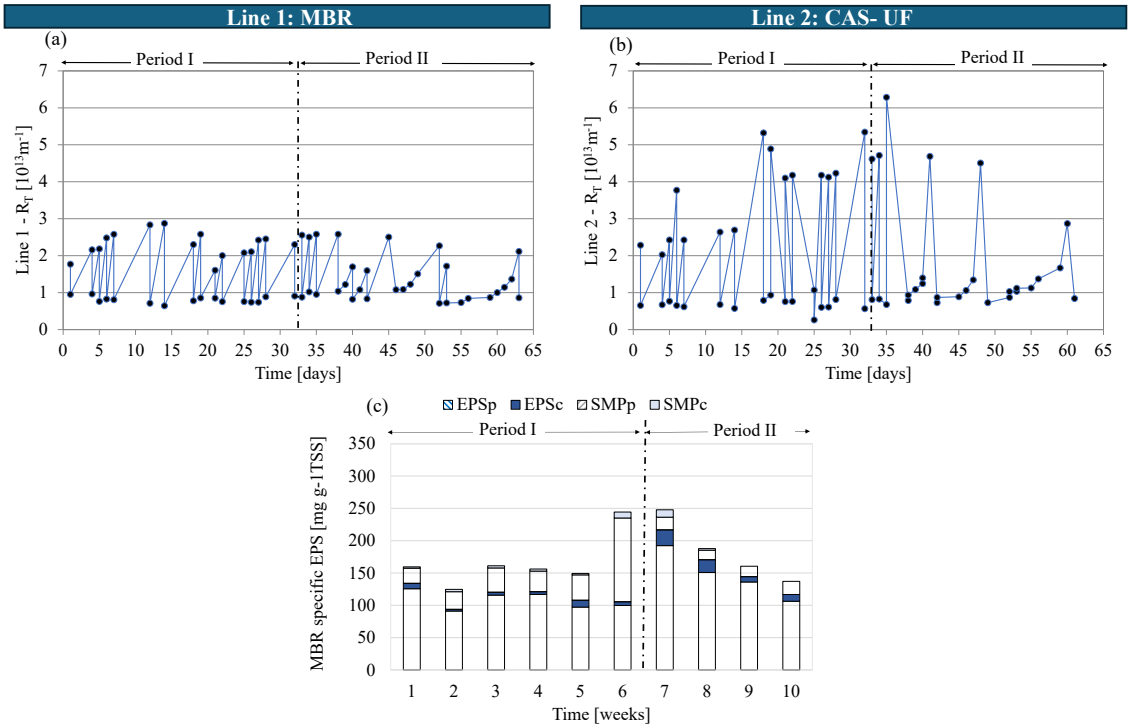

Figure 4, Total Resintance (RT) in Line I (a) and in Line II (b). EPS and SMP concentrations in Line 1 (c)

Regarding respirometry analysis, heterotrophic and autotrophic species activity was analysed. Regarding heterotrophic in Period I, the suspended biomass showed kinetic and stoichiometric values that were in line with the literature. However, the test performed on carriers did not show a significant activity of heterotrophic species, and it was not possible to process the respirogram charts. This result could be related to inhibition effects related to the intermittent aeration in Period I, which probably did not guarantee enough oxygen diffusion within the biofilm. In Period II, the suspended and attached heterotrophic species showed a good activity level. This result is confirmed by the increased COD removal rates achieved by the system in Period II. Regarding autotrophic species, no useful results were achieved in Period I, with biomass activity close to zero during the batch tests. This result could be related to the significant inhibition of nitrification that occurred in Period I, likely associated with the intermittent aeration; this result is proved by ammonia removal performance, which was very low during Period I. In Period II, continuous aeration enhanced nitrification, and the activity of nitrifying species showed moderate recovery.

4. Conclusion

This study compares the performance of two pilot plant configurations (Line I and Line II) operated in parallel in two different periods: Period I (with intermittent aeration) and Period II (with continuous aeration). In Line 1, the UF membrane operated as MBR, and Line II was composed of tertiary treatment (UF) after a CAS system connected by an IFAS reactor.The results demonstrate higher removal efficiency in Period II, especially in COD and nitrogen removal, in which Line II efficiency was slightly higher than Line I.
Period II registered lower N_2O emissions and a lower carbon footprint. This difference between Period I and II was also seen in terms of membrane fouling, which was lower in Period II than in the previous one.

Acknowledgements

This work forms part of a research project supported by a grant from the Italian Ministry of University and Research (MUR) through the Research project of national interest PRIN 2022 PNRR (D.D. n. 1409 del 14 September 2022) entitled “Innovative Membrane technologies for advanced and sustainable wastewater treatment in view of boosting a circular economy approach”.

References

[1] Ahmad, N.N.R., Ang, W.L., Teow, Y.H., Mohammad, A.W., Hilal, N., 2022. Nanofiltration membrane processes for water recycling, reuse and product recovery within various industries: A review. Journal of Water Process Engineering, 45, 102478.
[2] Christou, A., Beretsou, V. G., Iakovides, C. I., Karaolia, P., Michael, C., Benmarhnia, T., Chefetz, B., Donner, E., Gawlik, B. M., Lee, Y., Lim, T. T., Lundy, L., Maffettone R., Rizzo, L., Topp, E., Fatta-Kassinos, D.: Sustainable wastewater reuse for agriculture. Nature reviews earth & environment. (2024).
[3] Food and Agriculture Organization of United Nation (FAO) - Report on: The state of food and agriculture 2022 – leveraging agricultural automation for transforming agrifood systems. Rome, 2022
[4] Regulation (EU) 2020/741 of the European Parliament and of the Council of 25 May 2020 on minimum requirements for water reuse
[5] Gu, Y., Li, Y., Yuan, F., Yang, Q.: Optimization and control strategies of aeration in WWTPs: A review. Journal of Cleaner Production, Volume 418. (2023).
[6] Mannina, G., Alduina, R., Badalucco, L., Barbara, L., Capri, F.C., Cosenza, A., Di Trapani, D., Gallo, G., Laudicina, V.A., Muscarella, S.M., Presti, D., 2021. Water resource recovery facilities (Wrrfs): The case study of Palermo University (Italy). Water (Switzerland) 13. https://doi.org/10.3390/w13233413
[7] APHA, 2012. Standard Methods for the Examination of Water and Wastewater, Standard Methods. https://doi.org/ISBN 9780875532356
[8] Le-Clech, P., Chen, V., Fane, T.A.G., 2006. Fouling in membrane bioreactors used in wastewater treatment. J. Memb. Sci. 284, 17–53. https://doi.org/10.1016/j.memsci.2006.08.019.
[9] Boiocchi, R., Viotti, P., Lancione, D., Stracqualursi, N., Torretta,V., Ragazzi,M., Ionescu, G., Rada, E.C., 2023. A study on the carbon footprint contributions from a large wastewater treatment plant. Energy Reports 9, 274–286
[10] Di Bella, G., & Di Trapani, D. (2019). A brief review on the resistance-in-series model in membrane bioreactors (MBRs). Membranes, 9(2), 24.

Title: Transition to circular economy: the case study of Corleone wastewater treatment plant

Author(s): Alida Cosenza[1], Marika Carnesi[1], Daniele di Trapani[1], Hazal Gülhan[2], Antonio Mineo[1], Paulo Marcelo Bosco Mofatto[1] and Giorgio Mannina[1*]

[1] *Engineering Department, Palermo University, Viale delle Scienze, Ed.8, 90128 Palermo, Italy*
[2] *Environmental Engineering Department, Civil Engineering Faculty, Istanbul Technical University, Ayazaga Campus, Maslak, 34469 Istanbul, Turkey*

Keyword(s): wastewater treatments, water reuse, carbon footprint, circular economy, advanced technologies.

Abstract

The wastewater treatment plants (WWTPs) must be converted into Water Resource Recovery Facilities (WRRFs) to align with today's challenge in favour of a more environmentally sustainable approach adopting a circular economy scheme. Technological, regulatory, organizational, social and economic barriers hamper a straightforward transition. Within the EU project Wider-Uptake, a demonstration case study of Corleone's WWTP was set to break the above barriers and foster the transition to WRRFs. Innovative technologies were applied to Corleone's WWTP, such as the oxic-settling-anaerobic (OSA) system to reduce the production of waste-activated sludge. Water reuse was also applied by an ultrafiltration system, and carbon footprint was measured in view of a reduction by using mathematical modelling. The process showed that the effluent quality consistently met the Italian discharge limits. However, with the OSA process implementation, there was a decrease in ammonium removal efficiency. The sludge production in the OSA configuration decreased by 17.3% compared to the conventional activated sludge process. Nitrous-oxide measurements did not show a variation between CAS and OSA configurations.

Introduction

The urgency of sustainable development, highlighted by challenges like freshwater depletion and increasing sewage sludge production from wastewater treatment plants (WWTPs), has led to a global shift towards integrating circular economy principles into wastewater management [1]. Circular economy principles aim to reclaim water, energy, and materials from wastewater streams, mitigating environmental impacts and reshaping production systems. This transition often involves transforming traditional WWTPs into water resource recovery facilities (WRRFs), essential for sustainable water resource management [2]. Mannina et al. [3] highlighted that demonstrating case studies of resource recovery processes is vital since it helps educate the younger generations and end-users, creating awareness and convincing decision-makers to support full-scale applications.
In this context, this abstract presents the results of the Corleone WWTP case study, which is part of the EU project Wider-Uptake [4] and exemplifies the significance of plant optimization in mitigating sewage sludge production and reducing the carbon footprint (CF). This case study showcases the practical

application of the oxic-settling-anaerobic (OSA) process in sewage sludge reduction and its monitored impacts on effluent quality and greenhouse gas (GHG) emissions. Furthermore, the activation and monitoring of the plant's ultrafiltration (UF) section has been performed. The mathematical modelling has supported the optimal WWTP and UF to produce high effluent quality and increase plant sustainability.

Material and Methods

The Corleone WWTP (Figure 1) was initially designed to handle the domestic wastewater of 12,000 equivalent inhabitants, with a daily design flow rate of 3,700 m^3/d. The water treatment process includes preliminary treatment (i.e., screening and grit chamber units), biological treatment using the conventional activated sludge (CAS) process (2 aerobic tanks with a total volume of 768 m^3 each), secondary sedimentation (3 clarifiers with a total volume of 800 m^3) and disinfection. The sludge treatment involves aerobic digestion (two tanks with a combined volume of 330 m^3) and sludge dewatering (eight drying beds, each with a horizontal surface area of 40 m^2). The WWTP is not operating one aeration tank and one settler due to being underloaded compared to the initial design specifications. The effluent of the secondary clarifier was disinfected before discharge or treated by UF membrane to produce irrigation water. The UF membrane system was designed to treat a maximum flow rate of 51.35 m^3 h^{-1}. The UF system comprises two sand filters for pre-filtration, two membrane modules and a clean-in-place (CIP) reactor. Each module comprises 36 PVDF hollow fiber membranes (porosity of 0.04 µm). The membranes were operated with a cycle of 22 min of filtration (filtration flow rate, QF = 0.83 m^3 min^{-1}) and 3 min backwashing (backwashing flow rate, QB = 2.5 $m^3 min^{-1}$). Since one of the two modules is not in operation, the maximum net flowrate now equals 28 $m^3 h^{-1}$. The CIP is heated until 30-35°C. Chemical cleaning is operated every 14 days. To perform CIP, water collected inside the storage tank was firstly dosed with sodium hypochlorite (300 mg L^{-1}) and then with sulphuric acid and backwashed from the inner to the outer part of the fiber.

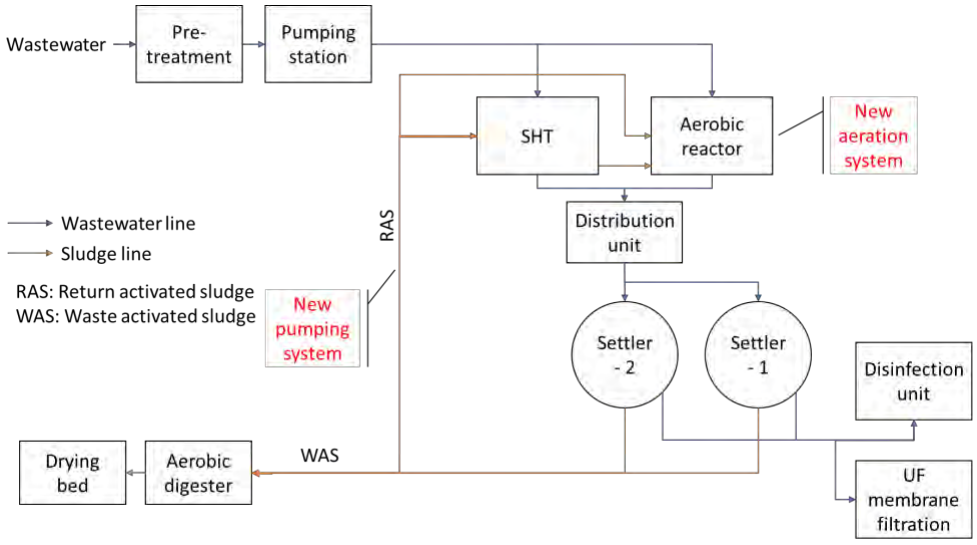

Figure 1. Corleone WWTP configuration with SHT reactor in the RAS line

Moreover, Corleone WWTP's main wastewater treatment line was upgraded with a sludge holding tank (SHT) (to realize the OSA configuration) by modifying one of the existing aerobic reactors. The

wastewater fed to the aerobic reactor was equal to 126 m^3/h (average value), whilst the effluent mixed liquor from the aerobic reactor was split into the two circular clarifiers, each characterized by a net diameter of 12 m. The fraction of the recycled activated sludge (RAS) stream (74 m^3/h) from the final settlers pumped to the SHT was defined as the internal ratio (IR). In contrast, the remaining portion was directly recycled to the aerobic reactor. Specifically, two different IRs were tested: 50 % and 100 % of the overall RAS stream, with the plant layout referred to as OSA-1 and OSA-2, respectively. Furthermore, a new aeration system with blowers enabling the application of SMART control solutions was implemented for the remaining aeration reactor. Utilizing this SMART control, the intermittent aeration (IA) was tested on full scale to make denitrification processes possible and consequently improve the quality of the effluent while reducing energy consumption. This configuration was referred to as OSA-IA. The WWTP was monitored within the Wider Uptake project. During the monitoring campaign, influent and effluent samples from each plant configuration were withdrawn two times per week in view of analysing total COD -TCOD, soluble COD - sCOD, ammonia - NH_4-N, total nitrogen - TN and orthophosphate - PO_4. The analysis was performed according to Standard Methods [5]. To evaluate the carbon footprint (CF), the GHG emissions (including direct, indirect, and derived) were quantified according to the literature [6]. Direct N_2O emissions were sampled by using a device (namely "gas hood") specifically designed and realized and it encompassed a cross-sectional area of 1.0 m x 0.9 m). The parameters required by the EU 741/2020 regulation [7] were also monitored to classify the permeate quality. The development of sustainable wastewater treatment processes requires a comprehensive understanding of the intricate interplay between various operational parameters and environmental impacts. In this context, a novel modelling approach had been devised within the Wider Uptake Project to enhance the estimation of effluent quality and GHG emissions from full-scale WWTPs. Leveraging data from the Corleone WWTP for calibration and validation, this model integrates the activated sludge model no. 1 (ASM1) [8] with modifications tailored to simulate N_2O emissions [9, 10]. Furthermore, mathematical modelling was also performed to describe the UF system behaviour and the membrane fouling with the final aim of optimizing the operation.

Results

Figure 2 shows the trend of influent, effluent, and removal efficiencies for COD and NH_4-N concentration. All configurations successfully met the regulation limits for effluent quality. When the plant layout was switched from CAS-LL to OSA process configuration, similar organic matter removal behaviour was noticed, with comparable average removal efficiencies (76 and 74% for COD in CAS-LL and OSA-1, respectively). Indeed, from Figure 2a, it can be noted that COD removals were not significantly affected by the OSA configuration. In contrast, during the OSA-2 period, a slight increase in the COD removal efficiency was observed, reaching values very close to that observed during the CAS-HL period (83%) (Figure 2a). Concerning ammonia removal, high nitrification performances were observed in both CAS-HL and CAS-LL periods, with average efficiencies of 94 and 92% and effluent NH_4-N concentrations lower than 2 mg/L (Figure 2b). With the implementation of the OSA configuration, a significant decrease in the ammonium removal efficiency was observed, with an average value of 67% in the OSA-1 period, which further decreased to 63% during the OSA-2 period (Figure 2b). One reason could be the lower biomass production in the OSA periods, which implied a lower NH_4-N metabolic assimilation. While comparing CAS and OSA-IA similar NH_4-N removal efficiencies were obtained. Regarding phosphorus removal, while the original CAS layout was not designed for it, implementing the OSA process resulted in a significant increase in phosphate (PO_4-P) removal, possibly due to improved phosphate accumulating organisms (PAOs) or denitrifying phosphate accumulating organisms (DPAOs) under OSA operation, facilitated by the alternation of aerobic/anaerobic conditions. Intensive sampling campaigns indicated that Implementing the OSA configuration did not affect N_2O emissions from the aerobic reactor (the average was 0.2 mg/L in liquid), with lower N_2O concentrations observed in the SHT (Figure 3).

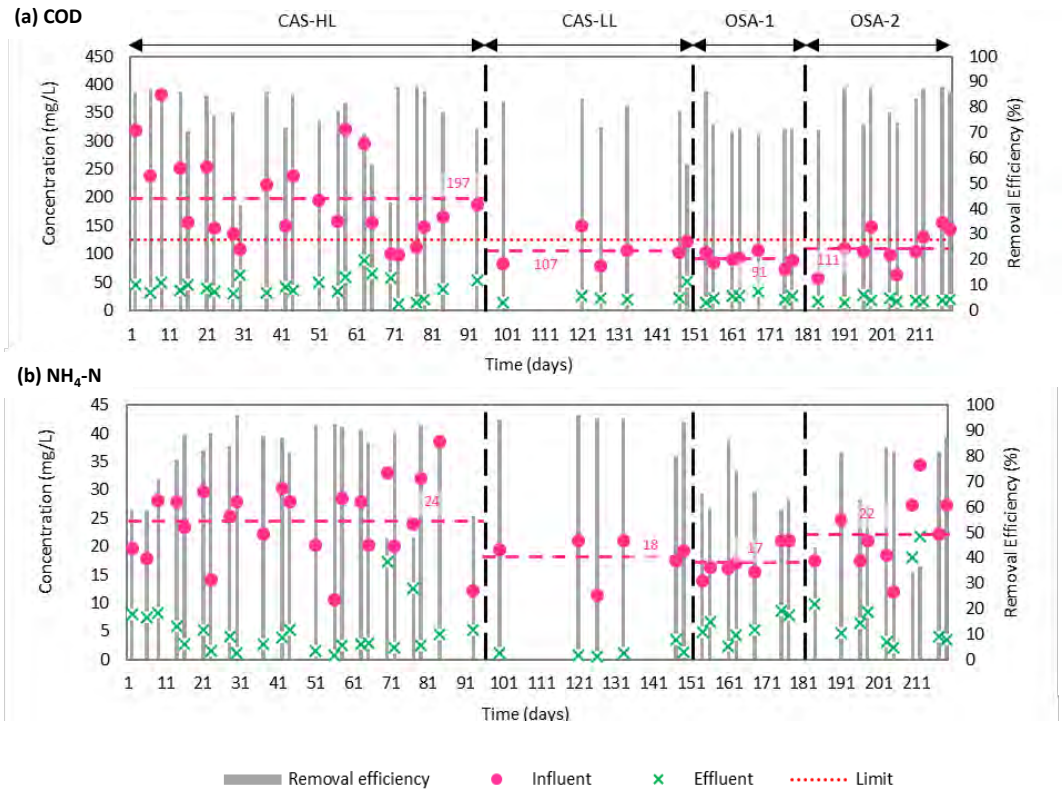

Figure 2. Influent and effluent concentrations and removal efficiencies of COD (a); and NH_4-N (c).

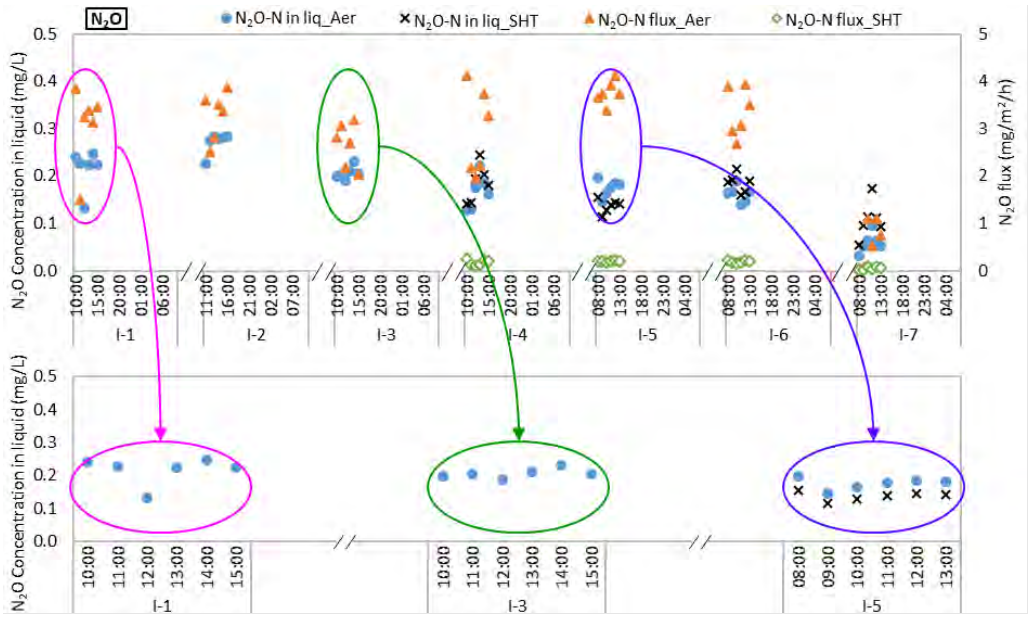

Figure 3. Intensive sampling campaign: N_2O-N concentrations in the liquid and gas samples and N_2O-N fluxes from the aeration tank and SHT.

The implementation of the OSA configuration reduced wasted sludge flow rates significantly (up to 17.3%) and improved phosphate removal (Figure 4) 11].

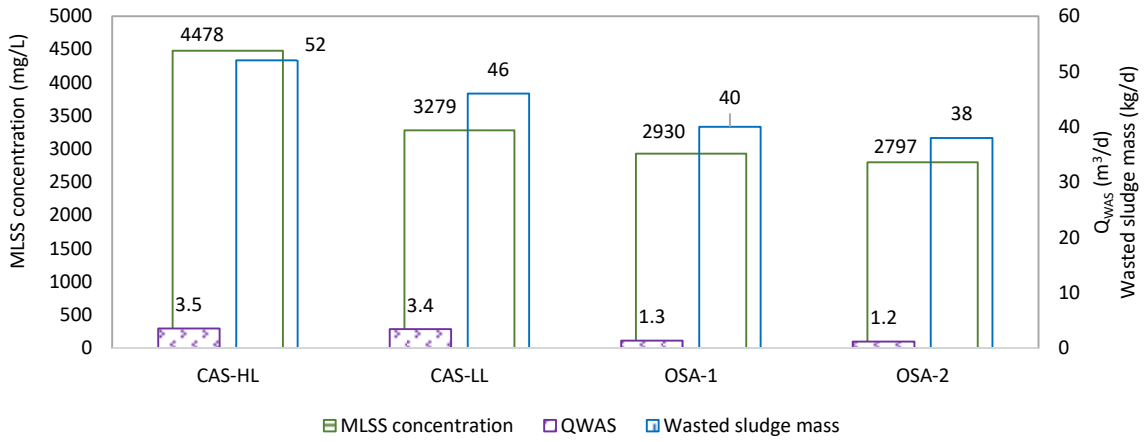

Figure 4. Averages of MLSS concentration, Q_{WAS}, and wasted sludge mass Intensive sampling campaign: N_2O-N concentrations in the liquid and gas samples and N_2O-N fluxes from the aeration tank and SHT.

The permeate effluent quality was classified as Class A or B of EU Regulation 2020/741 [7]. However, the membrane cleaning operation was a critical point of the membrane operation. In this regard, mathematical modelling of the UF system suggested the optimal chemical cleaning operation time to avoid the maximum transmembrane pressure achieved, as suggested by the manufacturer.

The dynamic simulations of the WWTP and scenario analysis underscore the complexity of optimizing wastewater treatment efficiency and sustainability. The findings highlight the importance of technological innovation and integrated decision-making processes in wastewater management.

Conclusions

In conclusion, the case study of Corleone WWTP exemplifies the imperative of optimizing WWTP for sustainable development. Through innovative approaches such as the OSA process, Corleone WWTP demonstrates tangible reductions in sewage sludge production and carbon footprint, aligning with circular economy objectives and European Commission recommendations. The implementation of the OSA configuration not only reduced wasted sludge flow rates significantly but improved phosphate removal, showcasing the potential for resource recovery and environmental stewardship. However, challenges remain, particularly in balancing trade-offs between effluent quality, energy consumption, and carbon footprint. In the future, the Water Reuse Risk Management Plans should be developed for the Corleone UF system to quantify the health and environmental risks and identify all the actions to reduce risks and improve sustainability.

Acknowledgements

This work was funded by the Project “Achieving wider uptake of water-smart solutions -- WIDER

UPTAKE" (Grant Agreement number: 869283) financed by the European Union's Horizon 2020 Research and Innovation Programme, in which Prof. Giorgio Mannina is Principal Investigator for the University of Palermo; local project website: https://wideruptake.unipa.it/.

References

[1] Mannina, G., Badalucco, L., Barbara, L., Cosenza, A., Di Trapani, D., Gallo, G., Laudicina, V. A., Marino, G., Muscarella, S. M., Presti, D., & Helness, H. (2021a). Enhancing a Transition to a Circular Economy in the Water Sector: The EU Project WIDER UPTAKE. Water, 13(7), 946. https://doi.org/10.3390/w13070946
[2] Kehrein, P., van Loosdrecht, M., Osseweijer, P., Garfí, M., Dewulf, J., & Posada, J. (2020). A critical review of resource recovery from municipal wastewater treatment plants – market supply potentials, technologies and bottlenecks. Environmental Science: Water Research & Technology, 6, 877-910. https://doi.org/10.1039/C9EW00905A
[3] Mannina, G., Gulhan, H., Ni, B., 2022. Water reuse from wastewater treatment: the transition towards a circular economy in the water sector. Bioresour. Technol. 363, 127951 https://doi.org/10.1016/j.biortech.2022.127951.
[4] Achieving wider uptake of water-smart solutions - WIDER UPTAKE" (Grant Agreement number: 869283)
[5] APHA, 2012. Standard methods for the examination of water and wastewater, 22nd edition edited by E. W. Rice, R. B. Baird, A. D. Eaton and L. S. Clesceri. American Public Health Association (APHA), American Water Works Association (AWWA) and Water Environment Federation (WEF), Washington, D.C., USA.
[6] Boiocchi, R., Viotti, P., Lancione, D., Stracqualursi, N., Torretta,V., Ragazzi,M., Ionescu, G., Rada, E.C., 2023. A study on the carbon footprint contributions from a large wastewater treatment plant. Energy Reports 9, 274–286
[7] Regulation (EU) 2020/741, 2023. Regulation (EU) 2020/741 of the European Parliament and of the Council of 25 May 2020 on Minimum Requirements for Water Reuse.
[8] Henze, M., Gujer, W., Mino, T., & van Loosdrecht, M. C. M. (2000). Activated Sludge Models: ASM1, ASM2, ASM2d and ASM3. London: IWA Publishing. https://doi.org/10.1007/978-981-10-1866-4
[9] Gulhan, H., Cosenza, A., & Mannina, G. (2023). Modelling greenhouse gas emissions from biological wastewater treatment by GPS-X: The full-scale case study of Corleone (Italy). Science of The Total Environment, 905, 167327.
[10] Mannina, G., Cosenza, A., Gulhan, H., Ng, H.Y., 2024. Ultrafiltration membrane modelling: comparison between two modelling approaches to the water reuse of Palermo and Corleone (Italy) case studies. Submitted to Chemosphere
[11] Mannina, G., Cosenza, A., Di Trapani, D., Gulhan, H., Mineo, A., Bosco Mofatto, P., 2024. Reduction of sewage sludge and N_2O emissions by an Oxic Settling Anaerobic (OSA) process: The case study of Corleone (Italy) wastewater treatment plant. Science of The Total Environment 906, 167793.

Nutrients removal in intermittently aerated IFAS systems: effects of operating conditions

Author(s): Santo Fabio Corsino*[1], Enrico Licitra[2], Michele Torregrossa[3], Gaetano Di Bella[4]

[1] *Department of Engineering, University of Palermo, Viale delle Scienze, 90128, Palermo, Italy, santofabio.corsino@unipa.it*
[2] *Department of Engineering and Architecture, University of Enna "Kore", Cittadella Universitaria, 94100 Enna, Italy, enrico.licitra@unikore.it*
[3] *Department of Engineering, University of Palermo, Viale delle Scienze, 90128, Palermo, Italy, michele.torregrossa@unipa.it*
[4] *Department of Engineering and Architecture, University of Enna "Kore", Cittadella Universitaria, 94100 Enna, Italy, gaetano.dibella@unikore.it*

Keyword(s): C/N; IFAS; Intermittent aeration; Nutrient removal; SRT.

Abstract

This study examined the impact of intermittent aeration (IA) strategy on nutrient removal in two Integrated Fixed film Activated Sludge reactors with two biofilm carriers (e.g., sponge and plastic). Short IA cycles (1 h) with a 2:1 aeration ratio showed high organic carbon and nitrification performance but lower denitrification and phosphorus removal. Adjusting the C/N ratio improved results, with longer IA cycles (2 h) enhancing performance. Sponge carriers outperformed plastic, offering better biofilm retention, nutrient removal, and resilience, simplifying IA implementation, and reducing operating costs.

Introduction

The Urban Waste Water Treatment Directive (91/271/EEC) has long regulated wastewater management in urban and industrial areas, targeting populations over 2,000 person equivalents (PE) [1]. Proposed updates, aligned with the European Green Deal, advocate secondary treatment for populations over 1,000 PE by 2030 and tertiary treatment (> 100,000 PE) for nitrogen and phosphorus removal by 2040 [2]. Conventional Activated Sludge (CAS) systems, common in small-medium WWTPs, struggle with nitrogen and phosphorus removal due to short solid retention times (SRTs). Therefore, to achieve process intensification and comply with stricter regulations, new strategies and advanced wastewater treatment technologies are necessary for retrofitting existing WWTPs. In this regard, enhancing the SRT and optimizing the existing treatment system are crucial. Advanced technologies like Intermittent Aeration (IA) and Integrated Fixed-film Activated Sludge (IFAS) should be useful to this aim. IA alternates aerated and not aerated period to allow nutrients removal processes, while IFAS combines suspended and attached biomass, aiding overloaded plants without new construction. Combining IA with IFAS enhances nutrient removal, but its optimization is crucial for achieving high performances. In this sense, design and operation of intermittent aeration systems are essential to ensure proper cycling between aerated and not-aerated phases, and it should be tailored to the influent nutrients load [3]. For this purpose, this study investigates the effect of IA cycles on nutrient removal in IFAS reactors with different biofilm carriers, simulating overloaded conditions and different nutrients loads. This research addresses a literature gap and contributes to optimizing wastewater treatment processes for regulatory compliance and environmental protection.

Materials and Methods

The study was conducted using two identical IA-IFAS systems, named plant A and plant B, at Kore Enna's Laboratory of Sanitary and Environmental Engineering. Each setup comprised a 15 L biological reactor and a 3.5 L vertical-flow settler, separated by a grid to prevent carrier passage. Plant A used plastic (polyethylene) carriers (Kaldnes™ K1) while Plant B used polyurethane sponge carriers

(LinPor™), both with a 33% filling ratio. Dedicated peristaltic pumps handled wastewater feeding and sludge recirculation, with air diffusers and mixers ensuring proper aeration and carrier/biomass suspension. Programmable Logic Control (PLC) managed aeration cycles. Synthetic wastewater, prepared based on literature [4], was adjusted for carbon, nitrogen, and phosphorous ratios. Figure 1 illustrates plant layout, while Table 1 details plant characteristics and carrier media.

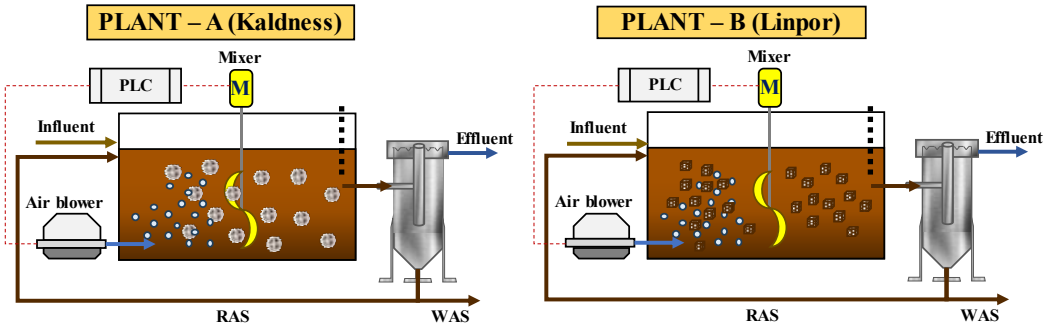

Figure 1. Plant layout

Table 1. Summary of the main characteristics of the IA-IFAS plants

Parameter	Units	Plant A	Plant B
Media carriers plant A	[-]	Kaldnes™ K1	LinPor™
Carriers material	[-]	Polyethylene	Polyurethane
Carriers size/shape	[mm]	12 mm / rings	15 mm / cubes
Media packing – plant A	[% v/v]	33	33
Number of carriers	[-]	3650	1000
Specific surface area for biofilm growth	[m^2 m^{-3}]	500	2000

The experiment lasted 200 days, divided into four periods. The first 50-day period (Period 0) involved continuous aeration to promote biofilm colonization. Subsequent periods implemented Intermittent Aeration (IA), with Periods 1 and 2 featuring 1-hour cycles (40 minutes aeration, 20 minutes not-aeration), and Period 3 doubling cycle duration (2 hours with 80 minutes aeration and 40 minutes not-aeration). The influent flow was 2 L h^{-1}, resulting in a hydraulic retention time (HRT) of 7.5 hours in the biological reactor. Nutrient ratios in the synthetic wastewater varied throughout the experiment, with Periods 0 and 1 having a C/N/P ratio of 11.7/1/1, reduced to 8.8/1/1 in Periods 2 and 3 by increasing nitrogen and phosphorous supply while keeping carbon dosage constant. To simulate plant overload, the SRT was maintained at 5 to 6 days by daily purging suspended biomass, ensuring a lower SRT than the washout SRT of autotrophic nitrifying bacteria, targeting a specific effluent ammonia concentration. All the physical-chemical analyses were performed according to Standard Methods [5]. Moreover, ammonia utilization rate (AUR) and nitrate utilization rate (NUR) assays were performed to evaluate nitrification and denitrification kinetics of both the suspended biomass and biofilm.

Results and discussion

Sponges as carriers allowed for higher biofilm concentrations (5000 mgTSS L^{-1}) compared to plastic ones (1000 mgTSS L^{-1}). Porous carriers like sponges trapped more biomass due to their greater surface area. On the other hand, plastic carriers in plant A faced more mechanical stress, limiting biofilm growth compared to sponge carriers in plant B. Any relationship was found between biofilm growth and plant operational modes in either system.

Referring carbon removal, at the beginning of the experiment, COD removal relied solely on suspended biomass due to poor biofilm growth on the carriers, achieving about 85%. When intermittent aeration was started in Period 1, Plant A experienced a slight decline in performance, taking about 35 days to regain similar COD removal as in Period 0, while Plant B continued to improve, reaching around 95% removal. This difference was attributed to higher biofilm concentration in Plant B. The transition to intermittent aeration likely reduced metabolic kinetics in Plant A due to lower electron acceptor availability, affecting COD removal temporarily. However, both plants gradually adapted, showing similar trends in Periods 2 and 3. Plant A experienced a longer initial performance decrease in Period 3, possibly due to extended anaerobic conditions within the biofilm.
Figure 2 depicts the nitrogen removal performances achieved during the experiment.

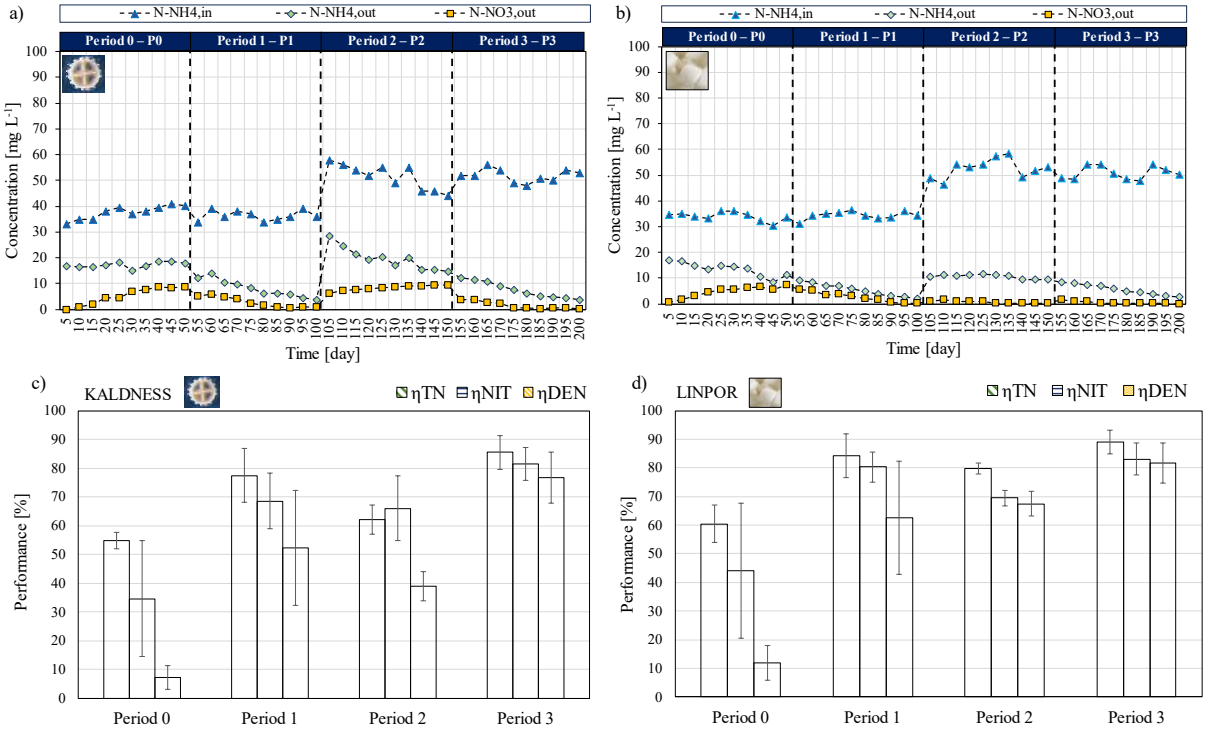

Figure 2. Trends of NH_4-N concentration in the influent, NH_4-N and NO_3-N in the effluents of plant A (a) and plant B (b). Average removals for TN, nitrification and denitrification observed in plant A (c) and plant B (d).

During Period 0, Plant A's effluent maintained a steady NH_4-N concentration at 18 mg L^{-1}, with a slight increase in NO_3-N to 10 mg L^{-1}. Nitrification commenced after 2-3 weeks with biofilm development, reaching 30% efficiency due to attached biomass. Plant B exhibited earlier nitrification due to sponge carriers facilitating biofilm growth. Denitrification was minimal but observed at the period's end. Introducing intermittent aeration in Period 1 increased total nitrogen removal efficiencies, with complete nitrification and improved denitrification (~ 60%). In Period 2, increased nitrogen load temporarily affected Plant A, while Plant B maintained stability. Period 3's extended aerated phase significantly improved nitrification and denitrification in both plants, showcasing high nitrogen removal efficiencies. Despite low SRT, both plants demonstrated high nitrogen removal efficiencies, with the sponge-based plant showing greater robustness, especially under modified operational conditions. Under optimal conditions, effluent total nitrogen concentration was well below regulatory limits for discharge into eutrophication-sensitive areas. Beginning in the experiment, plant B exhibited a slightly higher AUR of suspended biomass compared to Plant A (0.9 $mgNH_4$ $gVSS^{-1}h^{-1}$), while comparable values were

observed for biofilm AUR (0.4-0.5 $mgNH_4$ $gVSS^{-1}h^{-1}$). In subsequent periods, AUR of suspended biomass significantly increased in both plants to about 1.4 $mgNH_4$ $gVSS^{-1}h^{-1}$, likely due to the seeding effect from detached biofilm serving as continuous inoculum of nitrifying bacteria [6]. Nitrification kinetics of suspended biomass were influenced by variations in the C/N ratio and duration of aeration/non-aeration cycles. Increasing aerated phase duration resulted in slight improvement in AUR in both suspended biomass and biofilm of Plant A, while in Plant B, improvement was observed only in suspended biomass AUR, with over 25% reduction in biofilm AUR likely due to excessive biomass aging. Referring to phosphorous, during Period 0, over 90% of P removed was attributed to heterotrophs synthesis. In Period 1, under intermittent aeration, metabolism of phosphorus-accumulating bacteria (PAO) was observed. PAO's contribution was estimated at about 40%, enabling effluent TP concentration around 2 mg L^{-1}. In Period 2, despite increased influent phosphorus load, steady-state conditions were reached, with Plant B achieving over 80% removal due to higher biofilm concentration. Overall, longer non-aeration phases favored anaerobic processes, enhancing PAO-driven removal [7].

Conclusions

The findings of this research demonstrated the effectiveness of integrating IFAS systems with intermittent aeration to improve nutrient removal in overloaded plants, meeting environmental and regulatory requirements. The study emphasizes the importance of precisely controlling the intermittent aeration strategy, including adjusting cycle duration, and balancing aerated and non-aerated phases based on influent nutrient load. Additionally, sponge carriers offer benefits over plastic ones, as they enhance biofilm retention and require simpler management systems due to their superior resilience and adaptability to operational changes.

Acknowledgments

The research was carried out in the framework of the "SiciliAn MicronanOTecH Research And Innovation Center - **SAMOTHRACE**" project (MUR, PNRR-M4C2, ECS_00000022).

Part of the research was funded by the "**Smartee-Plants: Smart Energy-Efficiency wastewater treatment Plants**" project funded by "Programma Operativo F.E.S.R. Sicilia 2014/2020 l'Azione 1.1.5", Sicily, Italy.

References

[1] Directive 91/271/EEC, The urban waste water treatment directive. Available online on https://eur-lex.europa.eu/legal-content/EN/TXT/?uri=celex%3A31991L0271, (1991).
[2] European Parliamentary Research Service, Urban wastewater treatment : Updating EU rules [EU Legislation in Progress][Policy podcast], (2023) 1–3. https://epthinktank.eu/2023/03/01/urban-wastewater-treatment-updating-eu-rules-eu-legislation-in-progress/.
[3] M. Capodici, G. Di Bella, D. Di Trapani, M. Torregrossa, Pilot scale experiment with MBR operated in intermittent aeration condition: Analysis of biological performance, Bioresour. Technol. 177 (2015) 398–405. https://doi.org/10.1016/j.biortech.2014.11.075.
[4] J.J. Beun, A. Hendriks, M.C.M. Van Loosdrecht, E. Morgenroth, P.A. Wilderer, J.J. Heijnen, Aerobic granulation in a sequencing batch reactor, Water Res. 33 (1999)2283–2290.https://doi.org/10.1016/S0043-1354(98)00463-1.
[5] APHA, Standard Methods for the Examination of Water and Wastewater, 2012. https://doi.org/ISBN 9780875532356.
[6] D. Di Trapani, M. Christensson, M. Torregrossa, G. Viviani, H. Ødegaard, Performance of a hybrid activated sludge/biofilm process for wastewater treatment in a cold climate region: Influence of operating conditions, Biochem. Eng. J. 77 (2013) 214–219. https://doi.org/10.1016/j.bej.2013.06.013.
[7] P. Izadi, P. Izadi, A. Eldyasti, Enhancement of simultaneous nitrogen and phosphorus removal using intermittent aeration mechanism, J. Environ. Sci. (China) 109 (2021) 1–14. https://doi.org/10.1016/j.jes.2021.02.026.

PARALLEL SESSION: C7

Contaminated sites

Contaminated soil and water: remediation

Title: Application of an All-In-One ISCO Technology for the treatment of Monochlorobenzene, BTEX and Chloroform in groundwater at a Former Pharmaceutical Facility in Italy

Author(s): Alberto Leombruni *[1], Brant Smith[2], Mike Mueller[3]

[1] *Evonik Operations GmbH, Hanau, Germany, alberto.leombruni@evonik.com*
[2] *Evonik Operations GmbH, Hanau, Germany, mike.mueller@evonik.com*
[3] *Evonik Corporation LLC, Philadelphia, USA, brant.smith@evonik.com*

Keyword(s): Aquifer, Remediation, Injection, Monochlorobenzene, Chloroform, Hydrocarbons

Abstract

Activated Klozur® persulfate creates a multi-radical attack providing greater oxidation power capable of treating common and the most recalcitrant compounds alike. Klozur® persulfates include both sodium (SP) and potassium (KP) products. Both dissolve to provide the persulfate anion, which is typically stable for weeks to months. Sodium persulfate is highly soluble and available to react at the time of application whereas the low solubility of potassium persulfate has been observed to provide extended release of the persulfate anion over months to years. This allows immediate distribution in the subsurface with the stability providing a greater radius of influence and allowing more time to make contact and degrade a wide variety of contaminants in soil and groundwater [1], including chlorinated solvents, petroleum hydrocarbons, and PAH's. Klozur® CR, a blend of Klozur® SP (sodium persulfate) and PermeOx® Ultra (extended-release calcium peroxide), coupled with Klozur® KP has been selected as the best long-lasting treatment solution for the contaminants of this site by providing immediate treatment [2] with the Klozur® SP and extended treatment with both the PermeOx® Ultra and Klozur® KP.

Klozur technology has been successfully applied at several sites in Italy within the past few years. This presentation will discuss the broader program using specific sites as case studies. One of these specific sites was at a densely populated urban area site in the northern Italy. The site was characterized by historical contamination of various toxic compounds. The site, a dismantled former pharmaceutical facility, was impacted by the storage of Hydrocarbons and Chlorinates Solvents which have resulted in the groundwater contamination, including benzene (~ 1000 µg/L), monochlorobenzene (~ 250000 µg/L), chloroform (~ 54000 µg/L) and light TPHs (~ 16000 µg/L). In 2022, a successful pilot has been implemented injecting on site a total of 5600 kg of Klozur CR along with 1700 kg of Klozur KP in a 25% aqueous solution. In 2023, full scale has been completed applying approximately 29 MT of Klozur CR and 9 MT of Klozur KP in a 25% aqueous solution.

The combined remedy of ISCO followed by bioremediation has proven successful in treating petroleum hydrocarbon and chlorinated solvent contamination. With regard to the Northern Italy site, following 12 months after the full-scale application, the concentrations of contaminants had reached and maintained concentrations below the remediation goals in all monitoring piezometers in the treatment area. In particular, TPHs were reduced by greater than 85 percent, while MCB was reduced by greater than 95 percent. Monitoring data confirmed sustained elevation of oxidation-reduction potential (ORP) and dissolved oxygen (DO) as necessary subsurface conditions to support treatment [3].

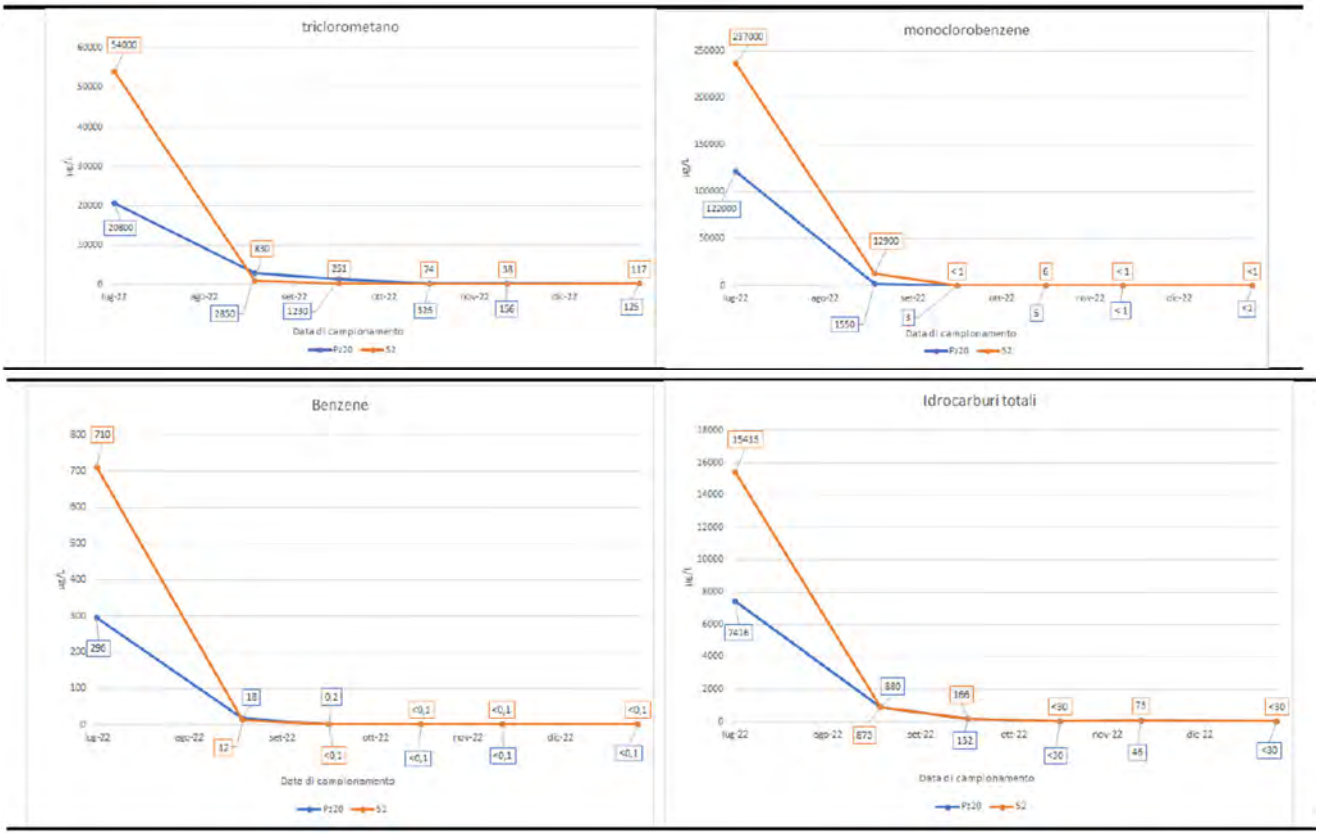

Figure 1. Post-application contaminant concentrations in the main monitoring points of the injection area

References

[1] N. Das and P. Chandran. (2010) 'Microbial Degradation of Petroleum Hydrocarbon Contaminants: An Overview.', Biotechnology Research International, Volume 2011.

[2] Joseph G. Leahy and Rita R. Colwell. (1990) 'Microbial Degradation of Hydrocarbons in the Environment', MICROBIOLOGICAL REVIEWS, Sept. 1990, p. 305-315

[3] Bruce E. Rittmann, Perry L. McCarty (2001) 'Environmental Biotechnology: Principles and Applications', McGraw-Hill, New York, NY.

Title: Advances in marine sediments remediation: performance comparison between activated carbon and single cell proteins as adsorbents in active capping for heavy metals removal in seawater

Author(s): Chiara Maraviglia*, Silvio Matassa, Alessandra Cesaro, Francesco Pirozzi

Department of Civil, Architectural and Environmental Engineering, University of Naples Federico II, Naples, Italy, chiara.maraviglia@unina.it; silvio.matassa@unina.it; alessandra.cesaro@unina.it; francesco.pirozzi@unina.it

Keyword(s): contaminants sequestration, brownfield, adsorption technology, water quality

Abstract

Marine sediments provide the largest habitat on planet earth and plays an essential role in shaping the structure and function of aquatic ecosystems, influencing both biotic and abiotic interactions within these environments [1].Unfortunately, they also serve as the primary repository for organic and inorganic contaminants in aquatic ecosystems, posing significant long-term risks to both human health and the environment.

Recent advances have highlighted the active capping as a prominent in-situ technology for contaminated marine sediments. This method involves placing a layer of a strong adsorbent clean material above the layer of contaminated marine sediments to control both sediment contamination and the transport of contaminants in the overlying water column (Figure 1). Significantly higher efficiencies are achieved when the capping layer is implemented using a selectively reactive material capable of binding or adsorbing target contaminants present in the sediment pore water [2].

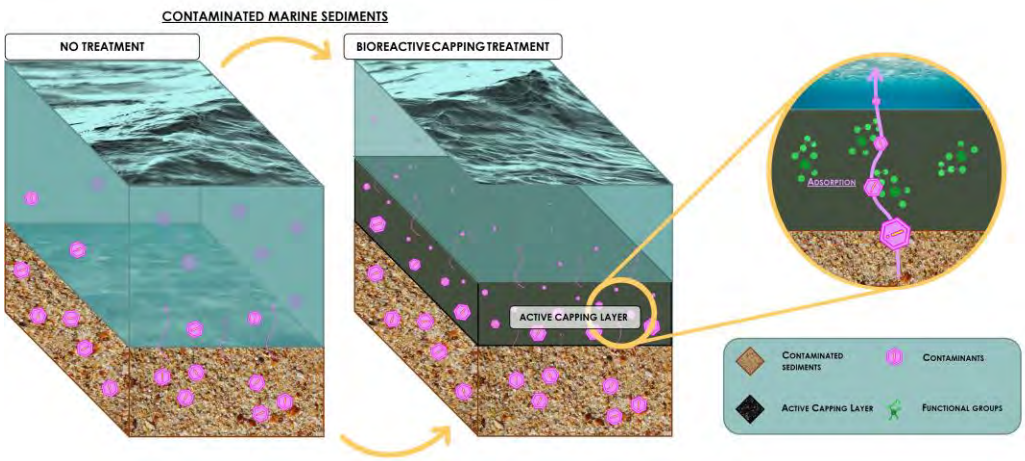

Figure 1. Active capping system scheme and mechanisms

The active capping technology is particularly suitable for multi-contamination scenarios, as it can be applied in the presence of both organic and inorganic contaminants. Its main advantage as an in-situ remediation technology lies in reducing the resuspension of contaminated sediments following their mobilization, and the consequent risk of contaminant transfer to the aquatic environment [3].

Different materials have been proposed in studies on the effectiveness of active capping [4-6], but it is not possible to determine unequivocally which materials, either alone or in combination, represent the best, as technological performances depend heavily on site-specific environmental conditions such as pH, salinity, and water currents [3].

This study focuses on single cell proteins (SCPs) as novel adsorbent material to be used in active capping system for the remediation of marine sediments contaminated by heavy metals. More specifically, SCP performances are compared to those of a conventional sorbent, namely the activated carbon, whose ability to adsorb metal ions has been largely reported [6]. Conversely, only few studies have proposed the use of protein-based materials, such as nanoparticles produced by means of the electrospinning technique from whey protein [7]. Another recent report [8] support the potential development of alternative adsorbent materials derived from proteins, due to the good encapsulation capacity of zinc ions on nanoparticles produced by desolvation in ethanol.

By elucidating the mechanisms underlying contaminant sequestration and evaluating the performance of the aforementioned materials, the upcoming findings are expected to contribute to the development of sustainable solutions for marine sediment remediation and offer practical insights for environmental practitioners and policymakers.

In the initial exploratory phase, the adsorptive capacity of commercial activated carbon (AC) and SCPs in zinc and chrome saline solutions (38 psu) was tested. As shown in Table 1, both single metals solution and their combination were considered, and two different doses of adsorbent materials were explored.

Table 1. Preliminary tests conditions

Description	Adsorbent dose [mg/L]
Zinc 150 mg/L Zinc 300 mg/L Chrome 150 mg/L Chrome 300 mg/L Zinc 75 mg/L, Chrome 75 mg/L Zinc 300 mg/L, Chrome 150 mg/L	5; 10

To this end, each test run was carried out in falcon tubes, with a working volume of 40 mL, kept in agitation for 48 hours at a speed of 70 rpm. For the study of adsorption kinetics, samples were taken after 24 and 48 hours from the beginning of the tests. The supernatant samples were analyzed to evaluate the residual concentration of zinc and chrome by means of atomic absorption spectroscopy and the adsorption efficiency was assessed as the ratio between the variation in heavy metal concentration against the control sample, measured at the same time interval, over the concentration of the control sample itself.

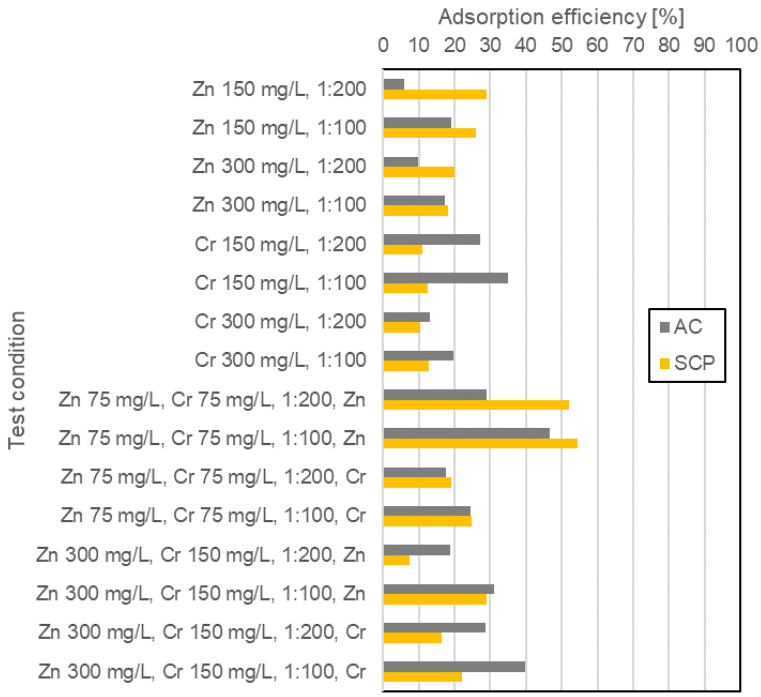

Figure 2. Adsorbent performance comparison at t=48 h

Figure 2 plots the results obtained in terms of adsorption efficiency. A high suitability of the SCPs to adsorb zinc ions is highlighted, regardless the absorbent dosages and heavy metal concentrations. SCPs were indeed observed to lead to metal removal ranging between 20% and 30%, higher than those achieved by commercial AC, whose performance do not exceed 20%. Additionally, the influence of the adsorbent material concentration, with the same zinc contamination, does not seem to significantly affect the performances for the SCPs, while increasing the adsorbent dosage in the system has a greater impact in the case of AC, with an increase in efficiency of 13% for tests carried out at a zinc concentration of 150 mg/L. However, when doubling the zinc concentration in solution, the AC performances remain more stable compared to that of SCPs, which experiences a decrease of about 8%.

Regarding the tests carried out in solutions contaminated with chrome, it can be noted that the performance of SCPs remains almost constant for varying metal concentrations, ranging around 10% for tests at a dosage of 5 g/L and around 13% for those carried out at 10 g/L. Conversely, using AC at a 5 g/L dosage, the efficiency decreases by about 50% when the contaminant concentration doubles; moreover, it increases of about 10% for both contamination conditions (i.e. 150 and 300 mg/L Cr) at the adsorbent dosage of 10 g/L.

For what concerns tests carried out in mixed metal solutions, results show that under all conditions the removal of zinc is favoured over that of chrome and adsorption efficiencies of zinc on SCPs reach levels of over 50%. Conversely, results on the chrome removal show similar efficiencies for both the materials tested.

Comparing results of these tests, carried out at a total heavy metal concentration of 150 mg/L, divided into 75 mg/L of zinc and 75 mg/L of chrome, with those of tests carried out at 150 mg/L of single metal,

an improvement of over 20% in the zinc adsorption process is evident for both dosages and materials tested. Furthermore, the variation in chrome removal in single and mixed metal solutions is different for the two tested materials as, while the chromium removal performance by AC decreases by about 10% for both tested dosages, SCPs are more efficient by the same percentage.

Finally, under the most severe multiple contamination conditions, namely in the presence of 300 mg/L of zinc and 150 mg/L of chrome, a general decrease in adsorption performance was observed for both materials compared to single metal tests. This was found to be more pronounced for zinc adsorption in the presence of SCPs, which decreases from 50% to about 20%. The only exception to this trend is found in chrome adsorption yields, which improve by about 10%.

In light of the findings from these preliminary tests, further studies are currently ongoing to better understand the mechanisms underlying the adsorption process as well as to verify the possibility to exploit any synergistic effect that the tested materials may display. This will enable the formulation of an active capping solution to maximize the simultaneous removal efficiency of the contaminants under study.

References

[1] J. S. Gray and M. Elliott, *Ecology of Marine Sediments*. Oxford University Press, 2009.

[2] D. Meric, S. M. Barbuto, A. N. Alshawabkeh, J. P. Shine, and T. C. Sheahan, “Effect of reactive core mat application on bioavailability of hydrophobic organic compounds,” *Science of The Total Environment*, vol. 423, pp. 168–175, Apr. 2012.

[3] C. Labianca, S. De Gisi, F. Todaro, M. Notarnicola, and I. Bortone, “A review of the in-situ capping amendments and modeling approaches for the remediation of contaminated marine sediments,” *Science of The Total Environment*, vol. 806, p. 151257, Feb. 2022.

[4] C. J. Hsu, Y. H. Cheng, A. Chung, Y. P. Huang, Y. Ting, and H. C. Hsi, “Using recoverable sulfurized magnetic biochar for active capping to remediate multiple heavy metal contaminated sediment,” *Environmental Pollution*, vol. 316, p. 120555, Jan. 2023.

[5] M.-Y. Ou *et al.*, “Using Mixed Active Capping to Remediate Multiple Potential Toxic Metal Contaminated Sediment for Reducing Environmental Risk,” *Water (Basel)*, vol. 12, no. 7, p. 1886, Jul. 2020.

[6] S.-J. Park, K. Kang, C.-G. Lee, and J.-W. Choi, “Remediation of metal-contaminated marine sediments using active capping with limestone, steel slag, and activated carbon: a laboratory experiment,” *Environ Technol*, vol. 40, no. 26, pp. 3479–3491, Nov. 2019.

[7] S. T. Sullivan, C. Tang, A. Kennedy, S. Talwar, and S. A. Khan, “Electrospinning and heat treatment of whey protein nanofibers,” *Food Hydrocoll*, vol. 35, pp. 36–50, Mar. 2014.

[8] İ. Gülseren, Y. Fang, and M. Corredig, “Zinc incorporation capacity of whey protein nanoparticles prepared with desolvation with ethanol,” *Food Chem*, vol. 135, no. 2, pp. 770–774, Nov. 2012.

Title: Effective Degradation of PAHs in Polluted Emulsions and Surfactant Recovery by Fenton and Solar Photo-Fenton Technologies

Author(s): Y. Moreno-Delafuente[*1], K. Ayedi[2], M. Herraiz-Carboné[1], M. Prisciandaro[2], S. Cotillas1, C.M. Domínguez[1], A. Santos[1]

1-Departamento de Ingeniería Química y de Materiales, Facultad de Ciencias Químicas, Universidad Complutense de Madrid, Avenida Complutense S/N, 28040 Madrid, España.
2-Department of Industrial and Information Engineering and Economics, University of L´Aquila, Piazzale Ernesto Pontieri, Monteluco di Roio, L´Aquila, 67100, Italy. (yaimor01@ucm.es)

Keyword(s): PAHs, Surfactant, Solar-Photo Fenton, Fenton

Abstract

In recent years, the growing presence of organic contaminants in soil and groundwater has significantly heightened scientific interest due to the potential environmental and health risks these substances pose. Among these contaminants, polycyclic aromatic hydrocarbons (PAHs) are particularly concerning due to their high toxicity and carcinogenic potential. PAHs are often found in soil and groundwater due to industrial waste discharges or ageing fuel spills [1]. These discharges percolate through the subsoil, eventually reaching groundwater sources.

Removing PAHs from surface soil and subsurface layers is challenging due to their high stability and low water solubility, classifying them as Hydrophobic Organic Compounds (HOCs). These compounds strongly adsorb onto soil or combine with other hydrocarbons to form Non-Aqueous Phase Liquids (NAPLs). Applying surfactants can enhance the solubility of PAHs, facilitating their extraction in Soil Washing processes or Surfactant Enhanced Aquifer Remediation (SEAR) techniques [2]. These methods, however, produce a contaminated aqueous emulsion that requires on-site treatment [3].

In this context, developing technologies for completely degrading organic contaminants in these polluted emulsions is crucial to minimize environmental risks. Over the past few decades, Advanced Oxidation Processes (AOPs) have been widely studied for the degradation of many organic compounds in aqueous matrices. AOPs primarily generate reactive species such as hydroxyl radicals ($OH^{\bullet}$), sulfate radicals ($SO_4^{\bullet-}$), and superoxide ($O_2^{\bullet-}$), all known for their high oxidation potential. Among these, the Fenton process stands out, utilizing hydrogen peroxide (H_2O_2) as the oxidant and iron (Fe^{2+}) as the catalyst, resulting in significant production of hydroxyl radicals [4]. This process must be conducted in an acidic environment to prevent catalyst precipitation, necessitating a subsequent neutralization stage before the treated effluent can be discharged. These constraints highlight the need for alternative methods that reduce post-treatment requirements. One promising approach involves using iron chelating agents, such as oxalate, which facilitates the complete solubilization of Fe^{2+} at a pH close to neutrality. This fact enables the formation of the ferrioxalate complex through reaction with Fe^{3+}, which can then be photochemically reduced under UV-visible light [5], forming Fe^{2+} that activates hydrogen peroxide and drives the Fenton reaction in what is known as the solar photo-Fenton process. The reactions involved in the catalytic iron cycle under solar light are summarized in Eqs [1] to [2].

$$Fe^{3+} + 3\ C_2O_4^{2-} \rightleftarrows [Fe^{III}(C_2O_4)_3]^{3-} \quad (1)$$

$$[Fe^{III}(C_2O_4)_3]^{3-} \xrightarrow{hv} Fe^{2+} + 2\ C_2O_4^{2-} + C_2O_4^{\bullet-} \quad (2)$$

This study aims to evaluate the Fenton and solar photo-Fenton processes for treating PAH-contaminated emulsions, focusing on pollutants like anthracene and benzo(a)pyrene. Sodium Dodecyl Sulfate, a commonly used surfactant in soil remediation, has been selected. The effects of varying concentrations of oxidants (60 - 230 mg H_2O_2 L^{-1}) and catalysts (2.5 - 10 mg Fe^{2+} L^{-1}) on PAH degradation were analyzed. The surfactant capacity of the treated samples was also assessed for potential reuse.

Experiments were conducted batchwise. For the Fenton process, acidic conditions (pH 2-3) were maintained in a stirred glass flask containing 0.4 L of the aqueous emulsion, thermostatized at 22°C. For solar simulation, experiments utilized a cylindrical borosilicate glass flat-plate reactor (0.4 L) with external recycling and a quartz window to ensure optimal UV-Vis light transmittance. The solar simulator acted as the radiation source, and a liquid pump recirculated the contaminated solution from a 2 L storage tank, kept at a constant temperature by a thermostatic bath. pH and temperature were continuously monitored in the storage tank, with a high recirculation rate (3 L min^{-1}), ensuring uniform conditions in the reactor and storage tank.

Parameters such as PAH and oxidant conversion, iron in solution, oxalate (in Photo Fenton experiments), pH, and remaining surfactant capacity were periodically measured throughout these experiments.

The results indicated that higher oxidant concentrations enhanced PAH degradation efficiency across both technologies (Figure 1). The Fenton process (Figure 1a) consistently achieved superior degradation rates under all conditions tested, facilitating faster PAH removal. Complete degradation of benzo(a)pyrene and over 85% anthracene degradation were achieved after 6 hours of reaction. Conversely, the solar photo-Fenton process (Figure 1b) resulted in up to 70% degradation of benzo(a)pyrene and 50% of anthracene, indicating a slower degradation rate. However, a pH close to neutrality (pH ≈ 7) was maintained throughout the 6-hour reaction period. Furthermore, the observed downward trend in the data suggests that extending the reaction time could lead to significantly higher degradation percentages.

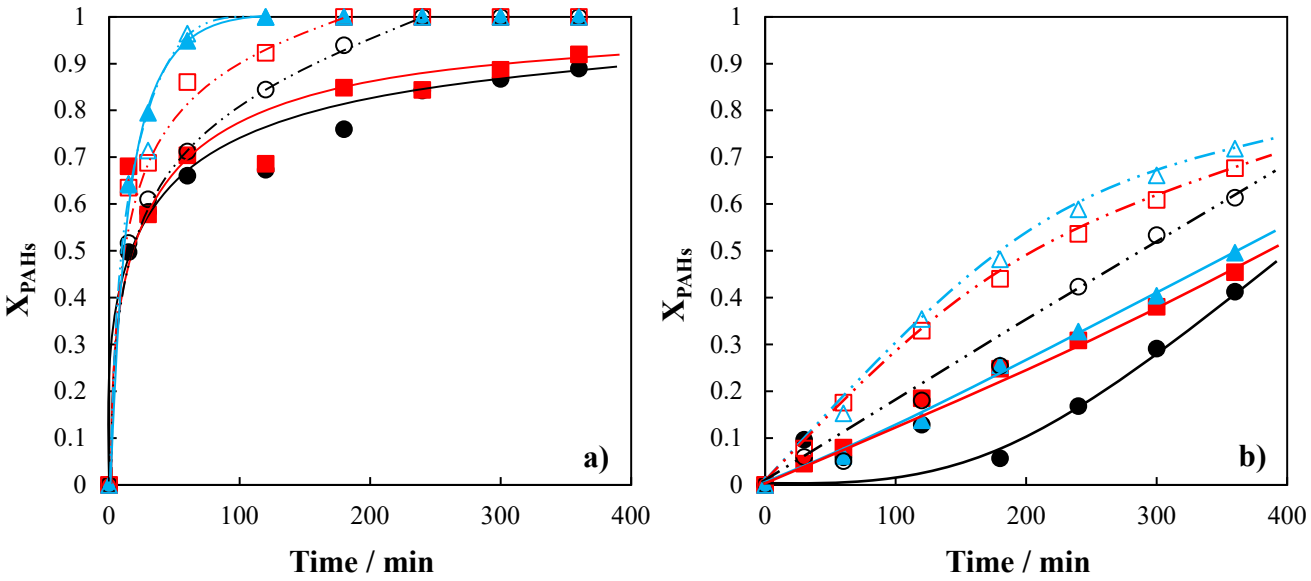

Figure 1. Influence of oxidant concentration on the degradation of PAHs during the application of **a)** Fenton process and **b)** solar-photo-Fenton process. (●) 60 mg L^{-1} H_2O_2, (■) 115 mg L^{-1} H_2O_2, (▲) 230 mg L^{-1} H_2O_2. $[PAHs]_0$ = 5 mg L^{-1} $[SDS]_0$ = 2.5 g L^{-1}. Solid symbols: anthracene; Hollow symbols: benzo(a)pyrene.

The surfactant capacity of the final samples (6 h) was evaluated by redissolving PAHs, and the values were compared with the initial capacity of SDS, which was considered 100% (Figure 2). In the Fenton process (Figure 2a), values close to 90% were observed in most cases. In contrast, in the solar-photo-Fenton process (Figure 2b), surfactant capacities up to 100% were obtained, demonstrating the reduced damage to the surfactant due to the soft conditions applied. These promising results may allow the reuse of the surfactant in subsequent soil washing processes for PAHs removal.

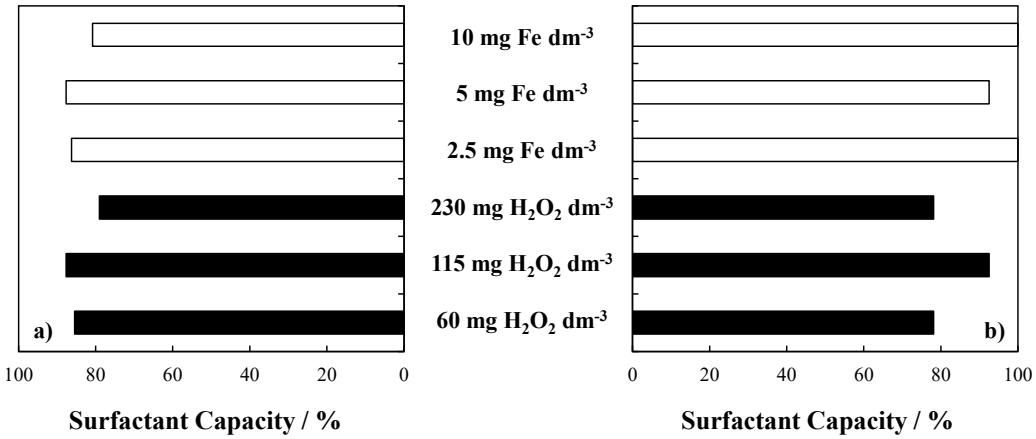

Figure 2. Surfactant capacity of SDS after the treatment of PAHs during the **a)** Fenton and **b)** solar-photo-Fenton processes. Black bars: oxidant concentration influence tests; white bars: catalyst concentration influence tests.

Acknowledgements

This research is part of the PID2022-137828OB-I00 project funded by MCIN/AEI/10.13039/501100011033 and FEDER/UE. Y. Moreno-Delafuente acknowledges the support of PREP2022-000074, funded by MICIU/AEI/10.13039/501100011033 and by the FSE+

References

[1] Janarthanam, V.A., Issac, P.K., Guru, A. Arockiaraj, J., “Hazards of polycyclic aromatic hydrocarbons: a review on occurrence, detection, and role of green nanomaterials on the removal of PAH from the water environment”, Environmental Monitoring and Assessment, 195(12), (2023).
[2] Trellu, C., Mousset, E., Pechaud, Y., Huguenot, D., van Hullebusch, E.D., Esposito, G. Oturan, M. A., “Removal of hydrophobic organic pollutants from soil washing/flushing solutions: A critical review”, Journal of Hazardous Materials, 306, 149-174, (2016).
[3] Cheng, H., Sabatini, D.A., “Separation of organic compounds from surfactant solutions: A review”, Separation Science and Technology, 42(3), 453-475, (2007).
[4] Neyens, E., Baeyens, J., “A review of classic Fenton's peroxidation as an advanced oxidation technique”, Journal of Hazardous Materials, 98(1-3), 33-50, (2003).
[5] Conte, L.O., Legnettino, G., Lorenzo, D. Cotillas, S., Prisciandaro, M., Santos, A., “Degradation of Lindane by persulfate/ferrioxalate/solar light process: Influential operating parameters, kinetic model and by-products”, Applied Catalysis B-Environmental, 324, (2023).

Title: Electrochemically assisted remediation of a highly chlorinated organic polluted sludge: a full-scale case study

Author(s): Jesús Fernandez-Cascan[1,2], Julia Isidro[2], Andrés Tiban-Anrango[2], Cristina Saez*[2], Joaquín Guadaño[3], Manuel A. Rodrigo[2]

[1] *Department of Agriculture, Livestock and Environment, Government of Aragon, Plaza San Pedro Nolasco, nº 7, 50001– Zaragoza, Spain.* Jjfernandezc@aragon.es

[2] *Department of Chemical Engineering, Universidad de Castilla-La Mancha, Campus Universitario s/n, 13071 Ciudad Real, Spain.* Julia.Isidro@uclm.es, bryanandres.tiban@uclm.es; Cristina.saez@uclm.es; Manuel.rodirgo@uclm.es

[3] *Empresa para la Gestión de Residuos Industriales SA (EMGRISA). C/ Santiago Rusiñol, 12, 28040 – Madrid.* jguadano@emgrisa.es

Keyword(s): Lindane; electrochemically assisted remediation; chlorinated hydrocarbons; volatilization; full-scale

Abstract

The lack of legal regulations regarding the industrial production of chemicals during years has contributed to the emerging of several highly polluted sites worldwide, associated to these past industrial activities. An example is the Sardas landfill, sited in Spain, that received all types of waste, including urban, chloroalkyls manufacturing waste and lindane manufacturing wastes during two decades of exploitation [1, 2]. Then, the surface sealing of the landfill was carried out with HDPE sheet, and the front of the landfill closure with a cement-bentonite screen. Additionally, in the nearness of this landfill there are many other highly polluted sites which needs for urgent actions to avoid extremely important environmental problems associated to the ageing and diffusion of hazardous pollution. This is the case of the leachate pond of the Sardas landfill, which was built to receive leachates drained from the bottom of the landfill and that after the appearance of a non-aqueous dense phase with lindane residues (DNAPL) in the ditch, also collected leachate pumped from different boreholes, which included contributions of DNAPL microdroplets.

The pond, built with HDPE sheet, has dimensions of 50x25 m^2 and accumulates a thickness of more than 0.5 m of a very plastic, adherent and difficult to handle sludge. It remains saturated, without compacting, and presents and heterogeneous distribution of contamination associated with HCH residues, from a few mg/kg to less than a dozen g/kg. Its location a few meters from the Sabiñánigo reservoir, and with the bottom less than 1 m from the alluvial, together with the time elapsed since its construction pose a serious risk, condition the possible actions on it because of the high risk of rupture of the sheet and contamination of the alluvial and the reservoir itself. Them, the dismantling of the pond is a critical operation, with a very high risk of affecting groundwater and ultimately the Sabiñánigo reservoir.

Considering the exposed background, this works proposes the use of electrochemically assisted technology for the dismantling of the leachate reservoir of the Sardas landfill. It is based on previous studies concerning the transport of lindane and other compounds contained in the dump and pond under the application of electric fields [3,4]. The electrokinetic process is intended to modify the texture of the sludge, its stabilization to geomechanical effects to facilitate its handling and extraction, enhancing to the extent that the degradation of chlorinated organic pollutants present in the sludge is compatible with this effect. At this point it will be important to consider not only the electrokinetic processes that may take place in the sludge, but also the magnitude of non-electrokinetic processes such as soil heating, which on a real scale can become the main mechanism.

To achieve the global technical objective, this work aims 1) to determine the mobility of pollutants in the sludge by the action of electric fields and the effect of the main manipulable variables (electric field, type of surfactant used as flushing fluid, type of electrodes), and 2) to verify at real scale (TRL7) the electrochemically-assisted remediation strategy of the sludge that allows the decontamination of the sludge in the pond and the textural improvement to facilitate the extraction of the sludge.

Two series of tests have been carried out: 1) bench scale tests in cells of 50 liters of capacity, to confirm the mobility of water and pollutants in the sludge under the application of electric fields using different electrodes and 2) a full-scale electrochemically assisted remediation test of 500 hours of operation in an enclosed area of 5 x 5 m^2. The move to a field scale in this type of treatment poses a significant engineering challenge due to the lack of references and the huge size of the polluted site. A floating platform with a plastic barrier was installed to enclose the area of treatment. This floating structure also supported the bubble chamber to isolate and facilitate the capture of the gases generated. The outer perimeter was isolated by a simple sheet piling to prevent the entry of water from the outside. The need of pumping was evaluated to prevent the leachate from exceeding the height of the sheet pile. Nine cylindrical carbon iron electrodes were inserted in the sludge and six different electric configurations were used. They were mechanized with grooves to allow the accumulation of the liquid removed from the sludge. Figure 2 shows the picture of both experimental systems.

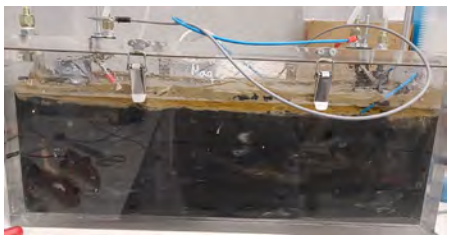

Bench scale reactor (50 dm^3)

Full scale prototype (12.5 m^3)

Figure 2. Electrochemically assisted remediation plants.

Results shown that electric fields applied to a highly polluted sludge in bench and full-scale tests promoted a considerable transport of water and pollutants, which were comparable to those observed in the treatment of silts with equivalent electric fields. Additionally, the addition of surfactants and high current densities seem to be detrimental for the performance of the further full-scale remediation, as uncontrolled dehydration was promoted. The addition of surfactant to the water reduced its mobility and does not improve the transport of pollutants, which is likely to be attributed to the lack of electrophoretic mobility of micelles. Maximum and average electro-osmotic fluxes ranged from 0.71 to 7.83 cm d^{-1} and 0.23 to 0.62 cm d^{-1} respectively, in both the bench and full-scale tests. The use of graphite electrodes induced higher volatilization of water, acidity in the surroundings of the anode and dehalogenation of chlorinated hydrocarbons, whereas iron electrodes enhanced the electrokinetic transport of water and reduced the acidification, which are critical aspects for the remediation of real sludges. Table 1 shows the COC removal attained with iron electrodes at two different cell potential (1 and 2 V/cm).

Table 1. Results of electrokinetic tests carried out with iron electrodes.

Conditions	Initial COC in sludge (mmol)	Final COC in sludge (mmol)	COC mobilized by electrokinetic transport (%)	COC volatilized (%)
1 V/cm	320.75	231.59	< 0.1	27.80
2 V/cm	284.71	39.00	< 0.1	86.30

Volatilization of the pollutants was determined to be the most important remediation mechanism in the treatment of this sludge, even more than electrokinetic mechanisms and dehalogenation. This is explained by the high temperatures that can be reached during the operation of full-scale tests. However, this also represents a critical risk, as the HDPE liner can be damaged, and this is a very critical parameter to be controlled during operation.

Finally, this work has allowed to delineate the primary components and auxiliary services that constitute an EKR and to integrate them into a control system that monitors key parameters indicative of the proper functioning of the eletrokinetic, electrochemical and physical mechanism involved in the overall process. Additionally, strict operational protocols and safety measures that are essential when conducting experiments at real industrial site have been established.

Acknowledgements
This work comprises the research project PID2022-140113OB-I00 granted by MCIN/ AEI/10.13039/501100011033/ and “Unión Europea NextGenerationEU/PRTR”. Government of Aragon is also grateful for providing the actual samples of contaminated waste used in this work and for support in analytical characterization.

References

[1] Santos A., Fernández J., Guadaño J., Lorenzo D., Romero, “A. Chlorinated organic compounds in liquid wastes (DNAPL) from lindane production dumped in landfills in Sabiñanigo (Spain),” Environmental Pollution, 242, 1616 (2018).
[2] García-Cervilla R., Romero A., Santos A., Lorenzo D. “Surfactant-Enhanced Solubilization of Chlorinated Organic Compounds Contained in DNAPL from Lindane Waste: Effect of Surfactant Type and pH,” International Journal of Environmental Research and Public Health, 17(12), 4494 (2020).
[3] Fernández-Cascán J., Isidro J., Guadaño J., Sáez C., Rodrigo M. A. “Electrochemically assisted transport of chlorinated hydrocarbons from aged to clean silt,” Electrochimica Acta, 451, 142297 (2023). https://doi.org/10.1016/j.electacta.2023.142297
[4] Fernández-Cascán J., Isidro J., Guadaño J., Sáez C., Rodrigo, M. A. “Electrochemically-assisted remediation of silt polluted with aged HCHs,” Electrochimica Acta, 464, 142934 (2023).

Title: Effect of Electric Field Intensity and Polarity Reversibility on the Transport of Hexachlorocyclohexanes in Contaminated Real Silt by Electrokinetic Techniques

Author(s): Gebran Bou-Habib[1], Ángela Moratalla*[1], Julia Isidro[1], Jesús Fernández-Cascán[2], Joaquín Guadaño[3], Manuel A. Rodrigo[1], Cristina Sáez[1]

[1]Department of Chemical Engineering, University of Castilla-La Mancha, Ciudad Real, Spain, angela.moratalla@uclm.es.
[2]Department of Agriculture, Livestock and Environment, Government of Aragon, Zaragoza, Spain, jfernandezc@aragon.es.
[3]Industrial Waste Management Company S.A., EMGRISA, Madrid, Spain, jguadano@emgrisa.es.

Keyword(s): Electrokinetic remediation, real contaminated silt, chlorinated organic compounds, hexachlorocyclohexanes

Abstract

In recent years there has been a great effort to develop effective remediation technologies for soil contaminated with hazardous substances. One of the main problems is the remediation of soils contaminated with synthetic pesticides, given their potential environmental and health impacts. The cause of this type of contamination is usually caused by accidental spills during the manufacturing process or uncontrolled dumping of waste. Hexachlorocyclohexane (HCH), an organochlorinated pesticide widely used in recent decades, has caused widespread contamination in various environmental sites, such as groundwater, soil and air, due to its volatility, solubility and long-range atmospheric transport capacity. Among them, worth to highlight the case of Sabiñánigo (Huesca) in north of Spain, where a company involved in the production of this pesticide operated there during almost two decades in the last century. The process produced a huge amount of wastes, associated with the low efficiency in the production of the active pesticide, and were buried for years in the landfills of Sardas and Bailin (Sabiñanigo). Thousands of tons of HCH and derivatives were aged for years [1]. Consequently, proper management and remediation of HCH-contaminated areas are of utmost importance.

In this regard, electrokinetic treatment has emerged as a good alternative. This treatment involves applying electric fields between anodes and cathodes inserted into polluted soil to transport pollutants through mechanisms such as electro-osmotic flux drag, electromigration (for pollutants with ionic groups) or electrophoresis (when flushing with surfactants fluids). Electric field intensity has been shown to be one of the key parameters in soil electrokinetic remediation, as higher electric field corresponds to higher expected rates of electrochemical processes generating acidic and basic fronts, as well as the rate of all electrokinetic processes. On the other hand, polarity reversibility can be an interesting strategy when transport of organic pollutant is very slow because it can help to mobilize pollutants for interaction with other reagents [2-6]. However, scaling up electrokinetic applications presents challenges due to the complexity of the control mechanisms involved. In many full-scale applications, ohmic heating often becomes the primary removal mechanism, where organics are volatilized and subsequently need appropriate management [7-9].

Considering this background, the present work aims to study the mobility of HCH and chlorinated organic compounds (COCs) in the aged and contaminated silts from the Sardas landfill and to assess the suitability of electrochemically assisted remediation technologies for the effective removal of highly contaminated sites. Thus, the effect of the intensity of the electric field and polarity reversibility on the treatment of these samples were studied.

For this research, soil samples were collected from three boreholes drilled in the alluvial area of the Sardas landfill, at depths ranging from 9.5 to 12 meters. The complete characterization of the soil was reported elsewhere [1]. In this soil, a silty layer contaminated with HCH and other COCs was identified. An additional sample was obtained from a central borehole, and it was utilized to analyze the initial concentration of HCH and COCs in the silty soil. To ensure similarity in soil and COCs composition, the samples were taken as close as possible to where the drilling machine could operate effectively. These samples were assembled with two compartments of standard PVC materials, as shown in Figure 1.

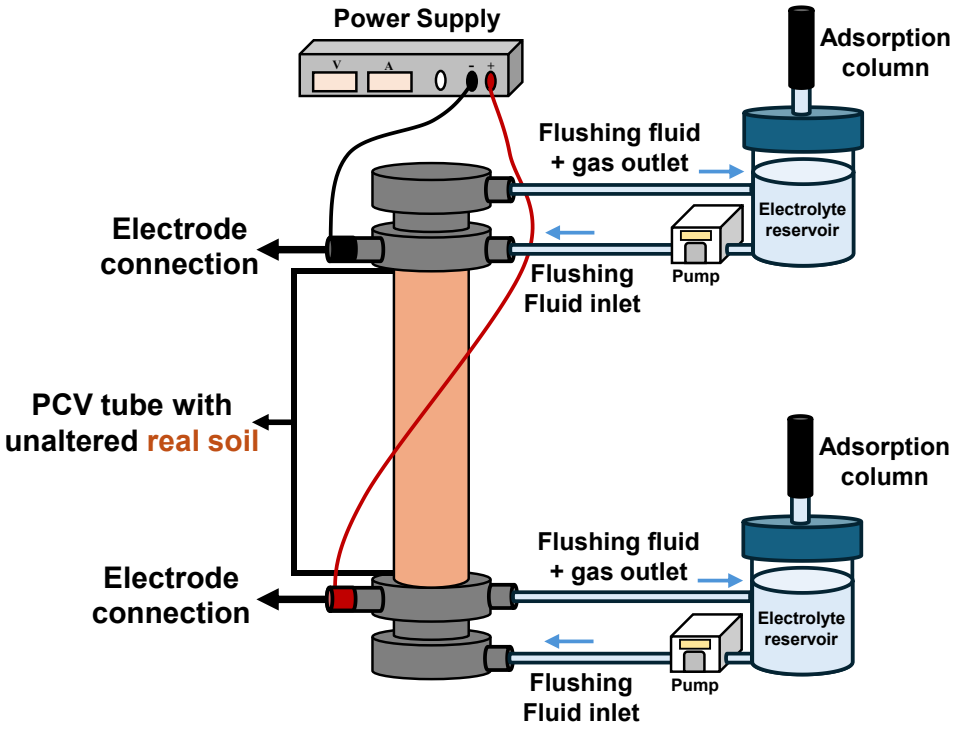

Figure 1. Experimental setup of electrokinetic remediation.

Thus, the experimental setup consists of two electrode chambers, one anodic and the other cathodic, alongside two reservoir tanks for water addition and collection, facilitating the electroosmotic flow from anode to cathode using tap water from the site served as the flushing fluid. Graphite was utilized for the anodes, while stainless steel was employed for the cathodes. Furthermore, a system of adsorption columns with activated carbon was included to retain organic compounds that could volatilise during the process. Throughout the operation, aqueous samples were extracted daily from the electrode chambers to monitor diverse physical and chemical parameter and organic pollutants. Both ends of each soil column were characterized before initiating each test, and a comprehensive post-mortem analysis of the entire soil column and the activated carbon (where the gases were retained) were conducted at the end of each test.

The experimental conditions are shown in table 1. On the one hand, three out of the six loam unaltered samples obtained during borehole drilling were selected for characterizing the influence of electric field intensity. In this process, the silt within the reactors was subjected to electric fields of 1.0, 2.0, and 4.0 V cm^{-1} (Experiment 1, 2 and 3, respectively) for a duration of one month, with anodes and cathodes positioned at the sample boundaries. Regarding the reversibility tests (Experiment 4, 5 and 6), an electric field of 1 V cm^{-1} was selected. In addition, a concentration of 15 g/L of sodium dodecyl sulphate (SDS) was incorporated into the flushing fluid as an anionic surfactant to enhance the mobilization and removal of HCH and COCs. To investigate the effect of SDS, in one silt sample (Experiment 4) polarity reversibility was not applied, while in the other two (Experiments 5 and 6) polarity was reversed every 7 days or every 15 days, respectively.

Table 1. Test parameters.

Study	Experiment nº and treatment time	Electric field	Reverse polarity time	Flushing fluid
Influence of electric field intensity	1 (30 days)	1 V/cm	-	Tap water
	2 (30 days)	2 V/cm	-	Tap water
	3 (30 days)	4 V/cm	-	Tap water
Influence of polarity reversibility	4 (30 days)	1 V/cm	-	SDS
	5 (30 days)	1 V/cm	15 days	SDS
	6 (30 days)	1 V/cm	7 days	SDS

The results indicate that higher electric field strengths lead to greater current intensities between electrodes and increased mobilization of electrolyte volumes. This results in average electroosmotic fluxes of 0.51, 0.72, and 1.47 cm/day for electric fields of 1.0, 2.0, and 4.0 V/cm, respectively, representing a consistent value of 0.3279 V/day. Changes in HCH and COCs were insignificant, with postmortem analysis revealing variability in concentrations compared to the initial sample silt and concentrations collected in wells and gas adsorption columns totalling less than 1.18E-2% for 1.0 V/cm, 2.93E-2% for 2.0 V/cm, and 6.92E-3% for 4.0 V/cm. However, what seems to be very important was the change in the number of chlorine substitutions in the cyclohexane molecules. The magnitude of the changes becomes larger as the electric flow increases passing from 5.55 down to 4.15 at 1.0 V cm^{-1}, 4.37 at 2.0 V cm^{-1} and 3.38 at 4.0 V cm^{-1}. This indicates the presence of a complex mixture of heptachlorocyclohexanes, HCH, pentachlorocyclohexenes, pentachlorobenzene, tetrachlorobenzenes, trichlorobenzenes, dichlorobenzenes, chlorobenzene and other aromatics compounds.

Regarding the impact of electric field reversibility and SDS addition, the addition of SDS did not demonstrate any effect on pollutant transport to the electrode wells, with collected concentrations being less than 0.1% of the total load in the raw loam and the concentration of COCs collected in the gas collection system were also negligible. This indicates that SDS is not able to solubilise and transport to the electrolyte compartment even the contamination in the proximity of these compartments and, therefore, that contrary to what has been found with respect to the transport of the same type of contaminant in clean matrices, ageing leads to a strengthening of the interaction between contaminants and loam. However, dehalogenation was observed when the polarity reversibility was applied, particularly evidenced by a significant decrease in cyclohexane molecule chlorination from 5.31 to 4.93 after two inversions (every 15 day), and further down to 3.87 after four inversions (every 7 day). This dehalogenation is important because the toxicity of the chlorinated cyclohexanes decreases with the number of chlorine substitutions. As the hazardousness of the species decreases importantly with the number of chlorine substitutions, electrokinetic treatment could help to decrease the hazardousness of

COC-contaminated soils. Therefore, it is proposed as a viable technological alternative for the treatment of sites highly contaminated with COCs. The technology developed in this study can serve as a reference for future research and management of other contaminated soil sites.

References

[1] J. Fernández, M.A. Arjol, C. Cacho, POP-contaminated sites from HCH production in Sabiñánigo, Spain, Environmental Science and Pollution Research, 20, 1937-1950 (2013).
[2] R. Ghobadi, A. Altaee, J.L. Zhou, E. Karbassiyazdi, N. Ganbat, Effective remediation of heavy metals in contaminated soil by electrokinetic technology incorporating reactive filter media, Science of The Total Environment, 794, 148668 (2021).
[3] E. Martens, H. Prommer, R. Sprocati, J. Sun, X. Dai, R. Crane, J. Jamieson, P.O. Tong, M. Rolle, A. Fourie, Toward a more sustainable mining future with electrokinetic in situ leaching, Sci Adv, 7 (2021).
[4] J. Vidal, M. Carvela, C. Saez, P. Cañizares, V. Navarro, R. Salazar, M.A. Rodrigo, Testing different strategies for the remediation of soils polluted with lindane, Chemical Engineering Journal, 381, 122674 (2020).
[5] Y. Wang, A. Li, C. Cui, Remediation of heavy metal-contaminated soils by electrokinetic technology: Mechanisms and applicability, Chemosphere, 265, 129071 (2021).
[6] J.M.M. Henrique, J. Isidro, C. Saez, R. Lopez-Vizcaíno, A. Yustres, V. Navarro, E.V. Dos Santos, M.A. Rodrigo, Combining Soil Vapor Extraction and Electrokinetics for the Removal of Hexachlorocyclohexanes from Soil, ChemistryOpen, 12, e202200022 (2023).
[7] R. López-Vizcaíno, C. Risco, J. Isidro, S. Rodrigo, C. Saez, P. Cañizares, V. Navarro, M.A. Rodrigo, Scale-up of the electrokinetic fence technology for the removal of pesticides. Part I: Some notes about the transport of inorganic species, Chemosphere, 166, 540-548 (2017).
[8] R. López-Vizcaíno, C. Risco, J. Isidro, S. Rodrigo, C. Saez, P. Cañizares, V. Navarro, M.A. Rodrigo, Scale-up of the electrokinetic fence technology for the removal of pesticides. Part II: Does size matter for removal of herbicides?, Chemosphere, 166, 549-555 (2017).
[9] J. Fernández-Cascán, J. Isidro, J. Guadaño, C. Sáez, M.A. Rodrigo, Electrochemically-assisted remediation of silt polluted with aged HCHs, Electrochimica Acta, 464, 142934 (2023).

Acknowledgements

This work has been supported by MCIN/AEI/10.13039/501100011033, the European Union (European Regional Development Fund) through the project PID2022-140113OB-I00.

PARALLEL SESSION: D7

Municipal and industrial waste

Anaerobic digestion

Pre-treatment strategy for polylactic acid biodegradability enhancement in anaerobic digestion process

Authors: Alberto Ferraro[1], Davide Giandomenico[1], Raffaele Morello[1], Danilo Spasiano[1], Umberto Fratino[1]

[1] *Dipartimento di Ingegneria Civile, Ambientale, del Territorio, Edile e di Chimica, Politecnico di Bari, via E. Orabona 4, 70125 Bari (BA), Italy, {alberto.ferraro, raffaele.morello, danilo.spasiano, umberto.fratino}@poliba.it, d.giandomenico@studenti.poliba.it*

Keywords: polylactic acid*, anaerobic digestion, pre-treatment, biodegradation*

Abstract

Since several decades, on a global scale, plastic materials manufacturing indeed represents one of the most productive industrial activities. In fact, from 1950s to the current days, a significant plastic production enhancement has been recorded with values increasing from 1.5 milliontonnes up to almost 400 milliontonnes [1].
Plastics are also involved in a wide range of manufacturing applications for common consumer goods and products (e.g. packaging, bags, utensils, etc.) due to their advantageous features such as chemical resistance, durability, proper malleability. However, some of these characteristics also provide concernment due to the adverse effects that can result on the environment once plastics are disposed as end-waste products. The resistance of conventional petroleum-based plastics to biodegradation phenomena in the environment leads to their very slow break down (over decades or centuries) [2]. The resulting wastes accumulation can provide several pathways for the contamination of different environmental compartments. For instance, anthropogenic plastic littering or waste disposal can represent a significant land-based source for marine environment contamination due to weather phenomena and surface water run off [3]. Besides, direct marine environment contamination by plastic materials can also be caused by anthropic activity such as fishing.
Based on their size, plastics can be classified as macroplastics and microplastics (< 5 mm). Despite both macro- and microplastics are widely found in the environment, the second group can be more easily ingested by aquatic species, biomagnify along trophic levels and represent a potential carrier of other pollutants in the food chain [4].
Starting from the last two decades, one strategy addressing to the environmental negative impacts of nonbiodegradable conventional petroleum-based plastics has been the production of alternative material identified as bioplastics. In general, the plastic materials classified as bio- include both biodegradable plastics (e.g. polycaprolactone, polyethersulphone, etc.) and bio-based plastics which are produced from biomasses or renewable resources [5]. The bio-based plastics can be either biodegradable (e.g. polylactic acid, polyhydroxybutyrate, etc.) or not biodegradable (e.g. polyethylene, nylon 11, etc.) [6]. Accounting for the biodegradable ones, these plastics can indeed be considered more environmentally sustainable products compared to the conventional material. Despite this, some drawbacks related to the bioplastics are nowadays also highlighted. For instance, bioplastics production requires higher process costs and the resulting material is generally characterized by lower mechanical properties than petroleum-based plastics [7]. Furthermore, landfilled bioplastics can undergo to natural decomposition by microorganism over time resulting in greenhouse gas emissions due to the products

from the biological degradation. By considering a complete bioplastic degradation in landfills, emissions from this waste end-of-life can achieve a value equal to the 80% of its life-cycle greenhouse emissions including the biogenic one [8].
Accordingly, proper strategies for the management of bioplastic wastes are fundamental in order to limit potential environmental impacts. A viable approach could be represented by degradation through biological treatments as alternative to conventional incineration or recycling. In this perspective, anaerobic digestion (AD) indeed represents a suitable process for potential energy recovery from biodegradable plastics decomposition. However, biodegradability rate of bioplastics can significantly differ according to the physical-chemical properties of the material (surface areas, molecular weight, crystallinity, etc.) [9] potentially hindering the AD effectiveness. Among different bioplastics, polylactic acid (PLA) has been thoroughly investigated as biodegradable substrate in AD however displaying slow degradation rate with consequent long-lasting treatment time required. For instance, it was observed that mesophilic AD carried out for over 150 days resulted in a 25% PLA degradation while higher biodegradation (above 70%) was achieved in over 60 days but through thermophilic condition [10,11]. Nonetheless, PLA is still widely used in many production fields such as food packaging, medical equipment, 3D printing, etc. [12]. Also, significant increase of the PLA production rate is still expected in future according to reported forecasts [13].
According to this, several studies investigated the effects of different pre-treatments strategies on the PLA biodegradability increase. For instance, alkaline pre-treatment of PLA resulted in an increased biodegradability rate due to the significant hydrolysis effect on the plastic compound [14]. A study focusing on a cold plasma treatment on PLA for food packaging also displayed an increase of the material hydrophilic nature and shorter molecular chains both providing better conditions for microbial attachment on the treated PLA surface and fragmentation [15]. Instead, for an alternative approach based on PLA co-digestion with food waste, a polymer weight loss of 53% in mesophilic AD conditions was reported [16].
In this perspective, the present work focused on the application of an AD process to test the potential biodegradability of PLA and on the efficiency of an alkaline pre-treatment for the enhancement of the plastic material degradation rate. The AD tests were simulated at lab-scale in batch condition and mesophilic temperature (35 °C) in glass bottles with total volume of 250 mL. For each test, digestate from a municipal wastewater treatment plant was used as inoculum while PLA filaments for 3D-printing (PLA Ingeo 850, white colored, Eolas Prints) were used as substrate. The PLA filament was characterized by a diameter and density of 1.75 mm and 1.24 g cm^{-3}, respectively.
A first set of experiments (SET-1) was carried out to compare the AD process efficiency between a control test (only digestate) and not pre-treated PLA. In order to investigate more in detail how the plastic material characteristics could influence the process, the biodegradability rate was tested on both the raw PLA filament and extruded PLA stick samples. The latter were obtained from the 3D-printing (195 °C) of plastic sticks by processing the initial raw PLA. Then, SET-1 was characterized by three tests namely control (C1), not-pretreated raw PLA (nr-PLA), and not-pretreated extruded PLA (ne-PLA) tests. For each batch test a digestate working volume of 150 mL was used which resulted in a total volatile solid (VS) content of 1.77 g. In both NR-PLA and NE-PLA tests, 0.65 g of plastic filament and stick were respectively used. This total amount was provided through 6 pieces of filaments and sticks in both corresponding tests. With the addition of 0.65 g of PLA, based on a theoretical value of 1.5 gCOD $gPLA^{-1}$, each test was characterized by a food/microorganisms (F/M) ratio equal to 0.55 gCOD gVS^{-1}. In a second set of experiments (SET-2), the comparison was still carried out among a batch AD control (C2) and tests with raw (pr-PLA) and extruded PLA (pe-PLA). However, in SET-2, both plastic substrates were pre-treated through alkaline washing prior to undergo to the AD process. Compared to SET-1 experiments, equal amount of digestate was also used for SET-2 as well as same PLA mass and number of plastic fragments provided in the corresponding tests.

The alkaline pre-treatment was performed on PLA fragments involved in SET-2 tests through a 2.5% concentrated (w/w) $Ca(OH)_2$ solution. Both raw and extruded PLA was immerged in 13 mL of the $Ca(OH)_2$ solution and the pre-treatment was carried out at 70 °C for 72 h. After the pre-treatment, the PLA fragments masses were measured. Moreover, the alkaline solutions were characterized in terms of COD content in order to assess possible increase of the soluble COD due to the plastic materials degradation. Finally, the pH of each 13 mL alkaline solution was adjusted, after the pre-treatment steps, to neutrality with HCl. Then, pre-treated raw and extruded PLA with the corresponding neutralized $Ca(OH)_2$ pre-treatment solutions were added to the digestate aliquots to complete the composition of the pr-PLA and pe-PLA tests, respectively. At different experimental times, produced biogas volumes from each reactor were measured through water volume displacement method. Then, gas samples were collected after each biogas volume measurement for further CH_4 and CO_2 content determination. The gaseous compound measurement was carried out by gas chromatography using a 8890GC System (Agilent) equipped with a thermal conductivity detector (TCD). For both SET-1 and SET-2, all the experiments were performed in triplicates.

Results from SET-1 experiments (**Figure 1a**) showed no significant differences among the performed tests in terms of biogas production. After the whole tests duration (63 days), the final CH_4 cumulative volume in the ne-PLA test was equal to 76.2 mL which almost corresponded to the final production observed in C1 (73.8 mL). Instead, the nr-PLA test resulted in a final cumulative CH_4 volume of 66.1 mL. Accounting for the CO_2, more similar final volumes equal to 39.1 mL, 41.2 mL, and 42.6 mL were measured for nr-PLA, ne-PLA, and C1 tests, respectively. These results confirmed that the PLA does not represent an easily biodegradable substrate and the observed CH_4 productions were mainly due to the degradation of the residual COD in the digestate. The higher cumulative values of CH_4 resulting from the ne-PLA test compared to the nr-PLA test could be ascribable to the effect on the PLA fragments of the high temperature involved during the 3D-printing extrusion. This could have caused a thermal degradation of the plastic material leading to a slight improvement of its biodegradability characteristic.

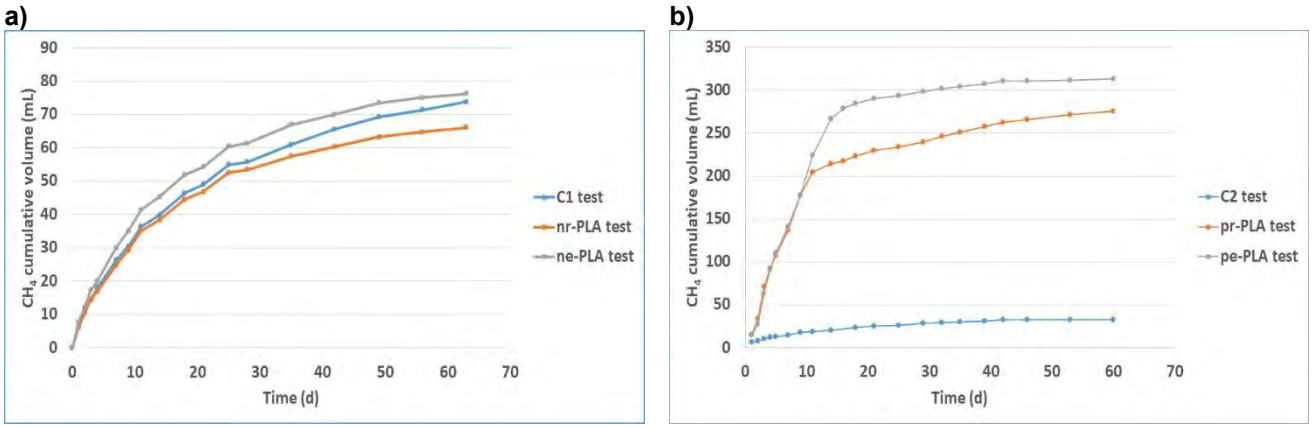

Figure 1. CH_4 cumulative volumes from a) SET-1 experiments and b) SET-2 experiments.

Accounting for the SET-2 experiments, more significant differences were observed among the two AD experiments with pre-treated PLA and the control (**Figure 1b**). After the alkaline pre-treatment, a weight loss of 32.8% and 52% was measured for the raw and extruded PLA, respectively. These weight losses contributed to soluble COD increase, in the alkaline pre-treatment solutions, to percentage values of 22.5% and 39.1% of the total PLA fragment COD for the raw and extruded PLA, respectively. Indeed, this result influenced the biogas production of both pr-PLA and pe-PLA tests with noticeable higher volumes compared to the C2 test. In particular, a significant CH_4 cumulative production rate was

observed for both tests with pre-treated PLA during the first 10-15 days and final volumes after 60 days were equal to 276.1 mL and 313.5 mL for pr-PLA and pe-PLA, respectively. According to these values, pr-PLA and pe-PLA tests showed final cumulative CH_4 volumes 9.8 and 8.6 times higher than C2. Based on the results, this study assessed the potential effectiveness of the alkaline pre-treatment on the PLA biodegradability enhancement. The outcomes also highlighted that effects from previous PLA processing can provide a more easily biodegradable material. Indeed, further in-depth studies focusing on the improvement of the PLA effectiveness as AD substrate are worth of investigation to provide a useful strategy for proper waste end-of-life management and environmental quality preservation.

References

[1] PlasticsEurope, Plastics – the fast Facts 2023. Annual production of plastics worldwide from 1950 to 2022 (in million metric tons). (2023). https://www.statista.com/statistics/282732/global-production-of-plastics-since-1950/

[2] Ibrahim N.I., Shahar F.S., Sultan M.T.H., Shah A.U.M., Safri S.N.A., & Mat Yazik M.H., Overview of Bioplastic Introduction and Its Applications in Product Packaging. *Coatings*, **11**, 1423, (2021).

[3] Venkatramanan S., Chung S.Y., Selvam S., Sivakumar K., Soundhariya G.R., Elzain H.E., & Bhuyan M.S., Characteristics of microplastics in the beach sediments of Marina tourist beach, Chennai, India. *Mar Pollut Bull*, **176**, 113409, (2022).

[4] Terzi Y., Gedik K., Eryaşar A.R., Öztürk R.Ç., Şahin A., & Yılmaz F., Microplastic contamination and characteristics spatially vary in the southern Black Sea beach sediment and sea surface water. *Mar Pollut Bull*, **174**, 113228, (2022).

[5] Atiwesh G., Mikhael A., Parrish C.C., Banoub J., & Le T.-A.T., Environmental impact of bioplastic use: A review. *Heliyon*, **7**, e07918, (2021).

[6] Tokiwa Y., Calabia B., Ugwu C., & Aiba S., Biodegradability of Plastics. *Int J Mol Sci*, **10**, 3722–3742, (2009).

[7] Thakur S., Chaudhary J., Sharma B., Verma A., Tamulevicius S., & Thakur V.K., Sustainability of bioplastics: Opportunities and challenges. *Curr Opin Green Sustain Chem*, **13**, 68–75, (2018).

[8] Rossi V., Cleeve-Edwards N., Lundquist L., Schenker U., Dubois C., Humbert S., & Jolliet O., Life cycle assessment of end-of-life options for two biodegradable packaging materials: sound application of the European waste hierarchy. *J Clean Prod*, **86**, 132–145, (2015).

[9] Bátori V., Åkesson D., Zamani A., Taherzadeh M.J., & Sárvári Horváth I., Anaerobic degradation of bioplastics: A review. *Waste Manag*, **80**, 406–413, (2018).

[10] Yagi H., Ninomiya F., Funabashi M., & Kunioka M., Mesophilic anaerobic biodegradation test and analysis of eubacteria and archaea involved in anaerobic biodegradation of four specified biodegradable polyesters. *Polym Degrad Stab*, **110**, 278–283, (2014).

[11] Yagi H., Ninomiya F., Funabashi M., & Kunioka M., Thermophilic anaerobic biodegradation test and analysis of eubacteria involved in anaerobic biodegradation of four specified biodegradable polyesters. *Polym Degrad Stab*, **98**, 1182–1187, (2013).

[12] Shrestha A., van-Eerten Jansen M.C.A.A., & Acharya B., Biodegradation of Bioplastic Using Anaerobic Digestion at Retention Time as per Industrial Biogas Plant and International Norms. *Sustainability*, **12**, 4231, (2020).

[13] European Bioplastics, Market update 2020: Bioplastics continue to become mainstream as the global bioplastics market is set to grow by 36 percent over the next 5 years. In: *15th EUBP Conference*. Berlin, Germany, (2020

[14] Benn N., & Zitomer D., Pretreatment and Anaerobic Co-digestion of Selected PHB and PLA Bioplastics. *Front Environ Sci*, **5**, 93, (2018).

[15] Song A.Y., Oh Y.A., Roh S.H., Kim J.H., & Min S.C., Cold Oxygen Plasma Treatments for the Improvement of the Physicochemical and Biodegradable Properties of Polylactic Acid Films for Food Packaging. *J Food Sci*, **81**, (2016).

[16] Hobbs S.R., Harris T.M., Barr W.J., & Landis A.E., Life Cycle Assessment of Bioplastics and Food Waste Disposal Methods. *Sustainability*, **13**, 6894, (2021).

Title: Application of an anaerobic sequencing batch reactor to control cheese whey fermentation towards bio-H_2 production.

Author(s): Tatiana Zonfa*[1]; Marica Falzarano[1]; Alessandra Polettini[1]; Raffaella Pomi[1]; Andreina Rossi[1]

[1] *Department of Civil and Environmental Engineering, Sapienza University of Rome (Italy)*
**tatiana.zonfa@uniroma1.it*

Keyword(s): dark fermentation; bio-hydrogen production; organic waste treatment.

Abstract

Dark fermentation is a promising biological process for the valorisation of organic residues and carbohydrate-rich wastewaters aimed at bio-H_2 production. Among others, cheese whey is considered a good option as the substrate due to the high organic content mainly consisting of lactose [1]. As a matter of fact, carbohydrates are the preferred substrate for H_2-producing microorganisms, which are involved in a complex set of metabolic reactions that lead to the production of various metabolites in addition to H_2 and CO_2, including organic acids in the liquid phase. It should be highlighted that the overall kinetics and yield of the H_2 production process is affected by the potential onset of competitive (e.g., H_2-consuming) or H_2-neutral metabolic pathways. For example, when a lactose-based substrate, such as cheese whey, is used, lactic acid production is typically found during the fermentative process and lactic acid bacteria (LAB) – that typically occur in dairy residues – could compete with the H_2-producing bacteria thus inhibiting H_2 production and adversely affecting the process stability [2,3]. However, some recent studies have shown that it is also possible to pursue H_2 producing pathways through lactic acid consumption, paving the way to LAB utilisation for this purpose [4–6]. Thus, identifying the most appropriate strategy for process control in view of increasing the performance and stability over time of H_2-producing communities is still a key research area in view of process scale-up. Moreover, further research is required to identify the most appropriate operating conditions that would allow the production of H_2 from lactate while counteracting the inhibitory effects of LAB.
This study aims to investigate the H_2 production by dark fermentation of cheese whey, taking advantage of the indigenous microbial community, under mesophilic conditions. The cheese whey used in this work is the by-product of the ricotta cheese processing coming from an Italian dairy industry located in the Lazio region; the results of the characterization are reported in Table 1, showing that the initial carbon content is mainly composed of carbohydrates, followed by a small amount of lactic acid and to a lesser extent acetic acid.

Table 1. Cheese whey characterization

Parameters	Unit of Measure	Value [1]
Total solids (TS)	% wet weight	4.60 ± 0.01
Volatile solids (VS)	% wet weight	3.96 ± 0.01
Total organic carbon (TOC)	gC/kg-sample	16.71 ± 0.03
Dissolved organic carbon (DOC)	gC/L	16.50 ± 0.01

Soluble carbohydrates [2]	gC-hexose/L	13.04 ± 0.53
Lactic acid (HLa) [2]	gC-HLa/L	2.29 ± 0.35
Acetic acid (HAc) [2]	gC-HAc/L	0.118 ± 0.003
pH	-	4.2 ± 0.05

[1] Average value ± standard deviation; [2] Values shown in terms of carbon content for ease of comparison.

The experimental set-up used a 1 L anaerobic Sequencing Batch Reactor (ASBR) coupled with a control system for automated operation of the sequential phases. The reactor is also equipped with a system for the continuous control of pH to the defined set point value by addition of NaOH. The experiments involved the following fixed operating parameters: pH = 6, T = 38 ± 1 °C, settling phase = 1 h and volume exchange ratio = 0.8, in combination with different hydraulic and cell residence times. Each condition was maintained for at least 10 cycles in order to select the H_2-producing biomass and to set a stable H_2 production. The biogas production was measured and automatically recorded over time thanks to a volumetric gas counter. The biogas was periodically sampled and analysed through a gas chromatograph for the determination of the H_2, CO_2 and, if any, N_2 and CH_4 content. The metabolic pathways are investigated through a sampling and characterization campaign of the slurry phase during the reaction stage of each cycle for the determination of the most relevant parameters: carbon content, solids, carbohydrates, volatile fatty acids (acetate, butyrate, propionate, valerate, caproate, heptanoate), lactic acid and ethanol. In addition, a preliminary investigation of the effects exerted by of the operating conditions on the microbial community composition, has been carried out.

Acknowledgement

This research was funded by the Italian Ministry for Public Education and Merit within the framework of the Enlarged Partnerships supported under the National Recovery and Resilience Plan (NRRP), Mission 4 Component 2 Investment 1.3 funded from the European Union – NextGenerationEU, name of the extended partnership: PE2 NEST – Network 4 Energy Sustainable Transition (project “Energy Sustainable Transition. Biological and non-conventional process for H2 production” CUP B53C22004070006).

References

[1] Asunis F, De Gioannis G, Dessì P, Isipato M, Lens PNL, Muntoni A, et al. The dairy biorefinery: Integrating treatment processes for cheese whey valorisation. J Environ Manage 2020;276:111240. https://doi.org/10.1016/j.jenvman.2020.111240.

[2] Ottaviano LM, Ramos LR, Botta LS, Amâncio Varesche MB, Silva EL. Continuous thermophilic hydrogen production from cheese whey powder solution in an anaerobic fluidized bed reactor: Effect of hydraulic retention time and initial substrate concentration. Int J Hydrogen Energy 2017;42:4848–60. https://doi.org/10.1016/j.ijhydene.2016.11.168.

[3] Gomes BC, Rosa PRF, Etchebehere C, Silva EL, AmâncioVaresche MB. Role of homo-and heterofermentative lactic acid bacteria on hydrogen-producing reactors operated with cheese whey wastewater. Int J Hydrogen Energy 2015;40:8650–60. https://doi.org/10.1016/j.ijhydene.2015.05.035.

[4] Ordoñez-Frías EJ, Muñoz-Páez KM, Buitrón G. Biohydrogen production from fermented acidic cheese whey using lactate: Reactor performance and microbial ecology analysis. Int J Hydrogen Energy 2024;52:389–403. https://doi.org/10.1016/j.ijhydene.2023.06.307.

[5] Asunis F, De Gioannis G, Isipato M, Muntoni A, Polettini A, Pomi R, et al. Control of fermentation duration and pH to orient biochemicals and biofuels production from cheese whey. Bioresour Technol

2019;289:121722. https://doi.org/10.1016/J.BIORTECH.2019.121722.
[6] Aranda-Jaramillo B, León-Becerril E, Aguilar-Juárez O, Castro-Muñoz R, García-Depraect O. Feasibility Study of Biohydrogen Production from Acid Cheese Whey via Lactate-Driven Dark Fermentation. Fermentation 2023;9. https://doi.org/10.3390/FERMENTATION9070644.

Title: Mater-Bi degradation during the semi-continuous anaerobic digestion of excess sludge and organic fraction of municipal solid waste

Author(s): Mariastella Ferreri*[1], Altea Pedullà[2], Paolo S. Calabrò[3]

[1] *Department of Civil, Energy, Environmental and Materials Engineering, Mediterranea University of Reggio Calabria, Reggio Calabria, Italy, mstella.ferreri@unirc.it*
[2] *Department of Civil, Energy, Environmental and Materials Engineering, Mediterranea University of Reggio Calabria, Reggio Calabria, Italy, altea.pedulla@unirc.it*
[3] *Department of Civil, Energy, Environmental and Materials Engineering, Mediterranea University of Reggio Calabria, Reggio Calabria, Italy, paolo.calabro@unirc.it*

Keyword(s): bioplastics, anaerobic digestion, biomethane, excess sludge, organic fraction of municipal solid waste

Abstract

The presence of bioplastics in the organic fraction of municipal solid waste (OFMSW) is increasing. The ensuing investigation delves into the impact of Mater-Bi presence on the anaerobic co-digestion process involving OFMSW and excess sludge.

Introduction

The organic fraction of municipal waste (OFMSW) constitutes a valuable resource for biomethane production via anaerobic digestion (AD). Bioplastics, commonly used in food-related packaging and collection bags, often are disposed of together with OFMSW and arrives in the plants destined to treat this fraction.

A study conducted by the Italian Composting Consortium (Consorzio Italiano Compostatori - CIC) and Corepla reveals a notable increase in the presence of UNI EN 13432:2002-certified compostable plastics within organic waste, rising from 1.5% in 2016/2017 to 3.7% in 2019/2020.

However, the actual biodegradability of these materials within the specific environments where they are managed has not been fully analysed especially in regard to anaerobic digestion plants.

In this study, compostable bags made from commercially available starch-based bioplastic (Mater-Bi®) were selected. Mater-Bi® is one of the most widely used commercial bioplastics on the market, utilized for shopping bags, waste collection bags, packaging, disposable products, and more. These bags were subjected to anaerobic degradability tests at laboratory scale.

The primary aims of the experimental activity entail assessing the impact of Mater-Bi on biomethane production and estimating the degradation of the investigated bioplastic at the end of the process.

Materials and methods

The experimental activity was conducted at laboratory scale through a semi-continuous anaerobic digestion system (Bioprocess Control Bioreactor, BPC Instruments). Four glass reactors with an operating capacity of 1.9 L and labelled with the letters A, B, C and D were used. The reactors were immersed in a thermostatic bath that kept temperature at 35°C (mesophilic conditions) and were equipped with a mechanical agitation system that provided uniform mixing and dispersion of the substrate. In addition, biomethane production was recorded by a system connected to the gas flow measuring device and remotely accessible.

The daily feeding of the substrate was performed manually through the inlet port and simultaneously the digestate was discharged from the outlet port.

The main substrate was a mixture, with a 50:50 ratio based on Volatile Solids (VS), of OFMSW and thickened excess sludge. Additionally, different percentages of bioplastics were introduced into each reactor. The investigated material was Mater-Bi cut into square-shaped pieces. More specifically, reactor A, served as a control, was bioplastic-free, while reactors B, C, and D contained 2%, 4% and 8% bioplastics referred to the amount of OFMSW.

Process operation was characterised by Organic Loading Rate (OLR) and Hydraulic Retention Time (HRT). In the initial phase the first parameter was set to 1 g_{VS}/L·d and then increased to 3 g_{VS}/L·d in the second phase, while HRT was set at 21 days during the entire experiment.

The initial phase, characterised by an OLR of 1 g_{VS}/L·d, ran for 9 weeks, equivalent to 3 HRT. Then, the second phase, featuring an OLR of 3 g_{VS}/L·d, lasted for a period of 6 weeks, corresponding to 2 HRT.

Biomethane production was subject to continuous monitoring, while digestate pH levels were assessed during each feeding operation, conducted five days per week. Furthermore, evaluations of pH, total solids (TS), volatile solids (VS), volatile fatty acids (VFAs) and the ratio between volatile fatty acids and buffering capacity (FOS/TAC) were performed on composite weekly digestate samples.

Result and discussion

During the initial 9-week phase of the experiment, characterized by an organic loading rate (OLR) set at 1 gVS/L·d, was observed that the presence of bioplastics did not produce a significant change in methane production. Compared with the control reactor A, reactor B (2%), C (4%) and D (8%) exhibited increases in production of 2.0%, 8.2% and 8.9%, respectively.

To assess the quality of the anaerobic digestion (AD) process, daily pH measurements were carried out, they revealed that all reactors kept a pH level between 7.1 and 7.5. The stability of the anaerobic digestion process is recognized within the pH spectrum of 6.3 to 7.8, beyond this range the survival of methanogenic bacteria is notably compromised [2].

Over the following 6 weeks, to investigate the effects of the augmented load, the OLR was increased to 3 g_{VS}/L·d. This adjustment had repercussions, particularly causing a significant increase in VFA concentration and the FOS/TAC ratio, both parameters providing insights into process stability.

Indeed, a rapid accumulation of volatile fatty acids leads to a decrease in pH and simultaneous inhibition in the growth of bacteria responsible for methane production [2]. These phenomena are particularly pronounced in reactor D, which contains the highest percentage of bioplastic, demonstrating how increased loading results in overloaded VFA accumulation, excessive medium acidification and a drastic reduction in methane yield. Consequently, specific measures were required between the 11th and 12th week to correct pH levels when they dropped below 6.5, achieved through the addition of 2 g/L of sodium bicarbonate to enhance the reactor's buffering capacity.

Moreover, due to the accumulation phenomena and the recurrent issues arising from overpressure within the D reactor caused by foam formation obstructing the pipes intercepting biogas flow, at the beginning of the 13th week the introduction of bioplastics as feedstock was halted and a feeding regimen identical to that of the control reactor was subsequently maintained.

As illustrated in *Figure 1*, upon the cessation of Mater-Bi feeding into the D reactor, discernible improvements in various parameters became evident. Specifically, methane yield began to slowly increase, while pH levels returned to optimal ranges. Furthermore, both the concentrations VFAs and the FOS/TAC ratio demonstrated a gradual decrease.

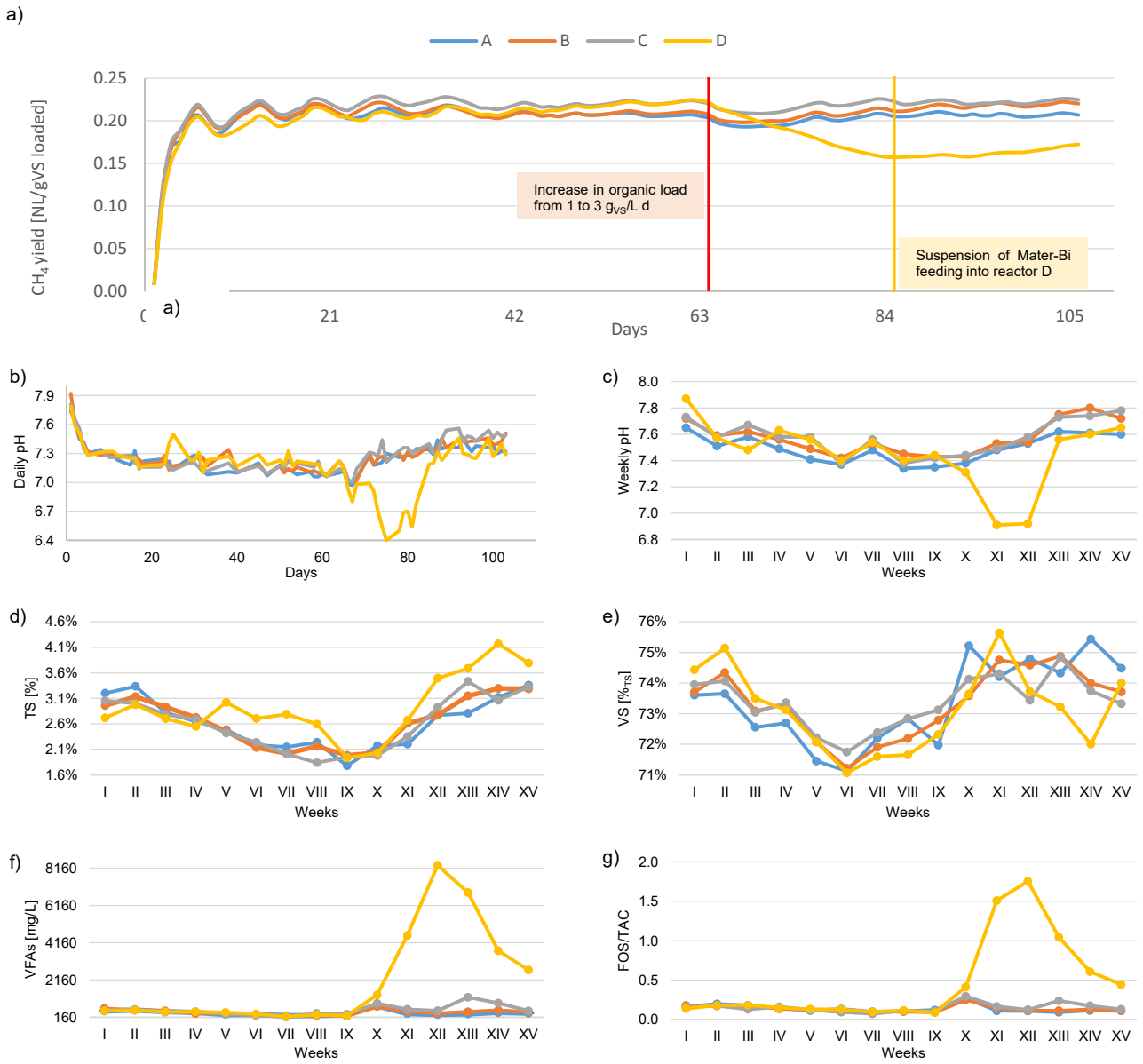

Figure 1. Semi-continuous results: (a) CH_4 yield, (b) daily pH, (c) weekly pH, (d) TS, (e) VS, (f) VFAs, (g) FOS/TAC

For the examination of Mater-Bi degradation during the anaerobic digestion process, the bioplastic pieces daily exiting with the digestate were isolated, meticulously cleansed, dried, and weighed. By recording the initial mass of bioplastics introduced into each reactor, it became feasible to determine the extent of bioplastics degradation and illustrate the trend in *Figure 2*.

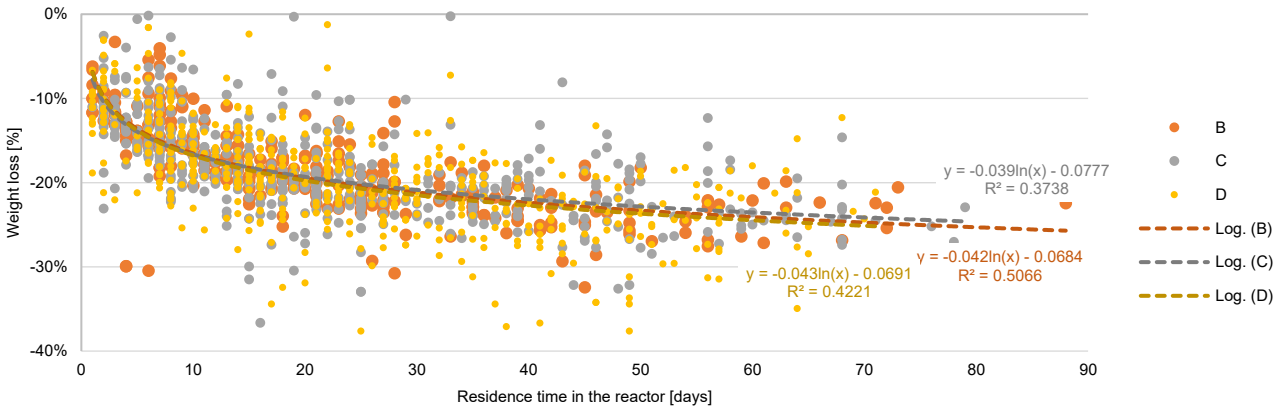

Figure 2. Bioplastic weight loss

The degradation pattern of Mater-Bi appears to follow a rather similar trend line across the different reactors. The trend line exhibits a logarithmic pattern, indicating that the weight loss is most prominent during the initial three weeks of the process before stabilising thereafter. Indeed, after a 3-week retention period in the three reactors, an average weight reduction of approximately 20% is observed, while after 12 weeks, a reduction of just 25% is observed.

Moreover, while in reactors B and C it was possible to discriminate between individual pieces of Mater-Bi, from approximately week 13 onwards, the collection of weight data for individual pieces within reactor D became impractical, as predominantly bioplastic shreds were discovered.

Conclusions

In conclusion, the semi-continuous anaerobic digestion experiment conducted demonstrated that the presence of Mater-Bi pieces does not significantly affect methane production. However, elevated concentrations appear to induce accumulation phenomena, leading to reactor acidification and inhibition of the anaerobic digestion process.

References

[1] Pangallo D., Gelsomino A., Fazzino F., Pedullà A. & Calabrò P. S. “The fate of biodegradable plastic during the anaerobic co-digestion of excess sludge and organic fraction of municipal solid waste”. Waste Management 168, 98–106 (2023).
[2] Prasanna Kumar, D. J., Mishra, R. K., Chinnam, S., Binnal, P. & Dwivedi, N. A comprehensive study on anaerobic digestion of organic solid waste: A review on configurations, operating parameters, techno-economic analysis and current trends. Biotechnology Notes 5, 33–49 (2024).

Title: Opportunities and challenges of combining sewage sludge thermal hydrolysis with thermophilic anaerobic digestion

Author(s): Pavel Jenicek*[1], Anna Magrova[1,2], Lise Appels[2]

[1] *University of Chemistry and Technology Prague, Department of Water Technology and Environmental Engineering, Technicka 5, 166 28 Prague, Czech Republic*
[2] *KU Leuven, Department of Chemical Engineering, Process and Environmental Technology Lab, Jan Pieter De Nayerlaan 5, Sint-Katelijne-Waver B-2860, Belgium*

Keyword(s): Anaerobic digestion intensification; sludge dewaterability; specific biogas production; thermal hydrolysis of sludge; thermophilic anaerobic digestion.

Abstract

Thermal hydrolysis (THP) of sludge is a proven technology for intensifying the anaerobic digestion of sewage sludge. However, there is a lack of data on the operational results of the combination of THP with thermophilic anaerobic stabilization (TAD). Therefore, three technological alternatives of THP and TAD were tested on a pilot scale at the WWTP Prague. The results showed that the combination of THP and TAD has its risks, which can be manifested by both instability of operation and a lower degree of improvement in biogas production compared to mesophilic conditions due to the higher level of basic biogas production. Although an improvement in sludge dewaterability and an increase in specific biogas production were achieved, after accounting for the energy consumption of the THP, this option was not evaluated as energetically advantageous for the WWTP Prague.

Introduction

The recent surge in energy prices has further increased the importance of energy efficiency in wastewater treatment plants (WWTP). Anaerobic digestion (AD) is among all WWTP processes the most important energy-positive technology that produces energy in the form of biogas. However, AD shows the limited degradation of sewage sludge that can be increased by pretreatment of these sludges by the thermal hydrolysis process (THP). The THP is based on the exposure of the sludge to high temperature and pressure, as a result of these conditions and the subsequent sudden release of high pressure, a highly efficient disintegration and solubilization of the sludge occurs.

A large amount of data on the effect of THP on solubilization, anaerobic sludge degradability, and biogas production can be found in publications by [1-3]. So far, literature references mentioning THP and thermophilic anaerobic digestion of sludge (THP-TAD) refer to results from laboratory experiments [4-5] and one pilot scale experiment [6]. However, the results of these studies are contradictory and relatively ambiguous. There is still a lack of data on the operational results of the technological variations of THP-TAD, as well as data on the effect of THP on highly optimized digestion with a high basic level of biogas production.

Therefore, continuous experiments were performed on a pilot scale with the aim of verifying the long-term effect of THP on anaerobic digestion in the specific context of WWTP Prague. Here AD is operated

under thermophilic conditions (55 °C) and achieves high specific biogas production even without THP (up to 0.6 m^3/kg VSS_{added}) [7]. The presented contribution provides an evaluation of these experiments.

Materials and Methods

The experiments were divided into 4 stages, the length of which was determined by achieving a steady state in the thermophilic digester. Individual stages differed by the technological variations of THP-TAD in the sludge line

Stage 1 (S1) – control stage without THP (20 days)
Stage 2 (S2) – THP of mixed raw sludge (15 and 20 days)
Stage 3 (S3) – THP of waste activated sludge (WAS) (20 and 25 days)
Stage 4 (S4) – THP of digested sludge and fugate recycling to anaerobic stabilization

In stages 2 and 3 different hydraulic retention times in TAD were also tested. In stage 4, hydrolysis took place in the same way as in stages 2 and 3, but the fugate of the hydrolyzed digested sludge was subjected to TAD in laboratory batch tests.

The THP unit consisted of a separate thermal hydrolysis reactor heated by steam to 160 °C. After a reaction time of 30 min, 150 L of hydrolysed sludge was released to the flash tank below the reactor. After spontaneous cooling, the sludge was fed into a continuously operated digester. The digested sludge was kept in an accumulation tank before dewatering in a pilot-scale dewatering unit.

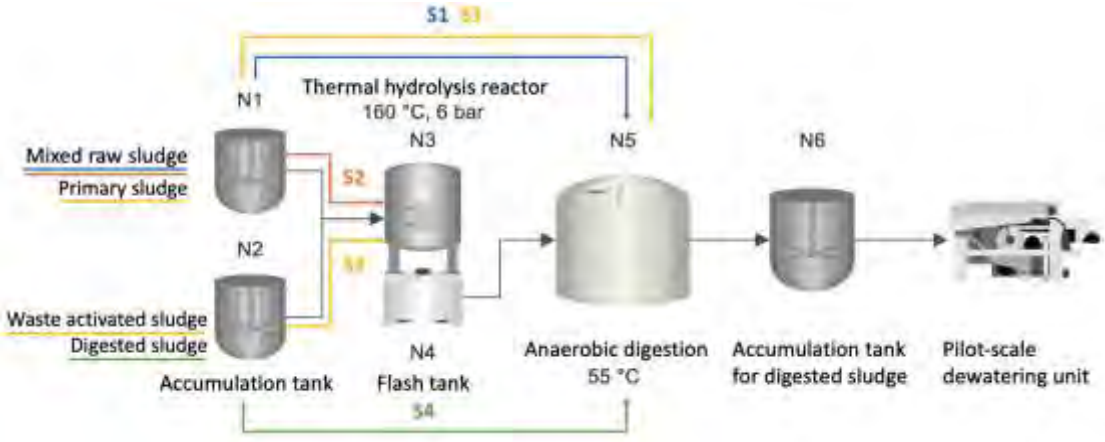

Figure 1: The **s**cheme of the pilot THP-TAD unit consisted of two storage tanks T1 and T2, a thermal reactor for the hydrolysis of sludge T3, a flash tank T4, a thermophilic digester T5 and a digested sludge storage tank T6.

Results and Conclusions

THP efficiency. The positive effect of hydrolysis is manifested by the conversion of the sludge from a solid to a liquid phase, which is significantly more accessible to anaerobic microorganisms. Therefore, the efficiency of hydrolysis is evaluated according to the increase of dissolved organic matter expressed as soluble COD (sCOD). The average hydrolysis efficiency shown in Table 1 was calculated as the efficiency of converting undissolved organic substances into dissolved substances. The results for both raw and WAS correspond to the values achieved in other studies [8-10]. The hydrolysis efficiency of digested sludge THP is lower, which corresponds to the hypothesis that during anaerobic digestion the proportion of biodegradable organic substances in the sludge decreases together with the proportion of

hydrolysable substances. However, even a hydrolysis efficiency of 14% provides a prerequisite for a significant increase in biogas production.

Table 1 The average efficiency of the hydrolysis process in different stages.

	Hydrolysis efficiency (%)	sCOD in hydrolysed sludge ($g.L^{-1}$)
Without THP	-	2.36 ± 0.56
THP of raw sludge	28	14.22 ± 0.97
THP of WAS	30	20.00 ± 0.71
THP of digested sludge	14	7.99 ± 4.24

Biogas production. During Stage 1 (THP of raw sludge), the specific biogas production increased to 0.51 $m^3.kg^{-1}$ VS_{added} (Table 2) which is an increase of almost 11% compared to the control without THP. This is a result at the lower end of the expected increase in biogas production (10-30%) reported by [3]. The results of Stage 3 (THP of WAS) were affected by the instability of the anaerobic process, and the value of specific biogas production in this case does not indicate a worse degradability of this sludge, but rather a potential inhibition.

Table 2 Average specific biogas productions and methane content in different stages.

	Specific biogas production ($m^3.kg^{-1}VS_{added}$)	Methane concentration in biogas (%)
Without THP	0.46	57.5
THP of raw sludge	0.51	60.8
THP of WAS	0.35	60.0
THP of digested sludge	0.18	76.9

In the last stage, when the thermal hydrolysis of the digested sludge was tested, the degradability of the fugate after dewatering, which would return to anaerobic stabilization, was tested using batch tests. These tests showed a specific biogas production of 0.18 $m^3.kg^{-1}VS_{added}$. Through VS mass balance and biogas production commonly achieved at WWTP Prague, the fugate of hydrolysed digested sludge would increase biogas production, which could increase by 9.5%.

Sludge dewaterability. The dewatering of the digested sludge was carried out in a pilot-scale centrifuge. Table 3 shows the highest dry matter achieved from the dewatered sludge after optimization of the type and dose of flocculant. The positive effect of THP on the dewaterability of sludge was confirmed. Although the improvement caused by hydrolysis of raw sludge and excess sludge cannot be considered technologically significant, the improvement of the dewaterability of hydrolyzed stabilized sludge by 4.5 percentage points can be evaluated as promising, however, the achieved values are lower than the values published in the literature 43- 47.5% [11,12].

Table 3 Maximum dry solids concentration of dewatered sludge in different stages.

	Dry solids concentration of dewatered sludge (%)
Without THP	23.8
THP of raw sludge	25.0
THP of WAS	24.8
THP of digested sludge	28.3

Thermal hydrolysis was tested in three technological scenarios for raw sludge, WAS, and digested sludge. In all cases, the presence of indicator pathogenic microorganisms was reduced below the values

required for sludge sanitation, in the case of raw sludge, even below the detection limit. In all cases, there was a slight improvement in sludge dewaterability. The best dewaterability was achieved when THP was applied to stabilized sludge. The specific production of biogas increased by about 10% when THP of raw sludge and digested sludge was combined with TAD. However, it is also necessary to consider the energy consumption of the THP process, which is assumed to be around 10% of the biogas produced, which is usually used to produce heat for THP (Barber, 2020). At the same time, surprisingly, the specific biogas production achieved on a pilot scale did reach the specific production of the full-scale two-stage TAD at the WWTP Prague.

Based on the pilot scale results, it can be stated that the combination of THP and thermophilic anaerobic stabilization shows risks that can be manifested both by instability of operation and a lower increase in specific biogas production than is expected for the combination of THP with mesophilic anaerobic digestion, however, the effect of THP must be evaluated comprehensively using a set of criteria that may have different weights in specific local cases.

References

1 Barber, W. (2020). Sludge thermal hydrolysis: Application and potential. IWA Publishing.

4 Braguglia, C. M., Carozza, N., Gagliano, M. C., Gallipoli, A., Gianico, A., Rossetti, S., Suschka, J., Tomei, M. C., & Mininni, G. (2014). Advanced anaerobic processes to enhance waste activated sludge stabilization. *Wat. Sci. Tech.*, 69(8), 1728–1734.

Braguglia, C. M., Gianico, A., Gallipoli, A., & Mininni, G. (2015). The impact of sludge pre-treatments on mesophilic and thermophilic anaerobic digestion efficiency: Role of the organic load. *Chem. Eng. J.*, 270, 362–371.

2 Carrère, H., Dumas, C., Battimelli, A., Batstone, D. J., Delgenès, J. P., Steyer, J. P., & Ferrer, I. (2010). Pretreatment methods to improve sludge anaerobic degradability: A review. *J. Hazard. Mater.*, 183(1), 1–15.

6 Chen, Z., Li, W., Qin, W., Sun, C., Wang, J., & Wen, X. (2020). Long-term performance and microbial community characteristics of pilot-scale anaerobic reactors for thermal hydrolyzed sludge digestion under mesophilic and thermophilic conditions. *Sci. Total Environ.*, 720, 137566.

5 Gianico, A., Braguglia, C. M., Cesarini, R., & Mininni, G. (2013). Reduced temperature hydrolysis at 134°C before thermophilic anaerobic digestion of waste activated sludge at increasing organic load. *Bioresour. Technol.*, 143, 96–103.

8 Han, D., Lee, C.-Y., Chang, S. W., & Kim, D.-J. (2017). Enhanced methane production and wastewater sludge stabilization of a continuous full scale thermal pretreatment and thermophilic anaerobic digestion. *Bioresour. Technol*., 245, 1162–1167.

9 Higgins, M. J., Beightol, S., Mandahar, U., Suzuki, R., Xiao, S., Lu, H.-W., Le, T., Mah, J., Pathak, B., DeClippeleir, H., Novak, J. T., Al-Omari, A., & Murthy, S. N. (2017). Pretreatment of a primary and secondary sludge blend at different thermal hydrolysis temperatures: Impacts on anaerobic digestion, dewatering and filtrate characteristics. *Water Res.*, 122, 557–569.

7 Jenicek, P., Bartacek, J., Kutil, J., Zabranska, J., & Dohanyos, M. (2012). Potentials and limits of anaerobic digestion of sewage sludge: Energy self-sufficient municipal wastewater treatment plant? *Wat. Sci. Tech.*, 66(6), 1277–1281.

3 Ngo, P. L., Udugama, I. A., Gernaey, K. V., Young, B. R., & Baroutian, S. (2021). Mechanisms, status, and challenges of thermal hydrolysis and advanced thermal hydrolysis processes in sewage sludge treatment. Chemosphere, 281, 130890.

11 Svennevik, O. K., Solheim, O. E., Beck, G., Sørland, G. H., Jonassen, K. R., Rus, E., Westereng, B., Horn, S. J., Higgins, M. J., & Nilsen, P. J. (2019). Effects of post anaerobic digestion thermal hydrolysis on dewaterability and moisture distribution in digestates. *Wat. Sci. Tech.*, 80(7), 1338–1346.

12 Svensson, K., Kjørlaug, O., Higgins, M. J., Linjordet, R., & Horn, S. J. (2018). Post-anaerobic digestion thermal hydrolysis of sewage sludge and food waste: Effect on methane yields, dewaterability and solids reduction. *Water Res.*, 132, 158–166.

10 Toutian, V., Barjenbruch, M., Unger, T., Loderer, C., & Remy, C. (2020). Effect of temperature on biogas yield increase and formation of refractory COD during thermal hydrolysis of waste activated sludge. *Water Res.*, 171, 115383.

Title: Strategic Enhancement of Lactic Acid Yields through Cavitation Pre-treatment in Food Waste Digestion

Author(s): Aisha Khan Khanzada*[1], Jacek Makinia[1]

[1] *Faculty of Civil and Environmental Engineering, Gdansk University of Technology, Gdansk, 80-233, Poland, aisha.khan.khanzada@pg.edu.pl*

Keyword(s): Anaerobic digestion, Cavitation, lactic acid, VFA, Inoculum-substrate ratio (ISR)

Abstract

This study explores the application of cavitation as a pretreatment method to enhance the anaerobic digestion of food waste, aiming to produce value-added products such as Lactic acid and volatile fatty acids (VFAs). Cavitation improves the hydrolysis of feedstocks like potatoes, subsequently increasing the bioavailability for microbial action and facilitating the breakdown into simpler molecules. Experiments conducted at varying Inoculum-to-Substrate Ratios (ISRs) in batch fermentation setups illustrate that cavitation significantly boosts the production of soluble chemical oxygen demand (sCOD) upto 10.86g/L at ISR 1:6, and L-lactic acid 4.71gCOD/L at ISR 1:4, indicating enhanced microbial accessibility and activity. Notably, cavitated treatments show a substantial increase in VFA production over five days compared to non-cavitated controls, with marked peaks in acetic, propionic, butyric, and valeric acids, particularly at higher ISRs. These findings suggest that cavitation not only optimizes fermentation processes but also potentially shortens digestion times, thereby improving operational efficiency and environmental sustainability in waste treatment facilities. This study confirms the potential of cavitation technology in augmenting anaerobic digestion, making it a promising approach for enhancing the sustainability and efficiency of Lactic acid production from food waste.

Introduction:

The significant increase in food waste due to population growth and economic development has prompted the exploration of sustainable solutions, such as converting waste into value-added products like organic acids, biogas, biohydrogen, and biodiesel through anaerobic digestion [1]. Key to this process is the efficient hydrolysis of feedstock, which can be enhanced by pretreatment techniques like cavitation. Cavitation method improve the bioavailability of waste for microbial action, facilitating the breakdown of complex molecules into simpler, more manageable forms [2]. Techniques such as acoustic cavitation are particularly effective in increasing the yield of desired products while also reducing the environmental impact by lowering emissions of acid rain-causing gases and other pollutants [3].

Methodology

In this study, potatoes were boiled, blended, and mixed with distilled water to create a homogeneous substrate, stored at 10°C with a concentration of 50g/L for fermentation. Using a bacterial culture from an anaerobic digester maintained at 20°C, the substrate and inoculum were analysed pre and post-pretreatment, revealing increased levels of TSS, VSS, glucose, and soluble COD, indicating enhanced fermentability. Batch fermentation experiments were conducted in 500ml flasks at 35°C and 100 RPM, adjusting pH levels with HCl and NaOH, monitoring daily for a week to study lactic acid production dynamics. A reactor, including a Hielscher UP400St operating at 20 kHz, were used

for pretreatment. Analyticaxxl assessments were performed using HPLC, GC, and SCOD measurement kits, thoroughly analysing the chemical composition, including total Kjeldahl nitrogen and VFAs, to gauge the effectiveness of the process and the impact of varying conditions on substrate bioconversion.

Results

Effect on sCOD

The graphs illustrate the effect of cavitation on soluble chemical oxygen demand (sCOD) over five days, comparing cavitated and non-cavitated substrates at two different Inoculum-to-Substrate Ratios (ISRs). At an ISR of 1:4, cavitated substrates peak at approximately 8.74 g/L after 1 day, surpassing the non-cavitated substrates that peak at 4.9 g/L after 2 days, with both showing a downward trend thereafter. Similarly, at an ISR of 1:6, cavitated substrates peak at around 10.86 g/L, significantly higher than the just over 5.43 g/L peak of non-cavitated substrates, indicating that cavitation enhances bioavailability and microbial breakdown of the substrate, thus potentially improving anaerobic digestion efficiency.

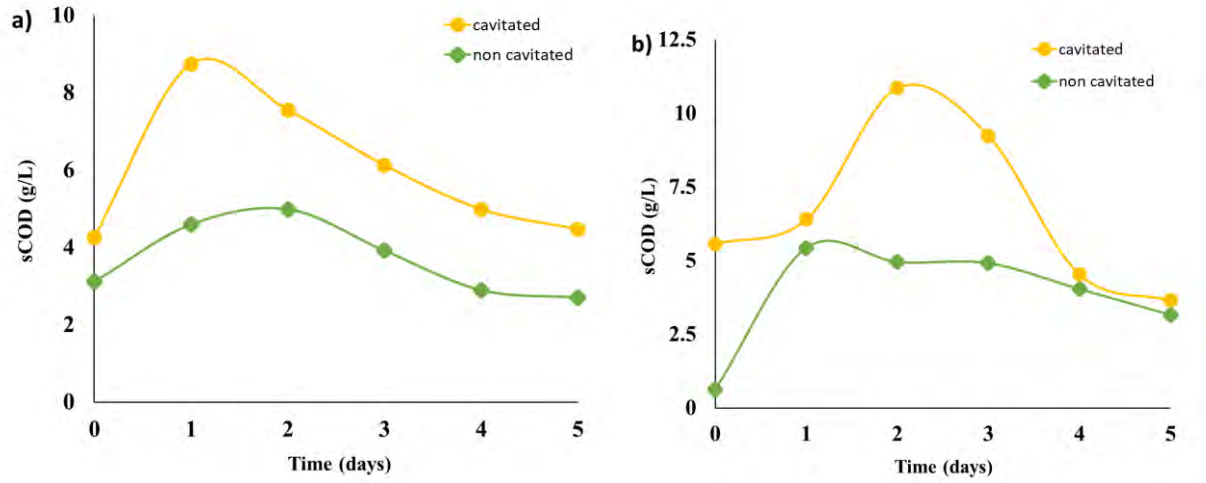

Figure 1. Effect of cavitation on sCOD at different ISR. a) sCOD at ISR 1:4, a) sCOD at ISR 1:6.

Effect on Lactic Acid

Figure 2 demonstrates the influence of cavitation on the production of L-lactic and D-lactic acid under different Inoculum-to-Substrate Ratios (ISRs) over five days. For L-lactic acid, at ISR 1:4 (Figure 2a), cavitated substrates peak at 4.71g/L gCOD/L after 1 day, which is notably higher than the non-cavitated substrates peaking at about 2.3 gCOD/L after 2 days; a similar pattern is observed at ISR 1:6 (Figure 2b) where cavitated substrates reach around 4.6 gCOD/L compared to 2.3 gCOD/L for non-cavitated substrates. D-lactic acid production also shows significant differences; at ISR 1:4 (Figure 2c), cavitated substrates peak early at 1.6 gCOD/L after 1 day, vastly outperforming non-cavitated substrates that plateau at 0.56 gCOD/L at 1:4, and at ISR 1:6 (Figure 2d), cavitated substrates again lead with a peak at 3.2 gCOD/L compared to just 0.99 gCOD/L in non-cavitated substrate setup. These trends indicate that cavitation markedly enhances lactic acid production, achieving higher concentrations more quickly than non-cavitated treatments, particularly evident at higher ISRs, suggesting that cavitation may optimize the availability and breakdown of fermentable substrates for microbial use.

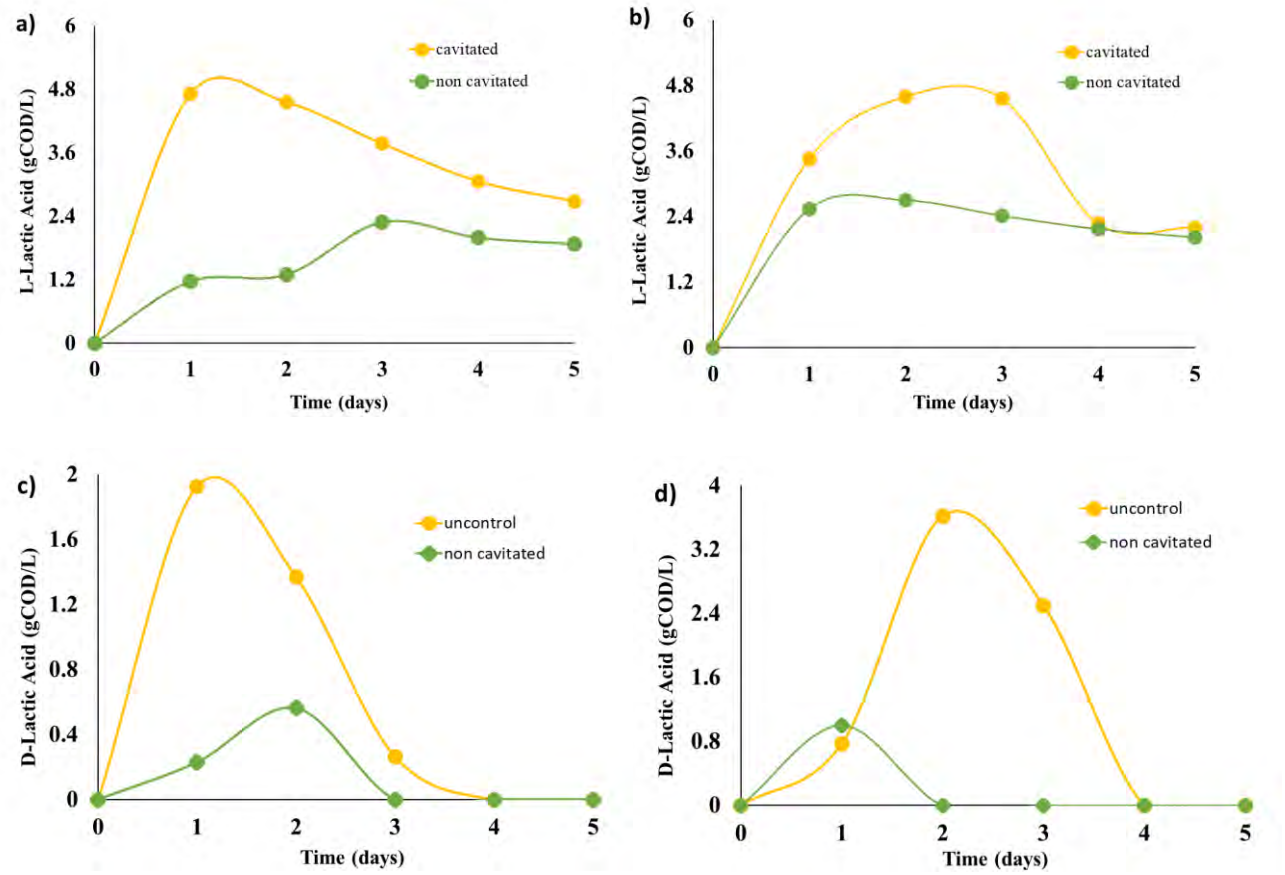

Figure 2. Effect of cavitation on lactic acid concentration. a) L-Lactic acid concentration at ISR 1:4, a) L-Lactic acid concentration at ISR 1:6. c) D-Lactic acid concentration at ISR 1:4, d) D-Lactic acid concentration at ISR 1:6.

Effect on VFA

Figure 3 displays the effect of cavitation on volatile fatty acid (VFA) concentrations across two Inoculum-to-Substrate Ratios (ISRs) over a period of five days. At ISR 1:4 (Figure 3a), cavitated treatments show higher overall concentrations of VFAs such as acetic, propionic, butyric, and valeric acids, with a noticeable peak in acetic and butyric acids on day 3, followed by a gradual decline. Acetic acid levels reach as high as approximately 0.189 g COD/L on day 2nd in the cavitated case, The non-cavitated treatments exhibit consistently lower concentrations throughout the period. The ISR 1:6 scenario (Figure 3b) presents a similar trend where cavitated treatments peak significantly higher, particularly for propionic and butyric acids on day 2, and maintain a substantial lead over the non-cavitated treatments, which show a slower increase and an earlier plateau. The trend of higher volatile fatty acid (VFA) concentrations in cavitated treatments observed in Figure 3 suggests several implications: improved bioavailability of substrates enhancing microbial access and consumption, stimulated microbial activity indicated by increased VFA production. Additionally, the increase in VFA production through cavitation could lead to reduced digestion times, increasing operational efficiency and making the process more economically viable while also reducing environmental impacts by enhancing the effectiveness of waste treatment and minimizing untreated organic material release.

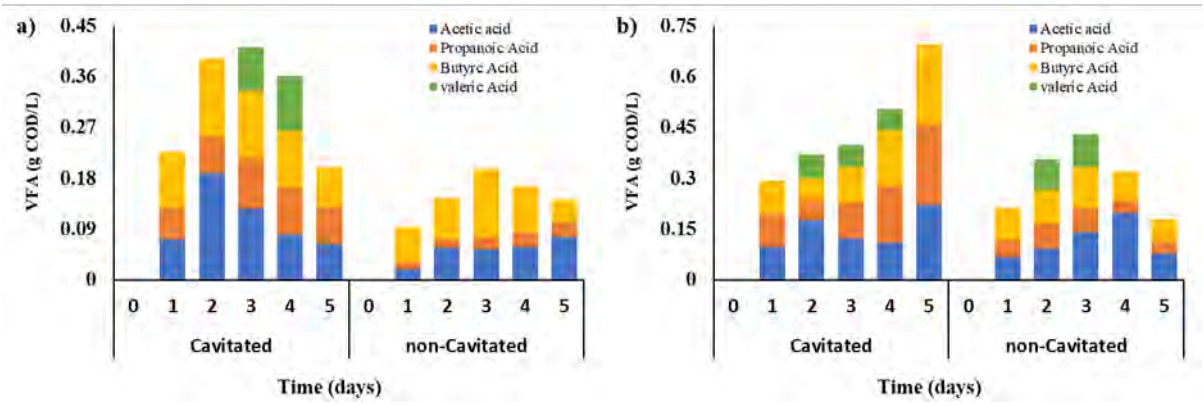

Figure 3. Effect of cavitation on VFA. a) VFA concentration at ISR 1:4, a) VFA concentration at ISR 1:6

References

[1] Dinesh, G.K.; Chauhan, R.; Chakma, S. Influence and Strategies for Enhanced Biohydrogen Production from Food Waste. *Renewable and Sustainable Energy Reviews* **2018**, *92*, 807–822, doi:10.1016/j.rser.2018.05.009.

[2] Askarniya, Z.; Kong, L.; Wang, C.; Sonawane, S.H.; Mąkinia, J.; Boczkaj, G. Tuning of Food Wastes Bioavailability as Feedstock for Bio-Conversion Processes by Acoustic Cavitation and SPC, SPS, or H2O2 as External Oxidants. *Chemical Engineering and Processing - Process Intensification* **2024**, *195*, 109626, doi:10.1016/j.cep.2023.109626.

[3] Wang, B.; Su, H.; Zhang, B. Hydrodynamic Cavitation as a Promising Route for Wastewater Treatment – A Review. *Chemical Engineering Journal* **2021**, *412*, 128685, doi:10.1016/j.cej.2021.128685.

PARALLEL SESSION: A8

Wastewater treatment

Sludge management optimization strategies

Minimization of sewage sludge production through the application of the OSA process

Author(s): Raffaele Morello[1], Francesco Di Capua[2], Danilo Spasiano[1], Giovanni Esposito[3], Francesco Pirozzi[3], Umberto Fratino[1]

[1] Dipartimento di Ingegneria Civile, Ambientale, del Territorio, Edile e di Chimica, Politecnico di Bari, Via Edoardo Orabona, 4, 70125 Bari (BA), Italy, {raffaele.morello,danilo.spasiano}@poliba.it
[2] Scuola di Ingegneria, Università degli Studi della Basilicata, Via dell'Ateneo Lucano 10, 85100, Potenza (PA), Italy, francesco.dicapua@unibas.it
3 Dipartimento di Ingegneria Civile, Edile e Ambientale, Università degli studi di Napoli "Federico II", Via Claudio, 21, 80125, Napoli (NA), {giovanni.esposito1, francesco.pirozzi}@unina.it

Keyword(s): *Sewage sludge; sludge minimization; oxic settling anaerobic; integrated fixed-film activated sludge; membrane bioreactor.*

Abstract

Sewage sludge production and management are among the most urgent problems for a wastewater treatment plant (WWTP) management nowadays [1,2]. For this reason, reducing sewage sludge production during the wastewater treatment cycle inside a WWTP is one of the most important challenges that research is facing in recent years. In particular, the strategies introduced in the last decades for minimizing sewage sludge production are conventionally grouped into two macro-categories: interventions along the water line and interventions along the sludge line [3].
The interventions along the water line act directly on the biological process used in the mainstream wastewater treatment. The interventions along the sludge line, on the other hand, aim to reduce as much as possible the sludge produced in the mainstream and can be distinguished in sludge pretreatments, strategies for enhancing volatile solids (VS) reduction during the anaerobic digestion (AD), and digestate post-treatments [1,3–5].
This research activity addresses the problem of sewage sludge production during mainstream biological wastewater treatment. Indeed, reducing sewage sludge production during the wastewater treatment cycle is fundamental as sludge minimization strategies in the water line act directly at the source of the problem and allow to reduce the negative burden connected to the downstream sludge treatment and disposal stages. Among the interventions along the water line, the oxic settling anaerobic (OSA) process proved its effectiveness in reducing sludge production during its early applications on a conventional activated sludge (CAS) cycle at different scales [2,6–11]. The process consists in the introduction of a sludge holding tank (SHT) along the recirculating activated sludge (RAS) line and, consequently, it submits the RAS to a cyclic alternation between aerobic and anoxic/anaerobic conditions [12]. The process triggers a series of mechanisms responsible for the reduction of the sludge yields and the increase of the decay rates including uncoupling metabolism, maintenance of metabolism, cell lysis-cryptic growth, selection of slow-growing bacteria, and EPS destruction [12,13]. The OSA process performances in reducing sludge production, as well as the predominant sludge reduction mechanisms, is influenced by several operating conditions such as the sludge retention time (SRT) [14,15], the hydraulic retention time inside the SHT (HRT_{SHT}) [6], the oxidation reduction potential (ORP) [16], temperature inside the SHT (T_{SHT}) [12] and the sludge interchange ratio (IR) [17,18].
One of the first goals of this research was to verify the performances of the OSA process in reducing

sludge production when combined to novel and more efficient bioreactor systems, in view of WWTPs upgrading. In particular, the bioreactors chosen during this activity were the integrated fixed-film activated sludge (IFAS) and the membrane bioreactor (MBR) systems, which can easily complement or replace an existing CAS [3,19].

During a first study, a lab-scale innovative IFAS-OSA system was implemented and operated under different operating conditions of HRT_{SHT} (6 and 12 h), T_{SHT} (ambient and 35°C), and SRT (between 39 and 126 d). The HRT_{SHT} and T_{SHT} were considered as main operating parameters of interest in order to identify the best combination of operating conditions enhancing sludge minimization, to investigate the impact of the OSA process on sludge dewaterability, as well as to elucidate the relationship between EPS and SMP trends and composition and sludge dewaterability itself [19].

The observed cell yield coefficient (Y_{obs}) for the reference IFAS system was 0.37 mgVSS/mgCOD (**Fig. 1a**). After the OSA process implementation, Y_{obs} decreased by 32% and between 46% and 65% at the HRT_{SHT} of 12 and 6 h, respectively, when T_{SHT} was at ambient values (**Fig. 1a**). When T_{SHT} was raised to 35°C, at the lower HRT_{SHT} of 6 h, Y_{obs} further decreased by 31% and 76% compared to the SHT operated at ambient temperature and to the reference IFAS, respectively (**Fig. 1a**). Thereby the OSA process exhibited the best performances in reducing sludge production at the lowest HRT_{SHT} tested and mesophilic temperature inside the SHT.

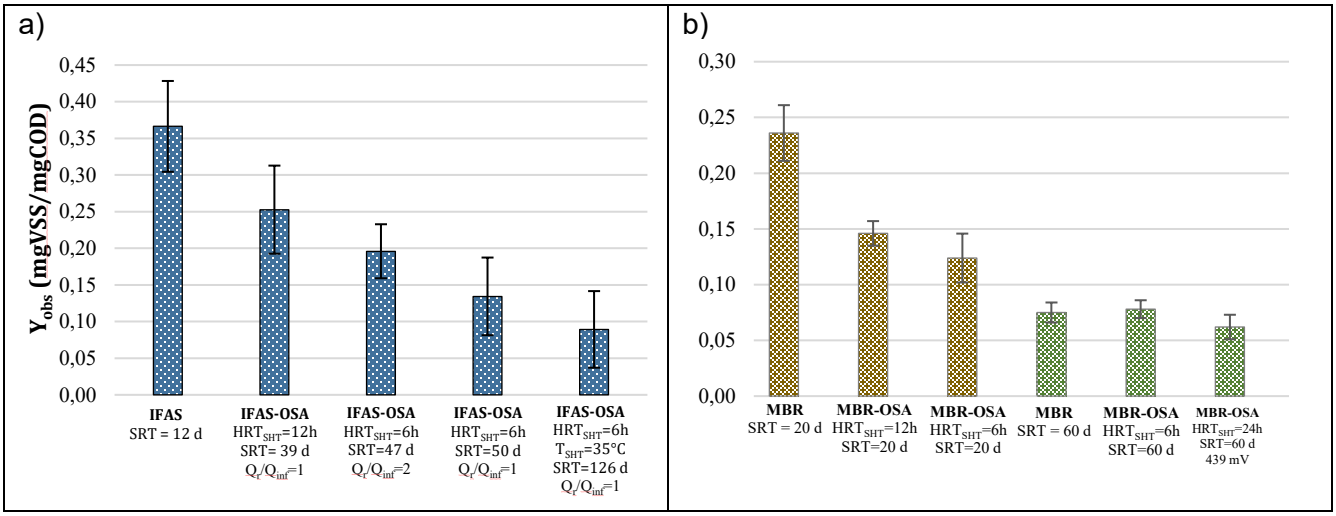

Figure 1 – (a) Evolution of Y_{obs} during the IFAS-OSA operation and (b) during the MBR-OSA operating phases.

Sludge dewaterability was evaluated in terms of capillary suction time (CST) at the end of each experimental period (**Table 1**). After the implementation of the OSA process, sludge dewaterability worsened under all the operating conditions tested, as CST passed from 39 s of the reference IFAS to 74-155 s of the IFAS-OSA system. The increase of the CST was probably related to the amount and composition of EPS released in the liquid medium, as a clear correlation between the CST and the concentration of EPS in the suspended phase was revealed (Pearson's coefficient = 0.87). The higher CST corresponded to the higher concentration of EPS, which was detected when the IFAS-OSA process was operated at the HRT_{SHT} of 12 h. This result confirms that the lower HRT_{SHT} of 6 h was the most suitable not only in terms of Y_{obs} reduction, but also for mitigating the worsening of sludge dewaterability.

Table 1 - EPS and SMP concentrations, and CST measured on the sludge from the IFAS at the end of each operational period.

Periods	EPS suspension (mg/g VSS)	EPS biofilm (mg/g VSS)	EPS_{TOT} (mg/g VSS)	SMP (mg/g VSS)	CST (s)
I	68±5	189±13	257±17	19±1	38
II	158±2	129±25	287±23	9±2	155
III	88±5	143±9	230±6	10±1	89
IV	72±2	105±10	177±12	5±1	84
V	54±3	92±11	147±9	25±1	74

During the IFAS-OSA operation, the SRT was not controlled in order to work with a stable biomass concentration inside the IFAS reactor along the study. Consequently, the SRT increased following the reduction of Y_{obs} and it was not possible to clearly discriminate between the effects of the OSA process implementation and SRT increase on the reduction of Y_{obs}. Hence, to better distinguish the effects of the SRT increase from the OSA process implementation on sludge production, during a second study two lab-scale MBR systems were operated at a fixed SRT of 20 d (MBR_{20}) and 60 d (MBR_{60}). Besides, to better understand the influence of both SRT and OSA implementation on the mechanisms governing sludge production and membrane operation, sludge characteristics in terms of EPS content, settleability, and filterability were monitored.

Y_{obs} was 0.236 and 0.075 mg VSS/mg COD for the reference MBR_{20} and the MBR_{60}, respectively (**Fig. 1b**). After the OSA process implementation, the MBR-OSA_{20} and MBR-OSA_{60} were operated at a HRT_{SHT} of 6-12 h and of 6-24 h, respectively. When the MBR-OSA system was operated at the SRT of 20 d, Y_{obs} reduced by 38% and 48% when the HRT_{SHT} was fixed to 12 and 6 h (**Fig. 1b**), respectively, indicating that the OSA process implementation and the lower HRT_{SHT} were more beneficial in reducing sludge production. No beneficial effect was observed for the MBR_{60}, as Y_{obs} did not significantly change at the HRT_{SHT} of 6 h (**Fig. 1b**), indicating a negligible effect on sludge production of the OSA process when microorganisms are subjected to a prolonged SRT. When the HRT_{SHT} was raised to 24 h, enhanced hydrolysis and acidogenic biomass fermentation positively affected sludge production, as Y_{obs} decreased by 17% (**Fig. 1b**).

The OSA process implementation did not negatively affect membrane operation, as transmembrane pressure (TMP) trend was similar for the reference MBR_{20} and the MBR-OSA systems (instant flux of about 15-18 LMH) at the different operating conditions tested, with a chemical cleaning frequency of the membrane that was comparable between the reference MBR_{20} (0.13 d^{-1}) and the MBR-OSA systems (0.08-0.25 d^{-1}). As regards the reference MBR_{60}, TMP was close to zero as it was operated with a lower flux (5 LMH) and no chemical washing was applied during its operation.

Table 2 – EPS concentration of the sludge from the MBR and SHT, and SVI, SRF and nCST measured on the sludge from the MBR at the end of each experimental period.

Periods	$EPS_{TOT,MBR}$ (mg/g VSS)	$EPS_{TOT,SHT}$ (mg/g VSS)	SVI (mL/gTSS)	SRF (m/kg)	nCST (s*L/g TSS)	Turbidity (abs)
I	15±0		116±1	3.28E+13	13±2	0.195±0.010
II	34±6	90±9	225±33	3.27E+14	18±1	n.a.
III	17±6	71±6	312±2	1.60E+14	32±4	0.273±0.068

I'	2±0		109±10	1.12E+13	5±0	0.065±0
II'	4±2	21±10	116±6	7.77E+13	19±3	0.120±0
III'	21±2	38±3	291±7	5.81E+13	19±4	0.881±0.195

n.a. = not available.

Sludge filterability was evaluated by means of both the specific resistance to filtration (SRF) and the normalized CST (nCST) at the end of each experimental period (**Table 2**). Regarding the MBR reference systems, both the SRF and the nCST were lower at the higher SRT of 60 d, showing that the higher SRT had a beneficial effect on sludge filterability, as also observed by Pontoni et al. [20] and Yilmaz et al. [21] . After the implementation of the OSA process, both the SRF and the nCST increased without showing a clear relationship with the operating conditions tested, revealing an overall worsening of sludge filterability after the OSA implementation. However, this phenomenon did not affect membrane operation and cleaning frequency. Sludge settleability was evaluated by means of the sludge volume index (SVI) after proper settling tests. After the OSA process implementation, SVI worsened at all the operating conditions tested. Similarly, by analysing the sludge supernatant obtained after the settling tests, it was observed also a significant increase of the turbidity after OSA implementation, independently from the SRT (**Table 2**). Increase of turbidity was positively correlated with the concentration of EPS_{TOT} in the MBR (Pearson's coefficient = 0.75). Furthermore, turbidity exhibited the worst value at the highest HRT_{SHT} tested of 24 h, consequently its worsening could also be the consequence of the increase in the concentration of dispersed microorganisms due to floc disruption at higher retention times in the MBR and SHT.

In terms of contaminants removal, during both studies the OSA process implementation did not affect chemical oxygen demand (COD) and ammonia (NH_4^+) removal (90-97% and 99-100%, respectively), but improved total nitrogen (TN) reduction (19-53%) due to the partial denitrification occurring inside the SHT. Indeed, TN removal improved due to a partial denitrification occurring under anoxic conditions inside the SHT following the release of organic carbon as a consequence of cell lysis, which served as an endogenous carbon source for microorganisms [8,19]. In contrast, the OSA process implementation negatively affected total phosphorous (TP) removal under most of the operating conditions tested. As the combined systems were not specially optimized for pursuing TP removal, this event is to be ascribed to the reduced bacterial growth and diminished uptake of phosphorous following the decline of Y_{obs} occurred after the implementation of the OSA process [19].

The main outcomes of these two studies can be summarized as follows. First of all, both the lab-scale IFAS and MBR systems exhibited better sludge productions compared to a CAS (**Fig. 1**), with a reduction between 14% and 81% compared to the typical Y_{obs} value reported in literature for a CAS system of 0.43 mg VSS/mg COD [22]. Secondly, the implementation of the OSA process to innovative bioreactors could be a practicable strategy for further reducing sludge production, especially when a high alternation frequency between oxic and anoxic/anaerobic conditions is ensured (at low HRT_{SHT} values). Furthermore, during the MBR-OSA operation, controlling the SRT at fixed values, it was possible to clearly distinguish between the effect of the SRT increase from the OSA process implementation on sludge production, suggesting that the application of the OSA process could be a valid solution when the SRT is controlled at a moderate value (e.g., ≤20 d), but its effect is expected to diminish when the sludge is already exposed to prolonged SRTs. This outcome represents an additional factor to take into account when considering the application of the OSA process as strategy for reducing sludge production. On the other hand, the OSA process implementation caused a worsening of sludge dewaterability due to the increased levels of exopolymeric substances in the suspended biomass of the IFAS system. Sludge dewaterability and membrane fouling did not significantly change after the implementation of the MBR, but sludge settleability worsened.

References

[1] M.C. Collivignarelli, A. Abbà, M.C. Miino, V. Torretta, What advanced treatments can be used to minimize the production of sewage sludge in WWTPs?, Applied Sciences (Switzerland) 9 (2019) 2650. https://doi.org/10.3390/app9132650.

[2] C.L. Martins, V.F. Velho, B.S. Magnus, J.A. Xavier, L.B. Guimarães, W.R. Leite, R.H.R. Costa, Assessment of sludge reduction and microbial dynamics in an OSA process with short anaerobic retention time, Environ Technol Innov 19 (2020). https://doi.org/10.1016/j.eti.2020.101025.

[3] R. Morello, F. Di Capua, G. Esposito, F. Pirozzi, U. Fratino, D. Spasiano, Sludge minimization in mainstream wastewater treatment: Mechanisms, strategies, technologies, and current development, J Environ Manage 319 (2022) 115756. https://doi.org/10.1016/j.jenvman.2022.115756.

[4] R. Ferrentino, M. Langone, L. Fiori, G. Andreottola, Full-Scale Sewage Sludge Reduction Technologies: A Review with a Focus on Energy Consumption, Water (Basel) 15 (2023) 1–20. https://doi.org/10.3390/w15040615.

[5] P. Foladori, G. Andreottola, G. Ziglio, Sludge Reduction Technologies in Wastewater Treatment Plants, 2010. https://doi.org/10.2166/9781780401706.

[6] S. Rodriguez-Perez, F.G. Fermoso, Influence of an oxic settling anoxic system on biomass yield, protozoa and filamentous bacteria, Bioresour Technol 200 (2016) 170–177. https://doi.org/10.1016/j.biortech.2015.09.106.

[7] M. Torregrossa, G. Di Bella, D. Di Trapani, Comparison between ozonation and the OSA process: Analysis of excess sludge reduction and biomass activity in two different pilot plants, Water Science and Technology 66 (2012) 185–192. https://doi.org/10.2166/wst.2012.153.

[8] R. Vitanza, A. Cortesi, M.E. De Arana-Sarabia, V. Gallo, I.A. Vasiliadou, Oxic settling anaerobic (OSA) process for excess sludge reduction: 16 months of management of a pilot plant fed with real wastewater, Journal of Water Process Engineering 32 (2019) 100902. https://doi.org/10.1016/j.jwpe.2019.100902.

[9] S.F. Corsino, M. Carabillò, A. Cosenza, F. De Marines, D. Di Trapani, F. Traina, M. Torregrossa, G. Viviani, Insights on mechanisms of excess sludge minimization in an oxic-settling-anaerobic process under different operating conditions and plant configurations, Chemosphere 312 (2023) 137090. https://doi.org/10.1016/j.chemosphere.2022.137090.

[10] A.L. Eusebi, P. Battistoni, Reduction of the excess sludge production by biological alternating process: Real application results and metabolic uncoupling mechanism, Environmental Technology (United Kingdom) 36 (2015) 137–148. https://doi.org/10.1080/09593330.2014.939230.

[11] R. Ferrentino, M. Langone, G. Andreottola, Sludge reduction by an anaerobic side-stream reactor process: A full-scale application, Environmental Challenges 2 (2021) 100016. https://doi.org/10.1016/J.ENVC.2020.100016.

[12] S.F. Corsino, M. Capodici, D. Di Trapani, M. Torregrossa, G. Viviani, Combination of the OSA process with thermal treatment at moderate temperature for excess sludge minimization, Bioresour Technol 300 (2020) 122679. https://doi.org/10.1016/j.biortech.2019.122679.
[13] T.S. de Oliveira, S.F. Corsino, D. Di Trapani, M. Torregrossa, G. Viviani, Biological minimization of excess sludge in a membrane bioreactor: Effect of plant configuration on sludge production, nutrient removal efficiency and membrane fouling tendency, Bioresour Technol 259 (2018) 146–155. https://doi.org/10.1016/j.biortech.2018.03.035.
[14] Semblante, F.I. Hai, H. Bustamante, W.E. Price, L.D. Nghiem, Effects of sludge retention time on oxic-settling-anoxic process performance: Biosolids reduction and dewatering properties, Bioresour Technol 218 (2016) 1187–1194. https://doi.org/10.1016/j.biortech.2016.07.061.
[15] Y. Wang, Y. Li, G. Wu, SRT contributes significantly to sludge reduction in the OSA-based activated sludge process, Environ Technol 38 (2017) 305–315. https://doi.org/10.1080/09593330.2016.1192223.
[16] S. Saby, M. Djafer, G.H. Chen, Effect of low ORP in anoxic sludge zone on excess sludge production in oxic-settling-anoxic activated sludge process, Water Res 37 (2003) 11–20. https://doi.org/10.1016/S0043-1354(02)00253-1.
[17] Z. Fida, W.E. Price, B.K. Pramanik, B.R. Dhar, M. Kumar, G. Jiang, F.I. Hai, Reduction of excess sludge production by membrane bioreactor coupled with anoxic side-stream reactors, J Environ Manage 281 (2021) 111919. https://doi.org/10.1016/j.jenvman.2020.111919.
[18] A. Karlikanovaite-Balikci, N. Yagci, Evaluation of sludge reduction in an oxic-settling-anoxic system operated with step feeding regime for nutrient removal and fed with real domestic wastewater, J Environ Manage 243 (2019) 385–392. https://doi.org/10.1016/j.jenvman.2019.05.042.
[19] R. Morello, F. Di, E. Sahinkaya, G. Esposito, F. Pirozzi, U. Fratino, D. Spasiano, Operational strategies enhancing sewage sludge minimization in a combined integrated fixed-film activated sludge – oxic settling anaerobic system, J Environ Manage 345 (2023) 118808. https://doi.org/10.1016/j.jenvman.2023.118808.
[20] L. Pontoni, M. Fabbricino, L. Frunzo, F. Pirozzi, G. Esposito, Biological stability and dewaterability of CAS and MBR sludge, Desalination Water Treat 57 (2016) 22926–22933. https://doi.org/10.1080/19443994.2016.1153904.
[21] T. Yilmaz, E.K. Demir, G. Asik, S.T. Başaran, E.U. Çokgör, S. Sözen, E. Sahinkaya, Effect of sludge retention time on the performance and sludge filtration characteristics of an aerobic membrane bioreactor treating textile wastewater, Journal of Water Process Engineering 51 (2023). https://doi.org/10.1016/j.jwpe.2022.103390.
[22] Metcalf & Eddy Inc., G. Tchobanoglous, H.D. Stensel, R. Tsuchihashi, F.L. Burton, Wastewater Engineering: Treatment and Reuse, 2014.

Title: Removal of emerging pollutants using biochar recovered from sewage sludge

Author(s): Maria Cristina Collivignarelli[1,2], Marco Baldi[3], Stefano Bellazzi[1], Sabrina Sorlini[4,5], Adele Papetti[6], Chiara Milanese[7]

1 *Department of Civil Engineering and Architecture, University of Pavia, Via Ferrata 3, 27100 Pavia, Italy; mcristina.collivignarelli@unipv.it (M.C.C.)*

2 *Interdepartmental Centre for Water Research, University of Pavia, Pavia, Via Ferrata 3, 27100 Pavia, Italy*

3 *Former professor Environmental Analytical Chemistry Department of Chemistry, University of Pavia, Via Taramelli 12, 27100 Pavia, Italy.*

4 *Department of Civil, Environmental, Architectural Engineering and Mathematics, University of Brescia, Via Branze 43, 25123 Brescia, Italy; franco.gomez@unibs.it (F.H.G.); a.masoud@unibs.it (A.M.N.M.); sabrina.sorlini@unibs.it (S.S.)*

5 *Research Center on Appropriate Technologies for Environmental Management in Limited Resources Countries (CeTAmb), University of Brescia, Brescia, Italy*

6 *Department of Drug Sciences, Nutraceutical & Food Chemical-Toxicological Analysis Laboratory, University of Pavia, Viale Taramelli 12, 27100 Pavia, Italy*

7 *Department of Chemistry, Physical Chemistry Section, University of Pavia, Via Taramelli 12, 27100 Pavia, Italy.*

Keyword(s): Natural material-based adsorbents; Adsorption; Biochar; Emerging Pollutants

Abstract

Due to the increase in human activity, emerging pollutants constitute a serious problem, becoming more real every year throughout the world. The purification of water from these pollutants is often difficult and not achievable through traditional biological treatments such as activated sludge. In this regard, the adsorption treatment with activated carbon is the most valid alternative that can be implemented. The adsorption treatment of persistent emerging pollutants is currently limited since the activated carbon regeneration phase is often not efficient in the desorption of the retained molecules. The idea of creating adsorbent materials from sewage sludge is therefore of great interest. The sewage sludge, produced by the purification of the water itself, can be engineered through a thermochemical pyrolysis process leading to the formation of biochar, a carbon-based material useful in the purification process thanks to its ability to adsorb, by a chemico-physical process, conservative micropollutants that escape traditional biological processes. In this way, the concept of circular economy is perfectly applied to sewage sludge, Figure1. At each treatment step the biochar must be analysed to study the transformations of the chemico-physical characteristics and the evolution of the adsorbent properties. The optimal operating conditions of thermochemical processes (temperature, contact time, chemicals, etc.) must be studied and optimized to ensure the technical, economic, and energetic sustainability of the treatment chain.

The work was focused on the removal of emerging pollutants such as AOX (Adsorbable Organic Halogens). The maximum removal efficiency was of about 25%. In addition to the application in quaternary sorption, the biochar was dosed in a laboratory-scale activated sludge biomass reactor, but no significant improvement in the overall performance yields was observed. The study therefore envisions future developments involving an optimization phase of the biochar activation procedure to achieve higher yields.

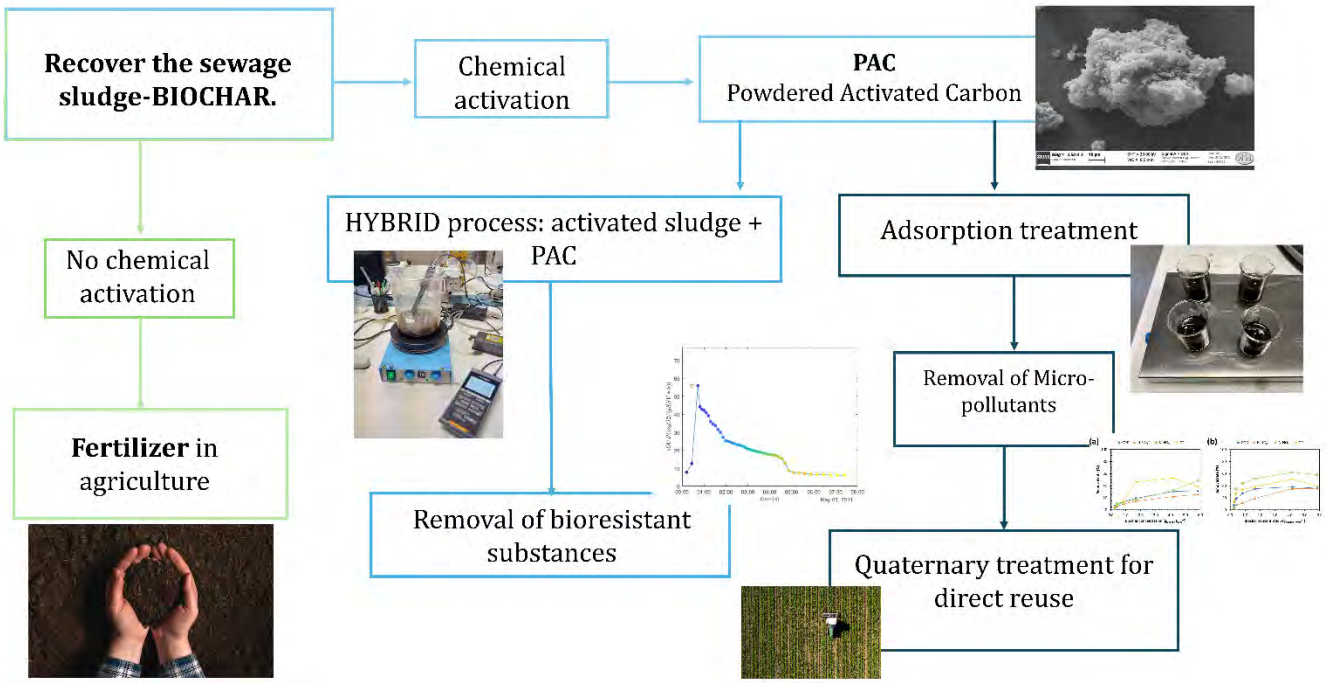

Figure 1. Methodological approach used for the valorisation of biological sludge through biochar.

Title: Life Cycle Assessment applied to sludges from wastewater treatment plant

Author(s): Lavinia Croce*[1], Paolo Viotti[1], Fabio Tatti[2]

[1] *Department of Civil, Construction and Environmental Engineering, Sapienza University of Rome, Via Eudossiana, 18, 00184, Rome, Italy*
[2] *Italian Institute for Environmental Protection and Research, ISPRA, Via Vitaliano Brancati, 48, 00144, Rome, Italy*

***Corresponding author:** lavinia.croce@uniroma1.it

Keyword(s): Life Cycle Assessment, Sludges, Wastewater treatment plant

Abstract

The study uses Life Cycle Assessment as a tool to analyse the impacts generated by the path of treatments of sludge from municipal wastewater treatment plants (CER 190805). Water treatment sludge is a residue resulting from wastewater treatment processes. This sludge contains a complex mixture of organic and inorganic substances, including suspended solids, biodegradable materials and other pollutants. The treatment and disposal of sludge is essential to prevent environmental pollution and protect public health and several rules from different countries give indication about the specific final use and disposal of this waste. Through the use of life cycle analysis, disposal/treatment options can be identified as generate a lower overall environmental impact. According to the UNI EN ISO 14040 [1] and ISO 14044 [2] standards, the LCA consists of four main steps: the definition of system boundaries, the inventory, the assessment of impacts and finally the interpretation of results. Through these different steps, it was possible to determine the emission impacts of sludge treatment and management in the different environmental categories. In fact, as wastewater regulations are increasingly stringent and the production of such sludge is considerable, it is important to place the methods of treatment and disposal of the sludge in line with the principles of environmental sustainability, minimizing the emissions and impacts generated. In the study, reference was made to the greenhouse effect (the one with the greatest impact due to energy use and transport), potential acidification and potential eutrophication. In Italy, various treatment methods are available, aimed at both reducing the water content of sludge and stabilizing it, such as thickening, anaerobic digestion with biogas production and possible energy recovery, methods involving the use of a centrifuge, belt press, etc. In addition to the treatment methods, which lead to the definition of different scenarios with different environmental impacts, one must also consider the different disposal methods, which can be landfill, composting, use in agriculture and incineration with energy recovery. In this study, different scenarios will be analysed to define these impacts and determine the most environmentally sustainable alternative, considering as functional unit 1 ton of mixed sludge (considering primary and secondary sludges) in dry basis. About the system boundaries it is considered the treatments of the mixed sludge, the transport of itself and the different disposal methods with their impacts. Non-commercial software was used for the analysis.

Sludge intended for use in agriculture must undergo stabilization to reduce its putrescibility and possible

hygienic effects, as well as not containing toxic, persistent or bio accumulative substances in concentrations harmful to the soil [3]. The main methods for stabilisation are anaerobic or aerobic digestion, both of which require energy to operate resulting in the production of carbon dioxide. In the former case, however, there is production of biogas that can be used for energy recovery.
For landfilling, the requirement is that the dry matter must not be less than 25 per cent, so methods to reduce the water content, such as dehydration and drying, are necessary [3].
For disposal by incineration processes, a distinction is made between plants dedicated to the disposal of municipal waste with prior thermal drying and plants for sludge with different moisture content (in which case we speak of wet phase oxidation) [3]. Stabilisation is not necessary, and in addition energy recovery can be achieved from the combustion of sludge according to its calorific value. Residual ash usually does not exceed 4% by volume of the dewatered sludge input, and it requires an adequate final disposal.
The main treatment technologies according to the different treatment methods are shown in Table 1:

Table 1. Sludge treatment considering different disposal methods [4]

Sludge treatment	Application on the soil	Disposal in landfills	Incineration
Dewatering	Moderate importance	Important	Important
Stabilization	Important	Moderate importance	Without importance

The study completes a previous paper [5] from the same authors which applies the LCA procedure to the management of a wastewater treatment plant in three different scenarios:

- Scenario A, considering a typical sludge-activated treatment plant;
- Scenario B, in which MBR technology was added to replace the secondary settler compared to the base case of scenario A;
- Scenario C, where the implementation of scenario A is the introduction of the anaerobic digester in the sludge line with energy recovery together with a photovoltaic plant in order to satisfy the energy demand of the plant itself.

As it is possible to evidence from Figure 1 the main impact comes from the CO_2 contribution to the Global Warming Potential (GWP) due to the large energy consumption and as a result of N_2O emissions in the effluent, which has a high conversion factor (298 times greater than that of CO_2 as reported by CML 2001) while acidification and eutrophication are due only to transport and partly to N_2O emissions in the effluent (just for the eutrophication) and remain unchanged in all three scenarios:

Figure 1. Comparison between Global Warming Potential (GWP) [kg CO_2 eq], Potential Acidification (PA) [kg SO_2 eq] and Potential Eutrophication (PE) [kg PO^{-}_4 eq] in scenario A [5]

Only in case of specific technologies for the energy recovery, such the ones reported in scenario C, (Figure 2) it is possible to reduce such important impact:

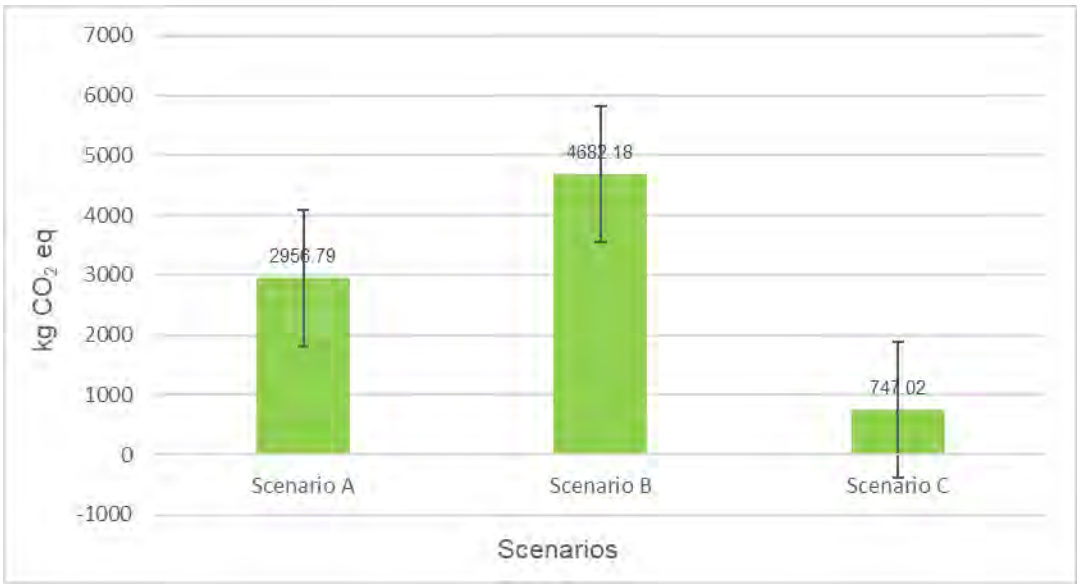

Figure 2. Comparison of GWP in the three different scenarios on a daily basis (related to energy consumption) [kg CO_2 eq] [5]

These considerations can be useful also in case of the other important phase of the wastewater recovery like the sludge's treatment and disposal as well as the construction of the plant itself [6]. The aim of this study is to find out if the correct combination of technologies can bring to a further step towards the sustainability also in the field of the Integrated Water Cycle with particular reference to the sludge treatment.

References

1. *Environmental Management-Life Cycle Assessment-Principles and Framework*; 1404;
2. Standard, I.; Preview, T.S. ISO 14044 Environmental Management-Life Cycle Assessment-Requirements and Guidelines Management Environnemental-Analyse Du Cycle de Vie-Exigences et Lignes Directrices ITeh STANDARD PREVIEW. **1404**, *2006*.
3. Angiuli, A.; Bonifazi, A.; Brunetti, G.; Caniani, D.; Ciola, G.; Colucci, V.D.; De Mattia, M.C.; Guariglia, D.; Iannone, R.F.; Lacarbonara, F.; et al. *Il Riutilizzo Dei Fanghi e Delle Acque Reflue in Agricoltura*; 2011; ISBN 9788880829218.
4. Andreoli, C.V.; Fernandes, F. *B I O L O G I C A L WA S T E WAT E R T R E AT M E N T S E R I E S TREATMENT*; Vol. 6; ISBN 9781843391661.
5. Viotti, P.; Tatti, F.; Bongirolami, S.; Romano, R.; Mancini, G.; Serini, F.; Azizi, M.; Croce, L.; Pubblica Sabina Sp, A. Life Cycle Assessment Methodology Applied to a Wastewater Treatment Plant. *Water 2024, Vol. 16, Page 1177* **2024**, *16*, 1177, doi:10.3390/W16081177.
6. Croce, L.; Viotti, P. Life Cycle Assessment applied to the construction phase of a wastewater treatment plant. 1st International Conference on Circularity, Sustainability and Resilience in Water, Wastewater and Sludge Management – CSRW24. Varese Conference 02/2024

Title: Unravelling the impact of thermo-alkaline pre-treatment of sewage sludge on the microplastics contained.

Author(s): Alberto Zoccali*[1], Alvise Vianello[2], Francesca Malpei[1], Jes Vollertsen[2]

[1] *Department of Civil and Environmental Engineering (DICA), Politecnico di Milano, Milan, Italy*
[2] *Department of the Built Environment, Aalborg University, Thomas Manns Vej 23, 9220 Aalborg, Denmark*

Keyword(s): PET and PA(66) particles, Mass evaluation, Chemical spectrum analysis

Abstract

Microplastics (MPs) are small-size plastics intentionally made or formed from large plastics due to sunlight, mechanical actions and other environmental stressors [1]. Recently, MPs has been classified as “small microplastics” and “large microplastics”, when their size ranging from 1 µm to 1 mm and from 1 mm to 5 mm, respectively. Furthermore, MPs have been recognized as Contaminants of Emerging Concern (CEC) due to the potential risk they pose to the environmental and human health [2].
MPs have been extensively studied across various environmental compartments, including air, water, and soil. Concerning the aquatic environment, their presence has been documented in surface freshwater, marine ecosystems, as well as in drinking water and wastewater [3]–[5]. The latter is widely investigated so far. In particular, wastewater treatment plants (WWTPs) have gathered attention as key contributors to MPs dispersion, serving as major terrestrial pathways for their release into aquatic ecosystems. Despite not being specifically designed for MPs removal, WWTPs demonstrate to be able to reach a MPs’ removal efficiency up to over 99% along the water treatment process [6]. However, it is worth noting that MPs’ removal within the WWTPs is mostly due to preliminary mechanical separation and entrapment in sludges. [7]–[9]. MPs concentration in sludge varies widely among different studies, ranging from 0.02 to 9379 MPs/g dry weight (DW) [10], [11]. Based on our own data processing of 55 papers, the average MPs concentration in dried sludge is about 125 ± 760 MPs/gDW. Such high variability may be due to different methods applied for the analysis and sampling. Sludge is therefore a very relevant path for MPs to enter into the environment, directly or indirectly. In the current WWTPs, the most common sludge stabilisation process employed is the anaerobic digestion (AD) [12]. Therefore, it is very important to study and investigate the fate and behaviour of MPs along the sludge line, including the effect of pre-treatments that are currently applied to enhance the anaerobic biodegradability of sludge [1], [13].
This topic has not been extensively investigate so far and, for this reason, the scope of this research is to evaluate experimentally if thermo-alkaline pre-treatment of synthetic sludge spiked with MPs can induce any MPs degradation.

A synthetic sludge free of MPs was prepared following the recipe of Baudez et al. [14] and spiked with specific MPs, as reported in Table 1. Tests were performed in stirred laboratory scale reactors, in duplicates.

Finally, the MPs were extracted from the treated samples and analysed. The MPs’ extraction protocol consisted of several subsequent steps (peroxidation with H_2O_2 (50%), SDS treatment, enzymatic treatments, Fenton oxidation and density separation) as described by Chand et al. [15]. The only difference is the solution used during the density separation that it was a zinc chloride solution of density 1.75 g/cm^3. The MPs’ extraction protocol required about 1 month per sample.

Table 1. Characteristics of the MPs and operating conditions of the thermo-alkaline pre-treatment tested.

Polymer types of MPs	PET and PA(66)
Shape of MPs	Fragment
Sizes of MPs	20 – 2000 µm
MPs added per sample	MPs >300 µm: 20 items for each polymer type MPs <300 µm: 0.38 mgPA(66) and 0.28 mgPET (consist of a total of about 500 MPs)
Dosages of NaOH or O_3	NaOH: 0, 0.5M and 10M
Volume deionized water or synthetic sludge	50 mL
Temperature	80°C and 120°C
Contact time	60 and 120 min

An evaluation of the mass (only for the MPs >300 µm) and the identification and characterization of the MPs has been performed before and after the treatments.
The mass of the MPs was measured using a Microbalance Sartorius CUBIS. The identification of the MPs >300 µm was done using a stereomicroscope (ZEISS, SteREO Discovery.V8), equipped with an Axiocam 105 color camera with a maximum 8x magnification. The particles' IR spectra were obtained with an Attenuated Total Reflection Fourier Transform Infrared (ATR-FTIR) microscopy (Agilent Cary 630 FTIR with a diamond ATR).
For the MPs <300 µm the characterization was carried out using a Focal Plane Array (FPA)-µFTIR microscope (Agilent Cary 620 FTIR microscope equipped with a 128 × 128 pixel FPA and coupled to an Agilent 670 IR spectroscope).
Thermo-alkaline pre-treatments caused the reduction of PET MPs, the more at increasing NaOH dosages, and up to about 100% at 10M dose (see an example in Figure 1). On the contrary, PA(66) did not show any mass losses, but only a very superficial degradation.

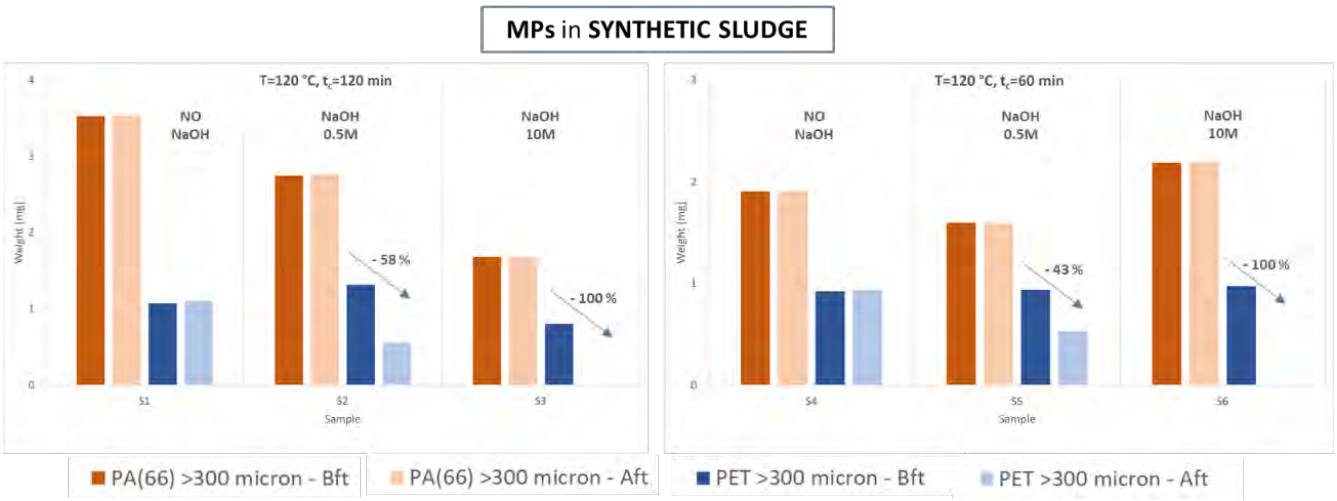

Figure 1. Example of mass evaluation of the MPs before and after the thermo-alkaline pre-treatment, for different operating conditions and NaOH dosages.

Considering the evaluation of the chemical spectrum of the MPs, with the thermo-alkaline pre-treatment, the PET particles showed the main changes in the spectral region between 1200 cm^{-1} and 1600 cm^{-1}. A principle component analysis (PCA) confirmed that the changes are function of the matrices and the NaOH dosages, as showed in Figure 2. On the contrary, the PA(66) did not show significant changes in

the chemical spectrum but only a slight formation of a peak in the spectral region 1730-1760 cm^{-1} (see Figurer 3).

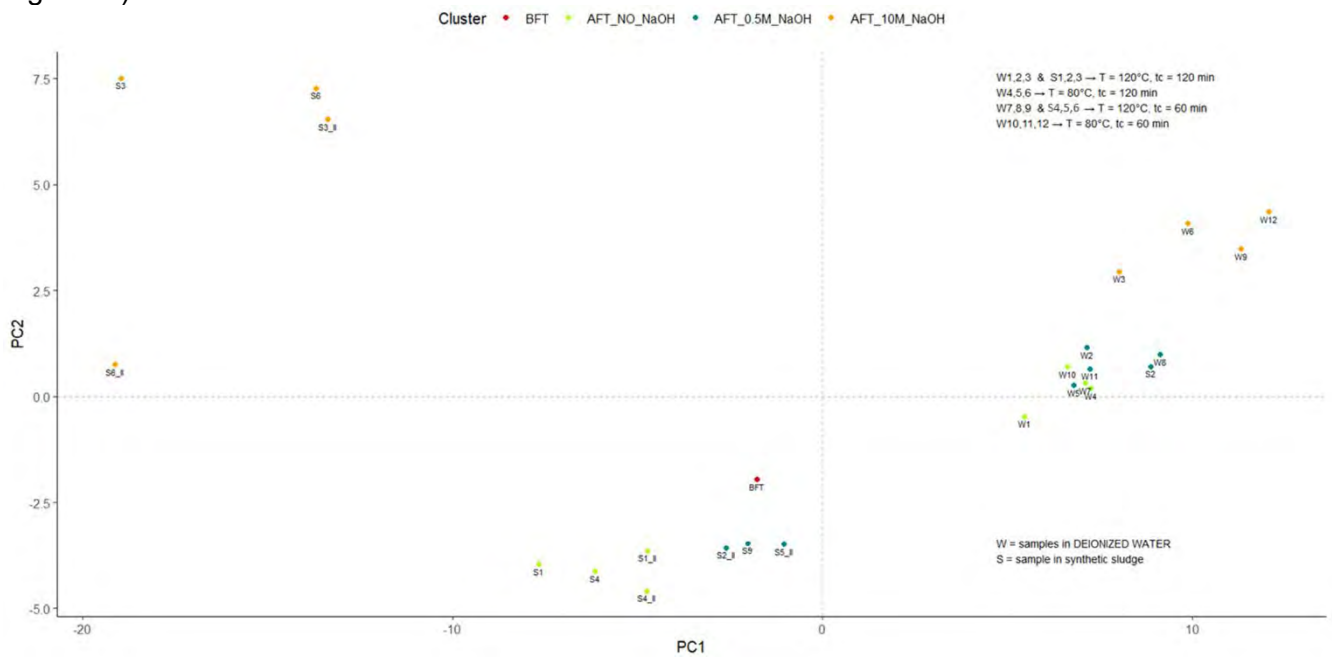

Figure 2. PCA analysis for the PET particles, considering the spectral region between 1200 cm^{-1} and 1600 cm^{-1}. All samples have been taken into account.

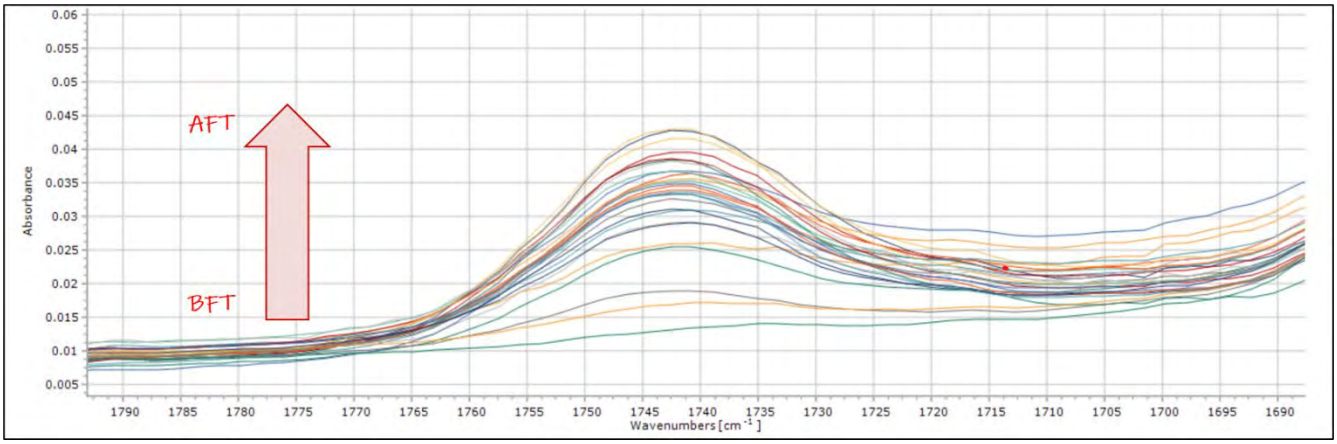

Figure 3. Formation of a peak in the spectral region 1730-1760 cm^{-1} for the PA(66) particles after the thermo-alkaline pre-treatment.

In conclusion, the thermo-alkaline pre-treatment has shown significant and marked changes in PET particles, as could be expected considering the reaction of NaOH with the ester bonds. On the contrary, the amide bonds of PA(66) particles, were less affective, showing just a superficial effect. These results are also interesting from an applied perspective, considering that the lower investigated dose is in line with that used in full-scale plants.

As future perspectives, research on other pre-treatments, other polymer types and on combined pre-treatment with AD are suggested to elucidate the potential reduction and changes in MPs' content.

This work is done within a Ph.D. thesis funded by FSE REACT-EU PON (XXXVII).

References

[1] J. Li, M. Dagnew, and M. B. Ray, "Microfibers in anaerobic digestion: Effect of ozone pretreatment," *J. Environ. Manage.*, vol. 346, no. June, p. 118792, 2023, doi: 10.1016/j.jenvman.2023.118792.

[2] M. Wagner and S. Lambert, *Microplastic pollution in inland waters focusing on Asia*, vol. 58. 2018.

[3] F. Belzagui, C. Gutiérrez-Bouzán, A. Álvarez-Sánchez, and M. Vilaseca, "Textile microfibers reaching aquatic environments: A new estimation approach," *Environ. Pollut.*, vol. 265, 2020, doi: 10.1016/j.envpol.2020.114889.

[4] R. Talbot and H. Chang, "Microplastics in freshwater: A global review of factors affecting spatial and temporal variations," *Environ. Pollut.*, vol. 292, no. PB, p. 118393, 2022, doi: 10.1016/j.envpol.2021.118393.

[5] M. Barchiesi, A. Chiavola, C. Di Marcantonio, and M. R. Boni, "Presence and fate of microplastics in the water sources: focus on the role of wastewater and drinking water treatment plants," *J. Water Process Eng.*, vol. 40, no. November 2020, p. 101787, 2021, doi: 10.1016/j.jwpe.2020.101787.

[6] J. Sun, X. Dai, Q. Wang, M. C. M. van Loosdrecht, and B. J. Ni, "Microplastics in wastewater treatment plants: Detection, occurrence and removal," *Water Res.*, vol. 152, pp. 21–37, 2019, doi: 10.1016/j.watres.2018.12.050.

[7] F. Murphy, C. Ewins, F. Carbonnier, and B. Quinn, "Wastewater Treatment Works (WwTW) as a Source of Microplastics in the Aquatic Environment," *Environ. Sci. Technol.*, vol. 50, no. 11, pp. 5800–5808, 2016, doi: 10.1021/acs.est.5b05416.

[8] K. Magnusson and F. Norén, "Screening of microplastic particles in and down-stream a wastewater treatment plant," *IVL Swedish Environ. Res. Inst.*, vol. C 55, no. C, p. 22, 2014.

[9] M. Lares, M. C. Ncibi, M. Sillanpää, and M. Sillanpää, "Occurrence, identification and removal of microplastic particles and fibers in conventional activated sludge process and advanced MBR technology," *Water Res.*, vol. 133, pp. 236–246, 2018, doi: 10.1016/j.watres.2018.01.049.

[10] A. A. Franco *et al.*, "Assessment and accumulation of microplastics in sewage sludge at wastewater treatment plants located in Cádiz, Spain," *Environ. Pollut.*, vol. 317, no. September 2022, p. 120689, 2023, doi: 10.1016/j.envpol.2022.120689.

[11] P. Salmi, K. Ryymin, A. K. Karjalainen, A. Mikola, E. Uurasjärvi, and J. Talvitie, "Particle balance and return loops for microplastics in a tertiary-level wastewater treatment plant," *Water Sci. Technol.*, vol. 84, no. 1, pp. 89–100, Jul. 2021, doi: 10.2166/wst.2021.209.

[12] A. Gianico, C. M. Braguglia, A. Gallipoli, D. Montecchio, and G. Mininni, "Land application of biosolids in europe: Possibilities, con-straints and future perspectives," *Water (Switzerland)*, vol. 13, no. 1, 2021, doi: 10.3390/w13010103.

[13] H. Li, C. Li, W. Liu, and S. Zou, "Optimized alkaline pretreatment of sludge before anaerobic digestion," *Bioresour. Technol.*, vol. 123, pp. 189–194, 2012, doi: 10.1016/j.biortech.2012.08.017.

[14] J. C. Baudez, P. Ginisty, C. Peuchot, and L. Spinosa, "The preparation of synthetic sludge for lab testing," *Water Sci. Technol.*, vol. 56, no. 9, pp. 67–74, 2007, doi: 10.2166/wst.2007.714.

[15] R. Chand, K. Kohansal, S. Toor, T. H. Pedersen, and J. Vollertsen, "Microplastics degradation through hydrothermal liquefaction of wastewater treatment sludge," *J. Clean. Prod.*, vol. 335, no. December 2021, p. 130383, 2022, doi: 10.1016/j.jclepro.2022.130383.

Biological vs. thermo-alkali pre-treatments: which is the best option for the valorization of WAS? Experimental tests and techno-economic analysis

Barbara Ruffino*, Giuseppe Campo, Alberto Cerutti, Mariachiara Zanetti

Department of Environment, Land and Infrastructure Engineering, Politecnico di Torino, Corso Duca degli Abruzzi 24, 10129 Torino, Italy (corresponding author e-mail: barbara.ruffino@polito.it)

Keywords: Techno-economic analysis; temperature-phased anaerobic digestion; biomethane; biogas upgrade; membrane; energy neutrality

Abstract

Improving the efficiency of anaerobic digestion (AD) of waste activated sludge (WAS) by means of pre-treatments is a critical step towards energy neutrality in wastewater treatment plants (WWTPs). This study was aimed at obtaining reliable outcomes for the future implementation of WAS pre-treatments in full-scale WWTPs, through pilot-scale continuous tests and a techno-economic analysis (TEA). Thermo-alkali (TA, 4 g NaOH/100 g TS, 90 ◦C, 90 min) and biological hydrolysis (BH, two-stage AD, 3 days, 55°C + 20 days, 38°C) pre-treatments were compared. The results showed that (i) TA was 3 times more efficient in COD solubilization than BH (40% vs. 15%); (ii) the specific methane production increase was of 110% and of only 24% for TA and BH, respectively, compared to the control system (untreated WAS). The surplus of biogas, over the amount necessary to sustain the AD process, was depolluted and upgraded to biomethane through an absorption tower, for H_2S and water removal, and a double-stage permeation membrane plant. According to the TEA outcomes, a biomethane selling price of at least 290 €/MWh was necessary to cover the costs associated with the "base" scenario (digestion of untreated WAS). Following enhanced biomethane production due to pre-treatments implementation, the selling price could decrease to around 250 €/MWh (BH) and 115 €/MWh (TA).

Introduction

Hydrolysis has been recognized as the limiting phase of anaerobic digestion (AD) of waste activated sludge (WAS). Energy recovery from WAS is still at quite low values, accounting for just around 7% of the energy available in wastewater [1]. That low value depends on the intrinsic nature of WAS. Specifically, the presence of protective extracellular polymeric compounds and the stiff structure of microbial cell walls determine low hydrolysis rate and low bio-methane output. Many efforts have been made to accelerate hydrolysis by using various types of pre-treatments [2]. Biological hydrolysis (BH) pre-treatments, among many others, try to improve hydrolysis in a stage preceding the principal digesting process. This reactors' configuration is known as two-phase AD (2PAD) or temperature phased AD (TPAD), because the first reactor is usually maintained at a higher temperature than the second reactor. There are only few reports of this type of pre-treatment applied to WAS as a mono-substrate in the literature [3].

In this study pilot-scale tests and a techno-economic analysis (TEA) were carried out to evaluate the feasibility of a BH process applied to WAS as a sole substrate. This scenario was compared with a "zero-scenario", that is where WAS was digested as it is, and with a scenario which included the application of the thermo-alkali (TA) pre-treatment (4 g NaOH/100 g TS, 90 ◦C, 90 min) already tested in a previous study [4]. The TEA was focused on both the digestion phase and the subsequent phases of depollution and upgrade of biogas to biomethane. The price at which biomethane must be sold to make the investment profitable was calculated by using the discounted cash flow (DCF) method.

Materials and Methods

Samples of WAS were collected from the outlet of the gravity pre-thickeners of a large Italian WWTP (2 M population equivalent). For the study purpose, WAS was thickened by gravity from its original TS content to approx. 2-2.5% by weight and stored at 4°C until use. The inoculum used for the start-up of the digesters was obtained from the full-scale digesters of the same WWTP.

The study included 3 pilot-scale tests aimed at comparing the performances of TA and BH pre-treatments with a reference system where the AD of the WAS was carried out under mesophilic conditions and no pre-treatments were applied. The operating conditions for the TA pre-treatment were 4 g NaOH/100 g TS, 90 ◦C, 90 min [4]. Both the raw and the TA pre-treated WAS were digested with a hydraulic retention time (HRT) of 20 days. In the third test, the WAS was subjected to a BH pre-treatment in a 12-L (working volume, 9 L) continuous stirred reactor (CRS) set at 55°C with a 3-day HRT. The pre-treated WAS was digested in a similar reactor (CSR, working volume 10 L), under mesophilic conditions (38°C), with a 20-day HRT.

The aim of the TEA was to calculate the price at which biomethane must be sold to compensate both the investment cost required to set up the plant for WAS valorization and biogas upgrade, and the annual operating costs.The TEA of the process considered a thickened WAS flow rate of 10 m^3/h with a TS content of 5% (VS/TS = 0.7). The WAS was treated according to the 3 different schemes described above, namely no pre-treatment, TA and BH (as detailed in Figure 1). In all the 3 schemes the biogas produced from the AD was split into two aliquots: (i) one was burned in a boiler, to obtain the heat necessary for the pre-treatment and/or the AD process; (ii) the other was subjected to processes of depollution and upgrade, to produce biomethane to be used as a natural gas substitute. The technical assessment included the heat balance related to the thermal sustainability of the whole AD process and the design of the principal components necessary for AD and biogas depollution and upgrade, which are depicted in Figure 1. Details of the methods used for the TEA are provided in a previous publication [5].

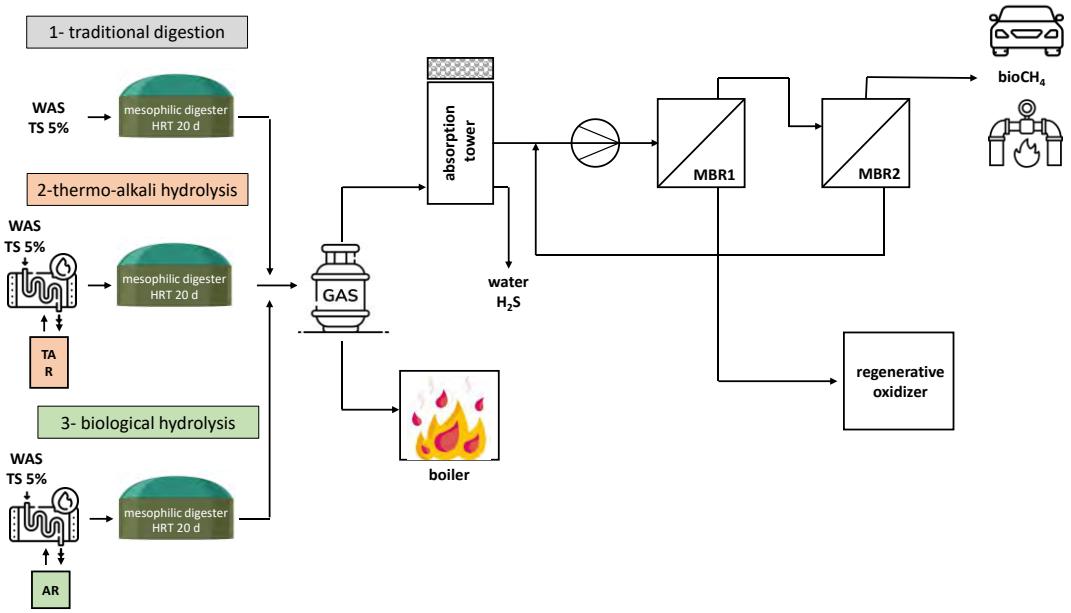

Figure 1. Scheme of biogas production and upgrade (some images are taken from www.flaticon.com)

Results and Discussion

After a phase of start-up, the digesters involved in the 3 tests run steadily for approx. 90 days, more than 4 HRTs. The TA pre-treatment was capable of increasing the amount of soluble COD (sCOD) in the substrate, thus determining a disintegration rate (DR) in the order of 40%, of the same order of that found at a smaller scale [6]. The SMP of the TA pre-treated WAS was of 0.330 Nm^3/kg VS fed, approx. 110% more than the control.
In the TPAD, the acidogenic reactor (AR) converts biodegradable COD to VFAs, through the processes of hydrolysis and fermentation. At the same time, the short HRT (3 days) controls the grow of methanogens and inhibits methane generation. The average sCOD at the AR outlet of the TPAD was of 5400 mg/L, thus determining a DR of approx. 15%. The production of methane in the AR was correctly maintained at low values (0.033 Nm^3/kg VS), around 17% of the overall production of the TPAD. As it can be seen from Figure 2, the apparent SMP of the methanogenic reactor (MR) was of 0.182 Nm^3/kg VS fed. The apparent SMP was determined by dividing the total methane produced by the amount of VS supplied into the second reactor (MR). The real methane production of the MR was of 0.163 Nm^3/kg VS fed, that is of only few percentage points more than that observed in the control. If both reactors are considered, the production of the TPAD reached the value of 0.196 Nm^3/kg VS fed, 24% more of that observed in the control. The study indicated that the TA pre-treatment outperformed the BH pre-treatment.

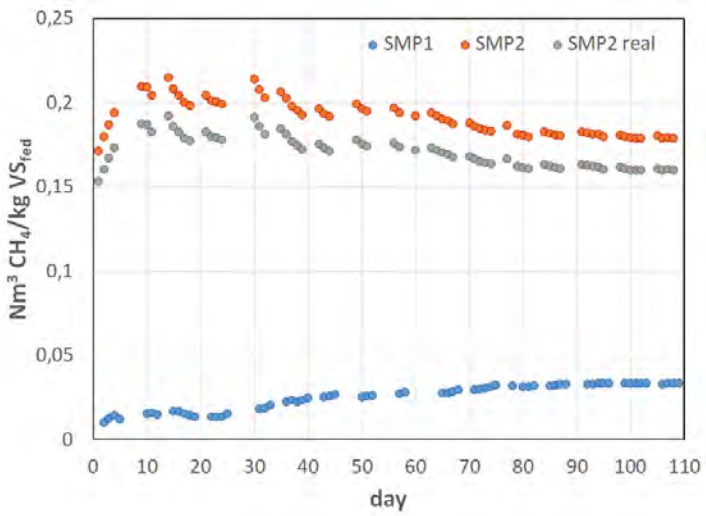

Figure 2. Specific methane production of the TPAD system, 1-AR, 2-MR

The key results of the technical assessment are detailed in Table 1. Based on the SMP found in Scenario 1 (control), 56.1% of the methane produced from the raw WAS was necessary for the thermal self-sustainability of the AD process in the absence of pre-treatments. The heat required for AD was obtained by burning the biogas in a boiler with a power of approx. 310 kW. A residual biogas flow rate of 36.6 Nm^3/h was depolluted and upgraded to obtain 22.5 Nm^3/h of biomethane with a purity of 97%. A membrane of 26 m^2 and a compressor with a power of 11 kW were deemed necessary for that operation. The CAPEX for Scenario 1 amounted to approx. 2.65 M€. The yearly energy cost was around 193 k€, while the price of biomethane capable of covering CAPEX and OPEX was calculated to be 290 €/MWh. The addition of the TA pre-treatment in Scenario 2 reduced the amount of biogas required to ensure the process's thermal self-sufficiency to 32.2%, which is 43% less than in Scenario 1. An amount equal to 60.5% of the heat required by the AD process was provided by the heat exchange between the WAS

exiting from the pre-treatment reactor and the raw WAS entering the sludge line at the ambient temperature (15°C). Scenario 2 could generate a flow rate of 73.1 Nm^3/h of biomethane with a purity of 97%, approx. 3 times more the amount produced in Scenario 1. The CAPEX increased to 3.28 M€, that is 23.7% more compared to the base scenario, because of the higher investments in the section of biogas depollution/upgrade and the presence of two additional pieces of equipment, namely the pre-treatment reactor and the heat exchanger. Specifically, the heat exchanger, with an exchanging surface of 60 m^2, had a purchase cost which was of about 15% of the overall CAPEX (data not shown). When compared to the base scenario, the purchase cost of the gasometer, membrane and compressor increased by 94%, 225% and 237%, respectively. However, because of the increased productivity due to the adoption of the TA pre-treatment, the price of biomethane capable of covering CAPEX and OPEX came to only 115 €/MWh. In this case, the OPEX included the purchase cost of the NaOH necessary for the TA pre-treatment. The annual amount of needed NaOH was 175 t, with a unit cost of 0.3 €/kg.

Table 2. Key parameters of the technical analysis

	Scenario 1	Scenario 2	Scenario 3
Biogas flow rate (Nm^3/d)	2058	4007	2450
Volume of the digester(s) (m^3)	6000	18 (PT) + 6000	900 (BH) + 6000
Heat necessary for the AD process (MJ/d)	26716	32207	29703
Boiler power (kWt)	309.2	372.8	343.8
Biogas to be upgraded (Nm^3/d)	903.3 (43.9%)	2717.2 (67.8%)	1218.1 (49.7%)
Biomethane (97% purity) (Nm^3/d)	540.6	1754.7	759.5
Permeate to be oxidized (Nm^3/d)	362.7 (16.1% CH_4)	962.5 (19.6%)	458.6 (17.8%)
Membrane area (m^2)	26.2	85.1	36.8
Compressor size (kW)	11	37	16

In the case of the TPAD (Scenario 3), the amount of biogas used to sustain the process (50.3%) was approximately of the same amount of that upgraded to biomethane (49.7%). The biogas which could be valorized increased by only 13% compared to Scenario 1. Scenario 3 could generate a flow rate of 31.6 Nm^3/h of biomethane with a purity of 97%, 40% more than Scenario 1. In Scenario 3 the price of biomethane capable of compensating CAPEX and OPEX was equal to approx. 250 €/MWh. This high value, which was only 14% lower than in the base scenario, was owing to both the high CAPEX, which was 30% higher than in Scenario 1, and the poor productivity of the biologically treated WAS. Specifically, the purchase cost of the AR contributed by more than 12% to the CAPEX of the plant. The difference in the CAPEX between the base scenario and the TPAD was noticeably greater than that indicated by Rajendran et al. (2020) [7], which was only of 3%. On the grounds of the results of above, the TA pre-treatment was more promising than BH for a further application at a commercial scale.

Conclusions

This study used tests in pilot-scale reactors and a TEA to compare the feasibility of applying BH, through a TPAD scheme, and TA pre-treatments to WAS. The results demonstrated a clear superiority of the TA pre-treatment over the BH, as here recalled:

1. The DR obtained with the BH was only one third of that of the TA process, that is 15% vs. 40%.
2. The SMP of the TA pre-treated WAS was 0.332 Nm^3/kg VS added, conversely the TPAD SMP was only 0.196 Nm^3/kg VS added. Those values were 110% and 24% higher than the control.
3. In the presence of the same boundary conditions, that is opportunity cost of the capital of 6% and project lifetime of 10 years, the price of biomethane capable of compensating the CAPEX and OPEX

for the project involving BH was more than twice than the price calculated for the digestion scheme including the TA pre-treatment, that is 250 €/MWh vs. 115 €/MWh.

References

[1] Wu S.L., Wei W., Ni B.J. Enhanced methane production from anaerobic digestion of waste activated sludge through preliminary pretreatment using calcium hypochlorite. J. Environ. Manage, 295, 113346 (2021). https://doi.org/10.1016/j.jenvman.2021.113346

[2] Wang X., Jiang C., Wang H., Xu S., Zhuang X. Strategies for energy conversion from sludge to methane through pretreatment coupled anaerobic digestion: potential energy loss or gain. J. Environ Manage, 330, 117033 (2023). https://doi.org/10.1016/j.jenvman.2022.117033

[3] Zhao X., Liu M., Yang S., Gong H., Ma J., Li C., Wang K. Performance and microbial community evaluation of full-scale two-phase anaerobic digestion of waste activated sludge, Sci Total Environ, 814, 152525 (2022). https://doi.org/10.1016/j.scitotenv.2021.152525.

[4] Campo G. et al. A modelling approach for the assessment of energy recovery and impact on the water line of sludge pre-treatments, Energy, 274, 127355 (2023). https://doi.org/10.1016/j.energy.2023.127355

[5] Campo G., Ruffino B., Reyes A., Zanetti M.C. Water-Energy Nexus in the Antofagasta Mining District: Options for Municipal Wastewater Reuse from a Nearly Energy-Neutral WWTP. Water, 15, 1221 (2023). https://doi.org/10.3390/w15061221

[6] Ruffino B., Campo G., Cerutti A., Zanetti M.C., Lorenzi E., Scibilia G., Genon G. Preliminary Technical and Economic Analysis of Alkali and Low Temperature Thermo-alkali Pretreatments for the Anaerobic Digestion of Waste Activated Sludge. Waste Biomass Valor. 7, 667-675 (2016). https://doi.org/10.1007/s12649-016-9537-x

[7] Rajendran K. et al. Advancing anaerobic digestion through two-stage processes: current developments and future trends, Renewable Sustainable Energy Rev, 123, 109746 (2020). https://doi.org/10.1016/j.rser.2020.109746

Title: Exploring alternate aeration strategies for improved sewage sludge stabilization

Author(s): Marta Domini*[1], Giorgio Bertanza[1]

[1] Dipartimento di Ingegneria Civile, Architettura, Territorio e Ambiente e di Matematica, Università degli Studi di Brescia. Via Branze 43, I-25123 Brescia, Italy

Keyword(s): aerobic digestion; sludge minimization; energy efficiency; wastewater treatment plant; cost reduction; dissolved oxygen

Abstract

Sewage sludge management is currently one of the major issues in the field of wastewater management. Sewage sludge is rich in nutrients and can be recovered for reuse in agriculture, biogas production, or incineration. Its high water content and the presence of microbiological and/or chemical contamination, pose challenges to sludge management, necessitating further treatment before reuse. Therefore, minimizing sludge production is a primary objective for wastewater treatment plant (WWTP) managers, to reduce management costs [2].
There are consolidated technologies to reduce the amount of sludge produced or its water content, as well as innovative processes or technologies, such as ultrasonic disintegration, wet oxidation, thermal hydrolysis, membrane bioreactors, enzymatic processes [3, 4, 5, 6, 7].
However, upgrading processes or installing new technologies is not always feasible and can be expensive. It is often advisable to assess the possibility of optimizing the functioning of the units already present in the plant through accurate monitoring, functionality tests on existing compartments, and the control of operational parameters [8].

This study aims to investigate the possibilities for reducing sludge production in a recently revamped WWTP in northern Italy, equipped with aerobic stabilization units, adopting different aeration strategies. In the first phase of the study, continuous aeration was assessed through two full-scale tests conducted in 2022, targeting a dissolved oxygen concentration (DO) of 1 mg/l (P1) and >3 mg/L (P2). Normalized results demonstrated that the Volatile Suspended Solids (VSS) abatement and sludge dewaterability, did not differ substantially with varying DO concentrations, considering a treatment duration of about 2 weeks, which aligns with current plant practice. Consequently, targeting a lower DO concentration resulted in lower energy consumption for the blowers [9].

The second phase of the study involved testing alternate aeration cycles at full scale. The first experiment (PCA) was carried out at the end of 2022, with alternate aerobic and anaerobic cycles active during the day and guided by redox potential and duration, for 22 days. Similarly to the first phase, no relevant differences were observed in VSS reduction or sludge dewaterability. However, energy consumption was lower, and there appeared to be advantages in terms of nitrogen removal [9].

Further full-scale tests using alternate cycles are undergoing (PCA-2 and PCA-3), intending to confirm previous results and verify the nitrogen removal improvement observed, by replicating the first PCA test. Methods included: test in batch for 22 days; dewatering of sludge at the beginning and the end of the test; stabilized and dewatered sludge samples collection for total suspended solids (TSS) and VSS concentrations analysis; analysis of the liquid fraction of the mechanically dewatered sludge for measuring TSS, VSS, COD, BOD_5, nitrogen, phosphorous; analysis of the liquid fraction of the

stabilized sludge (centrifugated manually, twice a week) for measuring nitrogen; monitoring of energy consumption; monitoring of DO, temperature, redox potential. PCA-2 differed from PCA for the following aspects: cycles running day and night; collection and analysis of additional samples of the liquid fraction of stabilized sludge (centrifugated manually); collection and analysis of recirculated sludge samples.

PCA-2 showed better performances than PCA in VSS abatement (32% compared to 25%), whilst VSS/TSS ranged from 69% to 59% (Figure 1). Also, during the test PCA-2, a higher reduction in the quantity of sludge produced was observed than in test PCA (25% and 15%, respectively). The additional data collected in test PCA-2 confirmed a decrease in nitrogen in the sludge.

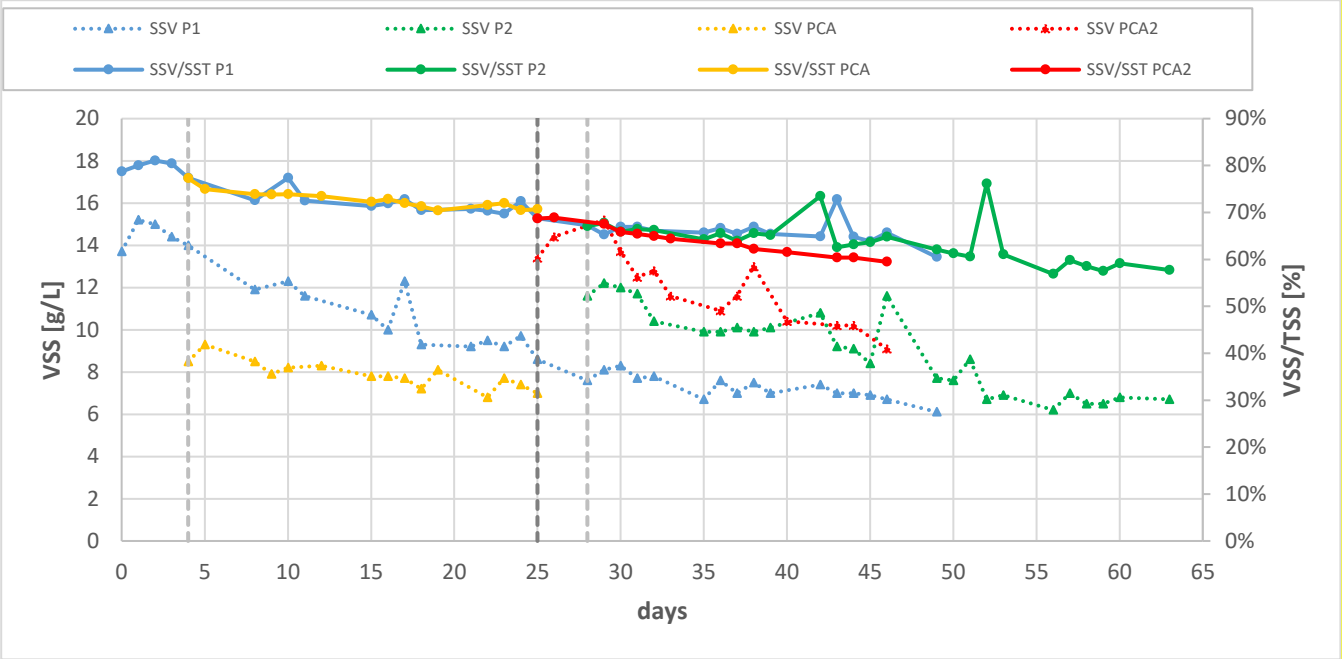

Figure 1. Comparison of tests (P1, P2, PCA, PCA-2) in terms of VSS removal and VSS/TSS ratio. The start of the curve for tests P2, PCA and PCA-2 corresponds to the day when the VSS content was the same as in test P1.

Based on the results obtained, we designed PCA-3 replicating the test PCA-2 with the following differences: analysis of additional parameters on the liquid fraction of stabilized sludge centrifugated manually (TSS, VSS, COD, BOD_5, phosphorous), continuous monitoring of DO and temperature, with automatic regulation of air blowers.
Results will be modeled and normalized following the method developed for previous tests and compared [9]. The final results will be presented at the conference.

The final objective is to develop operational recommendations, based on full-scale tests, to optimize sludge management and reduce associated costs, for which alternate cycle aeration appears to be a promising option.

Acknowledgments

The Authors acknowledge the staff of Acque Bresciane Srl, and the student Claudio Morari, for their support and contribution to data collection and field activities.

References

[1] Morello R., Di Capua F., Esposito G., Pirozzi F., Fratino U., Spasiano D., “Sludge minimization in mainstream wastewater treatment: Mechanisms, strategies, technologies, and current development”, Journal of Environmental Management, 319, 115756, (2022), https://doi.org/10.1016/j.jenvman.2022.115756.
[2] Domini M., Bertanza G., Vahidzadeh R., Pedrazzani R., “Sewage sludge quality and management for circular economy opportunities in Lombardy”, Applied Sciences, 12, 10391, (2022b), https://doi.org/10.3390/app122010391.
[3] Atay Ş., Akbal F., “Classification and effects of sludge disintegration technologies integrated into sludge handling units: an overview”, CLEAN–Soil, Air, Water, 44, 1198-1213, (2016)
[4] Bertanza G., Canato M., Heimersson S., Laera G., Salvetti R., Slavik E., Svanström M., “Technoeconomic and environmental assessment of sewage sludge wet oxidation”, Environmental Science and Pollution Research, 22, 7327-7338, (2015a)
[5] De Oliveira T.S., Corsino S.F., Di Trapani D., Torregrossa M., Viviani G, “Biological minimization of excess sludge in a membrane bioreactor: effect of plant configuration on sludge production, nutrient removal efficiency and membrane fouling tendency”, Bioresource Technology, 259, 146-155, (2018)
[6] Øegaard H.,“Sludge minimization technologies-an overview, Water Science and Technology”, 49, 31-40, (2004)
[7] Pérez-Elvira S.I., Nieto Diez P., Fdz-Polanco F., “Sludge minimization technologies, Reviews in Environmental Science and Bio/Technology”, 5, 375- 398, (2006)
[8] Bertanza G., Collivignarelli C., “Water treatment plants: operational control and functional testing”, (in Italian), Hoepli Editore, Milan, (2012)
[9] Domini, M., Volpi, A., & Bertanza, G. Potential of aerobic stabilization in drastic sludge reduction: a full-scale experiment. Environmental Engineering and Management Journal, 22(10), (2023)

PARALLEL SESSION: B8

Air quality and treatment

Emissions dispersion model

Title: Variability of equivalent Black Carbon aerosol in urban Barcelona by pedestrian mapping

Authors: Alessandro Bigi[1]*, Giorgio Veratti[1], Arunik Baruah[1,2], Laura Renzi[3], Martina Mazzini[3], Luca Di Liberto[3], Angela Marinoni[3], Marco Pandolfi[3], Grazia Ghermandi[1]

[1] *Dip. di Ingegneria 'Enzo Ferrari', Università di Modena e Reggio Emilia; Modena, Italy, *abigi@unimore.it*
[2] *IUSS Pavia, Pavia, Italy*
[3] *Istituto di Scienze per l'Atmosfera ed il Clima, ISAC-CNR, Italy*
[4] *IDAEA-CSIC, Barcelona, Spain*

Keywords: urban air quality, Black Carbon, aethalometer

Abstract

Equivalent Black Carbon (eBC) is an efficient indicator of air quality, endorsed by the latest WHO guidelines and included in the current proposal for a European air quality directive. In the summer of 2021 (July 19 - 31), an extensive observational campaign was conducted to evaluate eBC variability in Barcelona's urban environment. The study combined portable eBC sensors microaethalometers MA200 with reference instruments, the Aethalometer AE33 and the Multi Angle Absorption Photometer (MAAP), alternating between urban mapping and intercomparison at a reference station in Barcelona. Urban mapping involved pedestrian measurements along three distinct routes of approximately 3-4 km each: one representative of high-traffic areas, one in the historic center subject to traffic restrictions, and one near the city port. Each MA200 was assigned to a specific route; when not engaged in mapping, the MA200s were sampling from the same inlet at the reference site alongside the AE33, the MAAP, and other monitors. Intercomparison revealed a high level of consistency between MA200 devices. The eBC values provided by the MA200 firmware at 880 nm exhibited excellent agreement with both AE33-derived eBC and MAAP-derived eBC. The Absorption Ångström Exponent (AAE) derived from MA200 closely matched results from two out of three instruments, exhibiting a relative bias of the median AAE between -1% and 3%. Geographic Information System analysis of the collected data along the routes revealed discrete spatial and temporal variations, characterized by localized hotspots associated with local emission sources. These variations indicated significant differences within the same route, between routes, and between diurnal and weekly periods.

Introduction

Equivalent Black Carbon (eBC) is a insoluble refractory fraction of atmospheric aerosol arising from incomplete combustion of liquid and solid fuels and which has shown detrimental health effects, because it increases the risk of cardiovascular and respiratory diseases and it is therefore included in the latest WHO guidelines [1] and the current proposal of the European air quality directive [2]. Moreover, eBC plays a key role in atmospheric climate, as it absorbs solar radiation, contributing to atmospheric warming and altering cloud optical properties. Variability in eBC levels within urban areas is influenced by several sources, e.g. traffic, distance from roadways, vehicular fleet, urban morphology, domestic heating sources, industrial districts, and meteorological conditions. This variability leads to large differences in population exposure within a given urban setting [3]. Understanding eBC's sources and variability, particularly in urban areas is essential for mitigating both public health hazards and climate change.

Experimental equipment

The campaign covered the period 19 – 31 July 2021 and included both mapping of eBC across three different routes using portable samplers and the intercomparison of the portable samplers with reference instruments.
The samplers used are the lightweight portable micro-Aethalometer MA200 (AethLabs, San Francisco, USA): this is a filter absorption photometer that measures at five wavelengths (λ = 375, 470, 528, 625 and 880 nm) using polytetrafluoroethylene (PTFE) filter tapes. In order to correct for bias induced by particle build-up on the filter during sampling the instruments were used in dual-spot sampling mode and a compensation algorithm similar to the one by [4] was applied by the internal firmware, along with a multiple-scattering correction coefficient Cref = 1.3. Sampling flow was set to 150 ml min^{-1} and sampling interval was set to 30 seconds: given that the walking speed a ~1.04 m s^{-1} held while mapping, each eBC sample corresponds to a spatial average of 30 meters. Three different MA200s were used, one per route; all devices had the same firmware and the same setup. The flowrate of all MA200s was calibrated immediately prior the campaign. The MA200 of the urban traffic route had a malfunction in the early morning of July 25, therefore all data from that moment onwards were discarded from the analysis. For the location of each sampling point, we relied on the geographical coordinates provided by the internal GPS of the MA200.

Three different routes were mapped, representative of the air quality under urban traffic and urban background conditions, and next to the city harbour. Each route was between 3 and 4 km long. The urban background route was within the Low Emission Zone (LEZ) and followed a loop crossing part of the historical city centre, along small alleys and two large squares. The route is mainly pedestrian, with some streets upon to restricted traffic. 35 mins were generally needed to complete it. Several open air cafes and restaurants were present in both squares, with numerous customers, particularly in the evening. The urban traffic route was a loop following two major city roads, the Avenida Diagonal and the Gran Via de Carlos III, having a width of 20 meters and 35 m respectively. The path mapped both sides of both roads along the same stretch: the southern kerbside was mapped first and the northern kerbside was mapped on the way back. The latter kerbside is ~25 m wide, and it has regular trees and a two-lane cycling path. The harbour path is a single-direction route, 4 km long, flanking the harbour docks, with recurrent mooring of cruise/passenger ships and container ships. The urban background and urban traffic routes were mapped three times a day, starting at 9:30 local time (LT), 13:30 LT and 19:30 LT. The harbour route was mapped in the morning and evening, concurrently with the other routes. eBC mapping was repeated for 13 consecutive days.

Whenever not involved in mapping, the MA200s were deployed inside the atmospheric monitoring station within the grounds of the IDAEA-CSIC. The MA200s shared the same inlet, made of conductive material and not-conditioned. The station hosted several reference equipment for the determination of carbonaceous aerosols, including an Aethalometer AE33 (Aerosol d.o.o., Slovenia), a MAAP (Thermo Corp., USA), a semi-continuous online analyser for mass concentration of Elemental Carbon and Organic Carbon (Sunset Lab, Inc, USA) and a Single Particle Soot Photometer (SP2, Droplet Measurement Technologies, USA). Regarding the reference instruments, only the data from the AE33 and the MAAP were included in the analysis of the current study.

Data analysis protocol

In order to combine all mapping data and to allow the computation of a spatial average, each route was split in segments of ca. 90 meters, i.e. containing 3 measurement points. All mapping data was snapped to the closest route segment with a custom algorithm, granting also the correct temporal order of each

point. This procedure was needed due to the noise in the GPS coordinates of the MA200, particularly in the urban canyons of the background route. The snapped data was combined into weekday/weekend medians for the morning, noon and evening repetition of each route.
In order to assess the reliability of the portable instruments measurements, an intercomparison study was performed based on the deployment at the reference station. The eBC levels between the MA200 and the reference instruments were compared, as well as the Absorption Ångström Exponent (AAE) based on a linear fit over the absorption measured at 5 wavelengths from the MA200 and the AE33. The linear correlation between portable and reference instruments was estimated by Total Least Squares (TLS), which fits a linear model by minimizing errors in both the dependent and independent variables, i.e. accounting for the uncertainty in both equipment types. The performance of the intercomparison was computed on 5 minutes medians, i.e. aggregating ten consecutive 30-seconds readings for the MA200: this aggregation is indicative for the median computed on the mapping data aggregated based on the morning/noon/evening repetition of the route.

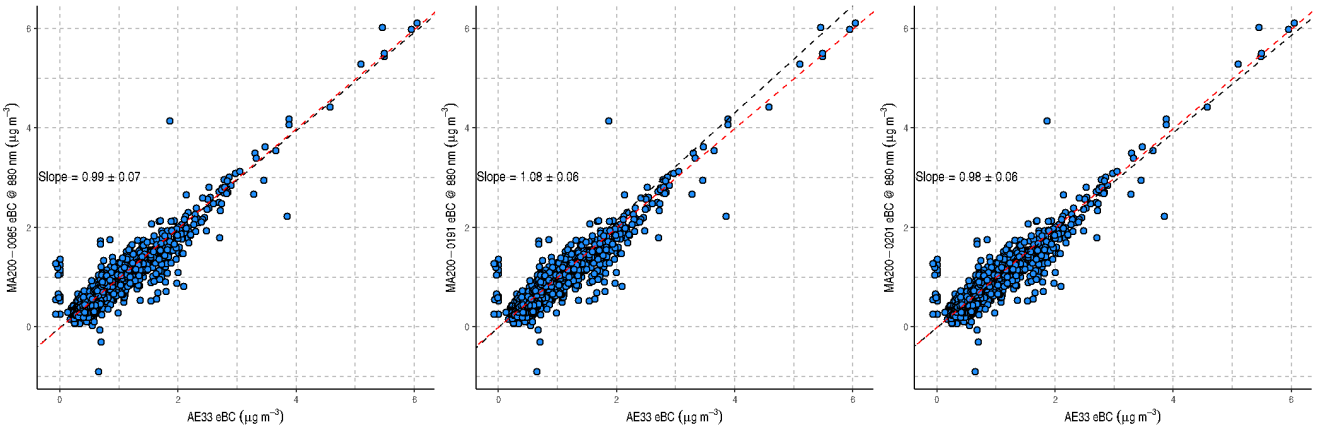

Figure 1. Scatterplot of 5-min median eBC from AE33 and MA200. The red dashed line indicates the 1:1 line, the black dashed line indicates the Total Least Square model (its slope is displayed in the plot).

Results

The eBC by MA200 showed an excellent linear correlation with MAAP for two units (TLS slope 1.02 and 1.04) and some overestimate by a unit (TLS slope 1.12). Similar performance was shown between the MA200 and AE33 (Figure 1), with two units showing excellent correlation for eBC (TLS slope 0.99 and 0.98) and one unit with lower performance (TLS slope 1.08). Similar pattern was shown by the spectral performance of the portable instruments, with two units having only a 2% bias in the AAE estimate, while one unit showed a bias of 12%. The eBC in the routes showed the effectiveness of the traffic restrictions in the LEZ in containing the eBC levels (Figure 2) compared to other routes. Largest eBC occurred in the morning at the traffic site, particularly along Gran Via de Carlos III. All routes had a minimum in the evening, probably due to the intense dispersion due to the increase of the land breeze.

References

[1] WHO, Global Air Quality Guidelines, WHO, Geneva (2021)
[2] European Commission (2022) 2022/0347
[3] Moreno T et al. “Urban air quality comparison for bus, tram, subway and pedestrian commutes in Barcelona”, Environmental Research, 142, 495-510, (2015)

[4] Drinovec L. et al. “The “dual-spot” Aethalometer: an improved measurement of aerosol black carbon with real-time loading compensation” 8, 1965–1979, (2015)

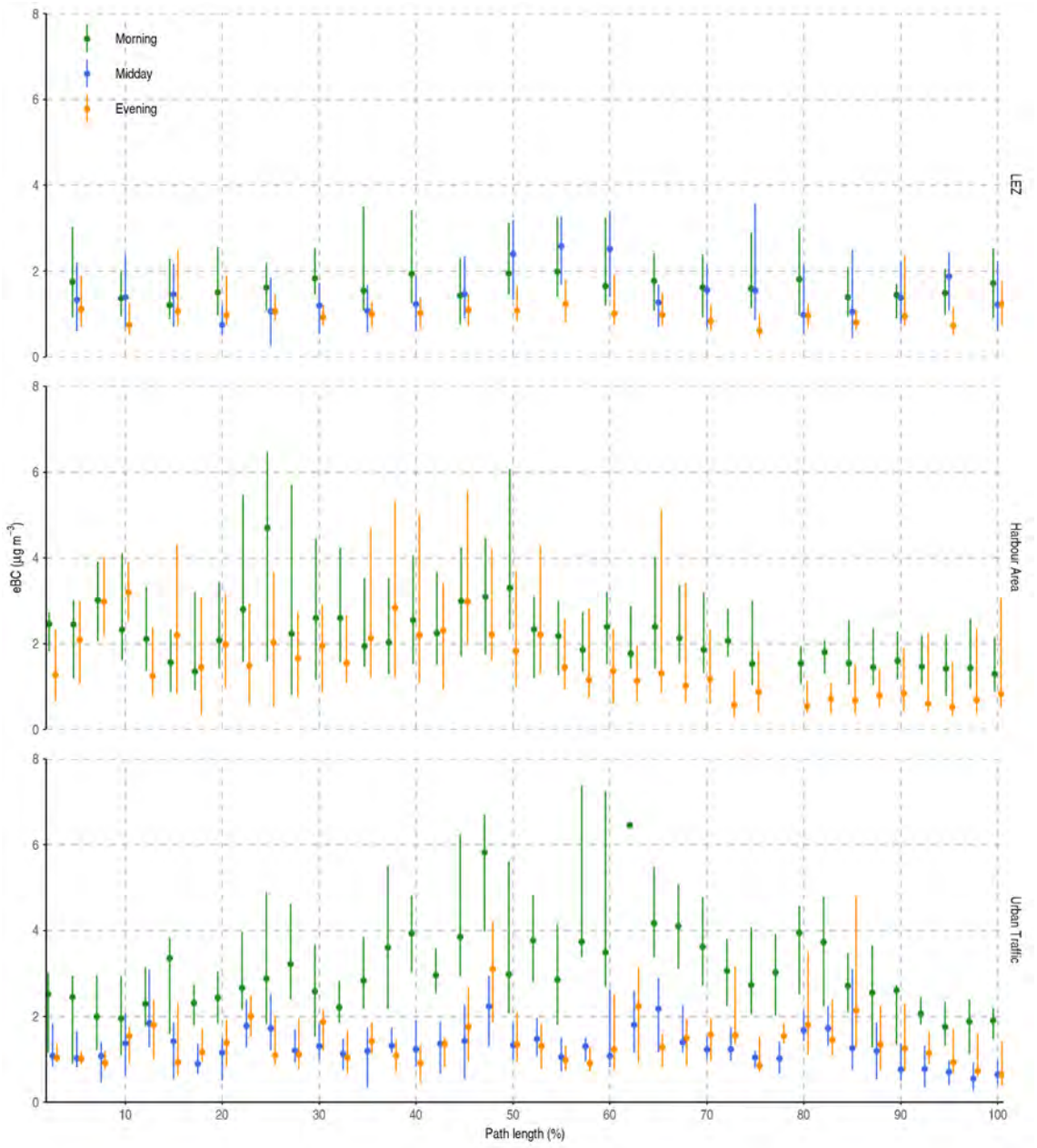

Figure 2. 25th, 50th and 75th quantiles of eBC along each route at morning, noon and evening.

Ackowledgements

This study was supported by the ‘Black Air project’ (CUP E94I19001080005) funded by the University of Modena and Reggio Emilia and Fondazione di Modena and by the ‘CAIAC project’ (I+D+I "Retos Colaboración", PID2019-108990PB-100) funded by the Ministerio de Ciencia, Innovación y Universidades.

Title: Influence of density-driven advection on vapor intrusion of chlorinated volatile organic compounds

Authors: Clarissa Settimi*[1], Iason Verginelli[1], Daniela Zingaretti[1], Renato Baciocchi[1]

[1] *Laboratory of Environmental Engineering, Department of Civil Engineering and Computer Science Engineering, University of Rome Tor Vergata, Via del Politecnico, 1, 00133 Rome*

settimi@ing.uniroma2.it

Keywords: chlorinated vapor intrusion; gas phase transport modeling; density-driven advection; column diffusion experiments

Abstract

Chlorinated volatile organic compounds (CVOCs), such as trichloroethylene (TCE) and tetrachloroethylene (PCE), released in the subsurface may cause the vapor intrusion (VI) into overlying buildings with consequent potential long-term risks to the health of the residents [1]. VI is typically an issue for CVOCs, due to their low biodegradability which does not allow an attenuation of the concentrations during the upward transport of contaminated vapors [2]. For an initial assessment of potential air risks related to VI, indoor concentrations of the contaminants of concern are calculated using attenuation factors (AFs), defined as the ratio of indoor and sub-slab or soil vapor concentrations [3]. In many regulatory programs, default values recommended by U.S EPA are used [4-5]. In the case of chlorinated compounds, in which no attenuation due to biodegradation is expected, the AFs are assumed to be constant with the source concentration [4]. However, Lahvis and Ettinger [3] and Abbasi et al. [6] collected soil gas measures of TCE and PCE concentrations from a large sample of buildings in California, observing a dependence of the AF from the subsurface concentration. In particular, by increasing the contaminants subsurface vapor concentration, a decreasing trend of the AFs was observed [3,6]. In general, there is evidence in literature that density-driven advection generated by density gradients could be relevant for compounds with high molecular weight and high permeability soils [7-9]. During upward diffusion of TCE or PCE vapors in the subsoil, the density of the vapors changes compared to the uncontaminated soil gas, and this density contrast results in a downward advective gas flow (i.e. density-driven transport) [7]. Typically, this phenomenon is not considered for VI evaluations, even for heavy chlorinated compounds [10]. However, many buildings in the US are constructed by posing the structure on high permeability granular fill layers useful for capillary break to avoid humidity intrusion [11] in which density-driven advection could affect the vapors transport.
This study investigates the influence of density-driven transport on the vapor intrusion pathway for CVOCs in such scenarios. For this purpose, a steady-state 1-D numerical model was developed using COMSOL Multiphysics considering two layers of soil with different permeabilities, thus simulating a scenario in which building foundations were constructed on a granular fill layer. In the model, the transport of chlorinated vapors from contaminated groundwater through the two layers of soil was considered affected by upward diffusion and downward density-driven transport. The developed model was validated with the results of an existing numerical model used to evaluate density-driven transport on TCE vapors diffusion [9]. From modeling results, subsurface vapor concentration and soil permeability emerged as influent factors affecting density-driven transport.

To provide further evidence, lab-scale column diffusion tests of TCE vapors were performed using different porous media fillings (i.e. sand and gravel) to examine the vertical soil gas concentration profile varying the permeability. In the column tests, the TCE concentration profiles were lower than expected under the assumptions of purely diffusive transport. Instead, the observed profiles closely matched the concentration values predicted by the developed model, which accounts for density-driven transport. Additionally, according to modeling results, the TCE vertical concentration profiles in the columns were found lower by increasing the filling porous medium permeability.
Similar outcomes were found by comparing the source to building AFs expected by the developed model with the ones observed by Lahvis and Ettinger [3] and Abbasi et al. [6] from field concentration data for TCE and PCE vapors as a function of the source concentration. In particular, the field AFs data were well described by the trends expected using the developed model considering a density-driven transport in the layer under the building foundations with high soil permeability values in the order of 10^{-6}-10^{-10} $m^{2,}$ which is the range of gravel. Thus, the obtained results suggest that density-driven transport could be relevant for chlorinated vapor intrusion, especially in the presence of granular fill layers under the buildings foundations.

References

[1] Verginelli, I., Capobianco, O., Hartog, N., Baciocchi, R., (2017). Analytical model for the design of in situ horizontal permeable reactive barriers (HPRBs) for the mitigation of chlorinated solvent vapors in the unsaturated zone. Journal of contaminant hydrology, 197, 50-61.
[2] U.S. EPA, (2012a). Petroleum Hydrocarbons and Chlorinated Solvents Differ in Their Potential for Vapor Intrusion, March 2012. https://www.epa.gov/sites/default/files/2014-09/documents/pvicvi.pdf
[3] Lahvis, M. A., Ettinger, R. A., (2021). Improving risk-based screening at vapor intrusion sites in California. Groundwater Monitoring & Remediation, 41(2), 73-86.
[4] U.S. EPA, (2012b). EPA's Vapor Intrusion Database: Evaluation and Characterization of Attenuation Factors for Chlorinated Volatile Organic Compounds and Residential Buildings. Office of Solid Waste and Emergency Response. EPA 530-R-10-002. March 16, 2012
[5] U.S. EPA, (2015). OSWER technical guide for assessing and mitigating the vapor intrusion pathway from subsurface vapor sources to indoor air. EPA OSWER Publication, 9200, 2-154.
[6] Abbasi, R., Bosan, W., Gallagher, D., (2023). Empirically Derived California Vapor Intrusion Attenuation Factors. Groundwater Monitoring & Remediation, 43(1), 60-68.
[7] Falta, R. W., Javandel, I., Pruess, K., Witherspoon, P. A., (1989). Density-driven flow of gas in the unsaturated zone due to the evaporation of volatile organic compounds. Water resources research, 25(10), 2159-2169.
[8] Mendoza, C. A., Frind, E. O., (1990). Advective-dispersive transport of dense organic vapors in the unsaturated zone: 2. Sensitivity analysis. Water Resources Research, 26(3), 388-398.
[9] Cotel, S., Schäfer, G., Barthes, V., Baussand, P., (2011). Effect of Density-Driven Advection on Trichloroethylene Vapor Diffusion in a Porous Medium. Vadose Zone Journal, 10(2), 565 581.
[10] Yao, Y., Shen, R., Pennell, K. G., Suuberg, E. M. (2013). A review of vapor intrusion models. Environmental science & technology, 47(6), 2457-2470.
[11] U.S. EPA, (2013). Moisture Control Guidance for Building Design, Construction and Maintenance, U.S. Environmental Protection Agency, 2013. https://www.epa.gov/sites/production/files/2014-08/documents/moisture-control.pdf.

Title: Micro-aethalometers and dispersion modeling for the identification of sources and levels of black carbon in a city of the central Po valley

Author(s): Giorgio Veratti*[1], Alessandro Bigi[1], Michele Stortini[2], Sergio Teggi[1], Grazia Ghermandi[1]

[1] *Department of Engineering "Enzo Ferrari", University of Modena and Reggio Emilia, Modena, Italy, {giorgio.veratti,alessandro.bigi,sergio.teggi,grazia.ghermandi}@unimore.it*
[2] *Struttura Idro Meteo Clima, Arpae Emilia-Romagna, Bologna, Italy, mstortini@arpae.it*

Keyword(s): Black carbon, atmospheric dispersion modeling, aethalometers, source apportionment

Abstract

Atmospheric aerosol particles significantly affect the Earth's radiation budget by directly scattering and absorbing solar and terrestrial radiation. They also serve as cloud condensation nuclei, influencing cloud formation and characteristics. Among these particles, black carbon (BC) is increasingly recognized as a significant component due to its broad-spectrum absorption capacity, ranging from ultraviolet to infrared wavelengths. This absorption leads to localized atmospheric heating and alters the distribution of solar radiation in the atmosphere. In addition to its climatic effects, BC poses significant public health risks, with exposure associated with aggravation of respiratory diseases, cardiovascular effects, impairment of lung function, and increased susceptibility to infection. Consequently, understanding the role of BC in atmospheric processes is critical to addressing both environmental and public health concerns.
Recent attention about health and climate impacts have led to a surge of research in urban areas, with a particular focus on BC concentrations identified as a key indicator of urban pollution. As a result, several studies have investigated the variability of BC mass concentrations in different urban locations. Despite the use of precise methods for BC determination, these studies have been limited to specific monitoring sites and have failed to provide continuous spatial data across the city, which is crucial to ensure consistent epidemiologic analyses.
This study aims to address this gap by conducting a comprehensive assessment of BC levels and source contributions in the urban environment of Modena, a medium sized city located in the central Po Valley. By employing a combination of field measurements and modeling techniques, we seeked to provide spatially resolved data on BC concentrations and identify key emission sectors. Such information is essential for informing policy decisions aimed at reducing urban pollution.

The measurement campaign conducted in this study was carried out from 4 February to 7 March 2020 and from 26 December 2020 to 21 January 2021, using two MA200 micro-aethalometers (microAeth® MA Series, Aethlabs, USA) equipped with PTFE filter tapes. These instruments quantify the absorption of light-absorbing carbonaceous aerosols at five different wavelengths (375, 470, 528, 625 and 880 nm), allowing for the estimation of the equivalent BC (eBC) concentrations by employing wavelength-specific mass absorption efficiencies. The sampling campaign strategically targeted two distinct locations within Modena. One sampling site was situated within a public park, chosen to represent typical background levels of BC in the city. The other location was selected for its proximity to heavy traffic, a well-known source of BC. The instruments operated at a flow rate of 100 ml min^{-1} in dual-spot sampling mode to compensate for filter loading effects and a constant correction factor of

1.3 was chosen to account for multiple light scattering within the filter fibers and between deposited particles and the filter. Absorption measurements from the MA200 devices were further partitioned into specific components, including BrC and BC, and their respective sources, namely fossil fuel (FF) and biomass burning combustion (BB), using the Multi-Wavelength Absorption Analyzer model [1].
To enhance the insights provided by the two micro-aethalometers and to gain a more detailed understanding of spatial BC levels, we implemented a hybrid Eulerian-Lagrangian modeling system tailored for the simulation of urban-scale BC concentrations. The approach uses the GRAMM-GRAL modeling system [2], chosen for its ability to simulate emission dispersion while taking into account the presence of obstacles when reconstructing flow fields, and the chemical transport model CHIMERE [3], chosen to estimate background concentrations from sources beyond the urban perimeter, to assess the impact of regional factors on BC levels in Modena.
CHIMERE has been configured over a domain covering a significant part of the Po Valley (from 8.78° E to 13.13° E longitude and from 43.57° N to 45.79° N latitude) with a fine horizontal resolution of 3 km. Meanwhile, simulations using the GRAMM mesoscale model were performed at 200 m resolution over a 30 km x 30 km domain centered on Modena. In addition, simulations with the Lagrangian model GRAL were performed at a resolution of 4 m over a domain of 10.2 km x 7.7 km, with boundary conditions derived from the large-scale wind fields of GRAMM.
City-scale traffic exhaust and non-exhaust emissions were estimated using a bottom-up approach combining modeled traffic data, road characteristics, fleet composition, and speed-dependent emission factors implemented in the traffic emission model VERT [4]. Resuspension emissions from vehicle movement were also included in the calculation using the reference emission factors from [5]. Anthropogenic emissions for other source sectors were taken from the regional emissions inventory regularly compiled by the local environmental agency, Arpae. Since emissions from biomass burning are subject to large uncertainties, we simulated five different emission scenarios based on different assumptions about source location and speciation conversion factors from total $PM_{2.5}$ emissions reported in the local regional inventory to BC emissions. To maintain consistency in the simulation, the same emission inventory was also used to perform simulations at the regional scale with the CHIMERE model.

Results from the measurement campaign showed that BrC concentrations were consistent and remarkably low throughout the day in both the analyzed periods (around 0.05 μg m^{-3} in the first, 0.1 μg m^{-3} in the second). On the other hand, FF, a marker for traffic-related emissions, showed distinct diurnal peaks during rush hours, in the morning (07:00 - 08:00 GMT) and in the evening (18:00 - 20:00 GMT) for both periods, with values up to 18.5 μg m^{-3} at the urban traffic site. In contrast, BB showed less diurnal variability, with a minimum in the early afternoon (15:00 - 17:00 GMT) and a peak in the evening (20:00 - 21:00 GMT), and generally lower concentrations compared to FF. A comparison of the two periods showed significant differences. The period from 26 December 2020 to 21 January 2021 had higher FF and BB concentrations, likely due to different meteorological conditions such as lower wind speeds and increased atmospheric stability, accentuated by frequent thermal inversions occurring even during daylight hours. In addition, lower temperatures likely led to more biomass burning for heating, which increased eBC concentrations.
In the second part of the study, the hybrid modeling system was used to provide spatially resolved BC concentration maps over the urban area of Modena and to elucidate the contribution of different sources. Figure 1 illustrates the average daily contributions of different modeled BC sources at the measurement sites, incorporating data from both the first and second simulated periods.
At the urban background site, BB emerges as the dominant source of BC throughout the day, with its total contribution (City+bck) ranging from 50% to 70%. Specifically, the average absolute BB contributions from urban and non-urban sources between 00:00 and 17:00 GMT are generally

comparable. For the city, the average values range from 0.31±0.22 μg m^{-3} to 0.78±0.38 μg m^{-3}, while for the background, they range from 0.37±0.07 μg m^{-3} to 0.62±0.1 μg m^{-3}. However, between 18:00 and 23:00 GMT, when local BB emissions are at their peak, local sources contribute more significantly to BB concentrations than the background, with average values ranging from 0.63±0.37 μg m^{-3} to 0.94±0.47 μg m^{-3} for the city and from 0.45±0.08 μg m^{-3} to 0.60±0.1 μg m^{-3} for the background. The second most significant contributor at the urban background site is FF combustion, which, like BB, is equally attributed to local and external sources from 00:00 to 17:00 GMT, resulting in average BC concentrations of around 0.17±0.06 μg m^{-3} for both the city and background. However, between 18:00 and 23:00 GMT, local sources of FF become more influential, with average values around 0.37±0.12 μg m^{-3}.

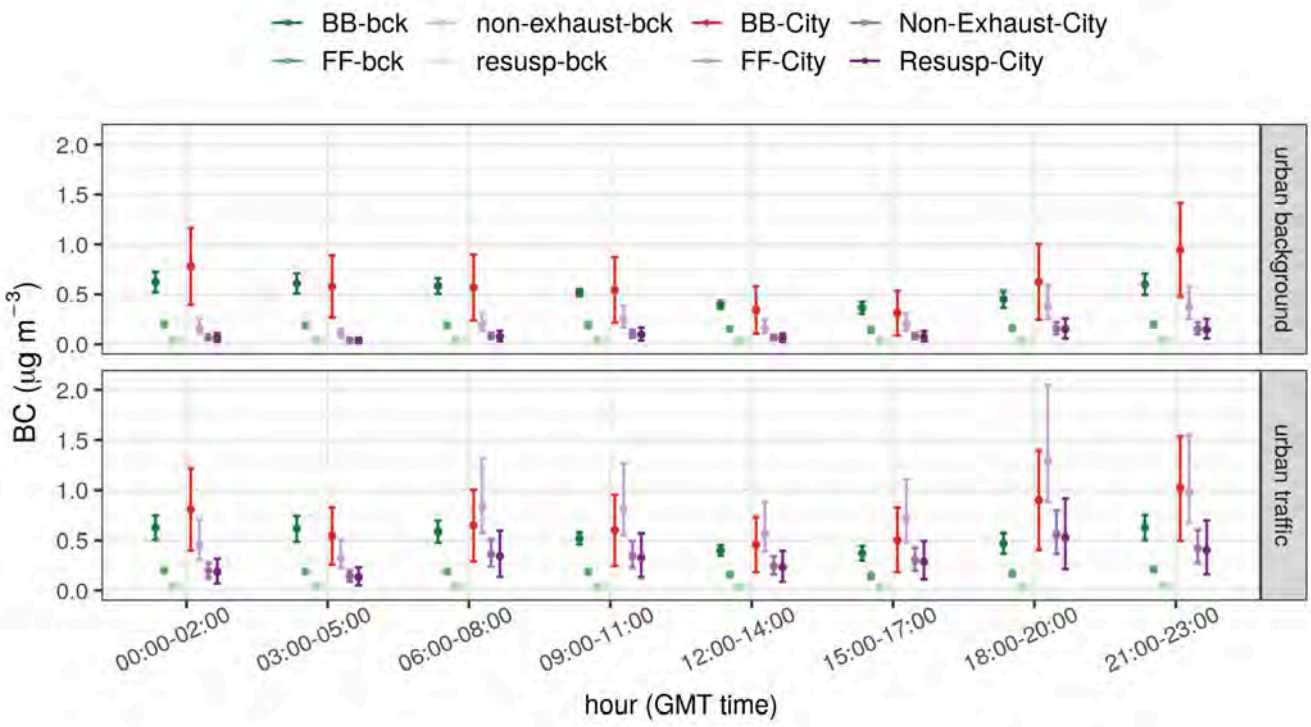

Figure 1. Average daily contributions of BC mass concentrations from various sources, including fossil fuel (FF), biomass burning (BB), traffic non-exhaust and resuspension, differentiating between urban (City) and background (bck) locations with respect to Modena urban area.

During daytime hours at the urban traffic site (from 06:00 to 20:00 GMT), as expected, local FF combustion takes the lead among the various sources with an average contribution from 0.56±0.18 μg m^{-3} to 1.3±0.41 μg m^{-3}, representing 27% and 32% of the relative contribution, respectively. The second most notable source is BB, contributing in the range of 0.60±0.36 μg m^{-3} to 0.91±0.5 μg m^{-3} during the same daytime window (21% and 23% of the relative contribution, respectively). In contrast, BB from local sources reaches its highest contribution during nighttime, specifically from 21:00 to 05:00 GMT, with an average maximum contribution of 1.02±0.52 μg m^{-3}, constituting 27% of the relative total. In addition, it's worth noting that in proximity to traffic-intensive areas, such as the selected traffic site in this study, the contribution of non-exhaust and resuspension sources cannot be overlooked, especially from 18:00 to 20:00 GMT when the overall relative contribution of these components reaches 29% (in absolute terms equal to 0.56±0.19 μg m^{-3} for local non-exhaust and

0.53±0.32 μg m^{-3} for background non-exhaust).
When the modeled concentrations are analyzed in terms of spatial averages over the entire urban area, it becomes evident that more than half (52%±10%) of the BC concentrations originate from local sources within Modena. Among these, biomass combustion is the main contributor with 35%±15%, followed by fossil fuel combustion with 9%±4%. However, long-distance transport also has an influence, contributing 48%±10% to the total BC concentrations. Within this, biomass combustion and fossil fuel combustion contribute 28%±1% and 15%±2%, respectively.
To validate model results, simulated BC concentrations at station locations were compared with observations from the two micro-aethalomters. During February-March 2020, the model showed good performance, with a mean bias of 0.02 μg m^{-3} (+2%) at the urban background site and -0.12 μg m^{-3} (-5%) at the traffic site. The linear correlation coefficients were also satisfactory (0.51 and 0.62 respectively). In particular, daily concentration peaks were accurately captured under different meteorological conditions, including high wind speed episodes. In the second simulation period (December 2020-January 2021), the model performance decreased due to challenging meteorological conditions (stable atmospheric conditions and frequent low wind speeds), but all statistical metrics considered remained within established acceptance criteria for urban dispersion modeling [6], see Table 1.

Table 1. Statistical analysis of hourly total BC concentrations at urban traffic and urban background sites

Station	Period	MB (μg m^{-3})	NMB (%)	NMSE	FAC2	r	FB	NAD
Traffic	1st period	-0.12	-5	0.34	0.80	0.62	0.05	0.02
Background	2nd period	0.03	2	0.34	0.67	0.51	0.05	0.02
Traffic	1st period	-0.92	-22	0.60	0.69	0.34	0.25	0.13
Background	2nd period	0.25	15	0.35	0.72	0.38	-0.13	0.06

MB represents the Mean Bias, NMB denotes the Normalized Mean Bias, NMSE stands for the Normalized Mean Square Error, *r* refers to the Pearson Correlation Coefficient, FB indicates the Fractional Bias, and NAD signifies the Normalized Average Difference.

The findings of this study, derived from both in-situ BC monitoring and the use of sophisticated modeling tools, underscore the importance of distinguishing between the contributions of biomass burning and traffic to black carbon at different spatial scales. The knowledge gained from this analysis can serve also as an important basis for the development of more robust air quality management strategies, not only in Modena, but also in other cities in the Po Valley region.

References

[1] Massabò, D., Caponi, L., Bernardoni, V., et al.: Multi-wavelength optical determination of black and brown carbon in atmospheric aerosols, Atmospheric Environment, 108, 1–12, 2015.
[2] Oettl, D.: Quality assurance of the prognostic, microscale wind-field model GRAL 14.8 using wind-tunnel data provided by the German VDI guideline 3783-9, Journal of Wind Engineering and Industrial Aerodynamics, 142, 104–110, 2015.
[3] Mailler, S., Menut, L., Khvorostyanov, D., Valari, M., Couvidat, F., Siour, G., Turquety, S., Briant, R., Tuccella, P., Bessagnet, B., Colette, A., Létinois, L., Markakis, K., and Meleux, F.: CHIMERE-2017: from urban to hemispheric chemistry-transport modeling, Geoscientific Model Development, 10, 2397–2423, 2017.
[4] Veratti, G., A. Bigi, S. Teggi and G. Ghermandi, 2024: Description and validation of VERT 1.0, an R-based framework for estimating road transport emissions from traffic flows. EGUsphere, 2024.
[5] Amato, F., Karanasiou, A., Moreno, T., Alastuey, A., Orza, J. A. G., Lumbreras, J., Borge, R., Boldo, E., Linares, C., and Querol, X.: Emission factors from road dust resuspension in a Mediterranean freeway, Atmospheric Environment, 61, 580–587, 2012.
[6] Hanna, S. and Chang, J.: Acceptance criteria for urban dispersion model evaluation, Meteorology and Atmospheric Physics, 116, 133–146, 2012.

CONSEQUENCES AND RISK MODELING OF NATECH IN INDUSTRIAL ENVIRONMENTS

Deborah Panepinto [1], Marco Ravina [1] and Mariachiara Zanetti [1]

[1] *Politecnico di Torino, DIATI, Corso Duca degli Abruzzi 24, 10129 Torino, Italy*

Keyword(s): *pollutant dispersion, Environmental compatibility, NaTech, air pollution*

Abstract

The objective of the work is to harmonize and integrate strategies to improve the quality management of the environmental matrixes in a complex industrial context, characterized by potential impacts on the environment and on human health due to NaTech hazards. In this work, the possible consequences of NaTech events on a complex industrial plant are considered. Particular attention is paid to the risk to the health of workers potentially present in the production plant. The consequences of a NaTech event on possible production processes involving hazardous substances are simulated, assessing the resulting environmental impacts, with particular regard to atmospheric emissions and the related risk to human health. By means of both established and innovative mathematical models, various modes of industrial accidents involving the release of hazardous substances on the ground and into the atmosphere are simulated. To this end, an existing industrial plant is considered as an example case study. A potential damaging event resulting from a NaTech event is applied to this scenario. In order to define the type of triggering event, a literature search has been conducted on the main existing NaTech databases. The results include the representation of the consequences of a NaTech event in terms of risk and environmental indices, with a view to contributing to the development of a possible integrated prevention methodology.

1. INTRODUCTION

Industrial sites, especially when characterized by a long-lasting operation in the past when adequate environmental legislation was still not in place, have been the source of impact on the environment due to emissions to air, water and soil. Actually, due to the enforcement of strict environmental legislation in the European community, the emissions of industrial activities are highly controlled (for example in the Environmental Integrated Authorization procedure concerning “big potential polluter” industries). Nevertheless, although emissions are within the limits imposed by the legislation, there is still a strong need to evaluate the environmental quality in a complex industrial context, characterized by potential impacts on the environmental and on human health due to, for example, NaTech (Natural and Technological) hazards, which refers to industrial triggered by natural events such as storms, earthquakes, flooding and lightning.
Such a kind of assessment is needed for:

- correct planning of future industries and activities on the potentially affected land. This is, for example, the case of the environmental impact evaluation foreseen by the Italian/European legislation for the evaluation of specific projects [Italian Republic, 2006; European Union, 2014];
- the definition of technical interventions useful to contain the environmental impact of actual industrial activities (for example, in the framework of the integrated environmental authorization) [Italian Republic, 2006; European Union, 2010];

- the analysis of the current environmental impact of operating industrial activities. This is, for example, the case of the environmental health impact assessment foreseen by the Italian/European law for specific industrial installations [Italian Republic, 2006; European Union, 2014].

A comprehensive impact assessment of industrial sites requires to consider the contribution of diffuse sources from the operating plants and from the eventually contaminated subsoil, besides the usual conveyed emissions from stacks, plus to correlate the concentration at the point of exposure with the potential health risks on the receptor.
The modeling approaches used to deal with all emissions potentially produced at an industrial site, i.e. diffuse or concentrated emissions from the operating plant and diffuse emissions from the contaminated sites, are fairly different [Swartjes, 2015]. Diffuse and conveyed emissions from industrial operating plants are usually evaluated using advanced dispersion models, which simulate the pollutant dynamics in the atmosphere (e.g. Gaussian or Lagrangian models like Calpuff, Spray, Aermod and others). On the one hand, these models allow to simulate the pollutant dispersion in case of multiple and complex emission sources, non-steady atmospheric conditions, and variable orography. On the other hand, these tools require detailed input datasets of the meteorology and geophysical features of the area under study. Also, running these models requires a high effort in terms of human resources and computational time, and their use is limited to specialists in the field [Holmes and Morawska, 2006; Khan and Assan, 2021]. Advanced dispersion models are currently applied to Health-Environmental Risk Assessment. Research activity has presently been taken to improve such integrated approach and the harmonization of these methodologies. The approach used to evaluate the impact of contaminated sites on the environment and potentially exposed human receptors is currently integrated into the Health-Environmental Risk Assessment. Health-Environmental Risk Assessment methodologies were internationally developed for contaminated sites (ASTM E1739, 1995; ASTM E2081, 2000) considering the evaluation of impacts due to specific chemical or physical agents in a particular site and time, with the aim of protecting human health at the local level. In Italy, the Health-Environmental Risk Assessment has been standardized for operators by ISPRA Public Agency with 2008 Guidelines and following modifications [ISPRA, 2008]. Presently, national and international software are available on the market (e.g., Risk-net, RBCA, RISC and others) performing level II risk analysis, which relies on the description of pollutants dynamics in air, water and soil through over-simplified analytical equations, which generally provide an approximate, and usually overestimated evaluation of the impact on the receptors.
In this work an existing industrial plant is considered as an example case study. A potential damaging event resulting from a NaTech event will be applied to this scenario. In order to define the type of triggering event, a literature search has been conducted on the main existing NaTech databases. The results will include the representation of the consequences of a NaTech event in terms of risk and environmental indices, with a view to contributing to the development of a possible integrated prevention methodology.

2. MATERIALS AND METHODS

2.1 Analysis of the Current situation and considerations

The starting point of the work was the review of the NaTech databases, collecting information on industrial accidents caused by natural events that caused the release of toxic gases into the atmosphere. The following databases were analyzed:

- Emars Database: incidents and situations without injuries in the European Union.
- eNATECH Database: a database on technological incidents caused by natural risks.

From the database the characteristics of a specific case was chosen in order to perform the current work. In particular we chosen a case where strong winds (up to 150 km/h) caused the uncontrolled movement of a crane, leading to its collapse and damaging an ethylbenezene storage tank. After a realistic scenario of an industrial settlement with complex configuration was taken into account (Figure 1) and solvent (ethylbenzene) atmospheric dispersion in normal operating conditions was simulated with a microscale lagrangian dispersion model (Figure 2, baseline scenario).

Figure 1. Plan view of the case study

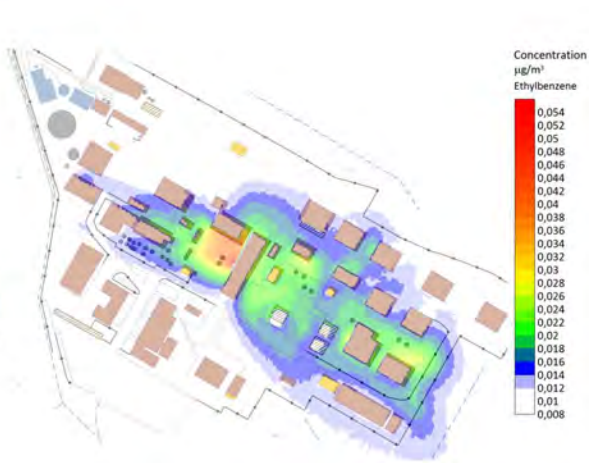

Figure 2. Average solvent concentration

The maps concerning the pollutant concentration was matched with the health environmental risk analysis (Figure 3). From the risk assessment point of view, it is important to note that:

- long- and short-term risk assessment was conducted on the baseline scenario
- carcinogenic risk (R) and hazard index (HI) were defined based on TLV-TWA exposure limits for occupational activities

$$- R = \frac{C_{air}}{RC_{canc}} * 10^{-6}$$

$$- HI = \frac{C_{air}}{RC_{no,canc}}$$

with

C_{air} = average pollutant concentrationin the air

RC_{canc} = reference concentration for carcinogenic effects

$RC_{no,canc}$ = reference concentration for non − carcinogenic (toxic)effects

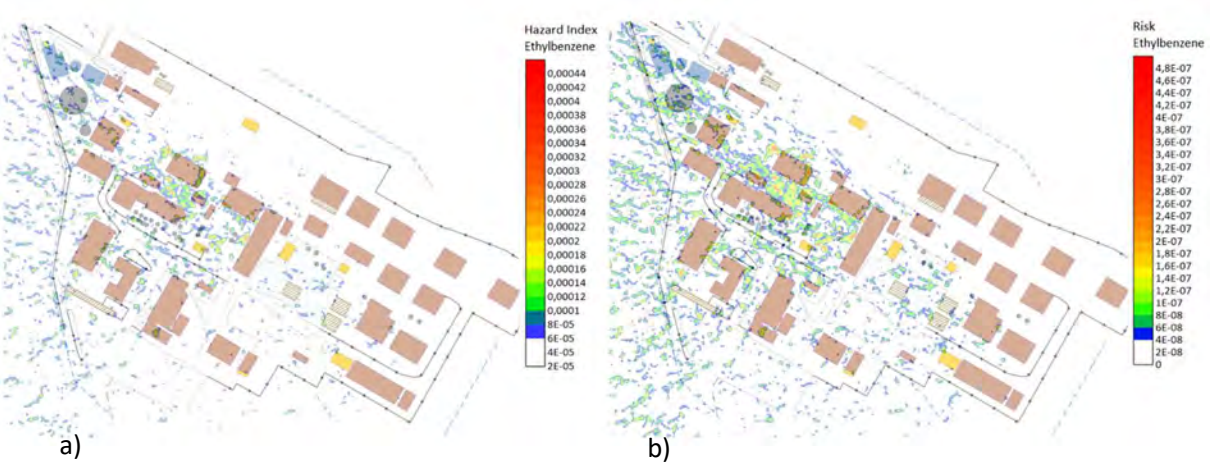

Figure 3. Hazard index (HI) (a) and Carcinogenic Risk (R) (b) for ethylbenzene inhalation, based on 98° pecentile modelled concentration

The current situation will be compared with the future situation (after the NaTech incident). In order to define the future situation, the procedure reported in the following flow chart (Figure 4) will be analyzed.

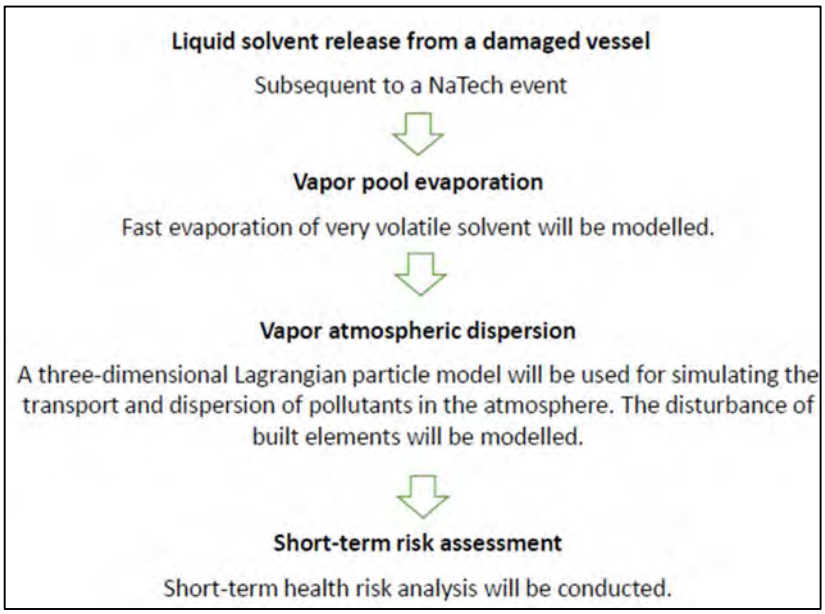

Figure 4. Procedure for future situation

With this comparison the main difference between the two situations can be highlighted and so it will be possible to analyze the main critical issues arising from this event.

3. CONCLUSION

The paper examines an existing industrial plant. For this baseline scenario the environmental impact (in

terms of emission coming from the industrial plant) and the actually risk were defined. A potential damaging event resulting from a NaTech event will be applied to this scenario. In order to define the type of triggering event, a literature search has been conducted on the main existing NaTech databases. The final results will include the representation of the consequences of a NaTech event in terms of risk and environmental indices. In particular the results in terms of concentration (coming from the implementation of a specific pollutant dispersion model) are used in order to evaluate (with the use of a specific risk model) the risk for the human health of a Natech event. The main is to try to contributing to the development of a possible integrated prevention methodology.

REFERENCES

European Union (2010). Directive 2010/75/EU of the European Parliament and of the Council of 24 November 2010 on industrial emissions (integrated pollution prevention and control).

European Union (2014). Directive 2014/52/EU of the European Parliament and of the Council of 16 April 2014 amending Directive 2011/92/EU on the assessment of the effects of certain public and private projects on the environment.

Holmes, N.S., Morawska, L., 2006. A review of dispersion modelling and its application to the dispersion of particles: An overview of different dispersion models available. Atmospheric Environment 40, 5902–5928. https://doi.org/10.1016/j.atmosenv.2006.06.003

Istituto superiore per la protezione e la ricerca ambientale (ISPRA) (2008). Criteri metodologici per l'applicazione dell'analisi assoluta di rischio ai siti contaminati (Rev.2).

Khan, S., Hassan, Q., 2021. Review of developments in air quality modelling and air quality dispersion models. Journal of Environmental Engineering and Science 16, 1–10. https://doi.org/10.1680/jenes.20.00004

Repubblica Italiana. Decreto Legislativo 3 aprile 2006, n. 152. Norme in materia ambientale. (GU Serie Generale n.88 del 14-04-2006 - Suppl. Ordinario n. 96)

Swartjes, F.A., 2015. Human health risk assessment related to contaminated land: state of the art. Environ Geochem Health 37, 651–673. https://doi.org/10.1007/s10653-015-9693-0

This study was carried out within the RETURN Extended Partnership and received funding from the European Union Next-GenerationEU (National Recovery and Resilience Plan – NRRP, Mission 4, Component 2, Investment 1.3 – D.D. 1243 2/8/2022, PE0000005) – SPOKE TS 2

Title: Modelling of Vegetative Environmental Buffer (VEB) effects on gas concentrations through AERMOD-View: comparison between observed and modelled data

Author(s): Luca Baccini*[1], Erin Cortus[2], Federico G.A. Vagliasindi[1]

[1] *Department of Civil Engineering and Architecture, University of Catania, Catania, Italy*
luca_baccini@outlook.it, federico.vagliasindi@unict.it
[2] *Department of Bioproducts and Biosystems Engineering, University of Minnesota – Twin Cities, Saint Paul, Minnesota (USA), ecortus@umn.edu*

Keyword(s): Vegetative Environmental Buffers, modelling, monitoring, correlation

Abstract

Vegetative Environmental Buffers (VEBs) are barriers made of trees and shrubs surrounding part or the entirety of a facility [1], [2], touted as cost-effective and easy to “install” and maintain solutions for airborne pollutant control [3], [4], [5].

Some authors investigated VEB effectiveness by comparing control sites without VEBs and sites with VEBs. Among these, [6] compared the concentration data recorded after the VEB with those measured on the barn side without a VEB. [7] used the concentrations recorded, at the same site, before the VEB was established and after it was planted. [8] compared the concentrations between a control site and a closely similar site with VEBs, while [9] made the comparison between a site with VEBs and a model validated on a different site without VEBs. Referencing a control site is questionable and challenging, because it is nearly impossible to have multiple barns with identical manure, layout, number, size and type of animals, and the same weather conditions. There is, however, a role for modelling, allowing a recreation of the site features and thus comparing scenarios with and without the VEBs.

A few modelling attempts evaluated VEB effects on downwind concentrations. [10], [11] used a k-ω CFD model to observe the effect of tree characteristics and weather conditions on odour plume size and length, respectively. [12], [13] using Envi-met, simulated different VEB types and layouts to determine the VEB effectiveness and the best design solution for mitigating particulate matter dispersion. Finally, [14] used AERMOD to validate bench-scale simulated VEBs and to evaluate the VEBs height effects on modelled downwind concentrations.

To increase the trust of these simulation tools, validation with onsite recorded downwind concentrations needs to be done. This work does a comparison between ammonia (NH_3) and hydrogen sulphide (H_2S) observed and modelled concentrations using AERMOD-View (version: 12.0.0, based on AERMOD version 23132). Recommendations on future efforts to model the VEBs are given.

NH_3 and H_2S concentrations as well as weather parameters, i.e., temperature, wind speed and direction, were recorded at two finishing pig barns with VEBs in Minnesota. The sites are referred to as Fairfax and Nicollet. The concentrations were recorded both at the source (continuously) and downwind the source (discontinuously), adopting a monitoring set-up depicted in Figure 1.

A geometrically similar site layout was simulated with AERMOD-View. AERMOD-View does not have built-in source types that represent barns, nor topographical features that represent VEBs. Thus, this analysis investigated three types of sources: Point Vertical (PV), Point Horizontal (PH), and Buoyline (BUOY). VEB porosity was simulated by varying the spacing between solid structures making up the VEB. Three types of VEB porosities (no porosity (S1), 50% porosity (S2), no VEB (S3)) were used in conjunction with the VEB height and width. To simulate the onsite monitoring settings, receptor grids

were deployed at 2.3, 4.6, and 9.2 m heights [Figure 2]. Two pollutants, NH_3 and H_2S, were modelled.

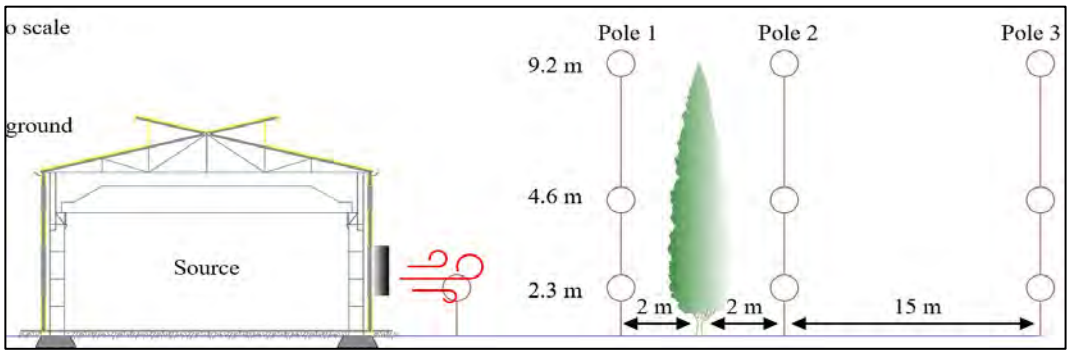

Figure 1. Representative scheme of the onsite set-up used for the monitoring activity.

Figure 2. Scenarios representation for the Fairfax site.

The comparison between observed and modelled concentrations was done using the following statistical parameters: R^2, Normalized Fraction Bias "FB" [15], and the p-values obtained through post-hoc paired t-test or Wilcoxon test. Given the limits of this abstract, only the best results will be reported.

The comparison through statistical parameters between the observed and modelled H_2S concentrations at the Fairfax site gave the following results: the R^2 ranges between 0.372-0.448 showing a middle-low agreement [Figure 3]; the FB values are close or slightly below the recommended good agreement threshold (|0.25|) [15], ranging between -0.356 and 0.000, suggesting that the model slightly underestimated the observed values; the p-values report no significant differences between the observed and modelled data. Moreover, the comparison between the observed and modelled concentration distributions show that the investigated porosities influenced the modelling outcomes more than the source types did [Figure 3].

For the Nicollet site the investigated porosities did not show differences in the concentration outcomes. This could be addressed to the fact that the plume generated by the source did not intercept the modelled VEBs. For these reasons only a comparison among the source types is reported. The outcomes of the comparison through statistical parameters between the observed and modelled NH_3 concentrations at the Nicollet site gave the following results: the R^2 values range between 0.563-0.917 showing a high correlation between the two data groups [Figure 4]; FB values range between -0.45 and -0.25 for BUOY and PV sources, respectively and 0.25 for PV source, suggesting that only the BUOY source modelled data slightly underestimated the observed concentrations; the p-values, showed that there are no significant differences between observed and modelled data. By increasing the Nicollet VEB heights from the onsite measured height (2023 height) up to the 20-year expected VEB height (2043 height), differences among scenarios with and without VEBs occurred, most likely because the

resulting plume intercepted the new VEB heights [Figure 4].

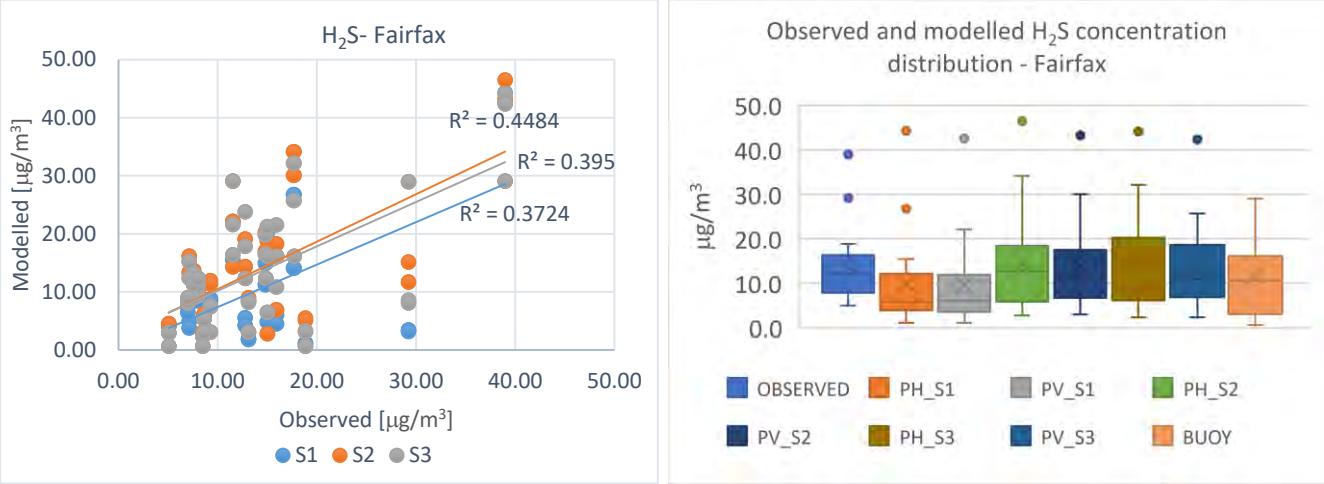

Figure 3. R^2 values for each investigated VEB porosity (scenario) (left). Observed and modelled H_2S concentration distributions for the Fairfax site (right).

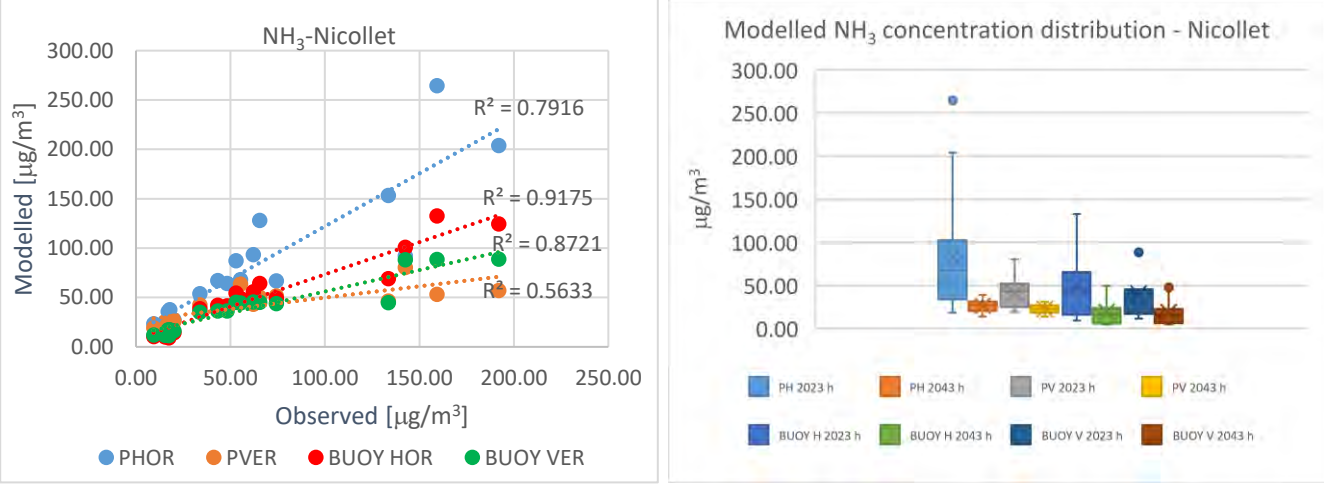

Figure 4. R^2 values for each investigated VEB porosity (scenario) (left). NH_3 comparisons between 2023 and 2043 height modelled concentration distributions for the Nicollet site (right).

Based on the weaknesses and strengths of this study the following recommendations can be drawn for future monitoring activities:

- Given that only three porosities were simulated, a recommendation is to investigate further porosities in the range between 0 % and 50%, to verify what noticed in this study,
- Considering that AERMOD does not have built-in settings to describe VEBs and barns, for future studies a broader variety of sources (i.e., point, area, volume, line sources) and porosities (i.e., within the range 0% and 50%) could be simultaneously investigated for comparison purposes.

From the results of this study the following conclusions can be summarized:

- VEBs characteristics, i.e., height and porosity as well as plume rise height had a major impact on the modelled outcomes,
- VEBs heights influenced the model outcomes more than the chosen source types did,
- There was not always agreement between modelled and observed data.

- Based on this work outcomes, future modelling approaches for VEBs simulation should focus on VEBs height, porosity, shape, and their effects on the pollutants plume.

Acknowledgement. The author wishes to acknowledge the University of Minnesota, especially to Prof. Kevin Janni for sharing preliminary useful training tools relative to the use of AERMOD-View, as well as Lakes Environmental Software and Dr. Greg Pratt for software assistance.

References

[1] J. Tyndall e J. Colletti, «Mitigating swine odor with strategically designed shelterbelt systems: a review», *Agroforest Syst*, vol. 69, fasc. 1, pp. 45–65, gen. 2007, doi: 10.1007/s10457-006-9017-6.
[2] J. Tyndall e R. A. Sudmeyer, «James R. Brandle Laurie Hodges», 2009.
[3] J. Tyndall, «Characterizing pork producer demand for shelterbelts to mitigate odor: an Iowa case study», *Agroforest Syst*, vol. 77, fasc. 3, pp. 205–221, nov. 2009, doi: 10.1007/s10457-009-9242-x.
[4] J. C. Tyndall e R. K. Grala, «Financial feasibility of using shelterbelts for swine odor mitigation», *Agroforest Syst*, vol. 76, fasc. 1, pp. 237–250, mag. 2009, doi: 10.1007/s10457-008-9140-7.
[5] H. E. “Gene” Garrett, S. Jose, e M. A. Gold, A c. di, «Front Matter», in *ASA, CSSA, and SSSA Books*, 1ª ed., Wiley, 2021. doi: 10.1002/9780891183785.fmatter.
[6] R. E. Nicolai, S. H. Pohl, R. Lefers, e A. Dittbenner, «Natural Windbreak Effect on Livestock Hydrogen Sulfide Reduction and Adapting an Odor Model to South Dakota Weather Conditions», 2004, [Online]. Disponibile su: https://www.researchgate.net/profile/Richard-Nicolai/publication/237621938_Natural_Windbreak_Effect_on_Livestock_Hydrogen_Sulfide_Reduction_and_Adapting_an_Odor_Model_to_South_Dakota_Weather_Conditions/links/558d331108ae591c19da4cae/Natural-Windbreak-Effect-on-Livestock-Hydrogen-Sulfide-Reduction-and-Adapting-an-Odor-Model-to-South-Dakota-Weather-Conditions.pdf
[7] B. J. Hofer, «EFFECT OF A SHELTERBELT ON H2S CONCENTRATIONS FROM SWINE BARNS», 2009.
[8] D. B. Parker, G. W. Malone, e W. D. Walter, «Vegetative Environmental Buffers and Exhaust Fan Deflectors for Reducing Downwind Odor and VOCs from Tunnel-Ventilated Swine Barns», *Transactions of the ASABE*, vol. 55, fasc. 1, pp. 227–240, 2011, doi: 10.13031/2013.41250.
[9] K. Ro *et al.*, «Enhanced Dispersion and Removal of Ammonia Emitted from a Poultry House with a Vegetative Environmental Buffer», *Agriculture*, vol. 8, fasc. 4, p. 46, mar. 2018, doi: 10.3390/agriculture8040046.
[10] X.-J. Lin, S. Barrington, D. Choinière, e S. Prasher, «Simulation of the effect of windbreaks on odour dispersion», *Biosystems Engineering*, vol. 98, fasc. 3, pp. 347–363, nov. 2007, doi: 10.1016/j.biosystemseng.2007.07.010.
[11] X.-J. Lin, S. Barrington, D. Choinière, e S. Prasher, «Effect of weather conditions on windbreak odour dispersion», *Journal of Wind Engineering and Industrial Aerodynamics*, vol. 97, fasc. 11–12, pp. 487–496, dic. 2009, doi: 10.1016/j.jweia.2009.06.012.
[12] D. Pauls e A. Christen, «Simulating the effect of adding vegetative buffers around poultry barns on mean wind and concentrations of PM10», University of British Columbia, Vancouver, Canada, nov. 2011. [Online]. Disponibile su: http://hdl.handle.net/2429/42449
[13] C. Adderley e A. Christen, «Evaluation of the performance of vegetative buffers for emission reduction of particulate matter from poultry facilities», Vancouver : University of British Columbia, ott. 2014. [Online]. Disponibile su: http://hdl.handle.net/2429/50843
[14] E. E. Weber, «The use of dispersion modeling to determine the feasibility of vegetative environmental buffers (VEBS) at controlling odor dispersion», Ph. D., University of Missouri--Columbia, 2012. doi: 10.32469/10355/15910.
[15] ASTM. Standard guide for statistical evaluation of indoor air quality models. D5157-97 (Reapproved 2003).

PARALLEL SESSION: C8

Contaminated sites

Contaminated soil and water: remediation

Title: Metal uptake and transport within Sorghum sp. from mining waste contaminated sites

Author(s): Andra-Maria Lăcureanu*[1], Mădălina-Flavia Ioniță[2], Emilia Dunca[3], Lăcrămioara Diana Robescu[4], Diana Mariana Cocârță[5,6]

[1]Research Centre for Advanced Materials, Products and Processes/CAMPUS, Laboratory for Analysis, Control and Remediation of Contaminated Soils, National University of Science and Technology POLITEHNICA Bucharest, Splaiul Independentei No. 313, Romania, andra.lacureanu@upb.ro
[2]IOSUD Department, University of Petroșani, University Street, no. 20, 332006 Petroșani, Romania, madalina.ionita96@yahoo.com
[3]Department of Environmental Engineering and Geology, Faculty of Mines, University of Petroșani, University Street, no. 20, 332006 Petroșani, Romania, emiliadunca@upet.ro
[4]Department of Hydraulics, Hydraulic Machinery and Environmental Engineering, Splaiul Independentei No. 313, Faculty of Energy Engineering, National University of Science and Technology POLITEHNICA Bucharest, 006042 Bucharest, Romania, diana.robescu@upb.ro
[5]Department of Energy Production and Use, Splaiul Independentei No. 313, Faculty of Energy Engineering, National University of Science and Technology POLITEHNICA Bucharest, 006042 Bucharest, Romania, diana.cocarta@upb.ro
[6]Academy of Romanian Scientists, 030167 Bucharest, Romania

Keyword(s): contaminated soil, tailing dumps, heavy metals, biomass, phytoextraction, mining waste

Abstract

The storage of mining waste represents a global environmental and public health problem, which leads to soil contamination through the absorption of metals in high concentrations. One of the methods used to remediate soils contaminated with metals is phytoextraction, which is based on the ability of certain varieties of high-biomass crops to extract these contaminants from soils. The current study aims to highlight the transfer mechanism of metals from soil to plants and to evaluate the potential of biomass crops to contribute to the restoration of soil health on unproductive land in the city of Petrella (tailing dump Branch IV Petrila, Romania). The obtained results show that sorghum can accumulate large amounts of metals and can be used as an energy crop.

Introduction

The storage of tailings resulting from the exploitation of natural mining resources represents an anthropogenic source of metal generation that affects the health and fertility of the soil [1].The most common metals identified in the environment are nickel (Ni), chromium (Cr), copper (Cu), arsenic (As), lead (Pb), cadmium (Cd), mercury (Hg), and iron (Fe). Metals such as Pb, Cd, and Hg affect the health of living organisms both in high and low concentrations [2]. Instead, Fe and Ni are needed in low concentrations because they allow the survival of all life forms. The types of waste, topography, runoff, and capture level are some of the factors that affect the concentrations of metals found in the soils close to waste mining deposits. Ingestion of a contaminated diet, which results from the transfer of metals from soil to plant and can be used as animal food or directly consumed by humans, is one significant way that humans are exposed to metals [2], [3]. Among the food products consumed by humans, vegetables are the most exposed to soil pollution. Plants uptake up metals from the soil and accumulate them in large enough quantities to cause various problems for both animals and humans [4].

Materials and Methods

In the framework of the current study, the Ramura IV tailings dump in Petrila was considered. For the experimental study, an area of 750 square meters was considered were located on which sorghum was sown. The sampling and collection of soil samples were performed according to the methodological norms provided in STAS 7184/1-84 [5] to carry out physico-chemical analyses at an accredited laboratory. The preparation of soil samples for the determination of metal concentrations in soil was carried out in accordance with the international standard ISO 11464:2006 [6]. Soil samples were air-dried and passed through a sieve of 2 mm openings in width. Then, the samples were homogenized with another amount of 20-30 g of soil. Onward, 0.5 g of soil were subjected to the acid digestion process according to the EPA 3051A method (US Environmental Protection Agency) [7]. The obtained digestate was analyzed by inductively coupled plasma atomic emission spectroscopy (ICP-OES).
After biomass harvesting, 2 g of air-dried soil were shaken with 100 mL of 1 N ammonium acetate solution [8]. After a 24-hour break, the samples were filtered, and the presence of heavy metals in the filtrate was analyzed by inductively coupled plasma mass spectrometry (ICP-MS) according to the ISO/TS 16965:2013 standard [9].

Results and discussion

Determination of metals concentration in soil

Eleven chemical compounds from the metals category were identified in the area under investigation after preliminary characterization. Mn and Fe were evaluated at the highest levels of concentration in soil, followed by the other heavy metals as following Fe>Mn>Zn>Cu>Ni>Cr>B>Co>Pb>Mo>Cd. According to the Romanian regulation in force, the Ministerial Order No. 756/1997 [10] thresholds were considered to assess the level of contamination in the investigated area (alert and intervention thresholds for the industrial use of the site were considered) (Table 1). Evaluation of the achieved results evidenced that the metals concentrations in the soil are below the limit of the intervention and alert thresholds, excepting B, for which the concentration in soil was 14.31 mg/kg$_{d.w}$ (with 4.31 mg/kg$_{d.w}$ higher than the reference value for intervention threshold) and Fe for which no limit of concentration is foreseen. It follows that a remediation strategy needs to be established. Sorghum was sown in this experimental research using the phytoextraction method.

Table 1. Romanian alert and intervention thresholds concentrations of pollutants in soils (mg/kg$_{d.w.}$) [10]

Contaminant	Normal Values	Alert Threshold Industrial Soil Use	Intervention Threshold Industrial Soil Use
		Less Sensitive Land Use	Less Sensitive Land Use
Cadmium	1	5	10
Nickel	20	200	500
Lead	20	250	1000
Total Chromium	30	300	600
Zink	100	700	1500
Cobalt	15	100	250
Manganese	900	2000	4000
Iron	-	-	-
Copper	20	250	500
Molybdenum	2	15	40
Barium	200	1000	2000

The concentrations of the metals (Mn, Zn, Cu, Fe) that have been identified are shown in Figure 1 following the harvesting of biomass (sorghum).

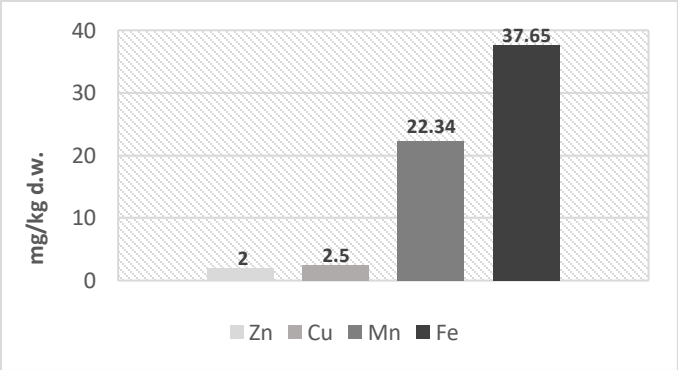

Figure 1. Metals identified in the soil after biomass harvesting

As a result, following the sorghum-based phytoextraction technique, the primary findings showed that the concentration of each of the metals found in the soil had considerably decreased. The concentrations in the soil for most of the chemical elements under analysis were below the limit of detection. Specific soil concentrations for elements like Zn, Cu, Mn, and Fe were the only ones that were identified.
It should be highlighted, however, that none of these elements' maximum allowed limit in the soil was exceeded (in accordance with the current Romanian regulation). The following sequence of decreases in concentration level was noted for these metals: Zn (98.51%)>Cu (96.83%)>Mn (94.4%). The results obtained are similar to those of Gorelova [[11], who demonstrated that sorghum has the capacity of absorbing a considerable amount of Fe from contaminated soils, followed by Mn, V, and Cu.

Conclusion

Phytoextraction is an economical method of extracting metals from plants. The success of such a remediation strategy depends both on the availability of the metal for absorption and on the ability of the plant to absorb and accumulate metals in its aerial parts. In this case study, sorghum, which can be tolerant to metals, was integrated to remediate the contaminated land evidencing important results in this regard.
Within the current geopolitical context, coal continues to be a significant global energy source. Surface coal mining results in several issues, one of which is heavy metal pollution from the disposal of mining waste. Coal mining waste contains heavy metals like As, Fe, Cd, and Pb, which can contaminate soil in many ways. The results of the current experimental study demonstrated Sorghum's important capacity to accumulate various metals in its tissue. Just four of the 11 metals that were originally found in the contaminated area were found after the phytoextraction procedure was used. Following the identification of metal loading in harvested sorghum, research is still being conducted to determine the metal concentrations in sorghum.

Acknowledgement

This research was supported by project Establishment and operationalization of a Competence Center for Soil Health and Food Safety – CeSoH, Contract no.: 760005/2022, specific project no.2, with the title: *Restoring soil health on unproductive land through biomass crops for sustainable energy - Soil- Bio mass- Sustainable*, Code 2, financed through PNRR-III-C9-2022 – I5 (PNRR-National Recovery and Resilience Plan, C9 Support for the private sector, research, development and innovation, I5,

Establishment and operationalization of Competence Centers).

References

[1] Saha T. R., Khan Md. A. R. K., Kundu. R., Naime. J, Karim K. Md. R. K., Ara M. H., "Heavy metal contaminations of soil in waste dumping and non-dumping sites in Khulna: Human health risk assessment," *Results in Chemistry,* Volume 4, pp. 100434, (2022).

[2] Nyiramigisha P., Komariah, Sajidan, "Harmful Impacts of Heavy Metal Contamination in the Soil and Crops Grown Around Dumpsites," *Reviews in Agricultural Science,* Volume 9, pp. 271-282, (2021).

[3] Ulmanu M., Matsi T., Anger I., Gament E., Olanescu G., Predescu C., Sohaciu M, "The Remedial Treatment of soil polluted with heavy metals using fly ash," *UPB Scientific Bulletine,* Volume 69, No. 2, (2007).

[4] Jolly Y. N., Islam A., Akbar S., "Transfer of metals from soil to vegetables and possible health risk assessment," *SpringerPlus 2,* 385 (2013).

[5] STAS 7184/1-84, Soils. Collection of samples for pedological and agrochemical studies.

[6] ISO 11464:2006, Soil quality, Pretreatment of samples for physico-chemical analysis.

[7] U.S. EPA. 2007. Method 3051A (SW-846): Microwave Assisted Acid Digestion of Sediments, Sludges, and Oils," Revision 1. Washington, DC.

[8] Standard operating procedure: 1N ammonium acetate, pH 7.0 method.

[9] ISO/TS 16965:2013, Soil quality — Determination of trace elements using inductively coupled plasma mass spectrometry (ICP-MS).

[10] ORDER no. 756 of November 3, 1997 for the approval of the Regulation.

[11] Gorelova S., V., Kolbas A. P., Muratova A. Y., Frontasyeva M.V., Zinicovscaia I., Okina O., I., "Prospects for the Use of Sorghum Bicolor for Phytoremediation of Soils Contaminated with Heavy Metals in Temperate Climates", Phytoremediation: Management of Environmental Contaminants, Volume 7, Springer International Publishing, pp. 263-301, (2023).

Treatment of hydrocarbon-contaminated soil with biosurfactants obtained from agricultural waste

Teklit Ambaye[1], Adriana Bava[2], Fabrizio Beltrametti[2], Andrea Franzetti[3], Mentore Vaccari[1]*

[1]*University of Brescia, Dep. of Civil, Environmental, Architectural Engineering and of Mathematics, Via Branze 43, 25123 Brescia, Italy*
[2] *BioC-CheM Solutions Srl, Via R. Lepetit, 34, 21040 Gerenzano (VA), Italy*
[3] *University of Milano-Bicocca, Dept. of Earth, and Environmental Sciences -DISAT, Piazza della Scienza 1, 20126 Milano, Italy*

Keyword(s): biosurfactant, agricultural waste, microbial electrochemical treatment, landfarming, petroleum hydrocarbon, bioremediation

Abstract

ABSTRACT: Petroleum and petroleum product exploration, transportation, and processing negatively impact soil ecosystems and cause severe damage. Hence, a study was conducted to evaluate the performance of microbial electrochemical treatment (MET) and landfarming in terms of biodegradation with petroleum hydrocarbon-polluted soil by adding rhamnolipid and surfactin biosurfactant at different doses of 50, 100, and 150 mg/kg_{dw} and 10, 25, and 50 mg/kg_{dw}, respectively. After the addition of an optimal dose of rhamnolipid (50 mg/kg_{dw}) to MET and landfarming treatment, the maximum petroleum hydrocarbon reduction rates of 78 and 62% were achieved in 20 days, respectively. However, adding surfactin did not enhance hydrocarbon biodegradation for both MET and landfarming treatments. The Germination index (GI) using Lepidium sativum L. seeds for measuring the toxicity of the soil after and before treatment using MET revealed the soil has high phytotoxicity except for 50 mg/kg of rhamnolipid addition, which shows a decrease in about 68.5% of the toxicity. Overall, the findings demonstrated that the effectiveness of landfarming and MET treatment for the degradation of soil polluted with petroleum hydrocarbons depends on the dose of the biosurfactant.

Keywords: biosurfactant, agricultural waste, microbial electrochemical treatment, landfarming, petroleum hydrocarbon, bioremediation

1. Introduction

Petroleum hydrocarbons (PHCs) are a toxic mixture of paraffinic, aliphatic, and aromatic components and have become a serious environmental problem due to their ability to pollute soil and water [1]. Various biological techniques are used to remove hydrocarbons from the environment through the metabolism of bacteria or other microorganisms; however, these processes have some limitations, such as the low biological availability and low water solubility of PHCs [2].

As a naturally green material, biosurfactants are presently gaining significant importance because they are eco-friendly, like biodegradation and bioremediation techniques. Compared with chemical surfactants, biosurfactants have many potential advantages, such as high selectivity, biodegradability, biocompatibility, bioavailability, and ecological acceptability, as well as higher efficacy under extreme

temperature and salt concentration conditions. Biosurfactants are successfully applied in microbial oil recovery, pharmaceuticals, cosmetics, wastewater treatment, and sludge treatment [3]. The application of biosurfactants makes it possible to increase the bioavailability of hydrocarbons in soil by increasing the rates of microbial biodegradation [3]. This phenomenon depends on the ability of biosurfactants to enhance hydrophobic and hydrophilic interactions in reducing surface tension, thus promoting oil mobilization and micelle formation [3]. However, due to the higher cost, the application of biosurfactants compared with chemical ones is still falling behind. Therefore, for large-scale production of biosurfactants, cheaper and more widely available substrates need to be used. In this regard, much attention has recently been paid to the production of biosurfactants from agro-industrial wastes [4]. Cereal wastes are agro-industrial wastes composed of hemicellulose, cellulose, and sugars that can be used for cost-effective biosurfactant production. This paper summarizes the main results obtained in the treatment of hydrocarbon-contaminated soils using biosurfactants produced from agricultural wastes in bioremediation technologies.

2. Materials and methods

2.1 Microcosm tests with Landfarming treatments

Mesocosm tests of landfarming treatments with 2 kg of petroleum hydrocarbon-contaminated soil were used to study degradation. 20-liter cylindrical glass with aeration, tilling, and adding water to the treatment are carried out to increase microbial activity for about 20 days.

The following operating conditions were tested:

(i) Control = 2 kg of contaminated soil.
(ii) (ii) Rhamnolipid (RH) = Contaminated soil (2 kg) + broth RH (50 mg/kg_{dw}).
(iii) (iii) Rhamnolipid (RH) = Contaminated soil (2 kg) + broth RH (100 mg/kg_{dw}).
(iv) (iv) Rhamnolipid (RH) = Contaminated soil (2 kg) + broth RH (150 mg/kg_{dw}).
(v) (v) Surfactin (SF) = Contaminated soil (2 kg) + broth SF (10 mg/kg_{dw}).
(vi) (vi) Surfactin (SF) = Contaminated soil (2 kg) + broth SF (25 mg/kg_{dw}).
(vii) Surfactin (SF) = Contaminated soil (2 kg) + broth SF (50 mg/kg_{dw}).

The addition of biosurfactants for the degradation of petroleum hydrocarbons was measured by GC FID gas chromatography (Agilent 6890) (DB5 column (I=30-60m)).

2.2 Microbial electrochemical treatment (MET)

The MET was prepared in rectangular glass cylinders (height 46 cm, diameter 7 cm, and capacity 2,000 cm^3) with granular graphite electrodes as anode and cathode. The cylinders were thoroughly filled with the soil polluted with petroleum hydrocarbon (2kg) to a height of 37.5 cm, corresponding to a capacity of 2 L. In all experiments, a potential of 0.8 mV was applied to the MET. The effect of biosurfactant concentration on the degradation efficiency of petroleum hydrocarbons in the MET was studied using rhamnolipid and surfactin biosurfactants in three different concentrations of the broth: rhamnolipid at 50, 100, and 150 mg/kg_{dw}, and surfactin at 10, 25, and 50 mg/kg_{dw}. In addition to the abiotic control, another negative control was also planned with the same conditions as the biotic systems but without the use of biosurfactants. The addition of biosurfactants for the degradation of petroleum hydrocarbons was measured by GC FID gas chromatography (Agilent 6890; DB5 column, I = 30–60 m).

2.3 Germination Index (GI)

Lepidium sativum L. seeds were cultivated on untreated and treated soil samples to calculate the germination index. To conduct the experiment, 5 g of dry soil was placed in Petri dishes, and the proper volume of deionized water was added to keep the soil moist. These Petri dishes were coated with Whatman filter paper #1 after roughly 24 hours. Ten unharmed, healthy *Lepidium sativum* seeds were added to each Petri dish. All seeded Petri dishes were then incubated in the darkroom for 72 hours at 27 °C. Seeds that had germination (G) were then counted. All interventions, including the control relative root length (L), were measured. Each seed germination test was performed three times. According to

Ambaye et al. [2], the germination index, or GI (%), was computed as follows: (G * L) / (Gc * Lc) x100 = GI (%).

3. Results and discussion

3.1 Microcosm tests with Landfarming treatments

The addition of various doses of rhamnolipid improved hydrocarbon removal yields compared with the control. Among the various doses, the maximum TPH degradation efficiency of 62% was attained with 50 mg/kg of RH addition due to the increased bioavailability of the pollutant by the biosurfactant (Figure 1). However, adding surfactin did not enhance hydrocarbon biodegradation. This suggests that surfactin caused some form of inhibition of biodegradation in these mesocosms.

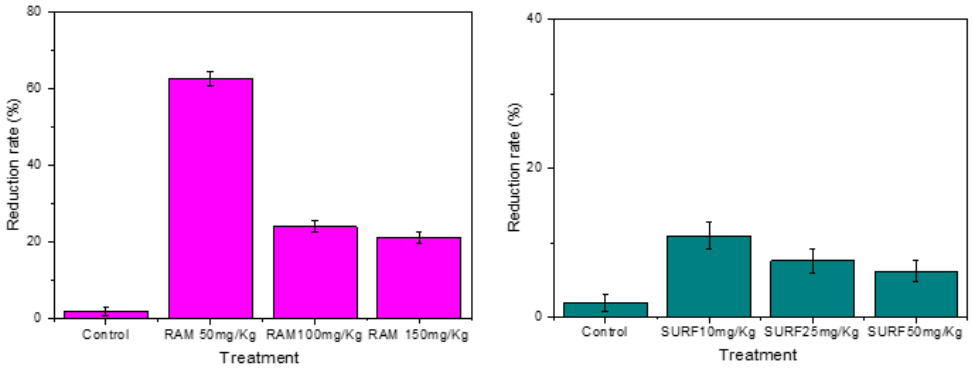

Figure 1. Total petroleum hydrocarbon reduction rate using rhamnolipid (pink color) and surfactin (blue color) in landfarming and the addition of different amounts of biosurfactant. Data are means of duplicates, and error bars show standard deviations.

3.2 Microbial electrochemical treatment

The addition of biosurfactants for the degradation of petroleum hydrocarbons during the double chamber MET process for 20 days leads to a maximum TPH degradation efficiency of 78% with 50 mg/kg of RH addition, which was 20 times as efficient compared to the control one (4%) while adding surfactin did not enhance hydrocarbon biodegradation as shown in Fig. 2. This shows adding RH to MET is significantly improved, implying an increase in the bioavailability of petroleum hydrocarbons; however, surfactin caused some form of inhibition due to its toxic nature.

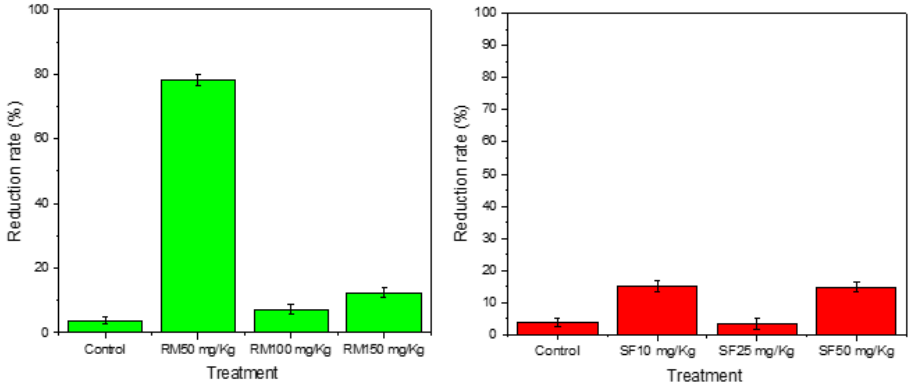

Figure 2. Total petroleum hydrocarbon reduction rate using rhamnolipid (green color) and surfactin (red color) in MET and the addition of different amounts of biosurfactant. Data are means of duplicates, and error bars show standard deviations.

3.3 Soil phytotoxicity assessment

Figure 3 illustrates the phytotoxic effect on the germination index (GI). A GI value greater than 100% indicates an effect that stimulates plants; a GI value between 50% and 80% indicates moderate phytotoxicity; and a GI value greater than 80% indicates no phytotoxicity. The GI with a 50 mg/Kg addition of rhamnolipid is about 68.5%, whereas in all the remaining treatments, the GI was below 50%.

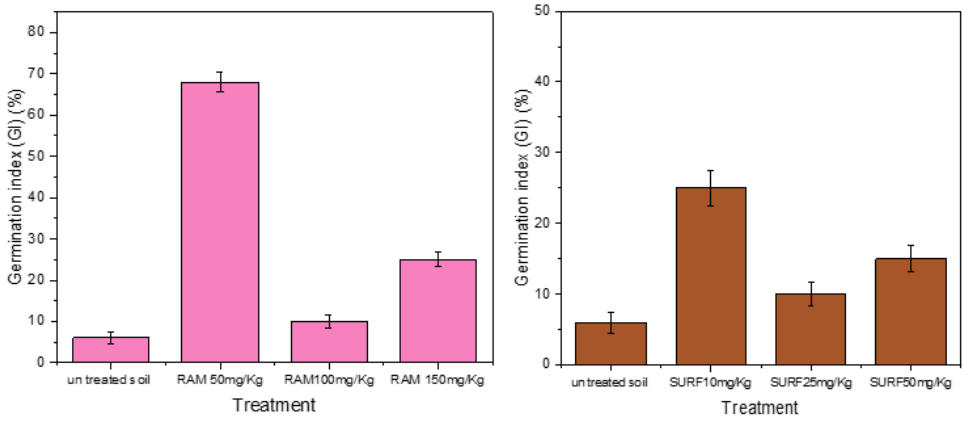

Figure 3. Germination index of *Lepidium sativum* L. seed growth in the soil before and after the MET using rhamnolipid (pink color) and surfactin (brown color) in MET and the addition of different amounts of biosurfactant. Data are means of duplicates, and error bars show standard deviations.

4. Conclusions

In short, the results show that adding rhamnolipid significantly increases the removal of hydrocarbons from contaminated soils in both landfarming and bioelectrochemical processes. This study's findings also demonstrated that the dose of biosurfactant affects the efficiency of landfarming and MET.

Acknowledgements

The results presented in this paper were obtained within the frame of the project "RICREA - Cereal waste for bioremediation" (https://www.progetto-ricrea.org), a research project co-funded by the Italian Ministry of the Environment and Energetic Security - General Directorate for the Circular Economy.

References

[1] Ambaye, T.G., Chebbi, A., Formicola, F., Prasad, S., Gomez, F.H., Franzetti, A. and Vaccari, M., 2022. Remediation of soil polluted with petroleum hydrocarbons, and their reuse for agriculture: Recent progress, challenges, and perspectives. Chemosphere, 133572.https://doi.org/10.1016/j.chemosphere.2022.133572

[2] Ambaye, T.G., Chebbi, A., Formicola, F., Rosatelli, A., Prasad, S., Gomez, F.H., Sbaffoni, S., Franzetti, A. and Vaccari, M., 2022. Ex-situ bioremediation of petroleum hydrocarbon contaminated soil using mixed stimulants: Response and dynamics of bacterial community and phytotoxicity. J. Environ. Chem. Eng. 10(6), 108814. https://doi.org/10.1016/j.jece.2022.108814

[3] Ambaye, T.G., Vaccari, M., Prasad, S. and Rtimi, S., 2021. Preparation, characterization, and application of biosurfactant in various industries: A critical review on progress, challenges, and perspectives. Environ. Technol. Innov, 24, 102090. https://doi.org/10.1016/j.eti.2021.102090

[4] Chebbi, A., Tazzari, M., Rizzi, C., Gomez Tovar, F.H., Villa, S., Sbaffoni, S., Vaccari, M. and Franzetti, A., 2021. *Burkholderia thailandensis* E264 as a promising safe rhamnolipids' producer towards a sustainable valorization of grape marcs and olive mill pomace. Appl Microbiol Biotechnol 105, 3825–3842 (2021). https://doi.org/10.1007/s00253-021-11292-0

Chemical enhanced oxidation with surfactants: a comparison of the effectiveness of two oxidants for the remediation of hydrocarbon-contaminated soils

Author(s): Federica De Marines[1,*], Marco Capodici[1], Gaetano Di Bella[2], Enrico Licitra[2], Gaspare Viviani [1], Daniele Di Trapani[1]

[1] *Department of Engineering, University of Palermo, Palermo, Italy, federica.demarines@unipa.it*
[2] *Faculty of Engineering and Architecture, University of Enna "Kore", Enna, Italy*

Keyword(s): TPHs, Chemical Oxidation, Surfactants, Potassium Ferrate, Soil Remediation

Abstract

This study aimed to assess the feasibility of the combined use of oxidants and surfactants for remediating diesel-contaminated soil. Potassium ferrate(VI) and potassium permanganate were evaluated in terms of oxidation efficiency. The results have shown that the combined use of surfactant and oxidant allows for high removal efficiencies. These were higher when using ferrate(VI) (>90%) compared to permanganate (~70%), mainly due to ferrate activation by the organic matter present in soil.

Introduction

Non-aqueous phase liquids (NAPLs) are caused by improper management or discharge of petroleum products and organic solvents; they represent a serious risk of contamination due to their persistence and mobility [1]. Generally, they consist of hydrophobic organic substances, such as petroleum hydrocarbons, which tend to be trapped in the soil pores, becoming a long-term source of contamination [2]. Chemical oxidation is a widely used remediation technique for the reclamation of contaminated soil due to its treatment speed. However, since oxidation reactions generally occur in the aqueous phase, the efficiency of the technique is limited by the availability of NAPL for oxidation [3]. To overcome this limitation, research has focused on the combined chemical oxidation and surfactant technology [4]; this is a promising strategy due to the high efficiency of desorption and solubilization of contaminants enabled by surfactants. In fact, surfactants, thanks to their amphiphilic structure, reduce the interfacial tension between NAPL and the liquid phase, thereby increasing the solubilization of NAPL [2]. However, the interactions between surfactants, oxidation systems, and contaminants have not been fully understood. Commonly used oxidizing agents include potassium permanganate, hydrogen peroxide, and ozone. However, in recent years, a new oxidant for chemical oxidation, potassium ferrate (K_2FeO_4), has gained the attention. Ferrate (Fe(VI)) has been widely used in the field of drinking water; however, its use for environmental remediation is an emerging field [5]. In this context, the aim of this study was to investigate the feasibility of the combined use of oxidant and surfactant for remediating diesel-contaminated sandy soil. Tests were conducted in slurry mode (100 g of soil and 500 mL of solution) by means of Jar Test. Specifically, the concentration of oxidants and surfactant were evaluated in terms of their effectiveness in solubilizing and oxidizing Total Petroleum Hydrocarbons (TPH). Additionally, the effect of both compounds on the residual phytotoxicity of the soil was studied.

Materials and Methods

The experimental campaign was divided into two phases. The first phase involved the dosage of Fe(VI) and SDBS, while the second one involved the addition of potassium permanganate ($KMnO_4$) and SDBS. In both cases, tests lasted 48 hours and oxidants were dosed 24 hours after SDBS. Each test analysed: (i) the influence of surfactant (0.1%, 0.2%, and 0.4% by weight) and oxidant (0.5%, 1%, and 1.5% by weight) concentration in terms of solubilization and oxidation efficiency of TPHs, and (ii) the germination index to assess the soil's phytotoxic characteristics. Additionally, a water test served as blank control. Each test was carried out in 3 replicates. The soil sample used, consisting of 63% sand, 22% silt, and 15% clay, was artificially contaminated with a known quantity of diesel (1% by weight) to achieve an initial TPH concentration of approximately 5000 mg/kg_{SS}. Prior to the start of the tests, the contaminated soil sample was manually mixed for 15 days to allow the volatilization of the most volatile components. The measurement of TPH concentrations in the solid matrix was conducted according to "Procedure for the analysis of hydrocarbons >C12 in contaminated soils - Manuals and Guidelines 75/11" proposed by ISPRA [6]; the measurement of hydrocarbons in the liquid phase was conducted in accordance with the standard "Oil Index" UNI EN ISO 9377-2 [7]; phytotoxicity was assessed through germination tests on *Lepidium sativum* (Garden cress) following the APAT procedure [8].

Results

The results obtained from the tests conducted in both experimental phases showed, in general, high removal efficiencies of TPHs from soil (Figure 1). In particular, the highest removal rates were found in the tests conducted with Fe(VI). Indeed, in all tests, the obtained efficiencies were higher than 90%, reaching, in some cases, values close to 96% (Figure 1a). On the contrary, results from tests with potassium permanganate showed removal rate consistently close to 70% (Figure 1b).

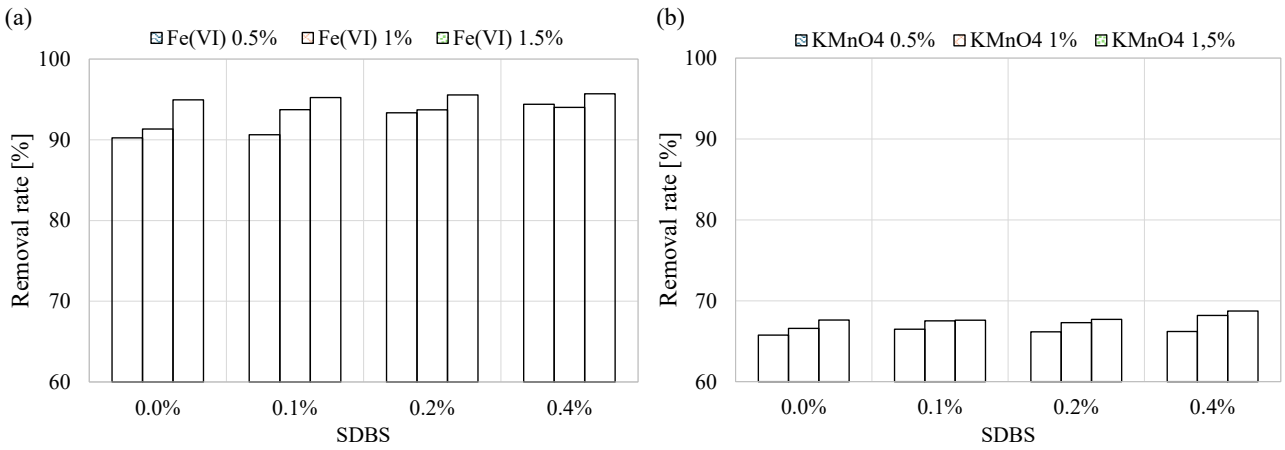

Figure 1. Removal efficiency of TPHs in soil as a function of Fe(VI) (a) and permanganate (b) doses.

These results are in contrast with those outlined in the study of Johansson et al. [9], which evaluated the oxidation of IPA and NAPL in sterile soil using Fe(VI) and $KMnO_4$. In fact, in their study, permanganate exhibited higher removal efficiencies (between 98% and 100%) compared to Fe(VI) (less than 65%). However, both findings of this study and those from Johansson and co-authors [9] are supported by the study of Ritoré et al. [10], which highlighted the influence of natural organic matter (NOM) on permanganate oxidation rate. Specifically, the study revealed that an increase in NOM content leads to a decrease in $KMnO_4$ oxidation. The divergence in results between this study and that of Johansson et al. [9] can be attributed to variations in NOM content: in the present experimentation, the soil has a TOC of 31.4 g/kg; conversely, in the one conducted by Johansson and co-authors [9],

sterile sand was used (TOC=0). Moreover, several studies reported in the literature [11, 12] showed that the presence of NOM, particularly humic acids, leads to the activation of ferrate and its reduction to Fe(V) and Fe(IV), molecules having reactivity up to 2-5 orders of magnitude higher than Fe(VI) [13]. Considering this, while organic matter in the soil has decreased the oxidation efficiency of $KMnO_4$, it has simultaneously enhanced that of Fe(VI).
Results of germination index determined on soil samples treated with ferrate and permanganate are reported in Table 1. In all tests GI values were very low (<45%) compared to the blank control (GI = 100%) indicating a negative impact on *Lepidium sativum* growth.
These results could be explained by the toxicity of SDBS [14]. Moreover, ferrate may have further contributed to the inhibition of seed germination due to the strongly alkaline environment (pH >13) that is established in its presence. Finally, permanganate also influenced seed germination by inhibiting growth. This result is consistent with the findings reported by Sirguey et al. [15], where permanganate was shown to have a negative impact on ryegrass (*Lolium multiflorum*) growth.

Table 1. Average values of GI of soil samples after tests (in brackets the standard deviation)

SDBS concentration	*Fe (VI) concentration*			*KMnO4 concentration*		
	0.5%	***1%***	***1.5%***	***0.5%***	***1%***	***1.5%***
—	34.1.8 ± 2.3	7.3 ± 1.2	6.5 ± 2.3	40.9 ± 3.61	14.5 ± 2.9	15.8 ± 2.6
0.1%	7.6 ± 2.5	-	-	-	5.4 ± 1.6	6.2 ± 1.1
0.2%	-	-	-	6.2 ± 1.4	9.1 ± 2.1	2.3 ± 1.4
0.4%	5.1 ± 0.8	-	-	2.2 ± 0.7	7.3 ± 1.3	-

Figure 2 shows seeds germination and roots elongation in the blank control and in the treated soil samples. As it can be seen, in treated soil samples, there is a noticeable decrease in seeds germination compared to the blank control; additionally, it is noted that permanganate exhibited a slightly lower phytotoxicity than ferrate.

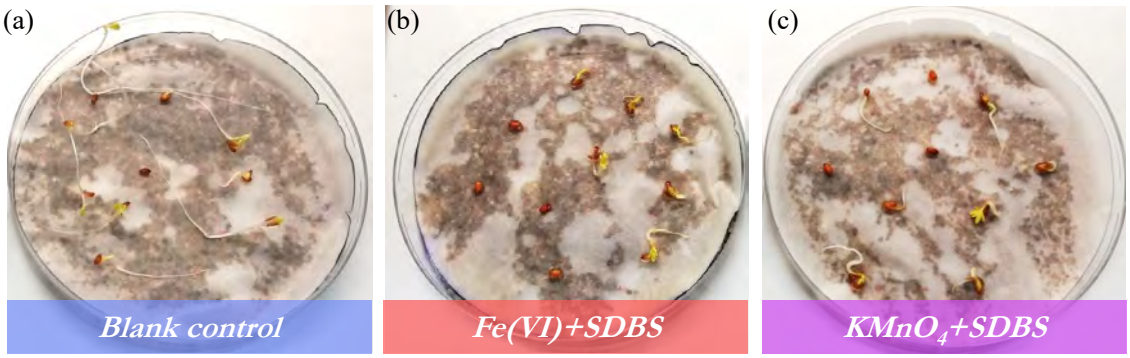

Figure 2. Seeds germination in: blank control (a), soil treated with Fe(VI) and SDBS (b) and soil treated with $KMnO_4$ and SDBS (c)

Conclusions

The conducted study confirmed the effectiveness of the combined oxidant and surfactant treatment. The tests conducted highlighted how the process efficacy is strongly influenced by the organic matter present

in the soil, particularly by humic acids. These, indeed, contributed to the activation of ferrate and its reduction to Fe(V) and Fe(IV), molecules with reactivity up to 2-5 orders of magnitude higher than Fe(VI). At the same time, NOM reduced the oxidation efficiency of permanganate. Results from phytotoxicity test showed low GI values, indicating an inhibitory effect on *Lepidium sativum* growth.

Acknowledgements

This study was carried out within the RETURN Extended Partnership and received funding from the European Union Next-GenerationEU (National Recovery and Resilience Plan – NRRP, Mission 4, Component 2, Investment 1.3 – D.D. 1243 2/8/2022, PE0000005).

References

[1] Gupta, P.K., Yadav, B.K., 2020. Three-Dimensional Laboratory Experiments on Fate and Transport of LNAPL under Varying Groundwater Flow Conditions. J. Environ. Eng. 146, 1–10. https://doi.org/10.1061/(asce)ee.1943-7870.0001672.
[2] Huo, L., Liu, G., Yang, X., Ahmad, Z., Zhong, H., 2020. Surfactant-enhanced aquifer remediation: Mechanisms, influences, limitations and the countermeasures. Chemosphere 252. https://doi.org/10.1016/j.chemosphere.2020.126620.
[3] Xu, J.C., Yang, L.H., Yuan, J.X., Li, S.Q., Peng, K.M., Lu, L.J., Huang, X.F., Liu, J., 2022. Coupling surfactants with ISCO for remediating of NAPLs: Recent progress and application challenges. Chemosphere 303, 135004. https://doi.org/10.1016/j.chemosphere.2022.135004
[4] Bouzid, I., Pino Herrera, D., Dierick, M., Pechaud, Y., Langlois, V., Klein, P.Y., Albaric, J., Fatin-Rouge, N., 2021. A new foam-based method for the (bio)degradation of hydrocarbons in contaminated vadose zone. J. Hazard. Mater. 401, 123420. https://doi.org/10.1016/j.jhazmat.2020.123420.
[5] Kumar Rai, P., Lee, J., Kailasa, S.K., Kwon, E.E., Tsang, Y.F., Ok, Y.S., Kim, K.H., 2018. A critical review of ferrate(VI)-based remediation of soil and groundwater. Environ. Res. 160, 420–448. https://doi.org/10.1016/j.envres.2017.10.016.
[6] ISPRA, 2011. Procedura per l'analisi degli idrocarburi >C12 in suoli contaminati - Manuali e Linee Guida 75/11.
[7] UNI EN ISO 9377-2:2002. Qualità dell'acqua- Determinazione dell'indice di idrocarburi - Metodo mediante estrazione con solvente e gascromatografia.
[8] APAT, 2004. Guida tecnica su metodi di analisi per il suolo e i siti contaminati - Utilizzo di indicatori biologici ed ecotossicologici 72–81.
[9] Johansson, C., Bataillard, P., Biache, C., Lorgeoux, C., Colombano, S., Joubert, A., Pigot, T., Faure, P., 2020. Ferrate VI oxidation of polycyclic aromatic compounds (PAHs and polar PACs) on DNAPL-spiked sand: degradation efficiency and oxygenated by-products formation compared to conventional oxidants. Environ. Sci. Pollut. Res. 27(1):704-716. http://doi.org/10.1007/s11356-019-06841-0.
[10] Ritoré, E., Morillo, J., Arnaiz, C., Coquele, B., Usero, J., 2023. Chemical oxidation of hydrocarbon-contaminated soil: oxidant comparison study and soil influencing factors. Environ Eng Res. 28(6): 220610. http://dx.doi.org/10.4491/eer.2022.610.
[11] Barışçı, S., 2017. The disinfection and natural organic matter removal performance of electro-synthesized ferrate (VI). J. Water Process Eng. 20, 84–89. https://doi.org/10.1016/j.jwpe.2017.10.005.
[12] De Marines, F., Corsino, S.F., Castiglione, M., Capodici, M., Torregrossa, M., Viviani, G., 2024. Ferrate as a sustainable and effective solution to cope with drinking water treatment plants challenges. J. Environ. Chem. Eng. 12, 112884. https://doi.org/10.1016/j.jece.2024.112884.
[13] Sun, S., Jiang, J., Qiu, L., Pang, S., Li, J., Liu, C., Wang, L., Xue, M., Ma, J., 2019. Activation of ferrate by carbon nanotube for enhanced degradation of bromophenols: Kinetics, products, and involvement of Fe(V)/Fe(IV). Water Res. 156, 1–8. https://doi.org/10.1016/j.watres.2019.02.057.
[14] Di Trapani, D., De Marines, F., Greco Lucchina, P., Viviani, G., 2023. Surfactant-enhanced mobilization of hydrocarbons from soil: Comparison between anionic and nonionic surfactants in terms of remediation efficiency and residual phytotoxicity. Process Saf. Environ. Prot. 180, 1–9. https://doi.org/10.1016/j.psep.2023.09.071.
[15] Sirguey, C.,de Souza e Silva, P.T., Schwartz, C., Simonnot, M.O., 2008. Impact of chemical oxidation on soil quality. Chemosphere. 72(2): 282-289. https://doi.org/10.1016/j.chemosphere.2008.01.027.

Title: Degradation of chlorinated solvents vapors in the unsaturated zone through horizontal permeable reactive barriers

Author(s): Daniela Zingaretti*[1], Clarissa Settimi[1], Iason Verginelli[1], Renato Baciocchi[1]

[1] *Department of Civil Engineering and Computer Science Engineering, University of Rome Tor Vergata, Rome, Italy* zingaretti@ing.uniroma2.it

Keyword(s): Zero-valent iron, bimetals, chlorinated solvents vapors, diffuse contamination

Abstract

Chlorinated solvents, such as trichloroethylene (TCE), have been used in various civil and industrial applications in the past decades due to their chemical and physical properties. These compounds are characterized by high mobility and low biodegradability at the same time, with consequent persistence in the environment. As a result, many groundwater bodies are currently characterized by diffuse contamination by chlorinated compounds, which can cause potential long-term risks to human health. In particular, the presence of these contaminants in groundwater is challenging for the management of the migration pathway of chlorinated solvents vapors to ambient air or into buildings (i.e., vapor intrusion). In sites characterized by diffuse contamination of chlorinated solvents, traditional remediation techniques are not technically and economically sustainable as they typically require high amounts of reagents or energy. In this scenario, it is more suitable to adopt risk management strategies to mitigate the volatilization pathway of chlorinated solvents vapors.
In the last years, we proposed to use horizontal permeable reactive barriers (HPRBs) placed in the unsaturated zone aimed at treating upward volatile organic compounds (VOCs), in imitation of vertical PRBs for the treatment of groundwater contaminated by chlorinated solvents. Initially, Zero-valent iron (ZVI) was investigated as reactive material for HPRBs and tested for TCE degradation in the gas phase through reductive dehalogenation [1]. Different types of granular zero-valent iron were tested in anaerobic batch experiments at room temperature analysing the degradation of TCE and the production of byproducts at discrete time intervals. Depending on the type of iron used, reductions of TCE gas concentration from 30% up to 99% were observed for treatments of 6 weeks [1]. The manufacturing process of the iron powder and the water content of the materials were found to play only a limited role whereas the pretreatment of the iron powder with HCl was found to enhance the reactivity of the iron. In all the experiments, the main byproducts of the reactions were C_4–C_6 alkenes and alkanes which can be attributed to a hydrogenation of the C-Cl bond [1]. To better understand the performance achievable with HPRBs filled with iron powders, a further study performed in our group examined the performances of different iron powders commercially available from different manufacturers and characterized by different specific surface areas [2]. The obtained results confirmed that the use of horizontal zero-valent iron barriers placed in the unsaturated zone to treat volatile compounds flowing upward can represent an attractive risk management option at sites contaminated by chlorinated solvents. As to the technical feasibility of this application, it was estimated that a barrier of 1 m filled with ZVI can ensure an attenuation of TCE vapor concentration of 99.9% [2].

In the last years, zero-valent bimetals based on iron and a secondary transition metal have also been widely investigated for the enhancement of chlorinated compounds degradation in the aqueous phase. In particular, the addition of a secondary transition metal (e.g., Cu or Ni) to iron increases the rate of reduction of chlorinated contaminants, as these metals are catalysts of iron corrosion reaction and of the dissociation of molecular hydrogen on the surface of the material. Following these findings, we decided to investigate the production and use of iron-based bimetals as filling materials for HPRBs [3-4].

Firstly, different disc-milled zero-valent Fe–Cu and Fe–Ni bimetals were produced by milling iron and secondary metal powders for 1 h at 700 rpm using a disc mill [3]. It was decided to generate bimetals with three different percentages by weight of secondary metal (Cu or Ni), i.e. 1%, 5%, and 20%, obtaining six different samples. The morphology of the produced bimetals, in terms of particles dimension, elemental composition, and mapping, was analysed by scanning electron microscopy (SEM) equipped with energy dispersive X-ray spectroscopy (EDS). The crystallographic structure of the tested materials was investigated by X-ray diffraction (XRD) analysis whereas the specific surface area (SSA) of the samples was evaluated by the Brunauer–Emmett–Teller (BET) method.

SEM analysis showed that the produced bimetals are characterised by particles with micrometric dimensions that allow their potential use as filling materials in HPRBs avoiding problems of particle aggregation. Furthermore, EDS analysis showed a homogenous distribution of Cu and Ni particles in Fe phase in the bimetals produced, that represent a fundamental characteristic for the enhancement of the reactivity toward dehalogenation reaction of chlorinated compounds [3]. Finally, XRD analysis confirmed that in the produced materials, especially in those with a Ni or Cu percentage lower than 20%, the secondary metal was entirely incorporated in Fe particles forming a bimetallic phase.

Afterward, the performances achievable with the different Fe–Cu and Fe–Ni bimetals were evaluated by means of anaerobic batch experiments at room temperature analysing the degradation of TCE and the production of byproducts at discrete time intervals. Regarding Fe–Cu bimetals (Fig. 2a–c), the highest TCE dechlorination performances were obtained using Fe-1%Cu with a 99.9% TCE reduction in 2 days. Using Fe-5%Cu and Fe-20%Cu, lower dechlorination performances were obtained in the degradation tests, with a 99.9% removal of TCE in 3–4 days [4]. Conversely, using Fe–Ni bimetals, better results were obtained compared to Fe–Cu ones in terms of TCE degradation performances, and a 99.9% TCE removal was achieved in maximum 2 days [4]. These results showed a significant enhancement in TCE removal compared to using ZVI alone which required minimum 3 weeks for an almost complete degradation of TCE vapors [2]. The byproducts detected at the end of the TCE degradation tests, were similar to those found by Zingaretti et al. [1-2]. Indeed the only detectable byproducts in the tested conditions were C_3–C_6 hydrocarbons, with no presence of vinyl chloride (VC) or dichloroethylene (DCE). These results suggest that the addition of Cu or Ni on iron did not influence the degradation pathway of TCE, but only catalyzed the degradation reactions [4].

In view of using the tested bimetals as constituents for HPRBs to treat chlorinated solvent vapors in the subsoil, the experimental results achieved were integrated into an analytical model to simulate the reactive transport of contaminated vapors through the barrier. According to this theoretical calculation, a thickness of the HPRB in the order of 20 cm could be potentially sufficient to efficiently degrade TCE vapors [4]. This could represent a significant improvement compared to previous estimations performed by Zingaretti et al. [2] that for ZVI alone estimated that a barrier of 1 m was needed to attenuate the TCE vapor concentrations of 99.9%.

Finally, the iron consumption due to oxidation of the HPRB was estimated and resulted in the range of 40–70 years [4], i.e., higher than other filling materials proposed in the literature (e.g. $KMnO_4$).

Although further investigations are needed before a full scale application, these results suggested that the use of these bimetals as constituents for HPRBs could be a promising option for effectively treating chlorinated solvent vapors

References

[1] Zingaretti D., Verginelli I., Baciocchi R., “Dehalogenation of trichloroethylene vapors by partially saturated zero-valent iron”, Science of The Total Environment, 647, 682-689 (2019)
[2] Zingaretti D., Verginelli I., Luisetto I., Baciocchi R.”Horizontal permeable reactive barriers with zero-valent iron for preventing upward diffusion of chlorinated solvent vapors in the unsaturated zone”, Journal of Contaminant Hydrology, 234, 103687 (2020)
[3] Settimi C., Zingaretti D., Sanna S., Verginelli I., Luisetto I., Tebano A., Baciocchi R., “Synthesis and Characterization of Zero-Valent Fe-Cu and Fe-Ni Bimetals for the Dehalogenation of Trichloroethylene Vapors”, Sustainability 14, (2022)
[4] Settimi C., Zingaretti D., Verginelli I., Baciocchi R.. “Degradation of trichloroethylene vapors by micrometric zero-valent FeCu and FeNi bimetals under partially saturated conditions”, Journal of Contaminant Hydrology, 257, 104204,(2023)

Title: The use of Liquid Activated Carbon (LAC) in microwave thermal treatment of PAH-contaminated soils: laboratory decontamination and columns leaching tests

Authors: Pietro P. Falciglia[1]*, Guido De Guidi[2], Monica Granetto[3], Tiziana Tosco[3], Rajandrea Sethi[3] and Federico G.A. Vagliasindi[1]

[1] *Dipartimento di Ingegneria Civile e Architettura, Università di Catania, Via S. Sofia, 64, 95125 - Catania*
[2] *Dipartimento di Scienze Chimiche, Università di Catania, Via S. Sofia, 64, 95125 - Catania*
[3] *Dipartimento* di *Ingegneria dell'Ambiente, del Territorio e delle Infrastrutture, Politecnico di Torino, Corso Duca degli Abruzzi, 24, 10129 - Torino*

Keywords: Liquid activated carbon; soil nanoremediation; microwave in-situ thermal treatment; in-situ soil remediation

Abstract

Introduction
Polycyclic Aromatic Hydrocarbon (PAH) – contaminated soils are a very important concern worldwide due to the high environmental persistence and strong affinity of adsorbed contaminants with solid particles. The PAH carcinogenic nature makes essential the search for rapid and cost-effective clean-up techniques [1].
Recent literature demonstrated that *MicroWave Heating (MWH)* can be exploited as a powerful tool in several environmental applications, among which treating organic-contaminated soils, sludge or toxic wastes. It showed a great ability to combine a rapid and effective contaminant removal with high flexibility and low costs. The soil decontamination process is based on the MW dielectric heating principle. The key factor is represented by the mechanism of partial conversion of the MW energy absorbed by the irradiated matrix into heat, which in turns results in a temperature increase. Contaminants adsorbed on soil grains are mainly removed by conventional “thermal desorption” or “selective heating”. The latter requires the lower energy consumption and it is activated in the presence of high-dielectric contaminants [2].
MWH was shown to be effective for short time removal of a large number of low-medium boiling point contaminants such as nitrobenzene, HCB, antibiotics and diesel–fuel. Research also demonstrated that the dielectric features of both contaminants and soils may represent the major driving force, which strongly decreases the energy requirements and makes MW a very cost-effective and sustainable solution. The dielectric properties of the irradiated medium influences in fact the MW penetration ability, heating and, consequently, contaminant thermal desorption process. Consequently, MWH was demonstrated as relatively effective for the removal of persistence organics from soils [2] due to the poor dielectric features of the irradiated media. Moreover, literature [3] showed that MW heating ability can be improved by adding external materials (artificial MW absorbers or enhancers) to the contaminated matrix before its irradiation. Activated Carbon (AC) is one of the most used MW-catalysts in environmental applications. Other materials are Cu_2O, NaOH, MnO_2, graphite, carbon nanotubes. The AC enhancing process is based on the concept of “hotspots” in MW-absorbing where AC surface can reach temperatures over 600 °C in very short irradiation times (after ~ 1 min).
Despite these advantages, AC solid nature limits the enhanced-MW heating treatment only to the ex-situ applications (soil excavation requirement). In the continuous search for liquid enhancing agents,

Liquid Activated Carbon (LAC) is a novel non-hazardous material that could represent a very favourable alternative. LAC use in enhanced-MW treatments, still unexplored, would allow to combine the high dielectric properties of solid AC jointly with the potential of in situ applications. However, studies usually report a high LAC mobility in the porous medium, on average higher than other nano- or micro-materials typically applied for in-situ remediation. If an extremely high mobility can be potentially a concern when applied in groundwater, this characteristic represents a positive factor in view of their possible application in soils.
The main goal of this work was the lab-scale investigation of an innovative LAC-enhanced MW treatment to decontaminate PAH-contaminated soils. Transport tests were also performed to assess the potential mobility of LAC suspensions in unsaturated porous media under the effect of gravity.

Materials and methods
A model sandy soil was artificially contaminated with PAHs. The contamination procedure was carried out by mixing a solution containing selected PAHs in dichloromethane (DCM) with the soil. Soil and spiking solution were shacked for 1 h and then the solvent was entirely separated from soil by means of a rotavapor system.
For the MW experiments, commercial LAC doses from 2.5 to 10.0% were mixed with the soil before irradiation. MW and LAC-MW heating treatments were simulated using a custom-made bench-scale oven, irradiating 15 g of PAH-contaminated soil samples (with or without LAC addition) for a maximum time of 5 min (Power range = 440 – 1000 W). The oven cavity was hydraulically connected to a dedicated exhaust gas line. A 1.5mm type-k thermocouple system was included for the soil sample temperature (T) recording. After MW treatment, the soil samples were cooled down, and then stored, sealed at 4 °C before analysis for PAH-residual concentrations (C) assessment. Residual PAHs were recovered with DCM applying the EPA method 3540C.
The mobility of LAC in unsaturated porous media was investigated in column transport tests performed diluting LAC in deionized water or tap water. A vertical plexiglass column (ID 1.6 cm, L 18 cm) was wet-packed with silica sand and 53 ml (corresponding to 1 pore volume) of concentrated LAC suspension (113 g/L) was let drain through it under gravity. Effluent samples were collected at a frequency of 10 s, thus allowing determination of the effluent discharge (by measuring volume) and LAC concentration (via UV-vis spectrophotometry) over time. At the end of the test, the column was extruded and dissected in 9 or 10 aliquots to determine the profile of retained LAC particles [4].

Results and Discussion
The soil temperature profiles (Figure 1a) show an almost increasing linear trend due to the progressive rise in MW energy absorbed by the irradiated samples over the time. Specifically, the LAC addition resulted in maximum T values in the 400 - ~1100 °C range. The highest temperature value was achieved for the 440 – LAC 10 (440 W – LAC 10% w/w) treatment after just 2 min. This is attributable to the increased dielectric properties of medium given by LAC, which in turns sharply increase its capability in concerting the MW electric field into heat (max heating rate = 370 °C min^{-1}). On the other hand, temperatures lower than 100 °C were found in absence of LAC even applying the power of 1000 W. This results in a decrease in PAH-concentration with irradiation time with a rapidity depending on the conditions investigated (Figures 1b). This revealed that the temperature effect and the relation between the treatment temperature and contaminant vaporization temperature are the key factors in organic contaminant removing.

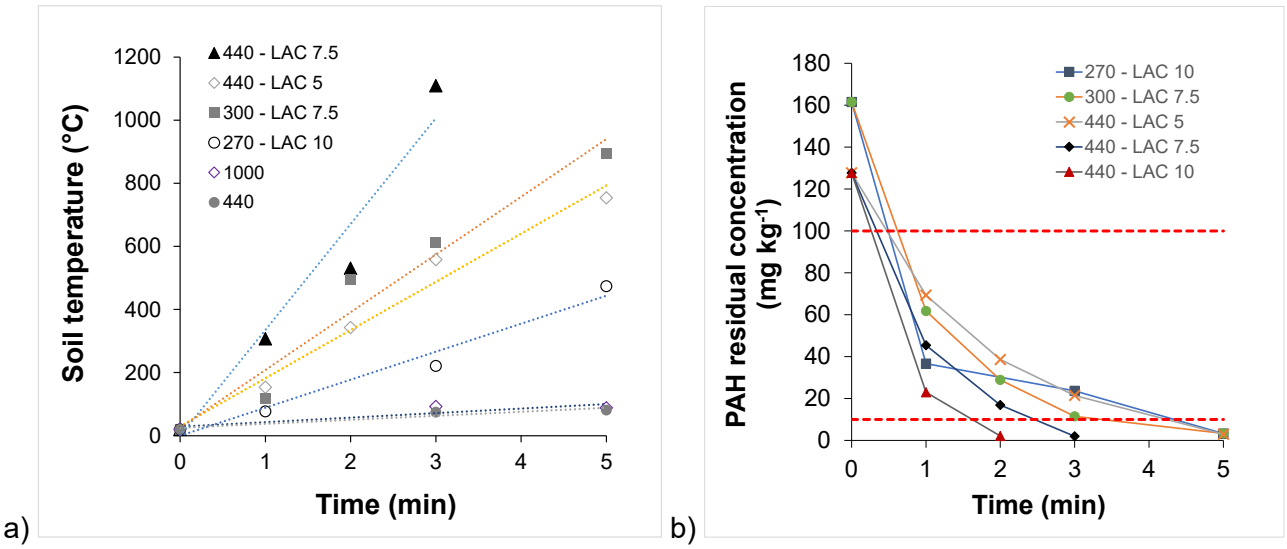

Figure 1. a) Temperature profile for MW and LAC-enhanced MW treatments. b) PAH residual concentration in soil after the MW irradiation.

LAC-enhanced treatment allows the achievement of severe Italian regulatory limit (L.D. 152/2006) for total PAHs of 10 mg kg^{-1} in just 5 min also when the minimal power was applied (270 – LAC 10). Shorter times of 4.4 or 4.2 min can be sufficient for higher powers and lower LAC doses (300 – LAC 7.5 or 440 LAC, respectively). The shortest time of 1.4 min is achievable when the maximum power and dose are applied. LAC colloidal particle aggregates adsorbed on the soil surface act as “hot spots” (Figure 2) with the ability in transforming the absorbed MW energy into a large a rapid local temperature increase up to values even much higher than those recordable by the measurement system. This results in thermal desorption of PAHs [5].
From literature, it is evident that current available PAH-contaminated soil remediation technologies cannot lead to a similar rapid and total decontamination goal.

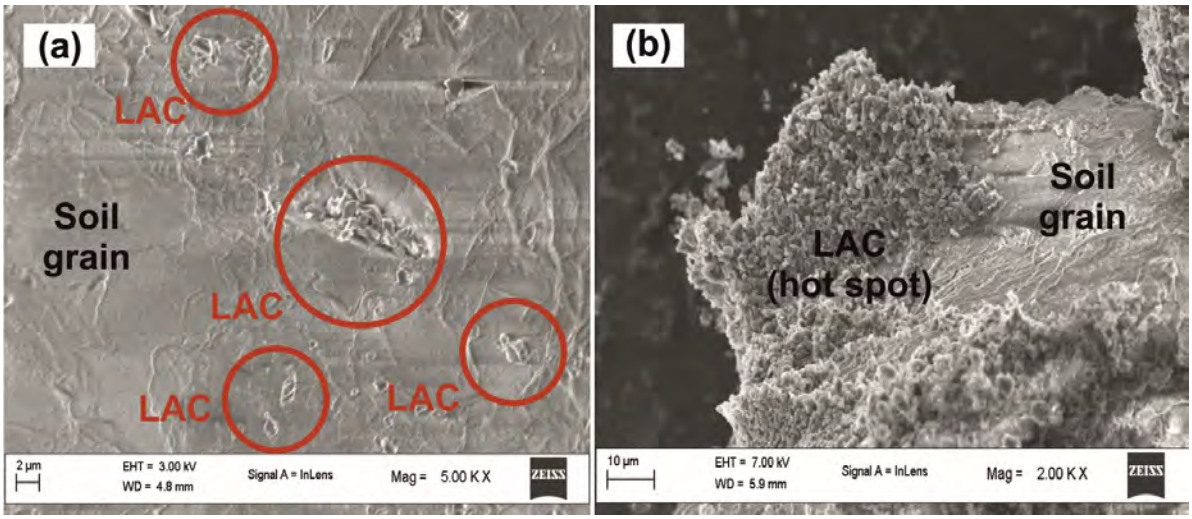

Figure 2. SEM images of LAC-soil mixture before irradiation with 5%-LAC dose (a) and 10%-LAC dose [5].

The column leaching tests showed LAC to be highly mobile when dispersed both in deionized and tap water. LAC outflow concentration equalled the applied one in less than 100s (Figures 2a), with a cumulative mass recovered of 63% and 69% in DiW and TapW, respectively (Figures 2b). The mass of LAC retained in the column increased with depth in the first 5 cm and then remained constant in the bottom part of the column. The higher concentration measured at the bottom column outflow is likely due to the column configuration. The shape of the vertical profiles (neither exponential nor hyper-exponential) suggested the absence of mechanical filtration and/or ripening, and blocking seemed to be the controlling interaction mechanism.

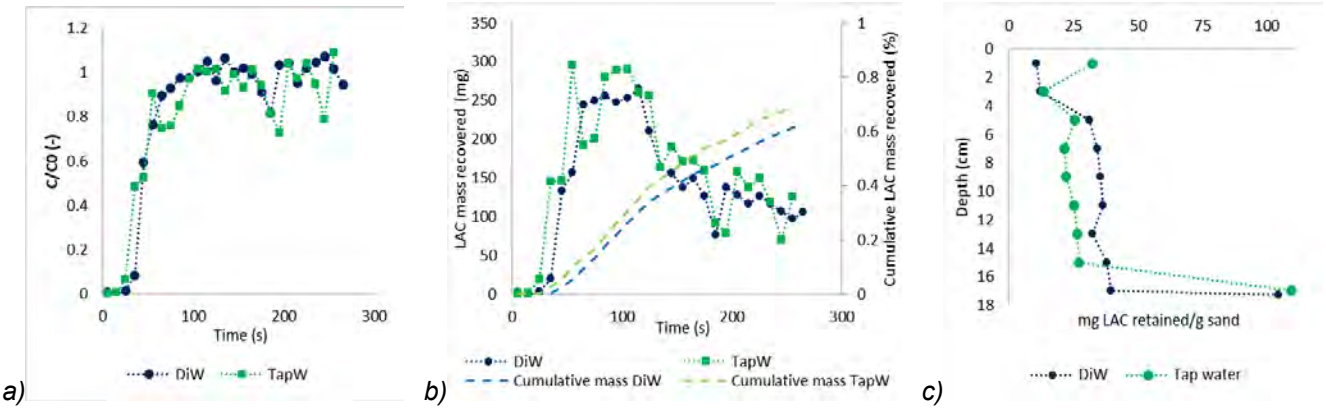

Figure 2. a) LAC breakthrough curves when suspended in deionized water and tap water, b) Recovered mass of LAC over time and its cumulative distribution, c) Vertical profile of LAC at the end of leaching tests.

Conclusions

The obtained results proven that the addition of liquid activated carbon (LAC) in soil largely increase the heating capacity of the irradiated media and, consequently, the very rapid and effective PAH removal from soils. The good LAC mobility observed in column transport tests opens optimistic perspectives for an effective delivery via gravity of the LAC suspensions, at least in permeable soils. Results show the potentiality of the investigated treatment in terms of clean-up time, decontamination effectiveness and environmental sustainability.

References

[1] Falciglia P.P., Catalfo A., Finocchiaro G., Vagliasindi F.G.A., Romano S., De Guidi G., Microwave heating coupled with UV-A irradiation for PAH removal from highly contaminated marine sediments, Chem. Eng. J. 334, 2018, 172–183.
[2] Falciglia P.P., De Guidi G., Catalfo A., Vagliasindi F.G.A., Remediation of soils contaminated with PAHs and nitro-PAHs using microwave irradiation, Chem. Eng. J. 296, 2016, 162–172.
[3] Chen J., Zhong D., Hou H., Li C., Yang J., Zhou H., Hu L., Wang L., Ferrite as an effective catalyst for HCB removal in soil: Characterization and catalytic performance, 294, 2016, 246–253.
[4] Mondino F., Piscitello A., Bianco C., Gallo A., de Folly D'Auris A., Tosco T., Tagliabue M., Sethi R., Injection of Zerovalent Iron Gels for Aquifer Nanoremediation: Lab Experiments and Modeling, Water 2020, Vol. 12, Page 826.
[5] Falciglia P.P., De Guidi G., Vento F., Finocchiaro G., Castro E., Granetto E., Tosco T., Vagliasindi F.G.A, Liquid activated carbon (LAC) – Enhanced microwave remediation of PAH – Contaminated soils, Separation and Purification Technology, 331, 2024, 125628.

Title: Degradation of 1,2-dichloroethane in real polluted groundwater under aerobic and anaerobic laboratory-scale conditions

Author(s): Michele Carabillò*[1], Marco Capodici[1], Valentina Catania[2], Gaetano Di Bella[3], Daniele Di Trapani[1], Maria Gabriella Giustra[3], Paola Quatrini[2], Roberto Scaffaro[1], Laura Scirè Calabrisotto[2], Gaspare Viviani[1]

*[1] Dipartimento di Ingegneria, Università degli Studi di Palermo, Viale delle Scienze ed. 8, 90128 Palermo, *michele.carabillo@unipa.it*
[2] STEBICEF Dipartimento di Scienze e Tecnologie Biologiche, Chimiche e Farmaceutiche, Università di Palermo, Viale delle Scienze ed. 16, 90128 Palermo
[3] Università di Enna KORE, Facoltà di Ingegneria e Architettura, Cittadella Universitaria, 94100 Enna, Italy

Keyword(s): Chlorinated solvents, Permeable reactive barrier, Poly-β-hydroxybutyrate, Biological reductive dichlorination, Direct or cometabolic aerobic oxidation

Abstract

Chlorinated solvents are a subgroup of organ-halogen compounds belonging to the class of chlorinated aliphatic hydrocarbons. They have been widely used in various industrial sectors as degreasers, dry cleaning, and solvents in the chemical-pharmaceutical industry [1]. Improper handling and disposal practices often lead to their release into the environment, where they can contaminate various environmental matrices, especially the aquifers [2]. Currently, the interest is directed towards the development of new in situ remediation technologies, including permeable reactive barriers (PRBs) based on biological processes [3]. Biodegradation can occur through an aerobic or anaerobic reaction, via a direct or cometabolic pathway [4]. In direct aerobic oxidation, the chlorinated compound acts as electron donor and growth substrate for microorganisms, while oxygen is the electron acceptor. Conversely, in aerobic cometabolism, oxygenase enzymes, synthetized by microorganisms for the uptake of growth substrates, fortuitously catalyze the oxidation of the chlorinated compound. Oxidative processes require nicotinamide adenine dinucleotide - hydrogen (NADH) as a source of reducing energy, which is regenerated through the oxidation of the growth substrate. However, in aerobic cometabolism, NADH cannot be regenerated, and biodegradation continues until the available reducing energy is depleted [5]. Generally, low-chlorinated compounds are degraded through an oxidative direct pathway, while polychlorinated compounds can be effectively degraded via reductive dechlorination. Biological reductive dechlorination (BRD) is an anaerobic respiratory process, called dehalorespiration, and microorganisms able to respire chlorinated compounds, utilizing them as terminal electron acceptors, are called organohalide respiring bacteria (OHRB) [6]. To date, BRD can be enhanced and supported using poly-β-hydroxybutyrate (PHB), which is effective both as a slow-release electron donor and as a reactive medium in a PRB. Its fermentation, in fact, simultaneously releasing electron donors and carbonaceous substrate, can support the long-term growth of dechlorinating bacteria [7]. The aim of this work was to gain insights about the feasibility of chlorinated solvents removal through biostimulated and bioaugmented biological processes in laboratory-scale permeable reactive barriers

(PRBs) under both anaerobic and aerobic scenarios. The novelty of this study relies in the use of real groundwater collected from an aquifer mainly contaminated by 1,2-DCA. Our results can provide useful preliminary indications towards the evaluation of 1,2-DCA anaerobic and aerobic biodegradation pathways when treating real contaminated groundwater.
The experimental campaign was divided into two periods, namely Period I(anaerobic) and Period II (aerobic); it is worth noting that Period II is currently in progress. Figure 1 shows the experimental apparatus during both periods.
Anaerobic period had an overall duration of 126 days. During the first 45 days, enrichment cultures were set up from the groundwater contaminated by chlorinated solvents, to favor the autochthonous dechlorinating bacterial population. A dechlorinating anaerobic bacterial consortium was enriched in presence of PHB powder, as electron donor for the BRD process, under anaerobic conditions. During the subsequent 81 days, a pilot study was carried out on a laboratory-scale plant fed with the real contaminated groundwater, inoculated with the dechlorinating bacterial consortia.
Aerobic period will have the same duration of Period I. Bioremediation relies on biodegradation of CAHs, that is carried out by specialized bacteria under aerobic conditions. Bioremediation relies on biodegradation of CAHs, that is carried out by specialized bacteria under aerobic conditions. To enrich the dechlorinating components of the autochthonous bacterial communities, different aerobic biostimulation treatments in microcosm were tested, using groundwater samples and appropriate culture media amended with 1,2-DCA and additional substrates, if required, to stimulate different biodegradative processes. Aerobic conditions in the column were achieved using Oxygen Release Compound (ORC); these methods stimulate the natural activity of soil self-purification by promoting the growth of natural bacterial families that metabolise hydrocarbons, once in the aquifer, tiny particles of ORC produce a slow controlled release of oxygen, for periods up to 12 months.
It should be noted that the materials and methods as well as results reported refer to the anaerobic period only, as the "aerobic" trial is currently in progress. Enrichment cultures in microcosm were set up using the real groundwater sample from the contaminated aquifer to enrich the autochthonous 1,2-DCA dechlorinating bacterial community. It was carried out by microorganisms, abiotic controls were set up in parallel to the biologically active treatments (Gu, 2016) using filter-sterilized groundwater. All microcosms were prepared in triplicate. At the end of four established incubation times (0, 15, 30 and 45 days), a set of microcosms of each condition was analyzed by gas-chromatography.
The experimental apparatus in Period I (Figure 1a) consisted of a 20-liter PVC feed bag, containing water from the contaminated aquifer, connected via a five-way distributor to an extremely precise MasterFlex multichannel peristaltic pump that feeds a system consisting of four lines in parallel, denoted by the letters A, B, C and D, identical in geometric configuration. Each line consisted of two columns placed in series: one made of glass, and one made of plexiglass. The four glass columns, filled with silica sand, simulate the PRBs and differentiated the four configurations of the experimental apparatus; in fact, the first represents the biotic control blank, characterized by the inoculation of a consortium of 1-2-DCA-degrading bacteria, the second represented the abiotic control blank while the third and fourth, in addition to the bacterial inoculum, were characterized by the presence PHB; in particular, in the third line PHB was present in the form of granules and powder, while in the fourth line PHB was present within highly engineered and environmentally sustainable biodegradable scaffolds to be used at the same time both as a physical support for the growth of the microbial population and as an electron donor to support the biological process. Plexiglass columns, placed downstream of the PRBs, were all filled with silica sand and simulated a portion of the aquifer downstream of the PRB itself. The operating conditions of this system consisted of a feed rate of 6 ml/h and a hydraulic detention time (TDI) of 25 hours. The experimental apparatus in Period II was characterized by four identical plexiglass columns in parallel, each with specific composition, as reported in Figure 1b.
Acetate concentration (Figure 2) values showed a different behaviour of the two forms of PHB used,

with higher values observed in line D than in line C. The increased fermentation obtained in line D could be linked to the high specific surface of the biopolymer itself (scaffold).

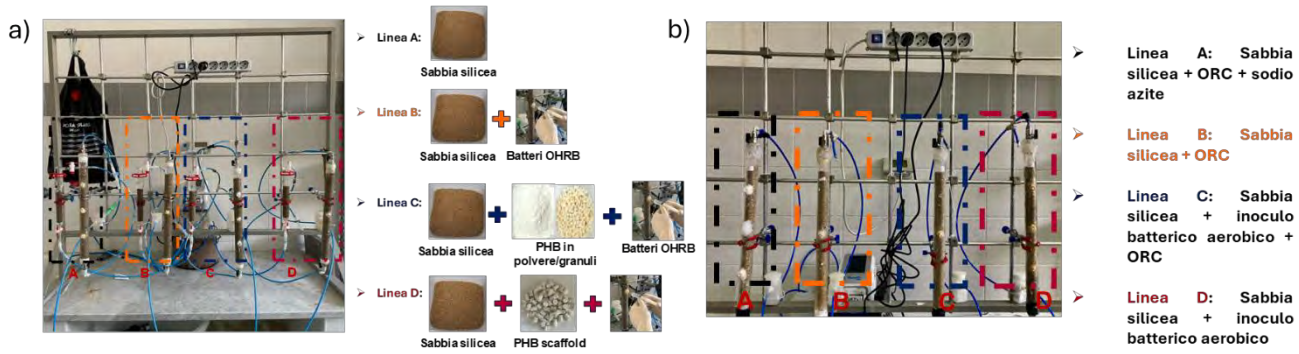

Figure 1. The experimental apparatus used during Period I (a) and Period II (b), respectively

The results obtained showed, after 81 days of testing, concentrations of acetate up to 500 mg/l in line C and 767 mg/l in line D. In addition, in both lines, the highest values were observed when leaving the PRB: this behaviour is probably due to the hydrolysis of PHB in the reactive columns resulting in the production of acetate, while in the simulation columns the aquifer was consumed by microorganisms and used as a substrate in the dechlorination process.

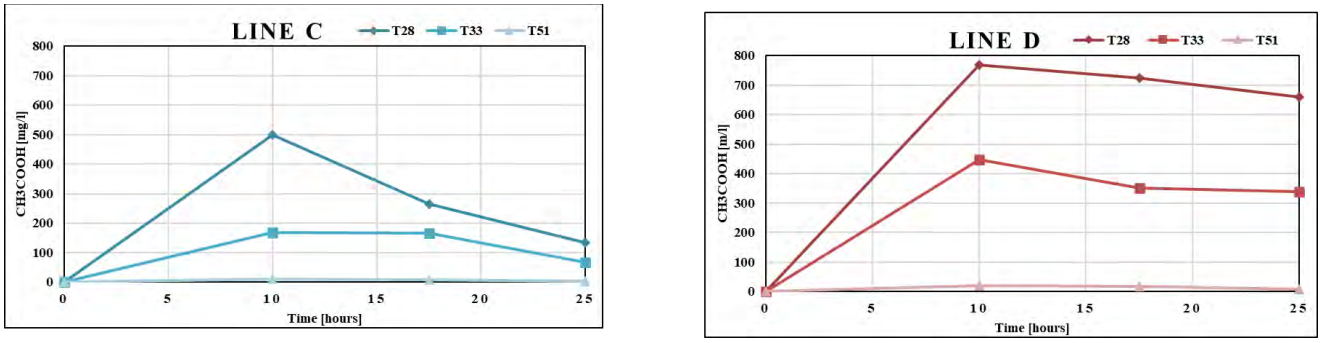

Figure 2. Acetate concentration values in Period I

Chemical monitoring of 1,2-DCA concentration by Gas Chromatography-Mass Spectrometry, revealed high removal efficiency in different anaerobic conditions. The mean removal efficiencies of 1.2-DCA in lines A, B, C and D (Figure 3) at the end of the trial were 15%, 25%, 60% and 70% respectively. From the data obtained, it was therefore observed that in the presence of PHB fermentation products the microbial consortium was more capable of degrading 1-2 DCA.

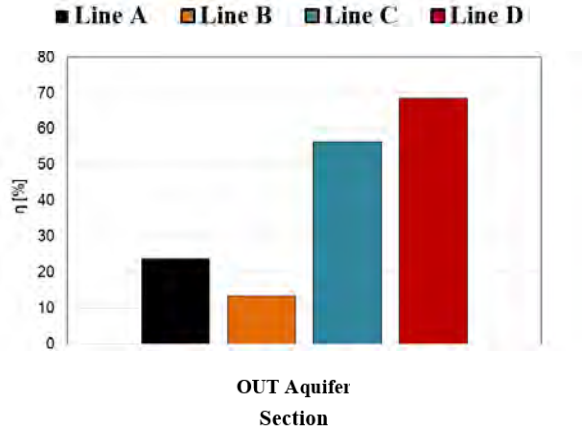

Figure 3. Removal efficiencies of 1.2-DCA in Period I

In the present study, aerobic and anaerobic biostimulation and bioaugmentation treatments were investigated for the bioremediation of a real groundwater mainly polluted by 1,2-DCA, by exploiting the biodegradation potential of the autochthonous bacterial communities. We demonstrated that both aerobic and anaerobic dehalogenating activity can be stimulated effectively in the same site and that the two obtained enriched consortia were composed of partially/putatively known dehalogenating bacteria. Our results highlight that a variety of biological processes can be effectively stimulated for the remediation of aquifers contaminated by chlorinated solvents.

Acknowledgements
This study was carried out within the RETURN Extended Partnership and received funding from the European Union Next-GenerationEU (National Recovery and Resilience Plan – NRRP, Mission 4, Component 2, Investment 1.3 – D.D. 1243 2/8/2022, PE0000005).

References
[1] Chang, C.H., Yang, H.Y., Hung, J.M., Lu, C.J., Liu, M.H., 2017. Simulation of combined anaerobic/aerobic bioremediation of tetrachloroethylene in groundwater by a column system. Int. Biodeterior. Biodegrad. 117, 150–157. https://doi.org/10.1016/ j. ibiod.2016.12.014.
[2] Nguyen, T.M., Chen, H.H., Chang, Y.C., Ning, T.C., Chen, K.F., 2023. Remediation of groundwater contaminated with trichloroethylene (TCE) using a long-lasting persulfate/biochar barrier. Chemosphere 333, 138954. https://doi.org/10.1016/j. chemosphere.2023.138954.
[3] Li, J., Hu, A., Bai, S., Yang, X., Sun, Q., Liao, X., Yu, C., 2021. Characterization and performance of lactate-feeding consortia for reductive dechlorination of trichloroethene. Microorganisms 9 (4), 751. https://doi.org/10.3390/ microorganisms9040751.
[4] Frascari, D., Zanaroli, G., Danko, A.S., 2015. In situ aerobic cometabolism of chlorinated solvents: a review. J. Hazard Mater. 283, 382–399.
[5] Van Hylckama Vlieg, J.E.T., De Koning, W., Janssen, D.B., 1996. Transformation kinetics of chlorinated ethenes by Methylosinus trichosporium OB3b and detection of unstable epoxides by on-line gas chromatography. Appl. Environ. Microbiol. 62, 3304–3312. https://doi.org/10.1128/aem.62.9.3304-3312.1996.
[6] Song, J., Li, Y., Wu, N., Li, P., Zhang, J., Rong, L., Song, Y., 2023. Impact of electron donors on chlorinated ethane degradation and native bacteria response in aged contaminated groundwater: a systematic study with insights. Int. Biodeterior. Biodegrad. 178 https://doi.org/10.1016/j.ibiod.2022.105548.
[7] Amanat, N., Matturro, B., Villano, M., Lorini, L., Rossi, M.M., Zeppilli, M., Rossetti, S., Petrangeli Papini, M., 2022. Enhancing the biological reductive dechlorination of trichloroethylene with PHA from mixed microbial cultures (MMC). J. Environ. Chem. Eng. 10, 107047 https://doi.org/10.1016/j.jece.2021.107047.

PARALLEL SESSION: D8

Municipal and industrial waste

Advanced waste processes and management

Title: Modelling material flow networks for industrial symbiosis in the metallurgical context

Author(s): Reza Vahidzadeh*[1], Giorgio Bertanza[2], Marta Domini[3]

[1] *Department of Civil, Environmental, Architectural Engineering and Mathematics (DICATAM), University of Brescia, Brescia, Italy, reza.vahidzadeh1@unibs.it*
[2] *Department of Civil, Environmental, Architectural Engineering and Mathematics (DICATAM), University of Brescia, Brescia, Italy, giorgio.bertanza@unibs.it*
[2] *Department of Civil, Environmental, Architectural Engineering and Mathematics (DICATAM), University of Brescia, Brescia, Italy, marta.domini@unibs.it*

Keyword(s): industrial waste, industrial symbiosis, circular economy, metals, network analysis, material recovery, green economy

Abstract

Industrial symbiosis (IS) includes the interaction of flows of material and energy among the traditionally separated companies in which the under-utilized residues of one company become resources for another. At this time, there is no widely accepted method of evaluation for IS performance especially at a system level for a group of industries. This study presents the results of the collaboration of the University of Brescia with the EU-funded project “Creation Of new value chain Relations through novel Approaches facilitating Long-term Industrial Symbiosis (CORALIS)”. CORALIS proposed 6 technological solutions for the valorization of metallurgical wastes including various metal powders, filter dusts and slags. In 2018, the total waste generated in the metallurgical sector under ATECO code 24 in Lombardy was 2,498,551.4 tons that forms 13.6 % of the total special waste produced in the region in the same year. In this study, the potential of resource recovery in a network of material exchange in the Lombardy region according to the IS solutions developed by CORALIS was evaluated. The potential regional IS networks in the metallurgical sector were characterized using social network analysis (SNA). SNA, as a specific field of graph theory, permits to visualize and to evaluate the interfirm resource exchanges. The method has been used in literature and practice for evaluating IS in Eco-industrial parks and small industrial districts, in which data on existing companies and their flows are available, such as the Kalundborg district [1] and the Lubei eco-industrial park [2]. Also, in supply chain management studies, the SNA is used as a tool for solving optimization and logistic problems at the interfirm level, e.g., for the minimization of the costs of transport among a big refinery and its raw material suppliers [3]. Theoretical works have been carried out on defining the parameters and indicators from SNA which can be useful for studying the organization of IS networks [4].
The potential contribution of the technological solutions under development by CORALIS in reducing the total waste generated in the sector was estimated for six IS scenarios. The impact of centralization and decentralization strategies on the network characteristics, and the efficiency of the networks in terms of treated waste and recovered resources, were estimated for 11 modelled networks. The network indicators including density and betweenness centrality showed a remarkably high potential of new IS linkages among the involved companies. The maximum network size may be obtained in a Combined scenario of all the 6 proposed technological solutions which involves 103 nodes and 222 ties under the decentralization condition and could effectively shorten the distance of material transportation. Comparing the different technologies, the maximum recovery can be achieved through the production

of pig iron by the reducing furnace, briquetting and the ferroalloy production processes.

Acknowledgements
This research was conducted within the MICS (Made in Italy – Circular and Sustainable) Extended Partnership and received funding from: Next-GenerationEU (Italian PNRR – M4 C2, Invest 1.3 – n. 1551.11-10-2022, PE00000004); and CORALIS project funded by the European Union's Horizon 2020 research and innovation program (grant agreement n.958337).

References

[1] Chopra, S.S., Khanna, V., "Understanding resilience in industrial symbiosis networks: Insights from network analysis," Journal of Environmental Management 141, 86–94, (2014).
[2] Zhang, X., Chai, L., "Structural features and evolutionary mechanisms of industrial symbiosis networks: Comparable analyses of two different cases," Journal of Cleaner Production 213, 528- 539, (2019).
[3] Shukery, M.F., Hashim, H., Lim, J.S., "Optimal location and allocation for the development of oil palm eco-industrial town (EIT): case study in state of Johor," Chemical Engineering Transactions, 56, 1417-1422, (2017).
[4] Ashton, W., "Understanding the organization of industrial ecosystems: A social network approach," Journal of industrial ecology, 12 (1), 34-51, (2008).

Title: Environmental and economic analyses of an innovative automatic system for sorting waste in public areas: case study of an airport

Author(s): Giovanni Dolci*[1], Alessandro Manea[2], Giulia Cavenago[3], Camilla Tua[4], Mario Grosso[5]

[1] Civil and environmental engineering department (DICA), Politecnico di Milano, Milan, Italy, giovanni.dolci@polimi.it
[2] DICA, Politecnico di Milano, Milan, Italy, alessandro.manea@mail.polimi.it
[3] DICA, Politecnico di Milano, Milan, Italy, giulia.cavenago@polimi.it
[4] DICA, Politecnico di Milano, Milan, Italy, camilla.tua@polimi.it
[5] DICA, Politecnico di Milano, Milan, Italy, mario.grosso@polimi.it

Keyword(s): Airport waste, waste management in public areas, life cycle assessment, cost analysis, automatic sorting

Abstract

Introduction
In the last decades the aviation sector has seen a rapid increase in the number of passengers transported all over the world, only stopped and temporarily reversed by the COVID-19 pandemic [1]. Among the waste generated by this sector, the municipal solid waste from the public areas of airport terminals (e.g. shops, check-in, restaurant, and café areas) is generally affected by a bad quality of the separate collection [2]. For this type of waste, a key aspect which contributes to a better management is passengers' behaviour and awareness. Indeed, the waste collection quality is affected by people's haste or negligence and by different familiarity with the waste collection system among the airport customers, i.e. people from various countries.
With the recent advancement in artificial intelligence methods, there are now opportunities to make a difference by adopting smart technologies to improve the segregation of recyclable materials at the very beginning of the waste value chain. The idea behind these methods is to improve the waste sorting at the source of waste generation, thus leading to higher amounts and higher quality of recyclable materials.
In this framework, this study aimed at exploring the environmental and economic effects of the implementation of an automatic system for sorting the municipal solid waste in public areas of airports focusing on Milano Malpensa as a case study.

Materials and methods
Examining the public areas of the Malpensa airport, about 155 tonnes of municipal solid waste are collected every year inside quadripartite bins for the separate collection of four fractions: residual waste, paper, plastic, and glass/aluminium.
First, the current waste composition was determined by means of waste composition analyses performed along a period of 2 months. The quality of the current manual separate collection was then evaluated by means of two parameters:

- The *classification accuracy*. Defined for each fraction, it is the ratio between the weight of the i-th fraction present in the correct bag and the total weight of the i-th fraction introduced in all the four bags.

- The *bag accuracy*. Defined for each bag, it is the ratio between the mass of the correct fraction in each bag and the total mass of waste in that bag.

Starting from data on the current waste characteristics, the collection quality expected with the use of an automatic sorting bin was estimated. The bin [3] is a prototype manufactured by the WiSort start-up company which is capable of autonomously sorting the waste in four different fractions (residual waste, paper, plastic, and glass/aluminium) through image recognition and a machine learning algorithm. A WiSort bin was installed in a public area of the airport of Milano Malpensa to perform the research.

Based on data on the current (manual) and the expected (automatic) collection qualities, the two systems were then compared from the environmental and the economic points of view, considering the whole waste management chain (i.e. waste collection in the airport, transportation to the waste treatment plants and material/energy recovery processes).
In such analyses, three scenarios were identified and evaluated:

- Manual sorting for energy recovery (MSE). Despite being collected in the four different bins, all the waste from the public areas of the airport is currently sent to the incineration with energy recovery. This is because of the bad quality of the sorting performed by passengers (the current average bag accuracies of the four collection bags, as shown in Table 1, are lower than the thresholds of the Italian packaging consortium for sending the separately collected fractions to material recovery [4]).
- Manual sorting for recycling (MSR). In this scenario, material recovery is introduced for paper and glass/aluminium bags, although not currently performed. They were assumed to be sent to sorting and material recycling processes. The extraneous fraction of bags was assumed to be sent to energy recovery after sorting. The plastic bag was assumed to be sent to sorting for being recovered as solid recovered fuel in a cement plant, while the management of the residual waste bag is the same modelled in the MSE scenario.
- Automatic sorting (AS). The waste is supposed to be automatically sorted by a WiSort bin and collected in the four bags. Two *classification accuracy* values were considered: 70% (AS70) and 90% (AS90). The former is slightly higher than the value of the current manual sorting, while the latter is the target for the WiSort bin, defined according to the performances of similar automatic machines on the market [5, 6]. The waste bags were assumed to be managed as modelled in the MSR scenario, except for plastic bags assumed to be firstly sent to sorting for polyethylene terephthalate (PET) recovery.

As regards the environmental aspects, a life cycle assessment (LCA) was performed considering as functional unit the management of 1 tonne of municipal solid waste with the composition measured by means of the waste composition analyses.
The 16 midpoint impact indicators of the Environmental Footprint method, version 3.0 [7] were included in the analysis.
The system boundary was set according to the “zero-burden approach”, i.e. the impacts of the upstream processes and activities connected to the supply chain of the product before it becomes a waste were not considered, being common in all the analysed scenarios. All the waste management stages were included, together with the life cycle of the bins (quadripartite or WiSort bin) and of the collection bags. Cases of multi-functionality related to the recovery of energy and materials in the valorisation of the waste were solved by expanding the system boundary [8] with an attributional approach.
Regarding data quality, the foreground system was mainly described with primary data collected from the waste composition analyses or provided by the airport operator and by the WiSort company. For the background system, data from literature and the ecoinvent database (version 3.8) were used [9].

Focusing on the economic assessment, a cost analysis from the perspective of the airport operator was performed to compare the scenarios. It included:

- the costs for cleaning operations (e.g. personnel costs for emptying the bins and moving the waste);

- the costs for internal and external transportations (i.e. costs for the transportation of waste to the treatment facilities);
- the waste treatment costs (i.e. the fees for processing the waste at the final plants);
- the costs of the bins (quadripartite or WiSort bin) and of the collection bags.

Results

Table 1 reports the average *bag accuracy* for the four collection bags in all the analysed scenarios. For the current situation (MSE scenario), values for all of the four collection bags are lower than the thresholds of the Italian packaging consortium for sending the separately collected waste to material recovery (i.e. 85%, 80%, and 93.5% respectively for paper, plastic, and glass/aluminium [4]).
The average *classification accuracy* of the current collection (weighted on fractions amounts) resulted 61.8%.

Table 1. Average *bag accuracy* for the four collection bags in the analysed scenarios

Bin (scenario)	Bag			
	Residual waste	Paper	Plastic	Glass/aluminium
Quadripartite bin (MSE and MSR)	65.3%	59.8%	78.5%	59.3%
WiSort bin (AS70)	55.8%	77.6%	84.4%	80.2%
WiSort bin (AS90)	83.0%	93.0%	95.4%	94.0%

Table 2 reports the potential environmental impacts of the MSE scenario and the potential impacts changes among scenarios.
Results indicate that the current management based on energy recovery (MSE) causes additional burdens (positive value of the indicator) on ten out of the 16 examined impact categories, and benefits (negative value of the indicator) on the six remaining ones. When examining the introduction of the recycling (MSR), impacts savings are observed for 14 categories. Finally, the automatic sorting (AS70 and AS90) allows for benefits in all the categories excluding *Resource use, minerals and metals*.
When compared to the current management (MSE), the MSR scenario allows for lower burdens or higher benefits in all the examined impact categories excluding *Water use*. The automatic sorting with a 70% *classification accuracy* (AS70) would allow for further benefits in six impact categories. On the contrary, AS70 is worse than MSR for four categories (and changes lower than 10% are observed in the remaining six categories). When a 90% *classification accuracy* is assumed (AS 90) the use of the automatic bin performs better than MSR in all impact categories excluding *Ionising radiation* and *Resource use, minerals and metals* (due to the production of the WiSort bin components).

Finally, the economic assessment indicates the following management costs: 450 €/t of waste - MSE, 425 €/t of waste - MSR, 441 €/t of waste - AS70, and 415 €/t of waste - AS90. Accordingly, the recycling after manual sorting (MSR) allows for a costs saving (-6%) compared to the current energy recovery (MSE). On the contrary, when the automatic sorting is implemented with a *classification accuracy* slightly higher than the current one (AS70), costs are higher than those of MSR scenario (+4%), due to the costs of the WiSort bin. Differently, with a 90% *classification accuracy* (AS90), costs are lower than both MRE (-8%) and MRS (-2%) scenarios.

Table 2. Potential impacts of MSE scenario (per functional unit) and impacts changes among scenarios (a negative percentage change indicates an improvement, while a positive percentage change indicates a worsening). For each scenario, negative values of the indicators (i.e. environmental benefits) are underlined.

Impact category (unit of measurement)	Impact	Impact change		
	MSE	(MSR-MSE) /|MSE|	(AS70- MSR) /|MSR|	(AS90- MSR) /|MSR|
Climate change (kg CO_2 eq/FU)	4.45E+02	-121%	-38%	-175%
Ozone depletion (kg CFC11 eq/FU)	-1.52E-05	-465%	-339%	-447%
Ionising radiation (kBq U-235 eq/FU)	-1.82E+01	-105%	+10%	-3%
Photochemical ozone formation (kg NMVOC eq/FU)	1.33E-01	-831%	-19%	-52%
Particulate matter (disease inc./FU)	-3.63E-06	-806%	+4%	-19%
Human toxicity, non-cancer (CTUh/FU)	3.72E-06	-231%	+18%	-31%
Human toxicity, cancer (CTUh/FU)	7.16E-07	-99%	-190%	-2215%
Acidification (mol H^+ eq/FU)	-6.78E-01	-313%	+5%	-16%
Eutrophication, freshwater (kg P eq/FU)	5.17E-02	-202%	-1%	-60%
Eutrophication, marine (kg N eq/FU)	8.93E-03	-3802%	-4%	-34%
Eutrophication, terrestrial (mol N eq/FU)	4.72E-01	-792%	-4%	-37%
Ecotoxicity, freshwater (CTUe/FU)	-5.53E+02	-1382%	+14%	-11%
Land use (Pt/FU)	7.81E+01	-2649%	-6%	-36%
Water use (m^3 depriv./FU)	1.56E+01	+12%	-419%	-463%
Resource use, fossils (MJ/FU)	4.03E+02	-1324%	-17%	-42%
Resource use, minerals and metals (kg Sb eq/FU)	-3.70E-04	-287%	+217%	+177%

Conclusions

According to the outcomes of the study, the automatic waste sorting performed directly inside the bin has a potential in reducing both environmental impacts and costs of the management of waste generated in public places, provided that it reaches a high level of sorting accuracy. The positive effects of such a system could be applied to other public areas such as shopping centres and train stations, making this waste stream more and more circular.

References

[1] World Bank, “Air transport. passengers carried”, (2020). https://data.worldbank.org/indicator/IS.AIR.PSGR?locations=1W
[2] Tjahjono M., Ünal E., Tran T.H., “The Circular Economy Transformation of Airports: An Alternative Model for Retail Waste Management”, Sustainability, 15, 3860, (2023). https://doi.org/10.3390/su15043860
[3] WiSort, “Smart Waste Management”, 2023. https://wisort.eu/
[4] CONAI, “Accordo quadro ANCI CONAI (Anci-Conai framework agreement” of the Italian national consortium of packaging materials)”, 2023. https://www.conai.org/regioni-ed-enti-locali/accordo-quadro-anci-conai/
[5] Bin-e, “Revolutionizing the waste management system”, 2023. https://www.bine.world/#home
[6] Cleanrobotics, “Smart bins for smarter recycling”, 2023. https://cleanrobotics.com/trashbot/
[7] Fazio S., Castellani V., Sala S., Schau EM., Secchi M., Zampori L., Diaconu E., “Supporting information to the characterisation factors of recommended EF Life Cycle Impact Assessment method. New models and differences with ILCD.”, JRC Technical Reports, 2018. https://publications.jrc.ec.europa.eu/repository/handle/JRC114822
[8] Finnveden G., Hauschild MZ., Ekvall T., Guinée J., Heijungs, R., Hellweg, S., Koehler, A., Pennington, D., Suh, S., “Recent developments in life cycle assessment”, Journal of Environvental Management, 91 (1), 1-21, 2009. https://doi.org/10.1016/j.jenvman.2009.06.018
[9] Ecoinvent centre, “Ecoinvent version 3.8 database”, 2021. http://www.ecoinvent.org/

Title: PERSPECTIVES OF RESIDUAL MUNICIPAL SOLID WASTE MANAGEMENT FROM AN ITALIAN CASE STUDY

Author(s): Marco Ragazzi*[1], Marco Tubino[2], Luca Adami[3], Marco Schiavon[4]

[1] *Department of Civil Environmental and Mechanical Engineering, University of Trento, Trento, Italy, Email address: marco.ragazzi@unitn.it*
[2] *Department of Civil Environmental and Mechanical Engineering, University of Trento, Trento, Italy, Email address: marco.tubino@unitn.it*
[3] *Department of Civil Environmental and Mechanical Engineering, University of Trento, Trento, Italy, Email address: luca.adami@unitn.it*
[4] *Department of Agronomy, Food, Natural Resources, Animals and Environment, University of Padova, Legnaro, Italy, Email address: marco.schiavon.2@unipd.it*

Keyword(s): management, municipal, residual, solid, waste

Abstract

In recent years [1], the Province of Trento, Italy, has addressed the issue of planning the management of residual urban waste in a scenario of particularly efficient selective collection: currently around 80% of residual municipal solid waste (MSW) is sent to the various recycling circuits. Of course, these streams generate residues that need to be considered for a correct analysis of the sector, depending on users' behaviour and technical aspects of the treatments.
The starting point of recent investigations in this area was the establishment of a research team from the University of Trento and the Bruno Kessler Foundation, on the initiative of the Environmental Protection Agency of Trento, which made available qualitative and quantitative data relating to the MSW sector.
The preliminary assessment also considered the special-waste sector. However, following the indications of the Province of Trento, the in-depth analysis only focused on the MSW sector, leaving to political or administrative decision-makers the opportunity to integrate the assessment with the inclusion of special waste.
The MSW sector has been strongly affected by the pandemic period. Therefore, to provide an initial overview at the end of 2021, it was deemed appropriate to refer to the 2019 data, with the recommendation to update the situation once the context had returned to normality; this is also because updated information allows a better calibration of the sizing of any treatment option that may be chosen in the selected scenarios. Furthermore, in the preliminary phase of the analysis it emerged, from the information made available by the Province, that in recent years, in contrast to the target of reducing the production of urban waste by 5%, an increase of approximately 1% per year had instead been noted. It was therefore agreed that a possible long-term objective could be to maintain the 2019 quantity.
The scenarios covered by the research were characterized by a contrast between pre-treated waste landfill and energy recovery. An indication from the European Union is included in this dichotomy which sets the objective of sending no more than 10% of urban waste produced to landfill by 2035 [2]. Whatever option is chosen, an economic indication always comes from the European Union: the recovery of material is a priority, but it must take into account the economic sustainability of the choices to be compared.

With reference to the Trentino context, the information produced by the Province in the pre-COVID period (2019 and early 2020) about the composition of residual MSW in Trentino was particularly useful. From these data it was possible to obtain the percentage of recyclable materials that are still present in unsorted municipal waste. In practice, these data highlight that with a further increase in the efficiency of separate-waste collection, also by reviewing the flows of materials of interest, it is possible to get significantly closer to the 10% limit mentioned above.
At the decision-making level, two macro-scenarios were envisaged:
a) close the cycle with a landfill (thus increasing the available volumes over time) accepting the possibility of not respecting the 10% objective of the European Union;
b) close the cycle with an energy recovery option.
In the in-depth analyses requested upon indication of the Province, only the second macro-scenario was considered. In this regard it should be noted that, if this were the political-administrative decision:

- the scale of the plant would be reduced, with a consequent technological orientation that could include systems other than direct combustion in a dedicated plant (which is more affected by a scale effect);
- the possibility of managing part of the flow of residual MSW at a regional level (as permitted by law) should however be verified, given the presence of the Bolzano incinerator within a useful distance.

Furthermore, if the solution of a dedicated plant located in Trentino is chosen:

- the energy content of the waste expected to enter the plant should be characterized in adequate detail, in order to optimize the sizing; as a first approximation, a calorific value of input waste was considered equal to 13 MJ/kg, but recent investigations have highlighted the possibility that residual MSW is settling towards a LHV of 17 MJ/kg; this aspect is relevant in terms of technological choice since the most widespread solution is generally adopted for lower values of LHV;
- the possibility of aiming for a solution that closes the treatment with on-site energy recovery or with the generation of products (e.g. methanol, dimethyl ether, etc.) to be used off-site should be examined, because the sector is evolving, but experiences on residual MSW are lacking;
- a suitable site for the location of the plant should be identified (through a comparative study), taking care that the available local meteorological data are adequate to have a reliable input for modelling the dispersion and deposition of the pollutants emitted into the atmosphere (in this case the plant would not have zero emissions into the atmosphere).

The work carried out during the above-mentioned collaboration also contains specific indications for integrating the existing legislation regarding environmental impact, in order to take into account the latest research findings in this sector. In particular, the present work underlines two aspects emerged from the analyses before and after the conclusion of the collaboration:

- the need for a complete health risk characterization that properly considers the potential problem of air pollutants (with specific attention to heavy metals) released by waste combustion technologies [3];
- the need for detailed environmental monitoring plans (EMPs) and monitoring and control plans (MCPs) [4].

Regarding the first aspect, the problem is partly related to the atmospheric dispersion of air pollutants released by thermal waste-to-energy plants, which, in mountainous regions like Trentino, is limited by the complex terrain morphology. The latter amplifies the probability of contact between pollutants and resident population, potentially determining exposure levels that are higher than in other geographical contexts (e.g., coastal areas or flat areas with greater air exchange). This problem has been dealt with in a series of publications since 2005 on topics related to the health risk from waste management and other activities characterized by similar types of emissions (e.g., steel-making plants).

The following main considerations can be drawn from the analysis of these publications.
First, based on the results of a work on the residual MSW incinerator of Bolzano [5], the combination of environmental monitoring campaigns and numerical simulations of atmospheric dispersion of the emitted air pollutants turns out to be crucial to completely characterize the situation around a waste combustion plant before and after its construction. Specifically, this combination of tools allows distinguishing between the expected impact of the plant alone and the other potential sources already existing in the surroundings of the plant. Well-planned soil, ambient air and deposition monitoring approaches [6,7] are also the key to characterize the baseline before the construction of an important emitter like a MSW incinerator.
Second, the continuous improvements in the environmental technologies used in the thermal waste-to-energy sector have considerably reduced the emissions of persistent organic pollutants (POPs). This has made other pollutants prevail in terms of potential health risk, like heavy metals. A weak legislation framework that sets a single concentration limit value at the emission level for a large group of heavy metals with different toxicity levels further complicates the matters. In fact, this group not only includes both non-carcinogenic and carcinogenic metals, but also does not distinguish the hexavalent chromium (Cr VI), which is carcinogenic, within the total chromium (Cr) (this one may include the non-carcinogenic Cr III). Thus, considering regulatory limit values may lead to underestimate the potential health risks associated with exposure to heavy metals, and this aspect should be considered when carrying out a health risk assessment.
Regarding the second aspect, EMPs are documents that are part of the environmental impact assessment procedure. The proponents of new or substantially upgraded activities must prepare them to present the environmental monitoring strategy before, during and after the construction of the new activities. Chemicals like POPs, polycyclic aromatic hydrocarbons and arsenic may require specific attention in an EMP in terms of both ambient air and deposition/soil sampling, if their role in the determination of the overall cancer risk is verified by a health risk assessment. Such substances are carcinogenic and affect the human body particularly through ingestion of contaminated food and accidental soil ingestion. Conventional monitoring approaches could be integrated with unconventional monitoring techniques, like the characterization of pond sediments, sewage sludge of local municipal wastewater treatment plants or conifer needles as natural markers.
Conversely, heavy metals like cadmium and chromium VI (Cr VI) are carcinogenic mainly by inhalation of contaminated air. Thus, for these compounds, an EMP should rather focus on ambient air monitoring. Cr VI, in particular, exceeds cadmium in terms of cancer potency by almost two orders of magnitude. Unfortunately, the detection limit of Cr VI in air samples was found to be relatively high by Huang et al. [8], specifically 0.33 ng/m^3. According to its toxicological profile [9], the long-term exposure by inhalation to Cr VI would result in an acceptable cancer risk when its maximum air concentration does not exceed 1/10 of its detection limit. Thus, it would be impossible to verify the compliance with the acceptable cancer risk by on-field measurement. To solve this issue, Cr VI concentration should be monitored at the stack (where the concentration is higher) and the compliance with the acceptable cancer risk level should be verified by estimating Cr VI ambient air concentration at ground level through atmospheric dispersion modeling. In 2021, a methodology was proposed with the objective of defining an emission limit value for Cr VI monitored at the stack of a waste combustion plant [10]. This may give an additional tool to MCPs to check the environmental performance of a plant during its operation, which is the main purpose of the document that the environmental authority in charge issues to the plant's owners. Monitoring Cr VI requires Cr speciation, which is a difficult task, even though different methodologies for Cr speciation have been developed in the last 30 years [11–14]. However, if the input waste is almost constant in terms of composition, there will be no need for frequent Cr speciation and the final check could be made on total Cr, which is regularly monitored at the stack of waste-to-energy plants.

References

[1] Agenzia Provinciale per la protezione dell'ambiente di Trento, 2023. 5° aggiornamento del Piano provinciale di gestione dei rifiuti, rifiuti urbani. Available at: https://www.appa.provincia.tn.it/Documenti-e-dati/Documenti-tecnici-di-supporto/5-aggiornamento-del-Piano-provinciale-di-gestione-dei-rifiuti-rifiuti-urbani
[2] EU, 2018, Directive (EU) 2018/850 of the European Parliament and of the Council of 30 May 2018 amending Directive 1999/31/EC on the landfill of waste, OJ L 150, 14.6.2018, p. 100-108., 32018L0850
[3] Tubino, M., Ragazzi, M., Adami, L., & Schiavon, M. (2023). Criteria for the Assessment of Health Risk from a Waste Gasification Plant. Environmental and Climate Technologies, 27(1), 654-665.
[4] Adami, L., Ragazzi, M., Tubino, M., & Schiavon, M. (2023). Criteria for Enhanced Monitoring and Control Plans for a Waste Gasification Plant. Environmental and Climate Technologies, 27(1), 570-580
[5] Ragazzi M., Tirler W., Angelucci G., Zardi D., Rada E. C., "Management of atmospheric pollutants from waste incineration processes: The case of Bozen", Waste Management and Research, 31, 235–240, 2013.
[6] Rada E. C., Ragazzi M., Tubino M., Gambaro A., Turetta C., Argiriadis E., Vecchiato M., Rossi B., Tava M., "Characterization of metals in air and soil near a steel making plant in the North part of Italy", Management of Environmental Quality: An International Journal, 27, 441–451, 2016.
[7] Rada E. C., Ragazzi M., Schiavon M., "Assessment of the local role of a steel making plant by POPs deposition measurements", Chemosphere, 110, 53–61, 2014.
[8] Huang L., Yu C. H., Hopke P. K., Lioy P. J., Buckley B. T., Shin J. Y., Fan Z., "Measurement of Soluble and Total Hexavalent Chromium in the Ambient Airborne Particles in New Jersey", Aerosol & Air Quality Research, 14, 1939–1949, 2014.
[9] United States Environmental Protection Agency. Chromium(VI). Available at: https://iris.epa.gov/ChemicalLanding/&substance_nmbr=144
[10] Rada E. C., Schiavon M., Torretta V., "A regulatory strategy for the emission control of hexavalent chromium from waste-to-energy plants", Journal of Cleaner Production, 278, 123415, 2021.
[11] Nusko R., Heumann K. G., "Cr(III)/Cr(VI) speciation in aerosol particles by extractive separation and thermal ionization isotope dilution mass spectrometry", Fresenius' Journal of Analytical Chemistry, 357, 1050–1055, 1997.
[12] Li Y., Pradhan N. K., Foley R., Low G. K. C., "Selective determination of airborne hexavalent chromium using inductively coupled plasma mass spectrometry", Talanta, 57, 1143–1153, 2002.
[13] Shah P., Strezov V., Nelson P. F., "Speciation of chromium in Australian coals and combustion products", Fuel 102, 1–8, 2012.
[14] Miyake Y., Tokumura M., Iwazaki Y., Wang Q., Amagai T., Horii Y., Otsuka H., Tanikawa N., Kobayashi T., Oguchi M., "Determination of hexavalent chromium concentration in industrial waste incinerator stack gas by using a modified ion chromatography with post-column derivatization method", Journal of Chromatography A, 1502, 24–29, 2017.

Title: Risk assessment applied to a quarry backfilling: comparison between the use of different filling materials

Author(s): Flavio Cioli[1], Sabrina Sorlini[1], Mentore Vaccari[1]

[1] *Department of Civil, Environmental, Architectural Engineering and Mathematics, University of Brescia, Brescia, Lombardy, Italy*

Keyword(s): Construction and Demolition Waste, Industrial Waste, Recycled Aggregate, Risk assessment, Leaching properties

Abstract
This study simulates the modelling of leaching pollutants present in a quarry backfilling consisting of Electric Arc Furnace Slag (EAFS), Waste Foundry Sand (WFS) or Recycled Aggregates (RA) from Construction and Demolition Waste (CDW), and, based on its geometry and the characteristics of the surrounding environment, estimates the expected concentrations in the groundwater beneath. For the study, concentrations in the leachate were evaluated using data from leaching tests conducted on materials using UNI-EN 12457-2 standard [2]. To evaluate the attenuation suffered by the concentration of contaminant due to transport from the backfilling to the aquifer, due to the infiltration of water into the unsaturated layer of soil and subsequent dilution in the surface aquifer, the leaching factor (LF) foreseen as part of the risk analysis for contaminated sites was considered. The potential impact on the groundwater resulting from waste leaching was assessed considering the Groundwater contamination threshold concentrations defined by Legislative Decree 152/06 [3] as reference limits.

Introduction
Nowadays, 165 Mtons of special waste are produced in Italy [4]; of these 47% is represented by CDW (chapter 17 of EWC), and 7% by waste from thermic processes (chapter 10). To limit the consumption of raw materials and the disposal in landfills, it is appropriate to encourage the recovery of material from waste, always considering the consequences that their reuse has on the environment and human health. Mostly of these wastes is recovered after treatment as road sub-base, for backfilling and for embankments replacing natural materials; these unencapsulated uses present the highest potential for release of a material and its constituents because the material is not chemically or physically bound. On the other hand, encapsulated reuses (e.g. in concrete, ceramics, glass etc.) prevents water from percolating through the wastes and minimizes the potential for leaching and the impact on environment. As of today in Italy, environmental assessment related to waste recovery is exclusively based on the use of the leaching test (D.M. 186/2006 [1]), and there is no existing methodology for risk assessment related to the recovery of these materials through Risk Analysis that takes into account the usage scenario and site-specific conditions. A risk-based approach should be pursued when reusing waste in scenarios that can impact the environment and human health. The risk assessment procedure is widely applied to landfills and contaminated sites. In recent years, the risk assessment methodology has also been applied to waste reuse in unbound applications. To make an effective risk assessment, the following are important: (i) identification of hazardous substances associated with the material; (ii) definition and quantification of reuse scenarios; and (iii) conceptual models of sources, pathway and receptors [5].
The objective of this work is to estimate the impact on the groundwater caused by the release of pollutants due to the filling of an exhausted quarry with three different materials: recycled aggregate from construction and demolition waste, electric arc furnace slag, and waste foundry sands.

Materials and methods

The study was conducted following the approach outlined by the Italian Environmental Agency for health and environmental risk assessment of contaminated sites [6]. The attenuation of contaminant concentration due to transport from the backfill to the groundwater is determined by the leaching factor (LF), a parameter that accounts for water infiltration into the unsaturated soil layer (SAM), that considers the path the pollutant takes to reach the water table, and dilution in the aquifer (LDF), that takes into account the dilution that the contaminant undergoes once it reaches the aquifer, during the transition from unsaturated soil to saturated soil.

Figure 1 represents the schematization of the transport mechanism in the case study. To assess the impact on the groundwater due to leaching, the threshold contamination concentrations for groundwater (CSC_{GW}) defined by Legislative Decree 152/2006 Part IV, Title V, Annex 5, Table 2 [3], and for parameters for which there was no predefined value, were considered other reference limits; in particular for Nitrates, Chlorides and Vanadium the Legislative Decree 30/2009 [7], while for Barium the ISTISAN Report 14|21 [8]. The risk was calculated for each considered pollutant as the ratio between the expected concentration in the groundwater and the CSC_{GW}. The risk is considered acceptable when the observed value is less than 1.

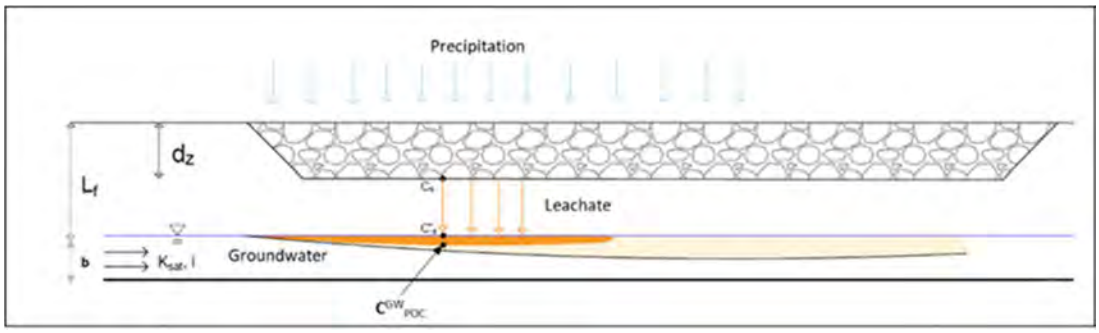

Figure 1. Schematization of the transport mechanism

For the application of the model, the geometric characteristics of the intervention (backfill thickness: d_z=17.75m; backfill extension in the direction of the aquifer flow: W=159m) and site-specific characteristics (aquifer depth from top of the source: L_f= 25.5m; hydraulic gradient: i=0.0009; hydraulic conductivity: k=8.25E-05 m/s; aquifer thickness: b=10m; annual cumulative precipitation: P=997mm/y) were collected from documentation and online database. The release of contaminants from the steel slag was evaluated according to the batch leaching test (UNI EN 12457-2) [2]. The eluate obtained was chemically characterized, detecting the parameters required by the Ministerial Decree 186/2006 (M.D. 186/2006) [1] for the recovery and reuse of special waste. Three different materials were considered as filling materials and eluates characteristics has been evaluated:

- RA: produced through the recovery of construction and demolition materials (183 samples);
- EAFS: slag is a by-product of steelmaking industry (69 samples);
- WFS: a discarded material coming from ferrous and non-ferrous metal casting industry (25 samples).

Results

The 80th percentile and Upper Confidential Limit 95% (UCL 95%) concentrations were calculated; the concentrations calculated at the 80th percentile is higher, hence providing a higher safety margin, and was therefore considered and shown in Table 1. The concentration of Fluoride and Copper in WFS are higher than the threshold defined by [1].

Table 1. Leachate concentrations from RAs (183 samples), EAFS (69 samples) and WFS (25 samples) tested according to the EN 12457-2. (80th percentile concentration is reported)

Parameter	U.o.M.	Limit value [1]	RA	EAFS	WFS
NO_3^-	mg/l	50	18.16	0.5	3
F^-	mg/l	1.5	0.51	0.2	**5**
Cl^-	mg/l	100	10.00	2.04	13.36
SO_4^{2-}	mg/l	250	80.56	1.6	101.60
CN^-	µg/l	50	10.00	10	20
Ba	mg/l	1	0.10	0.4	0.11
Cu	mg/l	0.05	0.04	0.005	**0.05**
Zn	mg/l	3	0.10	0.005	0.27
Be	µg/l	10	1.00	5	1.80
Co	µg/l	250	5.00	10	40.20
Ni	µg/l	10	5.70	5	9.08
V	µg/l	250	31.90	136.4	25.00
As	µg/l	50	7.20	10	7.42
Cd	µg/l	5	0.50	3	1
Cr	µg/l	50	43.76	5	13.60
Pb	µg/l	50	5.90	5	10
Se	µg/l	10	5.32	5	5
Hg	µg/l	1	0.50	0.1	0.6

With data used SAM results 0,696, LDF results 1,857 and LF 0,37. The risk related to the evaluation of the environmental risk assessment for groundwater obtained with the study are reported in Table 2.

Table 2. Risk calculated

Parameter	U.o.M.	CSC_{GW}	RA		EAFS		WFS	
			C'_s	Risk R_{GW}	C'_s	Risk R_{GW}	C'_s	Risk R_{GW}
NO_3^-	mg/l	50	6.81	0.14	0.19	0.00	1.11	0.02
F^-	mg/l	1.5	0.19	0.13	0.07	0.05	1.85	**1.23**
Cl^-	mg/l	250	3.75	0.02	0.75	0.00	4.94	0.02
SO_4^{2-}	mg/l	250	30.20	0.12	0.59	0.00	37.59	0.15
CN^-	µg/l	50	3.75	0.08	3.70	0.07	7.40	0.15
Ba	mg/l	0.7	0.04	0.38	0.15	0.21	0.04	0.06
Cu	mg/l	1	0.01	0.01	0.00	0.00	0.02	0.02
Zn	mg/l	3	0.04	0.01	0.00	0.00	0.10	0.03
Be	µg/l	4	0.37	0.09	1.85	0.46	0.67	0.17
Co	µg/l	50	1.87	0.04	3.70	0.07	14.87	0.30
Ni	µg/l	20	2.14	0.11	1.85	0.09	3.36	0.17
V	µg/l	50	11.96	0.24	50.47	**1.01**	9.25	0.19
As	µg/l	10	2.70	0.27	3.70	0.37	2.75	0.27
Cd	µg/l	5	0.19	0.04	1.11	0.22	0.37	0.07
Cr	µg/l	50	16.40	0.33	1.85	0.04	5.03	0.10
Pb	µg/l	10	2.21	0.22	1.85	0.19	3.70	0.37
Se	µg/l	10	1.99	0.2	1.85	0.19	1.85	0.19
Hg	µg/l	1	0.19	0.19	0.04	0.04	0.22	0.22

In the hypothesized site-specific scenario, results are different for each material tested:

- RA: the risk is acceptable for all considered parameters;
- EAFS: the risk results not acceptable for vanadium (value 1.01);
- WFS: the risk results not acceptable for fluorides (value 1.23).

Concluding Remarks

In the considered case study, was found to be acceptable (with R_{GW} < 1) using the eluate concentrations at the 80th percentile with two exceptions: for vanadium considering EAFS as filling materials and for fluoride when WFS are used.

However, it should be noted that input data in favour of safety were used to develop the model. It should also be taken into consideration that concentrations data are obtained from leaching tests with a liquid-to-solid ratio (L/S) of 10 l/kg, a ratio that is not representative in the context of waste recovery and is more characteristic for assessing leaching process in landfills; furthermore, leaching test used considers material with particle size lower than 4 mm, which rarely corresponds to the physical characteristics of the material used for recovery operations. In this specific case, the recovered material indeed has a particle size ranging from 0 to 90 mm. To overcome these limitations, different leaching tests could be used that employ a different liquid-to-solid ratio (e.g., EN 12457-1: L/S = 2 l/kg [9]), column percolation tests or other type of leaching tests in situ that better simulate the real conditions.

However, to conduct an accurate risk analysis, it is necessary to look for additional parameters in addition to those required by the recovery standard. Greater focus should be directed towards monitoring organic compound presence in eluates, regardless of whether national legislation sets specific limits. Additionally, even if concentrations of individual pollutants fall below anticipated thresholds, their collective impact could still pose environmental challenges.

References

[1] Ministero Dell'ambiente E Della Tutela Del Territorio. Decreto Ministeriale n. 186/2006. Regolamento Recante Modifiche Al Decreto Ministeriale 5 Febbraio 1998. Gazzetta ufficiale 2006, n.115.
[2] EN 12457 - Characterization Of Waste - Leaching - Compliance test for leaching of granular waste materials and sludges - Part 2: One stage batch test at a liquid to solid ratio of 10 l/kg for materials with particle size below 4 mm (without or with size reduction).
[3] DECRETO LEGISLATIVO 3 aprile 2006, n. 152. Norme in materia ambientale. Gazzetta ufficiale 2006, n.88.
[4] ISPRA. Rapporto rifiuti speciali – Edizione 2023
[5] Cioli, F., Abbà, A., Alias, C., & Sorlini, S. (2022). Reuse or Disposal of Waste Foundry Sand: An Insight into Environmental Aspects. Applied Sciences, 12(13), 6420.
[6] APAT (2008). Criteri metodologici per l'applicazione dell'analisi assoluta di rischio ai siti contaminati, Rev.2.
[7] DECRETO LEGISLATIVO 16 marzo 2009, n. 30 Attuazione della direttiva 2006/118/CE, relativa alla protezione delle acque sotterranee dall'inquinamento e dal deterioramento.
[8] Rapporti ISTISAN 14|21. Linee guida per la valutazione e gestione del rischio nella filiera delle acque destinate al consumo umano secondo il modello dei Water Safety Plan
[9] EN 12457 - Characterization Of Waste - Leaching - Compliance test for leaching of granular waste materials and sludges - Part 1: One stage batch test at a liquid to solid ratio of 2 l/kg for materials with particle size below 4 mm (without or with size reduction)

Title: Assessing Uncertainty in Waste Characterization: Experimental Analysis of Variability in Plastic Waste Sampling and Analysis

Author(s): Giovanni Beggio*[1], Maria Cristina Lavagnolo[2]

[1] Department of Civil, Environmental and Architectural Engineering, University of Padova, Via Marzolo 9, 35131, Padova, Italy (giovanni.beggio@unipd.it)

Keyword(s): Waste characterization, Sampling

Abstract

In the field of waste management and recycling, decisions made upon uncertain characterization data could force waste managers to adopt overprecautionary measures influencing significantly the economic sustainability of treatment plants and in general, of the circular economy. To address this trend, in determining whether regulatory limits are respected, the data uncertainty upon which decisions are made shall be properly considered. Uncertainty can be quantified by the variability (i.e., variance) of data generated by the materials characterization process. It is now recognized that this variability is mainly determined by the performed sampling procedures, while a minor role is played by the consolidated analytical techniques. A powerful tool to assess the total variability is represented by the so-called Replication Experiments (RE) [1]. By replicating the sampling performance in “fully nested experiments”, RE allow to calculate the value of the generated total variance together with its components (i.e., sampling and analysis), through nested ANOVA. Whether these experiments are often included in QA/QC procedures for goods production (e.g., food production, pharma, etc.), no examples can be found in the scientific literature about the application of RE on waste characterization, likely due to the logistic complexity of the experimental activities. Only “simplified” design were applied so far [2].
As first of his genre, this work shows and discusses the results of a RE applied to evaluate the efficiency of the sampling phase defined within a characterization plan aimed at classification of plastic waste derived from waste plastic selection plant.
The experimental activity was carried out at a plastic selection and recovery plant owned by multiutility company operating in Northern Italy. The material under investigation is commonly referred to as “fine PLASMIX” and consists solely of the <50mm undersieve generated from the screening of the plastic waste processed by the plant. Fine PLASMIX thus produced is usually classified under the code EWC 191212, and with this code, it is subsequently sent for further treatment at the adjacent solid recovered fuel (SRF) production facility.
The followed experimental design is shown in Figure 1. It was consistent with the so-called “Collaborative Trial in Sampling”, which involves the duplicate performance of a single sampling plan on a single sampling target, by 4 sampling teams, at 2 different times [1]. A batch representative of the daily production (approximately 20 tons and 140 m³ each) was chosen as the “sampling target”. This means that every laboratory sample collected was considered representative of the average composition of the reference batch.
The tested sampling plan was thoroughly optimized starting from the existing practical instructions given to the samplers while applying the requirements for probabilistic sampling given in the international

waste-sampling standards [3].

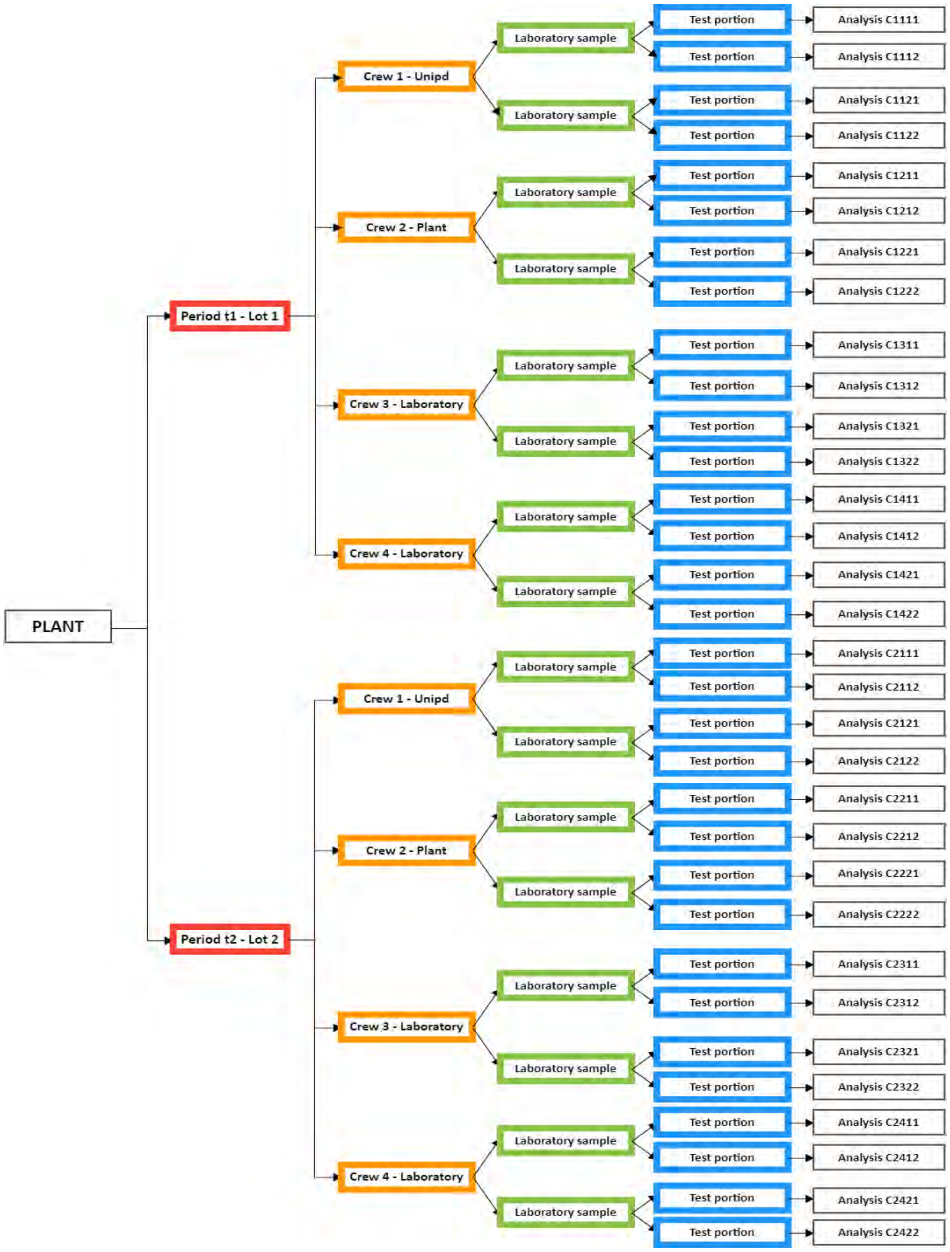

Figure 1. The design of the Replication Experiment

Duplicate analysis was performed on each so-collected laboratory sample. In total, 16 laboratory samples were collected, resulting in 32 analytical values for each investigated chemical-physical parameters (on solid samples: pH, TS, VS, LHV, TC, TOC, Cl, Ba, Mg, Ni, Pb, Cu, Sn, Hydrocarbons C10-C40). The experimental design allowed to calculate the total variance (for each set of 32 data) together with its components through a balanced fully nested ANOVA. In particular, the variance components quantified by the statistics were:

1. The variability generated by a possible seasonality of the physico-chemical characteristics of the waste (temporal variability);

2. The variability generated by the execution of the sampling action by different sampling teams (sampling reproducibility);
3. Variability generated by the execution of the sampling action by a single sampling team (i.e., sampling variability or sampling repeatability);
4. Variability generated by the analytical phases of test portion preparation and data quantification (i.e., analytical variability).

The results obtained by the fully nested ANOVA are shown in Figure 2. Results are expressed as the coefficient of variation to facilitate their interpretation.

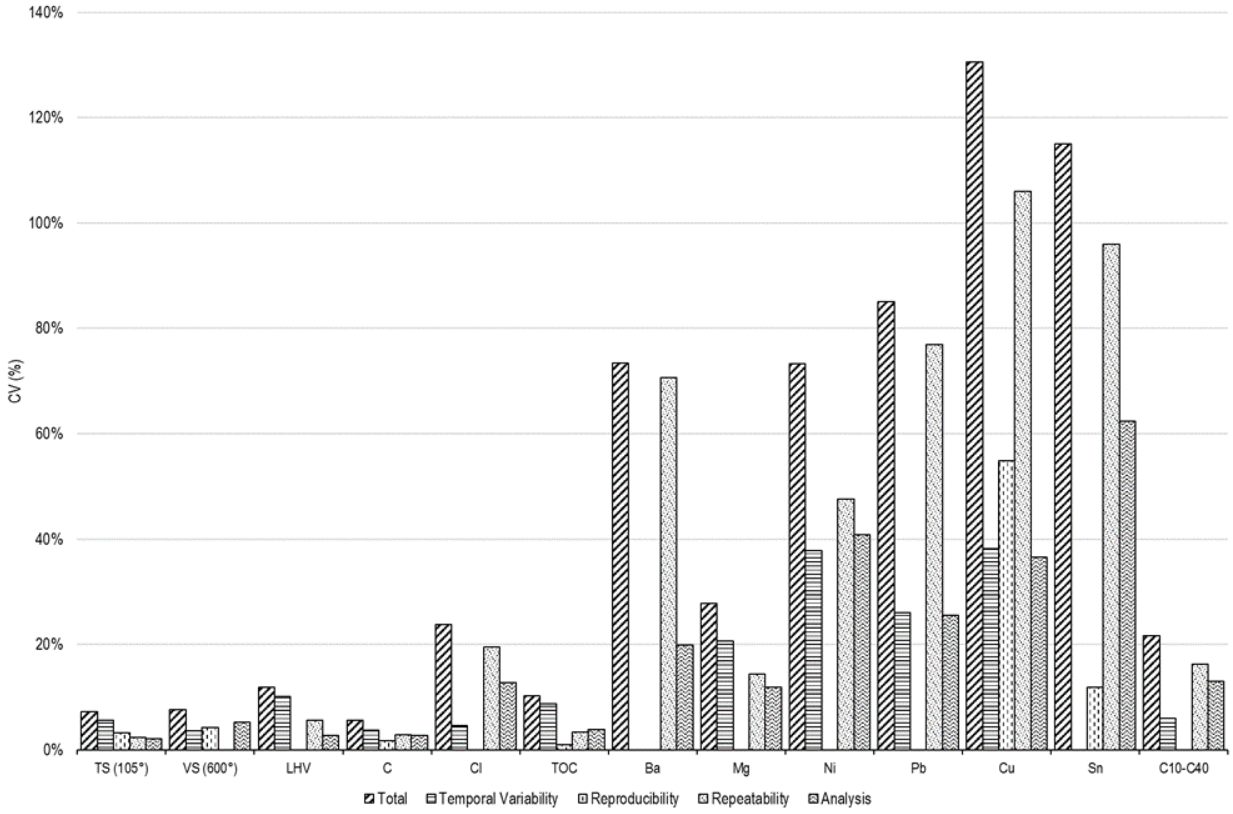

(a)

Figure 2. Components of the total variability (expressed in terms of coefficients of variation CV %) of the characterisation data for the parameters analysed on the solid sample.

Two classes of parameters can be identified based on the results obtained. The first class, which includes all analytes defined as macro-parameters (i.e., TS, VS, LHV, C, Cl, TOC, and C10-C40, along with Mg), is characterized by a total variability, expressed in terms of CV, of less than 30%. Therefore, further discussion for this set of parameters is of relative importance. The remaining parameters, represented by trace contaminants quantified in the samples (i.e., Ba, Ni, Pb, Cu, and Sn, for which the properties of interest are asymmetrically distributed in the population, with only some 'rare' particles showing the presence of the analyzed constituents), are characterized by significantly higher CV values, ranging from 73% (Ba and Ni) to 131% (Cu). That said, it is noted that for all analytes in this second group, the major contribution is determined by the repeatability of the sampling, with CV values ranging from 48% (Ni) to 106% (Cu), suggesting a general difficulty of the sampling plant in producing samples representative of the population to be characterized. It is recalled that the variability generated by the

repeatability of sampling is due to i) potential systematic errors deriving from the ambiguous application of the defined sampling instructions and ii) the high 'local' (i.e., spatial) heterogeneity of the parameter sought within the population to be characterized on the defined scale. In this context, the spatial variability of the analyzed components could have been too high to be effectively summarized in the produced samples. These results could indeed be due to the so-called 'nugget effect'.
Considering these results, it is necessary to emphasize that the degree of optimization characterizing the practical instructions followed by each sampling team (quantitative and qualitative, see Paragraph 2.3.2) is fully consistent with the requirements of probabilistic sampling as described in technical standards and therefore difficult to improve further (i.e., increasing the sample mass), without the obvious cost implications. In this context, this further optimization could be justified based on a cost-benefit analysis relative to the proximity of the absolute concentrations of these contaminants to the regulatory limits used for waste classification. In this context, it is important to remember that the sampling variability, can be reduced through appropriate optimizations of the sampling plan up to a minimum limit, which is constituted by the intrinsic variability of the material at the considered scale, also called “constitutional heterogeneity” [4,5].

Acknowledgements
This study was carried out within the MICS (Made in Italy – Circular and Sustainable) Extended Partnership and received funding from Next-GenerationEU (Italian PNRR – M4 C2, Invest 1.3 – D.D. 1551.11-10-2022, PE00000004).

References

[1] Eurachem, CITAC: Measurement uncertainty arising from sampling. 102 (2019)
[2] Khodier, K., Viczek, S.A., Curtis, A., Aldrian, A., O’Leary, P., Lehner, M., Sarc, R.: Sampling and analysis of coarsely shredded mixed commercial waste. Part I: procedure, particle size and sorting analysis. Int. J. Environ. Sci. Technol. 17, 959–972 (2020). https://doi.org/10.1007/s13762-019-02526-w
[3] CEN: CEN/TR 15310-1. Characterization of waste — Sampling of waste materials — Part 1: Guidance on selection and application of criteria for sampling under various conditions, (2006)
[4] Gy, P., 2004. Sampling of discrete materials - A new introduction to the theory of sampling: I. Qualitative approach. Chemom. Intell. Lab. Syst. 74, 7–24. https://doi.org/10.1016/j.chemolab.2004.05.012
[5] Hennebert, P., & Beggio, G. (2021). SAMPLING AND SUB-SAMPLING OF GRANULAR WASTE: SIZE OF A REPRESENTATIVE SAMPLE IN TERMS OF NUMBER OF PARTICLES. *Detritus*, *17*. doi: 10.31025/2611-4135/2021.15139

Title: A Combined Approach to Microalgae Cultivation: Efficiency and Carbon Capture in South Sardinia, a case study.

Author(s): Vincenzo A. Riggio[1*], Deborah Panepinto[1] and Mariachiara Zanetti[1]

[1] *DIATI - Dipartimento di Ingegneria dell'Ambiente, del Territorio e delle Infrastrutture, Politecnico di Torino, Italy*

Keyword(s): Microalgae cultivation, solar radiation, incinerator, CO2 bio fixation, bubble column.

Abstract

Microalgae demonstrate an impressive capacity to convert biologically sequestered CO2 into complex organic compounds with high efficiency. These compounds include a range of valuable biomolecules such as lipids, carbohydrates, pigments, and hydrocarbons. Consequently, microalgae biomass is a versatile resource with applications in various industries. Products derived from microalgae, including biopolymers, fertilizers, live feed, medicines, and food supplements, are economically valuable and have already established niche markets. However, despite the promising potential of microalgae cultivation, operational challenges prevent its widespread adoption. High production costs hinder the economic feasibility of microalgae cultivation, making it viable only for certain high-value products and in specific geographic regions. Furthermore, cultivating microalgae requires precise environmental control to ensure successful and economically viable production. The objective of this study is to address the challenges and opportunities in microalgae cultivation. Specifically, this research aims to develop a methodology for dimensioning outdoor, naturally illuminated microalgae cultivation plants and apply it in a real-case scenario, determining the plant's size based on the capacity of the selected commercially available centrifuge. The case study involves utilizing flue gases emitted from a waste incinerator plant in south Sardinia as a carbon source for cultivating *Chlorella sp.* This introduction sets the stage for a comprehensive investigation into the technical, economic, and environmental aspects of microalgae cultivation for carbon dioxide sequestration. By integrating scientific principles with real-world applications, this study seeks to advance our understanding of microalgae-based solutions to mitigate greenhouse gas emissions and foster sustainable resource utilization.

The methodology encompasses a multi-step approach, including literature review, solar radiation modelling, reactor design optimization, and nutrient analysis. Species selection based on CO2 tolerance and illumination strategies was followed by solar radiation modelling using PVGIS data. Reactor designs were optimized using the Lambert-Beer law to model irradiance diffusion within bubble column photobioreactors [1]. Biomass production estimation utilized the Molina growth model [2], considering continuous culture conditions and fixed centrifugation flow rates. Nutrient requirements were determined based on elemental composition, with considerations for waste stream utilization. Carbon dioxide capture and compression energy requirements were assessed to evaluate the energy balance of the integrated system. A literature review on lab and pilot scale experiment was done to select the most promising species according to their capability to withstand both high percentages of CO2 in the feed gas and low pH of the cultivation medium. The former condition was settled to promote the absorption of gaseous CO2 directly by the microalgae. *Anabaena sp*, *Euglena gracilis*, *Scenedesmus obliquus* and *Chlorella sp.* were selected as the most promising species. An ulterior selection on this experiment was done based on the illumination strategy. Only those experiments where illumination was natural or followed dark/light cycle which would resent natural illumination (12:12) were kept. After all these

selections, the only remaining species was *Chlorella sp*. Hourly solar radiation data for South Sardinia were acquired from PVGIS European Portal, a model to consider the adoption of automatic shading nets for irradiance control and irradiance diffusion was adopted. The irradiance was accordingly modified when it was above the saturation limit of *Chlorella*. The Lamber-Beer light dispersion law was then applied in order to model the hourly irradiation profile along numerous points inside a generalized cross section of a vertical, bubble column photobioreactor of 5 cm diameter and 2 meter height. For comparison, a second bubble column photobioreactor with an empty cylindrical volume inside was also considered. The dimension of this last one was 2 meter height, outer cylinder of 10 cm diameter an inner cylinder of 5 cm diameter. Reactor design optimization suggested that active shading systems significantly improve productivity as well as an optimal column design. This consideration is well visible in the following graph (Fig. 1 and 2).

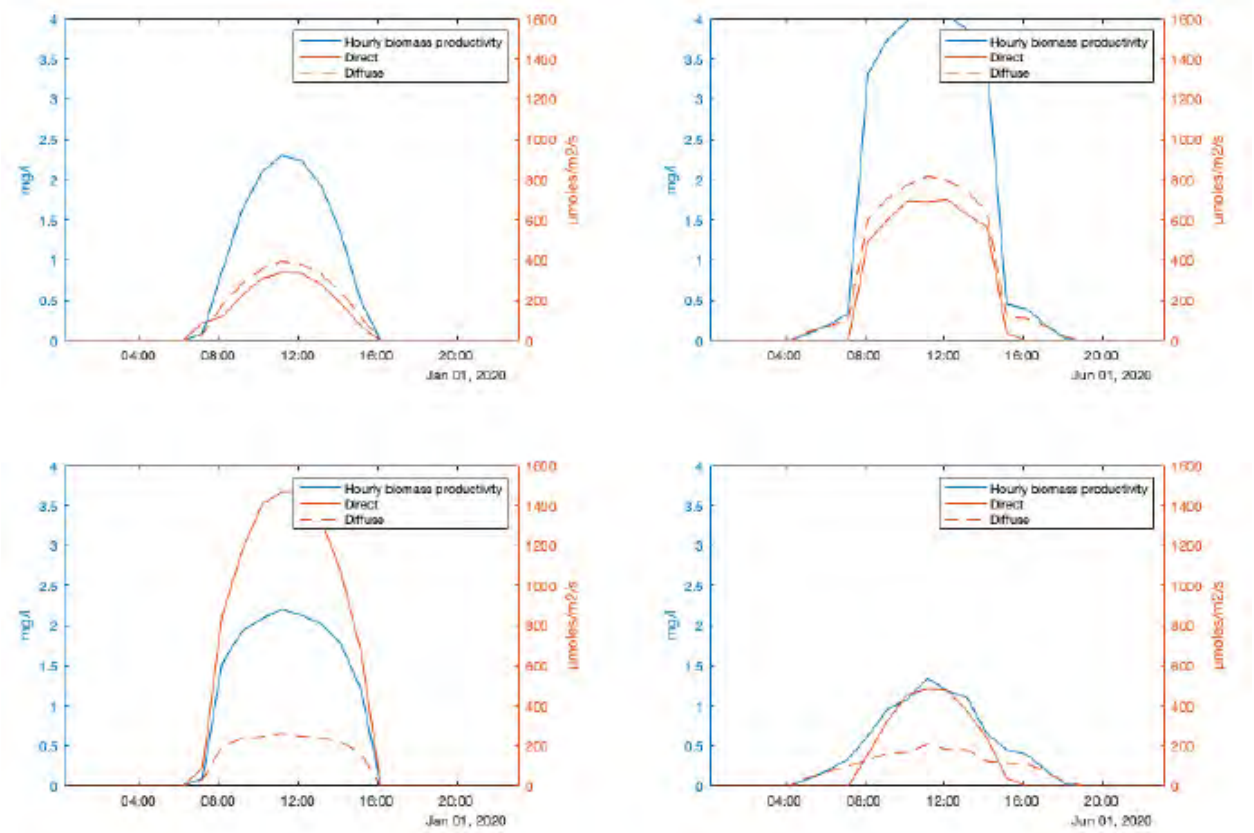

Figure 1: Hourly productivity and radiation components for a winter and summer day with (upper) and without (lower) active shading system. Standard bubble column

A static harvesting concentration of 0.8 g/l was settled as a conservative value for industrial harvesting and 500 l/h for 16 hours per day was adopted as harvesting flow rate. This is a real value as the sizing of the harvesting was performed based on the real specification of a commercial centrifuge (Alfa Laval Clara-20). Consequently, the irradiation profiles were incorporated into Molina growth model to have an estimation of the specific growing rate of the selected microalgae.

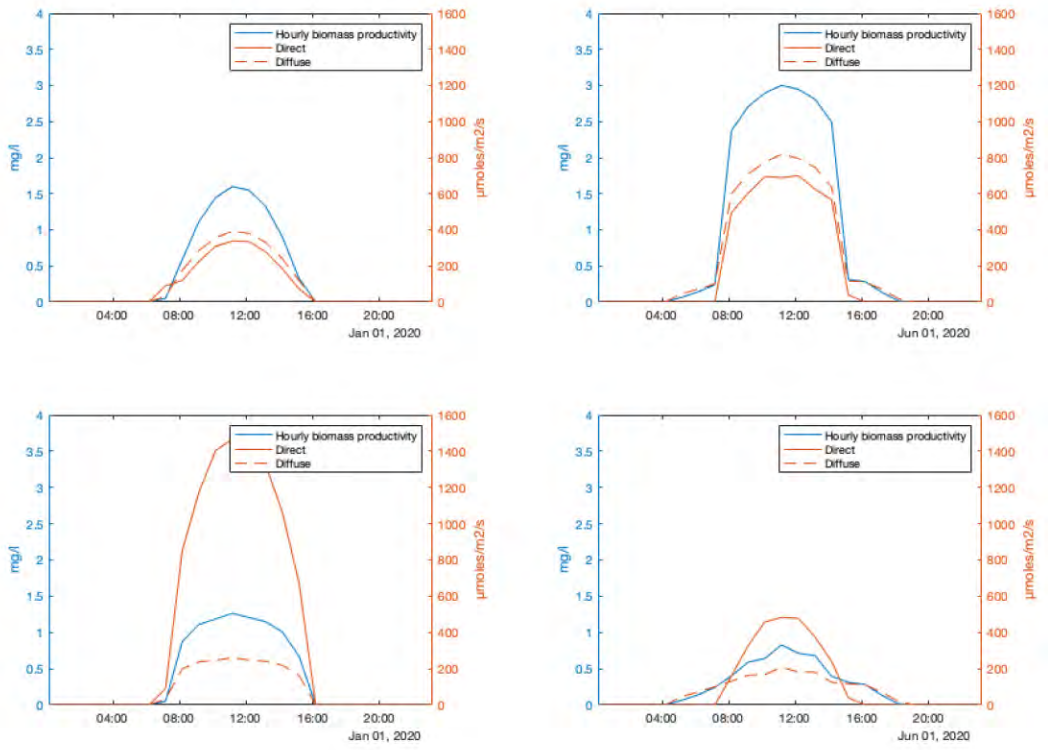

Figure 2: Hourly productivity and radiation components for a winter and summer day with (upper) and without (lower) active shading system. Bubble column with inner empty volume.

Overall, the system with active shading nets performed better. Among the two-reactor design, the one with 5 cm diameter without inner empty volume was found as the better one. The 5 cm diameter rector performed similarly to those found in literature. The hourly specific growing rate with and without the active shading system of this reactor were found respectively as $1.6x10^{-3}h^{-1}$ and $9.4x10^{-4}h^{-1}$. For what concerns the productivity, it was found as 0.0210 and 0.0127 g/l d for respectively the scenario with and without active shading system. The reactor with an empty cylindrical volume inside was less productive. The hourly specific growing rate with and without the active shading system of this last reactor design were found respectively as $1.1\ x10^{-4}h^{-1}$ and $6x10^{-4}h^{-1}$. For what concerns the productivity, it was found as 0.0151 and 0.0081 g/l d for respectively the scenario with and without active shading system. The results suggest that the adoption of a system to control irradiance would double the productivity and be beneficial for the cultivation. The specific growing rate and productivity values were lower than those found in literature for outdoor, naturally illuminated cultivation. This lower productivity could be linked to a higher harvesting concentration and a higher diameter assumed for the bubble column, both factors which influence light penetration across the cultivation medium and therefore have an effect on productivity.

Given this biomass production and by using the elemental composition of *Chlorella sp*, the carbon, nitrogen, phosphorus, and sulfur annual requirement were found. The cultivation medium was assumed as BG11, being this one already largely used for *Chlorella*. The results are summarized in Table 1.

Table 1: Annual biomass production and annual requirement of macronutrients.

Biomass	Annual production (tons) 40		
Element	**Macronutrient**	**Macronutrient requirement per year (tons)**	**Element requirement per year (tons)**
C	CO_2	77.12	21.05
N	$NaNO_3$	27.1	4.46
P	K_2HPO_4	4.48	0.86
S	$MgSO_4$	0.632	0.168

These requirements would represent a significant expense for the plant. One way to lower the mineral nutrient requirement could be the use of waste flows from various sources. Macchiareddu's industrial district accounts for several of those potential flows. Among the possible sources one is Ichnusa brewery, whose wastewater are remarkably rich in sugars and other compounds which can be used in microalgae production plant [3]. Another possible source of nutrient could be the nearby anaerobic digestor which is under refurbishment and expansion [4]. Finally, CACIP itself, the consortium which owns Tecnocasic waste incinerator plant, has a dedicated line for the treatment of industrial wastewater which is then sold for agriculture field irrigation thanks to its high content of nutrient. All these options could represent concrete alternatives for the nutrient supply of the cultivation. The carbon dioxide requirement of 77.12 tons was instead prospected to be entirely full filled by gaseous carbon dioxide. This amount was increased by a 10% to consider the loss of gaseous CO2 during the de-gasing of the photobioreactors. All this carbon was assumed to be provided by capturing the CO2 from the flue gases of Tecnocasic's municipal waste incineration plant whose CO2 concentration reaches a standard 10%. The annual requirement of carbon dioxide was found as the 0.11% of what is currently emitted by the incineration plant. Monoethanolamide capture system was assumed as the carbon dioxide capture method followed by a compression of the gas at 25 bar in order to have a temporary storage of CO2. An annual energy requirement of 67.8 MWh and 9.4 MWh were found for respectively the heat and electricity consumption of the capture and compression. Finally, using these annual cumulative energy consumption, specific energy requirement per tons of burned waste were found to assess the eventual downside of the carbon capture on the energy production of Tecnocasic's incineration plant. Results showed that capturing and compressing the required CO2 to 25 bar for storage purposes would have an almost negligible effect on the energy production of the waste incineration plant being the heat and electricity subtraction per ton of burned waste orders of magnitude lower than what is generated for the same unit weight of waste.

References

[1] Chini Zittelli, Graziella & Biondi, Natascia & Rodolfi, Liliana & Tredici, Mario, 2013. Photobioreactors forMass Production ofMicroalgae. 10.1002/9781118567166.ch13.
[2] E.Molina Grima, F.G. Acien Fernandez, F. Garcia Camacho, Yusuf Chisti, 1999. Photobioreactors: light regime, mass transfer, and scaleup, Editor(s): R. Osinga, J. Tramper, J.G. Burgess, R.H. Wijffels, Progress in Industrial Microbiology, Elsevier, Volume 35, Pages 231-247, ISSN 0079-6352, ISBN 9780444503879, https://doi.org/10.1016/S0079-6352(99)80118-0.
[3] Barbera, Alberto Bertucco, Sandeep Kumar, 2018. Nutrients recovery and recycling in algae processing for biofuels production, Renewable and Sustainable Energy Reviews, Volume 90, Pages 28-42, ISSN 1364-0321, https://doi.org/10.1016/j.rser.2018.03.004.
[4] V.A., "Efficiency and adaptation of the plant composting site at the Macchiareddu environmental platform" https://cacip.it/wp-content/uploads/Contenuti-per-sito-web-1.pdf

PARALLEL SESSION: S9

One health and environmental safety

Advanced monitoring and risk assessment

Title: Advanced Monitoring of Urban River: an integrated perspective

Author(s): Camilla Di Marcantonio*[1], Margherita Barchiesi[1], Francesca Mangiagli[1], Maria Rosaria Boni[1], Roberto Magini[1], Giuseppe Sappa[1], Paolo Viotti[1], Marco Seminara[2], Salvatore De Bonis[3], Eduardo Di Marcantonio[4], Massimo Marchiesi[4], Luigi Dallai[4], Agostina Chiavola[1]

[1] *Sapienza University of Rome, Department of Civil, Building and Environmental Engineering, Rome, Italy, camilla.dimarcantonio@uniroma1.it, margherita.barchiesi@uniroma1.it, Francesca.mangiagli@uniroma1.it, mariarosaria.boni@uniroma1.it, Roberto.magini@uniroma1.it, Giuseppe.sappa@uniroma1.it, paolo.viotti@uniroma1.it, agostina.chiavola@uniroma1.it*
[2] *Sapienza University of Rome, Department of Environmental biology, Rome, Italy*
[3] *ARPA Lazio, Sez. Prov.le di Roma Department of Environmental Status, Rome, Italy, salvatore.debonis@arpalazio.it*
[4] *Department of the Earth Sciences, Rome, Italy, Eduardo.dimarcantonio@uniroma1.it, Massimo.marchiesi@uniroma1.it, luigi.dallai@uniroma1.it*

Keyword(s): Contaminants of Emerging Concern, Monitoring, Urban River Ecosystem

Introduction

The quality of urban rivers is strictly connected with the quality of city's life. At both national and international level there is a lack of a comprehensive evaluation of the river water status in the urban district. This is mainly due to the parameters used for the definition of the status, which are unable to highlight the complexity of all the players engaged, as well as to a deficit in the monitoring objectives. Indeed, the environmental policy in force neglects the investigation of the causes of the water quality status, which is a compulsory element to design effective actions for restoration or protection of the urban river ecosystem.

The dynamic and complex state of rivers in urbanized areas, the often-limited self-purification capacity, as well as their dependence on external factors, such as land use and climatic factors, make difficult to identify the nature and location of all the sources of pollutants and their dispersion. All these factors impair the efforts spent in the proper management of urban rivers [1]. Understanding the relationships and connections among hydrological properties, storm water flow and characteristics of the different inflows to the river in urban areas is crucial for an effective and resilient river management. The main inflow of pollutants into urban aquatic environments are well known: wastewater treatment plants (WWTPs) effluents, storm-water runoff, combined sewer overflows (CSOs) [2]. Due to the effects of climate change which determine an increase in the intensity and frequency of rainy events and as a consequence of overflows, these factors are becoming increasingly important.
Degeneration of river ecosystems in urban areas was theorized by [3] who proposed the term "urban river (stream) syndrome". This "syndrome" concept can be used to describe newer or previously unknown types of river ecosystem degradation, due to additional pollutant sources such as plastics and contaminants of emerging concern (CECs). It has been demonstrated that CECs highly affect the ecosystems quality, causing, for example, the development of antibiotic-resistant strains and intersex in aquatic animals [4]. However, the characteristics of the urban river contaminants' inflows with respect to CECs and the interactions with the urban river water status are still to be elucidated [5,6]. Many CECs are excluded from the monitoring activities due to the lack of data/knowledge, instead of the evidence

of “no harm” [7]. It was underlined that one of the main reasons for not achieving the European Water Framework Directive goal of “good water status” is the insufficient monitoring to identify the causes of degradation [8].

The stable isotope analysis was recently proposed as an additional innovative tracking tool for the observation of the dynamics between urban river and its contaminant inflows [10]. Indeed, changes in stable isotope composition allows interpreting fundamental processes of interaction between the receiving environment and its inflows. Isotope tracking is usually applied to hydrogeological studies to trace the fate and behaviour in different matrices of organic and inorganic pollutants or to the observation of anthropogenic contaminants biomagnification into the food chain [11]. They have been successfully applied in monitoring groundwater contamination processes [12]. The multi-isotope approach, through the identification of Carbon, Nitrogen and Oxygen stable isotopes signature, as in rain waters as in groundwater, is an effective tool for contamination processes outcoming.

Considering this background, the present study aims to propose an integrated monitoring approach to characterise, quantify and describe the entire system made by the river and the surrounding interacting urban environment, with specific focus on sources and fate of traditional and emerging pollutants. The monitoring procedure will allow the identification of the causes of the water status taking advantage of an intersectoral approach and advanced tracking techniques (i.e. stable isotope signature). Indeed, the core of the evaluation will be the contaminants of emerging concern, including microplastics, with reference to their sources and background level.

Methodology

The case-study area is a stretch of the Tiber River in the northern part of Rome, being representative of the extreme complexity of these systems. Indeed, this area includes many of the possible contamination sources of an urban river (see Figure 1). Specifically, the investigated area extends approximatively from the Castel Giubileo dam to the bridge called “Ponte Tor di Quinto”. The monitoring activity on this stretch of Tiber river includes 6 sampling campaigns, starting from November 2023 and ending in October 2024. In each sampling campaign, grab samples are collected from 4 points with respect to the river stretch of interest: up-stream (Figure 2), down-stream to the effluent release from the WWTP, storm-water runoff spillway, down-stream. In the collected samples, the following classes of analytes are determined: CECs, traditional water quality parameters (including nutrients and metals), stable isotopes (δ13C) and microplastics.

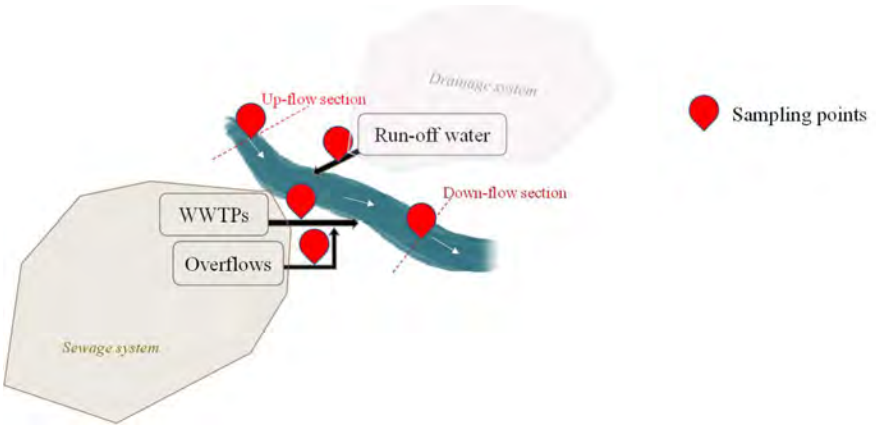

Figure 1 Schematic representation of the river stretch and type of sampling points.

Figure 2 Sampling location of the up-flow section.

Preliminary results and conclusions

The sampling campaign is on-going. Therefore, only preliminary and partial results are available at the moment. Figure 3 reports the occurrence of the target CECs measured in the first two days sampling. It can be highlighted the presence of the cocaine metabolite, caffeine and three pharmaceuticals.

More results will be presented at SIDISA 2024.

CEC	NOVEMBER 2023			FEBRUARY 2024		
	U	E	D	U	E	D
THC-COOH						
amphetamine						
benzoylecgonine						
cocaine						
methamphetamine						
caffeine						
carbamazepine						
ketoprofen						
lincomycin hydrochloride						
sulfadiazine						
sulfadimethoxine						
sulfamethoxazole						
trimethoprim						
warfarin						

Figure 3 Preliminary results about CECs occurrence in the main sampling points. Grey cells indicate concentrations below the Minimum Reporting Level (MRL equal to 0.05 µg/L for ketoprofen, 0.1 µg/L for THC-COOH, amphetamine, caffeine and 0.01 µg/L for the other contaminants) of the analytical method (UHPLC–MS/MS); orange cells indicate concentrations above the MRL. U=up-stream, E=down-stream to the effluent of the WWTP, D=down-stream.

Acknowledge

The study is funded by Sapienza University of Rome (Progetti Grandi di Ateneo 2022).

References

[1] M. Everard, H.L. Moggridge, Rediscovering the value of urban rivers, Urban Ecosyst. 15 (2012) 293–314. https://doi.org/10.1007/s11252-011-0174-7.

[2] A.M. Bisimwa, F.M. Amisi, C.M. Bamawa, B.B. Muhaya, A.B. Kankonda, Water quality assessment and pollution source analysis in Bukavu urban rivers of the Lake Kivu basin (Eastern Democratic Republic of Congo), Environ. Sustain. Indic. 14 (2022) 100183. https://doi.org/10.1016/j.indic.2022.100183.

[3] C.J. Walsh, A.H. Roy, J.W. Feminella, P.D. Cottingham, P.M. Groffman, R.P.M. Ii, R.A.P.M.O. Ii, The urban stream syndrome: current knowledge and the search for a cure Source : Journal of the North American Benthological Society , Vol . 24 , No . 3 (Sep ., 2005), Published by : The University of Chicago Press on behalf of the Society for Freshwater, 24 (2005) 706–723.

[4] M. Richardson, M. Soloviev, The urban river syndrome: Achieving sustainability against a backdrop of accelerating change, Int. J. Environ. Res. Public Health. 18 (2021). https://doi.org/10.3390/ijerph18126406.

[5] C. Di Marcantonio, A. Chiavola, V. Gioia, S. Leoni, G. Cecchini, A. Frugis, C. Ceci, M. Spizzirri, M.R. Boni, A step forward on site-specific environmental risk assessment and insight into the main influencing factors of CECs removal from wastewater, J. Environ. Manage. 325 (2023) 116541. https://doi.org/10.1016/j.jenvman.2022.116541.

[6] C. Di Marcantonio, A. Chiavola, D. Spagnoli, B. Meşe, F. Margarita, V. Gioia, A. Frugis, S. Leoni, G. Cecchini, M. Spizzirri, M.R. Boni, Linking conventional activated sludge treatment plant performances for micropollutants removal to environmental risk and SimpleTreat model assessment, Int. J. Environ. Sci. Technol. (2024). https://doi.org/10.1007/s13762-024-05476-0.

[7] W. Brack, V. Dulio, M. Ågerstrand, I. Allan, R. Altenburger, M. Brinkmann, D. Bunke, R.M. Burgess, I. Cousins, B.I. Escher, F.J. Hernández, L.M. Hewitt, K. Hilscherová, J. Hollender, H. Hollert, R. Kase, B. Klauer, C. Lindim, D.L. Herráez, C. Miège, J. Munthe, S. O'Toole, L. Posthuma, H. Rüdel, R.B. Schäfer, M. Sengl, F. Smedes, D. van de Meent, P.J. van den Brink, J. van Gils, A.P. van Wezel, A.D. Vethaak, E. Vermeirssen, P.C. von der Ohe, B. Vrana, Towards the review of the European Union Water Framework management of chemical contamination in European surface water resources, Sci. Total Environ. 576 (2017) 720–737. https://doi.org/10.1016/j.scitotenv.2016.10.104.

[8] L. Carvalho, E.B. Mackay, A.C. Cardoso, A. Baattrup-Pedersen, S. Birk, K.L. Blackstock, G. Borics, A. Borja, C.K. Feld, M.T. Ferreira, L. Globevnik, B. Grizzetti, S. Hendry, D. Hering, M. Kelly, S. Langaas, K. Meissner, Y. Panagopoulos, E. Penning, J. Rouillard, S. Sabater, U. Schmedtje, B.M. Spears, M. Venohr, W. van de Bund, A.L. Solheim, Protecting and restoring Europe's waters: An analysis of the future development needs of the Water Framework Directive, Sci. Total Environ. 658 (2019) 1228–1238. https://doi.org/10.1016/j.scitotenv.2018.12.255.

[9] C. Di Marcantonio, C. Bertelkamp, N. van Bel, T.E. Pronk, P.H.A. Timmers, P. van der Wielen, A.M. Brunner, Organic micropollutant removal in full-scale rapid sand filters used for drinking water treatment in The Netherlands and Belgium, Chemosphere. 260 (2020) 127630. https://doi.org/10.1016/j.chemosphere.2020.127630.

[10] E. Calizza, F. Favero, D. Rossi, G. Careddu, F. Fiorentino, S. Sporta Caputi, L. Rossi, M.L. Costantini, Isotopic biomonitoring of N pollution in rivers embedded in complex human landscapes, Sci. Total Environ. 706 (2020) 136081. https://doi.org/10.1016/j.scitotenv.2019.136081.

[11] P.M. Glibert, J.J. Middelburg, J.W. McClelland, M. Jake Vander Zanden, Stable isotope tracers: Enriching our perspectives and questions on sources, fates, rates, and pathways of major elements in aquatic systems, Limnol. Oceanogr. 64 (2019) 950–981. https://doi.org/10.1002/lno.11087.

[12] S. Iacurto, G. Grelle, F.M. De Filippi, G. Sappa, Karst Recharge Areas Identified by Combined Application of Isotopes and Hydrogeological Budget, Water. 13 (2021) 1965. https://doi.org/10.3390/w13141965.

Title: A risk-based methodology based on the results of leaching and ecotoxicological tests for assessing the environmental compatibility of the use of products from bottom ash treatment

Author(s): Luigi Acampora[1], Giulia Costa*[1], Francesco Lombardi[1], Lorenzo Maggi[2], Claudia Mensi[3], Silvia Messinetti[2], Erica Tediosi[2], Iason Verginelli[1]

[1] *Department of Civil Engineering and Computer Science Engineering, University of Rome Tor Vergata, Rome, Italy, costa@ing.uniroma2.it*
[2] *LabAnalysis Life Science, Novate Milanese, Italy*
[3] *A2A Ambiente S.p.A., Giussago, Italy*

Keyword(s): bottom ash, circularity, end of waste, leaching, ecotoxicity, risk assessment

Abstract

Waste-to-Energy is an established technology for residual waste management in Europe, which allows to recover not only energy but also valuable materials from the treatment of its most abundant solid residue: bottom ash (BA). Technologies for ferrous and non ferrous metals recovery from BA are being increasingly implemented all over Europe [1]. The mineral fraction (over 75% by weight) of BA is currently employed in construction applications in several Countries, but neither harmonized procedures, nor End of Waste criteria have been issued at a European level for establishing the environmental requirements for its utilization [2]. Each Country has developed its own rules that make use of different methodologies, mainly based on total content values and the results of leaching test methods. In Italy, which presents one of the highest utilisation rates (85%) [3], BA is typically sent to large-scale treatment plants that, besides ferrous and non ferrous metals recovery, separate mineral fractions that are generally employed as aggregates or sand substitutes in concrete or asphalt mixtures, or in cement or ceramics manufacturing. End of waste criteria have not been issued for the mineral fraction products and utilisation is decided by local authorities case by case, leading to uncertainties for BA producers, treatment plants and final users of the products. The main potential risk posed to the environment and human health by these materials is the release of metals, metalloids and salts (mainly chlorides and sulphates) into percolating rainwater that may subsequently migrate to contaminate soil, groundwater and surface water, therefore potentially impacting terrestrial and aquatic ecosystems, as well as drinking water quality.
In this work, we present a methodology that was applied to assess if the use as unbound fillers or aggregates of mineral fractions from BA treatment may pose potential risks to the environment and human health. This approach employs of the results of both leaching and ecotoxicological tests carried out on products collected from full-scale industrial plants and evaluates them through a risk assessment procedure, assuming worst reasonable scenarios. Specifically, ten different products collected from four Italian BA treatment plants, termed in this paper 1, 2, 3 and 4, were analysed. As for the analysis of the leaching behaviour of the products, three types of standardized tests (i.e. column percolation test - EN 14405, batch compliance test - EN 12457-2 and pH dependence test - CEN/TS 14429) were carried out. The samples collected were analysed for their content of major constituents (such as Ca, Mg, Al, and Fe), trace elements, including metals (e.g. Pb, Zn, Cu), metalloids (such as Cr, Mo and Sb) and anions (such as chlorides and sulphates), and Dissolved Organic Carbon (DOC).
Composite samples of the eluates of the column percolation tests were also employed to carry out acute and chronic ecotoxicological tests on aquatic organisms that are typically employed for waste

classification according to the EU's CLP regulation, i.e. the OECD 201 Freshwater Alga and Cyanobacteria Growth Inhibition test, the OECD 202 Daphnia sp. Acute Immobilisation test, the OECD 203 Fish Acute Toxicity test and the OECD 211 Daphnia magna Reproduction test. For the mineral fractions that are typically utilised as aggregates or fillers, terrestrial ecotoxicological tests were also carried out employing organisms of different groups (plants, soil organisms and microorganisms).
As for the evaluation of risk-based guideline values to which compare the obtained leaching test concentrations, following a conservative approach, it was considered that the products would be employed as unbound fillers or aggregates in large parking lots or road sub-base layers. As shown in Figure 1, the results of the different types of characterization leaching tests applied, which allow also to assess the release mechanism (e.g. solubility or washout), were used as input data, and depending on the scenario considered, different dilution factors were calculated according to fate and transport models reported in the ASTM (2000) guidelines to estimate the concentrations resulting in the groundwater (point of compliance). To evaluate the risks for the groundwater resource, two different approaches were adopted. The first consists in comparing the concentrations expected at the point of compliance with drinking water quality criteria set by specific legislation. In the second approach the risks were instead calculated for the water ingestion pathway using the equations proposed by ASTM (2000).

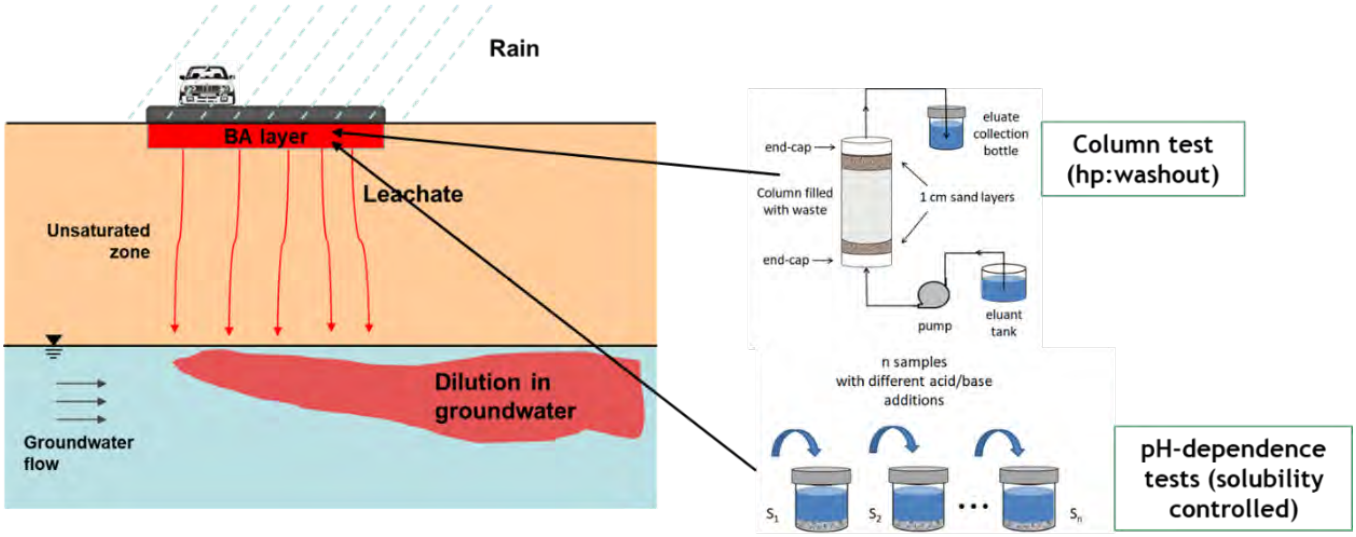

Figure 1. Scheme of the risk assessment procedure adopted.

To evaluate the risks for aquatic organisms, the results of the ecotoxicological tests were expressed as dilution factors and compared to the ones calculated for the assumed utilisation scenarios. Finally, also the results of the terrestrial ecotoxicity tests were statistically analysed to derive EC50 and EC10 to evaluate the risk for different scenarios.
Figures 2 and 3 show examples of the results obtained for a major element (Al), trace constituents (Cu and Cr) and anions (Chlorides) applying the two types of characterization leaching tests employed in this work, plotted as a function of the applied liquid to solid ration (L/S) for the percolation tests (Figure 2) and pH, in the case of the pH-dependence test (Figure 3). For most of the analysed constituents, the trends of the release curves obtained applying either type of test were quite consistent for the ten different samples analysed, although concentrations values showed to vary (e.g. of 1 order of magnitude in the case of Cu) depending on the type of sample. Based on the results of the leaching tests, the concentrations of the target contaminants to be used for the risk assessment were identified. For the pH-dependence leaching test, the maximum concentration obtained for pH values higher than 7 was selected, whereas for the percolation test, the maximum concentration values obtained for all of the

tested L/S ratios were considered. The maximum concentrations detected from the different types of leaching tests were compared with the limit values calculated considering three utilisation scenarios and the associated Leaching Factors. For the use of the product without restrictions ("no restrictions"), the maximum concentrations in the eluate obtained from the pH dependence leaching tests and the column percolation tests for most of the target contaminants showed to be incompatible with utilisation. In particular, the most critical constituents in terms of exceedance of the risk-based limits set for the no restrictions scenario were Al, Cr, Cu, Mo, Pb, Sb, chlorides and fluorides. For the use of the products as aggregates in unbound form for large-scale applications, excluding some specific isolated cases, the maximum concentrations detected for the different indicator contaminants in the different leaching tests were lower than the calculated limit values. For the use of the products in unbound form as road sub-base materials ("worst reasonable case") no exceedance of the limit concentrations was detected for any of the indicator contaminants.
Interestingly, the results of the ecotoxicological tests provided the same type of response, indicating that the risk for aquatic organisms related to use with no restrictions would not be acceptable, while that for large-scale applications safe in most cases, and that for worst-reasonable cases always acceptable.

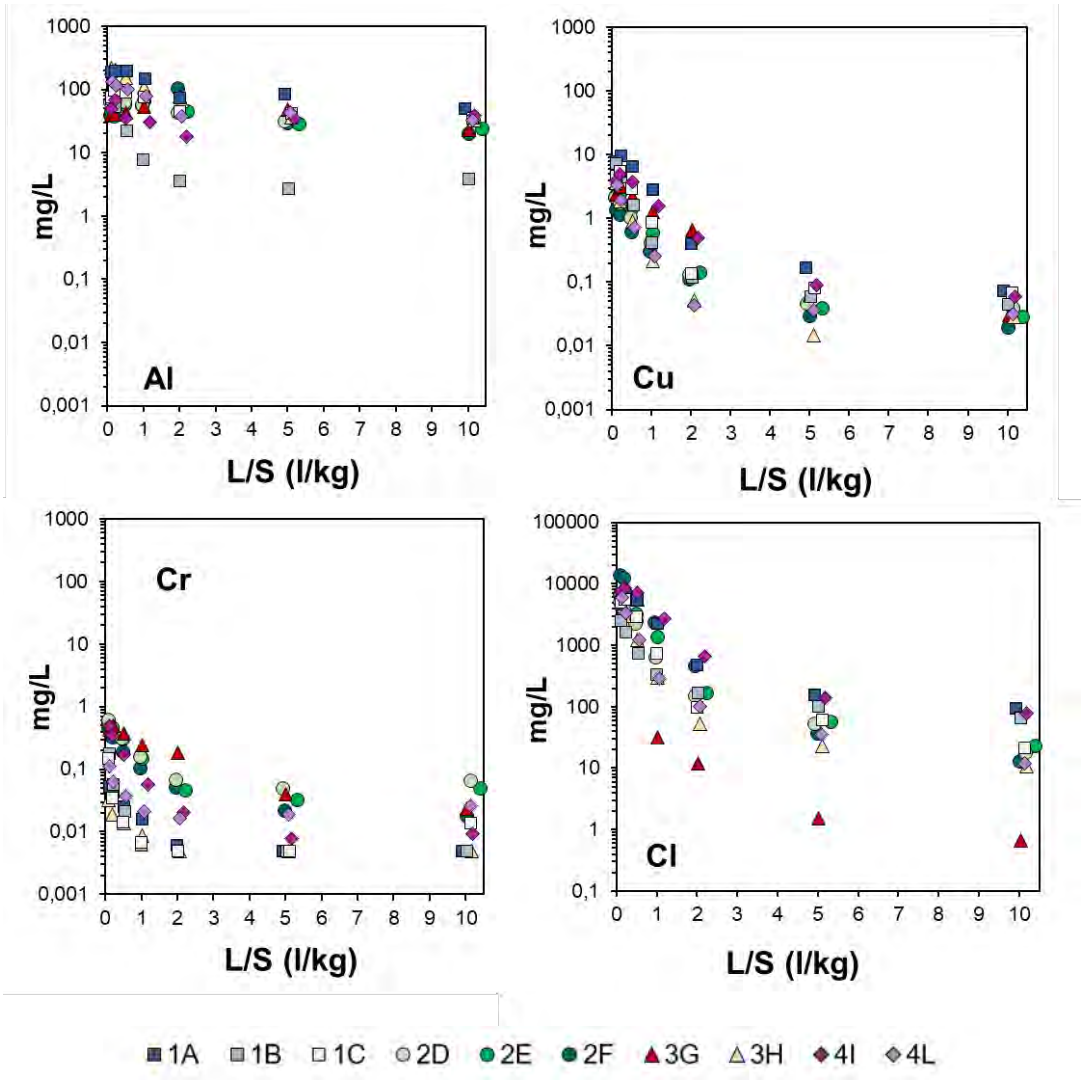

Figure 2. Examples of the average results of the percolation leaching test performed on each type of sample.

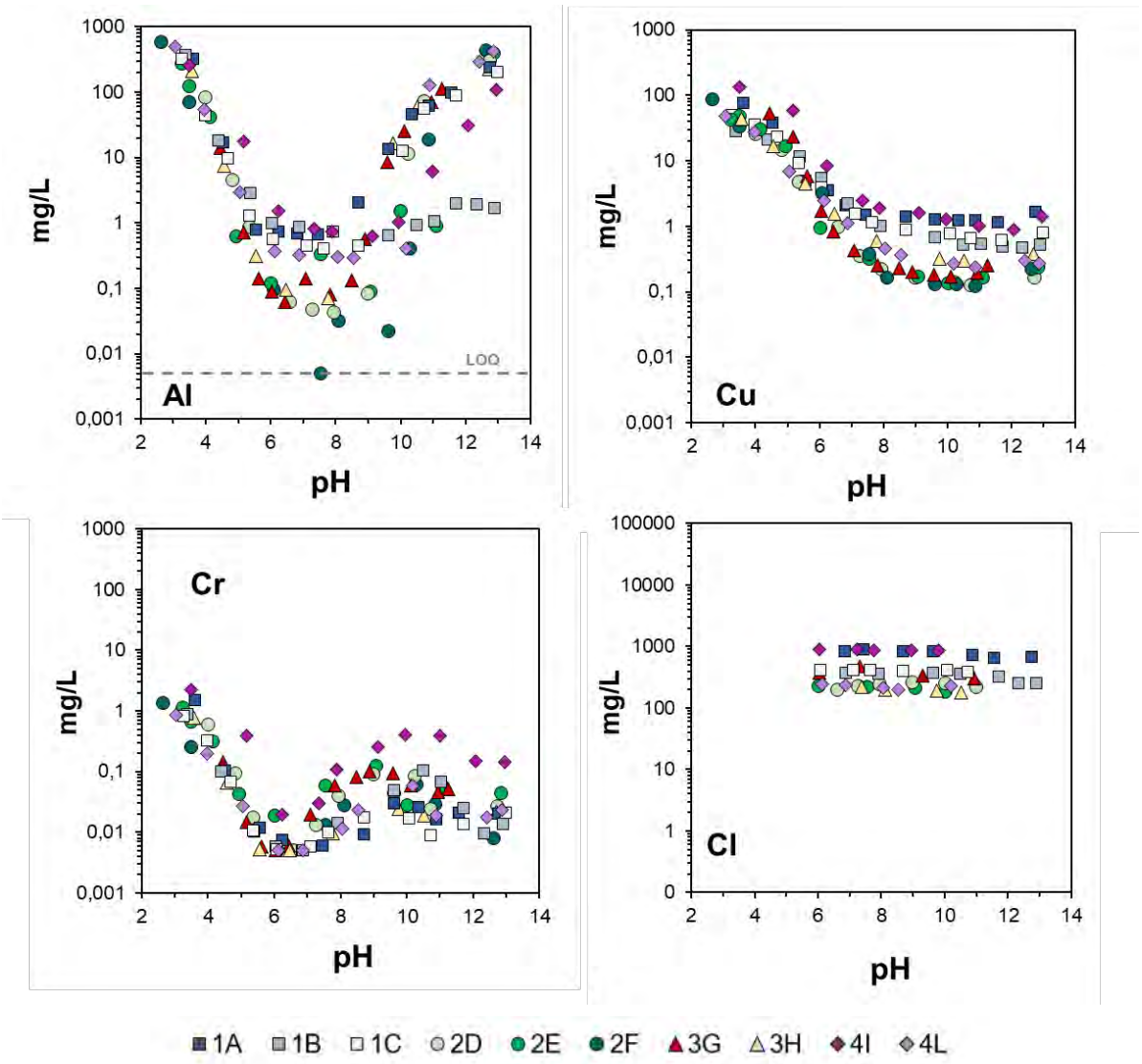

Figure 3. Examples of the average results of the pH-dependence leaching test for each type of sample.

References

[1] Šyc, M., Simon, F.G., Hyks, J., Braga, R., Biganzoli, L., Costa, G., Funari, V. & Grosso, M., 2020. Metal recovery from incineration bottom ash: State-of-the-art and recent developments. J. Hazard. Mater. 393, 122433.
[2] Saveyn H., Eder P., Garbarino E., Muchova L., Hjelmar O., van der Sloot H., Comans R., van Zomeren A., Hyks J. & Oberender A., 2014. Study on methodological aspects regarding limit values for pollutants in aggregates in the context of the possible development of end-of waste criteria under the EU Waste Framework Directive. Institute for Prospective Technological Studies: Seville, Spain.
[3] Blasenbauer D., Huber F., Lederer J., Quina M.J., B. Biscarat D., Bogush A., Elza Bontempi E., Blondeau J., Chimenos J.M., Dahlbo H., Fagerqvist J., Giro-Paloma J., Hjelmar O., Hyks J., Keaney J., Lupsea-Toader M., O'Caollai C.J., Orupõld K., Pajak T., Simon F.G., Svecova L., Šyc M., Ulvang R., Vaajasaari K., Van Caneghem J., van Zomeren A., Vasarevičius S., Wégner K. & Fellner J., 2020. Legal situation and current practice of waste incineration bottom ash utilisation in Europe. Waste Manage. 102, 868-883.
[4] ASTM, 2000. Standard Guide for Risk-Based Corrective Action. American Society for Testing and Materials. Standard E2081-00. West Conshohocken, PA.

Title: One Health: air pollution and human health under the environmental perspective

Authors: Lucia D'Elia*[1], Giuseppina Oliva[1], Tiziano Zarra[1], Vincenzo Belgiorno[1], Vincenzo Naddeo[1]

[1] *Sanitary Environmental Engineering Division (SEED), Department of Civil Engineering, University of Salerno, Via Giovanni Paolo II 132, 84084 Fisciano, SA, Italy*

Keyword(s): Air pollution, One health, Environmental Health, Health risk assessment, Air Pollution-Related Diseases

Abstract

Nowadays many scientific studies are focused on understanding how the environment, human health and animal health are connected. Air pollution is the first environmental risk factor threatening human health. Every year, poor air quality leads worldwide to the appearance of numerous diseases and the premature death of about 7 million people. Exposure to air pollutants can induce both short- and long-term effects. The first ones are connected to exposure to acute doses of contaminants, which are often temporary and affect the respiratory tract. Long-term effects are often irreversible and may affect many systems and functions of the human body. About 70% of air pollution-related diseases are non-communicable. These effects are endemic because they are observable even after exposure to low concentrations of pollutants and on days when air is good according to monitoring activities.
In this context, many plans and programs have been implemented at European and global level with the aim of protecting public health. The European Commission's Proposal for a New Directive on Air Quality at the start of 2024 is proof of the significance of this problem. It will align the limits of pollutants with those suggested by the World Health Organization in 2021 to protect public health. In this context, it is necessary, on the one hand to develop strategies to control air pollution and, on the other, to develop precise and reliable risk forecasting models to inform the population in real time in order to safeguard human health.

Introduction

The One Health approach, describes complex interconnections between humans, animal and environmental health. Urbanization, population growth, and economic development have undoubtedly led to progress, but they have also stress ecosystems by altering their functions and stability [1]. According to literature, pollution is the greatest risk factor for human health comparable only to smoking. In 2019 pollution was responsible of 9 million of premature deaths, of which about 7 million related to air [2]. According to the World Health Organization (WHO), 99% of the world's population breathe bad air [3]. Actions of individual nations are ineffective if not included in a regional framework of joint actions due the transboundary nature of the phenomenon [4]. Atmospheric agents transport contaminants for long distances. Particulate originated from the Sahara desert has been found in southern Europe and the Middle East [5]. In the next paragraphs, major effects of air pollution on public health as well as major strategies for air quality management and control in the world with particular attention to Europe will be illustrated. The presentation will also give an overview of future scientific research possibilities.

Effects of air pollution on human health

Air pollution is responsible for about 11% of total deaths among women and 12% among men for a total

of about 7 million premature deaths worldwide each year [6]. Deaths generally increase with age but numbers reveal a peak in the post-neonatal range and between 1 and 4 years. [7]. This results in a total decrease in life expectancy of 2.9 years [8]. Air pollution is also one of the elements that most affect the quantification of DALYs (disability adjusted life years) which is the sum of years of life lost due to premature mortality and years of life lived with disability or illness [6]. In this case the maximum in the post-neonatal age group in which each case leads to a high number of years of health lost [7]. About 70% of diseases related to air pollution are non-communicable. In these cases the risk is proportional to the exposure [7]. Short-term exposure is commonly associated with respiratory issues such as cough, shortness of breath, breathlessness, and asthma, but it could led also to eye inflammation, skin irritation, and headache [9]. Long-term effects may include respiratory, cardiovascular, metabolic, mental, or perinatal problems. Chronic obstructive pulmonary disease (COPD), strokes, obesity and hypertension are the most prevalent [10,11]. In general, the frequency of occurrence has an inverse relationship with the severity of the impact [12]. These numbers are alarming especially considering that they probably underestimate the real situation. In addition to the practical difficulties of collecting and processing data in many parts of the world, it should be stressed that often only some of the most easily detectable pollutants (particulate matter and ozone) are considered neglecting all others that nevertheless pose health risks. These estimates do not include all health effects of emerging contaminants such as micro(nano)plastics and PFAS (perfluorinated alkylated substances) that may also be found in the atmosphere. Ultimately, recent studies show that the negative effects of air pollution can be observed at very low concentrations and that there are no observable thresholds below which exposure can be considered safe [13].

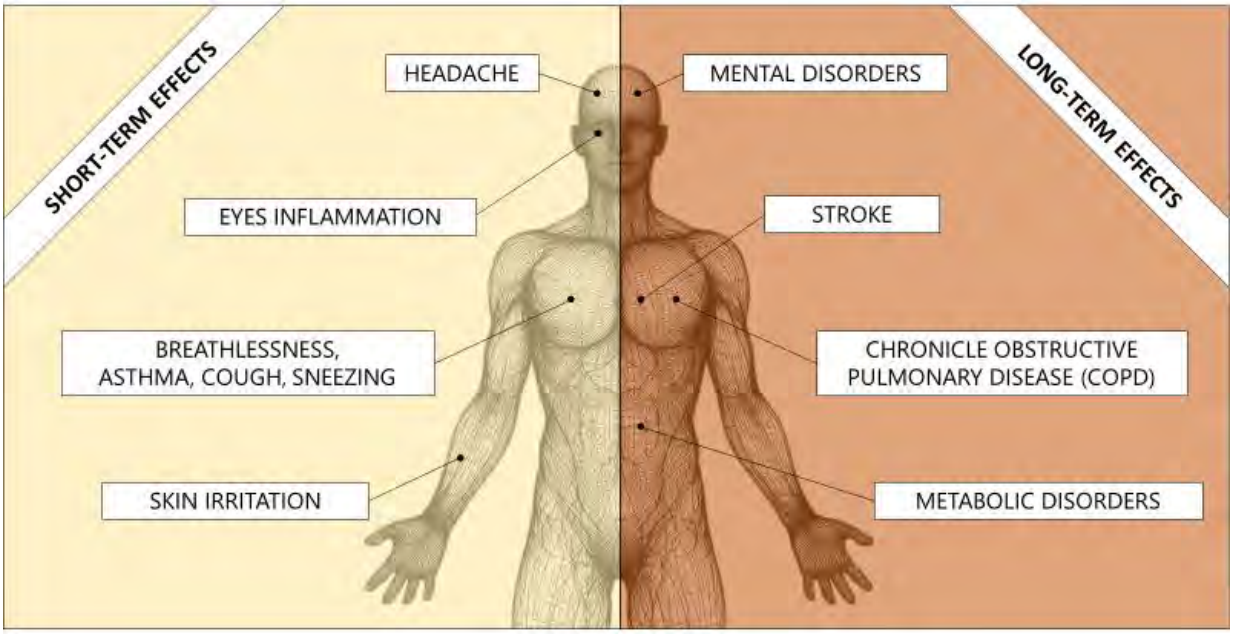

Figure 1. Main effects of air pollution on human health

Environmental strategies to protect public health from air pollution

In recent years, the number of environmental actions and programmes for the protection of public health has increased. WHO, the United Nations and the European Commission are only some agencies that are working to define solutions for this situation. Actions of individual nations are ineffective if not included in a wider regional framework. Practical implementation has also slowed down due to differences in the cultures, interests and environmental laws of countries that must collaborate and

sometimes to public opinion [4]. Therefore, the process should be fully participatory at all stages in order to raise public awareness of environmental issues and their impact on public health [14].

In the 2030 Agenda of the United Nations General Assembly, Target 3.9 of Sustainable Development Goal 3 (Good health and well-being) aims at substantially reducing the number of deaths and diseases from hazardous chemicals and air, water and soil contamination [15]. The European Commission in 2021 has defined within the plan "Towards Zero Pollution for Air, Water and Soil" the goal of reducing by 55% by 2030 the effects on health and premature deaths due to air pollution [16]. The WHO in 2021 defined new global guidelines for air quality (AQG2021) that, although they have no regulatory value, support institutions around the world to define policies for air pollution control. Contaminants limit values has been determined after a comprehensive study of the results obtained by authoritative bodies such as the Committee on the Medical Effects of Air Pollutants of United Kingdom, Health Canada, and United States EPA [17]. Over 100 medical, public health, scientific societies and patient representative organisations also signed these Guidelines through a joint statute carried out by the European Respiratory Society and the International Society for Environmental Epidemiology [5]. At the end of 2022 The European Commission presented the proposal for a new Air Quality Directive to replace and update the contents of Directives 2008/50/EC [18]. In February 2024, the Council Presidency and representatives of the European Parliament reached a provisional political agreement on a proposal to set EU air quality standards to achieve a zero pollution target [19].

Monitoring air pollution levels

To measure air quality levels and record changes over time, monitoring actions are necessary. Indices are used to evaluate and quantify air pollution and inform citizens promptly and recommend them behaviours to reduce the pollution-related health risks [20]. The most used index in the world is Air Quality Index (AQI): it is a dimensionless index defined in 1999 by US EPA. It expresses through a numerical value the level of pollutants defined in the atmosphere in a given time interval. Rising values represent increasing levels of air pollution that require increasingly stringent recommendations for citizens [21]. The calculation of AQI is based on the identification of the pollutant with the highest concentration. It fails to calculate the effects of exposure to multiple pollutants or those without thresholds [22]. To cope to these limits, the Air Quality Health Index (AQHI) has been defined by the Healthy Environments and Consumer Safety Branch of Canada in 2005 [22]. According to this model, behavioural advice is different for vulnerable individuals defined as "at risk" and all others [23]. Although AQI and AQHI are both reliable for predicting national daily mortality risk, AQHI is more flexible because it allows to choose different pollutants but also a specific population target to evaluate [20].

Future perspective

Worldwide, many programs exist for reducing the concentration of pollutants in the air for the protection of public health. Control policies based on innovative methodologies using technologically advanced tools must be developed. Air quality control models must be dynamic to give instant indications of pollution levels. At the same time, methodologies should aim to assess health effects to provide real-time guidance on the best behaviour to adopt to protect humans. Once effective models have been defined, it will be necessary to focus on the groups most vulnerable to air pollution because they are those on which the effects can be very significant even for low exposure levels. The Canadian model with the AQHI index could be optimized and applied by other Countries in the world where the AQI index is still used.

References

[1] FAO, UNEP, WHO, and WOAH (2022) One health joint plan of action (2022–2026): working together for the health of humans, animals, plants and the environment. .

[2] Fuller, R., Landrigan, P.J., Balakrishnan, K., Bathan, G., Bose-O'Reilly, S., Brauer, M., et al. (2022) Pollution and health: a progress update. *The Lancet Planetary Health*. 6 (6), e535–e547.
[3] (2022) World health statistics: monitoring health for the SDGs, sustainable development goals. Geneva: World Health Organization; 2022. Licence: CC BY-NC-SA 3.0 IGO. .
[4] Ren, C., Yu, C.W., and Cao, S.-J. (2023) Development of urban air environmental control policies and measures. *Indoor and Built Environment*. 32 (2), 299–304.
[5] Hoffmann, B., Boogaard, H., de Nazelle, A., Andersen, Z.J., Abramson, M., Brauer, M., et al. (2021) WHO Air Quality Guidelines 2021–Aiming for Healthier Air for all: A Joint Statement by Medical, Public Health, Scientific Societies and Patient Representative Organisations. *International Journal of Public Health*. 0.
[6] GBD 2019 Risk Factors Collaborators (n.d.) Global burden of 87 risk factors in 204 countries and territories, 1990-2019: a systematic analysis for the Global Burden of Disease Study 2019. *Lancet (London, England)*.
[7] Landrigan, P.J., Fuller, R., Acosta, N.J.R., Adeyi, O., Arnold, R., Basu, N. (Nil), et al. (2018) The Lancet Commission on pollution and health. *The Lancet*. 391 (10119), 462–512.
[8] Lelieveld, J., Pozzer, A., Pöschl, U., Fnais, M., Haines, A., and Münzel, T. (2020) Loss of life expectancy from air pollution compared to other risk factors: a worldwide perspective. *Cardiovascular Research*. 116 (11), 1910–1917.
[9] Larrieu, S., Lefranc, A., Gault, G., Chatignoux, E., Couvy, F., Jouves, B., et al. (2009) Are the Short-term Effects of Air Pollution Restricted to Cardiorespiratory Diseases? *American Journal of Epidemiology*. 169 (10), 1201–1208.
[10] Hu, X., Nie, Z., Ou, Y., Lin, L., Qian, Z., Vaughn, M.G., et al. (2023) Long-term exposure to ambient air pollution, circadian syndrome and cardiovascular disease: A nationwide study in China. *Science of The Total Environment*. 868 161696.
[11] Manisalidis, I., Stavropoulou, E., Stavropoulos, A., and Bezirtzoglou, E. (2020) Environmental and Health Impacts of Air Pollution: A Review. *Frontiers in Public Health*. 8 14.
[12] (2001) World Health Organization. Regional Office for Europe. Quantification of health effects of exposure to air pollution : report on a WHO working group, Bilthoven, Netherlands 20-22 November 2000. Copenhagen : WHO Regional Office for Europe. .
[13] Dominici, F., Schwartz, J., Di, Q., Braun, D., Choirat, C., and Zanobetti, A. (2019) Assessing Adverse Health Effects of Long-Term Exposure to Low Levels of Ambient Air Pollution: Phase 1. *Research Reports: Health Effects Institute*. 2019 200.
[14] Mirabelli, M.C., Ebelt, S., and Damon, S.A. (2020) Air Quality Index and air quality awareness among adults in the United States. *Environmental Research*. 183 109185.
[15] UN General Assembly (2015) Transforming our world: the 2030 Agenda for Sustainable Development.
[16] European Commission (2021) Communication from the commission to the european parliament, the council, the european economic and social committee and the committee of the regions Pathway to a Healthy Planet for All EU Action Plan: 'Towards Zero Pollution for Air, Water and Soil. .
[17] World Health Organization (2021) WHO global air quality guidelines: particulate matter (PM2.5 and PM10), ozone, nitrogen dioxide, sulfur dioxide and carbon monoxide. .
[18] European Commission (2022) Proposal for a DIRECTIVE OF THE EUROPEAN PARLIAMENT AND OF THE COUNCIL on ambient air quality and cleaner air for Europe (recast). .
[19] Council of the European Union (2024) Air quality: Council and Parliament strike deal to strengthen standards in the EU.
[20] Du, X., Chen, R., Meng, X., Liu, C., Niu, Y., Wang, W., et al. (2020) The establishment of National Air Quality Health Index in China. *Environment International*. 138 105594.
[21] U.S. Environmental Protection Agency (2018) Technical Assistance Document for the Reporting of Daily Air Quality – the Air Quality Index (AQI).
[22] Stieb, D.M., Burnett, R.T., Smith-Doiron, M., Brion, O., Shin, H.H., and Economou, V. (2008) A New Multipollutant, No-Threshold Air Quality Health Index Based on Short-Term Associations Observed in Daily Time-Series Analyses. *Journal of the Air & Waste Management Association*. 58 (3), 435–450.
[23] Canada, E. and C.C. (2007) About the Air Quality Health Index.

Title: The fate of micropollutants in the water environment from sources to humans: planning removal treatments and assessing the risk in a one-health approach

Author(s): Jessica Ianes, Luca Penserini, Elena Sezenna, Sabrina Saponaro, Beatrice Cantoni, Manuela Antonelli*

Politecnico di Milano, Department of Civil and Environmental Engineering (DICA), Piazza Leonardo da Vinci 32, 20133 Milan, Italy

Keyword(s): combined sewer overflows, contaminants of emerging concern, risk assessment, wastewater reuse

Introduction

Micropollutants represent an emerging challenge in water management as they are increasingly detected in water systems globally. These compounds encompass a diverse array of synthetic chemicals, such as pharmaceuticals, personal care products, pesticides, Per- and Poly-Fluoroalkyl Substances (PFAS), alkylphenols, and Polycyclic Aromatic Hydrocarbons (PAHs). Despite their low concentrations (ng L^{-1} - µg L^{-1}), micropollutants exert significant adverse effects, potentially disrupting ecosystems, compromising drinking water (DW) safety, and posing risks to human health. However, many sources of uncertainty arise, due to the knowledge gaps in micropollutants release, occurrence, fate in the environment and toxicity effects. Managing water quality in urban water systems is challenging due to multiple pollutant sources, pathways, and receptors. Micropollutants in urban areas are released by several sources, including point sources, such as industrial and municipal wastewater treatment plant (WWTP) discharges, and non-point sources, such as stormwater runoff, accumulating in surface water bodies and groundwater. This poses a threat to the environment, particularly when water reservoirs are exploited for drinking and recreational purposes.
Given the widespread and ubiquitous presence of micropollutants, it is fundamental to identify the main sources, to properly allocate monitoring efforts and mitigation strategies. Besides municipal and industrial WWTPs, combined sewer overflows (CSOs) exacerbate micropollutant contamination: during rain events, when the system capacity is exceeded, CSOs and WWTP bypass (BP) discharge a mixture of untreated wastewater and stormwater directly into surface waters [1]. Agricultural activities also play a significant role, with pesticides and fertilizers leaching into surface water bodies through runoff. Moreover, in case of direct and indirect reuse of reclaimed wastewater, micropollutants potentially present in the irrigation water can be transferred to the edible crops, whose consumption can pose a risk to human health [2]. In addition, the presence of a diverse range of micropollutants in water bodies used for DW supply asks for proper management. Finally, the materials in contact with DW can be an additional source of micropollutants [3]. To address the inherent complexity of micropollutants spread and to ensure effective environmental protection, an integrated approach is essential, involving comprehensive monitoring and analysis of multiple sources and rigorous fate modelling frameworks. Preventive risk assessments can be the key to identify the most effective mitigation and management scenarios.
The goal of this research is to explore the potential of integrated risk assessment procedures for prioritizing contaminants and compartments to be monitored in urban water systems, and determining the mitigation strategies that maximize the overall expected risk reduction. Based on the outputs of the integrated risk assessment, (i) preventive approaches can be preferred for selected micropollutants, such as regulatory measures curbing the entrance of potentially harmful contaminants in the

environment [4]; and/or (ii) effective removal strategies can be designed to target specific micropollutants in DW treatment plants and WWTPs [5,6].

Materials and Methods

The developed risk assessment procedure includes several steps. Firstly, the analyzed system boundaries were defined, to consider the compartments and the contaminants involved in the process, from sources to the final endpoint (whether it is the environment or human health). A schematic overview is reported in Figure 1. As for the exposure assessment step, micropollutants concentration data were collected from the literature for each compartment of interest. Additional modeling of micropollutant fate was used to predict their concentrations at the endpoint knowing the concentrations in each source and modelling the transport system. Then, in the hazard assessment step, the toxicological characterization for each micropollutant was retrieved from the literature. Finally, exposure and hazard assessment steps were combined in the risk characterization step, to quantitatively estimate environmental or human health risk for micropollutants in different compartments.

Figure 1. Conceptual scheme of the integrated urban water system, indicating the main families of micropollutants and the compartments involved.

As for the environmental risk assessment, the Risk Quotient (RQ) or the Risk Quotient for antibiotic resistance development (RQ_{ARB}) were estimated as the ratio between environmental concentration (MEC) and the Predicted No-Effect Concentration (PNEC), or the Predicted No-Effect Concentration for the antibiotic resistance development in bacteria ($PNEC_{ARB}$). Equations are as follows:

$$RQ = \frac{MEC}{PNEC} \quad (1)$$

$$RQ_{ARB} = \frac{MEC}{PNEC_{ARB}} \quad (2)$$

As for human health risk assessment, the Benchmark Quotient (BQ) was calculated as the contaminant exposure concentration (C_{EXP}), typically originating from crop or DW consumption, divided by its reference dose (RfD), as follows:

$$BQ = \frac{C_{EXP}}{RfD} \quad (3)$$

The proposed procedure included uncertainty analyses to account for knowledge gaps, input data uncertainties and tempo-spatial variabilities, and modeling uncertainties to provide decision-makers with the confidence level of the risk estimation. This was done through Monte-Carlo simulations by building the probabilistic distributions of the input variables and propagating such uncertainty distributions in the risk characterization step.

The developed procedure was applied to assess different types of risks in three different case studies:
1) The environmental risk for the receiving water body originated by the discharge of Benzo(a)pyrene by all discharges of an integrated wastewater system.
2) The human health risk contribution of different exposure routes (i.e., consumption of tap water, cereals and fruits and vegetables) due to the presence of two alkylphenols, bisphenol A (BPA) and nonylphenol (NP), frequently detected in DW and crops.
3) The simultaneous estimation of environmental, antibiotic resistance development and human health risks originating from the indirect reuse of reclaimed wastewater.

Results

Risk estimation can be beneficially used to quantitatively rank the different mitigation strategies based on their contribution to risk reduction.
Examples are reported in Figure 2 referring to the results of the first two case studies. In the first case study (Figure 2a), the environmental chronic risks posed by CSOs, BP, and WWTP effluent (EFF) were assessed and compared on an annual basis. CSOs result to pose the highest risk to surface water, followed by BP, and EFF, indicating that mitigation strategies should be prioritized on CSOs. In the second case study (Figure 2b), although the risk due to NP was not negligible, the calculated risk for human health due to BPA was significantly higher, and cereals and fruits and vegetables consumption determined a higher risk compared to tap water. Thus, interventions on soil, would be more effective in reducing the overall risk, especially targeting BPA.

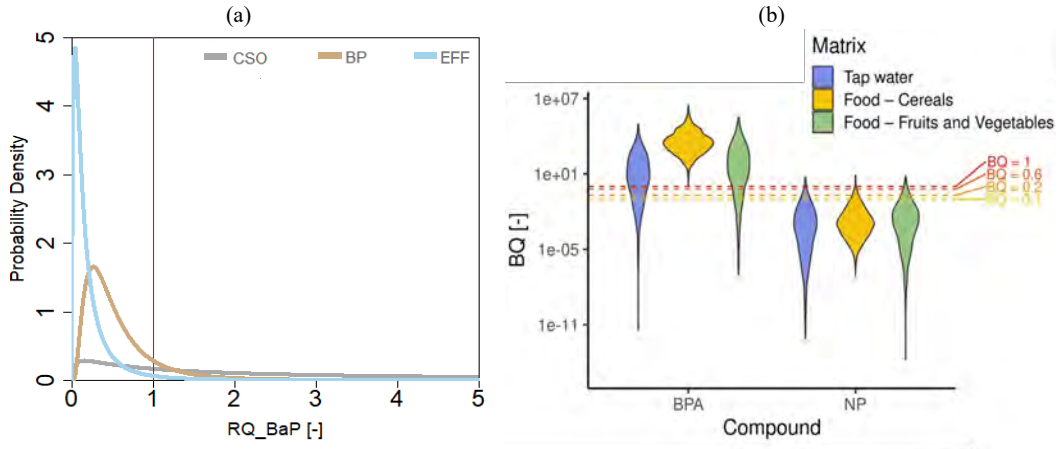

Figure 2. Estimated risk distributions: (a) RQ due to benzo(a)pyrene for each discharge type from an integrated wastewater system (red line represents the risk threshold RQ=1 [1]); BQ due to alkylphenols related to the consumption of food and water (dashed lines indicate BQ equal to the warning thresholds (0.1, 0.2, 0.6) and to the risk presence threshold (1) [2]).

Finally, a One Health approach is proposed for the indirect reuse of reclaimed wastewater in agriculture, to consider the risks to the environment where the reclaimed wastewater is released, and for human health, due to the consumption of irrigated crops. Results of risk estimation are shown in Figure 3 for three pharmaceuticals and three antibiotics. Estimated human health risk is substantially lower than the warning threshold (BQ equal to 0.1) for all the considered micropollutants. Thus, the presence of these micropollutants in reclaimed wastewater, used after dilution with the natural surface water for crop irrigation, does not pose a risk to human health. However, both the environmental risk and the risk of antibiotic resistance development significantly contribute to the overall risk. Hence, special attention would be recommendable in terms of regulatory measures or additional targeted monitoring campaigns.

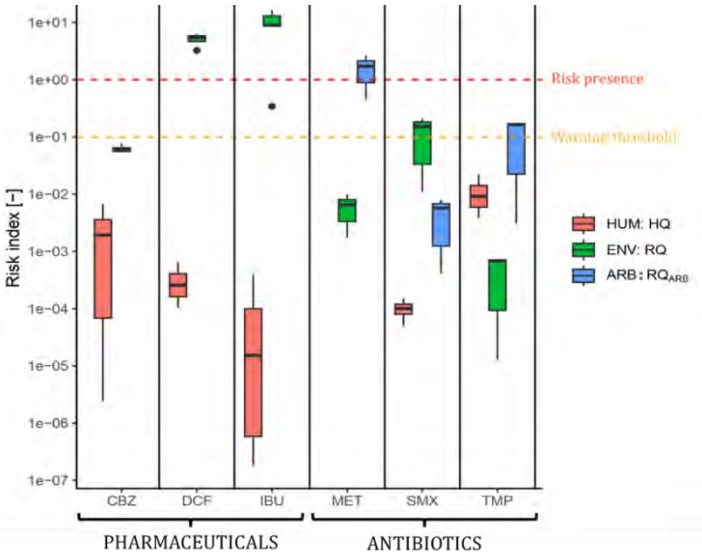

Figure 3. Risk indices distributions for human health, environmental, and antibiotic resistance risk for: carbamazepine (CBZ), diclofenac (DCF), ibuprofen (IBU), metronidazole (MET), sulfamethoxazole (SMX) and trimethoprim (TMP). MET concentration in crops was always below the limit of detection, making the human health risk not quantifiable. Dashed lines indicate risk indices equal to the warning threshold (0.1) and the risk presence threshold (1).

Conclusions

Results underscore the importance of holistic risk assessments employing integrated approaches to address the complex challenges posed by micropollutants in the water system. By integrating comprehensive source monitoring, innovative treatment technologies, and quantitative risk assessment methodologies, it is possible to support the decision-making process in safeguarding water quality and protecting human health.

The research is being funded by PNRR MUR - M4C2 Project “Return: Natural, man-made and environmental risks” (Project ID: PE-0000005, CUP D43C22003030002).

References

[1] Ianes, J., Cantoni, B., Remigi, E.U., Polesel, F., Vezzaro, L., Antonelli, M., 2023. A stochastic approach for assessing the chronic environmental risk generated by wet-weather events from integrated urban wastewater systems. Environ. Sci: Water Res. Technol. 9, 3174-3190.

[2] Penserini, L., Cantoni, B., Gabrielli, M., Sezenna, E., Saponaro, S., Antonelli, M., 2023. An integrated human health risk assessment framework for alkylphenols due to drinking water and crops’ food consumption. Chemosphere 325, 128259.

[3] Penserini, L., Cantoni, B., Vries, D., Turolla, A., Smeets, P.W.M.H., Bokkers, B.G.H., Antonelli, M., 2022. Quantitative chemical risk assessment for mixtures: Application to alkylphenol mixtures and phthalate mixtures in tap and bottled water. Environmental International 165, 107294.

[4] Cantoni, B., Bergna, G., Baldini, E., Malpei, F., Antonelli, M., 2024. PFAS in textile wastewater: An integrated scenario analysis for interventions prioritization to reduce environmental risk. Process Safety and Environmental Protection 183, 437-445.

[5] Cantoni, B., Ianes, J., Bertolo, B., Ziccardi, S., Maffini, F., & Antonelli, M. (2024). Adsorption on activated carbon combined with ozonation for the removal of contaminants of emerging concern in drinking water. Journal of Environmental Management, 350.

[6] Cantoni B., Turolla, A., Wellmitz J., Ruhl A.S., Antonelli, M., 2021. Perfluoroalkyl substances (PFAS) adsorption in drinking water by granular activated carbon: Influence of activated carbon and PFAS characteristics. Science of the Total Environment 795, 148821.

Title: **Remote sensing mapping of protected agriculture in Italian agricultural soils using a Sentinel-2 Imagery-based workflow**

Author(s): Daniele la Cecilia[1], Francesca Despini*[2], Sergio Teggi[2]

[1] *Department of Civil, Environmental and Architectural Engineering, University of Padua, Italy – daniele.lacecilia@unipd.it*
[2] *Department of Engineering Enzo Ferrari, University of Modena and Reggio Emilia, Italy – francesca.despini@unimore.it; sergio.teggi@unimore.it*

Keyword(s): Protected Agriculture, Remote Sensing, Sentinel-2, OPAC Classifier

Abstract

Protected agriculture is a significant aspect of European agriculture, especially in southern regions, substantially contributing to agricultural output. It encompasses greenhouse horticultural production and the growth of fruits, berries and vegetables on top of plastic-mulching. However, there are concerns over freshwater exploitation and environmental pollution from plant protection products and plastics. Accurately identifying and mapping these greenhouse surfaces is crucial for effective land management and policy-making [1,2]. Remote sensing techniques provide a valuable means to achieve this goal by offering comprehensive data on land cover types.

This study presents a workflow using the Open Field and Protected agriculture land cover Classifier (OPAC) [3], a random forest-based classifier, deployed in the Google Earth Engine platform to map protected agriculture over Italian agricultural soils. Sentinel-2 satellite images were selected for this study due to their free accessibility, comprehensive global coverage, and suitability for agricultural analysis.

Our methodology integrates several key steps to ensure accurate and reliable mapping results. These steps include atmospherically correcting Sentinel-2 images to enhance data quality, applying cloud masking algorithms to remove interference from cloud cover, aggregating images to minimize temporary reflective pixels, and incorporating auxiliary datasets such as Corine Land Cover, water masks and snow and elevation masks to further refine classification accuracy.

Validation of the classification model for protected agriculture, vegetated, and baresoil classes shows high overall accuracy. Mapping reveals significant areas of protected agriculture in Italy, the third European country by protected agriculture extension.

This methodology's strengths lie in a possible continuous and periodic mapping of protected agriculture, leveraging global datasets for rapid implementation and accessibility. Despite high accuracy, challenges persist in misclassifications, particularly in areas with reflective terrains, due to spectral ambiguities. Future improvements should focus on refining classification algorithms and incorporating more localized data to enhance accuracy and applicability all across Europe and beyond.

Figure 1. Detail of the classification showing protected agriculture (pink), baresoils (sienna), and vegetation (green) using the OPAC classifier over the agricultural area as per the CORINE Land Cover in the area near Salerno (southern Italy).

References

[1] Gruda, N., Bisbis, M., & Tanny, J. “Influence of climate change on protected cultivation: Impacts and sustainable adaptation strategies-A review.” Journal of Cleaner Production, *225*, 481-495. (2019)
[2] Perilla, G. A., & Mas, J. F. “High-resolution mapping of protected agriculture in Mexico, through remote sensing data cloud geoprocessing.” European Journal of Remote Sensing, *52*(1), 532-541 (2019).
[3] la Cecilia, D., Tom, M., Stamm, C., & Odermatt, D. “Pixel-based mapping of open field and protected agriculture using constrained Sentinel-2 data.” ISPRS Open Journal of Photogrammetry and Remote Sensing, 8, 100033 (2023)

Title: Innovative system for the well-being and protection of fish and consumers

Author(s): Eloise Pulvirenti*[1], Gea Oliveri Conti[1], Paola Rapisarda[1], Maria Castrogiovanni[1], Claudia Favara[1], Antonio Cristaldi[1], Margherita Ferrante[1].

[1] *Department of Medicine, Surgery and Advanced Technologies "G.F. Ingrassia", University of Catania*

Keyword(s): Aquaculture, MPs, fish, human health.

Abstract

Aquaculture is a practice of farming fish, molluscs and crustaceans in controlled environments, such as ponds, lakes or tanks [1,2]. This sector is emerging as a key element in the European Union, contributing to food security and sustainability [3]. The “sAMpEI” project of the University of Catania has developed a closed-cycle multitrophic intensive aquaculture model, which uses company reservoirs for fish fattening. The main objective is to promote aquaculture and exploit unused basin resources, creating opportunities for rural businesses interested in fish farming in inland areas. This approach is aligned with regional strategies for the integrated management of the water cycle and for supporting companies, with the aim of increasing profits linked to the use of internal waters and offering new job opportunities in the agricultural sector.
The analyzes using EP n.3788344 20 July 2022 entitled "Method for the extraction and determination of microplastics in organic and inorganic samples" and related determination in scanning electron microscopy (SEM) coupled to the EDX detector carried out on aquaculture fish in a lake environment showed a concentration of MPs smaller than 10 microns of 4.08E+03 p/g, and a concentration of MPs larger than 10 microns of 7.40E+01 p/g.
These values are lower than the MPs concentrations at time zero before being introduced into the aquaculture plant, with values of 1.21E+04 p/g and 2.08E+02 p/g respectively for MPs smaller and larger than 10 microns.
Aquaculture represents a precious resource for food security, sustainability and the creation of economic opportunities in inland areas. By harnessing untapped basin resources and promoting innovative practices, we can ensure sustainable growth and a central role for aquaculture in our future.

References

[1] Fiorella KJ, Okronipa H, Baker K, Heilpern S. Contemporary aquaculture: implications for human nutrition. Curr Opin Biotechnol. 2021 Aug;70:83-90.
[2] Miao C, Zhang J, Jin R, Li T, Zhao Y, Shen M. Microplastics in aquaculture systems: Occurrence, ecological threats and control strategies. Chemosphere. 2023 Nov; 340:139924. doi: 10.1016/j.chemosphere.2023.139924. Epub 2023 Aug 23.
[3] Toni M, Manciocco A, Angiulli E, Alleva E, Cioni C, Malavasi S. Review: Assessing fish welfare in research and aquaculture, with a focus on European directives. Animal. 2019 Jan;13(1):161-170.

Title: The use of vegetation indexes and proximity models in the study of population exposure to green spaces

Authors: Niccolò Martini*[1], Sofia Costanzini[1], Francesca Despini[1], Sergio Teggi[1], Tommaso Filippini[2], Marco Vinceti[2]

[1] *DIEF Department of Engineering "Enzo Ferrari", University of Modena and Reggio Emilia, Modena (Italy)*
[2] *Department of Biomedical, Metabolic and Neural Sciences, University of Modena and Reggio Emilia, Modena (Italy)*

Keywords: Case-Control Study, Green Spaces, Proximity Model, NDVI, Greenness

Abstract

The evaluation of the exposure of the population to environmental risk factors is a key point in epidemiological studies, as it allows to estimate the correlations between these factors and the occurrence of diseases.
Several studies have been conducted so far, the latest involved the relation between passive exposure to pesticides and risk of Amyotrophic Lateral Sclerosis (ALS) [1], outdoor artificial light and risk of early onset dementia [2], the impact of meteorological factors (temperature, relative humidity and ultraviolet radiation) on the spread of COVID-19 [3], and particulate matter from vehicular traffic and risk of dementia [4].
Currently, research efforts are mainly focused on two projects (one local UNIMORE FAR 2023 and one national PRIN 2022) aimed at studying the association between exposure to green spaces and light pollution on the risk of neurodegenerative diseases (dementia and amyotrophic lateral sclerosis, respectively).
Here the focus is to assess the exposure of each subject to green spaces. Epidemiological studies suggest that green space availability appears to be a relevant asset to improve population health, particularly mental health, thus decreasing the risk of cognitive impairment and dementia [5, 6].
The dataset used to study patients' exposure to green spaces is composed of 2434 people in the provinces of Modena, Parma and Reggio Emilia (Fig. 1). The residence address has been collected as of the recruitment date, provided it has been stable for the last 5 years.

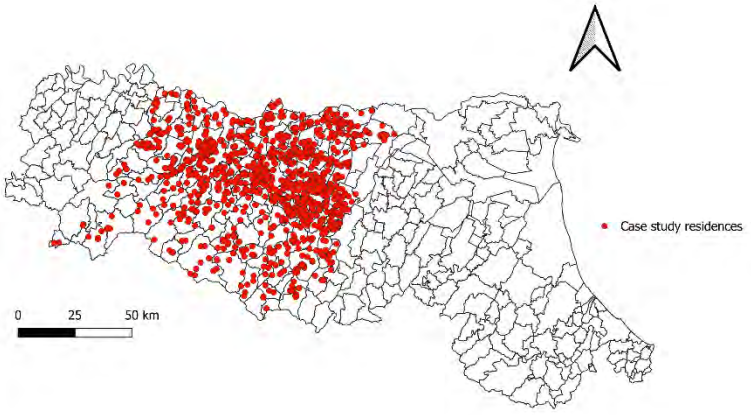

Fig. 1 Distribution of the case studies in the provinces of Modena, Parma and Reggio Emilia, Northern Italy.

Green spaces exposure assessment procedure:

For this purpose, we choose two indicators to model the amount of green spaces that is available for each receptor:

- The NDVI (Normalized Difference Vegetation Index) [7] is the main satellite indicator of the presence of vegetation on the Earth's surface and its evolution over time. The index is calculated from satellite images containing information in the red (R: 0.7 μm) and near-infrared (NIR: 0.9 μm) ranges. It evaluates the presence of photosynthetic activity, as it relates to the absorption in the red spectrum by the chlorophyll pigments, and the high reflectance of the leaves in the near-infrared necessary to prevent overheating;
- Greenness, an indicator of the presence of green areas obtained through a data transformation of a satellite image called Tasseled Cap [8]. This transformation reorganizes data into a new set of orthogonal axes, and it's designed to analyze vegetation changes detected by satellite sensors. The TC transformation provides 3 components. The primary axis, called Brightness, is calculated as the weighted sum of the reflectances of all spectral bands. Orthogonal to the first component, the second component is associated with green vegetation (Greenness), while the third component is orthogonal to the first two components and is associated with soil moisture and the presence of water (Wetness) [8].

The green areas indicators NDVI and Greenness were calculated from satellite images provided by the Landsat series satellites, and in particular the images acquired by Landsat 5, Landsat 7 and Landsat 8 were used to cover a total of 36 years, from 1985 to 2020. The diagnosis of both diseases can be affected by past exposure, so it is important to do a retrospective study as far back as possible in time. A Google Earth Engine procedure has been developed to extract the NDVI and Greenness values associated with each receptor (Fig. 2).

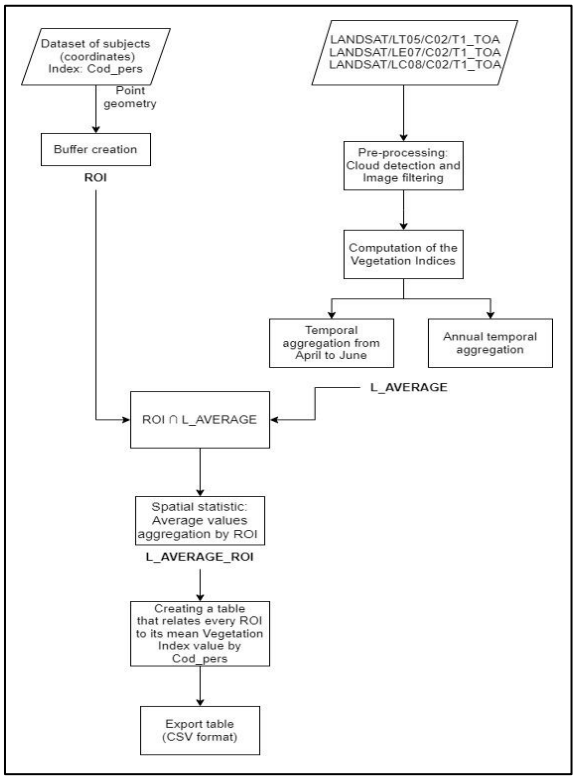

Fig. 2 Flowchart of the Google Engine procedure to extract the Vegetation Indices.

The selected images have been processed to remove unwanted conditions such as clouds and cloud shadows. For each pixel of each image the NDVI index and the Greenness have been calculated.
Once the two indexes are obtained for every pixel of every image, an annual mean of the NDVI and Greenness values is calculated to have only one image for each reference year. Given the high seasonal variability of these vegetation indexes, we also computed a mean of the values referred to the months April-May-June (AMJ) of each year to study the differences between the two approaches (annual vs AMJ).
Using the geographical coordinates of the subjects, their locations were overlapped with the satellite imageries. The exposure of the receptors was estimated according to the definition of a significant distance from the receptor considered, thus for each subject a buffer was created. The use of buffers to assess case study exposure has already been validated by previous epidemiological studies [9, 10]. The adoption of proximity models is a simplified approach compared to other models (i.e. dispersion models), and they can lead to over/underestimations. However, it has been shown that for assessments of long-term effects (multiple time-averaged exposure scenarios), and for spatially extended domains the geostatistical approach provides a good approximation of exposure even when compared with more accurate models [11]. In this study the calculation of the exposure was initially performed with the 100 m size buffer, according to [1]. Then, to assess the influence of the size of the buffers, the procedure was repeated even with 200 m buffers to compare the results. Finally, the mean value of the pixels within each buffer is performed. After these operations, we obtained the exposure as the annual or AMJ-averaged value of NDVI and Greenness for each buffer.

Results

The exposure scenarios calculated with different buffer sizes show similar results.
To assess the influence of green spaces on the considered diseases, the correlation between the aforementioned indexes and their temporal averaging was analyzed. In particular, we focused on the correlation between NDVI and Greenness evaluated on the same buffer dimension. Thus we assess how the temporal averaging (annual vs AMJ) affects the exposures.
Correlations have been calculated considering a 100 m buffer, especially between annual-averaged NDVI and Greenness and AMJ-averaged NDVI and Greenness. Fig. 3A shows an example of results obtained for the 2015 annual average.

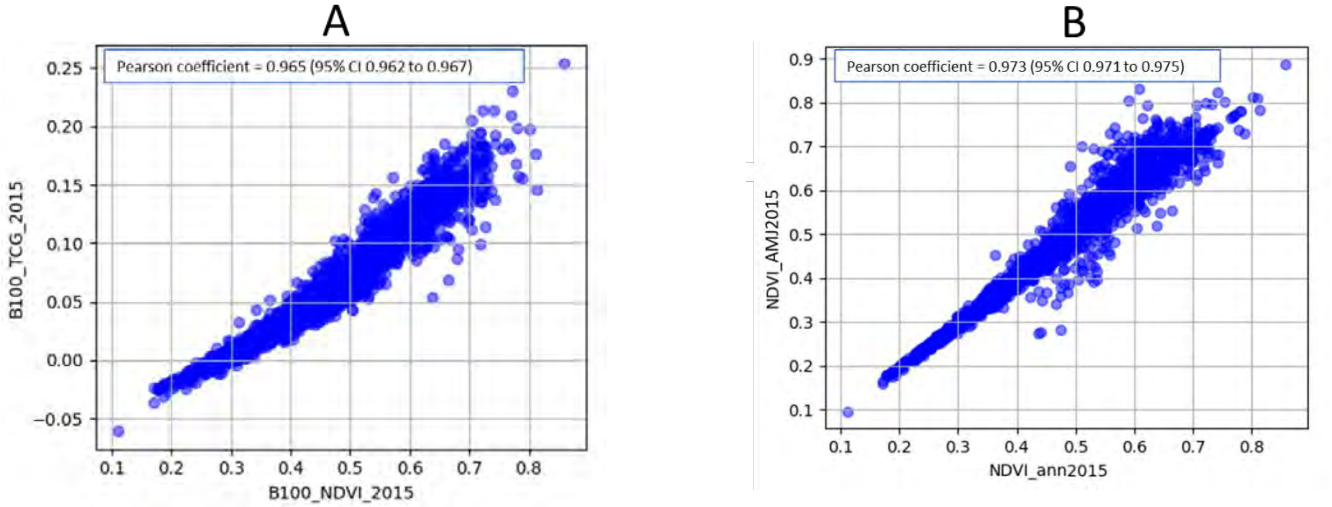

Fig.3 A.Correlation between NDVI and Greenness calculated with a buffer of 100m for the year 2015; B. Correlation between the annual mean of NDVI and the AMJ mean of NDVI for the year 2015.

Correlations, evaluated with the Pearson coefficient, show values up to 0.94 for all the years.
Finally, the influence of the temporal averaging, i.e. annual vs AMJ has been assessed (Fig. 3B). Here, we noticed a more pronounced variability with the coefficient values ranging from 0.985 to 0.771. This may be due to the availability of the less number of images in the AMJ period, in some cases very few (2 - 3 images). If the images were taken at the start of the considered period, for example, they could not be representative of the true variability of the indexes. Moreover, the pre-processing masking cloudy pixels would lead to a further loss of data.

Conclusions

In conclusion, the main findings of this application were that using Greenness or NDVI leads to similar exposures although NDVI could be preferred because of the simpler formulation.
In addition, the use of annual or seasonal averages may affect exposure estimation as both indexes vary strongly according to the phenological state of vegetation. Compared to the annual indexes, the use of indexes calculated with seasonal averages (AMJ) allows to obtain a more representative statistic of the presence of green spaces. Due to the high seasonal variability typical of the NDVI, an annual average may bias the estimates towards lower values of vegetation index, making it difficult to identify the targets exposed to green spaces, especially where there are mixed pixels of vegetation and impervious surfaces. Using instead a mean computed in the period where the vegetation is more flourishing (April-May-June) the pixels containing green spaces stand out more clearly, making it easier to identify them and to evaluate the exposure, thus reducing risk of misclassification.
Overall, the study provides a foundation for the subsequent use of such green space indexes for the evaluation of their association with neurodegenerative disease risk.

References:

[1] M. Vinceti *et al.*, “Pesticide exposure assessed through agricultural crop proximity and risk of amyotrophic lateral sclerosis,” *Environ Health*, vol. 16, (2017).
[2] E. Mazzoleni *et al.*, “Outdoor artificial light at night and risk of early-onset dementia: A case-control study in the Modena population, Northern Italy,” *Heliyon*, vol. 9, (2023).
[3] E. Balboni *et al.*, “The influence of meteorological factors on COVID-19 spread in Italy during the first and second wave,” *Environ Res*, vol. 228, (2023).
[4] T. Urbano *et al.*, “Particulate matter exposure from motorized traffic and risk of conversion from mild cognitive impairment to dementia: An Italian prospective cohort study,” *Environ Res*, vol. 222, (2023).
[5] Slawsky, Erik D. *et al.*, “Neighborhood greenspace exposure as a protective factor in dementia risk among U.S. adults 75 years or older: a cohort study”, *Environmental Health: A Global Access Science Source,* vol. 9, (2022)
[6] Bagheri, Nasser et al. “The Impact of Built and Social Environmental Characteristics on Diagnosed and Estimated Future Risk of Dementia”, *Journal of Alzheimer's Disease,* vol. 84, (2021)
[7] J. Weier and D. Herring, “Measuring vegetation (ndvi & evi),” *NASA Earth Observatory*, (2000).
[8] E. P. Crist and R. C. Cicone, “A Physically-Based Transformation of Thematic Mapper Data-The TM Tasseled Cap”, (1984).
[9] C. Malagoli *et al.*, “Passive exposure to agricultural pesticides and risk of childhood leukemia in an Italian community,” *Int J Hyg Environ Health*, vol. 219, pp. 742–748, (2016).
[10] K. P. Wittich and J. Siebers, “Aerial short-range dispersion of volatilized pesticides from an area source,” *Int J Biometeorol*, vol. 46, pp. 126–135, (2002).
[11] S. Costanzini *et al.*, “Atmospheric dispersion modeling and spatial analysis to evaluate population exposure to pesticides from farming processes,” *Atmosphere (Basel)*, vol. 9, (2018).

Title: Selection of fungi for the biofertilisation of phosphorus ($Ca_3(PO_4)_2$) in arid soils

Author(s): Rim Werheni Ammeri[1,2], El Bouali Sonia[2], Hammami Rania[2], Najla Sadfi-Zouaoui[2]

[1] *National Bone Marrow Transplant Center, Laboratory Ward, Tunis Rue Djebel Lakhdar 1006,Tunisia rimwerheni@gmail.com*
[2] *Laboratory of Mycology, Pathologies and Biomarkers (LR16ES05), Faculty of Sciences of Tunis, University Tunis El Manar, 2092 Tunis, Tunisia. : najla.sadfi@fst.utm.tn*

Abstract

The sustainable development of agriculture can be stimulated by the great market availability of bio-inputs, including phosphate-solubilizing microbial strains. However, these strains are currently selected using imprecise and questionable solubilization methodologies in solid or liquid media. We hypothesized that the hydroponic system could be a more efficient methodology for selecting phosphate-solubilizing strains as plant growth promoters. This methodology was tested using the plant Glycine max as a model. The growth-promoting potential of the strains was compared with that of the Biomaphos® commercial microbial mixture. The obtained calcium phosphate (CaHPO4) solubilization results using the hydroponic system were inconsistent with those observed in solid and liquid media. However, the tests in liquid medium demonstrated poor performances of *Codinaeopsis* sp. (328EF) and *Hamigera insecticola* (33EF) in reducing pH and solubilizing CaHPO4, which corroborates with the effects of biotic stress observed in G. max plants inoculated with these strains. Nevertheless, the hydroponic system allowed the characterization of *Paenibacillus alvei* (PA12), which is also efficient in solubilization in a liquid medium. The bacterium *Lysinibacillus fusiformis* (PA26) was the most effective in CaHPO4 solubilization owing to the higher phosphorus (P) absorption, growth promotion, and physiological performance observed in plants inoculated with this bacterium. The hydroponic method proved to be superior in selecting solubilizing strains, allowing the assessment of multiple patterns, such as nutritional level, growth, photosynthetic performance, and anatomical variation in plants, and even the detection of biotic stress responses to inoculation, obtaining strains with higher growth promotion potential than Biomaphos®. This study proposed a new approach to confirm the solubilizing activity of microorganisms previously selected in vitro and potentially intended for the bio-input market that are useful in P availability for important crops, such as soybeans

Keywords: phosphorus, fungi, soil, solubilization

PARALLEL SESSION: Poster

Title: Study of the Adsorption Process of Methyl Violet Dye in Sugar Cane Bagasse

Author(s): Mateus Felipe Pereira Fonseca[1], Patrícia Procópio Pontes*[2]

[1] *Chemistry Department, CEFET-MG, Belo Horizonte, Brazil, mateus.felipe.k@hotmail.com*
[2] *Chemistry Department, CEFET-MG, Belo Horizonte, Brazil, patriciaprocopio@yahoo.com.br*

Keyword(s): Textile dyes, sugar cane bagasse, adsorption, bioadsorption

Abstract

The textile industry is responsible for the production of effluents contaminated with dyes that are generally recalcitrant, carcinogenic, mutagenic and harmful to aquatic life [1]. It is therefore necessary to treat these effluents in order to avoid environmental impacts. Adsorption is a viable treatment alternative, as it can be carried out with residues from other production processes, such as sugarcane bagasse and sawdust, which are bioadsorbents with great adsorption potential.

To facilitate the separation of bioadsorbents from the liquid effluent, one of the alternatives is the immobilization of these bioadsorbents, through a process that creates a matrix that is easily separated from the treated effluent.

The present work aimed to study the removal of textile dye using free and immobilized sugarcane bagasse as an adsorbent.

Material and Methods

The experiments were performed in triplicate using orbital shaker under stirring at 130 rpm and methyl violet dye synthetic effluent in order to compare process variables such as adsorbent granulometry, contact time and effect of immobilization and pretreatment of adsorbent on dye adsorption efficiency. Adsorption column experiments were also performed in laboratory scale.

The first stage of the treatment process was drying the sugarcane bagasse, which occurred at approximately 250 °C. Then, the adsorbent went through a comminution and sieving process obtaining different particle sizes (Table 1).

Table 1. Adsorbent Granulometry

Granulometry	Mesh	Dimension (mm)
1	>35	< 0,500
2	20<x<35	0,500 <x< 0,841
3	10<x< 20	0,841<x< 2,00

Part of the sieved bagasse was pretreated with 0.5 $mol.L^{-1}$ sodium hydroxide solution. For the pretreatment, 25 mL of the solution were used for 1.0 g of adsorbent. The pretreatment occurred by agitating the bagasse with NaOH for 1 hour in a Cienlab orbital shaker at 130 rpm.

The treatment of effluent containing methyl violet dye was carried out in batch using an orbital shaker under agitation at 130 rpm. For the experiments, 1.0 g of free adsorbent and 50 mL of methyl violet solution with a concentration of 50 $mg.L^{-1}$ were added in a erlenmeyer flask. During the agitation period, aliquots were removed at different time intervals for analysis. These aliquots were filtered through a syringe filter to eliminate any trace of the adsorbent and then their absorbance was determined using a spectrophotometer at a wavelength of 576 nm. These analyzes were carried out in triplicate for the three previously selected sugarcane bagasse particle sizes. For these experiments, both sugarcane bagasse previously treated with NaOH and bagasse without pretreatment were used.

In addition to these batch processes, experiments were also carried out in an adsorption column (Table 2). The methyl violet solution with a concentration of 50 $mg.L^{-1}$ was treated in a column filled with sugarcane bagasse of particle size 2 (between 0.5 and 0.841 mm), with and without pretreatment and immobilized. The column height for both cases was 15 cm, the column diameter 2 cm and the flow rate 0.1 $mL.s^{-1}$. Then, the same process was repeated for the free sugarcane bagasse, varying the column height to 10 cm and the flow rate to 0.5 and 1.0 $mL.s^{-1}$, maintaining the diameter in 2 cm. The effluent was analyzed using a spectrophotometer to determine the efficiency of the processes.

Table 2. Experiments in adsorption column using methyl violet solution with a concentration of 50 $mg.L^{-1}$

Adsorbent	Granulometry	Column Height (cm)	Flow ($mL.s^{-1}$)
Immobilized Sugarcane bagasse	2	15	0.1
Free Sugarcane bagasse	2	10 and 15	0.1; 0.5; 1.0

Results and Discussion

It is known that the greater the surface area of an adsorbent, the greater the tendency for the adsorption process to become more efficient, since this occurs precisely on the surface [2]. Therefore, reducing the size of an adsorbent is an efficient way to increase its surface area and, therefore, the efficiency of the process.

In this research, the results obtained for the methyl violet adsorption process for different particle sizes of sugarcane bagasse indicated that the three particle sizes showed very similar efficiencies in tests with and without pre-treatment, with average efficiency values varying from 93% (with pre-treatment) to 96% (without pre-treatment) with 15 to 30 minutes of contact time (Figure 1). It was possible to observe that the smaller the particle size, the greater the efficiency of the process, as previously predicted. However, the difference in efficiency from the most comminuted bagasse to the least was not significant and, therefore, it was more viable to use a larger granulometry, as it provides high efficiency and is easier to obtain.

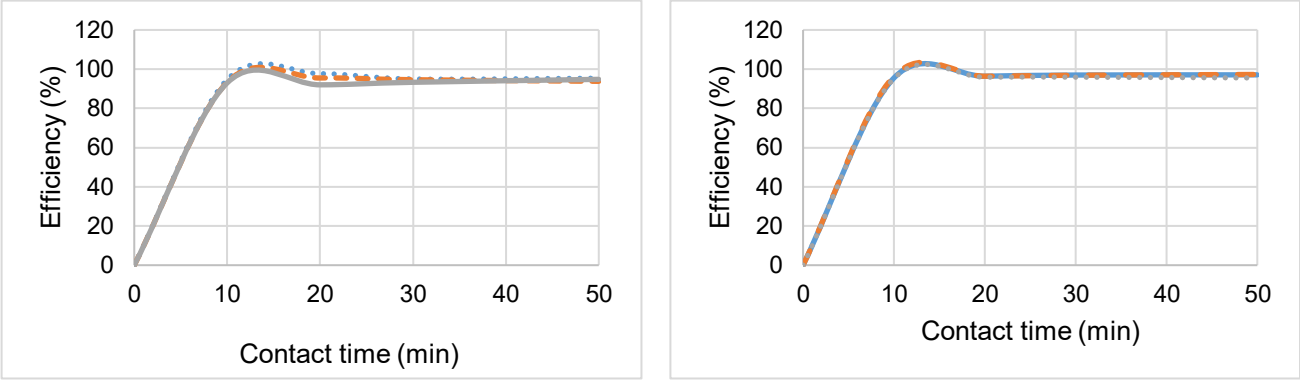

Figure 1. Removal efficiency of methyl violet (50 mg.L^{-1}) as a function of contact time for three different particle sizes of sugarcane bagasse (a) pretreated with 0.5 mol.L^{-1} NaOH and (b) without pretreatment.

Where:
- Sugarcane bagasse: granulometry >35 mesh
- Sugarcane bagasse: granulometry 20<x<35 mesh
- Sugarcane bagasse: granulometry 10<x< 20 mesh

Based on these data, a particle size between 20 and 35 mesh was selected as the best alternative as it does not need to undergo much fragmentation and still presents satisfactory efficiencies. Even though the larger particle size also offered good efficiency results, it was decided to select the particle size between 20 and 35 mesh as it provided an adsorbent that is easy to handle and obtain.

The pretreatment of the adsorbent was carried out to compare the impacts it would provide on the removal efficiency of the methyl violet dye. It was used pretreatment with a basic solution due to the fact that the dye studied is cationic. Using a basic solution for treatment would increase negative functional groups on the surface of sugarcane bagasse due to the action of hydroxide anions. Furthermore, pretreatment also eliminates water-soluble groups, increasing the surface area of the adsorbent [3].

Differently from expectations, sugarcane bagasse without pretreatment provided a higher removal efficiency than bagasse with basic pretreatment, although the difference was small (Figure 1). This may have occurred due to the fact that the bagasse already had functional groups that interacted well with the dye, not requiring pretreatment, which may have replaced some functional groups with others that interact less efficiently with methyl violet. However, it must also be considered that the difference in adsorbent efficiency was very small and this may indicate that the pretreatment did not affect the adsorbent characteristics significantly.

Evaluating the results of the experiment, it was noticeable that the longer the contact time, the greater the efficiency of the process up to a certain limit at which it stabilized. In the cases studied, it was observed that between approximately 10 and 15 minutes, maximum removal efficiency was already reached.

Table 3 presents the results obtained for the column adsorption experiments. For all cases, the column diameter was 2 cm and the initial concentration of methyl violet in the effluent was 50 mg.L^{-1}.

Table 3. Experiments in adsorption column using methyl violet solution with a concentration of 50 mg.L^{-1}

Adsorbent	Granulometry	Column Height (cm)	Flow (mL.s^{-1})	Average Efficiency (%)
Immobilized Sugarcane bagasse	2	15	0.1	64.8
Free Sugarcane bagasse	2	15	0.1	99.4
Free Sugarcane bagasse	2	10	0.1	98.5
Free Sugarcane bagasse	2	15	0.5	97.1
Free Sugarcane bagasse	2	15	1.0	96.4

Conclusions

The results indicated that the dye removal efficiency reached values above 90%, confirming the possibility of textile dye adsorption in sugarcane bagasse.

Particle size between 20 and 35 Mesh was the best alternative for the adsorbent because it did not have to undergo much fragmentation and had satisfactory efficiencies.

Unlike expected sugarcane without pretreatment provided higher removal efficiency than bagasse cane with pretreatment.

References

[1] Lellis,B., Favaro-Polonio, C.Z., Pamphile, J.A., Polonio, J.C. Effects of textile dyes on health and the environment and bioremediation potential of living organisms, Biotechnology Research and Innovation, Vol. 3, 2, 275-290, 2019.
[2] Nascimento, R. F. D. et al. Adsorção: aspectos teóricos e aplicações ambientais. UFC, Fortaleza 2014.
[3] Silva, W. L. L.; Oliveira, S. P. Modification of the sorptive characteristics of sugarcane bagasse for removing methylene blue from aqueous solutions. Scientia Plena, Vol. 8, 9, p. 1-8, 2012.

Evolution of wastewater purification: a historical perspective on innovation, regulation and knowledge transfer

Author(s): Bartolomeo Cosenza[1], Angelo Siragusa[2], Giovanni Mappa[3],

[1] *Dipartimento di Ingegneria Civile e Industriale, Università degli studi di Pisa, Largo Lucio Lazzarino, 56122 Pisa (PI), Italy, bartolomeo.cosenza@unipi.it*
[2] *Independent Researcher, Palermo (PA), Italy, angelo.siragusa@gmail.com*
[3]*Innovation Manager c/o ANOVA Studi, Napoli (NA), g.mappa@anovastudi.com*

Keyword(s): *purification, wastewater, technology, management, experience.*

Abstract

Over the centuries, humanity has embarked on a journey towards understanding and managing its water resources, especially when it comes to wastewater purification. This journey has spanned eras of discovery, innovation and challenges, shaping an intricate landscape of methodologies, technologies and regulations. From the simple observation of nature to the digital revolution, the wastewater purification sector has undergone a radical transformation, driven by increasingly stringent and intransigent environmental, regulatory and scientific needs. The aim of this work is to offer a historical overview of the evolution of wastewater purification, highlighting the crucial role of environmental and regulatory challenges and the importance of incorporating the latest technological innovations to optimize efficiency and ensure sustainability of purification processes. In parallel, this works intends to promote targeted and continuous training of the personnel involved, offering valuable guidance based on the experience accumulated by experts in the sector. The growing interest of the scientific community and professionals in preserving and sharing with future generations the entire wealth of experiences accumulated over time is closely linked to the history of wastewater management. Before the introduction of wastewater purification plants, the main purification mechanism was natural self-purification. Culturally and operationally, the management of water purification processes begins with this fundamental principle. However, it was in 1914 that the scholars Arden and Lockett, attracted by the concept of the "self-purifying power" of waterways, began to study the phenomena related to aerated biofiltration. From here the idea of the "activated sludge" process was born, which has represented for many decades, and still continues to represent today, the most widespread method in the world to purify wastewater [1],[2]. This process has undergone evolutions over time, thanks to the introduction and adoption of new emerging technologies, which have contributed to improving its efficiency and sustainability.In the 1970s and 1980s, numerous wastewater treatment plants were built in Italy, the management of which was often based on the "West Method" criterion (in Italy better known as "Occhio di lince") [3]. This approach, developed in the United States, was based on direct observation and interpretation of activated sludge characteristics such as: consistency, color, odor and foaming. These visual and sensorial signals provided operators with crucial indications on the functioning of the purification process and on the need for any corrective interventions. It is important to note that the West Method cannot be classified as a real control method but rather an aid and support aimed at assisting operators in identifying the quality of the activated sludge and the general state of the purification process, and in make decisions based on the information collected. In subsequent years, with the advent of more advanced technologies, such as real-time monitoring systems and process automation, the

management of purification plants has been further optimised, allowing for greater efficiency and better quality of wastewater treatment. Among the tools for verifying the functionality of an activated sludge purification plant, the classic "Imhoff cone tests" [4] must certainly be mentioned, later replaced by other more precise evaluation methods (such as the sedimentability tests of the sludge in oxidation tanks and recycling in 1 liter cylinder). These techniques allow the evaluation of both the sedimentation capacity of the sludge and the concentration of suspended solids, thus providing a more accurate assessment of the overall quality of the sludge. Initial guidance on COD (Chemical Oxygen Demand)-based nutrient fractionation and spirometric testing was essential to understanding the composition and biodegradability of wastewater [5]. The centrifugal machines widely used in purification plants were initially designed for oil mills and were then adapted for use in sludge treatments, even though they often performed poorly. New centrifugal machines then took over. Machines designed to be slimmer and with a lower center of gravity, ensuring greater operational efficiency [6]. Among the innovations are also the low energy consumption screw presses, which work continuously 24 hours a day. These technologies represent an important step forward in sludge management, offering greater efficiency, energy savings and reduction of operating costs. Turbidity measurements on treated wastewater required field sampling and the use of laboratory benchtop turbidimeters. This process was simplified with the introduction of continuous process cabin instruments where the measurement sensors were inserted. Today, measurement occurs continuously with optical sensors immersed directly in the purified water discharge channels, ensuring real-time and highly precise monitoring [7]. In the past, to monitor the level of sludge in the final settlers, the sedimentation disk method was used, which consisted of manually observing the deposition of the sludge on a graduated disk. This technique, however, was limited by its subjective nature and the need for accurate interpretation by the operator. With the advancement of technology, sludge level meters have become the prevalent choice in modern plants. These devices can provide automated and more precise measurement of sludge levels, minimizing the risk of human error and improving the overall efficiency of the purification process [8]. Previously, during the monitoring of the plant, the restoration of the faulty machines was done manually by the operating operators. This implied direct involvement of the staff to check for any tripping of circuit breakers or blown fuses. Subsequently, more automated solutions were introduced, such as contactors with motorized reset and fuses that reset automatically. The advent of PLCs has further improved operational efficiency, allowing automated control of each machine via a dedicated hour meter and simplifying exchange between machines [9]. Microscopic observations of activated sludge have always played a crucial role in diagnosing the health of the purification process. Using phase contrast microscopes, it was possible to identify filamentous bacteria and ciliated protozoa, providing valuable information on the quality of the treatment. With the introduction of the FISH technique and the use of diagnostic software based on numerical counting, the analysis has become more detailed and accurate, helping to identify dominant species. The microscopic control of the activated sludge floc has become standard practice in every laboratory inside or outside the plant. These analyzes provide predictive information on toxicity or nutrient deficiency phenomena, allowing operators to take timely action to preserve biomass and maintain effective water purification [10]. Regarding the monitoring of Purification Indices (ID) [11], in the past, reliance was placed on synoptic panels, akin to those used in industrial plants, to visualize the operational status of the plants. These panels were equipped with visual indicators, such as red, green, or yellow lights, to indicate correct operation or any anomalies. However, the system could be complex for the staff, particularly given the different conventions established for reporting faults or anomalies, often denoted by the color orange. Today, digitalization is revolutionizing the management processes of purification plants. Data centralization enables unified, real-time control of different processes, facilitating optimization through advanced predictive control [12]. This approach uses algorithmic models that learn from past situations and are able to predict and resolve issues proactively, keeping operational variables at optimal levels. All this not only increases the overall efficiency of the purifiers, but also provides greater robustness to

the processes, reducing the risk of failures and improving the quality of wastewater treatment. In modern "control rooms", screens show the monitored sections in real time, allowing remote control operators to supervise operations. In case of anomalies, an alarm is automatically activated, even on non-working days, and the available operators are ready to intervene. The centralized approach offers several opportunities [13], such as the ability to predict the quality of collected water, automate the dosing of coagulant reagents, simulate the properties of chemicals in storage, monitor the performance of decanters and intelligently plan filter washing. Furthermore, energy efficiency [14] is also improved by optimizing storage and pumping, considering electricity tariffs and photovoltaic generation (if available). Similarly, the manual compilation of the machine maintenance log has been replaced by the use of dedicated maintenance apps. These apps allow operators to scan QR codes to document the steps during scheduled and extraordinary maintenance operations. In addition to simplifying the registration process, maintenance apps offer more accurate tracking of activities performed, ensuring more efficient and timely maintenance. These advancements reflect an evolution towards more automated and computerized management of industrial operations, improving precision, efficiency and transparency in the execution of production and maintenance activities. Practices are also subject to change. The practice of manually filling out the driving booklet, for example, is just a distant memory. Thanks to the advent of new generation PLCs it is possible to automatically compile the register using the information collected from the control systems and process sensors. PLCs constantly monitor machine counts and process parameter values, updating the register in real time without the need for manual intervention. Even environmental impact considerations due to treatment plants have not been exempt from the change, fortunately [15], [16]. The problem of atmospheric emissions from sludge lines, for example, never received the necessary attention until the introduction of article 272 paragraph 2 of Legislative Decree 152/2006 and subsequent amendments. This article obliges the managers of purification plants with sludge treatment lines, operating in establishments dedicated exclusively to the treatment of wastewater, with a treatment capacity of at least 10,000 equivalent inhabitants for biological treatments and/or at least 10 m3/h of treated water for chemical/physical treatments, to comply with certain standards. This legislation introduced greater responsibility of plant managers in the control of air emissions deriving from sludge treatment operations, highlighting the importance of also addressing this critical aspect of water purification. The first activated sludge simulations were performed using programs such as "PFA and Denitrogest", stored on floppy disks. Over time, modeling has become more sophisticated, making use of increasingly complex and detailed models such as ASM1 and ASM2 [17], together with various applications such as SWATER (https://swater-saas.com/), capable of simulating the operation of purification plants in detail. These models allow you to create a digital twin of the plants [18], combining the modeling of each compartment with real data from sensors in the field. New technologies, such as drones equipped with IR ray systems allow aerial monitoring of plant areas, while cameras continuously monitor critical sections of the plants. Trained robots can perform specific inspections at certain times or based on certain conditions [19]. And innovative sensors, such as toxicity “sentinels,” are increasingly used to detect hazardous substances in wastewater. These technologies help increase the reliability of plant management, reducing human errors to a minimum. Over the decades, purification plants have undergone considerable technological progress, with the introduction of increasingly efficient tools and more sophisticated processes. However, this progress has not been accompanied by an effective handover between generations of industry professionals. Older chemical engineers, with decades of experience, have accumulated valuable knowledge, but the blocking of public competitions in management companies, often tied to an old organizational mold, has limited the entry of new talent. This generation gap has caused a loss of knowledge and skills, with a lack of connection between the vast experience gained over the years and the new generation of inexperienced professionals. Without adequate knowledge transfer, young professionals may find themselves unprepared to face emerging challenges and make full use of new available technologies. The handover

is essential to preserve and transmit the experience accumulated over time, allowing continuity in the management of the purification plants. New generations can bring innovation and freshness, but they need the guidance and support of older experts to fully develop their skills. Addressing this gap requires a commitment from institutions and companies to promote mentoring and professional development programs, as well as foster an inclusive and collaborative work environment. Only in this way will it be possible to guarantee optimal management of purification plants and adequately prepare future generations of professionals in the sector.

References

[1] Awasthi M. K., Ganeshan P., Gohil N., Kumar V., Singh V., Rajendran K., ... & Taherzadeh M. J., Advanced approaches for resource recovery from wastewater and activated sludge: A review. Bioresource Technology, 129250,(2023).
[2] Jenkins D., Richard MG, & Daigger GT, Manual on the causes and control of activated sludge bulking and foaming – Water Research Commission and U.S.EPA (1986).
[3] Manual of instruction for wastewater treatment plant operators - New York State Dept. Of Enviromental Conservation- vol. I, 5-35.
[4] Wertz, C. F.. Routine Tests for Operation of Sewage Treatment Works. *Sewage Works Journal*, *3*(4), 669-675, (1931).
[5] Mainardis, M., Buttazzoni, M., Cottes, M., Moretti, A., & Goi, D. (2021). Respirometry tests in wastewater treatment: Why and how? A critical review. *Science of the Total Environment*, *793*, 148607.
[6] Alt, C., Centrifuges for sludge treatment. In Water, Wastewater, and Sludge Filtration (pp. 249-273). CRC Press, (2020).
[7] Kitchener B. G., Wainwright J., & Parsons A. J. A review of the principles of turbidity measurement. Progress in Physical Geography, 41(5), 620-642, (2017).
[8] Ahmad T., Ahmad K., & Alam M., Sludge quantification at water treatment plant and its management scenario. Environmental Monitoring and Assessment, 189, 1-10, (2017).
[9] Rajhans A. R., More S. S., Gambhir S. V., & Deshmukh V. H. Review paper on wastewater treatment plant using PLC & SCADA. International Journal of Engineering Applied Sciences and Technology, 4(12), 2455-2143, (2020).
[10] Mesquita D. P., Amaral A. L., & Ferreira E. C., Activated sludge characterization through microscopy: A review on quantitative image analysis and chemometric techniques. Analytica Chimica Acta, 802, 14-28, (2013).
[11] Quevauviller P., Thomas O., & Derbeken A. V., Wastewater quality monitoring and treatment. John Wiley & Son, (2006).
[12] Matheri A. N., Mohamed B., Ntuli F., Nabadda E., & Ngila J. C., Sustainable circularity and intelligent data-driven operations and control of the wastewater treatment plant. Physics and Chemistry of the Earth, Parts A/B/C, 126, 103152, (2022).
[13] Pasciucco F., Pecorini I., & Iannelli R. (2022). Planning the centralization level in wastewater collection and treatment: A review of assessment methods. Journal of Cleaner Production, 375, 134092.
[14] Molinos-Senante M., & Maziotis A., Evaluation of energy efficiency of wastewater treatment plants: The influence of the technology and aging factors, Applied Energy, 310, 118535, (2022).
[15] Rashid S. S., Harun S. N., Hanafiah M. M., Razman K. K., Liu Y. Q., & Tholibon D. A., Life cycle assessment and its application in wastewater treatment: a brief overview. Processes, 11(1), 208, (2023).
[16] Lin J., Ye W., Xie M., Seo D. H., Luo J., Wan Y., & Van der Bruggen B.. Environmental impacts and remediation of dye-containing wastewater. Nature Reviews Earth & Environment, 4(11), 785-803, (2023).
[17] Duarte M. S., Martins G., Oliveira P., Fernandes B., Ferreira E. C., Alves M. M., ... & Novais P. A Review of Computational Modeling in Wastewater Treatment Processes. ACS ES&T Water (2023).
[18] Liu W., He S., Mou J., Xue T., Chen H., & Xiong W. Digital twins-based process monitoring for wastewater treatment processes. Reliability Engineering & System Safety, 238, 109416, (2023).
[19] Tempea I., Contributions on the use of mobile robots in wastewater treatment plants. Annals of'Constantin Brancusi'University of Targu-Jiu. Engineering Series/Analele Universităţii Constantin Brâncuşi din Târgu-Jiu. Seria Inginerie, (2), (2023).

Analysis of textile waste streams for regional planning: the Lombardy region case study

Authors: Samuele Abagnato*[1], Mario Grosso[1], Lucia Rigamonti[1]

[1] *Dipartimento di Ingegneria Civile e Ambientale, Politecnico di Milano, Piazza Leonardo da Vinci 32, 20133 Milano (MI), Italy, {samuele.abagnato,mario.grosso,lucia.rigamonti}@polimi.it*

Keywords: textiles, waste management, flow analysis

Abstract

Textile waste management is becoming a topic of great interest, because of the high environmental impacts of the textile industry and because of the spreading of business models that encourage a short service life of textile products, especially of garments [1]. These aspects of high concern brought the European Commission to adopt the “EU Strategy for Sustainable and Circular Textiles” [2] and to develop new policies. The Waste Framework Directive [3] establishes the mandatory separate collection of textiles as a fraction of the municipal waste by 2025 for Member States. In addition, the institution of Extended Producer Responsibility (EPR) schemes for textile products is proposed [4]. The amount of textile waste that will be collected and that will need a proper management is going to increase in the following years. For this reason, the quantification and the mapping of this waste stream are very important to plan efficient waste management system addressed to textiles.
Different researches proposed case studies about textile waste management, investigating different scenarios of separate collection, reuse and recycling rates [5, 6] or focusing on the composition of the textile waste [7, 8]. The quantification of textile waste streams through a material flow analysis can be the first step to assess the environmental impacts of textile waste management in a life cycle perspective [9].
Previous studies are mainly focused only on one type of textile waste stream, usually the municipal textile waste separately collected. The goal of the present work is to give a picture of all the textile waste streams at a regional scale. To this purpose, Lombardy (Italy) was identified as case study. First, the methodology adopted for the data elaboration is explained. Then, different analyses are carried out to understand which are the main characteristics of the current textile waste management system in Lombardy in order to support future policies. In the end, future research pathways are suggested.
The first step is the selection, through a screening of the European list of waste [10], of the types of textile waste to include in the analysis. In the present work, pre-consumer, post-consumer and textiles from the mechanical treatment of waste were considered, as summarised in Table 1.

Table 1 – Textile waste streams considered in the analyses.

Type of textile waste	Waste description and code according to the European list of waste
Pre-consumer textile waste	Waste from unprocessed textile fibres (04 02 21) Waste from processed textile fibres (04 02 22)
Post-consumer textile waste	Clothes from separate collection (20 01 10) Textile products from separate collection (20 01 11)
Textiles from waste treatments	Textiles from the mechanical treatment of waste (19 12 08)

The analysis was carried out with data referred to year 2021.
For each type of textile waste, several data were provided by ARPA Lombardia (the Regional

Environmental Agency), in particular: (i) the amount of waste produced with the list of producers; (ii) the amount of waste collected by waste transporters and received by the treatment plants; (iii) the amount of waste that each waste producer or treatment plant sent to other plants; (iv) the amount of waste treated by each receiving plant. To avoid the double counting of waste streams, the data referred only to transport operations were not considered. For each treatment plant, the amount of textile waste received, sent to other plants, and addressed to recovery or disposal was identified. For each treatment plant, the mass balance was verified. The sum of the quantities was calculated in order to obtain the total streams for each type of textile waste analysed.

The waste in input to the plants was split between "primary flow" (waste received from primary producers) and "secondary flow" (waste received from other plants). The primary flow was then split according to the geographical origin of the waste producer. Similarly, the waste stream sent outside the plants was split according to the location of the receiving subject. In addition, the waste generated in Lombardy and directly sent outside the region by waste producers was considered. The different treatment operations were defined according to [11] and grouped in four categories: (i) disposal; (ii) energy recovery; (iii) material recovery; (iv) preliminary operations or storage. The sum of the amount addressed to these operations is the total of the waste treated.

The results of the waste flows for the three different types of textile waste are summarised in Figure 1. The amount of pre-consumer and post-consumer textile waste received in input by plants in Lombardy resulted quite similar (35.1 kt and 38.5 kt respectively), while textiles from waste treatment were lower (10.5 kt). 70% of the total pre-consumer textile waste comes from Lombardy, while for the post-consumer waste this share is higher (87%). For textiles from waste treatment, instead, 55% came from other Italian regions. For post-consumer textile waste, the amount of waste sent outside the regional boundaries was very relevant (30.6 kt, corresponding to 73% of the total post-consumer waste), while for the other two types of textile waste almost all the waste in input was treated by the plants in Lombardy.

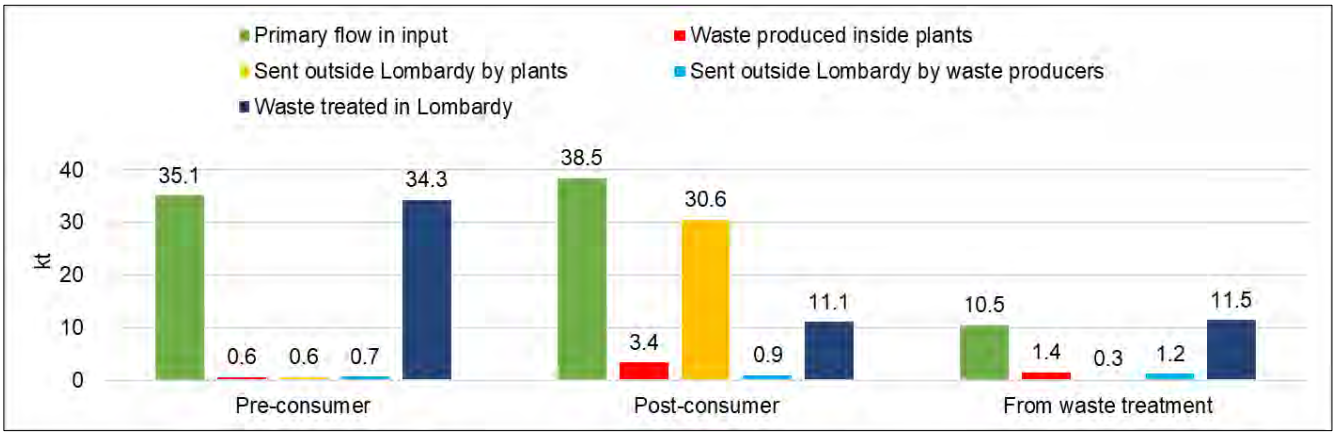

Figure 1 – Waste flows for each type of textile waste.

Among the waste treatment operations, 48%, 82% and 28% of the treated waste was addressed to material recovery respectively for pre-consumer waste, post-consumer waste and textile waste from previous treatments. Preliminary operations or storage covered an important share of the treatment operations (51%, 17% and 39% respectively for the three waste categories). Only for textiles from previous waste treatment the energy recovery was relevant (33%). To gather information about the material recovery processes, some interviews to the main textile waste management companies of the region have been carried out. For post-consumer textile waste, about 70% of the material recovery consists in the preparation for reuse (sanitization, sorting and sale on the global second-hand market),

and around 30% consists in recycling (mainly downcycling to produce industrial wipes, insulation or filler materials). About the pre-consumer textile waste, the recovery processes consist in a sorting step, where impurities are removed, and bales of homogeneous composition are obtained. The bales can be directly sold to downstream customers or sent to an unraveling process, where the textile fibres are opened in order to mechanically recycle them.
After the definition of the textile waste streams in Lombardy, different analyses about the number of the plants and about their size were carried out (Table 2). In total, in Lombardy in 2021, 180 subjects declared to manage the textile waste streams considered in this work. 79% of these subjects treated only one type of the aforementioned textile waste streams, 18% managed two types of textile waste, 3% treated three of them. Most of the plants treated pre-consumer waste, as can be seen in Table 2.
The plants were classified into classes according to the amount of managed waste (0-100 t, 100-300 t, 300-500 t, 500-1000 t, > 1000 t). For all three types of textile waste, most of the plants were in the first class, with less than 100 t managed in 2021 (Table 2).
In order to consider the size, the plants were ordered decreasingly according to the amount of waste managed. Then, the number of plants that contributed to at least 50% of the total waste managed was identified. This indicator was called N50. The share between N50 and the total number of plants is reported in Table 2. The low values of this share for all the waste types confirms that in Lombardy there are few plants that contribute to manage most of the waste. For instance, for post-consumer textile waste, only 6% of the plants treated half of the total waste in input to the plants of the region.

Table 2 – Number and size of the plants for each type of waste. The % of plants on the total is shown for each size class. With N50 is indicated the number of plants that contributed to reach 50% of the total waste, after that the plants were ordered in decreasing order according to the amount of waste managed.

Type of textile waste	N° of plants	0-100 t (%)	100-300 t (%)	300-500 t (%)	500-1000 t (%)	> 1000 t (%)	N50 / N tot (%)
Pre-consumer	132	55%	19%	9%	11%	6%	8%
Post-consumer	72	67%	6%	4%	8%	15%	6%
Textile from waste treatment	20	45%	10%	25%	5%	15%	10%

In the end, the textile waste composition was estimated. Since pre-consumer textile waste comes from the manufacturing processes of textile fibres, its composition was estimated from data about the Italian textile industry production in 2021 [12]. The composition of post-consumer textile waste was assumed from the literature [13]. The third type of waste (textiles from mechanical treatment of waste) is likely to come from previous operations on other textile waste streams. To verify this hypothesis, a screening about the sources of this type of waste in Lombardy was carried out. It was found that 79% of the textiles from waste treatment came from plants managing other types of textile waste streams (94% from pre-consumer and 6% from post-consumer). The remaining 21% was assumed to have unknown composition, because there were no data to support any assumption about this. So, the composition of the last type of textile waste was calculated as a weighted average of the previous two. Based on these assumptions, the composition of the different waste streams resulted as represented in Figure 2. Synthetic fibres are an important fraction for all the three types of waste streams (29% of pre-consumer, 24% of post-consumer and 23% of textiles from waste treatment). Cotton covers a more important share in post-consumer textiles (26%) than in the other two streams. Blended fibres are mainly present in post-consumer textiles (29%), where the presence also of non-textile materials (11%), such as buttons or zippers, is not negligible. A large part of pre-consumer waste and of textiles from waste treatment has still an unknown composition. The assumptions about the waste composition should be validated in

future works with direct investigation and samplings of the waste in input to the plants.

Future developments of this work are the investigation of the various disposal or recovery processes in Lombardy, with the collection of data about the specific processes. Subsequently, the Life cycle assessment methodology could be used to estimate the environmental benefits and burdens of the regional textile waste management system.

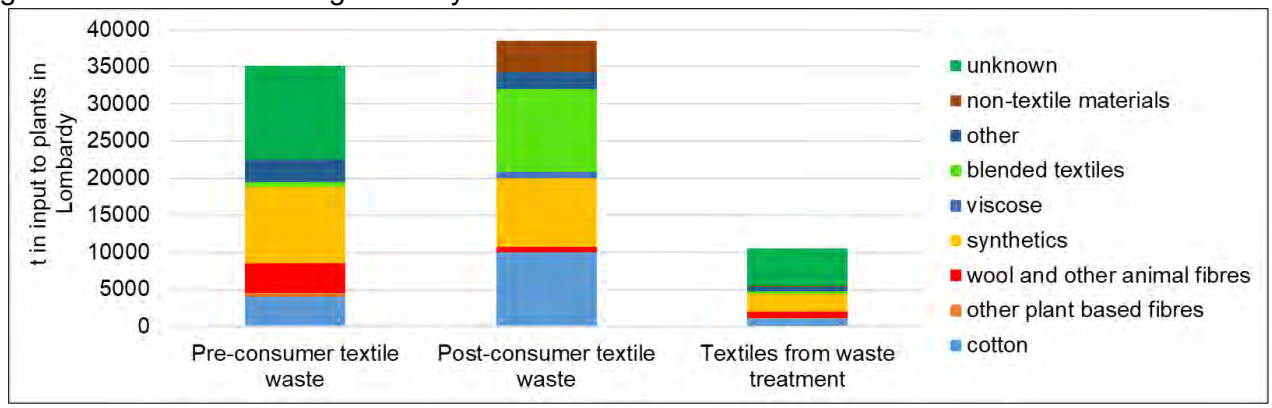

Figure 2 - Composition of the three different textile waste streams.

References

[1] Ellen MacArthur Foundation, A new textiles economy: Redesigning fashion's future, (2017, http://www.ellenmacarthurfoundation.org/publications accessed on 20th March 2024).
[2] European Commission, Communication from the Commission to the European Parliament, the Council, the European Economic and Social Committee and the Committee of the Regions: EU Strategy for Sustainable and Circular Textiles. Brussels, 30.3.2022 COM(2022) 141 final
[3] European Parliament, Directive 2008/98/EC of the European Parliament and of the Council of 19 November 2008 on waste and repealing certain Directives
[4] European Commission, Proposal for a Directive of the European Parliament and of the Council amending Directive 2008/98/EC on waste. Brussels, 5.7.2023 COM(2023) 420 final
[5] Amicarelli, V., Bux, C., "Quantifying textile streams and recycling prospects in Europe by material flow analysis", Environmental Impact Assessment Review, 97 (2022).
[6] Dahlbo, H., Aalto, K., Eskelinen, H., & Salmenperä, H., "Increasing textile circulation - Consequences and requirements", Sustainable Production and Consumption, 9, 44–57 (2017).
[7] Weber, S., Weber O., Habib, K., Dias, G.M., "Textile waste in Ontario, Canada: Opportunities for reuse and recycling", Resources, Conservation & Recycling, 190 (2023).
[8] Nørup, N., Pihl, K., Damgaard, A., Scheutz, C., "Quantity and quality of clothing and household textiles in the Danish household waste", Waste Management, 87, 454-463 (2019).
[9] Nørup, N., Pihl, K., Damgaard, A., Scheutz, C., "Evaluation of a European textile sorting centre: Material flow analysis and life cycle inventory", Resources, Conservation and Recycling, 143, 310-319 (2019).
[10] European Commission, Commission decision of 3 May 2000 replacing Decision 94/3/EC establishing a list of wastes pursuant to Article 1(a) of Council Directive 75/442/EEC on waste and Council Decision 94/904/EC establishing a list of hazardous waste pursuant to Article 1(4) of Council Directive 91/689/EEC on hazardous waste
[11] Decreto Legislativo 3 aprile 2006, n. 152, "Norme in materia ambientale"
[12] Istituto Nazionale di Statistica database (http://dati.istat.it/Index.aspx?QueryId=8914 accessed on 27th March 2024)
[13] Huygens, D., Foschi, J., Caro, D., Caldeira, C., Faraca, G., Foster, G., Solis, M., Marschinski, R., Napolano, L., Fruergaard Astrup, T. and Tonini, D., "Techno-scientific assessment of the management options for used and waste textiles in the European Union", Publications Office of the European Union (2023).

Title: Bimetallic Metal-Organic Frameworks: Efficient Catalysts for Water Disinfection via Advanced Oxidation Processes

Author(s): A. Fdez-Sanroman[1], D. Terron[1], B. Lomba-Fernández[1], E. Rosales[1], M.A. Sanromán[1], M. Pazos[1]*

[1] *CINTECX, Department of Chemical Engineering, Universidade de Vigo, Vigo, Spain, mcurras@uvigo.es*

Keyword(s): MOF, AOP, bimetallic, *Escherichia coli*, *Lactobacillus crispatus*

Abstract

In the last decade, there has been a worrying growth in the presence of contaminants in water, a phenomenon that has gained importance due to the rapid increase in population in urban areas around the world. However, this increase is not only due to population growth, but also to the inability of wastewater treatment plants to completely remove these contaminants. Among the most disturbing elements are pathogens, whose persistence in wastewater treatment facilities has generated concern, especially after events such as the SARS-CoV-2 crisis. This concern has been aggravated by the possible association of pathogens with microplastics present in water, which act as vectors and considerably increase the risk of contamination [1].

Wastewater treatment is a critical process to ensure the safety and quality of water resources. However, conventional treatment methods have limitations in the effective removal of pathogens and other micropollutants, which has generated the need to explore innovative approaches. A promising strategy is the adoption of innovative technologies based on Advanced Oxidation Processes (AOPs), which allow pathogens to be inactivated and micropollutants to be mineralized more efficiently [2]. Within these technologies, AOPs based on the Fenton reaction offer viable alternatives. These methods are based on the generation of highly oxidizing radicals, such as hydroxyl and/or sulfate radicals, capable of dismantling the cellular barriers of microorganisms and effectively disinfecting water.

In this study, two different approaches based on the Fenton and Fenton-like reactions will be presented. Specifically, the electro-Fenton process, an electrochemical method in which hydroxyl radicals are generated through the catalytic decomposition of electrochemically produced hydrogen peroxide, will be evaluated. In addition, the effectiveness of sulphate radicals will be examined, which have been shown to have significant degradation capacities, since they can be generated in the presence of catalysts by various oxidizing agents, including peroxymonosulphate (PMS) o persulphate.

Both Fenton and Fenton-like based processes require the presence of catalysts, mainly transition metals, and in this context Metal-Organic Frameworks (MOF) are postulated as attractive catalytic materials. MOFs are engineering materials known for their high surface area and unique crystalline structure comprising metal atoms linked by organic ligands. These qualities provide them appropriate catalytic properties, enabling the effective generation of reactive species in AOP. Currently, the most studied MOFs in AOPs are monometallic ones. However, some investigations have shown that

bimetallic MOFs have a key advantage by incorporating two transition metals in their structure, which promotes selectivity in the elimination processes and presents specific improvements, such as greater stability compared to monometallic MOFs.

The aim of the present communication was to investigate the effectiveness of bimetallic MOF in AOPs, specifically in the elimination of pathogens in wastewater. On the one hand, Zn-MIL53(Fe), a newly developed bimetallic MOF, was synthesized by solvothermal method, where H_2BDC, $FeCl_3 \cdot 6H_2O$ and $Zn(NO_3)_2 \cdot 6H_2O$ were mixed in N,N dimethylformamide (DMF) until fully homogenized. The Fe-Zn ratio was adjusted to 4:1, followed by three washes with DMF and absolute ethanol, respectively. Subsequently, the material was dried overnight in a dry vacuum at 11 mbar and 60ºC. After that, the material was used as a catalyst in heterogeneous electro-Fenton processes with the objective of eliminating pathogens in wastewater. This MOF demonstrated exceptional performance in inactivating both Gram-negative and Gram-positive bacteria. Complete elimination of gram-negative bacteria *(Pseudomonas aeruginosa*) in log8 and gram-positive bacteria *(Lactobacillus crispatus*) in log8 was achieved in just 5 minutes at 25 mA, with a catalyst dose of 4.32 g/L. Furthermore, Zn-MIL53(Fe) has shown to be a reusable material, capable of three complete disinfection cycles for both types of bacteria, making it highly promising for more efficient wastewater treatment applications involving the Fenton rection.
On the other hand, several CuFe MOFs were synthesized following previous procedure developed by Fdez-Sanromán et al [3]. The physical-chemical characterization confirmed the synthesis of distinct MOFs with different morphological structures based on their Fe/Cu ratios. These MOFs were ascertained in the generation of sulphate radicals through the activation of PMS, highlighting their effectiveness in the disinfection of *Escherichia coli*. Among them, $CuFe(BDC\text{-}NH_2)_1$, emerged as a promising candidate for disinfection, showing superior antibacterial activity attributed to its higher copper content. The optimization of the operational conditions suggested a potential reduction in MOF and oxidant concentrations required, improving the sustainability in water treatment.

Accordingly, both studies revealed the potential of bimetallic MOFs in improving water disinfection technologies with significant implications for wastewater treatment. In addition, the possibility of optimizing the conditions for the use of MOF and oxidant to improve sustainability in water treatment is highlighted.

References

[1] Ma, Y., Wang, L., Wang, T., Chen, Q., Ji, R., “Microplastics as vectors of chemicals and microorganisms in the environment”. In: Bolan, N.S., Kirkham, M.B., Halsband, C., Nugegoda, D., Ok, Y.S. (Eds.) Particulate Plastics in Terrestrial and Aquatic Environments. CRC Press, pp. 209-230 (2020).
[2] Lama, G., Meijide, J., Sanromán, A., Pazos, M. “Heterogeneous Advanced Oxidation Processes: Current Approaches for Wastewater Treatment”. Catalysts, 12, 344 (2022).
[3] Fdez-Sanromán, A., Lomba-Fernández, B., Pazos, M., Rosales, E. Sanroman, A. “Peroxymonosulfate activation by different synthesized CuFe-MOFs: Application for dye, drugs, and pathogen removal”. Catalyst, 13, 820 (2023).

Title: Enhancing pollutant adsorption and adsorbent regeneration via Electro- or Photochemical integration

Author(s): A. Fdez-Sanroman[1], N. Bermudez[1], B. Lomba-Fernández[1], A. Díez[1], E. Rosales[1], M.A. Sanromán[1], M. Pazos[1]*

[1] *CINTECX, Department of Chemical Engineering, Universidade de Vigo, Vigo, Spain, mcurras@uvigo.es*

Keyword(s): Adsorption, adsorbents, adsorbent regeneration, AOP, electro-sorption

Abstract

In the past century, significant changes have occurred in both life and society. The widespread use of pharmaceuticals, particularly antibiotics, has undoubtedly saved countless lives by effectively combating pathogens and commensal microorganisms. However, the increased consumption of human and veterinary medications, driven by global population growth, heightened life expectancy, increased healthcare investments, and Research and Development advancements, has raised environmental concerns. Organic compounds and their metabolites from these medications have been detected in various water sources, posing environmental risks. Trace levels of these compounds, ranging from ng/L to mg/L, have been found in surface water, wastewater, sediments, groundwater, and drinking water. The inherent toxicity and resistance of these compounds make complete elimination through biological processes challenging, necessitating alternative water treatment technologies to prevent their entry into aquatic ecosystems via sewage effluents.

The lack of regulation of these compounds and their potential effect on the environment, and, therefore, on society, require the adoption of appropriate technological solutions. It is necessary to develop comprehensive treatments applicable anywhere wastewater treatment is necessary. Among these technologies, adsorption has emerged as a promising method due to its simplicity, operational versatility, and high efficiency. The success of this process is greatly compromised by the type of adsorbent and the properties of the adsorbate; as well as by the composition of the wastewater itself. The main drawbacks detected in adsorption studies are the limited adsorption ability of several green materials and that this technology does not degrade pollutants and therefore an environmental problem can be generated derived from the accumulation of adsorbents. Therefore, the disposal of organic contaminant-laden adsorbents is a major challenge, and the development of novel regeneration techniques is needed to make adsorptive technologies more sustainable [1].

By direct polarization of carbonaceous materials, under sufficient applied electric fields, conductive particles can polarize, forming microelectrodes with both anodic and cathodic sides, inducing electrosorption and even electrolytic degradation of adsorbed compounds. Thus, electrosorption presents a viable option for eliminating ionizable pollutants from aqueous solutions by electrochemically polarizing electrodes to enhance adsorption capacity. Utilizing a three-dimensional (3D) electrode system proves beneficial for wastewater treatment, offering increased electroactive surface area and shorter mass transfer distances [2]. Moreover, the electrochemical process or photocatalyst processes could be used for the *in-situ* regeneration of saturated carbon electrodes or materials used in the

electrosorption process or adsorption processes. In addition, the inclusion of photocatalysts such as graphitic carbon nitride (g-C_3N_4) [3] could increase the feasibility of the process and open a new kind of adsorbent material with improved adsorption ability and properties for its regeneration by electro- or photo-catalyst processes.

In this context, in this study several actions were proposed to improve the adsorption process: (i) synthesis of several carbonaceous materials under the principles of circular economy, (ii) electrosorption; and (iii) hybrid technologies: adsorption in combination with sequential mode or successive with electro- or photochemical processes.

Initially, several carbonous materials were synthesised. To do that, a selection of agroindustry residues, including spent coffee, banana, chestnut peels, pine cones… were washed, dried and grounded before the synthesis. Hydrochars (HCs) were obtained by hydrothermal synthesis in a 50 mL autoclave, where 40 mL of water and 8 g of the agroindustry residue were added. Then, the synthesis took place for 2 h at 220ºC. For biochars (BC), N_2-calcination synthesis in a tubular furnace (Aero-360) was carried out and N_2 was fixed at 2 L/min. Initially, 400 or 800ºC were essayed, although the best performant materials were further optimized. In all cases, the residues were heat-treated for 2 h, having reached the fixed temperature at a rate of 10ºC/min. The assessment of the adsorption capabilities of the synthesized materials revealed noteworthy findings. The selection of the synthesis process was found to significantly influence the adsorption performance, with better levels for HCs. Concerning the temperature, its effect was related to the type of raw material used and should be determined for each waste material. For this preliminary study, it is concluded that the best adsorbents were the HCs of coffee and banana (HC_{coffe} and HC_{banana}, respectively) obtained both at 220ºC.

On the other hand, the HC of pine cone ($HC_{pine\text{-}cone}$) revealed satisfactory adsorption capacity. In this case, it was explored the use of both powdered and whole pine cone pieces, as their sizes and structures allow for the fabrication of electrodes directly applicable in the electrosorption process. In all tests, it was demonstrated that electrostatic interactions play a pivotal role in adsorption processes involving carbonaceous materials, often influenced by solution pH due to the interplay between the dissociated forms of pollutants and the surface chemistry of adsorbents. This material offers a dual benefit, serving as both electrode and adsorbent. Consequently, with this material a configuration of 3D electrode system was tested. This setup proved beneficial for the wastewater treatment of the different pollutants tested, offering increased electroactive surface area and shorter mass transfer distances.

Based on these results with the different HCs, the best adsorbents were used to synthesise different HC/g-C_3N_4 composites (from 1 to 20% g-C_3N_4) by hydrothermal treatment and the resultant material was electrodeposited on the surface of carbon felt to test in electrosorption and its regeneration by electro- and photocatalyst processes. In previous experiments, it was established that HC_{coffee}/g-C_3N_4 could serve as a photocatalyst for degrading pharmaceutical compounds such as sulfamethizole. Thus, the devised approach was to assess the effectiveness of this material as an electrosorbent and its subsequent regeneration via a photocatalytic process. Among the different combinations of HCs and g-C_3N_4 the most promising outcomes were achieved with composites of HC_{coffee}/g-C_3N_4 (10%) were electrodeposited onto carbon felt. The impact of applied voltage was evaluated within a range of 0.8 to 1.3 V, with maximum removal efficacy observed at 1.2 V (Figure 1). Although the adsorption capacity diminished over successive electrosorption cycles, operational viability was maintained.

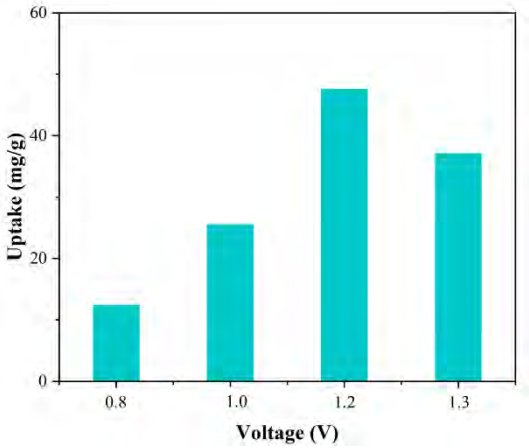

Figure 1: Uptake obtained over a period of 120 minutes under different voltages (0.8 V - 1.3 V) using HC_{coffee}/g-C_3N_4 (10%) deposited on a carbon felt electrode.

Addressing the disposal challenge of spent adsorbents, regeneration of HC_{coffee}/g-C_3N_4 composites by direct LED visible lamp radiation (80 W) for 2 h was performed. This regeneration strategy yielded successful results, restoring the composites to their initial adsorption capacity and thereby extending the operational life of synthesized adsorbents. Having validated the effectiveness of the HC_{coffee}/g-C_3N_4 composites, the influence of the water matrix and additional contaminants in the solution were analysed. It was evidenced that the presence of other compounds led to the saturation of the adsorbent diminishing the process's effectiveness.

Furthermore, Microtox® assays confirmed the suitability of these new adsorbents for removing ionizable pharmaceuticals by electrosorption process. Consequently, it is proposed the application of an electric field as a functional tool for improving the adsorption affinity of the pollutant and the application of photocatalysis for its regeneration. Based on these promising results, it can be concluded that the proposed strategies offer viable alternatives for removing emerging pollutants from water streams.

Acknowledgements
This research was funded through the join 2019-2020 Biodiversa & Water JPI joint call for research proposals, under the BiodivRestore ERA-Net COFUND programme with the Project PCI2022-132941 funded by MCIN/AEI /10.13039/501100011033, Project PDC2021-121394-I00 funded by MCIN/AEI/10.13039/501100011033 and by the European Union Next Generation EU/PRTR; PID2020-113667GBI00, funded by MCIN/AEI/10.13039/501100011033 and Xunta de Galicia, and the European Regional Development Fund (ED431C 2021-43).

References

[1] Fdez-Sanromán, A., Pazos, M., Rosales, E., Sanromán, M.A. “Unravelling the environmental application of biochar as low-cost biosorbent: A review”. Applied Sciences (Switzerland), 10 (21), art. no. 7810, pp. 1-22. (2020).
[2] Fdez-Sanromán, A., Pazos, M., Rosales, E., Sanromán, M.Á. Advancing in wastewater treatment using sustainable electrosorbents. Current Opinion in Electrochemistry, 44, art. no. 101450, (2024).
[3] Fdez-Sanromán, A., Torres-Pinto, A., Rosales, E., Silva, C.G., Faria, J.L., Pazos, M., Silva, A.M.T. Optimisation of a photoelectrochemical system for the removal of pharmaceuticals in water using graphitic carbon nitride. Catalysis Today, 432, art. no. 114578 (2024).

Assessing Environmental Performance and Sustainability in Industrial Sectors: A Methodological Approach

Authors: Stefano Castelluccio[1], Claudio Comoglio[1], Silvia Fiore[1].

[1]*DIATI, Department of Environment, Land and Infrastructure Engineering, Politecnico di Torino, Turin, 10129, Italy.*
stefano.castelluccio@polito.it, claudio.comoglio@polito.it, silvia.fiore@polito.it.

Keywords: environmental sustainability, industrial plants, methodology, EMAS.

Abstract

Introduction

Enhancing the environmental sustainability of industrial plants is critical for pursuing sustainable development. According to the latest report by the European Environmental Agency [1], in 2021, the environmental and health costs of European industrial sites, considering air pollution alone, amounted more than € 268 billion (totaling 2% of European GDP). This calculation factored in externalities related to air pollution, impacts on human health through inhalation and exposure to contaminated food and drink, harm to ecosystems, and damage to infrastructures and buildings. Therefore, improving the environmental sustainability of industrial facilities can have a decisive impact on pollution control and on limiting climate change effects, and it is increasingly recognized as a promising option [2], [3]. Given that a limited number of installations is often responsible for a substantial share of the collective impact of industrial facilities [1], targeted interventions in these installations can yield significant results. Nonetheless, the absence of a standardized methodology for evaluating the sustainability of industrial facilities remains a challenge.

Assessing the environmental sustainability of industrial sites has involved various methodologies, each presenting unique strengths and challenges. Individual or sets of indicators, such as those outlined by the Institution of Chemical Engineers (IChemE) and the Global Reporting Initiative (GRI) guidelines, are pivotal for transparent assessments and easy to implement. However, their efficacy can be hindered by factors such as indicator selection, data normalization, and impact aggregation. Conversely, Life Cycle Analysis offers comprehensive insights but has limitations in terms of functional unit selection, boundary setting, and identification of characterization factors. Furthermore, LCA requires specialized expertise and difficult-to-obtain analytical data, which constitute a critical limiting factor for its widespread implementation [4]. Similarly, environmental accounting methods like Cost–Benefit Analysis and Environmental Management Accounting may pose significant challenges, since various environmental parameters must be translated into the respective cost, alongside uncertainty and subjectivity limitations [4]. Balancing complexity with coverage of key sustainability issues is crucial for environmental sustainability assessments across industries. Despite the potential benefits, small and medium-sized industries often hesitate to engage in sustainability assessments due to data requirements and perceived lack of benefits. Material and energy flow analysis are positioned between indicator use and LCA in terms of complexity and can be particularly valuable when the main impacts of industrial processes are linked to material flows or energy usage. Among other approaches, Environmental Risk Assessment must be mentioned as an exhaustive and rigorous method but dependent on the local scale [5] and primarily requested by authorities. Combining approaches like multi-criteria analysis demonstrates promise and growing interest, yet standardization remains lacking [5]. Overall, evaluating environmental sustainability in industrial settings is a multifaceted endeavor, requiring a balance between comprehensiveness and feasibility. Enhancing standardization is imperative to facilitate result comparison, while the general lack of reference targets to judge the sustainability of installations is a crucial limitation [4].

In this context, our work addresses two limitations in the current state of the art: firstly, the lack of comprehensive evaluation methodologies for assessing the environmental sustainability of industrial plants using validated and easily available data; secondly, the limited understanding regarding how industrial organizations currently evaluate their environmental sustainability and their improvement strategies. The presented methodology analyzes the Environmental Statements (ESs) from industrial plants registered with the European Eco-Management and Audit Scheme (EMAS). EMAS, alongside ISO 14001, is the reference environmental management system for European companies. EMAS-registered organizations must publicly disclose their environmental performance through an ES, which is validated by an independent verifier. Our approach aims to advance current knowledge about two main research questions:

RQ1. Is it possible to provide a comprehensive analysis of the environmental performance of industrial plants using easily available and validated data?
RQ2. How do organizations quantify and address their environmental impacts, and what is the effectiveness of these efforts?

Methodology

We employed the outlined methodology across several industrial sectors. The first step involves identifying sectors where the number of companies registered with EMAS is large enough to guarantee a representative sample of the entire sector. Secondly, the environmental statements of registered companies are collected, and the disclosed data is analyzed. Regarding RQ1, the performance data disclosed in the ESs can be evaluated by comparison with reference values, such as the ones set in the sectorial Best Available Techniques Reference Documents (BREFs), by analyzing trends, and by quantifying the influence of the plant's characteristics on environmental performance. About RQ2, ESs' data allows to determine: which environmental aspects are considered significant by the companies; which aspects are quantified through indicators and the metrics used; which aspects are considered when defining improvement objectives; which are the objectives set by the companies; and how the budget is allocated between the various aspects.

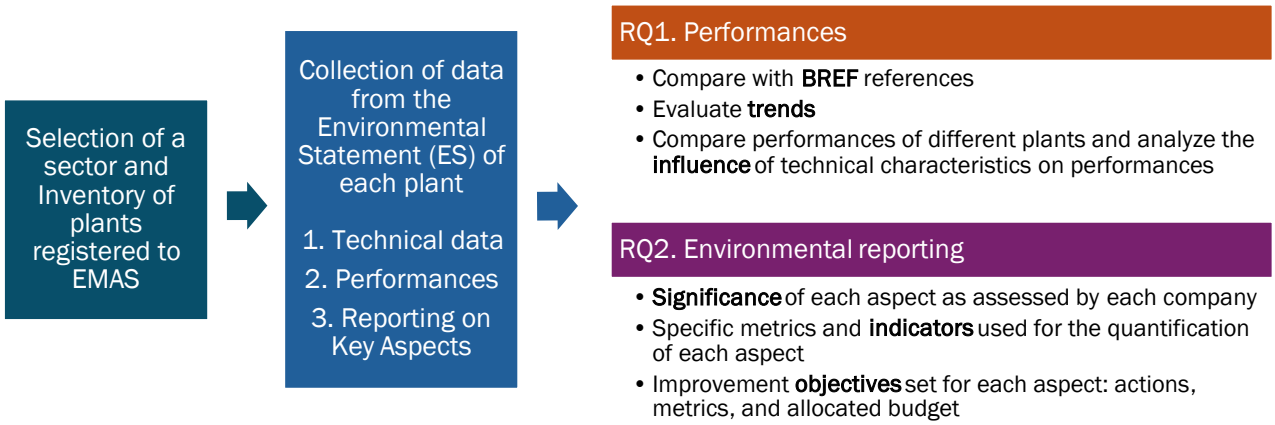

Figure 1. Illustration of the methodology steps.

RQ1. Evaluating the environmental sustainability of industrial plants

Case study 1 – Waste incineration sector

We conducted a comparative analysis of 15 incinerators against the Best Available Technique-Associated Emission Levels (BAT-AELs) [6]. Our assessment investigated emissions to air (dust, HCl, SO_x, NO_x, CO, total volatile organic compounds, NH_3, HF), reagents consumption (NaOH, $Ca(OH)_2$,

$NaHCO_3$, ammonia water), waste production (bottom and other ashes), and electricity consumption. The results underscored excellent performance across most indicators. For instance, emissions to air were often below the lower BAT-AEL, which represents excellent performance, and consistently below the upper BAT-AEL, as illustrated in Figure 2 from Comoglio *et al.* [7].

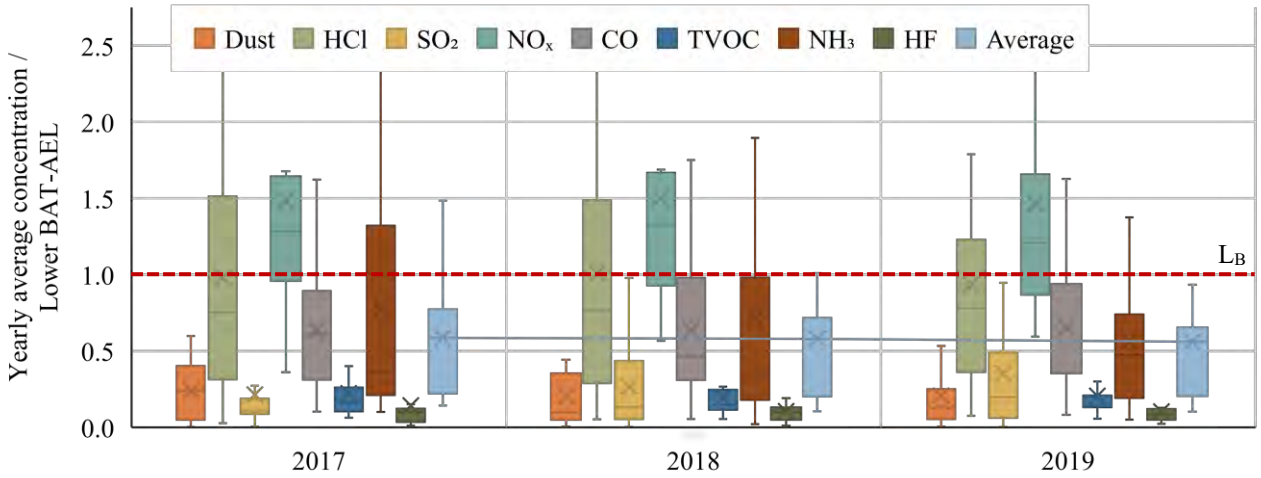

Figure 2. Flue-gas concentrations of pollutants emitted to air normalized with the respective lower BAT-AEL [7].

Case study 2 – Thermal energy sector

Expanding our scope, we analyzed a considerably larger sample of 73 thermal power plants over an extended period of 8 years. These improvements facilitated a more robust evaluation of trends and the influence of plant characteristics. As expected, natural gas and combined heat and power plants regularly outperformed other plants, and the performance differences were quantified (e.g., median cooling water use = 118 m^3/MWh for natural gas vs. 298 m^3/MWh). Surprisingly, plant age, size, and operational hours demonstrated limited effects on environmental performance. Trends varied notably based on the type of fuel used. Natural gas plants' performance improved across all indicators (-18% overall), whereas coal plants declined according to most indicators (+72% overall).

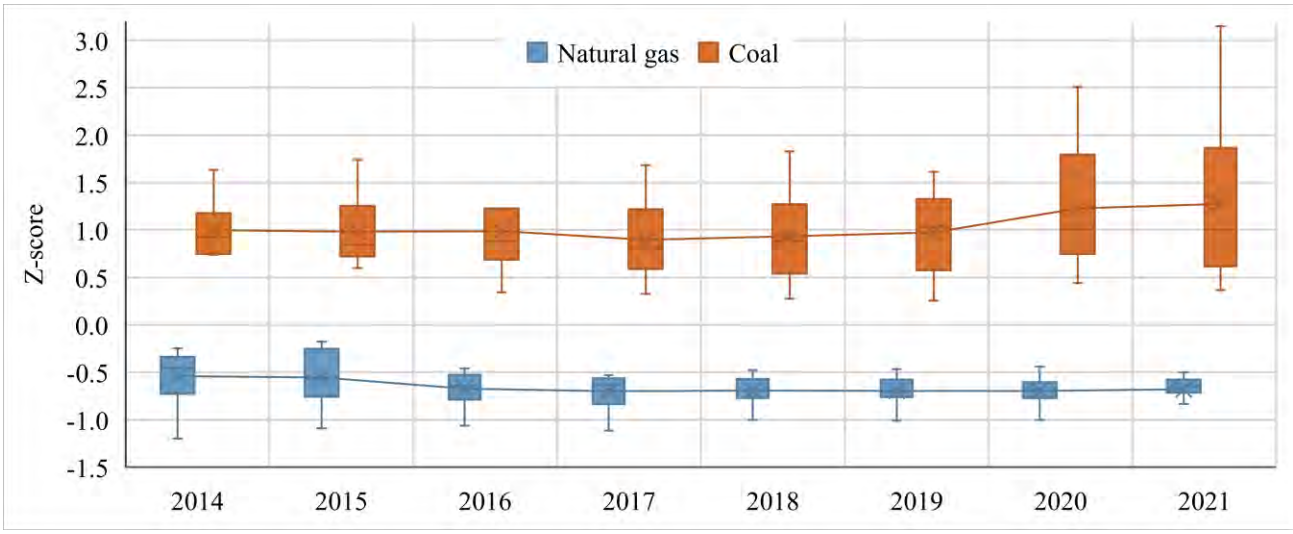

Figure 3. Overall temporal performance trends. Negative values indicate better performance.

RQ2. How organizations evaluate their environmental sustainability and improve it

Case study 3 – Hydropower sector

Our analysis included 206 hydropower (HP) plants, representing 29% of overall Italian HP production in 2019 [8]. Descriptions of the environmental state of the site were often neglected, and they rarely included quantitative indicators. The aspects considered most significant were soil contamination, biodiversity, waste production, risk of environmental accidents, water pollution and flow management, all of which received considerable attention in the sectorial literature. Interestingly, no correlation was found between the number of indicators used, the number of objectives set, the budget allocated, and the significance of each aspect [8]. For instance, 76% of the budget was directed towards technical aspects such as process management or energy production and not linked to any environmental improvement. Similar results were obtained when analyzing other industrial sectors. Moreover, organizations of the HP sector misrepresented their impact on biodiversity using mostly irrelevant metrics, such as total site area, while scarcely reporting their impacts on aquatic ecosystems and mitigation measures.

Conclusion

Our approach has proven to be a valuable and effective tool for assessing the environmental sustainability and performance of industrial plants using publicly available, certified, and independently validated data. When available, we suggest using BAT-AELs as reference targets to judge the sustainability of installations. Moreover, our methodology successfully quantified the disparities in environmental performance among plants with varying characteristics. These results indicate our methodology as an applicable tool in the multifaceted context of the evaluation of the environmental sustainability of industrial facilities.

On the other hand, our results highlight the need for sector-specific guidelines to bolster the efficiency of environmental reporting and sustainability assessment by organizations. Notable gaps include the inefficient allocation of improvement objectives and budget and the need for more effective indicators.

References

[1] EEA, “The costs to health and the environment from industrial air pollution in Europe - 2024 update,” European Environment Agency, Briefing Briefing No 24/2023, 2023.doi: 10.2800/912907
[2] R. Patnaik, “Impact of Industrialization on Environment and Sustainable Solutions – Reflections from a South Indian Region,” *IOP Conf. Ser. Earth Environ. Sci.*, vol. 120, no. 1, p. 012016, 2018, doi: 10.1088/1755-1315/120/1/012016.
[3] X. Cheng, L. Fan, and J. Wang, “Can Energy Structure Optimization, Industrial Structure Changes, Technological Improvements, and Central and Local Governance Effectively Reduce Atmospheric Pollution in the Beijing–Tianjin–Hebei Area in China?,” *Sustainability*, vol. 10, 2018, doi: 10.3390/su10030644.
[4] K. Angelakoglou and G. Gaidajis, “A review of methods contributing to the assessment of the environmental sustainability of industrial systems,” *J. Clean. Prod.*, vol. 108, 2015, doi: 10.1016/j.jclepro.2015.06.094.
[5] M. Herva and E. Roca, “Review of combined approaches and multi-criteria analysis for corporate environmental evaluation,” *J. Clean. Prod.*, vol. 39, pp. 355–371, 2013, doi: 10.1016/j.jclepro.2012.07.058.
[6] F. Neuwahl, G. Cusano, S. Roudier, S. Holbrook, J. Gómez Benavides, and J. Gómez Benavides, *Best Available Techniques (BAT) reference document for waste incineration: Industrial Emissions Directive 2010/75/EU (Integrated Pollution Prevention and Control)*. LU: Publications Office of the EU, 2019.
[7] C. Comoglio, S. Castelluccio, A. Scarrone, M. Onofrio, and S. Fiore, “Assessing the environmental performances of waste-to-energy plants: The case-study of the EMAS-registered waste incinerators in Italy,” *Waste Manag.*, vol. 153, pp. 209–218, 2022, doi: 10.1016/j.wasman.2022.09.005.
[8] C. Comoglio, S. Castelluccio, and S. Fiore, “Environmental reporting in the hydropower sector: analysis of EMAS registered hydropower companies in Italy,” *Front. Environ. Sci.*, vol. 11, 2023, doi: 10.3389/fenvs.2023.1178037

Design and development of nanostructured systems based on mesoporous silica for the capture of environmental contaminants

Anthropogenic pressures, energy-intensive technologies, and industrial/agricultural activities [1, 2] contribute to environmental deterioration, depleting water reserves. Uncontrolled emissions of CO_2, NOx, CH_4, VOCs, and POPs pose an imminent threat [3-4].

Addressing this requires both reducing emissions and remediating already polluted environments, employing techniques like oxidation, ion exchange, reverse osmosis, and adsorption [5]. Mesoporous nanostructured silica systems represent one of the most promising, specific and selective scavengers for organic and inorganic pollutants (such as CO_2 and heavy metals).

Two extensively studied families are SBA-15 and MSU-2. While lacking a regular channel packing order, MSU-2 materials exhibit a three-dimensional wormhole porous framework with uniform channel diameters, enhancing the diffusion rate of species within the pores [6]. SBA materials, present two-dimensional hexagonal array of uniformly distributed mesopores significantly facilitates the easy diffusion of substrate molecules compared to conventional solid supports. The thicker walls of SBA-15 contribute to greater thermal and mechanical stability when compared to other nanomaterials. The synthesis of these materials involves a non-ionic template (Pluronic 123) in an acidic medium with a pH ~ 1.[7]. These type of nanomaterials are characterized with a variety of techniques, including nitrogen adsorption porosimetry, thermogravimetry, XRD, SEM, TEM, infrared spectroscopy, and Zeta potential measurements, were employed to provide an in-depth characterization of their physical-chemical properties.

The synthesized nanostructured systems are modified by exploiting the reactivity of -OH groups, using ligands suitable for the capture of CO_2 and environmentally significant metals, as well as industrially relevant ones such as lithium. For lithium adsorption in particular, has been created **a manganese-lithium spinel type oxide ion sieve** and an **hybrid system with APTES-Glutaraldheyde-Crown ether** will be tested for the adsorption of Li^+ and Hg^{2+}

Bibliografia

[1] Grisolia, Antonio, et al. "Hybrid polymer-silica nanostructured materials for environmental remediation." *Molecules* 28.13 (2023): 5105.

[2] Devanathan, Ram. "Energy penalty for excess baggage." Nature nanotechnology 12.6 (2017): 500-501

[3] Zeb, Shakeel, et al. "Silica-based nanomaterials as designer adsorbents to mitigate emerging organic contaminants from water matrices." Journal of Water Process Engineering 38 (2020): 101675

[4] Li, Xiuquan, et al. "Adsorption materials for volatile organic compounds (VOCs) and the key factors for VOCs adsorption process: A review." Separation and Purification Technology 235 (2020): 116213

[5] Alharbi, Omar ML, Rafat A. Khattab, and Imran Ali. "Health and environmental effects of persistent organic pollutants." Journal of Molecular Liquids 263 (2018): 442-453.

[6] Pérez-Quintanilla, Damián, et al. "Synthesis and characterization of novel mesoporous silicas of the MSU-X family for environmental applications." Journal of Nanoscience and Nanotechnology 9.8 (2009): 4901-4909.

[7] Verma, Priyanka, et al. "Functionalized mesoporous SBA-15 silica: recent trends and catalytic applications." Nanoscale 12.21 (2020): 11333-11363.

[8] Weng, Ding, et al. "Introduction of manganese based lithium-ion Sieve-A review." *Progress in Natural Science: Materials International* 30.2 (2020): 139-152.

Sustainable use of water sources as a response to climate change challenge

Authors: Alena Vlašić[1], Daria Čupić[2]

[1]*Croatian Waters, Sector for Development and Water Management Planning, Zagreb, Croatia, alena.vlasic@voda.hr*
[2]*Croatian Waters, Sector for Development and Water Management Planning, Zagreb, Croatia, daria.cupic@voda.hr*

Keywords: alternative sources of water, climate change, strategy, water management, desalination, water reuse, directives, circular economy, sustainable development.

Abstract

1. Introduction

The Republic of Croatia is exposed to high risks of climate change, which is becoming a growing threat and a challenge. In several Mediterranean countries there are now regions where water abstraction disturbs the sustainability of water resources and the environment, with such condition easily worsening in the future. In the long term, climate change will affect the sea level rise, long-lasting droughts, and decrease of drinking water sources. Such conditions will directly affect human health, leading to diseases not typical for the Croatian climate [1]. Water is the basic natural and strategic resource. One of the basic concepts of the economics of natural resources and the environment is the concept of sustainable development. In line with that, sustainable development of water resources requires the hydrological cycle to be respected so that the capacity of renewable water resources does not decrease after prolonged use.

2. Regulations

The Croatian National Security Strategy identifies climate change as a “security threat, risk and challenge for Croatia”, recognizing the creation of Ecological Croatia as one of the main strategic goals [1]. Since climate change has a potential to cause significant damage to human health, physical structures and economic activities, particularly in agriculture, fisheries, biodiversity, tourism, transport, and production of electricity, the Croatian National Development Strategy until 2030 is an overarching strategic planning document streamlining long-term socio-economic development concerning all the above issues important for Croatia [2]. With the aim of more efficient water resource management and adaptation of our systems to climate change, a measure of high importance related to the strengthening of resilience of urban areas to human pressures caused by climate change included in the Climate Change Adaptation Strategy for the Period up to 2040 with a View to 2070 is an analysis of the

possibilities of reusing water and stormwater and developing a plan for rationalisation of water use in cases of increased demand caused by adverse hydrological conditions due to climate change [3]. As a guideline for low-carbon development until 2030, the Croatian Low-Carbon Development Strategy until 2030 with a View to 2050 specifies that it is necessary to analyse the possibilities to reuse water to irrigate agricultural land [4]. One of the main goals of the Croatian Sustainable Development Strategy is to ensure during the planning of economic activities, and in particular exploitation projects, rational use of non-renewable natural resources and sustainable use of renewable natural resources [5]. According to the Water Management Strategy, sustainable use will be achieved reusing water for irrigation [6]. The basic aim of water management is to ensure sustainable water use to be achieved by analysing the possibilities of reusing water and stormwater. The Sustainable Tourism Development Strategy unitl 2030 is a strategic planning document to design and implement tourism development policies and complies with national and European policies related to tourism and general socio-economic development [7]. The section “Environment and Space” of the National Plan for the Development of Islands 2021-2027 puts special emphasis on water and wastewater, waste management, nature and environmental protection, pure energy, production of energy, renewable sources of energy, and climate change adaptation and mitigation [8]. The Water Act regulates the legal status of water, water estate and hydraulic structures, water quality and quantity management, protection from adverse effects of water, detailed amelioration drainage and irrigation, special activities for water management, institutional structure for the provision of such activities, and other issues related to water and water estate [9]. The Mediterranean Strategy for Sustainable Development is focused on integrating environmental interests into the key sectors of economic development, taking into account social and cultural dimensions [10]. Abstraction volumes have to be sustainable in order to ensure the management and protection of water resources and the associated ecosystems. The objective of the EU Water Framework Directive is to prevent further water degradation, protect and improve the status of ecosystems, and establish a system of sustainable water use based on long-term protection of water resources [11]. The list of supplementary measures of the Directive contains, among other things, measures for water reuse and for the use of desalination procedures. The upcoming recast of the Urban Wastewater Treatment Directive in synergy with the evaluation of the Sewage Sludge Directive will contribute to raising the level of ambition to remove nutrients from wastewater and prepare the treated water and sludge for reuse, thus supporting circular agriculture with less pollution [12]. The EU Regulation on minimum requirements for water reuse lays down minimum requirements for water quality and monitoring and provisions on risk management, for the safe use of reclaimed water in the context of integrated water

management [13]. The purpose of the Regulation is to guarantee that reclaimed water is safe for agricultural irrigation, thereby ensuring a high level of protection of the environment and of human and animal health, promoting the circular economy, supporting adaptation to climate change, and contributing to the objectives of the Water Framework Directive.

3. Climate change and sustainable use of resources

It is expected that climate change will reduce water availability and increase the abstraction of water for irrigation in the Mediterranean region. Droughts have an important impact on regional economy, environment, and quality of life. They can bring losses in agriculture, adversely affecting freshwater ecosystems and leading to plant and animal species dying out. Last but not the least, droughts lead to water supply issues. In several Mediterranean countries, there are now regions where water abstraction disturbs the sustainability of water resources and the environment, with such condition easily worsening in the future. The preservation of water resources is a hydrological reponse to that issue. Water reuse is an important component of the water resource preservation strategy. Other solutions can also be applied, such as desalination of brackish or seawater, and Managed Aquifer Recharge (MAR). MAR in the Mediterranean aquifers could be such possible source. Water reuse and artificial aquifer recharged was highlighted as an important possible measure for further EU action in the 2012 Water Blueprint [14]. The future situation with sustainable water resources will basically depend on the status of water resource recharge, which will be affected by climate change and pollution, as well as on the pressures to water abstraction which depend on water use, tourism, population growth, and industrial development. Sustainable development enables harmony between man and nature in which the use of natural resources will not put them at risk or eradicate them. Since water resources are the basic elements of the quality of life, economy and tourism, they have to be managed systematically and responsibly, ensuring the required water volumes even under complex climate conditions, particularly during the tourist season. That very specific problem requires special water resource management infrastructure and strategy which can be faced with the said events. Good water resource planning is therefore extremely important, particularly in coastal regions and on islands in accordance with the needs of tourism, as well as adjusting the tourism development strategy with regard to the availability of water resources. Increased water demand is expected in tourist regions because of the expected increase in the number of tourists and achievement of a higher category of tourist services. The seasonal type of tourism makes resolving the issue of public water supply more difficult due to big differences in water consumption during the season and off-season. An EU report on the development of blue economy stresses continuous development of desalination as a key emerging sector within the Blue

Economy [15]. The report identifies growing dependence on the brackish water desalination technology in the Mediterranean basin, foreseeing strong sectoral growth over the next several years.

4. Possibility of using alternative water sources in Croatia

There are different treatment technologies which more or less successfully treat wastewater for irrigation needs, as well as for other needs such as watering of green spaces, recreation zones, camp sites, washing of public urban areas, and as technological water within a plant. A number of wastewater treatment plants (WWTP) has been constructed or is under construction in the Istria Pensinsula for which water reuse is foreseen for the irrigation of urban green spaces. Four WWTPs with membrane wastewater treatment technology have been built in Poreč. The total wastewater treatment capacity of all the WWTPs is 137,500 population equivalent (PE). These are state-of-the art plants which through membrane ultra-filtration and additional UV disinfection achieve the highest, tertiary level of wastewater treatment. This not only protects the environment and our most valuable resource - the sea; but it will also be possible to reuse water for the watering of green spaces and other public needs, in order to protect water resources. As part of a project of collection and treatment of wastewater in the Rovinj agglomeration, the Rovinj WWTP with a capacity of 63,000 PE, MBR technology and foreseen water reuse has been built, thus achieving efficient water resource management in the Istria area. This has a positive impact on the sustainability of drinking water resources in Istria County which is one of the few areas in Croatia now faced with difficulties in water availability (during dry years in the peak of the tourist season). Water reuse has a positive impact on potential effects of climate change by reducing the use of groundwater resources and reducing seawater infiltration. Several larger projects are still in implementation in Istria. There is also a number of wastewater treatment plants of smaller capacity that treat wastewater to the level suitable for the irrigation of green spaces and agricultural areas, sports fields, and washing of streets and other similar activities where water can be reused. Water supply is definitely one of the most important factors of sustainable development of tourism, particularly on islands. During seasonal population increase, it often happens that these are also periods with minimum or low recharge of natural resources. Big islands closer to the mainland are mostly connected to mainland karst springs through submarine pipelines. Smaller islands further away from the mainland are in a particularly unfavourable position due to insufficiently developed infrastructure, which is the cause of increased depopulation. The development of tourism on such islands leads to a big discrepancy in water demand in the summer and winter periods. Since water resources are the basic elements of the quality of life, economy and tourism, they have to be managed systematically and responsibly, providing, in the complex climate conditions, the required quantities of water, particularly during the

tourist season. Desalination is today an applicable method of providing the required water volumes in many areas, particularly on islands which are characterised by water shortages in the summer months, when the water demand is at the same time the highest, both for tourism and for agriculture. The problem of supplying their islands with drinking water is resolved through desalination procedures by other Mediterranean countries as well. Their experience has already demonstrated long-term sustainability of applying such innovations in new and existing desalination plants with the use of renewable sources of energy, thus helping ensure sustainable future in which water availability and environmental protection are the same thing [16]. The cohesion policy funds will be used in the highest amount so far to further strengthen the economy and support green transition, which will mitigate the impact of energy and climate challenges on the economy and society as a whole, with a strong focus on villages and islands. In Croatia, there are several examples of using water obtained from a desalination procedure on islands. On the island of Unije, brackish water is treated at a desalination plant with a capacity of 4 m3/h. The island of Susak uses the water obtained from a seawater desalination procedure at a plant with a capacity of 8 m3/h. On the island of Krk there are two brackish water desalination plants in Stara Braška with capacities of 5 m3/h and 25 m3/h. In Povljana on the island of Pag there is a brackish water desalination plant with a capacity of 104 m3/h. Water supply through desalination plants is foreseen on the islands of Olib (Q=4 m3/h), Premuda (Q=12 m3/h) and Silba (Q=12 m3/h) [17]. There is also an idea about installing a Q= 173 m3/h desalination plant at the Vrčići water abstraction site on the island of Pag. One example from the coastal region is that design documents have been prepared for supplying water to the settlement of Doli in the Dubrovnik area through a desalination plant from two wells with a capacity of up to 29 m3/h of water, i.e. 18 m3/h after desalination. Due to a big distance of the settlement of Porozina on the island of Cres from the existing public water supply system of the Town of Cres, Porozina is foreseen to be supplied with water from an individual system with the construction of a seawater desalination plant with a planned capacity of 5.25 m³/h. For the same reason, a design for the settlement of Beli on the same island has been prepared, foreseeing an individual system and the construction of a seawater desalination plant with a capacity of 3.3 m³/h.

5. Conclusion

The role of alternative water sources will become more important in the future, and they will be increasingly used for different purposes in water supply, agriculture, fire protection, recreation, etc, where demand exists. The current situation in Croatia shows that despite individual examples of reusing water and desalination procedures in tourist regions or islands the use of alternative sources of water is still not widespread enough because water is still thought of as an infinite resource. In order to increase

trust in the use of alternative water sources, in particular water reuse, the public should be informed. In particular, water reuse projects can rarely be implemented without social acceptance. However, it is important to make sure that designing the use of alternative water sources is properly integrated into the planning processes. The use of alternative water sources complies with water management according to the sustainable development principles, and is at the same time one of the measures to preserve and improve receiving water quality. With a framework to monitor and analyse data about relevant indicators of sustainable tourism which may affect the procedure of adoption of strategic, development and investment decisions which affect the environment, control of implementation of statutory provisions, and implementation of measures and activities defined by strategic documents, it can be said that using alternative water sources is a good response to the climate change challenge. The sustainability of the aquatic system requires a balance between water supply and demand, with one of the solutions being the use of alternative sources of water such as desalination of brackish and sea water, water reuse, and Managed Aquifer Recharge (MAR). According to the Croatian National Development Strategy until 2030, projects to increase climate resilience in water supply and wastewater management will intensify. It is expected that the implementation of measures from all the mentioned key strategies and pieces of legislation will help develop procedures to increase Croatia's climate change resilience.

References

[1] Croatian National Security Strategy (OG 73/17)
[2] Croatian National Development Strategy until 2030 (OG 13/21)
[3] Climate Change Adaptation Strategy for the Period up to 2040 with a View to 2070 (OG 45/20)
[4] Croatian Low-Carbon Development Strategy until 2030 with a view to 2050 (OG 63/21)
[5] Croatian Sustainable Development Strategy (OG 30/09)
[6] Water Management Strategy (OG 91/08)
[7] Sustainable Tourism Development Strategy until 2030 (NN 02/23)
[8] National Plan for the Development of Islands 2021-2027
[9] Water Act (OG 66/19, 84/21, 47/23)
[10] Mediterranean Strategy for Sustainable Development (2005)
[11] Water Framework Directive (2000)
[12] Council Directive 91/271/EEC of 21 May 1991 concerning urban waste-water treatment
[13] Regulation (EU) 2020/741 on minimum requirements for water reuse
[14] EU action in the 2012 Water Blueprint (EEA, 2012)
[15] Smart Specialisation in the Context of Blue Economy – Desalination Sector, EC, 2021
[16] Reverse osmosis desalination systems powered by solar energy; Shalaby et.al.,Elsevier,Vol. 251, 2022
[17] Evaluation of water supply solutions on islands - Study, Hidroprojekt-ing and SI Consult, Zagreb 2015

Title: Treatment of NAPL-contaminated emulsions by temperature-intensified alkaline persulphate

Author(s): Aurora Santos*[1], Andrés Sánchez-Yepes[1], Arturo Romero[1], David Lorenzo[1].

[1] *Chemical Engineering and Materials Department, Complutense University of Madrid, Spain*

Keyword(s): TPHs, alkaline persulphate, remediation, advance oxidation process, surfactant.

Abstract

Contamination of soil and groundwater by organic compounds from accidental or uncontrolled discharge or from industrial activities poses a high environmental risk [1, 2]. The uncontrolled release of these hydrophobic organic compounds results in the formation of non-aqueous liquid phases or NAPLs. NAPLs exhibit different properties and behaviour with respect to dissolved compound contamination plumes.

Depending on their origin, NAPLs can be less dense than water, they are called light non-aqueous phase liquids or LNAPLs. Most of these phases originate from petrol spills (BTEX compounds) or fuel oil spills (with heavier and less soluble compounds in the aqueous phase, generally known as total petroleum hydrocarbons, TPHs). Due to their low density, LNAPLs are found in areas above the phreatic water level [3, 4]. A simplified diagram of LNAPL migration is shown in Figure 1.

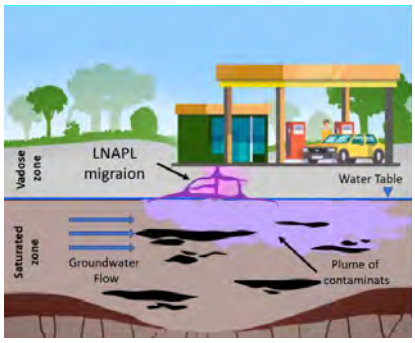

Figure 1. Conceptualization of LNAPL migration in the subsurface

A traditional approach to treating contaminated sites such as pumping or in situ chemical oxidation may be limited by the low solubility of contaminants [5]. The injection of aqueous solutions containing surfactants into the subsurface and subsequent extraction of contaminated emulsions was efficient solution to remove the residuals LNAPL [6]. This technology is known as surfactant enhanced aquifer remediation (SEAR). The main drawback of the SEAR process was that contaminants in the soil were transferred to the emulsion phase and must be managed [6, 7]. In the following work, an advanced oxidation process (AOPs) was proposed for the removal of LNAPLs present in the emulsion composed of E-Mulse 3® (EthicalChem, E3) by temperature-intensified alkaline persulfate (PS) oxidation. The LNAPL phase used consisted of a mixture of aliphatic and PAHs compounds obtained from a protected area.

The experimental conditions and concentrations of the different reagents used are summarised in Table 1. First, the oxidation of the contaminant-free surfactant was studied by thermal PS and temperature-intensified alkaline PS (Runs R1 and R2). The degradation of the TPHs-E3 emulsion was carried out by temperature-intensified alkaline PS (Runs R3). The reactions were carried out in 25 mL vials (each associated with a reaction time) containing the emulsion (E3 or TPHs-E3 respectively). The vials were placed in a temperature-controlled bath at 50°C. Once the temperature was reached, the vials of R1 were added the corresponding amount of PS to reach the initial concentration, while the vials of reactions R2 and R3 were also dopped with 2:1 NaOH/PS molar ratio (time zero). The blanks of each reaction contained only emulsion without oxidant or NaOH.

Table 1. Experimental conditions of the runs carried out to study the removal of TPHs from emulsions with E3. All experiments were carried out maintaining: $C_{E3,0}$ = 3.5 g·L^{-1}, $C_{PS,0}$ = 10 g·L^{-1}, T = 50ºC and 1440 min of reaction time.

RUN	$C_{TPHs,0}$ (mg·L^{-1})	$C_{E3,0}$ (g·L^{-1})	$C_{PS,0}$ (g·L^{-1})	NaOH/PS (mol·mol^{-1})	T (°C)	time (min)
R1	0	3.5	10	-	50	1440
R2	0	3.5	10	2:1	50	1440
R3	300	3.5	10	2:1	50	1440

The TPH concentration were identified and quantified by Gas Chromatography (GC). From the emulsion with TPHs, the fraction corresponding to aliphatic and polyaromatic (PAHs) compounds respectively was studied by SPE separation. E3 concentration was measured by GC equipped with a flame ionisation detector (FID). PS concentration was determined by colorimetric titration using an indicator solution of KI (64 g·L-1) and NaHCO3 (3.2 g·L-1). Short-chain acids and sulphates were measured by inorganic chromatography (IC) using a Metrohm 761 Compact IC system with anionic chemical suppression and a conductivity detector.

First, the reduction of the E3 concentration was studied using PS (R1) and alkaline PS (R2) both at 50°C. Figure 2 shown the oxidant consumption and the reduction of the surfactant with time for both oxidative processes. As shown in Figure 2, the reduction in E3 was independent of the oxidative process used. For both cases, the elimination was higher than 90% with a PS consumption of around 60%. For the oxidation with thermal alkaline PS, the oxidant consumption was a bit higher than 60% due to the alkaline activation of the oxidant.

The degradation of the emulsion with dissolved TPHs was represented in Figure 3. In Figure 3a the PS consumption was represented with respect to the surfactant removal and in Figure 3b with respect to the TPHs removal. As can be seen in Figure 3 the PS consumption was almost 80%, a higher value compared to the PS consumption for E3 degradation represented in Figure 2b, the presence of the contaminants in the emulsion increased the consumption of sulphate radicals and thus the oxidant consumption.

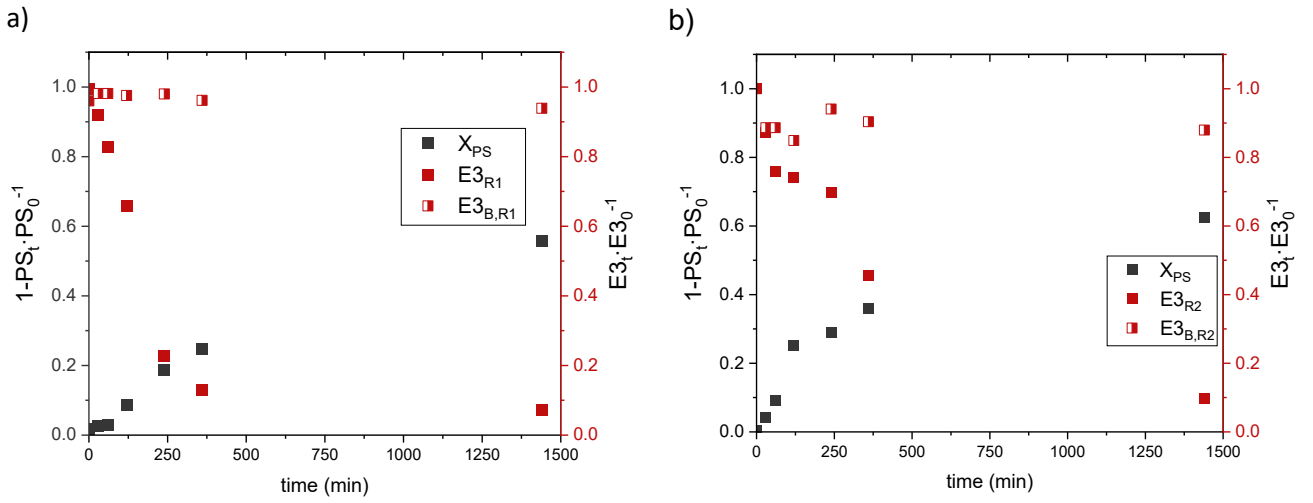

Figure 2. PS consumption and E3 reduction in the reaction using a) thermal PS and b) temperature-intensified alkaline PS. Conditions: $C_{E3,0}$ = 3.5 g·L^{-1}, $C_{PS,0}$=10 g·L^{-1}, 2:1 NaOH/PS, 50°C and 1440 min. Data compared to reaction blanks.

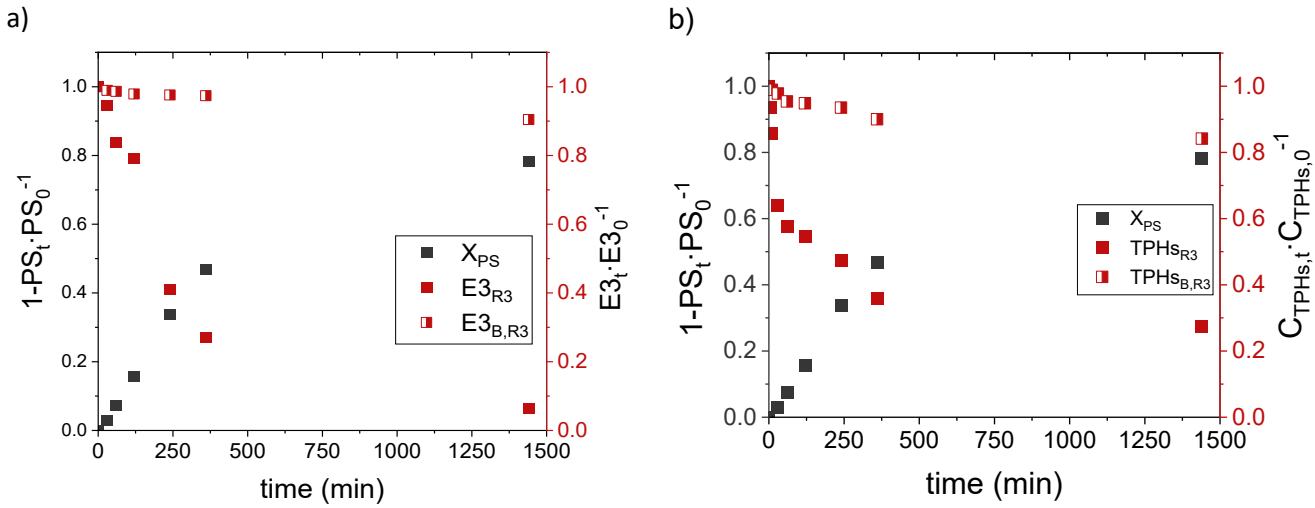

Figure 3. PS consumption and a) E3 and b) TPHs reduction for the degradation reaction of the TPHs-E3 emulsion using temperature-intensified alkaline PS. Conditions: $C_{TPHs,0}$ = 300 mg·L^{-1}, $C_{E3,0}$ = 3.5 g·L^{-1}, $C_{PS,0}$=10 g·L^{-1}, 2:1 NaOH/PS, 50°C and 1440 min. Data compared to reaction blanks.

As can be seen in Figure 3a, the degradation of E3 was not affected by the presence of TPHs dissolved in the emulsion in comparation to the values shown in Figure 2b. The removal of TPHs, represented in Figure 3b, was close to 80%, mostly removed during the first 6 hours of reaction. Analysing the reaction blanks (in the absence of oxidant and NaOH), it could be concluded that the surfactant was not thermally degraded and that the reduction of TPHs by evaporation was minimal.

The proportion of aliphatic compounds and PAHs in the emulsion was studied in the initial emulsion and in the aqueous after the reaction. The results were summarised in Table 2. In the initial emulsion, aliphatic compounds accounted for 70% of the TPHs and 30% were PAHs. At the end of the reaction, the final concentration of TPHs was 27%, of which 48.5% were aliphatic compounds and more than

50% were non-degraded PAHs. With these results it was concluded that the oxidation was more selective towards linear compounds than towards aromatics compounds. As shown in Table 2, the removal of aliphatic compounds was higher than 80%. In Table 2, the reduction in organic carbon (TOC) of the emulsion was only a 13%, indicating that there as hardly any mineralisation at the end of the reaction.

Table 2. Initial and final concentration and conversion of TOC, TPHs and the corresponding aliphatic compounds and PAHs in the TPHs-E3 emulsion. Degradation reaction of the TPHs-E3 emulsion using temperature-intensified alkaline PS. Conditions: $C_{TPHs,0}$ = 300 mg·L^{-1}, $C_{E3,0}$ = 3.5 g·L^{-1}, $C_{PS,0}$=10 g·L^{-1}, 2:1 NaOH/PS, 50°C and 1440 min. Data compared to reaction blanks. X represent the conversion.

	TPHs	Aliphatic	PAHs	TOC
$C_{Initial}$ (mg·L^{-1})	300.00	209.57	90.43	1878.60
C_{Final} (mg·L^{-1})	82.01	39.82	42.50	1639.20
X	0.73	0.81	0.53	0.13

Throughout the reaction, the concentrations of sulphate and short-chain acids were analysed as compounds associated with the consumption of PS and the degradation of organic matter in the emulsion. At the end of the reaction, the concentration of sulphate in solution was 7.80 g·L^{-1}, which is equivalent to the stoichiometric PS consumed. The concentration of short-chain acids was lower than 50 mg·L^{-1}, which is explained by the small reduction of the TOC value at the end of the reaction, as shown in Table 2.

Acknowledgement: This research is part of the project PID2022-137828OB-I00 (EMULREM) and PDC2022-133095-I00 funded by MCIN/AEI/10.13039/501100011033. This work was supported by the EU LIFE Program (LIFE17 ENV/ES/000260). A.S.-Y. would also like to thank the Ministry of Science and Innovation for supporting predoctoral contracts under FPI grant PRE2020-093195.

References

[1] R. Naidu, Recent Advances in Contaminated Site Remediation, Water, Air, & Soil Pollution, 224 (2013) 1705 https://doi.org/10.1007/s11270-013-1705-z.
[2] P. Panagos, M. Van Liedekerke, Y. Yigini, L. Montanarella, Contaminated sites in Europe: review of the current situation based on data collected through a European network, J Environ Public Health, 2013 (2013) 158764 https://doi.org/10.1155/2013/158764.
[3] A.H. Sulaymon, H.A. Gzar, Experimental investigation and numerical modeling of light nonaqueous phase liquid dissolution and transport in a saturated zone of the soil, J Hazard Mater, 186 (2011) 1601-1614 https://doi.org/10.1016/j.jhazmat.2010.12.035.
[4] K. Soga, J.W. Page, T.H. Illangasekare, A review of NAPL source zone remediation efficiency and the mass flux approach, J Hazard Mater, 110 (2004) 13-27 https://doi.org/10.1016/j.jhazmat.2004.02.034.
[5] R. Siegrist, M. Crimi, T. Simpkin, In Situ Chemical Oxidation for Groundwater Remediation, 2011.
[6] L. Huo, G. Liu, X. Yang, Z. Ahmad, H. Zhong, Surfactant-enhanced aquifer remediation: Mechanisms, influences, limitations and the countermeasures, Chemosphere, 252 (2020) 126620 https://doi.org/10.1016/j.chemosphere.2020.126620.
[7] A. Sánchez-Yepes, A. Santos, A. Romero, D. Lorenzo, Sustainable application of surfactants in soil remediation: Selective pollutants adsorption and hydrogen peroxide-driven adsorbent regeneration, Science of The Total Environment, 926 (2024) 171847 https://doi.org/10.1016/j.scitotenv.2024.171847.

Utilize HTC products for sustainable Biogas production through Anaerobic Digestion of Sewage Sludge

Author(sd): Annalinda Capone[1], Antonio Panico[1], Lucio Zaccariello[2], Biagio Morrone[1],

[1] *Dipartimento di Ingegneria, Università degli studi della Campania, Aversa, 81031 Caserta (CE), Italy, {annalinda.capone,antonio.panico, biagio.morrone}@unicampania.it*
[2] *Dipartmento DiSTABiF, Università degli Studi della Campania "Luigi Vanvitelli", Caserta (CE), Italy, lucio.zaccariello@unicampania.it*

Keyword(s): *Sewage sludge, Anaerobic digestion, Hydrochar, Hydrothermal Carbonization, recovery, Biogas, Waste management.*

Abstract

Sewage sludge, a byproduct of wastewater treatment plants, poses considerable challenges in waste management due to its potential to spread contaminants into the environment, including potentially toxic elements (PTEs), chemicals and pathogens. On the other hand, sewage sludge also can contain valuable organic compounds and essential nutrients, making it interesting for recovering materials as well as energy in various applications [1]. The comprehensive challenges of sewage sludge management, including its substantial volume and complex disposal requirements, have been extensively studied with the aim at exploring solutions through Anaerobic Digestion (AD). These challenges concern not only the quantity of sludge produced but also the environmental and regulatory constraints governing its disposal. Efforts have been dedicated to investigating various methods to address these aspects while enhancing the AD process performance. A significant focus lies in optimizing the biogas production, thereby offering a sustainable solution to energy needs while mitigating the environmental impact of sludge disposal.

The entire AD process takes place thanks to the presence of different strains of microorganisms, naturally present in the biomass, which differ along the process depending on the specific occurring environmental conditions. The conversion of biomass into biogas is the result of the sequence of four different phases, where different groups of microorganisms act: hydrolysis, acidogenesis, acetogenesis, and methanogenesis. In the first phase, bacteria that are capable of transforming the organic substances present in the sludge into fatty acids (formic, propionic, butyric, etc.) act [2]. Then, other microorganisms prevail and metabolize these acids, leading the process to the final products of low molecular weight, in particular carbon dioxide and methane.

However, sewage sludge management requires more than just optimizing biogas production. Environmental regulations, public health concerns, and the need for sustainable resource utilization demand innovative solutions involving the entire sewage sludge management lifecycle [3].

This work sheds lights on these complexities, particularly focusing on the role of the Hydrothermal Carbonization (HTC) process in transforming biomasses like sewage sludge into a valuable resource (i.e. hydrochar) that can also be integrated into AD [1] to boost the biogas production, thus closing entirely the cycle.

HTC is a thermochemical process that converts biomass into hydrochar by carbonization reactions with mild conditions at quite low temperatures for several hours. This process is particularly interesting because it can process wet biomass without a previous drying process. Three by-products result from

the HTC process: a gas, a liquid, and a solid phase, which is the hydrochar. Several researchers are studying different applications of this solid HTC by-product: soil amendment and solid biofuel are the more common uses of hydrochar. Moreover, this product seems to be a promising booster agent for methane production. Hydrochar has been found to improve AD performance when it is added to AD systems, increasing methane yield, improving operational efficiency and digestate dewatering and reducing the content of heavy metals in digestate [4].
By strategically combining these processes, biogas production can be enhanced, and the challenges associated with sewage sludge disposal can be mitigated. The sequential integration of HTC with AD represents a promising opportunity for maximizing resource utilization and process efficiency while addressing the pressing issues of sewage sludge management. Through this integrated approach, hydrochar can be added to substrates in AD, thus enhancing biogas production and minimizing waste disposal.

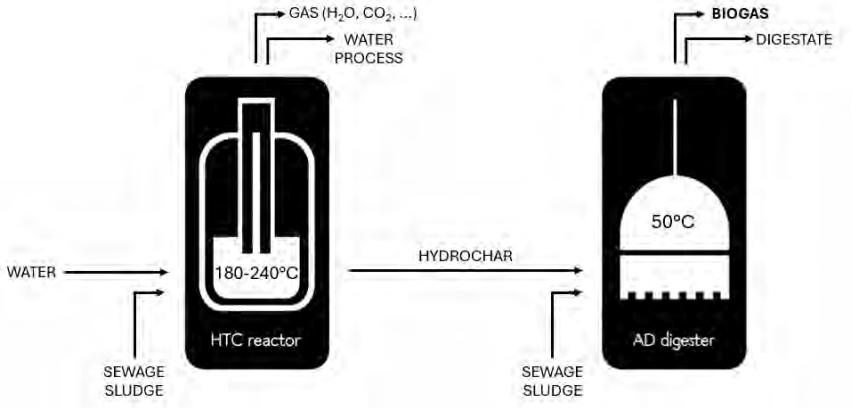

Figure 1. Sequential HTC and AD Processes Scheme

Hydrochar actually exhibits significant potential in enhancing the performance of an AD process. Extensive investigations into the composition and properties of hydrochar have shed light on its role in optimizing the AD process. These studies have clarified fundamental aspects of the interaction between hydrochar and AD substrates, including insights into electron transfer fate, microbial community dynamics, bioprocess mechanisms and the impact of reactions [5].
The characteristics of hydrochar, such as feedstock composition, HTC temperature and carbonization time, as well as modifications and dosage, significantly influence its efficacy in enhancing AD performance. For instance, shorter HTC times and lower temperatures may yield higher concentrations of oxygen-containing functional groups (OCFGs) on the hydrochar surface, thereby enhancing methane production potential [6].
This study aims at optimizing the HTC and AD processes by integrating them in series configuration to recover by-products from the first process and use them in the second process. The investigation focuses on assessing the effectiveness of different dosages of hydrochar mixed with a constant quantity of sewage sludge to determine the optimal concentration at thermophilic conditions (50°C).
Experiments were conducted at laboratory scale using 250 ml Duran bottles as reactors. These reactors were placed on a magnetic mixer to ensure substrate homogeneity as well as an efficient contact between microorganisms and substrates and prevent foam formation. A liquid displacement level system was employed to measure the volume of produced biogas. This system consisted of a 500 ml bottle connected to each reactor, enabling the passage of biogas. As biogas is going to be accumulating in the headspace of the bottle, the gas pressure increase, thus causing the liquid displacement (Figure

2). This liquid is then addressed into another bottle through a piping system, which serves as a collection tank.
Each reactor is heated by an electric resistance connected to a Labview program, which ensures fast temperature control and stability through a PI system.
At the top of each reactor, a valve system is installed, enhancing connectivity with the MicroGC pipe for analyzing the composition of the biogas. For the extraction process, tube connected through the reactor's bottle cap allows the gas collection system. Gas samples are drawn using a syringe and analyzed by a 990 Agilent MicroGC, allowing identification of gas composition in the biogas mixture.
The experimental Biomethane potential tests (BMP) tests were aimed at investigating the property of hydrochar to act as substrate and/or an AD performance booster. The experimental setup involves two AD reactors working in parallel, one is filled with only sewage sludge and used as blank control. The second reactor is filled with the same quantity of sewage sludge and a specified amount of hydrochar. The food-to-microorganism (F/M) ratio was fixed equal to 1 in terms of total volatile solids (TVS).
To prevent the solubilization of CO_2 in the liquid of the biogas measurement system a 0.1 molar solution of water and HCl was used with a resulting pH of 1.2.

Figure 2. Liquid Displacement System

Parameters such as biogas production yield, methane percentage in the biogas, or biogas production time are considered to optimize process.
The preliminary results have demonstrated that hydrochar shows considerable potential to enhance the performance of the AD process. It is a valuable by-product compound with promising capacity to increase AD performance process (Figure 3). Notably, it can enhance methane production, increasing the total yield by 18% to 30%, depending on the quantity added to the sewage sludge in the anaerobic digestion (AD) process.
Furthermore, interest in other products derived from HTC is being explored, particularly the liquid fraction of the HTC process, which primarily consists of water with the presence of volatile fatty acids (VFAs) [7]. Depending on the biomass feedstock and HTC conditions, the liquid phase can contain up to 2-5 g/L of VFAs like acetic, propionic, and butyric acids. Techniques such as liquid-liquid extraction and membrane filtration have been demonstrated to efficiently isolate these acids at high purities, enhancing their commercial value. Optimizing the HTC process to maximize VFA production not only transforms waste biomass into valuable biochemicals but also improves the sustainability and economic viability of the integrated HTC-anaerobic digestion (AD) process, potentially increasing the overall VFA yield by up to 20%. This approach presents a strategic method to enhance biomass utilization and support circular

economy initiatives. Following the HTC process, extraction of VFAs from the liquid phase can be conducted, further enhancing the potential applications and sustainability of the HTC-AD integrated approach.

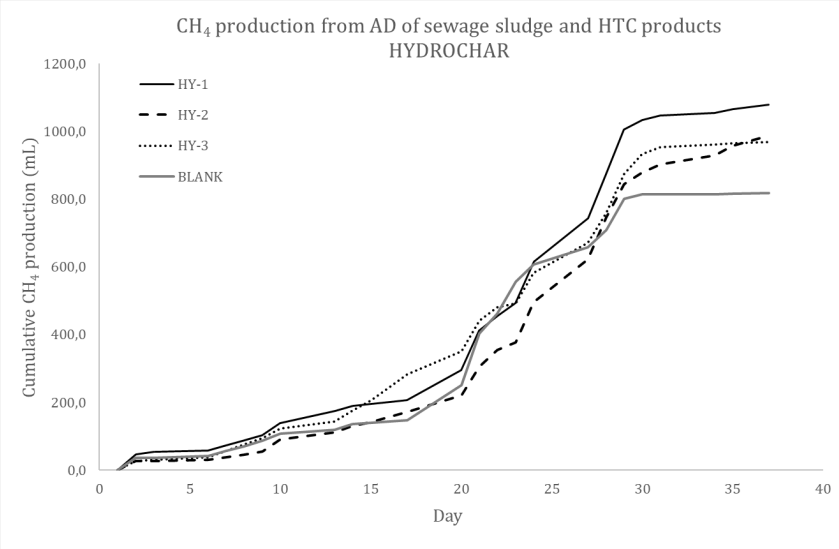

Figure 3. Methane production from AD of sewage sludge and various dosages of Hydrochar (HY 1-3)

References

[1] M. U. B. Khawer, S. R. Naqvi, I. Ali, M. Arshad, D. Juchelkov, M. W. Anjum e M. Naqvi, «Anaerobic digestion of sewage sludge for biogas & biohydrogen production: State-of-the-art trends and prospects,» *Fuel,* 2022.

[2] S. W. T. S. S. A. N. M. P. S. V. S. K. K. J. W. M. K. A. M. J. T. S. Harirchi, «Microbiological insights into anaerobic digestion for biogas, hydrogen or volatile fatty acids (VFAs): a review,» *Bioengineered,* pp. 13:3, 6521-6557, 2022.

[3] X. e. a. Ma, «Alkaline fermentation of waste activated sludge with calcium hydroxide to improve shot-chain fatty acids production and extraction efficiency via layered double hydroxides.,» *Bioresource technology,* vol. 279, pp. 117-123, 2019.

[4] J. Z. Q. Y. J. S. C. P. F. C. Q. X. S. W. D. W. X. L. a. G. Z. X. Wang, «Evaluating the potential impact of hydrochar on the production of short-chain fatty acid from sludge anaerobic digestion,» *Bioresource Technology,* pp. 234-241, 2017.

[5] R. Ferrentino, F. Merzari, L. Fiori e G. Andreottola, «Coupling Hydrothermal Carbonization with Anaerobic Digestion for Sewage Sludge Treatment: Influence of HTC Liquor and Hydrochar on Biomethane Production,» *Energies,* pp. 13, 6262, 2020.

[6] Q. e. a. Xu, «Hydrochar mediated anaerobic digestion of bio-wastes: Advances, mechanisms and perspectives.,» *Science of the Total Environment,* n. 163829, 2023.

[7] S. M. M. A. G. Divya Gupta, «Investigation on hydrochar and macromolecules recovery opportunities from food waste after hydrothermal carbonization,» *Science of The Total Environment,* vol. 749, n. 142294, 2020.

Environmental impact assessment involving advanced multispectral techniques to characterize pollution phenomena and improve situational awareness: a case study on the Avernus Lake

M. Ajaoud[1,*]; C. Ciccarelli[1,*] and M. Lega[1].

[1]*Department of Engineering, University of Naples Parthenope (Italy)*

Corresponding author: massimiliano.lega@uniparthenope.it

* These authors contributed equally to this work.

Keyword(s): Environmental Impact Assessment, Situational Awareness, Multispectral Techniques

Abstract

Recently, environmental preservation gained a central role in the general discourse, reflecting a growing recognition of our responsibility to safeguard natural resources. To preserve the environmental balance, environmental impact assessment activities have become integral to various project developments and sustainability initiatives, as Lega et al. emphasized the importance of comprehensive monitoring in Environmental Impact Assessment (EIA) [1].

To better describe, survey and model contaminated soil and water resources, the scientific realm is involved in using advanced techniques. A pivotal aspect of this research lies in the interdisciplinarity of the approach, which facilitates understanding the complex connection within the environmental systems. Therefore, it's necessary to have a multidisciplinary method which employs various methodologies and technologies to enhance the process.

Responding to this imperative, our research group has developed an innovative approach to environmental monitoring, integrating on-site surveys with proximal/remote sensing-based technologies such as multispectral and thermal analysis.

The combination of these methods enables the collection of diverse environmental data, enhancing our ability to observe, detect, and predict environmental changes over different scales and time periods, an illustration of that is the Fast Detection Strategy for Cyanobacterial blooms and associated Cyanotoxins [2]. Through the use of this methodology, we aim to enhance situational awareness for the environment.

Our case study focused on the multilayered characterization of an environmental anomaly in Avernus Lake, Italy. Utilizing multispectral analysis techniques, we performed a survey on the water body across various years, particularly during periods associated with harmful algal blooms, for example the phenomenon of April 2022, as Esposito et al. thoroughly studied [3]. Subsequently, we focused on the source area of these blooming and, employing thermal fingerprint analysis, we were able to characterize

a wastewater discharge. The thermal imaging revealed a distinct temperature differential in the form of a plume, indicating the presence of a wastewater discharge point, probably linked to human activities that are conducted in the area. Furthermore, Lega et al. underscored the efficacy of remote sensing in distinguishing water quality characteristics and spatial features of plumes [4].The in-situ sampling and chemical analysis gave confirmation to the thermal observation, showing the presence of different components in the water.

This case study demonstrates the potential of such interdisciplinary and multilayered approaches in advancing our understanding of complex environmental phenomena, particularly in the realm of pollution dynamics, ultimately promoting a more sustainable and responsible management of our natural resources.

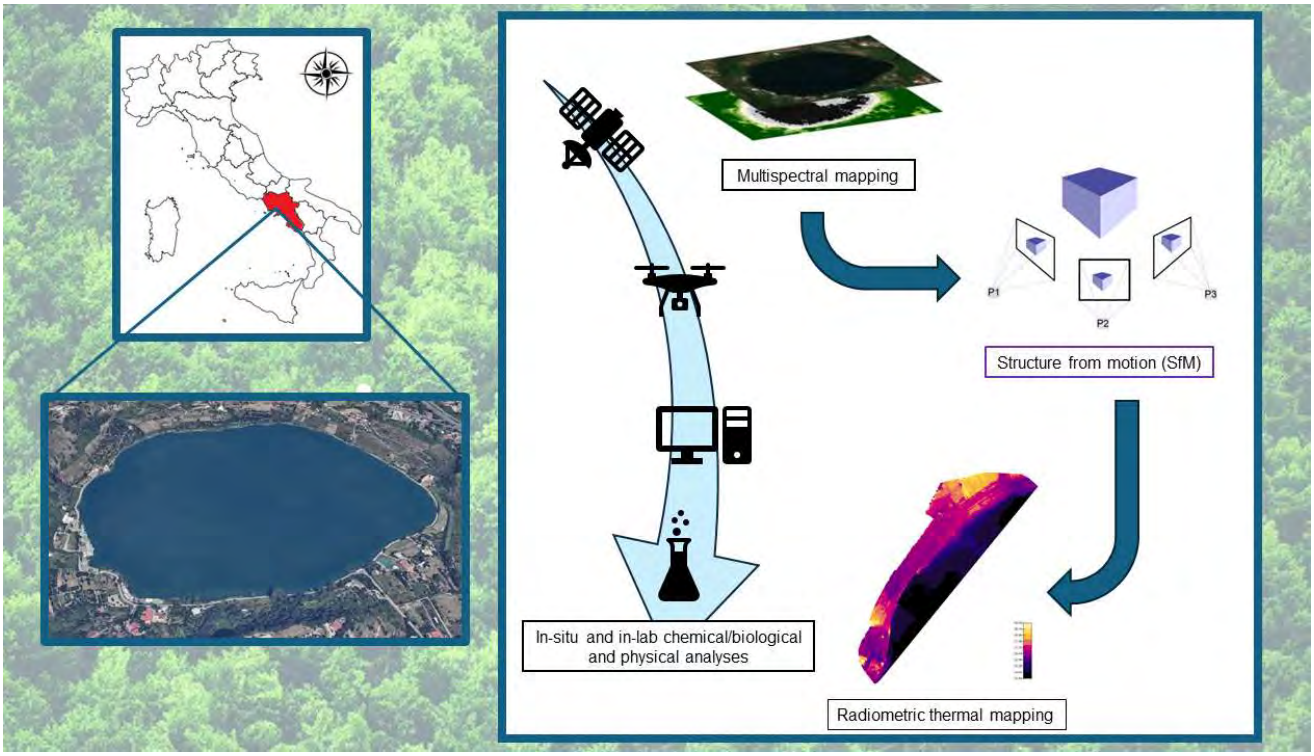

Figure 1: Synthesis of the workflow.

Acknowledgments: Some authors conducted the activities described here within the framework of the international PhD program and the UNESCO Chair 'Environment, Resources and Sustainable Development,' thanks also to a specific contribution of the Italian Aerospace Research Centre (CIRA).

The authors' activities were also supported by the project 'STOPP - Strumenti e Tecniche di Osservazione della Terra in Prossimità e Persistenza' (STOPP - Tools and Techniques for Earth Observation in Proximity and Persistence), managed by the Italian Space Agency (ASI) and involving several Italian universities, institutions, and research centres.

References

[1] Lega, M., Casazza, M., Teta, R., & Zappa, C. J., Environmental impact assessment: A multi-level, multi-parametric framework for coastal waters, International Journal of Sustainable Development and Planning, 13(8), 1041-1049, (2018). https://doi.org/10.2495/SDP-V13-N8-1041-1049.

[2] Esposito, G., Teta, R., Marrone, R., De Sterlich, C., Casazza, M., Anastasio, A., ... & Costantino, V., A Fast Detection Strategy for Cyanobacterial blooms and associated cyanotoxins (FDSCC) reveals the occurrence of lyngbyatoxin A in Campania (South Italy). Chemosphere, 225, 342-351, (2019). https://doi.org/10.1016/j.chemosphere.2019.02.201.

[3] Esposito, G., Glukhov, E., Gerwick, W. H., Medio, G., Teta, R., Lega, M., & Costantino, V., Lake Avernus Has Turned Red: Bioindicator Monitoring Unveils the Secrets of “Gates of Hades”. Toxins, 15(12), 698, (2023). https://doi.org/10.3390/toxins15120698.

[4] Lega, M., & Endreny, T., Quantifying the environmental impact of pollutant plumes from coastal rivers with remote sensing and river basin modelling, International Journal of Sustainable Development and Planning, 11(5), 651-662, (2016). https://doi.org/10.2495/SDP-V11-N5-651-662.

Title: CIRCULAR ECONOMY IN THE TREATMENT OF ALUMINIUM SCRAP METAL

Authors: Dorcas Adejunmobi*[1], Sabrina Sorlini[1], Alessandro Abbà[1]

[1] *Department of Civil, Environmental, Architectural Engineering and Mathematics, University of Brescia, via Branze 43, 25123 Brescia, Italy, dorcas.adejunmobi@unibs.it, sabrina.sorlini@unibs.it, alessandro.abba@unibs.it*

Keywords: Aluminium, Shredder Residue, Recycling, Energy and Material Recovery

Abstract

Primary aluminium (PAl) produced through energy-intensive processes results in significant environmental impacts including deforestation, soil erosion, water pollution, and greenhouse gas emissions (GHG) such as CO_2 [1]. The global production of aluminium (Al) accounts for 3% of GHG emissions in 2022 with about 1.1 Gt of CO_2 per year [2]. Al production requires approximately 1% of global energy consumption. However, the recycling of Al called secondary aluminium (SAl) offers substantial energy savings, reduction of air pollutants, and water conservation compared to PAl production [3]. According to the U.S. Aluminium Association, Al recycling requires only 5% of the energy needed to produce the PAl, resulting in GHG emissions of 0.5t CO_2 equivalent/t recycled Al [4]. With the increase in demand for Al, the production of SAl is experiencing a significant increase [5]. Globally, the amount of SAl has continued to increase, in 2019 20 Mt of Al was produced from old scrap compared to the 1 Mt produced in 1980 [2]. 26% of the SAl was from old scraps originating from packaging, 13% from engineering and cables, 33% from transport and 16% from building applications [2]. In the process chain of SAl production, the shredder process is the mechanical scrap sorting of Al scrap, and it is an essential prerequisite to obtain an excellent product property with high yield of SAl [6].

The development of the processes for recovering Al has reached a steady stage. However, the shredder process produces a residual waste, substantial amounts of the residual waste result from the removal of materials with less conductivity (like stainless steel and non-metallic fractions) during eddy current treatment of scrap. Additionally, residual waste can also come from the separation of lightweight fractions during density sorting of the scrap. The recovery and recycling of these residual wastes are still not fully developed as most of these wastes are mostly disposed into landfill. These residual wastes, called Shredder Residues (SR), consist of plastics, metal, rubber, foam, paper, wood, glass, stones, etc. It is usually assumed that the SRs are not economically valuable [7].

In this study a review is done on the SR by focusing on the composition of the SR and the treatment methods applied. The aim of this study is to give a general understanding of the SR produced by a company called Rottami Padana in the Province of Brescia which could be built upon for the development of solutions for SR management.

The scheme of the Al scrap recycling process is illustrated in the **Figure 1** (yellow arrow shows the flow of the metal scrap undergoing treatment, green arrow - the production, and red arrow - the waste).

The facility recovers ferrous and non-ferrous metals from two types of scrap:

- Type 1: Metal scrap from construction, particularly window profile;
- Type 2: Metal scrap from industrial wastes which include the mixture metal scrap from all sectors like factory waste, automotive parts, etc.

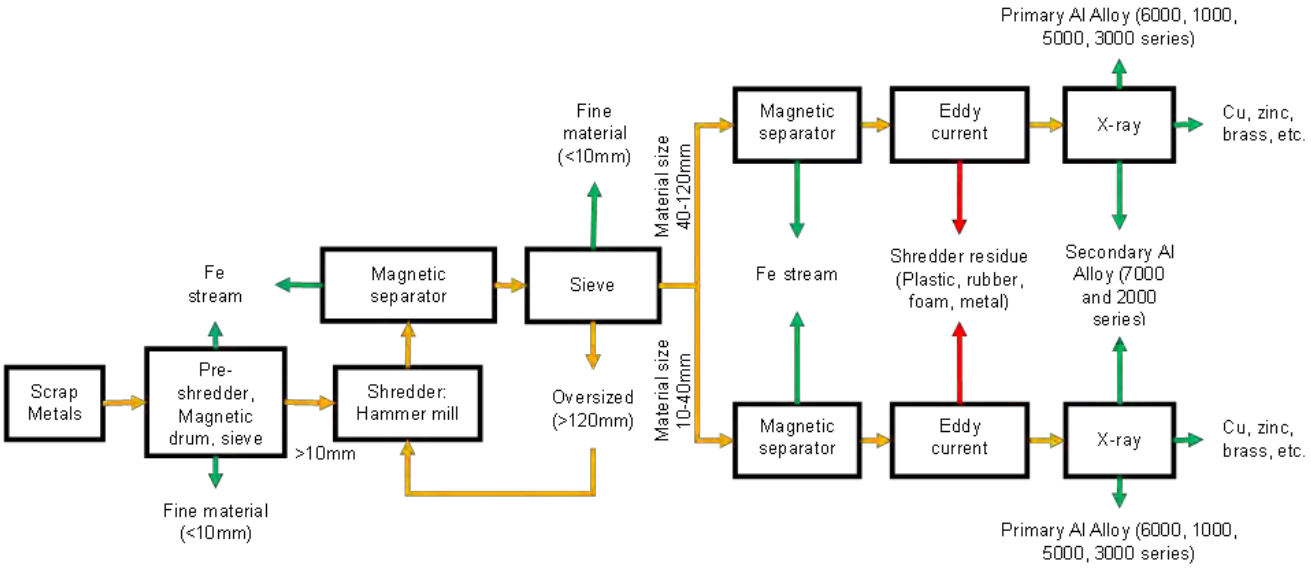

Figure 1. The scheme of the treatment process (shredder facilities)

Hitherto, to the best of authors' knowledge, research solely on SR from other sources of Al scraps asides from the automotive cannot be found in literatures. The composition of SR is similar to the composition of Automotive Shredder Residues (ASR). Literatures [8] focused on the SR as a mixture of ASR with some other residues originating from different sources (like white goods, industrial bulky waste, metal scrap). Some authors [9] stated that ASR comprises approximately 50% of total SR; while other authors [10] focused on the treatment of ASR.
A characterization was done on the SR collected from the shredder plant. **Table 1** shows the percentage of output of the shredder facility. **Table 2** and **Figure 2** reported the average composition of the SR from the facility.

Table 1. Average percentage distribution of output of the shredder facility

	Type 1	**Type 2**
Metal Output	92.42%	93.10%
Primary Aluminium Alloy*	83.20%	76.84%
Secondary Aluminium Alloy + Heavy Metal****	4.16%	11.63%
Iron	5.06%	4.63%
Fine material	3.88%	4.05%
Shredder Residues (SR)	3.66%	2.74%
Weight Loss	0.04%	0.11%

*Primary Aluminium Alloy includes 6000, 1000, 5000 and 3000 series.
**Secondary Aluminium Alloy includes 7000 and 2000 series.
***Heavy Metal includes Copper, Bronze, Zinc, Zamak.

Table 2. Average Material Composition of Shredder Residues (SR)

	Type 1 (Avg %)	Type 2 (Avg %)
Metal	20.00	20.50
Plastics	36.32	27.50
Light Plastics	8.25	30.66
Rubber	28.20	10.24
Wood	2.81	3.53
Foam	1.48	1.94
Textile	2.94	3.35
Stone	0	2.28

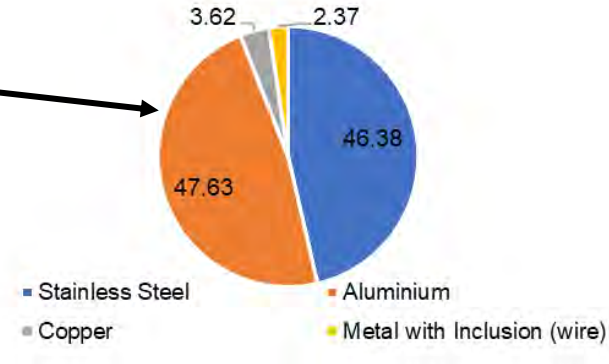

Figure 2. Average composition metal residues (%)

The heterogeneity of the SR is the major challenge in its treatment in a cost effective and environmentally friendly manner [12]. Different treatment methods have been applied to SR for the purpose of recovering energy and materials, these methods can be grouped into two, mechanical sorting, and thermal treatment: the mechanical sorting is aimed at concentrating material fractions that can be recycled and/or reducing pollutant release before further recovery processes or disposal, while the thermal treatment (pyrolysis, incineration, gasification) is aimed at energy recovery.
The treatment of SR begins with the removal of metal fractions (non-ferrous and ferrous metal except stainless steel). This is typically done using technology similar to that found in shredder facilities (see **Figure 1**), therefore, to further decrease the metal content in the SR, SR can undergo a second pass through shredder facilities. Also, a high-intensity magnet can then be used to separate weakly magnetic particles like stainless steel [13]. The upcycling of plastics from SR when mixed plastics are recovered as new product is a method to recycling plastics from SR where the individual separation of the different plastics is not easy nor economical effective. Some authors [14] considered the use of fine fraction of ASR in concrete paving blocks to replace the natural fine aggregate through the Portland cement solidification/stabilization technique with a 20% substitution content of the fine sand for the fine fraction of ASR. The resulting concrete paving block could be used as a potential solution to reduce the environmental impact from landfilling disposal.
Some authors have studied the production of SRF (solid recovered fuel) from the non-metal fraction of ASR [15] while [16] studied SR as a potential feedstock for cement manufacturing. SRF are solid fuels prepared from non-hazardous waste to be used for energy recovery in incineration plants. SRF was characterised and classified by the ISO 21640:2021, this classification is based on three major indicators lower heating value, chlorine and mercury content. The main barriers to the recovery of SR are the presence of contamination like PVC which increases the chlorine content of the SRF; the heterogeneity and variability of the SR which make some properties of the SR always varying, thus challenging to design a fixed treatment process or suitable co-combustion path in cement kiln.
In conclusion, despite the benefits of SAI, challenges persist in effectively managing SR generated in the process, characterized by its diverse composition and inherent variability. Mechanical sorting with material recovery and thermal treatment methods are essential for extracting value from SR. Innovative strategies such as the second passing of the waste through the shredder facilities, the sustainable upcycling of industrial mixed plastic from SR, and utilizing non-metal fraction of SR as SRF show promise in addressing these challenges. However, the presence of contaminants and the heterogeneous nature of SR necessitate further research and collaborative efforts to develop sustainable SR management practices in the aluminium industry. Most of the research on this kind of waste are majorly tailored towards the management of residual waste from the treatment of End-of-Life

vehicles (i.e. ASR) with less attention on the SR from the treatment of other types of scrap. More research attention needs to be given to other types of SR to advance innovative treatment solutions.

Acknowledgement

This work is supported by Rottami Padana (Castegnato, Brescia – Italy), which is co-funding the research activities in the Ph.D. Programme in Civil and Environmental Engineering, International Cooperation, and Mathematics (DICACIM).

References

[1] S. Carlisle and E. Friedlander, 'The influence of durability and recycling on life cycle impacts of window frame assemblies', *Int J Life Cycle Assess*, vol. 21, no. 11, pp. 1645–1657, Nov. 2016, doi: 10.1007/s11367-016-1093-x.
[2] D. Raabe *et al.*, 'Making sustainable aluminum by recycling scrap: The science of "dirty" alloys', *Progress in Materials Science*, vol. 128, p. 100947, Jul. 2022, doi: 10.1016/j.pmatsci.2022.100947.
[3] U.S. Environmental Protection Agency, 'Environmental Facts: Recycling Saves Energy and Reduces Pollution', U.S. Environmental Protection Agency. [Online]. Available: https://www.epa.gov/facts-and-figures-about-materials-waste-and-recycling/environmental-facts-recycling-saves-energy
[4] W. T. Choate and J. A. S. Green, 'U.S. Aluminum Production Energy Requirements: Historical Perspective, Theoretical Limits, and New Opportunities', 2003.
[5] V. K. Soo, J. R. Peeters, P. Compston, M. Doolan, and J. R. Duflou, 'Economic and Environmental Evaluation of Aluminium Recycling based on a Belgian Case Study', *Procedia Manufacturing*, vol. 33, pp. 639–646, 2019, doi: 10.1016/j.promfg.2019.04.080.
[6] G. Gaustad, E. Olivetti, and R. Kirchain, 'Improving aluminum recycling: A survey of sorting and impurity removal technologies', *Resources, Conservation and Recycling*, vol. 58, pp. 79–87, Jan. 2012, doi: 10.1016/j.resconrec.2011.10.010.
[7] Cheminfo Services Inc, 'Background Study on the Content of Shredder Residue'. Jan. 2014.
[8] N. Ahmed, H. Wenzel, and J. B. Hansen, 'Characterization of Shredder Residues generated and deposited in Denmark', *Waste Management*, vol. 34, no. 7, pp. 1279–1288, Jul. 2014, doi: 10.1016/j.wasman.2014.03.017.
[9] GHK and Bio Intelligence Service, 'Annex 3: Post-Shredder Technologies – Review Of The Technologies And Costs'. 2006.
[10] S. K. Vijayan and S. Bhattacharya, 'Processing of automotive shredder residues: Economic evaluation of a process for energy and high-value metals recovery', *Cleaner Chemical Engineering*, vol. 6, p. 100103, Jun. 2023, doi: 10.1016/j.clce.2023.100103.
[11] R. Cossu *et al.*, 'ITALIAN EXPERIENCE ON AUTOMOTIVE SHREDDER RESIDUE: CHARACTERIZATION AND MANAGEMENT', 2012.
[12] S. K. Vijayan, M. A. Kibria, M. H. Uddin, and S. Bhattacharya, 'Pretreatment of Automotive Shredder Residues, Their Chemical Characterisation, and Pyrolysis Kinetics', *Sustainability*, vol. 13, no. 19, p. 10549, Sep. 2021, doi: 10.3390/su131910549.
[13] W. Ge, A. Encinas, E. Araujo, and S. Song, 'Magnetic matrices used in high gradient magnetic separation (HGMS): A review', *Results in Physics*, vol. 7, pp. 4278–4286, 2017, doi: 10.1016/j.rinp.2017.10.055.
[14] J. A. Caetano, V. Schalch, and J. M. Pablos, 'Characterization and recycling of the fine fraction of automotive shredder residue (ASR) for concrete paving blocks production', *Clean Techn Environ Policy*, vol. 22, no. 4, pp. 835–847, May 2020, doi: 10.1007/s10098-020-01825-y.
[15] E. Acha *et al.*, 'Combustion of a Solid Recovered Fuel (SRF) Produced from the Polymeric Fraction of Automotive Shredder Residue (ASR)', *Polymers*, vol. 13, no. 21, p. 3807, Nov. 2021, doi: 10.3390/polym13213807.
[16] Bob Boughton, 'Evaluation of Shredder Residue as Cement Manufacturing Feedstock'. Mar. 2006.

Title: Complex water treatment – from pharmaceuticals to microplastics

Author(s): Marketa Spacilova*[1], Pavel Dytrych[1], Martina Dlaskova[1], Olga Solcova[1]

[1] *Department of Catalysis and Reaction Engineering, Institute of Chemical Process Fundamentals of the CAS, Rozvojova 135, 165 00 Prague, Czech Republic*

Keyword(s): removal of contaminants; micropollutants; microplastics; biochars; sorption

Abstract

The presence of a wide range of diverse micropollutants in water sources is one of the greatest global challenges of our time [1]. These compounds usually pass through some sewage treatment plant without changes. Most of these micropollutants (pharmaceuticals, hormones, pesticides, etc.) are known to pose a major threat to many organisms as they can cause significant acute and chronic ecotoxicological effects even at low concentrations [2,3]. Microplastics have recently been added to this group of pollutants, making the search for new and effective ways to remove them a necessity. Their widespread use in recent years has led to micropollutants accumulation in the environment and their penetration into living organisms through the food chain [4]. Therefore, the removal of these substances from water is getting extremely important for our health and environment. For these reasons, the aim of this work was to find new effective and well-applied natural-based sorbents whose effectiveness was tested in the removal of selected micropollutants including microplastics from wastewater.

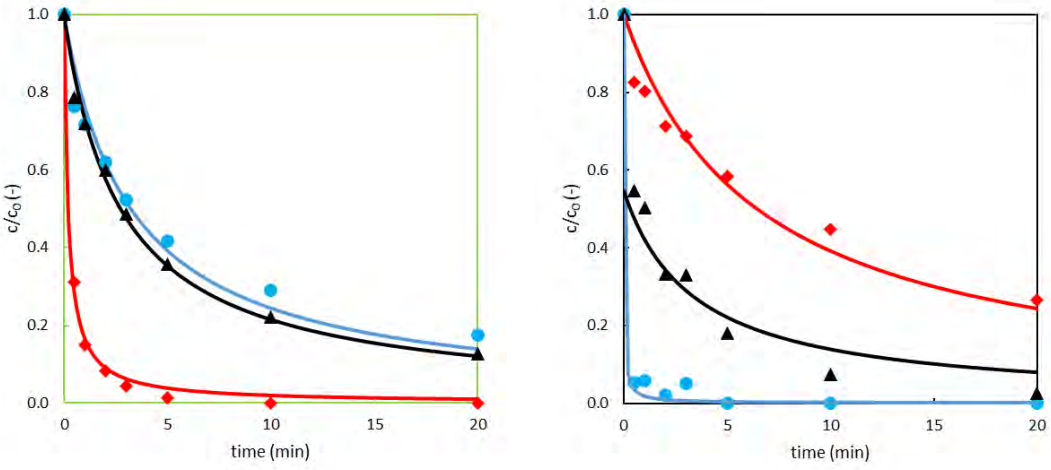

Figure 1 Comparison of sorption rates of the tested pollutants (**diclofenac**, **naproxen**, **acetaminophen**) to prepared microalgae biochar (left) and activated carbon Supersorbon (right)

Biochar-based sorbents were prepared using three types of waste plant materials (marine macroalgae originating in the Atlantic, sunflower seed husks and biomass from microalgae chlorella after extraction) to remove micropollutants. The effectiveness of the prepared sorbents was verified on selected pharmaceuticals present in wastewater, namely diclofenac, naproxen, acetaminophen and triclosan. The removal efficiency related to this approach reached up to 96%, whereas the commercial activated

carbon of Supersorbon achieved only 69%. A competitive sorption of a mixture of these substances was also tested to approximate real wastewater (Fig. 1).
In addition, the removal of a currently very problematic group of micropollutants – microplastics, was tested using economically inexpensive natural sorbents, bentonites. The obtained data contributed significantly to the design and implementation of a semi-operational column. The developed column was tested during a several-month campaign at the Central Wastewater Treatment Plant in Prague with high removal efficiency [5].

Acknowledgement

The financial support from the Technology Agency of the Czech Republic project TN02000044 is gratefully acknowledged.

References

[1] da Barcello, D.S., Procopiuck M., Bollmann H.A., Management of pharmaceutical micropollutants discharged in urban waters: 30 years of systematic review looking at opportunities for developing countries, Sci. Total Environ., 809 (2022), 10.1016/j.scitotenv.2021.151128.
[2] Yu Y., Tong D., Yu Y., Tian D., Zhou W., Zhang X., Shi W., Liu G., Toxic Effects of Four Emerging Pollutants on Cardiac Performance and Associated Physiological Parameters of the Thick-Shell Mussel (Mytilus Coruscus). Environmen Pollut, (2023), 334, 122244. https://doi.org/10.1016/j.envpol.2023.122244.
[3] Tenorio-Chávez P., Cerro-López M., Castro-Pastrana L. I., Ramírez-Rodrigues M. M., Orozco-Hernández J. M., Gómez-Oliván L. M., Effects of Effluent from a Hospital in Mexico on the Embryonic Development of Zebrafish, Danio Rerio. Sci Total Environ, (2020), 727, 138716. https://doi.org/10.1016/j.scitotenv.2020.138716.
[4] Li X., Liu Y., Yin Y., Wang P., Su, X., Occurrence of Some Legacy and Emerging Contaminants in Feed and Food and Their Ranking Priorities for Human Exposure. Chemosphere, (2023), 321, 138117. https://doi.org/10.1016/j.chemosphere.2023.138117.
[5] Spacilova M., Dytrych P., Lexa M., Wimmerova L., Masin P., Kvacek R., Solcova O., An Innovative Sorption Technology for Removing Microplastics from Wastewater. Water. (2023), 15(5):892. https://doi.org/10.3390/w15050892.

Title: Fluidized bed co-combustion of used toner cartridges with sewage and paper mill sludge

Author(s): Hana Snajdaufova*[1], Milan Carsky[1], Marek Jadlovec[2], Stanislav Honus[2], Olga Solcova[1]

[1] *Institute of Chemical Process Fundamentals CAS, v.v.i., Rozvojova 135/1, 16500 Prague 6, Czech Republic, snajdaufova@icpf.cas.cz*
[2] *Technical University of Ostrava, Department of Energy, Ostrava, Czech Republic*

Keyword(s): Toner cartridges, combustion, fluidized bed

Abstract

The paper addresses increasing world volumes of waste, namely sewage sludge, paper mill sludge, and electronic waste; and its use as an alternative fuel. Half of collected empty printer and toner cartridges can be reused to save greenhouse gas emissions. There are either “original toner cartridges” bearing the same trademark as the corresponding printer and copier or “compatible toner cartridges” with a different trademark. However, the latter ones are not reused and go mostly into material recycling or combustion [1]. Crushed toner cartridges (from the original toner cartridges) were combusted with sewage sludge (and its blends with paper mill sludge) pellets in a fluidized bed of sand at the temperature of 800-900°C. The pilot plant combustor used [2, 3] is shown in Fig.1. After reaching a steady state, the flue gas was analysed for Hg, CO, CO_2, NO_x, SO_2, NH_3, HF, HBr and HCl at the oxygen flue gas concentration of 11 %. The results of the analysis are given in Tables 1, 2, and 3.

Table 1. Flue gas concentration at combustion of crushed toner cartridges (10%) with a pelletized sewage sludge (90%)

CO_2 %	CO mg/m³	NH_3 mg/m³	NO_x mg/m³	SO_2 mg/m³	HF mg/m³	HBr ppm	HCl mg/m³	Hg µg/m³
4,4	211	1,9	572,3	995,7	2	0,041	62,2	50,2

Table 2. Flue gas concentration at combustion of crushed toner cartridges (10%) with a pelletized 4:1 blend of a sewage and paper mill sludge (90%)

CO_2 %	CO mg/m³	NH_3 mg/m³	NO_x mg/m³	SO_2 mg/m³	HF mg/m³	HBr ppm	HCl mg/m³	Hg µg/m³
4,5	176,3	2,3	564,7	933,2	2,3	1,7	42,9	37,3

Table 3. Flue gas concentration at combustion of crushed toner cartridges (10%) with a pelletized 2:1 blend of a sewage and paper mill sludge (90%)

CO_2 %	CO mg/m³	NH_3 mg/m³	NO_x mg/m³	SO_2 mg/m³	HF mg/m³	HBr ppm	HCl mg/m³	Hg µg/m³
4,6	213	2	383,5	717,7	1,6	0,056	16,7	32,2

The concentrations of pollutants were below acceptable limits agreed on in most EU countries, with the exceptions of SO_2, HCl, CO, and NO_x, indicating a need for a downstream flue gas cleaning. Mercury concentration in the flue gas decreased substantially with the addition of paper mill sludge. Carbon dioxide concentration in the flue gas was not significantly affected by the addition of paper mill sludge. The concentrations of Carbon monoxide have to be lowered by a secondary air input. While a usual flue gas cleaning is still necessary, this alternative fuel may be used for fluidized bed combustion.

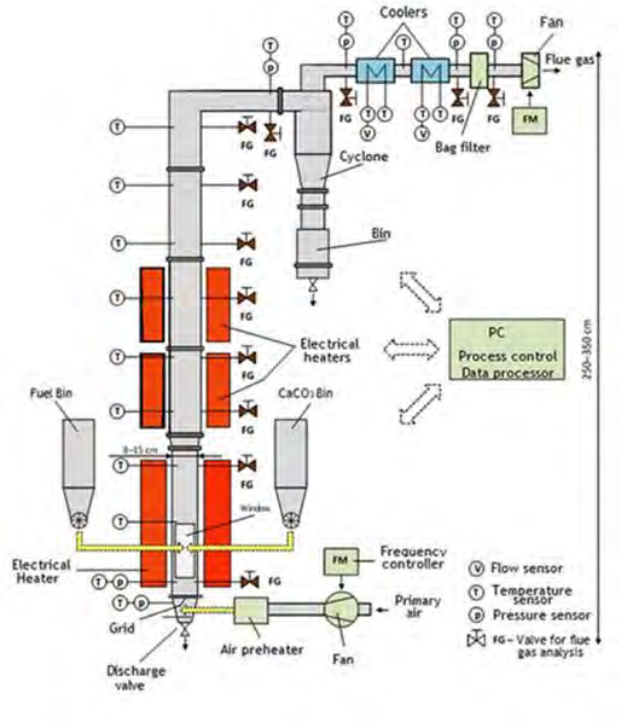

Figure 1. Fluidized bed combustor

Acknowledgement:

The financial support from the Technology Agency of the Czech Republic project TN02000044 is gratefully acknowledged.

References

[1] Interzero, “Reuse of toner cartridges: Study proves concrete environmental benefit” https://www.interzero.de/en/media/service-for-journalists/press-releases/detail/reuse-of-toner-cartridges-study-proves-concrete-environmental-benefit/ ,Accessed 21 May 2024.
[2] Carsky M., Solcova O., Soukup K., Kralik T., Vavrova K., Janota L., Vitek M., Honus S., Jadlovec M., Wimmerova L., “Techno-Economic Analysis of Fluidized Bed Combustion of a Mixed Fuel from Sewage and Paper Mill Sludge”, Energies, *15*(23), (2022), 8964
[3] Vavrová K., Kralik T., Janota L., Solcova O., Carsky M., Soukup K., Vítek M., “Process Economy of Alternative Fuel Production from Sewage Sludge and Waste Celluloses Biomass”, Energies, 16, (2023), 518

Title: Farmland from brownfields by animal waste hydrolysate

Author(s): Lenka Moravkova*[1], Martina Dlaskova[1], Frantisek Kastanek[1], Olga Solcova[1]

[1] *Institute of Chemical Process Fundamentals CAS, v.v.i., Rozvojova 135/1, 16500 Prague 6, Czech Republic, moravkova@icpf.cas.cz*

Keyword(s): soil contamination, animal waste hydrolysate, brownfields, heavy metal contamination

Abstract

Metal contamination of soils is one of the phenomena which have a negative impact on human health. Therefore, a hydrolysate obtained by thermal pressure hydrolysis of animal wastes (poultry feathers) [1] was applied as a chelating agent for the leaching of heavy metals from brownfields - industrial soils contaminated with heavy metals after years of metallurgical and coking activities.
Hydrolysates were prepared in a stainless steel stirred 25 l autoclave in a weakly acidic environment (malic acid) at the temperature of 140 °C for 5 h at inert atmosphere. 2 kg of waste frozen material was placed in 15 l of water with 100 g of malic acid added. The composition of the hydrolysate is a set of amino acids with predominantly aspartic acid, peptides, proteins and water. The amount of amino acids represented 5-8 g/l, and the sum of peptides and proteins up to 40 g/l. The representation of individual amino acids is shown in the Fig. 1.

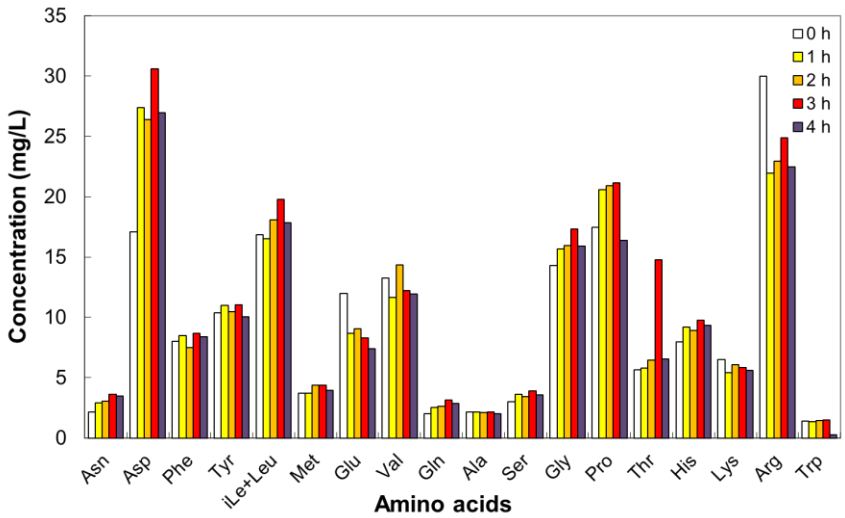

Figure 1 Representation of individual amino acids in hydrolysate

The hydrolysate, when specifically used as a chelating agent, was doped with small proportions of thiourea (1.5%) and citric acid (3%). The soil samples were, firstly, sieved to the grain size of 1.25 mesh, mixed with hydrolysates and stirred at room temperature for 72 h, then filtered and analysed for the

metal content by MP-AES. The extraction efficiencies of hydrolysates were compared with the extraction efficiency of EDTA (Ethylenediaminetetraacetic acid).

The metal extraction efficiency of the hydrolysate was on average in small units of % for most heavy metals (Cu, Mn, Pb, Zn). The extraction efficiency of the hydrolysate was compared under standard 24 h conditions with an EDTA-based wash solution. In the case with EDTA, the heavy metal leaching was also similar or even lower than with the hydrolysate.

Table 1. Metal extraction after 4 days

Metal extraction		**Cu** %	**Fe** %	**Mn** %	**Pb** %	**Zn** %
Hydrolysate of poultry feathers	S1	34,4	0,6	29,5	9,5	19,8
	S2	6,2	0,3	7,5	2,6	11,5
	S3	7,8	0,1	5,3	3,7	11,8
EDTA	S1	14,0	0,0	2,8	2,2	9,1
	S2	10,5	0,1	2,7	3,6	20,0
	S3	8,2	0,0	1,1	1,5	8,7

However, the composition of the hydrolysate, compared to synthetic chelating agents such as EDTA, allowed a significant bioaccumulation of soil sporo-forming bacteria up to several orders of magnitude [2], here in particular of the genus Bacillus, after a contact time (at least four days) with the soil, producing biosurfactants. That resulted in an indirect decrease in the surface tension and a direct increase in the extraction efficiency of the hydrolysate for heavy metals, in contrast to the comparative extraction of metals from the same soil samples under identical conditions involving EDTA. The leaching efficiency of all common heavy metals increased significantly after soil biostimulation with hydrolysate for 4 days. Furthermore, under the application of the animal hydrolysate, it allowed leaching of Ni and Cr, which cannot leach with EDTA even under increased contact times. After washing the soil with EDTA solutions, there was no increase in soil bacteria and no formation of biosurfactants.
It became evident that, apart from chelating effects, the hydrolysate was a very good biostimulant for soil bacteria (as determined by DNA analysis of soil samples). Even after 24 h, there was a noticeable increase in plant-friendly bacteria such as *Bacillus*, *Paenibacillus*, *Pseudomonas*, *Flavobacterium*, *Streptomyces*, and many others. Nitrogen and carbon content of microbial biomass in samples after hydrolysate treatment was determined by fumigation-extraction method. The results were compared with soil treated with water only. The increase of microbial carbon in the hydrolysate treated soil was more than 30-fold and that of nitrogen even 100-fold. No increase in carbon and nitrogen was evident in the EDTA-treated samples.
The animal hydrolysate appears to be a new promising and affordable biodegradable chelating and biostimulating agent based on natural amino acids and peptides for sustainable and cost-effective leaching of heavy metals from real soils contaminated for many years by industrial activities. In addition, the treated soil is enriched with beneficial soil bacteria that support crop growth.

Acknowledgement:

The financial support from the Strategy AV21 project Food for Future and the Technology Agency of the Czech Republic project TN02000044 is gratefully acknowledged.

References

[1] Solcova O., Knapek J., Wimmerova L., Vavrova K., Kralik T., Rouskova M., Sabata S., Hanika J., “Environmental aspects and economic evaluation of new green hydrolysis method for waste feather processing”, Clean Techn Environ Policy 21, 1863-1872, (2021). https://doi.org/10.1007/s10098-021-02072-5
[2] Solcova O., Rouskova M., Sabata S., Dlaskova M., Demnerova K., Bures J., Kastanek F., “Removal of heavy metals from Industrial brownfields by hydrolysate from waste chicken feathers in intention of circular bioeconomy”, Environmental Advances 16, 100521, (2024). https://doi.org/10.1016/j.envadv.2024.100521

Title: Early warning system and decision support system for catchment

Author: Marcello DI Vincenzo

Keyword(s): water scarcity, flooding, climate changes, river modelling, hydraulic model

Abstract

XVPGA EWS is a technological solution that generates key automatic alerts in the identification of a flood and its potential effects, reservoir management, and notification to Civil Protection and the population in crisis situations. It's based on the Hydraulic model of the catchment and it can be used also to face water scarcity phenomena, taking in consideration the groundwater, dams and reservoir levels, the melting snows, the precipitation forecast and specific applications to optimize the water use in irrigation.

Picture 1. Predicted floding area in the town

XVPGA EWS integrates an Early Warning System and a Decision Support System onto GIS. It's is a scalable product designed for use by large organizations responsible for water resource planning and management, such as River Basin Authorities, as well as small private users in need of a powerful hydrological management system. This solution can be used in:
-ordinary situation, allow for the exploitation, management, and planning of water for the medium to long term (Hydrological Year).
-extraordinary situation. Droughts, allows the exploitation, management, and planning of seasonal water during periods of water-scarcity
-extraordinary situation.floodings, enable the exploitation, management, and planning of water during flood events (Hourly-Minute).

Picture 2. Rainfall sensors are matched with methereological radar maps

Description:

EWS is a complex simulation system joining different meteorological, hydrological and hydrodinamic models with the aim to modelize catchments as well as possible and the objective of flows forecasting. This expert system needs high technical skills and the incomes are static data regardless of when they were ingested (historical or real time).

It Is an hydrometeorological warning service transforming measured of estimated data in alerts by thresholds crossing in real time. It includes hydrologic simulation and historical information, but functionalities and capabilities are oriented to real time and warnings management and dissemination.

EWS will enable a more efficient and sustainable management of water resources, optimizing their use and minimizing the environmental impact and risks associated with extraordinary situations.

Users will be able to make informed decisions based on data and advanced analytics, leading to improved planning and allocation of water resources for multiple purposes

Simulation and emergency planning will help reduce the risks of floods and other water-related disasters, safeguarding communities and critical infrastructure.

Swift alerting during flood episodes will enable better preparation and response to flood events, minimizing associated risks and damages, and facilitating communication among different emergency management agencies (Civil Protection, police, municipalities, water authorities, etc.). The tool displays indicators for operations and management to the user. Additionally, it provides the capability to generate graphic information, allowing for holistic management and visualization based on user types and assigned roles.

The proposed solution provides the user with a comprehensive map-based visualization of public asset data deployed in the study area

GoAigua-EWS adapts to the user's characteristics and systems. This adaptability allows for continuous improvement as information and needs expand.

The system enables fast and reliable predictions and monitoring of adverse weather phenomena based on predefined and customized thresholds. It allows the creation of user groups based on the type of alert.

Methodology:

The first step is the **data ingestion (Big Data)** from:

- Accessing to hydro-climatical sensors networks.
- Weather forecast numerical models.
- Precipitation maps: areal interpolation.
- Accessing meteorological RADAR.
- Setting rainfall in sensors.
- Geostatistical methods: Kriging, CoKriging CoLocalized, Kriging with External Drift.
- Territory zonify.

After the system realize a **Precipitation analysis(fast flood)** through a real-time computation of a real precipitation, having as objective an immediate detection of risk areas, both current and forecasted. To do that are considered:

- Observed precipitation maps.
- Forecasted precipitation maps.
- Risk areas maps + risk zones (rainfall accumulation in ToC).
- Flow estimations.
- Hydrological Event and Recession Model with Antecedent Moisture Establishment, Highly parameterizable and extensible.

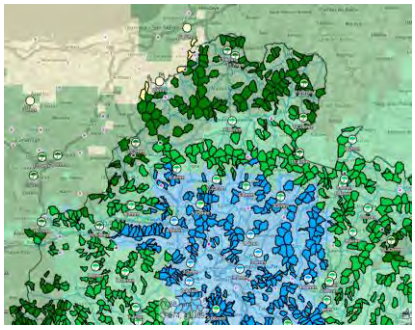

Picture 4. ToC1h

EWS can can provide estimated hydrograph at the discharge points of all watersheds. Zoning by different ToC (1h, 2h, 3h, 6h, 12h, etc.). Any ToC can be included. Proceding in this way is possible to integrate rainfall in catchments, to do a Concentration time analysis, with Intensity-Duration-Frequency curves and a Unitarian hydrologic modelling

River analysis (river flood)

In the same time a continuous river analysis is implemented: continuous hydrologic and hydrodynamic modelling in full basin providing estimations for hydrologic variables (snow cover & resources, precipitation, runoff flows, flow rate, dam maneuvers):

- Snowmelt model.
- Rainfall-Runoff model.
- Hydrograph transmission model.
- Reservoirs management model: the rese rvoir evolution given outflows setting by a technician and automatic recommendation of maneuvers during a flood event.

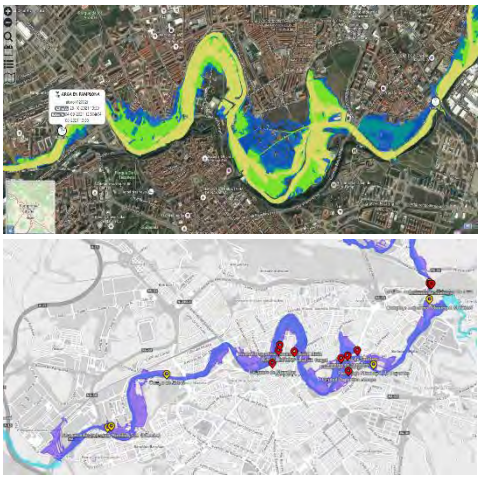

Picture 5. River Hydrograph model

The Objective is determining event severity, current and forecast, Observed flows, Forecasted flows,, Return periods maps, providing estimations for hydrologic variables (snow cover & resources, precipitation, runoff flows, flow rate, dam maneuvers).

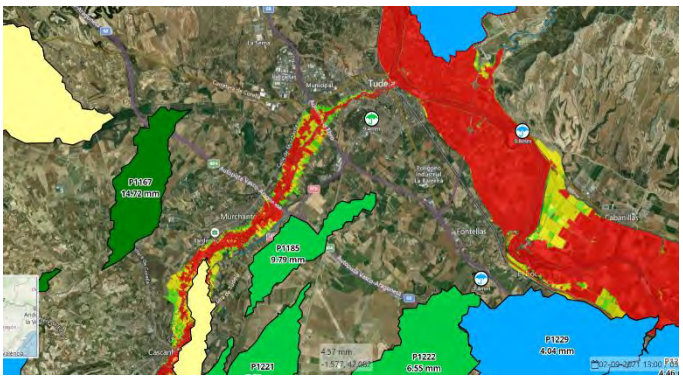

Picture 5. Risk area map

Matching together all these data in a unique catchment model is possible to have an immediate detection of risk areas, both current and forecasted. It could be extrapolated an Observed precipitation maps, a forecasted precipitation maps, a Risk areas maps + risk zones (rainfall accumulation in ToC) as shown in the Picture 5, and Flow estimations.

Event monitoring and alert dissemination

Finally it's possible to proceed with a configuration allows setting alerts by:

- Weather variables thresholds.
- Hydrological variables thresholds.
- Lineal combination of different variables.
- For ALL THE DATA stored.

Each actor in the event management must have only the information they need and understand. A stackholder adaptation is done according the Location, the Responsibility and Technification skill.
Ian automatic dissemination is possible through instant messaging to cell phones or other methods (email, SMS, etc.).

We can submit 2 case studies concerning the Hebro catchment in Spaing implemented in 2020

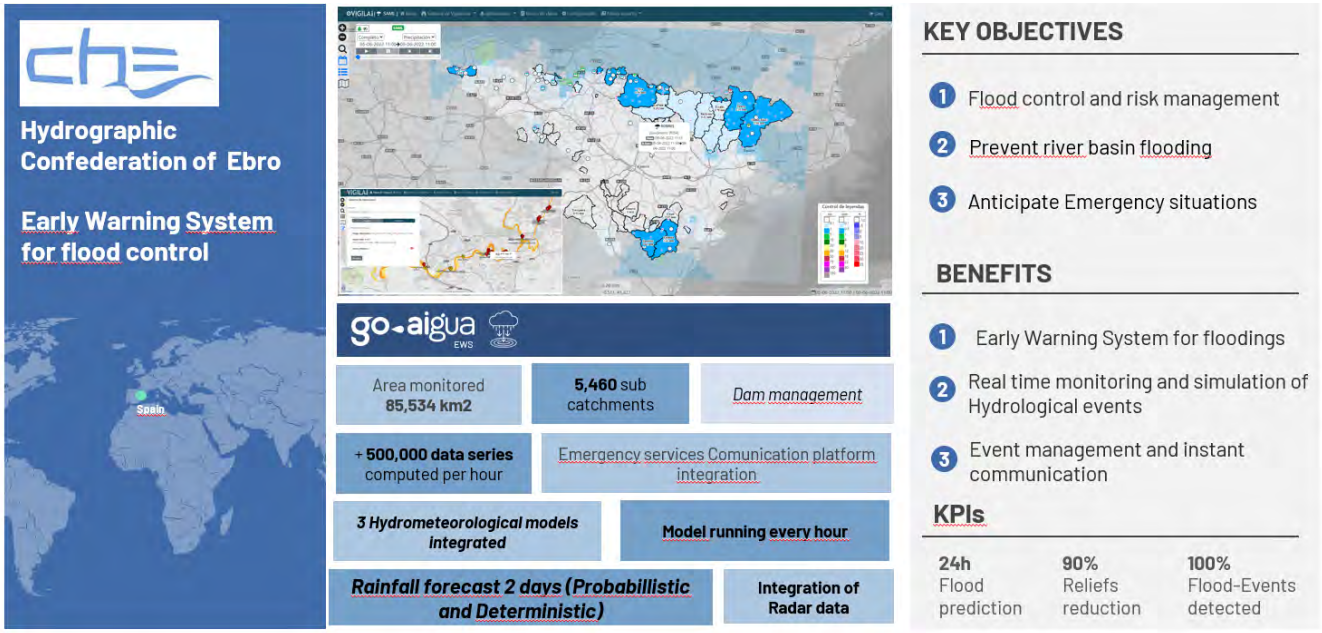

And Navarre Region also implemented in 2022:

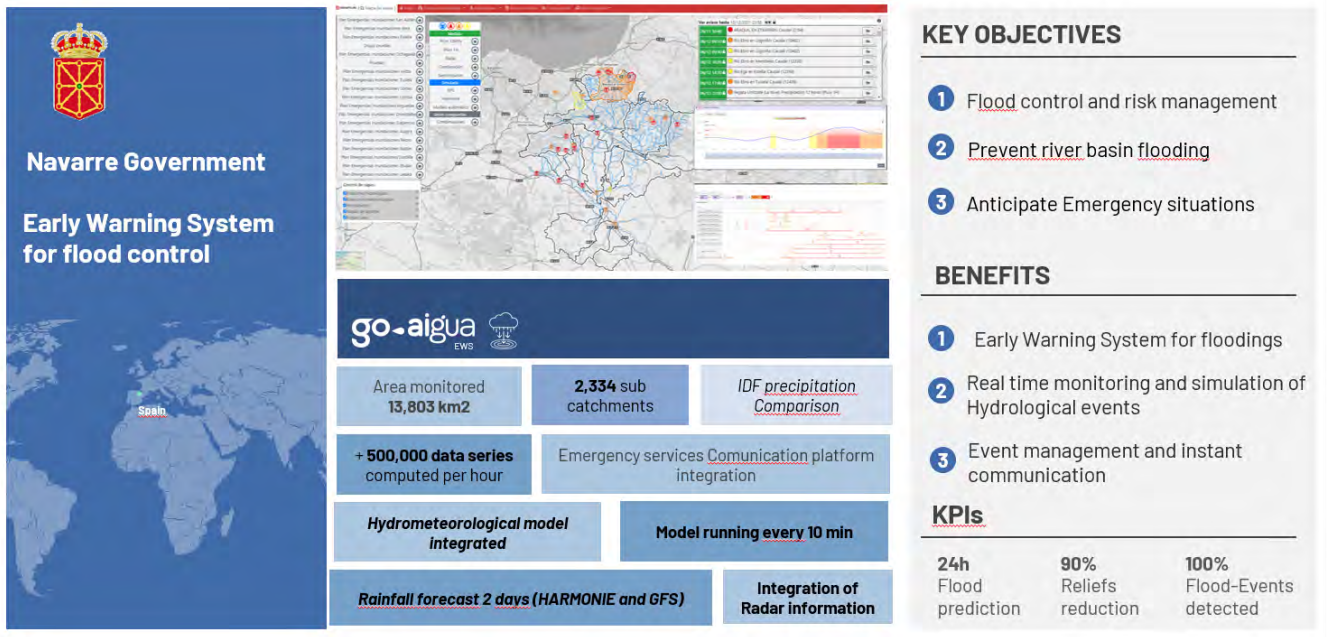

Title: Exploring the role of wastewater treatment plants in microplastics management: a scoping review on fate and occurrence.

Author(s): Alberto Zoccali*[1], Francesca Malpei[1]

[1] *Department of Civil and Environmental Engineering (DICA), Politecnico di Milano, Milan, Italy*

Keyword(s): Data repository, Microplastics, Removal, Wastewater treatment plant

Abstract

In the recent years, microplastics (MPs) have become a global environmental concern due to their widespread occurrence and potential ecological and human health risks. For these reasons, the scientific community considers their presence one of the most interesting recent environmental issues and has exponentially increased its efforts to study the problem in all its aspects. MPs have been identified as Contaminants of Emerging Concern (CEC) [1] and their widespread presence in any environmental compartments and some biota has been confirmed by numerous studies. Among the different sources of MPs into surface water, wastewater treatment plants (WWTPs) discharges are considered as the main terrestrial pathways of MPs emissions into aquatic ecosystems [2]–[5]. Although WWTPs were not designed for MPs removal, they exhibit a wide removal efficiencies, ranging from 48% up to over 99% in water line [6], [7]. Even when equal or very similar wastewater treatment processes are employed, the removal efficiency of MPs can differ widely. This variability is related to several factors: local conditions, composition of the mixture and sizes of the MPs investigated, WWTP configuration, operational parameters of the treatment process units and last, but not least, methods of sampling and identification and characterization procedures among the studies. Nevertheless, it is not properly correct to talk about “removal” when we refer to the MPs occurrence in WWTPs. In fact, it is worth saying that the MPs trapped during their trip within the water line of the WWTPs are then transferred to the sludge line. Moreover, mechanical stress in WWTPs can fragment MPs, making them harder to trap.

In this scenario of high variability, there are many gaps to be filled, including a lack of knowledge and uncertainty regarding the removal efficiency of microplastics and their abundance within WWTPs at worldwide level, and how engineering-related aspects (e.g. HRT and SRT) could affect MPs removal in WWTPs.

To address these gaps, a scoping review is undergoing to collect relevant data from published paper referred to full scale WWTPs. The final aim is to investigate not just presence, fate, removal, analytical methods, but also the effect of operating conditions.

To reach the aims, a wide literature survey was carried out. All the papers were extracted from Scopus database, using the following keywords: “Wastewater treatment plants”, “Removal” and “Microplastics”. A total of 496 papers published before September 2024 were found, of which 147 were eligible for data repository. The database contains more than 250 information fields and a total number of around 550 different WWTPs. Within the database, both qualitative and quantitative information has been collected, including: a) general information (i.e. geographical location, country, publication year, ...); b) WWTPs characteristics (i.e. population served, type of wastewater treated, flow rate); c) parameters of influent,

effluent, and sludge (i.e. pH, TSS concentration, …); d) operating parameters (i.e., HRT and SRT); e) plant configuration; f) MPs removal efficiencies (after each treatment level with respect to the influent); g) sampling, pre-treatment and identification/characterization methods; h) MPs concentration (in the influent, after preliminary, primary, secondary and tertiary treatments and in sludge); i) characteristics of detected MPs (in terms of shape, polymer type and size).

Descriptive and statistical analyses were conducted to elucidate the most relevant and useful relation from an engineering point of view. The analysis were carried out, grouping for geographical continent where the WWTPs are located (except for Africa for which the data available were insufficient), treatment level of WWTPs and MPs characteristics, such as polymer type, size and shape. Concerning the MPs abundance in different geographical areas and treatment levels, the results are reported in Figure 1, in terms of polymer type, size and shape.

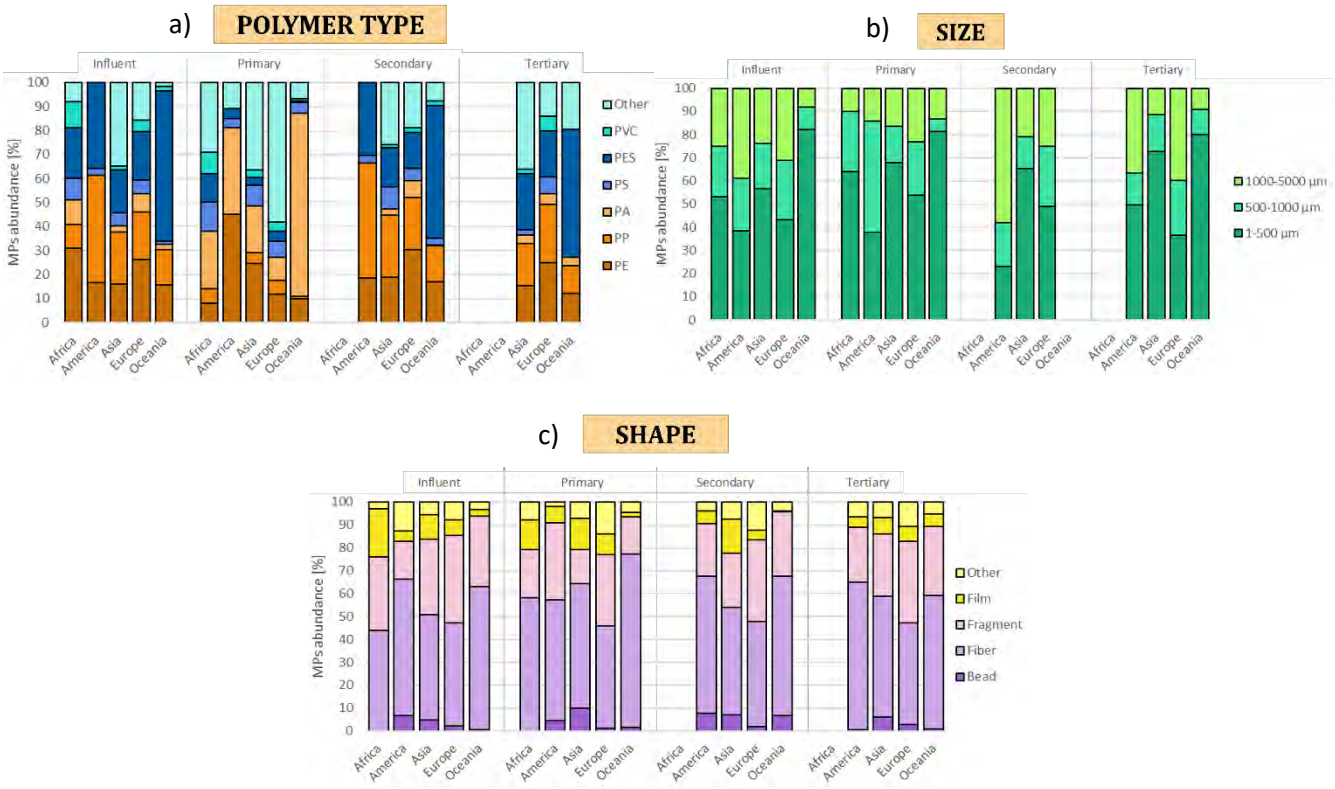

Figure 1. MPs abundance grouped by treatment level, geographical location of WWTPs and characteristics of MPs (a) polymer type, b) size, c) shape).

The results show that for the shape, the composition of the MPs mixture is similar with not too much variability, while both for the polymer type and size, the trend would seem to be the opposite. Moreover, looking at the MPs characteristics as a whole, we can conclude that the most common polymers found are PE, PP and PES, as fibers or fragments, with a size ranging from 1 to 500 µm.
Moving to the MPs concentration, data analyses showed that the average values were 790±3,498, 651±1,684, 149±660, 40±191 MPs/L of wastewater for influent, primary, secondary, and tertiary treatment steps, respectively. The average concentration of MPs in digested sludge was 145±799 MPs/g dry weight.

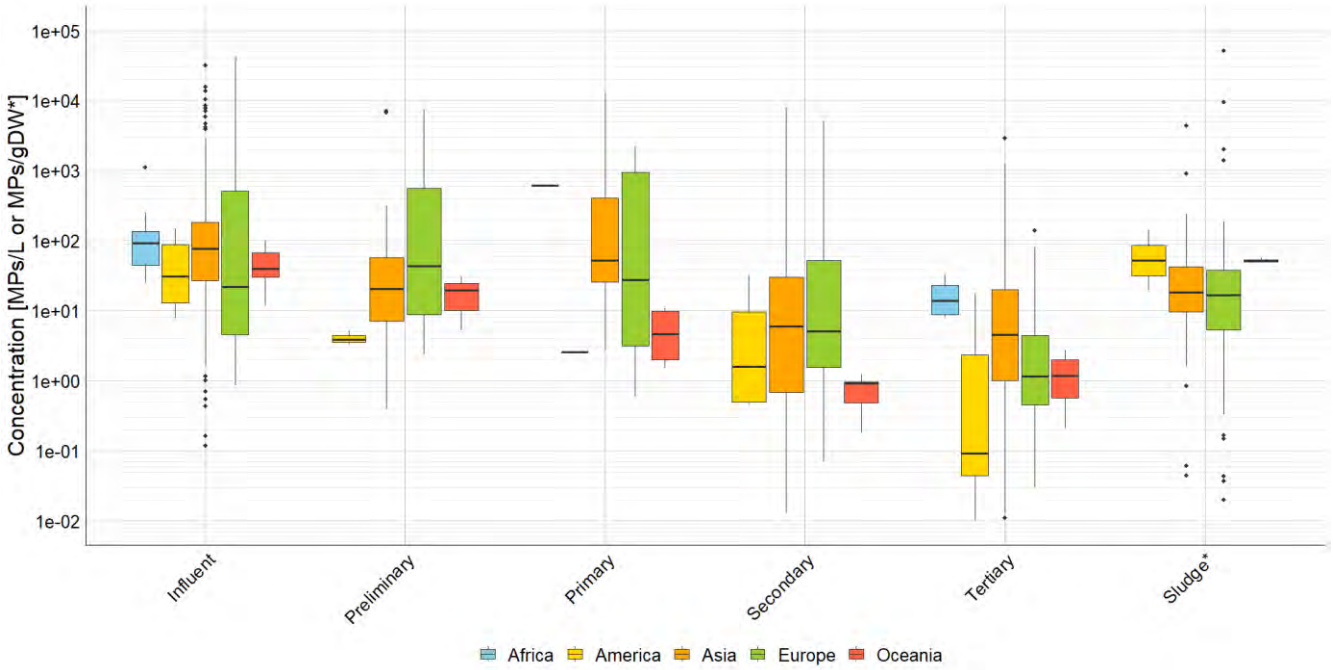

Figure 2. MPs concentration in the influent, in the effluent of each treatment level and in the sludge, grouped by geographical location of WWTPs.

Moreover, as shown in Figure 2, moving from influent to tertiary effluent, when the treatment level of WWTPs increase, the MPs concentration decrease. Consequently, the removal efficiency of MPs in water line tends to increase.
Finally, it is worth saying that the data were so heterogeneous and the variability is high. This may reflect not just local features and wastewater characteristics, but also different sampling volume, different microplastic characterization, sampling and identification methods used among the paper, as shown in Figure 3. Furthermore, only few case studies have investigated some geographical areas (e.g. Africa and Oceania) and missing data regarding operating conditions of the process treatment units.

In conclusion, the database connected to the scoping review, which will be updated continuously, can provide an in-depth analysis of engineering factors related to the removal of microplastics in WWTPs and establish a data repository of significant value for the scientific and technical community interested in this increasingly environmental issue. Nevertheless, the scientific community needs both for standardized MPs sampling, identification and characterization methods and for shared rules about the minimum information (e.g. the operating parameters of the treatment units) that should be included in publications.

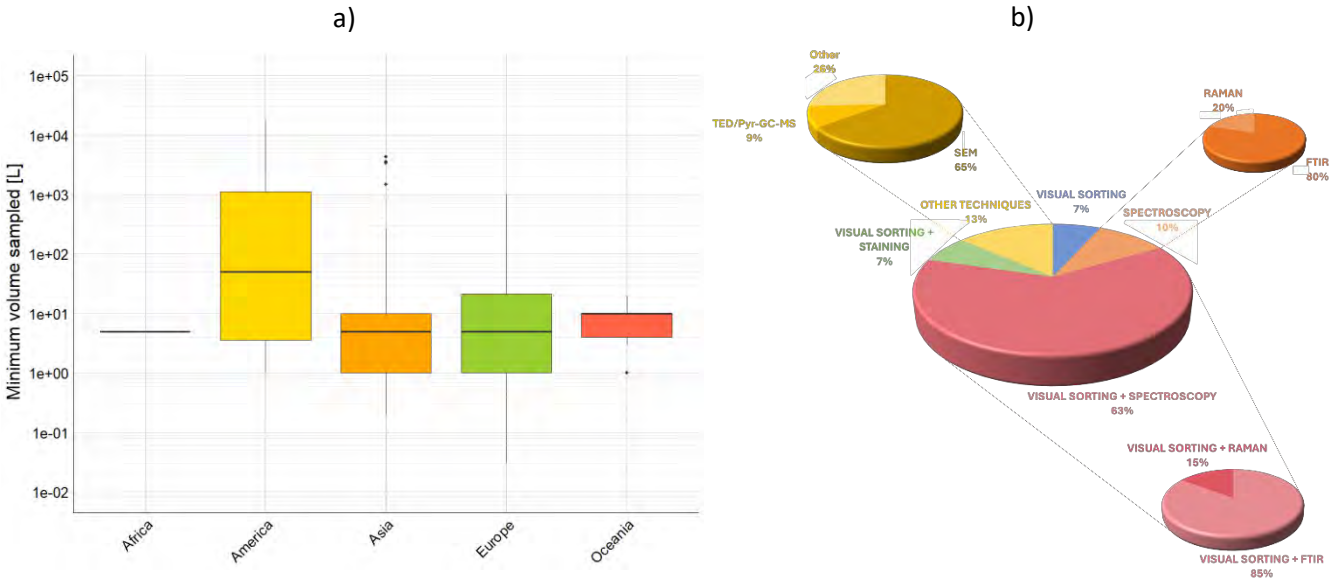

Figure 3. a) Minimum volume sampled, grouped by geographical location of the WWTPs. b) MPs identification and characterization methods currently used in the case studies stored in the database.

This work is done within a Ph.D. thesis funded by FSE REACT-EU PON (XXXVII).

References

[1] M. Wagner and S. Lambert, *Microplastic pollution in inland waters focusing on Asia*, vol. 58. 2018.
[2] J. Talvitie *et al.*, “Do wastewater treatment plants act as a potential point source of microplastics? Preliminary study in the coastal Gulf of Finland, Baltic Sea,” *Water Sci. Technol.*, vol. 72, no. 9, pp. 1495–1504, 2015, doi: 10.2166/wst.2015.360.
[3] C. Bretas Alvim, M. A. Bes-Piá, and J. A. Mendoza-Roca, “Separation and identification of microplastics from primary and secondary effluents and activated sludge from wastewater treatment plants,” *Chem. Eng. J.*, vol. 402, no. July, p. 126293, 2020, doi: 10.1016/j.cej.2020.126293.
[4] C. Edo, M. González-Pleiter, F. Leganés, F. Fernández-Piñas, and R. Rosal, “Fate of microplastics in wastewater treatment plants and their environmental dispersion with effluent and sludge,” *Environ. Pollut.*, vol. 259, 2020, doi: 10.1016/j.envpol.2019.113837.
[5] J. Sun, X. Dai, Q. Wang, M. C. M. van Loosdrecht, and B. J. Ni, “Microplastics in wastewater treatment plants: Detection, occurrence and removal,” *Water Res.*, vol. 152, pp. 21–37, 2019, doi: 10.1016/j.watres.2018.12.050.
[6] R. Z. Habib, T. Thiemann, and R. Al Kendi, “Microplastics and Wastewater Treatment Plants—A Review,” *J. Water Resour. Prot.*, vol. 12, no. 01, pp. 1–35, 2020, doi: 10.4236/jwarp.2020.121001.
[7] C. Akarsu, H. Kumbur, K. Gökdağ, A. E. Kıdeyş, and A. Sanchez-Vidal, “Microplastics composition and load from three wastewater treatment plants discharging into Mersin Bay, north eastern Mediterranean Sea,” *Mar. Pollut. Bull.*, vol. 150, no. September 2019, 2020, doi: 10.1016/j.marpolbul.2019.110776.

Title: Behavior of membrane distillation in the treatment of a diverse range of real and industrial water streams: challenges and future perspectives

Author(s): L. Craveri[1,*], E.Bertozzi[1], M.Malaguti[1], M. Frappa[3], F. Macedonio[3], A. Figoli[3], A.Tiraferri[1,2]

[1] *Department of Environment, Land and Infrastructure Engineering, Politecnico di Torino, Torino 10129, Italy*
[2] *Clean Water Center, Politecnico di Torino, Torino 10129, Italy*
[3]*Institute on membrane Technology, National Research Council of Italy (CNR-ITM), Rende (CS), 87036, Italy*
lorenzo.craveri@polito.it

Keyword(s): Membrane distillation, Industrial wastewaters, Desalination, Fouling, Wetting

Abstract

Membrane distillation (MD) is a membrane technology that exploits a vapor pressure gradient (generally obtained through a temperature gradient) across a porous hydrophobic membrane. One of the main applications for this technology is desalination, even if it is gaining attention for several application for water treatment and reuse [1].

In this work, MD was challenged with real water and wastewater samples derived from a diverse range of sources (such as aquaculture, textile, and food and beverage industries) with the aim of water reuse. In particular, the following wastewaters were investigated: (i) two samples deriving from the textile dying process (named “Textile 1” and “Textile 2”); (ii) two samples from aquaculture, one with low salinity (“Aquaculture fresh”) and one with seawater salinity (“Aquaculture sea”); (iii) a sample from the wastewater treatment plant of a brewery.

First, the wastewaters were characterized by analysis of the total organic carbon (TOC), total nitrogen, pH, electrical conductivity (EC), and surface tension. Table 1 shows the results of said characterization, highlighting the diversity in composition of the samples tested. Such diversity allowed the investigation of the potential of MD to target an ample range of water streams.

Table 1. Characterization of the analysed wastewaters.

Parameter	Unit of measurement	Textile 1	Textile 2	Aquaculture fresh	Aquaculture sea	Brewery
Electrical conductivity	mS/cm	54.2	2.4	2.9	53.5	2.9
pH	-	11.0	9.5	7.8	7.1	7.7
Total Organic Carbon	mg/L	229.5	4.1	20.1	32.3	9.5
Total Carbon	mg/L	421.5	116.4	53.8	90.8	348.1
Inorganic Carbon	mg/L	191.2	114.0	33.8	58.4	338.6
Total Nitrogen	mg/L	38.2	10.3	53.1	8.2	14.9
Surface Tension	mg/L	31.5	38.7	73.5	69.2	73.8

Direct contact membrane distillation (DCMD) tests were carried out with PVDF membranes in a bench-scale system. Two types of tests were performed for each water stream: (i) the behaviour of the membrane with a constant feed composition was evaluated in closed-loop batch experiments to understand the fouling and wetting behaviour (roughly 5 days); (ii) high-recovery tests were used to assess the productivity and the effectiveness of the process. MD performance was evaluated with continuous measurements of distillate electrical conductivity (used as a proxy for salt rejection) and by evaluation of the organic content (TOC) of the distillate at the end of the tests.

For what concerns textile wastewaters, both fouling and recovery test showed an immediate development of wetting phenomenon, detected visually (passage of dye from the feed to the permeate), and through the swift increase of the distillate EC. This result may be explained by the presence of surfactants, which influence the surface tension of the feed solution and impact the membrane hydrophobicity. However, literature results [2] with synthetic wastewaters report that a good separation of dye and organic content can be obtained with MD. Therefore, a pre-treatment step was added to degrade the surfactants and increase the surface tension of the solution. Different pre-treatments were considered, among which granular active carbon (GAC) adsorption and photocatalysis seemed the more promising. GAC adsorption, in particular, allowed to significantly reduce the influence of wetting in the filtration process, as shown by higher values of electrical conductivity rejection (used as a proxy for salt rejection and reported in Figure 1), and organic content rejection, that was assessed at value close to 100%. Figure 1 shows the results concerning two recovery tests carried out in the same conditions after GAC adsorption.

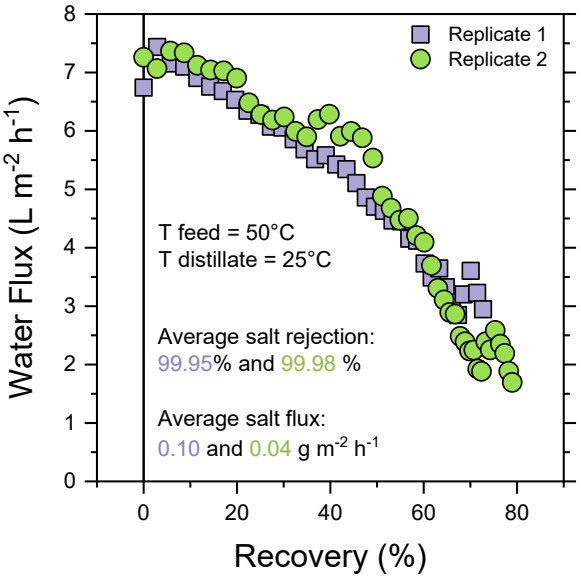

Figure 1. Results of tests carried out with textile wastewater 1 after GAC adsorption.

Samples of aquaculture wastewaters showed similar behaviour in both fouling and recovery tests. The former showed a fast decrease of flux at the beginning of the tests, followed by a stable flux (around 50-60% of the initial one) for the rest of the test. Seawater displayed a higher salt flux throughout the whole test, but electrical conductivity rejection value as high as 99.6%; however, the membrane performance appeared to worsen over time, as underlined by a progressive decrease of the rejection values. Recovery tests showed a continuous decrease of the flux, likely due to the development of fouling phenomena on the membrane. Seawater presented again a higher salt flux, but rejection values up to 99.8%. Distillate organic content (TOC) was measured to evaluate the performance of the separation, and revealed an overall rejection of ~80%, pointing out that, despite a good salt rejection, a pre-treatment may be needed to lower effect of fouling and improve the performance of the membrane. Figure 2 shows the results of recovery tests for a) fresh and b) sea aquaculture wastewater.

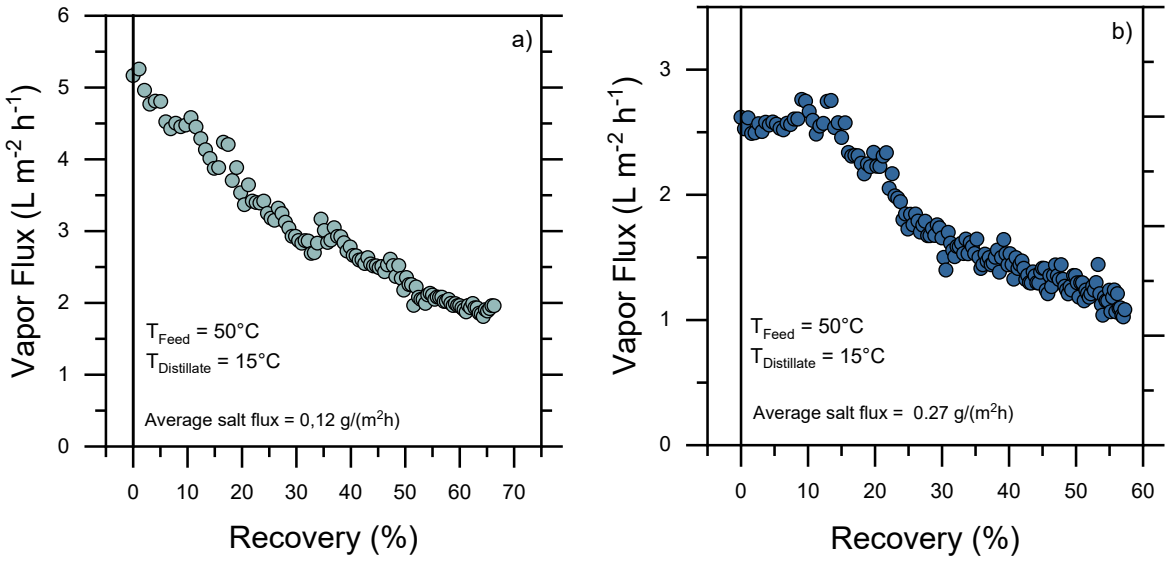

Figure 2. Results of tests carried out with a) fresh and b) sea aquaculture wastewater.

Wastewater from the brewery treatment plant showed promising results for what concerns wetting phenomena and salt rejection. However, scaling (salt deposition on the membrane surface) emerged as the main hindrance to the process. In fact, the precipitation of salts over time (probably due to the high concentration of calcium and phosphate, that were detected with further analysis) was evident; this turned out to be an issue not only for the membrane (with lower fluxes and worse performance in terms of rejection), but for the whole system, since salt deposition may damage the mechanical components (such as pumps). In fact, all the test carried out revealed pump clogging at value of recovery between 40 and 50%. Therefore, a pre-treatment may be needed to make the process feasible in the long-term and achieve high recovery values. Figure 3 shows results concerning three replicates of recovery tests.

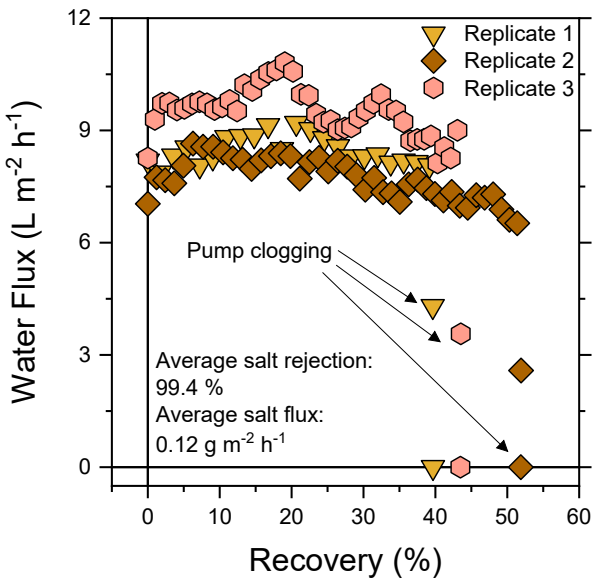

Figure 3. Results of tests carried out with brewery wastewater with no pre-treatment.

Overall, the feed waters derived from the industrial sources investigated showed promising results for the MD treatment, even if several issues emerged during the tests: wetting, fouling, and scaling phenomena were in fact a hindrance to the process in most cases. However, results show that MD could be suitable for the treatment of a few types of feed waters derived from various sources and industries with an appropriate pre-treatment.

References

[1] Drioli, E., Ali, A., & Macedonio, F. (2015). Membrane distillation: Recent developments and perspectives. *Desalination*, *356*, 56-84.

[2] Reddy, A. S., Kalla, S., & Murthy, Z. V. P. (2022). Textile wastewater treatment via membrane distillation. *Environmental Engineering Research*, *27*(5).

Acknowledgments

Funded by the European Union (Grant Agreement #101091915, MEloDIZER, HORIZON-CL4-2022-RESILIENCE-01). Views and opinions expressed are however those of the author(s) only and do not necessarily reflect those of the European Union or the European Health and Digital Executive Agency (HADEA). Neither the European Union nor the granting authority can be held responsible for them.

Title: Exploring the effect of citrus industry by-products as nitrogen fertilizer for wheat growth

Author(s): Caterina Lucia*[1], Carlotta Conigliaro[1], Felicia Macina[1] Sofia Maria Muscarella[1], Vito Armando Laudicina[1,2].

[1] *Department of Agricultural, Food and Forestry Sciences, University of Palermo, Palermo, Italy, *caterina.lucia@unipa.it*
[2] *NBFC, National Biodiversity Future Center, Palermo, Italy*

Keyword(s): citrus industry by-products, sustainable waste management, circular economy.

Abstract

Wastewater generation is a significant global challenge driven by various human activities and industries. This issue has been intensified due to rapid population growth, urbanization, and industrialization, creating major obstacles to the sustainable management of water resources and posing threats to human health and the environment [1]. The main challenge in wastewater treatment operations is the production of sludge, which comes from urban, industrial, and agricultural sources. Although often considered a by-product, sewage sludge has the potential to be a sustainable source of energy and resources [2]. The use of sludge as a raw material in various industries is in line with circular economy principles and promotes effective waste management. Proper sludge management can promote sustainable agricultural practices, energy production, and resource conservation. The application of sewage sludge in agriculture can potentially reduce dependence on conventional fertilizer production. Sewage sludge provides benefits as a fertiliser, especially in those areas where low-fertile soils cannot supply nutrients needed for plant growth. The addition of sludge as a recovery material could offer a considerable improvement in terms of the supply of N, P, K to plants and organic carbon in the soil, particularly in arid and semi-arid areas where organic matter is continuously decreasing [3]. The citrus industry is estimated to yield a sludge production ranging from 0.10 to 0.30 kg of sludge per kg of chemical oxygen demand (COD) [4]. The citrus sewage sludge (CSS) had a subalkaline pH and high electrical conductivity, although it is lower than 4 dS m^{-1}. CSS has usually a high content of total N, so the C/N ratio is about 6. Among macronutrient cations, Ca is the most abundant, followed in order by Mg, P, K, and Na [5]. Based on the above considerations, a pot experiment was conducted to explore the ability of CSS and CSS biochar, obtained at two different temperature (300 and 400 °C), to act as a nitrogen fertilizer for wheat growth. The experiment was carried out in a greenhouse using black plastic pots (10x10x17 cm) and filled with 800 g of soil previously sieved to 4 mm and homogenised. Two distinct soil types were employed: Calcic Rhodoxeralf (S1) and Typic Haploxeralf (S2). The main characteristics of soils used for this experiment are reported in Table 1. Soils were mixed with 20% of perlite, in volume, and amended with CSS, CSS biochar at 300°C temperature (B300), CSS biochar at 400°C temperature (B400) or fertilised with ammonium sulphate and chicken manure to supply 30 mg of N per plant. Three wheat seeds were transplanted into each pot. The plants were irrigated three times a week with a nutrient solution having the following composition: K_2SO_4, KCl, KH_2PO_4 and micronutrients. Five replicates per treatment were performed for a total of 60 samples (Figure. 1).
Soil samples were collected at the end of the experiment for the analysis of nitrate and ammonium content. These samples were dried and sieved at <2 mm. Mineral N extraction from the soil was performed using 2M KCl. This extraction was conducted using 2 g of soil in 20 mL of extractant in

polyethylene falcon tubes, end-over-end shaken at 180 rpm for 30 minutes. Ammonium (NH_4^+) and nitrate (NO_3^-) were quantified through colorimetric analysis employing the Berthelot method [6] and the Spectroquant® Nitrate test, using a spectrophotometer (UVmini-1240, Shimadzu Italia srl, Milan, Italy) after the formation of a yellow-green and red complex, respectively.
Root and shoot samples were removed from the pots, oven-dried at 65 °C for 72 hours and dry weight noted. Then, the roots, stems, gluma and wheat grain were collected separately and underwent grinding for subsequent analysis. The replacement value of fertilizer product, CSS, (MFRV) was calculated adapting the equation applied by Ayeyemi et al. [7] from the amount of commercial mineral N fertilizer saved or replaced when using an alternative fertilizer while achieving the same N uptake or yield. It can be interpreted as the percentage of commercial mineral fertilizer that can be replaced by alternative fertilizers. It was estimated based on N_{uptake} for each N applying the eq. 4:

$$MFRV = \frac{N_{uptake_i} - N_{uptake_c}}{N_{uptake_s} - N_{uptake_c}} \; x \; 100 \qquad (4)$$

where, N_{uptake_i} is the N_{uptake} by the crop in the treatment with alternative fertilizer i, N_{uptake} is the average N_{uptake} in the control treatment, and N_{uptake_s} is the average *N* uptake in the mineral fertilizer treatment at the same N rate as i.
The replacement value (RV) was also estimated on a total dry matter basis as (eq. 5):

$$RV = \frac{DM_i - DM_c}{DM_s - DM_c} \; x \; 100 \qquad (5)$$

where DM_i is the dry matter of the crop in the treatment with alternative fertilizer i, DM_c is the average dry matter of the control treatment, and DM_s is the average dry matter of the mineral fertilizer treatment at the same N rate as i.

Table 1. Main characteristics of the soil samples used for the experimental design.

Sample	pH	E.C.	Available P	Total N	Total Organic C	clay	silt	sand	Total carbonates
		dS m^{-1}	mg kg^{-1}	mg g^{-1}	g kg^{-1}	%	%	%	%
S1	8.44	0.25	9.93	1.67	12.7	16	16	68	51.7
S2	8.18	0.01	2.25	2.23	16.7	16	20	64	2.3

Figure 1. The experiment designed as a Randomized Complete Block Design (RCBD) with five replications for each treatment.

In soil S1, nitrate values increased in all treatments except for soils treated with B400. In soil S2 it only increased in soils where chicken manure was added (Figure 2). In general, regardless of soil type, the lowest nitrate values were found in the B400 treatment. This is probably due to a higher uptake by wheat plants.

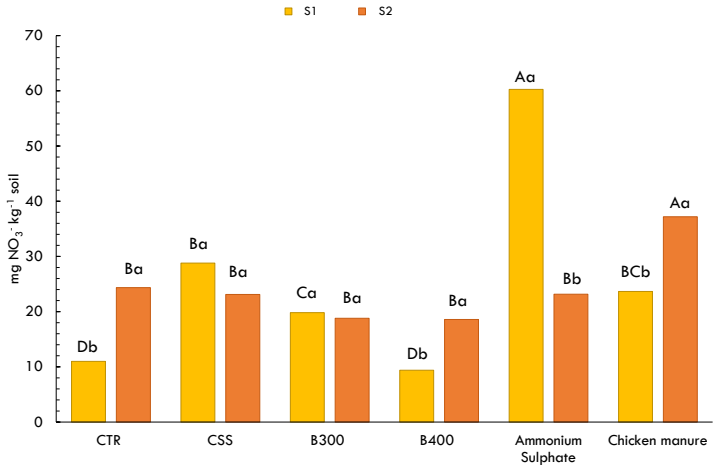

Figure 2. Nitrate content determined in soils after the experiment. Different capital letters indicate significant differences (P < 0.05) among treatments within the same soil; lowercase letters indicate significant differences (*P* < 0.05) among soils within the same treatment.

Concerning the ammonium content determined in soils with different treatments, a decrease in B400, poultry manure and ammonium sulphate was found in soil S1. In soil S2, the highest ammonium content was found only in soils treated with chicken manure (Figure 3).

Figure 3. Ammonium content in soils tested. Different capital letters indicate significant differences (P < 0.05) among treatments within the same soil; lowercase letters indicate significant differences (*P* < 0.05) among soils within the same treatment.

By measuring the dry weight of wheat plants, the RV was determined. Among all the treatments, the CSS was the most efficient. Indeed, in comparison with inorganic fertilizer, it can replace fertilizer in a range between 70-90%, while in comparison with organic fertilizer, it can replace fertilizer in a range between 100-120% (Figure 4).

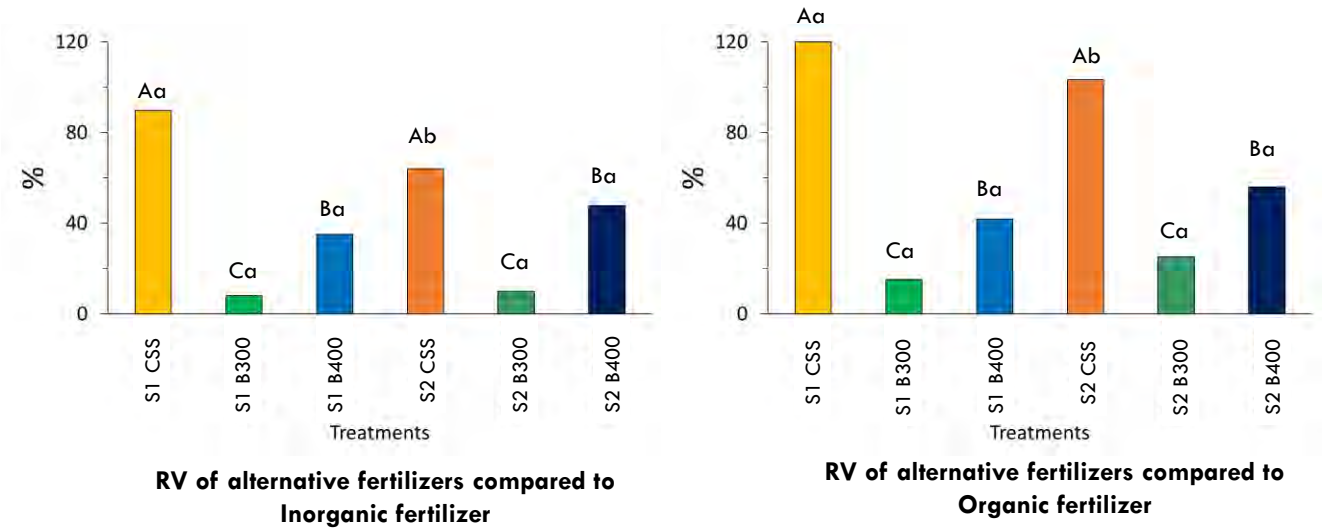

Figure 4. Replacement value of alternative fertilizers compared to inorganic and organic fertilizer.

Based on these preliminary results, it is possible to state that there was a soil effect. In fact, CSS had a greater effect in soil S1, while B300 and B400 had a significantly effect in soil S2. Moreover, the comparison of alternative fertilizers with inorganic and organic fertilizer showed that the RV of CSS was between 70-120%, of B300 was between 15-40% and, of B400 was between 35-60%. Therefore, it can be concluded from these data that both sludge and biochar, obtained at two different temperatures, can exert a nitrogenous fertilising effect.

References

[1] Gherghel A., Teodosiu G., De Gisi S. “A review on wastewater sludge valorisation and its challenges in the context of circular economy”. Journal of Cleaner Production, 228, 244-263, (2019).
[2] Aleisa E., Alsulaili A., Almuzaini Y. “Recirculating treated sewage sludge for agricultural use: Life cycle assessment for a circular economy”. Waste Management, 135, 79–89, (2021).
[3] Abdoli M. “Sustainable Use of Sewage Sludge in Soil Fertility and Crop Production”. Sustainable Management and Utilization of Sewage Sludge, 297-333, (2022).
[4] Corsino S.F., Di Trapani D., Torregrossa M., Viviani G. “Aerobic granular sludge treating high strength citrus wastewater: analysis of pH and organic loading rate effect on kinetics, performance and stability”. Journal of Environmental Management, 214, 23–35, (2018).
[5] Lucia C., Pampinella D., Palazzolo E., Badalucco L., Laudicina V.A. “From Waste to Resources: Sewage Sludges from the Citrus Processing Industry to Improve Soil Fertility and Performance of Lettuce (Lactuca sativa L.)”. Agriculture,13, 913. (2023).
[6] Mulvaney R. L. Nitrogen—inorganic forms. Methods of soil analysis: Part 3 Chemical methods, 5, 1123-1184. (1996).
[7] Ayeyemi T., Recena R., García-López A. M., Delgado A. Circular Economy Approach to Enhance Soil Fertility Based on Recovering Phosphorus from Wastewater. Agronomy, 13(6), 1513. (2023).

Title: Combined sewer overflows as a critical source of microplastics input to the aquatic environment

Author(s): Giuseppe Beringheli*[1], Santo Fabio Corsino[1], Marco Carciola[1], Michele Torregrossa[1]

[1] *Department of Engineering, University of Study of Palermo, Palermo, Italy, giuseppe.beringheli@unipa.it*

Keyword(s): microplastics, combined sewer overflow, CSO, wastewater

Abstract

Nowadays, the release of microplastics (MPs) into the aquatic environment is a critical current topic. In addition to effluents from wastewater treatment plants, a significant source of MPs input into this environment is represented by the discharges from combined sewer overflows (CSOs) during storm events. This issue has been the focus of this work and the first results allowed defining that CSOs are indeed a possible critical source of MP input to the aquatic environment.

Introduction

Plastics were invented in 1860 and have since become popular globally due to their low production cost and properties of durability, light weight, low thermal and electrical conductivity, and corrosion resistance [1, 2]. European plastic production in 2022 was about 400.3 million tonnes [3]. Despite their many benefits, polymeric materials pose a significant threat to the environment when they reach the end of their life cycle. Specifically, their improper disposal causes them to enter the environment; where, taking more than a hundred years to degrade, they result in damage to nature's biota by altering its ecological balance [4]. In recent decades, there is a particular focus on the study of microplastics as emerging pollutants in water, their presence in marine and terrestrial ecosystems, and their health and environmental impacts [5].
Microplastics (MPs) are small polymer fragments generally less than 5 mm in size, resulting from the physical, photochemical and biological deterioration of plastic materials (secondary MPs) or produced directly as microparticles in manufacturing industries (primary MPs) [6].
The release of microplastics into the environment can occur in several ways [7]. Urban drainage systems and wastewater treatment plants (WWTP) are a possible source of microplastic input into natural ecosystems [8, 9, 10]. During intense rainfall events, the urban surface runoff causes microplastics to leach from road pavement and building roofs. The surface runoff, containing microplastics, once intercepted by the urban drainage network reaches the WWTP resulting in the increase of the influent concentration of MPs compared to typical dry weather values [11]. Recently, the scientific community has wondered about possible sources of pollution from the activation of combined sewer overflows (CSOs) during intense rainfall events [12]. Water discharged into receiving water bodies due to the activation of CSO is not treated (except for the "first flush" water). In this context, CSO represent a pathway through which microplastics can reach aquatic environments [13, 14].
Considering this, the main objective of the present work was to determine the concentration of MPs in the CSO's discharge during rainfall events that resulting in the activation of the CSO.

Materials and methods

The experimental activity was carried out at the Laboratory of Environmental Sanitary Engineering “Prof. Luigi Gagliardi” of the Department of Engineering, University of Palermo. The experimental campaign began in September 2023. During the campaign, the presence of microplastics in raw sewage entering the WWTP of Palermo (“Acqua dei Corsari”) was analyzed in both dry weather (no rain) and rain weather. Fourteen dry weather samples were used to determine the baseline of MPs concentrations under normal operation. The experiment lasted 9 months, during which samples were periodically collected from September 2023 until May 2024. All the samples in dry weather conditions were 24-h composite, taken with the automatic instrumentation present in the plant upstream of the screening unit. Thirteen instantaneous samples were withdrawn manually during rain events. Specifically, samples referring to 25/09/2023, 22/11/2023, 10/02/2024, 20/02/2024, 24/02/2024, 28/02/2024, 05/03/2024 and 08/05/2024 were collected during the sewer overflow, after the influent flowrate exceeded the average daily flow rate during dry weather by five times. The other samples are referred to rain weather, without the activation of CSO. All samples were stored at 4°C. Microplastics were isolated from wastewater using a multi-step approach. First, 500 mL of sample was filtered through a stainless-steel screen with 5-mm mesh, to remove particles larger than the upper limit of the size range of microplastics. Hereafter, to remove organic materials, 10 ml of 30% H_2O_2 was added to the 500-ml sample in a Pyrex beaker. Then, the sample was heated to 65°C and mixed at 100 rpm for 12 hours. After this time, MPs flotation was achieved by adding 50 ml of saturated aqueous NaCl solution and leaving the sample settling for 24 hours. The supernatant was then filtered through a nylon filter with 20 µm mesh size. The filter was finally placed in a glass Petri dish and dried at 40 °C in an oven for 24 hours. The MPs were analyzed using a stereomicroscope with 20-80x magnification equipped with a Leica digital camera. Specifically, the number of microplastics were manually counted and then classified by shape into “fragments”, “films”, “fibers” and “spheres” [11]. In Figure 1, a picture of MPs is reported.

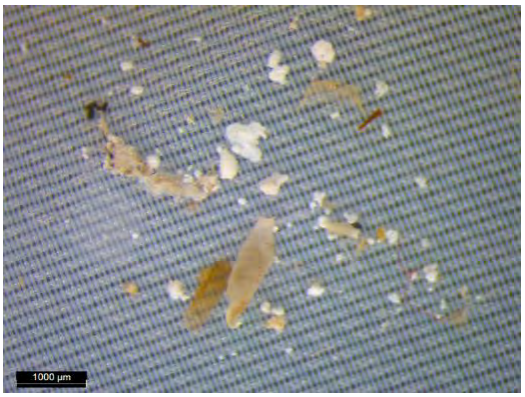

Figure 1. Microplastics particles at 40x of magnification

Results and discussion

Figure 2 shows MPs concentration (as total elements per liter of wastewater) in all the collected samples. As can be seen in Figure 3, the total number of MPs was significantly higher during rainy weather conditions (blue box), with values ranging from 4284 to 10476 MPs/L, whereas during dry weather (green box) the MPs concentration was between 1739 and 6277 MPs/L. Overall, the average MPs concentrations were 6952 ± 2303 MPs/L and 3596 ± 1331 MPs/L during rainy weather and dry weather, respectively. Samples represented graphically by red bars in Figure 2 refer to CSO discharge events. It

is worth to note that during these events, MPs concentrations were found significantly above the average dry weather values and the rain events when CSO discharge did not occur. These early results allowed us to highlight the emerging problematic of MP discharge into water bodies during CSO-triggered events. In the continuation of the experimental work, we will want to relate MP values in discharge from CSOs to some influential factors such as, for example, Antecedent Dry Days (ADD) of the CSO event and precipitation event characteristics.

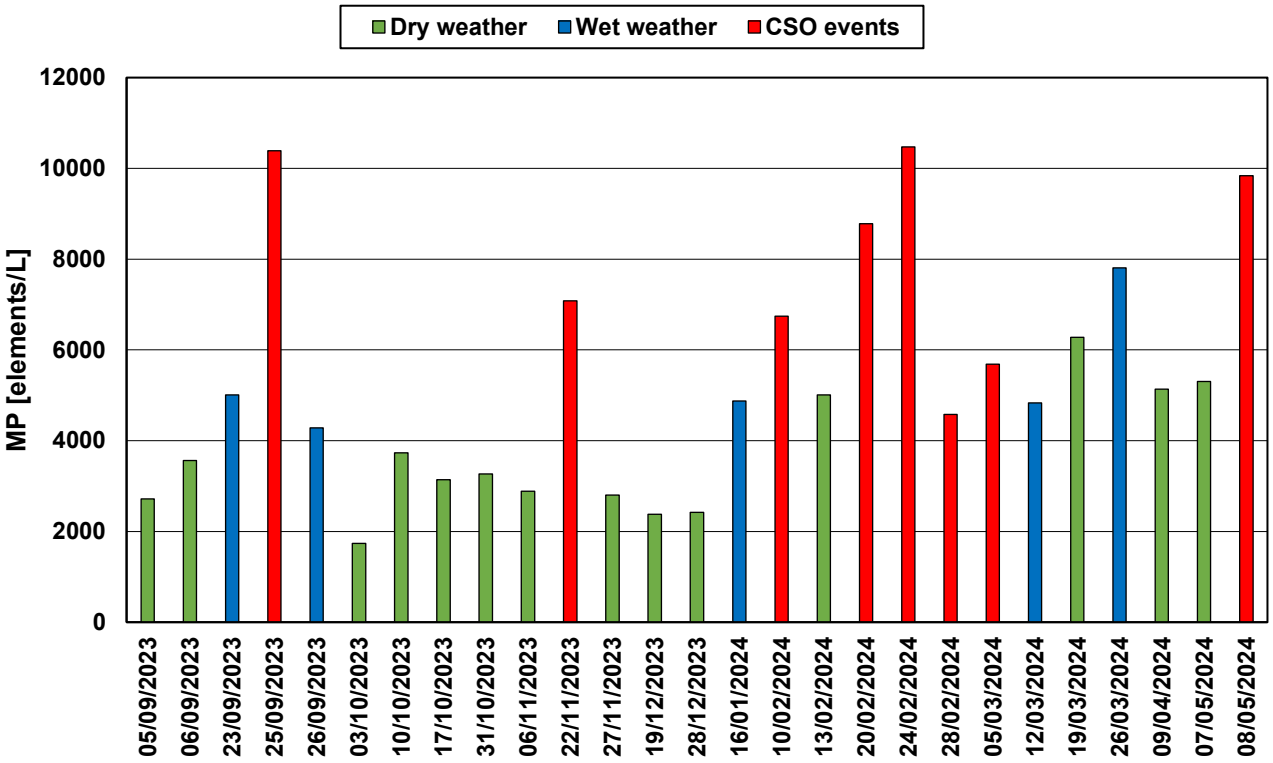

Figure 2. MPs concentration in the wastewater samples during rainy and dry conditions

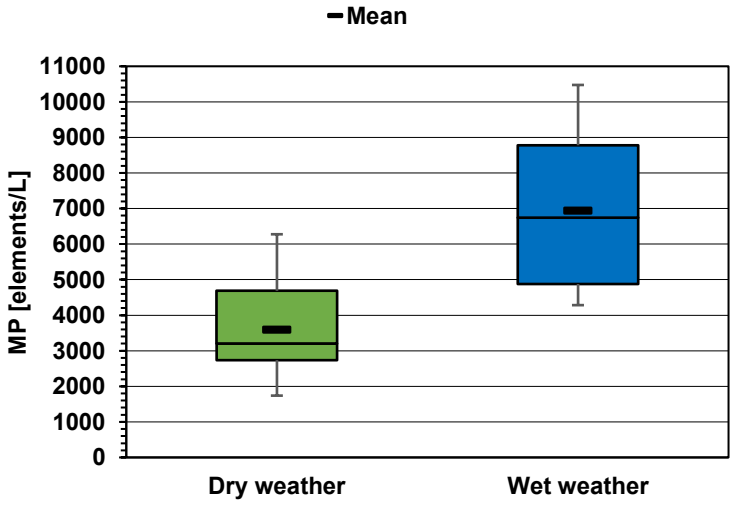

Figure 3. Box-plot of dry and wet weather MPs concentration

Conclusions

This study pointed out that the number of microplastics in wastewater influent to municipal WWTP is not negligible. The concentration of MPs increased during meteoric events likely because of the meteoric runoff collected in urban drainage systems. Moreover, when CSO occurred the MPs concentration further increased. Since in these cases, effluent is discharged without any treatment into receiving water bodies, there would be a serious risk of abundant release of microplastics into the environment when extreme rain events occur. Due to this relevant environmental issue, it is possible to state that it is necessary to further investigate the influence of CSO on microplastic pollution of receiving water bodies, so that possible solutions can be found to mitigate the environmental risks associated with this type of discharge.

References

[1] B. Chae, S. Oh, and D. G. Lee, “Is 5 mm still a good upper size boundary for microplastics in aquatic environments? Perspectives on size distribution and toxicological effects,” *Mar. Pollut. Bull.*, vol. 196, no. August, p. 115591, 2023, doi: 10.1016/j.marpolbul.2023.115591.

[2] Y. Cho, W. J. Shim, S. Y. Ha, G. M. Han, M. Jang, and S. H. Hong, “Microplastic emission characteristics of stormwater runoff in an urban area: Intra-event variability and influencing factors,” *Sci. Total Environ.*, vol. 866, no. October 2022, p. 161318, 2023, doi: 10.1016/j.scitotenv.2022.161318.

[3] Plastics Europe, “The Circular Economy for Plastics A European Analysis,” no. March, pp. 1–114, 2024.

[4] M. Zhang, J. Yao, X. Wang, Y. Hong, and Y. Chen, “The microbial community in filamentous bulking sludge with the ultra-low sludge loading and long sludge retention time in oxidation ditch,” *Sci. Rep.*, vol. 9, no. 1, pp. 1–10, 2019, doi: 10.1038/s41598-019-50086-3.

[5] F. Yang *et al.*, “Characteristics and the potential impact factors of microplastics in wastewater originated from different human activity,” *Process Saf. Environ. Prot.*, vol. 166, no. June, pp. 78–85, 2022, doi: 10.1016/j.psep.2022.07.048.

[6] N. A. Khan *et al.*, “Microplastics: Occurrences, treatment methods, regulations and foreseen environmental impacts,” *Environ. Res.*, vol. 215, no. May, 2022, doi: 10.1016/j.envres.2022.114224.

[7] S. Saud, A. Yang, Z. Jiang, D. Ning, and S. Fahad, “New insights in to the environmental behavior and ecological toxicity of microplastics,” *J. Hazard. Mater. Adv.*, p. 100298, 2023, doi: 10.1016/j.hazadv.2023.100298.

[8] C. Baresel and M. Olshammar, “On the Importance of Sanitary Sewer Overflow on the Total Discharge of Microplastics from Sewage Water,” *J. Environ. Prot. (Irvine,. Calif).*, vol. 10, no. 09, pp. 1105–1118, 2019, doi: 10.4236/jep.2019.109065.

[9] H. Chen *et al.*, “The occurrence of microplastics in water bodies in urban agglomerations: Impacts of drainage system overflow in wet weather, catchment land-uses, and environmental management practices,” *Water Res.*, vol. 183, p. 116073, 2020, doi: 10.1016/j.watres.2020.116073.

[10] N. Obermaier and A. Pistocchi, “A Preliminary European-Scale Assessment of Microplastics in Urban Wastewater,” *Front. Environ. Sci.*, vol. 10, no. July, pp. 1–12, 2022, doi: 10.3389/fenvs.2022.912323.

[11] M. S. Ross *et al.*, “Estimated discharge of microplastics via urban stormwater during individual rain events,” *Front. Environ. Sci.*, vol. 11, no. January, pp. 1–12, 2023, doi: 10.3389/fenvs.2023.1090267.

[12] S. A. Forrest, D. McMahon, W. A. Adams, and J. C. Vermaire, “Change in microplastic concentration during various temporal events downstream of a combined sewage overflow and in an urban stormwater creek,” *Front. Water*, vol. 4, 2022, doi: 10.3389/frwa.2022.958130.

[13] F. Di Nunno, F. Granata, F. Parrino, R. Gargano, and G. de Marinis, “Microplastics in combined sewer overflows: An experimental study,” *J. Mar. Sci. Eng.*, vol. 9, no. 12, 2021, doi: 10.3390/jmse9121415.

[14] Y. Zhou *et al.*, “Microplastics discharged from urban drainage system: Prominent contribution of sewer overflow pollution,” *Water Res.*, vol. 236, no. April, p. 119976, 2023, doi: 10.1016/j.watres.2023.119976.

Title: Advance in SODIS through the addition of a photosensitive agent

Author(s): Elisabetta Gover*[1], Clara Comuzzi[2], Marilena Marino[2], Daniele Goi[1].

[1] *Polytechnic Department of Engineering and Architecture, University of Udine, Via del Cotonificio 108, Udine, 33100, Italy, gover.elisabetta@spes.uniud.it*
[2] *Department of Agricultural Food Environment and Animal Sciences, University of Udine, Via Sondrio 2/A, 33100 Udine, Italy*

Keyword(s): Solar Water Disinfection, microorganisms, photoactive agent

Abstract

In developing countries, consumption of contaminated water can lead to gastrointestinal diseases, posing a significant risk to public health and resulting in high mortality rates. To address this issue, Solar Water Disinfection (SODIS) is an effective and inexpensive method for providing safe drinking water. This technique involves filling transparent plastic or glass containers, typically 2-liter PET beverage bottles, with water and leaving them in the sun for 6 to 48 h. After this time the water is drinkable and must be consumed within 24 hours to prevent recontamination. Additionally, SODIS is an accessible method since it does not necessitate the use of chemical disinfectants.[1] The effectiveness of SODIS depends on factors like radiation intensity, temperature, water turbidity, and water height to predict mortality from waterborne disease.[2] When exposed to UV radiation, both endogenous photosensitizers (e.g., quinones, flavins, and porphyrins) and exogenous photosensitizers (e.g., humic acids) become activated and generate reactive oxygen species (ROS), which react with biomolecules to inactivate microorganisms.[3] Exposure to sunlight can increase temperatures, leading to the degradation of proteins in microorganisms and causing oxidative damage due to the interaction with dissolved oxygen and heat. The effectiveness of solar disinfection mainly depends on the intensity of the sun, which is influenced by weather conditions and location, which is why it is more effective in tropical or subtropical regions.[4] Despite its benefits, SODIS reduces microorganisms by only 3-logs [5] and lowers diarrheal disease prevalence by 31%,[6] indicating the need for improved methods. To enhance the antimicrobial effect of SODIS, it is reasonable to add catalysts to the aqueous solution, such as photosensitizing organic dyes. These compounds, including salts of thionine, xanthene, and porphyrin derivatives, increase the production of ROS, leading to potentially disinfection of the water. Therefore, to make it easier to remove the photosensitizer once the treatment is finished, they must be incorporated into polymeric matrices.[7] Recent studies have shown that of various porphyrins can be incorporated into a PVC matrix for water disinfection, proving a reduction of 4-logs *vs Staphylococcus aureus*.[8]

In view of this remarkable result, we proposed a new antimicrobial material that utilizes a porphyrin photosensitizer immobilized on bio-renewable and environmentally friendly polymeric supports, resulting in reduce environmental impact. This new matrix is derived from the assembly of vanillin, which is derived from lignin, a widely available waste product of the wood industry. Vanillin is used as the main building block to synthesize a linear polymer network that is functionalized with

diamine. The network is then incorporated with Meso-Tetra (4-methylphenyl) porphine (4MeP) and tested against microorganisms to ensure its efficacy. This combination has also been tested to address any period of cloudiness that may arise, thereby improving the overall efficacy of the SODIS treatment process. This development is expected to ensure that populations living in water-scarce regions can access clean and healthy water.

References

[1] McGuigan K. G., Conroy R. M., Mosler H. J., du Preez M., Ubomba-Jaswa E., & Fernandez-Ibanez P., "Solar water disinfection (SODIS): a review from bench-top to roof-top." *Journal of hazardous materials* 235: 29-46, (2012).
[2] Pichel N., Vivar M., and Fuentes M., "The problem of drinking water access: A review of disinfection technologies with an emphasis on solar treatment methods." *Chemosphere* 218: 1014-1030, (2019).
[3] Silverman A. I., Peterson B. M., Boehm A. B., McNeill K., & Nelson K. L. "Sunlight inactivation of human viruses and bacteriophages in coastal waters containing natural photosensitizers." *Environmental science & technology* 47.4: 1870-1878, (2013).
[4] World Health Organization. Results of round II of the WHO international scheme to evaluate household water treatment technologies. World Health Organization, (2019).
[5] Luzi S., Tobler M., Suter F., & Meierhofer R., "SODIS manual: Guidance on solar water disinfection." *SANDEC, Department of Sanitation, Water and Solid Waste for Development: Eawag, Switzerland* 1-18, (2016).
[6] Sobsey M. D., Stauber C. E., Casanova L. M., Brown J. M., & Elliott M. A., "Point of use household drinking water filtration: a practical, effective solution for providing sustained access to safe drinking water in the developing world." *Environmental science & technology* 42.12: 4261-4267, (2008).
[7] García-Fresnadillo D. "Singlet Oxygen Photosensitizing Materials for Point-of-Use Water Disinfection with Solar Reactors." *ChemPhotoChem* 2.7: 512-534, (2018).
[8] Comuzzi C., Marino M., Poletti D., Boaro M., & Strazzolini P. New antimicrobial PVC composites. Porphyrins self-aggregation in tuning surface morphologies and photodynamic inactivation towards sustainable water disinfection. *Journal of Photochemistry and Photobiology A: Chemistry*, *430*, 113967, (2022).

Title: An innovative solar greenhouse for enhanced sewage sludge drying: a case study

Author(s): Alice Sorrenti*[1], Santo Fabio Corsino[1] and Michele Torregrossa[1]

[1]Department of Engineering, University of Palermo, Viale delle Scienze,90128 Palermo, Italy;
*Corresponding author, alice.sorrenti@unipa.it

Keyword(s): sludge reduction; convective drying; greenhouse; renewable energy; solar sludge drying; sustainable sludge management.

Abstract
In recent years, the continuous growth of the urban population, the improvement of the quality of human life and the development of agriculture and industry have made the topic of sludge treatment and disposal the subject of considerable and growing interest. Today it represents one of the major critical issues in the wastewater treatment cycle and is assuming growing importance at both a national and international level. In light of this, this work illustrates the design and testing of three different prototypes of solar greenhouses based on the principle of heat convection to achieve better sludge drying. The main objective of this work was to develop an efficient and sustainable drying system for sewage sludge. These prototypes, in fact, were powered by a renewable energy source such as solar energy, allowing not only to obtain a direct environmental benefit in terms of reduction of sewage sludge but also an indirect environmental benefit due to the use of a source of renewable energy.

Introduction
Due to the increase in industrialization and the growth of the world population – projected to reach an additional 8.6 billion people by 2030, according to the United Nations – many countries are implementing stricter laws on wastewater discharge standards [1]. To meet these, new wastewater treatment plants (WWTPs) will be constructed and the existing ones will be retrofitted to enhance the treatment capacity. This will result in a significant increase in sewage sludge generation which treatment and disposal will pose several environmental and economic concerns. Considering this, researchers are focusing on innovative technologies to achieve excess sludge minimization, with the aim to reduce the amount of sludge to be disposed [2]. Currently, both thermal and solar drying techniques are widely applied for sludge drying [3]. Thermal drying implies significant energy consumption, either from electrical vectors or directly from fossil fuels, leading to increased energy consumption. In order to adopt eco-friendly practices and leverage renewable energy, employing solar greenhouse drying systems emerges as a viable and advantageous solution for medium-small WWTPs located in climate zones with high solar radiation. Conventional solar greenhouses utilize both solar-generated hot water and the greenhouse effect to harness energy. Previous studies carried out on open and closed-static greenhouse dryers demonstrated that approximately 55 – 80% and 90% of dry solid concentration could be obtained in less than 2 months [4,5]. A recent study demonstrated that use of a forced ventilation system to provide hot air for sludge drying instead of hot water below the wet sludge enabled to achieve approximately 95% of dry solid concentration in about 25 days [6]. This study has laid the groundwork for the development of a technology for solar greenhouses based on the use of hot air produced by a solar panel. In light of this, the present work illustrates the design and testing of three different prototypes of solar greenhouses based on the principle of heat convection to obtain enhanced sludge drying. The main objective of this

work was the development of an efficient and sustainable drying system for sewage sludge. Indeed, these prototypes were fed by a renewable energy source such as solar energy, allowing not only to obtain a direct environmental benefit in terms of sewage sludge reduction but also an indirect environmental benefit due to the use of a renewable energy source.

Materials and methods

The pilot scale greenhouses were designed and constructed using a polyvinylchloride (PVC) tank of 0.97 m length, 0.64 m width. The horizontal surface area of each greenhouse was equal to 0.62 m^2 and the overall volume was 0.42 m^3. The roof had a height of 1 m at the top and it was constituted by two 10 mm transparent polycarbonate sheets inclined at 45 degrees. The bottom of the PVC tank was shaped by a thin concrete layer to provide a slope of approximately 1% toward a drainage pipe placed along the longitudinal axis of the tank. A drainage layer consisting of about 0.20 m of gravel with different particle size distribution (20–30 mm and 4–8 mm) and 0.05 m of sand was placed on the bottom of the tank. Each of the solar greenhouse was equipped with a forced ventilation system to provide hot air for sludge drying and to overcome the hydraulic head losses through the drainage and wet sludge layers. To this aim, a side-channel air blower (engine power of 0.2 kW) was installed. Air was introduced through two different inlet points: a perforated pipeline (6 mm medium-sized holes) placed within the drainage sand layer and above the sludge layer by means of three orifices (6 cm diameter) horizontally arranged. A properly shaped stainless-steel profiled sheet was placed on the perforated pipeline to ensure a homogeneous distribution of the air and to avoid the water percolation inside it. Hot air was produced by an aero-thermal flat solar panel (courtesy of SolarAir) (1.30 m^2) tilted at a 30-degree angle and south-oriented. Two dedicated flowmeters allowed the air flow regulation. The main components of the solar greenhouse system are below reported:

- Solar hot air system: composed of a Twin Solar 1.3 solar collector with a surface of 5.87 m^2 oriented to the south with a tilt of 40°.
- Solar greenhouse box: made of PVC, with a total volume of 0.34 m^3 (0.97 m × 0.64 m), coated with thermal insulation material, except for the roof made of honeycomb polycarbonate.
- Mini-electro fans: installed to ensure adequate air turbulence inside the greenhouses, with a size of 80 mm × 80 mm × 25 mm, operating at a voltage of 12 Volts with a current of 0.41 A.
- Side channel blower: with an electrical power of 0.2 kW and a flow rate of 40 m^3/h. This system is timed using a timer, drawing air from outside to the solar collector and pushing it inside the solar greenhouse (inlet air).
- Drained water and condensation water collection system.
- Photovoltaic system: feeding all electrical devices.

During the experiment, the three prototypes worked in parallel using the same excess sludge (initial humidity equal to 96%) taken from the wastewater treatment plant where the greenhouses were installed. Solar greenhouses worked in different modes. Specifically, solar greenhouse A worked by blowing hot air over the sludge layer; solar greenhouse B worked with insufflation under the sludge layer, while prototype C worked as a traditional bed.

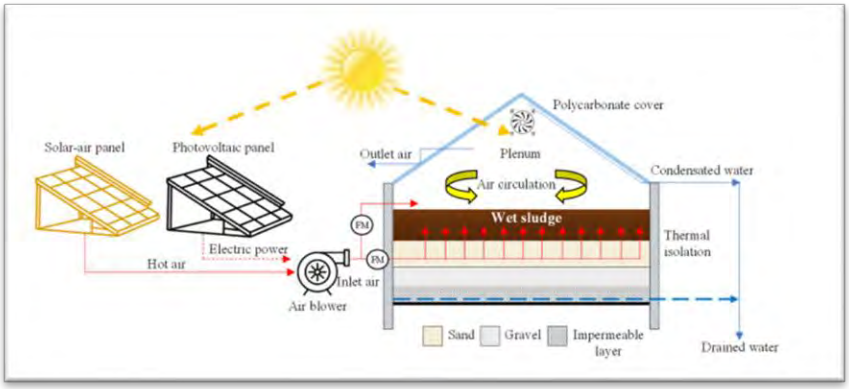

Figure 1. Schematic view of the static solar greenhouse

Results and discussion

To date, some interesting results have been obtained in this first phase of the experimental campaign. The air flow rate per unit area was initially set at 8 m/h and then, to study the effects of this flow rate on the humidity reduction yields, it was brought to 24 m/h from the 7th day until the end of the test.

The behavior of the sludge during the drying process has a trend in which 4 periods can be distinguished (Figure 2): the first section of the curve drying represents the removal of free water; then we observe a succession of two decreasing rates, respectively relative the removal of interstitial and surface water; while the last part of the curve is a short interval in which the bound water is removed and where an equilibrium humidity value of the mixture is reached. From a drying kinetic point of view, the first stretch is characterized by an almost constant drying kinetic, it subsequently takes on gradually decreasing values due to the fact that the free water has been removed, while longer times are required to remove the interstitial and surface water.

At the end of the first experimental campaign, which lasted 30 days, a reduction in sludge humidity of 53% was obtained for prototype greenhouse B, followed by 30% for greenhouse A versus 17% for the traditional drying bed. The weight of the sludge also went from the initial 115 kg to 7.88 kg after 30 days for greenhouse B. In general, the results show that the deformation of the sludge, the temperature, the drying kinetic and the intensity of solar radiation are the main factors that influence the sludge drying process.

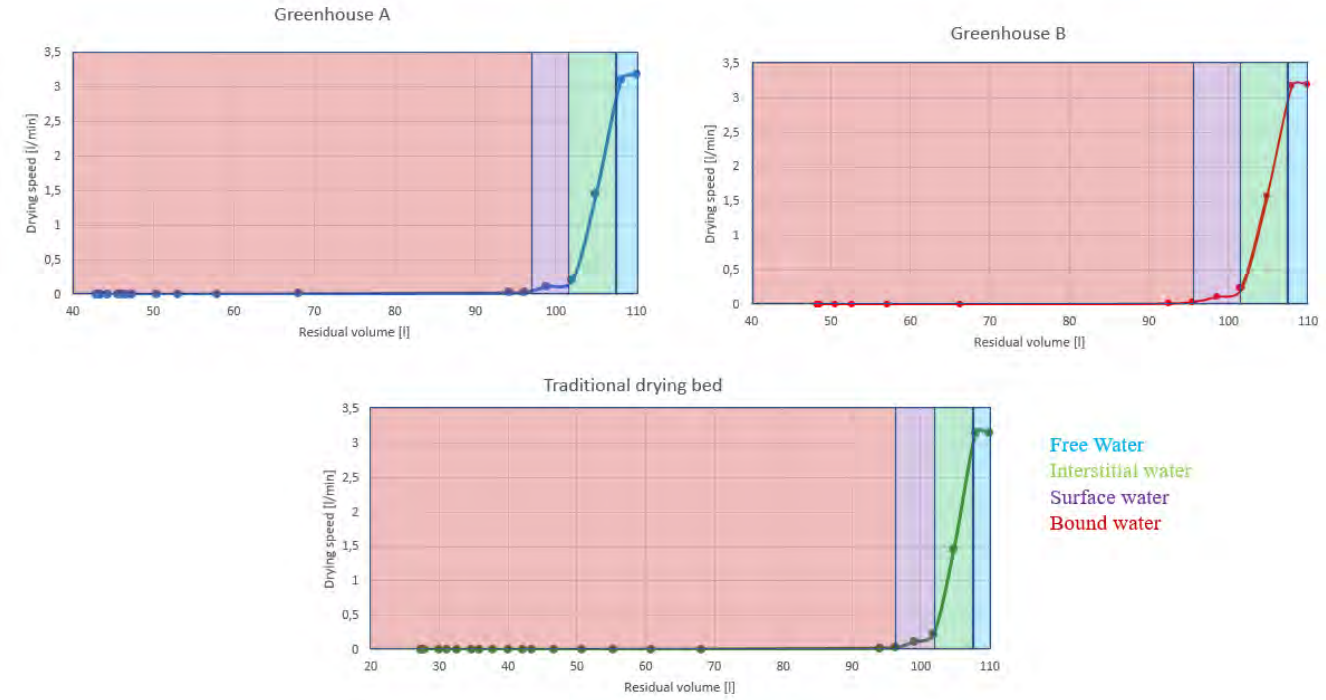

Figure 2. Drainage curves of three configurations

Conclusions

The results obtained during this experimental campaign highlight the system's benefits and validity compared to pre-existing systems in literature, without resort to traditional methods such as high temperature dehydration and incineration. The experimentation will continue through the analysis of further configurations by varying the main parameters: air flow rate, thickness of the sludge layer and initial characteristics of the sludge. In this way it will be possible to identify a system/technology that allows you to maximize drying performance, and identify the optimal values of the sizing parameters of this type of system.

References

[1] Belloulid, M.O., Hamdi, H., Mandi, L., Ouazzani, N., 2017. Solar Greenhouse Drying of Wastewater Sludges Under Arid Climate. Waste and Biomass Valorization 8, 193–202. https://doi.org/10.1007/s12649-016-9614-1
[2] Collivignarelli, M.C., Abbà, A., Miino, M.C., Torretta, V., 2019. What advanced treatments can be used to minimize the production of sewage sludge in WWTPs? Appl. Sci. 9. https://doi.org/10.3390/app9132650
[3]Mathioudakis, V.L., Kapagiannidis, A.G., Athanasoulia, E., Diamantis, V.I., Melidis, P., Aivasidis, A., 2009. Extended Dewatering of Sewage Sludge in Solar Drying Plants. Desalination 248, 733–739. https://doi.org/10.1016/j.desal.2009.01.011
[4]Morello, R., Di Capua, F., Esposito, G., Pirozzi, F., Fratino, U., Spasiano, D., 2022. Sludge minimization in mainstream wastewater treatment: Mechanisms, strategies, technologies, and current development. J. Environ. Manage. 319, 115756. https://doi.org/10.1016/j.jenvman.2022.115756
[5]Salihoglu, N., Pinarli, V., Salihoglu, G., 2007. Solar drying in sludge management in Turkey. Renew. Energy 32, 1661–1675. https://doi.org/10.1016/j.renene.2006.08.001
[6]Sorrenti, A., Corsino, S.F., Traina, F., Viviani, G., Torregrossa, M., 2022. Enhanced Sewage Sludge Drying with a Modified Solar Greenhouse. Clean Technol. 4, 407–419. https://doi.org/10.3390/cleantechnol4020025

Title: Utilizing Agro-food Waste as Soil Amendment to Mitigate Pesticide Leaching into Subsoil

Authors: Monica Granetto*[1], Carlo Bianco[1], Rajandrea Sethi[1], Tiziana Tosco*[1]

[1] DIATI – Dipartimento di Ingegneria dell'Ambiente, del Territorio e delle Infrastrutture, Politecnico di Torino, Torino, Italy, tiziana.tosco@polito.it

Keywords: Soil amendments, Zeolite, Biochar, Corncob, Pesticide leaching, Pesticide sorption

Introduction

Maintaining high-quality surface and groundwater is a global challenge, particularly with pollution from urban, industrial, and agricultural sources. Agricultural pollutants include excess nutrients (P and N), pesticides, and pharmaceuticals from localized spills or diffuse sources like manure application and fertilization. Controlling diffuse contamination is particularly challenging. Soil amendments, especially agricultural waste (e.g., sawdust, mowing, biochar) and minerals (e.g., zeolites), can be effective. While biochar and zeolites improve soil properties and water retention, their production is energy-intensive. Therefore, sustainable soil amendments obtained from agro-food waste with minimal energy use are desirable. Milled corncob and spent coffee grounds, due to their availability and porous structure, are promising candidates and were studied in this work in comparison with biochar and a zeolite for the adsorption of water contaminated by copper sulphate and dicamba. Copper sulphate is commonly used in organic farming as a fungicide for various crops and tends to accumulate in the soil, potentially remobilizing with changes in pH and salinity. It can also contaminate water resources through runoff. Dicamba, a broad spectrum herbicide, has high water solubility, leading to significant infiltration potential and moderate air volatilization [1]. In this work the use of the four soil amendments mixed with sand in varying proportions has proven effective in reducing leaching and, consequently, the contamination potential of these two pesticides [2]. The approach developed in this study can also be adapted for using these amendments in water treatment (e.g., biobeds or filter beds) or contaminated soils.

Materials and methods

The chosen soil amendments include zeolite, biochar, corncobs, and spent coffee grounds. The corncobs (Agrindustria) come from the inner part of corn cobs, obtained through extraction, drying, and grinding. The spent coffee grounds were washed with deionized water and dried. These materials were manually ground and characterized for morphology (SEM-EDX) and composition (XRD). They were then mixed with silica sand (Dorsilit 8, Dorfner, Germany) in proportions from 1% to 20% by weight. The mixtures were characterized for bulk density, pH, electrical conductivity, and water holding capacity (WHC) according to biochar certification standards [3].
Adsorption tests for copper sulphate ($CuSO_4$*$5H_2O$, Scharlab - Spain) and dicamba (Alfa Chemistry-US) were conducted at room temperature and pressure. Specifically, 2.5 g of each mixture were mixed with 25 ml of copper sulphate solution (124 to 624 mg/l) or dicamba solution (250 to 1500 mg/l). After 24 hours, the samples were centrifuged, and residual concentrations were measured using a UV-VIS spectrophotometer (Specord S600-Analytic Jena) and colorimetric detection with Zincon, following Ghasemi's method [4].

Leaching tests for dicamba and copper were conducted in vertical glass columns (4.1 cm diameter), packed with 320 g of pure sand or sand mixed with 5% zeolite, biochar, or corncobs. The material was saturated, and columns were weighed to determine porosity. After drainage, a water flow of 0.4 ml/min (infiltration rate of 0.028 cm/min) was established to maintain unsaturated conditions. A tracer test with 10 mM KBr was conducted, and electrical conductivity was recorded. Then, a solution of 624 mg/l copper sulphate or 1500 mg/l dicamba was injected for at least 7.5 hours, followed by flushing with potable water for another 7.5 hours. The concentrations in the column effluent were measured using the same methods as the adsorption tests. Results from the tracer and contaminant injection tests were interpreted with HYDRUS1D software (PC Progress) to obtain information on porosity, hydraulic conductivity, and the interaction of contaminants with the sand and amendments mixtures.

Results

SEM images (not reported) were processed to obtain the particle size distribution of the studied amendments. The average particle sizes (d_{50}) vary between 0.45, 0.4, 0.7, 0.55, and 0.6 mm for sand, zeolite, biochar, corncobs, and spent coffee grounds, respectively.
The water holding capacity (WHC) increases with increasing amendment percentage in the amendment-sand mixtures, following the trend: spent coffee grounds > biochar > corncobs > zeolite. At a 20% dose, spent coffee grounds have higher values compared to other materials, with a WHC of 0.62 g/g compared to 0.54, 0.55, and 0.34 g/g for mixtures with corncobs, biochar, and zeolite. The pH values of the pure materials are 7.45, 6.8, 8.4, 5.52, and 4.2 for sand, zeolite, biochar, corncobs, and spent coffee grounds, respectively. On average, adding amendments to sand causes a pH variation, increasing values by 11% with biochar or decreasing them by 9%, 34%, and 61% with zeolite, corncobs, and spent coffee grounds, respectively.
Figure 1 (top) displays the copper sulphate adsorption isotherms in terms of the mass of $CuSO_4$ adsorbed on the mixtures (sand+amendment) as a function of the equilibrium concentration reached in the liquid phase. The adsorption capacity follows the sequence biochar > spent coffee grounds > zeolite > corncobs: biochar performs the best, with the maximum adsorbed mass reaching 6 mg/g. The adsorption isotherms of biochar for doses below 5% show an asymptotic trend, indicating material saturation, while for higher doses, a distinctly linear trend is observed. Zeolite and spent coffee grounds exhibit comparable removal efficiencies, with isotherms showing similar trends and material saturation reached for doses below 20%. Lastly, corncobs show nearly linear isotherm trends at all sand ratios.
As for dicamba (Figure 1 bottom) the sorption isotherms show that the overall removal efficiency is higher for spent coffee grounds and corncobs, followed by biochar and zeolite. Dicamba is known to have a greater affinity for matrices with high organic content, such as corncobs and spent coffee grounds (Villaverde, 2008). The isotherms exhibit a distinctly linear trend, with no material saturation reached within the range of investigated concentrations.
Figure 2 illustrates breakthrough curves (concentration exiting the column normalized to the inlet concentration) for copper sulphate (left) and dicamba (right) in various column tests performed in partially saturated conditions, mimicking vertical percolation of water contaminated by the pesticides through soil. The tested porous materials include pure sand and sand mixed with zeolite, biochar (each at a 5% content). Porosity, determined gravimetrically, measured 0.405 for pure sand, 0.41 for the zeolite blend, 0.45 for corncobs, and 0.48 for biochar. Unsaturated water content ranged from 0.22 cm^3/cm^3 for sand alone to 0.21, 0.24, and 0.32 cm3/cm3 for the zeolite, corncobs, and biochar mixes, respectively.

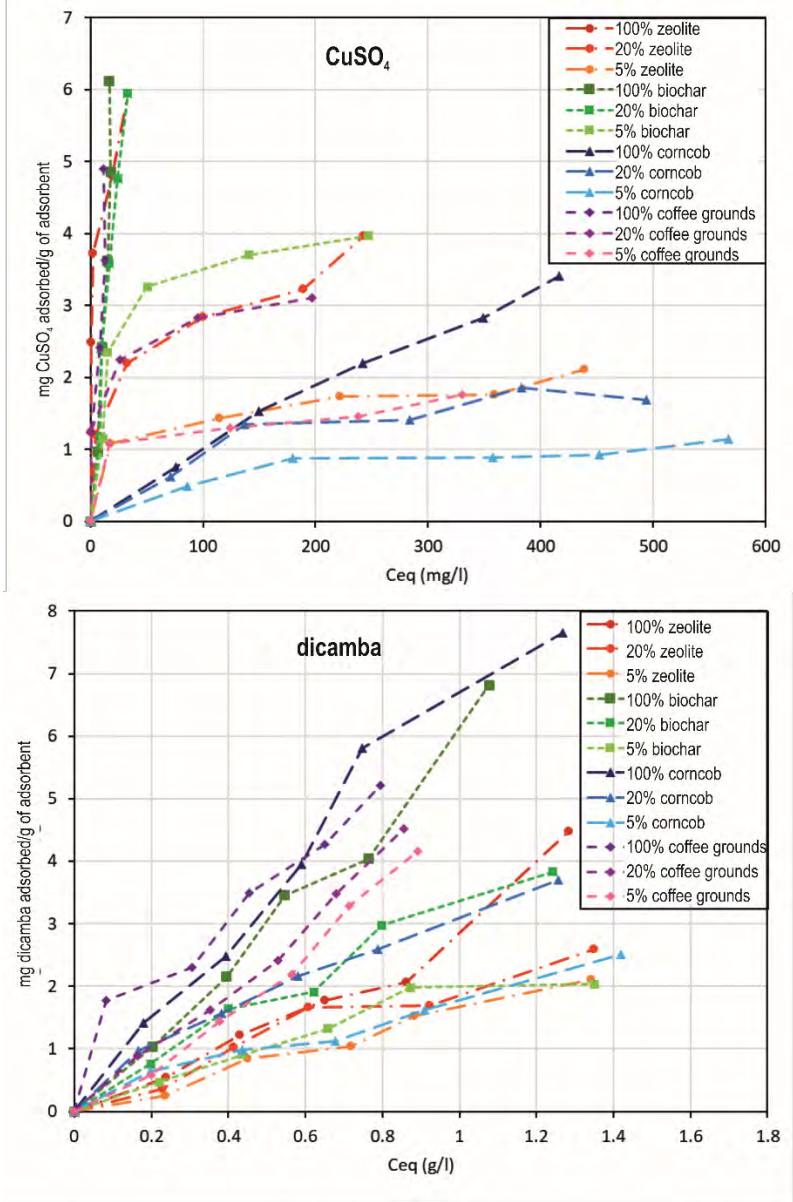

Figure 1. Copper sulphate and dicamba sorption isotherms on the sand-amendment mixtures

Regarding copper adsorption and its subsequent delay in column exit (figure 2 left), a pattern emerged: sand < sand and corncobs < sand and zeolite or biochar. In pure sand, copper sulphate exit experienced a delay, with C/C_0 values rising after 1.5 PV. Conversely, in mixtures involving zeolite, biochar, or corncobs, copper exit during injection was absent, suggesting a significant interaction (adsorption and/or precipitation) of the metal with the sand and amendment blends. These interactions were also evident from pH fluctuations during injection. However, for corncobs alone, post-injection flushing with water resulted in copper sulphate release, attributed to varying conditions such as ionic strength and pH. This finding suggests corncobs may be less suitable for field applications where soil hydrochemical conditions fluctuate.

Dicamba (Figure 2 right) in pure sand exited the column without delay, reaching plateau C/C_0 values

close to 0.9. Similarly, the sand-zeolite mixture did not exhibit a delayed breakthrough curve, maintaining a concentration C/C_0 of 0.8. Although biochar showed a similar plateau C/C_0 value, its exit from the column was delayed (around 1.5 PV). Notably, corncobs displayed a pronounced delay in dicamba exit (around 2.5 PV), with plateau concentrations C/C_0 at 0.6. These results align with batch adsorption tests, indicating corncobs' superior affinity for dicamba compared to biochar and zeolite.

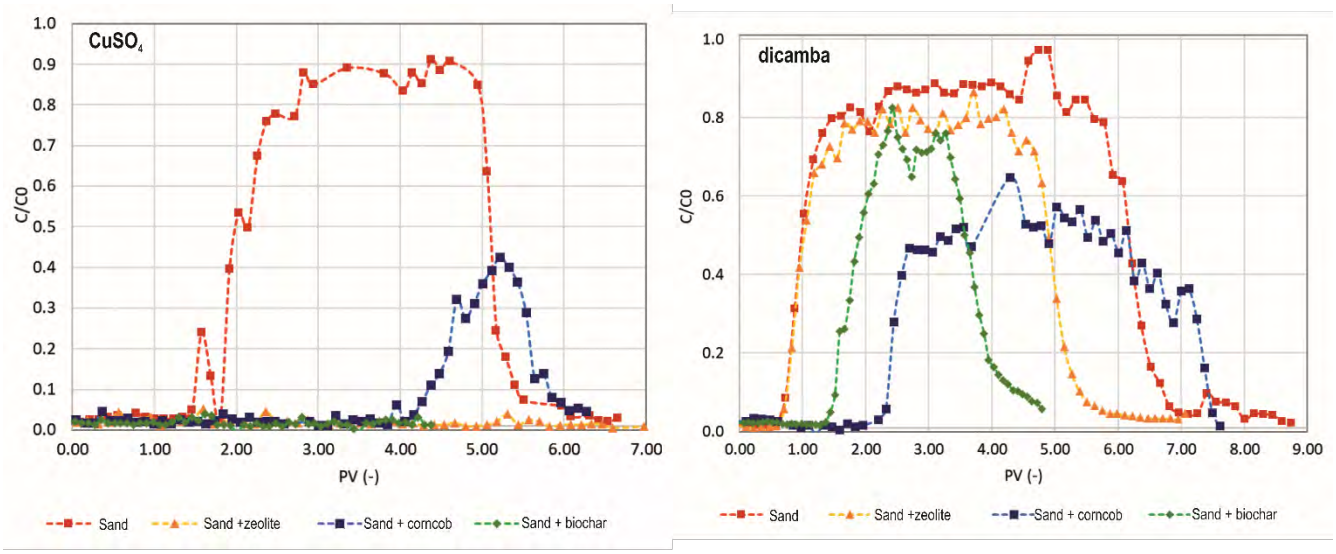

Figure 2. Breakthrough curves of copper sulphate (left) and dicamba (right) in partially saturated columns packed with sand-amendment mixtures (amendment mass ratio of 5%)

Conclusions

This study investigated the interaction between selected soil amendments and two pesticides, copper sulphate and dicamba, in laboratory conditions. Milled corncob, a byproduct of corn cultivation, and spent coffee ground were tested in comparison with a zeolite and a biochar sample under static and dynamic conditions to assess their adsorption potential and ability to reduce pesticide leaching in soils. The results suggest these amendments are highly effective in reducing pesticide leaching, indicating their potential use in agriculture to prevent contamination. In particular, milled corncob, despite the minimal pre-processing, showed comparable or higher efficacy with respect to biochar toward the organic pesticide and is thus a good candidate as soil amendment in view of a circular, low impact approach to the valorisation of agricultural waste.

References

[1] Granetto, M., Serpella, L., Fogliatto S., Re, L., Bianco C., Vidotto F., Tosco T. (2022) Natural clay and biopolymer-based nanopesticides to control the environmental spread of a soluble herbicide. Science of the total environment, 806 (3), 151199.
[2] Granetto, M., Bianco C., Sethi R., and Tosco T. (submitted). The role of soil amendments in limiting the leaching of agrochemicals: laboratory assessment for copper sulphate and dicamba.
[3] Schmidt, H.-P. (2015) European Biochar Certificate (EBC) - guidelines version 6.1.
[4] Ghasemi, J., Ahmadi, S., Torkestani, K., 2003. Simultaneous determination of copper, nickel, cobalt and zinc using zincon as a metallochromic indicator with partial least squares. Analytica Chimica Acta 487, 181-188.

Comparison between continuous stirred tank reactor (CSTR) and plug-flow reactor (PFR) for excess sludge minimization in CAS-ASSR-based process

Sara Mulone*[1], Marco Capodici[2], Santo Fabio Corsino[3], Michele Torregrossa[4]

[1] *Dipartimento di Ingegneria, Università degli Studi di Palermo, Palermo, Italia, sara.mulone@unipa.it*
[2] *Dipartimento di Ingegneria, Università degli Studi di Palermo, Palermo, Italia, marco.capodici@unipa.it*
[3] *Dipartimento di Ingegneria, Università degli Studi di Palermo, Palermo, Italia, santofabio.corsino@unipa.it*
[4] *Dipartimento di Ingegneria, Università degli Studi di Palermo, Palermo, Italia, michele.torregrossa@unipa.it*

Keyword(s): activated sludge, continuous stirred tank reactor, excess sludge minimization, plug-flow reactor, wastewater treatment

Abstract: The aim of this study was to investigate how the hydrodynamics of the anaerobic reactor affected excess sludge minimization performance in a CAS-ASSR based process. The research involved comparing two plants with identical configurations based on the ASSR process: one featuring a completely stirred tank anaerobic reactor (CSTAR), and the other employing a plug-flow-like (PFAR) hydrodynamic. Both the plants operated under the same AET (anaerobic exposure time) ranging between 13-8 h/d. The preliminary results suggested that the PFAR enabled better sludge minimization performances while operating at the same AET, because the exacerbation of metabolic stress conditions for biomass.

Introduction

Minimizing excess sludge from wastewater treatment plants is a critical issue due to increasing sludge production and stricter environmental regulations. Current research is focusing on the upgrading of conventional activated sludge (CAS) system with the aim to trigger excess sludge minimization, while resulting in low-cost and environmentally friendly technologies. One such method involves the anaerobic side-stream reactor (ASSR) process, which involves the insertion of an anaerobic tank in the return activated sludge (RAS) line toward which the entire flux or a portion of the settled sludge is subjected to anaerobic conditions [1]. This triggers mechanisms like uncoupling metabolism, sludge decay, and cell lysis that reduce bacterial growth [2].

Key parameters affecting sludge reduction in ASSR systems are considered the hydraulic retention time (HRT) and sludge interchange ratio (SIR). The HRT, meaning the duration sludge is held into the ASSR, ranges from a few hours to several days, with higher HRT generally improving sludge reduction. On the other hand, SIR, the fraction of RAS entering the ASSR, also impacts sludge reduction, though results vary widely. Several studies showed that both high and low HRT and SIR can yield similar sludge minimization efficiencies [3]–[5], suggesting other factors might be at play. Indeed, one critical factor is the frequency of sludge exposure to anaerobic conditions, which depends on the HRT of the mainstream reactors and RAS flux. This frequency can affect daily anaerobic contact time and overall sludge reduction efficiency. A previous study investigated the role of anaerobic exposure time (AET), calculated based on exposure frequency and HRT, in sludge reduction. Applying this concept, it was demonstrated a clear relationship between the AET and the sludge reduction yield [6]. In the literature, there is a lack of novelty regarding the role of the hydrodynamic of the anaerobic reactor on the sludge minimization yield.

Considering this, the aim of this work was to study the effects of the hydrodynamics of the ASSR reactor on the performance of excess sludge minimization. Specifically, the study was based on a comparison between two plants with the same configuration, based on the ASSR process: one equipped with a completely stirred tank anaerobic reactor (CSTAR) and the other with a plug-flow-like (PFAR) hydrodynamic.

Materials and methods

In this study, a laboratory-scale plant configured according to a CAS system was used. The plant consisted of an aeration basin with a variable volume of 15 to 25 liters and a 14.5-liter vertical-flow clarifier connected by gravity. The plant was fed with a synthetic medium at a constant flow rate of 2 L/h. Using synthetic influent helped control operational parameters (e.g., food to microorganism ratio - F/M) while varying the HRT of the aerobic reactor, and ensured results were not influenced by the qualitative characteristics of the influent. For details on the synthetic medium composition, refer to the literature [7]. The aerobic reactor was equipped with two porous-stone diffusers connected to an air blower providing a constant airflow of 5 L/min, maintaining a dissolved oxygen concentration of approximately 2 mg/L. To prevent poorly mixed zones, a vertical impeller was installed. The clarifier was equipped with a peristaltic pump that continuously extracted settled sludge from the hopper and recirculated it to the aeration basin at a constant flow rate of 2 L/h. Effluent wastewater was collected in a tank designed to trap suspended solids escaping the clarifier for more accurate solids mass balance calculations.

The ASSR configuration included an anaerobic reactor in line with the RAS, with the recirculated sludge passing entirely through the ASSR (SIR = 100%). The study was divided into two periods: during the first a 12-liter CSTAR was used, whereas in the second this was replaced by a 12-liter PFAR. The CSTAR was equipped with a vertical impeller and three vertical baffles placed at 120 degrees to ensure complete mixing. The PFAR was constituted by a rectangular basin divided into 6 zones, each mixed by a dedicated impeller.

Figure 1 illustrates a schematic layout of the plant.

The anaerobic exposure time was calculated as follows:

$$AET = \frac{V_{ASSR} \cdot x_{RAS} \cdot 24}{(V_{aerobic} + V_{clarifier}) \cdot x_{ML} + V_{ASSR} \cdot x_{ASSR}} = \frac{x_{RAS} \cdot 24}{\frac{(V_{aerobic} + V_{clarifier})}{V_{ASSR}} \cdot x_{ML} + x_{ASSR}} \quad \left[\frac{h}{day}\right] \qquad (eq.1)$$

Each plant operated into 3 phases, named phase I, phase II and phase III, characterized by different AETs (13 h/d, 10 h/d, and 8 h/d). This was achieved by increasing the volume of the aerobic reactor from 15 L to 20 L and 25 L.

The HRT in the ASSR was equal to 6 h. To maintain the same F/M, the biochemical oxygen demand (BOD) in the synthetic medium was increased to obtain 0.25 kgBOD/kgTSS·d, and the nutrients (nitrogen and phosphorus) dosage increased proportionally to maintain the same nutrients (carbon, nitrogen, phosphorous) ratio.

Effectiveness of the ASSR in terms of excess sludge minimization was assessed by means of the observed yield coefficient (Y_{obs}). This was calculated dividing the cumulative mass of total suspended solids (TSS) produced by the cumulative mass of COD removed (eq. 2).

$$Y_{obs} = \frac{mass\ of\ TSS\ produced}{mass\ of\ COD\ removed} = \frac{\Delta X}{Q_i \cdot (COD_{in} - COD_{out})} \quad \left[\frac{gTSS}{gCOD}\right] \qquad (eq.2)$$

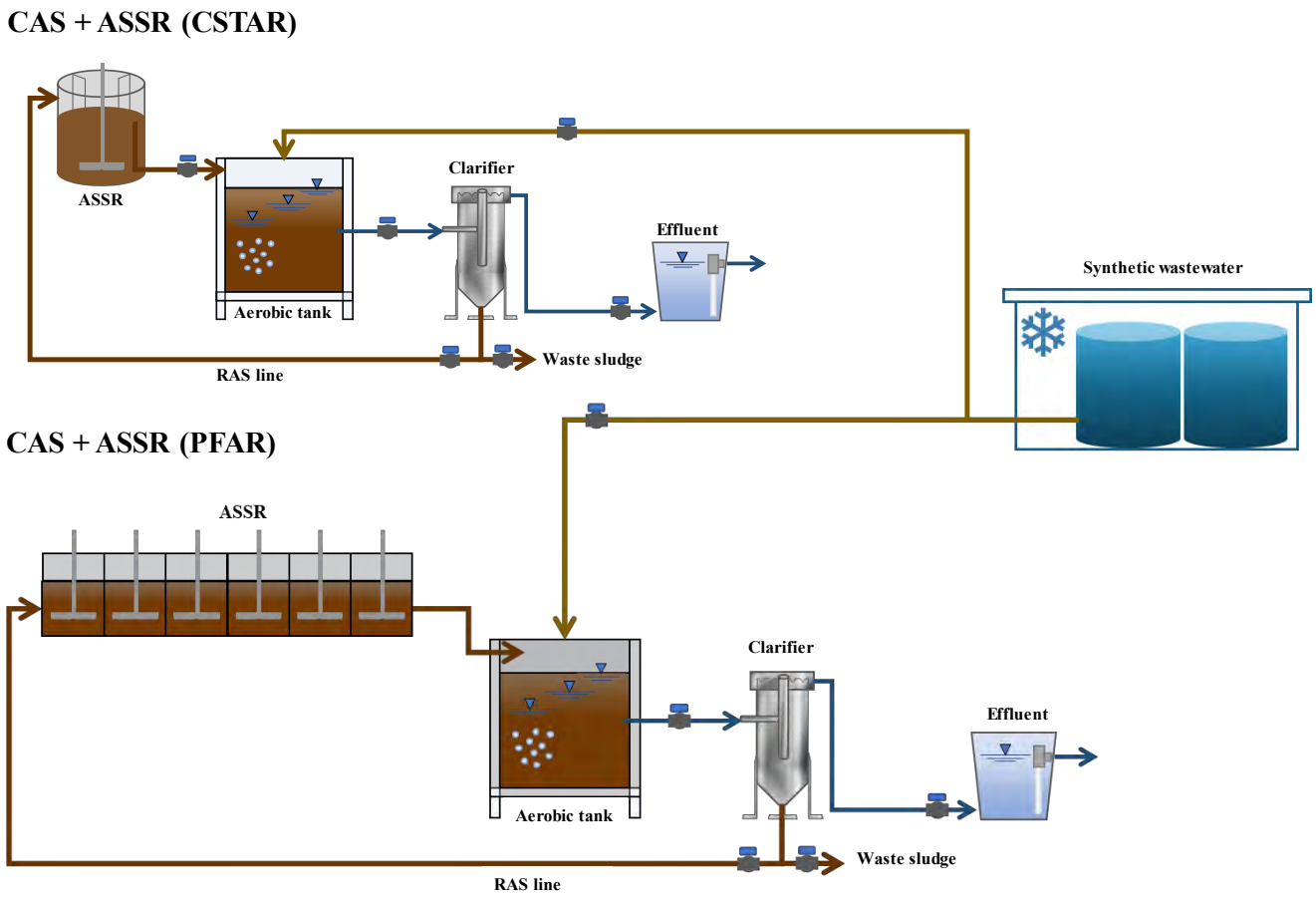

Figure 1: Plant layouts

Results and discussion

When operating with the CSTAR, excess sludge production was successfully reduced (10-60%) with the increase of the AET (8 – 13 h/d), although maintaining the same HRT in the ASSR and a constant sludge interchange ratio (SIR) (100%). In more detail, when the CSTR was operated with AET of 13 h/d, the observed yield coefficient began to decrease, stabilizing at approximately 0.27 gTSS/gCOD, leading to about 60% efficiency in excess sludge minimization. When the AET was decreased to 10 h/d, the observed yield coefficient stabilized at around 0.40 gTSS/gCOD, resulting in approximately 38% excess sludge minimization compared to the CAS configuration. A similar pattern was observed in the following stage, where the AET was further decreased to 8 h/d (Yobs = 0.58 gTSS/gCOD, meaning -10% of excess sludge minimization). Overall, when operating with CSTAR at low AET (< 6 h), the main mechanisms for sludge reduction were maintenance and uncoupling metabolism. Increasing the AET (> 8 h) favored the occurrence of extracellular polymeric substances (EPS) hydrolysis and endogenous decay mechanisms, leading to improved excess sludge reduction.
Results obtained with the PFAR during phase I (AET = 13 h/d) indicated that the observed yield reduction was greater than that observed in the ASSR with the CSTAR configuration. Indeed, at steady state, the Y_{obs} was equal to 0.20 gTSS/gCOD, thereby resulting in about 25% of sludge reduction improvement. Kinetic parameters indicated that biomass from the ASSR-PFAR was characterized by a

higher endogenous decay rate (3.4 d^{-1} vs 2.5 d^{-1}) than the CSTAR-ASSR, and the hydrolysis of extracellular polymeric substances (EPS) was more evident as suggested by the higher concentration of soluble EPS in the bulk (85 mg/gTSS vs 50 mg/gTSS). This suggested that at equal of AET, the plug-flow hydrodynamic occurred in the PFAR enhanced stressful conditions for activated sludge, leading to improved sludge minimization yields. Moreover, it was noticeable to note that the achievement of steady state during phase I was much faster in the PFAR (4 weeks vs 8 weeks).

Conclusions

The experimental activity is still ongoing, but preliminary results seem to confirm that the PFAR configuration ensures a quicker system response and a higher yield in reducing excess sludge production, even with the same AET, due to more intense metabolic stress conditions compared to the CSTAR-ASSR configuration.

References

[1] C. Park and D.-H. Chon, “High-Rate Anaerobic Side-Stream Reactor (ASSR) Processes to Minimize the Production of Excess Sludge,” *Water Environ. Res.*, vol. 87, no. 12, pp. 2090–2097, 2015, doi: 10.2175/106143015x14362865227355.

[2] R. Morello, F. Di Capua, G. Esposito, F. Pirozzi, U. Fratino, and D. Spasiano, “Sludge minimization in mainstream wastewater treatment: Mechanisms, strategies, technologies, and current development,” *J. Environ. Manage.*, vol. 319, no. July, p. 115756, 2022, doi: 10.1016/j.jenvman.2022.115756.

[3] C. L. Martins *et al.*, “Assessment of sludge reduction and microbial dynamics in an OSA process with short anaerobic retention time,” *Environ. Technol. Innov.*, vol. 19, p. 101025, 2020, doi: 10.1016/j.eti.2020.101025.

[4] R. Vitanza, A. Cortesi, M. E. De Arana-Sarabia, V. Gallo, and I. A. Vasiliadou, “Oxic settling anaerobic (OSA) process for excess sludge reduction: 16 months of management of a pilot plant fed with real wastewater,” *J. Water Process Eng.*, vol. 32, no. February, p. 100902, 2019, doi: 10.1016/j.jwpe.2019.100902.

[5] S. F. Corsino, T. S. de Oliveira, D. Di Trapani, M. Torregrossa, and G. Viviani, “Simultaneous sludge minimization, biological phosphorous removal and membrane fouling mitigation in a novel plant layout for MBR,” *J. Environ. Manage.*, vol. 259, no. October 2019, p. 109826, 2020, doi: 10.1016/j.jenvman.2019.109826.

[6] S. Mulone, S. F. Corsino, M. Capodici, and M. Torregrossa, “The anaerobic exposure time (AET) as a novel process parameter in the anaerobic side-stream reactor (ASSR)-based process for excess sludge minimization,” *Water Res.*, vol. 254, no. February, p. 121380, 2024, doi: 10.1016/j.watres.2024.121380.

[7] S. F. Corsino, T. S. de Oliveira, D. Di Trapani, M. Torregrossa, and G. Viviani, “Simultaneous sludge minimization, biological phosphorous removal and membrane fouling mitigation in a novel plant layout for MBR,” *J. Environ. Manage.*, vol. 259, p. 10986, 2020, doi: 10.1016/j.jenvman.2019.109826.

Assessment of early warning capacity of wastewater-based epidemiology for SARS-CoV-2 and Influenza virus: a synthesis of a 4-year experience in Sicily, Italy

Walter Priano*[1], Roberta Palermo[1], Fabio Tramuto[1,2], Walter Mazzucco[1,2], Gina Andolina[2], Francesca Rita Iaia[1], Arianna Russo[2], Viviana Giangreco[2], Giorgio Graziano[2], Francesco Vitale[1,2], Carmelo Massimo Maida[1,2]

[1] *Dipartimento di Promozione della Salute, Materno Infantile, Medicina Interna e Specialistica d'Eccellenza, Università di Palermo, Palermo, Italia*
[2] *Sicilian reference COVID-19 laboratory, UOC Epidemiologia Clinica, Azienda Ospedaliera Universitaria Policlinico "P. Giaccone", Palermo, Italia*

Keyword(s): wastewater-based epidemiology, wastewater, COVID-19, SARS-CoV-2

Abstract

Introduction

Originating in the 1920s to monitor typhoid fever in England, Wastewater-Based Epidemiology (WBE) has been extensively used for environmental surveillance of flaccid paralysis since the 1940s [1] as a proxy for the circulation of illicit substances and chemical exposure in the 1980s [2-4] and as a tool to provide early warnings for outbreaks of common pathogenic viruses such as hepatitis A [5] and E [6], poliovirus, and norovirus [7,8], as well as other viruses belonging to different families [9] (e.g. measles [10]). It represents an innovative, rapid, accurate, and cost-effective surveillance tool that provides essential aggregated qualitative and quantitative information about the health and behaviour of populations by detecting urinary and faecal markers in wastewater at the inlet of treatment plants, ensuring privacy. Although many factors can impact the shedding rate of viruses in the faeces, including viremia, the duration, severity, age and stage of the disease [11], studies have shown that SARS-CoV-2 is excreted in faeces early during the clinical course of the disease also in an asymptomatic population, representing an ideal target for wastewater monitoring [12]. Thus, routine wastewater epidemiological detection of SARS-CoV-2 has gained approval, as supported by numerous national and international projects (e.g., SARI, SARS-CoV-2 WBE NSF RCN, COVIDPoops19, SCORE, Global Water Pathogen Project) underscoring the importance of this tool at monitoring circulation of viruses in the population and identifying outbreaks, even before cases are reported to the healthcare system. Our working group operated in the framework of the national surveillance program by collecting and processing samples from wastewater plants located across the Sicilian region during SARS-CoV-2 spread. The aim was to investigate the relationship between the presence of the virus in wastewater and the trend of infection cases in the population of the Region, thus evaluating the potential of WBE as an early warning system, firstly for SARS-CoV-2 circulation and, in 2023, for Influenza virus.

Methods: **Collection of samples, Viral RNA extraction and RT-qPCR assays performing:** For each wastewater treatment plant (WTP), 1L of a 24-hour composite sample of raw sewage was collected, stored at +4°C, and analyzed to detect SARS-CoV-2 RNA. Samples were treated at 56°C for 30 minutes, concentrated using a polyethylene glycol (PEG)-based procedure [13], and centrifuged. The viral pellet was resuspended in lysis buffer for RNA extraction using a semi-automated method with magnetic silica. RT-qPCR assays targeting ORF1b were conducted using a thermal protocol that included reverse transcription, denaturation, and cycling. Positive results had Ct<40 within 40 cycles. SARS-CoV-2 quantification used 10-fold dilutions of dsDNA standards to create RT-qPCR standard curves, and results were expressed in GC/day/inhabitant. PCR inhibition was checked by comparing Ct

values of samples spiked with control RNA to water controls. The assay's limit of detection (LoD) was set at 2 GC/L. Concentration/extraction efficiency was evaluated using Murine Norovirus, with efficiency acceptable if ≥ 1%. The same protocol was used for Influenza virus detection, with quantification performed using synthetic double-stranded plasmid dilutions and LoD determined by spiking wastewater extracts.

Clinical data, statistical analysis and results:

Our first aim was to correlate the number of geo-referenced COVID-19 cases within the area served by a wastewater treatment plant with SARS-CoV-2 detection in wastewaters adducted to that plant to estimate the specificity of the method. Thus, eligible SARS-CoV-2 patients were residents/domiciled in Sicily with a confirmed positive RT-PCR test between **January 1, 2020**, and **August 31, 2021**. Subjects were anonymized, geocoded, and attributed to areas served by 9 WWTP's. For each area, we calculated the daily **prevalence** (number of active SARS-CoV-2 cases/residents*100,000) and **incidence** (number of new SARS-CoV-2 cases/residents*100,000) of active SARS-CoV-2 cases. A logistic regression model was calculated to evaluate the association between the active SARS-CoV-2 incidence rates and the probability of positive PCR results of wastewater samples; then, results were used to calculate the fitted predicted values for positive and negative PCR results of wastewater samples (Figure 1). ROC curve was used to assess the active SARS-CoV-2 incidence rates for each PCR sample (Figure 2A) and to identify an optimal cut-off value that could predict the active SARS-CoV-2 incidence rate (Figure 2B).

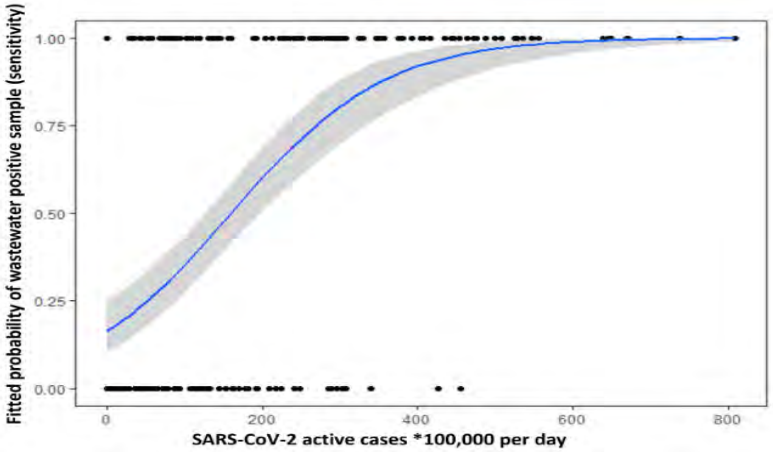

Figure 1. Predicted probability of positive wastewater according to the active SARS-CoV-2 cases.

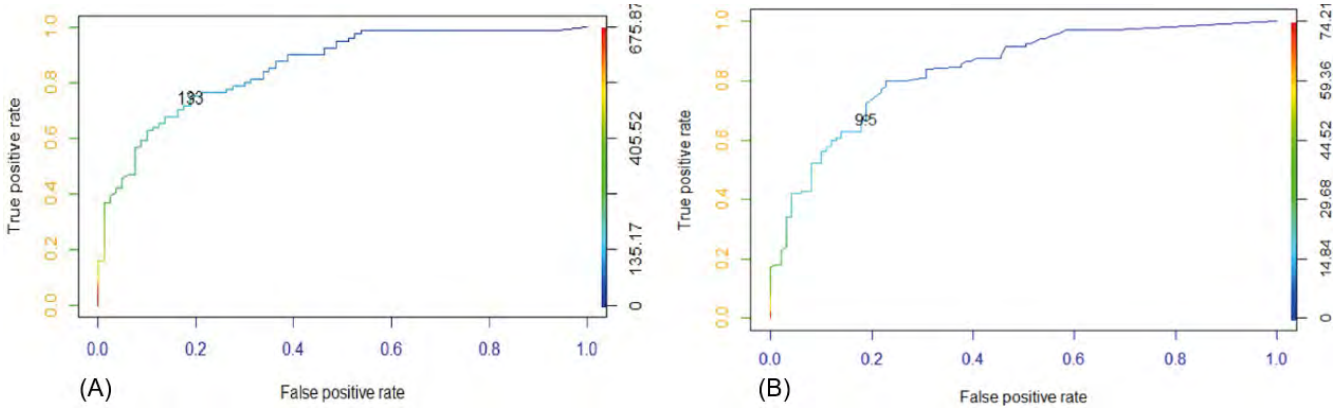

Figure 2: ROC curve to predict the number of A: SARS-CoV-2 active cases/100,000 inhabitants: best cut-off

133/100,000 residents; sensitivity=80.3%(69.2%–88.2%); specificity=76.5% (65.8%–84.7%); AUC=78.3% (70.9%–84.2%); and B: SARS-CoV-2 new cases/100,000 inhabitants: best cut-off **9.5/100,000 residents**; sensitivity=78.5% (69.3%–85.6%); specificity=78.8% (69.2%–86.1%); AUC=78.6% (72.3%–83.9%).

Our second evaluation was made to assess the early warning capacity of WBE for SARS-CoV-2 outbreaks by performing correlation analyses between the weekly amount of SARS-CoV-2 GC/L assessed I, samples, and clinical outcomes: hospitalizations, deaths, and ICU admissions of eligible SARS-CoV-2 positive cases between **October 1, 2021**, and **August 31, 2022**. Pearson's correlation test, log-linear regression analyses, and significance tests were performed to compare the mean weekly prevalence of cases with the mean weekly viral load (GC/L) detected at different periods (0-6 months, 7-12 months, and 12 months) and times (t0, t7, and t14) as shown in Figure 3 and 4.

		t0 Prevalence			t7 Prevalence			t14 Prevalence			Severe Clinical Outcomes		
	Time Periods (Months)	R	r^2	*p*-Value	R	r^2	*p*-Value	R	r^2	*p*-Value	R	r^2	*p*-Value
GC/L *	0–6	0.90	0.82	<0.001	0.89	0.79	<0.001	0.87	0.76	<0.001	0.93	0.61	<0.001
	7–12	0.77	0.59	<0.001	0.79	0.62	<0.001	0.69	0.47	<0.001	0.75	0.53	<0.001
	0–12	0.85	0.72	<0.001	0.87	0.76	<0.001	0.86	0.74	<0.001	0.90	0.51	<0.001

Figure 3: Pearson's correlation index and p-values for correlation analyses

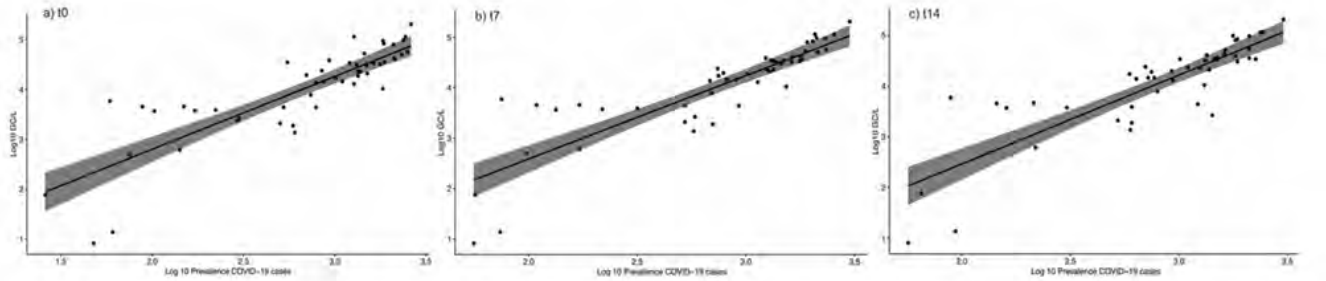

Figure 4: Correlation graphs between the viral load detected in wastewater and the prevalence of active cases reported in the communities during the 12-month COVID-19 surveillance at t0 (a) (R=0.85; p-value<0.001), t7 (b) (R=0.87; p-value<0.001), and t14 (c) (R=0.86; p-value<0.001).

Finally, we assessed WBE's early warning capacity for the Influenza virus. In detail, we accessed Influnet data to retrieve ILI incidence per 1,000 inhabitants in Sicily from week 42/2022 to week 17/2023. Regional swab data were also retrieved for this period. Influenza data were aggregated weekly, as the viral load obtained from 5 Sicilian WTPs (summed and log-transformed for analyses). Thus, using "sampling week" and "ILI incidence/1,000 inhabitants", the incidence was set at weeks 0, 1, and 2, and we performed correlation and significance tests, as shown and described in Figure 5.

	time	R	r^2	*p-value*
ILI x 1000 inhabitants (regional) x Influenza viral load GC/day/inhabitant	w0	0.60	0.30	<0.001
	w1	0.78	0.47	<0.0001
	w2	0.75	0.61	<0.0001
n° of IAV+IBV positive swabs (regional) x Influenza viral load GC/day/inhabitant	w0	0.66	0.21	<0.001
	w1	0.74	0.30	<0.0001
	w2	0.80	0.40	<0.0001

Figure 5: Correlation analysis between the mean weekly viral load in wastewaters and, respectively, the weekly

incidence of regional ILI x 1,000 inhabitants in Sicily and the cumulative number of IAV+IBV positive swabs detected in the Region at weeks 0,1 and 2.

Conclusion:

To conclude, as we portrayed throughout text and figures, an extensive validation for the early warning capacity of the WBE tool was assessed, not only for SARS-CoV-2, but for the Influenza virus too. Integrating WBE surveillance into clinical one could prove invaluable insights, estimating the prevalence of undiagnosed infections and predicting the spread of pathogens and genetic variants, aiding public health authorities in decision-making regarding implementation of containment measures.

References

[1] O'Reilly, K.M., Verity, R., Durry, E. et al. Population sensitivity of acute flaccid paralysis and environmental surveillance for serotype 1 poliovirus in Pakistan: an observational study. BMC Infect Dis 18, 176 (2018). https://doi.org/10.1186/s12879-018-3070-4
[2] Choi PM, Tscharke B, Samanipour S, Hall WD, Gartner CE, Mueller JF, Thomas KV, O'Brien JW, "Social, demographic, and economic correlates of food and chemical consumption measured by wastewater-based epidemiology", in Proc. Natl. Acad. Sci. U.S.A., vol. 116, n. 43, Oct. 2019, pp. 21864-21873, DOI:10.1073/pnas.1910242116, PMC 6815118, PMID 31591193
[3] Daglioglu N, Guzel EY, Kilercioglu S, "Assessment of illicit drugs in wastewater and estimation of drugs of abuse in Adana Province, Turkey, in Forensic Sci. Int., vol. 294, Jan 2019, pp. 132-139, DOI:10.1016/j.forsciint.2018.11.012, PMID 30529037
[4] Cosenza A, Maida CM, Piscionieri D, Fanara S, Di Gaudio F, Viviani G, Occurrence of illicit drugs in two wastewater treatment plants in the South of Italy, in Chemosphere, vol. 198, maggio 2018, pp. 377-385, DOI:10.1016/j.chemosphere.2018.01.158, PMID 29421753
[5] Hellmér, Maria, et al. "Detection of pathogenic viruses in sewage provided early warnings of hepatitis A virus and norovirus outbreaks." Applied and environmental microbiology 80.21 (2014): 6771-6781.
[6] Alfonsi, Valeria, et al. "Hepatitis E in Italy: 5 years of national epidemiological, virological and environmental surveillance, 2012 to 2016." Eurosurveillance 23.41 (2018): 1700517.
[7] Anthony I. Okoh, Thulani Sibanda e Siyabulela S. Gusha, Inadequately Treated Wastewater as a Source of Human Enteric Viruses in the Environment, in International Journal of Environmental Research and Public Health, vol. 7, n. 6, MDPI AG, 14 giugno 2010, pp. 2620-2637, DOI:10.3390/ijerph7062620, ISSN 1660-4601
[8] Y Guillois-Bécel, E Couturier, JC Le Saux, AM Roque-Afonso, FS Le Guyader, A Le Goas, J Pernès, S Le Bechec, A Briand, C Robert, E Dussaix, M Pommepuy e V Vaillant, An oyster-associated hepatitis A outbreak in France in 2007., in Euro surveillance : bulletin Europeen sur les maladies transmissibles = European communicable disease bulletin, vol. 14, n. 10, 12 marzo 2009, ISSN 1025-496X
[9] Anthony I. Okoh, Thulani Sibanda e Siyabulela S. Gusha, Inadequately Treated Wastewater as a Source of Human Enteric Viruses in the Environment, in International Journal of Environmental Research and Public Health, vol. 7, n. 6, 2010, pp. 2620-2637, DOI:10.3390/ijerph7062620, ISSN 1660-4601
[10] Benschop, Kimberley SM, et al. "Polio and measles down the drain: environmental enterovirus surveillance in the Netherlands, 2005 to 2015." Applied and environmental microbiology 83.13 (2017): e00558-17.
[11] Chen, Y., Li, L., 2020. SARS-CoV-2: virus dynamics and host response. Lancet Infect. Dis. 20 (5), 515–516. https://doi.org/10.1016/S1473-3099(20)30235-8.
[12] Sandra Westhaus, Frank-Andreas Weber, Sabrina Schiwy, Volker Linnemann, Markus Brinkmann, Marek Widera, Carola Greve, Axel Janke, Henner Hollert, Thomas Wintgens e Sandra Ciesek, Detection of SARS-CoV-2 in raw and treated wastewater in Germany – Suitability for COVID-19 surveillance and potential transmission risks, in The Science of the total environment, vol. 751, Elsevier BV, 10 gennaio 2021, p. 141750, DOI:10.1016/j.scitotenv.2020.141750, ISSN 0048-9697.
[13] Wu,F.; Zhang, J.; Xiao, A.; Gu, X.; Lee, W.L.; Armas, F.; Kauffman, K.; Hanage, W.; Matus, M.; Ghaeli, N.; et al. SARS-CoV-2 Titers in Wastewater Are Higher than Expected from Clinically Confirmed Cases. mSystems 2020, 5, e00614-20.

ANALYSIS OF THE PFAS TREATMENT AND REGULATION

Deborah Panepinto [1], Barbara Ruffino [1] , Silvia Frisario [2] and Mariachiara Zanetti [1]

[1] *Politecnico di Torino, DIATI, Corso Duca degli Abruzzi 24, 10129 Torino, Italy*
[2] *Eni Rewind Spa, Piazza Boldrini 1, San Donato Milanese, Italy*

Keyword(s): PFAS, PFAS regulation, thermal treatment

Abstract

PFAS, which stands for Per- and Polyfluoroalkyl Substances, are a group of human-made chemicals that have been used in a wide range of products for their water- and grease-resistant properties. These chemicals have been used in products like non-stick cookware, water-repellent clothing, food packaging, and in firefighting foams.

They are often referred to as "forever chemicals" because they do not break down easily in the environment. The main sources of PFAS contamination include:

- Manufacturing Facilities: PFAS are used in the production of a variety of consumer and industrial products, including non-stick cookware, waterproof clothing, stain-resistant fabrics, and firefighting foams. Manufacturing plants that produce these products may release PFAS into the environment.
- Firefighting Foams: Aqueous film-forming foams (AFFF) containing PFAS have been used by firefighters to combat liquid fuel fires at airports, military bases, and other locations. The use of PFAS-containing firefighting foams has led to PFAS contamination of soil and water in these areas.
- Wastewater Treatment Plants: PFAS can enter wastewater treatment systems when products containing these chemicals are used or disposed of. Treatment plants may not effectively remove PFAS from the water, leading to contamination of surface waters.
- Landfills and Waste Sites: Products containing PFAS are often disposed of in landfills, which can leach PFAS into the surrounding soil and groundwater.
- Air Emissions: Some PFAS compounds can become airborne during manufacturing processes or from the use of products containing PFAS. These PFAS can be deposited onto land and water, contributing to contamination.
- Agricultural Runoff: PFAS can be found in biosolids (sewage sludge) that are sometimes used as fertilizer in agriculture. This can lead to PFAS entering the soil and groundwater and potentially accumulating in crops.

- Consumer Products: PFAS can be present in various consumer products, including non-stick cookware, food packaging, and stain-resistant carpets. Over time, these products may release PFAS into the environment.
- Contaminated Drinking Water: In areas where PFAS have contaminated groundwater or surface water, drinking water supplies can become a source of exposure. This can occur through runoff from contaminated sites or leaching from landfills.
- Industrial Discharges: Industrial facilities that use or produce PFAS-containing products may discharge PFAS into nearby water bodies.
- Dust and Soil: PFAS can settle in dust and soil, and people can be exposed through ingestion, inhalation, or skin contact with contaminated dust or soil.

PFAS are of concern because they are highly persistent in the environment and the human body, and some of them have been associated with various health risks. These health risks include:

1. Toxicity
2. Bioaccumulation
3. Environmental Contamination

Due to these concerns, there has been increased regulatory scrutiny and efforts to phase out the use of certain PFAS chemicals in various products. Some countries and regions have set limits on the use of certain PFAS compounds, and there are ongoing research and regulatory efforts to better understand and address the risks associated with these substances.

It's important to note that not all PFAS chemicals have the same level of toxicity or persistence, and ongoing research is aimed at better understanding the specific health and environmental risks associated with different types of PFAS.

When it comes to wastewater treatment plants, addressing PFAS can be a complex challenge. Here are some key points to consider:

- Source of PFAS: Wastewater treatment plants can receive PFAS from various sources, including industrial discharges, stormwater runoff, and domestic wastewater. Identifying the sources of PFAS in the influent is an important step in managing their presence.
- Treatment Technologies: Traditional wastewater treatment processes, such as primary and secondary treatment, are not effective at removing PFAS from water. Specialized treatment technologies are required to remove PFAS, such as granular activated carbon (GAC) adsorption, ion exchange, and advanced oxidation processes (AOPs). These technologies can be integrated into existing treatment plants.
- Granular Activated Carbon (GAC): GAC is a common method for removing PFAS. It involves passing the wastewater through a bed of activated carbon, which adsorbs the PFAS compounds. Over time, the GAC media becomes saturated and must be replaced or regenerated.
- Regulatory Standards: Regulations regarding PFAS in wastewater vary by region and can change over time. It's essential for wastewater treatment plants to stay informed about local and national regulations and standards.
- Sludge Management: The treatment of PFAS-contaminated wastewater can lead to the concentration of PFAS in the sludge generated during the treatment process. Proper management of this sludge is crucial to prevent further environmental contamination.

In summary, addressing PFAS in wastewater treatment plants requires specialized treatment technologies and close attention to regulations and also public concerns.

In this work a comprehensive investigation was conducted to analyze the temporal evolution of limits established for Perfluoroalkyl Substances (PFAS) in various environmental matrices (EPA, 2023). The analysis included limits for water intended for human use, including drinking water, surface waters, groundwater, and air. Countries such as the United States, Canada, the United Kingdom, Denmark, Sweden, and Germany played a significant role in developing regulations on PFAS. The European Union has set limits for PFAS in drinking water through Directive 2020/2184.

In Italy, the Veneto and Piedmont regions have shown particular interest in PFAS, setting limits for both drinking water and discharge. Italian regulations, such as Legislative Decree 18/2023 for drinking water, Legislative Decree 172/2015 for surface waters, and Ministerial Decree of July 6, 2016, for groundwater, reflect the country's commitment to managing the environmental impacts of PFAS. Currently, there are no European directives establishing limits for the presence of PFAS in groundwater.

From the point of view of the treatment, from the literature, it is evident that currently, thermal treatment is recognized as the only established solution to destroy PFAS, utilizing high temperatures to break C-F bonds (EPA, 2020) (Junli Wang, 2022) (Anushka Garg, 2023). Among various thermal treatment methods, incinerators are designed to maximize the destruction of organic compounds, minimizing the formation of incomplete combustion products.

Literature reveals that wastewater treatment plants exhibit concentrations of PFAS both in the influent and effluent, including the sludge from the treatment process ((Grace K. Longendyke, 2022) ((Bommanna G. Loganathan, 2007). Incineration appears to be one of the primary disposal methods for PFAS-contaminated treatment sludge.

In general, optimal conditions for achieving high yields in PFAS destruction through incineration indicate a temperature between 600 and 1000°C. This temperature varies based on the specific type of PFAS, suggesting that longer molecular chains require higher temperatures. The optimal residence time in the post-combustion chamber ranges from 2 to 10 seconds, emphasizing the importance of strong turbulence in the combustion chamber. According to scientific literature, efficiency in PFAS destruction, regardless of the considered matrix, reaches 99% under optimal operating conditions.

REFERENCES

Anushka Garg, N. P. (2023). Treatment technologies for removal of per- and polyfluoroalkyl substances (PFAS) in biosolids. Chemical Engineering Journal.

Bommanna G. Loganathan, K. S. (2007). Perfluoroalkyl sulfonates and perfluorocarboxylates in two wastewater treatment facilities in Kentucky and Georgia. ScienceDirect.

EPA. (2020). Per- and Polyfluoroalkyl Substances (PFAS): Incineration to Manage PFAS Waste Streams.

EPA. (2023). PFAS National Primary Drinking Water.

EPA. (2023). Proposed PFAS - National Primary Drinking Water Regulation.

Grace K. Longendyke, S. K. (2022). PFAS fate and destruction mechanisms during thermal treatment: a comprehensive review. Royal Society of Chemistry.

Junli Wang, Z. L. (2022). Critical Review of Thermal Decomposition of Per- and Polyfluoroalkyl Substances: Mechanisms and Implications for Thermal Treatment Processes. Environmental Science & Technology.

Preliminary results of Sequencing Batch Reactor (SBR) and Integrated Fixed Activated Sludge Reactor (IFAS) inoculated with solar saltern sediments in the treatment of hypersaline wastewater

Alex Ricoveri[1,2,3*], Riccardo Campo[1], Daniele Bacchi[3], David Gabriel[2], Giulio Munz[1]

[1] Department of Civil and Environmental Engineering University of Florence, Via S. Marta n. 3, 50139 Florence, Italy
[2] Department of Chemical, Biological and Environmental Engineering, Escola d'Enginyeria, Universitat Autònoma de Barcelona, 08193 Bellaterra, Spain
[3] Italprogetti Spa, Lung'Arno Pacinotti 59/A, 56020 Montopoli In Val D'Arno, Pisa, Italy.

Keywords (3-6): hypersaline wastewater, halophilic community, total organic carbon removal, carriers, biofilm.

INTRODUCTION

Lefebvre and Moletta [1] reported that, in 2006, approximately 5% of total wastewater consisted of saline and hypersaline wastewater. The increasing world population and growing industrialisation drive an increase in the production of saline wastewater [2]. Hypersaline wastewater (salt concentration >35 g NaCl/L) is generated by various industrial sectors (agri-food, tanning, pharmaceutical, oil, and gas) and is often associated with a high organic load [3].
The objective of treating saline and hypersaline wastewater is not to decrease the salt concentration (mainly NaCl) but rather to focus on reducing the concentration of Chemical Oxygen Demand (COD) and nutrients (N and P).
The conventional approach to treating this wastewater is the use of chemical-physical processes. This is reflected in the high costs of the depuration process and the possibility of generating further pollution due to the reagents used during wastewater treatment [4]. Despite the potential positive aspects of cost reduction and greater environmental sustainability, the full-scale implementation of biological processes under these conditions is lacking. Conventional microbial consortia cannot be used under hypersaline conditions due to the absence of strategies to regulate osmotic pressure and prevent cell death [5]. Otherwise, halophilic microorganisms live and thrive in hypersaline conditions [6].
Studies are scarce in the literature regarding the utilisation of these microorganisms for wastewater treatment. The metabolic limitations of halophilic biomass and the commonly reported challenges, such as oxygen diffusion, inadequate biomass sedimentation, corrosion issues, and effluent turbidity, may have deterred further investigation in this area [4].
This study aims to evaluate the preliminary performance of a sequentially operated reactor (SBR) and an integrated fixed activated sludge reactor (IFAS). The reactors were inoculated with hypersaline sediments and synthetic saline wastewater containing sodium acetate (70%), yeast (10%), and diethylene glycol (20%) (a pollutant present in some wastewaters produced by the oil and gas industry).

MATERIALS AND METHODS

Sequencing batch reactors

Two plexiglass reactors (SBR and IFAS) were equipped with a dissolved oxygen optical probe, pH meter, aeration pipeline, and flowmeters (Figure 1). In addition, an overhead mechanical stirrer ensures mixing (at 160 rpm) in the SBR reactor. The temperature was kept constant at 27°C using a thermostatic bath, while the airflow rate was adjusted to 140 L/h to prevent oxygen limitation in saline conditions. Polyethylene plastic carriers measuring 1.2 x 1 cm were used to fill approximately one-third of the IFAS reactor's apparent volume. Around 20 g of saline sediments from the Trapani solar saltern were used as inoculum for the SBR and IFAS reactors. The turn-on/off of the influent and effluent pumps, aeration, and mixing were controlled by an Arduino-based microcontroller. The reactors were run in a sequence of phases: feeding (8.6 min), reaction (283 min), sedimentation (60 min), and discharge (8 min) for an overall cycle length of 6 hours.

The influent solution was prepared keeping the organic carbon substrate separate from the nutrients in a different tank. In addition, once prepared, the organic carbon influent solution was kept at 4°C to avoid degradation. The solution was warmed and then dosed into the bioreactors. The C/N/P ratio was kept at 100/10/1 and the composition of the medium per litre of solution was:

NaCl 110 g, KCl 2 g, $MgCl*6H_2O$ 1.5 g, $MgSO_4*7H_2O$ 1.5 g, NaBr 0.15 g, $CaCl_2*2H_2O$ 0.05 g, KI 0.035 g, 1.04 g CH_3COONa, 0.163 g DEG, 0.109 g Yeast, 0.199 g $(NH_4)_2SO_4$, g 0.0185 KH_2PO_4 and 1 ml of trace element solution.

Organic carbon influent and effluent analyses were performed with a total organic carbon analyser multi-N/C (Analytic Jena, Germany). Influent and effluent samples were filtered at 0.45µ previous analysis. During 40 days of operation, hydraulic retention time (HRT) and organic loading rate (OLR) were 1.18 and 1.15 days and 163±15.4 mg C/L*day and 167±15.9 mg C/L respectively for the SBR and IFAS reactors.

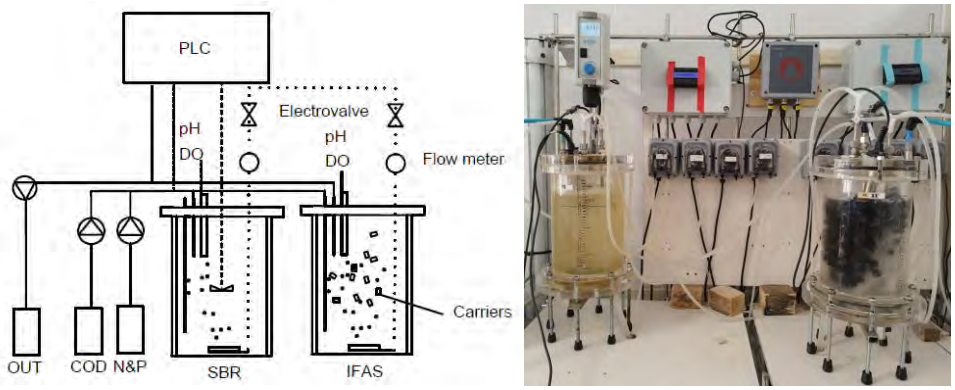

Figure 1. *Schematic representation of the reactors (sx) and image of the experimental set-up (dx).*

RESULTS AND DISCUSSION

As shown in Figure 2, the saline sediments had a fast response in terms of organic substrate degradation under aerobic conditions. SBR and IFAS influent varied 192.7±18.6 mgC/L and 191.8±14.3 mgC/L respectively. During the 40 days of the experiment, a halophilic microbial community was developed with a removal efficiency of 70.7±8.7% and 68.1±9% for SBR and IFAS, respectively. Acetate and yeast were the most probable substrates consumed. In a study conducted by Oren (2016) [7], they observed that halophilic microorganisms rapidly consumed acetate during dissolved oxygen tests in an Eilat salt pond.

Nevertheless, under the bioreactors' conditions, it appears that DEG was either not degraded or only partially degraded. The study conducted by Gotvajn and Zagorc-Koncan [8] describes DEG as a

compound exhibiting borderline characteristics of rapid biodegradability. In the simulation test conducted in a wastewater treatment plant using activated sludge (initial inoculum 2500 mg SS/L), complete removal of DEG was observed after four days, starting with an initial concentration of 150 mg/L.
To adequately assess the degradation of glycol under our experimental conditions, a higher concentration of biomass is required and a reduction in easily biodegradable substrates, specifically sodium acetate.
Following 38 days of operation, the plastic carriers were observed. The internal faces of an opened carrier are depicted in Figure 3. It is possible to see an incipient biofilm layer. The images obtained under the optical microscope show an aggregation of biological (production of extracellular polymeric substances) and inorganic (salt crystals) material. This approach could ensure that the biomass remains within the reactor bulk, preventing washout resulting from insufficient settling [9]. Furthermore, according to Hasanzadeh et al. 2020 [9], the biofilm structure may exhibit enhanced resilience to fluctuations in salinity and organic loading.

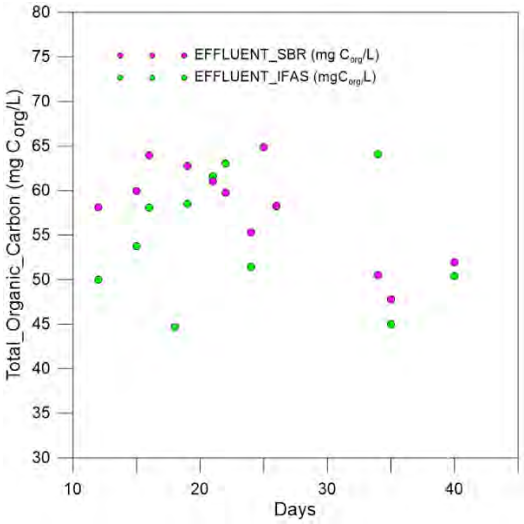

Figure 2 Total organic carbon concentration in SBR and IFAS effluent.

Figure 3 The carrier's internal surface shows an incipient biofilm after 38 days (sx). Detail of the biofilm (40 x magnification).

CONCLUSIONS

In this preliminary study, it was observed that biomass exhibits rapid activation and growth upon inoculation into the consumption of easily biodegradable compounds under hypersaline conditions, leading to a total organic carbon removal efficiency of approximately 70%. Furthermore, the IFAS configuration is promising, as shown by early biofilm formation on the carriers within the initial 38 days of testing. This has the potential to offer a solution to issues associated with biomass sedimentation under saline conditions. Furthermore, a higher concentration of biomass in the IFAS configuration would provide more definitive insights into the degradability of DEG under hypersaline conditions.
The presentation of these preliminary results could potentially afford a significant contribution to the utilisation of halophilic communities in industrial hypersaline wastewater treatment.

Acknowledgements

The present study received funding from the European Union's Horizon 2020 research and innovation programme under grant agreement No. 872053 (MSCA RISE RECYCLES).

References

[1] Lefebvre, O., & Moletta, R. (2006). Treatment of organic pollution in industrial saline wastewater: A literature review. In Water Research (Vol. 40, Issue 20, pp. 3671–3682). Elsevier Ltd. https://doi.org/10.1016/j.watres.2006.08.027

[2] Cui, Y. W., Zhang, H. Y., Ding, J. R., & Peng, Y. Z. (2016). The effects of salinity on nitrification using halophilic nitrifiers in a Sequencing Batch Reactor treating hypersaline wastewater. Scientific Reports, 6. https://doi.org/10.1038/srep24825

[3] Lefebvre, O., Vasudevan, N., Torrijos, M., Thanasekaran, K., & Moletta, R. (2005). Halophilic biological treatment of tannery soak liquor in a sequencing batch reactor. Water Research, 39(8), 1471–1480. https://doi.org/10.1016/j.watres.2004.12.038

[4] Zhao, Y., Zhuang, X., Ahmad, S., Sung, S., & Ni, S. Q. (2020). Biotreatment of high-salinity wastewater: current methods and future directions. In World Journal of Microbiology and Biotechnology (Vol. 36, Issue 3). Springer. https://doi.org/10.1007/s11274-020-02815-4

[5] Castillo-Carvajal, L. C., Sanz-Martín, J. L., & Barragán-Huerta, B. E. (2014). Biodegradation of organic pollutants in saline wastewater by halophilic microorganisms: A review. In Environmental Science and Pollution Research (Vol. 21, Issue 16, pp. 9578–9588). Springer Verlag. https://doi.org/10.1007/s11356-014-3036-z

[6] Oren, A. (2008). Microbial life at high salt concentrations: Phylogenetic and metabolic diversity. Saline Systems, 4(1). https://doi.org/10.1186/1746-1448-4-2

[7] Oren, A. (2016). Probing saltern brines with an oxygen electrode: What can we learn about the community metabolism in hypersaline systems? In Life (Vol. 6, Issue 2). MDPI AG. https://doi.org/10.3390/life6020023

[8] Zgajnar Gotvajn, A., & Zagorc-Koncan, J. (2003). Comparison of diethylene glycol and phenol biodegradability by different test methods. *Arhiv za higijenu rada i toksikologiju*, *54*(3), 189–195.

[9] Hasanzadeh, R., Abbasi Souraki, B., Pendashteh, A., Khayati, G., & Ahmadun, F. R. (2020). Application of isolated halophilic microorganisms suspended and immobilized on walnut shell as biocarrier for treatment of oilfield produced water. Journal of Hazardous Materials, 400. https://doi.org/10.1016/j.jhazmat.2020.123197

Title: Microbial Quality Control on Soil irrigated by treated secondary wastewater: case tomato plant

Author(s): *Rim Werheni Ammeri[1,2], El Bouali Sonia[2], Oueslati Maroua[2], Najla Sadfi-Zouaoui[2]

[1] *National Bone Marrow Transplant Center, Laboratory Ward, Tunis Rue Djebel Lakhdar 1006,Tunisia rimwerheni@gmail.com*
[2] *Laboratory of Mycology, Pathologies and Biomarkers (LR16ES05), Faculty of Sciences of Tunis, University Tunis El Manar, 2092 Tunis, Tunisia. : najla.sadfi@fst.utm.tn*

Abstract

Treated wastewater, also called effluent, can be a valuable resource for irrigation, especially in regions facing water scarcity. However, its use requires careful consideration of both the benefits and challenges involved. Our study is an evaluation of microbiological and chemical analysis soil irrigated by treated secondary wastewater as part of the international SWIRIPS.
The samples were collected from Tunisian agricultural soil. Firstly, we made the monitoring of the physical and chemical microbiological analysis to have an independent and complementary cross-check of the soil quality. After the pilot system is installed and running at the demo sites, water and soil samples will be taken out and in-lab tested. In addition, the effect on crop production irrigated with the purified wastewater produced will be studied, in order to study the possible onset of diseases that could be related to the water reuse and any beneficial or non-effects of using recycled water rich in nutrients.

Keywords: soil, wastewater, microbial quality, irrigation

Title: Diversity and Toxicological Potential of Fungal Contaminants in Tunisian Citrus Fruits: Implications for Food Safety and Public Health

Author(s): *Dorra Souei[1], Sabrine Abidi[1], Rania Hammami[1], Ichrak Hamdene[1], Carlos Lus[2], Giuseppe Meca De Caro[2], Najla Sadfi-Zouaoui[1]*

[1] Laboratory of Mycology, Pathologies and Biomarkers (LR16ES05), Faculty of Sciences of Tunis, University Tunis El Manar, 2092 Tunis, Tunisia. : souaidorra06@gmail.com; najla.sadfi@fst.utm.tn
[2]Laboratory of Agrifood Biotechnology, Faculty of Pharmacy, university of Valencia-SpainGiuseppe.Meca@uv.es

Abstract

The presence of fungi in agricultural products, particularly in Citrus fruits, poses significant risks to food safety due to their ability to produce toxic compounds known as mycotoxins. This study conducted in Tunisia aims to comprehensively investigate the toxin-producing capabilities of fungi isolated from Citrus fruits, shedding light on the potential health hazards associated with fungal contamination in the food supply chain.
Through rigorous examination processes, Citrus fruits displaying symptoms of fungal infection underwent isolation and identification of pathogenic fungi. The identified fungi species included Alternaria alternata, Aspergillus niger, Aspergillus flavus, and Penicillium sp., all renowned for their capacity to produce mycotoxins.
To confirm the toxin-producing potential of these fungi, axenic cultures were established and monitored. Results revealed a significant diversity in mycotoxin production among the different fungal strains. Particularly, Penicillium strains exhibited the highest mycotoxin production, with 42 different mycotoxins identified, followed by Alternaria and Aspergillus strains producing 32 and 30 mycotoxins, respectively. This extensive mycotoxin production underscores the pressing need to understand and mitigate fungal contamination in agricultural products.
Furthermore, molecular analysis was employed to explore the genetic basis of mycotoxin production in isolated fungi. The findings unveiled that Aspergillus flavus possessed genes responsible for Fumonisin, Aflatoxin, and trichothecenes mycotoxins, indicating its potential to produce multiple toxic compounds. Conversely, Aspergillus niger (Y18) was found to only harbor the trichothecene gene, suggesting a more limited mycotoxin production profile.
Among the Alternaria strains examined, the majority were found to possess the gene responsible for Alternariol monomethyl ether (AME), further highlighting the diversity of mycotoxin-producing capabilities within this genus.
Utilizing advanced analytical techniques such as UPLC-ESI-MS-TOF analysis, the study identified Citrinin, Alternariol monomethyl ether (AME), and Funalenone as the primary mycotoxins produced by Penicillium, Alternaria, and Aspergillus strains, respectively. This detailed characterization of mycotoxin profiles provides valuable insights into the potential health risks associated with fungal contamination in Citrus fruits.
In conclusion, this research significantly contributes to our understanding of the fungal ecology of Citrus fruits and emphasizes the critical need to implement effective strategies to mitigate fungal contamination and minimize mycotoxin exposure in the food supply chain, thereby safeguarding public health.

Keywords: UPLC-ESI-MS-TOF, toxinogenic fungi, mycotoxins, Citrus fruits

Title: Gamifying Training to Enhance Sustainable Occupational Health and Safety in Waste Treatment Plants: the SOHS project

Author(s): Barbara Rita Barricelli[1], Roya Biabani Reshtehroudi[1], Federica Caffaro[2], Raffaele Cioffi[3], Giuseppe De Palma[1], Daniela Fogli[1], Matteo Gremo[2], Niccolò Leonardi[4], Margherita Micheletti[3], Niccolò Pampuro[4], Emma Sala[1], Mentore Vaccari*[1]

[1] *Università degli Studi di Brescia, Brescia, Italy, {firstname.lastname}@unibs.it*
[2] *Università degli Studi Roma Tre, Rome, Italy, {firstname.lastname}@uniroma3.it*
[3] *Università degli Studi di Torino, Turin, Italy, {margherita.micheletti, r.cioffi}@unito.it*
[4] *Consiglio Nazionale delle Ricerche, Turin, Italy, {firstname.lastname}@stems.cnr.it*

Keyword(s): Occupational Safety and Health; Human Work Interaction Design; Gamification; Digital twin

Abstract

European municipal solid waste management (MSWM) strategies have notably evolved, adopting integrated methods that prioritize recycling and resource recovery [1]. This shift has led to more waste sorting and recovery facilities, thereby expanding the workforce engaged in waste management tasks [2] [3]. The increased complexity of these integrated MSWM systems introduces new occupational safety and health (OSH) risks that need to be carefully addressed.
Data from INAIL, the Italian public body overseeing mandatory insurance against workplace accidents and occupational diseases, indicates a troubling trend: from 2018 to 2022, the waste management sector reported over 10,000 work accidents and 1,000 work-related illnesses annually [4]. Beyond physical hazards, individual and psychosocial factors also negatively impact occupational safety and health (OSH). Unsafe behaviours, low risk perception, and failure to follow safety protocols significantly heighten the risk of accidents and illnesses [5] [6]. Effective training, a key component of OSH prevention as required by Italian legislation [7], has been shown to foster safe work practices, alleviate stress, and strengthen safety commitment, especially when interactive methods like hands-on demonstrations are used [8].
Gamification, which involves incorporating game-like elements into training, provides a cost-effective and flexible method that can deliver realistic simulations and support learner-centred education [9] [10] [11]. This method enhances engagement and knowledge retention, leading to improved safety outcomes. Current research has identified a significant gap in understanding the occupational safety and health (OSH) risks faced by workers in the expanding waste management sector, emphasizing the need for highly engaging safety training tailored to these specific OSH requirements [12].
In this paper, we provide a brief overview of the SOHS Project (Sustainable Occupational Health and Safety in Waste Treatment Plants: A Gamified Training Tool for Workers), a two-year research initiative funded by the PRIN 2022 Programme (Italian Research and University Ministry and European Union NextGenerationEU). The main objectives of this study can be summarized as follows: First, to conduct a comprehensive occupational risk assessment at three selected waste treatment plants, covering biomechanical, chemical, biological, and psychosocial risk factors encountered during on-site waste processing. This assessment will help define risk scenarios that include individual behavioral

components. Second, to design and develop a digital twin prototype, which is a virtual model of a waste management plant, to study various identified scenarios for workers' training. These scenarios will be incorporated as gamified elements to help workers recognize on-site hazards and learn correct and safe behaviors. Third, to test the prototype's usability in terms of effectiveness, efficiency, and satisfaction with diverse groups of workers, representing a wide range of human variability, including age, gender, cultural differences, and work expertise. Evaluating and improving the interactive system based on user feedback will effectively minimize the risk of the system failing to meet user or organizational needs. For this, the SOHS Project involves researchers from four institutions, each contributing complementary expertise in risk assessment, scenario identification, and the design, development, and usability evaluation of a gamified training prototype. Università degli Studi Roma Tre leads the project through its Department of Education, specializing in mixed-methods analysis of how individual and psychosocial variables impact occupational safety and health (OSH) and the overall efficiency and sustainability of work systems. The Italian National Research Council participates with the Institute of Sciences and Technologies for Sustainable Energy and Mobility (STEMS) in Turin, focusing on managing waste from the agri-food chain, monitoring greenhouse gas emissions from composting, and developing processes to convert agro-industrial by-products into organic fertilizers.

Università degli Studi di Torino contributes through its Department of Life Sciences and Systems Biology, focusing on anthropometric and biomechanical variability and its impact on human interaction with work environments and technology. This includes ergonomic analysis to improve health, safety, comfort, and overall well-being at work. Università degli Studi di Brescia is involved through three departments: the Sanitary and Environmental Engineering research group (Department of Civil, Architectural, and Environmental Engineering and Mathematics), which focuses on pollution phenomena and waste management technologies; the Occupational Health and Industrial Hygiene group (Department of Medical and Surgical Specialties, Radiological Sciences, and Public Health), which concentrates on occupational health and risk assessment using industrial hygiene methods; and the Human-Computer Interaction group (Department of Information Engineering), which brings expertise in Human Work Interaction Design, usability, and user experience for non-IT professionals deeply knowledgeable in their work domains.

To achieve the objectives of SOHS Project, two case studies have been selected to represent the majority of processes and working procedures related to Municipal Solid Waste Management (MSWM). The first plant is a social cooperative established in Brescia in 1995, which integrates social and environmental initiatives. The cooperative's activities and services in the environmental sector contribute to waste reduction, decreased consumption, and support innovative and cooperative efforts for the creative recovery and enhancement of human and natural resources. The second plant is a facility in Parma managed by a leading company in Emilia-Romagna specializing in the recovery of recyclable materials. Founded in 1963, this company has become a key player in non-hazardous waste recovery, focusing on paper and cardboard. With over 50 years of experience, the company offers comprehensive waste management solutions, providing appropriate equipment and leveraging advanced technology to meet customer needs.

The ongoing on-field risk assessment has yielded some initial findings. Key hazard zones include conveyor belts, loading/unloading stations, transit areas, and machinery/vehicle handling areas. Postural and biomechanical discomfort during task performance was observed but not always perceived by workers. Discomfort varied based on workers' anthropometric characteristics, such as height. Valuable feedback from domain experts regarding training needs will inform the creation of engaging and effective scenarios. Gamification strategies will be employed to motivate workers' participation through rewards and recognition systems.

References

[1] Chen X., Geng Y., Fujita T., “An overview of municipal solid waste management in China,” Waste Management 30(4), 716–724 (2010).
[2] Song J., Feng R., Yue C., Shao Y., Han J., Xing J., Yang W., “Reinforced urban waste management for resource, energy and environmental benefits: China’s regional potentials,” Resources, Conservation and Recycling 178, 106083 (2022).
[3] Szulc J., Okrasa M., Majchrzycka K., Sulyok M., Nowak A., Szponar B., Górczyńska A., Ryngajłło M., Gutarowska B., “Microbiological and toxicological hazard assessment in a waste sorting plant and proper respiratory protection,” Journal of Environmental Management 303, 114257 (2022).
[4] INAIL Istituto Nazionale Assicurazione contro gli Infortuni sul Lavoro. Banca dati statistica. Retrieved 07/05/2024 (2023).
[5] Caffaro F., Micheletti Cremasco M., Roccato M., Cavallo E., “It does not occur by chance: a mediation model of the influence of workers’ characteristics, work environment factors, and near misses on agricultural machinery-related accidents,” Int. J. Occup. Environ Health 23(1), 52–59 (2017).
[6] Glasscock, D. J., Rasmussen, K., Carstensen, O., Hansen, O. N., “Psychosocial factors and safety behaviour as predictors of accidental work injuries in farming,” *Work & Stress*, *20*(2), 173-189 (2006).
[7] D.lgs 81/2008. Testo coordinato con il d.lgs. 3 agosto 2009, n. 106. Testo unico sulla salute e sicurezza sul lavoro (2008).
[8] Ricci F., Chiesi A., Bisio C., Panari C., Pelosi A., “Effectiveness of occupational health and safety training: A systematic review with meta-analysis,” Journal of Workplace Learning 28(6), 355–377 (2016).
[9] Brahm F., Singer M., “Is more engaging safety training always better in reducing accidents? evidence of self-selection from chilean panel data,” Journal of Safety Research 47(1), 85–92 (2013).
[10] Mohd N.I., Ali K.N., Ebrahimi S.S., Ahmad Fauzi A.F.A., “Understanding the level of self-directed learning and decision-making style of construction-related workers,” International Journal of Interactive Mobile Technologies 13(07), 44–53 (2019).
[11] Vigoroso L., Caffaro F., Micheletti Cremasco M., Cavallo E., “Innovating occupational safety training: A scoping review on digital games and possible applications in agriculture,” International Journal of Environmental Research and Public Health 18(4), 1868 (2021).
[12] Jedynska A., Kuijpers E., van den Berg C., Kruizinga A., Meima M., Spaan S. , “Biological agents and work-related diseases: results of a literature review, expert survey and analysis of monitoring systems,” Tech. rep., European Agency for Safety and Health at Work (2019).

Title: REMOVAL OF ALUMINIUM FROM A LOW - MINERAL CONTENT GROUNDWATER: A CASE STUDY

Author(s): Salvatore Nicosia[1], Gaspare Viviani[1]

[1] *Department of Engineering, University of Palermo, Palermo, Italy, salvatore.nicosia@unipa.it*

Keywords: aluminium removal, chemical water treatment, drinking water, flocculation, filtration

Abstract

Introduction

Aluminium is the most abundant metal in Earth's crust, and is also an ubiquitous one; yet, there is today a diffuse drive towards a severe reduction of Al content in drinking water. An actual case study – raised by a Municipality in Sicily, Italy - gave us the occasion to try at the laboratory bench the selective removal of Al ions from a low-mineral content groundwater, based on their transformation into Al hydroxide, which is the only insoluble form among the many that this element can have in water.

The groundwater of our interest came from some natural springs in the *Madonie Massif* (Western Sicily, Italy), and had electrical conductivity 82 ÷ 96 mS/cm; pH = 6,8 ÷ 7,2; hardness just 2 - 4°F; and negligible turbidity. Recorded values of its aluminium content range between 400 and 800 mg/l, which is higher than the ceiling (200 μg/l) that is today recommended by WHO. It probably comes from some *laterite lenses* intercalated between the main limestone strata.

Indeed, the excellent general chemical quality of this groundwater for the consumer does not help in the task of removing Al only, because: 1. the very low original Al concentration range retards all the reactions; 2. the low mineral content provides the water with almost no buffer power; and, 3. none of the treatments aimed at Al removal can benefit here from synergies like e.g. the one with turbidity, which helps supplying nuclei in flocculation process.

A process arrangement in which a granular bed of calcium carbonate is used to stabilize pH at its optimum value, that is between 7 and 8; then a silica filter bed retains the particles just formed; proved itself effective at the bench scale in making Al to flocculate. To complete the treatment train, between the two columns an appropriate dose of lime can be dissolved into the water as a source of available OH ions.

To make the overall process' effectiveness more consistent, two more reagents were actually required: a small amount of a strong acid, and a polyelectrolyte as flocculation aid. The reasons will be explained in the following.

The Chemistry of Aluminium

Aluminium is an *amphoteric* element; one of the practical consequences is that, while metal hydroxides are generally just weakly soluble - or insoluble at all - the aluminium hydroxides, after formation and possible precipitation from water, in a strongly basic environment can re-ionize themselves and re-dissolve as anions. The Aluminium hydroxides equilibria are defined by the equation below (leftwards: basic behaviour; rightwards: acid behaviour):

$$[Al(H_2O)_6]^{3+}(aq) \overset{-\,3\,H_3O^+}{\underset{+\,3\,H_3O^+}{\rightleftarrows}} Al(OH)_3(H_2O)_3(s) \overset{+\,OH^-}{\underset{-\,OH^-}{\rightleftarrows}} [Al(OH)_4]^-(aq) + 3\,H_2O$$

Catione di un generico sale di Al idrato | Idrossido di Al | Anione idrossi-alluminato

Some remarks on this chemical equation:

- ✓ all the chemical species involved are hydrate: Al ions are aquo-ions, such as the hexa-aquo-ion $[Al(H_2O)_6]^{3+}$;
- ✓ Al hydroxide is the only neutral species; on account of neutrality, it is practically insoluble, and susceptible of precipitation;
- ✓ on the passage from aquo-cation to Al-hydroxide, the former loses 3 H_3O^+ and transfers them to water. This entails the *use* of 1 g-eq of water alkalinity per g-eq Al that turns itself into hydroxide.

Our Experimental Strategy to Remove Aluminium from Water

The first campaign of experiments we had made had demonstrated that in solution the rate and the extent of the theoretical steps of the equation written above are actually unreliable.

This is probably because the water molecules behave as a *barrier* between the targeted Al ion and the reagents, which are purposely added.

Therefore only the flocculation – filtration experiments following, made in filter beds (either reacting or inert) will be reported on here (Table 1).

Granular calcite (calcium carbonate) acts establishing the conditions of 1) pH; 2) stoichiometric alkalinity; and, 3) calcium ions availability; that are considered necessary to make aluminium to flocculate.

Silica shows itself chemically inert as it is supposed to be (Table 2). The dissolution – hydrolysis of calcite effectively sets the pH at 8.3 – 8.4, which is right for Al flocculation; while providing a small amount of hydroxyls. However, $Al(OH)_3$ generation in a water of such chemical composition could require also some free hydroxyls, coming from the careful addition of a strong base such as lime:

$$[Al(H_2O)_6]^{3+} + 3\,OH^- \rightleftarrows Al(OH)_3 + 6\,H_2O.$$

Table 1. Strategy and variables of the experiments of flocculation – filtration made in filter beds

REAGENTS ADDED / DESCRIPTION	$Ca(OH)_2$ at 2‰	H_3PO_4 1 M	Poly-electrolyte solution at 1%	$AlCl_3$ at 200 mgAl/l	Granular calcite	Granular Silica 0,6÷0,8
Phase A: Experiments in *mild conditions*; municipal supply water non-Al enriched						
					■	■
Phase B: Experiments in *drastic conditions*; municipal supply water enriched in Al						
		■		■	■	■

Table 2. Chemical changes taking place in the two filter beds.

Filtering medium / Reacting system	Calcite				Silica sand			
90 ml calcite bed + 50 ml sand bed + supply water enriched of Al to 1 mg/l	pH		E.C., (µS/cm)		pH		E.C., (µS/cm)	
	before	after	before	after	before	after	before	after
After continuous flow of V = 40 Bed Volumes	6.9	8.4	87.3	108	8.4	8.3	108	106

The Bench-scale Pilot Plant

The bench-scale pilot plant which was set up in the Department's *Laboratory of Sanitary and Environmental Engineering* puts in practice the 2nd and the final units of a possible complete chain for Al removal from water (Figure 1). In Figure 2 the hydraulic setup of the pilot plant (left) and a picture with the 2 columns in series, with calcite beds (background) and silica (foreground) are reported. The main characteristics of the pilot plant are reported in Table 3.

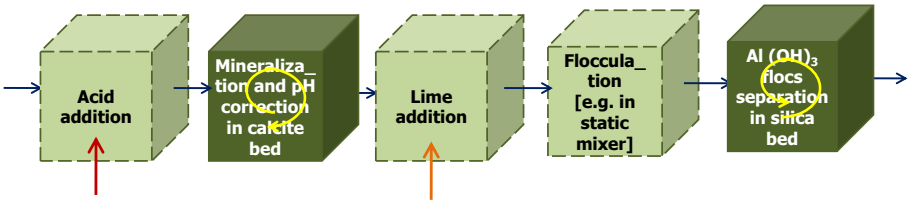

Figure 1. A possible treatment chain for Al removal

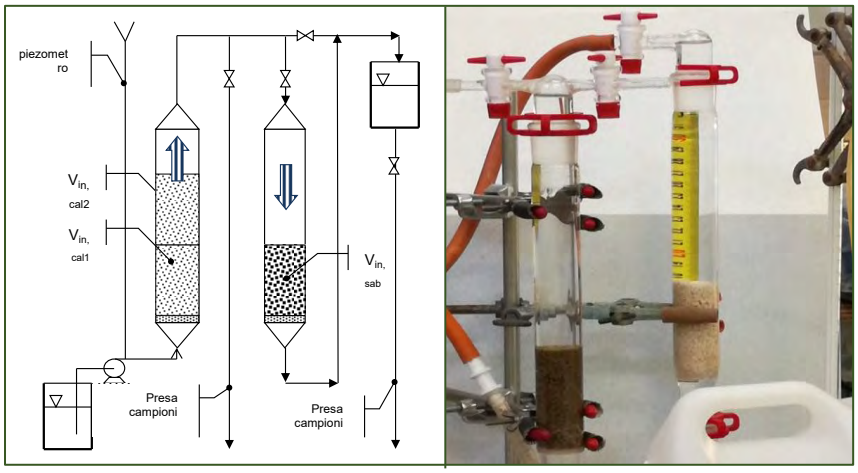

Figure 2. The pilot plant

Table 3. Design and operation parameters of the pilot plant.

FEATURE	VALUE	FEATURE	VALUE
Column internal diameter, D_i (cm)	3	Feed flow rate, F	1 100 cm^3/h; 10 BV/h for the calcite column; 20 for the sand
Column gross length, L (cm)	30	Empty Bed Contact Time (calcite bed)	(V/F) = (110 / 1.100) × 60 = 6 min
Bed depth, Z (cm)	17 for the calcite column; 8 for the sand one	Empty bed approach velocity, u = F / A (m/h)	1,4
Empty column cross section, A (cm^2)	7,1	*Particle Reynolds Number*, Re(p) = ($\rho \cdot u \cdot d_p / \mu \cdot e$)	(1000 × (1.4 / 3600) × 0.001) / (0,001 × 0.4) = 1.1
(Z/D_i) ratio	5,7	Empty column Reynolds Number, Re = ($\rho \cdot u \cdot D_i / \mu$)	13 → laminar flow pattern
Bed volume, V (cm^3)	110 for the calcite column; 8 for the sand one	Total head loss of the two filters in series (clean)	70 cm water column

Results and discussion

The four experiments that we ran with the pilot plant described above gave the following results. Alkalinisation by granular $CaCO_3$ proved itself to be the core reaction, and filtration in a silica bed an effective means of retaining suspended solids; nevertheless - in our case study - their efficiency when applied alone was rather low (about 50%).

A pre-treatment with acid did improve the process' effectiveness, probably demolishing the shield of water molecules. The most suitable acids are the phosphoric or the cheaper sulphuric; either dosed at 0,30 meq/l to get at about pH = 5. In our experiments this additional unit process increased the overall efficiency to about a valuable 90%.

Table 4. Efficiency of the filtration processes tested in removing Al from water

RELEVANT FEATURES	Acid before	Calcite	Sand	Lime	Poly-electrolyte	Inlet Al, µg/l	Outlet Al, µg/l	Removal Efficiency (Al), %
PHASE A						192,14	90	53
PHASE B						1.000	110	89
							90	91
							80	92

Conclusions

This lab-scale experiences showed that Aluminium can be selectively removed from natural waters intended for drinking use, simply by relying on its basic chemical behaviour with regard 1) to ambient pH, and 2) to the availability of Ca and OH; and making the conditions effective at their best.

In our case study, among the several reactions and processes that were tried, a sequence of 2 granular beds (calcite + silica) proved itself effective in the range 200 – 1 000 µgAl/l. This arrangement appears reliable, and also affordable even for a local Water Supply Service. The units for the addition of three reagents (an acid + lime + a polyelectrolyte), and an advanced mixing system, should be added to the chain in order to make up a real treatment plant.

References

[1] Hem, J. D. and Roberson,C. E. *Form and Stability of Aluminum Hydroxide Complexes in Dilute Solution. Determination of the effect of pH on aluminum solubility*. Geological Survey, Water Supply Paper 1827-A. U.S. Government Printing Office, Washington D.C. (1967)

[2] Lobo-Recio M. A., Rodrigues C., Custodio Jeremias T., Lapolli F., Padilla I. e Lopez Delgado A. *Highly efficient removal of aluminum, iron, and manganese ions using Linde type-A zeolite obtained from hazardous waste*. Chemosphere 267, 128919; https://doi.org/10.1016/j). (2021)

[3] Prakash K. H., Kumar R., Ooi C. P., Cheang P., and Khor K. A. *Apparent Solubility of Hydroxyapatite in Aqueous Medium and Its Influence on the Morphology of Nanocrystallites with Precipitation Temperature*. *Langmuir*, 22,11002-11008. (2006)

[4] Frommell, D.M.; Feld, C.M.; Snoeyink, V.L.; Melcher, B., and Feizoulof, C. *Aluminum residual control using orthophosphate*. J. Am. Water Works Assoc., 96(9): 99–109. (2004)

Acknowledgements

- *Mrs. Rosa D'Addelfio, Technician in charge of the Laboratory, took care of the instruments and of the pilot plant, and contributed to all the phases of the experimental work.*
- *Dr Geol Laura Ercoli (Università degli Studi di Palermo) contributed to this research with her sound knowledge of the stratigraphy and mineralogy of the Madonie Massif.*

Title: Advanced oxidation processes applied to microplastics degradation: a preliminary experimental study

Author(s): Federico Cecchini*[1], Valentina Innocenzi[2], Marina Prisciandaro[3]

[1] *Department of Industrial and Information Engineering, and of Economics, L'Aquila, Italy, federico.cecchini@graduate.univaq.it*
[2] *Department of Industrial and Information Engineering, and of Economics, L'Aquila, Italy, valentina.innocenzi1@univaq.it*
[3] *Department of Industrial and Information Engineering, and of Economics, L'Aquila, Italy, marina.prisciandaro@univaq.it*

Keyword(s): wastewater, microplastics, Fenton, advanced oxidation

Abstract

Microplastics, defined as plastic particles smaller than 5mm, have recently become a source of concern due to their potential threat to both aquatic species and humans. Microplastics do not have life-threatening effects on living organisms, but they can cause chronic toxicity [1], which is a major concern in long-term exposure. Microplastics can be classified as primary or secondary.
Primary microplastics are those that were initially produced to be less than 5 mm in size; they are commonly found in textiles, medicines, and personal care products such as face and body exfoliants [2]. These primary microplastics can be transported in both freshwater and seawater environments via rivers, discharges from water treatment plants, wind, and surface runoff [3].
Secondary microplastics result from the fragmentation of plastic debris due to physical, chemical, and biological interactions, but mainly due to processes such as photo-oxidative degradation, i.e. induced by ultraviolet radiation [4]. The basic mechanism of photo-oxidative degradation for the two plastics used in the highest volume and, thus, most numerous in marine debris, PE and PP, is well known [5].
Several studies ([6],[7]) report different values of microplastic removal by different sections of Wastewater Treatment Plants (WWTPs). However, the results are strongly influenced by the stages of sample collection, pretreatment, characterization, and quantification of microplastics. Both studies also highlight the presence of microplastics in effluents.
Several studies have shown how plastics are subject to photodegradation [4]. The basic mechanism of photo-oxidative degradation for the two plastics used in the highest volume and, therefore, most numerous in marine debris, PE and PP, is well known [5]. It is, therefore, conceivable to degrade microplastics through advanced oxidation processes.
This paper reports the results obtained in two experimental trials aimed at degrading microplastics using advanced oxidation process (AOP).

Materials and methods

A sample of Plasmix fragments, supplied by Montello Spa, a company based in Bergamo (Italy) that deals with the recycling of post-consumer plastic packaging, was used to carry out the laboratory tests. Plasmix is defined as a collection of heterogeneous plastics included in post-consumer packaging and not recovered as individual polymers. What comes from urban waste from the separate collection of plastics is sorted and sent for recycling for use in different applications.

To characterize the size distribution of the plastic fragments, a particle size analysis was carried out using a stack of sieves. The sieves used were in the order of 800 μm, 710 μm, 600 μm, 500 μm, 425 μm, 250 μm, 180 μm, 90 μm, 45 μm and 26 μm. The results of the sieving operation carried out on a 1g sample are shown below. To make the distribution more homogeneous, fragments larger than 800 μm were discarded because they could have caused problems during the experimental tests due to their large size. The results of the measurement are shown in the Table 1.

Table 1. Sample particle size.

Fraction (μm)	Weight (g)	%
<26	0.007	0.714
26-45	0.003	0.306
45-90	0.065	6.633
90-180	0.182	18.571
180-250	0.185	18.878
250-425	0.301	30.714
425-500	0.059	6.020
500-600	0.070	7.143
600-710	0.068	6.939
710-800	0.040	4.082
total	0.98	-

FTIR is the most used method for analyzing microplastics in wastewater treatment plants. FTIR analysis was performed on a sample of microplastics to obtain a precise chemical characterization and determine which polymers were most abundant among the fragments examined. The emission spectra are shown in Figure 1. The FTIR analysis revealed that polyethylene terephthalate (PET) was the most abundant polymer among the sample's fragments.

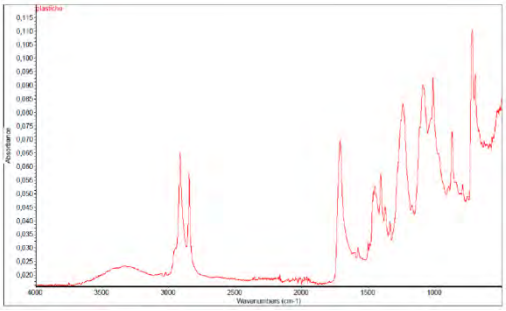

Figure 1. FTIR emission spectrum before the oxidation treatment.

The Fenton process is often used to remove organics from wastewater samples extracted from the WWTP. However, this treatment may impact the surface chemistry and size of microplastics.
The Fenton test was performed by mixing in a flask:

- 1g sample of microplastics.
- 1.1g ferrous sulfate hydrate (heptahydrate) $FeSO_4 \cdot 7H_2O$.
- 200 ml distilled water.
- 0.1 ml of concentrated H_2SO_4 sulphuric acid.
- H_2O_2 hydrogen peroxide in a 1:1 ratio with the ferrous sulphate.

The solution was left to stir using a magnetic stirrer to achieve complete mixing and for the oxidation reaction to occur. At the end of the process, a pH value of 3.74 was measured. Subsequently, the solution was filtered to regain the microplastics, which were left in an oven at 40°C for about 24 hours

to repeat the particle size analysis on the dry sample.
Another type of advanced oxidation that could be very efficient in the degradation of microplastics is acoustic cavitation. Acoustic cavitation occurs when ultrasonic waves cause pressure changes in a liquid. This process cyclically leads to the formation and collapse of cavitation bubbles.
Using a sonicator, the sample of microplastics was subjected to ultrasound to approximate the effects of acoustic cavitation. The sample of microplastics was placed inside a beaker containing water, and then the beaker was placed inside the sonicator to subject the plastics to ultrasound. The Plasmix solution was kept in the ultrasonic bath for a couple of hours and was then filtered to concentrate the microplastics. The resulting concentrated sample was dried in an oven at 50 °C for about a day before repeating the particle size analysis to assess any changes in particle size.

Results and Discussion
Table 2 displays the results of particle size analysis following oxidation treatments.

Table 2. Particle size analysis of treated microplastics.

Fraction (μm)	Post Fenton Weight (g)	Post Fenton %	Post Sonication Weight (g)	Post Sonication %
<26	0.000	0.000	0.000	0.000
26-45	0.003	0.321	0.000	0.000
45-90	0.045	4.813	0.014	1.781
90-180	0.135	14.439	0.139	17.684
180-250	0.130	13.904	0.161	20.483
250-425	0.227	24.278	0.249	31.679
425-500	0.070	7.487	0.048	6.107
500-600	0.103	11.016	0.068	8.651
600-710	0.108	11.551	0.052	6.616
710-800	0.114	12.193	0.055	6.997
total	0.935	-	0.78	-

Comparison of the particle size analysis carried out on the original sample with that carried out after the oxidation process shows an increase in all cuts larger than 425 μm, while the percentages for the smaller size classes decrease. Contrary to what might have been expected, following oxidation with the Fenton reagent, the amount of the larger particles increased, while the smaller ones decreased. In a nutshell, we can state that the degradation process does not take place, the phenomenon of the increase in size could be linked to an agglomeration of the microplastic particles because of the addition of the reagents, which act, probably under the operating conditions under consideration, as flocculants.
When comparing the emission spectra of the FTIR analysis of the sample subjected to the oxidation reaction using the Fenton reagent, shown in Figure 2, to those of the original sample, a difference in the spectra can be seen, most likely due to the presence of iron ions and OH molecules after treatment, which create interference and thus a modified spectrum compared to the initial one.
Research in the literature concerning the Fenton treatment of plastics shows that the reaction is ineffective in degrading microplastics. In fact, a study conducted by Tagg et al. in 2017 [8] analyzed the effects of Fenton's reagent on four different types of polymers (PE, PP, PVC, nylon). After experimenting with this advanced oxidation process on the polymers, also using different concentrations of hydrated ferrous sulphate (10, 20, 30 mg ml^{-1}), it was concluded that Fenton's reagent did not significantly affect the particle size of any of the four polymers, let alone the infrared absorption spectra derived from the FTIR analysis.

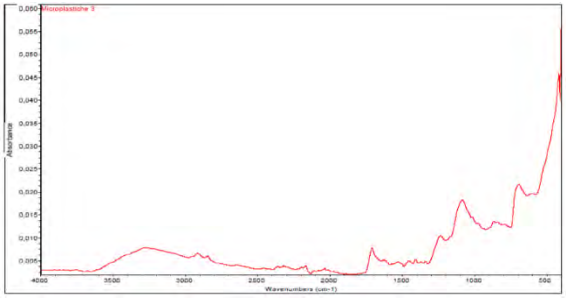

Figure 2. FTIR emission spectrum after Fenton treatment.

Comparing the particle size analysis carried out on the original sample and the one carried out following the sonication test, we can see that there is no significant change in size except for a slight decrease in the percentages for the smaller cuts. This means that the ultrasound-induced degradation failed to change the morphology of the plastic particles, most likely due to the too-low frequency at which the machinery used was working. For this reason, it would be interesting to evaluate the effect of the ultrasonic bath on microplastics when the frequency is higher.

Conclusion

Based on these preliminary findings, degrading microplastic particles using appropriate advanced oxidation methods is not currently considered a viable solution to microplastic pollution. This is because, in several experimental studies, oxidative techniques have failed to break the bonds that form the polymer particles, and because degrading microplastics risks producing fragments that are even smaller in size and thus more difficult to remove from wastewater.
However, the Fenton process results should not be interpreted as entirely negative. In fact, increasing the average sample size can improve particle separation. Future research could be conducted to validate the results obtained in this trial using specific coagulants, with the goal of further investigating pre-treatment steps that use flocculation processes to agglomerate microplastic particles before sending the effluent to a sedimentation basin, thereby increasing the efficiency of microplastic separation.

References

[1] Lee Y., Cho J., Sohn J., Kim C. “Health Effects of Microplastic Exposures: Current Issues and Perspectives in South Korea.” Yonsei Med J 2023, 64, 301, doi:10.3349/YMJ.2023.0048.
[2] Gouin T., Roche N., Lohmann R., Hodges G. “A Thermodynamic Approach for Assessing the Environmental Exposure of Chemicals Absorbed to Microplastic.” Environ Sci Technol 2011, 45, 1466–1472, doi:10.1021/ES1032025/SUPPL_FILE/ES1032025_SI_001.PDF.
[3] Gall S.C., Thompson R.C. “The Impact of Debris on Marine Life.” Mar Pollut Bull 2015, 92, 170–179, doi:10.1016/J.MARPOLBUL.2014.12.041.
[4] Andrady A.L., Hamid H.S., Torikai A. “Effects of Climate Change and UV-B on Materials.” Photochemical and Photobiological Sciences 2003, 2, 68–72, doi:10.1039/B211085G/METRICS.
[5] Singh B., Sharma N. “Mechanistic Implications of Plastic Degradation.” Polym Degrad Stab 2008, 93, 561–584, doi:10.1016/J.POLYMDEGRADSTAB.2007.11.008.
[6] Carr S.A., Liu J., Tesoro A.G. “Transport and Fate of Microplastic Particles in Wastewater Treatment Plants.” Water Res 2016, 91, 174–182, doi:10.1016/J.WATRES.2016.01.002.
[7] Murphy F., Ewins C., Carbonnier F., Quinn B. “Wastewater Treatment Works (WwTW) as a Source of Microplastics in the Aquatic Environment.” Environ Sci Technol 2016, 50, 5800–5808, doi:10.1021/ACS.EST.5B05416/SUPPL_FILE/ES5B05416_SI_001.PDF.
[8] Tagg A.S., Harrison J.P., Ju-Nam Y., Sapp M., Bradley E.L., Sinclair C.J., Ojeda J.J. “Fenton’s Reagent for the Rapid and Efficient Isolation of Microplastics from Wastewater.” Chemical Communications 2016, 53, 372–375, doi:10.1039/C6CC08798A.